2nd INTERNATIONAL SYMPOSIUM

AGROECOINFO

VOLOS, GREECE 30/6/2022-2/7/2022

AGROECOINFO

Edited by:

Nicolas R. Dalezios,University of Thessaly,Greece

Alfonso Dominguez Padilla, University of Castilla-La-Mancha (UCLM), Albacete, Spain

Gilles Belaud, Institut Agro -UMR G-eau, Montpellier, France

ISBN 978-618-84403-8-8

University of Thessaly, 2022

PREFACE

Agricultural production highly depends on climate conditions and is adversely affected by anthropogenic climate change, and it is foreseen that climate extremes, such as droughts, heatwaves, and floods, are expected to increase in the future. As a result, agricultural production risks could become an EU-wide issue. As yield variability intensifies, the food supply is at increasing risk. Climate change adaptation is being mainstreamed in new initiatives under the European Green Deal, including the EU Biodiversity Strategy, the Farm to Fork Strategy, the Circular Economy Action Plan, among others. The new Adaptation strategy anticipates the demands created by other initiatives in supplying a larger array of solutions and information on adaptation.

At the present time, the intensive crop production sector in Europe is at a crossroads, where it is faced with the challenging task of finding the direction that leads into a sustainable and resilient future. For example, intensive irrigated agriculture is a major pillar of global and national food security and often the only driver of rural economies, while it is also the largest water consumer and a major soil and water polluter, especially in Southern Europe. As a result, more sustainable crop management strategies and new incentives and policies are required for ensuring the sustainability of agriculture and ecosystem services without compromising environmental integrity. The challenge for sustainable and resilient crop production is to achieve optimized yield (in quantity and quality) and farm income with a minimum of inputs (nutrients, water, energy, pesticides, herbicides, land, labor, but also capital), while preserving the environment and nurturing flourishing social communities.

There is a range of technology available for implementing time-space precision farming- and sensor-based monitoring of agricultural production, although operational field applications are not commonly available. Due to the complex nature of databases, geoinformatics tools are increasingly employed to facilitate strategic and tactical applications at the farm, district/basin, and policy levels. Often these technological means are used without the necessary integrated view, addressing only isolated points or elements, which are impossible to evaluate in their effect on the overall yield. Indeed, an integrated approach is missing. Thus, it is necessary to consider a thorough spatiotemporal evaluation process to provide meaningful and timely advisory services to farmers. This process will also help orient the farmer in each moment on the optimum selection of measures along the crop growth cycle. Scientific and technical advances indicate that there is still a significant potential to increase the quantity and quality of crop production per surface unit in intensive production systems (irrigated and rainfed), as well as in small farms which have even less facilities to use decision support tools. The key to improving crop production efficiency and reducing its environmental impact is fine-tuning variability management, both in space (geographic location, topography, soils) and time (climate, weather, phenological growth stage). The elements that a farmer needs to manage are conceptually simple (selection of species and variety, soil preparation system, plant protection, nutrients management, and irrigation if needed). However, managing their space-time variability is far from being simple or easy. In the International Symposium “Ecosystems Sustainability and Geoinformatics: AGROECOINFO22”, the sustainability issue is presented and exposed along with technological and other tools and strategies for this purpose.

It is also necessary to develop new policies, new ways to involve farmers in the innovation process as well as adequate procedures and governance settings to overcome bottlenecks that prevent real scale adoption of improved new technologies within the farmers’ communities in Europe. This requires a performance assessment of selected measures from the field to the regional level. The overall objective remains to develop smart farming- and sensor-based monitoring to ensure sustainability and resilience of agriculture and ecosystem services, which are expected to improve yields and minimize the possible environmental risks at different scales, from farm to district and European scales. The key to improving the efficiency of crop production and reducing its environmental impact is the consideration of its temporal variability due to climate, which affects plants and phenology, as well as the spatial variability in terms of topography, soil type and geographical location. In the International Symposium “Ecosystems

Sustainability and Geoinformatics: AGROECOINFO22", tools and strategies are presented, which consider economic and environmental impacts and support farmers and decision makers at the farm, district and European levels.

The International Symposium "Ecosystems Sustainability and Geoinformatics: AGROECOINFO22" is held at the Park Hotel, Volos Greece, 30/6 – 2/7/2022. The International Symposium is jointly organized by:

1. University of Thessaly (UTH), Volos Greece
2. Sustainable production in water limited environments of Mediterranean Agro-ecosystem (SUPROMED) Project of the PRIMA 2018 program of the European Commission.
3. Open Innovation Hub for Irrigation Systems in Mediterranean Agriculture (HUBIS) project of the PRIMA 2019 program of the European Commission.
4. COST FAIRNESS action of the European Commission.
5. 3D S.A., General Aviation Applications, Thessaloniki, Greece.

The contents of the Proceedings cover a range of topics related to **Ecosystems Sustainability and Geoinformatics** including sessions on:

- **Climate Variability and Change: Impacts – Mitigation – Adaptation**
- **Ecological Management**
- **Environmental Hazards and Extremes**
- **Water Resources for Agriculture**
- **Digital Agriculture - Geoinformatics**
- **Ecosystems Sustainability**
- **Implementation in Water-Limited Environments**

AGROECOINFO22 aims to bring together professionals, experts and researchers working on **Ecosystems Sustainability and Geoinformatics**, emphasizing on solutions and innovations to real ecosystem cases and the respective challenges. We are pleased to report that this Proceedings Volume contains the ninety-four (94) accepted papers of the International Symposium "Ecosystems Sustainability and Geoinformatics: AGROECOINFO22". The accepted contributions are the result of a review process and follow the appropriate scientific and methodological procedures to present research results in the above-mentioned subjects.

Finally, the Proceedings Volume owes its appearance to the many efforts of the Scientific Committed, the Organizing Committed, the reviewers and above all the contributors themselves from many countries. It is believed that Europe provides a complex and challenging environment to develop and implement fruitful research in this significant and appealing field of **Ecosystems Sustainability and Geoinformatics,** which constitutes a current issue in Europe and internationally.

Volos, October 3, 2022

The Editors of this Proceedings Volume of the International Symposium "Ecosystems Sustainability and Geoinformatics: AGROECOINFO22":

Nicolas R. Dalezios, University of Thessaly (UTH), Volos, Greece

Alfonso Dominguez Padilla, University of Castilla-la-Mancha (UCLM), Albacete, Spain

Gilles Belaud, Institut Agro -UMR G-eau, Montpellier, France

LOCAL ORGANIZING COMMITTEE

Nicolas Dalezios, University of Thessaly Greece

Nikitas Mylopoulos, University of Thessaly, Greece

Nicholas Dercas, Agricultural University of Athens, Athens Greece

Dimitrios Skepastianos, 3DSA, General Aviation Applications, SA, Greece

Panagiotis Vlastaridis, University of Thessaly, Greece

Marios Spiliotopoulos, University of Thessaly, Greece

Ioannis Faraslis, University of Thessaly, Greece

Maria Stamou, University of Thessaly, Greece

Konstantina Giannousa, University of Thessaly, Greece

Georgios Tziatzios, University of Thessaly, Greece

Stavros Sakellariou, University of Thessaly, Greece

Nikos Alpanakis, University of Thessaly, Greece

Polychronis Velentzas, University of Thessaly, Greece

SCIENTIFIC COMMITTEE

Costin Badica, University of Craiova, Romania

Gilles Belaud, Institut Agro Montpellier, France

Dimitrios Bouranis, Agricultural University of Athens, Greece

Zhour Bouzidi, University Meknes Moulay Ismail, Morocco

Maria Do Rosario Cameira, University of Lisbon, Portugal

Olga Christopoulou, University of Thessaly Greece

Nicolas Dalezios, University of Thessaly Greece

Nicos Danalatos, University of Thessaly Greece

Nicholas Dercas, Agricultural University of Athens, Greece

Guido Durso, University of Naples Federico II, Italy

Josef Eitzinger, University of Natural Resources and Life Sciences, Austria

Eleftherios Eleftherohorinos, Aristotle University of Thessaloniki, Greece

Ioannis Faraslis, University of Thessaly, Greece

Athanasios Fragkou, University of Thessaly Greece

Rafael Angel Ferrer Martinez, Hispatec, Spain

Pedro Gavilán, Instituto Andaluz de Investigación y Formación Agraria Pesquera, Spain

Theofanis Gemtos, University of Thessaly, Greece

Athanasios Gertsis, Perrotis College, Greece

Anne Gobin, Katholic University of Leuven, Belgium

Evangelia Golia, Aristotle University of Thessaloniki, Greece

Tarik Hartani, University of Tipaza, Algeria

Ali Hammani, Institut Agronomique et Vétérinaire Hassan II, Morocco

Jari Hyvaluoma, Hame University of Applied Sciences, Finland

Kostas Kalabokidis, University of Aegean, Greece

Vasilis Kanakoudis, University of Thessaly, Greece

Theodoros Karakasidis, University of Thessaly, Greece

Fadi Karam, UL, Lebanon

Vanessa Katsardi, University of Thessaly, Greece

Nikos Katsoulas, University of Thessaly, Greece

Evangelos Keramaris, University of Thessaly, Greece

Kalliopi Kravari, Aristotle University Thessaloniki, Greece

Livari Kunttu, Hame University of Applied Sciences, Finland

Chrysi Laspidou, University of Thessaly, Greece

Ramón López-Urrea, ITAP, Spain

Athanasios Loukas, Aristotle University of Thessaloniki, Greece

José Antonio Martínez López, University of Castilla-La Mancha, Spain

Benoit Masquin, GAC Group, France

Luciano Mateos, Agencia Estatal Consejo Superior de Investigaciones Científicas (CSIC), Spain

Dimitris Melas, Aristotle University of Thessaloniki, Greece

Carlo De Michele, Ariespace, SME, Napoli Italy

Luca Montanarella, JRC, Joint Research Center-EU, Italy

Nikitas Mylopoulos, University of Thessaly, Greece

Panagiotis Nastos, University of Athens

Pavol Nejedlik, ESI, Earth Science Institute of the Slovac Academy of Sciences. Slovakia

Claas Nendel, Leibniz Center for Agricultural Landscape Research,Germany

Alberto Oikawa Lucas, Hispatec, Spain

Alfonso Domínguez Padilla, University of Castilla-La Mancha, Spain

Paula Paredes, University of Lisbon, Portugal

Lisa Pourcher, GAC Group, France

Nciri Radhouan, National Agronomic Institute of Chott-Mariem, Tunisia

Gonçalo Rodrigues, Centro Operativo e de Tecnologia de Regadio (COTR), Portugal

Gianni Quaranta, MEDES Foundation, Italy

Stavros Sakellariou, University of Thessaly, Greece

Athanasios Sfouggaris, University of Thessaly, Greece

Dimitrios Skepastianos, 3DSA, General Aviation Applications, SA, Greece

Petros Spachos, University of Thessaly, Greece

Pantelis Sidiropoulos, University of Thessaly,Greece

Marios Spiliotopoulos, University of Thessaly, Greece

Anamaria Tarquis, Universitad Politécnica de Madrid, Spain

Jose María Tarjuelo Martín-Benito, University of Castilla-La Mancha, Spain

Christos Tsantilas, *ELGO* Dimitra,Greece

Lampros Vasiliades, University of Thessaly, Greece

Polychronis Velentzas, University of Thessaly, Greece

Panagiotis Vlastaridis, University of Thessaly, Greece

Francesco Vuolo, University of Natural Resources and Life Sciences, Vienna. Austria

Abdelaziz Zairi, Institut National de la Recherche en Génie Rural, Eaux et Forêts (INRGREF), Tunisia

Christos Zerefos, Academy of Athens

Alí Zidi, Hispatec Analytics, Spain

CONTENTS

SESSION 1:
CLIMATE CHANGE

ASSESSMENT OF CLIMATE CHANGE IMPACTS ON SOIL DEGRADATION AND THE PERFORMANCE OF THE PRINCIPAL FIELD CROPS IN THESSALY, CENTRAL GREECE

Karamanos, A.J.[1], Voloudakis, D.[3], Kairis, O.[2], Kosmas, C.[2], Kapsomenakis, J.[3], Douvis, C.[3], and Zerefos, C.[3,4]

[1] Corresponding author, Agricultural University of Athens, Faculty of Crop Science, Athens, Greece
[2] Agricultural University of Athens, Laboratory of Soil Science and Agricultural Chemistry, Athens, Greece
[3] Academy of Athens, Research Centre of Atmospheric Physics and Climatology, Athens, Greece
[4] Academy of Athens, Biomedical Research Foundation, Greece

Abstract. An assessment of climate change impacts on the yields and production of wheat, maize and cotton in the Region of Thessaly, Central Greece, using the emission scenarios RCP4.5 and RCP8.5 by the middle (2041-2060) and the end of this century (2081-2100) considering soil resources was attempted. High-resolution climatic simulations using the regional climatic model RCA4 were performed on 11x11 km grids in three study areas producing daily values of the main climatic parameters for the period 1970-2100. The crop simulation model AquaCrop (version 6.0) was used for predicting crop yields. Soil degradation data (erosion and salinization) were taken into account for the prediction of both yield and production figures. Air temperatures are projected to increase by 1.6 to 1.85 ^{o}C by the middle and end of the century respectively for RCP4.5. The corresponding values for RCP8.5 are 2.25 to 4.9^{o}C. Water deficits caused by decreasing precipitation and increasing potential evaporation are predicted to be more intense by the end of the century in both scenarios. In comparison with the reference period (1981-2000) and in the deepest soils, wheat yields are predicted to increase by 21.03 to 61.67% in both scenarios; the yields of maize are projected to decrease by 15.36 to 27.17%, and those of cotton to decrease by 1.11% to 25.35%. Yields are predicted to fall with decreasing soil depth, more drastically in maize and cotton than wheat. These findings are discussed in terms of the different responses of the three crops to the elevated values of both air temperature and CO_2-concentration as well as to soil depth. The predicted production figures of Thessaly for the two emission scenarios and periods ranged between -7.21 to +32.09% for wheat, -26.21 to -42.57% for maize and -21.6 to -37.17% for cotton, in comparison with the reference period. It appears that the inclusion of the effects of soil erosion and salinization in the calculation of crop yields and production brings the predictions for climate change impacts closer to reality.

1 Introduction

According to the Sixth IPCC Report (IPCC, 2021), the Mediterranean Basin will be among the areas more adversely affected in terms of a rise in temperature, a decrease in the overall water balance leading to agricultural and ecological drought, and a high frequency of extreme weather events. In an extensive national study using three emission scenarios (CCSIC, 2011) it was found that Greece is expected to experience these negative effects in all sectors of the economy by the middle and the end of this century. Among them, agricultural production has been identified as the most vulnerable.

According to the findings of this study, the agricultural production in the Region of Thessaly, located in the central and eastern part of Greece, is predicted to suffer losses equal or greater than 10% in agricultural production (Karamanos et al., 2011). Such figures are of particular interest, in view of the importance of this Region on the national agricultural productivity, mainly based on the production of field crops: Thessaly accounts for 37.5% of cereal and 35.8% of cotton production on a national basis (ELSTAT, 2018). In a more elaborate study focusing on Thessaly, Karamanos and Voloudakis (2017) using the AquaCrop crop simulation model predicted yield increases of about 20% for wheat and 10-20% for cotton and up to 10% decrease for maize, in comparison with the period 1981-2000. Similar figures were predicted for the same three crops under the emission scenario A1B in Thessaly by Georgopoulou et al. (2017), whereas Kapetanaki and Rosenzweig (1997) predicted a decrease by 8.8% in maize yields by the middle of this century.

All these predictions are based on the adoption of GHG-emission scenarios, simulations of future climatic data using regional climatic models, and applications of crop simulation models. Some of the crop simulation models are using as inputs soil parameters, such as soil depth, texture, hydraulic conductivity, field capacity, and permanent wilting point, which are usually considered steady in time. However, a more accurate prediction would require the inclusion of the effects of both climate change and agricultural management on land

degradation (Le Houérou, 1996; Webb et al., 2017). Thus, the projected decrease in the depth of fertile soil caused by mechanical and water erosion should also be taken into account when implementing crop simulation models for yield predictions.

The assessment of the quality of agricultural lands under climate change is essential when estimating future agricultural production on a local, regional or national basis. The existing methodologies of Environmentally Sensitive Areas land degradation assessment (Kosmas et al., 1999; Ferrara et al., 2020), mechanical and water erosion (e.g. Govers et al., 1994; Kosmas et al., 1997), and soil salinization risk assessment (Kosmas et al., 2014) provide useful tools towards this direction.

Following the lines suggested by Rosenzweig and Tubiello (1997), the assessment of yield and production of the three main crops of Thessaly (wheat, maize and cotton) under two emission scenarios (RCP4.5 and RCP8.5) in the middle and the end of the century will be the subject of the present work. High-resolution climatic simulations using a contemporary regional climatic model will produce daily values of the main climatic parameters in three representative study areas of Thessaly for the periods 2041-2060 and 2081-2100. The crop simulation model AquaCrop (Doorenbos and Kassam, 1979), suitable for crops growing under water deficits, will be used for yield assessments. Values of soil depth derived from estimates of mechanical and water erosion in the two periods and the three study areas will be included in the model and accounted for in yield computations. Production estimates for each crop will be derived as products of yields by the corresponding areas of agricultural lands, taking into account soil degradation due to primary salinization. The projected responses of these crop species may act as useful indicators of the responses of crops growing on different water resources (dryland vs. irrigated) as well as on different thermal requirements (winter vs. summer crops).

2 Materials and Methods

2.1 Study areas

Three plain study areas expressing to a significant extent the climatic and soil conditions prevailing in Thessaly and cultivated with field crops were chosen. The three areas were located in the municipalities of Kileler (Sotirio and Zappeio) and Trikala. 11x11 km grids with the following coordinates were studied in the areas of Trikala (43º 75΄00΄΄- 43º 85΄ 00΄΄ N, 30º 25΄ 00΄΄- 31º 35΄ 00΄΄ W), Sotirio (43º 67΄ 50΄΄ - 43º 78΄ 00΄΄ N, 38º 30΄ 00΄΄ - 39º 40΄ 00΄΄ W), and Zappeio (43º 64΄ 00΄΄ - 43º 79΄ 00΄΄ N, 36º 15΄ 00΄΄- 37º 15΄ 00΄΄ W).

2.2 Climatic simulation

Future climatic projections are based on greenhouse gas emission scenarios (Representative Concentration Pathways, RCPs). Two of these scenarios were used in this study, namely the RCP4.5 (intermediate emissions: Clarke et al., 2007; Thomson et al., 2011) and the RCP8.5 (drastic increase in the emissions: Riahi et al., 2007, 2011). For each scenario, the results of 11x11km high resolution climatic simulations of the EUROCORDEX initiative (https://euro-cordex.net/) covering a daily time analysis for the period 1970-2100 at the study areas were used. The simulations were run with the regional climatic model RCA4 (Samuelsson et al., 2011) using initial and boundary conditions from the global climatic model MPI-ESM-LR (Giorgetta et al., 2013), from which the daily values of the following climatic parameters for each study area for the periods 2041-2060 and 2081-2100 were derived: air temperature (minimum, average, maximum), precipitation, relative humidity, solar irradiance, and wind speed. Potential evapotranspiration (ET_o) was calculated according to Allen et al. (1998) following the modified Penman-Monteith equation (1965).

2.3 Soil degradation

Detailed information on the soil characteristics of the study areas was obtained from the soil map of Thessaly compiled under the auspices of the Hellenic Ministry of Rural Development and Food at a scale 1:30,000 (OPEKEPE, 2014). The soil mapping units (SMUs) were characterized by a set of soil parameters expressed by alphanumeric characters. A detailed correspondence of the classes of each parameter to the alphanumeric characters is described by Kairis et al. (2020).

Both soil mechanical and water erosions are processes leading to the reduction of soil depth in the upper and middle parts of a hillside and its increase in the lower parts. Soil displacement during mechanical erosion was calculated according to Govers et al. (1994), taking into account the plowing depth, soil bulk density, the slope of the soil surface, and a diffusion coefficient. Based on a 30 m detailed Digital Elevation Model (DEM), derived from NASA's Shuttle Radar Topography Mission satellite data (https://www2.jpl.nasa.gov/srtm/), the area of each SMU was divided into 20x20 m grids and the shape of each square was estimated in terms of

the curvature based on the relief of the surface. For each square, the difference between the loss of soil material to the lower square and the addition of material from the upper square was calculated based on the above equation. In grids with a convex or a straight surface the result after plowing was usually the loss of soil material, while in grids with a concave surface the final result was the addition of material. The decrease or increase of soil depth at a location was calculated according to Tsara et al. (2001).

Soil water erosion was calculated by using an empirical second-degree polynomial of the annual precipitation derived by statistical analyses of long-term experimental data obtained from areas of the Mediterranean (Kosmas et al., 1997).

Primary salinization risk, induced by the upward movement of poor-quality groundwater, was assessed by means of the Salinization Risk index (SR) only in one of the three study areas (Sotirio), because of the insufficient soil drainage regime met in SMUs of the lowlands in this area. SR was calculated from an empirical equation derived from a statistical analysis in 258 field sites of Greece, Europe and Africa (Kosmas et al., 2014). Potential evapotranspiration, quality of irrigation water, degree of groundwater utilization, soil drainage, flooding frequency, land ownership, distance from the coastline, percentage of irrigated agricultural land, population density are the variables used in this equation. Based on the values of the SR, the salinization risk of a specific soil is estimated according to Karavitis et al. (2020).

2.4 Crop simulation, yields and productivity

The version 6.0 (2018) of the AquaCrop crop growth simulation model (Raes et al., 2009; Steduto et al., 2009) was used to project crop yields, taking into account the variability of the climatic parameters derived by the climate model, the increase in CO_2-concentration of each emission scenario, soil, and crop parameters. The model has been satisfactorily validated in Greece (Voloudakis et al., 2015, 2018). Apart from the standard initial values of the soil properties required as inputs, the changes in soil depth caused by erosion were also taken into account. AquaCrop has been used in the case of cotton (e.g. García-Vila et al., 2009; Voloudakis et al., 2015), maize (e.g. Hsiao et al., 2009; Katerji et al., 2013) and wheat (e.g. Andarzian et al., 2011; Iqbal et al., 2014) crop simulations.

The depths of soils were classified into three groups: deep (>100cm), medium (61-100cm), and shallow (<60cm). Accordingly, three figures of yields were produced for each crop, depending on soil depth. The average yield of each crop for the whole region was derived as the mean of the values obtained from each study area for a given group of soil depth.

The total production of each crop on a regional basis was derived as the sum of the products of the average yields from the three study sites for each soil group and the land area of the region corresponding to the specific groups of soil depth taken from the soil map of Thessaly (OPEKEPE, 2014).

3 Results

3.1 Climatic parameters

The values of the climatic parameters derived from the application of the adopted meteorological model are shown in Table 1. In comparison with the data produced by the model for the reference period, the average maximum daily air temperatures for the RCP4.5 scenario is expected to rise by 1.62^{o}C in 2041-2060 and by 1.85^{o}C in 2081-2100 on the average for all study areas. For the RCP8.5 scenario, the corresponding average rise is predicted to reach 2.26^{o}C in 2041-2060 and 4.98^{o}C in 2081-2100.

The predicted increases in the average minimum daily air temperatures are 1.60 and 1.84^{o}C in 2041-2060 and 2081-2100 for RCP4.5 respectively. The corresponding increases for RCP8.5 are 2.24 and 4.84^{o}C in 2041-2060 and 2081-2100.

The average annual precipitation is predicted to exhibit minor fluctuations in comparison with the reference period for the scenario RCP4.5: it is higher by 8.24 (2081-2100) to 8.69% (2041-2060) in Sotirio and lower by 4.01 (2041-2060) to 2.32% (2081-2100) in Trikala; in Zappeio it is lower by 3.23% in 2041-2060 and higher by 3.29% in 2081-2100. For the RCP8.5, however, consistently lower values by 5.82 to 13.58% are projected in 2041-2060 and by 19.11 to 26.67% in 2081-2100 over the three study areas.

The average daily potential evapotranspiration is predicted to rise in comparison with the reference period in both scenarios, more intensively for RCP8.5. For the RCP4.5 increases between 8.3 to 17.3% are predicted in the middle and the end of the century. For the RCP8.5 increases are foreseen to reach 11.4 to 20.4% in 2041-2060 and 25.3 to 33.9% in 2081-2100.

In comparison with the reference period, the predicted rises in CO_2-concentration will reach 133.6 ppm (37.8%) in 2041-2060 and 180.6 ppm (51.1%) in 2081-2100 for RCP4.5. For RCP8.5, the corresponding increases will reach 191.8 ppm (54.2%) in 2041-2060 and 496.5 ppm (140.4%) in 2081-2100.

Table 1. The average values of: (a) the daily maximum (T_{max}) and minimum (T_{min}) air temperatures, annual precipitation (P), and daily potential evapotranspiration (ET_o) in the reference period (1981-2000) and in the periods 2041-2060 and 2081-2100 for the emission scenarios RCP4.5 and RCP8.5 in the three study areas of Thessaly derived from the adopted meteorological model; (b) the CO_2-concentration in the same periods and emission scenarios. The [CO_2]-value for the reference period was calculated from the data of the World Meteorological Organization.

(a)

		Sotirio		Zappeio		Trikala	
		RCP4.5	RCP8.5	RCP4.5	RCP8.5	RCP4.5	RCP8.5
T_{max} (°C)	1981-2000	20.80		21.39		22.01	
	2041-2060	22.33	22.97	23.02	23.68	23.70	24.32
	2081-2100	22.55	25.60	23.22	26.39	23.97	27.16
T_{min} (°C)	1981-2000	8.97		9.52		9.95	
	2041-2060	10.54	11.19	11.10	11.73	11.61	12.25
	2081-2100	10.77	13.76	11.31	14.31	11.88	14.88
P (mm)	1981-2000	364.90		458.09		363.83	
	2041-2060	396.62	343.65	443.29	395.89	349.23	324.16
	2081-2100	394.47	295.16	473.18	335.89	355.38	248.64
ET_o (mm)	1981-2000	3.67		4.11		3.93	
	2041-2060	4.25	4.38	4.45	4.58	4.61	4.73
	2081-2100	4.24	4.88	4.41	5.14	4.60	5.26

(b)

[CO_2] (ppm)	1981-2000	353.60	
		RCP4.5	RCP8.5
	2041-2060	487.20	534.20
	2081-2100	545.40	850.10

3.2 Soil depth

The percentage of land surface in the three areas of study, grouped according to the depth of their soils, as depicted in the corresponding SMUs in the soil map of Thessaly in three different periods (2014, 2060, and 2100) is shown in Table 2. Soils were characterized as deep (>100cm), medium (61-100cm) and shallow (<60cm).

The changes in the relative proportions of land with different soil depths in the course of time are caused by the combined action of mechanical and water soil erosion. No differentiation between the scenarios RCP4.5 and RCP8.5 either in 2060 or in 2100 was predicted.

	Sotirio			**Zappeio**			**Trikala**		
Soil depth	**2014**	**2060**	**2100**	**2014**	**2060**	**2100**	**2014**	**2060**	**2100**
>100 cm	84.50	84.50	78.50	15.27	15.27	15.27	94.60	94.60	94.60
61-100 cm	12.10	12.10	7.40	46.74	46.74	15.80	0	0	0
<60 cm	3.40	3.40	14.10	37.99	37.99	68.93	5.40	5.40	5.40

Table 2. Distribution of the land areas (%) in the three areas of study on the basis of the depth of their soils, as depicted in the corresponding soil map units in the soil map of Thessaly in three different periods (2014, 2060, and 2100). No difference between the scenarios RCP4.5 and RCP8.5 is foreseen for 2060 and 2100.

Considering the present situation, a clear difference between the three study areas was observed, as a result of their different relief. Thus, Zappeion, consisting mostly of hilly areas, exhibits a small proportion of deep soils (15.27%) and much greater proportions of medium (46.74%) and shallow soils (37.99%). To the other end, in Trikala, consisting mainly of plains, the proportion of deep soils exceeds 90%. In Sotirio, with a small percentage of hilly areas, the proportion of deep soils is 84.5%, whereas those of medium and shallow soils are quite low (12.1% and 3.4% respectively).

In 2060, no differentiation in the proportion of all classes of soils in all areas is predicted. In 2100, however, a partial transition of the medium to shallow soils is foreseen, especially in the hilly areas of Zappeion, as a result of the enhanced soil erosion.

3.3 Soil salinization

Major primary salinization risks occur only in the poorly drained soils of Sotirio. Figure 1 indicates the predictions for salinization in 2041-2060 and 2081-2100 in comparison with the reference period. It can be seen that the SMUs experiencing no salinization risk in the reference period will remain in the same class up to the end of the century. However, the soils initially characterized of low and medium risk are predicted to be degraded by two classes and become of high and very high risk already by 2060. No difference between the scenarios RCP4.5 and RCP8.5 is predicted. Thus, 59.4% of the land in this study area will become by 2060 unsuitable for cultivation.

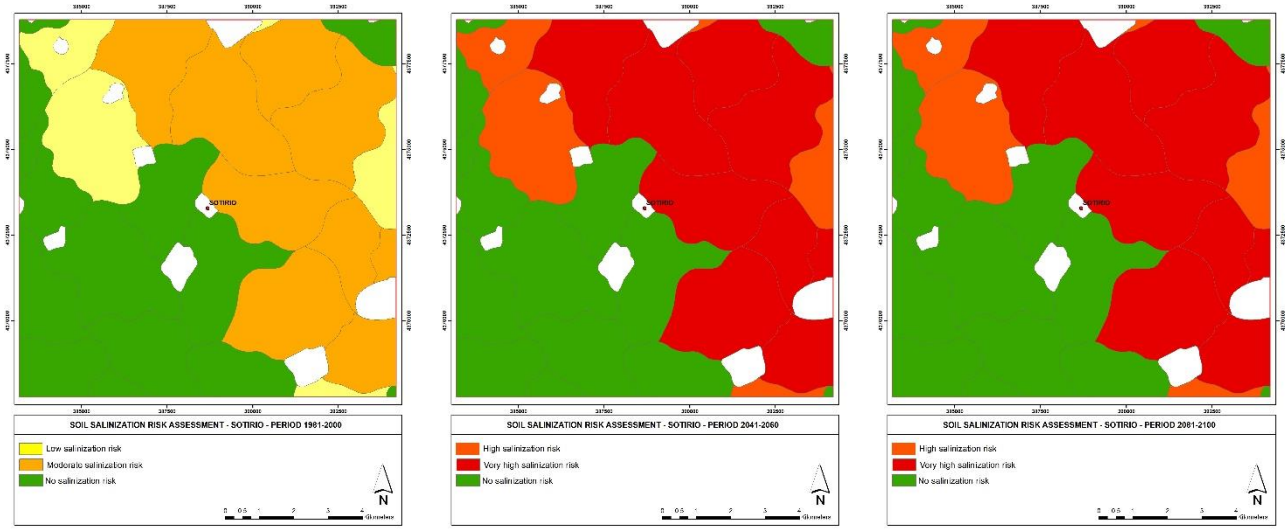

Figure 1. Spatial distribution of salinization risk of the study site of Sotirio in the year of publication of the soil map (2014, left), 2041-2060 (middle), and 2081-2100 (right). No difference is predicted between the scenarios RCP4.5 and RCP8.5.

3.4 Crop yields

The predicted proportional differences in the yields of the three crops in 2041-2060 and 2081-2100 in soils of different depths in Thessaly, in comparison with the reference period 1981-2000, averaged over the three study areas, are shown in Figure 2. Positive differences are predicted only for wheat yields. For RCP4.5 (Fig. 2a) these differences will rise up to 21.03% in 2041-2060 and 27.36% in 2081-2100 in the deep soils. The differences are reduced in soils of medium depth (by 11.67 and 5% in 2041-2060 and 2081-2100 respectively) and become negative in the shallow soils (-19.05 and -9.52% in 2041-2060 and 2081-2100 respectively). For the scenario RCP8.5 (Fig. 2b) the positive yield differences are higher than those projected for RCP4.5: 25.81 and 61.67% in deep, 16.67 and 63.3% in medium, and -5.56 and 34.91% in shallow soils in 2041-2060 and 2081-2100 respectively.

Maize yields are predicted to decline substantially in comparison to 1981-2000 in all cases. The yield reductions are greater as soils become shallower and are similar either in the middle or in the end of the century. For RCP4.5 (Fig. 2a), the projected reductions in 2041-2060 and 2081-2100 will be -21.32 and -15.36% in the deep, -36.7 and -36.28% in the medium and -54.49 and –56.14% in the shallow soils respectively. For RCP8.5 (Fig. 2b), the corresponding reductions are predicted higher: -27.17 and -24.37% in the deep, -49.87 and -46.04% in the medium, and -75.49 and -85.48% in the shallow soils, in 2041-2060 and 2081-2100 respectively.

As in maize, cotton yields are also predicted to decline in comparison to 1981-2000. For both scenarios, yield reductions are relatively small in the deep soils, but they become substantial in the medium and especially in the shallow soils. For RCP4.5 (Fig. 2a), the projected reductions were found to be -20.5 and -1.11% in the deep, -46.55 and -43.1% in the medium, and -91 and -79.89% in the shallow soils in 2041-2060 and 2081-2100 respectively. For RCP8.5 (Fig. 2b), the corresponding

values for the two periods are predicted to reach -25.35 and -13.18% in the deep, -53.45 and -55.17% in the medium, and -100 and -95.02% in the shallow soils.

3.5 Crop production

The predicted proportional differences in the production of the three crops in the Region of Thessaly in comparison with the reference period 1981-2000, are shown in Table 3.

The predictions show increases in wheat production by 4.71 up to 32.09% for both scenarios, except for the period 2041-2060 in RCP8.5 where a small decrease by 7.21% is recorded. The increases are higher in 2081-2100 under both scenarios. Definite decreases in productivity are foreseen for both maize and cotton. In maize, the decreases will range between 26.21 and 27.37% for RCP4.5 and 40.25 and 42.47% for RCP8.5, with roughly similar reductions in 2041-2060 and 2081-2100 for both scenarios. In cotton, the decreases will range between 21.6 and 37.17% for RCP4.5 and 33.66 and 34.15% for RCP8.5 with smaller reductions in 2081-2100 than in 2041-2060.

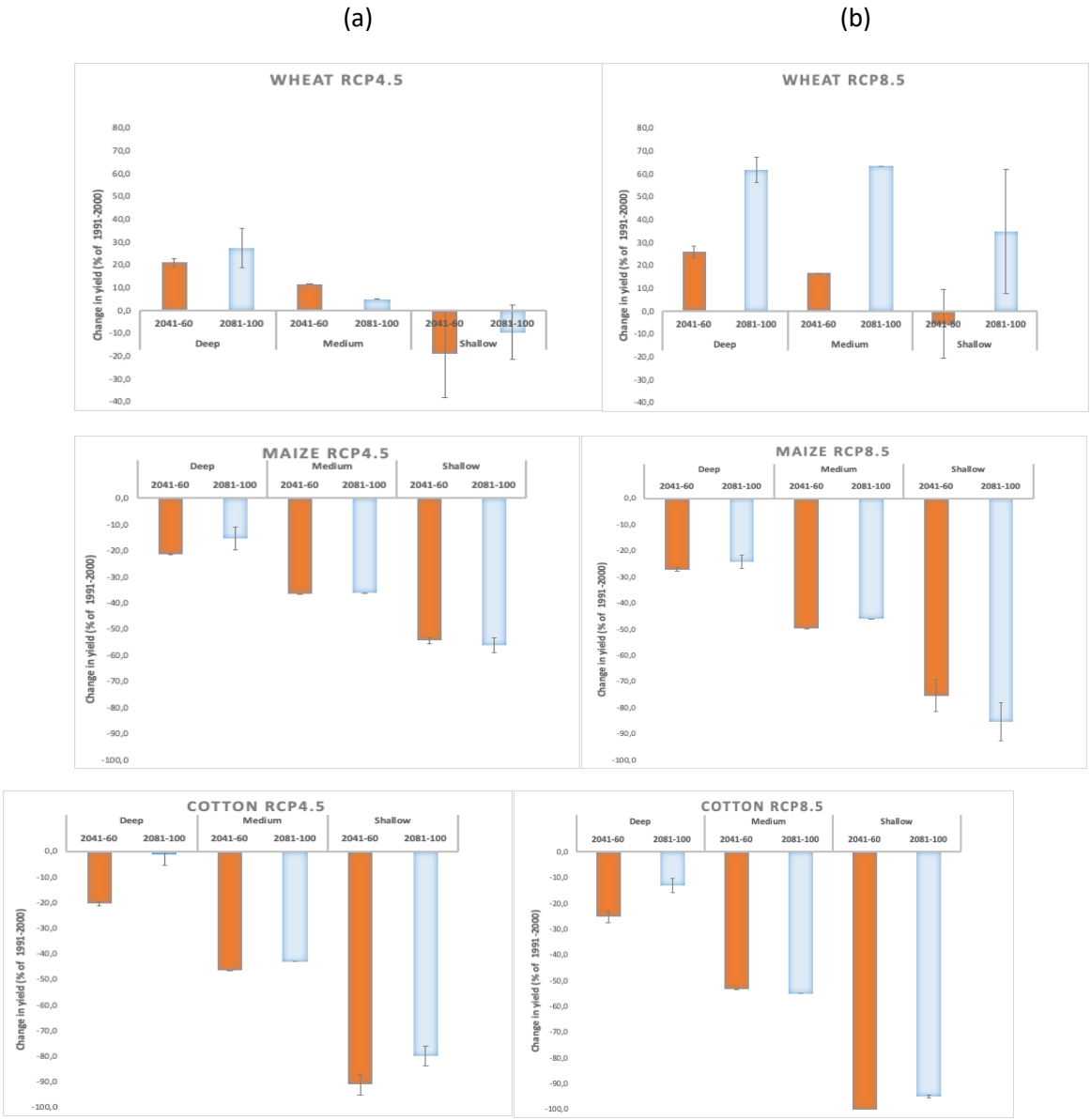

Figure 2. The predicted proportional differences (%) in the yields of wheat, maize, and cotton in 2041-2060 and 2081-2100 in comparison with the reference period (1981-2000), averaged over the three study areas of Thessaly for deep (>100 cm), medium (60-80 cm) and shallow (<60 cm) soils. Scenarios RCP4.5 (a), RCP8.5 (b). The bars indicate the standard errors of the means.

4 Discussion

For the mild scenario RCP4.5, the projected differentiations in the course of the century are mainly focused on temperature increases reaching values close to 2ºC by 2081-2100. The impacts on water balance will be achieved through the projected increases in ET_o already by 2041-2060, in view of the predicted fluctuating pattern of annual precipitation. For RCP8.5, however, the projected increases in both maximum and minimum temperatures will be substantially higher, exceeding 2ºC by the middle and approaching 5ºC by the end of the century. At the same time, significant water deficits will be induced by both the expected decreases in annual precipitation and the increase in ET_o.

Crop species	Reference period (1981-2000) (tn)	RCP4.5		RCP8.5	
		2041-2060 (tn) (%)	2081-2100 (tn) (%)	2041-2060 (tn) (%)	2081-2100 (tn) (%)
Wheat	323878.7	339130.0 (+4.71%)	367177.3 (+13.37%)	300533.4 (-7.21%)	427797.5 (+32.09%)
Maize	240539.9	174693.4 (-27.37%)	177499.4 (-26.21%)	138133.0 (-42.57%)	143725.4 (-40.25%)
Cotton	219803.4	138103.9 (-37.17%)	172320.0 (-21.60%)	144746.0 (-34.15%)	145826.5 (-33.66%)

Table 3. The projected productions and their proportional changes (in brackets) of the examined crops in the Region of Thessaly in comparison with the reference period 1981-2000. The results were calculated from the average yields of each crop in the three study sites for each group of soil depth and the corresponding land areas of the Region. Areas characterized of high and very high salinization risk in 2041-2060 and 2061-2100 were not taken into account.

Both mechanical and water erosion are considered as important components of soil desertification process, resulting in a removal of the soil surface from the top of the hill downwards and a decrease in soil depth. Our analysis (Table 2) shows that the soil loss predicted for the middle and end of the century in the study areas will be observed mainly in soils with depth between 60-100 cm. The higher proportion of this group of soils is observed in the hilly area of Zappeion, which has experienced extended erosion due to the intensive cultivation for a number of decades. In this area, the percentage of shallow soils with depth less than 60cm is predicted to rise from 37.99% in 2060 to 68.94% in 2100. This result confirms the findings of Kosmas et al. (1997) in other hilly areas of Greece cultivated with cereals in the last decades. The mostly deep and plain soils of the other two study areas do not appear to be threatened by erosion. The lack of differentiation in the predicted soil displacement by erosion between the two emission scenarios implies that the processes involved are not expected to depend on the intensity of change of the principal climatic parameters. Instead, the progressive aggravation of the consequences of soil erosion towards the end of the century points to the detrimental effects of the existing inappropriate soil management and to the urgent necessity of adopting soil conservation practices.

Salinization risks were projected only in the study area of Sotirio, where the hydromorphic characteristics of the SMUs in the lowlands of the alluvial land induce poor drainage and favour salt accumulation via upward soil water flux. The risks are further aggravated by the small distance of this area from the coastline, which favors sea water intrusion. On the account of its definition, the SR-index is expected to be affected by climate change through the rise in both ET_o and soil water conductance. The high vulnerability of the SMUs in this area to salinization is visible from the predicted sudden transition of soils from low and medium into high and very high-risk classes even under the mild emission scenario already by 2060, without any further aggravation in 2100 (fig. 1). The lack of differentiation between the two emission scenarios implies a minor impact of the climatic parameters on soil salinization in comparison with the other factors involved.

Positive impacts of climate change on wheat yields at levels similar to those reported in this work were predicted for the same area and emission scenarios, but using different climatic models, by Karamanos and Voloudakis (2017). Wheat yield increases, though at lower proportions, were also predicted by Georgopoulou et al. (2017). Negative predictions for maize yields in Thessaly reaching -8.8% by 2050 were first reported by Kapetanaki and Rosenzweig (1997), followed by Georgopoulou et al. (2017), Karamanos and Voloudakis

(2017), and Voloudakis et al. (2018). The predictions for cotton yields found in this work are more negative than those reported for the same region (Voloudakis et al., 2015, 2018). Cotton yield increases by 10 to 20% were also predicted by Karamanos and Voloudakis (2017) and by 9.8% by Georgopoulou et al. (2017). The deviations in the predicted yield fluctuations reported in this work from the above findings are possibly due either to the implementation of different crop simulation models or/and to the adoption of different regional or local climatic models (Voloudakis et al. 2015), as well as to the spatial approach applied in the present work. The inclusion of the fluctuations in soil depth caused by mechanical and water erosion in the crop simulation model may have also contributed towards more precise predictions.

Yields are predicted relatively stable up to a depth of about 100 cm for all three crops. For a given emission scenario, yields are predicted to decline when soil depth decreases below 100 cm, more abruptly in both maize and cotton than wheat, reaching virtually zero values at depths around 40 cm (Figure 2). Thus, wheat yields appear to be the most resilient in soil depth restriction exhibiting marginal values between 1-2 tn ha^{-1} in soils as shallow as 30 cm. The decrease in soil depth below a certain extent is expected to reduce crop yields due to an overall decline in the volume of the rhizosphere and the concomitant decrease in the water and nutrient availability to crops. The observed different behaviour among the three crops could be explained by means of the type of their root systems, which has been taken into account in the AquaCrop model. The profuse fibrous root system of wheat and maize can exploit better the restricted soil mass of the shallow soils than the tap root system of cotton (Oosterhuis, 1990), which is better adapted for deep soils. On this account, the poor performance of cotton in shallow soils is justifiable.

As already known, elevated CO_2-concentrations positively affect the rate of photosynthesis (Gaastra, 1963) and induce higher crop yields (Kimball, 1983). However, the extent of this positive influence depends on the metabolic pathway of CO_2-fixation, being more enhanced in C_3 and marginal in C_4- crop species (Lawlor, 1997). This fact may explain the predicted positive yield responses to climate change of wheat, a cool-season C_3-crop. The predicted negative yield responses of maize, a warm-season C_4-crop, can be attributed both to its low response to the elevated CO_2 and to its negative response to the high temperatures expected to prevail during summer (Kim et al., 2007). The predicted marginal to negative responses of cotton yields, less intense in comparison with maize, could partly attributed to the fact that cotton is a C_3 summer crop. The projected high spring and summer temperatures inducing lower rates of dry matter accumulation via higher dark respiration rates, in combination with the shortening of the crop's biological cycle appear to have offset the positive responses of the elevated CO_2-concentration expected for a C_3-crop (Morison and Lawlor, 1999; Allen, 2019).

The production figures of the crops on a regional basis are the products of their yields and the area on which they are cultivated. The reduction in soil depth caused by mechanical and water erosion has been taken into account in yield computations using the crop simulation model. In addition, the detrimental effects of land degradation caused by salinization in 2041-2060 and 2081-2100 have been accounted for when considering the cultivation areas for each crop. Thus, an area of 6870.9 ha, salinized at high and very high levels in Sotirio, was left out as unsuitable for cultivation already by 2041-2060. When comparing the proportional changes in yields with those of production of all three crops (Figure 2 and Table 3) for the corresponding periods and emission scenarios, it is evident that the production figures are more negative than those predicted for yields in the deep soils. Thus, the consideration of the effects of soil erosion in the calculation of crop production resulted in figures more negative than those expected if the cultivated land were regarded as a plain area with uniform depth. It seems that the approach adopted in this work is closer to reality, by taking into account all information available on the soil resources of Thessaly under the influence of climate change.

References

Allen Jr, L.H., 2019. Simplifying crop growth response to rising CO_2 and elevated temperature. Agric. Environ. Lett., 4, 1-4.

Allen, R.G., Pereira, L.S., Raes, D. and Smith, M., 1998. Crop evapotranspiration: Guidelines for computing crop water requirements. Irr. Drain. Paper 56, UN-FAO, Rome

Andarzian, B., Bannayan, M., Steduto, P., Mazraeh, H., Barati, M.E., Barati, M.A. and Rahnama, A., 2011. Validation and testing of the AquaCrop model under full and deficit irrigated wheat production in Iran. Agric. Water Manag., 100,1–8.

Clarke, L.E., Edmonds, J.A., Jacoby, H.D., Pitcher, H., Reilly, J.M. and Richels, R., 2007. Scenarios of greenhouse gas emissions and atmospheric concentrations. Sub-report 2.1a of Synthesis and Assessment

Product 2.1. Climate Change Science Program and the Subcommittee on Global Change Research, Washington DC.

CCSIS, Climate Change Impacts Study Committee, 2011. The Environmental, Economic and Social Impacts of Climate Change in Greece, Bank of Greece, Athens.

Doorenboos ,J. and Kassam, A.H., 1979. Yield Response to Water, Irrigation and Drainage Paper n.33, FAO, Rome.

ELSTAT, Hellenic Statistical Authority, 2018. Agricultural Statistics, Athens.

Ferrara, A., Kosmas, C., Salvati, L., Padula, A., Mancino, G. and Nolè, A., 2020. Environmentally sensitive areas to land degradation and desertification (LDD) at the global level: updating the MEDALUS-ESA framework for worldwide LDD assessment. Land Degrad. Dev., doi:10.1002/ldr.3559

Gaastra, P., 1963. Climatic control of photosynthesis and respiration. In: L.T. Evans (ed.), Environmental Control of Plant Growth, Academic Press, New York, 113-138.

García-Vila, M., Fereres, E., Mateos, L., Orgaz, F. and Steduto, P., 2009. Deficit irrigation optimization of cotton with AquaCrop. Agron. J., 101, 477–487.

Georgopoulou, E., Mirasgedis, S., Sarafidis. Y., Vitaliotou, M., Lalas, D.P. et al., 2017. Climate change impacts and adaptation options for the Greek agriculture in 2021–2050: A monetary assessment. Clim. Risk Manag., 16, 164-182. doi: 10.1016/j.crm.2017.02.002

Giorgetta, M., Jungclaus, J., Reick, C.H., Legutke, S., Bader, J. et al., 2013. Climate change from 1850 to 2100 in MPI-ESM simulations for the coupled model intercomparison project phase 5. J. Adv. Model Earth Syst., 5, 572-597. doi: 10.1002/jame.20038

Govers, G., Vandaele, K., Desmet, P., Poesen, J. and Bunte, K., 1994. The role of tillage in soil redistribution on hillslopes. Eur. J. Soil Sci., 45, 469-478.

Hsiao, T.C., Heng, L.K., Steduto, P., Rojas-Lara, B., Raes, D. and Fereres, E., 2009. AquaCrop - The FAO crop model to simulate yield response to water: III. Parameterization and testing for maize. Agron. J., 101, 448-459.

Iqbal, M.A., Shen, Y., Stricevic, R., Pei, H., Sun, H. et al., 2014. Evaluation of the FAO AquaCrop model for winter wheat on the North China Plain under deficit irrigation from field experiment to regional yield simulation. Agric. Water Manag., 135, 61–72.

IPCC, Intergovernmental Panel on Climate Change, 2021. Summary for Policymakers. In: V. Masson-Delmotte et al. (eds), Climate Change 2021: The Physical Science Basis. Contribution of Working Group I to the Sixth Assessment Report of the Intergovernmental Panel on Climate Change, Cambridge University Press

Kairis, O., Dimitriou, V., Aratzioglou, Ch., Gasparatos, D., Yassoglou, N., Kosmas, C. and Moustakas, N., 2020. A comparative analysis of a detailed and semi-detailed soil mapping for sustainable land management using conventional and currently applied methodologies in Greece. Land, 9, 154, https://doi.org/10.3390/land9050154.

Kapetanaki, G. and Rosenzweig, C., 1997. Impact of climate change on maize yield in Central and Northern Greece: A simulation study with Ceres-Maize. Mitig. Adapt. Strateg. Glob. Chang., 1, 251-271. doi: 10.1023/B:MITI.0000018044.48957.28.

Karamanos, A., Skourtos, M., Voloudakis, D., Kontogianni, A. and Machleras, A., 2011. Impacts of climate change on agriculture. In: The Environmental, Economic and Social Impacts of Climate Change in Greece, Climate Change Impacts Study Committee, Bank of Greece, Athens, 186-196.

Karamanos, A.J. and Voloudakis, D., 2017. Predictions and adaptation measures of the impacts of climate change on the principal arable crops of Thessaly. Presentation in the Conference *Local Governance and Thessaly in front of the Global Challenge* (Karditsa, 9-10/6/2017) http://www.pedthessalias4clima.gr/media (in Greek)

Karavitis, C., Tsesmelis, D., Oikonomou, P., Kairis, O., Kosmas, C. et al., 2020. A desertification risk assessment decision support tool (DRAST). Catena, 187. doi: 10.1016/j.catena.2019.104413.

Katerji, N., Campi, P. and Mastorilli, M., 2013. Productivity, evapotranspiration, and water use efficiency of corn and tomato crops simulated by AquaCrop under contrasting water stress conditions in the Mediterranean region. Agric. Water Manag., 130, 14-26.

Kim, S.H., Gitz, D.C., Sicher, R.C., Baker, J.T., Timlin, D.J. and Reddy, V.R., 2007. Temperature dependence of growth, development, and photosynthesis in maize under elevated CO_2. Environ. Exp. Bot., 61, 224-236.

Kimball, B.A., 1983. Carbon dioxide and agricultural yield: an assemblage and analysis of 430 prior observations. Agron. J., 75, 779-788.

Kosmas, C., Danalatos, N., Cammeraat, L.H., Chabart, M., Diamantopoulos, J. et al., 1997. The effect of land use on runoff and soil erosion rates under Mediterranean conditions. Catena, 29, 45-59.

Kosmas, C., Kirkby, M. and Geeson, N., 1999. Manual on: Key indicators of desertification and mapping environmentally sensitive areas to desertification, European Commission, Energy, Environment and Sustainable Development, EUR 18882.

Kosmas, C., Kairis, O., Karavitis, C., Ritsema, C., Salvati, L. et al., 2014. Evaluation and Selection of Indicators for Land Degradation and Desertification Monitoring: Methodological Approach. Environ. Manag., 54, 951-970.

Lawlor, D.W., 1997. Response of crops to environmental change conditions. J. Agric. Meteorol., 2, 769-778

Le Houérou, H.N., 1996. Climate change, drought and desertification. J. Arid Environ., 34, 133-185.

Monteith, J.L., 1965. Evaporation and environment. Symp. Soc. Exp. Biol., 29, 205-234.

Morison, J. and Lawlor, D.W., 1999. Interactions between increasing CO2 and elevated temperature. Plant Cell Environ., 22, 659-682.

Oosterhuis, D.M., 1990. Growth and development of a cotton plant. In: W.N. Milney and D.M. Oosterhuis (eds), Nitrogen Nutrition of Cotton: Practical Issues, American Society of Agronomy, Madison Wisc.,1-24.

OPEKEPE, Greek Payment and Control Agency for Guidance and Guarantee Community Aid, 2014. Development of a unified system for geospatial soil data and the delineation of the rural areas of the country. Ministry of Rural Development and Food. https://iris.gov.gr/SoilServices/js/pdf/SOIL MAP OF GREECE e-SOILBOOK.pdf (in Greek)

Raes, D., Steduto, P., Hsiao, T.C. and Fereres, E., 2009. AquaCrop – The FAO crop model to simulate yield response to water II: main algorithms and software description. Agron. J., 101, 438-447.

Riahi, K., Grübler, A. and Nakicenovic, N., 2007. Scenarios of long-term socio-economic and environmental development under climate stabilization. Technol. Forecast Soc. Change, 74, 887–935.

Riahi, K., Krey, V., Rao, S., Chirkov, V., Fischer, G. et al., 2011. RCP-8.5: exploring the consequence of high emission trajectories. Clim. Change, 109, 33. doi:10.1007/s10584-011-0149-y

Rosenzweig, C. and Tubiello, F.N., 1997. Impacts of global climate change on Mediterranean agriculture: Current methodologies and future directions. Mitig. Adapt. Strateg. Glob. Chang.,1, 219-232. doi: 10.1023/B:MITI.0000018269.58736.82.

Samuelsson, P., Jones, C.G., Willén, U., Ullerstig, A., Gollvik, S. et al., 2011. The Rossby Centre Regional Climate Model RCA3: model description and performance. Tellus Ser. A ,63, 4–23.

Steduto, P., Hsiao, T.C., Raes, D. and Fereres, E., 2009. AquaCrop—the FAO crop model to simulate yield response to water, I. Concepts. Agron. J., 101, 426–437.

Thomson, A.M., Calvin, K.V., Smith, S.J., Kyle, G.P., Volke, A. et al., 2011. RCP4.5: a pathway for stabilization of radiative forcing by 2100. Clim. Change, 109, 77. doi:10.1007/s10584-011-0151-4.

Tsara, M., Gerontidis, S., Marathianou, M. and Kosmas, C., 2001. The long-term effect of tillage on soil displacement of hilly areas used for growing wheat in Greece. Soil Use Manag., 17, 113-120.

Voloudakis, D., Karamanos, A., Economou, G., Kalivas, D., Vahamidis, P. et al., 2015. Prediction of climate change impacts on cotton yields in Greece under eight climatic models using the AquaCrop crop simulation model and discriminant function analysis. Agric. Water Manag., 147, 116–128.

Voloudakis, D., Karamanos, A., Economou. G., Kapsomenakis, J. and Zerefos, C., 2018. A comparative estimate of climate change impacts on cotton and maize in Greece. J. Water Clim. Change, 9, 643-656. doi:10.2166/wcc.2018.022

Webb, N.P., Marshall, N.A., Stringer, L.C., Reed, M.S., Chapell, A. and Herrick, J.E., 2017. Land degradation and climate change: building climate resilience in agriculture. Front. Ecol. Environ., 15, 450-459.

Climate change projections of crop-specific temperature- and precipitation- related indices for Greece from EURO-CORDEX simulations in the 21st century

Mavrommatis T.[1], A.K. Georgoulias[1], D. Akritidis[1], D. Melas[2], P. Zanis[1]

[1]Department of Meteorology and Climatology, School of Geology, Aristotle University of Thessaloniki
[2]Laboratory of Atmospheric Physics, School of Physics, Aristotle University of Thessaloniki

Abstract. In the framework of the "National Network on Climate Change and its Impacts (CLIMPACT)" an updated assessment of projected climate change over Greece in the near future and at the end of the 21st century is presented, focusing on crop-specific temperature- and precipitation- related indices. The analysis is based on an ensemble of 11 high-resolution EURO-CORDEX regional climate model (RCM) simulations covering the historical period 1950–2005 and the future period 2006–2100 under the influence of a strong, a moderate, and a no mitigation Representative Concentration Pathway (RCP2.6, RCP4.5 and RCP8.5, respectively). The statistical robustness of climate change signals is also assessed. Because of the robust warming projected for Greece from these simulations for the different scenarios, crop-specific indices related to maximum (the number of days in spring with TASMAX > 30 ºC (tropical days)) and minimum (including the number of days with TASMIN < -8 ºC in winter and with TASMIN < 3 ºC in spring) daily temperature are anticipated to increase and decrease, respectively. The number of days with PR > 1mm (wet days) on an annual basis is expected to be statistically reduced only at the end of the 21st century over specific regions.

1 Introduction

Agriculture, an important sector of the economy for Greece, is directly impacted by weather and climate in a number of ways and this will continue in the future. Climate change (and particularly the combined effects of changes in temperature, rainfall and atmospheric CO_2 concentration) impacts on the agriculture sector are different across European regions. These among others include increases in heat extremes and risk of droughts, augmented water demand and decreases in precipitation and crop yields (see Figure 3.1 in EEA 2019). The combined effects of rising temperatures and decreases in rainfall patterns are expected to have direct effects on crop yields and indirect effects through changes in irrigation water availability. Higher temperatures will eventually reduce yields of desirable crops while encouraging weed and pest proliferation. Precipitation decreases are expected to increase the likelihood of short-run crop failures and long-run production declines (Nelson et al., 2009).

Georgoulias et al. (2022) presented an updated assessment of projected climate change over Greece in the near future and at the end of the 21st century, focusing on near surface temperature (TAS), precipitation (PR), and heat-, cold- and drought- related climate indices. They found a statistically robust TAS increase over the southeastern Europe both in the near future and at the end of the century under three different IPCC AR5 Representative Concentration Pathways (RCPs). The projected warming among the RCPs differentiates after 2030 and is larger over the continental part of Greece than over the sea. TAS is projected to increase by 1.2º C, on average, in the near future (2021-2050; NF) and by 1.4 ºC at the end of the century (2071-2100; EOC) under RCP2.6 (a strong mitigation scenario where greenhouse gas (GHG) concentrations are bound to decrease by -70% in the period 2010-2100 (van Vuuren et al., 2011)). Under the moderate mitigation scenario RCP4.5, TAS is expected to increase by 1.4 ºC and 2.3 ºC, respectively, while for the scenario with no future environmental and climate change policies and continuous increases in GHG concentrations (RCP8.5; Riahi et al., 2011), by 1.6 ºC and 4.3 ºC, respectively. Robust reductions in PR totals over areas in Greece, southern Turkey and over the sea below ~38 ºN at the end of the century for RCP8.5 only were identified (Georgoulias et al. 2022).

On this context, this study, in the framework of the "National Network on Climate Change and its Impacts (CLIMPACT)", presents an updated assessment of projected climate change over Greece in the near future and at the end of the 21st century, focusing on crop-specific temperature- and precipitation- related indices.

2 Data and methods

Daily near surface maximum and minimum air temperature (TASMAX and TASMIN, respectively; in ºC) and precipitation (in mm day^{-1}) from 11 regional climate model (RCM) simulations at a horizontal resolution of 0.11º (~12.5 km), derived from the EURO-CORDEX initiative (https://www.euro-cordex.net/) (Jacob et al., 2020, 2014; Vautard et al., 2013), were used. The simulations are a product of various RCMs driven by various global climate models (GCMs) (**Table 1**). Each set incorporated four different simulations: a historical (Hist) simulation

for the period 1950-2005 and three simulations for the period 2006-2100 under the three different RCPs mentioned in **section 1**.

Table 1. List with the EURO-CORDEX simulations used in the present study.

	RCM	Driving GCM	Realization	Hist	RCP2.6	RCP4.5	RCP8.5
1	ALADIN63.v2	CNRM.CNRM-CERFACS-CNRM-CM5	r1i1p1	x	x	x	x
2	CCLM4-8-17.v1	CLMcom.ICHEC-EC-EARTH	r12i1p1	x	x	x	x
3	HIRHAM5.v2	DMI.ICHEC-EC-EARTH	r3i1p1	x	x	x	x
4	RACMO22E.v1	KNMI.ICHEC-EC-EARTH	r12i1p1	x	x	x	x
5	RACMO22E.v2	KNMI.MOHC-HadGEM2-ES	r1i1p1	x	x	x	x
6	RACMO22E.v2	KNMI.CNRM-CERFACS-CNRM-CM5	r1i1p1	x	x	x	x
7	RCA4.v1	SMHI.MOHC-HadGEM2-ES	r1i1p1	x	x	x	x
8	RCA4.v1	SMHI.MPI-M-MPI-ESM-LR	r1i1p1	x	x	x	x
9	RCA4.v1	SMHI.ICHEC-EC-EARTH	r12i1p1	x	x	x	x
10	REMO2009.v1	MPI-CSC.MPI-M-MPI-ESM-LR	r1i1p1	x	x	x	x
11	REMO2009.v1	MPI-CSC.MPI-M-MPI-ESM-LR	r2i1p1	x	x	x	x

Four agricultural related indices (3 of these are based on temperature and one is on PR) (**Table 2**) were calculated on a grid cell basis for each one of the RCM simulations separately and then they were averaged to compile the ensemble mean values. The projected changes in the climate related indices over Greece are reported for the NF (2021-2050) and the EOC (2071-2100) 30-year periods relative to the reference period (1971-2000). The changes are calculated on a grid cell basis for each RCP separately, and the results are presented by means of maps. Following recent studies (e.g., Jacob et al., 2014), a difference between two climate projections is considered statistically robust if the differences for at least 7 out of the 11 simulations, constituting each ensemble, have the same sign with the ensemble difference and are statistically significant at the 95% confidence level according to the non-parametric Mann-Whitney test (Mann and Whitney, 1947).

Table 2. Crop specific indices related to agriculture for the historical and the three RCP scenarios.

	Crop	Indices	Season	Related to
1	Olive/Grape/Wheat	Days with TASMAX > 30ºC	Spring	Flowering
2	Wheat	Days with TASMIN < 3 ºC	Spring	Late frost
3	Olive	Days with TASMIN < -8 ºC	Winter	Survival
4	Grape/Wheat/ Tomato/Potato	Days with PR > 1 mm (wet days)	Annual	-

3 Results

Figure 1 shows the projected ensemble changes in the number of spring days with TASMAX > 30 ºC (tropical days) for the near-future and the end-of-the-century periods under the three RCPs. Analysis revealed generally statistically non-robust increases for this vital for olive, grape and wheat cultivations index under the examined scenarios (except for RCP4.5 and RCP8.5 (when statistically robust increases up to 10 days/yr all over Greece are expected) in the EOC period), except for limited areas only (mainly in Macedonia and Thessaly).
The projected ensemble changes in the number of days with TASMIN < -8 ºC (**Figure 2**), an important index of olive winter survival, are characterized by statistically robust decreases over the mountain topography of west Macedonia and Pindus, increasing in magnitude (but not spatially) from the NF to EOC period and from the strong (RCP2.6)- to no- mitigation scenario (RCP8.5).
Similar, statistically robust, maximum decreases up to 12 days with TASMIN < 3 ºC in spring, spatially expanding from the mountainous inland to lowland coastal regions as moving from the strong (RCP2.6)- to no-mitigation scenario (RCP8.5), are anticipated over the Greece in the NF period (not shown). A similar regional expansion but more intensive in magnitude (up to 28 days) is expected in the EOC period.

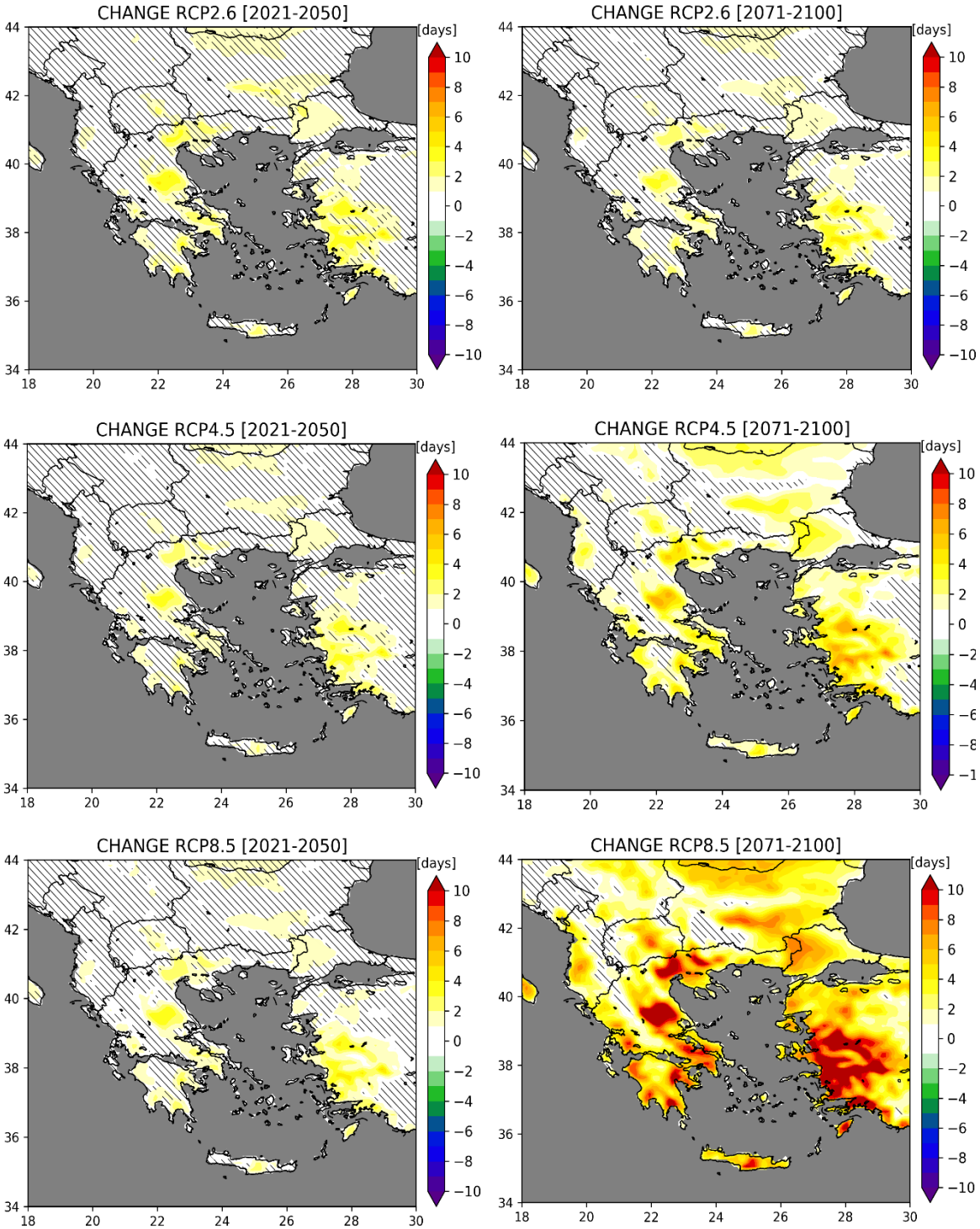

Figure 1. Differences in the frequency of days with TASMAX > 30ºC in spring) fields from the EURO-CORDEX ensemble between the near-future (2021-2050) (left column maps) and the end-of-the-century (2071-2100) (right column maps) and the reference period (1971-2000) for southeastern Europe for the emission scenarios RCP2.6, RCP4.5 and RCP8.5. Hatching indicates areas where the differences are not statistically robust.

The analysis regarding the change patterns of number of days with PR > 1mm (wet days) on annual basis (Figure 3) found statistically robust decreases only in the EOC, of up to 16 days for the RCP4.5 below the ~39o N and by up to 28 days for the RCP8.5 all over the country (not shown). Rajczak and Schär (2017) reached to the same conclusions on annual basis with decreases in wet day frequency of EURO-CORDEX runs over the Mediterranean region to agree with these of the EU-ENSEMBLES for both time periods for

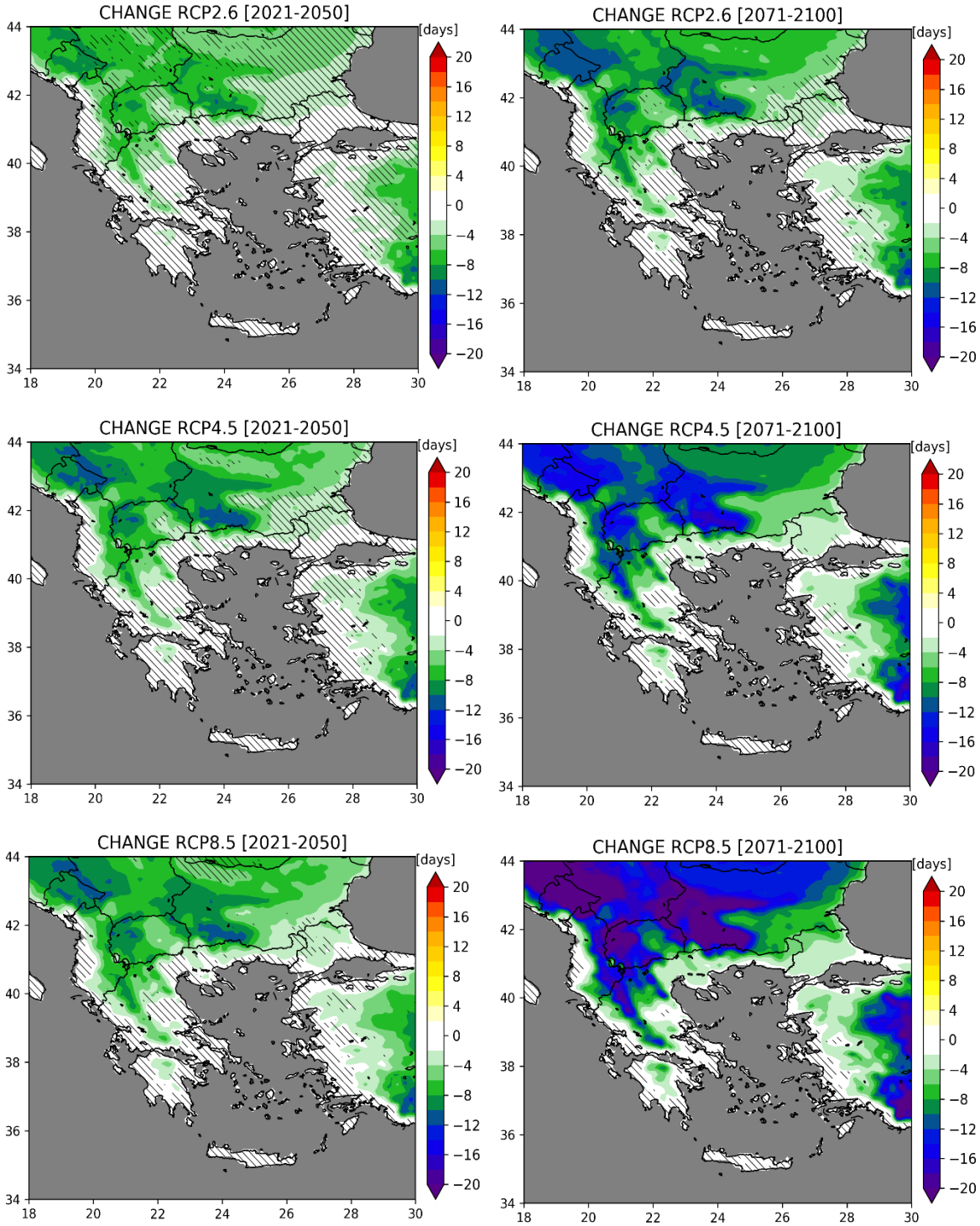

Figure 2. The same as Figure 1 but for days of TASMIN < -8 ºC in winter.

RCP8.5 (-23% for NF and -77% for EOC (EURO-CORDEX) vs -21% for NF and -74% for EOC (EU-ENSEMBLES)) and to underestimate these under the RCP4.5 (-15% for NF and -37% for EOC (EURO-CORDEX)).

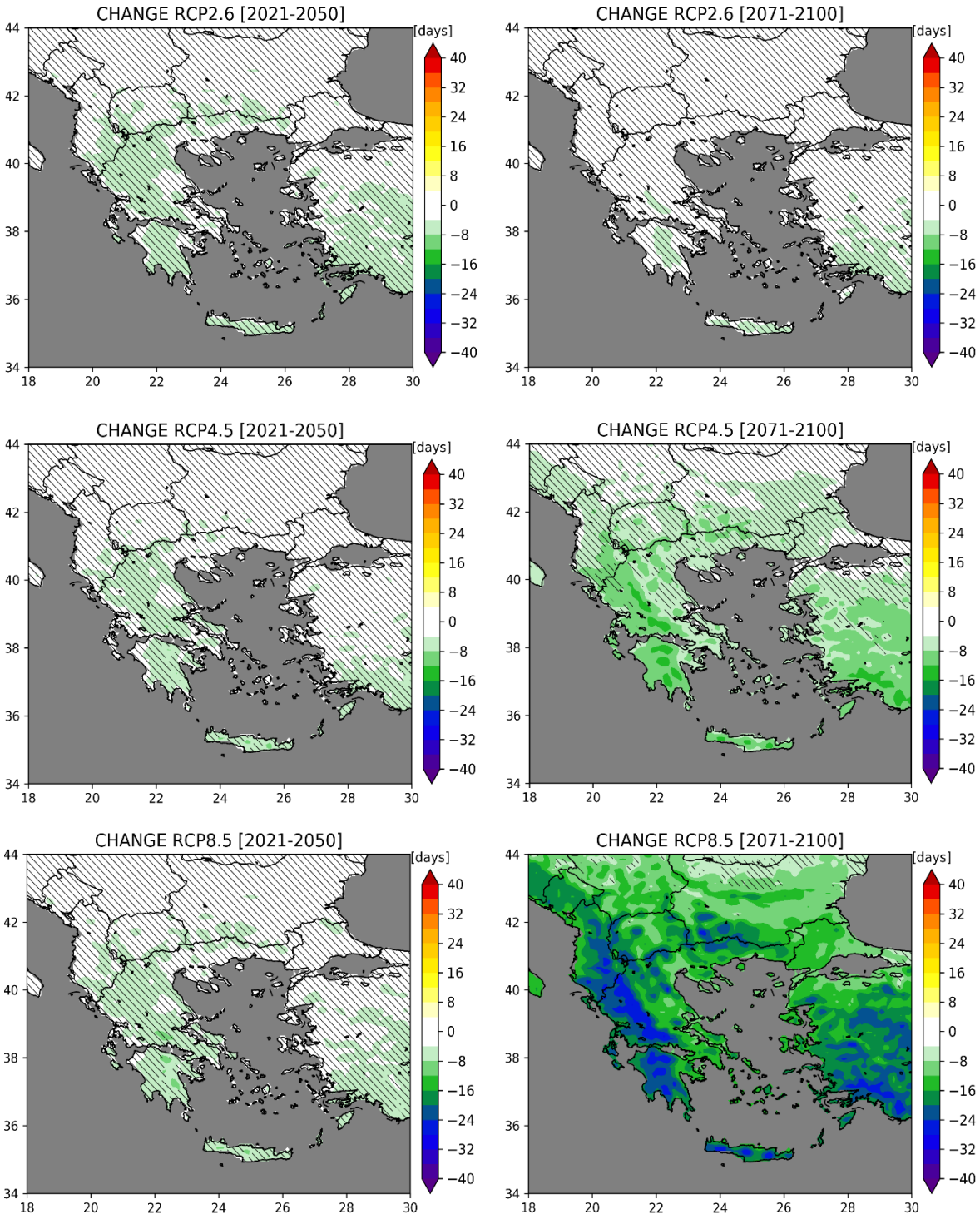

Figure 3. The same as Figure 1 but for days with PR > 1mm on annual basis.

4 Summary

In the framework of the "National Network on Climate Change and its Impacts (CLIMPACT)" an updated assessment of projected climate change over Greece in the near future and at the end of the 21st century, focusing on crop-specific temperature- and precipitation- related indices, is presented. The analysis is based on an ensemble of 11 high-resolution EURO-CORDEX regional climate model simulations covering the historical period 1950–2005 and the future period 2006–2100 under the influence of the three most recent emission scenarios: RCP2.6, RCP4.5 and RCP8.5. Because of the robust warming projected for Greece from

these simulations for the different scenarios, crop-specific indices related to maximum (the number of days in spring with TASMAX > 30 ºC (tropical days)) and minimum (the number of days with TASMIN < -8 ºC in winter and with TASMIN < 3 ºC in spring) daily temperature are anticipated to increase and decrease, respectively. The number of days with PR > 1mm (wet days) on annual basis is expected to be statistically reduced only at the end of the 21st century at specific regions only.

References

EEA, 2019. Climate change adaptation in the agriculture sector in Europe. European Environment Agency (EEA), doi:10.2800/537176

Georgoulias, A.K., Akritidis, D., Kalisoras, A., Kapsomenakis, J., Melas, D., Zerefos, C.S., Prodromos Zanis,P., 2022. Climate change projections for Greece in the 21st century from high-resolution EURO-CORDEX RCM simulations, Atmospheric Research 271, https://doi.org/10.1016/j.atmosres.2022.106049.

Jacob, D., Petersen, J., Eggert, B., Alias, A., Christensen, O.B., Bouwer, L.M., Braun, A., Colette, A., Déqué, M., Georgievski, G., Georgopoulou, E., Gobiet, A., Menut, L., Nikulin, G., Haensler, A., Hempelmann, N., Jones, C., Keuler, K., Kovats, S., Kröner, N., Kotlarski, S., Kriegsmann, A., Martin, E., van Meijgaard, E., Moseley, C., Pfeifer, S., Preuschmann, S., Radermacher, C., Radtke, K., Rechid, D., Rounsevell, M., Samuelsson, P., Somot, S., Soussana, J.-F., Teichmann, C., Valentini, R., Vautard, R., Weber, B., Yiou, P., 2014. EURO-CORDEX: new high-resolution climate change projections for European impact research. Reg Environ Change 14, 563–578. https://doi.org/10.1007/s10113-013-0499-2

Jacob, D., Teichmann, C., Sobolowski, S., Katragkou, E., Anders, I., Belda, M., Benestad, R., Boberg, F., Buonomo, E., Cardoso, R.M., Casanueva, A., Christensen, O.B., Christensen, J.H., Coppola, E., De Cruz, L., Davin, E.L., Dobler, A., Domínguez, M., Fealy, R., Fernandez, J., Gaertner, M.A., García-Díez, M., Giorgi, F., Gobiet, A., Goergen, K., Gómez-Navarro, J.J., Alemán, J.J.G., Gutiérrez, C., Gutiérrez, J.M., Güttler, I., Haensler, A., Halenka, T., Jerez, S., Jiménez-Guerrero, P., Jones, R.G., Keuler, K., Kjellström, E., Knist, S., Kotlarski, S., Maraun, D., van Meijgaard, E., Mercogliano, P., Montávez, J.P., Navarra, A., Nikulin, G., de Noblet-Ducoudré, N., Panitz, H.-J., Pfeifer, S., Piazza, M., Pichelli, E., Pietikäinen, J.-P., Prein, A.F., Preuschmann, S., Rechid, D., Rockel, B., Romera, R., Sánchez, E., Sieck, K., Soares, P.M.M., Somot, S., Srnec, L., Sørland, S.L., Termonia, P., Truhetz, H., Vautard, R., Warrach-Sagi, K., Wulfmeyer, V., 2020. Regional climate downscaling over Europe: perspectives from the EURO-CORDEX community. Reg Environ Change 20, 51. https://doi.org/10.1007/s10113-020-01606-9

Mann, H.B., Whitney, D.R., 1947. On a Test of Whether one of Two Random Variables is Stochastically Larger than the Other. Ann. Math. Statist. 18, 50–60. https://doi.org/10.1214/aoms/1177730491

Nelson, G.C, Rosegrant, M.W., Jawoo Koo, J., Robertson, Sulser, R.T., Zhu, T, Ringler, C., Msangi, S., Palazzo, A., Batka, M., Magalhaes, M., Valmonte-Santos, R., Ewing, M., and Lee, D., 2009. Climate Change Impact on Agriculture and Costs of Adaptation. Food policy Report, IFPRI, doi: 10.2499/0896295354

Rajczak, J., Schär, C. (2017). Projections of future precipitation extremes over Europe: A multimodel assessment of climate simulations. Journal of Geophysical Research: Atmospheres, 122, 10,773–10,800. https://doi.org/10.1002/ 2017JD027176

Riahi, K., Rao, S., Krey, V., Cho, C., Chirkov, V., Fischer, G., Kindermann, G., Nakicenovic, N., Rafaj, P., 2011. RCP 8.5—A scenario of comparatively high greenhouse gas emissions. Climatic Change 109, 33–57. https://doi.org/10.1007/s10584-011-0149-y

van Vuuren, D.P., Stehfest, E., den Elzen, M.G.J., Kram, T., van Vliet, J., Deetman, S., Isaac, M., Klein Goldewijk, K., Hof, A., Mendoza Beltran, A., Oostenrijk, R., van Ruijven, B., 2011. RCP2.6: exploring the possibility to keep global mean temperature increase below 2°C. Climatic Change 109, 95–116. https://doi.org/10.1007/s10584-011-0152-3

Vautard, R., Gobiet, A., Jacob, D., Belda, M., Colette, A., Déqué, M., Fernández, J., García-Díez, M., Goergen, K., Güttler, I., Halenka, T., Karacostas, T., Katragkou, E., Keuler, K., Kotlarski, S., Mayer, S., van Meijgaard, E., Nikulin, G., Patarčić, M., Scinocca, J., Sobolowski, S., Suklitsch, M., Teichmann, C., Warrach-Sagi, K., Wulfmeyer, V., Yiou, P., 2013. The simulation of European heat waves from an ensemble of regional climate models within the EURO-CORDEX project. Clim Dyn 41, 2555–2575. https://doi.org/10.1007/s00382-013-1714-z

Evaluation of Rainwater Harvesting Systems' Efficiency for Domestic Water Needs in Greek Islands under Climate Change Scenarios

Panagiotis T. Nastos[1] and Elissavet Feloni[1,2]

[1]Laboratory of Climatology and Atmospheric Environment, Department of Geology and Geoenvironment, National and Kpodistrian University of Athens, 15784, Athens, Greece
[2]Department of Water Resources and Environmental Engineering, School of Civil Engineering, National Technical University of Athens, 15780 Athens, Greece

Abstract. Rainfall is always part of our lives. Due to climate change, there are several periods of intense droughts, heatwaves, and, on the other hand, storms of high intensity and severe flooding. Thus, there is a need for proper water resources management, especially regarding rainwater. Meeting water requirements in areas of poor water potential, such as the Greek Islands, is an intertemporal issue since they were first inhabited. Rainwater Harvesting (RWH) Systems are proposed as an efficient solution to address water scarcity. In this research work, the simulation of such a system was performed for two islands in Greece that are characterized by different rainfall regime: Corfu and Naxos. Particularly, several scenarios were investigated, and the system's reliability is determined comparatively after considering synthetic timeseries of daily rainfall that incorporate climate change. More specifically, according to the latest IPCC, seven low/medium (RCP 4.5) and seven high (RCP 8.5) emissions scenarios were selected for a future period of 60 hydrological years and the reliability is determined as a function of the model's parameters (collection area: 40 to 140m^2, rainwater tank volume: 5 to 30m^3, number of household members: 2, 4), for a predetermined percentage of coverage (30%) on the total daily water demand (180 l/d). In addition, taking into consideration that it is a closed-type tank, the effect of evapotranspiration is considered negligible. Regarding the results obtained for these two islands, a RWH system for the island of Corfu, seems to be particularly efficient for all scenarios examined, due to the local high-rainfall regime, compared to the island of Naxos, where, in many cases, system cannot fully meet the demand-target, not even for the largest tank of 30m^3. In conclusion, this research contributes to the evaluation of similar RWH systems and has shown that these systems can be considered as a "green" solution of relatively low cost, especially for areas where there is a more favorable rainfall regime, but water supply is currently achieved through transportation of water from the mainland or other islands using tank vessels and where desalination units have not been yet installed.

Keywords. Rainwater harvesting systems (RWH), rainwater tank, daily water balance models, IPCC, RCP, daily consumption, efficiency, Corfu, Naxos, urban water demand at household level.

1 Introduction

The lack of sufficient available water resources to meet the demands of urban water usage in areas, such as the Greek Islands, is a common problem towards local water resources management and there are many techniques regarding water collection and storage that are investigated to potentially contribute to reduce the problem. Among them, Rainwater Harvesting (RWH) Systems is a common practice usually operating at a household scale, ensuring the provision of water that is suitable for a number of uses, such as laundry, toilet, garden, etc. RWH tanks cannot be formulated, because the size is strongly affected by various local variables, such as local rainfall, the collection surface area, the demand and the number of served residents. Methods for RWH tank sizing vary from country to country depending on standards and regulations adopted by each country (e.g., Handia et al.,2003; Ward et al., 2011; Campisano and Modica, 2012; Londra et al., 2015), and the size can be determined either by using the daily or monthly water balance method (behavioral models) (Tsihrintzis and Baltas, 2013; application for Greece) or using the dry period demand method. One advantage of the behavioral methods is that they can measure several variables of the system over time, such as volumes of consumed and overflowed rainwater, percentage of days in which rainwater demand is met (Ghisi et al., 2009), etc. The main disadvantage of these methods is that there is no guarantee of similar results when using different rainfall data from the same region, as the simulation is based on a water mass balance equation (Basinger et al., 2010). The water balance method is based on recordings of local rainfall data used directly as hydrological input data in the system. Overall, the capacity of rainwater harvesting tanks cannot be formulated because is strongly influenced by several local variables, such as local rainfall, the collection surfaces, demand and the number of routes residents (Londra et al., 2015).
In Greece, the main reasons that cause problems in the use and rational management of water resources are both the unequal distribution of water resources and demand in space and time (Londra et al., 2015). It is worth noting that there is not a proposed methodology to calculate the size of rainwater harvesting tank in

Greece. The aim of this study is the investigation of such a system's operation under various combinations regarding the number of residents, the collection area and the tank size, for two Greek Islands that are characterized by different rainfall regime. On the one hand, Corfu Island (Ionian Sea, NW Greece) appears one of the highest annual precipitation depth in Greece, and, on the other site, Naxos Island (Aegean Sea, Eastern Greece) is an area of low precipitation depth. The entire analysis is performed after developing and implementing a daily water balance model, which allows to calculate the efficiency coefficient (Reliability, *Re (%)*) of the system for various combinations. Finally, the corresponding results given in graphs are capable for sizing the rainwater harvesting tanks in RWH systems Greece for domestic use and for a standard Re (%). The analysis is performed using the historic daily precipitation timeseries for these two islands and, also, after applying several climate change scenarios. Results show that the local precipitation regime affects the system's performance, that is satisfactory only for Corfu. In Naxos Island, especially in case of households with more than two members and for small collection areas, the system cannot meet the demand, even after using the maximum tank size that is investigated.

2 Study areas and Datasets

There are two areas that are investigated through this analysis, the first one named Corfu is linked to a high precipitation regime, while the second, which is the island of Naxos, is linked to a low precipitation regime. The island of Corfu, located in the Ionian Sea, belongs to the complex of Ionian Islands. The population of the island is about 102071 people, but this number increases during summer periods because of the tourism. Naxos Island, located in the Aegean Sea, belongs geographically to the Cyclades complex of islands. The population of the island is now 18340 residents, but, as in Corfu, this number increases during summer periods due to tourism.

For the present study, the available historic timeseries of daily rainfall provided by the Hellenic National Meteorological Service for the period October 1980 to September 2019, were analyzed and processed. The analysis presented corresponds to 39 hydrological years, in order to follow the minimum hydrological standards for sizing a RWH tank (at least 30 years). Figures 1a and 1b show the daily variation of the rainfall depth (in mm) for the station of Corfu and Naxos, and for the period that the model is initially performed (October 1980 - September 2019).

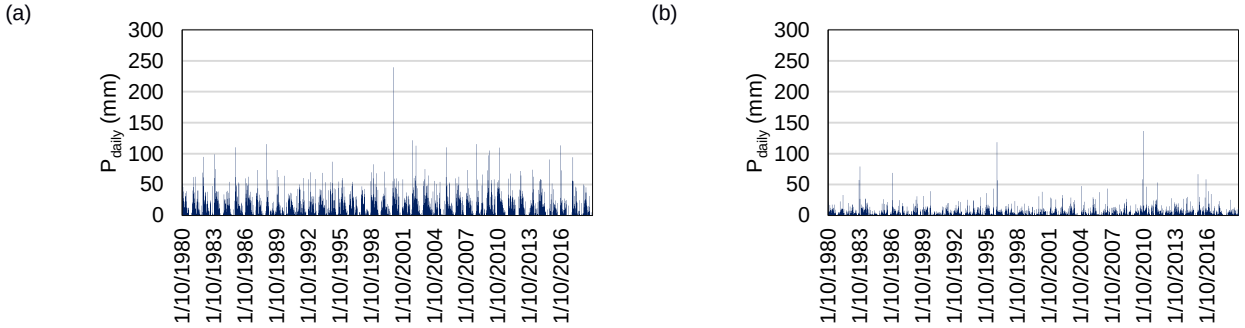

Figure 1. Daily rainfall depth (Historical timeseries) for the period 1980-2019 (a) Corfu, (b) Naxos.

Furthermore, synthetic timeseries from the CORDEX (Coordinated Regional Downscaling Experiment) are also used to further investigate the system's performance under climate change conditions. Timeseries are freely accessed through the DEAR-Clima (Data Extraction Application for Regional Climate) website: http://meteo3.geo.auth.gr:3838/ (last accessed on May 19, 2022), that is a user-friendly interface that visualizes and provides a variety of variables, temporal intervals and GCM-RCM models, to a high spatial resolution and for the period up to 2100. The current analysis uses the daily rainfall timeseries of the models presented in Table one and for two RCPs scenarios: 4.5 and 8.5.

Table 2. Global and Regional Climate Models for the timeseries of climate change scenarios.

Global and Regional Climate Models (RCP 4.5, 8.5)	
1. CLMcom-CCLM4-8-17	1.1 CNRM-CERFACS-CNRM-CM5
	1.3 MPI-M-MPI-ESM-LR
2. CNRM-ALADIN53	2.1 CNRM-CERFACS-CNRM-CM5
3. SMHI-RCA4	3.1 CNRM-CERFACS-CNRM-CM5
4. KNMI-RACMO22E	4.1 ICHEC-EC-EARTH
5. IPSL-INERIS-WRF331F	5.1 IPSL-IPSL-CM5A-MR
6. MPI-CSC-REMO2009	6.1 MPI-M-MPI-ESM-LR

3 Model description

Daily water balance model

In the frame of this study, a daily water balance model was implemented for the sizing of rainwater harvesting tank. The water balance equation is:

$$S_t = S_{t-1} + R_t - D_t, \qquad 0 \le S_{t-1} \le V_{tank}$$

where:

S_t, the stored volume at the end of the day (m^3); S_{t-1}, the stored volume at the beginning of the day (m^3); R_t, the harvested rainwater volume at the end of the day (m^3); D_t, the daily water demand (m^3); and, V_{tank}, the capacity of rainwater tank (m^3).

Daily harvested rainwater volume (R_t)

The daily harvested rainwater volume (runoff), from a roof area, is calculated as:

$$R_t = C \times A \times P_{eff,t} \ (m^3)$$

where:

C, the runoff coefficient; A, the rain collection area (m^2); and, $P_{eff,t}$, the daily effective rainfall depth at the end of the day (m).

The runoff coefficient can take different values, depending on the material of the collection surface. In the present study, the coefficient is 0.90 (Tsihrintzis and Baltas, 2013). The daily effective rainfall is equal to daily rainfall minus the first flush.

$P_{eff,t} = P_t - 0.33$ (mm)

where:

P_t, the daily rainfall; and 0.33, the value for the first flash.

Daily water demand (D_t)

The daily water demand of a household is calculated as:

$$D_t = N_{cap} \times q \times (\tfrac{p}{100})$$

where:

N_{cap}, the number of residents (cap); q, the daily water use per day (m^3/cap/day); and, p, the percentage of total water use satisfied by harvested rainwater.

Tank size

Considering the equations of the water balance and the daily water demand, the daily rainwater stored volume is calculated as:

$$S_t = S_{t-1} + C \times A \times P_{eff,t} - N_{cap} \times q \times (\tfrac{p}{100}) \text{ , με } 0 \le S_{t-1} \le V_{tank}$$

The daily difference between runoff (inflow) and demand (outflow) is calculated as follows:

$$\Delta S_t = C \times A \times P_{eff,t} - N_{cap} \times q \times \left(\frac{p}{100}\right)$$

The equation for the daily water stored volume can be rewritten as: $S_t = S_{t-1} + \Delta S_t$

The calculation of the daily storage volume is iterative and starts from an initial value $S_{t-1} = S_0$ for t= 0. The lower value for the volume zero, referring to an initially empty tank (S_0= 0). When it is partially full, the volume can take any value, while the maximum value is equal to the volume of the tank itself ($S_0 = V_{tank}$). In this study, it was considered an initially full rainwater tank.

The following repeated process is:

$$if\ (S_{t-1} + \Delta S_t) > V_{tank}\ then\ S_{t,tank} = V_{tank},\ if\ (S_{t-1} + \Delta S_t) < V_{tank}\ then\ 0,\ else\ S_t = S_{t,tank} = S_{t-1} + \Delta S_t$$

where:

$S_{t,tank}$, the actual available stored water volume in the tank at t day.

When the tank is full, there is a volume which overflows (O_t) and is calculated as:

$$if\ S_t \ge V_{tank}\ then\ O_t = S_t - V_{tank},\ else\ O_t = 0$$

In the case that the volume of rainwater collected and stored ($S_{t,tank}$) is not enough to meet the demand, then the demand will be satisfied, in parts or in whole, with an additional amount of water delivered from the local public water supply, the tap (T_t), which can be calculated as: $if\ (S_t < D_t)\ then\ T_t = D_t - S_{t,tank}\ ,\ else\ T_t = 0$

Reliability coefficient (Re)

The reliability coefficient (Re) is defined as the percentage of the total number of days that the water stored in the tank serves the needs of the individuals exclusively, to the total number of days that the rain data has been recorded and used in the model (i.e., days of model simulation):

$$Re\ (\%) = \frac{\sum days\ without\ tap\ water}{\sum simulation\ days}$$

4 Results & Discussion

To investigate the reliability of the rainwater collection system, various scenarios were created, taking into account the characteristics of the two areas. Among the scenarios analysed, each one refers to a different number of residents (N_{cap}) and all examine a range of rain collection areas (A) and tank size (V_{tank}). At all cases, the system's efficiency is determined using a target p=30%, of the total water demand q=180 L/cap/day and number of members (Ncap) equals to 2 and 4. In order to investigate system's reliability for several combinations, a collection area (A) from 40 to 140 m^2 and a rainwater tank volume (V_{tank}) from 5 to 30 m^3 were considered. Figures 2 and 3 present indicatively the reliability coefficient (Re) as a function of roof area (A) and rainwater volume tank (V_{tank}) for the two islands and for 2 and 4 household members, respectively.

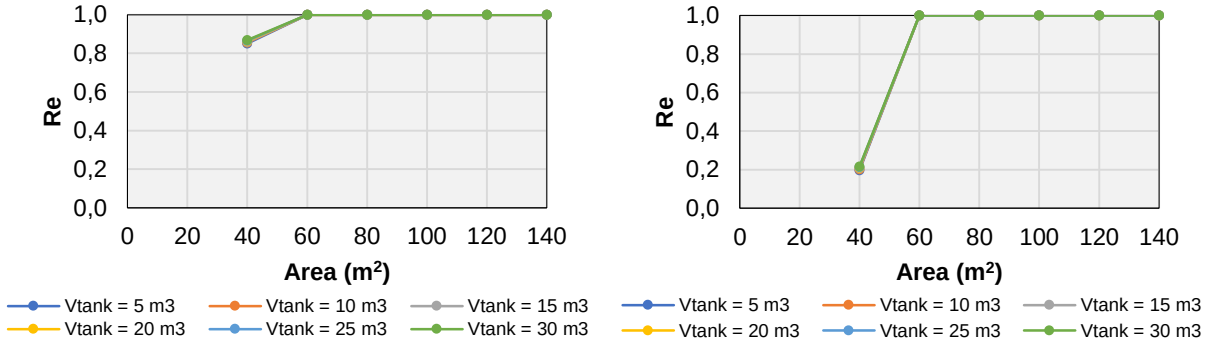

Figure 2. RWH reliability coefficient (Re) for different range of roof area (A) and rainwater volume tank (V_{tank}), for N_{cap}= 2, using the historic timeseries for (a) Corfu, (b) Naxos.

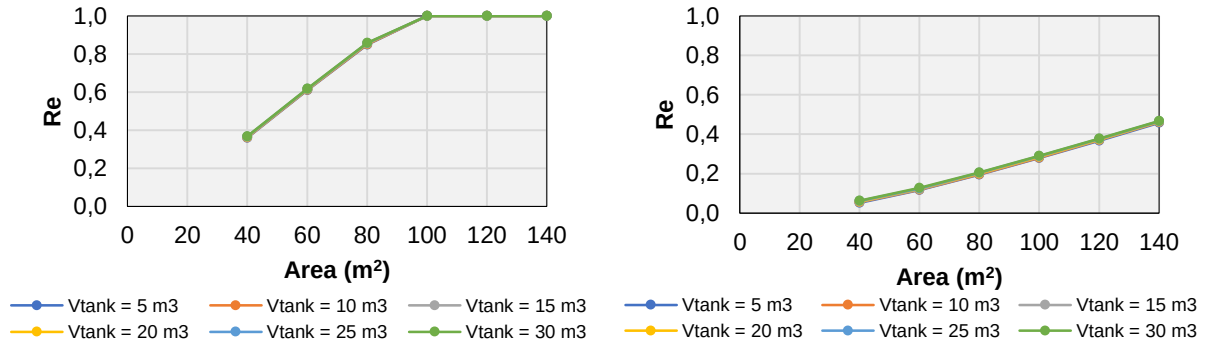

Figure 3. RWH reliability coefficient (Re) for different range of roof area (A) and rainwater volume tank (V_{tank}), for N_{cap}= 4, using the historic timeseries for (a) Corfu, (b) Naxos.

Finally, the analysis performed under several climate change scenarios (Table 1). The combination between the selected Regional Climate Models and the Global Climate Models (Driver) resulted in seven models that examined for two RCP scenarios; the average, RCP4.5, and the worst-case scenario, RCP8.5. All 14 timeseries were considered to estimate the RWH system's reliability coefficient for all A-V_{tank}-N_{cap} combinations for both islands. Table 2 summarizes the minimum and maximum reliability estimated for each scenario, which corresponds to a scenario using the smallest A=40m^2 and V_{tank}=5m^3 and the biggest one (A=140m^2 and V_{tank}=30m^3), respectively.

5 Summary and Conclusions

The RWH system simulation that is presented through this work highlights the variation in reliability after considering various combinations regarding members per household, collection area and tank size. Additionally, as expected, rainfall regime is decisive for the performance, as shown through the analysis for two Greek islands that are characterized by different rainfall regime. A rainwater harvesting system that may operate at the island of Corfu seems to be a very efficient solution for a water supply of 30% of the domestic daily water demand. On the other hand, in Naxos, the system's performance is not satisfactory for the examined tank volumes (up to 30m^3). As a general conclusion, by increasing the water tank volume and simultaneously increasing the roof area, the system becomes more efficient, in all examined combinations.

Finally, the analysis under climate change scenarios shows a wide range in the results regarding RWH system's reliability, as the corresponding analysis is driven by the daily rainfall timeseries patterns.

Table 2. Minima and maxima RWH Re (%) using the timeseries of climate change scenarios.

Combination of Regional Climate Model and Global Climate Model (Driver)	Climate Scenario	Re (%)	Corfu	Naxos	Corfu	Naxos
			N_{cap}=2		N_{cap}=4	
1.1 CNRM-CERFACS-CNRM-CM5	RCP 4.5	*min*	100.0%	19.7%	52.3%	5.0%
		max	100.0%	100.0%	100.0%	46.4%
	RCP 8.5	*min*	100.0%	20.9%	50.3%	5.9%
		max	100.0%	100.0%	100.0%	47.2%
1.3 MPI-M-MPI-ESM-LR	RCP 4.5	*min*	59.8%	20.0%	21.0%	5.2%
		max	100.0%	99.8%	100.0%	46.2%
	RCP 8.5	*min*	54.6%	18.0%	19.4%	4.9%
		max	100.0%	91.9%	100.0%	41.0%
2.1 CNRM-CERFACS-CNRM-CM5	RCP 4.5	*min*	82.9%	35.2%	27.5%	7.6%
		max	100.0%	100.0%	100.0%	81.3%
	RCP 8.5	*min*	80.5%	31.7%	26.6%	7.1%
		max	100.0%	100.0%	100.0%	73.9%
3.1 CNRM-CERFACS-CNRM-CM5	RCP 4.5	*min*	74.9%	37.2%	27.0%	11.1%
		max	100.0%	100.0%	100.0%	75.9%
	RCP 8.5	*min*	71.3%	37.7%	25.7%	11.6%
		max	100.0%	100.0%	100.0%	76.9%
4.1 ICHEC-EC-EARTH	RCP 4.5	*min*	77.2%	40.9%	29.4%	12.1%
		max	100.0%	100.0%	100.0%	81.4%
	RCP 8.5	*min*	76.4%	38.5%	28.5%	11.7%
		max	100.0%	100.0%	100.0%	77.4%
5.1 IPSL-IPSL-CM5A-MR	RCP 4.5	*min*	99.8%	66.6%	51.5%	23.5%
		max	100.0%	100.0%	100.0%	100.0%
	RCP 8.5	*min*	100.0%	62.6%	68.3%	21.7%
		max	100.0%	100.0%	100.0%	100.0%
6.1 MPI-M-MPI-ESM-LR	RCP 4.5	*min*	60.5%	48.6%	20.2%	16.6%
		max	100.0%	100.0%	100.0%	92.9%
	RCP 8.5	*min*	55.9%	47.1%	19.2%	16.5%
		max	100.0%	100.0%	100.0%	90.3%

References

Basinger, M., Montalto, F. and Lall, U., 2010. A rainwater harvesting system reliability model based on nonparametric stochastic rainfall generator. Journal of Hydrology, 392(3-4), pp.105-118.

Campisano, A. and Modica, C., 2012. Optimal sizing of storage tanks for domestic rainwater harvesting in Sicily. Resources, Conservation and Recycling, 63, pp.9-16.

Ghisi, E., da Fonseca Tavares, D. and Rocha, V.L., 2009. Rainwater harvesting in petrol stations in Brasilia: Potential for potable water savings and investment feasibility analysis. Resources, Conservation and Recycling, 54(2), pp.79-85.

Handia, L., Tembo, J.M. and Mwiindwa, C., 2003. Potential of rainwater harvesting in urban Zambia. Physics and chemistry of the earth, parts a/b/c, 28(20-27), pp.893-896.

Londra, P.A., Theocharis, A.T., Baltas, E. and Tsihrintzis, V.A., 2015. Optimal sizing of rainwater harvesting tanks for domestic use in Greece. Water Resources Management, 29(12), pp.4357-4377.

Tsihrintzis, V. and Baltas, E., 2013, September. Sizing of rainwater harvesting tank for in-house water supply. In 13th International Conference on Environmental Science and Technology, Athens, Greece (pp. 5-7).

Ward, S., Memon, F.A. and Butler, D., 2012. Performance of a large building rainwater harvesting system. Water research, 46(16), pp.5127-5134.

LIFE ADAPT2CLIMA tool: A decision support tool for adaptation to climate change impacts on the Mediterranean islands' agriculture

Christos Giannakopoulos[1], Anna Karali[1], Giannis Lemesios[1], Christina Papadaskalopoulou[2], Konstantinos V. Varotsos[1], Maria Papadopoulou[3], Marco Moriondo[4], Camilla Dibari [5], Maria Loizidou[2]

[1]Institute for Environmental Research and Sustainable Development, National Observatory of Athens, Athens, Greece
[2]School of Chemical Engineering, National Technical University of Athens, Athens, Greece
[3]Laboratory of Physical Geography and Environmental Impacts, School of Rural and Surveying Engineering, National Technical University, Athens, Greece
[4]Institute of BioEconomy, National Research Council (IBE-CNR), Florence, Italy
[5]Department of Agricultural Sciences and Technologies, University of Florence, Florence, Italy

Abstract. Climate change may affect many economic sectors, and agriculture is one of the most exposed, as it directly depends on climatic factors such as temperature and precipitation for its viability. The potential negative impacts of climate change on agriculture, include reduced crop yields due to high temperatures, increased water demand for irrigation and reduced water availability due to prolonged periods of droughts and water scarcity, which will in turn lead to conflicting water demands between agriculture and other usage. The EU LIFE ADAPT2CLIMA project aims to increase knowledge on the vulnerability of Mediterranean agriculture to climate change and to facilitate the development of adaptation strategies for agriculture by deploying an innovative decision support tool. The ADAPT2CLIMA tool assess the impacts of climate change on crop production and the effectiveness of selected adaptation options in decreasing vulnerability to climate change in three Mediterranean islands i.e., Crete-Greece, Sicily-Italy and Cyprus.
The tool construction was closely monitored by the project steering committees comprising of climate and crop scientists, policy makers as well as farm association executives who were interacting to tailor make the final product perfectly suited to their needs. In particular, the tool provides: i) future projections of climatic indicators relevant to agriculture; ii) future hydrological conditions; iii) crop performance indicators for six crops; (iv) socio-economic indicators used in the climate change impact assessment; (v) impact and adaptation assessments for each crop together with an evaluation of the proposed adaptation options for the three islands. Finally, the tool can potentially be replicated in all regions of Greece, Italy and Cyprus. Once certain input requirements are met, an impact assessment may be calculated and visualized for the region of interest towards more effective selection of areas in need and choice of adaptation measures.

1 Introduction

Climate change may affect many economic sectors, and agriculture is one of the most exposed, as it directly depends on climatic factors such as temperature and precipitation for its viability. The potential negative impacts of climate change on agriculture, include reduced crop yields due to high temperatures, increased water demand for irrigation and reduced water availability due to prolonged periods of droughts and water scarcity, which will in turn lead to conflicting water demands between agriculture and other usage. In addition, the extensive exploitation of coastal aquifers for irrigation, may lead to seawater intrusion and water and soil salinization which can seriously damage plants and soils. Negative effects on agriculture will be exacerbated by damages to crops caused by extreme weather events. Impacts may also occur due to the climate change impacts on soil fertility, such as increased vulnerability of soil organic matter and risk of soil erosion due to rising temperatures and higher occurrence of droughts and rainfall.
LIFE ADAPT2CLIMA project aims to increase knowledge on the vulnerability of EU Mediterranean agriculture to climate change and to support decision making for adaptation planning. The project implementation areas are three islands located in the Mediterranean i.e., Crete (Greece), Sicily (Italy) and Cyprus. While all EU countries are expected to be affected by climate change, the islands located at the Mediterranean basin, such as the islands of Crete, Sicily and Cyprus are considered particularly vulnerable. This is due to the fact that: (i) they lie in the Mediterranean basin, which is a climate change hot spot, (ii) they depend solely on their own water resources and therefore are highly sensitive to changes in precipitation (iii) the fertility of their soils and the quality of water resources for irrigation may be affected due to the consequences of climate change. The project methodology is based on the deployment of a set of climate, hydrological and crop simulation models for the assessment of climate change impacts on agriculture.
The main project outcome was the development and demonstration of a user friendly and interactive decision support tool, assessing the impacts of climate change on crop production and the effectiveness of selected

adaptation options in reducing crops' vulnerability to climate change. The implementation of the tool in the three project islands led to the development of adaptation strategies of the agricultural sectors of the islands.

2 ADAPT2CLIMA tool structure

The tool provides quantitative information through interactive maps and graphs within a GIS-based environment on:

a) agriculture relevant climatic indicators,
b) hydrologic and drought indicators for the project's pilot areas,
c) crop performance indicators for different sowing seasons and precocity levels for six crops (olives, vineyards, wheat, barley, tomatoes and potatoes),
d) socio-economic indicators used in the climate change impact assessment of the agricultural sector,
e) evaluation of available adaptation measures for addressing climate change impacts on crops against several adaptation related criteria,
f) total climate change impact assessment for each crop under study with or without the implementation of selected adaptation measures

The tool is accessible at the following link: https://tool.adapt2clima.eu/en/home/ in three languages (Greek, English, Italian).

2.1 Climatic indicators

This section provides information on current and future projections of climatic indices relevant to agriculture, based on state-of-the-art Regional Climate Model (RCM) output developed within the EURO-CORDEX initiative (11km horizontal resolution) for the areas under study. After an extensive evaluation analysis two RCMs (HadGEM2-ES/RCA4 (Collins et al., 2011; Strandberg et al., 2014) and the MPI-ESM-LR/RCA4 (Popke et al., 2013; Strandberg et al., 2014) were found to adequately reproduce the climatic conditions of the islands and were used in order to assess the impact of climate change on agriculture. Future projections are based on the intermediate mitigation scenario (RCP4.5) and the extreme emission scenario (RCP8.5). Moreover, two main future climatic perspectives are provided. The mean future period (2031-2060) which enables long-term adaptation planning for decision makers and extreme climatic conditions, i.e., intense cold/warm years and dry/wet years which can be used for short-term adaptation planning by farmers, in case such extreme climatic conditions occur in the near future. In the framework of the project, climate indices mainly related to temperature and precipitation affecting agriculture were constructed. These indices are related to the different phenological stages of the plant, plant production and crop quality as well as plant's survival such as: the number of days with minimum temperature less than 13°C in summer related to grain development of wheat, the number of days with maximum temperature greater than 30°C in spring related to the flowering of olives and vineyard.

2.2 Hydrologic indicators

To estimate hydrologic indicators, ground water flow and contaminant transport simulation models were developed using Visual MODFLOW Flex as a processor for the MODFLOW and SEAWAT groundwater simulation algorithms (Waterloo Hydrogeologic, 2017). The required hydrologic data and hydrogeological characteristics were derived from the literature data or obtained by contacting the local authorities (e.g., Water Development Department, Agricultural Research Institute of Cyprus), whereas historic meteorological data were derived from the E-OBS gridded dataset (Papadopoulou et al., 2020). These were developed for selected pilot sites for the driest year in the 2031-2060 period under both emission scenarios. In the tool the groundwater level variability between a reference hydrological year and future climatic scenarios together with the drought index (SPEI) evolution near selected water sources are provided.

2.3 Agronomic indicators

Crop yield changes were assessed utilizing three crop simulation models which were first calibrated using crop specific parameters concerning crop phenology and growth. These models are the following: a) CropSyst (version 3.2) (Stöckle et al., 2003) for wheat, barley, tomato and potato, b) OLIVEmodel.CNR (Moriondo et al., 2019) for olives and c) UNIFI.GrapeML (Leolini et a., 2018) for grapevines. For each crop, traditional sowing seasons and precocity levels were examined. More specifically, for the annual crops (barley, wheat, tomato and potato) the simulations were run considering four different periods for sowing that can be conceptually summarized as follows: early, early medium, medium late and late. For each crop, different dates were identified to represent the four sowing periods. Regarding the perennial crops (grapevine and olive tree),

precocity levels were set based on the bud-break date and the flowering date, respectively. Except for crop yield different crop performance indicators (flowering date, maturity date, actual evapotranspiration-AET, potential evapotranspiration-PET, AET/PET) are presented in the tool.

2.4 Socio-economic indicators

Several socio-economic indicators used in the climate change vulnerability assessment of the agricultural sector are presented for each one of the three islands. These indicators are the following: a) agricultural population (farm holders and family members, permanent and seasonal employees), b) dependence of farmers on agriculture, expressed as the percentage of farmers whose exclusive or main occupation is agriculture, c) age of farmers and in particular, the percentage of farmers aged over 65 years old, d) contribution of the pilot crops to the local rural economy, in terms of total revenues and price. The socio-economic data were obtained by the National Statistical Institutes and are provided at municipal level for each island.

2.5 Total impacts & adaptation

In this section, the magnitude of total climate change impacts for each crop and island under study, as well as the potential for enhancing crops resilience through the implementation of selected adaptation measures are presented. The assessment of total climate change impacts on agriculture was based on the relevant terminology presented within the 5th Assessment Report (AR5) of the IPCC (2014).

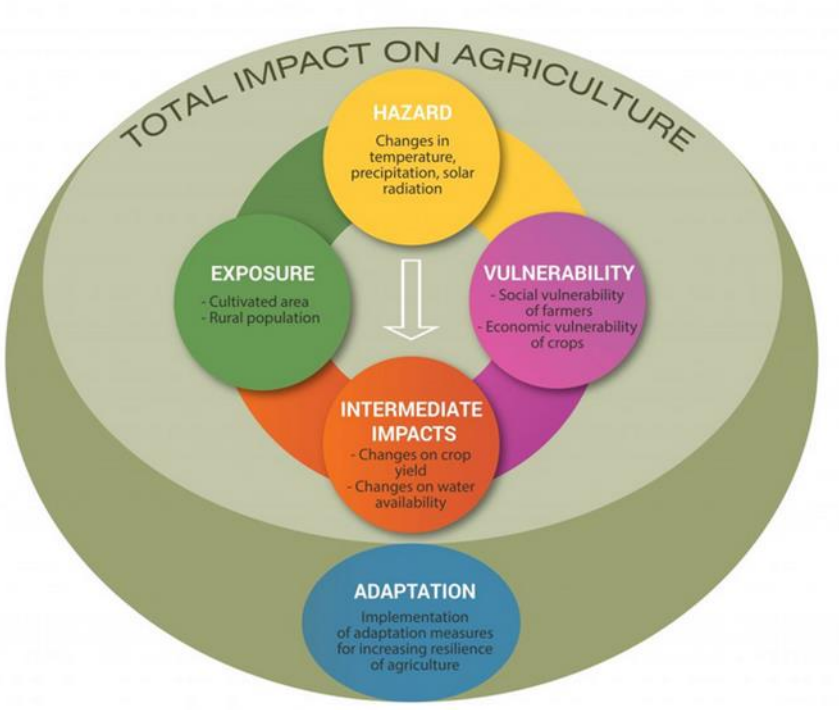

Figure 1. Total impact assessment methodology based on the IPCC (2014) framework.

According to the latter, the total impacts are a result of the interaction of climate change (hazard) and the vulnerability of the exposed system and population. In the current study, the climatic hazard refers to the expected changes in temperature, precipitation and solar radiation. Exposure refers to the cultivated areas of the examined crops and to the concentration of agricultural population, while vulnerability refers to the size and dependency of population to agriculture and the economic importance of crops in terms of revenues and value (Figure 1).

It was found that for the three islands, summer crops (olives, grapes and tomatoes in open-field conditions) are more negatively impacted than winter crops, as they grow during peak periods of drought and heat stress. For example, for grapes in Cyprus and Sicily yield is projected to decrease by 11% and 13%, respectively, under the RCP8.5; while olive yield is anticipated to decrease by 5-6% in Crete and Cyprus. Although winter

crops overall are less impacted, in some cases, such as barley in Cyprus (12% yield reduction at island level under RCP8.5), significant impacts are estimated. Following these estimated reductions in yield, the project team conducted a total impact assessment taking into account socio-economic aspects for each region as mentioned above (Figure 2). Thus, farmers and government should take targeted action to increase the resilience of the agricultural sector, with a special focus on these areas and crops. In this direction, the project proposes a clear set of adaptation measures that can greatly ameliorate the intensity of the impacts on each crop (Section 2.6).

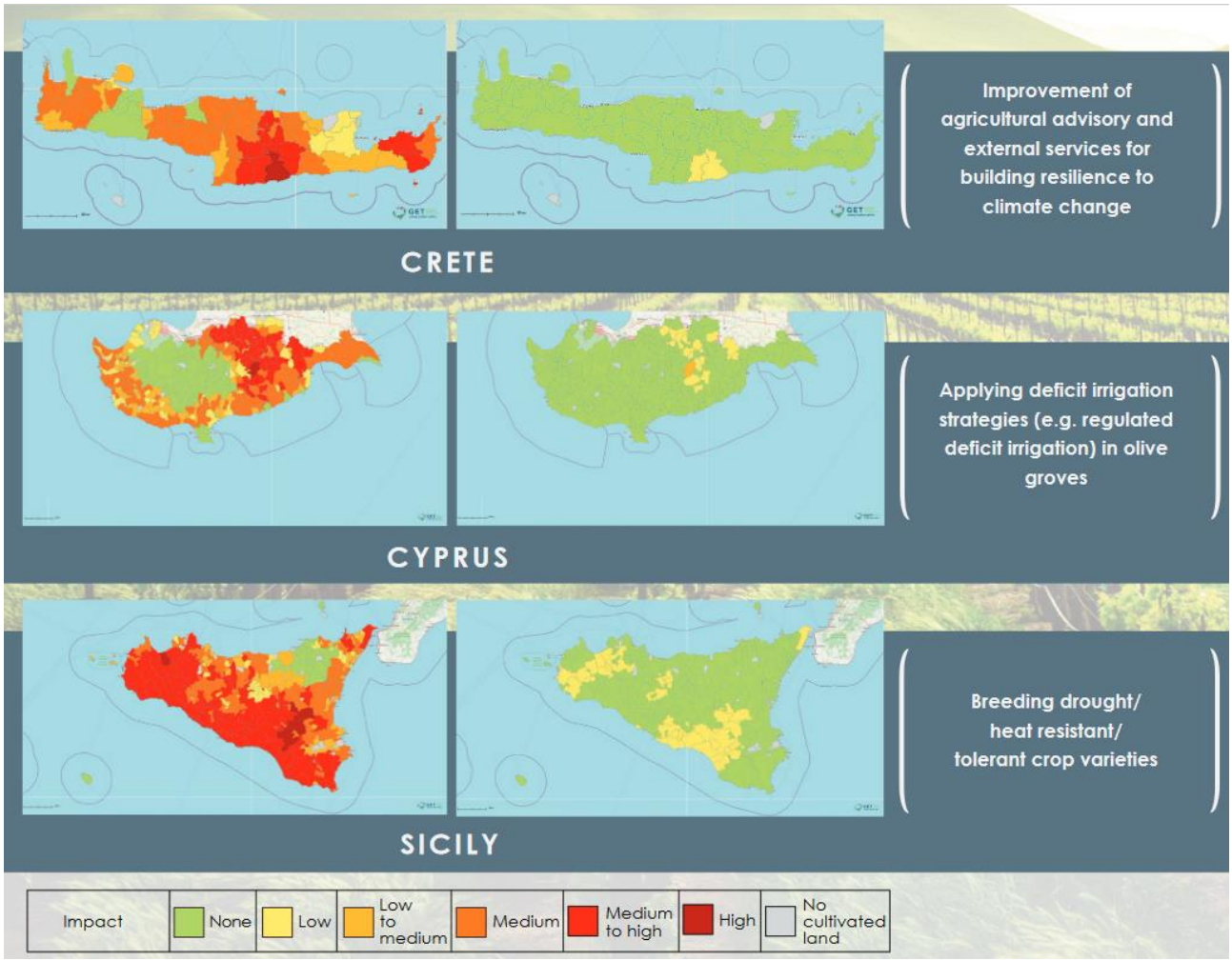

Figure 2. Examples of high total climate change impact on crops (left) and their reduction by implementing selected adaptation measures (right).

2.6 Adaptation measures

The list of the available adaptation measures for addressing climate change impacts on crops provided, was based on an extensive literature review by the project partners. The measures were compiled into a questionnaire that was distributed to selected experts and stakeholders from Cyprus, Greece and Italy. In this way, the measures were evaluated in terms of their effectiveness, contribution to climate change adaptation, and economic viability. The adaptation measures were then ranked using the multi-criteria analysis (MCA) method. The highest-ranking adaptation measures applicable to all crops included: efficient irrigation systems; development/improvement of early warning systems; improvement of agricultural advisory and external services; better on-farm water harvesting; improved local institutional support; drought/heat resistant/tolerant crop varieties; and a database with long-term monitoring data for crop pests and diseases.

2.7 Apply the tool to your area

There is a separate section of the tool, called “Apply the tool to your area”, which aims at replicating the tool to other regions of Greece, Italy and Cyprus and/or to other crops of the three project countries. The minimum data required for conducting a climate change impact assessment refer to the expected crop yield change (%) and the cultivated area at municipal level, as well as some economic data related to the examined crops. Following the data are assessed based on the ADAPT2CLIMA impact assessment methodology and the relevant results are presented in the form of maps and tables. Based on the results of the assessment, the competent authorities may decide on the specific areas and crops where adaptation measures should be implemented.

3 Summary

The LIFE ADAPT2CLIMA project developed a decision support system, the ADAPT2CLIMA tool, for demonstrating the impact of climate change on the agricultural sector of Sicily (Italy), Cyprus and Crete (Greece). The implementation of the tool in the three project islands, in close collaboration with project stakeholders, led to the development of sectoral adaptation strategies for the three islands.

ADAPT2CLIMA tool provides interactive features enabling users to explore climate change projections (for a specific area under two emission scenarios); future hydrological and crop yield assessment; impact assessment (for different crop types); and adaptation assessment (how different adaptation options address crop impact). The latter, enables regional authorities and farmers to target action to increase the resilience of the agricultural sector, for which the project proposed a clear set of adaptation measures to ameliorate the intensity of impacts.

The ADAPT2CLIMA tool has a scalable architecture that can be easily replicated at the national level for Greece, Italy and Cyprus. Finally, the fact that the three islands are representative of the wider Mediterranean region with respect to the crops cultivated, climate regime and associated impacts, is expected to enhance replicability and transferability of the tool in the Mediterranean region.

Acknowledgements

The ADAPT2CLIMA decision support tool was developed with co-funding from the EU in the context of the project LIFE ADAPT2CLIMA (LIFE14 CCA/GR/000928).

References

Collins, W. J., Bellouin, N., Doutriaux-Boucher, M., Gedney, N., Halloran, P., Hinton, T., Woodward, S., 2011. Development and evaluation of an Earth-System model – HadGEM2. Geosci. Model Dev., 4(4), 1051–1075, doi:10.5194/gmd-4-1051-2011.

IPCC, 2014. Summary for policymakers. In: Climate Change 2014: Impacts, Adaptation, and Vulnerability. Part A: Global and Sectoral Aspects. Contribution of Working Group II to the Fifth Assessment Report of the Intergovernmental Panel on Climate Change [Field, C.B., V.R. Barros, D.J. Dokken, K.J. Mach, M.D. Mastrandrea, T.E. Bilir, M. Chatterjee, K.L. Ebi, Y.O. Estrada, R.C. Genova, B. Girma, E.S. Kissel, A.N. Levy, S. MacCracken, P.R. Mastrandrea, and L.L.White (eds.)]. Cambridge University Press, Cambridge, United Kingdom and New York, NY, USA, 1-32.

Leolini, S. Bregaglio, Moriondo, M., Ramos, M.C, Bindi, Ginaldi, F., 2018. A model library to simulate grapevine growth and development: software implementation, sensitivity analysis and field level application. European Journal of Agronomy, 99, 92-105. https://doi.org/10.1016/j.eja.2018.06.006.

Moriondo, M., Leolini, L., Brilli, L., Dibari, C., Tognetti, R., Giovannelli, A., Rapi, B., Battista, P., Caruso, G., Gucci, R., Argenti, G., Raschi, A., Centritto, M., Cantini, C., Bindi, M., 2019. A simple model simulating development and growth of an olive grove. European Journal of Agronomy,105,129-145. https://doi.org/10.1016/j.eja.2019.02.002.

Papadopoulou, M.P., Charchousi, D., Spanoudaki, K., Karali, A., Varotsos, K.V., Giannakopoulos, C., Markou, M., Loizidou, M., 2020. Agricultural Water Vulnerability under Climate Change in Cyprus. Atmosphere, 11, 648. https://doi.org/10.3390/atmos11060648.

Popke, D., Stevens, B., Voice, A., 2013. Climate and climate change in a radiative-convective equilibrium version of ECHAM6, J. Adv. Model. Earth Syst. 5(1), 1-14, doi:10.1029/2012MS000191.

Stöckle, C.O., Donatelli, M., Nelson, R., 2003. CropSyst, a cropping systems simulation model. European Journal of Agronomy 18, 289–307.

Strandberg, G., Bärring, A., Hansson, U. et al., 2014. CORDEX scenarios for Europe from the Rossby Centre regional climate model RCA4. Reports Meteorology and Climatology, ISSN: 0347-2116.

Waterloo Hydrogeologic, 2017. Visual MODFLOW Flex 4.1 Integrated Conceptual & Numerical Groundwater Modeling; Waterloo Hydrogeologic: Waterloo, ON, Canada, p. 86.

Climate change mitigation through enhanced weathering: agricultural field trials in Greece

Evangelou, E.[1], I. Smet[2], C. Tsadilas[1], and M. Tziouvalekas[1]

[1]Hellenic Agricultural Organization "DEMETER", Institute of Industrial and Forage Crops, 1 Theophrastos str. 41335, Larisa Greece
[2]Fieldcode Greece M.I.K.E., Vasilissis Sofias Avenue 97, 11521, Athens, Greece

Abstract.

Humanity faces many challenges among which food security and climate change are the major ones. Whereas worldwide a million hectares of farming land are lost every year, there are no more areas left to expand our agricultural activities. So, in order to achieve food security, agricultural production must become more efficient. Such intensification of agricultural production should be obtained through sustainable methods which protect the environment as well as reduce greenhouse gas (GHG) emissions.
In order to avoid the worst scenarios of climate change, besides drastically cutting our GHG emissions we also need to remove previously emitted carbon dioxide (CO_2). One proposed carbon dioxide removal (CDR) method is based on the natural process of rock weathering where, in the presence of water, silicate minerals react with CO_2 to produce nutrients and water-soluble (bi) carbonates. These carbonates can either react with Ca^{2+} to form insoluble $CaCO_3$ precipitated within the soil profile or reach the groundwater and end up in rivers and oceans. However, this process is too slow to satisfy the need for urgent climate change mitigation. Recently, enhanced weathering (EW) through the application of specific silicate rock powders on irrigated agricultural lands has gained great attention as a CDR option with potential benefits to crops.
In the present study, we investigate the potential of CO_2 capture through EW of silicate rock dust on a cotton field in Thessaly, central Greece. An experiment was conducted with cotton including seven treatments with olivine-rich rock dusts mixed with the soil, one of them in combination with biochar, in a randomized complete block design with four replications of each treatment, besides a control treatment without rock dust.CO_2 removal was based on the assessment of soil solution composition (pH, CO_3^{2-}, HCO_3^-, Ca^{2+}, Mg^{2+}, alkalinity, pH) sampled after each irrigation. Furthermore, nineteen soil properties, including heavy metals, were measured in soil samples taken before rock dusts application, during flowering, and after the harvesting stage time. Possible effects of rock dust application on nutrient uptake by the crop, cotton yield, and fiber quality were also determined. This paper presents the results of the first year of the field experiment.

1 Introduction

In order to avoid the worst scenarios of climate change, it has become clear that besides drastically cutting greenhouse gas (GHG) emissions we also need to remove previously emitted GHG. A greenhouse gas removal technology (GGRT) or negative emission technology (NET) is one capable of removing GHG from the atmosphere (Fuss et al., 2018). Carbon dioxide (CO_2) is the most abundant GHG and its atmospheric levels increased almost 50% since the start of the industrial revolution. Many research groups therefore focus on finding carbon dioxide removal (CDR) technologies. One such method that received increasingly more interest in the past decade is enhanced weathering (EW), defined as the process by which CO_2 is sequestered from the atmosphere through the dissolution of silicate minerals on the land surface (Renforth et al., 2011).
Over geological timespans, natural weathering of silicate rocks played a significant role in the regulation of Earth's climate through removal of atmospheric CO_2 (Berner and Kothavala, 2001). This process is the chemical dissolution of minerals which react with water and CO_2, thereby liberating base cations (generating alkalinity) and converting CO_2 into dissolved inorganic carbon (principally hydrogen carbonate ions HCO_3^-) that is removed via soil drainage waters. These weathering products are transported via land surface runoff to the oceans where they may eventually form carbonate rocks with a carbon storage lifetime exceeding 100,000 years. However, due to the average slow rate of natural rock weathering, its effect on a human time scale is too slow to compensate for the manmade artificial changes in atmospheric CO_2 composition (Taylor et al., 2017). To accelerate the natural weathering process, EW focuses on (1) using minerals which show the highest reactivity with CO_2 (Ca-Mg silicates such as olivine), (2) grinding rocks containing these minerals to increase the reactive surface (promoting mineral dissolution and thus CO_2 capture rate), and (3) placing CO_2-reactive rock dust in optimal conditions for mineral dissolution (plenty of CO_2, water and high temperatures).
The worldwide magnitude of carbon capture potential through EW varies depending on the application area considered, the type of rock used and the application rate (Beerling et al., 2018).

Many EW studies use ultramafic rocks such as peridotite or dunite because they contain a lot of olivine, a mineral that has a high CO_2 drawdown relative to its mass (Renforth et al., 2015). This Ca-Mg silicate mineral, however, also contains nickel and chromium that can be released during its dissolution. To avoid these heavy metals entering the environment in too high concentrations, careful monitoring of soil type and application rate is needed (Amann et al., 2020). A good alternative EW rock is basalt: another abundant and fast-weathering rock with lower amounts of olivine – and hence lower heavy metal contents. Added benefit of basalt is that upon dissolution it releases more plant nutrients and hence represents potential co-benefits for soil health and crop production when combined with farming (Hartmann et al., 2013).
Indeed, terrestrial EW research focuses on agricultural land because spreading olivine rich rock dust on croplands means introducing it to a favorable environment: soil microorganisms and plant roots generate weak organic acids and higher levels of CO_2 which enhance the chemical reactions of rock weathering (Amann & Hartmann, 2019). There is also a practical reason to combine EW with agriculture as it could easily fit into everyday farmer's life. For example, farmers routinely apply granular fertilizers and lime, which suggests that annual applications of rock dusts could be feasible at large scales with existing farming equipment. Existing irrigation practices in croplands furthermore provide the water needed to accelerate rock dissolution. Incentives for farmers to become part of much needed EW carbon capture are that added minerals can improve both crop yields and soil quality, and the possibility of negative emissions credits. Global cropland (arable, forage, fiber, fruit and so on) covers approximately 12 X 10^8 ha (12 million km^2), and an additional 1–10 X 10^8 ha of marginal agricultural land may be available where treatment with those materials could rejuvenate degraded soils (Beerling et al. 2018).
Like other potential large-scale CDR strategies, EW is relatively immature and requires further research, development and demonstration across a range of crops, soil types and climates, as well as across spatial scales. This paper presents preliminary results of the first EW experiment in Greece. Different olivine containing silicate rock dusts are applied to a cotton field in Thessaly, central Greece, in order to assess any effect on the yield or quality of the cotton and the potential of CO_2 capture in the cotton field soil.

2 Materials and methods

A field experiment with cotton was conducted in the area of Niki village, 25 km SE of Larissa and about 30km NE of Volos central Greece. The field is located in the former lake Karla, and its soil classifies as Entisol developed on alluvial deposits. This soil´s texture consists of 48% clay, 28% silt and 24% sand it is characterized by 23.8% $CaCO_3$, pH 8.4, a slope < 3% and no significant soil properties variability within the field. Eight experimental treatments were randomly assigned in plots, within each of four blocks to follow a randomized complete block design with plot dimensions of 4 X 8 m.
The 8 treatments are (1) control where no material is applied, (2) basalt from Germany, (3) olivine-rich rock from Norway, (4) olivine-rich rock from Italy, (5) olivine-rich rock from Spain, (6) Greek olivine-rich rock from Grecian Magnesite, (7) Greek olivine-rich rock from Vitruvit and (8) a combination of Vitruvit Greek olivine rich rock and biochar. All rock dusts had a grain size <250μm and were manually added at an application rate of 4kg/m² (40ton/ha) 10 days before sowing. The biochar was activated by soaking in a mixture of water and 12-15-15 liquid fertilizer prior to addition to the soil. At the same time, the farmer uniformly applied pre-plant fertilizer (15–15–15 type) at 300 kg/ha to provide adequate N supply during early season at P and K sufficiency. All experimental materials were incorporated in the upper 25 cm of soil by farmer machinery. Sowing of cotton (*Gossypium hirsutum L*., 332 Delta Pine variety) at a density of 22 seeds/m and 0.95 m inter-row spacing (23 kg seeds ha^{-1}) took place on 23 April 2021.
Soil samples were collected from the four control plots prior to rock dust application to allow characterization of the initial soil conditions. Soil samples were subsequently collected from all 32 plots from a depth of 0-30 cm both at the end of July during flowering and just before cotton harvesting late September. Soil samples were air dried, crushed, sieved with a 2 mm sieve and analyzed for the following properties. pH and electrical conductivity in a suspension 1:1 water: soil, cation exchange capacity by sodium acetate method, exchangeable K and Mg with the ammonium acetate method, organic matter after wet oxidation procedure with the potassium dichromate method, available P with the sodium bicarbonate method, total N with the Kjeldahl method, and available B with the hot calcium chloride extraction method.
During the flowering period in late July plant sampling took place to examine potential differences in nutrition of cotton across the 8 treatments. Nutrient concentrations of N, P, K, Ca, Mg, Fe, Mn, B, Cu and Zn in the cotton plants were estimated according to Page et al 1982.
Within each plot, five macrorhizons were installed in the soil in order to collect soil water at a depth of 30 cm, mostly after irrigation. In-season drip irrigation was performed every 5-6 days from mid-June to the end of August. In season nitrogen fertilization was applied with irrigation water (fertigation) until flowering at the end of July. A total of twelve soil water sampling sessions were conducted throughout the growing period. All soil

water analysis was performed according to APHA, 1992. CO_3^{2-} and HCO_3, by titration with H_2SO_4 0.1 N using phenolphthalein and helianthine as color indicator, respectively. Total alkalinity (TA) expressed as mg/l $CaCO_3$, pH and electrical conductivity (EC) determined with a pH and conductivity meter respectively, K measured by Corning 410 flame photometer, Ca & Mg analysed by a Varian AA400 Plus atomic absorption spectrometer and heavy metals Cr and Ni by atomic absorption supplied with furnace graphite.
A manual cotton harvest took place on 4 October within each plot from the central 2 cotton rows along the inner 3m. After cotton yield estimations based on the weight of the collected cotton, subsamples of cotton were sent to the the Cotton Classification Centre in Karditsa for fiber quality analysis.
Statistical analysis performed with SPSS includes one way analysis of variance (ANOVA) with LSD test to evaluate any differences in soil properties, soil water and cotton yield and quality parameters which might reflect the effect of the different dust rocks applications. Person correlation was also used to detect any potential correlations.

3. Results and discussion

No statistically significant differences were found between the treatments for either the cotton yield or any of the studied cotton quality parameters. A non-significant cotton yield variability was observed however, between treatments with the biochar plots to have the higher cotton yield values reflecting probably the particular Biochar properties in regard to absorption and slow release of nutrients. Overall, the application of the 6 different olivine rich rock dusts does not seem to negatively affect cotton yield or fiber quality (Table 1).

Table 1. *Average values of cotton yield and fiber quality parameters of the 2021 EW experiment*

Cotton parameters	Control	DE basalt	NO olivine	ES olivine	IT olivine	GR olivine GM	GR olivine VV	GR VV + Biochar
Cotton Yield, kg/ha	4009,1 a*	3779,5 a	3355,4 a	3526,2 a	3503,3 a	4412,0 a	4019,5 a	4662,5 a
Lint weight,%	0,46 a	0,46 a	0,47 a	0,47 a	0,47 a	0,47 a	0,48 a	0,48 a
SCI	153,82 a	137,59 a	140,63 a	143,94 a	139,75 a	153,37 a	144,02 a	153,75 a
Moisture,%	7,06 a	6,95 a	7,06 a	7,45 a	7,13 a	6,97 a	7,13 a	7,42 a
Micronaire	4,78 a	4,90 a	4,72 a	4,72 a	4,71 a	4,55 a	4,74 a	4,62 a
Maturity	0,85 a	0,85 a	0,85 a	0,85 a	0,85 a	0,85 a	0,85 a	0,85 a
UHML, mm	30,14 a	29,22 a	29,13 a	28,90 a	29,17 a	29,47 a	29,58 a	30,22 a
Length uniformity	84,18 a	82,88 a	83,20 a	83,92 a	82,85 a	84,65 a	83,24 a	84,29 a
SFI	8,05 a	8,16 a	8,28 a	7,97 a	8,41 a	7,80 a	8,20 a	7,80 a
Strength	35,59 a	33,14 a	33,20 a	34,07 a	33,74 a	34,80 a	34,27 a	34,96 a
Elongation	8,75 a	9,13 a	9,04 a	9,10 a	8,99 a	8,86 a	8,69 a	8,73 a
Reflectance%	76,19 a	76,00 a	75,91 a	72,66 a	74,48 a	74,59 a	75,12 a	75,68 a
Yellowness +b	8,16 a	8,18 a	8,07 a	7,80 a	8,02 a	7,58 a	7,81 a	7,91 a

* *For each parameter same letter for different treatments shows no significant difference for $p<0.05$ according to the LSD post hoc test.*

Data on nutrient concentrations in the cotton plants reveal similar results. Apart from P, no nutrients seem affected by the rock dust applications as they don´t show a significant difference compared to the control (table 2). Cotton plants in the plots with biochar, however, show high values for most nutrients and even significantly higher P contents. Nutrient uptake is generally reported to improve with the application of biochar to soil as it can serve as a nutrient reservoir for plants besides improving soil properties. In this study, however, it is unclear whether the seemingly higher bioavailability of macronutrients in the biochar treatment is due to the activation of the biochar with a “dense” fertilizer, or due to the interaction of the biochar with the soil chemistry. The second highest P content is found in the treatment with basalt, perhaps reflecting its distinct mineralogical composition that includes phosphorus rich minerals which are not present in the olivine rich rock dusts.
Most soil properties show distinct seasonal variations but no significant variability between different treatments at any given time, suggesting that EW did not have any measurable effects during the first 5,5 months of this cotton field experiment. Instead, it seems that the ´background´ physical, chemical and biological processes affect most of soil properties in the same way throughout the cotton season. For example, a significant variation of soil pH values is recorded in all eight treatments, including the control. A steady increase in cation exchange capacity for all treatments from early April through to late September coincides with a similar trend observed for the basic cations contributing to the CEC. The steady increase in exchangeable Ca that is statistically significant for all eight treatments, however, is not mirrored by a continuous increase of exchangeable Mg that is statistically confirmed for the control, IT and ES olivine treatments.

***Table 2**. Average values of the nutrient concentrations of cotton plants in the different treatments*

Plant nutrients	Control	DE basalt	NO olivine	ES olivine	IT olivine	GR olivine GM	GR olivine	GR VV + Biochar
K (%)	1,03 a	1,08 a	0,85 a	0,86 a	0,96 a	1,05 a	0,86 a	1,12 a
Ca (%)	2,80 a	2,86 a	2,74 a	2,64 a	2,72 a	2,84 a	2,89 a	3,03 a
Mg (%)	0,78 a	0,75 a	0,77 a	0,72 a	0,74 a	0,80 a	0,81 a	0,83 a
N (%)	3,00 a	3,28 a	2,97 a	2,98 a	3,04 a	3,34 a	3,02 a	3,26 a
P (%)	0,177 bc	0,206 ab	0,1864	0,162 c	0,175 bc	0,194 abc	0,187	0,217 a
Fe (mg/kg)	375,75 a	257,75 a	250,00 a	279,00 a	353,50 a	379,75 a	291,75 a	231,25 a
Zn (mg/kg)	76,50 a	107,25 a	33,00 a	76,00 a	66,00 a	32,75 a	35,00 a	62,75 a
Cu (mg/kg)	7,05 a	5,56 a	4,92 a	2,40 a	7,32 a	6,05 a	5,52 a	6,70 a
Mn (mg/kg)	131,25 a	128,25 a	112,75 a	121,25 a	112,00 a	121,25 a	126,50 a	118,75 a
B (mg/kg)	77,25 a	77,25 a	83,50 a	76,75 a	72,50 a	75,75 a	78,75 a	65,75 a

For each parameter same letter for different treatments shows no significant difference for p<0.05 according to the LSD post hoc test.

Nickel and chromium are those heavy metals that dissolution of olivine is expected to release into the soil. Figure 1 shows that control has lower Ni concentrations in second and third soil sampling compared with the initial conditions of the 1st sampling where no materials have been applied. These differences are not statistically significant for any treatments at the 2nd sampling where all treatments show the same seasonal trend of elevated Ni contents. But at the 3rd sampling, when Ni contents had again overall decreased, the higher amounts observed for all olivine rich rock dusts are statistically significant for the Italian olivine and the Greek Vitruvit & Biochar treatments.

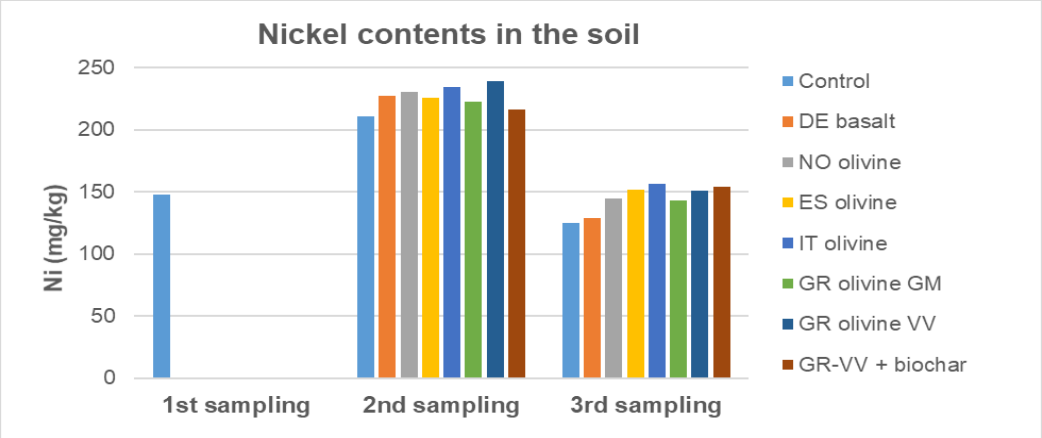

***Figure 1**. Evolution of soil Ni concentrations in the growing period of the cotton (1st sampling: initial conditions before materials applied, 2nd sampling: Flowering period, 3d sampling: harvest period).*

Soil chromium does not follow the exact same trends as Ni since the Cr contents do not have a clear seasonal variation but show a large variability in the second sampling where the control has one of the highest concentrations (Figure 2). At harvest time, however, control and basalt treatments do have overall lower Cr soil contents compared to the treatments with olivine-rich rocks. Overall, it seems that some differences in (pseudo) total Ni and Cr soil contents developed about 5.5 months after rock dust application could reflect the dissolution of olivine.

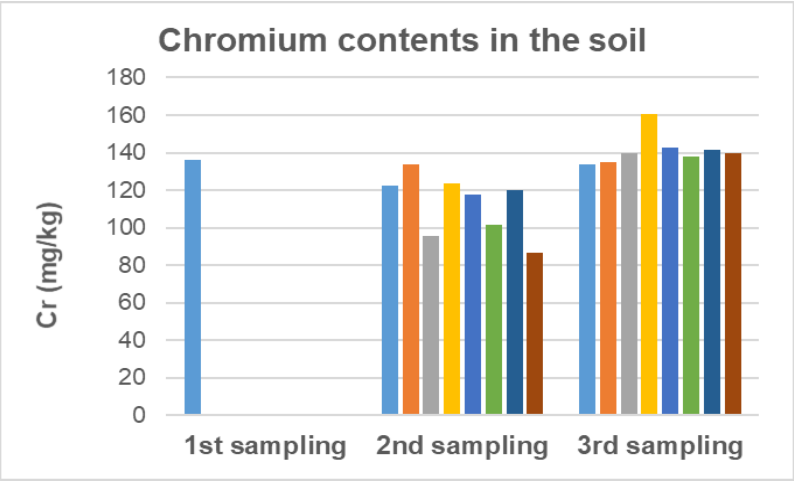

***Figure 2**. Evolution of soil Ni concentrations in the growing period of the cotton (1st sampling: initial conditions before materials applied, 2nd sampling: Flowering period, 3d sampling: harvest period).*

A strong positive correlation (R^2 = 0.92) between soil contents of (pseudo) total Ni and Cr observed at harvest time also suggests that the concentrations of these heavy metals are coupled to one another, as for example within the crystal structure of a specific mineral. Only the treatment with Spanish olivine does not fit on this strong correlation between Ni and Cr contents in the soil 5,5 months into the experiment (Figure 3). Compared to the other olivine rich rocks, the Spanish olivine material has a different mineralogical composition with almost twice as much serpentine as olivine that might result in a different Ni/Cr ratio upon dissolution. More research is needed to better understand and evaluate potential soil contamination with Ni and Cr by repeated applications of olivine rich rock dusts in a range of different soil conditions.

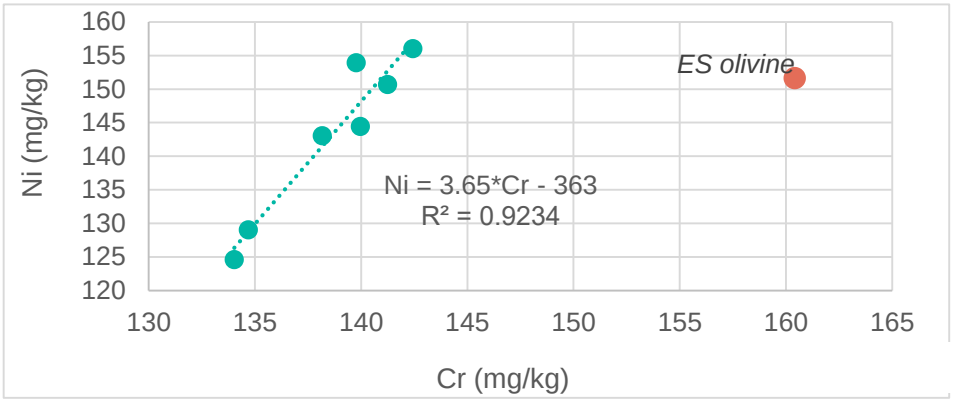

***Figure 3**. Relationship between (pseuodo) tota soill Cr and Ni contents at harvest time.*

The soil water properties generally show little to no statistically significant variability between the eight treatments within a single sampling session. Exception to this is only the *Greek Vitruvit olivine with biochar* that revealed distinctly higher Ca^{2+}, Mg^{2+} and K^{+} concentrations on the 5th water sampling (mid-June). A few weeks later, however, this trend was reversed, and the biochar treatment had the lowest cation contents, reflected in a significantly different EC. Biochar addition seems to affect also heavy metal concentrations in the soil water: the biochar treatment has the overall highest Ni contents for 6 out of 12 samplings (Figure 4) and the by far highest soil water Cr level at the end of the growing season (data not shown).

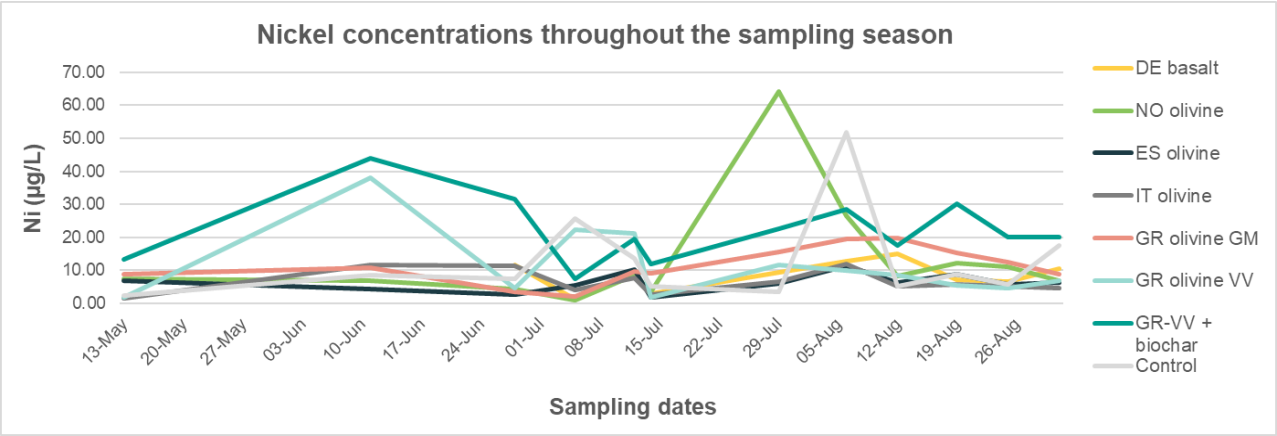

***Figure 4**. Soil water Ni concentrations throughout the 12 samplings*

Total alkalinity (TA) does not show any statistically significant difference between the treatments at a given time, but it does show roughly the same seasonal trend for all eight treatments (Figure 5). The higher TA values observed at the start of the experiment start to decrease mid-June and reach an overall low by early July. The fluctuation across treatments, showing peaks again towards the end of July and in late August. The same seasonal variability of soil water properties is also observed for pH, CO_3^{2-}, HCO^{3-}, EC, Ca^{2+}, Mg^{2+} and K^+ across all eight treatments. The control treatment thereby fluctuates between the olivine rich rock dust treatments, suggesting that the soil water does not reflect any enhanced weathering or olivine dissolution. Instead, these patterns seem to reflect changes in soil water chemistry due to agricultural management like irrigation and fertilization, besides a naturally fluctuating background of physical, chemical and biological processes.

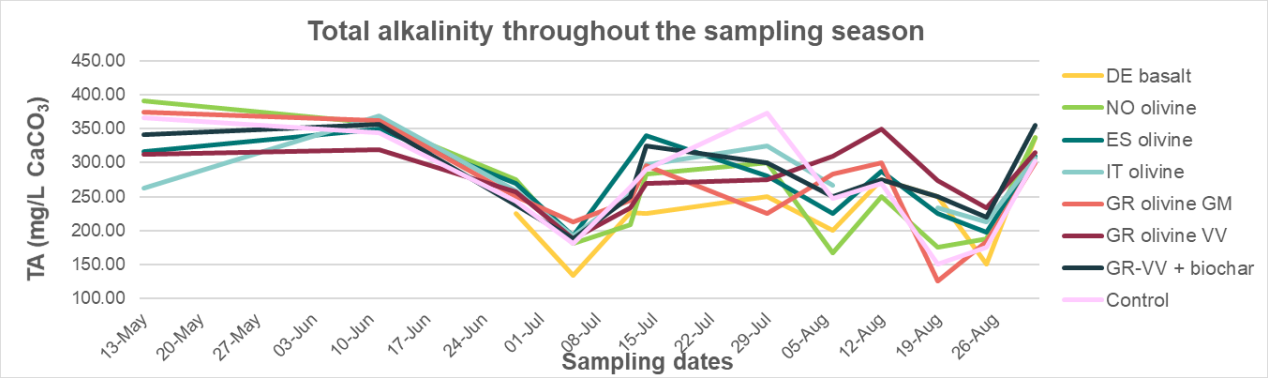

***Figure 5**. Seasonal variation of total alkalinity of soil water samples*

4. Conclusions

The first EW field experiment carried out in Greece involves the addition of 6 different olivine rich rock dusts and a biochar to a cotton field at an application rate of 40ton/ha. Preliminary results from the first 6 months of the experiment indicate there are no negative effects on cotton yield, fiber quality or nutrient uptake by the plants suggesting that cotton cultivation could be a potential crop suitable for EW in Greece. Although an increase in soil Ni and Cr contents about 6 months after rock dust application points to dissolution of the added materials, no clear signal of carbon sequestration through EW could be detected in the soil water.
The current EW field experiment will be continued, as it is known that application of this CDR technique on a field scale needs more time to reveal measurable results. Special attention will thereby be paid to the monitoring of heavy metals Ni and Cr that are released in the soil environment upon olivine dissolution, and to assessing the potential of CDR through EW in combination with cotton cultivation in Greece. More of this type of EW field experiments are needed across a variety of soil types with different pH as the EW reactions are affected directly by initial soil properties.

5. References

Amann, T, and Hartmann, J. 2019. Ideas and perspectives: Synergies from co-deployment of negative emission technologies. Biogeosciences, 16, 2949–2960.

Amann Markus Kiesewetter Gregor, Schöpp Wolfgang, Klimont Zbigniew, Cofala Janusz, Rafaj Peter, Höglund-Isaksson Lena, Gomez-abriana Adriana, Heyes Chris, Purohit Pallav, Borken-Kleefeld Jens, Wagner Fabian, Sander Robert, Fagerli Hilde, Nyiri Agnes, Cozzi Laura Pavarini Claudia 2020. Reducing global air pollution: the scope for further policy interventions. Phil. Trans. R. Soc. A.3782019033120190331

Beerling, D. J., Leake, J. R., Long, S. P., Scholes, J. D., Ton, J., Nelson, P. N., … Hansen, J. 2018. Farming with crops and rocks to address global climate, food and soil security. Nature Plants, 4, 138– 147.

Berner, R.A., and Kothavala, Z., 2001, GEOCARB III: A revised model of atmospheric CO2 over Phanerozoic time: American Journal of Science, v. 301, p. 182–204.

Fuss S et al. 2018 Negative emissions - Part 2: costs, potentials and side effects Environ. Res. Lett. 13 063002

Hartmann, J., West, A. J., Renforth, P., Köhler, P., De La Rocha, C. L., Wolf-Gladrow, D. A., Dürr, H. H., Scheffran, J. 2013. Enhanced chemical weathering as a geoengineering strategy to reduce atmospheric carbon dioxide, supply nutrients, and mitigate ocean acidification. Reviews of Geophysics, 51, 2, 113-149.

Renforth P., C.L. Washbourne, J. Taylder, D.A.C. Manning 2011.Silicate production and availability for mineral carbonation. Environmental Science and Technology, 45, pp. 2035-2041.

Renforth, P., A.E. Pogge von Strandmann, G.M. Henderson, 2015. The dissolution of olivine added to P.soil: Implications for enhanced weathering.Applied Geochemistry, Volume 61: 109-118.

Taylor L.L., D.J. Beerling, S. Quegan, S.A. Banwart 2017. Simulating carbon capture by enhanced weathering with croplands: an overview of key processes highlighting areas of future model development Biol. Lett., 13.

Page, A.L. et al. (Ed.) (1982). Methods of soil analysis. Part 2: Chemical and microbiological properties, 2nd ed. American Society of Agronomy, Madison, Wisconsin, USA.

Climate change projections of wheat development and yield with Ceres-Wheat over north Greece from EURO-CORDEX simulations with two calibration strategies

Nikou M. [1,2], Mavromatis T. [1]

[1]Department of Meteorology and Climatology, School of Geology, Aristotle University of Thessaloniki
[2]Soil and Water Resources Institute, Hellenic Agricultural Organization (H.A.O.) - "DEMETER", 570 01 Thessaloniki, Greece

Abstract. Although, yield trials (i.e., experiments with which a set of cultivars is usually assessed to make genotype recommendations) are usually labor intensive, time consuming, and expensive, they do not record crop- and site-specific information required for crop model calibration and validation. In this study, yield gap-based calibration on potential mode and a "traditional" for rainfed experiments strategy will be used to estimate the genetic coefficients of two winter wheat cultivars in north Greece with the crop simulation model Ceres-Wheat. Afterwards, climate change projections of simulated wheat development and yield, based on an ensemble of 11 high-resolution EURO-CORDEX regional climate model (RCM) simulations covering the historical period 1981 – 2005, the near-future (2021–2050) and the end-of-the-century (2071-2100) periods under the influence of the moderate Representative Concentration Pathway RCP4.5, will be attempted. The preliminary results show the superiority of the Yield gap-based calibration. Climate change projections of wheat development and yield, based on an ensemble of 11 high-resolution EURO-CORDEX regional climate model simulations imply that anthesis is anticipated to occur earlier and potential grain yield will show a decrease over time.

1 Introduction

Agricultural decision-making increasingly incorporates crop simulation models. Calibration is a challenging and essential step in the development and application of a model. (Lobell and Ortiz-Monasterio 2006). The unavailability of reliable historical data for model calibrations is a constant challenge for crop model simulation, particularly for future crop performance projections and impact studies under varying conditions. In some cases, the quantity and quality of available input data, like climate, soil physical and chemical properties, agronomic and management practices, and cultivar characteristics, may not be sufficient for crop model calibration. As a result, crop simulation model's effectiveness for projections can be hindered by data limitations (Kephe et al. 2021). This challenge is exacerbated in regions with a Mediterranean climate (such as Greece) that are characterized by unfavorable growth conditions (especially for rainfed crops such as wheat) resulting from water stress, low soil fertility, and/or poor agronomic practices. On this context, there is an urgent need for an approach that will allow the determination of genotype's characteristics (particularly these related to grain and growth characteristics rather to development) required by crop models and will minimize the required data from field experiments.

In this study, we attempted to calibrate the Ceres-Wheat crop model (which simulates wheat growth, development and yield considering the interactions between weather, genetics, soil and crop management) (Hoogenboom et al. 2010) and estimate the required genetic coefficients for two winter durum wheat cultivars in north Greece by (a) developing a methodology based on the concept of yield gap and (b) exercising a traditional calibration strategy (trial and-error approach). The yield gap is a crucial biophysical indication of the available room for crop production increase with current land and water resources. It is defined as the difference between actual farm yield and the yield potential (Rattalino Edreira et al. 2021). Firstly, the two calibration strategies were evaluated with crop data that covered the years 2004 to 2010 for two durum wheat cultivars collected from the Aristotle University Farm in Thessaloniki, Greece. Then, climate change projections of wheat development and yield with the Ceres-Wheat based on an ensemble of 11 high-resolution EURO-CORDEX regional climate model (RCM) simulations (Georgoulias et al. 2022), under the influence of the moderate Representative Concentration Pathway RCP4.5 which assumes moderate mitigation, covering the historical period 1981 - 2005 and the future periods 2021 – 2050 (near future) and 2071-2100 (the-end-of-the-century), were also attempted.

2 Data and methods

2.1 Data

Yield trials for two durum wheat cultivars (Mexicali and Sifnos) were conducted at the farm of the Cereal Institute (40º 31` N; 23º 00` E; 15m altitude) in Thermi, during 2004- 2010. The experiments (9 for the former cultivar and 10 for the latter, **Figure 1**) were laid out in randomized complete block design (RCBD) with four replications. The plot in the fields had seven rows at 25 cm apart from each other. Recommended seed rate of 180 kg ha^{-1} was used.

Soil surface parameters namely soil pH, organic carbon, nitrogen, cation exchange capacity and bulk density were estimated in Soil Science Institute of Thessaloniki. Albedo and drainage rate were determined by Jones and Kiniry (1986) and Suleiman and Ritchie (2001), respectively. Soil physical properties, such as the lower limit of soil water content, the water content at the drained-upper limit, the saturation water content, and the saturated hydraulic conductivity, were estimated at the Land Improvement Institute of Thessaloniki. Main management inputs included plant population, planting depth, and planting date. Emergence date, end ear growth date, and final grain yield were all observed. In 2009-10, anthesis and physiology maturity date, thousand grain weight, and individual grain weight were also collected (Symeonidis, 2011). Phosphorous and nitrogen applied to all treatment. Diseases, weeds and pest infestations were controlled. The crop model's minimum weather requirements, daily solar radiation, maximum and minimum air temperature, and precipitation were collected from the site's meteorological station.

2.2 Calibration strategies

Traditional calibration

Before a crop model's application, one has to estimate first the characteristics of the specific cultivar if they have not been previously determined. Although, yield trials (i.e., experiments with which a set of cultivars is usually assessed to make genotype recommendations) are usually labor intensive, time consuming, and expensive, they do not record crop- and site-specific information required for crop model calibration. The initial soil water conditions, a requirement by the crop model if it is to run on rainfed mode, of the experiments considered were not known. To overcome this limitation, the soil profile, for all experiments, was assumed to be full at the first wet day before planting (this constitutes the traditional calibration strategy in this study). This is a common assumption when initial soil water information is missing.

Calibration based on yield gap analysis

Although, cultivar characteristics should ideally be defined on potential production level (i.e., the crop growth rate) and thus yield is determined only by solar radiation, temperature and atmospheric CO_2 and is not limited by water supply and nutrients (Van Ittersum et al. 2013), they traditionally estimated, even for rainfed crops, based on crop observations/measurements made under water- and/or nitrogen stress conditions (i.e., water- and/or nutrient-limited production level). As a result, during the process of calibration, the limiting effects of water and nutrient stresses (deficits or excesses) on crop development and particularly on growth reflect (the degree depends the severity and duration of the water and nutrient stresses) on the estimation of the genetic coefficients are related to development and grain and growth characteristics, respectively. As opposed to the "traditional" procedure, a procedure based on yield gap analysis is proposed: the crop model is run on potential mode and the simulated yield for each year i ($Yp_{(i)}$) was then adjusted by the relative yield gap ($Yrg_{(i)}$) to achieve agreement with the actual, for the specific year i, harvested yield ($Yac_{(i)}$):

$$\mathrm{Yrg(i)} = \frac{Yg_{(i)}}{Ysp_{(i)}} \times 100 \quad (1)$$

the yield gap ($Yg_{(i)}$) is calculated as the difference between potential site yield ($Ysp_{(i)}$) (also called yield potential) and the actual yield ($Yac_{(i)}$). Since $Ysp_{(i)}$ depends on climate, is not only site specific but also year specific. At least four methods can be distinguished to estimate yield gaps at a local level: (1) field experiments, (2) yield contests, (3) maximum farmer yields based on surveys, and (4) crop model simulations (Van Ittersum et al. 2013). In this

study, the site- and year- specific Yrg(i) values from the global yield gap atlas (www.yieldgap.org) were used. The WOFOST crop model (de Wit et al. 2019) was used for their estimation as described a by van Ittersum et al. (2013). The yield gaps between actual yield and potential yield for the specific yield trials ranged from 1.9 t dm/ha to 6,3 t dm/ha for Mexicali, and from 1.7 t dm/ha to 6.6 t dm/ha for Sifnos **(Figure 1)**. The higher Yrg occurred in 2005 early plantings for both cultivars (71% for Mexicali and 74% for Sifnos), and the lower in 2004 late plantings (15% for Mexicali and 14% for Sifnos) which also coincided with the higher and the lower Ya, respectively, for both cultivars.

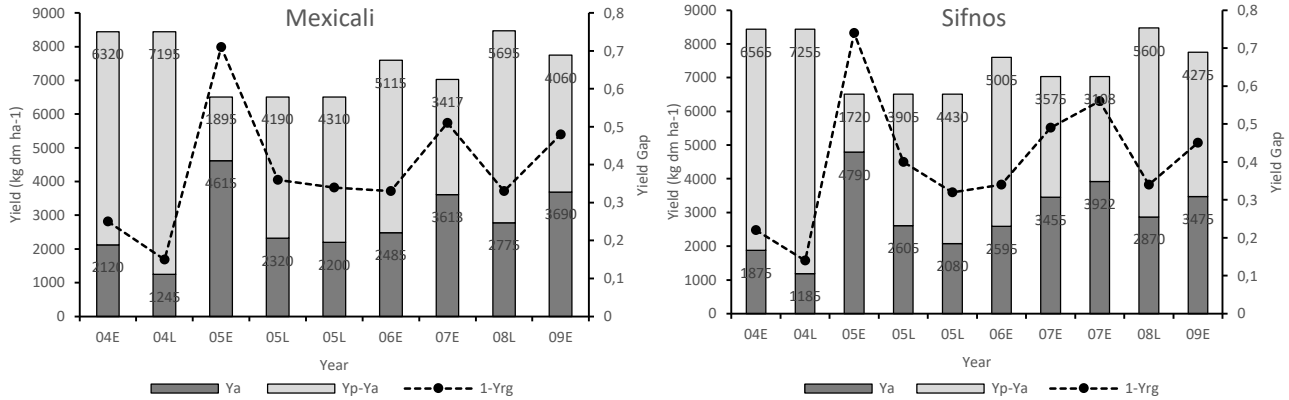

Figure 1 Actual Yield (Ya) (kg dm/ha), Yield Gap (Yp-Ya) (kg dm/ha) and relative Yield Gap (1-Yrg) for Sifnos and Mexicali. On the horizontal axis, E represents early plantings and L late plantings in the reported year.

2.3. Genotype parameter estimation

The genetic coefficients required by the CERES-Wheat for each cultivar were estimated by adjusting coefficients until close match were achieved between simulated and observed crop observations/measurements (trial-and-error method). This method is simple and widely used, but it is ineffective, especially when there are a large number of parameters to consider (Hsiao et al. 2009). Various systematic algorithms have been developed for model parameter estimation (Ceglar et al. 2011).

In this study, genetic parameters were estimated using the generalized likelihood uncertainty estimation (GLUE) method, a frequently employed Bayesian method that is integrated into the DSSAT software (Hoogenboom et al., 2010; He et al., 2010). The parameters of P1V (days for optimum vernalizing temperature required to complete vernalization) and P1D (the percentage reduction in development rate in a photoperiod 10h shorter than the threshold relative to that at the threshold) were adjusted firstly, using the GLUE method, to match the observed anthesis dates. Next, the grain characteristic parameters, G1 (kernel number per unit canopy weight at anthesis (number/g), G2 (the standard kernel size under optimum conditions (mg)) and G3 (the standard non-stressed dry weight (including grain) of a single tiller at maturity (g)), were optimized to match the grain yield.

2.4. Statistical measures

Several statistical measures, including the coefficient of determination (R^2), root mean square error (RMSE), mean bias error (MBE), and mean absolute error (MAE), were used to evaluate the relationship between predicted and observed values, as follows:

$$RMSE = \sqrt{\left(\sum_{i=1}^{n}\left(P_i - O_i\right)^2\right)\Big/ n}$$

$$MBE = \frac{1}{n}\sum_{i=1}^{n}\left(P_i - O_i\right)$$

$$MAE = \frac{1}{n}\sum_{i=1}^{n}\left|P_i - O_i\right|$$

where n is the number of observations, P_i is the model predictions and O_i is the observed value, for year i. Regression analysis was also used to evaluate the two calibration strategies.

3 Results

Anthesis date (days to end ear growth) and yield grain values were calculated according to the two calibration strategies. Although high correlation (r^2>0.62) (Hinkle et al.1994) for anthesis dates was found for both calibration strategies, the yield gap procedure produced higher values for Mexicali (r^2 was 0.699 vs 0.621) and marginally worse values for Sifnos (r^2 was 0.757 vs 0.767, respectively) (**Figure 2**). In contrast to MBE, MAE and RMSE were also in favor of yield gap. The differences in statistical measures between the two strategies could partially be attributed to the different mode the crop model was run (potential mode for yield gap vs. rainfed mode for "traditional" calibration).

The yield gap-based calibration strategy was more effective than the "traditional" strategy as all statistical measures were better. While very strong associations (r^2>0.981) were found with the former strategy for both cultivars, only moderate (Sifnos) and high (Mexicali) association produced from the latter strategy was found between actual and simulated yields (**Figure 2**). MBE, MAE and RMSE were also substantially lower with yield gap calibration.

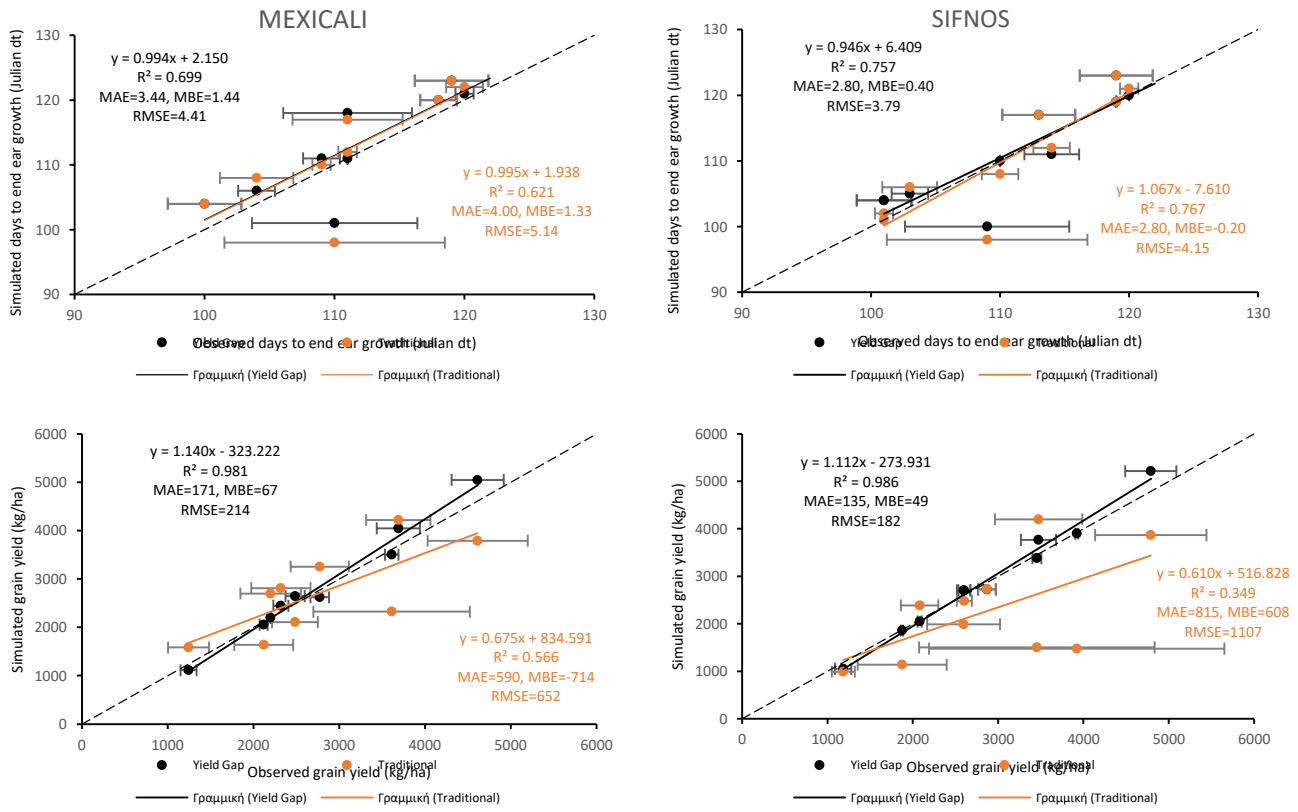

Figure 2. Comparison of the two calibration strategies ("Traditional" vs "Yield gap") for a) end ear growth (top plots) and b) grain yield (lower plots) for Mexicali (left plots) and Sifnos (right plots). Bars indicate standard deviations of observations in relation to the average. The solid lines represent the linear regression fits to crop data, while the dotted line represents the 1:1 line.

Figure 3 depicts the anticipated differences in mean daily solar radiation, maximum and minimum air temperature, and precipitation from the EURO-CORDEX ensemble between the near-future (2021-2050) and the end-of-the-century (2071-2100) with the reference period (1981-2005) (REF) for Thermi under the emission scenario RCP4.5. The average maximum and minimum temperatures in Thermi during growing season are expected to increase by approximately 1.2ºC and 1.1ºC, respectively, for NF period, and even higher (by approximately 2.1ºC and 2.0ºC, respectively), for EOC. Solar radiation and precipitation will slightly increase (by about 1.3% and 1.7%) and decrease (by almost 0.01 mm/day and 0.03 mm/day) for NF and EOC periods, respectively.

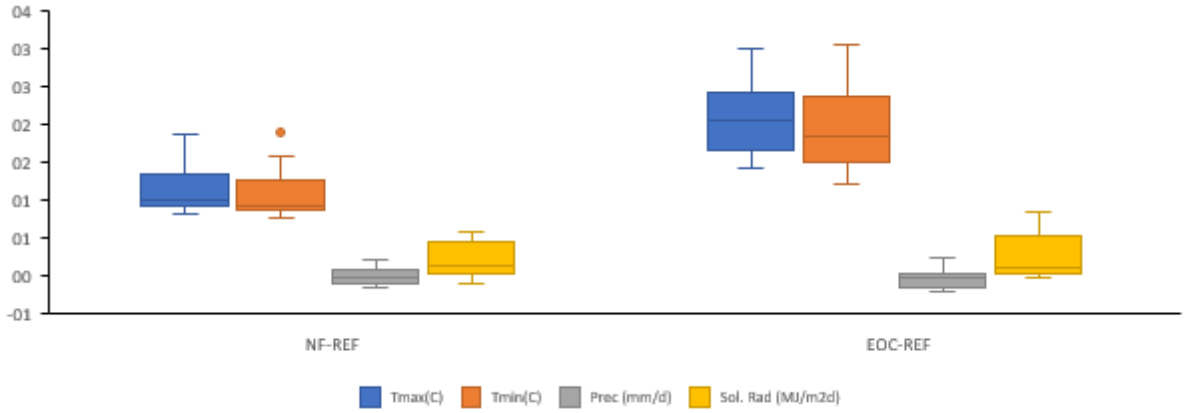

Figure 3 Differences in maximum and minimum air temperature, daily solar radiation, and precipitation during the growing season (Dec 1 – Jun 30) from the EURO-CORDEX ensemble between the near-future (2021-2050) (NF-left part) and the end-of-the-century (2071-2100) (EOC-right part) and the reference period (1981-2005) (REF) for Thermi (northern Greece) for the emission scenario RCP4.5.

When the historical time series from the site's meteorological station (covering the period 1979-2010) were adjusted based on the differences expected in NF and EOC (**Figure 3)** and the yield gap-based estimates genetic coefficients were used, crop simulated anthesis is anticipated to occur earlier (by 9 days for NF period and 14 days for EOC for Sifnos and by 8 days for NF period and 13 days for EOC for Mexicali (**Figure 4**)), which is primarily due to increasing temperatures in Figure 3. On the other hand, the mean and median values of potential grain yield are expected to show a similar decrease for both cultivars, varying from 3 to 4% for NF period, and from 6 to 7% for EOC period.

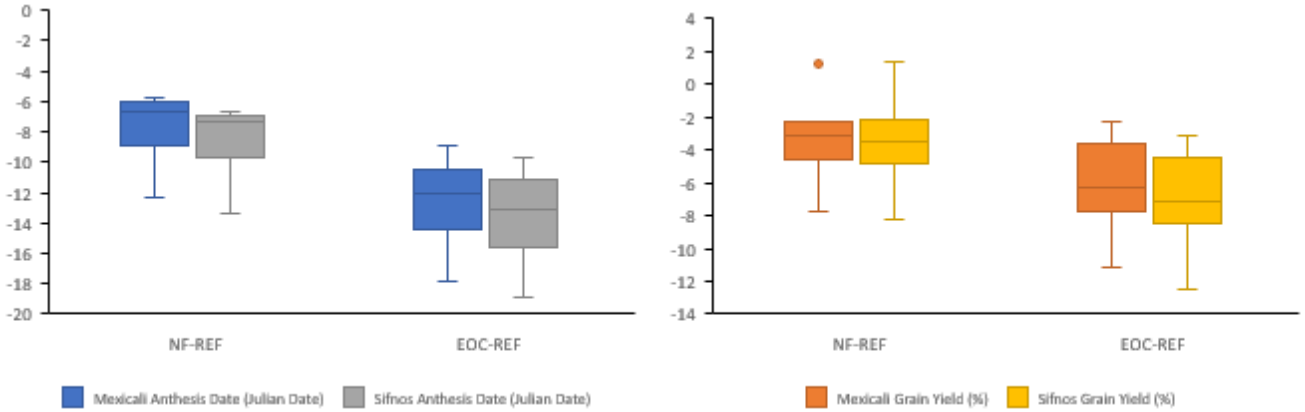

Figure 4 Differences in mean crop simulated anthesis (days) and grain yield (%) between the NF and REF periods, as well as the EOC and REF periods

4 Summary

The preliminary results highlight the superiority of the Yield gap-based calibration in expense of the "traditional" strategy in estimating the genetic coefficients of two winter wheat cultivars in north Greece with the Ceres-Wheat crop model. Climate change projections of crop simulated wheat development and yield, based on an ensemble of 11 high-resolution EURO-CORDEX regional climate model simulations imply that anthesis is anticipated to occur earlier and potential grain yield will show a decrease over time.

References

Ceglar, Andrej, Zalika Črepinšek, Lučka Kajfež-Bogataj, and Tjaša Pogačar. 2011. The Simulation of Phenological Development in Dynamic Crop Model: The Bayesian Comparison of Different Methods. Agricultural and Forest Meteorology 151 (1): 101–15. https://doi.org/10.1016/j.agrformet.2010.09.007

de Wit, A., Boogaard, H., Fumagalli, D., Janssen, S., Knapen, R., van Kraalingen, D., Supit, I., van der Wijngaart, R., van Diepen, K., 2019. 25 years of the WOFOST cropping systems model, Agricultural Systems, 168, 154-167, https://doi.org/10.1016/j.agsy.2018.06.018.

Georgoulias, A.K., Akritidis, D., Kalisoras, A., Kapsomenakis, J., Melas, D., Zerefos, C.S., Prodromos Zanis,P., 2022. Climate change projections for Greece in the 21st century from high-resolution EURO-CORDEX RCM simulations, Atmospheric Research 271, https://doi.org/10.1016/j.atmosres.2022.106049.

Hinkle, D., W. Wiersma, and S. Jurs. 1994. Applied statistics for the behavioral sciences (3rd ed.). Houghton Mifflin Company, Boston.

Hoogenboom, G., Jones, J.W., Porter, C.H., Wilkens, P.W., Boote, K.J., Hunt, L.A., Tsuji, G.Y. (Eds.), 2010. Decision Support System for Agrotechnology Transfer Version 4.5. Volume

Hsiao, Theodore C., Lee Heng, Pasquale Steduto, Basilio Rojas-Lara, Dirk Raes, and Elias Fereres. 2009. Aquacrop-The FAO Crop Model to Simulate Yield Response to Water: III. Parameterization and Testing for Maize. Agronomy Journal 101 (3): 448–59. https://doi.org/10.2134/agronj2008.0218s.

Ittersum, Martin K. Van, Kenneth G. Cassman, Patricio Grassini, Joost Wolf, Pablo Tittonell, and Zvi Hochman. 2013. Yield Gap Analysis with Local to Global Relevance-A Review. Field Crops Research 143: 4–17. https://doi.org/10.1016/j.fcr.2012.09.009.

Jacob, Daniela, Juliane Petersen, Bastian Eggert, Antoinette Alias, Ole Bøssing Christensen, Laurens M. Bouwer, Alain Braun, et al. 2014. EURO-CORDEX: New High-Resolution Climate Change Projections for European Impact Research. Regional Environmental Change 14 (2): 563–78. https://doi.org/10.1007/s10113-013-0499-2.

Jones, Charles Allan. CERES-Maize; a simulation model of maize growth and development. No. 04; SB91. M2, J6. 1986.

Kephe, Priscilla Ntuchu, Kingsley Kwabena Ayisi, and Brilliant Mareme Petja. 2021. Challenges and Opportunities in Crop Simulation Modelling under Seasonal and Projected Climate Change Scenarios for Crop Production in South Africa. Agriculture and Food Security 10 (1): 1–24. https://doi.org/10.1186/s40066-020-00283-5.

Lobell, David B., and J. Ivan Ortiz-Monasterio. 2006. Regional Importance of Crop Yield Constraints: Linking Simulation Models and Geostatistics to Interpret Spatial Patterns. Ecological Modelling 196 (1–2): 173–82. https://doi.org/10.1016/j.ecolmodel.2005.11.030.

Rattalino Edreira, Juan I., José F. Andrade, Kenneth G. Cassman, Martin K. van Ittersum, Marloes P. van Loon, and Patricio Grassini. 2021. Spatial Frameworks for Robust Estimation of Yield Gaps. Nature Food 2 (10): 773–79. https://doi.org/10.1038/s43016-021-00365-y.

Soltani, Afshin, Holger Meinke, and Peter De Voil. 2004. Assessing Linear Interpolation to Generate Daily Radiation and Temperature Data for Use in Crop Simulations. European Journal of Agronomy 21 (2): 133–48. https://doi.org/10.1016/S1161-0301(03)00044-3.

Suleiman, A. A.; Ritchie, J. T. Estimating saturated hydraulic conductivity from soil porosity. Transactions of the ASAE, 2001, 44.2: 235.

Symeonidis K., 2011. Contribution to the study of growth and harvest of grains in Greece with agrometeorological models, (Master thesis), doi: 10.26262/heal.auth.ir.129044.

An easy-to-use climate service tool for the olive and wine sectors -results from the Med-Gold project

Varotsos K. V.[1], Gratsea M. [1], Giannakopoulos C. [1*], Alessandro Dell'Aquila[2]; António Graça[3]; Marta Teixeira[3]; Natacha Fontes[3]; Nube Gonzalez-Reviriego[4]; Raul Marcos-Matamoros[4,5]; Chihchung Chou[4]; Marta Terrado[4]; Federico Caboni[6]; Riccardo Locci[6]; Martina Nanu[6]; Sara Porru[6]; Giulia Argiolas[6]; Marta Bruno Soares[7]; Michael Sanderson[8], Javier López Nevado[9], Silvia López Feria[9]

1 National Observatory of Athens, Institute for Environmental Research and Sustainable Development
2 ENEA, SSPT-MET-CLIM, CR Casaccia, Via Anguillarese 301, 00123, Rome Italy
3 Sogrape Vinhos SA, Rua 5 de outubro, 4527, 4430-852 Avintes, Portugal
4 Earth Sciences Department, Barcelona Supercomputing Center, Plaça d'Eusebi Güell, 1-3, Barcelona
08034, Spain
5 Department of Applied Physics, University of Barcelona, Av. Diagonal 647, Barcelona 08028, Spain
6 Lutech S.p.A Cagliari, Italy
7 Sustainability Research Institute, School of Earth and Environment, University of Leeds, Leeds, United
Kingdom
8 Met Office, Fitzroy Road, Exeter, EX1 3PB, United Kingdom
9 DCOOP Sociedad Cooperativa, Andalusia, Spain

*corresponding author e-mail: cgiannak@noa.gr

Abstract: Olive oil and wine production are characteristic of a well-defined area around the Mediterranean Sea, a hot spot for climate change, with increasing extreme phenomena, such as droughts and heatwaves. The MED-GOLD projects aims to make European agriculture and food systems more resilient, sustainable and efficient towards climate change. This study reports on the climate service tool – the Dashboard - developed in the frame of the MED-GOLD project for the olive and wine sectors. The MED-GOLD Dashboard is a web-based application that allows the users to easily visualize, interact and even download climate data and indices referring to seasonal or longer time scales (historical climate, seasonal forecasts, long-term projections). The aim of the specific tool is to enable a wide range of end-users (e.g. policymakers, farmers, agronomists) to adapt their decision making strategies to the climate conditions and climate change. The tool was designed, developed and improved in accordance with the needs and the continuous feedback of the end-users. The calculation of the indices and the essential climate values (ECVs), which are the main products of the Dashboard, have been developed in collaboration with the end-users who have helped with the identification of the needs for each sector and provided continuous feedback for the evaluation and improvement of the tool.

1 **Introduction**

Climate change is causing extreme weather events, such as droughts and heat waves. In recent years, the crop management has become a real challenge for olive oil and wine producers. In the future, with the ongoing climate change, anticipating these events will be essential for adaptations in the olive oil and wine sectors, crops with great socio-economic importance. For instance, a decrease in the suitability of the olive orchards in southern Europe due to extreme heat and water stress is suggested by several studies (e.g. Ponti et al., 2014; Rodriguez et al., 2020).

In the frame of the MED-GOLD project, such a climate service tool - the Dashboard - has been developed for these sectors. The MED-GOLD dashboard is an easy-to-use visualization tool, which provides access to information on past climate and predictions of future climate at different time scales. The tool has been co-developed with users to ensure that it addresses their needs and expectations. The selected bio-climatic indicators presented in the tool, have been identified by several interactions with the end-users and the key climate-related information provided for the decision making, relies on a robust and well-established scientific background. The aim of this climate service tools is to enable

the end-users to adapt their decision-making strategies to the climate conditions and climate change. The tool is presented separately for the three-time scales - historical climate, seasonal forecasts, climate projections - in the results section.

2 Data and Methodology

During the first year of the MED-GOLD project, the engaged partners (i.e. cooperatives or organizations operating in the sectors of our interest) contributed to understanding the needs of each sector in terms of climate information through participatory workshops. The Dashboard tool was co-developed with the partners since the provided climate information was based on the partners' needs; several online surveys and participatory workshops were organized throughout the project for the continuous assessment of the added value of the provided climate services.

Eventually, essential climate values (ECV) and bioclimatic indicators identified by professional agronomists as appropriate for the olive oil and wine sectors, have been calculated for the past (historical climate) and the future (seasonal forecasts, long-term projections).

For the development of the historical climate section, hourly climate data has been downloaded from the Copernicus' Climate Data Store (CDS), focusing on the ERA5 reanalysis, which combines model data with observations into a globally complete and consistent dataset (Hersbach et al., 2020). The bioclimatic indicators and the risk indices were computed based on these datasets and the produced data was finally included in the Dashboard system.

The seasonal predictions climate service was based on the ECMWF SEAS5 seasonal predictions dataset obtained from the Climate Data Store of the Copernicus Climate Change Service (CDS-C3S). The products obtained from this component of the climate service included statistically downscaled essential climate variables (ECVs; i.e. mean temperature, maximum temperature, minimum temperature and precipitation), bioclimatic indicators and risk indices.

For the computation of the long-term projections an ensemble of five different Regional Climate Model (RCM) simulations from the EURO-CORDEX datasets was used (Jacob et al., 2014). The PTHRES dataset has been used for the bias correction of the daily RCM data for the temperature variables (daily maximum, minimum and mean) as well as daily accumulated precipitation for the Douro Valley region.

3 Results - The tool

The Dashboard tool can be accessed through the MED-GOLD website, where log-in credentials can be requested. A user guide has been designed to provide documentation for the people who wish to use the tool; it contains step-by-step instructions on how to log on, use the tool, download and interpret the results.

The Dashboard can provide end-users with information on essentials variables (temperature, precipitation) and bioclimatic indices at three different time scales for the two main sectors (olive and grape) and it is under development for the durum wheat sector (Fig. 1). The bioclimatic indices take into account the climate and the phenology of the crops. In addition, certain risk indicators developed for the wine sector, represent the possibility of sanitary heat risks.

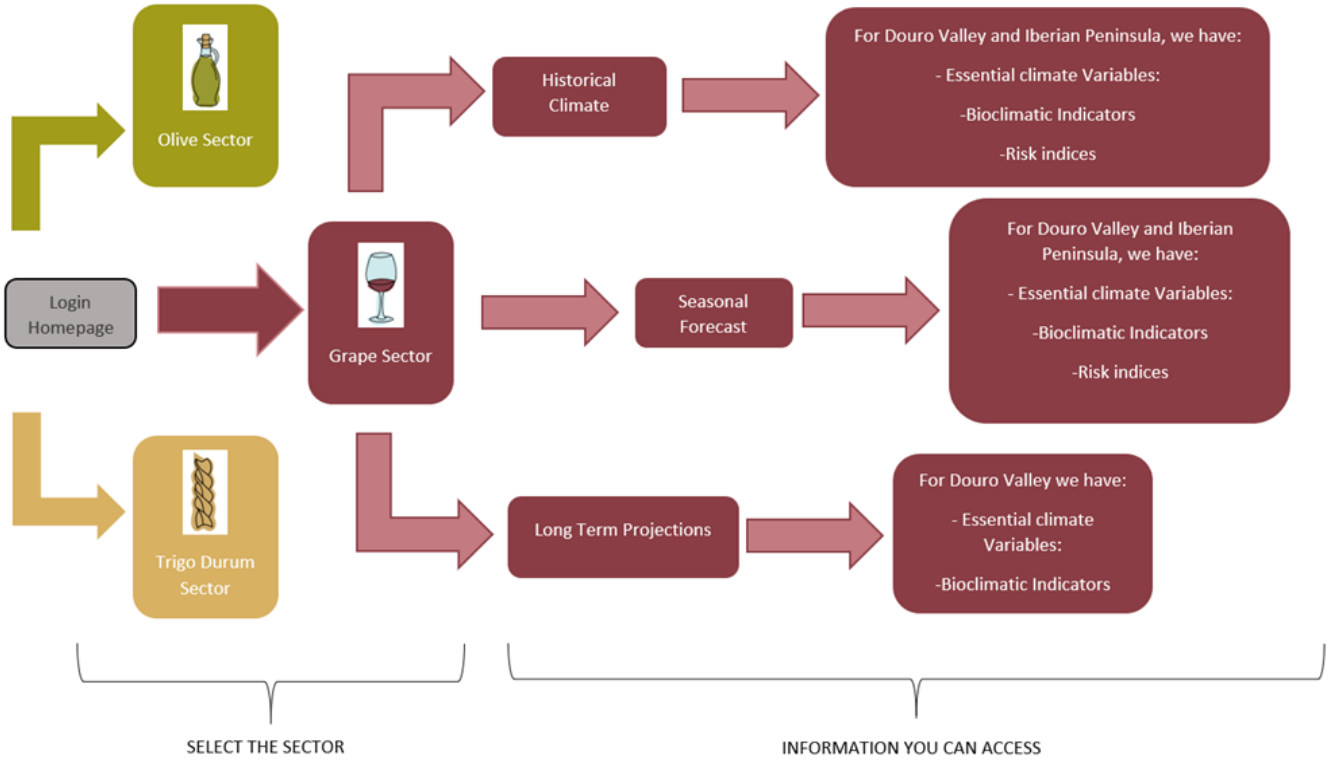

Figure 1. Information provided in the Dashboard tool.

The tool's homepage is easy to navigate and provides the following selection options (Fig. 2):
(1) Timescale selection (historical climate, seasonal forecasts, long-term projections)
(2) Location selection ((search by geographic coordinates, city or country)
(3) Type of variables (climate variables, bioclimatic indicators, wine risk indicators)
(4) Region of interest (Douro region or Iberian Peninsula)
(5) Variable or index of interest
(6) Time period of interest
(7) Filter (Data for each year or averaged over a period)
(8) Export data (ascii, netcdf or jpg format)

For example, after making the appropriate selections in the fields described above, the end-user can see that the climate for the reference period 1981-2010 with respect to 1951-1980, over the region of interest for the MED-GOLD wine service, is generally warmer. This implies reduced need of additional sanitary treatments and an increase of possible heat stress for the grapes.

Regarding longer time scales, the analysis of the climate projections reported in the Dashboard revealed robust increasing changes between both the near and the distant future compared to the reference period for the temperature related indices under both RCP scenarios. On the contrary, the changes in the precipitation related indices were found less pronounced for the near future period under both RCP4.5 and RCP8.5, while the highest and more robust decreases were identified for the distant future period under RCP8.5

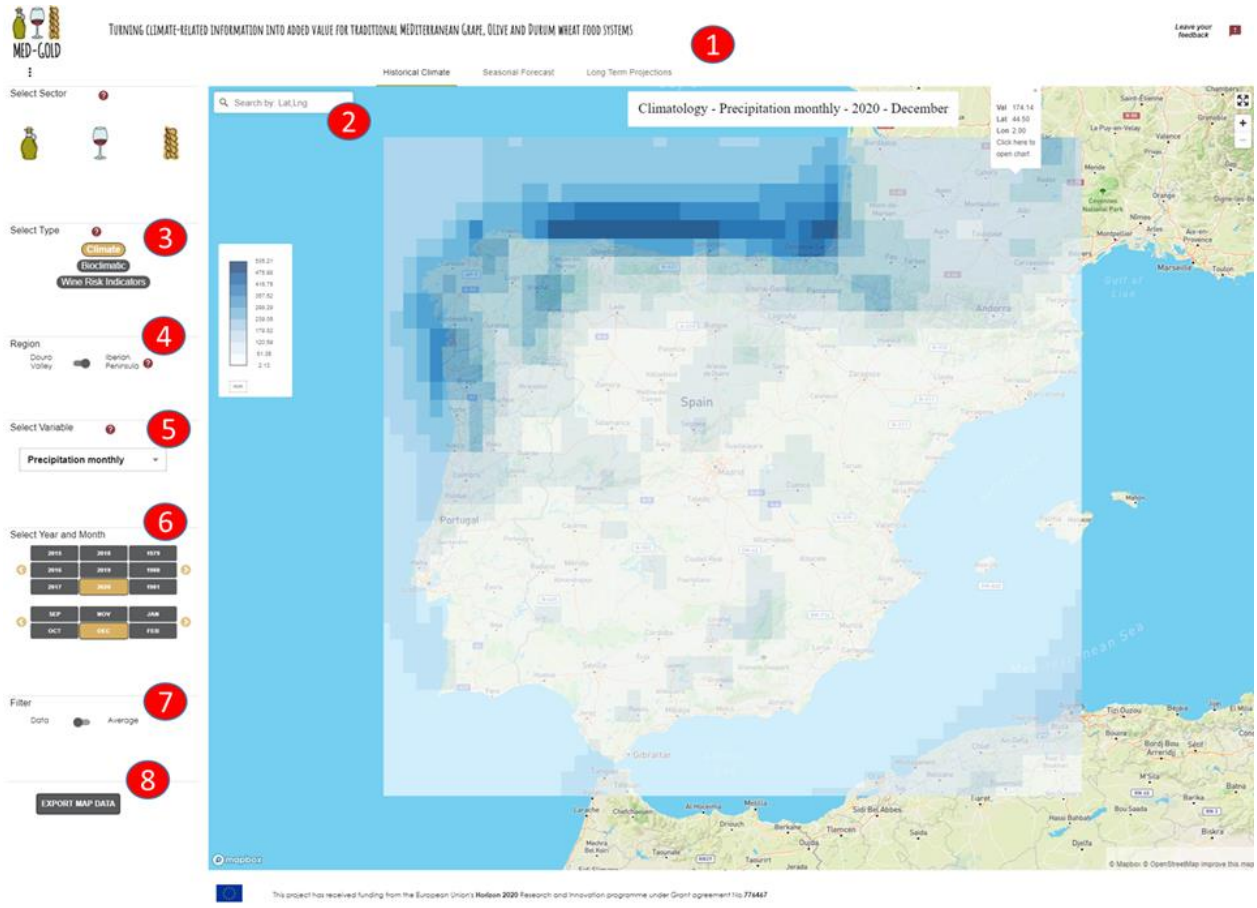

Figure 2. Dashboard homepage

4 **Conclusions**

The co-development of the Dashboard tool contributed to the creation of a simple and user-friendly tool. It resulted in appropriate timeliness of the climate information, spatial scale, appropriate selection of variables, and understandable presentation format (visualization), which in turn can be helpful for decisions such as pest control, harvest planning and production prediction. The Dashboard tool can be further improved, providing more climate information to the end-users. The lessons learnt during the development of the indices for the olive and wine sectors can pave the way for more crops and more areas to be included in the tool. Overall, the tool can contribute to more resilient to climate risk crops, by encouraging at the same time eco-friendly farming practices.

Acknowledgments This project has received funding from the European Union's Horizon 2020 research and innovation program 'MEDiterranean Grape, OLive and Durum wheat food systems, MED-GOLD' under grant agreement No 776467.

References

Hersbach H., Bell B., Berrisford P., Hirahara S., Horanyi A., Munoz-Sabater J., Nicolas J., Peubey C., Radu R., Schepers D., Simmons A., Soci C., Abdalla S., Abellan X., Balsamo G., Bechtold P., Biavati G., Bidlot J., Bonavita M., De Chiara G., Dahlgren P., Dee D., Diamantakis M., Dragani R., Flemming J., Forbes R., Fuentes M., Geer A., Haimberger L., Healy S., Hogan R.J., Hólm E., Janisková M., Keeley S., Laloyaux P., Lopez P., Lupu C., Radnoti G., de Rosnay P., Rozum I., Vamborg F., Villaume S., Thepaut J.N.: The ERA5 global reanalysis, Quartely Journal of the Royal Meteorological Society, 146:, 1999-2049, doi: 10.1002/qj.3803, 2020

Ponti L., Gutierrez A.P., Ruti P.M., Dell'Aquila A.: Fine-scale ecological and economic assessment of climate change on olive in the Mediterranean Basin reveals winners and losers. Proc. Natl. Acad. Sci. USA, 111, 5598–5603, 2014

Rodríguez Sousa A.A., Barandica J.M., Aguilera P.A., Rescia A.J.: Examining Potential Environmental Consequences of Climate Change and Other Driving Forces on the Sustainability of Spanish Olive Groves under a Socio-Ecological Approach. Agriculture, 10, 509, 2020

Jacob D., Petersen J., Eggert B., Alias A., Christensen O.B., Bouwer L.M., Braun A., Colette A., Déqué M., Georgievski G., Georgopoulou E., Gobiet A., Menut L., Nikulin G., Haensler A., Hempelmann N., Jones C., Keuler K., Kovats S., Kröner N., Kotlarski S., Kriegsmann A., Martin E., van Meijgaard E., Moseley C., Pfeifer S., Preuschmann S., Radermacher C., Radtke K., Rechid D., Rounsevell M., Samuelsson P., Somot S., Soussana J.F., Teichmann C., Valentini R., Vautard R., Weber B., Yiou P.: EURO-CORDEX: new high resolution climate change projections for European impact research, Regional Environmental Change, 14, 563–578, doi:10.1007/s10113-013-0499-2, 2014.

The Growing Degree Days' evolution for viticulture over the Mediterranean area via a high spatial resolution dataset.

Charalampopoulos, I[1], I. Polychroni[2], P.T, Nastos[2]

[1] Laboratory of General and Agricultural Meteorology, Department of Crop Science, Agricultural University of Athens, Greece.
[2] Laboratory of Climatology and Atmospheric Environment, Department of Geology and Geoenviroment, National and Kapodistrian University of Athens, University Campus, 15784 Athens, Greece.

Abstract. Climate change may be a challenge for the agricultural sector worldwide. The pressure by the altered thermal conditions drives the zonal shift for a wide variety of cultivations. This study presents the multiyear analysis of the Growing Degree Days (GDD) index over the Mediterranean Basin, focused on the high-value vine cultivation derived from the E-OBS dataset. In order to handle this big environmental dataset, R-language script and packages were used, along with the capabilities of GIS software. The analyzed time period is 1950 to 2018, and the performed analysis indicates a broad shift in areas of GDD > 2000 units.
The extracted results specify the areas where the GDD index significantly exceeds the suitable values for those valuable crops, increasing thermal stress risk. At the same time, in northern areas, the rising of the GDD may be a chance for new plantations of vine fields.

1 Introduction

Viticulture is one of the most important parts of the Mediterranean agricultural sector, in direct financial terms and as a cultural factor (Bindi et al., 1996; Droulia and Charalampopoulos, 2022). Moreover, the vine is one of the most resilient crops due to climate change, which will drive to more xerothermic conditions in southern Europe and northern Africa. So, it is of utmost importance to investigate yet model the changing environmental conditions that will affect the viticultural sector's quality and yield quantity. A group of important research is already published using the advantage of datasets such as Agri4Cast, ERA and other atmospheric datasets (Bandhauer et al., 2022; Charalampopoulos et al., 2021; Mavromatis and Voulanas, 2020; Photiadou et al., 2017). This research is preliminary research for modelling atmospheric suitability for viticulture over the Mediterranean basin, examining the time and spatial evolution of a critical index (or indicator) of the Growing Degree Days (GDD).

2 Data, area and methods

The selected area is the Mediterranean basin, one of the major epicentres of the vine world. Since the spatial shifting of critical GDD values occurred in an extended area, the results cover a wide area from central Europe to the Sahara Desert.
For the study, the high spatiotemporal resolution (~10X10 km) dataset of E-OBS (v19.0e) was utilized. As several comparison studies reviled, this dataset is the one of the most accurate and confident (Bandhauer et al., 2022; Mavromatis and Voulanas, 2020), and it is already used for a wide variety of similar research (Fraga et al., 2013; Fraga and Santos, 2017; Photiadou et al., 2017). In order to calculate the Growing Degree Days (GDD) the following classic formula was applied to the daily data of the E-OBS.

$$GDD = \sum_{G_b}^{G_e} \frac{T_{max} + T_{min}}{2} - T_{base} \qquad (1)$$

The calculations period starts from the year 1950 to the year 2018, and the input parameters are the daily minimum (T_{min}) and maximum (T_{max}) air temperature. The base temperature (T_{base}) was set at 10 ^{o}C and the growing period beginning (G_b) was set on April and the end (G_e) on the end of October. The essential equation (1) is utilized with the adjustment of $T_{min} = T_{base}$ if $T_{min} < T_{base}$ and $T_{max} = T_{base}$ if $T_{max} < T_{base}$ (Charalampopoulos et al., 2021). In order to facilitate a large amount of data and to conduct the calculations, a R-language (R Core Team, 2018) script was utilized along with the QGIS software (QGIS Development Team, 2009) to map the results.

3. Results and discussion

The GDD accumulates the thermal environment which is necessary for the biological cycle of a crop. The crucial threshold for the vines is defined as the 2000 GDD (yearly), but there is also cool - climates viticulture even under climatic conditions of less than 1000 GDD (Schultze and Sabbatini, 2019).
In order to examine the spatial evolution (swift) of the zones with GDD>2000, a map (figure 1) of the overlapping areas of the selected time periods was produced. In addition, multiple barplots of the total surface with GDD> 2000 for each country are presented in figure 2.
It is crucial to pinpoint that the GDD values are only one of the crucial factors of the atmospheric yet environmental requirements for successful (quantitatively and qualitatively) vine cultivation. So, GDD>2000 is not evidence of environmental suitability for such cultivation because the farmers should consider the frost frequency, the thermal stress, the soil texture and fertility and the water availability of the area.

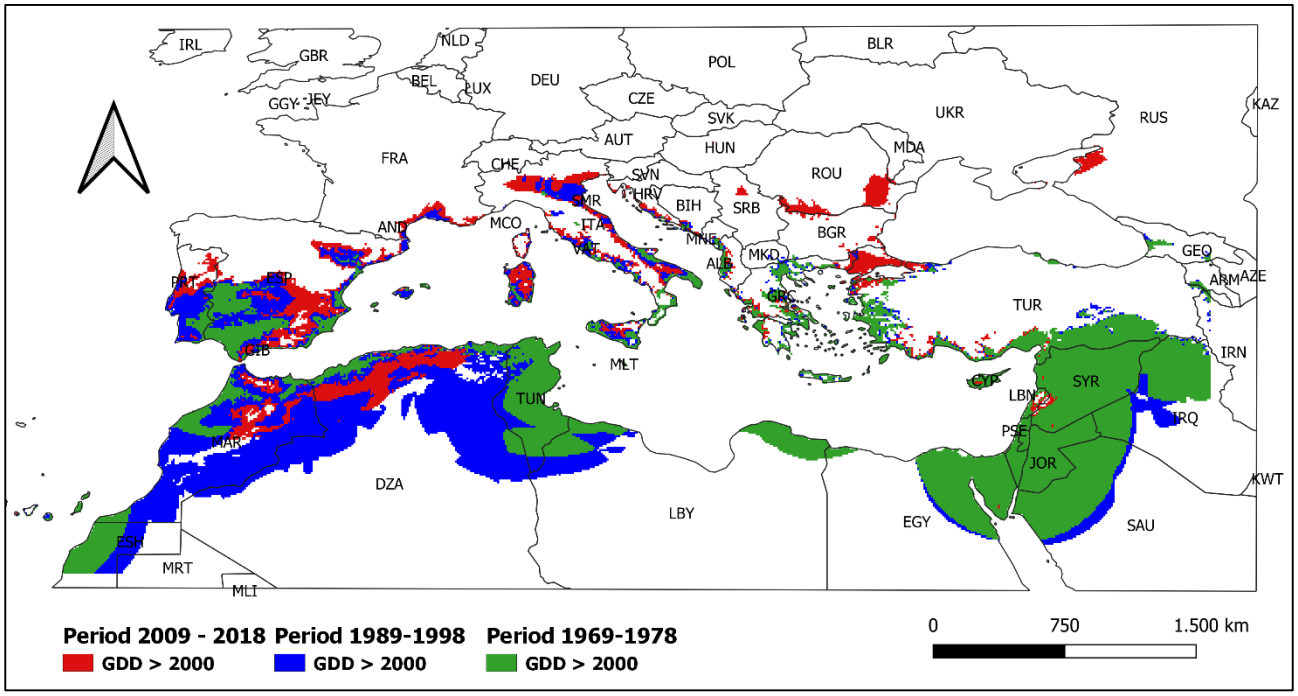

Figure 1. The areas with GDD> 2000 for the selected time periods.

As we can see in the map (fig. 1), the areas with GDD> 2000 for the period of 1969-1978 occurred mainly in the southeastern part of the Mediterranean basin, covering the whole of Israel, Jordan, and Syria, Palestine and a part of Lebanon lowlands. Moreover, a significant part of the Saudi Arabia desert (the southeastern spatial limit of the dataset) and arid western Iraq accumulated GDD>2000, along with the south part of Turkey. The above areas, along with the Aegean seashore and the greater part of Cyprus and a part of northern Libya is a historical wine regions. The E-OBS dataset with a pixel of ~100 km^2 detected some regions over the Caucasus (Georgia and Azerbaijan) for the same period. It is anticipated that the half southern part of seaside Italy and the Adriatic shoreline of Albania, Montenegro and Croatia are under the climatic conditions of GDD> 2000. Moving to the western part of the Mediterranean basin, we see that a great part of Tunisia, and a narrow strip of northern Algeria, along with the shoreline of Morocco, fulfil the criterion of GDD. Finally, the southern part of the Iberic Peninsula (Spain and Portugal) is in the zone of GDD> 2000 for this period. It is worth mentioning that the E-OBS dataset cannot detect GDD> 2000 zone in the northern traditional wine regions of France and central Europe. T

The areas with GDD> 2000 during the next period (1989-1998) are shown in the blue colour in figure 1, indicating an expansion to higher altitudes and latitudes over the European part of the study area. So, there is an extended area in the northern part of Italy (the valley from Milan to Venice), fulfilling the criterion and the Mediterranean shore of France. During the same period, the subregion of Catalonia and a great part of central Spain fulfilled the criterion along with an extended area of Portugal in south Lisbon.

The third period (2009-2018), coloured with red, indicates a significant expansion of the areas with GDD> 2000 to northern regions such as a part of the Russian territory on the Black Sea, the European part of Turkey, a region over the boarders of Bulgaria – Romania and an area of Romania near the black sea. The GDD> 2000

areas are spread over some mountainous areas of Greece mainly in the wester part of the country. But, the greatest advancements are over the eastern Italy, Sardinia island and the shore line of France. Moreover, the southern part of Spain is under conditions of GDD> 2000.

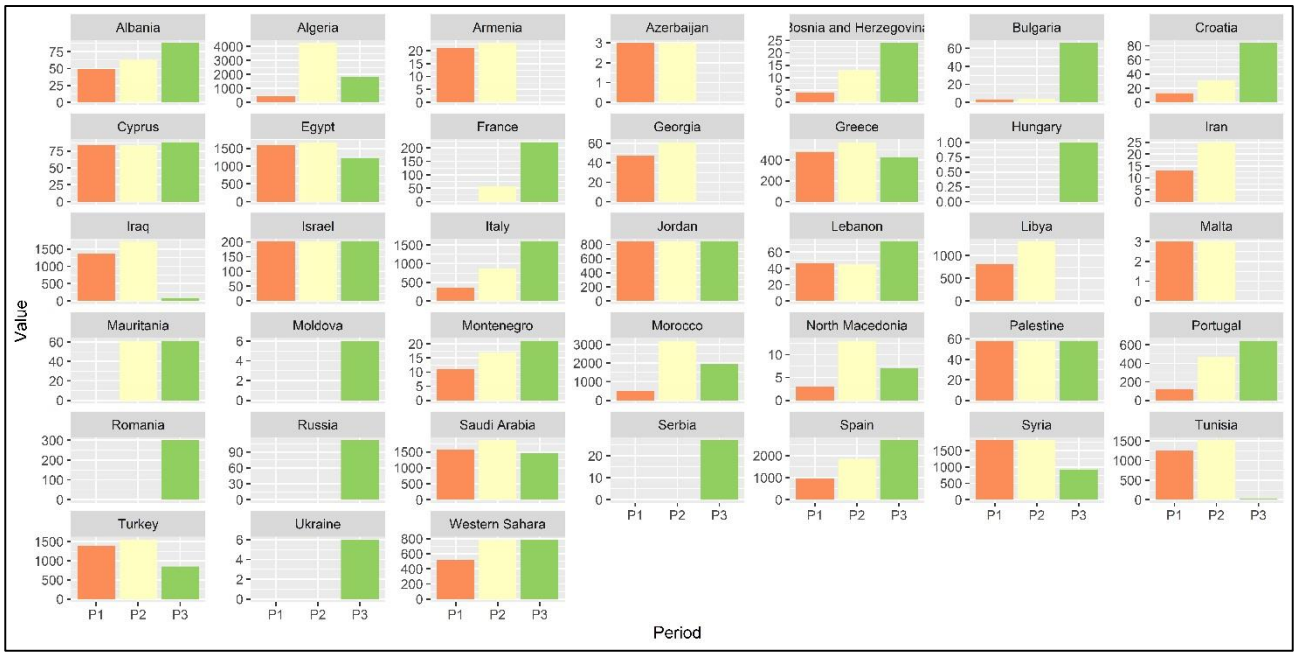

Figure 2. The time evolution of area of GDD> 2000 per country. The value is X100 km^2 and P1 is 1969 -1978, P2 is 1989 - 1998 and P3 is 2009 - 2018 time periods.

The area (covered by GDD> 2000) per country reveals the phenomenon's time evolution. It is very important to mention that the E-OBS dataset has some gaps (empty cells) mainly in the perimeter during the last 15 years. To avoid serious mistakes and false conclusions we decided to remove the pixels with non-complete series of data. That is the reason we see no areas covered by GDD> 2000 in the third period (P3) over Tunisia, Iran, Libya, Malta, Georgia, Armenia, and Azerbaijan. And that's the reason of the reduction of the covered area from second period (P2) to the third (P3) one, in countries such as North Macedonia, Greece, Syria, Morocco, Saudi Arabia, Algeria etc, since there is no climate cooling recorded. The multiple barplots in figure 2 indicates a steady increment of the surface under climatic conditions of GDD> 2000 due to climate change. All the above findings are in corroboration with previous related research, which indicates extensive shifting of GDD and vine areas to northern (in Europe) and higher areas *(Charalampopoulos et al., 2021; Droulia and Charalampopoulos, 2022; Omazić et al., 2020; Patriche and Irimia, 2022; Santos et al., 2020; Spinoni et al., 2015)*.

4 Summary

Based on the finding of this research, it is evident that the rising temperature over the Mediterranean leads to an expansion of suitable areas for viticulture. This will be a chance for agricultural development over higher (mountainous) and northern areas, which will fulfil the vines' water and thermal needs. To draw a safer conclusion about the atmospheric suitability should examine the spatial and temporal distributions of more atmospheric indicators and parameters, such as frost, precipitation, evapotranspiration etc.

Despite the gaps in its spatial perimeter, the E-OBS dataset is a valuable asset for the agroclimatic assessment of the Mediterranean area. The time resolution (daily data) and the accuracy of the estimated parameters of the dataset are very important. Its spatial resolution is a limiting factor for such research since the 10X10 km resolution hides some significant narrow agricultural regions. However, the E-OBS can be fine scaled utilizing downscaling methods. So, this dataset could be the basis for extended bioclimatic modelling for important cultivation such as vines.

References

Bandhauer, M., Isotta, F., Lakatos, M., Lussana, C., Båserud, L., Izsák, B., Szentes, O., Tveito, O.E., Frei, C., 2022. Evaluation of daily precipitation analyses in E-OBS (v19.0e) and ERA5 by comparison to regional high-resolution datasets in European regions. International Journal of Climatology 42, 727–747. https://doi.org/10.1002/joc.7269

Bindi, M., Fibbi, L., Gozzini, B., Orlandini, S., Miglietta, F., 1996. Modelling the impact of future climate scenarios on yield and yield variability of grapevine. Clim. Res 7, 213–224.

Charalampopoulos, I., Polychroni, I., Psomiadis, E., Nastos, P., 2021. Spatiotemporal Estimation of the Olive and Vine Cultivations' Growing Degree Days in the Balkans Region. Atmosphere 12, 148. https://doi.org/10.3390/atmos12020148

Droulia, F., Charalampopoulos, I., 2022. A Review on the Observed Climate Change in Europe and Its Impacts on Viticulture. Atmosphere 13, 837. https://doi.org/10.3390/atmos13050837

Fraga, H., Malheiro, A.C., Moutinho-Pereira, J., Santos, J.A., 2013. Future scenarios for viticultural zoning in Europe: ensemble projections and uncertainties. Int J Biometeorol 57, 909–925. https://doi.org/10.1007/s00484-012-0617-8

Fraga, H., Santos, J. a., 2017. Daily prediction of seasonal grapevine production in the Douro wine region based on favourable meteorological conditions. Australian Journal of Grape and Wine Research 23, 296–304. https://doi.org/10.1111/ajgw.12278

Mavromatis, T., Voulanas, D., 2020. Evaluating ERA-Interim, Agri4Cast and E-OBS gridded products in reproducing spatiotemporal characteristics of precipitation and drought over a data poor region: The Case of Greece. International Journal of Climatology n/a. https://doi.org/10.1002/joc.6950

Omazić, B., Prtenjak, M.T., Prša, I., Vozila, A.B., Vučetić, V., Karoglan, M., Kontić, J.K., Prša, Ž., Anić, M., Šimon, S., Güttler, I., 2020. Climate change impacts on viticulture in Croatia: Viticultural zoning and future potential. International Journal of Climatology 40, 5634–5655. https://doi.org/10.1002/joc.6541

Patriche, C.V., Irimia, L.M., 2022. Mapping the impact of recent climate change on viticultural potential in Romania. Theor Appl Climatol. https://doi.org/10.1007/s00704-022-03984-y

Photiadou, C., Fontes, N., Graça, A.R., Schrier, G. van der, 2017. ECA&D and E-OBS: High-resolution datasets for monitoring climate change and effects on viticulture in Europe. BIO Web Conf. 9, 01002. https://doi.org/10.1051/bioconf/20170901002

QGIS Development Team, 2009. QGIS Geographic Information System. Open Source Geospatial Foundation.

R Core Team, 2018. R: A Language and Environment for Statistical Computing [WWW Document]. URL https://www.R-project.org/ (accessed 2.5.20).

Santos, J.A., Fraga, H., Malheiro, A.C., Moutinho-Pereira, J., Dinis, L.-T., Correia, C., Moriondo, M., Leolini, L., Dibari, C., Costafreda-Aumedes, S., Kartschall, T., Menz, C., Molitor, D., Junk, J., Beyer, M., Schultz, H.R., 2020. A Review of the Potential Climate Change Impacts and Adaptation Options for European Viticulture. Applied Sciences 10, 3092. https://doi.org/10.3390/app10093092

Schultze, S.R., Sabbatini, P., 2019. Implications of a Climate-Changed Atmosphere on Cool-Climate Viticulture. J. Appl. Meteor. Climatol. 58, 1141–1153. https://doi.org/10.1175/JAMC-D-18-0183.1

Spinoni, J., Vogt, J., Barbosa, P., 2015. European degree-day climatologies and trends for the period 1951-2011. International Journal of Climatology 35, 25–36. https://doi.org/10.1002/joc.3959

Does changing climate in Serbia affect codling moth presence in Serbian orchards?

Marcic M.[1] and Lalic B[2]

[1]Forecasting and Warning Service in Plant Protection of Serbia, Novi Sad, Serbia
[2] Faculty of Agriculture, University of Novi Sad, Novi Sad, Serbia

Abstract. The codling moth is one of Serbia's most economically significant fruit pests. Since 2012 permanent monitoring of codling moth appearance in Serbia is conducted. Observation results indicate a significant time-shift of first trap catches compared to literature data - from the first decade of May to the beginning/end of April. We hypothesized that the cause of the determined shift is regional change of climate in Serbia, particularly the increase in winter temperatures. This study was designed to test this hypothesis. The biological data analyzed refer to the daily catches of adults on pheromone traps in the period from early April to the end of September in commercial apple orchards. For 16 locations, during the 2012–2021 period, 93 data sets were analyzed. According to all climate change scenarios, an increase in winter, spring and summer temperature is expected, increasing the suitability of conditions for an earlier beginning and prolongation of the seasonal duration of pests. It raises the question: "Should we expect prolonged exposure of apples to codling moth and an increased risk of apple damage?".

1 Introduction

The codling moth (*Cydia pomonella* Linne) is the most important pest of apple fruit, and it appears regularly every year in all apple orchards in Serbia (Almasi et al., 2004). The apple is the second most important variety in total fruit production with 23.737 hectares of apple orchards (Keserovic et al., 2012), which ranks the codling moth as one of Serbia's most economically significant fruit pests. The damage is caused by larvae, which burrow into the fruits. Infested fruits are unmarketable. In years with heavy infestations in untreated orchards, yield loss by *C. pomonella* damage reaches 80%. (EPPO, 1994). One of the most common ways to monitor the detection and population of the codling moth in agriculture is by using pheromone traps. Captures in traps baited with synthetic pheromone lures accurately show whether a specific insect is present and when its seasonal flight period starts. A simple and widespread strategy is to time insecticide sprays accordingly (Witzgall et al., 2010). Using pheromone traps makes it possible to determine the beginning and dynamics of the adult's flight during the vegetation.

The codling moth belongs to the class of insects whose phenology is greatly influenced by temperature. All physiological and biochemical processes that are important for the development of plants and harmful organisms are conditioned by the temperature of the environment in which they are located. Most often, the temperature determines when a process will start (lower limit temperature) or end (upper limit temperature), while the intensity of the process is proportional to the energy brought from the external environment into the biological system (Lalic et al., 2021). In many insect species (Macrolepidoptera), both an earlier beginning and prolongation of seasonal duration occurred in parallel with recent global warming (Altermatt, 2009). Solar radiation can affect the performance of herbivorous insects directly by increasing body temperature or indirectly through changes in the quality of the host plant or the activities of a natural enemy (Battisti et al., 2013). In the last climatological period in Serbia (1981–2010), there was an increase in temperatures and increased duration of insolation compared to the previous climatological period (1961–1990) (Lalic et al., 2021). The impact climate changes may have on the complex of pests that affect crops in specific regions, the persistence of pest problems, and the efficacy of options available to manage pests will need to be assessed (Strand, 2000). Guided by these facts, we assumed that there was a change in the seasonal flight dynamics of the codling moth. Therefore, our study addresses the following questions:

- Has there been a time-shift in the first occurrence of adults (biofix) in the observed ten-year period compared with the 1950ies, 1980ies and early 2000ies?
- What could be the reasons for changing the seasonal flight dynamics of the codling moth?

To answer the first question, we compared the data from the previous ten years with the literature data for Serbia from the past (Section 3.1). Monitoring of the codling moth has been carried out in Serbia since the 1950ies. From 1948 to 1950, monitoring was performed in the regions of Kragujevac, Cacak, Jagodina and Prokuplje. The first butterflies appeared from April 28th to May 13th (Lekic, 1950). During the 1980ies, the beginning of the adult flight was registered from May 5th to May 9th in the regions of Cacak and Valjevo (Stamenkovic, 1984). In the region of Belgrade during 2002 and 2003, the first adults were registered from April 29th to May 1st (Peric et al., 2004, Graora, Jerinic-Prodanovic, 2005). At the beginning of the 21st century

(2001–2003), in the region of Leskovac, the first adults in pheromone traps were caught in the period from April 14th to May 2nd (Nikolic, 2006).
To address the second question, we explored: a) correlation between average monthly temperatures before biofix and biofix DOY (day of year) during the 2012–2021 period and b) the climatic characteristics of Serbia in two climatological periods, 1961–1990 and 1981–2020 (Section 3.2). The answers to addressed questions are important because changes in the phenology dynamics of codling moth cause changes in the strategy of apple protection. As possible causes of time-shift in adults' occurrence, the air temperature and insolation are selected.

2 Material i method

2.1 Study region

Serbia is a meridional country. The terrain is predominantly flat in the north and is part of the Pannonian lowland. South of the Sava and Danube rivers, the altitude increases significantly so that in the far east and southwest, it reaches heights of over 2000 m. The climate of Serbia is moderately continental, with pronounced local characteristics, a temperature regime that in most parts of the country corresponds to the climate of the temperate zone and a precipitation regime that is characteristic of the continental climate (RHMZ, 2022).

Table 1. Selected locations

Region	Locality	Year of monitoring	Apple variety	Anti-hail nets	Irrigation	Plant protection measures against CM	Density	Latitude	Longitude	Elevation (m)
Beograd	Padinska Skela	2013-2014 2016-2018	Idared, Golden Delicious	No	No	Yes	1,75 m x 4 m 2,5 m x 4 m	44°57'39"	20°25'57"	68
Cacak	Lipnica	2019-2021	Idared	No	No	Yes	3 m x 4 m	43°49'3"	20°25'30"	325
Jagodina	Santarovac	2015-2019	Idared, Golden Delicious, Granny Smith, Jonagold, Mutsu	No	Yes	Yes	1,5 m x 3,5 m	43°55'23.11"	21°10'32.941"	
Kikinda	Kikinda	2012-2021	Idared, Golden Delicious, Jonagold, Mutsu, Gloster	No	No	Yes	2 m x 4 m	45°51'17"	20°30'28"	105
Kragujevac	Vinca	2019-2021	Idared, Granny Smith, Mutsu	No	No	Yes	2,5 m x 4 m	44°12'43"	20°38'12"	328
Krusevac	Milutovac	2015-2018	Golden Delicious, Gala, Jonagold	No	Yes	Yes	1 m x 3,5 m	43°41'38"	21°7'27"	295
Novi Sad	Nestin	2012-2021	Idared, Golden Delicious	No	No	Yes	1,5 m x 3,2 m	45°13'52.0"	19°28'08.5"	130
Novi Sad	Cenej	2012-2021	Idared, Golden Delicious, Granny Smith	No	Yes	Yes	1,5 m x 3,2 m	45°23'54.0"	19°49'12.4"	85
Ruma	Irig-Kudos	2012-2020	Idared, Golden Delicious	No	Yes	Yes	1,2 m x 4 m	45°2'22.221"	19°49'58.703"	133
Senta	Kanjiza	2012-2016 2017-2021	Idared, Golden Delicious, Gala, Braeburn	No Yes	No Yes	Yes Yes	- 0,8 m x 3 m	- 46°03'12"	- 20°04'09"	- 73
Smederevo	Selevac	2014-2021	Idared, Granny Smith, Akane, Mutsu	No	No	Yes	1,1 m x 3,5 m	44°34'58"	21°5'1"	187
Smederevo	Suvodol	2019-2021	Idared, Granny Smith, Mutsu	No	No	Yes	1 m x 3,5 m	44°34'4"	20°53'48"	162
Subotica	Backi Vinogradi	2012-2018 2020-2021	Idared, Golden Delicious, Jonagold, Mutsu	No	Yes	Yes	1,8 m x 3,8 m	46°6'33"	19°53'4"	90
Vranje	Dubnica	2019-2021	Idared, Golden Delicious, Red Delicious, Jonagored, Mutsu	No	Yes	Yes	1,5 m x 4 m	42°31'42"	21°50'12"	523
Vrsac	Crvena Crkva	2012-2014	Idared, Golden Delicious, Granny Smith	No	Yes	Yes	1,5 m x 4 m	44°53'58"	21°21'26"	80
Zrenjanin	Sutjeska	2012, 2014-2019	Idared, Golden Delicious	No	No	Yes	1,2 m x 4 m	45°23'26.320"	20°41'42.421"	80

Data on adult catches on pheromone traps used in this study are coming from the codling moth monitoring by the Forecasting and Warning Service in Plant Protection of Serbia (PIS) network. This network operates all over the territory of the Republic of Serbia, organized in 34 regional offices. PIS conducts daily monitoring of the most important plant productions and harmful organisms' occurrence and presence. Pheromone traps are in use for monitoring 43 pests at over 900 locations every year. In addition to pheromone traps, other monitoring tools, such as visual observations, light lamps, and automatic weather stations are used to prepare recommendations for spraying and non-pesticide measures. More about PIS can be found in Lalic et al., 2020.

During one production year, monitoring of codling moth is carried out at about 60 locations. For the purpose of this study, only locations with a minimum of three years of continuous monitoring are selected from the 2012–2021 observation period. The traps were in production orchards where chemical protection measures against harmful organisms were regularly carried out. To avoid the impact of insecticides on possible errors in the first detection of adults, we selected only locations with a high insect population where over 100 individuals were registered on traps during the season. All locations where traps were not set in time to detect the first appearance of adults were excluded from the analysis. A total of 16 locations from 14 regions were analyzed. More details about apple orchards where pheromone traps were placed can be found in Table 1.

2.2 Data from pheromone traps and historical data

Historical data on the first occurrence of adults in the 1950ies are found in Lekic (1950) and refers to the regions of Kragujevac, Cacak, Jagodina and Prokuplje. Data for the 1980ies are found in Stamenkovic (1984) and include data for the regions of Čačak and Valjevo. Data from early 2000ies are found in Peric et al. (2004), Graora and Jerinic-Prodanovic (2004) and Nikolic (2006) and refer to the Leskovac and Belgrade regions.
Pheromone traps used at all locations during the 2012–2020 study period are manufactured by Chsalomon® (Hungary). Traps type RAG and a female pheromone were used to attract males. The traps are set at the 2 m height within the tree canopy. Typically, two traps were set - one on edge and one in the middle of the orchard. The pheromone was changed every four weeks, and the sticky inserts were changed every seven to ten days. Countings were performed on a daily basis, and the average value from both traps is considered a daily catch. A permanent monitoring of codling moth typically takes place from the beginning of April till the end of September.

2.3 Climatological data

Monthly air temperature changes are analyzed for two climatological periods, 1961–1990 and 1981–2020, for locations presented in Tab. 2. Changes in insolation are analyzed for two typical locations, in the northern (Rimski Sancevi) and the southern (Vranje) part of the country and presented in Tab. 3.

Table 2. Changes in normal air temperature for the selected period (December–February (DJF), March–May (MAM), Jun–August (JJA), September–November (SON), March–August (MA)) during the 1981–2020 in respect to the 1961–1990 climatology [source: RHMZ of Serbia].

Locality	DJF	MAM	JJA	SON	MA	Year
Palic	0.5	0.6	1.3	0.3	0.9	0.7
Kikinda	0.6	0.5	1.1	0.2	0.8	0.5
Sombor	0.5	0.6	1.1	0.3	0.9	0.7
Zrenjanin	0.3	0.5	1.2	0.5	0.9	0.6
R.Sancevi	0.5	0.5	0.8	0.1	0.6	0.5
S. Mitrovica	0.3	0.4	0.8	0.2	0.6	0.5
Beograd	0.6	0.6	1.1	0.3	0.9	0.6
V. Gradiste	0.4	0.3	0.9	0.0	0.6	0.4
Loznica	0.5	0.6	1.1	0.3	0.8	0.6
Sm. Palanka	0.5	0.4	1.0	0.2	0.7	0.5
Valjevo	0.5	0.5	1.0	0.3	0.8	0.5
Negotin	0.7	0.8	1.4	0.2	1.1	0.7
Crni Vrh	0.2	-0.1	0.9	-0.2	0.4	0.2
Kragujevac	0.5	0.4	1.2	0.2	0.8	0.6
Cuprija	0.3	0.3	1.0	0.1	0.6	0.4
Zajecar	0.5	0.6	1.3	0.1	1.0	0.6
Pozega	0.3	0.3	0.8	0.0	0.5	0.4
Zlatibor	0.6	0.6	1.0	0.1	0.8	0.6
Kraljevo	0.3	0.3	0.9	0.0	0.6	0.5
Krusevac	0.5	0.5	1.0	0.2	0.8	0.6
Nis	0.4	0.4	1.1	0.2	0.7	0.5
Sjenica	0.6	0.5	1.1	0.3	0.8	0.6
Kopaonik	0.6	0.9	1.5	0.7	1.2	0.9
Dimitrovgrad	0.1	0.2	0.8	-0.1	0.5	0.3
Leskovac	0.3	0.2	0.8	-0.1	0.5	0.3
Vranje	0.2	0.3	0.9	0.0	0.6	0.3

Table 3. Mean values of insolation (h) for the period 1961–1990 and 1981–2010 [source: RHMZ of Serbia].

Locality	Period	I	II	III	IV	V	VI	VII	VIII	XI	X	XI	XII	Year
Rimski Sancevi	1961-1990	68.1	88.6	147.9	176.8	231.5	249.7	289.2	272.2	207.0	172.8	83.4	55.2	2042.4
	1981-2010	64.8	99.0	156.4	190.1	250.8	269.4	303.6	285.8	205.7	158.9	92.4	58.4	2135.3
Vranje	1961-1990	67.2	94.4	141.3	176.6	219.9	247.8	303.8	291.4	221.9	171.3	91.5	58.7	2086
	1981-2010	73.8	100.7	151.3	176.2	230.5	274.3	316.1	294.8	209.8	153.4	87.5	55.5	2124

3 Results

3.1 First occurrence of adults

The subject of this analysis was the date of the first occurrence of adult – biofix. To make the data easier to compare, biofix is expressed as day of the year (DOY). Historical data are presented in Fig. 1, while results of PIS monitoring for 2012–2021 are presented in Fig. 2.

During the 1950ies, the biofix ranged from the end of April (118 DOY) until mid-May (134 DOY). The first occurrence of an adult during the 1980ies was reported in the first decade of May (125–129 DOY). Since the early 2000ies, there has been a noticeable shift in biofix to the last decade of April (106 DOY) and the very beginning of May (122).

In the region of Cacak during the period from 1948 to 1950, the first adults occurred from 118 to 131 DOY. During 1981 and 1982, the first adults occurred on 129 DOY. From 2019 to 2021, the first adults on traps were caught from 113 to 122 DOY. For the region of Belgrade, we can identify two periods in this century. During 2002 and 2003, at two localities, the first adults on traps were registered from 115 to 121 DOY. In the last decade, during 2013, 2014, 2016, 2017 and 2018, the first adults were registered from 95 to 118 DOY. A slight increase in biofix variability over the seasons can be noticed in the north-south direction (Tab. 4). This effect can be partially caused by complex orography and typically higher altitudes of locations below the 45th parallel.

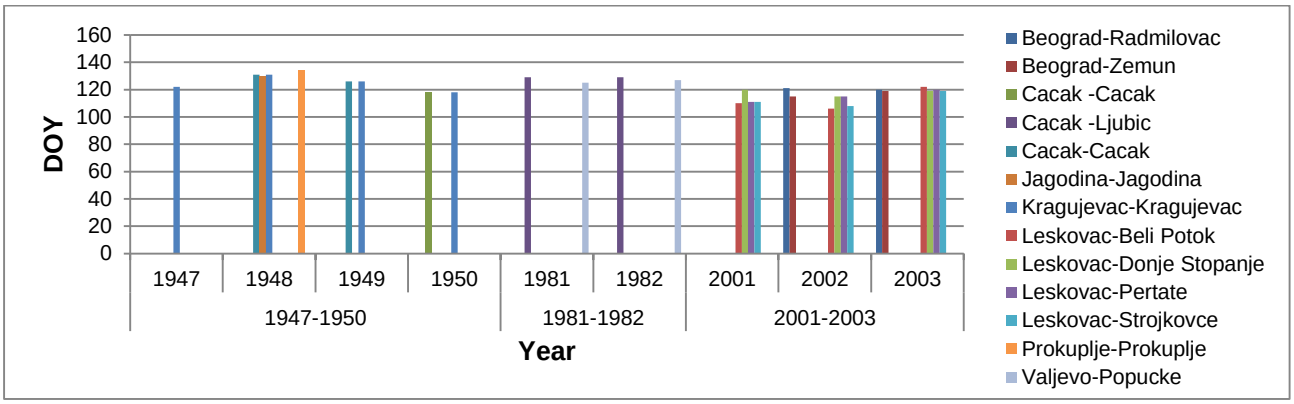

Figure 1. First occurrence of adults for selected periods: 1947–1950, 1981–1982, 2001–2003

During the 2012–2020 period, the first adults are caught during April, from the beginning of April (94 DOY) until the end of April (120 DOY) on all locations. Only in 2021, the first adults occur at the beginning of May (127) in three locations (Kanjiza 121 DOY, Lipnica 122 DOY and Dubnica 125 DOY) and in other locations during April (108-120 DOY). Based on the above data, it can be concluded that there was a chronological earlier shift in the biofix. In the region of Kragujevac, the earliest occurrence of adults during the 1950ies was in 1950 (118 DOY), and in the last three years in 2019 (104 DOY), which makes a difference of 14 days. For the Cacak region, such a difference is 8 days (1950 118 DOY and 2020 110 DOY). Changes are also noticeable during this century. According to data for the Belgrade region, the difference in the appearance of adults between 2002 (115 DOY) and 2014 (95 DOY) is 20 days.

Table 4. Biofix coefficient of variability (%) for selected locations for 2012–2021 period.

Backi Vinogradi	Kanjiza	Kikinda	Cenej	Sutjeska	Nestin	Irig Kudos	Padinska Skela
6	8	3	7	8	9	8	8
Crvena Crkva	Suvodol	Selevac	Vinca	Santarovac	Lipnica	Milutovac	Dubnica
16	16	13	15	13	5	8	12

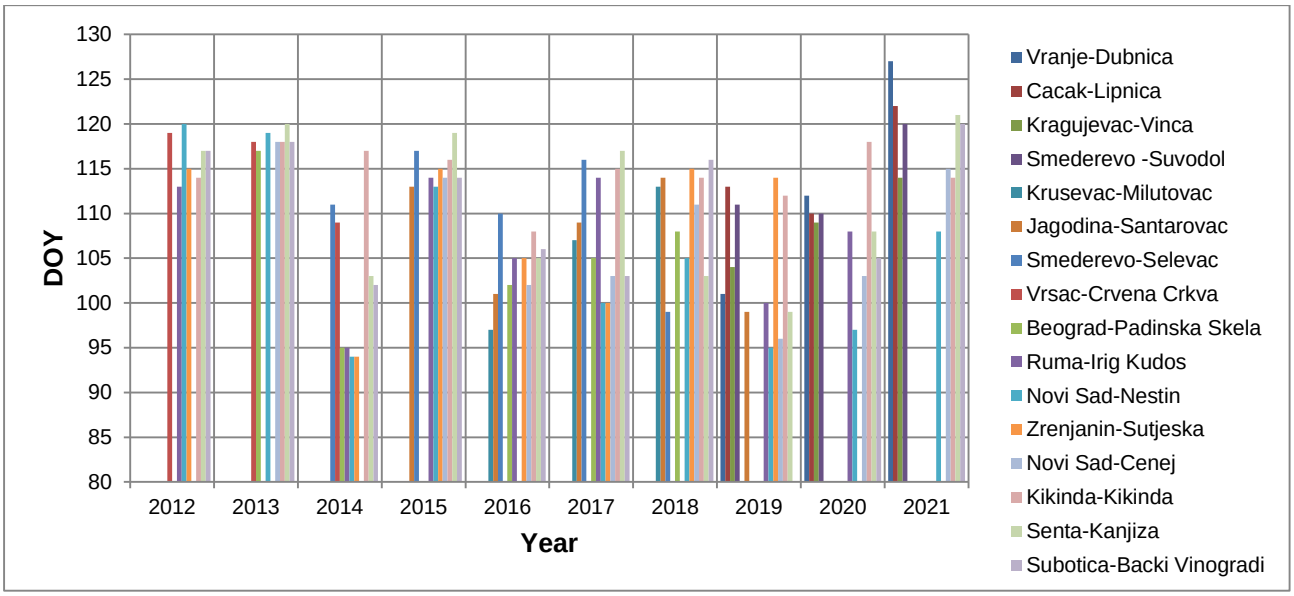

Figure 2. First catch of males of codling moth on pheromone traps (2012–2021)

3.2 Winter-spring temperature impact on biofix

For locations with at least five years of biofix observations, coefficient of correlation and p-value for monthly air temperature (January, February, March) and specific winter-spring period (January–March, January–April) and biofix DOY are calculated for the 2012–2021 period using data from the nearest climate station. Statistically significant results are obtained for only three locations in March and April (Tab. 5). It indicates that some factors other than temperature can affect overwintering and the time of the first appearance of adults in spring.

Table 5 Correlation coefficient between monthly temperature and time of biofix (%)

Location	Month	Correlation coeficient (%)	p-parametar (%)
Palic (Backi Vinogradi)	March	-73	2.3
Novi Sad (Cenej)	March	-82	1.2
Smederevska Palanka (Selevac)	April	-97	0.4

In order to discuss changes in biofix on a longer time scale (Fig. 1), temperature regime and insolation are analyzed for two climatological periods. During the last climatological period (1981–2010), the normal annual air temperature was 0.5 °C higher than in 1961–1990 (Tab. 2). However, from the point of view of interpreting the earlier occurrence of harmful organisms, the trend of increasing temperatures for the DJF and MAM are of upmost importance.

Table 3 shows the insolation changes for two locations, Rimski Sancevi and Vranje - northern and southern part of the country, respectively. According to Lalic et al. (2021), during the last climatological period, from February to August, the sunshine duration is higher than for 1961–1990 climatology at all inspected locations. As a result, an increase of incoming solar radiation, particularly in February, can affect plant and tree skin temperature leading to earlier occurrence of harmful organisms and thus the earlier timing of codling moth appearance.

4 Discussion and Conclusion

In order to predict future responses of species to a changed climate we first need to discover how species have responded to climate change in the past (Roy and Sparks, 2000). In this study, we analyzed changes in the first appearance of adults of the codling moth over about 70 years and saw that there were changes. Depending on the region and year, differences can be 20 days. Other authors also reported a shift in the first occurrence of other species belonging to the insect class. For example, Altermatt (2010) observed 263 species belonging to Macrolepidoptera in the period before and after 1980 in the area of Central Europe. He found that

in parallel to the changes in voltinism, the species shifted their flight to an earlier date. On average, the DOY of the first 25 per cent of all individuals of a species observed was 2.1 days earlier after 1980 compared with before 1980 for the first generation. Roy and Sparks (2000) analyzed 35 butterfly species in the British Isles in the period 1976–1998. They found that the first appearance of most species (26 species) is earlier in recent years. This relationship is significant for 13 species, most notably *Anthocharis cardamines* and *Vanessa atalanta* where appearance has advanced by 17.5 and 36.3 days, respectively, over the analyzed period.

In Serbia, shift of biofix timing during the 2012–2021 in respect to historical period is regional specific and varies from 8 days in Cacak region, to 14 days in the region of Kragujevac. During the last monitoring period highest variation of biofix is identified in the region of Belgrade - 20 days. Due to high variability of biofix on country level over the period of intensive monitoring, average values of biofix are not compared with historical data.

Many authors have dealt with estimates of expected climate change on the codling moth. Stoeckli et al. (2012) identified a significant two-week shift to earlier dates in phenological stages, such as overwintering adult flight for the period 2045–2074 in Switzerland. Juszczak et al. (2013) are found that in the Wielkopolska region in Poland, the average date of first imago flights occurred at about 137 DOY in the period of 1972–2005, and it may happen around 110–115 DOY in the period of 2040–2060.

We concluded that the most probable and most important causes of early shifting of biofix day are changes in air temperature in March and April and insolation in February and March. But what we should expect in future? To assess the impact of climate change on codling moth biofix, we analyzed expected air temperature changes from March until May (MAM) (typically available climate model output) for the 2001–2030 and 2071–2100 integration periods of climate models. According to available results, changes in the temperature range from -0.1 to 0.4 °C are expected for MAM at the beginning of the XXI century and from 3.3 to 3.8 °C at the end of the century (Lalic et al., 2020). It implies an even earlier time of biofix in the coming decades.

The earlier occurrence of adults will cause an earlier beginning of egg-laying and egg hatching, and thus the application of insecticides in the control of codling moth. The beginning of the adult's flight is important because it is close to the time for the application of insecticides before the start of egg-laying (juvenile hormone mimics). Plant protection from first-generation larvae is crucial for final fruit yield.

Of particular importance is to determine the exact number of generations over the season because it determines the exposure of apple fruits and the overall risk of damage. According to literature, the codling moth is developing two complete generations in Serbia (Lekic, 1950, Vukasovic et al., 1962, Camprag et al., 1983, Almasi et al., 2004) or 2–3 generations (Miletic et al., 2011). The changes in biofix that have already taken place and the expected changes raise many questions that need further study. It would be essential to determine the exact number of generations that the codling moth develops in Serbia during one year. We assume that the third generation is developing, which will be the subject of further research.

Acknowledgements

Monitoring of the codling moth with pheromone traps by Forecasting and Warning Service in Plant Protection of Serbia (PIS) is financed by the Ministry of agriculture, forestry and water management of the Republic of Serbia and the Provincial Secretariat for agriculture, water management and forestry of Vojvodina province, Republic of Serbia. The study was funded by the Ministry of Education, Science and Technological Development of the Republic of Serbia (Grant No. 451-03-68/2022-14/200117). Part of this study was carried out in context with the ACRP-13th Call Project RIMPEST (“The effect of changing climate on potential risks from important insect pests on plant production in Austria and related adaptation options”) funded by the Climate and Energy Fund.

References

Almasi, R., Injac, M. i Almasi, S., 2004. Stetni i korisni organizmi jabucastih vocaka. Poljoprivredni fakultet, Novi Sad. - in Serbian

Altermatt, F., 2009. Climatic warming increases voltinism in European butterflies and moths. Royal Society Publishing, 277, 1281–1287. doi: 10.1098/rspb.2009.1910

Batistti, A., Marini, L., Pitacco, A. and Larson, S., 2013. Solar radiation directly affects larval performance of a forest insect. Ecological Entomology, 38, 553–559. doi: 10.1111/een.12047

Camprag, D., Krnjaic, Đ., Maceljski, M., Macek, J., Maric, A. i Vrabl, S. 1983. Prirucnik izvestajne i prognozne službe zastite poljoprivrednih kultura. Savez drustava za zastitu bilja Jugoslavije, Beograd, 682. - in Serbian

EPPO Standard PP 2/1(1), 1994. Guideline on good plant protection practice: principles of good plant protection practice. OEPP/EPPO Bulletin 24, 233-240.

Graora, D. i Jerinic-Prodanovic, D., 2005. Dinamika leta i stetnost jabukovog smotavca (Cydiapomonella L). Biljni lekar, vol. 33, br. 6. - in Serbian

Juszczak, R., Kuchar, L., Lesny, J. And Olejnik, J., 2012. Climate change impact on development rates of the codling moth (*Cydia pomonella* L.) in the Wielkopolska region, Poland. International Journal of Biometeorology, 57**,** 31–44. doi: 10.1007/s00484-012-0531-0

Keserovic, Z., Magazin, N., Kurjakov, A., Doric, M. i Gosic, J., 2014. Popis poljoprivrede 2012. Poljoprivreda u Republici Srbiji. Vocarstvo. Republicki zavod za statistiku, ISBN 978-86-6161-118-6. - in Serbian

Lalic, B., Ejcinger, J., Dalamarta, A., Orlandini, S., Firanj Sremac, A. i Paher, B., 2021. Meteorologija i klimatologija za agronome. Univerzitet u Novom Sadu, Poljoprivredni fakultet u Novom Sadu. - in Serbian

Lalic, B., Marcic, M., Sremac, A.F., Eitzinger, J., Koci, I., Petric, T., Ljubojevic, M. and Jezerkic, B. 2020. Landscape Phenology Modelling and Decision Support in Serbia. In Landscape Modelling and Decision Support; Mirschel, W., Terleev, V.V., Wenkel, K.-O., Eds.; Innovations in Landscape Research; Springer International Publishing: Cham, Switzerland, pp. 567-593 ISBN 978-3-030-37420-4.

Lekic, M., 1950. Biologija jabucnog smotavca na teritoriji NR Srbije i mere za njegovo suzbijanje. Zastita bilja, 1, 32-65. - in Serbian

Miletic, N., Tamas, N. and Graora, D., 2011. The control of codling moth (Cydia pomonella L.) in apple trees. Žemdirbystė=Agriculture, vol. 98, No. 2, p. 213–218.

Nikolic, K., 2006. Pocetak leta leptira - znacajan momenat u prognozi jabukinog smotavca (Cydia pomonella). Biljni lekar, vol. 34, br. 2. - in Serbian

Peric, P., Dimic, N., Stamenkovic, S. i Marcic, D., 2004. Efektivnost lambda i gama-cihalotrina u suzbijanju Cydio pomonella L. i Aphis pomi Deg. Pesticidi i fitomedicina, vol. 19, br. 2. - in Serbian

RHMZ, Republicki hidrometeoroloski zavod, (https://www.hidmet.gov.rs) [accessed 19.5.2022.]

Roy, D.B. and Sparks, T.H., 2000. Phenology of British butterflies and climate change. Global Change Biology 6, 407-416.

Stamenkovic, S., Stamenkovic, T. i Pantelic, Ž.,1984. Fenologija leta jabukinog smotavca Cydia (Carpocapsa) pomonella L. (Lepidoptera - Tortricidae). Zastita bilja, 167, 37-46. - in Serbian

Strand, J.F., 2000. Some agrometeorological aspects of pest and disease management for the 21st century. Agricultural and Forest Meteorology, 103, 73-82, doi: 10.1016/S0168-1923(00)00119-2

Vukasovic, P. i sar, 1962. Stetocine u biljnoj proizvodnji. II specijalni deo, Zavod za izdavanje udžbenika SR Srbije, Beograd, 598. - in Serbian

Witzgall, P., Kirsch, P. and Cork, A., 2010. Sex Pheromones and Their Impact on Pest Management. Journal of Chemical Ecology, 36, 80-100, doi: 10.1007/s10886-009-9737-y

The use of the VIIRS active fire product for the determination of fire occurrence per land cover type and seasons for Thailand

Julia Borgman[1,2], Dimitris Stratoulias[1,3], Aekkapol Aekakkararungroj[1,3], Peeranan Towashiraporn[1,3] and Nektaria Adaktylou[4,*]

[1] Asian Disaster Preparedness Center (ADPC), Bangkok, Thailand
[2] Faculty of Geo-Information and Earth Observation (ITC), Enschede, The Netherlands
[3] SERVIR-Mekong, Bangkok, Thailand
[4] West Virginia University, Morgantown, USA

Abstract

In the context of fire monitoring, Earth Observation can provide information on the spatial and temporal relationship between fire occurrence, seasons and land cover that would otherwise be cumbersome to collect at a large scale. The current study explored the relation between VIIRS fire occurrence, seasons and landcover types within Thailand. The Moderate Resolution Imaging Spectroradiometer (MODIS) and Regional Land Cover Monitoring System (RLCMS) annual land cover classification maps of Thailand were compared, as well as the relation of their classes to fire occurrence for the most recent commonly available year, 2018. In addition, the fire occurrence per season was studied for the recent years 2017-2020. It was found that, for 2018, most detected fires occurred during the transition and dry seasons for the cropland classes of the RLCMS and MODIS annual land cover products. Furthermore, for the years 2017-2020, the highest fire count was observed in 2019. It is, therefore, argued that concurrently acquired VIIIRS and MODIS satellite data can provide insights on the land use classes for which fire occurs at large scale, which for the case of Thailand is agricultural cropland. This study aims to give an insight into the relationship between climate and fuel, which could be further investigated and used in policymaking and fire prevention.

1 Introduction

The occurrence of both anthropogenic and natural occurring fires in South-East Asian countries is a contemporary topic (Sirimongkonlertkun, 2012). Biomass burning, as a convenient way of preparing land for agricultural cultivation and disposal of crop residue, results in a seasonal reoccurring haze problem, especially in the annual dry season in Thailand (Arunrat, Pumijumnong, & Sereenonchai, 2018; Quah & Johnston, 2001). Agricultural burning results in immediate benefits for farmers, such as the ease of clearing the field after harvesting and fortification of nutrients to the soil as a substitution of industrial fertilizer. However, this practice may result in wider long-term negative environmental impacts (Sang-Arun, Yamaji, & Boonwan, 2010). In addition, the rising temperatures and altered precipitation patterns, often resulting in more extreme fire events, increase the importance of adequate fire risk monitoring mechanisms (Holsinger, Parks, & Miller, 2016). The occurrence and extent of fires are known to be affected by weather, topography and fuels, referred to as the fire triangle (Holsinger et al., 2016). The latter, the fuel availability, is an important factor that can be altered by human behavior. Understanding the relation between fire occurrence and fuels is essential for studying wildfire risk and assessing possible preventative mitigation measures. The evolution of remote sensing sensors and techniques provides new means of monitoring fire occurrence and fuel distribution at larger scales and in more efficient ways compared to previous field-based only

techniques (Nuthammachot, Askar, Stratoulias, & Wicaksono, 2022). Beside fuels, atmospheric parameters, such as humidity and temperature, dependent on the season, play a role in fire ignition and development. Studying the relation between fire occurrence and seasonal patterns can provide insights into time periods during which the wildfire risk is most severe. The seasons in Thailand can be described by different monthly time intervals and climatic conditions. According to Kliengchuay et al. (2018) the seasons can be divided into three periods. The rainy season spans from June to October and is characterized by frequent rains, where the wettest time period is August to September (Climatological Group Meteorological Department, 2015; Kliengchuay et al., 2018). The dry season runs from November to February, which is known to be the mildest weather period of the year (Kliengchuay et al., 2018). Lastly, the transitional season encompasses the months March to May and is characterized by a slowly increasing temperature leading up to the rainy season, where April is identified as the hottest month of the year (Climatological Group Meteorological Department, 2015; Kliengchuay et al., 2018).

The Visible Infrared Imaging Radiometer Suite (VIIRS) 375m active fire data enables near real-time fire detection with an improved resolution compared to earlier satellite-based fire datasets (Schroeder, Oliva, Giglio, & Csiszar, 2014). Additional metrics, such as the confidence of fire detection and fire radiative power, provide information that can be used for investigating fires and studying their relations with other data sources. In this study, the relationships between VIIRS fire occurrences, seasons and land cover in a South-East Asian country were studied. The focus was on the most recently available land cover and fire data for Thailand nationwide. Two land cover classification products were explored, namely the 500m resolution Moderate Resolution Imaging Spectroradiometer (MODIS) annual Land Cover Type Product (MCD12Q1) with the International Geosphere-Biosphere Programme (IGBP) class descriptions, and the annual Regional Land Cover Monitoring System (RLCMS) classification created by SERVIR-Mekong (SERVIR Mekong, n.d.; Sulla- Menashe & Friedl, 2018).

1.1 VIIRS Active Fire Product

VIIRS is onboard the NOAA-20 and Suomi NPP satellite missions (Schroeder & Giglio, 2017). The instrument collects environmental data, such as vegetation health, fire intensity and smoke plumes. The daily acquisition rate of high-resolution imagery enables near real-time earth monitoring services. For example, the SERVIR- Mekong Air Quality Explorer (MAQE) tool displays operational fire locations in the Mekong region based on the VIIRS I-band 375m active fire product (SERVIR Mekong, n.d.). Besides the location of fires, the VIIRS active fire data has multiple other informative attributes. For the application within the MAQE, the confidence attribute plays an important role, that is providing information on the level of certainty about the fire occurrence at the location, based on a confidence level retrieved from various algorithms. This value can serve as a quality filter during further processing of the VIIRS active fire data.

1.2 MODIS Land Cover Type Product

The MODIS Land Cover Type Product (MCD12Q1) consists of annual global land cover maps with a 500m spatial resolution (Sulla-Menashe & Friedl, 2018). The land cover maps are retrieved through a supervised classification following the decision tree algorithm of MODIS reflectance data. Training data is used to train the classifier and assess the classification results (Sulla-Menashe & Friedl, 2018). The MCD12Q1 product encompasses 13 distinct layers, consisting of different classification schemes and land cover classification systems. In addition, a quality assurance layer and land/water masks are supplemented to provide additional information. The created land cover maps are validated through cross-validation with the initial training data to assess their classification accuracy. At the time of writing, the most recent MODIS land cover map is of 2020.

1.3 SERVIR RLCMS

The MODIS Land Cover Type Product (MCD12Q1) consists of annual global land cover maps with a 500m spatial resolution (Sulla-Menashe & Friedl, 2018). The land cover maps are retrieved through a supervised classification following the decision tree algorithm of MODIS reflectance data. Training data is used to train the classifier and assess the classification results (Sulla-Menashe & Friedl, 2018). The MCD12Q1 product encompasses 13 distinct layers, consisting of different classification schemes and land cover classification systems. In addition, a quality assurance layer and land/water masks are supplemented to provide additional information. The created land cover maps are validated through cross-validation with the initial training data to assess their classification accuracy. At the time of writing, the most recent MODIS land cover map is of 2020. The RLCMS is created through a collaborative development process by multiple stakeholders (SERVIR Mekong, n.d.). The process is implemented in Google Earth Engine and due to its flexibility, it can be updated at any time using new datasets. Besides the available data, such as that related to elevation and infrastructure, the main basis for the RLCMS consists of the publicly available USGS Landsat data. After defining the requirements and collecting reference data, primitives are developed, which consist of mappable elements that describe a class and form a basis for making decisions. Within the RLCMS, the Monte Carlo analysis is used to assign land cover classes to primitives (SERVIR Mekong, n.d.). This method enables the creation of a deterministic decision tree, where the focus lies on using probability measures of belonging to a certain land cover class instead of numerical thresholds. The intermediate results are validated through an accuracy assessment, which consists of a visual interpretation to detect possible anomalies and a quantitative accuracy assessment (SERVIR Mekong, n.d.). The most recently updated RLCMS map from the SERVIR Mekong website dates back to 2018 at the time of writing.

2 Methodology

2.1 Data preprocessing and acquisition

The main objective of this research was to study the relation between VIIRS fire occurrences and land cover maps and establish a methodology which can be applied in other settings and time periods. Similar to previous research in the field of wildfire risk assessment, the focus of this study lied on the use of public domain geospatial data, which is freely available to the public (Adaktylou, Stratoulias, & Landenberger, 2020). For this research, the MCD12Q1 was directly downloaded from the NASA Land Processes Distributed Active Archive Center (LP DAAC) in tile format according to the extent of the study site using the R statistical programming language (R Core Team, 2020). The tiles in hdf format were converted to GeoTIFF, reprojected to the same coordinate system as the VIIRS data and clipped to the exact boundary of Thailand. The annual VIIRS product, in the form of a csv file, was directly read into R using web scraping commands. The R code was automated to enable creating landcover mosaics and reading VIIRS fire products for different years, by adjusting variables initialized in the code.

2.2 VIIRS filtering and land cover extraction

The VIIRS fire occurrence was filtered based on the confidence value “high”, to only include fires with a high likelihood of occurrence of an actual fire. A column was added to count possible fire duplicates that occurred at the same coordinates within the selected year, which can be used for further research. Apart from the annual fire count, the fire count per season was studied. The seasonal month ranges defined

by the Climatological Group (2015) were used to define the seasons within this study. In this study, the dry season spans from November to February, the transitional season from March to May and the rainy season from June to October. The acquisition date of each fire was used as an input for classifying the fire into one of the three seasons. To find the corresponding land cover class for each fire occurrence, the corresponding land cover raster values were extracted for each fire using the coordinates. The resulting data frame includes the season in which the fire occurred and the land cover class, according to the MODIS or RLCMS land cover classification.

3.Results

3.1. VIIRS fire occurrences per season in Thailand from 2017-2020

As shown in figure 1, the number of fires is overall the highest during the transition season in recent years. However, in 2020, the number of fires in the dry and transition season have become comparable. It can be seen that the number of fires in the longest season, the rainy season, which lasts for 5 months, is significantly lower compared to the other seasons during all studied years.

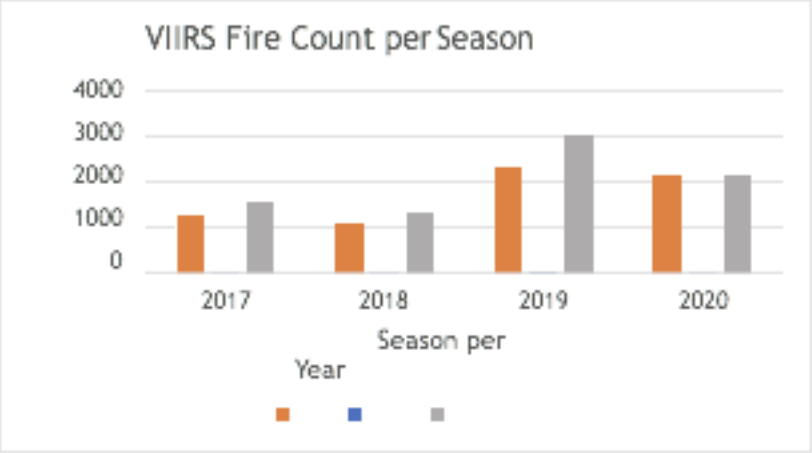

Figure 1: *Fire occurrences per land cover class for 2017-2020*

3.2 Comparison between the RLCMS and MODIS land cover and fire occurrences in Thailand for 2018

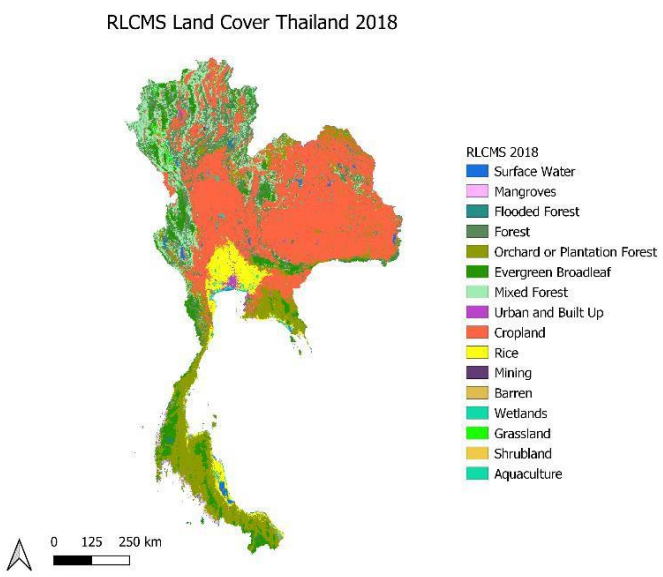
RLCMS Land Cover Thailand 2018
RLCMS 2018
Surface Water
Mangroves
Flooded Forest
Forest
Orchard or Plantation Forest
Evergreen Broadleaf
Mixed Forest
Urban and Built Up
Cropland
Rice
Mining
Barren
Wetlands
Grassland
Shrubland
Aquaculture
0 125 250 km

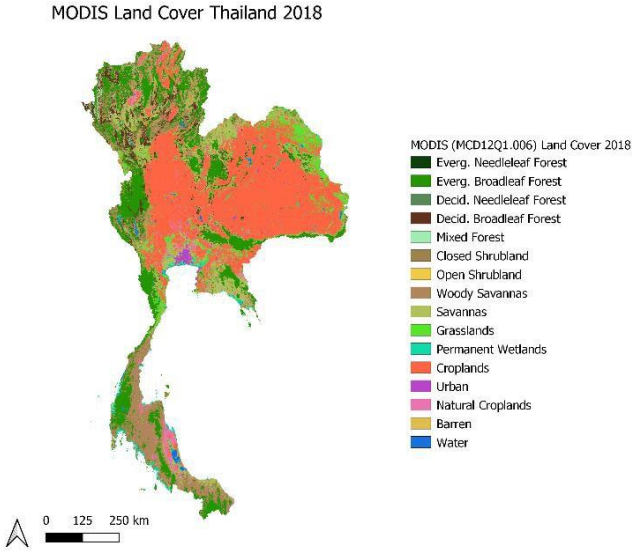
MODIS Land Cover Thailand 2018
MODIS (MCD12Q1.006) Land Cover 2018
Everg. Needleleaf Forest
Everg. Broadleaf Forest
Decid. Needleleaf Forest
Decid. Broadleaf Forest
Mixed Forest
Closed Shrubland
Open Shrubland
Woody Savannas
Savannas
Grasslands
Permanent Wetlands
Croplands
Urban
Natural Croplands
Barren
Water
0 125 250 km

Figure 2: *RLCMS land cover map*

Figure 3: *MODIS land cover map*

The MODIS and RLCMS land cover classification products include similar, as well as different land cover classes. As shown in figures 2 and 3, the overall distribution of cropland appears to be similar between both classifications, however the RLCMS map includes various land classes more specific for Thailand and the Mekong region, such as mangroves, plantation forest and rice cultivation. The MODIS land cover map consists of global land cover classes, of which some are non-existing in Thailand, such as needleleaf forests.

Figure 4 depicts the fire count percentages per land cover for the RLCMS land cover classes and figure 5 for the MODIS land cover for the year 2018. The fire count on cropland is significantly higher compared to the other classes for both land cover datasets. A potential explanation could be agricultural burning, which is a well-known practice in the region, especially in the north of Thailand during the dry season (Arunrat et al., 2018). For the RLCMS dataset, the second and third classes with the highest fire count are the mixed forest and forest classes, followed by rice cultivation.

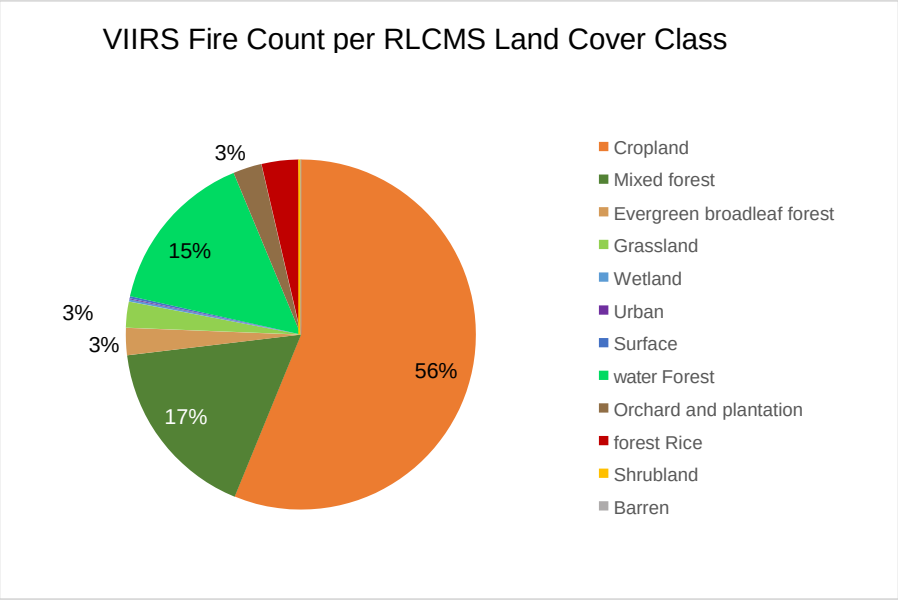

Figure 4: *Fire occurrences per land cover class for the RLCMS land cover data in 2018*

For the MODIS land cover map, the second and third highest fire counts can be observed for the woody savanna and savanna classes, followed by grasslands and broadleaf forest classes.

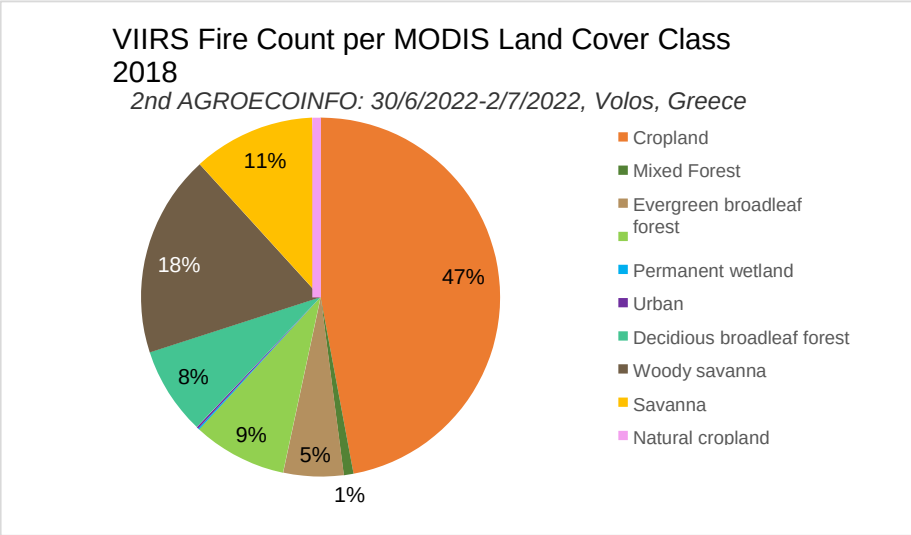

For the MODIS land cover map, the second and third highest fire counts can be observed for the woody savanna and savanna classes, followed by grasslands and broadleaf forest classes.

Figure 5: *Fire occurrences per land cover class for the MODIS land cover data in 2018*

Overall, it can be seen that both land cover classifications indicate that the highest number of fires occur on cropland for the year 2018. The main differences consist of the fires occurring on woody savannas and savannas for the MODIS data compared to forest and mixed forest for the RLCMS data. Lastly, the RLCMS data indicates that fires have occurred on land classified as rice cultivation, which is a class that is not included in the MODIS classification.

4 Summary

In this study, the distribution of high confidence VIIRS fire observations has been studied over three different seasons. The longest season, the rainy season, depicts significantly less to almost no fires compared to the other two seasons, while the transition season has the highest fire count. This is an observation that could be dependent on the season definitions used during this study and could be further investigated in future studies. However, the fire occurrence gap between the transition and dry season decreased in the year 2020. Overall, between the studied years, 2019 has the highest fire count. The fire occurrences per land cover class for the year 2018 have been compared between the MODIS and RLCMS land cover classification products. The classifications show similarities within their land cover classes, but also differences. The RLCMS data is more adapted to the Mekong region compared to the MODIS classes, the latter being more globally oriented. When comparing the fire count per land cover class, the croplands clearly showed the highest fire count, which could be potentially linked to agricultural burning. For the MODIS data, other classes with high fire counts were woody savannas and savannas. Whereas for the RLCMS data, other classes with high fire counts were forests and mixed forests.

Acknowledgements
The VIIRS fire dataset was accessed through the NASA FIRMS website. The RLCMS land cover map was provided by the SERVIR-Mekong land cover tool and the MODIS dataset was downloaded through the NASA open directory.

References
Adaktylou, N., Stratoulias, D., & Landenberger, R. (2020). Wildfire Risk Assessment Based on Geospatial Open Data: Application on Chios, Greece. ISPRS International Journal of Geo-Information 2020, Vol. 9, Page 516, 9(9), 516. https://doi.org/10.3390/IJGI9090516

Arunrat, N., Pumijumnong, N., & Sereenonchai, S. (2018). Air-Pollutant Emissions from Agricultural Burning in Mae Chaem Basin, Chiang Mai Province, Thailand. Atmosphere 2018, Vol. 9, Page 145, 9(4), 145. https://doi.org/10.3390/ATMOS9040145

Climatological Group Meteorological Department. (2015). The Climate Of Thailand. Retrieved from https://www.tmd.go.th/en/archive/thailand_climate.pdf

Holsinger, L., Parks, S. A., & Miller, C. (2016). Weather, fuels, and topography impede wildland fire spread in western US landscapes. Forest Ecology and Management, (380), 59–69. https://doi.org/10.1016/j.foreco.2016.08.035

Kliengchuay, W., Meeyai, A. C., Worakhunpiset, S., & Tantrakarnapa, K. (2018). Relationships between meteorological parameters and particulate matter in Mae Hong Son province, Thailand. International Journal of Environmental Research and Public Health, 15(12). https://doi.org/10.3390/ijerph15122801

Nuthammachot, N., Askar, A., Stratoulias, D., & Wicaksono, P. (2022). Combined use of Sentinel-1 and Sentinel-2 data for improving above-ground biomass estimation. Geocarto International, 37(2), 366–376. https://doi.org/10.1080/10106049.2020.1726507

Quah, E., & Johnston, D. (2001). Forest fires and environmental haze in Southeast Asia: Using the 'stakeholder' approach to assign costs and responsibilities. Journal of Environmental Management, 63(2), 181–191. https://doi.org/10.1006/JEMA.2001.0475

R Core Team. (2020). R: A Language and Environment for Statistical Computing. Vienna, Austria. Retrieved from https://www.r-project.org/

Sang-Arun, J., Yamaji, E., & Boonwan, J. (2010). Promoting Plant Residue Utilization for Food Security and Climate Change Mitigation in Thailand, 343–352. https://doi.org/10.1007/978-90-481-9914-3_34

Schroeder, W., & Giglio, L. (2017). Visible Infrared Imaging Radiometer Suite (VIIRS) 750 m Active Fire Detection and Characterization Algorithm Theoretical Basis Document 1.0.

Schroeder, W., Oliva, P., Giglio, L., & Csiszar, I. A. (2014). The New VIIRS 375m active fire detection data product: Algorithm description and initial assessment. Remote Sensing of Environment, 143. https://doi.org/10.1016/j.rse.2013.12.008

SERVIR Mekong. (n.d.). Portal User Guide and Manual. Retrieved May 2, 2022, from https://gdoc.pub/doc/e/2PACX- 1vQWuDUyC3KO0GMrqxvP2uc_LvUgkCAnU-cAIqJx5G0A0h7V7UyNF3gEkXMjorwE059Y06DwpyJCVfcb

Sirimongkonlertkun, N. (2012). Effect from Open Burning at Greater Mekong Sub-Region Nations to the PM10 Concentration in Northern Thailand: A Case Study of Backword Trajectories in March 2012 at Chiang Rai Province. Retrieved from https://mfuic2012.mfu.ac.th/electronic_proceeding/Documents/00_PDF/O-SC-D/O-SC-D- 008.pdf

Sulla-Menashe, D., & Friedl, M. A. (2018). User Guide to Collection 6 MODIS Land Cover Product. https://doi.org/10.5067/MODIS/MCD12Q1

Seasonal Standardized Precipitation Index (SPI) over the Mediterranean region

Iliana D. Polychroni[1], Ioannis Charalampopoulos[2], Panagiotis T. Nastos[1] and Maria Hatzaki[1]

[1]Laboratory of Climatology and Atmospheric Environment, Department of Geology and Geoenviroment, National and Kapodistrian University of Athens, University Campus, GR 15784 Athens, Greece
[2] Laboratory of General and Agricultural Meteorology, Agricultural University of Athens, Athens 118 55, Greece

Abstract. Mediterranean region is an area with unique geophysical, historical and cultural history. According to IPCC 2014, the surface temperature is projected to rise over the 21st century and the mean precipitation is likely to decrease in mid-latitude dry regions. Consequently, we confronted the challenge to study the drought over the Mediterranean region, by means of the Standardized Precipitation Index (SPI), defined as the difference from the mean for a specified time period divided by the standard deviation, where the mean and standard deviation are determined from past records. The upcoming climate change will affect the water resource system of the Mediterranean; thus drought is a long-range phenomenon that has severe environmental, economic and social impacts. The objective of this study is to assess and analyze the spatio-temporal evolution of the SPI for 6-month timescale, during the period 1950-2018. More specifically, we investigate the SPI_6 for March and SPI_6 for September concerning the following two 6-month seasons: the Winter-Half, which consists of the months of October, November, December, January, February and March, and the Summer-Half, which consists of April, May, June, July, August and September, respectively. We choose these specific two 6-month SPI timescale, because SPI at the end of March would provide useful information of the amount of precipitation that has fallen during the wet season period from October through March for certain Mediterranean locales. Towards this purpose, we processed the high resolution gridded daily precipitation dataset (0.1° x 0.1°; v.19e), based on the E-OBS dataset from European Climate Assessment & Dataset (ECA&D). The SPI_6 values were calculated with the package 'SPEI' in R-project. Mean SPI_6 patterns and trends covering the Mediterranean region, for the entire period (1950-2018) and for consecutive 30-year periods (eg. 1950-1979, 1951-1980 etc.) were estimated using R-project.
.

1 Introduction

The Intergovernmental Panel on Climate Change in 2014 (IPCC, 2014) reported that the surface temperature is projected to rise over the 21st century and the mean precipitation will likely decrease in mid-latitude dry regions. These changes are expected to affect the human activities in the upcoming years, since the frequency and intensity of major extreme weather events such as heat waves, floods and droughts will change. As reported by FAO & WWC (2015), climate change can affect both surface- and ground- water quality and quantity, and as a result modify the agricultural production and the associated ecosystems. These impacts are considered to be greater in arid regions, on shallow aquifers, and on ecosystems already stressed (Kløve et al., 2014; Menberg et al., 2014).
Drought is a natural either local or regional phenomenon and refers to a prolonged period (weeks, months, seasons or years) of drier than normal conditions resulting in reduction of water availability. The main drought types concern meteorological, climatological, hydrological, atmospheric, agricultural, socioeconomic and water management (Wilhite and Glantz, 1985). Generally, drought is characterized by three parameters: intensity, duration and spatial extent (Rossi et al., 1992). Droughts considered to be natural disasters and they may have severe impacts on various sectors of agriculture, economy, environment and society. According to literature, a number of drought indices have been applied during the twentieth century in order to quantify, monitor and analyze drought events, among those are: the Palmer Drought Severity Index (Palmer, 1965), the Crop Moisture Index (Palmer, 1968), the Surface Water Supply Index (Shafer and Dezman, 1982), the Standardized Precipitation Index (SPI) (McKee et al., 1993) and the Reconnaissance Drought Index (Tsakiris and Vangelis, 2005; Tsakiris et al., 2007). SPI is an index simple to calculate, since the only meteorological parameter required is the precipitation and it is also flexible as it can be computed for multiple timescales (McKee et al., 1993; WMO, 2012). Therefore, the use of the SPI index lately has been increased by many scientists in order to assess the drought intensity in different countries of the world (Manasta et al., 2010; Blain, 2012; Shahabfar and Eitzinger, 2013; Mathbout et al., 2017) and especially in the Mediterranean region (Karavitis et al., 2011; Buttafuoco et al., 2015; Paparrizos et al., 2016; Kostopoulou et al., 2017, Caloiero et al., 2018, Achite et al., 2022).

The objective of this study is to analyze the drought severity in the Mediterranean region during the period 1950-2018 by applying the SPI index for two 6-months seasons: the Winter-Half and the Summer-Half. The spatiotemporal evolution of the means and trends of SPI index could provide us useful information and help us to understand how the water resources system of the Mediterranean is influenced by changes in climate conditions.

2 Study area, data and methods

The study area of this research is the wider Mediterranean region. Mediterranean region has a very specific climate with warm, dry, sunny summers and mild, wet winters (Csa, Csb, according to Köppen classification) which makes it very sensitive to potential climatic changes (Philandras et al., 2011; Nastos et al., 2013).
SPI index is defined as the difference from the mean precipitation for a specified time period divided by the standard deviation, where the mean and standard deviation are determined from past records. According to Guttman (1999), the SPI is probability based and was designed to be a spatially invariant indicator of drought that recognizes the importance of time scales in the analysis of water use and water availability. For computational accuracy of the SPI, Guttman (1994) suggested that there must be at least 30 years of monthly precipitation data, with 50-60 years being preferred. For the calculation of SPI for any location, the long-term monthly precipitation data for a period is fitted to a gamma probability distribution and turned into the normal distribution, so that the mean SPI for the examined location and period is zero (Edwards and McKee, 1997), that is the values of SPI are actually seen as standard deviations from the median. The classification of drought conditions by means of SPI classes are shown in Table 1. Positive/negative SPI values indicate higher/lower than median precipitation.

Table 1. Classification of drought conditions according to SPI (McKee et al., 1993).

SPI values	Category
≥ 2.00	Extreme wet
1.50 to 1.99	Severe wet
1.00 to 1.49	Moderate wet
0 to 0.99	Mild wet
0 to -0.99	Mild drought
-1.00 to -1.49	Moderate drought
-1.50 to -1.99	Severe drought
≤ -2.00	Extreme drought

For this study, high resolution gridded daily precipitation datasets were processed covering the period January 1, 1950 - December 31, 2018, based on the E-OBS dataset (0.10° x 0.10°; v.19e) from the European Climate Assessment & Dataset (ECA&D, Klein Tank et al., 2002; www.ecad.eu).
All the calculation along with the spatiotemporal analysis were carried out by using R-project. More specifically, the package 'SPEI' was used for the calculation of SPI. The SPI_6 values were calculated for each month of the year for the period 1950-2018 over the Mediterranean region. The SPI_6 for March and SPI_6 for September refer to the following two 6-month seasons; namely, the Winter-Half, which consists of the months of October, November, December, January, February and March, and the Summer-Half, which consists of April, May, June, July, August and September, respectively. Moreover, the SPI_6 means and trends were calculated for consecutive 30-year periods (eg. 1950-1979, 1951-1980, 1952-1981 etc) for the examined area.

3 Results

Regarding the SPI_6 means for March and September for the period 1950-2018 (figure 1), it is obvious that in many regions of the Mediterranean the values are below zero with slight decreases, meaning that the conditions there are mild dry. More specifically, the lowest means (near to -0.4) of SPI_6 for March (1950-2018) appear in central Spain, Italy, Greece and in the southeastern part of the Mediterranean (Cyprus, Jerusalem, Egypt) but as far as it concerns the lowest means of SPI_6 for September, they are spotted in north Morocco, northwest Algeria, south Spain, Corsica, coastal zone of south France and northwest Italy, and in North Greece. Looking at the SPI_6 trends for March and September during the period 1950-2018, one could remark statistically significant decreasing trends (from -0.02 to -0.05) for both seasons in many areas (north Portugal, central Morocco, north Algeria, Tunisia, Libya, Sicily, north Italy, south Greece and Turkey) against increasing trends mainly for March (from 0.02 t0 0.05) in central Italy, Austria, Croatia, Romania and Jerusalem.

The evolution of SPI_6 means and trends for March and September over consecutive 30-years periods (1951-1980, 1961-1990, 1971-2000 and 1981-2010), are depicted in figure 2 and 3, respectively. Taking into consideration the evolution of SPI_6 means for March and September over consecutive 30-years periods, the lowest values, in both cases, are observed during the periods 1971-2000 and 1981-2010 in most areas of the Mediterranean, especially within the last period 1981-2010, indicating that the Mediterranean region experiences drier conditions (less than median precipitation) nowadays. More specifically, it should be mentioned that lower values appeared in all evolution maps of SPI_6 means for March than in SPI_6 means for September, over consecutive 30-years periods, meaning that in the Winter-Half season prevailed more dry conditions than in the Summer-Half.

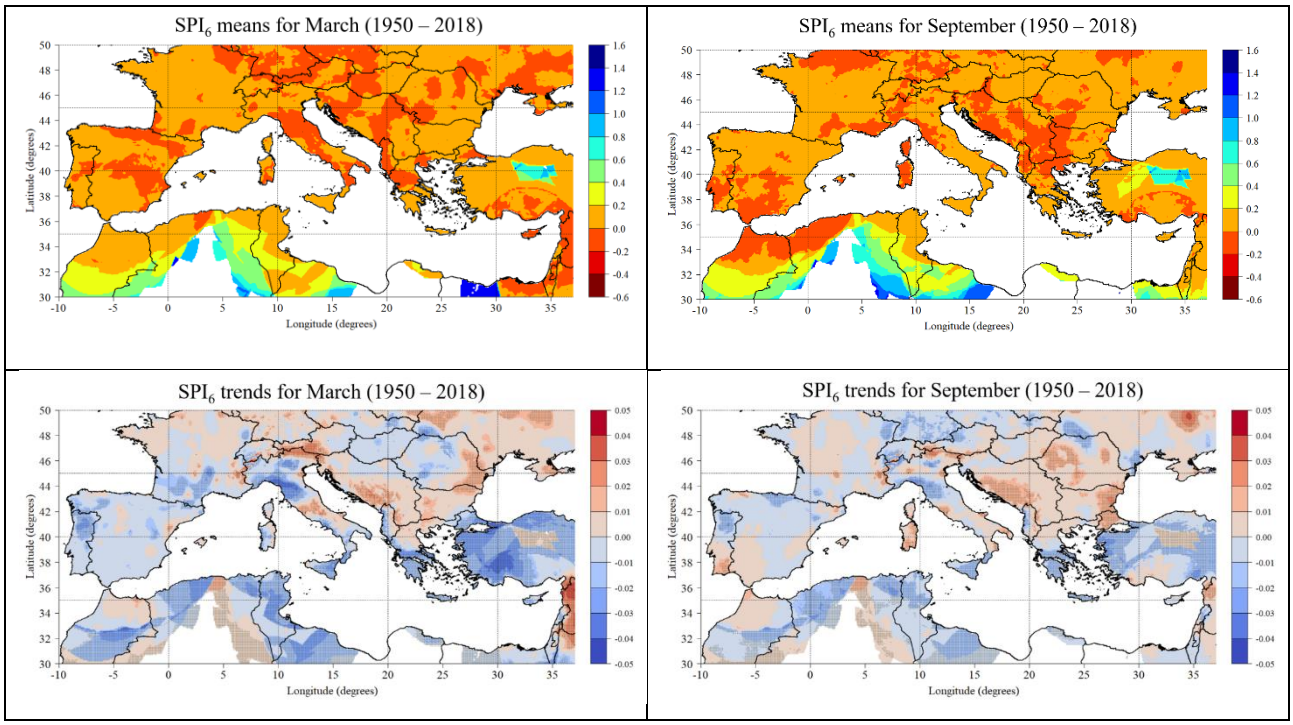

Figure 1. SPI_6 means for March and September during the period 1950-2018. SPI6 trends for March and September during the period 1950-2018. The values with asterisk (*) refer to statistically significant trends at 95% cl.

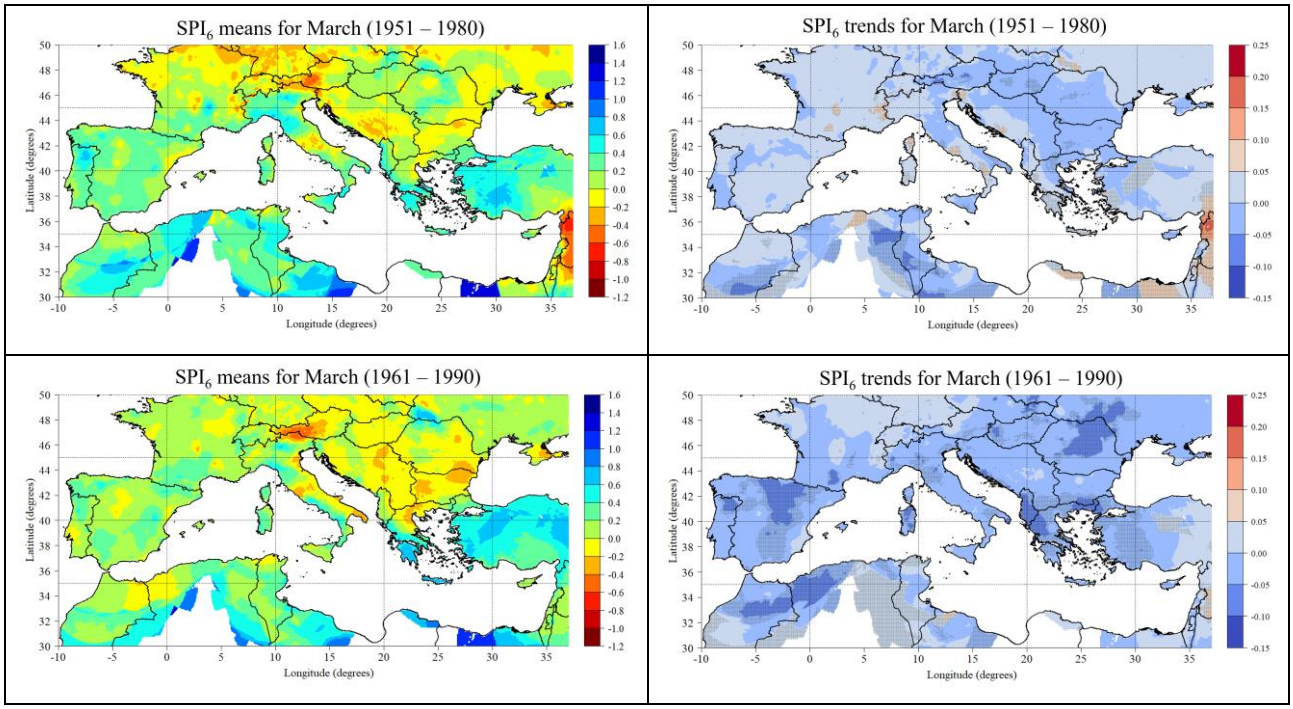

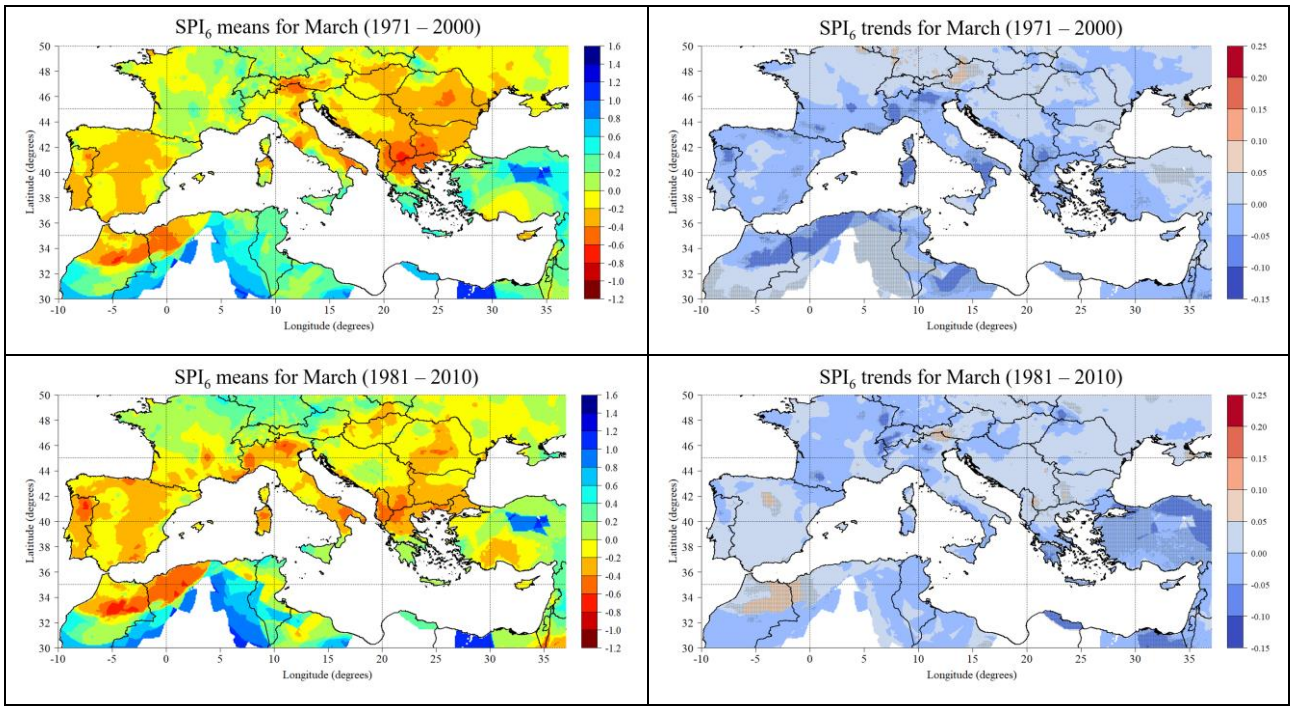

Figure 2. Evolution of March SPI_6 means and trends over consecutive 30-years periods. The values with asterisk (*) refer to statistically significant trends at 95% cl.

Looking the SPI_6 trends for March and September over consecutive 30-years periods, there are generally decreasing trends in most areas of the Mediterranean region. Regarding the period 1961-1990 of SPI_6 trends for March, there are found the lowest decreasing statistically significant trends (at 95% C.L.) in Iberian Peninsula, Morocco, Greece and Turkey. Moreover, within the period 1981-2010 for SPI_6 for March, there are some increasing trends (0.15) in Austria, central Spain and Morocco. It is worth noting that within the period 1951-1980 there are increasing SPI_6 trends for September in Italy, Croatia, Romania and Ukraine against decreasing trends in Morocco, Tunisia and Austria. This situation changed and in period 1981-2010, there are statistically significant increasing SPI_6 trends for September in north Greece, Austria and Bulgaria against decreasing not statistically significant trends which prevail in most areas.

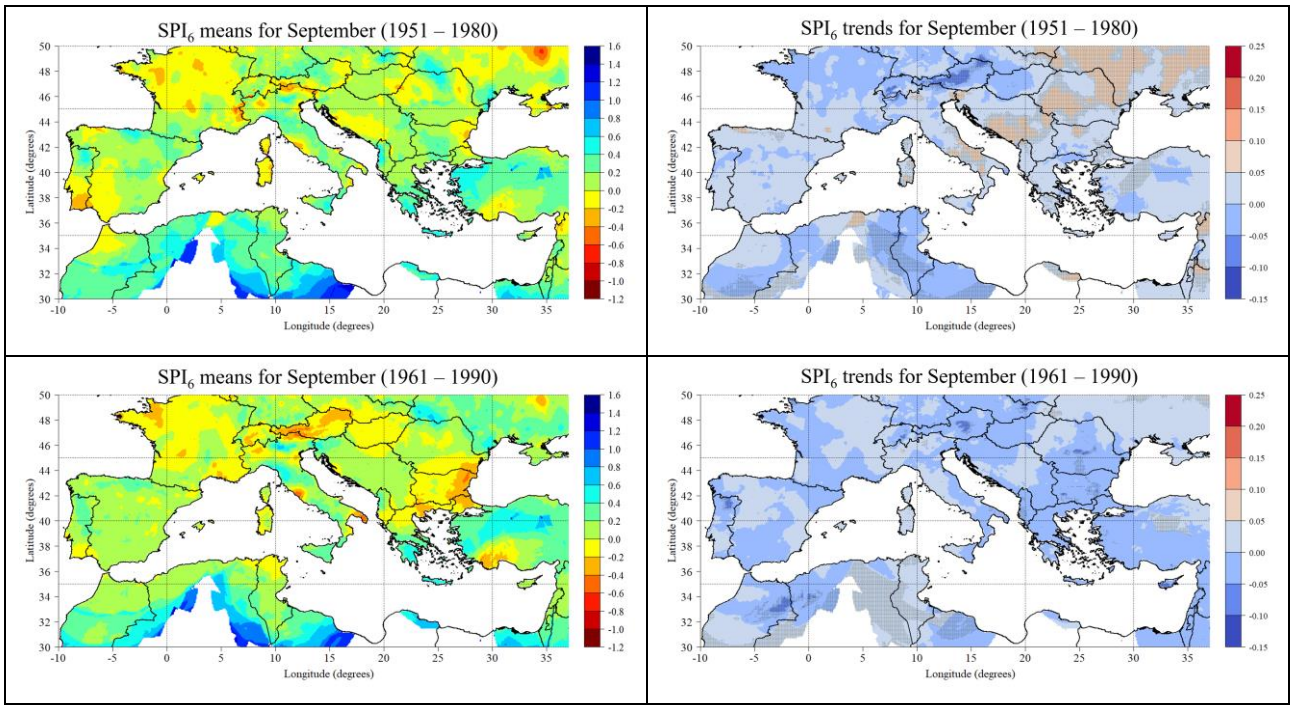

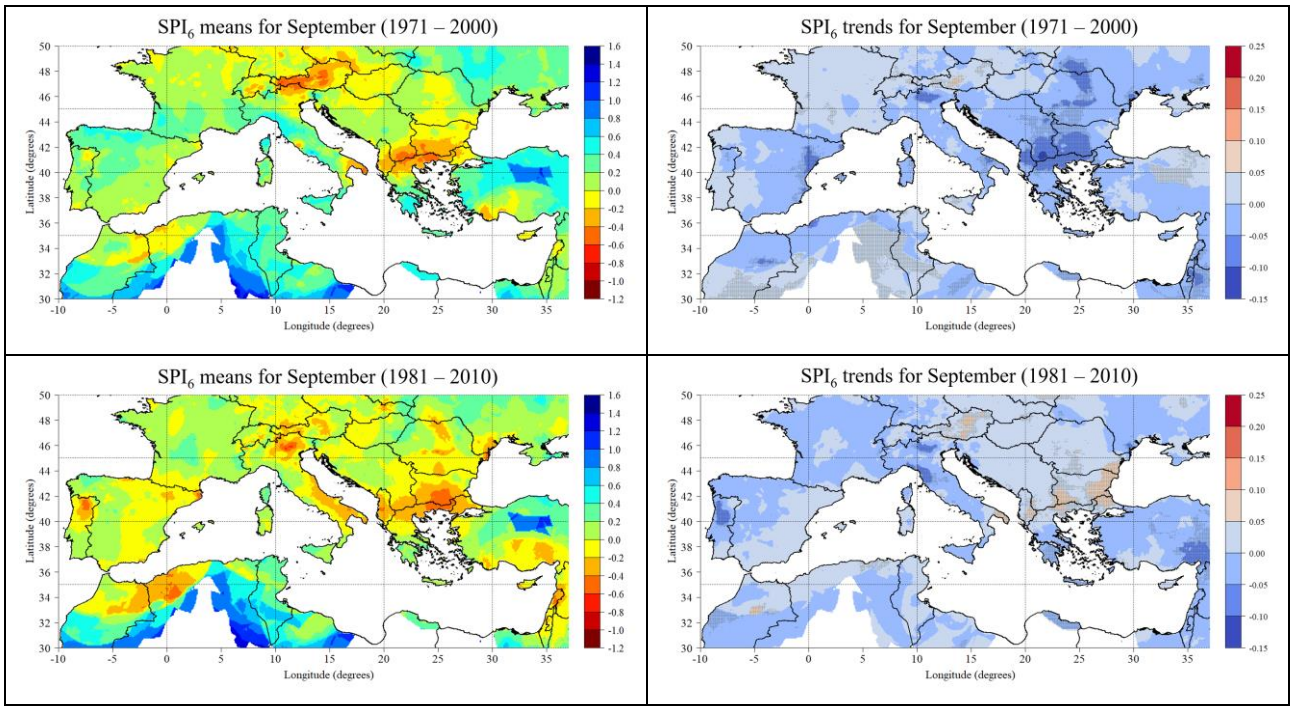

Figure 3. Evolution of September SPI_6 means and trends over consecutive 30-years periods. The values with asterisk (*) refer to statistically significant trends at 95% cl.

4 Summary

The main findings of this study are summarized as follows:

- Regarding the SPI_6 means for March and September for the period 1950-2018, it is obvious that in many regions of the Mediterranean the values are below zero with slight decreases, meaning that the conditions there are mild dry.
- The evolution of SPI_6 means for March and September over consecutive 30-years periods showed that the lowest values, in both cases, are observed during the periods 1971-2000 and 1981-2010 in most areas of the Mediterranean, especially within the last period 1981-2010, indicating that the Mediterranean region experiences drier conditions (less than median precipitation) nowadays.
- As the evolution of the SPI_6 trends for March and September over consecutive 30-years periods are concerned, there are generally decreasing trends in most areas of the Mediterranean region.

References

Achite, M., Bazrafshan, O., Azhdari, Z., Wałęga, A., Krakauer, N.; Caloiero, T., 2022. Forecasting of SPI and SRI Using Multiplicative ARIMA under Climate Variability in a Mediterranean Region: Wadi Ouahrane Basin, Algeria. Climate, 10, 36.

Blain, G.C., 2012. Monthly values of the standardized precipitation index in the State of São Paulo, Brazil: trends and spectral features under the normality assumption. Bragantia, 71(1): 460-470.

Buttafuoco, G., Caloiero, T. and Coscarelli R., 2015. Analyses of Drought Events in Calabria (Southern Italy) Using Standardized Precipitation Index. Water Resources Management, 29: 557–573.

Caloiero T, Veltri S, Caloiero P, Frustaci F., 2018. Drought Analysis in Europe and in the Mediterranean Basin Using the Standardized Precipitation Index. Water, 10(8):1043.

Edwards, D.C and McKee, T.B., 1997. Characteristics of 20th century drought in the United States at multiple time scales. Atmospheric Science Paper, 634: 1–30.

FAO (Food and Agriculture Organization of the United Nations) and WWC (World Water Council), 2015. Towards a water and food secure future: Critical Perspectives for Policy-makers. FAO/WWC, Rome/Marseille.

Guttman, N.B., 1994. On the Sensitivity of Sample L Moments to Sample Size. Journal of Climate, 7: 1026-1029.

Gutmann, N.B., 1999. Accepting the standardized precipitation index: a calculation algorithm. Journal of American Water Resources Association, 35(2): 311–322.

IPCC (Intergovernmental Panel on Climate Change), 2014. Climate Change 2014: Synthesis Report. Contribution of Working Groups I, II and III to the Fifth Assessment Report of the Intergovernmental Panel on Climate Change [Core Writing Team, R.K. Pachauri and L.A. Meyer (eds.)]. IPCC, Geneva, Switzerland.

Karavitis, C.A, Alexandris, S., Tsesmelis, D.E. and Athanasopoulos, G., 2011. Application of the standardized precipitation index (SPI) in Greece. Water, 3: 787–805.

Klein Tank, A.M.G. and Coauthors, 2002. Daily dataset of 20th-century surface air temperature and precipitation series for the European Climate Assessment. International Journal of Climatology, 22: 1441-1453.

Kløve, B., Ala-Aho, P., Bertrand, G., Gurdak, J.J., Kupfersberger, H., Kværner, J., Muotka, T., Mykrä, H., Preda, E., Rossi, P., Uvo, C.B., Velasco, E. and Pulido-Velazquez, M., 2014. Climate change impacts on groundwater and dependent ecosystems. Journal of Hydrology, 518: 250-266.

Kostopoulou, E., Giannakopoulos, C., Krapsiti, D. and Karali, A., 2017. Temporal and Spatial Trends of the Standardized Precipitation Index (SPI) in Greece Using Observations and Output from Regional Climate Models. In: Karacostas T., Bais A., Nastos P. (eds) Perspectives on Atmospheric Sciences. Springer Atmospheric Sciences. Springer, Cham.

Manatsa, D., Mukwada, G., Siziba, E. and Chinyanganya, T., 2010. Analysis of multidimensional aspects of agricultural droughts in Zimbabwe using the Standardized Precipitation Index (SPI). Theoretical and Applied Climatology, 102: 287–30.

Mathbout S., Lopez-Bustins J., Martin-Vide Jm, Bech J., Rodrigo F., 2018. Spatial and temporal analysis of drought variability at several time scales in Syria during 1961–2012, Atmospheric Research, 200,153-168.

McKee, T.B., Doesken, N.J. and Kleist, J., 1993. The relationship of drought frequency and duration to time scales. In Proceedings of the 8th Conference on Applied Climatology, Boston, MA: American Meteorological Society, 17(22): 179-183.

Menberg, K., Blum, P., Kurylyk, B.L. and Bayer, P., 2014. Observed groundwater temperature response to recent climate change. Hydrology and Earth System Sciences, 18(11): 4453-4466.

Nastos, P., Kapsomenakis, J. and Douvis, K., 2013. Analysis of precipitation extremes based on satellite and high-resolution gridded data set over Mediterranean basin. Atmospheric Research, 131: 46–59.

Palmer, W.C., 1965. Meteorological drought. US Department of Commerce Weather Bureau Research Paper No. 45.

Palmer, W.C., 1968. Keeping track of crop moisture conditions, nationwide: The new crop moisture index. Weatherwise, 21: 156-161.

Paparrizos, S., Maris, F., Weiler, M. and Matzarakis, A., 2016. Analysis and mapping of present and future drought conditions over Greek areas with different climate conditions. Theoretical and Applied Climatology, doi:10.1007/s00704-016-1964-x.

Philandras, C.M., Nastos, P.T., Kapsomenakis, J., Douvis, K.C., Tselioudis, G., and Zerefos, C.S., 2011. Long term precipitation trends and variability within the Mediterranean region, Natural Hazards and Earth System Sciences, 11: 3235-3250, doi:10.5194/nhess-11-3235-2011, 2011.

Rossi, G., Benedini, M., Tsakiris, G. and Giakoumakis, S., 1992. On regional drought estimation and analysis. Water Resources Management, 6(4):249-277.

Shahabfar A, Eitzinger J., 2013. Spatio-Temporal Analysis of Droughts in Semi-Arid Regions by Using Meteorological Drought Indices. Atmosphere, 4(2):94-112.

Tsakiris, G. and Vangelis, H., 2005. Establishing a drought index incorporating evapotranspiration. European Water, 9/10: 3-11.

Tsakiris, G., Pangalou, D., and Vangelis, H., 2007. Regional drought assessment based on the reconnaissance drought index (RDI). Water Resources Management, 5(21): 821–833.

Wilhite, D.A. and Glantz, M.H. (1985). Understanding: the drought phenomenon: the role of definitions. Water international, 10(3):111-120.

World Meteorological Organization, 2012. Standardized Precipitation Index User Guide (M. Svoboda, M. Hayes and D. Wood). (WMO-No. 1090), Geneva.

SESSION 2:
ECOLOGICAL MANAGEMENT

FAIRness of Micrometeorological Data and Responsible Research and Innovation: an Open Framework for Climate Research

Branislava Lalic,[1] Ivan Koci,[2] Mark Roantree[3]

[1]Faculty of Agriculture, University of Novi Sad, Novi Sad, Serbia
[2] Forecasting and Reporting Service for Plant Protection of the Republic of Serbia (PIS)

[3] Insight Centre for Data Analytics, School of Computing, Dublin City University, Ireland.

Abstract. During the XX century, the atmospheric science community became one of the major "big data" sources, and micrometeorological measurements are an important part of it. This trend is still going strong, supported by networks of so-called "unconventional" measurements and SMART technologies (citizen weather networks and meteorological instruments on different mobile devices, for example). The potential weakness of data coming from such diverse sources is the lack of **f**indability, **a**ccessibility, **i**nteroperability, and **r**eusability (FAIR). The opportunity for improvement is "to define a minimal set of related but independent and separable guiding principles and practices, which enable both machines and humans to find access, interoperate and reuse research data and metadata" (PwC EU Services, 2018). Enhanced FAIRness of micrometeorological data strongly supports almost all main pillars of Responsible Research and Innovation (RRI), particularly in STEM and STEM-related fields, leaving room for different levels of accessibility since FAIRness does not imply Open data status.
In a case study, an initial FAIRness assessment is performed for micrometeorological data measured in an orchard within the Forecasting and Reporting Service for Plant Protection of the Republic of Serbia (PIS) observational network.

1 Introduction

RRI concept. In an ideal World, Responsible Research and Innovation (RRI) projects and initiatives would be redundant. The collective consciousness of the research community will be enough to:

a) provide Open Access (OA) to research results (publications, data, models, methodologies),
b) pursue high-quality Science Education (SE) by committing our collective knowledge through science textbooks for all educational levels-from elementary to graduate schools;
c) develop equal opportunity research environments regardless of gender (Gender Equality), race, nationality, or religion;
d) provide whole Public Engagement (PE) in research and SE by maintaining communication with the general and specialized public and supporting Citizen Science (CS) initiatives;
e) overcome all ethical issues (Ethics) by constructive discussions with all interested parties;
f) participate in Governance (GOV) and convince policymakers that research results should be fully considered while designing strategic, long-term, and short-term plans.

However, a survey conducted in 2017 involving about 3100 researchers receiving H2020 funding revealed that most of them were unaware of the RRI concept (Novitsky, Bernstein, Blok, Braun, Chan, Lamers, Loeber, Meijer, Lindner & Griessler, 2020). This realization should be an alarm for the scientific community and society. Recent COVID19 pandemics confirmed that the scientific community could respond to today's greatest challenges. However, the growing anti-vaxxer campaign has confirmed our vulnerability and lack of RRI when conducting scientific research.

FAIR data concept. An important goal on the road map of future responsible research and innovation society is related to data management. Namely, during recent decades, the volume of data generated has been growing exponentially. "The total amount of data created, captured, copied, and consumed globally is forecast to increase rapidly, reaching 64.2 zettabytes in 2020. Over the next five years up to 2025, global data creation is projected to grow to more than 180 zettabytes. In 2020, the amount of data created and replicated reached a new high" (Statista, 2022). All forms of professional work, particularly in research, involve some degree of data management. The lack of data findability, accessibility, interoperability, and reusability (FAIR) costs Europe a minimum of €10.2bn per year - approximately 78% of the Horizon 2020 budget per year (PwC EU Services, 2018). Making data FAIR is essential for the development of responsible research and the innovation society.

RRI and FAIR data. In the context of RRI, the FAIR data concept is commonly associated with Open Access to (research) data. Nevertheless, we would like to challenge the FAIR data concept concerning all RRI principles.

a) **Open Access**. Even though openness is considered a component of FAIR data, it is important to have in mind that it does not equate to open data (Mons et al., 2017) and vice versa. Namely, while open data may be findable and accessible, this does not guarantee that the same data are interoperable and reusable. In addition, findable and accessible data can be open according to specific conditions and restrictions or not open at all.
b) **Science Education**. SE is at a critical point. Anti-vaxxers' impact on reducing vaccination, the growing number of flat-Earth believers (it is not "knowing" it is "believing" since it is not based on facts), and climate change skepticism often using extreme examples, indicate that the SE paradigm must be changed. Enhanced FAIRness of data and methodologies with appropriate publicity and presence on social media can significantly contribute to this effort.
c) **Gender Equality**. Due to different social or professional circumstances, some researchers can have reduced physical approach to labs (work from home for different reasons, for example). In that case, a lot of research can be done if FAIR data are available.
d) **Public Engagement**. Citizen science and PE, as two sides of one "science & society coin" are strongly boosted by the FAIRness of data and methodologies as their integral part.
e) **Ethics**. Due to new legislation related to data privacy protection, all FAIR data must be clearly in line with appropriate ethics criteria. However, additional data anonymization will be a helpful addition to already FAIR data.
f) **Governance**. Hopefully, enhanced FAIRness of data would make them more acceptable for policy- and decision-makers.

The greatest challenges of the 21st century, such as climate change, natural hazards, biodiversity and ecosystem functions, food risks, deforestation, vector born (human, animal and plant) diseases, air quality, and urbanization, are either affected by or affect atmospheric conditions, particularly on the micro-scale.
Reliable and sufficient knowledge of environmental conditions or processes delivered from micrometeorological and microclimatological data play a central role in assessing and modeling trends and effects of climate change (CC) and adverse weather events on the environment and ecosystems on all spatial and temporal scales. Enormous efforts have already been made at the European level to centralize data from ground-based (synoptic scale) and satellite measurements, weather, and climate simulations and make them available for public use (COPERNICUS, ECMWF database, e-OBS, for example). These well-established data sources are broadly and successfully used in research, education, and economics. However, beyond specific initiatives (The European Eddy Fluxes Database Cluster, The Pan-Eurasian Experiment, for example), they are still missing one vital component – micrometeorological data, i.e., data addressing meteorological conditions of the microenvironment (few kilometers scale) open and available for various application potentials and user groups.
Micrometeorological data are usually collected as a part of scientific projects and observational networks developed for different purposes but they often "languish" in reports and institutional data silos. To address this shortfall, FAIRness of micrometeorological data should be enhanced. There are a number of existing projects and initiatives that aim to implement FAIR data principles.

- The GO FAIR initiative (https://www.go-fair.org/) is a bottom-up, stakeholder-driven and self-governed initiative that intends to offer an open and inclusive ecosystem for individuals, institutions and organizations through three implementation networks: GO CHANGE, GO TRAIN and GO BUILD.
- The FAIRsFAIR project (Koers et al., 2020) provies a detailed description of FAIR assessment frameworks and tools for datasets, repositories, and digital objects.
- FAIR data self assessment tool (https://ardc.edu.au/resources/aboutdata/fair-data/fair-self-assessment-tool/) developed by Australian Research Data Commons (ARDC) (Wilkinson et al., 2013; Wilkinson et al., 2016) is designed to make easier FAIR self-assessment and enhancement of datasets.
- In this paper, we will use micrometeorological data measured within the Forecasting and Reporting Service for Plant Protection of the Republic of Serbia (PIS) network (Lalic et al., 2020) to demonstrate some elements as proof of concept behind the FAIRness of micrometeorological data and ongoing CA20108 FAIRNESS Cost action (D Milošević, B Lalić, S Savić, B Bechtel, M Roantree, S Orlandini, 2022).

2 Methodology

2.1 PIS micrometeorological network

PIS micrometeorological network of automated weather stations (AWSs) was established in 2010, intending to provide information about meteorological conditions following the development of harmful organisms in agricultural production to support the work of plant protection specialists of PIS and producers. The network was initially designed, and AWSs were installed according to WMO recommendations for the special meteorological measurements, while all stations were purchased from licensed manufacturers with calibrated sensors. AWS locations were set within plant canopies using GPS. According to location settings, all AWSs can be classified as fixed (orchards, vineyards) and flexible - shifted among crop canopies during one season. For more detail about PIS micrometeorological data and metadata, please refer to Lalic et al. (2022).

2.2 FAIRness validation methodology

We used a simplified methodology designed by Jones and Grootveld (2017) to discuss the extent to which the PIS micrometeorological data is FAIR and the measures required to improve the FAIRness of this data. The methodology is designed in the form of a checklist to simplify the initial steps toward enhanced data FAIRness. We selected data measured within an apple orchard at the Cenej location, in the Novi Sad region for this study.

3 Results and Discussion

In the framework of CA20108 FAIRNES Cost action activities, an extensive self assessment of PIS micrometeorological data is in progress. It includes following phases:
i) initial self assessment – intended to identify lack of basic features using Jones and Grootveld (2017) and ARDC self assessment tools;
ii) qualitative self assessment – intended to test quality of exsisting solutions and room for improvement. Some examples of good practices presented by Wilkinson et al. (2016) and Jacobsen et al. (2019) forms the starting point for the interpretation of results and implementation considerations;
iii) methodology pipeline design – identifies tools, methods and algorithms necessary to implement findings from phase i) and ii);
iv) execution and testing of methodology pipeline – one segment of PIS micrometeorological database will be used to test designed framework and to prepare fully FAIR data satisfiying European Open Science Cloud (EOSC) repository criteria.

Table 1. Findability – Data can be found by humans or machines

Ref	Metric	Test	Current	CA20108 Enhancement Plan
F1	A persistent identifier is assigned to data	True	AWS ID	DOI for every dataset
F2	There are rich metadata describing the data	Partial	Scientific paper (where available)	Metadata Description
F3	The metadata are online in a searchable resource	Partial	Scientific paper (where available)	Searchable Metadata Repository
F4	The metadata record specifies the persistent identifier	True	Paper DOI	Permanent Metadata Repository.

Table 2. Accessibility – humans or machines can gain access to data under specific conditions or restrictions

Ref	Metric	Test	Current	CA20108 Enhancement Plan
A1	Following the persistent ID will lead to data or associated metadata	True	AWS ID	DOI for every dataset & searchable metadata repository
A2	The protocol by which data can be retrieved follows recognized standards	Partial	http for most data with remaining data in csv format.	Online searchable repository
A3	The access procedure includes authentication and authorization steps	Partial	Mixed Username/password in open access catalogue	Registration required for Cost Action online repository.
A4	Metadata accessible where possible (even when data are not)	True	Paper DOI	Searchable Metadata Repository with access to data.

Table 3. Interoperability – data and metadata conform to recognized formats and standards in order to be combined and exchanged.

Ref	Metric	Test	Current	CA20108 Enhancement Plan
I1	Data is provided in commonly understood and preferably open formats	Partial	Partly JSON, partly (interactively) csv, Excel.	WMO GAMP with downloadable data & metadata in CSV format.
I2	The metadata provided follows relevant standards	True	WMO GAMP	WMO GAMP
I3	Controlled vocabularies, keywords, thesauri or ontologies are used where possible	Partial	According to best practice	WMO GAMP
I4	Qualified references and links are provided to other related data	Partial	Aggregated with other tools	CA20108 metamodel facilitates embedded links.

Table 4. Reusability – data and metadata are licensed, conforming to community norms and allowing users to know what kinds of reuse are permitted.

Ref	Metric	Test	Current	CA20108 Enhancement Plan
R1	Data are accurate, well described with many relevant attributes	Partial	Basic quality control checks.	Automated Quality Control checks including data imputation.
R2	The data have a clear and accessible data usage license	True	Data is free to use	Data is free to registered researchers.
R3	It is clear how, why and by whom the data have been created and processed	True	Fully documented.	Part of the Metadata specification.
R4	The data and metadata meet relevant domain standards	Partial	Both data and metadata meet standards for micrometeorological measuremets in a field/canopy layer.	WMO GAMP.

Tables 1-4 present the first results of phase i) - initial self assessment. While none of the FAIR metrics can be categorised as fail, none are the 4 categories have passed all of the assessments. Of the 16 metrics, only 7 could be deemed as being met in full while the remained 9 metrics are deemed partially true. Thus, there is a clear case for improvement and the primary goal of the CA20108 Cost Action to to provide a Knowledge Portal and Data Repository where all datasets meet the 16 FAIR requirements in full. For the PIS case study, the immediate attention is devoted to metadata standardisation, keywords and vocabulary following CA20108 ongoing activities.

3.1 Discussion

In this section, we examine the FAIR metrics in detail and discuss what is required to ensure that micrometeorological experiments and datasets conform to the FAIR standard and in that respect, the work that is planned by the CA20108 Cost Action.

When considering the Findability metric, which states that data can be found by humans or machines, the metrics require that metadata is rich, searchable and permanent with a DOI for each dataset. The PIS requires richer metadata with a proper (metadata) search engine. The Accessibility metric requires that data can be retrieved under specific conditions or restrictions. It stipulates the use of username/password, a DOI for data retrieval and standard communication protocols. While it is accepted that data will not always be freely avaialble, it requires that metadata is always accessible. An online portal can deliver on all of these requirements and for the PIS case study, the lack of online repository meant that two of the metrics were only partially achieved.

The Interoperability metric is potententially the most difficult metric to achieve as it requires the careful specification of a climate metamodel. The requirement that data and metadata conform to recognized formats

and standards for the purpose of data integration and exchange will necessitate the formal specification of metadata that conforms to a recognised international standard. For the CA20108 Cost Action, the metamodel specification will conform to WMO standards (WMO GAMP 2012) which ensures the first 3 requirments (in table 3) are met and in addition, the Cost Action metadata will facilitate links to external online sources. For the PIS case study, I4 is partially achieved as data is aggregated with other tools (pheromone traps, light traps, volumetric spore catchers, visual examinations of host plants and harmful organisms), processed and calculated data. The Reusability metric requires that the metadata specification is as exhaustive as possible (many relevant attributes), usage license, and data provenance. To maximize reusability, the Cost Action plans to include automated data quality checks and the inclusion of gap filling methods.

4 Summary

The FAIRNESS Cost action intends to enhance FAIRNESS by improving standardization and integration between databases and datasets of micrometeorological measurements that are part of research projects or local/regional observational networks established for special purposes (agrometeorology, urban microclimate monitoring). The PIS case study provides an example of an initial FAIRness self assessment and possible implementations. Additionally, the distinction between Open data and FAIR is addressed with a discussion of all 16 FAIR metrics in order to clarify these, sometimes, mismatching topics.

The actual return on investment in the implementation of FAIR data and RRI principles is almost impossible to assess due to unquantifiable elements such as 1) the value of improved research quality; 2) higher inclusiveness of low performing countries and individuals in STEM research; and 3) reduction of "crowding out" effect on high performing countries and other indirect positive spill-over effects in the longer term.

It is important to remember that FAIR data supports RRI but at the same time, RRI practitioners are making data FAIR. This is the positive feedback we are hoping to achieve. Therefore, our duty as professionals, whose work and results are directly or indirectly related to the general population and everyday life, is to embrace RRI principles, ensuring that this is the sole mechanism for conducting research.

Acknowledgements

The study was funded by the Ministry of Education, Science and Technological Development of the Republic of Serbia (Grant No. 451-03-68/2022-14/200117) and H2020 - Co Change project (Grant No.873112). Micrometeorological measurements and phenological observations in crop canopies, orchards and vineyards by Forecasting and Reporting Service for Plant Protection of the Republic of Serbia (PIS) are financed by the Ministry of Agriculture, Forestry and Water Management of the Republic of Serbia and Provincial Secretariat for Agriculture, Water management and Forestry of the Vojvodina province, Republic of Serbia. Mark Roantree is funded by Science Foundation Ireland under grant number SFI/12/RC/2289-P2. The authors would like to acknowledge the CA20108 Cost Action - FAIRNESS.

References

Jones, S., Grootveld, M., 2017. How FAIR are your data? https://doi.org/10.5281/zenodo.5111307

Lalic, B., Marcic, M., Sremac, A.F., Eitzinger, J., Koci, I., Petric, T., Ljubojevic, M., Jezerkic, B., 2020. Landscape Phenology Modelling and Decision Support in Serbia. In: W. Mirschel, V.V. Terleev, K.-O. Wenkel (eds.), Landscape Modelling and Decision Support, Innovations in Landscape Research, Springer International Publishing, Cham, Switzerland, 567–593.

D Milošević, B Lalić, S Savić, B Bechtel, M Roantree, S Orlandini 2022. FAIRNESS Project-FAIR NEtwork of micrometeorological measurements, EGU22-971, Copernicus Meetings, March 2022.

Mons, B., Neylon, C., Velterop, J., Dumontier, M., da Silva Santos, L.O.B., Wilkinson, M.D., 2017. Cloudy, Increasingly FAIR; Revisiting the FAIR Data Guiding Principles for the European Open Science Cloud. Information Services & Use, 37, 49–56. DOI 10.3233/ISU-170824

Novitzky, P., Bernstein, M.J., Blok, V., Braun, R., Chan, T.T., Lamers, W., Loeber, A., Meijer, I., Lindner, R., Griessler, E., 2020. Improve Alignment of Research Policy and Societal Values. The EU Promotes Responsible Research and Innovation in Principle, But Implementation Leaves Much to be Desired. Science, 369, 6499, 39–41. DOI: 10.1126/science.abb3415

PwC EU Services, 2018. The cost of not having FAIR research data. DOI 10.2777/02999

Statista Research Department, 2022. Amount of data created, consumed, and stored 2010-2025. (https://www.statista.com/statistics/871513/worldwide-data-created/#:~:text=The%20total%20amount%20of%20data,replicated%20reached%20a%20new%20high.)

Koers, H., Gruenpeter, M., Herterich, P., Hooft, R., Jones, S., Parland-von Essen, J., Staiger, C., 2020. Assessment report on 'FAIRness of services' (1.0). Zenodo. https://doi.org/10.5281/zenodo.3688762

Wilkinson, M.D., Dumontier,M., Aalbersberg, I.J., Appleton, G., Axton, M., Baak, A., Blomberg, N., Boiten, J.-W., da Silva Santos, L. B., Bourne, P.E., Bouwman, J., Brookes, A.J., Clark, T., Crosas, M., Dillo, I., Dumon, O., Edmunds, S., Evelo C.T., Finkers, R., Gonzalez-Beltran, A., Gray, A. J.G., Groth, P., Goble, C., Grethe, J.S., Heringa, J., Hoen, P.A.C. 't, Hooft, R., Kuhn, T., Kok, R., Kok, J., Lusher, S.J., Martone, M.E., Mons, A., Packer, A.L., Persson, B., Rocca-Serra, P., Roos, M., van Schaik, R., Sansone, S.-A., Schultes, E., Sengstag, T., Slater, T., Strawn, G., Swertz, M.A., Thompson, M., van der Lei, J., van Mulligen, E., Velterop, J., Waagmeester, A., Wittenburg, P., Wolstencroft, K., Zhao, J., Mons, B., 2016. The FAIR Guiding Principles for scientific data management and stewardship. Sci. Data, 3**,** 160018. https://doi.org/10.1038/sdata.2016.18

Wilkinson, M.D., Dumontier, M., Sansone, S.-A., da Silva Santos, L.A.B., Prieto, M., Batista, D., McQuilton, P., Kuhn, T., Rocca-Serra, P., Crosas, M., Schultes, E., Wlkinson, M.D., Dumontier, M., Sansone, S.A. et al*.,* 2019. Evaluating FAIR maturity through a scalable, automated, community-governed framework. Sci Data, 6, 174. https://doi.org/10.1038/s41597-019-0184-5

Jacobsen, A., de Miranda Azevedo, R., Juty, N., Batista, D., Coles, S., Cornet, R., Courtot, M., Crosas, M, Dumontier, M., Evelo, C. T., Goble, C., Guizzardi, G., Hansen, K.K., Hasnain, A., Hettne, K., Heringa, J., Hooft, R.W.W., Imming, M., Jeffery, K.G., Kaliyaperumal, R., Kersloot, M.G., Kirkpatrick, C.R., Kuhn, T., Labastida, I., Magagna, B., McQuilton, P., Meyers, N., Montesanti, A., van Reisen, M., Rocca-Serra, P., Pergl, R., Sansone, S.-A., da Silva Santos, L. O. B., Schneider, J., Strawn, G., Thompson, M., Waagmeester, A., Weigel, T., Wilkinson, M. D., Willighagen, E. L., Wittenburg, P., Roos, M., Mons, B., Schultes, E., Jacobsen, A., de Miranda Azevedo, R., Juty, N., Batista, D., Coles, S., Cornet, R. Schultes, E., 2020. FAIR principles: Interpretations and implementation considerations. Data Intelligence, 2, 10–29. doi: 10.1162/dint_r_00024

WMO GAMP 2012, Guide to Agricultural Meteorological Practices (GAMP) (WMO-No.134) Edition: 2010, WMO, 2012.

Monitoring the effect of foliar application of cysteine and methionine in combination with hydrogen peroxide as potential crop boosters during low temperature regime, on optical properties of durum wheat (*Triticum durum* cv. antalis) leaves

Andriani Tzanaki[1,2], Despina Dimitriadi[2], Styliani N. Chorianopoulou[1,3], Dimitris Bouranis[1,3]

[1]Plant Physiology and Morphology Laboratory, Crop Science Department, Agricultural University of Athens, Greece; [2] Karvelas AVEE, Ypato, Viotia, Greece; [3] PlanTerra Institute for Plant Nutrition and Soil Quality, Agricultural University of Athens, Greece

Abstract. Durum wheat growth and development is affected by atmospheric temperature. In this ongoing research, a durum wheat crop was established in December 2021, at Ypato, Viotia, Greece. Aqueous solutions of cysteine and methionine were applied foliarly, alone or each one in combination with hydrogen peroxide and a silicon-based wetter, as potential boosters of crop response during low temperature periods. Fv/F0, SPAD, and PRI values were taken 4-, 7-, 12-, and 25-days post spraying, to monitor the effect of spraying on leaf optical properties, as potential indices of leaf reaction to foliar application in relation to temperature fluctuation. Results showed fluctuations in the values of indices, indicative of the reaction of leaf to hydrogen peroxide application. The data suggest that the applied combinations of Met/H_2O_2/SW7 and Cys/H_2O_2/SW7, especially that with methionine, could play the role of crop booster against low temperature stress, whilst the combination with the silicon-based wetter seems to be an effective one.

1 Introduction

The atmospheric temperature constitutes a key player during wheat growth and development. Low temperatures can slow or even cease plant growth and have detrimental effects on total grain yield. Wheat optimal temperatures range between 17-23 ^oC, while at about 2-3 ^oC roots and shoots stop growing. Lower temperatures cause the leaves to stop developing and below -17 ^oC conditions can be lethal to plants (Porter et al 1999).

Exogenous application of several substances seems to help alleviate low temperature effects by priming the plant to prepare it for the upcoming adverse conditions or boost its metabolism to overcome them. Among them, is hydrogen peroxide (H_2O_2), a member of the reactive oxygen species. Application of H_2O_2 enables the plant to boost its antioxidant machineries and to acclimatize prior to abiotic stress exposure. Thus, H_2O_2-treatment seems to harden the plant to better cope with suboptimal conditions, including cold and heat (Banerjee and Roychoudhurry 2019).

Methionine (Met) is a sulfur amino acid (AA) and in addition to its participation as a structural component of proteins, it serves as the precursor of sulfur-adenosyl-methionine, known as SAM, a key metabolite. SAM feeds various metabolic pathways, one of which is the production of ethylene. SAM is a methyl donor in many metabolic pathways and therefore contributes to dealing with adverse crop conditions in various levels, thus supporting the crop to cope effectively with the adverse conditions (Mentzos et al, 2020).

Cysteine (Cys) is the first sulfur amino acid, with a thiol side chain. Cysteine plays a structural main function in proteins as well as role as a precursor for essential biomolecules, such vitamins, and some defense compounds, such as glucosinolates and thionins. Cysteine is the precursor molecule of glutathione, the predominant non-protein thiol, which plays an important role in plant stress responses. (Sadak et al., 2020).

Plant response was monitored by measuring Chlorophyll Fluorescence (Fv/F0), SPAD and PRI index.

Photochemical Reflectance Index (PRI) is measured by comparing leaf reflectance in two narrow wavelength bands centered to 531 nm and 570 nm. The Photochemical Reflectance Index (PRI) is sensitive to changes in carotenoid pigments that are indicative of changes in photosynthetic light use efficiency, the rate of CO2 uptake and as a water-stress index. As such, it is used in studies of vegetation productivity and stress. PRI is calculated by the equation (R531 – R570) / (R531 + R570) and correlates with the epoxidation state of xanthophyll cycle pigments and photosystem efficiency (Sellers 1985).

The SPAD index corresponds to the amount of chlorophyll present in the plant leaf. The values are calculated based on the amount of light transmitted by the leaf in two wavelength regions in which the absorption of chlorophyll is different. The peak absorption areas of chlorophyll are in the blue and red regions, with low absorption in the green region and almost no absorption in the infrared region. Based on this, the wavelength ranges chosen to be used for measurement are the red area where absorption is high and unaffected by carotene, and the infrared area where absorption is extremely low. SPAD value = k [logT940- logT650] + c, T940 = I'940/I940, where I': the intensity of the radiation that fell on the surface of the leaf, and I: the intensity of the radiation that came out of the leaf.

Fv/F0, the ratio of variable fluorescence to minimum fluorescence, is a very sensitive stress detector, more sensitive than Fv/Fm (Kuckenberg et al. 2009). Changes in leaf photosynthesis rate can be easily estimated by chlorophyll fluorescence (Lichtenthaler and Rinderle 1988; Scholes and Rolfe 1996). This technique provides information on the potential and current efficiency of photosynthesis and the integrity of photosynthetic apparatus even at very early stages of stress conditions (Baker and Rosenqvist 2004).
In this study, we studied these three indices, i.e., Fv/F0, SPAD, and PRI, to monitor the response, if any, of durum wheat leaves, after spraying with Cys, Cys + H_2O_2, Met, Met + H_2O_2. We also recorded the minimal and maximal values of atmospheric temperature. We discuss the fluctuations of indices values in relation to temperature fluctuations for each treatment after the foliar application in a period of 25 days.

2 Experimental

2.1 Plant material

Durum wheat (*Triticum durum* cv. antalis) was showed on December 22nd, 2021, at Ypato, Viotia, Greece and the appropriate agronomic treatments were applied. The dimensions of the experimental plots were 1.5m x 4m (Fig.1) and crop did not receive irrigation. Low temperatures below zero took place between 12 and 16 March, 2022. Was this a potential injurious period at this growth stage of wheat? On March 17th, 2022, i.e., at the stage of 3 tillers and 3 leaves on the main stem (BBCH-23), we applied the following aquatic solutions as potential boosters towards relieving cold stress.

2.2 Foliar applications

Cysteine 5 mM or methionine 5 mM, with or without the addition of hydrogen peroxide 2.5 mM aqueous solutions were applied foliarly, against water as control. A silicon-based wetting agent (SW7) was used. Thus, the following five treatments were tested: water (C), SW7 (0.5 mL/L), Cys/SW7, Cys/H_2O_2/SW7, Met/SW7, Met/H_2O_2/SW7.

2.2 Leaf optical properties dynamics

The PlantPen model PRI 210 was used to measure PRI values. The SPAD values were measured by the Chlorophyll Meter SPAD-502. Fm/Fv was measured by OS30p+, OptiSciences chlorophyll fluorometer.
SPAD, PRI, and chlorophyll fluorescence measurements were taken 4-, 7-, 12-, and 25-days post spraying. SPAD and PRI measurements were taken at the newest mature leaf, at about ½ of leaf's length, between 09:00-12.00. Four measurements were taken per leaf from each of 10 random plants and average of all plants per plot was calculated. Chlorophyll fluorescence measurements were taken at the newest mature leaf, between 09:00-12:00, at about 1/3 of leaf's length (from the base of the leaf). One measurement per leaf was taken from each of 10 random plants; plants were dark adapted for 1 hour. Leaves were collected and dried at 40 ^oC, the corresponding fresh and dry weight were recorded, and the water content was calculated and expressed as percentage.

Figure 1. View of the plots at Ypato, Viotia, Greece, on March 17th, 2022. Durum wheat crop was at the stage of 3 leaves and 3 tillers.

3 Results and Discussion

3.1 Temperature profile during the experiment

Prior to foliar application, crop experienced a gradual decrease of temperature from 10 ºC to 0 ºC (Fig.2). Then, it reversed from 0 ºC to 8 ºC and applications took place. Post spraying, the temperature fluctuation pattern can be devided into four, short-term periods. Between d0 and d4, the mean temperature followed a descending pattern again and low temperatures prevailed (8 to 3 ºC; period *a*). At d3 post spraying, pattern reversed and followed a new ascending pattern (from 3 ºC to 15 ºC; period *b*). Thereafter, it fluctuated around 15 ºC (period *c*), and a new decrease took place (period *d*). At d25, mean temperature was the same as that of d4, i.e., 7 ºC.

The variations of temperature can result in both cold and heat stress in plant species. Exogenous application of H_2O_2 induced acclimation to short-term cold stress in tomato seedlings (Iseri et al., 2013). The acclimatized plants exhibited high RWC. After H_2O_2 application the endogenous antioxidant machinery remains active before encountering abiotic stress. The stress-induced injuries are less, and post-stress recovery is enhanced, promoting tolerance (Banerjee and Roychoudhurry 2019). Interestingly, leaf water content at d4 was higher by 5.6% in Cys/H_2O_2 against Cys, and 5.3% in Met/H_2O_2 against Met (Table 1).

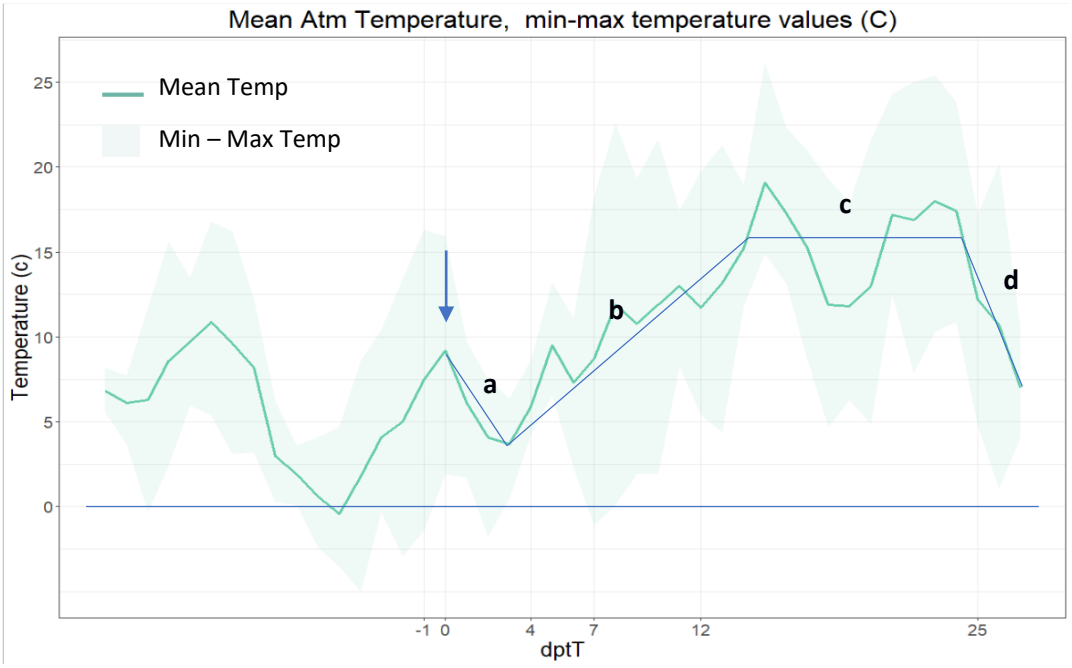

Figure 2. Mean atmospheric temperature (green solid line) and min and max temperatures (light green coloured area) from March 1st to April 13th). Dpt: days post spraying. Dpt0 marks the day of the spraying (March 17th).

Table 1. Leaf water content at day post transplantation (dpt) d4 and d12.

	C	SW7	Cys	Cys/H_2O_2	Met	Met/H_2O_2
dpt	**leaf water content (%)**					
d4	79.1	78.3	79.8	**84.3**	78.7	**82.9**
d12	80.3	82.2	79.4	81.0	80.7	81.3

3.2 The Fv/F0 index

The ratio of variable fluorescence [Fv=(Fm-F0)] to minimal fluorescence of control plants, Fv/F0, increased with time (Fig.3). At d4 (period *a*), there was an effect of treatments on the index. Cys and Met provided lower Fv/F0, whilst the combination with H_2O_2 increased the index values. At d7, all values were the same. At d12,

Cys, Met, and Met/H_2O_2 provided higher values. Period *d* provided lower values in all four treatments with AAs and combinations with H_2O_2.

3.3 SPAD index dynamics

At d4, i.e., at the end of period *a*, SPAD values (Fig.4) presented increased standard deviations. At d7, values restored, with Met/H_2O_2 to provide good score. At d12 and d25, only Met is comparable to control. The rest provided higher values. It is worth mentioning that SW7 provided higher values compared with control.

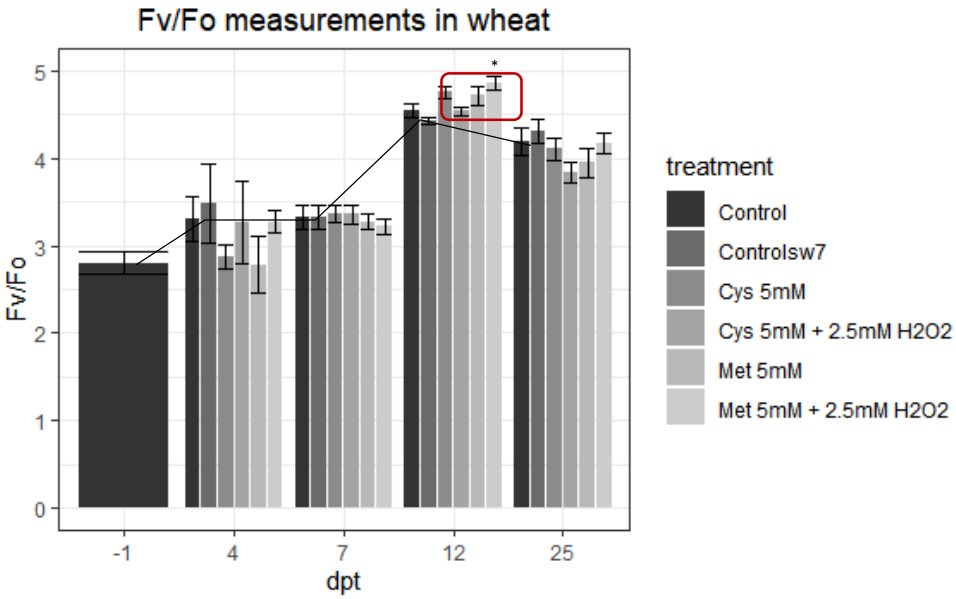

Figure 3. Fv/F0 index values of the measuring days. Level of significance (Dunnet's test-comparing with Control): '*' 0.05

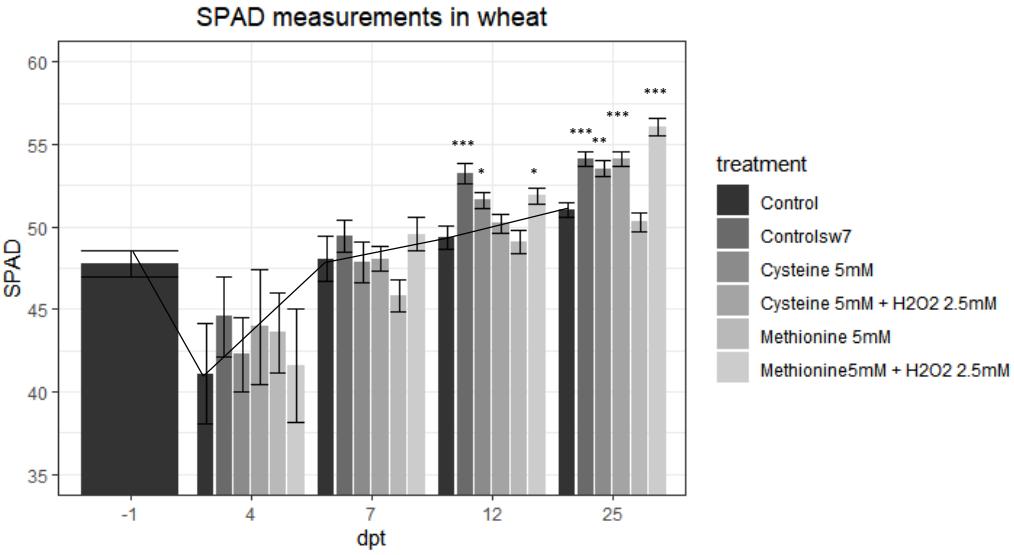

Figure 4. SPAD values for the 5 measuring days with error bars. Level of significance (Dunnet's test-comparing with Control): '.' 0.1, '*' 0.05, '**' 0.1, '***' 0.01

3.4 PRI dynamics

PRI presented an interesting pattern at d4 (Fig.5), with Cys/H_2O_2 to show statistically improved values compared with control, however, at d7 the pattern reversed, a behaviour that needs further study for explanation. D12 and d25 showed positive values and no differences between treatments.

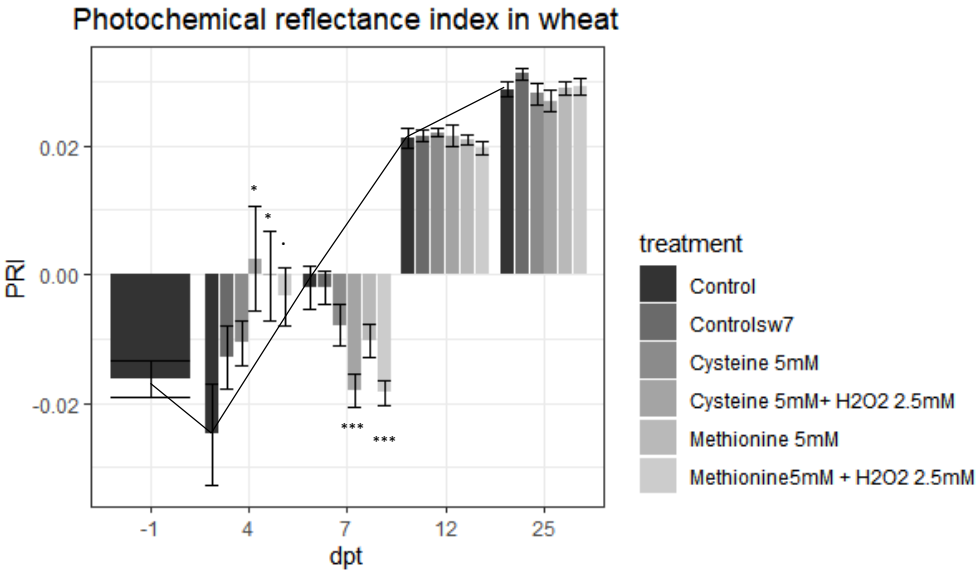

Figure 5 PRI values of the measuring days. Level of significance (Dunnet's test-comparing with Control): '.' 0.1, '*' 0.05, '***' 0.01

4 Summary

Temperature fluctuations seem to have affected all three measured indices, with the period from d0 to d7 to represent a transition state. Especially, the fluctuations of Fv/Fo suggest that the applications did not induce stress to sprayed plants, whilst the fluctuations of PRI at d4 perhaps suggest that changes in the responding photochemical system may have been induced by the applications of methionine alone, or its combination with hydrogen peroxide. This seems to hold true with both combinations of cysteine, or methionine, with hydrogen peroxide at d7. Interestingly, SPAD values were affected by the application, after d7. Taken together, the discussed fluctuations may suggest that the coexistence of S-containing amino acids along with hydrogen peroxide could play the role of crop confronter of the effect of low temperatures, and this suggestion should be verified by biochemical stress indicators, within a week post spraying.

References

Baker, N. R., & Rosenqvist, E. (2004). Applications of chlorophyll fluorescence can improve production strategies: An examination of future possibilities. Journal of Experimental Botany, 55, 1607–1621. doi: 10.1093/jxb/erh196.

Banerjee A., A. Roychoudhurry (2019) Abiotic stress tolerance in plants by priming and pretreatment with hydrogen peroxide. In: M. Hasanuzzaman, V. Fotopoulos (Eds), Priming and pretreatment of seeds and seedlings. Implication in plant stress tolerance and enhancing productivity in crop plants. pp.417-426. Springer Nature Singapore Pte Ltd. ISBN 978-981-13-8625-1.

Gamon J.A., L. Serrano, J.S. Surfus (1997) The photochemical reflectance index: an optical indicator of photosynthetic radiation use efficiency across species, functional types, and nutrient levels. Oecologia 112, 492−501.

Iseri OD, Koerpe DA, Sahin FI, Haberal M (2013) Hydrogen peroxide pretreatments of roots enhanced oxidative stress response of tomato under cold stress. Acta Physiol. Plant. 35, 1905-1913.

Kuckenberg J., I. Tartachnyk, G. Noga (2009) Temporal and spatial changes of chlorophyll fluorescence as a basis for early and precise detection of leaf rust and powdery mildew infections in wheat leaves. Precision Agric 10, 34-44.

Lichtenthaler, H. K., & Rinderle, U. (1988). The role of chlorophyll-fluorescence in the detection of stress conditions in plants. CRC Critical Reviews in Analytical Chemistry, 19, 29–85.

Mentzos G. D. Dimitriadi, K. Lagos, A. Tzanaki, V. Constantinou-Kokotou, S. Chorianopoulou, D. Bouranis (2020) Crop biofortification with sulfur: Methionine as fertilizer additive. In: Proceedings of the 28th International Symposium of CIEC, Fertilization and Nutrient Use Efficiency in Mediterranean Environments. Bouranis D.L., Haneklaus S.H., Chorianopoulou S.N., Li J., De Kok L.J., Schnug E., Ji L. (Eds.), Utopia Publishing, ISBN: 978-618-5173-62-3., p.149-153.

Porter, J. R., & Gawith, M. 1999. Temperatures and the growth and development of wheat: a review. European Journal of Agronomy, 10(1), 23–36. doi:10.1016/s1161-0301(98)00047-1

Reddie, K. G., & Carroll, K. S. 2008. Expanding the functional diversity of proteins through cysteine oxidation. Current Opinion in Chemical Biology, 12(6), 746–754. doi:10.1016/j.cbpa.2008.07.028

Sadak M. Sh., A. R. A. El-Hameid, F. S. A. Zaki, M. G. Dawood, M. E. El-Awadi (2020) Physiological and biochemical responses of soybean (Glycine max L.) to cysteine application under sea salt stress. Bulletin of the National Research Centre 44:1, https://doi.org/10.1186/s42269-019-0259-7

Scholes, J. D., & Rolfe, S. A. (1996). Photosynthesis in localised regions of oat leaves infected with crown rust (Puccinia coronata): Quantitative imaging of chlorophyll fluorescence. Planta, 199, 573–582. doi: 10.1007/BF00195189.

Sellers P. J. (1985) Canopy reflectance, photosynthesis, and transpiration. International Journal of Remote Sensing, 6, 1335-1372.

Microalgae production using waste nutrient sources: effect on environmental impact indicators

Sofoklis Bouras[1], George Kountrias[1], Ioannis T. Karapanagiotidis[2], Dimitrios Antoniadis[1], Dimitrios Papanastasiou[1], Vasileios Anestis[1], Nikolaos Katsoulas[1*]

[1]Laboratory of Agricultural Constructions and Environmental Control; Department of Agriculture Crop Production and Rural Environment; University of Thessaly; Fytokou Street; 38446; Volos; Greece
[2]Aquaculture Laboratory; Department of Ichthyology and Aquatic Environment; University of Thessaly; Fytokou Street; 38446; Volos; Greece

* Corresponding author. Email: nkatsoul@uth.gr

Abstract

Fish oil is a critical nutrient component in aqua feeds since it is rich content in n-3 polyunsaturated fatty acids (PUFA). Inflated prices due to unsustainable conventional extraction practices have led the aquaculture industry to exploit alternative sources of PUFA besides wild fish stocks. Microalgae can serve as alternative component in aqua feeds due to their high nutritional value (Vitamins, antioxidants, proteins, lipids and PUFA). They serve as an effective tool to remediate a several waste streams derived from the biofuel industry, valorising by that low-cost alternative sources for the production of high cash yield compounds utilized by the pharmaceutical industry. In this study, we assessed the potential cultivation of the rich in the PUFA docosahexaenoic acid (DHA) heterotrophic marine microalgae *Schizochytrium limacinum* SR21, in a growth media containing two different alternative nutrient sources, crude glycerol derived from biofuel industry as a carbon source and effluent digestate from the production of biogas livestock decomposition, as a source of nutrients and trace elements at increasing concentrations in order to assess their effect on biomass productivity, lipid accumulation, proximate composition, carbon assimilation and DHA content. It was shown that *Schizochytrium limacinum* SR21 can be used to remediate waste streams from the biofuel industry as alternative nutrient sources in a sustainable and environmental friendly way with the optimal concentration being 48% (v/v), which promoted biomass productivity, lipid accumulation and DHA Yield, 49.2 g L^{-1}, 8.47 g L^{-1} and 0.635 g L^{-1} respectively. Moreover the utilization of effluent digestate and a inorganic nitrogen source resulted in a substantial decline of 16 environmental impact indicators, 73-100% when organic nitrogen sources were replaced with 48% (v/v) effluent digestate. Although this study did not achieve to reach industrial production standards with regards to the DHA content, a further assessment of other culture parameters (nitrogen concentration, oxygen dilution, temperature) is needed in order to optimise DHA production.

Keywords: microalgae; docosahexaenoic acid; greenhouse production; aqua feed; sustainability; waste management

1 Introduction

Natural ecosystems have been severely degraded, as a result of environmental pollution due to the heavy industrialization of the 21st century, a phenomenon which made energy resources scarce and limiting. In order to compensate for the draining reserves of fossils fuels, since 1992 most of the countries of the European union are producing green alternative fuels such as biodiesel at an industrial scale. In 2015 it was estimated that the annual production of biodiesel was 11.8 billion litters (Eryilmaz et al., 2016).

For every ton of biodiesel, 100 kg of crude glycerol is generated. Since it has low economic value its purification it's is not profitable and disposal of crude glycerol in landfills can be harmful for the environment (McNutt and Yang, 2017). However crude glycerol can be utilized as an alternative carbon source in microbial fermentation, replacing by that glucose and other expensive organic carbon sources (Thompson and He, 2006).

Another important waste stream which is contributing to the pollution of the environment is animal manure, since Europe generates approximately 1500 million tons of animal manure which is responsible for 18% of gas house emissions related to livestock farming (Holm-Nielsen et al., 2009). An innovative modern approach to remediate this particular pollutant is co–digestion of livestock manure for the production of biogas. However, this potential solution produces also waste streams such as the effluent digestate, which are the residues of the anaerobic digestions. This particular waste stream since it's a rich source of nitrogen, phosphorous, potassium and trace elements can be implemented as a supplementary fertilization source, however uncontrolled land applications can lead to excess nutrient leaching and eutrophication (Campbell et al., 2009; Zhu et al., 2016).

These waste streams, crude glycerol and effluent digestate, have been successfully utilized in microalgae cultivation media as a phycoremidiation tool and expensive conventional nutrient component replacements in

the pharmaceutical industry for the production of health compounds such as docosahexaenoic acid (DHA) an n-3 polyunsaturated fatty acid (PUFA) which can be utilized as a sustainable replacement of fish oil which is an important ingredient in aqua feeds (Phang et al., 2015).
Schizochytrium sp., is a non-photosynthetic marine protist (Leyland et al., 2017), that produces lipids rich in DHA. The strain *Schizochytrium limacinum* SR21, accumulates up to 50 % of its dry weight in lipids yielding 35% DHA of its total lipid content in short 7-10 days (Sun et al., 2014).
The aim of this research was to assess the effects of use of waste streams derived from the biofuel industry, on the growth, biomass and DHA production of *Schizochytrium limacinum SR21*. In particular, the effects of using crude glycerol (alternative carbon source) and effluent from anaerobic digestates derived from crop and livestock farming residues enriched with inorganic nitrogen (alternative macronutrients and trace elements source) on the above production parameters and environmental impact indicators will be assessed.

2 Material and Methods

2.1 Heterotrophic Cultivation

The alga strain *Schizochytrium limacinum* SR21 (*Aurantiochytrium limacinum* SR21, ATCC ® MYA-1381 ™) was obtained from the American Type Culture Collection (ATCC). Activation of cells in order to develop the inoculum was performed according to the ATCC protocol, in a 250 mL Erlenmeyer flask containing 50 mL of ATCC 790 growth medium, composed of 5 g L^{-1} glucose, 1 g L^{-1} peptone and 1 g L^{-1} yeast extract, micronutrients and 20 g L^{-1} sea salts mixed with distilled water (Bouras et al., 2020). Sea salts were purchased from Aquaforest sp. O.o., Brzesko, Poland.
After 2 days of cultivation cells were sub cultured for 5 days in a seed culture medium according to Chen et al. (2016) and stored in 20% glycerol (v/v) at −20 ºC (Sun et al., 2014) for future studies. In short elemental composition of micronutrient solution was: 0.001 g L^{-1} $ZnSO_4 \cdot 7H_2O$, 0.002 g L^{-1} $MnSO_4 \cdot 4H_2O$, 0.01 g L^{-1}, H_3BO_3, 0.001 g L^{-1} $Co(NO_3)\ 2 \cdot 6H_2O$, 0.001 g L^{-1} $Na_2MoO_4 \cdot 2H_2O$, 0.0005 g L^{-1} $CuSO \cdot 5H_2O$, 0.7 g L^{-1} $FeSO_4 \cdot 7H_2O$ and 0.8 g L^{-1} EDTA whereas ASW contained: 30 g L^{-1} NaCL, 1.2 g L^{-1} Mg, 0.742 g L^{-1} K and 0.33 g L^{-1} Ca.
In order to determine the optimal carbon and nitrogen concentration which would promote cell proliferation and lipid biosynthesis, a batch experiment (experiment 1) was carried out with different concentrations of crude glycerol and organic nitrogen sources (yeast extract and peptone) in ASW. Cells were grown at four different crude glycerol concentrations (30, 60, 90, 120 g L^{-1}) and five nitrogen concentrations (1.1, 2.2, 3.3, 4.4, 5.5 g L^{-1}). The nitrogen concentration levels derived by combining equal amounts of yeast extract (10, 20, 30, 40, 50 g L^{-1}) and peptone (10, 20, 30, 40, 50 g L^{-1}). The experiment was carried out with the same inoculum, micronutrients and supplementary minerals at the same conditions of the abiotic environment as mentioned previously. According to our findings, the optimal concentration of total nitrogen and crude glycerol was 3.3 g L^{-1} and 120 g L^{-1}, respectively.
Taking into consideration the results from experiment 1 in experiment 2 microorganisms were in grown in a fermentation medium that contained 120 g L crude glycerol (carbon source) and pretreated effluent at five different concentrations: 0%, 8%, 16%, 32% and 48% v/v. Furthermore, in order to accomplish a nitrogen concentration of 3.3 g L^{-1} ammonium chloride (NH4CL) was added at the needed quantities. The rest of the macronutrients concentrations (phosphorus, potassium and magnesium) were regulated for comparison reasons to the concentration equal to that of the experiment 1, with the addition of KH_2PO_3 and $MgSO_4 \cdot 7H_2O$, while micronutrients were added only to the control treatment and not to the media containing the effluent. Thus, the composition of the control fermentation medium (0% effluent) was 120 g L^{-1} crude glycerol, 12.5 g L^{-1} NH_4Cl, 1.5 g L^{-1}, KH_2PO_3, 0.7 g L^{-1} $MgSO4 \cdot 7H_2O$ and micronutrients. The rest of the treatments (8%, 16%, 32%, 48% v/v effluent) contained 120 g L^{-1} crude glycerol, 3.3 g L^{-1} nitrogen, P, K, 8%, 16%, 32%, 48% v/v effluent and 92%, 84%, 68% and 52% v/v ASW, respectively.
The experiment was carried out in 500 mL shake flasks (DURAN ® GLS 80 ® Laboratory Bottle Wide Mouth) with 400 mL working volume containing and 10% (v/v) inoculum of the seed culture of the microorganisms. Cultures were incubated in a growth chamber at 25 o C for 7 days on an orbital shaker set at 120 rpm. Ionic concertation was constantly corrected with 2M KOH. Oxygen was sparged into the medium with compressed air at a rate of 150L h −1. During the experiment, dissolved oxygen (DO) level was maintained at 50% of saturation by regulating the oxygen supply. Prior to inoculation, the pH of the medium was adjusted to designated target values with 2M KOH or 1N HCL and autoclaved at 121◦ C for 15 min. The experiment was carried out for 7 days.
Elemental composition of crude glycerol and effluent was from the same batch as mentioned in previous research by Bouras et al. (2016). In short physical characteristics of crude glycerol were the following: glycerol 80.4% (w/w), methanol 0.7% (w/w), pH 1.9, Ash 2.2 (m/m), moisture 11.9 (w/w) whereas the elemental composition of the pre-treated waste effluents (in mg L-1) was: Total N (161), P (91), Ca (1000), Mg (260), S (330), Cu (5.6), Co (30), Zn (12), Mn (11), Fe (110). The physical characteristics were: total solids (2.2 w/w),

conductivity (15.05 mS cm-1), Optical density at 660 nm(0.7), pH (7.7), Ash (1 w/w), Moisture (97.8 w/w), COD (1 g L-1).
All measurements were conducted according to Bouras et al. (2016). In short biomass was determined daily, gravimetrically by cell dry weight. Total lipids were extracted according to Folch et al. (2016) with a solution of Chloroform/Methanol (C:M 2:1/v/v) whereas fatty acid methyl esters (FAME) were prepared by acid catalyzed transesterification according to Christie and Han (2003). FAMEs were quantified by gas-liquid chromatography with Perkin Elmer Clarus 680 coupled with a Col-Elite FAME Wax capillary column (30 m × 0.25 mm id, film thickness 0.25 μ m) (PN N9316694, Perkin Elmer, Waltham, MA, USA). The crude protein content was determined with Kjeldahl analyses. Ash content was measured by dry ashing the samples at 600 ◦ C for 5 h. Calorific value was determined with an IKA calorimeter (C5000, IKA Werke, Staufen, Germany). Crude carbohydrate content was quantified by subtracting the sum of the percentages of crude protein, total lipid, moisture and ash from 100. Total organic carbon was quantified with a total organic carbon analyzer (TOC-L, Shimadzu Corp, Kyoto, Japan).

2.2 Environmental Life Cycle Assessment

Scope and goal Definition. The evaluation of the potential environmental impact during the upscale of the heterotrophic microalgae cultivation (1000 L total volume) of the strain *Schizochitrium Limacinum Sr21* utilizing waste streams from the biofuel industry was investigated by assessing the median environmental impacts of three different cultivation media components: 1) a conventional Medium **(CM)** were organic nitrogen sources (40 g L^{-1} Yeast Extract and 40 g L^{-1}Peptone) 120 g L^{-1} crude glycerol, 12.5 g L^{-1} NH_4Cl, 1.5 g L^{-1} KH_2PO_3, 0.7 g L^{-1} $MgSO4{\cdot}7H_2O$ and 5 ml/L micronutrient were added, 2) a control medium **(CoM)** which contained 0% v/v effluent and additionally 120 g L^{-1} crude glycerol, 12.5 g L^{-1} NH_4Cl, 1.5 g L^{-1} KH_2PO_3, 0.7 g L^{-1} $MgSO4{\cdot}7H_2O$ and 5 ml/L micronutrient were added and 3) an alternative medium **(AM)** which contained 48% v/v and additionally 120 g L^{-1} crude glycerol, 12.5 g L^{-1} NH_4Cl, 1.2 g L^{-1} KH_2PO_3 and 0.13 g L^{-1} $MgSO4{\cdot}7H_2O$ were added.
Life Cycle Inventory Compilation. The complete list of the materials and quantities utilized for the formulation of the three different cultivation media at a working volume of 1000L each, are listed in table 1. Modeling, supply chain and electricity inputs were based on life cycle inventory datasets (Ecoinvent v. 3.4 database available in Simapro v.8.5.2.0 and ReCiPe 2016 Midpoint (H) V1.02 for impact environmental impact assessment).

3. Results and Discussion

The highest biomass productivity was achieved when the cultivation media was enriched with pretreated effluent digestate at a concentration of 16% and 32% (v/v), 64.3 ± 1.9 and 64.2 ± 2.1 respectively (Table 1). Organic nitrogen sources such yeast and peptone are frequently used in microbial fermentation due to their essential content in amino acids vitamins and trace elements. However due to their high cost, alternative nitrogen sources have been tested with promising results, such as ammonium sulfate urea and ammonium acetate (Yokochi et al., 1998). In this current study expensive cultivation media components (yeast and peptone) were successfully substituted with cost effective inorganic nitrogen sources (NH_4CL) since biomass productivity was 3 times higher compared to yeast and peptone. This comes into to agreement with previous research where organic nitrogen sources inhibited cell growth since they were utilized for synthesis of intracellular cell components (Sun et al., 2014).
Besides the importance of selecting the correct organic nitrogen sources due to their species specificity, micronutrients are also an important component of the cultivation media since their influencing several different biochemical processes. Research in the particular topic is limited especially with regards on their effect on thraustochytrids. However according to previous research under limiting conditions of Fe, Cu, Zn and Mn biomass productivity was inhibited in several *Schizochytrium* strains and fungi (Nagano et al., 2013; Philpott, 2006) which come into agreement with our results since increasing concentrations of effluent increased cell proliferation. However biomass productivity declined at high effluent concentrations (48% v/v) probably due to high concentrations of copper (5.6 mg L^{-1}) and zinc (12 mg L^{-1}) which come into agreement with previous research which indicates that high copper concentrations above 0.5 mg L^{-1} can affect negatively cell reproduction in several *Schizochytrium* strains (Lin et al., 2010). Moreover the increased lipid content which was exhibited at moderate and high influent concentrations was induced probably due to the increase of the elemental content of Fe, since several studies reported that there is a positive relationship with regards, Fe concentration and lipid biosynthesis in oleogenus fungi (Dediukhina et al., 2011; Pádrová et al., 2016).
Oxygen levels is an important abiotic culture parameter, since previous research indicates that DHA biosynthesis is optimized under low oxygen levels ranging from 10-30% (Ganuza et al., 2008). However high oxygen levels ranging from 40-50 % promote cell proliferation in the expense of lipid productivity and DHA content (Chi et al., 2007) . This comes into agreement with our results since compared to previous studies

(Zhu et al., 2008) the substantially high biomass (49.2 ± 2.7 g L^{-1}) was followed by low DHA levels (635 ± 00.1 mg L^{-1}).

Table 1. *Inventory of ingredient inputs and energy consumption per cultivation media.*

Inputs/Outputs	Cultivation Media		
	Conventional Medium	Control Medium	Alternative Medium
Products Output			
Harvested Dry Matter,g/L	32	17	49
Materials			
Crude Glycerol, kg	120	120	120
NaCl, g	17.952	17.952	10.348
Mg, g	0.718	0.718	0.414
Kg, g	0.443	0.443	0.256
Ca, g	0.198	0.198	0.114
$ZnSO_4 \cdot 7\ H_2O$, g	0.005	0.005	
$MnSO_4 \cdot 4\ H_2O$, g	10^{-5}	10^{-5}	
$H_3BO_3\ Co(NO_3)_2 \cdot 6\ H_2O$, g	$5*10^{-5}$	$5*10^{-5}$	
$Na_2MoO_4 \cdot 2\ H_2O$, g	$5*10^{-6}$	$5*10^{-6}$	
$CuSO_4 \cdot 5\ H_2O$, g	$25*10^{-6}$	$25*10^{-6}$	
$FeSO_4 \cdot 7\ H_2O$, g	$35*10^{-5}$	$35*10^{-5}$	
EDTA, g	$4*10^{-3}$	$4*10^{-3}$	
$MgSO_4$, kg	0.15	0.15	0.15
KH_2PO_4, kg	0.7	0.7	0.7
Yeast Extract, kg	35		
Peptone, kg	35.2		
NH_4CL, kg		31.5	31.5
Glucose, kg	5	5	5
Biogas effluent, kg			385.2
Deionized Water, kg	902.4	902.4	517.3
Electricity			
Cell Culture Chamber,KWh,	480	480	480
Radial mixer/Impeller	30.24	30.24	30.24
UV Sterilizer	8.34	8.34	8.34
Air Blower	873.6	873.6	873.6

With regards the environmental impact, of the treatments where organic nitrogen sources (CM), 0% (CoM) and 48 % (AM) effluent were used, from lab to pilot scale which included 1000 L working volume open pond bioreactors, the utilization of effluent digestate and inorganic nitrogen source resulted in a substantial decline of 16 environmental impact indicators, 57-99% and 73-100% when Com and AM was used instead of the CM (Figure 1). Interesting is the fact that the relative contribution of NH_4CL and effluent digestate to the decline of the enviromental pollution indicators, utilized as the primary sources of nitrogen nutrition and micronutrients, was more than 60 % with regards the nitrogen sources and 41 % when effluent was used (Figure 2). When waste streams from the biofuel industry, in our case effluent digestate derived from biogas production is utilized in order to grow microalgae, environmental impact indicators are reduced severely since the particular waste stream is not leached towards the environment in landfills and reused in the frame of the circular economy concept.

Table 2. *Biomass productivity (Dry weight), Crude lipid production as % of dry weight biomass, total lipid content of dry biomass, Protein content as % of dry weight biomass DHA content as % of total lipids, total DHA content of dry biomass and residual of organic carbon after 7 days of dried algal biomass of S. limacinum grown on medium containing yeast and peptone (y&p), varying levels of effluent digestate (0%, 8%, 16%, 32% 48% (v/v))*

Cultivation Media (Treatments)	Dry Weight (g L^{-1})	Crude Lipid (%)	Total Lipid (g L^{-1})	DHA Fraction (%)	Total DHA (mg L^{-1})	Organic Carbon (g L^{-1}
Y & P	17 ± 0.8^{a}	47 ±1.4^{a}	7.9± 0.1^{a}	9±0.25^{a}	710±0.01^{a}	18±0.01^{a}
0%	31 ± 1.2^{b}	8.9±1.4^{b}	2.7± 0.8^{b}	3.33±1.7^{b}	89±0.02^{b}	35±0.03^{b}
8%	29 ± 0.5^{b}	5.3±0.6^{c}	1.5± 0.9^{b}	0.56±0.1^{b}	8.4±0.03^{c}	37±0.3^{b}
16%	64 ± 1.9^{c}	7.8±0.8^{c}	4.9±0.2^{c}	N.D	N.D	35.3±0.48^{b}
32%	64 ± 2.1^{c}	17.1±3.4^{d}	10.94±0.1^{a}	4.34±0.5^{b}	530±0.05^{a}	29±1.2^{c}
48%	49 ± 2.7^{d}	17.3±3.5^{d}	8.47±0.31^{a}	7.5±1.2^{a}	635±0.01^{a}	21±0.1^{c}

[1]Values (percentages) are represented as the mean ± standard deviation of triplicates, whereas letters (a, b, c and d) indicate statistical differences analysed at a level of $p < 0.05$.

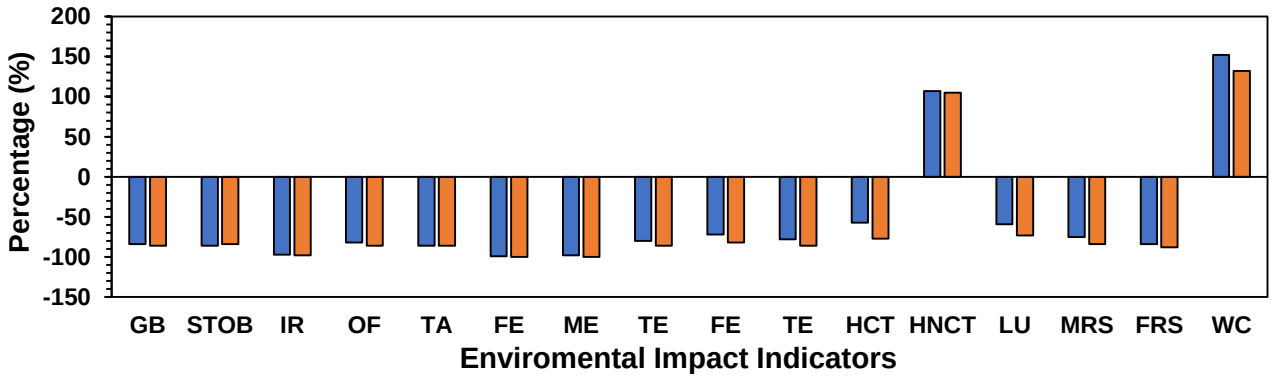

Figure 1. *Relative reduction (%) of environmental impact indicators per kg of produced dry biomass. Symbols : ■ Control medium (0% effluent) vs Conventional medium (Yeast & Peptone), ■ Alternative medium (48% effluent) vs Conventional medium (Yeast & Peptone). Environmental Impact Indicators (**GB** : Global Warming, **STOB** : Stratospheric ozone depletion, **IR** : Ionizing Radiation, **OF** : Ozone formation impact on human health, **TA** : Terrestrial Acidification, **FE** : Fresh water Acidification, **TE** : Terrestrial Eco toxicity, **FE** :Freshwater eco toxicity, **HCT** : Human Carcinogenic toxicity, **HNCT** : Human non-carcinogenic toxicity, **LU** : Land use, **MRS** : Mineral Resource Scarcity, **FRS** : Fosil resource Scarcity, **WC** : Water Consumption)*

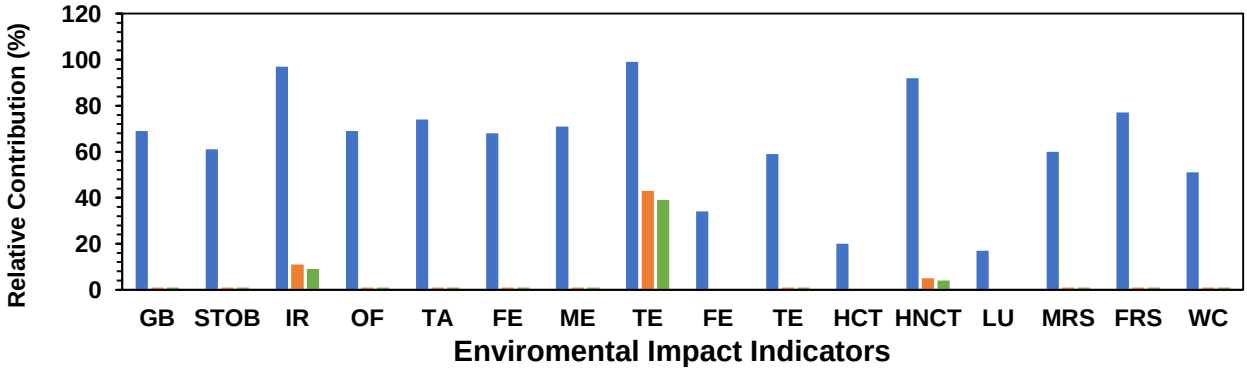

Figure 2. *Relative contribution of peptone to on environmental impact indicators per kg of produced dry biomass. Symbols : ■ **Conventional medium** (Yeast & Peptone), ■ **Alternative medium** (48% effluent) and ■ **Control Medium** (0% effluent). Environmental Impact Indicators (**GB** : Global Warming, **STOB** : Stratospheric ozone depletion, **IR** : Ionizing Radiation, **OF** : Ozone formation impact on human health, **TA** : Terrestrial Acidification, **FE** : Fresh water Acidification, **TE** : Terrestrial Eco toxicity, **FE** :Freshwater eco toxicity, **HCT** : Human Carcinogenic toxicity, **HNCT** : Human non-carcinogenic toxicity, **LU** : Land use, **MRS** : Mineral Resource Scarcity, **FRS** : Fosil resource Scarcity, **WC** : Water Consumption*)

4 Summary

The marine protist *S. limacinum* SR21 can serve as an effective bioremediation tool to handle waste streams from the biofuel industry. The optimal effluent concentration in order to maximize DHA production was 48% v/v, yielding 49.7 g L^{-1} biomass and 0.8 g L^{-1} DHA. Although this study did not achieve to reach industrial production standards with regards to the DHA content, environmental impact indicators were substantially lowered when organic nitrogen sources and micronutrients were replaced with low cost nitrogen sources and effluent digestate. However, a further assessment of other culture parameters (nitrogen concentration, oxygen dilution, temperature) is necessary to be conducted in order to standardize DHA production for aquaculture feeds.

Acknowledgements`

This research has been co-financed by the European Union and Greek national funds through the Operational Program Competitiveness, Entrepreneurship and Innovation, under the call RESEARCH – CREATE – INNOVATE (project code: T1EDK-01580).

References

Campbell, J. E., Lobell, D. B., and Field, C. B. (2009). Greater transportation energy and GHG offsets from bioelectricity than ethanol. *Science* **324**, 1055-1057.

Chi, Z., Pyle, D., Wen, Z., Frear, C., and Chen, S. (2007). A laboratory study of producing docosahexaenoic acid from biodiesel-waste glycerol by microalgal fermentation. *Process Biochemistry* **42**, 1537-1545.

Dediukhina, É., Chistiakova, T., and Vaĭnshteĭn, M. (2011). Biosynthesis of arachidonic acid by micromycetes (review). *Prikladnaia Biokhimiia i Mikrobiologiia* **47**, 125-134.

Eryilmaz, T., Yesilyurt, M. K., Cesur, C., and Gokdogan, O. (2016). Biodiesel production potential from oil seeds in Turkey. *Renewable and Sustainable Energy Reviews* **58**, 842-851.

Ganuza, E., Anderson, A., and Ratledge, C. (2008). High-cell-density cultivation of Schizochytrium sp. in an ammonium/pH-auxostat fed-batch system. *Biotechnology letters* **30**, 1559.

Holm-Nielsen, J. B., Al Seadi, T., and Oleskowicz-Popiel, P. (2009). The future of anaerobic digestion and biogas utilization. *Bioresource technology* **100**, 5478-5484.

Lin, Y.-C., Leaño, E. M., and Pang, K.-L. (2010). Effects of Cu (II) and Zn (II) on growth and cell morphology of thraustochytrids isolated from fallen mangrove leaves in Taiwan.

McNutt, J., and Yang, J. (2017). Utilization of the residual glycerol from biodiesel production for renewable energy generation. *Renewable and Sustainable Energy Reviews* **71**, 63-76.

Nagano, N., Taoka, Y., Honda, D., and Hayashi, M. (2013). Effect of trace elements on growth of marine eukaryotes, tharaustochytrids. *Journal of bioscience and bioengineering* **116**, 337-339.

Pádrová, K., Čejková, A., Cajthaml, T., Kolouchová, I., Vítová, M., Sigler, K., and Řezanka, T. (2016). Enhancing the lipid productivity of yeasts with trace concentrations of iron nanoparticles. *Folia microbiologica* **61**, 329-335.

Phang, S.-M., Chu, W.-L., and Rabiei, R. (2015). Phycoremediation. *In* "The Algae World", pp. 357-389. Springer.

Philpott, C. C. (2006). Iron uptake in fungi: a system for every source. *Biochimica et Biophysica Acta (bba)-molecular cell research* **1763**, 636-645.

Sun, L., Ren, L., Zhuang, X., Ji, X., Yan, J., and Huang, H. (2014). Differential effects of nutrient limitations on biochemical constituents and docosahexaenoic acid production of Schizochytrium sp. *Bioresource technology* **159**, 199-206.

Thompson, J. C., and He, B. B. (2006). Characterization of crude glycerol from biodiesel production from multiple feedstocks. *Applied engineering in agriculture* **22**, 261-265.

Yokochi, T., Honda, D., Higashihara, T., and Nakahara, T. (1998). Optimization of docosahexaenoic acid production by Schizochytrium limacinum SR21. *Applied Microbiology and Biotechnology* **49**, 72-76.

Zhu, L., Yan, C., and Li, Z. (2016). Microalgal cultivation with biogas slurry for biofuel production. *Bioresource technology* **220**, 629-636.

Zhu, L., Zhang, X., Ren, X., and Zhu, Q. (2008). Effects of culture conditions on growth and docosahexaenoic acid production from Schizochytrium limacinum. *Journal of Ocean University of China* **7**, 83-88.

Coping with urban soil pollution by heavy metals in Volos, Greece.

P. S. C. Aslanidis[1],*, E. E. Golia[2,3], S. G. Papadimou[3], O. D. Kantzou[2], A. M. Charitodiplomenou[2], K. Parcharidou[3], M. Androudi [3] and N. G. Tsiropoulos[4]

[1]Department of Planning and Regional Development, University of Thessaly, Volos, Greece
[2]Department of Agriculture Crop Production and Rural Environment, Laboratory of Soil Science, University of Thessaly, Volos, Greece.
[3]Department of Agriculture, Laboratory of Soil Science, Aristotle University of Thessaloniki, Thessaloniki, Greece.
[4]Department of Agriculture Crop Production and Rural Environment, Laboratory of Analytical Chemistry and Pesticides Laboratory, University of Thessaly, Volos, Greece.

Abstract. The impacts of heavy metals (HMs) or potentially toxic elements (PTEs) are undoubtedly a burning question in order to observe and breakdown urban soil pollution. At the present study light would be shed on the total concentration of PTEs during the years 2018 – 2021. As a case study Volos was selected because of its Mediterranean and peculiar (micro-) climate. While, at the same time 62 soil samples per year were collected in a study area that covers around 3.5km^2. Moreover, the imaginary triangle, which was observed, is bordered by the historic train station, the stations of buses and the maritime port. Furthermore, five drivers that push environment into instability are: rampant population growth, urbanization, (de-) industrialization, energy (fuel) poverty, and COVID – 19. However, these drivers would be explained by the principles of Circular Economy (CE), Sustainability, Sustainable Development Goals (SDGs) 11 – 12, and European Green Deal (EGD). Apparently, the impacts of PTEs are profound on (urban) biodiversity, and that would be also a matter of discussion. The depiction of total concentrations via thematic maps was achieved via the use of program QGIS 16. As a solution of the current environmental enigma of PTEs a proposed way out is phytoremediation. One matter of phytoremediation is intertwined with two aspects of CE, while the other with SS. To come to the point, CE, sustainability, SDGs, and EGD would constitute the theoretical background of the necessity of phytoremediation as a nature-based solution (NbS) in the mitigation of urban soil pollution by PTEs.

1 Introduction

The changes in society, in economy, and last but not least the instability on the environment were the core of Club of Rome in 1968. There were potent driving forces which destabilize the environment, for instance, the growth of population, disordered urban sprawl, industrialization, energy poverty, and the world pandemic. Moreover, the measures of preserving soil, its quality, and fertility were exhibited (Meadows et al., 1972).
The present case would focus on heavy metals (HMs) or alternatively potentially toxic elements (PTEs). The PTEs: Cu, Zn, Mn, Ni, and Co in narrow traces are essential for the functions of human beings, the flora and fauna. Nevertheless, when PTEs surpass the critical values, there is great augmentation of risks towards the people and the environment. For example, PTEs might provoke unwanted effects like diseases or illnesses. Some people have been diagnosed with arrhythmia or nausea, while other have experienced cancers (WHO, 2017, 2019; Lermen et al., 2021).

1.1. Drivers of change

Population growth is one driver of change that renders environmental stability at stake. Population growth is tightly interconnected with urbanization. Hence, it is imperative that focus be given on these two drivers and their impacts on the levels of PTEs (Golia et al., 2021a, 2021b; Peng et al., 2022). Areas with vivid commercial activities and trade-offs might be potential sources of environmental pollution by PTEs. Industrialization plays an important role on an area's economy, however, around industries there are possible accumulation of PTEs. Soil quality was exacerbated due to the utilization chemical ameliorants (World Commission on Environment and Development, 1987). Furthermore, the present study monitors the triangle: port, train station, and two bus terminals as fields with probable accumulation of PTEs (Braniš, 2006; Mueller et al., 2011; Golia et al., 2021a). The global pandemic from 2020 to 2021 resulted on the discontinuity of peoples' normality (Anastasiou and Duquenne, 2021). As an immediate result was the change of heating periods and means. This change on heating means is connected with energy poverty, because some households utilize less appropriate wood–fuel types as an alternative way (Streimikiene et al., 2021). This creates a vicious cycle with PTEs which adhere to GHGs and aggravate atmospheric conditions. Ultimately, when atmospheric particles sink to soil with PTEs on them, they pose a tremendous risk on soil conditions.

1.2. Circular Economy and Sustainability

The transition from linear to circular economy was never the easy option, either for entrepreneurs, or policymakers. Although, the importance of circular economy lies on its ability to maintain a product (ultimately) to eternity. Of course, this could not happen due to technological constraints, but it is an extremely auspicious strategy for entrepreneurs.
Resources, waste, and toxicity are at the core of eco-efficiency, although as a term could not address redesign of the linear system and economic growth (Braungart et al., 2007). The way-out of this quagmire is the adoption of two circular economy's schools of thought. On the one hand, there is the 'cradle to cradle' (C2C) which enables the economy to effectively use its components (McDonough and Braungart, 2002). On the other hand, put the environment at the core of experimentation to understand the know-how through the principles to live sustainably and not abusing the remaining raw resources (Benyus, 2002).

1.3. The role of SDGs and EGD

There are 17 SDGs which promote environmental respect and protection in different institutional ways. For instance, SDGs 11 and 12 focus on the amelioration of urban environment and sustainable consumption or production. In addition, SDGs 3 and 15 exemplifying the improvement of citizens' wellbeing and the amelioration of life on land respectively (Arana et al., 2020; Federico, 2020).
Accordingly, Agenda 2030 under EGD might render EU as the global leader of circular economy by implementing three roadmaps. Firstly, it is necessary to address the capabilities of circular economy, then it is the promotion of the durability of bioeconomy, and the preservation of biodiversity (Von-der-Leyen, 2019). The adoption of EGD paves the way to enhancing the notion of 'farm-to-fork' (Montanarella and Panagos, 2021).

1.4. How to cope with urban soil pollution?

Factories, industrial areas, mines have been monitored for their accumulations of PTEs (Kelepertzis, 2014; Pappa et al., 2018). However, there are also the most populated coastal cities in Greece which could be described by familiar areal typical features referring to urban soil pollution by HMs (Koliadima et al., 1998; Sakellariadou et al., 2001; Bourliva et al., 2018; Kelepertzis et al., 2020; Golia et al., 2021a; 2021b).
One eco-friendly way to cope with urban soil pollution by PTEs is the adoption of NbS. One type of grass (Brassica Napus) and willow (Salix Nigra) are capable ways of phytoremediation (Mleczek et al., 2009; Massenet et al., 2021). The success of phytoremediation is attributed to the production of great quantities of biomass (Akpor and Muchie, 2010; Labrecque et al., 2020; Golia et al., 2021a; Rajendran et al., 2022). On might also propose the use of NbS in three scales: inside, around and outside of the cities (Christopoulou et al., 2007; UNEP, 2021). One of the proposed NbSs is Salix Nigra, although Salicaceae plants might irritate allergic unwanted effects to individuals, however this downside is outweighed by willow's advantages.

2. Materials and Methods

The collection of totally 248 soil samples took place during 2018 – 2021. The samples were collected by wooden shovel, they have been put into plastic bags and then air-dried with a 2mm sieve. In addition, several physicochemical parameters and the pseudo-total concentrations were measured via Aqua Regia method. The total concentrations of the examined PTEs were extracted using acidic and alkaline solutions (Page et al., 1982). All of the PTEs were monitored according to ISO 11446 via an atomic absorption spectrophotometer. Lastly, the European Council Directive 86/278/EEC was important for the categorization of the PTEs according to their acceptable limits.
There was also the creation of thematic maps via QGIS. 16. Thematic maps constitute a way of monitoring PTEs with great accuracy, especially when referring to studies of urban soil pollution (Bourliva et al., 2018; Kelepertzis et al., 2020; Golia et al., 2021a).

3. Results and Discussion

The total concentrations of Cd and Zn in 2021 could be examined in Figure 1. The PTEs are divided into four classes, however the categorization has different limits for each PTE. Cd has almost 54 samples (out of 62) under the lowest limit. This is auspicious result, because Cd has detrimental effects on human health. Additionally, Zn has only 1 value (out of 62) that surpasses the upper limit and only 10 values are under the lower limit. However, Zn has beneficial effects on people and on plants, but only in short quantities.

PTEs could derive from anthropogenic or natural sources. For instance, Zn and Cd concentrations in cities could reside on car brakes, Zn could also exist on the rails of trains. Another possible source of pollution is cars, especially the parts of brakes and fuel system (Kabata-Pendias and Pendias, 2010; Golia et al., 2021a; 2021b).

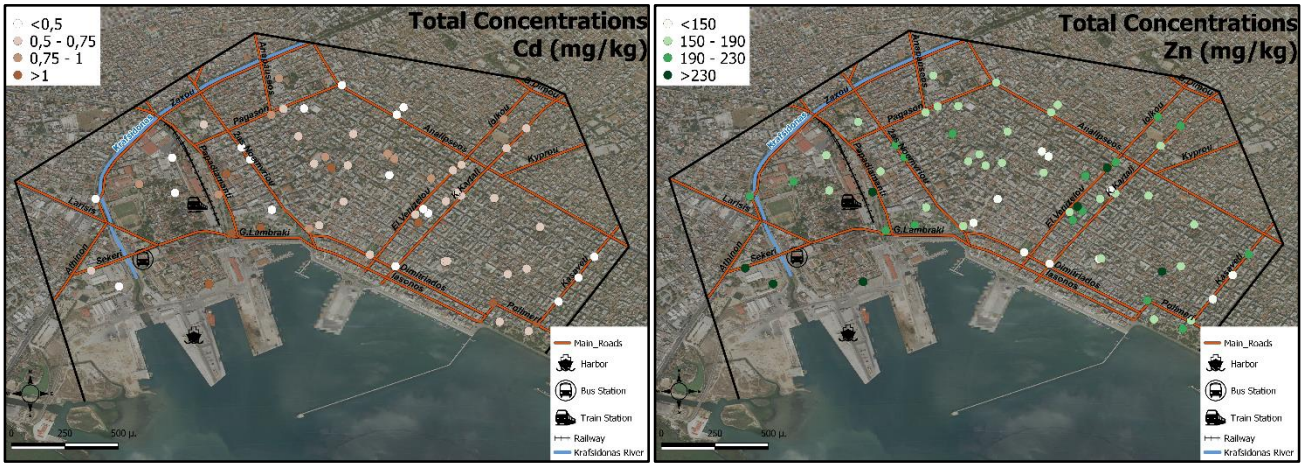

Figure 1. (left) total concentrations of Cd (mg*kg^{-1}) in 2021; (right) total concentrations of Zn (mg*kg^{-1}) in 2021.

Referring to total concentration of Cu and Pb were observed via thematic maps as well in Figure 2. Cu has positive potential effects on human health and in year 2021 there were 27 samples (out of 62) under the lower limit (0.5 mg*kg-1) of Directive 86/ 278/EEC. Further, Pb illustrated a bit more positive pattern of 43 samples (out of 62) under the lower limit (150 mg*kg-1). Both PTEs have zero samples above the higher limit of the European Directive.

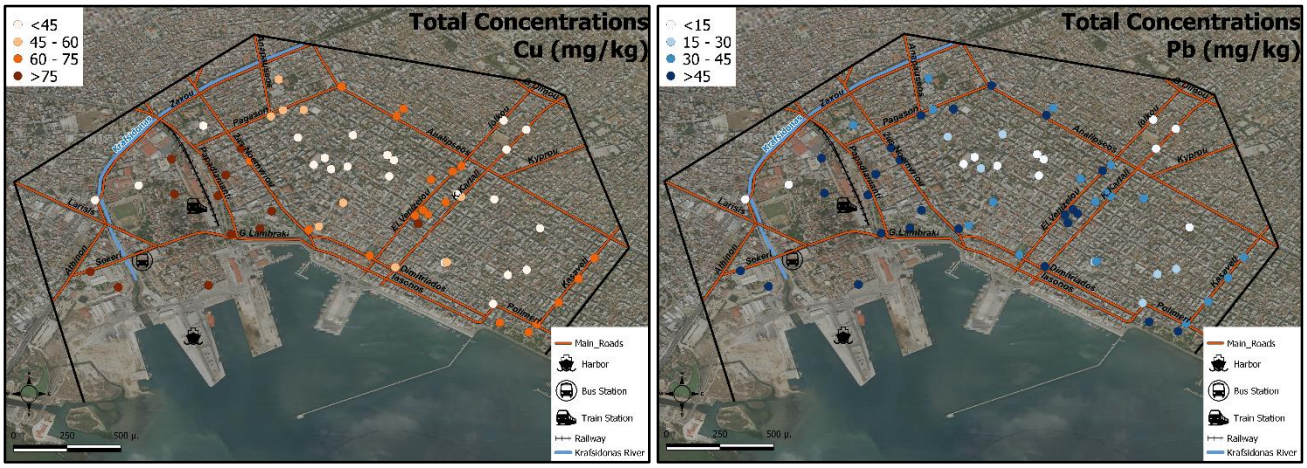

Figure 2. (left) total concentrations of Cu (mg*kg^{-1}) in 2021; (right) total concentrations of Pb (mg*kg^{-1}) in 2021.

Circular economy's schools of thought and sustainability provide the necessary theoretical background for examining PTEs, because these two perspectives enable the scientific community to monitor and at the same time to understand easier the notions of hazardous materials. As well as the institutional backdrop from SDGs and EGD, which promote actions like NbS, as phytoremediation in order to cope with PTEs.
Ultimately, the drivers of change as they have been stated in introduction, they pose several threats to urban sustainability. Thus, it is of utmost importance that PTEs be studied more thoroughly by interdisciplinary studies. Undoubtedly, the requirement of forecasting methods is imperative. Especially, when policymakers ought to care for the wellbeing of citizens in cities. A further focus should be given to coastal cities as well, due to the augmented maritime activity.

4 Summary

Present study's focus shed light on (1) drivers of change of urban soil pollution, (2) PTEs in urban soils of Volos, and (3) the identification of the natural or anthropogenic sources of PTEs via thematic maps. PTEs were examined under the scope of Sustainability, Circular Economy, and European Green Deal. In short, one quote

that illustrates the bitter reality is that of McDonough and Braungart (2002), which is ‘’a world of abundance, not one of limits, pollution, and waste’’.

Acknowledgements

The authors would like to express their gratitude to the Postgraduate Program of the University of Thessaly, entitled: Sustainable Management of Environmental Change and Circular Economy. Part of the results derive from the post-graduate dissertation of student Sotiria G. Papadimou.

References

Akpor, O.B., Muchie, M. 2010. Remediation of Heavy Metals in Drinking Water and Wastewater Treatment Systems: Processes and Applications. Int. J. Phys. Sci. 5, 1807–1817.

Anastasiou, E., Duquenne, M.N. 2021. First-Wave COVID-19 Pandemic in Greece: The Role of Demographic, Social, and Geographical Factors in Life Satisfaction during Lockdown. Soc. Sci., 10.

Arana, C., Franco, I., Joshi, A., SedhaiJyoti. 2020. SDG 15 Life on Land: A Review of Sustainable Fashion Design Processes - Upcycling Waste Organic Yarns. In Actioning the Global Goals for local impact: Towards sustainability science, Franco, I.B., Chatterji, T., Derbyshire, E., Tracey, J., Ed., Springer, pp. 247–264 ISBN 9789813299276.

Bourliva, A., Kantiranis, N., Papadopoulou, L., Aidona, E., Christophoridis, C., Kollias, P., Evgenakis, M., Fytianos, K. 2018. Seasonal and Spatial Variations of Magnetic Susceptibility and Potentially Toxic Elements (PTEs) in Road Dusts of Thessaloniki City, Greece: A One-Year Monitoring Period. Sci. Total Environ., 639, 417–427.

Braniš, M. 2006. The Contribution of Ambient Sources to Particulate Pollution in Spaces and Trains of the Prague Underground Transport System. Atmos. Environ., 40, 348–356.

Christopoulou, O., Polyzos, S., Minetos, D. 2007. Peri-Urban and Urban Forests in Greece: Obstacle or Advantage to Urban Development? Vol. 18, ISBN 9608934508.

Federico, M.B. 2020. SDG 3 Good Health and Well-Being. In Actioning the Global Goals for local impact: Towards sustainability science, policy, education and practice, Franco, I.B., Chatterji, T., Derbyshire, E., Tracey, J., Ed., Springer, pp. 39–55, ISBN 978-981-329-926-9 978-981-329-927-6.

Golia, E.E., Papadimou, S.G., Cavalaris, C., Tsiropoulos, N.G. 2021a. Level of Contamination Assessment of Potentially Toxic Elements in the Urban Soils of Volos City (Central Greece). Sustain. 2021, 13, 1–12.

Golia, E.E., Angelaki, A., Giannoulis, K.D., Skoufogianni, E., Bartzialis, D., Cavalaris, C., Vleioras, S. 2021b. Evaluation of Soil Properties, Irrigation and Solid Waste Application Levels on Cu and Zn Uptake by Industrial Hemp. Agron. Res., 19, 92–99.

International Organization for Standardization ISO/DIS 11466. 1994. Environment Soil Quality., Geneva, Switzerland.

Benyus. J.M.2002. Biomimicry: Innovation Inspired by Nature. HarperCollins e-books 2002.

Kabata-Pendias, A. and Pendias, H. 2010. Trace Elements in Soils and Plants, Third Edit., CSR Press, Vol. 2, ISBN 0-8493-1575-1.

Kelepertzis, E. 2014. Investigating the Sources and Potential Health Risks of Environmental Contaminants in the Soils and Drinking Waters from the Rural Clusters in Thiva Area (Greece). Ecotoxicol. Environ. Saf., 100, 258–265

Kelepertzis, E., Argyraki, A., Chrastný, V., Botsou, F., Skordas, K., Komárek, M., Fouskas, A. 2020. Metal (Loid) and Isotopic Tracing of Pb in Soils, Road and House Dusts from the Industrial Area of Volos (Central Greece). Sci. Total Environ., 725, 138300.

Koliadima, A., Athanasopoulou, A., Karaiskakis, G. 1998. Particulate Matter in Air of the Cities of Athens and Patras (Greece): Particle-Size Distributions and Elemental Concentrations. Aerosol Sci. Technol., 28, 292–300.

Labrecque, M., Hu, Y., Vincent, G., Shang, K. 2020. The Use of Willow Microcuttings for Phytoremediation in a Copper, Zinc and Lead Contaminated Field Trial in Shanghai, China. Int. J. Phytoremediation, 22, 1331–1337.

Lermen, D., Weber, T., Göen, T., Bartel-Steinbach, M., Gwinner, F., Mueller, S.C., Conrad, A., Rüther, M., von Briesen, H., Kolossa-Gehring, M. 2021. Long-Term Time Trend of Lead Exposure in Young German Adults – Evaluation of More than 35 Years of Data of the German Environmental Specimen Bank. Int. J. Hyg. Environ. Health, 231.

Massenet, A., Bonet, A., Laur, J., Labrecque, M. 2021. Co-Planting Brassica Napus and Salix Nigra as a Phytomanagement Alternative for Copper Contaminated Soil. Chemosphere, 279, 130517

McDonough, W., Braungart, M. 2002. Cradle to Cradle: Remaiking the Way We Make Things., North Point Press.

Meadows, D.H., Meadows, D.L., Randers, J., BehrensIII, W.W. 1972. Limits to Growth, A POTOMAC ASSOCIATES BOOK, ISBN 9780444641304.

Mleczek, M., Rissmann, I., Rutkowski, P., Kaczmarek, Z., Golinski, P. 2009. Accumulation of Selected Heavy Metals by Different 736 Genotypes of Salix. Environ. Exp. Bot, 66, 289–296.

Montanarella, L., Panagos, P. 2021. The Relevance of Sustainable Soil Management within the European Green Deal. Land use policy, 100, 104950.

Mueller, D., Uibel, S., Takemura, M., Klingelhoefer, D., Groneberg, D.A. 2011. Ships, Ports and Particulate Air Pollution - An Analysis of Recent Studies. J. Occup. Med. Toxicol., 6, 1–6.

Page, A.L., Miller, R.H., Keeney, D.R. 1982. Methods of Soil Analysis,2. Chemical and Microbiological Properties., A.L., P., R.H., M., D.R., 748 K., Eds., American Society of Agronomy, Madison, Wisconsin, USA.

Pappa, F.K., Tsabaris, C., Patiris, D.L., Androulakaki, E.G., Eleftheriou, G., Betsou, C., Michalopoulou, V., Kokkoris, M., Vlastou, R. 2018. Historical Trends and Assessment of Radionuclides and Heavy Metals in Sediments near an Abandoned Mine,Lavrio, Greece. Environ. Sci. Pollut. Res., 25, 30084–30100,

Peng, C., Zhang, K., Wang, M., Wan, X., Chen, W. 2022. Estimation of the Accumulation Rates and Health Risks of Heavy Metals in Residential Soils of Three Metropolitan Cities in China. J. Environ. Sci. (China), 115, 149–161.

Rajendran, S., Priya, T.A.K., Khoo, K.S., Hoang, T.K.A., Ng, H.S., Munawaroh, H.S.H., Karaman, C., Orooji, Y., Show, P.L. 2022. A Critical Review on Various Remediation Approaches for Heavy Metal Contaminants Removal from Contaminated Soils. Chemosphere, 287, 132369.

Sakellariadou, F., Dassenakis, M., Michailidou, L., Haralambides, L. 2001. Metal Pollution in Piraeus Port, a Major Mediterranean Port. Fresenius Environ. Bull., 10, 73–79.

Streimikiene, D., Kyriakopoulos, G.L., Lekavicius, V., Siksnelyte-Butkiene, I. 2021. Energy Poverty and Low Carbon Just Energy Transition: Comparative Study in Lithuania and Greece, Springer Netherlands, Vol. 158.

UNEP Smart, Sustainable and Resilient Cities: The Power of Nature-Based Solutions. 2021, 1–32. https://wedocs.unep.org/bitstream/handle/20.500.11822/36586/SSRC.pdf?sequence=1&isAllowed=y (accessed on 20 April 2022).

Von-der-Leyen, U. A 2019. Union That Strives for More: My Agenda for Europe. Eur. Crim. Law Rev.

WHO 2017. Guidelines for Drinking-Water Quality, https://www.who.int/publications/i/item/9789241549950 (accessed on 20 571 April 2022)

WHO 2019. Prevenint Diesease Through Healty Environments: Exposure to Cadmium: A Major Public Health Concern. Prev. Dis. Through Heal. Environ. https://apps.who.int/iris/handle/10665/329480 (accessed on 20 April 2022)

World Commission on Environment and Development. 1987. The Brundtland Report: “Our Common Future”.

Silvopastoralism in the Mediterranean with special emphasis in Greece

Anastasia Pantera[1], Konstantinos Mantzanas[2], Vasilios Papanastasis[2], Andreas Papadopoulos[1]

[1]Department of Forestry and Natural Environment Management, Agricultural University of Athens, Karpenissi
[2] Department of Forestry and Natural Environment, Aristotle Univeristy of Thessaloniki, Thessaloniki, Greece

Abstract. The Mediterranean basin is characterized by a variety of bioclimates, species and farming systems adapted to local needs and environments with agroforestry being one of the most ancient land uses. Agroforestry is the practice of deliberately integrating woody vegetation (trees or shrubs) with crops and/or animal systems to benefit from the resulting ecological and economic interactions. Silvopastoralism has been one of the older agroforestry land uses, supporting rural population through time under adverse, sometimes, environments. Silvopastoral are the systems where there is a joint wood and animal production. The diverse forests of the Mediterranean region, predominated by the coniferous *Pinus* sp., *Abies* sp., *Juniperus* sp., or broadleaved mainly of *Quercus* sp., grazed by domesticated livestock mostly of sheep and goats, have provided numerous products. These products include dairy and meat and their byproducts supporting local economy and forming the basis of an exemplary circular economy. The combinations of plant and animal species are numerous and depend on local environmental and local conditions, a respectable example of sustainable land use, including sedentary, with a permanent base throughout the year, or transhumant with seasonal movement of the animals. Well known silvopastoral systems are the Dehesa in Spain and the Montado in Portugal. Similar systems, however not well known, are the Greek oak silvopastoral systems mostly of valonia oak. Pollarding is still a living practice throughout the Mediterranean although confined due to law restrictions. Some other well distributed throughout Greece, mainly in mountainous regions, are the chestnut and walnut silvopastoral or grazed forests. Grazing has been accused for soil erosion however it is getting attention lately as a fire management tool. In particular, grazing may reduce the flammable understory vegetation reducing forest fire risk while providing products and supporting local communities. Existing research indicates that appropriate application of agroforestry principles and practices is a key mean by which the European Union might achieve more sustainable production methods whilst producing both profits for farmers and environmental benefits for society.

Key words: Agroforestry**,** grazing, husbandry, livestock, forests

1 Introduction

Eastern Mediterranean is characterized by a variety of ecosystems traditionally used by humans for the past millennia, providing numerous services and products. Eastern Mediterranean areas have never been glaciated except of local glaciers in the highest mountains permitting the uninterrupted evolvement of flora and fauna for long periods. Additionally, isolation such as in the Greek islands, favored the multiplication and subspeciation of many species (Curry-Lindahl, 1964). Some of the world's greatest civilizations flourished in its countries and, possibly no other place on earth has witnessed so many historical events in the past 3000 years. All of the above factors, in combination to the climatic conditions, contributed to the formation of forests and forested areas rich in plant species and life forms, providing shelter and forage for grazing animals. Raising livestock in the eastern Mediterranean began as early as 10000 BC whereas by 3000 BC it had already spread to the western part of the region Le Houerou (1981). Livestock became part of the landscape with forest being the first element to be affected (Papanastasis, 2009). Evidence show livestock grazing in Roman olive and orange groves (Nair, 1993). Agroforestry represents the traditional land use system that combines the woody, the livestock and the annual crop component (Mosquera-Losada et al, 2018). The agroforestry system in which trees/shrubs are combined with livestock and pasture production on the same unit of land is defined as silvopastoral (AFTA, 1997; Alavapati and Nair 2001; Mosquera-Losada, 2009, Moreno et al 2018, Pantera et al, 2018). Mediterranean forests can be characterized as silvopastoral systems since their relatively open crowns, due to the light tolerance of the dominant tree species as well as due to their past mismanagement, permit the growth of a lush understory of herbaceous and woody species, mostly evergreen, which means that green leaves and twigs are available as forage throughout the year (Papanastasis, 1996 and 2009).

Silvopastoral are complex systems accompanied by a number of advantages and disadvantages (Wilson and Kang, 1981; Nair, 1984; MacDicken and Vergara, 1990). However, all of their disadvantages can be overcome by proper management. It is the purpose of this paper to describe the basic components of silvopastoral systems in eastern Mediterranean with special emphasis in Greece and the management applied

so far. The later depend on their components which, according to Papanastasis (1996, 2004), are tree (species composition), animals & pastures (pastures-management) and the presence of man (ownership-management). All of these components affected and were affected, positively or negatively, to each other and to the physical environment of a specific area.

2 Woody component and silvopastoral management

Woody represent the first component which provide numerous products such as timber, fuel wood, fencepost, charcoal, fodder, fruits and nuts, serving multiple purposes from water and nutrient absorption, nitrogen fixation, shade, windbreaks and hedgerows, boundary markets, erosion control, and were managed accordingly, that is based to the individual needs of the local population and to the available natural resources of each area. These parameters, in combination to products' demand and availability of resources, shaped a variety of systems based on local peculiarities and environmental conditions.
Actually, the silvopastoral are multistrata ecosystems rich in plant species and can be characterized based on their overstory tree and by their understory plant species (Papanastasis and Noitsakis, 1992). Based on the woody component, three major categories of silvopastoral systems can be distinguished in eastern Mediterranean, the coniferous such as of *Pinus* sp., *Abies* sp., *Juniperus* sp., *Cupressus* sp. etc, the evergreen and the deciduous (including semi-deciduous) broadleaved tree species such as of oak, olives, walnuts, almonds, poplar etc. (Papanastasis and Noitsakis, 1992). In space, the trees in all categories may be spontaneous or planted whereas the understory is composed of shrubs, grasses and other low vegetation (Papanastasis, 2004).
In Greece, two silvopastoral systems can be distinguished, the open forests, with tree canopy less than 40%, where animal production is the main and wood production the secondary use and the grazable (dense) forests, with tree canopy exceeding 40%, where there is a joint wood and animal production (Papanastasis, 1996). A detailed description based on the tree component is presented in the following sections.

2.1 Coniferous silvopastoral systems

Pine forests cover about 5% of the total area of Mediterranean basin and about 25% of the total area under forest and are the ones most frequently affected by human interventions and forest fires (Richardson and Rundel, 1998). Several pine species form silvopastoral systems in eastern Mediterranean region (Grove and Rackham, 2001; Papanastasis, 2004) providing a great number of products, as mentioned before.
An important coniferous silvopastoral system in Greece is that of Aleppo pine (*Pinus halepensis* ssp. *halepensis*), combining a large variety of evergreen sclerophyllous shrubs of *Pistacia* sp*., Erica* sp*., Quercus* sp*., Phillyrea* sp*., Arbutus* sp*., Cistus* sp*.,* etc providing fodder for bees, sheep and mainly goats (Schultz et al., 1987). This system evolved in time mostly for its resin value, for livestock grazing and honey produced. Farmers sustained this system by clearing its understory by collecting the understory vegetation for fuel wood and for better access to the resin collection areas and by grazing these areas. However, the substitution of resin with chemical, and basically cheaper, chemical substances as well as the decreased grazing of these forests favored the development of a dense, flammable understory biomass partly responsible for the frequent forest fires and the subsequent change in land use as will be discussed in the brutia pine systems.

Brutia pine (*Pinus halepensis* ssp. *brutia*), forms similar silvopastoral systems in Greece, Cyprus and Turkey. In Greece it contains *Quercus coccifera* trees and/or almonds, walnuts, apples, wild and tame pears, grapes, figs, (Schultz et al., 1987) whereas in Turkey is accompanied with maquis vegetation (Geray and Özden, 2003), both used for grazing by goats and sheep. Products from this system vary from timber, fruits, honey, fuel wood, resin, wildlife, meat, and recreation (Papanastasis et al., 2009). In the Greek island of Thassos, the economic revenue from honey production of the brutia pine forest is multiple times greater than that from timber production (Eleftheriadis, 1987). At present, this system is seriously degraded from overgrazing and illegal lumbering, without any specific management regime (Geray and Özden, 2003; Papanastasis et al., 2009). Forest fires represent a frequent menace and its only present economic revenue depends on meat/dairy products, honey production and tourism. It is of vital importance that a management plan is immediately applied involving grazing that may suppress the dense understory reducing forest fires risk. A major threat applied to all systems is land use change after wild fires to forestry, agriculture and mostly to numerous civil uses. Papanastasis (2004) warns that the aforestation of agrosilvopastoral systems may lead to the degradation of their original vegetation.

Pinus nigra forms silvopastoral systems in mountainous areas with herbaceous understory in Greece (Papanastasis et al., 2009), and with the same species (*Pinus nigra*) with *Cedrus libani* and *Abies nebrodensis* system in Turkey, used for grazing by the Anatolian black goats (Geray and Özden, 2003). In Cyprus, overstory of *Cedrus* sp. *Cupressus* sp., combined with *Pistacia* sp., *Juniperus* sp. etc, 11% carrigue of *Cistus* sp., *Thymus* sp. grazed by goats (Koutalianos, 2007). Papanastasis et al. (2009) describes a *Cupressus sempervirens* silvopastoral system in Greece used for grazing. Another important system is the Greek fir tree (*Abies cephalonica* and *Abies borissi regis)*, with understory vegetation of *Juniperus* sp., *Quercus* sp. and a variety of herbaceous species, used for grazing primarily by sheep and less by cattle and goats. These systems have supported the local economy in many poor mountainous regions where availability of other resources is limited during the winter period but decreased in time due to legal restrictions (grazing by goats prohibited by law), rural abandonment and apostrophe to traditional practices such as pastoralism in favor to the more attractive ones such as tourism.

2.2 Broadleaved silvopastoral systems

Acorns have been multiple times praised for their nutritional value (Fraser, 1922). Many oak forest of *Quercus infectoria*, *Q. cerris*, *Q. pubescens* spread in many parts of Turkey as well as forested areas of *Q. brantii* in S.E. Anatolia and *Q. ithaburensis* in W. & S. Anatolia (Davis, 1982), used for grazing (Dufour-Dror, 2007). *Quercus ithaburensis* ssp. *ithaburensis* and *Q. calliprinos* forests found in many parts of Israel, accompanied by shrubs and other herbaceous species, are a valuable and suitable environment for cattle grazing (Dufour-Dror, 2007). *Q. ithaburensis* with its subspecies is an east-Mediterranean species (Pantera et al., 2008) forming distinctive silvopastoral system in Greece. *Q. ithaburensis* was used in the past for its wood, acorns as well as for tannery (Grispos, 1936; Cristodoulopoulos, 1937; Tsitsas, 1978) but nowadays in Greece is mainly used for grazing (Figure 1), especially by sheep and is declining mostly due to abandonment (Pantera and Papanastasis, 2003). The species has currently ecological rather than economic importance (Pantera and Papanastasis, 2003). The understory of such systems is composed mainly of holm oak*,* almonds*,* olives, carobs, mulberries, several bushes or dwarf shrubs, providing fodder for sheep, goats, and hogs (Pantera *et al*., 2008). Nowadays farmers are switching them to olive groves and/or agricultural fields. In Turkey there is still a great interest for *Q. ithaburensis* used for organic tannery derived products such as leather goods, tapestry etc.

Kermes *(Quercus coccifera)* and holm oak (*Quercus ilex),* accompanied by shrubs, both grazed by sheep and goats (Papanastasis et al., 2009) form other silvopastoral systems. They provide a variety of products ranging from meat and dairy products to charcoal. Managed for heir values, these systems are rapidly degrading to extinction, due to overgrazing, illegal lumbering, forest fires and abandonment. The decreasing grazing rates favor the growth of a dense understory that increases forest fir risk but also renders them inaccessible for future use as silvopastures. Thus, a better management needs soon to be applied for such systems, not only because their extinction would be detrimental to the local economy and the system itself, but also for their value as traditional land use systems.

Chestnut (*Castanea sativa*) and walnut (*Juglans regia*) form significant silvopastoral systems, mostly in mountainous areas, combined with a variety of other plant species (*Fagus* sp.*, Ilex aquifolium*, *Tilia* sp., *Caprinus orientalis, Aesculus hippocastanum*, apple and pear orchards), sustaining a number of domesticated but also wild animals such as wolves, wild dogs, wild boars, greatly contributing to the biodiversity of the area (Schultz et al., 1987; Papanastasis et al., 2009). Their multiple products include nuts, quality timber, fruits, honey, fuel wood, wildlife, meat, recreation etc. and was intentionally cultivated in certain areas for the past 400 years (Pantera and Mouflis, 1996). Since in many areas it is a sub-climax community, its cultivation included the clearing of invading species, grafting wild chestnuts and lopping branches (Pantera and Mouflis, 1996). These systems are abandoned lately due to the low-price value of the nuts, the scarce and expensive manual labor but mainly due to the fact that locals get a better income from tourism rather that farming. Another major threat is a fungal disease which has been devastating chestnut trees in the past few years.

Olive orchards are frequently described in the bible as the grazing land of thousands of sheep. Its silvopastoral systems in Greece include oranges, almonds, walnuts, apricots, fig, poplars, and various grazing animals (Mantzanas et al., 2006; Papanastasis et al., 2009). There is a growing interest lately for olive-tree organic products among the numerous other products it offers however farmers are switching them to monocultures which are easier to manage. A major threat to this system is the intrusion of the pest *Oxalis pes-caprae* in its substratum replacing other valuable to livestock grazing species. This system needs to be preserved, among others, for its great non-timber and traditional value.

Two systems with increasing interest and value lately are the ones formed by carob (*Ceratonia siliqua*) and mastic tree (*Pistacia lentiscus*). The former combines with olives, cypresses, and its pods are nutritious for

sheep and goats (Schultz et al., 1987; Papanastasis et al., 2009), but also for human consumption replacing chocolate. Mastic-tree can be found in many areas (Athanasiadis, 1986), however, in the island of Chios, Greece, produces the valuable gum and its secondary products (oil, lotions, etc.) (Savidis, 2000). Meat and dairy products from the grazing animals of the system are additional income sources however, the locals, due to the increasing price of the mastic, are switching it to monoculture (Schultz et al., 1987).
Other species of interest include *Erica arborea* and *Morus alba*–silkworm (Schultz et al., 1987; Papanastasis et al., 2009), fig and the poplar-sheep silvopastoral systems. Usually fig trees (*Ficus carica*) spread in many areas providing a number of products (Athanasiadis, 1986). It is a very old system, well adapted to the dry and poor areas providing fodder for sheep and goats (Papanastasis et al., 2009). No specific management has been applied so far and, as with many other systems.

3 Animal-pasture component and silvopastoral management

Goats and sheep represent the major livestock component in Mediterranean silvopartoral systems (Vidal, 2002) mostly due to the available forage (Mosquera-Losada et al., 2009; Papanastasis, 2009). Goats and sheep numbers are multiple times higher than those of cattle in Jordan, Palestine, Greece, Syria, Cyprus, Lebanon, Albania, Turkey and equal in Egypt and Israel. Goats outnumber sheep only in Cyprus (FAO, 2006; Papanastasis, 2009). Apiculture and silkworm cultures are special types of silvopastoral systems involving honeybees using aphid nectar on pine trees as well as flower nectar to produce honey, and silkworms using mulberry (*Morus alba)* as feed for the caterpillars and *Erica arborea* to suspend cocoons (Schultz et al., 1987; Papanastasis et al., 2009). Goats have been blamed many times as the main cause for the destruction of the natural environment of many greek areas even thought overgrazing rather than goat grazing should be blamed for it (Papanastasis, 2009). In Greece, during the Ottoman period and up to a few decades ago, people lived in small villages farming and herding. Nowadays grazing is prohibited by law under certain conditions such as inside fir, burned or under regeneration forests and forested areas (Giannakouros, 2002). Efforts for the improvement of pastures in forested land include the construction of watering, salting and sheltering points even thought during the past decade emphasis and funding has switched to the construction/opening of new roads (Pantera et al., 2003).
The diverse physiognomy of Greece (flat areas at sea level up to mountainous locations of over 2,000 m a.s.l.), combined to the limited available fodder for livestock during the winter, have contributed to the formation of two husbandry types, the *sedentary* with a permanent base throughout the year, and the *transhumant* with seasonal movement of the animals. Similar grazing regime is reported for Turkey by Geray and Özden (2003). Today, however, sedentary livestock production appears to be more common, largely because seminomadic communities have become settled villagers.

Figure 1. Valonia oak silvopastoral system

An important contribution of grazing animals is that of reducing understory biomass and, subsequently reduce forest fire risk. This raises a very important issue, especially after the devastating forest fires of 2007 and 2021 and needs to be further investigated. Many times and mainly due to the lack in personnel, the after-fire control on the actual grazing stock is minimal. The resulting overgrazing caused and still causes severe damages to both regeneration and trees but also creates a false idea to many people as of the devastating results of grazing.

4 Human component and silvopastoral management

Forest and other wooded land in Mediterranean basin countries, with the exception of Lebanon, are public-owned in contrast to the western ones (FAO, 2009a). Mismanagement including overgrazing (FAO, 2009b) is another common characteristic. There are indications of intensive grazing from Crete to Macedonia (N. Greece). In Cyprus, the Acama-Randi Forest is seriously degraded with desertification signs mostly due to overgrazing, uneven distribution of the livestock in the area and uncontrolled grazing (Papanastasis, personal communication). The Israeli Tabor oak forests (*Quercus ithaburensis* ssp. *ithaburensis*), have been destroyed by man through time, especially in the western part due to wood harvest in the past, as well as by overgrazing (Dufour-Dror, 2007).

Most silvopastoral systems are traditional of high environmental value that have supported financially local communities providing people the means to survive through eras of famine and wars. Greece has a minor part of its land suitable for agricultural use and even less for intensive agriculture. So, even in the lowlands, silvopastoral systems were, are and must continue to be used for their multiple products and services. The lack of a holistic management has resulted to the gradual degradation of many traditional silvopastoral systems. Abandonment is a major reason for their degradation driven by the low money revenue of these systems as compared to other practices. The present unwillingness of farmers to practice silvopastoralism and inherent their knowledge to the next generation posses a major threat for the lack and disappearance. As mentioned before, pastoralism faces the apostrophe of young people who prefer more attractive professions such as those involved with tourism. In many areas the price value of land has increased tremendously for recreation purposes which, in combination to the high man-labour cost, has driven many locals to employ other occupations (mostly within the tourist industry) rather than farming and pastoralism. Additionally, overgrazing in combination to frequent forest fires has seriously degraded the environment in certain areas prohibiting any further agricultural or pastoral use.

5 Conclusions

Farmers are an important component of silvopastoral systems and they must understand the ecological, economic and traditional role of these systems. Special incentives must be given to farmers, maybe through subsidies, to sustain the existing form of their land management and even establish new silvopastoral systems. A great effort is on the way, and must be further supported by the local authorities, for public awareness, on several of these systems, stressing out that these systems are not only a part of the local economy and environment but also a part of Greek history and tradition.
Silvopastoral systems are very rich and viable with great ecological, economic and environmental importance. A sound management must emphasize the outstanding role of silvopastoral systems taking into account their great economic and ecological value.

References

Alavapati, Jr.R. and Nair PKR., 2001. Socioeconomics and institutional perspectives of agroforestry. In: Palo M. Uusivuori J (eds.) World forests, society and environment: markets and policies. Kluwer, Dordrecht, The Netherlands.

Association for Temperate Agroforestry (AFTA), 1997. The status, opportunities and needs for agroforestry in the United States, AFTA, Columbia, MO.

Athanasiadis N., 1986. Forest Botany (Trees and shrubs of the greek forests), Part II, Pub. Giahoudi-Giapoudi, Thessaloniki, 309 pp.

Cristodoulopoulos A., 1937. Paragogi kai ekmetalefsi valanidiou [Production and use of the oak acorns], Forest Life, 87: 51 – 52 (In Greek).

Curry-Lindahl K., 1964. Eden in a ruined landscape: The Mediterranean lands. In: EUROPE: A NATURAL HISTORY, pp. 14-28, NY, 299 pp.

Dufour-Dror, J.M., 2007. Influence of cattle grazing on the density of oak seedlings in a Tabor oak forest in Israel, Acta oecologia 31: 223-228.

Eleftheriadis N., 1987. Management of brutia and Aleppo pine forests. Proceedings from the scientific meeting “Aleppo and brutia pine forests”, pp. 169-186, (In greek).

FAO 2009a, http://www.fao.org/forestry/32182/en/.

FAO 2009b, http://www.fao.org/ag/agl/agll/terrastat/wsrout.asp?wsreport=4&region=2&search=Display+statistics+%21.

FAO Statistical Yearbook 2005-2006, http://www.fao.org/es/ess/yearbook/

Frazer J.G., 1922. The magic art and the evolution of Kings. Vol II. MacMillan and co. London.

Geray U., Özden S., 2003. Silvopastoralism in Turkey's Mountainous Mediterranean Region Mountain Research and Development 23(2):128-131.

Giannakouros P.E. 2002. Forest code and forest laws. Book, Sakkoula Pub., Athens-Komotini, 633 pp. (In Greek).

Grispos P., 1936. The acorns extracts in forest industry. *Forest Life* 44 – 45: 157 – 160 (In Greek with English summary).

Grove A.T., Rackham O., 2001.The nature of Mediterranean Europe, An Ecological History. Yale University press, London.

Koutalianos A., 2007. The fire protection system of Cyprus, Proceedings of 13th Panhellenic conference, Hellenic Forestry Society, Kastoria, October 2007, pp. 174-184.

Le Houerou, H.N., 1981. Impact of man and his animals on Mediterranean vegetation. Mediterrannean-Type Shrublands, Elsevier Sci. Publ. Co. N.Y. pp. 479-521.

Mantzanas K., Tsatsiadis E., Ispikoudis I., Papanastasis V.P., 2006. Agrosilvopastoral systems in Greece. In: Platis etl. (eds.), Rangelands and semi-mountainous areas: means of rural development, Proceeding if the 4th Panhellenic Rangeland Congress, Volos, 10-12 November 2004, pp: 297-303.

Moreno, G., Aviron, S., Berg, S., Crous-Duran, J., Franca, A., García de Jalón, S., Hartel, T., Mirck, J., Pantera, A., Palma, J.H.N., Paulo, J.A., Re, G.A., Sanna, F., Thenail, C., Varga, A., Viaud, V., Burgess P.J. (2017). Agroforestry systems of high nature and cultural value in Europe: provision of commercial goods and other ecosystem services. Agroforestry Systems (2017). https://doi.org/10.1007/s10457-017-0126-1

Mosquera-Losada, M.R., J.H. Mcadam, R. Romero-Franco, J.J. Santiago-Freijanes, And A. Rigueiro-Rondriguez, 2009. Definitions and components of agroforestry practices in Europe. A. Rigueiro-Rondriguez et al. (eds.), Agroforestry in Europe: Current Status and Future Prospects, Pub. Springer, pp. 3-19.

Mosquera-Losada, R.M., Santiago-Freijanes J.J., Moreno, G.M, den Herder M, Aldrey JA, Rois-Diaz M, Ferreiro-Domíguez, N., Pantera A, Rigueiro-Rodriguez A, 2018, Agroforestry definition and practices for policy makers, 4th European Agroforestry Conference – Nijmegen, 28-30 May 2018 Agroforestry as Sustainable Land Use.

NAIR, P.K.R., 1993. An introduction to agroforestry, Book, Kluwer Academic Publishers, Dordrecht, The Netherlands, 499 pp.

Pantera A., Karageorgos G., Loukas P. Fakas I., 2003. Mountainous rangelands of the prefecture of Evritania. Proceedings of the 3rd Pan-Hellenic Rangelands Congress, Pub. No 10, 25-33pp, (In Greek with English summary).

Pantera A., Mouflis G., 1996. Agroforestry: the union of forestry, agriculture and/or pasture. *In*: Proccedings of the 1st Panhellenic Rangeland Society, Drama, pp. 46-52, (In greek with English summary).

Pantera A., Papadopoulos A., Fotiadis G., Papanastasis V.P., 2008. Distribution and phytogeographical analysis of *Quercus ithaburensis* ssp. *macrolepis* in Greece, *Ecologia Mediterranea,* 34: 73-82.

Pantera A., Papanastasis V.P., 2003. Valonia oak (Quercus ithaburensis Decaisne subsp. macrolepis (Kotschy) Hedge & Yalt.) in Greece. Geotechnical Scientific Subjects, 14(1): 33 – 44, (In Greek with English summary).

Pantera, A., Burgess, P.J., Mosquera-Losada, R.M., Moreno, G.M., López-Díaz, M.L., Corroyer, N., McAdam, J., Rosati, A., Papadopoulos, A.M., Graves, A., Rigueiro Rodríguez, A., Ferreiro-Domíguez, N., Fernández Lorenzo, J.L., González-Hernández, M.P., Papanastasis, V.P., Mantzanas, K., Van Lerbergerhe, P., Malignier, N. (2018). Agroforestry for high value tree systems in Europe. *Agroforestry Systems*. https://doi.org/10.1007/s10457-017-0181-7

Papanastasis V.P., 1996. Silvopastoral systems and range management in the Meditarrenean region, In: Etienne, M. (ed.) Western European Silvopastoral Systems INRA, Paris, France, pp. 143-156.

Papanastasis V.P., 2004. Vegetation degradation and land use changes in agrosilvopastoral systems. *In*: Agrosilvopastoral systems of the Mediterranean, CATENA VERLAG, Reiskirchen, pp.1-12.

Papanastasis V.P., 2009. Grazing value of mediterranean forests. In: «Modelling, Valuing and Managing Mediterranean Forest Ecosystems», M. Palahi, Y. Birot, F. Bravo, E. Goritz (eds.), EFI proceedings No. 57, pp. 7-15.

Papanastasis VP, Mantzanas K, Dini-Papanastasi O, Ispikoudis I., 2009. Traditional agroforestry systems and their evolution in Greece. In: Rigueiro-Rodrigez A et al (eds) Agroforestry in Europe: current status and future prospects. Springer, Berlin, pp 89–109

Papanastasis V.P., Noitsakis V., 1992. Rangeland ecology. Giahoudi-Giapouli Pub., Thessaloniki, 244 pp. (In Greek).

Richardson D.M., Rundel P.W., 1998. Pine ecology and biogeography – An introduction. *In*: Ecology and biogeography of *Pinus*. D.M. Richardon (ed.), Cambridge University press, Cambridge, pp. 1-40.

Savidis TH., 2000. The mastic tree of Chios. Book, Pub. Kiriakidi Brothers, Thessaloniki, 135 pp.

Shultz Am, Papanastasis V, Katelman T, Tsiouvaras C, Kandrelis S, Nastis A., 1987. Agroforestry in Greece, Pub. Aristotle University of Thessaloniki, Thessaloniki, Greece.

Tsitsas S., 1978. The Wildtrees of the Mountain and the Hills, History - Mythology - Laography -Poetry – Physiolatry, Athens, (In Greek).

Vidal C., 2002.Holdings with grazing livestock have different paths. Statistics in Focus 25:1-7. vol_1_1/index_en.asp, cited at 25-4-2009.

Wilson, G.F. And B.T. Kang, 1981. Developing stable and productive cropping systems for the humid tropics. In: Stonehouse, B. (ed.), Biological husbandry: A scientific approach to organic farming. Butterworths, London, pp. 87-94.

Impact of heavy metal contamination to the hydrodynamics of a layered soil sample

Angelaki A.[1], Dionysidis A.[1], Golia E.E.[2]

[1] Department of Agriculture, Crop production & Rural Environment, University of Thessaly, Fytokou Str., 38446, Volos, Greece

[2] School of Agriculture, Laboratory of Soil Science, Aristotle University of Thessaloniki, University Campus, 541 24, Thessaloniki, Greece.

Abstract. Complete knowledge of the water movement into the vadose zone could be a key solution to most hydrological, environmental and agricultural issues, that are in the spotlight due to climate change along with the increasing pollution. The aquifer recharge, the irrigation doses, rates, frequency, the movement of pollutants, nutrients, trace elements and the water management in total, are affected by the hydrodynamics of the vadose zone. Since soil profiles in nature appear in layers, this study focuses on the water and heavy metal solution movement through soil layers with different characteristics. In order to investigate the potential changes to the hydrodynamics, two different soil layers were contaminated with Cu solution of high concentration and the adsorption, along with hydraulic parameters of the layers were calculated. For the purposes of the current research, experiments were carried out in the laboratory and the physicochemical behaviour of the soil-water complex with and without contamination was investigated. Results showed that the hydraulic properties of the more cohesive layer (loam) were significantly affected by the presence of Cu cations, while the layer with low rate of fine granular particles (sand), was not significantly affected by the prior Cu contamination.

1 Introduction

The ability of soil to hold water, depends on many factors such as porosity, hydraulic conductivity, sorptivity etc. The complete knowledge of infiltration mechanism through various soil types comprises an important and necessary tool for water management. Layered soils are very common in nature, which lead many researchers to focus on infiltration rate, drainage and generally water movement through unsaturated layers of soil. Hill and Parlange (1972) proved that when the lower layer has hydraulic conductivity much greater than the hydraulic conductivity of the upper layer, moisture head becomes unstable and infiltration at the lower layer starts when the upper layer comes to saturation. If hydraulic conductivity ratio is greater than 20, then cylindrical fingers of water appear during infiltration of the lower soil layer (Samani et al, 1989). Sharma et al, (2014) showed that the order in which the soil layers were stratified in a water-saturated profile did not influence the effluent solute concentration distribution. In order to estimate the layers' hydraulic parameters, Mohammadzadeh-Habili and Heidarpour (2015) proposed a theoretical method using the Green–Ampt model for layered soils, based on infiltration test data. One of the crucial properties of the unsaturated soil that affects infiltration mechanism is Sorptivity (Angelaki et al, 2021). Sorptivity can be estimated by using the equation (Philip 1969), which is valid at the very early time of the phenomenon:

$$I = St^{1/2} \quad (1)$$

where I is the cumulative infiltration, S is Sorptivity and t is time. At the very early time of infiltration, the phenomenon is dominated by capillary forces. Sorptivity S is the slope of the straight line of cumulative infiltration I versus square root of time, before gravity forces begin to act to water (Angelaki et al, 2004, 2021). The use of pesticides, fertilizers and sewage sludge are considered to be possible sources of copper inflow into the soils of cultivated areas. The agglomeration, dispersion and charge of the soil solution are greatly influenced by the pH of the soil and the ionic strength of the soil solution. Copper in low concentrations is beneficial to plants, but its toxic effect is significant if its concentration exceeds certain limits (Berkowitz et al, 2008, Golia et al, 2015, Khanam 2020). Soil accumulation is known to be associated with heavy metal concentrations (Sparks 2005. Kabata-Pendias 2011, Alloway 2013). However, information on the distribution of heavy metals in soil agglomeration is still scarce. Soil pollution with heavy metals at high concentrations affect aggregation and can lead to changes of the soil structure

and hydraulic properties, the most cohesive the soil is (Ciu et al 2016, Xiao et al 2016, Angelaki et al, 2022). Zhou et al. (2016) investigated the leaching and the transformation of fertilizers in layered soils, applied with irrigation. As soil profiles in nature usually appear in layers, researching the impact of a high concentration heavy metal solution to the hydrodynamic parameters of a layered soil is a challenge.

2 Materials and Methods

The experiments of the present study were performed at the Laboratory of Agricultural Hydraulics of the Department of Agriculture Crop Production & Rural Environment of University of Thessaly. Two well-dried in 105 ^{0}C soil samples of different hydraulic properties (loam and sand), were used to fill a transparent column with an inner diameter of 6 cm, at two layers. The soil samples were collected from Almyros area, Magnesia (Golia et al. 2015, 2019). At the bottom of the column soil samples were supported by a geotextile of hydraulic conductivity at saturation greater than that of the soil samples. In order to obtain the particle size distribution, the soil samples were sieved using a specific device with classified sieves. Into the column, the soil samples were packed uniformly, using a specific method for filling the column and the loam-layer was placed above the sand-layer. In order to obtain cumulative infiltration data and estimate the sorptivity of the upper layer, a steady load of about 2 mm distilled water was applied at the soil surface, simulating surface irrigation. Hydraulic conductivity at saturation was measured using a separate experimental procedure for each soil sample, called the constant head method. According to Darcy (1856):

$$Q = K_s A(\Delta H)L^{-1} \quad (2)$$

where, Q is the flow rate, K_s is the saturated hydraulic conductivity, A the soil surface area, ΔH is the water load over the soil sample and L is soil's height. Thus, K_s was calculated by measuring Q, A, ΔH and L in the laboratory. In order to contaminate the layered soil column, a Cu 400 mgL^{-1} solution was used as "incoming solution" and the Cu concentration at the leaching solution was measured. Distilled water (2 mm load at the soil surface) was applied again and the impact of Cu contamination on the hydraulic parameters of the soil column was investigated.

3 Results and Discussion

The mean value of the soil moisture at saturation for the L soil was found 0.405 cm^3/cm^3 and for the S soil was found equal to 0.229 cm^3/cm^3.
Hydraulic conductivity at saturation (K_s) was obtained by equation (2) and the results are the following:
Loam (L): K_s = 0.13 cm/min.
Sand (S): K_s = 0.87 cm/min.
From the very early times of infiltration, when capillary forces are the ruling forces, an estimation of Sorptivity (S) for the upper layer was obtained from the cumulative infiltration versus square root of time diagram (Figure 2). The calculated value (from equation 1) of sorptivity for loam layer is: S_L = 1.9103 cm/min$^{1/2}$.

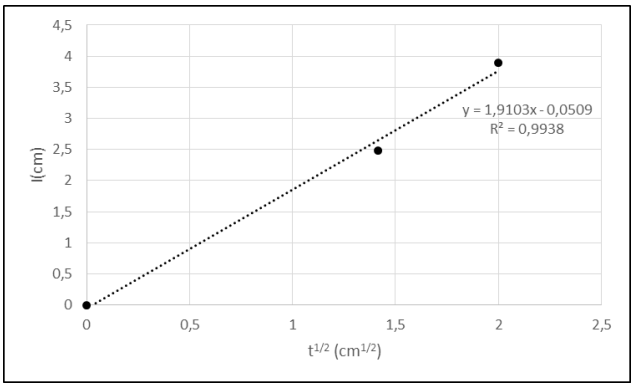

Figure 1. Estimation of Sorptivity for the upper layer.

Adsorption (A) was calculated as a subtraction of the Cu concentration at the leaching fluid from the incoming fluid. The lower soil layer (S) showed negligible adsorption, while at the upper layer (L) the adsorption of Cu cations was equal to 2.21 mg kg^{-1} dry soil.
Saturated hydraulic conductivity was re estimated after the contamination and the values are listed below:
Loam (L): K_s = 0.15 cm/min.
Sand (S): K_s = 0.86 cm/min.
Results show a 15.4% increase of saturated hydraulic conductivity of the upper layer (L), while no significant (-1.15%) impact of the contamination on saturated hydraulic conductivity found on the lower layer (S).
Sorptivity of the upper layer was found after contamination: S_L = 2.1820 cm/$min^{1/2}$, indicating an about 14% increase.
Cu cation capacity at sandy soils is low, which allows Cu cations movement either to lower depths, or to potential uptake by the crops. At more cohesive soils, Cu interacts with clay particles and organic matter showing increasing adsorption for pH>4 (Liu et al, 2018). Metals entering into the soil due to contact with the atmospheric air, due to infiltration, interact with clay and organic particles and accumulate into the soil (Kabata-Pendias 2011, Alloway et al. 2013, Volk and Yerokun 2016, Lasota el al 2020). Thus, the presence of Cu cations at the lower layer (S), had a negligible impact to the hydraulic parameters due to the negligible adsorption capacity. On the other hand, Cu cations had a quite considerable impact to the hydraulic parameters under investigation, due to the presence of fine clay and silt, which may lead to aggregation, because as heavy metals enter into the soil, there is an interaction with the clay and the organic particles which leads to accumulation (Lasota et al, 2020, Angelaki et al 2022).

4 Conclusions

The object of this research was to determine the impact of Cu contamination to the hydrodynamic properties at the vadose zone of a layered soil column. For this purpose, experiments were accomplished in the laboratory, at a layered soil sample. Results showed that the presence of Cu cations had no impact on hydraulic parameters of the sand-layer, while adsorption and increased saturated conductivity and sorptivity was found at the loam-layer, due to interaction of the heavy metal cations with the fine granular particles.

5 References

Alloway, B.J. Heavy Metals in Soils: Trace Metals and Metalloids in Soils and Their Bioavailability, 3rd ed.; Alloway, B.J., Ed.; Blackie Academic and Professional: London, UK, 2013; ISBN 9789400744691.

Angelaki A., Dionysidis A., Sihag P., Golia E. (2022) Assessment of contamination management caused by copper and zinc cations leaching and their impact on the hydraulic properties of a sandy and a loamy clay soil. Land, 11, 290. https://doi.org/10.3390/land11020290

Angelaki, A.; Sihag, P.; Sakellariou-Makrantonaki, M.; Tzimopoulos, C. The effect of sorptivity on cumulative infiltration. Water Sci. Technol. Water Supply 2021, 21, 606–614. https://doi.org/10.2166/ws.2020.297 .

Angelaki A., Sakellariou – Makrantonaki M., Tzimopoulos C. «Laboratory experiments and estimation of cumulative infiltration and sorptivity» (2004) Water, Air and Soil Pollution: Focus (WAFO) entitled: “Protection and Restoration of the Environment”, Kluwer Academic Publishers, 4: 241 – 251.

Berkowitz, B.; Dror, I.; Yaron, B. Sorption, retention, and release of contaminants. In Contaminant Geochemistry: Transport and Fate in the Subsurface Environment; Berkowitz, B., Dror, I., Yaron, B., Eds.; Springer: Heidelberg/Berlin, Germany, 2008; pp. 93–126.

Cui, H.; Ma, K.; Fan, Y.; Peng, X.; Mao, J.; Zhou, D.; Zhang, Z.; Zhou, J. Stability and heavy metal distribution of soil aggregates affected by application of apatite, lime, and charcoal. Environ. Sci. Pollut. Res. 2016, 23, 10808–10817. https://doi.org/10.1007/s11356-016-6271-7 .

Dalton F. N., Poss J. A., (1990) ‘Soil water content and salinity assessment for irrigation scheduling using time – domain reflectometry: Principles and application’. Acta Horic., 278, 1: pp., 381 – 393.

Darcy H., 1856. Les fontaines publiques de la ville de Dijon, Paris pp.590.

Drungil C. E.C., Abt K., Gish T. J., (1987) 'Soil moisture determination in gravelly soils with time domain reflectometry'. ASAE paper no. 87 – 2568, St. Joseph, MI.

Golia, E.E., Tsiropoulos, G.N., Füleky, G., Floras, S., Vleioras, S. 2019. Pollution assessment of potentially toxic elements in soils of different taxonomy orders in central Greece. Environ Monitor Assess, 191(2), 106.

Golia, E.E.; Dimirkou, A.; Floras, S.A. Spatial monitoring of arsenic and heavy metals in the Almyros area, Central Greece. Statistical approach for assessing the sources of contamination. Environ. Monit. Assess. 2015, 187, 399–412. https://doi.org/10.1007/s10661-015-4624-1.

Herkelrath W. N., W. M. Hamburg S. P., Murphy F., (1991) 'Automatic, real time monitoring of soil moisture in a remote field area with time – domain reflectometry'. Water Resour. Res., 27, pp., 857 – 864.

Hill, D.E. and Parlange J.Y., 1972. Wetting fond instability in layered soils. Proc. Soil Sci. Soc. Am. 36 (5): 697-702.

Kabata-Pendias, A. Trace elements in soils and plants: Fourth Edition; CRC Press; Taylor and Francis Group: Ann Arbor, MI, USA, 2011; ISBN 9781420093704.

Khanam, R.; Kumar, A.; Nayak, A.K.; Shahid, M.; Tripathi, R.; Vijayakumar, S.; Bhaduri, D.; Kumar, U.; Mohanty, S.; Pan-neerselvam, P.; et al. Metal(loid)s (As, Hg, Se, Pb and Cd) in paddy soil: Bioavailability and potential risk to human health. Sci. Total Environ. 2020, 699, 134330.

Lasota, J.; Blonska, E.; Lyszczarz, S.; Tibbett, M. Forest humus type governs heavy metal accumulation in specific organic matter fractions. Water. Air. Soil Pollut. 2020, 231, 80. https://doi.org/10.1007/s11270-020-4450-0 .

Liu, L.; Li, W.; Song, W.; Guo, M. Remediation techniques for heavy metal-contaminated soils: Principles and applicability. Sci. Total Environ. 2018, 633, 206–219.

Mohammadzadeh-Habili Jahanshir, Heidarpour Manouchehr, Application of the Green–Ampt model for infiltration into layered soils, Journal of Hydrology, Volume 527, 2015, Pages 824-832, https://doi.org/10.1016/j.jhydrol.2015.05.052.

Parlange J. – Y., (1972) 'Theory of water movement in soils. 6. Effect of water depth over soil' Soil Sci., Vol. 133, pp. 308 – 312.

Roth K., Shulin R., Fluhler H., Attinger W., (1990) 'Calibration of time – domain reflectometry for water content measurement using a composite dielectric approach' Water Resour. Res., 26, pp., 2267 – 2273.

Sakellariou-Makrantonaki M., A. Angelaki, C. Evangelides, V. Bota, E. Tsianou and N. Floros, (2016) «Experimental determination of Hydraulic Conductivity at unsaturated soil column», Procedia Engineering 162(2016), pp. 83–90, DOI 10.1016/j.proeng2016.11.019

Samani Z., Cheraghi A. and Willardson L., (1989). Water movement in horizontally layered soils. J. Irrig and Drain Div. ASCE 115 (3): 449-456.

P. K. Sharma, V. A. Sawant, S. K. Shukla & Zubair Khan (2014) Experimental and numerical simulation of contaminant transport through layered soil, International Journal of Geotechnical Engineering, 8:4, 345-351, DOI: 10.1179/1939787913Y.0000000014

Topp G. C., Davis J. L., Annan A. P., (1980) 'Electromagnetic determination of soil water content: Measurements in coaxial transmission lines'. Water Resour. Res., 16, pp. 574 – 582.

Volk, J.; Yerokun, O. Effect of application of increasing concentrations of contaminated water on the different fractions of Cu and Co in sandy loam and clay loam soils. Agriculture 2016, 6, 64. https://doi.org/10.3390/agriculture6040064.

Xiao, R.; Zhang, M.; Yao, X.; Ma, Z.; Yu, F.; Bai, J. Heavy metal distribution in different soil aggregate size classes from restored brackish marsh, oil exploitation zone, and tidal mud flat of the Yellow River Delta. J. Soils Sediments 2016, 16, 821–830. https://doi.org/10.1007/s11368-015-1274-4

ZHOU Jian-Bin, Jin-Gen XI, Zhu-Jun CHEN, Sheng-Xiu LI, Leaching and Transformation of Nitrogen Fertilizers in Soil After Application of N with Irrigation: A Soil Column, Pedosphere, 2006, Pages 245-252, https://doi.org/10.1016/S1002-0160(06)60050-7.

Water and nutrients use efficiency in Aquaponics

Aslanidou M.,[1] Mourantian A., [1] Levizou E., [1] Mente E.,[2] Katsoulas N. [1*]

[1]University of Thessaly, Dept. of Agriculture Crop Production and Rural Environment, Fytokou Str., 38446, 8 Volos, Greece

[2] University of Thessaly, Dept. of Ichthyology and Aquatic Environment, Fytokou Str., 38446, 8 Volos, Greece

* Corresponding author. Email: nkatsoul@uth.gr

Abstract. Aquaponics is an emerging system applied nowadays in the framework of circular economy representing a food production technology that combines aquaculture and hydroponic in an integrated recirculating system without soil. Aquaponics involves a dynamic interaction between fish, plants, bacteria, and their aquatic environment. In a closed aquaponics system (coupled), the aquaculture effluent flows through hydroponic troughs, and the resulted drainage solution is sent back to the fish-rearing tanks for reusing instead of being discharged. On the contrary, in a decoupled aquaponics set-up, the fish effluent and the nutrient/drainage solution of the plants recirculate independently in the subsystems providing full control and management of the water. Four experiments were carried out between May 2020 and July 2021 in the pilot scale aquaponic system of the University of Thessaly. The parallel application of coupled (AQ) and decoupled (CAP) aquaponics treatments in comparison to a control (hydroponics, HP) are presented for four cultivations (basil, cucumber, parsley, and tomato). Tilapia fish was reared in a pilot aquaculture system (9 m^3). The CAP treatment performed the greatest yield, while AQ had the lowest. Compared to HP, AQP and CAP resulted in lower fertiliser and water consumption.

1 Introduction

Nowadays the intensification of agricultural and fisheries food production systems leads to high energy and fossil fuel consumption, reduction of arable land, water scarcity, and the decline of fish stocks (Klinger & Naylor, 2012). On the other hand, the human population is predicted to reach 11 billion by the end of the century (FAO-ONU, 2017). It is consequently under concern how these production systems can correspond to the food needs of a high rising human population in a sustainable way. In the context of a sustainable hydroponic and recirculating aquaculture system circular economy provides Aquaponics as the most suitable solution for the elimination of eutrophication and natural resources scarcity and for water saving. Aquaponics combines intensive aquaculture and hydroponic system. According to Palm et al. (2018), ‘’Aquaponics is a production system of aquatic organisms and edible plants, where the major nutrient source (>50%), for plant nutrition, comes from the aquatic organisms’ faces’’ There are two types of aquaponic systems. In coupled one, the fundamental principle is the 100% recirculation of water between the aquaculture and the hydroponic system. In the decoupled one water recirculation is controlled and depends on the irrigation system of the plant cultivation (Goddek 2017).

High-yield hydroponic systems require a considerable amount of macro-and micronutrients of industrial and mining origin, leading to high energy (i.e., for production and transport) and finite resources use (e.g., phosphorus and oil) (Sverdrup and Ragnarsdottir, 2011). Also, in no-recirculating systems, intermittent disposal of considerable amounts of nutrient-rich water leads to high water consumption as well as surface and groundwater pollution (Gagnon et al., 2010). The regular exchange of water performed in conventional aquaculture systems is not necessary for

aquaponics as this system provides water reuse (i.e., 95%–99%) (Dalsgaard et al., 2013). Additionally, aquaponics utilizes the nutrients discharged from drainage solutions of the cultivation offering a great impact on the elimination of the eutrophication phenomenon. The aim of this study is the comparison of yield, water, and fertilizer consumption between a coupled pilot aquaponic system (AQP), a decoupled pilot aquaponic system, and a pilot hydroponic system. The cultivation periods concern 2 leafy and 2 fruit cultivations for further conclusions on the aquaponic effect.

2. Materials and methods

2.1. Facilities, plant, and fish material

Four experiments were held on the period of 18th May 2020 to 12th July 2021 in the climate-controlled experimental greenhouse of the Laboratory of Agricultural Constructions and Environmental Control of the University of Thessaly in Velestino (latitude 39_440 longitude 22_790, altitude 85 m), Greece. The cultivation area occupied 360 m^2 of the greenhouse and the aquaculture premises had the rest area of 80 m^2. For the basil, cucumber, parsley, and tomato cultivations, the media-based technique was applied via perlite slubs (ISOCON Perloflor Hydro 1, ISOCON S.A., Athens) and 18 hydroponic channels distributed in the three blocks in the greenhouse. The drip irrigation system was used for the irrigation and nutrition of the plants. The drainage solution from every 3 hydroponic channels was collected to a drainage tank and in the case of AQ was returned back to the aquaculture system at the end of the day. Basil plants (10 days old) (*Ocimum basilicum* var. Genovese) were transplanted (2.35 plants m^{-2}) into the slubs on the 18th of May 2020 and harvested after 35 and 55 days after transplanting (D35 and D55) (two harvests). In the 2nd experiment (21/8/2020 until 15/11/2020), 15-day-old cucumber plants (*Cucumis sativus* var. Aisopos in small Rockwool cubes were placed in each substrate (1.18 plants m^{-2}). Cucumber harvests started 21 days after transplanting and lasted at D86. In the 3rd experimental period, parsley plants (*Petroselinum crispum*) were transplanted at a plant density of 2.35 plants m^{-2} on the 7th of December 2020 and harvested on D70. In the 4th experiment tomato plants (*Solanum lycopersicum* var. Cabrera) were transplanted (1.76 plants m^{-2}) into the slubs on the 15th of March. Tomato harvests started at D71 and lasted at D120. The aquaculture system consisted of three fish tanks (1.3 m^3), a mechanical filter (0.65 m^3), a biofilter (0.5 m^3), and a clear tank (2.5 m^3). Tilapia fish (*Oreochromis mossambicus*) were stocked at a rate of 8 kg·m^{-3}. The water was recirculating constantly in the aquaculture system and controlled via a network of sensors and software installed on a computer (Argos Electronics, Evia, Greece).

2.2. Nutrient Solution Formulation and Control

The application of coupled system involved the treating of the fish effluent with sulfuric acid to a pH set point of 5.6. There was a complete recirculation of nutrient solution as the drainage solution of the AQ cultivation after disinfection, came back to the aquaculture system. In the decoupled case the fish solution was treated with a mix of sulfuric and nitric acid to achieve a pH set point of 5.6. Additionally, the appropriate quantities of fertilizers were added to reach the standard concentrations of the control cultivation (HP). The CAP and HP cultivations represented the open hydroponic system. The control of nutrient solutions for all cultivations was achieved by software installed on a computer (Argos Electronics, Evia, Greece).

2.3. Measurements

In 1st period, two harvests occurred for estimating the yield per plant. During the first sampling date (D35) the basil plants were harvested at the base of the plant 12 cm above the ground portion, in order to allow them to regrow until the final harvest at D55. Parsley plants were harvested at D70. The total biomass was weighted, and the resultant material (leaves and stems) was considered as

the total yield per plant. For the cucumber and tomato crops, harvests of fruits were performed weekly, and their weight was recorded. The average yield of fruits per predetermined plant (12 for cucumber and 6 for tomato cultivation) was converted as the total yield per cubic meter.

2.4. Calculations

The water use efficiency (WUE) was estimated by dividing the biomass produced by the volume of the water applied. It is considered that the AQP system is a closed system as the drainage solution was returned to the RAS system every experimental day. So, in this case the volume of water supplied for the calculation of WUE is the volume of water absorbed by the crop. The nutrient use efficiency (NUE) was calculated by dividing the biomass produced by the quantity of fertilizers consumed. It is known that only acids were added to the RAS solution for the AQP treatment's nutrient solution

3 Results

3.1. Yield

Among the treatments CAP cultivation appeared the most productive with values 1.72 kg m^{-2} (1^{st} basil), 1.81 kg m^{-2} (2^{nd} basil), 6.87 kg m^{-2} (cucumber), 0.68 kg m^{-2} (parsley) and 14.69 kg m^{-2} (tomato) respectively. The lowest yield corresponded to AQP plants in all cultivations except from basil 2^{nd} harvest where AQP plants were comparable with HP plants respectively. AQP treatment performed 0.91 kg m^{-2} (1^{st} basil), 1.46 kg m^{-2} (2^{nd} basil), 4.05 kg m^{-2} (cucumber), 0.21 kg m^{-2} (parsley) and 6.47 kg m^{-2} (tomato). HP treatment performed 1.58 kg m^{-2} (1^{st} basil), 1.52 kg m^{-2} (2^{nd} basil), 6.82 kg m^{-2} (cucumber), 0.62 kg m^{-2} (parsley) and 13.33 kg m^{-2} (tomato). It is found that the CAP yield of leafy cultivations appears clearly greater than HP. The differentiation percentage is just 0.77% for cucumber and 9.26% for tomato respectively. According to Delaide (2017) and Goddek (2017), CAP's better yield concerns the particular composition of aquaculture solutions. The presence of dissolved organic molecules (DOM) and plant growth-promoting rhizobacteria and/or fungi (PGPR and/or PGPF) in RAS solution may enhance plant growth.
The lowest percentage difference between AQP and HP & CAP plants performed basil (2^{nd}) cultivation (11.68%), followed by cucumber (40.78%), basil 1^{st} harvest (45%), tomato (53.68%), and parsley plants (70.76%) respectively. Castillo-Castellanos et al. (2016), Pinho et al. (2017), and Quillere et al. (1995), support that low nutrient concentrations in AQP solution have a negative effect on plant production. Delaide (2017), demonstrated no statistical differences in fresh weight of AQP and HP lettuce plants making recommendations for the application of AQP treatment. They found that the root biomass of AQP plants was greater than HP plants. This phenomenon was recorded only at the 2^{nd} harvest of basil plants with AQP (152.45 g), CAP (141.75 g) and HP (128.15 g) root biomass respectively. The low percentage differentiation of basil (2^{nd}) yield cultivation between AQP and HP (4.06%) demonstrates that AQP plants have a delayed growth rate because of the root biomass and low nutrient concentrations in the other cultivation cases.

3.2. WUE & NUE

The greatest Water Use Efficiency was presented from the AQP treatment except for the parsley cultivation with values of 13.1 (basil), 32 (cucumber), 6.06 (parsley), and 20 (tomato) respectively. The continuous recirculation of water in AQP treatment leads to water savings to an exceptional degree per unit produced. CAP treatment was calculated with higher WUE than HP cultivation with values of 12.5 (CAP) and 10.4 (HP) for basil cultivation, 27 (CAP) and 26 (HP) for cucumber, 11.32

(CAP) and 8.12 (HP) for parsley and 14 (CAP) and 13 (HP) for tomato cultivation respectively. This effect corresponds to the greater yield of CAP treatment than HP. There was lower fertilizer consumption in CAP treatment as a portion of nutrients was utilized from the aquaculture solution. So the Nutrient Use Efficiency for CAP treatment performed higher values than HP treatments: 11.56 (CAP) and 8.73 (HP) for basil cultivation, 9.3 (CAP) and 7.27 (HP) for cucumber, 2.24 (CAP) and 1.65 (HP) for parsley and 8 (CAP) and 4 (HP) for tomato cultivation respectively.

4 Summary

CAP treatment seems to be the greatest combining high yield and low environmental impact. This treatment represents the decoupled aquaponic system promoting the advantages of nutrient solution control and water quality of both aquaculture and hydroponic solutions. AQP treatment performed the lowest yield. However, this treatment demonstrated greater WUE values and zero fertiliser consumption. For this reason, more studies have to be done on AQP and CAP treatments as aquaponics seems to be hopefully more productive and environmentally friendly than hydroponic cultivation.

Acknowledgments

This research is co-financed by the European Union and Greek national funds through the Operational Program Competitiveness, Entrepreneurship, and Innovation, under the call RESEARCH – CREATE – INNOVATE (project code: T1EDK-01153)

References

Castillo-Castellanos, D., Zavala-Leal, I., Ruiz-Velazco, J. M. J., Radilla-García, A., Nieto-Navarro, J. T., Romero-Bañuelos, C. A., & González-Hernández, J. (2016). Implementation of an experimental nutrient film technique-type aquaponic system. *Aquaculture international*, *24*(2), 637-646.

Dalsgaard, J., Lund, I., Thorarinsdottir, R., Drengstig, A., Arvonen, K., & Pedersen, P. B. (2013). Farming different species in RAS in Nordic countries: Current status and future perspectives. *Aquacultural engineering*, *53*, 2-13.

Delaide, B. (2017). *A study on the mineral elements available in aquaponics, their impact on lettuce productivity and the potential improvement of their availability* (Doctoral dissertation, Université de Liège, Liège, Belgique).

FAO, F. (2017). The future of food and agriculture–Trends and challenges. *Annual Report*, 296, 1-180.

Gagnon, J., Raskin, M., Remache, J., & Sack, B. P. (2010). Large-scale asset purchases by the Federal Reserve: did they work?. *FRB of New York Staff Report*, (441).

Goddek, S. (2017). *Opportunities and challenges of multi-loop aquaponic systems* (Doctoral dissertation, Wageningen University).

Klinger, D., & Naylor, R. (2012). Searching for solutions in aquaculture: charting a sustainable course. *Annual Review of Environment and Resources*, 37, 247-276. *DOI :10.1146/annurev-environ-021111-161531*

Palm, H. W., Knaus, U., Appelbaum, S., Goddek, S., Strauch, S. M., Vermeulen, T. & Kotzen, B. (2018). Towards commercial aquaponics: a review of systems, designs, scales and nomenclature. *Aquaculture international*, 26(3), 813-842. https://doi.org/10.1007/s10499-018-0249-z

Pinho, S. M., de Mello, G. L., Fitzsimmons, K. M., & Emerenciano, M. G. C. (2018). Integrated production of fish (pacu Piaractus mesopotamicus and red tilapia Oreochromis sp.) with two varieties of garnish (scallion and parsley) in aquaponics system. *Aquaculture international*, *26*(1), 99-112.

Quilleré, I., Roux, L., Marie, D., Roux, Y., Gosse, F., & Morot-Gaudry, J. F. (1995). An artificial productive ecosystem based on a fish/bacteria/plant association. 2. Performance. *Agriculture, ecosystems & environment*, *53*(1), 19-30.

Sverdrup, H. U., & Ragnarsdottir, K. V. (2011). Challenging the planetary boundaries II: Assessing the sustainable global population and phosphate supply, using a systems dynamics assessment model. *Applied Geochemistry*, *26*, S307-S310. doi:10.1016/j.apgeochem.2011.03.089

Monitoring urban soil pollution using bioindicators: trees and shrubs

E. E. Golia[1*], P. S. C. Aslanidis[2] , I. Papadopoulos[1], K. Kanelli[1], E. Argyraki[1], R. Vogia[1] , Th. Arnaoutopoulou[1], N. Paraskevaidou[1] , K. Varvetsioti[1], V. Gkinou[1], P. Vasilikogiannaki[1]

[1]School of Agriculture, Laboratory of Soil Science, Aristotle University of Thessaloniki, University Campus, 541 24, Thessaloniki, Greece.
[2]Department of Planning and Regional Development, University of Thessaly, Pedion Areos, 383 34, Volos, Greece.

*Corresponding author: E-mail: egolia@auth.gr, Tel +30 2310998809

Abstract. The detection of deposition, accumulation, and distribution of heavy metals (HMs) or potentially toxic elements (PTEs) has been widely accomplished via the use of bioindicators. Bioindicators like the higher plant leaves are the most common practice. To exemplify, evergreen trees can be effectively brought into play in the bio-monitoring of pollutants in urban environments. Such bioindicators have plenty of advantages: simple sampling, effortless low-cost analysis, and long lifetime. The responses of plants to elevated concentrations of contaminants depended upon environmental conditions and by plant physiological status. Uptake and accumulation of elements in plants may follow different pathways, i.e. the foliar surface and the root system. The adsorption of significant amounts of HMs by leaves could be demonstrated by the comparison between the –washed and unwashed– leaves. The aim of this study was the monitoring of urban soil pollution by PTEs in the city of Thessaloniki (northern Greece). Hence, the assessment of concentrations and distribution of PTEs was audited, firstly in urban soils, and secondly in the leaves of the trees and shrubs thriving in the green areas of the city. Heavy metal concentrations were determined in leaf dust, plant tissues and respective soil samples. Concentrations showed high correlations among them. At the same time, the determination of the transferring indices of HMs took place, foremost from the soil to the root system of the plant, next in order, in the inner part of the plant. Moreover, HM indices were determined from the basement to the aboveground part of the plants. The results of the present research indicate, that in the specific soil and climatic conditions, the studied plants seemed to be a promising tool for monitoring urban soil pollution.

1 Introduction

A conceptual environmental problem related to urban development in space and time is increased pollution (Nriagu, 1990). The rapid urbanization and industrialization due to the migration of people from rural to urban areas in recent decades includes the demand for transport and energy, with increasing anthropogenic activities, such as vehicle traffic or industrial activities (Grigoratos et al., 2014), and this demand is directly related to atmospheric anthropogenic emissions. Nowadays, air pollution is one of the most significant problems in urban environments (Sawidis et al., 2012) and plays a vital role due to dry or wet deposition in soil. On the other hand, It is well known, that long-term environmental pollution is reflected in the soil (Kabata-Pendias and Pendias, 2001). Pollutants containing potentially toxic elements are released from numerous anthropogenic sources such as industry (Kaitantzian et al., 2013), mining (Lv et al., 2014, Odumo et al., 2014), combustion of fossil fuels in vehicular traffic (Argyraki and Kelepitzis, 2014), and energy production. Among them transport is a major source of atmospheric pollution in urban areas and therefore special attention should be given) to traffic pollutants, such as heavy metals (like Pb, Zn, Cr, Ni or Cd) (Sawidis et al., 2011).

Elemental analysis of plant samples has, for many years, been an low-effort, alternative and effective way of conducting ecological research in urban areas (Markert, 1995, Aksoy et al., 2000). Nowadays) It is widely accepted that plants can be used effectively as biomonitors of environmental pollution. The accumulation of a trace element in plants confirms its availability in the soil, but many plants accumulate trace elements or PTEs in their aerial parts (leaves/barks) at levels many times higher than those in the soil solution (Baker et al., 2000), (Ma et al., 2001). Despite the fact that it is commonly difficult to determine the source of heavy metals (Oliva and Mingorance, 2006), trees can be used as effective biomonitors to detect low concentrations of pollutants both from soil and air. Although many plant species have been used to monitor pollution, pointing to their advantage, little attention has been attribute to evergreen trees (Sawidis et al., 2011).

As reported in similar studies, evergreen plants absorb a higher percentage of leaf nutrients than deciduous species. Therefore, evergreens are expected to be more resistant to contaminated environments and more suitable for biomonitoring purposes (Sawidis et al., 1995). Although, it is known that trees are not the best indicators for air pollution monitoring when compared to lower plants (fungi, algae, lichens or mosses) (Sawidis et al., 1995), they are unlike lichens or mosses, the main type of plant found in urban areas with a high degree of pollution (Wittig, 1993). So, they could be sampled by standard sampling and analytical techniques for intercomparison monitoring of the time-trend distribution of trace elements (Berlizov et al., 2007). Additionally, among the most striking advantages of using trees are that they are inexpensive alternatives to air sampling, they provide useful data for the design of deposition monitoring networks, and they greatly facilitate the detailed identification of trace elements (Sawidis et al., 2011).

The objectives of the present work were: (1) to estimate the soil pollution rate by potentially toxic element in the city of Thessaloniki (northern Greece) by using trees or shrubs as biomonitors or bioindicators, and (2) to examine the influence of various factors (traffic, industry, meteorological conditions, etc.) on their distribution pattern in the soil, as well as, in the air of the city. For this purpose, tree leaves of various botanical species were selected. Most of the selected tree species have been used for medicinal purposes due to their incorporating bioactive compounds), such as flavonoids, phenolics and essential oils. They are also located in the urban network of the city, in the courtyards of the houses, inside the parks, and playgrounds in the city centre of Thessaloniki.

2 Materials and methods

2.1 Site description and leaf sampling

Trees and shrubs of various botanical species are particularly widespread in the urban environment of Greek cities. They are found, in the urban network of the city, in the yards of the houses, and in the parks and playgrounds in the city center of Thessaloniki. The trees in the main streets, which were selected for sampling, have with 5 m distance from the traffic lights. Samples were collected from different sides of same age trees (about 10 - 15 years old) at the heights of 1.5 to 2 m above ground level. The leaves with defects, such as bird droppings, pesticide treatment, insect infestation, honeydew presence, chlorosis, necrosis, and unusual dust cover, were avoided in the collection process. Further clean up steps were not conducted on sampled leaves. The sampling process was conducted after a 10-day rainless period.

2.2 Analytical methods

Plant tissues and leaves from trees and shrubs were analyzed to determine nitrogen, phosphorus and potassium content. This was followed by digestion with a mixture of concentrated acids (Aqua Regia method) and determination of metals by atomic absorption spectrophotometer. In some cases, it was used the flame or graphite furnace component, in order to detect metals at lower limits.

3 Results

The concentrations of the thee leave from the sampling area of the present study are presented in Table 1. The highest values were observed for Zn, followed by Cu and Pb (mg kg^{-1}). According to the mean value of each element, the interregional variation of the element distributions in the studied city revealed differences in the accumulation of all elements studied. Heavy metal uptake in leaves of the studied trees showed that the areas located in close vicinity to the city centre are highly affected by air pollution, as they showed a distinctly high load of heavy metals.

Table 1. Total concentrations of potentially toxic elements in plant tissues (trees and shrubs)

	Cu	Zn	Cd	Pb
	mg kg^{-1} dry matter			
Minimum Value	4.8	9.4	0.01	5.5
Maximum Value	58.1	89.5	1.1	21.7
Average value	33.2	56.2	0.34	13.4

CV (%)	22.7	33.1	36.8	31.2

4 Discussion

The effect of urban pollution, which therefore means accumulation of heavy metals, varies between different species of trees and shrubs and among the parts of these plants. A critical factor which determines heavy metal uptake from a certain plant would be the structure of its leaf (Sawidis et al., 2011). Previous investigations (Vidal et al., 2020) have confirmed that plants, and particular trees produce high amounts of phenolic compounds as a response to the heavy metal stress. Hence, this capability renders them as suitable candidates for phytoremediation.

The increased Zn content in thee leaves throughout the sampling area of the present study was caused probably by anthropogenic activities, with tire and brake wear, diesel exhaust emissions, and corrosion of safety fence being the most common (Grigoratos and Martini, 2015). Average concentrations, however, were within normal levels, suitable for the smooth operation of plant growth systems. The highest Cu and Pb concentrations in the tree leaves were found, probably, due to the long-time and increased vehicle traffic along the highways. The mean Cu concentration values were higher than the normal range for plants (Kabata-Pendias and Pendias, 2001). The lower measured concentrations (<5 mg kg^{-1}) were below the normal range (5–30 mg kg^{-1}) for plants. Regarding Pb, high concentrations in tree leaves were measured, in the polluted sites, but in all cases were lower than the toxic limits. This can be attributed to the fact that the vehicles and industrial activities in the city contribute to the heavy metal pollution. Industrial and metallurgical processes along with the combustion of diesel oil produce the highest emissions of heavy metals, which can be toxic for the plants' physiological function (Sawidis et al., 2011).

The factories, located in the west area in the city of Thessaloniki, may contribute to the pollution of the area, especially when the weather conditions are favorable for the spread of pollutants (Bourliva et al., 2020, Kelepetzis and Argyraki, 2020,). It is also worth noting that Thessaloniki is a rural area surrounded by the Hortiatis mountain to the north and the Thermaikos gulf to the south, creating a microenvironment conducive to the frequent entrapment of air pollution like in Volos city (Antoniadis et al., 2019, Kelepetzis et al., 2020, Botsou et al., 2020). The burning of materials in the fireplaces of the houses of the study area may also contribute to the increase in heavy metals pollution. There is also evidence that the coal or crude oil used for household heating, gasoline, and diesel vehicle exhaust are of the major problems in urban soil pollution (Golia et al., 2021).

5 Conclusions

In conclusion, the exhaust gasses of motor vehicles, metalworking industries, and other anthropogenic sources are the main sources of air pollution and eventually of soil pollution in city of Thessaloniki. Further research is needed to investigate the influencing factors, such as the geomorphological status, the urban micro climate, the air circulation, along with the emission gasses levels, in order to find out the possible sources of pollution in the soils and plant leaves of the centre of Thessaloniki. The tree leaves can be considered effective heavy metal accumulator, and therefore a valuable tool for monitoring urban pollution, as they can be sampled systematically, using standardized sampling and analytical techniques. More studies would be necessary in the near future, in order to investigate the favorable plant species that could more clearly reflect and contribute to the monitoring of long-term soil pollution in urban environments.

References

Aksoy, A., Sahin, U. and Duman, F., 2000. Robinia pseudo-acacia L. as a possible biomonitor of heavy metal pollution in Kayseri Turk. J. Bot., 24, pp. 279-284.

Antoniadis, V., Golia, E.E., Liu, Y.T., Wang, S.L., Shaheen, S.M. and Rinklebe, J., 2019. Soil and maize contamination by trace elements and associated health risk assessment in the industrial area of Volos, Greece. Environ. Int., 124, 79–88.

Argyraki, A. and Kelepertzis, E., 2014. Urban soil geochemistry in Athens, Greece: the importance of local geology in controlling the distribution of potentially harmful trace elements. Sci. Total Environ., 482–483, pp. 366-377.

Argyropoulos, G., Manoli, E., Kouras, A. and Samara, C., 2012. Concentrations and source apportionment of PM10 and associated major and trace elements in the Rhodes Island, Greece. Sci. Total Environ., 432, pp. 12-22.

Baker, A.J.M., Mc Grath, S.P., Reeves, R.D. and Smith, J.A.C., 2000. Metal hyperaccumulator plants: a review of the ecology and physiology of a biological resource for phytoremediation of metal polluted-soils, N. Terry, G. Benuelos (Eds.), Phytoremediation of Contaminated Soil and Water, Lewis Publishers, London, pp. 85-107.

Berlizov, A.N., Blum, O.B., Filby, R.H., Malyuk, I.A. and Tryshyn V.V., 2007. Testing applicability of black poplar (Populus nigra L.) bark to heavy metal air pollution monitoring in urban and industrial regions. Sci. Total Environ., 372, pp. 693-706.

Botsou, F., Moutafis, I., Dalaina, S. and Kelepertzis, E., 2020. Settled bus dust as a proxy of traffic-related emissions and health implications of exposures to potentially harmful elements. Atmos. Pollut. Res., 11, 1776–1784.

Bourliva, A., Kantiranis, N., Papadopoulou, L., Aidona, E., Christophoridis, C., Kollias, P., Evgenakis, M., K. Fytianos K., 2018. Seasonal and spatial variations of magnetic susceptibility and potentially toxic elements (PTEs) in road dusts of Thessaloniki city, Greece: A one-year monitoring period. Sci. Total Environ, 639,417-427.

Golia, E.E., Papadimou, S.G., Cavalaris, C., and Tsiropoulos, N.G., 2021. Level of Contamination Assessment of Potentially Toxic Elements in the Urban Soils of Volos City (Central Greece). Sustainability, 13(4), 2029.

Grigoratos, T. and Martini, G., 2015. Brake wear particle emissions: a review. Environ. Sci. Pollut. Res. 22, 2491–2504.

Grigoratos, T., Samara, C., Voutsa, D., Manoli, E. and Kouras, A., 2014. Chemical composition and mass closure of ambient coarse particles at traffic and urban-background sites in Thessaloniki, Greece. Environ. Sci. Pollut. Res., 21, pp. 7708-7722.

Kabata-Pendias, A. and Pendias, H., 2001. Trace Elements in Soils and Plants (third ed.), CRC Press, Boca Raton, Florida, USA.

Kaitantzian, A., Kelepertzis, E. and Kelepertsis, A., 2013. Evaluation of the sources of contamination in the suburban area of Koropi–Markopoulo, Athens, Greece. Bull. Environ. Contam. Toxicol., 91, pp. 23-28.

Kelepertzis, E., Argyraki, A., Chrastný, V., Botsou, F., Skordas, K., Komárek, M. and Fouskas, A, 2020. Metal(loid) and isotopic tracing of Pb in soils, road and house dusts from the industrial area of Volos (central Greece). Sci. Total Environ., 725.

Lv, J., Liu, Y., Zhang, Z. and Dai, B., 2014. Multivariate geostatistical analyses of heavy metals in soils: spatial multi-scale variations in Wulian, Eastern China. Ecotoxicol. Environ. Saf., 107, pp. 140-147.

Ma, L.Q., Komar, K.M., Tu, C., Zhang, W., Cai, Y. and Kenelley, E.D., 2001. A fern that hyperaccumulates arsenic Nature, 409, p. 579.

Markert, B., 1994. Element Concentration Cadasters in Ecosystems. Progress Report on the Element Concentration Cadaster Project ECCE of INTECOL/IUBS. 25th General Assembly of IUBS, Paris.

Nriagu, J.O., 1990. Global metal pollution: poisoning the biosphere? Environ. Sci. Policy Sustain. Dev., 32, pp. 7-33.

Odumo, B., Carbonell, G., Angeyo, H., Patel, J., Torrijos, M. and Martín, J.R., 2014. Impact of gold mining associated with mercury contamination in soil, biota sediments and tailings in Kenya. Environ. Sci. Pollut. Res., pp. 1-10.

Oliva, S.R. and Mingorance, R.D., 2006. Assessment of airborne heavy metal pollution by aboveground plant parts. Chemosphere, 65, pp. 177-182.

Sawidis, T., Breuste, J., Mitrovic, M., Pavlovic, P. and Tsigaridas, K., 2011. Trees as bioindicator of heavy metal pollution in three European cities. Environ. Pollut., 159, pp. 3560-3570.

Sawidis, T., Krystallidis, P., Veros, D. and Chettri, M., 2012. A Study of Air Pollution with Heavy Metals in Athens City and Attica Basin Using Evergreen Trees as Biological Indicators. Biological Trace Element Research, 148:396–408.

Sawidis, T., Marnasidis, A., Zachariadis, G. and Stratidis, J., 1995. A study of air pollution with heavy metals in Thessaloniki city (Greece) using trees as biological indicators. Arch. Environ. Contam. Toxicol. 28, 118–124.

Vidal, C., Ruiz, A., Ortiz, J., Larama, G., Perez, R., Santander, C., Ferreira, P.A.A. and Cornejo, P. 2020. Antioxidant Responses of Phenolic Compounds and Immobilization of Copper in Imperata Cylindrica, a Plant with Potential Use for Bioremediation of Cu Contaminated Environments. Plants, 9:1397.

Wittig, R., 1993. General aspects of biomonitoring heavy metals by plants, Plants as Biomonitors. Indicators for Heavy Metals in the Environment, VCH, Weinheim, pp. 3-27.

Levels of Potentially Toxic Elements in Urban Soils of Thessaloniki (northern Greece)

E. E. Golia[1], P. S. C. Aslanidis[2], M. Androudi, M. Mamopoulos[1], M.L. Takatzoglou[1], A. Koropouli, I. Chatzisavvas, Th. Vretta[1], K. Livogianni[1], E. Tzika[1], O. Karadedos[1], M. Kontosis[1,] C. Adamantidou[1].

[1]School of Agriculture, Laboratory of Soil Science, Aristotle University of Thessaloniki, University Campus, 541 24, Thessaloniki, Greece.
[2]Department of Planning and Regional Development, University of Thessaly, Pedion Areos, 383 34, Volos, Greece.
*Corresponding author: E-mail: egolia@auth.gr, Tel +30 2310998809

Abstract. A major matter of public and academic concern is urban soil pollution provoked by heavy metals (HMs) or potentially toxic elements (PTEs). The existence of heavy metals is natural in urban and in agricultural soils as well. Nevertheless, contamination usually derives from excessive local and peripheral – human, agricultural, and industrial – activities. There are different impacts according to the sources of pollution: road traffic and combustion of fossil fuels are disturbing, agricultural runoffs are destructive, but activities from industry and waste incinerators are detrimental. Furthermore, the acute nature of/ and the toxicity of PTEs is an open debate because of their long-lasting persistence and non-biodegradable nature. Moreover, two main points of urban soil pollution is the aggravation of citizens' health and wellbeing. Especially when augmented concentrations of PTEs are found in green spaces – public parks and playgrounds– have immediate and direct impact to the people. The present study focuses on the monitoring of PTEs in Thessaloniki which is a – coastal and densely populated – city and located in central Macedonia, northern Greece. The soil samples were collected from pocket-sized green spaces, parks, and boulevards in the downtown and the vicinity of harbor. Additionally, statistical analysis has been conducted for the –total and available– concentrations of several HMs and their distribution in urban soils, in an attempt to determine the possible sources of pollution in the study area. The survey carried out on the soil samples, which in some cases, did not indicate levels above maximum thresholds. However, continuous study of PTE levels every year and during the year is necessary to monitor the pollution of the study area.
Keywords: heavy metals; anthropogenic effect; bioavailability; total content

1 Introduction

Over the last 3 decades, there has been a great global concern about attributing polluted environmental impacts on human health (Shifaw, 2018). The World Health Organization (WHO) estimates that about a quarter of the human diseases are due to exposure to environmental pollutants (Papadopoulou et al., 2014). Urban areas are the hot spots for environmental hazards on multiple scales, as a result of population growth, industrial development and vehicular transport growth (Puskas and Fairsang, 2009). In recent decades, there has been a rapid development of urbanization and increase in the urban population, as short-term and intensive human activities lead to large amounts both of organic (such as polyhalogenated compounds) and inorganic pollutants (such as potentially toxic metals) (Golia et al., 2021). Generally, soil is regarded as the ultimate sink for heavy metals released into the environment (Mohammadi et al., 2020). Therefore, urban soils, acting as a reservoir of contaminants, are excellent indicators of pollution (Martínez-Bravo and Martínez-del-Río 2019), while heavy metals in the soil are considered important indicators for monitoring the impact of human activities on soil environmental quality (Golia et al., 2021).
Even though potentially toxic metals are naturally present in the soil due to erosion and weathering of parent rocks (Tong et al., 2020), elevated concentrations of these elements are usually linked to human-induced activities (Antoniadis et al., 2017). The anthropogenic sources of pollution, such as industries (mainly non-ferrous industries, but also power plants and iron, steel and chemical industries), agriculture (irrigation with polluted waters, sewage sludge and fertilizer, especially phosphates, contaminated manure and pesticide containing heavy metals), transportation (combustion of fossil fuels and road traffic), and so on, are typically exacerbated

in cities due to the local concentration of humans and their activities (Gope et al., 2017). Undeniably, nowadays, soil of highly urbanized industrial areas and municipalities are vulnerable to degradation processes.

It is well known that Potentially Toxic Elements (PTEs), including heavy metals and metalloids, are among the most persistent soil pollutants because of their non-biodegradable nature and the long-term toxicity (Ma and Rao, 1997). Heavy metals in the soil can be absorbed by plants and enter the food chain. They also may contaminate surface and groundwater resources (Khoder et al., 2012, Logiewa et al., 2020). Continuous release of trace elements from man-made sources results in the considerable changes in the bio-geochemical cycle of those elements (Ali and Khan, 2018). In addition, previous work has shown that exposure to high concentrations of heavy metals in the soil can lead to many health problems. For example, long-term exposure to those pollutants can result in dermal lesions, skin cancer, peripheral neuropathy, kidney problems etc. (Mohammadi, 2020).

Therefore, it is vital to assess the contamination and determine the possible sources of heavy metals in urban and suburban areas, in densely populated areas, or in industrial soils in order to improve the environment and protect human health (Golia et al., 2020, Han et al., 2020). The main objectives of the present study were (1) to estimate heavy metal contents in the urban soils of Thessaloniki, (2) to analyze their sources and (3) to highlight the areas (locations) which are more at risk of pollution.

2 Materials and Methods

2.1 Site Description

The present work was carried out in the urban area of Thessaloniki, the second largest city in Greece and one of the most important trade and communication centers, situated in the heart of the Balkan Peninsula. With a permanent population of over 1,000,000 and having one of the most commercial ports very close to the city center, it is no coincidence that it is an important industrial center and attraction for tourists. Thessaloniki is a coastal city surrounded by numerous residential suburbs while an extended industrial area is located north westerly of the city. Despite the important size of the city, the absence of a developed public transport system led to increased road traffic into the city center daily (Bourliva et al., 2018).

Thessaloniki is located on the northern edge of the Thermaic Gulf on its east coast and is bound by Mount Chortiatis to its southeast. The climate in the broader Thessaloniki area is directly affected by the Aegean Sea, on which it is situated. Thessaloniki's climate is typically Mediterranean, characterized by low precipitation levels (rain during 33% of the year) and low wind velocity values. Generally, winters are relatively dry, with common morning frost, while summers are hot and quite dry.

2.2 Soil Sampling

A total of fourty-four soils samples, consisting of three sub-soils each, were collected at a depth of 0-10 cm from diverse green spaces, including parks, and playgrounds in the downtown, squares close to the harbor, flower beds located close to main streets, and the vicinity of harbor.

2.3. Chemical Analysis of Soil Samples

The physicochemical analyses of the fourty four soil samples were performed using the methods described by Page et al. (Trujillo-González et al., 2019). The analyses were preceded by air-drying the soil samples for three days and sieving them with a 2 mm sieve. Clay, sand, and silt percentage, as well as, cation exchange capacity (CEC), electrical conductivity, organic matter content, pH values (1:1) (soil: water), and the available metal concentration for the plants, were measured, using the solution of diethylene triamino-pentaxic acid (DTPA). Among other measures, total concentrations (Table 1), were measured using the Aqua Regia method (HCl-HNO_3 mixture, 3: 1) (ISO / DIS 11466 1994) [26]. Finally, the concentrations of metals Cu, Zn, Pb, and Cd were determined with an Atomic Absorption Spectrometer (AAS), flame component (F-AAS) or Graphite furnace (Golia et al., 2021).

3 Results

3.1 Physicochemical Properties of Soil Samples

Most soils had an alkaline pH (> 7.5), a low percentage of organic matter (<2.4%) and a high percentage of clay (22.3-36.5%). The percentage of calcium carbonate was quite high (6.3-14.6%). Only 14.5% the soil samples had pH values between 6.3-6.9 and an undetectable $CaCO_3$ value.

3.2 Levels of Potentially Toxic Elements

The mean values of metal concentrations during the research are presented in Table 1. The average values were found to be lower than maximum permitted values for all evaluated metals, except Cu. In particular, the mean Cu concentration was 335,16, while the other values were as follows: for Zn, the mean was 298,15, for Cd, the mean was 1,30, and for Pb, the average was 128,83. Average Cu concentration was higher than EU limits, while the Zn, Cd and Pb mean concentrations were lower than the background levels.

Table 1. Pseudo-total concentrations of potentially toxic elements (mean values of 44 soil samples).

-	Cu	Zn	Cd	Pb
-	mg kg−1			
Minimum Value	98	110	0,5	70
Maximum Value	630	450	2,1	206
Average value	335,16	298,15	1,30	128,83
EU Limits	140	300	3	300

It is worth noting that from the Cu concentrations measured, below the EU limits was only the 20%, while the remaining 80% was higher than them, with prices ranging from 98-630. Zn concentrations ranged from 110-450, of which only 43% were lower than the EU limits. As for Cd and Pb concentrations, ranged from 0,5-2,1 and 70-206, respectively, of which no price exceeds the EU limits. More specifically, Figure 1. shows the distribution of soil samples at different concentrations of Cu, Zn, Cd and Pb respectively. In each diagram the value of the concentration which is the limit of the European Union is of interest, as in some cases a large number of samples exceed this value.

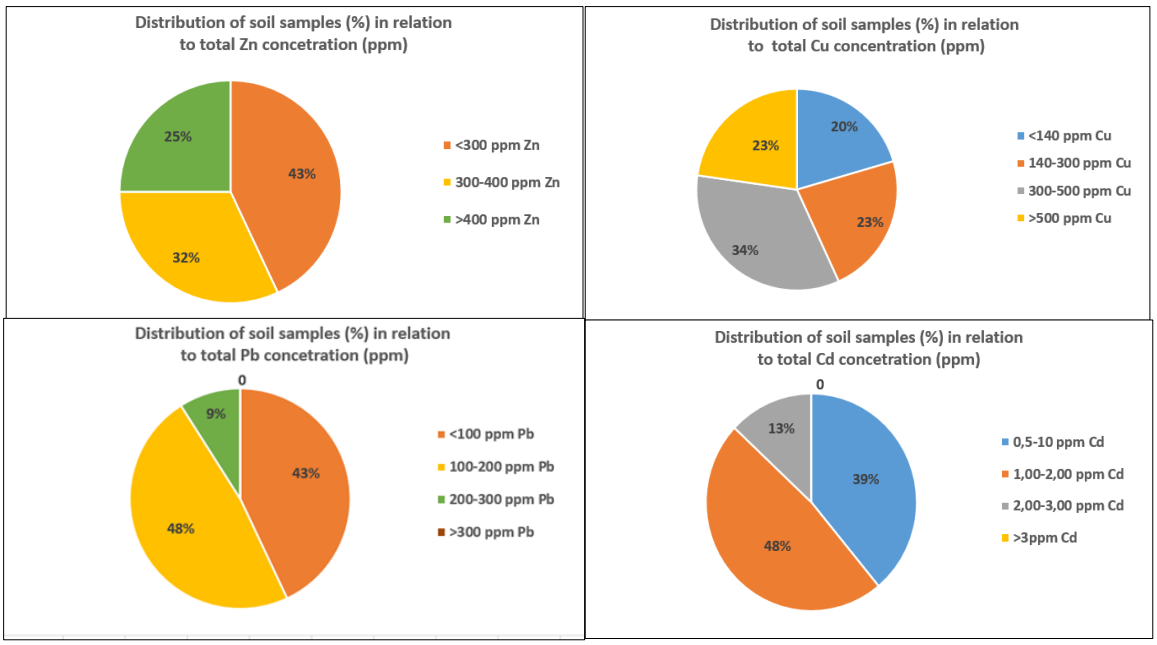

Figure 1. Distribution of soil samples (%) in relation to total Cu, Zn, Cd and Pb, respectively, concetration (ppm).

4 Discussion

4.1 Physicochemical Properties of Soil Samples

The physicochemical properties of the soil samples are representative of the samples of the urban fabric (Golia et al., 2021). However, in the case of Volos, no soil sample was found with a low pH value. A stronger correlation between metal concentrations and soil pH is therefore expected.

4.2 Levels of Potentially Toxic Elements

The presence of widely known as traffic-related elements (Kowalska et al., 2018, Massas et al., 2010) reveals that their possible source is vehicular emissions. Specifically, the high loading for Cu (630 mg kg^{-1}) known as the most abundant element in brake lining materials (Massas et al., 2010), along with the high loadings for Pb (206 mg kg^{-1}), typically used as frictional additives in brake friction materials (Wijesiri et al., 2015, Pan et al., 2018), suggest that total concentrations of potentially toxic elements are highly impacted from non-exhaust emissions and specifically brake wear emissions. That's why the highest concentrations of Cu and Pb occurred near the heaviest traffic roads (Monastiriou), as well as in the areas adjacent to the railway station, the bus stations, and the commercial port (Adimalla et al., 2020, Alexakis et al., 2015, Botsou et la., 2020), as mentioned in many studies.

Regarding Zn, an element significantly abundant in brake lining (Kelepertzis et al., 2020, Christoforidis and Stamatis, 2009), enforce brake wear as the potential source of the specific metal. Several sources of Zn in urban soils have been reported, both crustal and anthropogenic, with tire and brake wear, diesel exhaust emissions and corrosion of safety fence being the most common (Massas et al., 2010). Also, it is noteworthy that high concentrations of Zn found near the commercial port. Prolonged use and storage of metal objects and scrubs may have led to high Zn levels locally (Golia et al., 2021).

In general, high levels of metals are usually observed near ports (Antoniadis et al., 2017). It is well known that the concentration of metals in aquatic ecosystems, such as ports, is measured in water and sediments. Usually, metals are present in the highest concentrations in the sea sediments and in lower in water (Kelepertzis and Argyraki, 2015, Papadopoulou-Vrynioti et al., 2013). The permanent presence of metals near ports is a very worrying problem as their constant contact with salts and the high percentage of moisture provokes oxidizing conditions. Then, the metals corrode and their concentrations in the soils accumulate (Golia et al., 2021).

Finally, the high loadings of Cd that observed suggesting mixed sources of oil/fuel combustion and industrial activities. Cadmium is commonly used in lubricating oil (Kasa et al., 2014), while coal combustion could release Cd into the environment. The factories located around the city of Thessaloniki may contribute to the pollution of the area, especially when the weather conditions are favorable for the spread of pollutants (Alexakis et al., 2020). Moreover, the burning of materials in the fireplaces of the houses of the study area may also contribute to the increase in PTE pollution (Golia et al., 2021). There is also evidence that the coal or crude oil used for household heating, gasoline, and diesel vehicle exhaust is of the major problems in urban soil pollution (Golia et al., 2021).

5 Conclusions

The level of heavy metals in the soil samples of Thessaloniki were found to be lower than the maximum permitted values set by the European Union. Nevertheless, the presence of heavy metals seems to be significantly increasing near the commercial port of the city of Thessaloniki, close to the railway station, and in the intercity bus station along with the big and heaviest traffic roads of Thessaloniki. Continuous long-term monitoring for the evaluation of PTE levels is of the utmost importance, as high PTE levels could ultimately have a negative impact on the environment, food and consequently on the health of the citizens of Thessaloniki and neighboring communities. The present study could give rise to further and more thorough research in the future. Locating sources of contamination locally and nationally could control or even reduce the levels of PTEs in the area of interest.

References

Adimalla, N., Chen, J. and Qian, H., 2020. Spatial characteristics of heavy metal contamination and potential human health risk assessment of urban soils: A case study from an urban region of South India. Ecotoxicol. Environ. Saf., 194.

Alexakis, D., Gotsis, D. and Giakoumakis, S., 2020. Evaluation of soil salinization in a Mediterranean site (Agoulinitsa district—West Greece). Arab. J. Geosci., 8, 1373–1383.

Ali, H. and Khan, E., 2018. What are heavy metals? Long-standing controversy over the scientific use of the term 'heavy metals' – proposal of a comprehensive definition. Toxicological & Environmental Chemistry, Volume 100, Issue 1, Pages 6-19.

Antoniadis, V., Golia, E.E., Shaheen, S.M. and Rinklebe, J., 2017. Bioavailability and health risk assessment of potentially toxic elements in Thriasio Plain, near Athens, Greece. Environ Geochem Health, 39:319–330.

Botsou, F., Moutafis, I., Dalaina, S. and Kelepertzis, E., 2020. Settled bus dust as a proxy of traffic-related emissions and health implications of exposures to potentially harmful elements. Atmos. Pollut. Res., 11, 1776–1784.

Bourliva, A., Kantiranis, N., Papadopoulou, L., Aidona, E., Christophoridis, C., Kollias, P., Evgenakis, M. and Fytianos, K., 2018. Seasonal and spatial variations of magnetic susceptibility and potentially toxic elements (PTEs) in road dusts of Thessaloniki city, Greece: A one-year monitoring period. Science of The Total Environment, Volume 639, Pages 417-427.

Christoforidis, A. and Stamatis, N., 2009. Heavy metal contamination in street dust and roadside soil along the major national road in Kavala's region, Greece. Geoderma, 151, 257–263.

Golia, E.E., Antoniadis, V., Tsiropoulos, N. and Vleioras S., 2020. Investigation of Extraction Methods for the Assessment of the Pseudo-Total Concentration of Potentially Toxic Elements in Moderately Contaminated Soils of Central Greece. Water Air and Soil Pollution, Volume 231, Issue 9, Article number 484.

Golia, E.E., Papadimou, S.G., Cavalaris, C., and Tsiropoulos, N.G., 2021. Level of Contamination Assessment of Potentially Toxic Elements in the Urban Soils of Volos City (Central Greece). Sustainability, 13(4), 2029.

Gope, M., Masto, R.E., George, J., Hoque, R.R., and Balachandran, S., 2017. Bioavailability and health risk of some potentially toxic elements (Cd, Cu, Pb and Zn) in street dust of Asansol, India. Ecotoxicol. Environ. Saf., 138, 231–241.

Han, Q., Wang, M., Cao, J., Gui, C., Liu, Y., He, X., He, Y. and Liu, Y., 2020. Health risk assessment and bioaccessibilities of heavy metals for children in soil and dust from urban parks and schools of Jiaozuo, China. Ecotoxicol. Environ. Saf., 191.

Kasa, E., Felix-Henningsen, P., Duering, R.A. and Gjoka, F., 2014. The occurrence of heavy metals in irrigated and non-irrigated arable soils, NW Albania. Environ. Monit. Assess., 186, 3595–3603.

Kelepertzis, E. and Argyraki, A., 2015. Geochemical associations for evaluating the availability of potentially harmful elements in urban soils: Lessons learnt from Athens, Greece. Appl. Geochem., 59, 63–73.

Kelepertzis, E., Argyraki, A., Chrastný, V., Botsou, F., Skordas, K., Komárek, M. and Fouskas, A., 2020. Metal(loid) and isotopic tracing of Pb in soils, road and house dusts from the industrial area of Volos (central Greece). Sci. Total Environ., 725.

Khoder, M., Al Ghamdi, M. and Shiboob, M., 2012. Heavy Metal Distribution in Street Dust of Urban and Industrial Areas in Jeddah, Saudi Arabia. J. King Abdulaziz. Univ. Environ. Arid L. Agric. Sci., 23, 55–75.

Kowalska, J.B., Mazurek, R. and Gąsiorek Michałand Zaleski, T., 2018. Pollution indices as useful tools for the comprehensive evaluation of the degree of soil contamination–A review. Environ. Geochem. Health, 40, 2395–2420.

Logiewa, A., Miazgowicz, A., Krennhuber, K. and Lanzerstorfer, C., 2020. Variation in the concentration of metals in road dust size fractions between 2 μm and 2 mm: Results from three metallurgical centres in Poland. Arch. Environ. Contam. Toxicol., 78, 46–59.

Ma, L.Q. and Rao, G.N., 1997. Chemical fractionation of cadmium, copper, nickel, and zinc in contaminated soils, Volume 26, No.1, pp. 259-264. American Society of Agronomy, Crop Science Society of America, and Soil Science Society of America.

Martínez-Bravo, M. and Martínez-del-Río, J., 2019. Urban pollution and emission reduction. Sustainable cities and communities, pp. 905-915.

Massas, I., Ehaliotis, C., Kalivas, D. and Panagopoulou, G., 2010. Concentrations and availability indicators of soil heavy metals; The case of children's playgrounds in the city of Athens (Greece). Water. Air. Soil Pollut., 212, 51–63.

Mohammadi, A.A., Zarei, A., Esmaeilzadeh, M., Taghavi, M., Yousefi, M., Yousefi, Z., Sedighi, F. and Javan, S., 2020. Assessment of Heavy Metal Pollution and Human Health Risks Assessment in Soils Around an Industrial Zone in Neyshabur, Iran. Biological Trace Element Research, 195:343–352.

Pan, L., Wang, Y., Ma, J., Hu, Y., Su, B., Fang, G., Wang, L. and Xiang, B., 2018. A review of heavy metal pollution levels and health risk assessment of urban soils in Chinese cities. Environ. Sci. Pollut. Res., 25, 1055–1069.

Papadopoulou-Vrynioti, K., Alexakis, D., Bathrellos, G.D., Skilodimou, H.D., Vryniotis, D., Vassiliades, E. and Gamvroula, D., 2013. Distribution of trace elements in stream sediments of Arta plain (western Hellas): The influence of geomorphological parameters. J. Geochem. Explor., 134, 17–26.

Papadopoulou-Vrynioti, K., Alexakis, D., Bathrellos, G.D., Skilodimou, H.D., Vryniotis, D. and Vassiliades, E., 2014. Environmental research and evaluation of agricultural soil of the Arta plain, western Hellas. J. Geochemical Explor., 136, 84–92.

Puskas, I. and Fairsang, A., 2009. Diagnostic indicators for characterizing urban soils of Szeged, Hungary. Geoderma, 148, 267–281.

Shifaw, E., 2018. Review of Heavy Metals Pollution in China in Agricultural and Urban Soils. Journal of Health & Pollution, Volume 8, Issue 18, Article number 180607.

Tong, S., Li, H., Li, W., Tudi, M. and Yang, L., 2020. Concentration, Spatial Distribution, Contamination Degree and Human Health Risk Assessment of Heavy Metals in Urban Soils across China between 2003 and 2019—A Systematic Review. International Journal Environmental Research Public Health, Volume 17, Issue 9, Article number 3099.

Trujillo-González, J.M., Torres-Mora, M.A., Jiménez-Ballesta, R. and Zhang, J., 2019. Land-use-dependent spatial variation and exposure risk of heavy metals in road-deposited sediment in Villavicencio, Colombia. Environ. Geochem. Health, 41, 667–679.

Wijesiri, B., Egodawatta, P., McGree, J. and Goonetilleke, A., 2015. Process variability of pollutant build-up on urban road surfaces. Sci. Total Environ., 518–519, 434–440.

SESSION 3:
ENVIRONMENTAL HAZARDS AND EXTREMES

HAZE: An Agent-Based Methodology for Dealing with Environmental Hazards in Agriculture

Kravari K. [1], **C. Badica**[2] **and A. Kravaris**[1]

[1] Department of Industrial Engineering and Management, International Hellenic University, Greece
[2] Computer and Information Technology Department, University of Craiova, Romania

Abstract. Environmental risks in agriculture are increasingly affecting crops and farmers, leading to significant economic and social consequences. Problems with agriculture are exacerbated by, inter alia, climate change, water scarcity, and desertification, necessitating a credible and intelligent approach that will support agriculture and its stakeholders. To this end, the present work aims to enrich methods and techniques with the help of advanced information technologies and in particular Intelligent Agents (IAs) part of the symbolic Artificial Intelligence (AI). An autonomous agent is a system that is within and part of an environment that feels that environment and acts on it, over time, pursuing its own agenda. In other words, agents equipped with rules and facts are goal-oriented. Therefore, agents are clearly suited to changing environments (dynamic, unpredictable, unreliable). In this context, the article presents the first steps toward a holistic and easily adaptable methodology, called HAZE, a new approach that will allow both real-time monitoring and warning and decision-making. The HAZE Agent Frame will be powered by data from standard IoT sensors (eg in fields). More specifically, the goal is to create a human-like artificial intelligence environment without the need for oversight that represents every aspect of the pilot sites, including crops, stakeholders, and risks, as well as autonomy, reactivity, and preventive action of agents. This methodology will improve the way in which farmers, even stakeholders, react and handle an environmental hazard. The methodology will allow the right prognosis to be achieved by leading to timely and smart decisions that will help prevent potential damage. The first part of the methodology includes the development of a series of environmental hazard types and their characteristics along with effects while the second part will collect and reason on (IoT) data providing a smart control and decision-making application.

1 Introduction

The Internet of Things (IoT) is a rapidly evolving extension of the IT technology. It is a new paradigm that creates a world where Things, devices, services or even humans, will be connected and able to make decisions and communicate (Lee and Lee, 2015). An area that is expected to attract more attention, in this context, is Smart Farming and Precision Agriculture which due to the IoT emergence faces new challenges. Today, the IoT mostly sends data up towards the Cloud for processing. Many researchers believe that as both software and hardware continues to evolve, some of these processes may be bring back to the devices. Hence, in the IoT of tomorrow, value between devices and across industries could be uncovered using Intelligent Agents (IAs) that can add autonomy, context awareness, and intelligence (Lee and Lee, 2015; Gore et al. 2018). Actually, it is estimated that by the end of the year more than twenty-nine billion connected devices will forecast, most of which are related to the IoT. Hence, it is clear that as more devices get connected and gain smart features, more data will be gathered, and agriculture can be improved. In this context, we, as plenty others, propose a decentralized approach where devices combined with intelligent agents will become part of the Internet of Smart Things. In this context, Intelligent Agents are considered as an appropriate and promising technology since they form an alternative to traditional interactions among people and objects (Alioto, 2017; Amin et al., 2018). Intelligent agents are increasingly used among others in networking and mobile technologies in order to achieve automatic and dynamic behavior, high scalability and self- healing networking, promoting flexibility and trustworthiness (Amin et al., 2018). Their capability of autonomously representing people, devices or even services allows them to be applied in many real world applications, including crisis management and green growth.

Furthermore, environmental risks in agriculture are increasingly affecting crops, economy and society. Climate change, water scarcity, and desertification are only some of the underlying issues that raise problems to farms and stakeholders. To this end, the first attempt of HAZE took into account some of the most common cases of hazards classified by agricultural practice, by environmental issue and by disasters. In this context, the present study propose a rule-based methodology that will allow agents to provide monitoring, warning and decision-making without human intervention. Furthermore, this study combines the agent technology with the microservice architecture, a promising modular approach (Garriga, M., 2018). A core concept of the methodology is the proper information exchange among Agents and/or Things in order to assure safe and robust transactions, maximizing interoperability, reusability, automation and efficiency. Finally, the article is organized as follows, section 2 presents an overview of environmental hazards and their characteristics that

are taken into account in HAZE, and section 3 presents the valuable agent technology as well as the proposed HAZE approach while section 4 summarizes the added value of the article with some final remarks.

2 Environmental Hazards and Characteristics

The environmental hazards in agriculture involves impacts on a variety of different factors, such as the soil, water, air, animal and soil variety, people, plants, and the food itself. The international community acknowledging the great importance agriculture to society and environment has already committed to increasing sustainability of food production as part of Sustainable Development Goal 2: "End hunger, achieve food security and improved nutrition and promote sustainable agriculture" (United Nations, 2015). In this context, the first part of the proposed methodology is to decide upon the series of the environmental hazard types along with their characteristics that will be included in HAZE. Although, there are plenty of cases, for this first study only some were chosen, yet, the methodology is expandable and more types can be easily adopted. To this end, two main groups of cases where formed; the first consists of hazards related to agricultural practice while the second is related to environmental issue (Table 1).

Table 1. Environmental Hazards Categorization in HAZE.

By agricultural practice	By environmental issue	By disasters
Irrigation	Climate change	Flood/Drought
Pesticides	Pollutants	Fire
Plastics	Soil degradation	Earthquake

Agricultural practices can lead to serious threats, although there are efforts to limit their impact. Irrigation affects the quantity and quality of soil and water while its effects include among others alteration of hydrological conditions. For instance, if the soil is under irrigated, soil salinity is increased due to poor soil salinity control while irrigation with saline or high-sodium water could lead to the formation of alkaline soil. Furthermore, it is estimated that more than 98% of sprayed insecticides reach a destination other than their target since they are sprayed across larger areas or even whole fields (Miller, 2004). Hence, pesticides, being mainly toxic chemicals can lead to a variety of side effects to plants, animals, humans, and the environment. Today, it is estimated that over 60% of agricultural land is at pesticide pollution risk (Tang, 2021). As far as it concerns plastics, there is even the term plasticulture which refers to the practice of using plastic materials in agricultural applications. This practice includes may include, among others, soil fumigation film and plastic plant packaging. The main issue in this case is that plastic is hard to recycle while chemicals affect crops and the environment.

On the other hand, hazards related to environmental issues are even more. Global warming, as a result of climate change, has on temperature and precipitation while greenhouse gases such as carbon dioxide, methane, and nitrous oxide lead to various issues that affect agriculture. Additionally, agricultural pollution, due to biotic and abiotic byproducts of farming practices results in contamination or degradation of the environment while affecting the economy. This pollution may come from a variety of sources, such as water pollution. In this context, management practices play a crucial role in the amount and impact of these pollutants. Generally speaking, farming pollutants include, among others, sediments, pathogens, metals, and salts. Furthermore, soil degradation, defined as the decline in soil quality, can be a result of many agriculture factors. Salting, waterlogging, compaction, changes in soil acidity are some of the soil degradation attributes (Soil Erosion – Causes and Effects).

Finally, natural hazards may have a severe impact on agriculture while the crop subsector is the most affected by natural hazards leading to crop production losses. Natural disasters are generally meteorological, hydrological, geological or biological. Examples of meteorological and hydrological disasters include typhoons, floods and droughts. The impacts of natural disasters on agriculture and the environment can be direct or indirect as well as positive or negative. Floods and droughts, for instance, may reduce farm productivity, damage farm inputs, facilities and infrastructure while floods/fires can even damage farm supply routes (Ben Mhenni et al. 2021; Sivakumar, 2021).

3 Smart Control and Decision-Making Application

3.1 Intelligent Agents and Defeasible Logic

In order to provide real-time assessment, early warning and decision-making, HAZE uses as a core component of the system the agent technology. Intelligent Agents are a well-studied technology that can form a human-like artificial intelligence environment without the need for supervision. This technology offers plenty of

properties (Table 2), especially autonomy, reactivity, proactivity and communication ability. Autonomy means that an agent exercises exclusive control over its own actions and state. Reactivity means sensing or perceiving change in their environment and responding while all agents have the ability to communicate with other entities, such as human users, other agents, or objects. Furthermore, agents have the ability to plan and set goals, to maintain beliefs, to reason about their actions and others, including humans, and learn from past experience and machine learning techniques.

Table 2. Intelligent agents' properties.

Autonomy	Migration
Adaptability	Learning
Social ability (Collaboration/ Coordination/Interaction)	Reactivity
Persistence (execution)	Proactivity
Communication ability	Mobility

Although designing and building agents is not trivial, information systems based on intelligent agent technology form a dynamic and meaningful community, where each agent has its own role. Actually, a multi-agent system could be considered as a virtual social community, which reflects transactions among entities, services and devices. What is even more important is the ability of agents to think and learn, conducting inference. There is a number of logics, and subsequently reasoning, that can be used but for the present approach defeasible logic (DL), that introduced by Nute (2003), was chosen. DL is a simple and efficient rule based nonmonotonic formalism that deals with incomplete and conflicting information. It has the notion of rules that can be defeated; hence it derives plausible conclusions from partial and sometimes conflicting information. These conclusions, despite being supported by the currently available information, could nonetheless be rejected in the light of new, or more refined, information. Furthermore, compared to more mainstream non-monotonic approaches, the main advantages of defeasible reasoning are enhanced representational capabilities and low computational complexity (Maher, 2001).

More specifically, a defeasible theory D, which in HAZE is represented as a knowledge base, consists of three basic parts; namely a set of facts (F), a set of rules (R) and a superiority relationship (>). Hence, D can be represented by the triple (F, R, >). Additionally, the set of rules R consists of three distinct types of rules; namely strict rules, defeasible rules and defeaters. Strict rules are denoted by $A \rightarrow p$ and are interpreted in the typical sense that whenever the premises are indisputable, so is the conclusion. An example of a strict rule could be "Flood is hazard" which written formally is r_1: flood(X) → hazard(X). On the other hand, defeasible rules are rules that can be defeated by contrary evidence and are represented as $A \Rightarrow p$. An example of a defeasible rule could be "Any hazard is considered to be dangerous" which written formally is r_2: apartment(X) ⇒ acceptable(X). Finally, defeaters are rules that do not actively support conclusions, but can only prevent some of them. They are represented as $A \in p$. In other words, these rules can be used to defeat defeasible rules by producing evidence to the contrary. An example of such a rule could be "If a flood occurs, but its severity is under a threshold, then it might be not risky" which written formally is r_3: flood(X), severity(X,Y), Y>threshold ∈ ¬risky(X). Hence, this defeater can defeat, for instance, rule r_4: flood(X) ⇒ risky(X).

As far as it concerns the superiority relationship among the rule set R, it is an acyclic relation > on R. An example of such a relationship could be the following: given the defeasible rules r_2 and r_4, no conclusive decision can be made about whether the flood is risky or not since rules r_2 and r_4 contradict each other. Yet, if superiority relation > with $r_3 > r_4$ exists then r_3 overrides r_4 and the conclusion that the flood is not risky can be derived. In this case rule r_3 is called superior to r_4 and r_4 inferior to r_3. Another important element of defeasible reasoning is the notion of conflicting literals, where literals are considered to be conflicting and at most one of a certain set should be derived. An example of such a case is a negotiation about the amount of pesticides that should be used, where a proposal should be made by the potential stakeholder. The proposal can be determined by several rules, whose conditions may or may not be mutually exclusive. All rules have proposal(X) in their head, since a proposal is usually a positive literal. However, only one offer should be made. Therefore, only one of the rules should prevail, based on superiority relations among them. In this case, the conflict set is: C(proposal(x,y)) = {¬ proposal (x,y)} ∪ { proposal (x,z) | z ≠ y}. For instance, the following two rules make a proposal for a given field area, based on the farmer's requirements. However, the second one is more specific and its conclusion overrides the conclusion of the first one.

r_5: fieldSize(X,Y),Y≥45,annualCrop(X,Z) ⇒ proposal(X,250+2Z+5(Y−45))
r_6: fieldSize (X,Y),Y≥45, annualCrop (X,Z),nearUrban(X) ⇒ proposal(X,300+2Z+5(Y−45))
$r_6 > r_5$

3.2 HAZE approach

First of all, HAZE models three main types of system entities (Figure 1); namely agents that represent human or virtual entities, services and devices. All types of entities are represented as agents while microservice architecture was used for the implementation of services and devices, achieving the necessary functionalities and reducing the common issue of device handling. In this context, the methodology assigns an extendable list of characteristics C and preferences P to each entity (C_x^k & P_x^m | k,m ∈ [1, N], x ≡ entity) where k and m represent the number of characteristics and preferences, respectively. The C list contains the type of the entity, the assigned roles, the possible hazards risks, the type and amount of pollutants, the crop, in case of farm lands, and so on. On the other hand, preferences include information such as the desirable irrigation degree or the desirable level of security. For computational and priority purposes, each characteristic and preference is assigned with a value of importance (weight) at the range [0, 1]; namely W_c^k & W_p^m | k,m ∈ [1, N], c ≡ characteristic, p ≡ preference. This weight, actually, defines how much attention will be paid to each characteristic or preference, e.g. if there is a case of land that is endangered by floods, for instance, due to nearby rivers, etc, this land should be always monitored. Another case would be an environment with limited availability in water, this land would have priority among the rest areas. Additionally, the aforementioned environmental hazards (section 2) are represented following the same approach; namely HAZE assigns an extendable list of hazards H and characteristics CR to each case (H_y^i& CR_y^j | i,j ∈ [1, N], y ≡ environmental hazard) where i and j represent the number of hazards and characteristics, respectively. Hence, HAZE is able to include both stakeholders, such as farmers and farm lands, as well as environmental hazards, such as drought, combining all necessary information for the decision making.

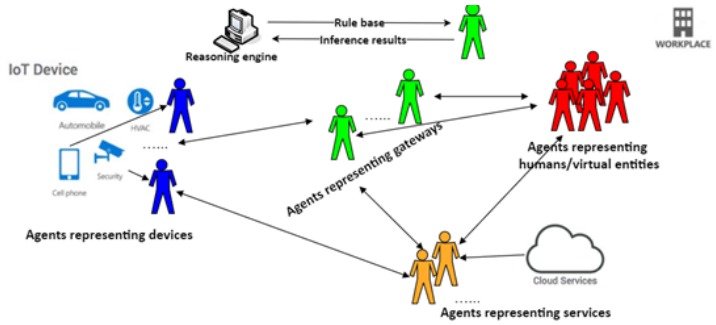

Figure 1. System entities.

More specifically, in the context of decision making, a logic programming language is used. Fusing the data extracted from a case, decisions are made triggering an informative message to the user. The message can range from suggestions to warnings or information for action. Examples include a simple overview of the overall hazards risks in a specific land area and warning messages for the next hours or days. In this context, it is necessary to define rating values in order to realize the decision-making mechanism which, of course, has to deal with a range of complex issues. Hence, HAZE aims at providing an estimation procedure much as experts do in the real world, where they build and maintain domain estimation over time. To this end, we simulate their decision making process, proposing a set of strict and defeasible rules, in a practical, intuitive approach. To this end, first of all, the sensors collect data, such as temperature or waterfall, while historical data, if any, are loaded. Then a confidence value and a value indicating the importance of the collected value is assigned depending on the aforementioned lists. When all values are got together, the rating mechanism adds the current time point (t), forming the final estimating value (r) as a tuple. An example of such a tuple (represented as fact) is presented below in the compact d-POSL syntax (Bassiliades, 2006) of defeasible RuleML (Kontopoulos 2011), which a compact way to express facts and rules.

rating(*id*→id_x, *t*→*?t*, temperature →*?temp*$_x$, depth→*?dep*$_x$, …., *confidence*→*?conf*$_x$, *importance*→*?imp*$_x$).

Of course, each case has different characteristics/parameters that are taken into account as well as a different degree of tolerance, thus, what may be low for a case could be high for another. Hence, each case has some thresholds that determine the lowest accepted value for each parameter. In this context, rule r_1, presented below, indicates that if all values are higher than the associated thresholds then the levels are considered good. Yet, this rule is strict and quite rare.

r_1: *good_level*(*time* → *?t*, *reason* → *all*) :-

temperature_*threshold*(*?temp*), depth_*threshold*(*?dep*), *…,*

rating(*id*→id_x, *t*→*?t*, temperature →$?temp_x$, depth→$?dep_x$, …., *confidence*→$?conf_x$, *importance*→$?imp_x$),

$?temp_x$>*?temp*, $?dep_x$>*?dep*, ….

Yet, usually, each case is classified in relation to a reason, e.g. pollutant value. In this context, the following rule characterize a characteristic case based on a specific reason.

r_2: *pollution_existence*(*time* → *?t*, *reason* → pollutant1) :-

rating(id→?idx, time → ?t, pollutant1→*?poll1x), poll1_threshold(?do), ? poll1x>? poll1.*

r_3: *internal_changes* (*time* → *?t*, *reason*→ *depth*):-

rating(*id*→$?id_x$, *time* → *?t*, *depth* →*? *dep_x*), depth_threshold*(*?dep*), $?dep_x$>*?dep*.

For instance, r_2 consists of two main clauses, a rating that includes the time that was reported the rating, if the value is greater than the threshold then the rule concludes that at a specific time point (*?t*), the environment appears pollution as far as it concerns the poll1 (a pollutant case) value. However, from each case's perspective a parameter could be more important than others. For instance, in a case poll1 value could be considered the most important aspect, perhaps not the only one, in deciding whether it's the environment could be characterized good or bad. In this context, rules r_2 and r_3 could be "replaced" by defeasible rules (r_3' – r_3'), while a priority relationship among them will define which reason is eventually more important. Of course, any potential theory could be formed, namely rule combination and priority relationship (e.g. r_2' > r_3') regarding the reasons, in order to represent preferences related to each case. Of course, we could classify a case in relation to more than one reasons. For instance, rule r_4 describes such a case. According to that "a case has good properties if it has good rating in at least three parameters".

r_4: *good_case_levels*(*time* → *?t*, *reason* → *at_least_3*):-

good_for(*time* → *?t*, *reason* → *?r1*), *good_for*(*time* → *?t*, *reason* → *?r2*),

good_for(*time* → *?t*, *reason* → *?r3*), *?r1 ≠ ?r2, ?r2 ≠ ?r3, ?r3 ≠ ?r1.*

The above is just part of the decision making mechanism but reveal the concept of the approach. Our intention is to enrich the rule set in order to detect even more case, simple and complex (Carrera et al., 2014).

4 Summary

This article discussed upon HAZE, which realizes an intelligent-based approach where both technical and practical guidelines support a decision-making methodology for dealing with environmental hazards in agriculture. It limits the common disadvantages of the existing distributed human-based approaches, by considering the agents as a network acting in the environment on behalf of humans. The heart of the procedure is a rule-based procedure that can take advantage of the data acquired by hazard classification and an appropriately developed sensor system that should be installed in the area that is monitored. As for future directions, our priority is to study the scalability the complexity of the model as well as the scalability of the multi-agent system. Hence, we will further improve the proposed model, attempting to reduce among others its complexity and enriching the hazard cases.

Acknowledgement

This research has received funding from the European Union´s UCPM-2020-KN-AG under grant agreement No 101017819 with the acronym RESISTANT.

References

Kravari, K., Bassiliades N., 2019. StoRM: A social agent-based trust model for the internet of things adopting microservice architecture. SIMPAT Journal 94: 286-302.

Whitmore A., Agarwal A., Xu L.D., 2014. The Internet of Things—a survey of topics and trends, Inf. S.. Front. 17 (2) 261–274, https://doi.org/10.1007/s10796-014-9489-2.

Nute, D., 2003 Defeasible Logic. Springer-Verlag: Web Knowledge Management and Deci-sion Support, 14th International Conference on Applications of Prolog, 151-169.

Lee, I., Lee, K., 2015. The Internet of Things (IoT): Applications, investments, and challenges for enterprises. Business Horizons 58(4), 431-440.

Garriga, M., 2018. Towards a Taxonomy of Microservices Architectures. Software Engineering and Formal Methods Lecture Notes in Computer Science, 203-218.

Gore, R., Lemos, C., Shults, F. L., and Wildman, W. J., 2018. Forecasting Changes in Religiosity and Existential Security with an Agent-Based Model. Journal of Artificial Societies and Social Simulation, 21(1). doi:10.18564/jasss.3596

United Nations, 2015. Resolution adopted by the General Assembly on 25 September 2015, Transforming our world: the 2030 Agenda for Sustainable Development (A/RES/70/1)

Miller, T.G., 2004. Sustaining the Earth: An Integrated Approach. Thomson/Brooks/Cole. pp. 211–216. ISBN 978-0-534-40088-0.

Tang, F. H. M., Lenzen, M., McBratney, A., Maggi, F., 2021. "Risk of pesticide pollution at the global scale". Nature Geoscience. 14 (4): 206–210.

Soil Erosion – Causes and Effects. www.omafra.gov.on.ca. Retrieved 20/5/2022.

Ben Mhenni, N., Shinoda, M. and Nandintsetseg, B., 2021. Assessment of drought frequency, severity, and duration and its impacts on vegetation greenness and agriculture production in Mediterranean dryland: A case study in Tunisia. Nat Hazards 105, 2755–2776. https://doi.org/10.1007/s11069-020-04422-w

Sivakumar, M. 2021. Climate Change, Agriculture Adaptation, and Sustainability. In: Kaushik, A., Kaushik, C.P., Attri, S.D. (eds) Climate Resilience and Environmental Sustainability Approaches. Springer, Singapore. https://doi.org/10.1007/978-981-16-0902-2_6 6

Alioto, M., 2017. Enabling the Internet of Things: From Integrated Circuits to Integrated Systems. Cham: Springer International Publishing.

Amin, E., Abouelela, M., & Soliman, A., 2018. The Role of Heterogeneity and the Dynamics of Voluntary Contributions to Public Goods: An Experimental and Agent-Based Simulation Analysis. Journal of Artificial Societies and Social Simulation, 21(1). doi:10.18564/jasss.3585

Maher, M.J., 2001. Propositional defeasible logic has linear complexity. Theory and Practice of Logic Programming 1(6):691–711.

Bassiliades, N., Antoniou, G., and Vlahavas, I., 2006. A Defeasible Logic Reasoner for the Semantic Web. International Journal on Semantic Web and Information Systems, 2(1):1-41.

Kontopoulos, E., Bassiliades, N., and Antoniou, G., 2011. Visualizing Semantic Web proofs of defeasible logic in the DR-DEVICE system. Knowledge-Based Systems, 24(3):406-419.

Carrera, A., Iglesias, C., García-Algarra, J., & Kolařík, D., 2014. A real-life application of multi-agent systems for fault diagnosis in the provision of an Internet business service. Journal of Network and Computer Applications, 37:146-154.

Agronomic simulation in a Mediterranean agricultural watershed. The case of Lake Karla

Georgios Tziatzios[1], Pantelis Sidiropoulos[1], Lampros Vasiliades[1], Aikaterini Lyra[1],Marios Spiliotopoulos[1], Nikitas Mylopoulos[1], Athanasios Loukas[2], Nicolaos Danalatos[3]

[1]Laboratory of Hydrology and Aquatic Systems Analysis, Department of Civil Engineering, School of Engineering, University of Thessaly, 38334 Volos, Greece.
[2] Laboratory of Hydraulic Works and Environmental Management, Department of Agronomy and SurveyingEngineering, Aristotle University of Thessaloniki, Thessaloniki, Greece
[3] Laboratory of Agronomy and Applied Crop Physiology, Department of Agriculture Crop Production and Rural Environment, University of Thessaly, Fytokou Street, Volos, 38446, Greece
* e-mail: getziatz@uth.gr

Abstract

Agronomic tools are a dynamic component in simulation systems to achieve sustainable water resources management in rural watersheds. Sustainable management of water resources is indissolubly linked to agriculture in Mediterranean countries where it is an essential mainstay of the economy. This article describes an integrated simulation system for modelling groundwater pollution by nitrates in Lake Karla watershed (Central Greece). The simulation is based on the APEX simulation model, and in this article, we give emphasis to the calibration and validation process. Data from 1980 to 2012 is used for the calibration, while the results are validated against data from 2012 to 2016. Automated calibration and sensitivity analysis of APEX is performed using the "APEX-CUTE" software. The calibration process shows that the crop yield depends on various parameters such as the field capacity, the wilting point, the water storage N leaching, Nitrate leaching ratio, for cotton and winter wheat yield while the nutrient losses indicate dependency on parameters such as biological mixing efficiency, maximum depth for biological mixing, coefficient modifying microbial activity with soil depth, the volatilization/nitrification partitioning coefficient and the standing dead fall rate coefficient. The described calibration process significantly improves model performance for most agronomic simulation model outputs, the crop yield and nutrient losses being the concerned parameters.

Introduction

Agriculture is a vital economic component in Mediterranean countries like Greece, Italy, Spain, and Portugal that contributes to social progress by raising the living standards and meeting the demands of an increasing global population. Furthermore, agriculture contributes significantly to an increased production volume and improved quality as the needs of modern consumers continue to increase. Excessive amounts of nitrogenous fertilizers are applied to improve crop production and product quality (Velten et al., 2015, Georgopoulou et al., 2017, Zulfiqar et al., 2019, Masia et al., 2021). Nitrogen is one of the most essential macronutrients required by plants to grow. Conversely, the intensification of agriculture combined with the low cost of inorganic fertilizers, although recently there has been a significant increase in these types of fertilizers as well. Moreover, rapid source of nutrients offered by the inorganic fertilizers to the plants has led to excessive fertilization of crops, which results in quality degradation and contamination of groundwater systems (Wick et al., 2012, Ahmed et al., 2017). The "Nitrates Directive" (91/676/CEE) is a European Union measure approved in 1991, intending to reduce water contamination caused or induced by nitrates from agricultural sources and prevent additional contamination (Wick et al., 2012, Serio et al., 2018). The aforementioned directive characterizes as vulnerable zones all areas where the nitrates concentration in

percolating waters exceeds or could exceed 50 mg/l. In vulnerable zones the intensive use of fertilizers impacts to environmental nitrate contamination, as recognized by a European Water Framework Directive (Giammarino and Quatto, 2015, Serio et al., 2018). In addition, The EU Directive 2006/118/EC suggests that the countries of the European Union establish quality standards, develop methodologies for assessing and monitoring groundwater quality, and implement measures to support groundwater protection, such as adjustments to agricultural practices and encouraging good agricultural practices. This is another attempt to protect groundwater against pollution and deterioration (91/676/CEE, Wick et al., 2012). Simulation models developed and widely applied, initially with the aim of understanding the functioning of physical systems as well as the various physical processes that take place in these systems, are extremely useful and valuable tools and are likely to solve real-world problems of groundwater pollution safely and efficiently (Karatzas, 2017). Simulation tools have been applied to agriculture with varying degrees of success for years. These tools intended to describe the major characteristics of a particular rural system that symbolize a complicated system. The complexity of the natural/real agricultural system (whether it is a field or an agricultural watershed) results in greater complexity in the model structure, with a large input data expected to reproduce and simulate such systems. Models that represent agricultural systems have become crucial tools for planning management practices, evaluating sustainable crop production, and reducing environmental impacts such as water pollution, greenhouses gases and carbon footprint of agri-food supply chain (Osorio et al., 2019). This paper documents the calibration and the validation of an agronomic tool using crop yield and nutrient losses as criteria

1. Materials and Methods

An integrated simulation system that consists of models simulating the surface runoff model (UTHBAL), groundwater flow model (MODFLOW), solute transport for solving advection, dispersion, and chemical reactions of contaminants in saturated groundwater flow systems (MT3DMS), reservoir balance (UTHRL), reservoir-aquifer interaction (LAK3), and agronomic model has been created and used for this study. The flow chart in Figure 1a illustrates the simulation system and the Figure 2b the Agricultural Policy Environmental eXtender (APEX) model in details. The studied area is a rural region of Central Greece, Lake Karla Basin the most intensively cultivated region in Greece the two dominant crops in the study area are wheat and cotton (Tziatzios et al., 2021).

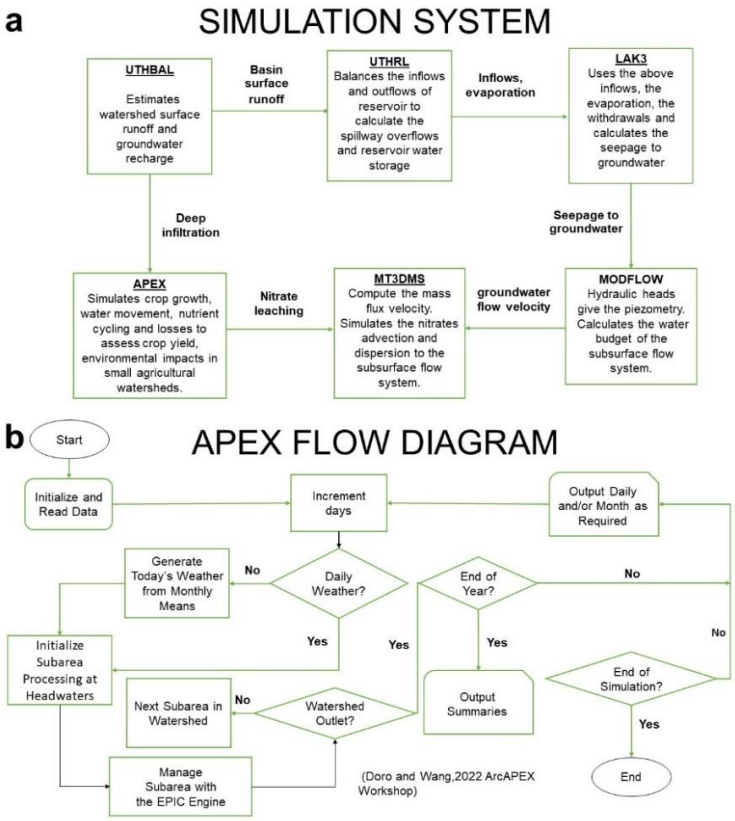

Figure 1a. The simulation system. **Figure 1b.** The APEX model flow diagram

APEX operates on a daily time step and is a model developed for whole farm and watershed management simulation (Wang et al., 2014, Mason et al.,2020). APEX simulates details of farming and land-use practices in small- to medium-sized watersheds up to about 10.000 km^2 (Taylor et al., 2015). APEX can simulate plant growth, water movement, and fate and transport of sediment, nutrients, and pesticides. APEX works by first subdividing the watershed into multiple subareas, homogeneous in terms of soil, slope, land use, management, and weather, before defining the routing structure for an APEX whole-farm or watershed simulation (Gassman et al., 2010). To achieve this process, APEX input includes topography characteristics, physical and chemical soil parameters, daily weather data, land use and management and conservation practices (Bosch et al., 2020). APEX functions can perform long-term continuous simulations and can be used for simulating the impacts of different nutrient management, tillage, conservation, and cropping practices on crop yield and the agricultural and physical environment.

ArcAPEX was designed to automate the parameterization of APEX model using readily available topographic, hydrologic, land use, and soils spatial datasets. In addition to automated identification of model topographic and landscape characteristics, ArcAPEX features direct integration with an APEX parameters database that contains plant, tillage, fertilizer, pesticide, and weather characteristics. The user interface for the tables in the APEX parameters geodatabase (operation schedules, crop, tillage, fertilizer, pesticide, monthly weather, and wind) allow users to add new records to the database tables (Tuppad et al., 2009). Input data provided to the APEX model as text files can also be modified (or created) using the APEXeditor. The APEXeditor is a simple, but powerful user interface for management of APEX input data (read and write), execution of individual APEX runs, and loading of output files into the spreadsheet for further processing and visualization (Osorio et al., 2019). The sensitivity analysis and the calibration and validation process can be conducted using the APEX-CUTE tool. APEX-CUTE tool uses an optimization algorithm with a dynamically dimensioned search (DDS) for automatic calibration of watershed models (Wang et al., 2014). In this article we used ArcAPEX in ArcGIS interface 10.7.1 with APEX v1501 for the subarea

delineation and definition of the routing scheme, APEXeditor to edit some input file after they were created in ArcAPEX, while the sensitivity analysis and automated calibration was performed in APEX CUTE v7.

2.1 APEX Subarea Delineation and Subarea Analysis

APEX extended the EPIC model's ability by allowing users to simulate hydrologically connected subareas instead of a single area, while routing water, sediment, nutrients, and pesticides from subarea to complex landscapes and channel systems to the watershed outlet (Wang et al., 2014). Subarea plan follows the Hydrologic Response Unit concept (HRU). When more than one outlet is selected, the entire watershed is divided in sub-watersheds (one for each outlet selected during the delineation process). Then, each sub-watershed is divided in subareas.
As a first step the watershed is divided into multiple subareas, and then the basic computation element is extracted. The model simulates all the subareas that contribute to bringing water to the outlet the user has defined during the delineation process. Each subarea is associated with a channel for routing runoff, sediment, nutrients, and pesticides from one subarea to another (Tuppad et al., 2009). In our case, the study area divided in thirty-four subareas and four sites (Figure 2). Site24 includes subarea 1 to subarea 24, and subarea 27. Site25 includes subarea 25, 28, and 29, Site26 consisted of only subarea 26, while Site31 includes subarea 30 to 34. DEM raster provided by Copernicus https://land.copernicus.eu/imagery-in-situ/eu-dem/eu-dem-v1.1.

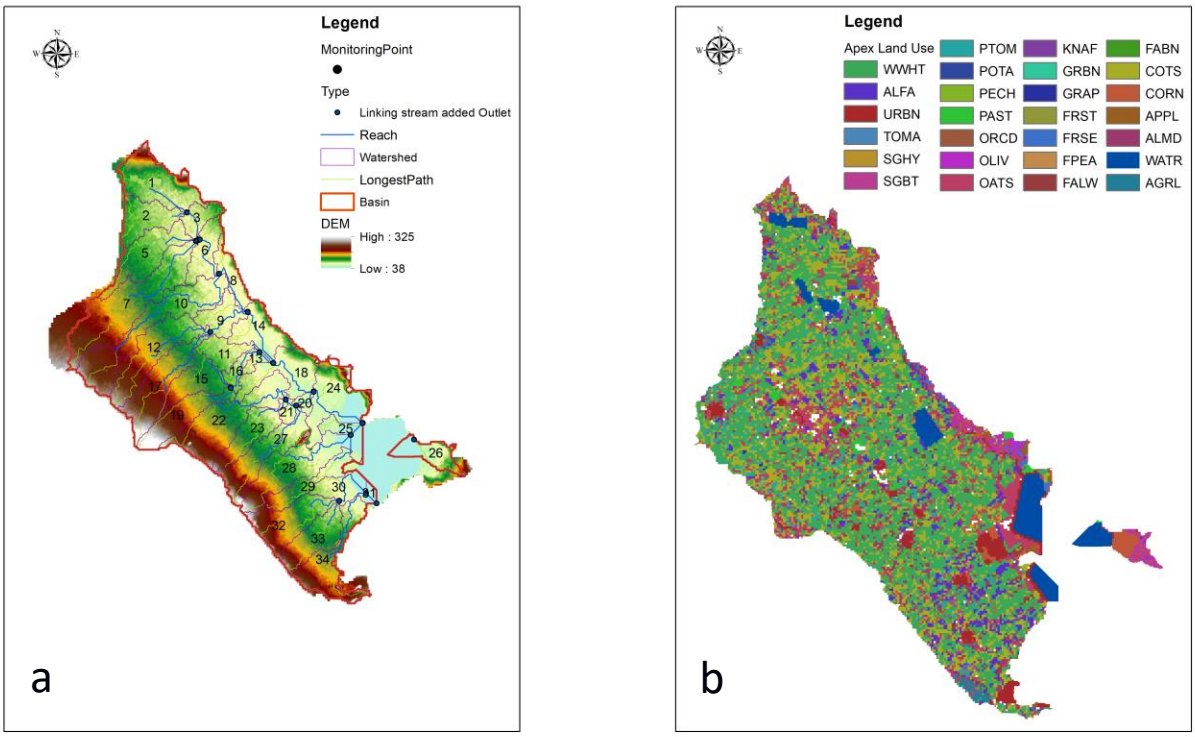

Figure 2a. The DEM, the delineation of watershed and the division of the watershed into multiple sub watersheds and subareas. **Figure 2b.** Land use map of the study area in 2009.

3 Results

3.1 Sensitivity analysis

The most important input parameters that need adjusting during the calibration process is presented analytically by Wang and her associates (2012). An APEX-CUTE sensitivity analysis was carried out to identify the parameters to be expected to have the greatest effect on nutrient losses calculated. APEX-CUTE take into consideration 34 parameters making 700 runs and the most influential parameters found to be biological mixing efficiency, maximum depth for biological mixing, coefficient modifying microbial activity with soil depth, the volatilization/nitrification partitioning coefficient and the standing dead fall rate coefficient. The findings also agree with the analysis of Mason et al., (2020).

3.2 APEX calibration and validation

The first step for successful agronomic modelling is to ensures that data is representative of the simulated conditions providing information on crop, tillage operations (including tillage depth and timing), the fertilizations including amount and type), time of planting and harvesting, irrigation (including amount and timing). Then the user can begin the calibration process by modifying several parameters and other factors of the simulation such as the WA: Biomass-Energy Ratio (CO2=330ppm), potential heat units required by the crop to reach maturity (Mason et al., 2020). The APEX-CUTE tool was used to calibrate data from 1980 to 2012 and for the validation process from 2012 to 2016. Mean yield values were used for winter wheat and cotton (Figures 3a and 3b) (Tavoularis,2012) The statistical criteria of coefficient of determination (R^2) and Nash – Sutcliffe efficiency (NSE) was used to check the model performance as presented in Table 1 according to Moriasi and his associates (Moriasi et al., 2007).

Table1. Statistical results for calibration and validation process

Crops	**Calibration Process (1980 - 2012)**		**Validation Process (2012 -2016)**	
Statistical Criteria	R^2	NSE	R^2	NSE
Winter Wheat	0.70	0.67	0.68	0.60
Cotton	0.71	0.65	0.67	0.55

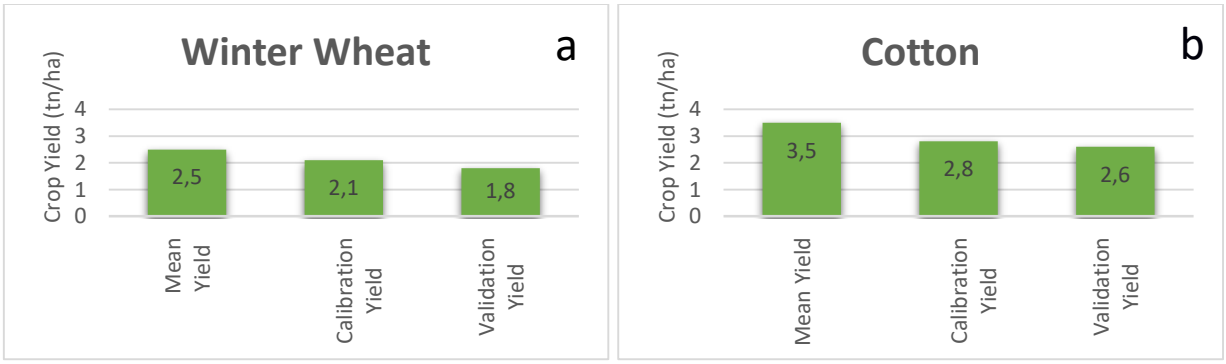

Figure 3a. The mean, calibration, and validation crop yield for winter wheat. **Figure 3b**. The mean, calibration, and validation crop yield for cotton

4. Conclusions

Agronomic simulation is an important tool in the protection of the environment and natural resources. In this paper we presented an APEX agronomic model calibrated and validated for crop yield of winter wheat, cotton, and nutrient losses. Field capacity, wilting point and nitrate leaching ratio are crucial as parameters for crop yield. APEX is a very useful tool for the simulation of fields in a watershed level and APEX CUTE a very useful tool for sensitivity analysis, calibration, and validation process in agricultural systems. After the calibration process, the APEX model was able to give satisfactory results in replicating the average yield of winter wheat and cotton for the 2012-2016 period.

References

Ahmed, M., Rauf, M., Mukhtar, Z., & Saeed, N. A. (2017). Excessive use of nitrogenous fertilizers: an unawareness causing serious threats to environment and human health. Environmental Science and Pollution Research, 24(35), 26983-26987 https://doi.org/10.1007/s11356-017-0589-7

Bosch, D. D., Doro, L. U. C. A., Jeong, J., Wang, X., Williams, J. R., Pisani, O., Endale, D.M & Strickland, T. C. (2020). Conservation tillage effects in the Atlantic Coastal Plain: An APEX examination. Journal of Soil and Water Conservation, 75(3), 400-415. https://doi.org/10.2489/jswc.75.3.400

Doro L. and Wang S. (2022). Agricultural Policy Environmental eXtender (APEX) model Basic Concepts. ArcAPEX for Agricultural Watershed Modeling - Virtual (Zoom Meeting) - 16-18 Mar 2022

European Commission. 1991. Council Directive Concerning the Protection of Waters Against Pollution Caused by Nitrates from Agricultural Sources (91/676/EEC).

Gassman, P. W., Williams, J. R., Wang, X., Saleh, A., Osei, E., Hauck, L. M., & Flowers, J. D. (2009). The Agricultural Policy Environmental EXtender (APEX) Model: An Emerging Tool for Landscape and Watershed Environmental Analyses (Technical Report No. 09-TR 49). Ames, Iowa: Center for Agricultural and Rural Development, Iowa State University.

Georgopoulou, E., Mirasgedis, S., Sarafidis, Y., Vitaliotou, M., Lalas, D. P., Theloudis, I., ... & Zavras, V. (2017). Climate change impacts and adaptation options for the Greek agriculture in 2021–2050: A monetary assessment. Climate Risk Management, 16, 164-182 http://dx.doi.org/10.1016/j.crm.2017.02.002

Giammarino, M., Quatto, P. (2015). Nitrates in drinking water: relation with intensive livestock production. Journal of preventive medicine and hygiene, 56(4), E187–E189.

http://europa.eu.int/comm/environment/water/water-nitrates/index_en.html.

https://doi.org/10.4236/jsea.2019.1210027

Karatzas GP. (2017) Developments on Modeling of Groundwater Flow and Contaminant Transport. Water Resources Management 31: 3235-3244. https://doi.org/10.1007/s11269-017-1729-z

Masia, S., Trabucco, A., Spano, D., Snyder, R. L., Sušnik, J., & Marras, S. (2021). A modelling platform for climate change impact on local and regional crop water requirements. Agricultural Water Management, 255, 107005. https://doi.org/10.1016/j.agwat.2021.107005

Mason, R., Gorres, J., Faulkner, J. W., Doro, L., & Merrill, S. C. (2020). Calibrating the APEX model for simulations of environmental and agronomic outcomes on dairy farms in the Northeast US: A step-by-step example. Applied Engineering in Agriculture, 36(3), 281-301. https://doi.org/10.13031/aea.13679

Osorio Leyton, J.M. (2019) APEXeditor: A Spreadsheet-Based Tool for Editing APEX Model Input and Output Files. Journal of Software Engineering and Applications, 12, 432-446. https://doi.org/10.4236/jsea.2019.1210027

Moriasi N. D., Arnold J. G, Van Liew M. W., Bingner R. L., Harmel R. D., Veith T. L. (2007). Model Evaluation Guidelines for Systematic Quantification of Accuracy in Watershed Simulations. Transactions of The Asabe 50(3), 885-900.doi: https://doi.org/10.13031/2013.23153

Serio, F., Miglietta, P. P., Lamastra, L., Ficocelli, S., Intini, F., De Leo, F., & De Donno, A. (2018). Groundwater nitrate contamination and agricultural land use: A grey water footprint perspective in

Southern Apulia Region (Italy). Science of the Total Environment, 645, 1425-1431. https://doi.org/10.1016/j.scitotenv.2018.07.241

Tavoularis K., (2012). Average Crop Yields in Greece. Ministry of Agricultural Development and Food Agricultural Policy and Documentation Directorate Department of Agricultural Statistics, Athens Greece.

Tuppad, P., M. F. Winchell, X. Wang, R. Srinivasan, and J. R. Williams. 2009. ArcAPEX: ArcGIS interface for Agricultural Policy Environmental eXtender (APEX) hydrology/water quality model. Intl. Agric. Eng. J. 18(1-2): 59-71.

Tziatzios, G., Sidiropoulos, P., Vasiliades, L., Lyra, A., Mylopoulos, N., & Loukas, A. The use of pilot points method on groundwater modelling for a degraded aquifer with limited field data: the case of Lake Karla aquifer https://doi.org/10.2166/ws.2021.133

Velten, S., Leventon, J., Jager, N., & Newig, J. (2015). What is sustainable agriculture? A systematic review. Sustainability, 7(6), 7833-7865. https://doi.org/10.3390/su7067833

Wang, X., Williams, J.R., Gassman, P.W., Baffaut, C., Izaurralde, R.C., Jeong, J. and Kiniry, J.R. (2012) EPIC and APEX: Model Use, Calibration, and Validation. Transactions of the American Society of Agricultural and Biological Engineers, 55, 1447-1462. https://doi.org/10.13031/2013.42253

Wang, X., Yen, H., Liu, Q., & Liu, J. (2014). An auto-calibration tool for the Agricultural Policy Environmental eXtender (APEX) model. Transactions of the ASABE, 57(4), 1087-1098. https://doi.org/10.13031/trans.57.10601

Wick, K., Heumesser, C., & Schmid, E. (2012). Groundwater nitrate contamination: factors and indicators. Journal of environmental management, 111, 178-186. http://dx.doi.org/10.1016/j.jenvman.2012.06.030

Zulfiqar, F., Navarro, M., Ashraf, M., Akram, N. A., & Munné-Bosch, S. (2019). Nanofertilizer use for sustainable agriculture: Advantages and limitations. Plant Science, 289, 110270. https://doi.org/10.1016/j.plantsci.2019.110270

Application of the Canadian Fire Weather Index at the Mediterranean area of Greece

Nikolaos Ntinopoulos, Marios Spiliotopoulos, Lampros Vasiliades and Nikitas Mylopoulos

Laboratory of Hydrology and Aquatic Systems Analysis, Department of Civil Engineering, University of Thessaly, Volos, Greece, e-mail: spilioto@civ.uth.gr

Abstract. Forest fires are of critical importance in the Mediterranean region. Fire weather indices are meteorological indices that produce information about the impact as well as the characteristics of a fire event in an ecosystem and have been developed for that reason. This study explores the spatiotemporal patterns of the FWI system, within a study area defined by the boundaries of the Greek state. The FWI has been calculated and studied for current and future periods using data from the CFSR model coming from the National Centers for Environmental Protection (NCEP), as well as data from NASA satellite programs and the European Commission for Medium Range Weather Forecasts (ECWMF) in the form of netCDF files. Data from the Hellenic National Meteorological Service (HNMS) were also used for the calculation of the Fosberg FWI which was used as an extra means of assessment regarding the spatiotemporal patterns of the FWI. The calculation and processing of the result was conducted in python programming language, with the exception being the calculation of the Fosberg FWI having been performed in Visual Basic for Applications (VBA). For the latter low volume of meteorological data stored in excel files deemed the use of VBA a more practical option. A similar pattern can easily be noted for all indices who seem to have their higher values concentrated in the southeast of the country owing that to the higher temperatures and more frequent drought events that affect the indices' behavior in both the current and future periods.

1 Introduction

The Mediterranean climate is characterized by increased aridity, high temperatures and extreme events during the summer period. An estimated 50,000 forest fire incidents occur annually in the region accounting to a total burned area of an estimated 470,000 ha (Pausas et al., 1999). Most forest fires in the region can be traced to human activity. Forest fires pose a complex threat to modern societies, comprised of environmental, socioeconomic and above all human costs ,posing a threat to functional and cultural infrastructure as well as human lives (Sakellariou et al., 2022). Thus, it is of critical importance that fire agencies possess adequate means for the prediction and prevention of fire events.

Forest fires being a common occurrence in the broad Mediterranean region, are expected to increase in both number of occurrences and intensity, due to climate change (Howden et al., 2001) Forest fires having their behavior closely tied to fuel moisture present increased sensitivity regarding climate change effects (Weber et al., 1997). Greece therefore presents an increased vulnerability regarding fire increase and climate change in general (Giannakopoulos et al., 2011), owing that to being located in the eastern edge of the Mediterranean Basin. Fire danger is used to express assessment of fixed and variable factors of the environment that determine ease of ignition rate of spread difficulty to control and fire impact (Merrill et al., 1987) .Out of the many indices used in literature (Merrill et al., 1987) the Canadian Fire Weather Index has been selected ,being the most reliable and frequently used one (Merrill et al., 1987) developed by the Canadian Forest Fire Danger Rating System (CFFDRS), along with the Fosberg Fire Weather Index (FFWI), both being meteorological indices requiring no information on the actual vegetation state ridding calculations of a degree of complexity (Di Giuseppe et al., 2020). Extracting correlations between the two indices, and climate related factors such as sub-indices of the FWI, and topography, can provide a better comprehension of the effect said factors on fire occurrence and fire vulnerability.

2 Materials and Methods

2.1 Study area

Greece is located in the most southeastern edge of Europe, in latitude from 35o 00' N to 42o 00' N and in longitude from 28o 00' E to 30o 00' E (Bedia et al., 2018). The Greek climate is classified as Mediterranean climatic type, being characterized by mild winters, relatively warm and dry summers and a long sunshine duration for the most part of the annual circle. The western part of the Greek territory is generally wetter, while the eastern part is much drier and windier, mainly during the summer season (Johnson et al., 2019). The fire season in Greece tends to range from March to October (Cloke et al., 2017).

2.2 Data acquisition

FWI calculations require daily meteorological data (temperature, wind speed at 10m, relative humidity, precipitation), whereas Fosberg FWI requires monthly values of wind speed temperature and relative humidity. Data for the calculation of the FWI were collected by the *National Centers for Environmental Protection (NCEP)* (https://globalweather.tamu.edu/), as point outputs from the CFSR model ,for the period 2010-2014.A total of 339 points inside a boundary box containing Greece, were obtained. Data from the Goddard Space Flight Center (https://portal.nccs.nasa.gov/datashare/GlobalFWI/v2.0/) of NASA were also used in the form of netCDF files, coming from NASA satellite missions and algorithms(IMMERG.v6 long term mean, GPM.v5-FINAL, TRMM.v5 long term mean, and GPCP long term mean) covering the periods 2001-2019, 2018, 1998-2014, and 1997-2014 respectively. For future predictions of the index ,data came as netCDF files provided by the European Commission for Medium Weather Forecasts (ECMWF) (https://cds.climate.copernicus.eu/cdsapp#!/software/app-tourism-firedanger-indicators-projections?tab=app) for the time periods 2041-2060 and 2079-2098, for RCP's 4.5 and 8.5 corresponding to the mean and worst case respectively. Data for the composition of the Fosberg FWI were obtained by the *Hellenic National Meteorological Service (HNMS*) (http://www.emy.gr/emy/en/) for the period March-October 2019. While the index was also calculated using the CFSR dataset.

2.3 FWI calculation and structure

The FWI index is calculated on a daily basis from the values corresponding to the previous day, while Fosberg FWI was calculated by mean monthly values. The FWI was calculated through the implementation of equations derived by ('Van Wagner et al., 1987', n.d.) ,in python programming language, according to the code provided by (Wang et al., n.d.).For the calculation of the Fosberg FWI Visual Basic for Applications (VBA) programming language was used .The FWI system is comprised by 5 sub-indices, three moisture and two behavioral indices ,these are the Fine Fuel Moisture Code (FFMC) the Duff Moisture Code (DMC) and the Drought Code (DC) and two behavioral indices ,the initial spread index (ISI) and the Buildup index (BUI). The Fire Weather Index (FWI) is the end result of the FWI system which is an index with no units within the range (0, +∞) that rates the general intensity of a fire. The Daily Severity Index (DSR) is a non linear transformation of the FWI that can provide information regarding the difficulty of suppression of a wild fire ,and can be averaged over time giving the Seasonal Severity Index (SSR). Two additional indices were calculated those being Days FWI >40, and Days FWI >50, in order to track the number of days within the fire seasons (March-October) of the dataset when the FWI surpassed said values classified as very high and extreme respectively according to ECMWF. The CFSR dataset provides the option of min, max temperature of the simulated day. It is advised that the system utilizes daily temperature measured at 12 p.m. Given the absence of such measurement the max temperature of the dataset was selected to account for the loss of extreme observations. The average values of the FWI might appear low for a Mediterranean ecosystem, however they represent the five year mean situation for each pixel. After obtaining the mean values of the FWI and the rest of the indices, the output data was converted to a point shapefile containing the mean values for the indices mentioned for each of the 339 points. The Kriging method was then applied in ARCGIS to obtain thematic maps for each index using as boundaries a shapefile with Greece's geographic boundaries obtained from (https://www.diva-gis.org/).The Fosberg FWI was calculated in Visual Basic for applications using monthly mean values for the variables needed for its computation. Regarding future projections of the FWI the dataset encompasses a broad region including the European domain thus, the boundaries were specified via coordinates that more specifically capture the geographic domain of Greece. The dataset includes but is not limited to information over the number of days per pixel for each simulation period with the FWI projected to surpass the three thresholds that have been set by ECMWF, that of 15,30,45 defining three distinct fire danger classes low, medium, and high fire danger respectively for both RCPs.

3 Results

3.1 General overview

A common pattern for all datasets, can be noted in the spatial distribution of the FWI and its related codes/ indices throughout the study area. That being the concentration of high values on the hot, dry south and east for both the current and historic period. This can be traced to the influence that the Greek climate and topography exert over the index. According to (Baijnath-Rodino et al., 2020) who found similar patterns in results the southern and eastern parts of Greece tend to be the most dry and hot throughout the annual period and hence the fire season. The Fosberg FWI although not related to the calculations of the FWI presents a similar spatial distribution.

3.2 Correlation Between FWI and moisture codes

As per the CFSR dataset outputs, similarities in patterns appear between the spatial distribution of the FWI, and its sub-indices (**Figure1**) all concentrating their high values in the dry, southern and eastern part of

Greece. For both the moisture and behavior indices, higher values can be attributed to conditions of heat and drought. Despite the non-linearity of the FWI calculations, a linear regression model was opted to study the relation between the FWI and its sub-indices, due high similarity in spatial distributions. The model has been written in python programming language. Various model runs were performed, out of which one is being displayed in this study as representative. The data was empirically split using train/test analogy of 65% / 35%. Table 1 shows in greater detail the statistics regarding the 7 sub-indices of the FWI system.

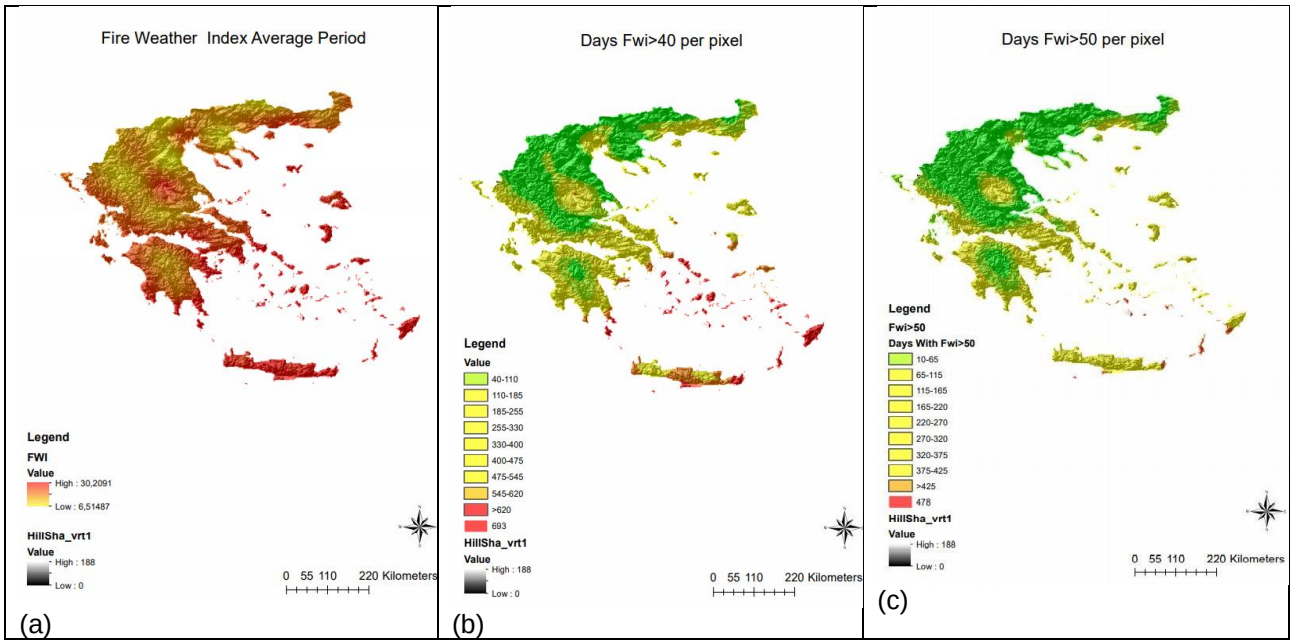

Figure 1 Thematic maps for the FWI (a) ,Days FWI > 40 (b) ,Days FWI > 50 (c) for the 2010-2014 period regarding the CSFR dataset.

The model, being a machine learning program will produce slightly different yet similar outputs each time it is run without alteration of its parameters. Most indices correlate well to the FWI, with the slight exception being the drought code (DC). Standard errors for all runs and all indices tend to be low signifying that the standard deviation of each train and test sample for every run is close to the standard deviation of the total series. The p-value also remains considerably low P>0.0001. The indices the Days FWI > 40 and Days FWI > 50 keep the best correlation coefficients R^2 for all runs, being all above 0.9. This means there exists a strong linear proportionality between mean values of the FWI and the number of days it exceeds the set thresholds of 40 and 50 for the fire-seasons of the study period. The mentioned claim can also be backed by the spatial patterns inf **Fig.1**.

Table 1. Description of statistics of the linear regression model between the FWI and its related indices (Representative Run).

Correlation to FWI	DC	DMC	FFMC	ISI	BUI	Days FWI>40	Days FWI>50
Run4							
R^2	0.632	0.81	0.943	0.964	0.817	0.983	0.954
Slope	-2.63E+01	6.33E-01	1.597	1.878	6.63E-01	3.6E-02	5.38E-02
Intercept	6.77E-01	-3.84	-8.14E+01	-3.5E-02	-5.24	6.877	8.751
p-value	6.44E-79	1.32E-129	5.45E-221	3.75E-239	2.66E-125	4.69E-303	6.05E-221
stdderr	2.71E-02	1.59 E-02	2.00E-02	2.06E-02	1.72E-02	2.54E-04	6.74E-04

4 Validation

FFWI and FWI seem to follow similar spatial distributions .Results of (Baijnath-Rodino et al., 2020) ,show the most affected areas by climate change to be located in the south and east of Greece. According to (Di Giuseppe et al., 2020) a very high number of extreme days were found for several regions mainly in the south and east of Greece, where most forest fires seem to occur.Regarding the computation of the FWI from the various NASA datasets, the latter come in accordance to the results from the CFSR dataset. Although time periods are not identical the results seem to be similar regarding average values of the index for (Table 5), as well as their spatial pattern, concetrating their higher values in the southeast of the country.

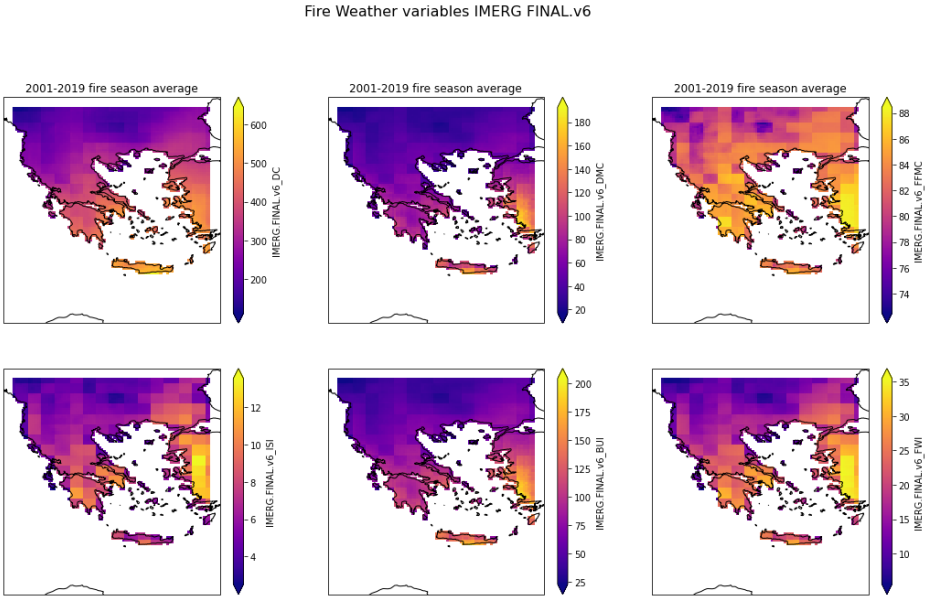

Figure 2. FWI system indices for Immerg.v6 dataset for 2001-2019 fire seasons (March-October) for a bounding box(lat=[33,43],lon=[19,28]).

Table 2. Description of statistics of FWI regarding the CFSR model and NASA datasets. Count is in points for CFSR Dataset and in pixels for NASA datasets.

FWI	Time period	Mean	Max	Std.dev	Count
CFSR	2010-2014	18.50	30.56	6.16	339
IMMERG- long term mean	2001-2019	18.38	35.44	6.67	3935
TRMM -long term mean	1998-2014	18.67	35.22	6.37	6.44
GPM - Final	2018	17.87	33.97	5.48	3425
GPCP	1997-2014	16.11	34.57	6.43	44

The CFSR dataset was also implemented for the calculation of the Fosberg FWI.Generally values from the CFSR dataset FFWI are higher than the HNMS ones derived from observed data .The mean FFWI values were 19.96 and 10.57 respectively. Differences can be attributed to different time periods of datasets ,and CFSR data being modeld outputs.The CFSR-produced FFWI seems to correlate well with the FWI. Linear regressions were performed between FWI and each monthly FFWI for the fire season as well as a multiple one including all monthly FFWI values . Most individual monthly regressions return a good score with the exception being those of August and October having an $R^2 = 0.584$ each,while the multiple linear regression returns a score $R^2 = 0.863$.

Table 3. Statistics of Individual linear regressions of fFWI-FWI for the CFSR dataset

Month	Slope	Intercept	p-value	R^2	Std.Error
Mar.	0.910	9.135	1.058E-94	0.718	0.031
Apr.	1.145	7.059	7.729E-110	0.771	0.034
May.	1.628	3.275	3.021E-123	0.809	0.043
Jun.	1.553	2.851	3.369E-129	0.824	0.039
July.	1.341	3.352	4.928E-66	0.719	0.046
Aug.	0.994	5.911	1.691E-84	0.584	0.046
Sep.	1.150	5.544	4.070E-66	0.676	0.043
Oct.	0.994	5.911	5.480E-109	0.584	0.046

5. Future projections

When it comes to future FWI projections we note increasing trends in both time periods(*2041-2060, 2079-2098*) and RCPs. Specifically the mean value for the CFSR dataset is 18.49,while mean values for the index for the RCP 4.5 are 36.94 period and 38.19 for the two periods.For the RCP 8.5 the values are 38.24 and 43.76 respectively. The max FWI for the CFSR dataset was 30.56 with the max future values being 88.55 and 89.73 for the two periods of RCP 4.5 and 91.37 and 99.84 for RCP 8.5. As per the days exceeding thresholds the numbers tend to increase for all fire danger classes low, medium , and high from the first to second period as well as from RCP 4.5 to 8.5 . The indices Days FWI > 40 and Days FWI > 50 of the CFSR dataset refer to the fire-seasons of the five year period (2010-2014) hence the number should be divided by 5 when examining the data on an annual basis. A common trend regarding the current and future projections in all periods and RCPs is the tendency of high FWI values and high numbers of threshold exceeding days to concentrate on the drier and hotter south and east of Greece. It should be highlighted here, that climate models are highly valueable tools in the domain of climate science providing useful otherwise unobtainable information. However as mentioned by (Moriondo et al., 2006) they are unavoidably accompanied by uncertainty that should be acounted for, regarding their application.

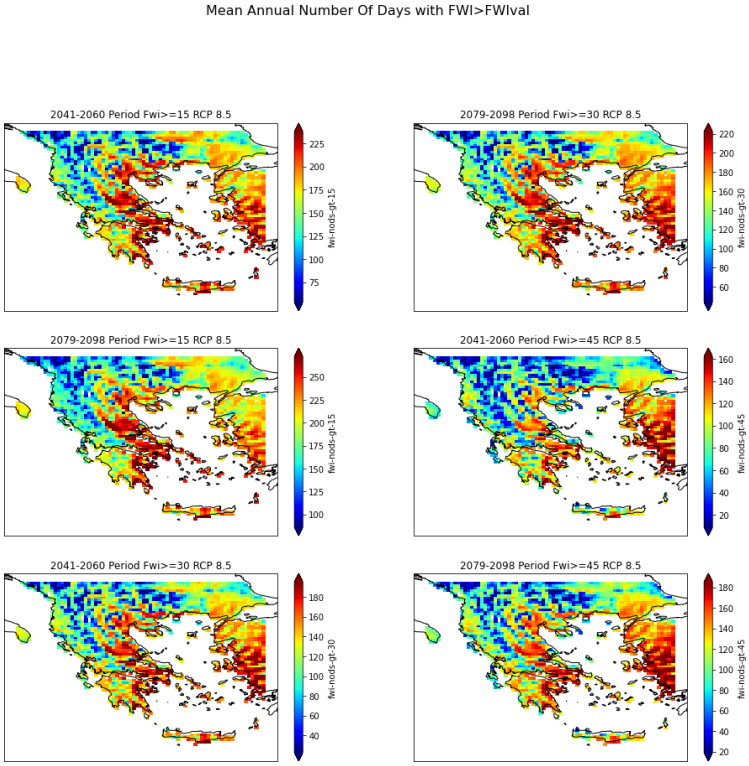

Figure 3. Graphic representation for the number of days per pixel the FWI exceeds the thresholds 15,30,45 defining the three fire danger classes as low, medium, and high for the time periods 2041-2060 as well as 2079-2098 regarding the worst case of the RCP 8.5

Table 4. FWI mean and max values for datasets and their corresponding study periods.

Dataset	Mean FWI	Max FWI	Std. dev
RCP 4.5 2041-2060	36.94	88.55	19.48
RCP 4.5 2079-2098	38.19	89.73	19.75
RCP 8.5 2041-2060	38.24	91.37	19.72
RCP 4.5 2079-2098	43.76	99.84	19.87
CFSR dataset 2010-2014	18.49	30.56	6.159

6. Conclusions

The aim of this study was to highlight the link between FWI and climate conditions - especially drought, among other factors that affect its spatial profile such as topography. Generally, the drier and hotter southern and eastern regions of Greece seem to concentrate both high values of FWI and higher numbers of fire events. The FWI alone cannot predict fire occurrence, being exclusively derived by meteorological information. It can only provide a measure assessing the favorability of weather conditions regarding fire occurrence in a region, further factors such as fuel structure ,road network characteristics,slope ,aspect and population statistics (Sakellariou et al., 2019) would need to be considered if fire occurrence preceisely was the aim of the study. The linear regression model of section 3 proved that high numbers of mean FWI signify high number of threshold exceeding days in an area. As highlighted by (Varela, 2015) areas with high number of days of extreme FWI tend to concentrate the majority of fire events. When studying the three moisture indices of the FWI system the best performing one regarding correlation is the FFMC, which rates the moisture content of

the top, fine, least compressed fuel beds of the ground that are the most flammable and according to (Moriondo et al., 2006) a non-significant increase in the FFMC can significantly contribute in the flammability of said fuel layers.

Acknowledgments: The authors acknowledge Prof. N.R. Dalezios for the encouragement for this research.

References

Baijnath-Rodino, J.; Foufoula-Georgiou, E.; Banerjee, T., 2020: *Reviewing the 'Hottest' Fire Indices Worldwide*.

Bedia, J.; Golding, N.; Casanueva, A.; Iturbide, M.; Buontempo, C.; Gutiérrez, J. M., 2018: Seasonal predictions of Fire Weather Index: Paving the way for their operational applicability in Mediterranean Europe. *Climate Services*., Climate services in practice: what we learnt from EUPORIAS, **9**, 101–110.

Cloke, H. L.; Pappenberger, F.; Smith, P. J.; Wetterhall, F., 2017: How do I know if I've improved my continental scale flood early warning system? *Environmental Research Letters*., **12**, 044006.

Di Giuseppe, F.; Vitolo, C.; Krzeminski, B.; Barnard, C.; Maciel, P.; San-Miguel, J., 2020: Fire Weather Index: the skill provided by the European Centre for Medium-Range Weather Forecasts ensemble prediction system. *Natural Hazards and Earth System Sciences*., **20**, 2365–2378.

Giannakopoulos, C.; Kostopoulou, E.; Varotsos, K. V.; Tziotziou, K.; Plitharas, A., 2011: An integrated assessment of climate change impacts for Greece in the near future. *Regional Environmental Change*., **11**, 829–843.

Howden, S. M.; Moore, J. L.; McKeon, G. M.; Carter, J. O., 2001: Global change and the mulga woodlands of southwest Queensland: greenhouse gas emissions, impacts, and adaptation. *Environment International*., **27**, 161–166.

Johnson, S. J.; Stockdale, T. N.; Ferranti, L.; Balmaseda, M. A.; Molteni, F.; Magnusson, L.; Tietsche, S.; Decremer, D.; Weisheimer, A.; Balsamo, G.; Keeley, S. P. E.; Mogensen, K.; Zuo, H.; Monge-Sanz, B. M., 2019: SEAS5: the new ECMWF seasonal forecast system. *Geoscientific Model Development*., **12**, 1087–1117.

Merrill, D. F.; Alexander, M. E., 1987: Glossary of forest fire management terms.

Moriondo, M.; Good, P.; Durao, R.; Bindi, M.; Giannakopoulos, C.; Corte-Real, J., 2006: Potential impact of climate change on fire risk in the Mediterranean area. *Climate Research*., **31**, 85–95.

Pausas, J. G.; Vallejo, V. R., 1999: The role of fire in European Mediterranean ecosystems. In: Chuvieco, E. (ed.), *Remote Sensing of Large Wildfires: in the European Mediterranean Basin*. Springer, Berlin, Heidelberg, pp. 3–16.

Sakellariou, S.; Tampekis, S.; Samara, F.; Flannigan, M.; Jaeger, D.; Christopoulou, O.; Sfougaris, A., 2019: Determination of fire risk to assist fire management for insular areas: the case of a small Greek island. *Journal of forestry research*.

Sakellariou, S.; Sfougaris, A.; Christopoulou, O.; Tampekis, S., 2022: Integrated wildfire risk assessment of natural and anthropogenic ecosystems based on simulation modeling and remotely sensed data fusion. *International Journal of Disaster Risk Reduction*., **78**, 103129.

Van Wagner et al., 1987: Development and Structure of the Canadian Forest Fire Weather Index System. — European Environment Agency, (n.d.). Methodology Reference, .

Varela, 2015: Fire Weather Index (FWI) classification for fire danger assessment applied in Greece. *Tethys, Journal of Weather and Climate of the Western Mediterrania*.

Wang, Y.; Anderson, K. R.; Suddaby, R. M., (n.d.) Updated source code for calculating fire danger indices in the canadian forest fire weather index system, 36.

Weber, M. G.; Flannigan, M. D., 1997: Canadian boreal forest ecosystem structure and function in a changing climate: impact on fire regimes. *Environmental Reviews*., **5**, 145–166.

An integrated hydrologic/hydrodynamic analysis of the Medicane "Ianos" flood event in Pamisos river basin, Greece

Vasiliades L.[1], P. Sidiropoulos[1] and N. Mylopoulos[1]

[1] Department of Civil Engineering, University of Thessaly, Volos, Greece

Abstract. On 18th September 2020 Medicane "Ianos" caused significant floods and structural damages on Pamisos river basin, Greece. This flood event is analysed and modelled using an integrated hydrologic/hydrodynamic modelling framework in order to estimate the flood hydrograph and the flood extent in the broader Mouzaki region. Extreme precipitation with high intensity rates were measured in 24-hour rain duration at five (5) selected meteorological stations in the wider study area, with estimated return periods of larger than 1000 years for the mountainous areas and 200 years for the plain regions, respectively. Areal precipitation is estimated at 15-min time intervals at subwatershed level and with the use of HEC-HMS software and the Natural Resources Conservation Service (NRCS) Unit Hydrograph method simulated flood hydrographs at important junctions are estimated and applied in HEC-RAS 2D model for flood routing and estimation of flood attributes (i.e., water depths and flow velocities), as well as mapping of inundated areas. The simulated flood extent closely matches the observed flooded region calculated from Sentinel images by the Copernicus Emergency Management Service. As a result, the modelling approach of this study may be developed into a methodological framework to assist flood hazard mitigation programmes in the region.

1 Introduction

Hydrometeorological hazards such as storms and floods are extreme hydrological phenomena mainly caused by meteorological anomalies and modified/intensified by catchment processes and human activities. Climate change and variability is producing significant alterations in hydrological dynamics, with a general tendency to intensify hydrological extremes (AghaKouchak et al., 2013). Therefore, the physical dependencies between global (climatic) and local (hydrologic) processes should be analyzed to better understand the key factors controlling changes and future scenarios.

Mediterranean Tropical Like Cyclones (TLC) known as Medicanes are accompanied by strong winds, heavy precipitation and thunderstorms, causing occasional severe damages in private property, agriculture and communication networks, or resulting in flooding of populated areas, posing a risk to human life (Nastos et al., 2018). Furthermore, there is a rising global awareness for flood impacts mitigation due to the increase in frequency, magnitude, and intensity of medicanes in the near future (González-Alemán et al., 2019). Hence, for accurate assessment and management of flood hazard, the hazard inundation identification, modelling and mapping and the associated risk evaluation should be applied using suitable and effective deterministic and/or probabilistic hydrologic/hydraulic approaches (Teng et al., 2017).

Flood hazard analyses provide an estimation of the extent and intensity of extreme scenarios and associate an exceedance probability to it. A common feature in all hazard loss models is the direct monetary hazard loss which is a function of the type or use of the building and the inundation depth. Such depth-damage functions are seen as the essential building blocks upon which hazard loss analyses are based, and they are internationally accepted as the standard approach to assessing urban loss (Merz et al., 2010; Smith, 1994). However, this type of curve should be derived specifically for the location in which it will be applied. There is a high possibility of error which somehow should be accounted for. Moreover, damage/losses cannot be uniquely related to the highest simulated inundation depth at each cell from a certain extreme episode. The damage/losses could be influenced by other hydraulic parameters, such as water velocity and inundation time which should be taken into account (Aronica et al., 2012). The objective of this study is to model and reconstruct the flood event caused by Medicane “Ianos” in Pamisos River basin (with toral basin area of 248 km^2), central Greece, using a CN-based unit hydrograph rainfall-runoff model and a 2D hydraulic/hydrodynamic model for flood routing and hazard mapping.

2 Study Area and Methodology

Medicane “Ianos” impacted Thessaly and had caused significant structural damages, and flash flood related impacts that resulted in four fatalities and extended infrastructure damages and landslides especially in the Prefecture of Karditsa (Lagouvardos et al., 2021). Extreme mountainous precipitation in terms of intensity and duration resulted in torrential flooding with subsequent landslides and debris flows and high structural damages on buildings, transportation infrastructure, and powerlines. In the low-relied areas of the Thessaly Plain, large scale flooding with the inundation of over 400 km^2 of agricultural and urban land caused widespread disruptions

to communities and severe impact on the economic activity, especially in the city of Karditsa (Zekkos and Zalachoris, 2020). Figure 1 shows the damage caused in the wider area and specifically in the road network (43 points mainly in the mountainous areas), in the hydrographic network (14 points in the lowland areas). Figure 1 also shows the flood overflow points (4 points) in the city of Karditsa.

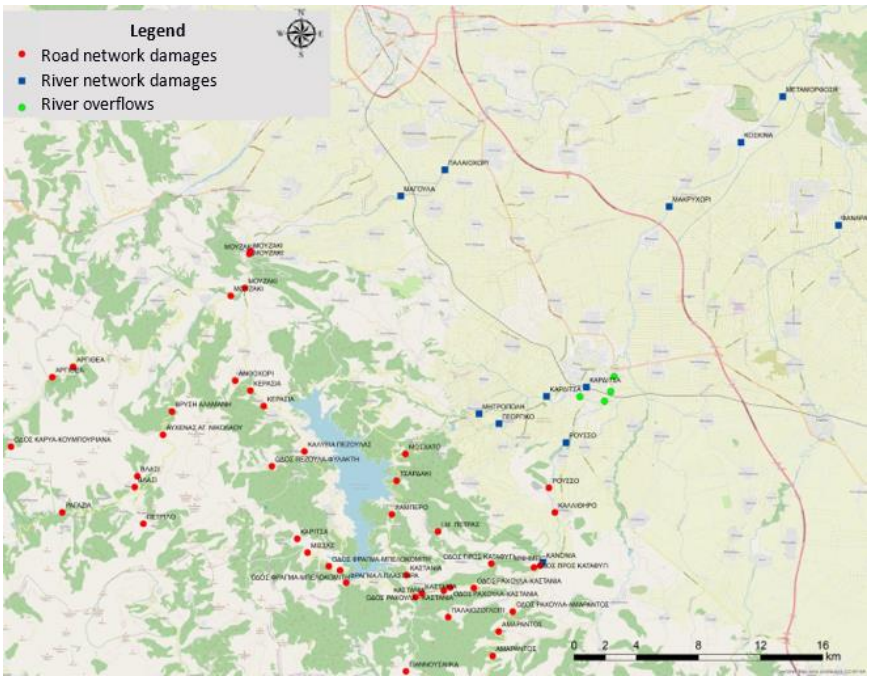

Figure 1. Damage points caused by Medicane "Ianos" in the Prefecture of Karditsa, Greece.

The hydrological approach is based on semi-distributed modelling of the rainfall-runoff process (at sub-watershed scale) using the HEC-HMS software and the SCS-CN method for estimating rainfall excess, as well as the unit hydrograph theory for propagating the surface runoff to the subbasin outlets. In this study, the estimation of the concentration time (t_c) of the watershed was based on the empirical approach of Giandotti formula. Moreover, to take account of the dependence of the response time of the basin against runoff, the kinematic wave theory-based semi-empirical formula was employed, considering that t_c is inversely proportional to the areal rainfall, $t_c(T) = t_c \sqrt{\frac{i(5)}{i(T)}}$ where $i(5)$ is the design rainfall intensity for return period T=5 years, for which the time of concentration is estimated by the Giandotti formula, and $i(T)$ is the calculated intensity of the Ianos return period, T (estimated from the Greek Intensity-Duration-Frequency IDF or ombrian curves). The spatially-averaged per subwatershed Curve Number (CN) parameter is estimated on the basis of distributed soil and land cover information, following the typical classification by NRCS, by means of detailed lookup tables for average antecedent soil moisture conditions (AMC II). The transformation of the excess rainfall over each sub-basin to flood hydrograph at the outlet junction (rainfall-runoff model) was achieved using the dimensionless curvilinear unit hydrograph approach of SCS, which is considered the prevailing modeling approach for ungauged basins. A key assumption of the method was the implementation of the concept of varying (i.e., runoff-dependent) time of concentration, which affects the shape of unit hydrographs, thus introducing further nonlinearities to overall modeling approach. Further details of the methodology could be found in Vasiliades and Mylopoulos, 2021.

The two dimensional (2D) HEC-RAS hydraulic-hydrodynamic model, developed by the Hydrologic Engineering Center (HEC) of United States Army Corps of Engineers, has been selected for flood inundation and mapping. The HEC-RAS model uses the sub-grid bathymetry approach that adopts a relatively coarse computational grid and information underlying the topography at a finer scale. The sub-grid bathymetry equations are derived from the full shallow water equations. Fundamental elements for an accurate flood inundation modeling and mapping, are the digital elevation model (DEM), the stream channel geometry (river flowpaths, banks, etc.), the hydraulic model configuration (i.e., initial and boundary conditions, roughness coefficients, technical works), and the representation of urban areas by considering the effect of the building blocks to the water flow. In this study, the flood hydrographs derived from the hydrological model were used as input hydrographs in the 2D HEC-RAS hydraulic–hydrodynamic model for flood inundation modelling and mapping. The DEM,

provided by the Greek National Cadastre and Mapping Agency S.A. (NCMA) with a resolution of 5 m, was used for flood modelling and mapping results and all examined reaches were modelled with flexible mesh sizes (ranging from 12.9 to 510 m^2), roughness coefficient values based on CORINE land cover data and a computation interval of 2.0 s. All hydrotechnical works (e.g., flood protection works, culverts, bridges, weirs) within the river and the adjacent areas were based on previous studies at the study area (Papaioannou et al., 2021).

3 Application of the Methodology - Results

A combined hydrological and hydraulic–hydrodynamic modelling approach is applied for flood inundation modelling and mapping at Kalentzis ungauged watershed. Figure 2 shows the study area with the important hydrographic network and with the selected discretization modelling scheme that include nine (9) subwatersheds, five (5) reaches and six (6) junctions. Pamisos river basin contains several hydraulic structures and flood protection works and downstream of the output junction J1 is merged with Pinior river.

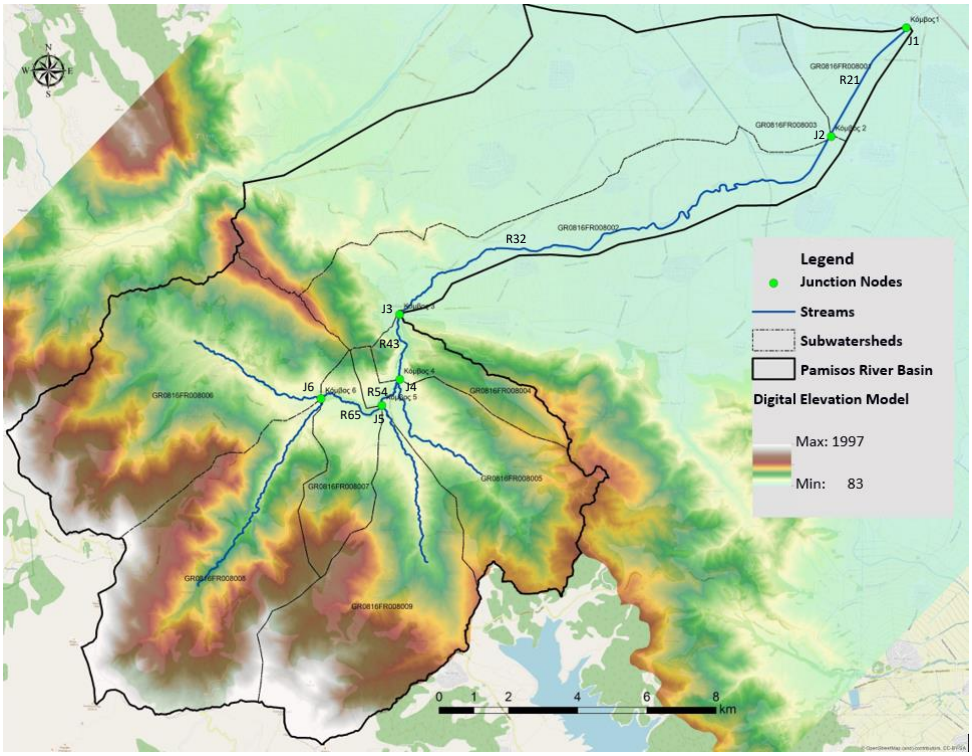

Figure 2. Pamisos River basin with the employed modelling components (selected sub-watersheds, stream reaches, junctions for flood inundation modelling and mapping).

Rainfall data of five meteorological stations (namely Argithea, Vrontero, Drakotrypa, Karditsa and Plastiras Dam) in the wider area at 15-min intervals are used to represent the spatiotemporal rainfall distribution of "Ianos" event and to estimate areal rainfall at subwatershed level. Areal rainfall at the subwatershed centroid was estimated using inverse distance square weighting and adjusted to the mean elevation of the subwatershed with the developed precipitation gradient. It should be noted that the observed extreme rainfall in the study rainfall stations had estimated return periods (estimated using the Greek IDF curves) for rain duration of 24 and 48 hours larger than 1000 for the mountainous and 200 years for the low elevation stations, respectively. Figure 3 shows areal rainfall timeseries estimated in two characteristic subwatersehds for the period 17-9-2020 until 20-9-2020 with a time interval of 15 min.

The application of the semi-distributed hydrological modelling procedure in Pamisos river basin led in the estimation of hydrographs at the junctions used for the hydrologic and hydrodynamic simulation of "Ianos" flood event for the period 17-9-2020 until 20-9-2020. For example, Figure 4 shows the estimated hydrographs at Pamisos river for one mountainous subwatershed GR0816FR008009 and the hydrograph hydrologic flood routing of the stream reach R32.

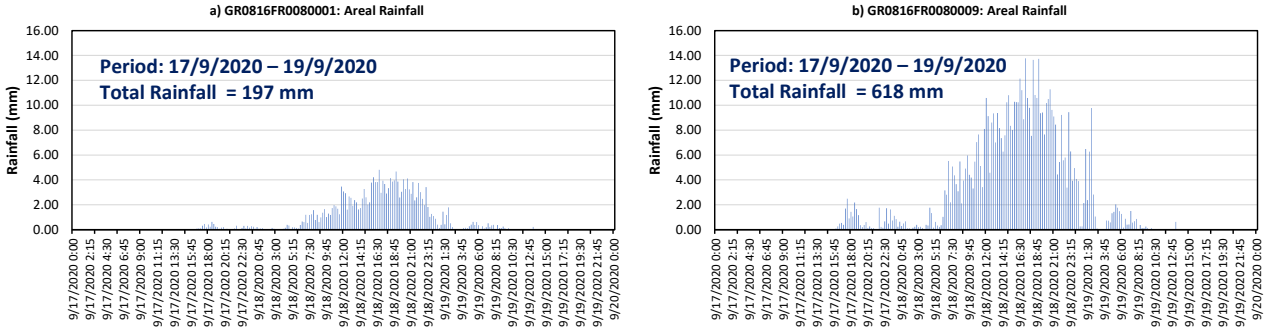

Figure 3. Estimated areal rainfall timeseries in a) plain GR0816FR008001 subwatershed and b) mountainous GR0816FR008009 subwatershed.

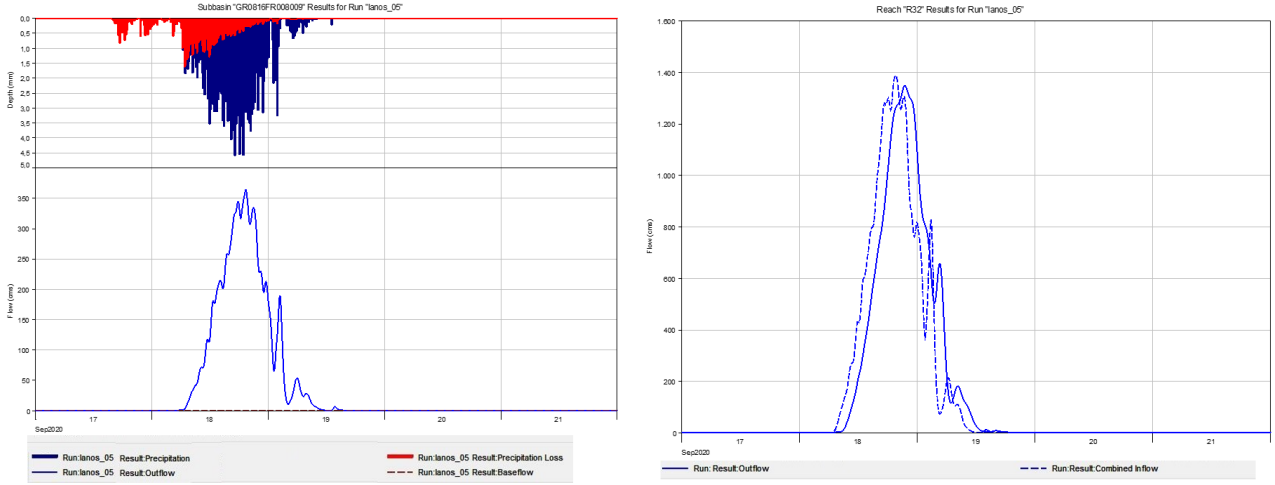

Figure 4. Simulated hydrographs in the mountainous subwatershed GR0816FR008009 and the stream reach R32.

Conventional and non-conventional flood data and impact records of the extreme flash-flood event that occurred on 18th September 2020 were used for the comparison of the simulated flood extent of the "Ianos" Medicane in the greater area of Karditsa Perferture. Figure 5 illustrates the water depths and the estimated flood extent resulted from the rainfall-runoff and the hydrodynamic flood routing modelling processes for the Sunday 20-09-2020 and greek local time 12:00. It is interesting to note that the simulated flood extent of Figure 5 (estimated about 69 km^2) is in close agreement with the observed flooded area estimated from Sentinel images by the Copernicus Emergency Management Service (EMSR465: Floods in Thessaly Region, Greece) at the study area.

Table 2. Combined flood hazard curves - vulnerability thresholds classification limits (based on Smith et al., 2014) of Medicane "Ianos".

Flood Hazard Vulnerability Classification	Classification Limit (D and V in combination)	Limiting Still Water Depth (D)	Limiting Velocity (V)	Flooded Area (km^2)
H1 = generally safe for vehicles, people and buildings	D * V ≤ 0.3	D ≤ 0.3	V ≤ 2.0	79.05
H2 = unsafe for small vehicles	D * V ≤ 0.6	D ≤ 0.5	V ≤ 2.0	1.47
H3 = unsafe for vehicles, children and the elderly	D * V ≤ 0.6	D ≤ 1.2	V ≤ 2.0	17.37
H4 = unsafe for vehicles and people	D * V ≤ 1.0	D ≤ 2.0	V ≤ 2.0	7.94
H5 = unsafe for vehicles and people. All buildings vulnerable to structural damage. Some less robust buildings subject to failure	D * V ≤ 4.0	D ≤ 4.0	V ≤ 4.0	2.73
H6 = Unsafe for vehicles and people. All building types considered vulnerable to failure	D * V> 4.0	-	-	1.09

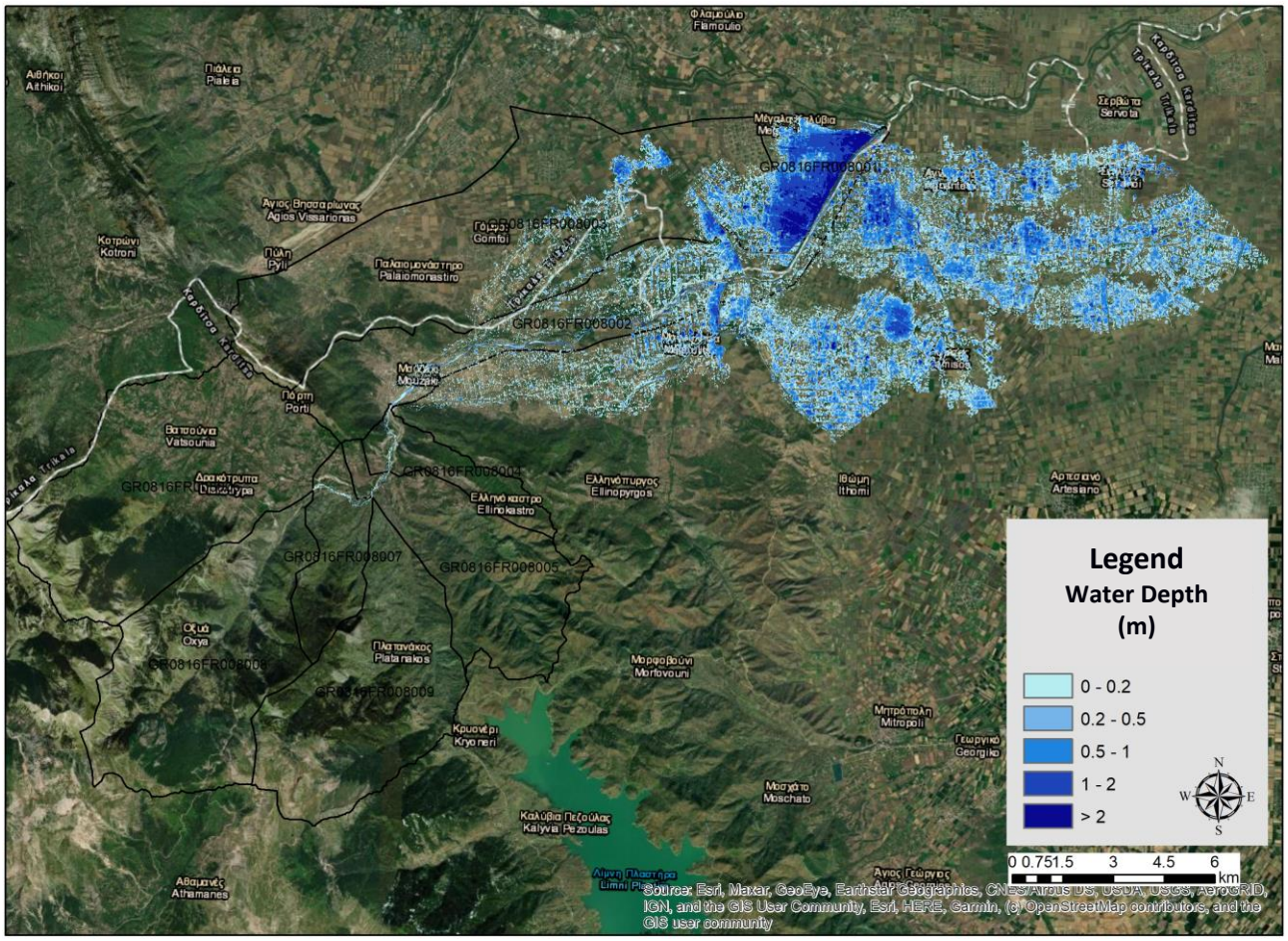

Figure 5. Simulated flood extent and water depths in Pamisos River basin for Sunday 20-09-2020 12:00 Greek local time.

The base data that underpins assessment of floodplain risk typically comprises the flow characteristics (the flow depth and velocity) in the flood-affected areas of Pamisos river basin. Flood hazard is estimated in this study using the DV criterion (DV = Maximum Water Depth * Maximum Water Velocity), which incorporates people, vehicle and structural (building) stability criteria in the resistance/resilience of the above categories on floods (Smith et al., 2014). Table 1 presents the flood hazard assessment categories of the DV criterion (Figure 6) and the flood hazard area per category caused by the Medicane “Ianos” in Pamisos river basin.

4 Summary

The flood event that occurred on 18th September 2020 in Pamisos river basin due to the Medicane “Ianos”, was reproduced using an integrated hydrologic/hydrodynamic modelling framework. Using the HEC-HMS software and the Natural Resources Conservation Service (NRCS) Unit Hydrograph procedure in semi-distributed mode (at subwatershed level) simulated flood hydrographs at important tributaries junctions were estimated and applied in HEC-RAS 2D model for flood routing and estimation of flood attributes (i.e., water depths and flow velocities), as well as mapping of inundated areas. The characteristics of the flood (depth and velocity of the simulated flood wave) were combined to estimate flood hazard using the DV criterion and finally the damage caused by Medicane "Ianos" was evaluated. Simulated flood extent is in close agreement with the observed flooded area estimated from Sentinel images by the Copernicus Emergency Management Service. As a result, the modelling approach of this study may be developed into a methodological framework to assist flood hazard mitigation programmes in the region.

Acknowledgements

Rainfall data for Argithea, Drakotrypa, Pastiras Dam, Vrontero meteorological stations were provided by the Greek Public Power Corporation and Meteoclub Network supplied the data for Karditsa meteorological station.

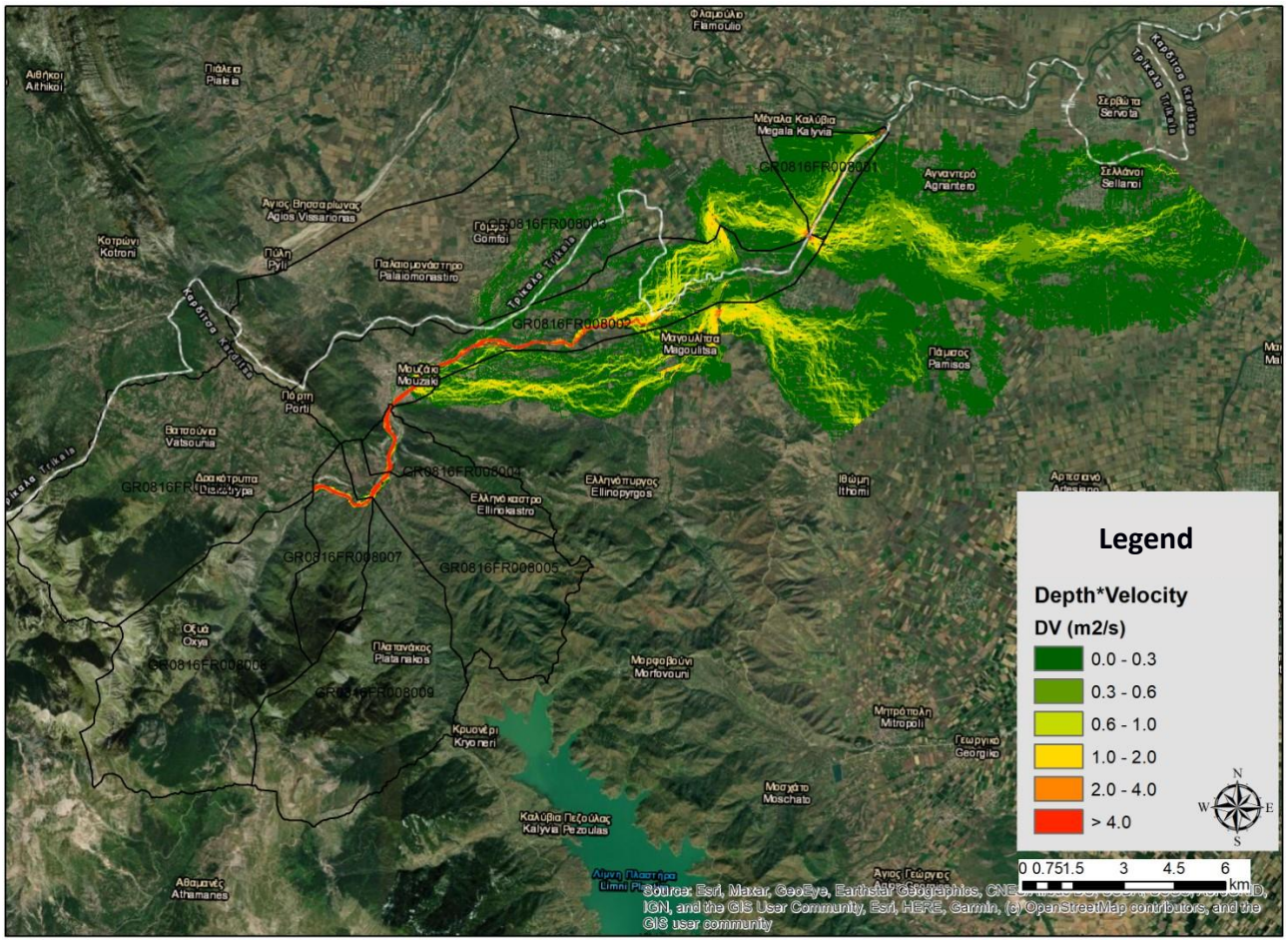

Figure 6. Flood hazard mapping caused by Medicane “Ianos” in Pamisos River basin using the DV criterion.

References

AghaKouchak, A., Easterling, D., Hsu, K., Schubert, S., Sorooshian, S. (Eds.), 2013. Extremes in a Changing Climate, Water Science and Technology Library. Springer Netherlands, Dordrecht. https://doi.org/10.1007/978-94-007-4479-0

Aronica, G.T., Candela, A., Fabio, P., Santoro, M., 2012. Estimation of flood inundation probabilities using global hazard indexes based on hydrodynamic variables. Physics and Chemistry of the Earth, Parts A/B/C 42–44, 119–129. https://doi.org/10.1016/j.pce.2011.04.001

González-Alemán, J.J., Pascale, S., Gutierrez-Fernandez, J., Murakami, H., Gaertner, M.A., Vecchi, G.A., 2019. Potential Increase in Hazard From Mediterranean Hurricane Activity With Global Warming. Geophys. Res. Lett. 46, 1754–1764. https://doi.org/10.1029/2018GL081253

Lagouvardos, K., Karagiannidis, A., Dafis, S., Kalimeris, A., Kotroni, V., 2021. Ianos - A hurricane in the Mediterranean. Bulletin of the American Meteorological Society 1–31. https://doi.org/10.1175/BAMS-D-20-0274.1

Merz, B., Kreibich, H., Schwarze, R., Thieken, A., 2010. Review article "Assessment of economic flood damage". Nat. Hazards Earth Syst. Sci. 10, 1697–1724. https://doi.org/10.5194/nhess-10-1697-2010

Nastos, P.T., Karavana Papadimou, K., Matsangouras, I.T., 2018. Mediterranean tropical-like cyclones: Impacts and composite daily means and anomalies of synoptic patterns. Atmospheric Research 208, 156–166. https://doi.org/10.1016/j.atmosres.2017.10.023

Papaioannou, G., Vasiliades, L., Loukas, A., Alamanos, A., Efstratiadis, A., Koukouvinos, A., Tsoukalas, I., Kossieris, P., 2021. A Flood Inundation Modeling Approach for Urban and Rural Areas in Lake and Large-Scale River Basins. Water 13, 1264. https://doi.org/10.3390/w13091264

Smith, D.I., 1994. Flood damage estimation - A review of urban stage-damage curves and loss functions. Water SA 20, 231–238.

Smith, G.P., Davey, E.K., Cox, R.J., 2014. Flood Hazard. UNSW Australia Water Research Laboratory Technical Report 2014/07.

Teng, J., Jakeman, A.J., Vaze, J., Croke, B.F.W., Dutta, D., Kim, S., 2017. Flood inundation modelling: A review of methods, recent advances and uncertainty analysis. Environmental Modelling & Software 90, 201–216. https://doi.org/10.1016/j.envsoft.2017.01.006

Vasiliades, L., Mylopoulos, N., 2021. Expert Report for the 18th September 2020 Flood Event in the wider area of Argithea and Mouzaki Municipalities. Directorate of the Fire Service of Karditsa, Mouzaki, March 2021 (in Greek).

Zekkos, D., Zalachoris, G., 2020. The September 18-20 2020 Medicane Ianos Impact on Greece Phase I Reconnaissance Report Geotechnical Extreme Events Reconnaissance Association. https://doi.org/10.18118/G6MT1T

Evaluation of the performance of agrometeorological indicators in lead times of weather forecasts

Eitzinger J.[1], S.Thaler [1,2], G. Kubu [1], A. Manschadi [1], M. Palka [1] and S. Schneider[3]

[1] University of Natural Resources and Life Sciences (BOKU), Vienna, Austria
[2] CzechGlobe – Global Change Research Institute CAS, Brno, Czech Republic
[3] Zentralanstalt für Meteorologie und Geodynamik (ZAMG), Vienna, Austria

Abstract. Within the ACRP project AgroForeCast (AGROmeteorological FORECAST for improving resilience and sustainability of Austrian farming systems under changing climate), the application potential for short-term to seasonal forecasting and adaptation of relevant information for decision support was analysed. The accuracy of weather forecast based impacts (i.e. the overall level of agreement between forecasts and observations) is crucially important for building trusted relationships between providers of climate related risk information and farmers. With the help of the GIS (Geographical Information System)-based tool ARIS (Agricultural Risk Information System), various agroclimatic indicators can be calculated for the Austrian agricultural area at a 1 km grid scale, which can be used to monitor or forecast the impact of adverse weather conditions on crops. Our study presents results of the forecasting performance of selected agroclimatic risk indicators, such as yield depletion through drought and heat stress for three main arable crops, the grapevine related HUGLIN Index and pest risk of two varieties of grape berry moth for various sites over Austria. For all presented indicators it was shown that in general the forecast performance will mainly increase the less the future prediction target is away from the forecast start. However, also long-term predictions can perform in some years and sites better than updated forecasts with lower lead time.

1 Introduction

Rising demands for sufficient, safe, and nutritious food, environmental concerns, volatile agricultural prices, and diminishing profit margins for farmers are among the major challenges facing farming systems today. At the same time, the productivity and resilience of cropping systems is progressively being limited by climate change and increased climate variability (Lobell et al., 2015; Trnka et al., 2011; Eitzinger et al., 2013; IPCC 2014). Farmers must routinely make a range of critical decisions, both prior to and during the crop growing season, that strongly interact with current and seasonal weather conditions.

Using meteorological forecasting products of different time ranges to develop flexible, proactive strategies for managing climate variability and extreme weather events (e.g. frost, hail, water and heat stresses, pest prediction etc.) is considered as one of the most significant measures to improve the resilience of farming systems to climate change and increased climate variability (Hansen, 2005; Meza et al., 2008; Lalic et al. 2016, 2017). Considering these challenges, within the ACRP project AGROFORECAST (AGROmeteorological FORECAST for improving resilience and sustainability of Austrian farming systems under changing climate), the application potential for short-term to seasonal forecasting and adaptation of relevant information for decision support for Austrian conditions is analysed. The accuracy of weather forecast based impacts (i.e. the overall level of agreement between forecasts and observations) is crucially important for building trusted relationships between providers of climate related risk information and farmers.

With the help of the GIS (Geographical Information System)-based tool ARIS (Agricultural Risk Information System), various agro-climatic indicators can be calculated for the Austrian agricultural area at a 1 km grid scale, which can be used to monitor or forecast (using weather forecast products) the impact of adverse weather conditions on crops. Various abiotic and biotic risks are estimated for different main crops, including quantitative and qualitative assessments of the occurrence, severity of various types of weather-related impacts. This paper presents results of the forecasting performance of selected agro-climatic risk indicators, such as yield depletion through drought and heat stress for three main arable crops, the grapevine related HUGLIN Index and pest risk of two varieties of grape berry moth for various sites over Austria.

2 Material and Methods

2.1 ARIS Model input data

The weather data input into ARIS concerned INCA grid data (observed weather conditions) as well as forecasts of 10-days and 7-months global forecasts scaled down to 1km and comprising 16 ensemble members. The latest ECMWF long-range ensemble forecast system 5 (SEAS5, in operation since November 2017) with forecasts up to 7 months was used as meteorological input in combination with ECMWF medium-range forecasts (10 days). The study period was set from 2018 to 2022 and the various weather forecast data in ARIS were used for the evaluation in addition to the observed INCA data. Spatial downscaling methods were applied to the forecasts during the harvest season (spring, summer, and autumn) and included downscaled 10-day ECMWF data as well as downscaled 7-month seasonal forecasts of temperature (min, max), precipitation and global radiation on a daily basis with a resolution of 1x1 km.
For calculation of soil-crop water balance based on the FAO56 method (Allen et al., 1998) and soil water depletion as a drought stress factor ARIS is using available soil water holding capacity up to 1m soil depth developed from the Austrian electronic soil map (e-bod; https://bodenkarte.at/). For crop drought stress detection and related yield reduction in ARIS the main rooting zone of 0-40 cm is considered. The selected abiotic and biotic risks the different crops were simulated for 32 locations in Austria (Fig. 1) for the evaluation of the seasonal forecast performance (in comparison with INCA weather data input).

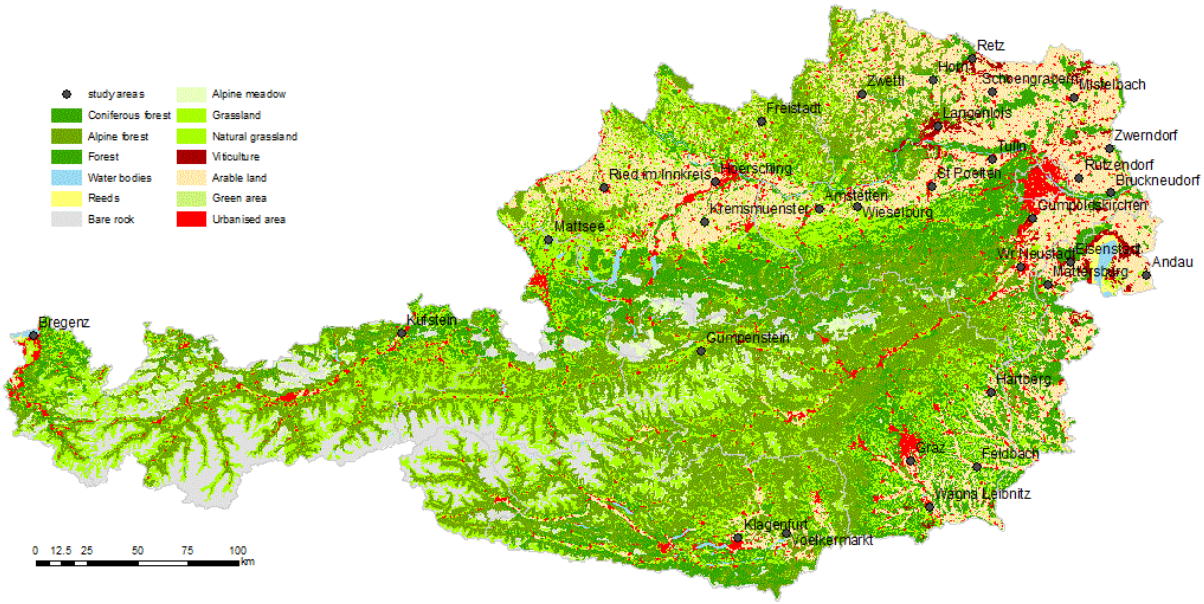

Figure 1. Land use types (CORINE 20212) and selected sites in Austria for the statistical evaluation of agrometeorological risk indicators based on weather forecasts.

2.2 Selected indicators

The HUGLIN index (Huglin, 1978) calculates the temperature sum (T_{max} and T_{mean}) above the temperature threshold of 10°C for vineyards during the growing period from the beginning of April to the end of September. The index value over one growing season can be used as a suitability criteria of various grapevine cultivars and type of wine quality.
The second indicator, the relative yield reduction factor, is an empirically based linear potential yield depression from optimum yield due to combined accumulated drought and heat stress during the crop growing season. It is calculated from the beginning of the crop specific growing season to maturity/harvest dates for winter wheat, spring barley and maize.
The third indicator is the first occurrence (by DOY) of European grapevine moth (Lobesia botrana) and the European grape berry moth (Eupoecelia ambiguella). Itis calculated by an empirical linear model based on mean daily temperatures, days < 11°C, days with precipitation and precipitation sum from January till May (Bluemel et al., 2020).

3 Results

The results of the HUGLIN Index seasonal forecast performance are shown in Fig. 2. The observed (red line) and predicted (blue line = mean value, grey area = max and min values of the 16-members ensemble) HUGLIN Index simulations for the years 2018 and 2019 at the Austrian vineyard site Retz (north-east of Austria). Seasonal forecasts starting from February to July, respectively, are displayed. In 2018, the HUGLIN Index was underestimated by the forecasts starting in February, March and April. The approximations with the observed values fit well from seasonal forecasts starting with May onwards. In 2019, deviations were smaller compared to the previous year; again, simulated values become more accurate from May onwards.

a) 2018

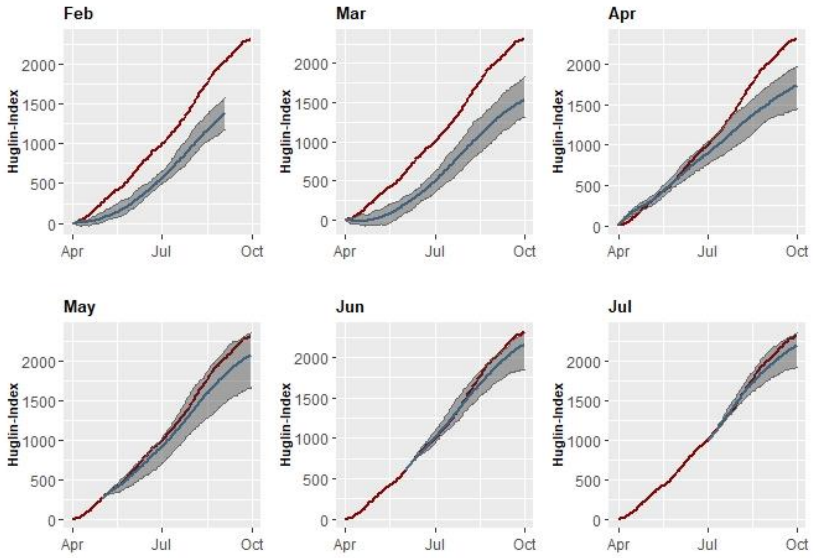

b) 2019

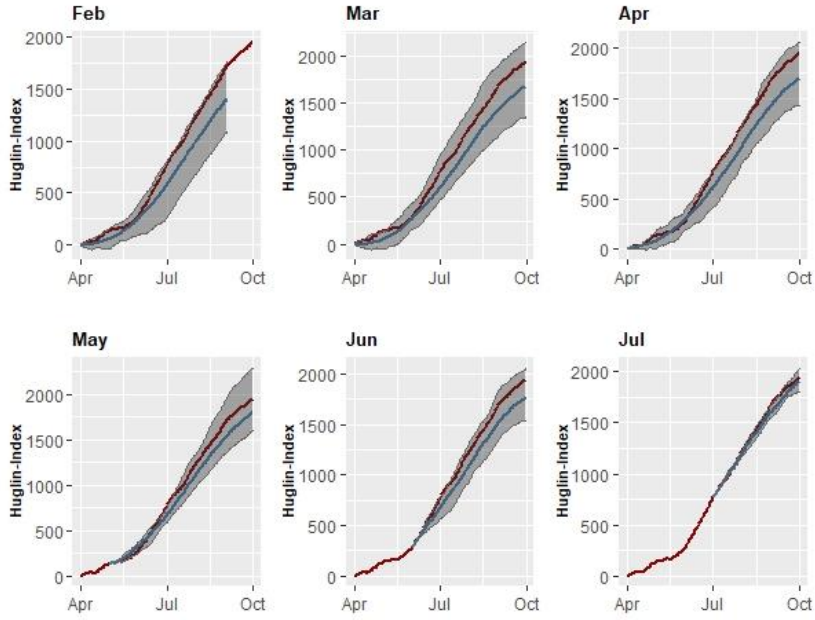

Figure 2a-b. HUGLIN Index for the years 2018 (a) and 2019 (b) at site Retz: observed weather data based simulation (red line) vs. weather forecast based simulations (blue line = mean value, grey areas mark max and min values of the ensemble); seasonal forecast from February, March, April, May, June and July.

Based on drought and heat stress level, the relative yield reduction factor is presented for different sites and crops (maize, winter wheat, spring barley) for the years 2020 and 2021 (Fig 3).

Opposed to the HUGLIN Index, precipitation is also taken into account together with temperature for calculating yield reduction through the considered soil water depletion. The results indicate that depending on the crop, region and time, variations in weather input data have different effects on yield reduction. For maize, site Hoersching (north-west of Austria, cool-humid climate) shows good maize yield forecast results in both years, while at site Hartberg (south-east of Austria, warm-humid climate) deviations are large, especially in 2021. For maize the variation within the ensemble members is significantly higher than for winter wheat and spring barley. For winter wheat, Rutzendorf (north-east of Austria, warm-dry climate) showed smaller deviations of the simulated forecasted yield reduction in comparison to simulated yield depletion by observed weather data in 2020, while modelled forecasts for Kufstein (west of Austria, humid climate) were more accurate in 2021. In 2020, Andau (east of Austria, warm-dry climate) and Voelkermarkt (south of Austria, warm moderate humid climate) displayed minor deviations of the simulations (forecast vs. observed weather data) for spring barley yield reduction, which were however considerably higher in 2021.

a) Maize yield depletion (relative)

2020

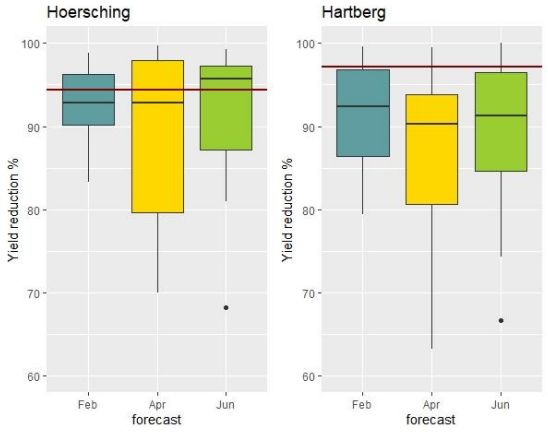

2021

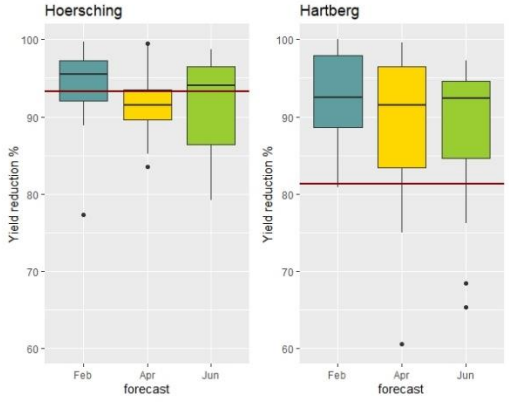

b) Spring barley yield depletion (relative)

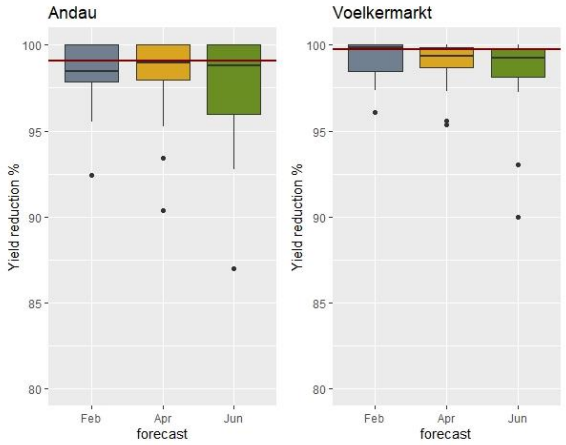

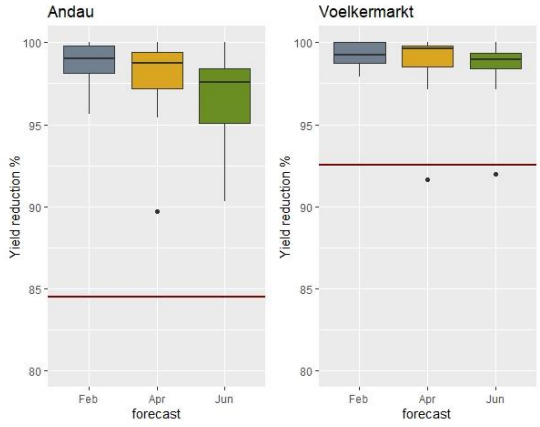

c) Winter wheat yield depletion (relative)

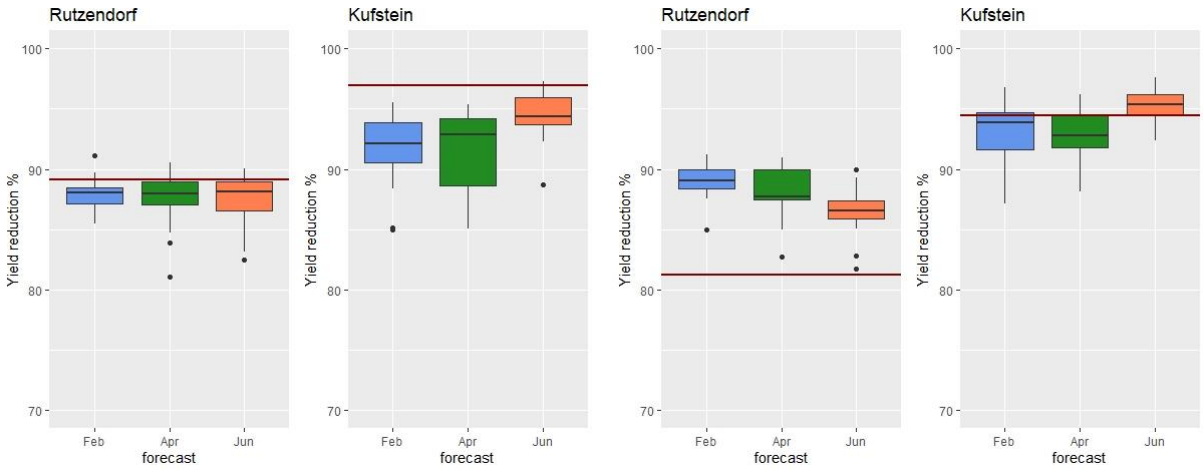

Figure 3a-c. Yield reduction for the years 2020 and 2021 in Hoersching and Hartberg (maize, a), Andau and Voelkermarkt (spring barley, b), Rutzendorf and Kufstein (winter wheat, c): observed weather data based simulation (red line), weather forecast based simulation (boxplots) from the 16-member ensemble forecasts February, April and June.

The pest occurrence prediction for grape berry moth show similar results for both varieties (Fig. 4a-b) as the driving forces of its phenological model are similar, with temperature as the main factor. The performance of the different seasonal weather forecasts start (February, March, April, May) is quite different between the 4 prediction years, where 2018 and 2021 had the highest deviations to the observed weather based simulation. For example, in 2021 (cool, but dry spring season) the early seasonal weather forecasts predicted warmer temperatures than observed ones leading to a high deviation of predicted first occurrence of about 10 days (in context, 2 days deviation is acceptable for pest warning). With some exception the April and May start of the seasonal forecast performed better than the earlier forecast starting dates and in years 2019 and 2020 all forecast starting dates performed relatively well. These deviations can be clearly related to the performance of seasonal weather forecasts.

a)

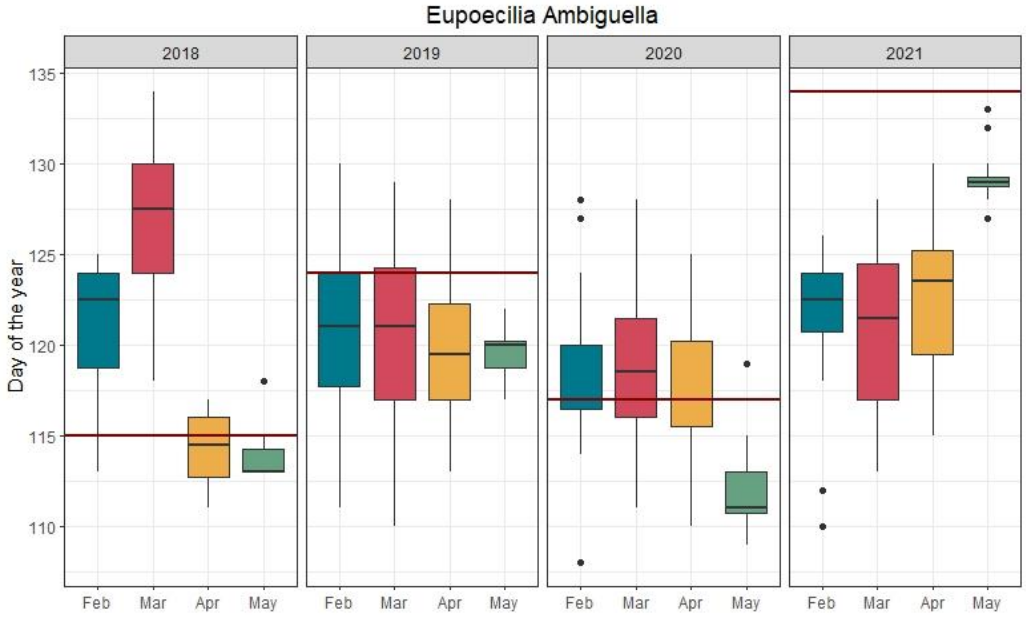

b)

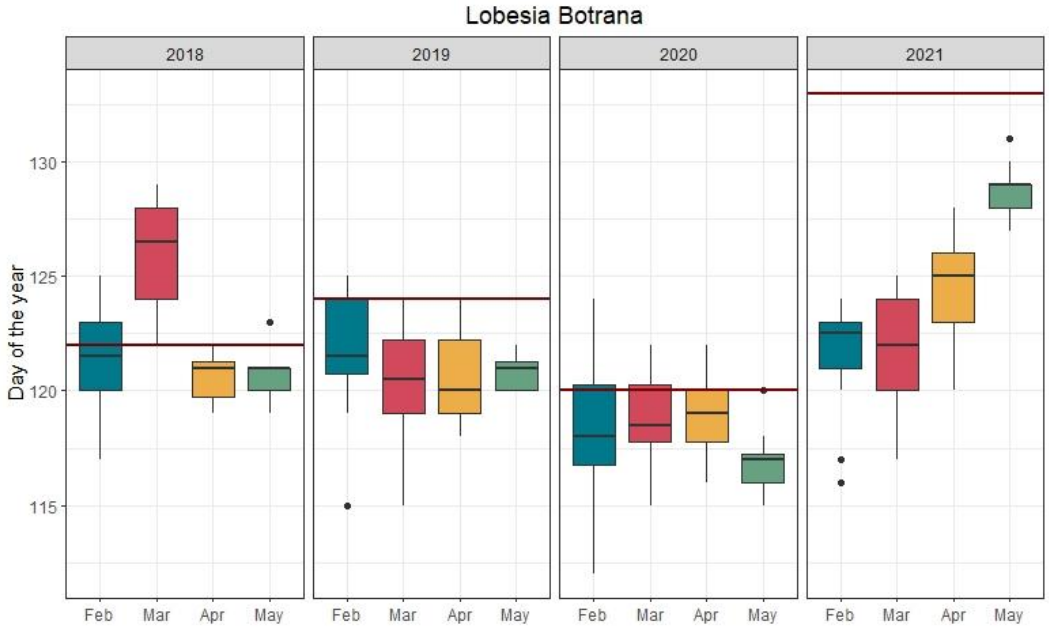

Figure 4a-b. Grape berry moths (L. Botrana (a) and E. Ambiguella (b)) first occurrence of adults at site Retz over 2018-2021. Observed weather data based simulation (red line) vs. weather forecast based simulation (boxplots) from the 16-members ensemble forecasts February, March, April and May.

4 Discussion and Conclusions

Within our study we tested the performance, sensitivity, and uncertainty of different agro-meteorological indicators for selected Austrian cropping sites using seasonal weather forecasts of different ranges as input for the ARIS.

For strongly temperature depending indices such accumulating temperature index (HUGLIN Index, Fig. 2) as well as thermophile insect pest development (grape berry moth, Fig. 4) it seems that prediction quality (accuracy and uncertainty within the ensemble members) is systematically increasing (with few exceptions) with reduced forecasting lead times.

Indicators where additionally precipitation is a forcing factor show a more mixed behaviour. Depending on the crop type, the performance of the yield risk indicator showed different performance in the various years as well as at sites. First results suggest that there is a higher uncertainty of yield predictions for summer crops such as maize, compared to winter crops (winter wheat) or spring crops with short growing season (spring barley). Remarkably, in our selected cases it seems that also long lead time (e.g. start with February forecast) can perform in some years very well, in other years not, which can be explained by probably sudden change of weather pattern during the crops growing season (e.g. spring barley and wheat in 2021, where a wet July/August followed by an extremely dry spring, affecting spring barley more than winter wheat). In regard to the underlying algorithm for yield reduction, which is based on regional calibration to drought and heat effect, further uncertainties are involved by an “averaged” impact of drought and heat stress over the related crop growing season, not considering effects of specific timing of strong stress occurrence.

Further it seems that the different annual weather conditions, the occurrence of short-term extreme climate events (such as drought and wet periods as well as heat waves) can cause deviations to seasonal forecast quality. For all presented indicators in our study it was shown that in general the forecast performance will increase the less the future prediction target is away from the forecast start. However, also long- term predictions can perform in some cases better than updated forecasts with lower lead time. We were however still not able to show if that is only arbitrary behaviour or not, due to the limited number of “test” cases obtained so far for a sound statistical analysis. It is also worth, to further investigate the prediction performance of the various indicators in regard to specific annual weather patters or local climate characteristics in regard to the frequency of limiting crop stress or risk parameters.

Acknowledgements

The database, simulations, and analysis were supported by the project AGROFORECAST of the Austrian Climate Research Program (ACRP) and dissemination from the COST Action CA20108 (FAIRNESS).

References

Bluemel, S; Eitzinger, J; Gruber, B; Gatterer, M; Altenburger, J; Hausdorf, H. (2020). Influence of weather variables on the first seasonal occurrence of the grape berry moths Eupoecilia ambiguella (lepidoptera: tortricidae) and Lobesia botrana (lepidoptera: tortricidae) in a case study region in Austria. Mitt. Klosterneuburg. 2020; 70(2): 115-128.

Eitzinger J., Trnka M., Semerádov, D., Thaler S., Svobodová E., Hlavinka P., Siska B., Takáč J., Malatinská L., Nováková M., Dubrovsk, M., Zalud Z. (2013). Regional climate change impacts on agricultural crop production in Central and Eastern Europe – hotspots, regional differences and 34 common trends. The Journal of Agricultural Science 151(6): 787-812.

Hansen J.W. (2005). Integrating seasonal climate prediction and agricultural models for insights into agricultural practice. Philosophical Transactions of the Royal Society, 360: 2037-2047.

Huglin, P. (1978). Nouveau mode d'évaluation des possibilités héliothermique d'un milieu viticole. Comptes Rendus Académie d'Agriculture 1978, 1117–1126.

IPCC (2014). Summary for policymakers. In: Climate Change (2014). Impacts, Adaptation, and Vulnerability. Part A: Global and Sectoral Aspects. Contribution of Working Group II to the Fifth Assessment Report of the Intergovernmental Panel on Climate Change [Field, C.B., V.R. Barros, D.J. Dokken, K.J. Mach, M.D. Mastrandrea, T.E. Bilir, M. Chatterjee, K.L. Ebi, Y.O. Estrada, R.C. Genova, B. Girma, E.S. Kissel, A.N. Levy, S. MacCracken, P.R. Mastrandrea, and L.L. White (eds.)]. Cambridge University Press, Cambridge, United Kingdom and New York, NY, USA, pp. 1-32.

Lalić, B; Firanj Sremac, A; Dekić, Lj; Eitzinger, J; Perišić, D. (2017). Seasonal forecasting of green water components and crop yields of winter wheat in Serbia and Austria. J AGR SCI, 1-17.

Lalic, B; Francia, M; Eitzinger, J; Podrascanin, Z; Arsenic, I. (2016). Effectiveness of short-term numerical weather prediction in predicting growing degree days and meteorological conditions for apple scab appearance. METEOROL APPL.; 23(1): 50-56

Lobell, D.B., G.L. Hammer, K. Chenu, B. Zheng, G. McLean and S.C. Chapman. (2015). The shifting influence of drought and heat stress for crops in Northeast Australia. Glob Chang Biol. doi:10.1111/gcb.13022.

Meza F.J., Hansen J.W., Osgood D. (2008). Economic value of seasonal climate forecasts for agriculture: Review of ex-ante assessments and recommendations for future research. Journal of Applied Meteorology and Climatology, 47: 1269-1286.

Trnka, M., Olesen, J. E., Kersebaum, K. C., Skjelvag, A. O., Eitzinger, J., Seguin, B., Peltonen-Sainio, P., Rötter, R., Iglesias, A., Orlandini, S., Dubrovsky, M., Hlavinka, P., Balek, J., Eckersten, H., Cloppet, E., Calanca, P., Gobin, A., Vucetic, V., Nejedlik, P., Kumar, S., Lalic, B., Mestre, A., Rossi, F., Kozyra, J., Alexandrov, V., Semeradova, D., Žalud, Z. (2011). Agroclimatic conditions in Europe under climate change. Global Change Biology, 17: 2298–2318. doi: 10.1111/j.1365-2486.2011.02396.x.

`A geographical analysis of wildfire fuel characteristics by cover type in Greece

Palaiologou P.[1], K. Kalabokidis[2] and C. Vasilakos[2]

[1]Department of Forestry and Natural Environment Management, Agricultural University of Athens, Karpenisi, Greece
[2]Department of Geography, University of the Aegean, Mytilene, Greece

Abstract. The main drivers of wildfire behavior are topography (e.g., slope), weather (e.g., wind and fuel moisture content) and fuel (e.g., quantity, arrangement, and continuity at both the surface and canopy levels). In this study, we examined how the fuel characteristics (fuelbed inputs grouped as fuel model, canopy cover and stand height) vary by cover type and across the different regions of Greece for the reference year of 2018. In addition, we investigated how the different fuel models vary in terms of canopy characteristics and topographic features. The analysis was conducted by combining vector and raster datasets. Canopy characteristics datasets were retrieved from open geospatial providers such as the Global Land Analysis and Discover team at the University of Maryland, USA, which used the Global Ecosystem Dynamics Investigation (GEDI) Lidar forest structure measurements to map forest height, and the Copernicus Tree Cover Density. The CORINE Land Cover vector dataset of 2018 served as the base mapping and analysis layer, supplemented by information from the National Forest Registry of Greece (circa 1992) to define vegetation species in each CORINE class. Results showed important regional variations of fuel model types that explain the regional differences in burned area. Also, the distribution of topographic features by fuel model is indicative of why certain fuel types burn more frequently and intensively than others. We provided a breakdown of canopy cover and height by species that can aid to the understanding of which are the forests that require management to reduce their density (high canopy cover) or can create more revenue (high stand height).

1 Introduction

The changes occurred on the Greek landscapes during the past three decades are phenomenal. It is not only the two seasons (2007 and 2021) of mega-fires that shook the societal and political *status quo* regarding the way we confront, manage and live with fires, but also the way that these mega-fires reshaped the biophysical and social realities. For example, the unpreceded 40,000 ha of 2021 in Evia destroyed the economic fabric of the region and huge funding were funneled there by the Greek government to maintain the social balance and change the established economic paradigm. In addition, the destruction of so many hectares of forested lands in an isolated islandic system, and the years required to regenerate, is paving the ground for more natural disasters such as increase flooding and soil erosion, rockfalls and soil loss. As we enter the era of mega-fires, we expect that similar wildfires will occur not only in regions prone to large fire propagation such as the Peloponnese, Attica and Evia, but also to high elevation ecosystems as those found in Central Greece and Epirus. By default, these ecosystems have reduced defenses from both the non-fire-resistant vegetation species that cover them and by the intense depopulation that led to land abandonment and in turn, fire deficiencies that enhance fuel accumulation. To put it simply, there is not a single region in Greece that can claim that will remain “fire-proof” during the era of mega-fires. From this standpoint, we ask where potential future fires will ignite and how they will propagate. Furthermore, how these future fires can affect populated places and other values-at-risk. One approach to examine this is through stochastic fire behavior modelling, producing thousands wildfire simulations. These simulations can in turn used to estimate community exposure and ecosystem risk and use the results to plan for potential preventive measures to reduce the estimated fire spread rate and intensity. To achieve this goal, it is important to create or find the necessary inputs for this fire behavior modelling software to run. In this study we created a combined dataset of basic fire simulation inputs (fuel models, elevation, slope, canopy cover and stand height) and critique their distribution across the Greek landscape.

2 Materials and Methods

Wildfire behavior models, such as those of Rothermel (1972) consider numerous empirical variables. While these inputs are important for equation outputs, they are often difficult and time-consuming, if not impossible, to measure for each fuel bed. A fuel model defines these input variables for a stylized set of quantitative vegetation characteristics that can be visually identified in the field. Depending on local conditions, one of several fuel models may be appropriate. As the base mapping layer, we used the CORINE Land Cover (CLC) (EEA 2022) inventory (2018 version) after intersecting its main forest related classes, i.e., Broad-leaved forest,

Coniferous forest, Transitional woodland-shrub and Mixed forest with a detailed vegetation species layer produced by the First National Forest Inventory of Greece that captured the species distribution and cover for reference year 1992 (Palaiologou et al. 2022). Then, based on knowledge retrieved through extensive inventories across different Greek ecoregions (Kalabokidis et al. 2016) and expert knowledge regarding the potential fire behavior of each vegetation class, we assigned one or more fuel models at each class depending on topographic and other conditions. For example, olive groves received three different fuel models depending on the slope of each pixel considering that smaller slopes are easier to treat and maintain in a low fuel state by their owners (≤5°; Fuel Model: GR1, Short, sparse dry climate grass), compared to those pixels with slopes between 5-15° (FM: GS1, Low load, dry climate grass-shrub) and >15° (FM: GS2, Moderate load, dry climate grass-shrub), where fuel is usually comprised of tall grass mixed with short shrubs and other vegetation. Similarly, grasslands burn differently across the elevation gradient, with higher altitudes be moister and with different plant properties, i.e., density, height, mixture with shrubs, dead fuel moisture of extinction and curing period. We assigned five different fuel models to grasslands and pastures based on the elevation gradient where the pixel was located, i.e., 0-600 m: GS2, >600-800 m: GS1, >800-1200 m: GR4, >1200-1700 m: GR2, and >1700 m: GR1 (see Table 1 for fuel model definitions). All pixels from the European Settlement Map Built-up areas, after resampling, were assigned with a non-burnable fuel model since those areas are mostly residential buildings or roads. For stand height, we used the ETH Global Canopy Height 2020 (Lang 2022), which is a product that fused the GEDI with Sentinel-2 though probabilistic deep learning model to retrieve stand height at 10 m ground sampling distance for the year 2020. Tree canopy cover was retrieved from the Copernicus portal, showing the level of tree cover ranging from 0 (all non-tree covered areas) to 100% for the reference year 2018 in 10 m spatial resolution. Lastly, using the University of Maryland Forest Loss per Year (Hansen et al. 2013), we retrieved the locations of pixels that faced forest loss during 2019 and assigned the fuel model GS1 to describe the conditions that prevail after a disturbance, mostly wildfires in our case, that is characterized by a mixture of tall, cured grasses during the summer mixed with short shrubs. For canopy layer, for disturbances occurred after the reference years of 2020 for tree height and 2018 for canopy cover, we assigned a pixel value of zero. All raster datasets, both the inputs and the final layers, were resampled at 30 m spatial resolution.

3 Results

The most widespread fuel model for forested areas is the TL6, assigned mostly to mixed broad-leaved forests (5.4%), *Quercus* spp. (4.24%) and *Fagus* spp. (1.5%) (Table 1). Next, TU1 was assigned to transitional woodland-shrub dominated by *Quercus* spp. (3.9%), sparse vegetation dominated by *Quercus* spp. (1.3%) and agricultural lands mixed with sparce *Quercus* spp. and other natural vegetation (1.4%) and broadleaf shrubs (0.5%). The TU5 was primarily assigned to *Pinus* spp.(2.5%), mixed broadleaf-coniferous forest (1.2%), *Pinus halepensis* (1.5%) and transitional woodland-shrub dominated by *Abies* spp. (0.7%). The TL9 was assigned mostly to high elevation conifers, such as *Abies* spp. (1.7%), and mixed broadleaf-*Abies* spp. (0.4%). Last, the TU4 fuel model was assigned mostly to sparse *Pinus halepensis* (1.10%). Regarding the non-forest fuel models, GS1 was assigned to natural grasslands with sparse wooden vegetation (8.2%), land principally occupied by agriculture, with significant areas of natural vegetation (5.4%), complex cultivation patterns (5.2%) and olive groves (5%). The SH5 was assigned to sclerophyllous vegetation (11.9%), natural grasslands with significant area covered with shrub (1.3%) and mixed forest with shrub understory (1%). The GR1 was assigned to non-irrigated arable land (8.9%), pastures (0.85%) and vineyards (0.6%). The GS2 was assigned to discontinuous urban fabric (1.6%), agricultural areas with natural vegetation and significant area covered with shrub (1.3%) and sparse vegetation with shrubs (0.55%). The GR4 was mainly assigned to natural grasslands (1.6%). Finally, the SH1 was assigned to fruit trees and berry plantations (1%) and pastures with sparse and short shrub (0.15%).

Table 1. Fuel models distribution over the Greek landscape

Fuel Model Type	Description	Area (ha)	Percent
GS1	Shrubs are about 1-foot high, low grass load. Spread rate moderate; flame length low.	3,648,959	24.68
SH5	Heavy shrub load, depth 4 to 6 feet. Spread rate very high; Flame length very high.	2,110,436	14.28
TL6	Moderate load, less compact. Spread rate moderate; Flame length low.	1,683,304	11.39
GR1	Grass is short, patchy, and possibly heavily grazed. Spread rate moderate; flame length low.	1,596,590	10.80
TU1	Fuelbed is low load of grass and/or shrub with litter. Spread rate low; flame length low.	1,075,986	7.28

TU5	Fuelbed is high load conifer litter with shrub understory. Spread rate moderate; flame length moderate.	950,141	6.43
NB3	Agricultural field, maintained in non-burnable condition.	932,250	6.31
GS2	Shrubs are 1 to 3 feet high, moderate grass load. Spread rate high; flame length moderate.	583,043	3.94
SH7	Very heavy shrub load, depth 4 to 6 feet. Spread rate lower than SH5, but flame length similar. Spread rate high; flame length very high.	437,221	2.96
TL9	Very high load broadleaf litter; heavy needle-drape in otherwise, sparse shrub layer. Spread rate moderate; flame length moderate.	309,797	2.10
GR4	Moderately coarse continuous grass, average depth about 2 feet. Spread rate very high; flame length high.	299414	2.03
NB8	Open water	253029	1.71
TU4	Fuelbed is short conifer trees with grass or moss understory. Spread rate moderate; flame length moderate.	194115	1.31
SH1	Low shrub fuel load, fuelbed depth about 1 foot; some grass may be present. Spread rate very low; flame length very low.	180016	1.22

In Figure 1, the fuel model map is presented, covering the entire Greece and a 20-km buffer zone expanding into Albania, North Macedonia, and Bulgaria. This zone has not been expanded to Turkey, since the river Evros that defines the border between the two countries was considered as a barrier to fire transmission, eliminating the need to further expand the study area.

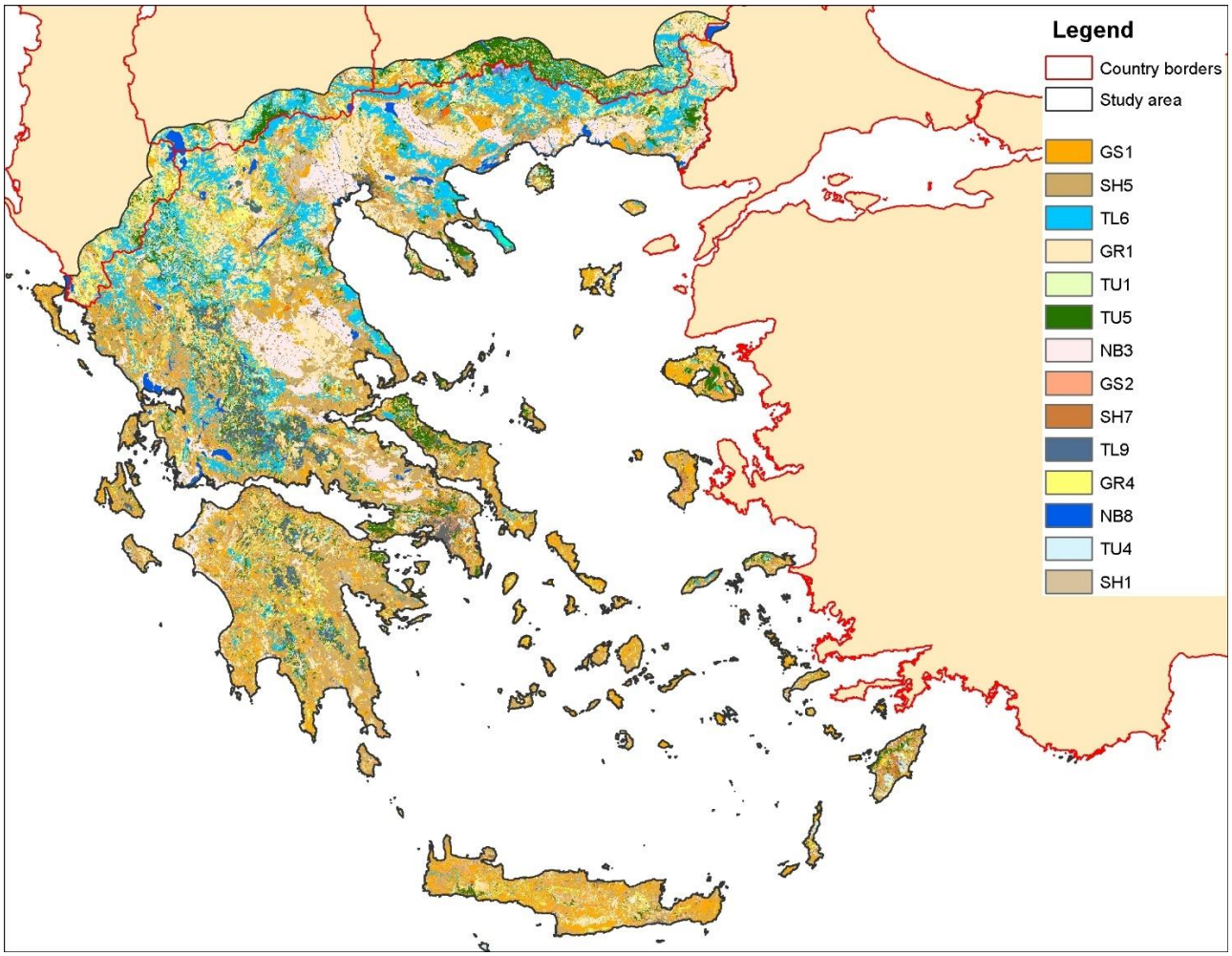

Figure 1. Fuel models of study area, including a buffer zone of 20-km at the northern borders of Greece.

Below, we examine the four main fuel models used for forested areas (TL6:186; TU1: 161; TU5: 165 and TL9: 189) based on their elevation, slope, stand height and canopy cover properties. In Figure 2, the TL6 fuel model that describes conditions of moderate load broadleaf litter is dominant mostly on elevations < 1300 m and on moderate to high slopes (between 12 and 30 degrees). The majority of pixels of stand height are in the range

of 17.5-37.5 m (77%), followed by a 14% with a height > 37.5 m. For the TU1 fuel model where the primary carrier of fire is low load of grass and/or shrub with litter that produces low spread rates and flame length (Figure 3), 30% of all pixels are in elevations < 600 m and 45% between 600 and 1000 m. Above 1000 and below 1450 m we find the 21% of all pixels with this fuel model. Regarding slope, 10% of all values are <5°, 33% between 12 and 21° and another 33 between 21 and 30 °. Almost 20% of all values are in slopes > 30°. This fuel model has an important percentage with low canopy cover (32% of pixels with <15% canopy cover), but on the other hand, 42% of all pixels have cover between 55-85%. For stand height, almost 60% of all pixels are in the range of 17.5-37.5 m, suggesting that mature old-growth forests exist there, while 33% have heights <2.5 m, an indicator that these are mostly shrublands.

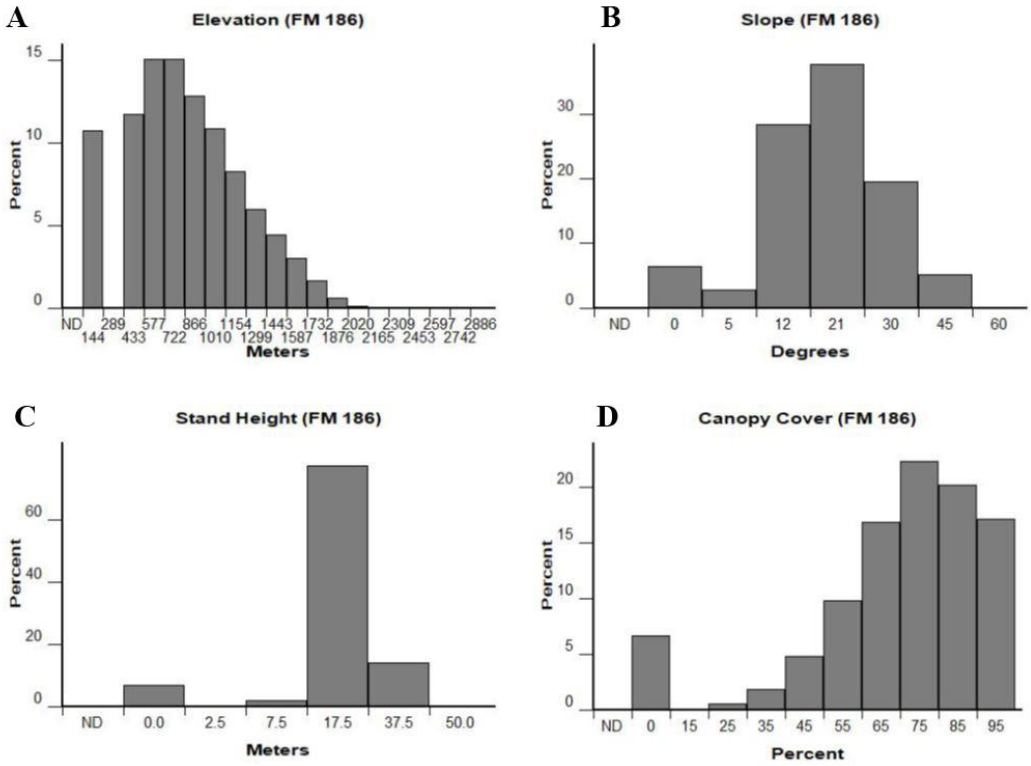

Figure 2. Characteristics and properties of the locations assigned with the fuel model TL6 - Moderate Load Broadleaf Litter. **(A)** Elevation. **(B)** Slope. **(C)** Stand height. **(D)** Canopy cover.

In Figure 4, the distributions of the TU5 fuel model are presented. For this fuel model, the primary carrier of fire is heavy forest litter with a shrub or small tree understory producing moderate spread rate and flame length. We found that 28% of all pixels with TU5 fuel model are located below 600 m elevation, and 25% between 600-1000 m. A very high percentage (46%) is located on very high elevations >1000 m above sea level. The most frequent slope category is the 21-30 degrees with 35% of all pixels, followed by the 12-21 degrees (27%) and 30-45 degrees (20%). Almost 80% of all pixels have canopy cover >55%, with a substantial percentage of 30% with cover >85%.

Last, in the stand height class of 175.-37.5 m falls the 58% of all pixels with this fuel model, with another 26% falling in the class of 37.5-50 m. An important finding is that 13% of all pixels have a height < 2.5, suggesting potential errors in the input datasets for that fuel model. Finally, for the fuel model TL9 (Figure 5) that describes conditions of very high load, fluffy broadleaf litter with moderate spread rate and flame length, we found that 80% of all pixels with that fuel model are in elevations between 1000-1600 m. In addition, a 16% of all pixels are in slopes steeper than 45°, with 65% falling in slopes between 21-45°. An impressive 44% of all pixels have closed canopies with >95% cover, with another 37% of pixels having canopy cover between 75-95%. Finally, these forests are very tall, with almost 40% of all pixels falling in the stand height class of 37.5-50 m, and 55% in the class of 17.5-37.5 m.

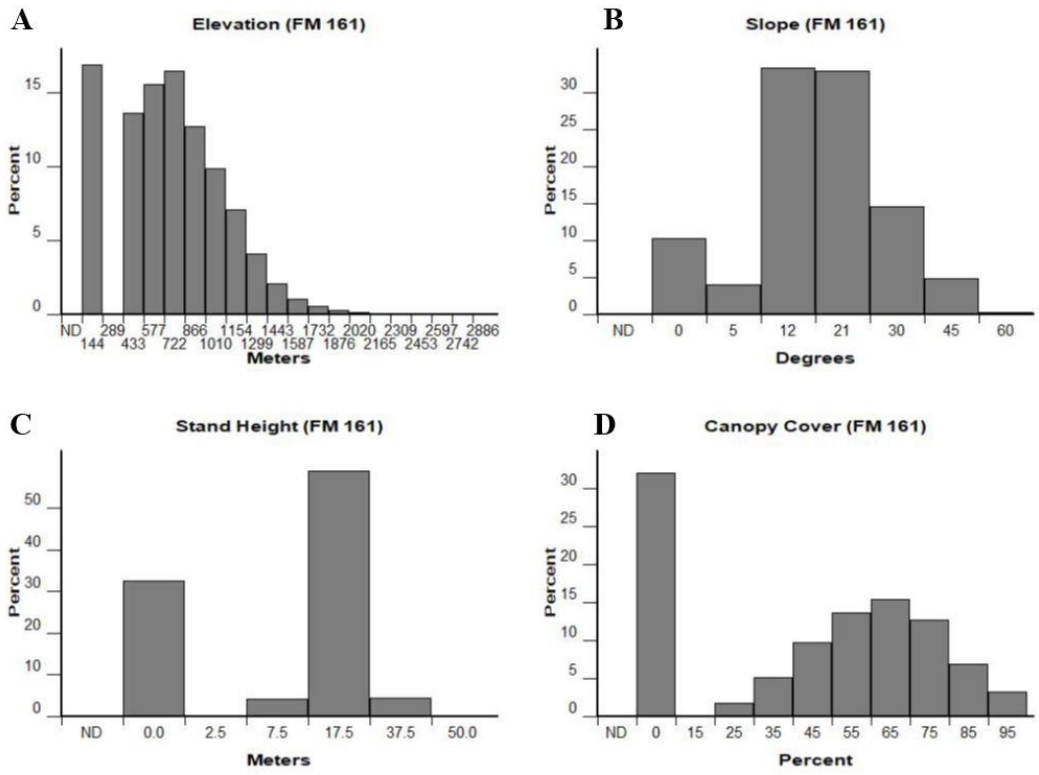

Figure 3. Characteristics and properties of the locations assigned with the fuel model TU1 - Low Load Dry Climate Timber-Grass-Shrub. **(A)** Elevation. **(B)** Slope. **(C)** Stand height. **(D)** Canopy cover.

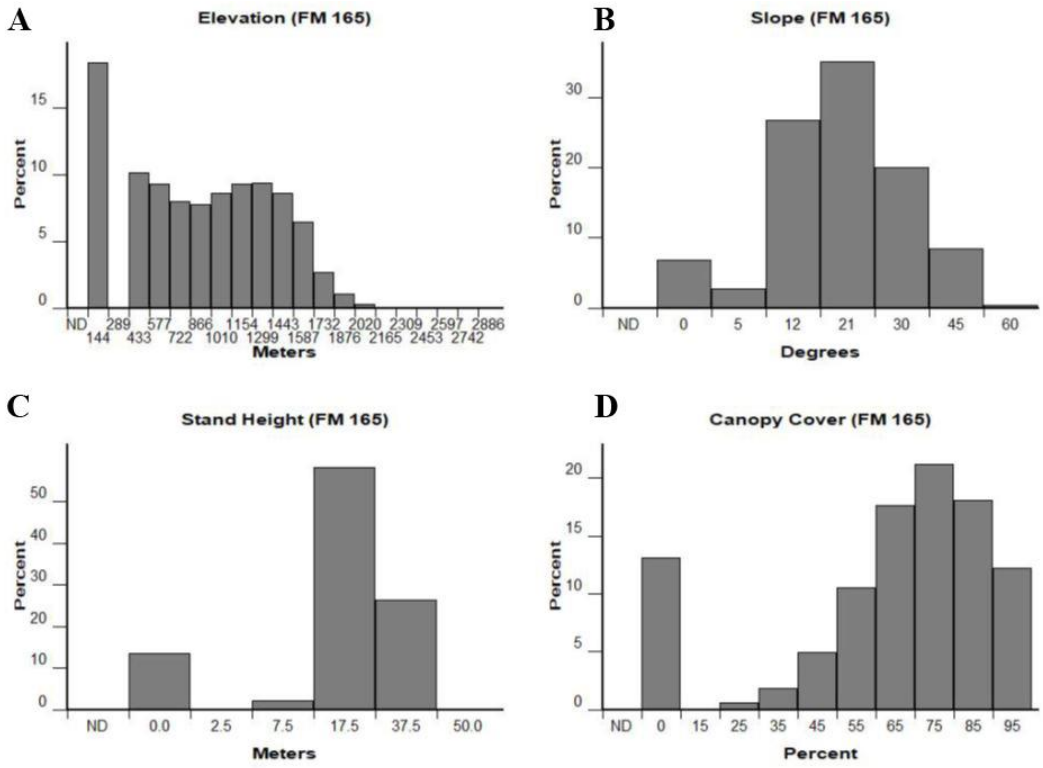

Figure 4. Characteristics and properties of the locations assigned with the fuel model TU5 - Very High Load, Dry Climate Timber-Shrub. **(A)** Elevation. **(B)** Slope. **(C)** Stand height. **(D)** Canopy cover.

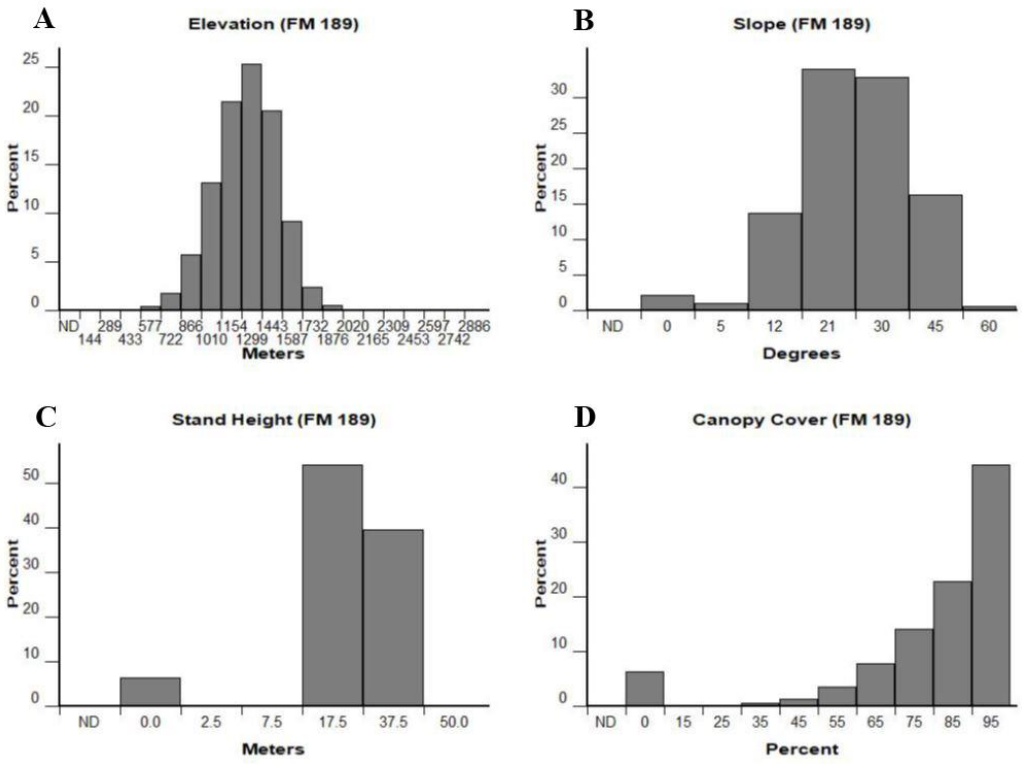

Figure 5. Characteristics and properties of the locations assigned with the fuel model TL9 - Very High Load Broadleaf Litter. **(A)** Elevation. **(B)** Slope. **(C)** Stand height. **(D)** Canopy cover.

3 Concluding remarks

Creating model-ready datasets and applying them to analyze wildfire risk and exposure for Greece is a tractable problem if Copernicus data and other datasets from trusted publishers/creators are used in conjunction with local knowledge and auxiliary datasets that describe the forest conditions and the fire history of each area. We found that large parts of Greece are covered by non-tree species, and little can be done there to reduce fire risk, except for suppression. Fuel models that exclusively describe forest stand conditions cover a much smaller portion of the landscape and there, it is possible to reduce the potential fire spread and intensity through fuel management. We also found that certain ecosystems can become more resilient if low intensity fuel treatments are applied there, for example, in tall forests covered with the TL9 fuel model or in very dense canopy cover areas, where thinning can promote both natural regeneration and reduce fuel load and canopy compactness.

Acknowledgements

We acknowledge current support from the European Union's Horizon 2020 research and innovation programme FIRE-RES under grant agreement No. 101037419.

References

EEA. Corine Land Cover (CLC) 2018, Version 2020_20u1. Available online: https://land.copernicus.eu/pan-european/corine-land-cover/clc2018 (accessed on 21 February 2022).

Hansen, M.C.; Potapov, P.V.; Moore, R.; Hancher, M.; Turubanova, S.A.; Tyukavina, A.; Thau, D.; Stehman, S.V.; Goetz, S.J.; Loveland, T.R.; et al. 2013. High-Resolution Global Maps of 21st-Century Forest Cover Change. *Science*, 342, 850-853.

Kalabokidis, K., Ager, A., Finney, M., Athanasis, N., Palaiologou, P. and Vasilakos, C., 2016. AEGIS: a wildfire prevention and management information system. *Natural Hazards and Earth System Sciences*, 16(3), 643-661.

Lang, N., Walter J., Konrad S. and Jan D.W., 2022. A high-resolution canopy height model of the Earth. arXiv, 2204.08322.

Palaiologou, P., Kalabokidis, K., Day, M.A., Ager, A.A., Galatsidas, S. and Papalampros, L., 2022. Modelling Fire Behavior to Assess Community Exposure in Europe: Combining Open Data and Geospatial Analysis. ISPRS International Journal of Geo-Information, 11(3), 198.

Rothermel, Richard C., 1972. A Mathematical Model for Predicting Fire Spread in Wildland Fuels. USDA Forest Service. Research Paper INT-115.

Flood hazard modelling and mapping of the Medicane "Ianos" in Kalentzis River Basin, Greece

Vasiliades L.[1], E. Farsirotou[2] and A. Psilovikos[2]

[1] Department of Civil Engineering, University of Thessaly, Volos, Greece
[2] Department of Ichthyology & Aquatic Environment, University of Thessaly, Volos, Greece

Abstract. The flood event that occurred on 18th September 2020 in Kalentzis river basin due to the Medicane "Ianos", is reproduced using an integrated hydrologic/hydraulic modelling framework to simulate the flood hydrograph and the flood extent in the greater area of Karditsa city. Extreme rainfall amounts were observed in the mountainous and lowland areas, with estimated return periods of 1000 and 200 years, respectively, for rain duration of 24 hours, and used to estimate areal precipitation at 15-min time interval at subwatershed level. Using the HEC-HMS software and the Natural Resources Conservation Service (NRCS) Unit Hydrograph procedure simulated flood hydrographs at important tributaries junctions are estimated and applied in HEC-RAS 2D model for flood routing and estimation of flood attributes (i.e., water depths and flow velocities), as well as mapping of inundated areas. Simulated flood extent is in close agreement with the observed flooded area estimated from Sentinel images by the Copernicus Emergency Management Service. Hence, the modelling procedure of this study could be expanded in a methodological framework to support flood hazard mitigation policies in the study area.

1 Introduction

Floods are among the most destructive water-related hazards and are mainly responsible for the loss of human lives, infrastructure damages and economic losses. In general, there are five distinct types of floods (i.e., flash, fluvial, pluvial, urban, and coastal floods), which may stem from various processes and sources. Flood impacts could be aggravated by human activities and interventions in the natural systems (e.g., deforestation, earthworks, water works, urbanization). Flash and fluvial (river) flooding is the most common type of flood in small and medium sized watersheds and several studies highlight the importance of flood hazard modelling using integrated hydrologic and hydrodynamic modelling procedures (Dottori et al., 2013; Teng et al., 2017).
Mediterranean Hurricanes or "Medicanes" also known as tropical-like cyclones (TLCs), are extreme cyclonic windstorms morphologically and physically similar to tropical cyclones occurring in the Mediterranean Sea (Nastos et al., 2018). Medicanes poses serious threats to human life and infrastructure, such as heavy rainfall and flooding, intense wind, lightning, tornadoes, and high waves and storm surge (Romero and Emanuel, 2013). Recent studies show that medicanes' intensity and frequency of occurrence are likely to increase due to climate change in the near future (González-Alemán et al., 2019; Koseki et al., 2021).
Between 2016 and 2020, four strong medicanes have developed in the Ionian Sea and have caused damage in Greece, with the most recent and most destructive case being the Medicane Ianos between 15 and 20 September 2020 (Dafis et al., 2020). Medicane "Ianos" impacted Greece and had caused significant wind damage, and precipitation related impacts that resulted in four fatalities and extended infrastructure damages and landslides in the Ionian Islands and in Central Greece (Lagouvardos et al., 2021). Extreme mountainous precipitation in terms of intensity and duration resulted in torrential flooding with subsequent landslides and debris flows and high structural damages on buildings, transportation infrastructure, and powerlines. In the low-relied areas of the Thessaly Plain, large scale flooding with the inundation of over 400 km^2 of agricultural and urban land caused widespread disruptions to communities and severe impact on the economic activity, especially in the city of Karditsa (Zekkos and Zalachoris, 2020). The objective of this study is to model and reconstruct the flood event caused by Medicane "Ianos" in Kalentzis River basin (with toral basin area of 654 km^2), central Greece, using a CN-based unit hydrograph rainfall-runoff model and a 2D hydraulic/hydrodynamic model for flood routing and hazard mapping.

2 Methodology

A combined hydrological and hydraulic–hydrodynamic modelling approach is applied for flood inundation modelling and mapping at Kalentzis ungauged watershed. Figure 1 shows the study area with the important tributaries (Gavras, Karampalis, Kalentzis and Lipsimos rivers) with the selected discretization modelling scheme which include 16 subwatersheds, six reaches and seven junctions. All selected streams drain near the city of Karditsa and contain multiple hydraulic structures and flood protection works. Table 1 presents the basic geographic and hydrologic attributes of the study subbasins and reaches.

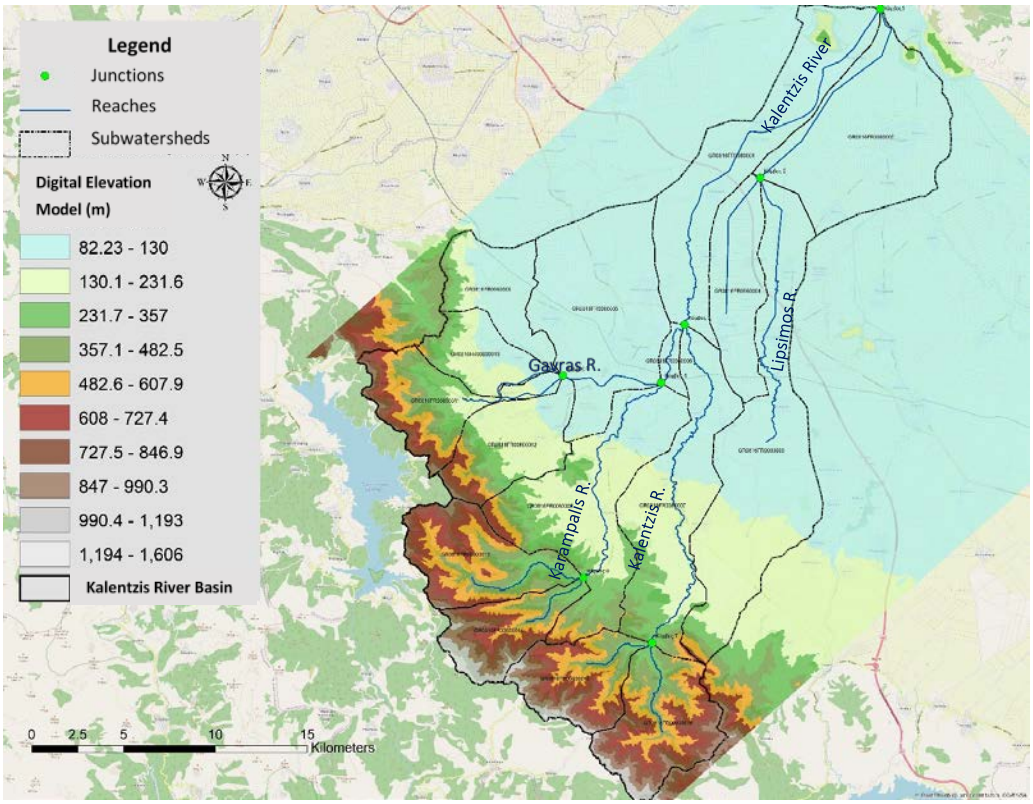

Figure 1. Kalentzis River basin with the employed modelling components (selected sub-watersheds, stream reaches, junctions for flood inundation modelling and mapping).

Table 1. Characteristics of the study subwatershed and sream reaches.

Characteristics of the study subwatersheds						
Subwatershed Code	**Reach**	**Outlet Junction**	**Area (km^2)**	**Mean Elevation (m)**	**Outlet Elevation (m)**	**Maximum Flow Length (km)**
GR0816FR0060001	R31	J1	61.105	96.607	88.2	23.600
GR0816FR0060002	R21	J1	66.716	92.272	88.2	14.991
GR0816FR0060003	IN	J2	84.907	137.512	91.7	26.928
GR0816FR0060004	IN	J2	28.536	99.392	91.7	7.987
GR0816FR0060005	R54	J4	66.508	123.801	113.6	20.036
GR0816FR0060006	R43	J3	3.791	108.433	105.8	4.646
GR0816FR0060007	R73	J3	57.165	184.312	105.8	26.931
GR0816FR0060008	R64	J4	63.631	244.069	113.6	19.844
GR0816FR0060009	IN	J5	24.002	143.525	115.6	9.997
GR0816FR00600010	IN	J5	18.683	189.329	115.6	7.303
GR0816FR00600011	IN	J5	28.889	456.465	115.6	13.976
GR0816FR00600012	IN	J5	29.533	280.219	115.6	12.045
GR0816FR00600013	IN	J6	34.016	565.397	271.4	14.619
GR0816FR00600014	IN	J6	22.991	719.821	271.4	11.498
GR0816FR00600015	IN	J7	26.884	682.405	255.4	10.246
GR0816FR00600016	IN	J7	36.545	659.979	255.4	11.910

Characteristics of the study reaches					
Reach Code	**Subwatershed**	**Inlet Junction**	**Outlet Junction**	**Length (km)**	**Mean Slope**
R21	GR0816FR0060002	J2	J1	14.990	0.0002
R31	GR0816FR0060001	J3	J1	23.600	0.0007
R43	GR0816FR0060006	J4	J3	4.640	0.0017
R54	GR0816FR0060005	J5	J4	5.893	0.0003
R64	GR0816FR0060008	J6	J4	32.904	0.0048
R73	GR0816FR0060007	J7	J3	25.325	0.0059

2.1 Hydrological modelling

The hydrological approach is based on semi-distributed modelling (at sub-watershed scale) of the rainfall-runoff process using the HEC-HMS software and the SCS-CN method for extracting the excess from the gross rainfall, and the unit hydrograph theory, for propagating the surface runoff to the subbasin outlets. In this study, the estimation of the concentration time (t_c) of the watershed was based on the empirical approach of Giandotti formula. Moreover, to take account of the dependence of the response time of the basin against runoff, the kinematic wave theory-based semi-empirical formula was employed, considering that t_c is inversely proportional to the areal rainfall, $t_c(T) = t_c \sqrt{\frac{i(5)}{i(T)}}$ where $i(5)$ is the design rainfall intensity for return period T=5 years, for which the time of concentration is estimated by the Giandotti formula, and $i(T)$ is the calculated intensity of the Ianos return period, T (estimated from the Greek Intensity-Duration-Frequency IDF or ombrian curves). The spatially-averaged per subwatershed Curve Number (CN) parameter is estimated on the basis of distributed soil and land cover information, following the typical classification by NRCS, by means of detailed lookup tables for average antecedent soil moisture conditions (AMC II). The transformation of the excess rainfall over each sub-basin to flood hydrograph at the outlet junction (rainfall-runoff model) was achieved using the dimensionless curvilinear unit hydrograph approach of SCS, which is considered the prevailing modeling approach for ungauged basins. A key assumption of the method was the implementation of the concept of varying (i.e., runoff-dependent) time of concentration, which affects the shape of unit hydrographs, thus introducing further nonlinearities to overall modeling approach. Further details of the methodology could be found in Vasiliades et al., 2021.

2.2 Hydrodynamic modelling

The two dimensional (2D) HEC-RAS hydraulic-hydrodynamic model, developed by the Hydrologic Engineering Center (HEC) of United States Army Corps of Engineers, has been selected for flood inundation and mapping. The HEC-RAS model uses the sub-grid bathymetry approach that adopts a relatively coarse computational grid and information underlying the topography at a finer scale. The sub-grid bathymetry equations are derived from the full shallow water equations. Fundamental elements for an accurate flood inundation modeling and mapping, are the digital elevation model (DEM), the stream channel geometry (river flowpaths, banks, etc.), the hydraulic model configuration (i.e., initial and boundary conditions, roughness coefficients, technical works), and the representation of urban areas by considering the effect of the building blocks to the water flow. In this study, the flood hydrographs derived from the hydrological model were used as input hydrographs in the 2D HEC-RAS hydraulic–hydrodynamic model for flood inundation modelling and mapping. The DEM, provided by the Greek National Cadastre and Mapping Agency S.A. (NCMA) with a resolution of 5 m, was used for flood modelling and mapping results and all examined reaches were modelled with flexible mesh sizes (ranging from 9.10-900 m^2), roughness coefficient values based on CORINE land cover data and a computation interval of 2.0 s. All hydrotechnical works (e.g., flood protection works, culverts, bridges, weirs) within the river and the adjacent areas were based on previous studies at the study area (Papaioannou et al., 2021).

3 Application of the Methodology

Rainfall data of five meteorological stations in the wider area at 15-min intervals are used to represent the spatiotemporal rainfall distribution of “Ianos” event and to estimate areal rainfall at subwatershed level. Figure 2 shows the temporal rainfall intensity distribution of two represantive meteorological stations (Karditsa and Plastiras Dam) from the period 17-9-2020 and time 18:00 (≈ onset date of onset of the medicane "Ianos") until 19-9-2020 and time 12:00 (≈ end date of "Ianos"). It should be noted that the observed extreme rainfall in the study rainfall stations had estimated return periods (estimated using the Greek IDF ombrian curves) for rain duration of 24 hours larger than 1000 and 200 years for the mountainous (Plastiras Dam) and plain (Karditsa) stations, respectively.

3.1 Hydrological and hydrodynamic modelling results

The application of the semi-distributed hydrological modelling procedure in Kalentzis river basin led in the estimation of hydrographs at the junctions used for the hydrologic and hydrodynamic simulation of “Ianos” flood event for the period 17-9-2020 until 20-9-2020. For example, Figure 3 shows the estimated hydrographs at Karampalis river for one mountainous subwatershed GR0816FR00600013 and the hydrograph flood routing of the stream reach R64.

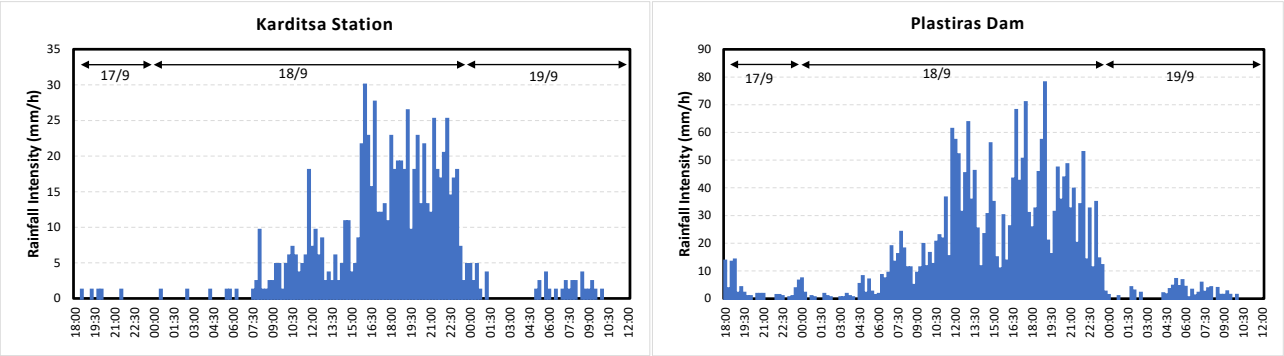

Figure 2. Rainfall intensity timeseries with 15-min time interval in two representative rainfall stations.

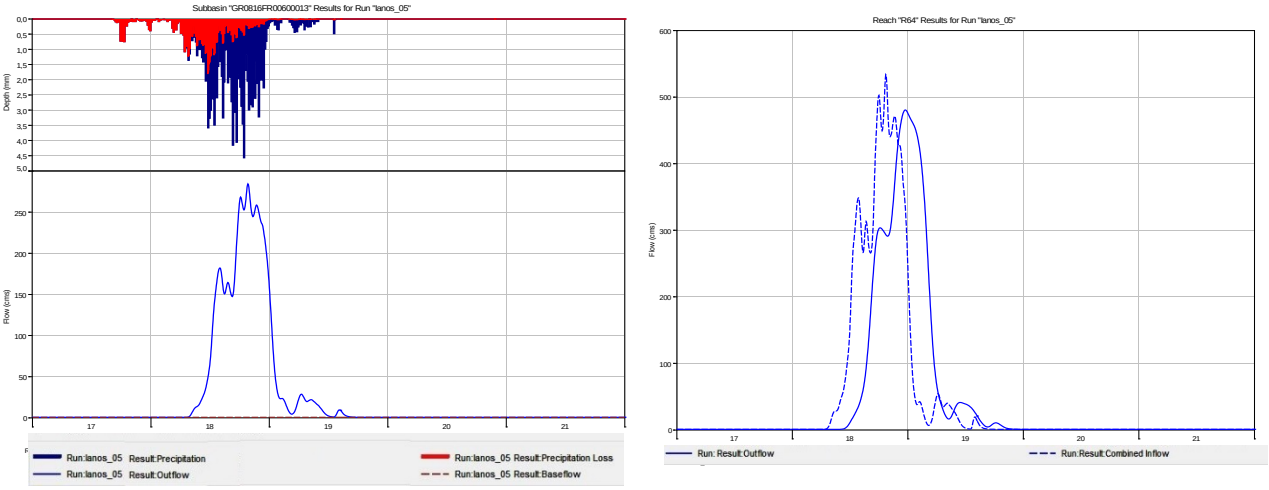

Figure 3. Simulated hydrographs in a selected subwatershed and a stream reach of Karampalis tributary.

Conventional and non-conventional flood data and impact records of the extreme flash-flood event that occurred on 18th September 2020 were used for the comparison of the simulated flood extent of the "Ianos" Medicane in the greater area of Karditsa city. Figure 4 illustrates the maximum water depths and velocities and the estimated flood extent resulted from the rainfall-runoff and the hydrodynamic flood routing modelling processes. It is interesting to note that the simulated flood extent of Figure 4 (estimated about 236 km^2) is in close agreement with the observed flooded area estimated from Sentinel images by the Copernicus Emergency Management Service (EMSR465: Floods in Thessaly Region, Greece).

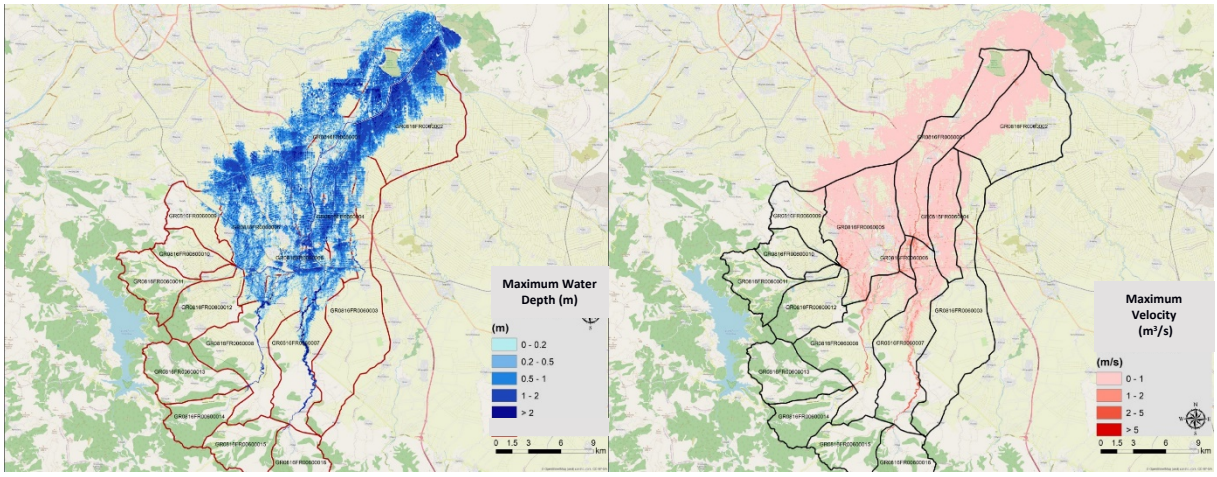

Figure 4. Simulated maximum flood extent and maximum water depths and velocities in Kalentzis River basin.

3.2 Flood hazard assessment

The base data that underpins assessment of floodplain risk typically comprises the flow characteristics (the flow depth and velocity) in the flood-affected areas of Kalentzis river basin. Flood hazard is estimated in this study using the DV criterion (DV = Depth * Velocity), which incorporates people, vehicle and structural (building) stability criteria in the resistance/resilience of the above categories on floods (Smith et al., 2014). Table 2 shows the flood hazard assessment categories of the DV criterion and the flood hazard area per category caused by the Medicane "Ianos" in Kalentis river basin is depicted in Figure 5.

Table 2. Combined flood hazard curves - vulnerability thresholds classification limits (based on Smith et al., 2014) of Medicane "Ianos".

Flood Hazard Vulnerability Classification	Classification Limit (D and V in combination)	Limiting Still Water Depth (D)	Limiting Velocity (V)	Flooded Area (km^2)
H1 = generally safe for vehicles, people and buildings	D * V ≤ 0.3	D ≤ 0.3	V ≤ 2.0	158.8
H2 = unsafe for small vehicles	D * V ≤ 0.6	D ≤ 0.5	V ≤ 2.0	3.1
H3 = unsafe for vehicles, children and the elderly	D * V ≤ 0.6	D ≤ 1.2	V ≤ 2.0	43.4
H4 = unsafe for vehicles and people	D * V ≤ 1.0	D ≤ 2.0	V ≤ 2.0	19.9
H5 = unsafe for vehicles and people. All buildings vulnerable to structural damage. Some less robust buildings subject to failure	D * V ≤ 4.0	D ≤ 4.0	V ≤ 4.0	8.8
H6 = Unsafe for vehicles and people. All building types considered vulnerable to failure	D * V> 4.0	-	-	2.2

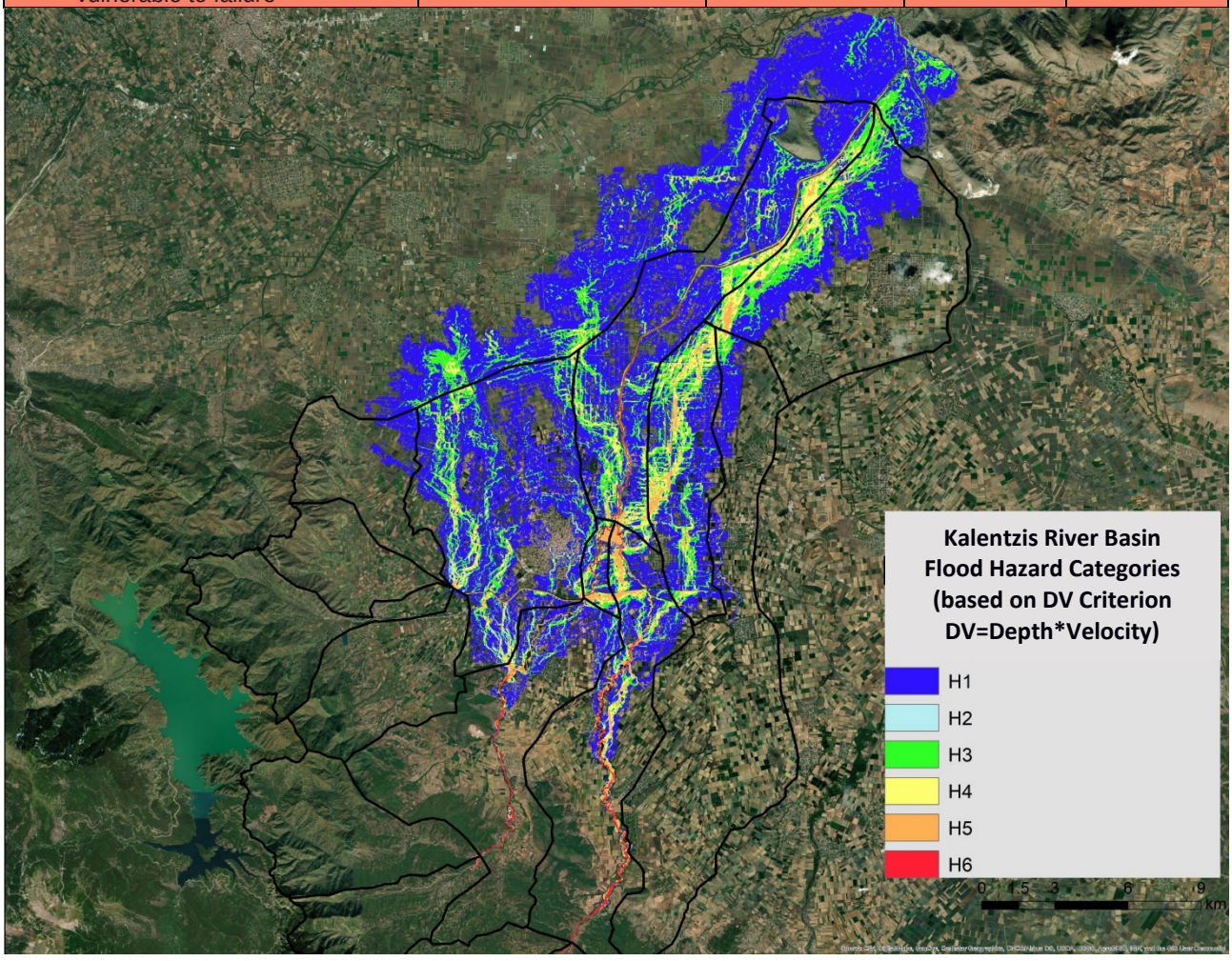

Figure 5. Mapping of flood hazard caused by Medicane "Ianos" in Kalentzis River basin.

4 Summary

The flood event that occurred on 18th September 2020 in Kalentzis river basin due to the Medicane “Ianos”, was reproduced using an integrated hydrologic/hydrodynamic modelling framework to simulate the flood hydrograph and the flood extent in the greater area of Karditsa city. Extreme rainfall amounts were observed in the mountainous and lowland areas, with estimated return periods of 1000 and 200 years, respectively, for rain duration of 24 hours, and used to estimate areal precipitation at 15-min time interval at subwatershed level for the period 17 September 2020 to 20 September 2020.

Using the HEC-HMS software and the Natural Resources Conservation Service (NRCS) Unit Hydrograph procedure in semi-distributed mode (at subwatershed level) simulated flood hydrographs at important tributaries junctions were estimated and applied in HEC-RAS 2D model for flood routing and estimation of flood attributes (i.e., water depths and flow velocities), as well as mapping of inundated areas. The characteristics of the flood (depth and velocity of the simulated flood wave) were combined to estimate flood hazard using the DV criterion and finally the damage caused by Medicane "Ianos" was evaluated. Simulated flood extent is in close agreement with the observed flooded area estimated from Sentinel images by the Copernicus Emergency Management Service. Hence, the modelling procedure of this study could be expanded in a methodological framework to support flood hazard mitigation policies in the study area.

Acknowledgements

Rainfall data for the four meteorological stations (Argithea, Drakotrypa, Pastiras Dam, Vrontero) were provided by the Greek Public Power Corporation and Meteoclub Network supplied the data for Karditsa meteorological station.

References

Dafis, S., Claud, C., Kotroni, V., Lagouvardos, K., Rysman, J., 2020. Insights into the convective evolution of Mediterranean tropical-like cyclones. Q.J.R. Meteorol. Soc. 146, 4147–4169. https://doi.org/10.1002/qj.3896

González-Alemán, J.J., Pascale, S., Gutierrez-Fernandez, J., Murakami, H., Gaertner, M.A., Vecchi, G.A., 2019. Potential Increase in Hazard From Mediterranean Hurricane Activity With Global Warming. Geophys. Res. Lett. 46, 1754–1764. https://doi.org/10.1029/2018GL081253

Koseki, S., Mooney, P.A., Cabos, W., Gaertner, M.Á., de la Vara, A., González-Alemán, J.J., 2021. Modelling a tropical-like cyclone in the Mediterranean Sea under present and warmer climate. Nat. Hazards Earth Syst. Sci. 21, 53–71. https://doi.org/10.5194/nhess-21-53-2021

Lagouvardos, K., Karagiannidis, A., Dafis, S., Kalimeris, A., Kotroni, V., 2021. Ianos - A hurricane in the Mediterranean. Bulletin of the American Meteorological Society 1–31. https://doi.org/10.1175/BAMS-D-20-0274.1

Nastos, P.T., Karavana Papadimou, K., Matsangouras, I.T., 2018. Mediterranean tropical-like cyclones: Impacts and composite daily means and anomalies of synoptic patterns. Atmospheric Research 208, 156–166. https://doi.org/10.1016/j.atmosres.2017.10.023

Papaioannou, G., Vasiliades, L., Loukas, A., Alamanos, A., Efstratiadis, A., Koukouvinos, A., Tsoukalas, I., Kossieris, P., 2021. A Flood Inundation Modeling Approach for Urban and Rural Areas in Lake and Large-Scale River Basins. Water 13, 1264. https://doi.org/10.3390/w13091264

Romero, R., Emanuel, K., 2013. Medicane risk in a changing climate. J. Geophys. Res. Atmos. 118, 5992–6001. https://doi.org/10.1002/jgrd.50475

Smith, G.P., Davey, E.K., Cox, R.J., 2014. Flood Hazard. UNSW Australia Water Research Laboratory Technical Report 2014/07.

Vasiliades, L., Farsirotou, E., Psilovikos, A., 2021. Expert Report for the 18th September 2020 Flood Event on the wider area of Karditsa. Directorate of the Fire Service of Karditsa, Karditsa, March 2021 (in Greek).

Zekkos, D., Zalachoris, G., 2020. The September 18-20 2020 Medicane Ianos Impact on Greece Phase I Reconnaissance Report Geotechnical Extreme Events Reconnaissance Association. https://doi.org/10.18118/G6MT1T

Frost climatology over southeastern Europe via a high spatiotemporal resolution gridded dataset

Charalampopoulos I.[1], F. Droulia[1], I. Tsiros[1]

[1]Laboratory of general and agricultural meteorology, Agricultural University of Athens, Greece

Abstract. The present study is aimed at analyzing the evolution of major climatic frost indices over the southeastern part of Europe. For this purpose, the Agri4Cast dataset of the JRC MARS Meteorological Database, derived from reanalysis and observations data, was utilized. This is a gridded dataset with high spatial (25 km) and temporal (daily) resolution. For the calculation of Last Spring Frost (LSF), First Autumn Frost (FAF), Free of Frost Days (FFD) and the sum of the Frost Days per year (FD), R-language scripts and packages along with GIS software were employed. Results for the studied period (1979 – 2020) indicate that the FFD is increasing, enabling the occurrence of a more extended growth period in most study areas.
On the contrary, LSF tends to occur later in the spring in some major agricultural areas of Greece, Romania, and Bulgaria, raising the crops' risk for severe frost damage. The FAF tends to be higher in most study areas except for the coastal Albania, the Thessaly plain in Greece, and the Crete island's eastern part. Moreover, the time evolution between 1980-1999 and 2000-2020 of the frost days (FD)indicates a general reduction over all the examined countries.

1 Introduction

Agricultural production is governed by local and regional climate change(Droulia and Charalampopoulos, 2021; Terando et al., 2012). The changing weather patterns along with the extreme weather events are challenging factors determining the development of crops and, ultimately,the promotion of theintra-seasonal production variations(Kogo et al., 2019).Moreover, future climate change in the Mediterranean basin maycause alterations in air temperature and extreme weather events(Droulia and Charalampopoulos, 2022; Moriondo and Bindi, 2007). A restriction yet damaging factor the agricultural production is the frost phenomenon. Using frost indices such as Free Frost Days (FFD), Frost Days (FD), Last Spring Frost (LSF) and First Autumn Frost (FAF) makes it possible to determine the potential frost damage and finally evaluate if a region is characterized by climatic conditions suitable enough for the growth and productivity of crops(Biazar and Ferdosi, 2020; Ci et al., 2016).
The present research is focused on ten countries of southeastern Europe for the period 1978 to 2020 and analyzes in detail the past and the present (by 2020) of the frost indices. It is particularly focused on southeastern Europe, a transitional climatic zone that is projected to face abrupt changes in the essential atmospheric parameters of temperature and precipitation, thus directly impacting crop sustainability (Alexandrov and Hoogenboom, 2000; Cheval et al., 2017; Giannakopoulos et al., 2011). So, it is of utmost importance to obtain reliable information related tothe abiotic factors to plan and implement the most appropriate mitigation strategies (Knox et al., 2016; Önol and H. M. Semazzi, 2009).

2 Data and Methods

2.1 Examined Area and Data

The study is focused on the countries of Albania, Bosnia and Herzegovina, Bulgaria, Croatia, Greece, Montenegro, North Macedonia, Romania, Serbia, and Slovenia. The criterion for this selection is twofold, considering the areas' agricultural production potential and their sensitivity to climate variations.To examine the frost regime, thefine-scale gridded meteorological dataset Agri4Cast of the JRC MARS Meteorological Database (Biavetti et al., 2014; Charalampopoulos et al., 2021) was utilized. This dataset contains meteorological observations from weather stations interpolated to a regular 25x25 km grid on a daily basis. For the selected study area, 1532 grid points cover canonically every part of the Balkan peninsula.

2.2 Methods

The acquired data consist of the grid number, the day/month/year and the temperature parameters (maximum and minimum) from 1978 to 2020, covering 42 years on a daily scale. Thus, the amount of data rows exceeds 22 million in total. For the purpose of managing and analyzing this extensive dataset, the R language(Charalampopoulos, 2020) and the specialized packages "dplyr"(Wickham et al., 2020) and "fst"(Klik and Collet, 2020) were employed. The mapping procedure was implemented in ArcMap 10.8.1. For the summary statistics calculations (median, max, min and kernel densities) and visualization, "gtsummary"(Sjoberg et al., 2021) and "ggpubr"(Kassambara, 2020) packages, respectively, were used.

2.3 Climatic frost indices

The FD (Frost Days) was calculated as the sum of days per year, where the minimum air temperature is equal to or below 0 ^{o}C (Terando et al., 2012). In addition, the FFD (Frost Free Days), which is a free of frost period of a year, was calculated, and it is the period between the LSF (Last Spring Frost and theFAF(First Autumn Frost). The LSF is the last frost occurrence from the beginning of the year to 15thJuly. This parameter is of utmost importance because crops cultivated in the examined area (e.g., maize and wheat) are of higher sensitivity in terms of frost damage during the spring. To be more precise, the late spring frosts are the most dangerous in the specific geographic area(Scheifinger et al., 2003; Wypych et al., 2017). Finally, the FAF is the first frost after 15th July. The frost parameters' related trends were also calculated. A least square regression was conducted for every grid point for the temporal parameters (Year) and the indexvalue. So, the trend is the regression's coefficient, and the related R^2 indicated significance. The spatial distribution of the indices and their trends have been implemented by interpolating the gridded data values. Specifically, the ordinary kriging method(Cressie, 2015) was implanted to take advantage of the gridded data(Terando et al., 2012).

3 Results and discussion

Results represent the frost indices of the study area calculated for the whole annual period of the most recent year(2020) and their trend derived from the analysis of the time period of 1979-2020. The primary scope of this study is to examine the spatial distribution and trends in the southeastern Europe.

3.1 First Autumn Frost (FAF)

In Figure 1, the lower values of the FAF are depicted over the Eastern Carpathian in the northern part of Romania, with the first frost occurrence calculated in late September. Similar FAF values have been shown for the mountainous areas of Montenegro. On the other hand, the coastal region from eastern Bulgaria to northern Croatia faces the first frost after the summer (FAF) in December.

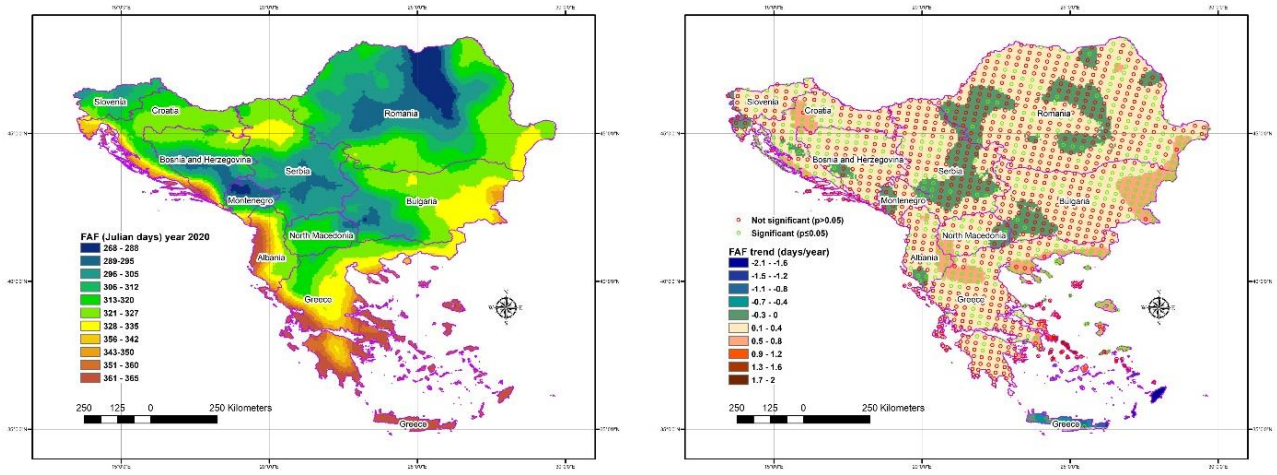

Figure 1. FAF Julian days spatial distribution in 2020 (left) and FAF trend in days/year (right).

Considering the FAF trends map (Figure 1, right), the negative values have been calculated over the southeastern Aegean Sea's islands (Crete, Rhode, etc.), in central Serbia and the plain area southwestern part of Bulgaria. Earlier autumn frosts are expected in the near future over the aforementioned areas. The opposite trend occurs in the rest areas of the studied area. However, as illustrated by the green and blue colors of the right map, the risk will be slightly higher in the agricultural areas. Furthermore, as displayed in the right map,the values are positive in all cases regarding the FAF trends, with the highest trend calculated for Greece (0.34 d/yr) and the lowest for Serbia (0.01 d/yr). As shown in the same map, the trend is clear but often non-significant, a finding which is in line with Wypych et al. (2017) for the frost in central Europe. The generalized result is that the first autumn frost shifts to the cold period, thus extending the cultivation period.

3.2 Last Spring Frost (LSF)

Figure 2presents the last spring frost (LSF) in Julian days and the related trend (right). Results indicate an almost free of frost spring for the Adriatic coast (western part of the map). On the contrary, there are some mountainous areas in northern Romania and in the south of Bulgaria, in which the LSF approachesthe second half of May.

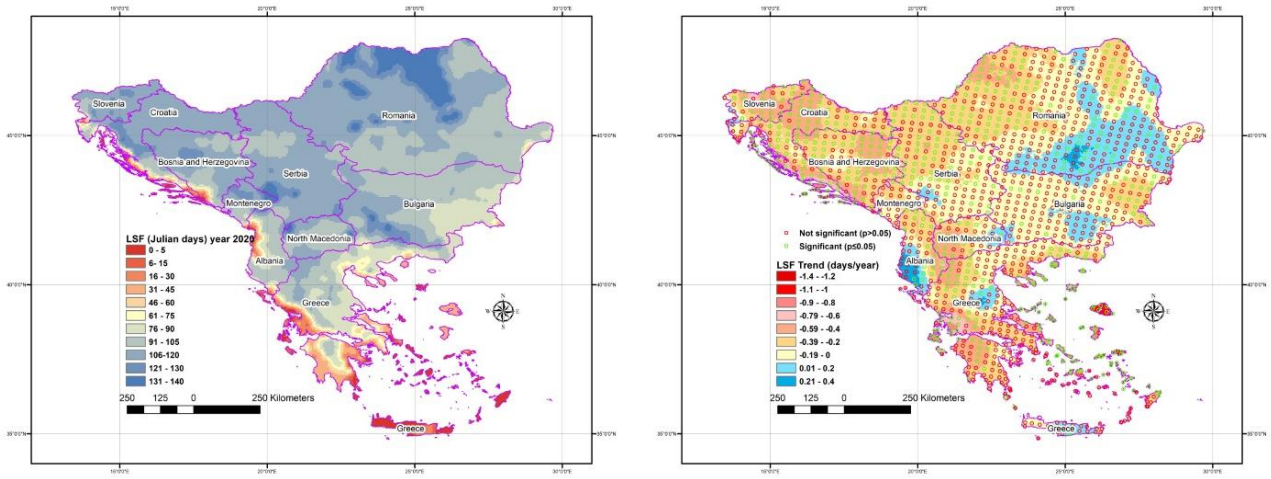

Figure 2. LSF *Julian days* spatial distribution in 2020 (left) and LSF trend *in days/ year* (right).

Considering that the spring frosts may endanger yields directly and indirectly(Lake et al., 2021; Risbey et al., 2019), a strip of land under low spring frost risk is shown. By combining this information with the right-hand side map, it is calculated that southern Albania has a positive trend from 0.01 d/yr to 0.4 d/yr. Therefore, this specific area will face increased spring frost risk in the years to come. A similar trend is recorded over the Thessalian plain in central Greece, which is one of the most productive areas of the country in terms of agricultural yields. Also, a positive LSF trend was calculated over the great Danubian plain on both sides of the Bulgarian – Romanian borders along with the Thracian basin in the southeastern part of Bulgaria. Negative trends result for the remaining area, indicating that the risk of late spring frost will be reduced in the following years.

3.3 Free of Frost Days (FFD)

Results on the FFD maygive helpful information about the length of the free frost period. Thus, the spatial distribution (Figure 3) for the year 2020 reveals beneficial conditions as a consequence of long FFD in the southern part of the Balkans and along the coastal strip of the Adriatic Sea. Also, the areas with a free frost window are located over the eastern part of Bulgaria and the Danubian plain. Contrarily, the central Balkan mountainous regions form a free of frost period with a duration smaller than 200 consecutive days.

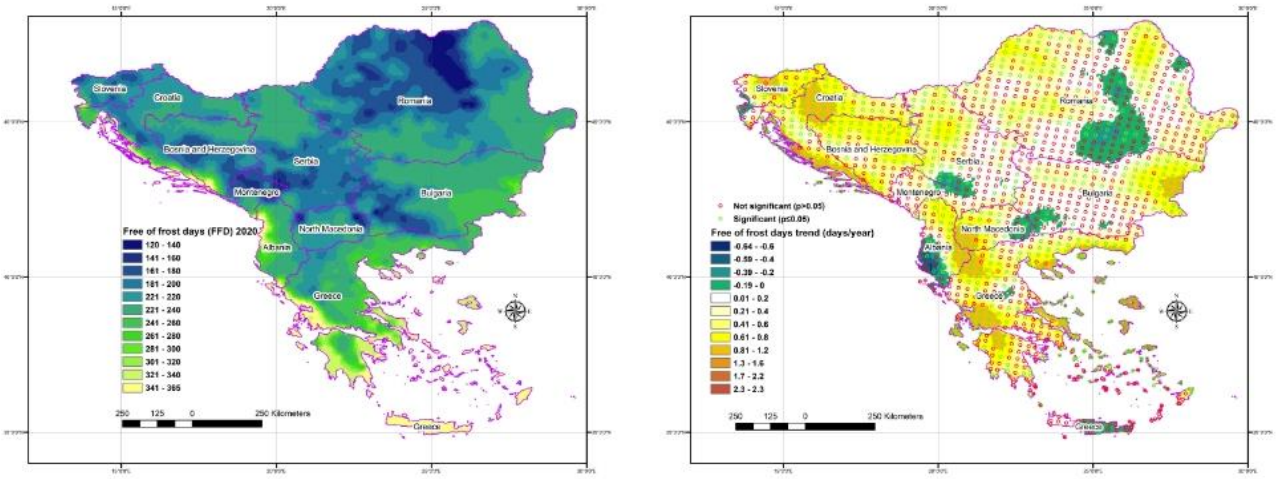

Figure 3. FFD number of days spatial distribution in 2020 (left) and FFD trend days/year (right).

It is important to mention that the regions in which a reduction of the free frost period will be shortened are the agricultural zone northern to the Romano-Bulgarian borders and the southern coastal part of Albania. The same trend is calculated for the eastern part of Crete Island and a small part of southwestern Serbia. On the other hand, the rest area is under a positive trend of FFD, indicating more extended cultivation periods between the LSF and FAF.

3.4 Frost Days (FD)

The following image in Figure 4 illustrates the FD probability density plots(Vermeesch, 2012) for two distinct time periods, 1980-1999 and 2000-2020, overall the studied countries. The alteration of the total frost days (FD) aggregated on an annual basis per country is displayed. In general, calculations demonstrate a high frost days reduction over all the countries examined. The highest reductions occurred in Slovenia, with 23 frost days annually for the 2000-2020 period compared withthe 1980-1999 period. Bosnia and Herzegovina followwith a reduction of 21 frost days between the two time periods. The lowest reduction is recorded forGreece (EL), with 4frost days.

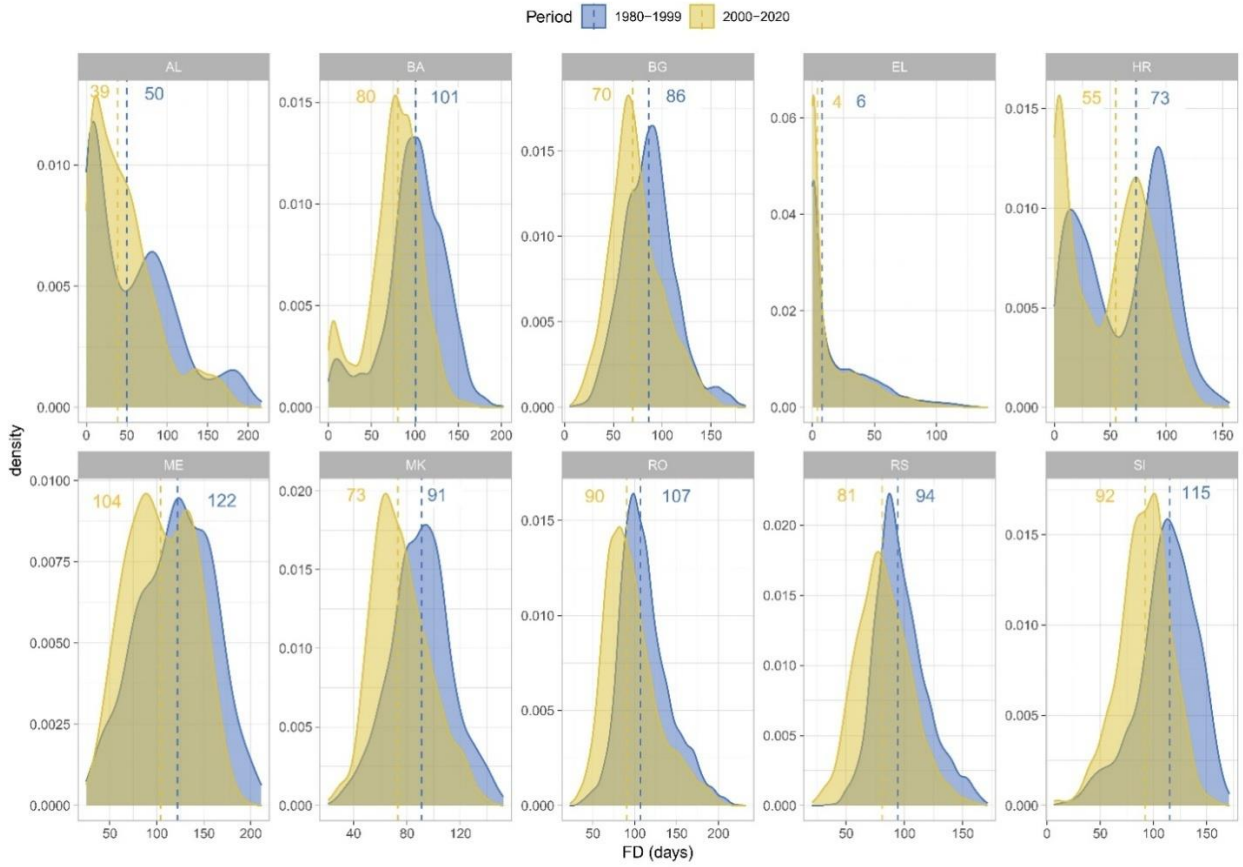

Figure 4. FD density plots per country.

In addition, the density distributions are unimodal in most cases. It is evident that the frost days demonstrate a decreasing tendency from 1980-1999 to the 2000-2020 period. The general outcome related to the reducing trend of the number of frost days on an annual basis is in accordance with similar research studies by Trnka et al. (2011), Kostopoulou and Jones (2005), Lavalle et al. (2009) and Ruml etal. (2012).

4 Summary

The results of the present study may lead to some conclusions related to the frost conditions and trends over the southeastern part of the European continent. First, in general, the frost phenomenon tends to be more sparse whereas its occurrence frequency will be reduced in the near future. The free of frost period will be explanting over most of the studied area, giving a longer uninterrupted growing season. In addition, the last spring frost, which is one of the most critical frost indices, will be reduced (lower Julian day). Still, there is a positive tension over some of the most important agricultural areas of the studied area. The first autumn frost tends to be reduced in most ten selected countries. Finally, the used dataset has the adequate spatiotemporal resolution to fulfil the needs of frost research like the presented one.

References

Alexandrov, V.A., Hoogenboom, G., 2000. The impact of climate variability and change on crop yield in Bulgaria. Agricultural and Forest Meteorology 104, 315–327. https://doi.org/10.1016/S0168-1923(00)00166-0

Biavetti, I., Karetsos, S., Ceglar, A., Toreti, A., Panagos, P., 2014. European meteorological data: contribution to research, development, and policy support, in: Second International Conference on Remote Sensing and Geoinformation of the Environment (RSCy2014). Presented at the Second International Conference on Remote Sensing and Geoinformation of the Environment (RSCy2014), International Society for Optics and Photonics, p. 922907. https://doi.org/10.1117/12.2066286

Biazar, S.M., Ferdosi, F.B., 2020. An investigation on spatial and temporal trends in frost indices in Northern Iran. Theor Appl Climatol 141, 907–920. https://doi.org/10.1007/s00704-020-03248-7

Charalampopoulos, I., 2020. The R Language as a Tool for Biometeorological Research. Atmosphere 11, 682. https://doi.org/10.3390/atmos11070682

Charalampopoulos, I., Polychroni, I., Psomiadis, E., Nastos, P., 2021. Spatiotemporal Estimation of the Olive and Vine Cultivations' Growing Degree Days in the Balkans Region. Atmosphere 12, 148. https://doi.org/10.3390/atmos12020148

Cheval, S., Dumitrescu, A., Birsan, M.-V., 2017. Variability of the aridity in the South-Eastern Europe over 1961–2050. CATENA 151, 74–86. https://doi.org/10.1016/j.catena.2016.11.029

Ci, H., Zhang, Q., Singh, V.P., Xiao, M., Liu, L., 2016. Spatiotemporal properties of growing season indices during 1961–2010 and possible association with agroclimatological regionalization of dominant crops in Xinjiang, China. Meteorol Atmos Phys 128, 513–524. https://doi.org/10.1007/s00703-015-0419-8

Cressie, N., 2015. Statistics for spatial data. John Wiley & Sons.

Droulia, F., Charalampopoulos, I., 2022. A Review on the Observed Climate Change in Europe and Its Impacts on Viticulture. Atmosphere 13, 837. https://doi.org/10.3390/atmos13050837

Droulia, F., Charalampopoulos, I., 2021. Future Climate Change Impacts on European Viticulture: A Review on Recent Scientific Advances. Atmosphere 12, 495. https://doi.org/10.3390/atmos12040495

Giannakopoulos, C., Kostopoulou, E., Varotsos, K.V., Tziotziou, K., Plitharas, A., 2011. An integrated assessment of climate change impacts for Greece in the near future. Reg Environ Change 11, 829–843. https://doi.org/10.1007/s10113-011-0219-8

Kassambara, A., 2020. ggpubr: "ggplot2" Based Publication Ready Plots [WWW Document]. URL https://CRAN.R-project.org/package=ggpubr (accessed 4.20.21).

Klik, M., Collet, Y., 2020. fst: Lightning Fast Serialization of Data Frames for R [WWW Document]. URL https://CRAN.R-project.org/package=fst (accessed 7.1.20).

Knox, J., Daccache, A., Hess, T., Haro, D., 2016. Meta-analysis of climate impacts and uncertainty on crop yields in Europe. Environ. Res. Lett. 11, 113004. https://doi.org/10.1088/1748-9326/11/11/113004

Kogo, B.K., Kumar, L., Koech, R., Langat, P., 2019. Modelling Impacts of Climate Change on Maize (Zea mays L.) Growth and Productivity: A Review of Models, Outputs and Limitations. Journal of Geoscience and Environment Protection. https://doi.org/10.4236/gep.2019.78006

Kostopoulou, E., Jones, P.D., 2005. Assessment of climate extremes in the Eastern Mediterranean. Meteorol. Atmos. Phys. 89, 69–85. https://doi.org/10.1007/s00703-005-0122-2

Lake, L., Chauhan, Y.S., Ojeda, J.J., Cossani, C.M., Thomas, D., Hayman, P.T., Sadras, V.O., 2021. Modelling phenology to probe for trade-offs between frost and heat risk in lentil and faba bean. European Journal of Agronomy 122, 126154. https://doi.org/10.1016/j.eja.2020.126154

Lavalle, C., Micale, F., Houston, T.D., Camia, A., Hiederer, R., Lazar, C., Conte, C., Amatulli, G., Genovese, G., 2009. Climate change in Europe. 3. Impact on agriculture and forestry. A review. Agron. Sustain. Dev. 29, 433–446. https://doi.org/10.1051/agro/2008068

Moriondo, M., Bindi, M., 2007. Impact of climate change on the phenology of typical Mediterranean crops. Italian Journal of Agrometeorology 3, 5–12.

Önol, B., H. M. Semazzi, F., 2009. Regionalization of Climate Change Simulations over the Eastern Mediterranean. J. Climate 22, 1944–1961. https://doi.org/10.1175/2008JCLI1807.1

Risbey, J.S., Monselesan, D.P., O'Kane, T.J., Tozer, C.R., Pook, M.J., Hayman, P.T., 2019. Synoptic and Large-Scale Determinants of Extreme Austral Frost Events. Journal of Applied Meteorology and Climatology 58, 1103–1124. https://doi.org/10.1175/JAMC-D-18-0141.1

Ruml, M., Vuković, A., Vujadinović, M., Djurdjević, V., Ranković-Vasić, Z., Atanacković, Z., Sivčev, B., Marković, N., Matijašević, S., Petrović, N., 2012. On the use of regional climate models: Implications of climate change for viticulture in Serbia. Agricultural and Forest Meteorology 158–159, 53–62. https://doi.org/10.1016/j.agrformet.2012.02.004

Scheifinger, H., Menzel, A., Koch, E., Peter, Ch., 2003. Trends of spring time frost events and phenological dates in Central Europe. Theor. Appl. Climatol. 74, 41–51. https://doi.org/10.1007/s00704-002-0704-6

Sjoberg, D.D., Curry, M., Hannum, M., Larmarange, J., Whiting, K., Zabor, E.C., Drill, E., Flynn, J., Lavery, J., Lobaugh, S., Wainberg, G.Z., 2021. gtsummary: Presentation-Ready Data Summary and Analytic Result Tables [WWW Document]. URL https://CRAN.R-project.org/package=gtsummary (accessed 4.21.21).

Terando, A., Easterling, W.E., Keller, K., Easterling, D.R., 2012. Observed and Modeled Twentieth-Century Spatial and Temporal Patterns of Selected Agro-Climate Indices in North America. J. Climate 25, 473–490. https://doi.org/10.1175/2011JCLI4168.1

Trnka, M., Brázdil, R., Dubrovský, M., Semerádová, D., Štěpánek, P., Dobrovolný, P., Možný, M., Eitzinger, J., Málek, J., Formayer, H., Balek, J., Žalud, Z., 2011. A 200-year climate record in Central Europe: implications for agriculture. Agron. Sustain. Dev. 31, 631–641. https://doi.org/10.1007/s13593-011-0038-9

Vermeesch, P., 2012. On the visualization of detrital age distributions. Chemical Geology 312–313, 190–194. https://doi.org/10.1016/j.chemgeo.2012.04.021

Wickham, H., François, R., Henry, L., Müller, K., 2020. dplyr: A Grammar of Data Manipulation [WWW Document]. URL https://CRAN.R-project.org/package=dplyr (accessed 4.25.20).

Wypych, A., Ustrnul, Z., Sulikowska, A., Chmielewski, F.-M., Bochenek, B., 2017. Spatial and temporal variability of the frost-free season in Central Europe and its circulation background. International Journal of Climatology 37, 3340–3352. https://doi.org/10.1002/joc.4920

SESSION 4:

WATER MANAGEMENT FOR AGRICULTURE

A Brief History of Wastewater Reclamation and Reuse

Andreas N. Angelakis[1] and Vasileios Tzanakakis[2]

[1] Joint IWA/IWHA-SG on Water History and Hellenic Union of Water Supply and Sewerage Enterprise, 41222 Larisa, Greece; angelak@edeya.gr
[2] Department of Agriculture, School of Agricultural Science, Hellenic Mediterranean University, Iraklion, 71410 Crete, Greece; vtzanakakis@hmu.gr

Abstract: This paper provides a brief overview of the evolution of water reuse over the last 5,000 years, along with current practice and recommendations for the future. Understanding the practices and solutions of the past, provides a lens with which to view the present and future.
From the beginning of the Bronze Age (*ca*. 3,200-1,100 BC), domestic wastewater (sewage) has been used for irrigation and aquaculture by a number of civilizations. In historic times (*ca.* 1000 BC-476 AD), wastewater was disposed or used for irrigation and fertilization purposes by the Greek and later Roman civilizations, especially in areas surrounding important cities (e.g. Athens and Rome). In more recent times, the practice of land application of wastewater for disposal and agricultural use was utilized first in European cities and later in USA. Today, water reclamation and reuse projects are being planned and implemented throughout the world. Recycled water is now used for almost any purpose including potable use.

Keywords: Water reuse history, sewage farms, water reuse trends and challenges, water reuse criteria, water reuse categories, potable reuse.

1. Prolegomena

The more you look back in the past, the more you see into the future
Sir Winston Leonard Spencer-Churchill (1874-1965).

Wastewater treatment and reuse has a long history. These practices passed through different development stages with time, in regards to knowledge of the processes, treatment technology, and evolution of regulations and/or guidelines Since prehistoric civilizations to Hellenic civilizations and later by Romans, reuse became a common practice serving disposal, irrigation, and fertilization purposes.(Tzanakakis et al. 2014) In more recent history, since 16th century to nowadays, wastewater reuse practices continue to evolve serving mainly irrigation and fertilization purposes. Despite the decline that occurred in the first half of the 20th century, reuse came to the fore again mainly in areas with water scarcity problems.

A review paper on water reuse is presented. This paper is organized as follows: Section 1 Prolegomena is an introductory to the theme and elements of the review, followed by Sections 2–5 that explain the distinct histories of water reuse from the prehistoric era to present time in a geographical and chronological view. Finally, Section 6 is the epilogue that includes conclusive remarks and highlights.

2. Prehistoric Times (*ca* 3,200-1,100 BC)

The first indications of the utilization of wastewater for irrigation and fertilization of agricultural lands extend back ca 5,000 years to the Bronze Age civilizations (e.g. Minoan and Indus Valley) (Angelakis *et al.,* 2018). Minoans developed advanced sewerage systems to dispose of wastewater to rivers (e.g., Palaces of Knossos), to the sea (e.g. Palace of Zakros), or to agricultural land for irrigation and fertilization purposes (e. g. Palace of Phaistos and Villa of Hagia Triada). A good example is in the Palace of Phaistos, where the end of the wastewater and stormwater sewage and drainage system is used to divert wastewater and stormwater to the farmland.

In the Indus Valley (modern-day Pakistan) similar advanced sewerage and drainage systems have been utilized dating back to ca 2,600 BC. These systems, such as those in the cities of Harappa and Mohenjo-Daro, are important because they made it possible to develop a thriving civilization in Indus

Valley (Angelakis et al., 2018). In the city of Harappa, every house was connected to the main sewer ensuring the proper removal of the wastes. To insure that the system functioned properly maintenance, inspection holes were provided (Gray, 1940). Local drains were covered and connected to larger sewers used to transport the collected wastewaters for disposal to agricultural lands. Use of human and other wastes for aquaculture was also practiced as early as ca 1,100 BC in various regions in China during the Yin dynasty.

3. Historical Times (*ca*. 1,100 BC-476 AD)

The Ionian philosopher Anaximander (ca 610-547 BC) first referred to meteorological phenomena and the hydrological processes and broadly speaking to water recycling: *Rains are generated from the evaporation (atmis) that is sent up from the earth toward under the sun* (Hippolytus Ref. I 6, 1-7-D. 559 W.10). Thereafter Aristotle (384-322 BC) understood the water phase change: *The sun causes the moisture to rise…….Even if the same amount of water does not come back ever year and in a given place, yet in a certain period all quantity has been abstracted is returned* (ibid, II.2, 355a 26) (Koutsoyiannis and Angelakis, 2003). He also reported that: *Salt water when it turns into vapour becomes drinkable [freshwater] and the vapour does not form salt water when it condenses again; this I know by experiment*. (Meteorologica II 3). Thus very early the truth is that all water is always reused.

Throughout the ages, human civilizations have paid close attention to wastewater and reused it in various ways. In arid climates, in particular, wastewater would pass through many reuse cycles, a fact attested to by both Classical Greek, and Jewish and Roman literature. Furthermore, unplanned, incidental or *de facto* reuse of wastewater had a very long history throughout the medieval periods (Angelakis and Rose, 2014).

4. Medieval Times (*ca* 476-1,400 AD)

During the post Roman period (ca 476-1400 AD) there was no improvement in methods of waste removal in Europe for many centuries. With the advent of the Dark Ages little progress was made for 1400 years, from the late forth century. However, in several Asian countries (e.g. China, India, and Vietnam) were implemented various types of sewerage and drainage systems in the religious temples developed under several dynasties, which disposed partially to the surrounding agricultural land.

In Europe during Medieval times, water technology and knowledge made little progress. During that period, the emphasis was on wars rather than on civilization. Sanitation, in the best cases, reverted to the basics, becoming very primitive in most towns. As a result, disease outbreaks were commonplace; epidemics decimated towns and villages. In Europe, during Medieval times at least 25 % of the population died due to cholera, plague, and other water borne diseases (Schladweiler, 2002). Gradually, as populations expanded, the disposal of human feces became an issue in large cities during the Middle Ages. Waste disposal was for the most part unregulated. For instance, in Paris it was only in 1530 that a municipal decree required property owners to construct cesspools in each new dwelling (Burian and Edwards, 2002). Generally, each neighborhood and community had a self-interested attitude towards water supply and municipal wastewater services. Citizens were willing to pay for sewers to drain their neighborhood, but only into the next one (Burian and Edwards, 2002). This vision was unfortunately exported to Australia and to the Americas once colonialized.

Although there was turmoil in Europe during medieval times, some innovative ways to reuse water were developed and used in early Central and South America before colonization. The *Chinampa* is one of these. *Chinampas* are a Mesoamerican agriculture practice that has been described as floating gardens. *Chinampas* do not need irrigation and are small but very high productive plots artificially built over wetlands, marshes, shallow lakes or flood plains using sediments, manure, compost, and vegetation debris (Angelakis et al., 2018). *Chinampas* are considered to be the most productive and ecologically sustainable form of agriculture in pre-Hispanic Mesoamerica, as they reclaim solid and liquid wastes improving and protecting local biodiversity (Morehar, 2012). The exact origin of *Chinampas* is not well known but Aztecs (ca 1,200-1,500 AD) were among the first civilizations documenting its use in pyramid paintings. Here again, observation of the benefits of animal and human waste must have played an important role in the development of the *Chinampas* (Coe, 1964).

5. Water Reuse in Early and Mid-modern Times (*ca.* 1400- 1900 AD)

Sanitation practices re-emerged in force in the mid-nineteenth century following the great epidemics in several regions of the world. During that period, authorities recognized the need for sanitation and this led to the development of effluent application practices, known as “sewage farms” as a means to protect public health and to control water pollution (Stanbridge, 1976; US EPA, 1979). For the first time in sanitation legislation, criteria with reference to “sewage farms” were developed. In the more recent history, the earliest documented ‘sewage farms’ (i.e. wastewater application to the land for disposal and agricultural use) were operated in Bunzlau (Silesia/Poland) in 1531 and in Edinburgh (Scotland) in 1650, where wastewater was used for beneficial crop production (Tzanakakis *et al*., 2014). At the end of 18th century, large ‘sewage farms’ were established in many rapidly growing cities of Europe and the United States as well as in Australia in 1897 (Reed *et al*., 1995; Tzanakakis *et al*., 2014). Other terms used for such operations were “broad irrigation,” and “land treatment” where sewage is applied intermittently to land at a low rate of flow, such that it does not interfere with the growth or harvesting of the cultivated crops. These practices were increasingly seen as a solution for the disposal of large volumes of produced wastewater, some of them are still in use as shown in Table 1. Land treatment was, in fact, the first wastewater treatment process applied on a large scale in the mid-19th century.

The first engineered systems of land application of urban wastewater for agricultural irrigation were implemented in Paris, France and Milan, Italy urban areas. Following the extension and modernisation of the Paris sewers in 1850s, the first regulation on water reuse by spreading was published in 1899 (Lazarova *et al*., 2013). Paris was a typical example with the first sewage farms established at Gennevilliers in 1872, handling, after an extension, the wastewater of the whole town. At the beginning of 20th century, the sewage farms reached their maximum extent in France established in four different areas; in Gennevilliers (900 ha), in Achères (Achères plain, 1400 ha), in Pierrelaye (2010 ha), and in Triel (950 ha), using the raw wastewater which was supplied by the Colombes pumping station in Paris (Jimenez and Asano, 2008; Lazarova *et al*., 2013). In Milan, the first irrigation consortium was constituted in 1881 for irrigation of 3,500 ha with urban sewage. In parallel, the first handbooks on sanitary engineering were published in France and Italy. In the United States, this practice was first used at the State Insane Asylum near Augusta, Maine, in 1876.

Table 1. Selected early land treatments and reuse systems (Angelakis et al., 2018).

Location	Date started	Type of land based system	Area (1000 ha)	Flow (m^3/d)
Europe				
Bunzlaw, Poland	1531	Sewage farms		
Edinburgh, UK[a]	1650	Sewage farms		
Croydon-Beddington, UK	1860	Sewage farms	0.25	17.4
Paris, France	1869	Irrigation	0.64	30.3
Leamington, UK	1870	Sewage farms	0.16	3.4
Berlin, Germany	1874	Sewage farms	2.7	N/A
Augusta, ME, USA	1876	Irrigation		
Milan, Italy	1881	Irrigation	3.5	
Wroclaw, Poland	1882	Sewage farms	0.80	10.6
Braunschweig, Germany	1896	Sewage farms	4.4	60.0
USA				
Calumet City, MI	1888	Irrigation	0.005	
South Framingham, MA	1889	Irrigation		
Woodland, CA	1889	Irrigation	0.07	15.5
Boulder, CO	1890	Irrigation		

Fresno, CA	1891	Irrigation	1.60	10.6
San Antonio, TX	1895	Irrigation	1.60	75.7
Vineland, NJ	1901	Rapid infiltration system	0.0026	3405.9
Ely, NV	1908	Irrigation	0.16	6.1
Lubbock, TX	1915	Irrigation		
Others				
Tula (Mezquital) Valley Mexico[b]	1896	Irrigation	90.00	
Melbourne, Australia	1897	Irrigation	4.16	189.3

Adapted from Jimenez and Asano, 2008; Metcalf and Eddy, Inc., 1991; Reed and Crites, 1984; Tzanakakis *et al.,* 2014.

[a]The value of wastewater as a fertilizer was well recognized in 1650.

[b]The initial irrigated area was of less than 2000 ha but currently is of 90,000 ha after reaching a maximum of 110,000 ha in 1995.

In Mexico, drainage canals were built around 1890 to take wastewater from Mexico City to provide irrigation water for agricultural lands in the Mezquital valley. The scheme now irrigates up to 90,000 ha of agricultural crops and is the largest scheme in the world. An added benefit has been the recharge of groundwater in the region (Jimenez and Asano, 2008). In Germany, the sewers introduced in cities during the 19th and 20th centuries led in many cases into systems of ponds and fields for direct recycling through sophisticated agriculture and aquaculture systems. In the Danish capital Copenhagen, in the early 20th century, new investments in a traditional dry sanitation system linking agriculture with the city was soon replaced by a sewer system discharging untreated sewage for decades into the Baltic Sea (Angelakis *et al.,* 2018).

6. Water Reuse in Contemporary Times (1900 AD-present)

The advent of 20th century brought significant technological innovations and growth in wastewater treatment plants that were able to handle large volumes of wastewater for direct discharge to waterways and the ocean. These plants were widely adopted by many major urban centres around the globe as they were compact and did not require large areas for treatment compared to sewage farms (Metcalf and Eddy, Inc., 1991; Jimenez and Asano, 2008; Lazarova et al., 2013).

Since the beginning of the 20th century, wastewater reclamation and reuse and resources management concept have been promoted by different regions and governmental agencies. As a result, a variety of water reuse criteria for use of reclaimed water for crop irrigation and other beneficial uses were developed and adopted. These rules and regulations have been developed primarily to protect public health and water resources. In England, in 1912, the “Royal Commission on Sewage Disposal” adopted for the first time standards for effluent discharge that included limits of 20 mg/L for BOD and 30 mg/L for suspended solids (US EPA, 1979). A few years later, in 1918, California State Board of Public Health set up the first regulations for use of sewage for irrigation purposes.

Establishing guidelines for water reuse is a challenge because of the absence of comprehensive international guidelines, and of a scientific consensus on the approach that should be adopted to issue such guidelines. This has also led to inconsistencies between the guidelines that are already implemented in countries. Additional research is therefore needed. The research should be directed towards reducing persistent uncertainty about the potential for adverse human health effects from exposure to recycled water and to increase confidence in water reuse.

Many things have changed in the water reclamation and reuse field during the last three decades. One of the most relevant is the recognition of reclaimed water as an essential component of integrated water resources management. Reclaimed water has become a new, additional, alternative, reliable water supply source for numerous uses in the diverse environment. The water reuse frontier has expanded from agricultural and landscape irrigation and restricted urban uses, to indirect potable reuse and even direct potable reuse at current time (Mujeriego, 2013). In this context, water reclamation and reuse are defined more precisely as follows (Asano *et al.,* 2007): (a) “Water reclamation” – Treatment or processing of

wastewater to make it reusable with definable treatment reliability and water quality criteria. And (b) "Water reuse" – The use of treated wastewater for a beneficial use, such as agricultural irrigation and industrial cooling. Applications and examples of water reuse are given in Table 2.

Table 2. Water reuse cases around the globe (Jones et al., 2021; Sato et al., 2013; Goyal, 2022)

S. No.	Region	Notable countries/cities	Reuse Volume (cubic km)	Applications	Examples
1.	North America	United States of America, Canada	9.1	Direct potable reuse, Environmental Recreation, Irrigation, Municipal, Industrial	Orange county DPR system, Big spring Texas IPR, Arizona, California (DPR), Pomona plant, Los Angeles, commercial buildings in British Columbia, Toronto Healthy house, Refinery complexes, Regina etc.
2.	South America	Argentina, Brazil, Chile, Colombia, Mexico, Peru	2.1	Irrigation	Mezquital Valley, Mexico, Caribbean Islands, irrigation and washing of roads and monuments, Sau Paulo and Fortaleza, Brazil
3.	Europe	Spain, Cyprus, Germany, Belgium, Malta, Greece, Italy, France	6.7	Agricultural, Environmental, Industrial	Direct aquifer recharge, Barcelona, Girona, (Golf course irrigation), Groundwater recharge in Flanders, Northern Belgium, Sant Antnin sewage treatment plant, Malta, Artificial surface and groundwater recharge, Berlin etc.
4.	Middle East and Africa	Israel, Namibia, Egypt, Kuwait, Tunisia, Ghana, Ethiopia, Saudi Arabia, South Africa, Jordan	7.7	Irrigation	Windhoek DPR plant, Namibia, IPR in Israel (Tel-Aviv, Dan region project), Agricultural and landscape irrigation in Tunisia, Durban Water recycling plant , Virginia Pipeline Project Adelaide, South Australia, Oil refineries in Geelong (Victoria), Kwinana Water Reclamation Plant etc.etc.
5.	Asia-Pacific	Japan, China, India, Hong Kong, Singapore, South Korea, Brisbane, Melbourne, Sydney, Perth	15	Agricultural, Industrial, Indirect potable reuse, Recreational	NEWater Reclamation Plant, Singapore, Toilet flushing, Shinjuku, Tokyo, Kitakyushu region (Fukuoka), and Tokai region
6.	Russia	Moscow, Vladivostok, St. Petersburg	0.99	Industrial	Oil Refineries in north western region

A number of factors such as costs reduction in pumping, necessity of maintaining dual-distribution systems and desirability of full reuse of available water in the metropolitan areas dictate that purified water will be destine to be a source of potable water supply in the future (Drewes and Khan, 2011; Tchobanoglous *et al*., 2011). Direct potable reuse will require, however, public confidence and acceptance, performance, efficiency, reliability and cost-effectiveness of treatment technologies to always produce water that is safe and acceptable to consume.

7. Epilogue

The intended water reuse applications must govern the degree of wastewater treatment required and the reliability of wastewater reclamation processes and operation, where technical solutions have to match capacities, and where urban source treatment should be implemented along a multiple-barrier approach combining treatment and different health protection measures. As water reuse for food crop production will remain a major option, the challenge is to integrate agriculture into urban sanitation concepts with the additional advantage of water and nutrient recycling as two of the major ways of closing the water and nutrients loops in the urban-rural interface addressing the water SDG targets.

A large variety of water reuse criteria exists. Efforts for making more consistency among different regulations and guidelines related to water quality should be fostered. For the sake of integrated water management and to gain public understanding and acceptance, water reuse regulations should be part of a set of consistent water regulations applying to drinking water, bathing water, irrigation water, discharge, etc.

Today, water reclamation technologies exist to produce water of almost any quality desired including purified water of quality equal to or higher than drinking water. Potable reuse studies and projects have demonstrated the capability of producing water of excellent quality and ensuring system reliability with health risks not greater than the existing water supplies. Among the most pressing issues, those repeatedly emphasized are “necessity and opportunities” for water reuse, public perception and acceptance, risks and safety of reclaimed water, water rights and economics of reclaimed water in the context of integrated water resources management.

References

1. Angelakis, A. N. and Rose, J., (Eds.) (2014). Evolution of Sanitation and Wastewater Management through the Centuries. IWA Publishing, London, UK, xxx, 529.
2. Angelakis, A. N., Asano, T., Bahri, A., Jimenez, B. E., and G. Tchobanoglous, G. (2018). Water Reuse: From ancient to the modern times and future. Front. Environ. Sci. 6 (26): 1-17, doi: 10.3389/fenvs.2018.00026.
3. Asano, T., F. L. Burton, H. Leverenz, R. Tsuchihashi, and G. Tchobanoglous (2007) Water Reuse: Issues, Technologies, and Applications, McGraw-Hill, New York. p. 38.
4. Burian, S. J. and Edwards, F. G. (2002). Historical Perspectives of Urban Drainage. Proceedings of 9th International Conf. on Urban Drainage, ASCE. Portland, OR, USA, http://dx.doi.org/10.1061/40644(2002)284).
5. Coe, M. D. (1964). The Chinampas of Mexico. Sci. Amer. 211 (1), 90-99.
6. Drewes, J.E. and S.J. Khan (2011). Water Reuse in Drinking Water Augmentation. In Water Quality & Treatment: A Handbook on Drinking Water, Edzwald, J.K. (ed.), McGraw-Hill, New York, USA.
7. Gray, H. F. (1940). Sewerage in Ancient and Medieval Times. Sewage Works J. 12 (5): 939–946.
8. Goyal kirti. Ph.d. thesis. Decision support system for treated wastewater reuse by department of hydro and renewable energy. Indian institute of technology roorkee, roorkee-247667 (India). February, 2022.
9. Jimenez, B. and T. Asano, (Eds.) (2008). Water Reuse: International Survey of Current Practice, Issues and Needs, Scientific and Technical Report No. 20, IWA Publishing, London, UK.
10. Jones, E. R., Van Vliet, M. T. H., Qadir, M., & Bierkens, M. F. P. (2021). Country-level and gridded estimates of wastewater production, collection, treatment and reuse. Earth System Science Data, 13(2), 237–254. https://doi.org/10.5194/essd-13-237-2021
11. Koutsoyiannis, D. and Angelakis, A. N. (2003). Hydrologic and Hydraulic Sciences and Technologies in Ancient Greek Times. The Encycl. of Water Sci., Markel Dekker Inc., (B.A. Stewart and T. Howell, Eds.), Madison Ave. New York, N.Y., USA, pp. 415-417.
12. Lazarova, V., Asano, T., Bahri, A. and Anderson, J. (Eds.) (2013). Milestones in water reuse – The best success stories. IWA Publishing, London, UK, ISBN: 9781780400075. pp. 408.
13. Metcalf and Eddy, Inc. (1991). Wastewater Engineering. Treatment, Disposal, Reuse. 3rd edition, McGraw-Hill Inc., New York, US.

14. Morehar, C.T. (2012). Mapping ancient chinampa landscapes in the Basin of Mexico: a remote sensing and GIS approach. J. Arch. Sci. 39, 2541-2551.
15. Mujeriego, R., (2013). Foreword, in Lazarova, V., Asano, T., Bahri, A. and Anderson, J. (Eds.). Milestones in water reuse – The best success stories. IWA Publishing, London, UK.
16. Reed, S. C., Crites, R. W., and Middlebrooks, E. J. (1995). Natural Systems for Waste Management and Treatment. Second Edition, McGraw Hill Co, New York, NY, USA.
17. Sato, T., Qadir, M., Yamamoto, S., Endo, T., & Zahoor, A. (2013). Global, regional, and country level need for data on wastewater generation, treatment, and use. Agricultural Water Management, 130, 1–13. https://doi.org/10.1016/j.agwat.2013.08.007
18. Schladweiler, J. C. (2002). Tracking down the roots of our sanitary sewers. Historian: Arizona Water & Pollution Control Association (Member Association - WEF, Section - AWWA), Phoenix, AZ, USA, http://www.sewerhistory.org/time-lines/tracking-down-the-roots-of-our-sanitary-sewers/
19. Stanbridge, H. H. (1976). History of Sewage Treatment in Britain, Part 5 Land Treatment. The Institute of Water Pollution Control, Maidstone, Kent, UK.
20. Tchobanoglous, G., Leverenz, H., Nellor, M. H. & Crook, J. (2011) Direct potable reuse: A path forward. WateReuse Research and WateReuse California, Washington, DC.
21. Tzanakakis, V.E., Koo-Oshima, S., Haddad, M., Apostolidis, N., and Angelakis, A. N. (2014). The history of land application and hydroponic systems for wastewater treatment and reuse. In: Evolution of Sanitation and Wastewater Management through the Centuries; (A.N. Angelakis and J.B. Rose, Eds.); IWA Publishing: London, UK, Ch. 24: 459-482.

US. EPA (1979). A history of land application as a treatment alternative. US. EPA, EPA 430/9-79-012, Apr. 1979. EPA, Washington DC, USA.

DEVELOPMENT OF A DECISION SUPPORT SYSTEM FOR THE IRRIGATION AND THE CONTROL OF *Helicoverpa armigera* IN GREECE

Dimitrios LEONIDAKIS[1], Vasilis PAPAKONSTANTINOU[1], Nikolaos KATSENIOS[2], Christoforos-Nikitas KASIMATIS[2], Evangelos PSOMAKELIS[3,4], Gabriel MAVRELLIS[5], Christos LEKARAKOS[2], Aspasia EFTHIMIADOU[2*]

[1] Farmacon G.P., K. Therimioti 25, Giannouli, Larisa, 41500 Thessaly, Greece

[2] Department of Soil Science of Athens, Institute of Soil and Water Resources, Hellenic Agricultural Organization-Demeter, Sofokli Venizelou 1, Lycovrissi,14123 Attica, Greece

[3] School of Electrical and Computer Engineering, National Technical University of Athens, 15780 Athens, Greece

[4] Department of Informatics and Telematics, Harokopio University of Athens, 17778 Athens, Greece

[5]Geospatial Enabling Technologies (GET), Athens, Greece

Abstract. Cotton (*Gossypium hirsutum*) is a plant cultivated in many regions of Greece and is of major significance for the Greek agricultural sector. There are two important factors that affect the quality and yield of cotton crops. The first factor is irrigation, as rainwater levels are inadequate, the use of irrigation water is mandatory most of the times. The second is the control of the pest *Helicoverpa armigera*, commonly known as cotton bollworm. Technological advances and the adoption of Decision Support Systems (DSSs) in the agricultural section have become an important tool in crop management and sustainable agriculture, since they could be used for reducing irrigation water and pest monitoring. DSSs are computerized systems that can assist in complex decision-making activities. Machine learning algorithms are integrated in those systems allowing the prediction of different scenarios, leading in evidence-based decisions. Therefore, the development of a DSS that will be used for advising farmers in cotton production providing them with advice regarding the management of cotton cultivation is necessary. The system will retrieve real-time data from IoT sensors and satellite data combined with the use of predictive entomological models and electronic pheromone traps to monitor insect population. The developed DSS will use real time data, aiming at predicting the irrigation water needed, as well as required spraying for pest protection. As a result, valuable resources will be saved. Moreover, responsible and sustainable use of inputs is promoted by limiting the use of excessive irrigation and input of chemicals in the aquatic ecosystem. Lastly, the goal of the developed DSS, is to reduce the irrigation times and the amount of required spraying for pest protection without affecting the quality and yield of the crops.

1 Introduction

Technological improvements nowadays have made traditional techniques seem time consuming as farmers need up-to-date information about their field. Agriculture faces enormous challenges given the demand for sustainability (Garnett et al., 2013). Moreover, agriculture is called to almost doubling the production and at the same time to decrease or at least maintain the existing ecological footprint (Sundmaeker et al., 2016). In order to manage the increase in the complexity of farming systems, various new technologies have an important role and especially the information and communication technologies (ICT) (Aubert et al., 2012). Various types of ICT systems and their applications, such as smart farming and precision farming (Precision Agriculture - PA), are expected to play an important role in managing complexity and achieving the goal (Sundmaeker et al., 2016). Specific types of information systems, also known as Agricultural Decision Support Systems (AgriDSS), have been developed for the application of precision farming or smart farming.

The Agricultural Decision Support Systems should contribute to the maximum for the sustainable development of the farmers' business with the least negative impact on the environment. Moreover, DSSs should not only be limited to provide up-to-date and relevant information on the state of the field, but they should also help improve the yield or the quality characteristics of the crops (Kasimatis et al., 2022)

Smartphones and tablets have been invaded in the rural population to a great extent, both in developed and developing countries. However, farmers with internet access are facing an over-information state from systems or digital tools that aim to support the decisions that the farmers are called to make (Rose et al., 2016; Schröer-Merker et al., 2016). There are few references to mobile agricultural tools available (Costopoulou et al., 2016; Karetsos et al., 2014; Patel and Patel, 2016; Schröer-Merker et al., 2016) and most of them are limited to a

specific geographical location, agricultural system and / or agronomic issue. The list of mobile applications is constantly changing, as new products are released or updated, while others become obsolete. Despite the amount of information that producers can receive through applications, there is an opportunity for group and targeted learning through low-cost applications. Those applications integrate geophysical databases with agricultural information and social networking . New technology by itself is insufficient for successful adaptation to agriculture (Navarro-Hellín et al., 2016) ,but a mobile application can make it easier for people to acquire the knowledge that leads to better decision-making (Eichler Inwood and Dale, 2019).

2 Materials and Methods

For the implementation of the system, we will use different types of technologies, such as wireless IoT sensor networks, satellite images, databases and internet applications. The system uses all these technologies to collect information from the environment, to manage them, and to display them in a simple and understandable form to the user, wherever he is.

These technologies provide, process and analyze data of high spatial and temporal analysis, obtained from many sources, in order to support the decision-making of agricultural production. The systems that contribute to the collection and processing of information are:

- graphical Information Systems (GIS) data
- Global Position System (GPS)
- GIS and mapping applications
- Yield Mapping Systems
- Variable Rate Application Technology
- Remote Sensing
- Crop Production Modelling
- Decision Support Systems

A DSS will be developed to support the decision-making of the farmer. The system will be based on the development of specialized models for the determination of irrigation needs, forecasting and assessment of green worm infestation as well as automatic calculation of the phenology stage of the crop.

A series of soil moisture and air temperature sensors will be installed in the two areas where cotton is a basic crop, Thessaly and Thrace, in cooperation with cotton growers. Also, central stations for collecting the necessary meteorological data will be installed along with the creation of the appropriate network for receiving and processing the meteorological data.

The irrigation model will be based in the calculation of the evapotranspiration and all the necessary data will be collected by the installed meteorological stations. At the same time soil moisture sensors will be installed in the study fields. These sensors in cooperation with the required soil analysis for the granulometric properties of the soil as well as the quantification of the organic matter, will provide all the required information about the time and dose of irrigation to the crop, depending on its phenological stage.

Using satellite images in spectra that are highly correlated with the water status of plants, an attempt will be made to check and calibrate the algorithms for calculating evapotranspiration and consequently the irrigation needs that exist in the international literature.

For the development of the model for the monitoring of the green worm, the creation of a model based on degree days will be created. In addition to that, electronic pheromone traps will be used which they will send the number of arrests at regular time intervals. The most appropriate time period for chemical intervention will be determined in combination with the local meteorological data and the intensity of the arrests. Conventional pheromone traps will also be installed in order to confirm and verify the number of arrests.

The calculation of the phenological stages of the crop will be based on growing degree days (GDD) models, which are described analytically in the international literature and with the simultaneous visual confirmation from visits to the selected fields. The models that will be developed will be compared with field measurements of:

- the yield of the crop,
- the phenological stages of the crop,

- the pests and diseases of the crops (use of conventional pheromone traps alongside with the electronic pheromone traps),
- the air and soil moisture.

All the above field measurements will take place in 6 different fields at least in the study areas and the crops will be monitored for the whole cultivation season. The first monitoring period will lead to the learning and optimization of the models and then the models will be evaluated again.

The information system will integrate both the data of the measurements by the IoT sensors that will be installed in the fields, as well as the data of the collection, analysis and processing of the Sentinel-2 satellite. Utilizing free Sentinel-2 satellite data is particularly important as it will enable the coverage of large areas with high spatial accuracy (10-20 meters). However, it is more than necessary to calibrate the indices produced based on real field data, in order to obtain a valid and reliable set of indices.

Automated satellite data collection and analysis will be based on utilizing the Sentinel Hub subscription platform which provides an API for capturing and analyzing Sentinel images in near real time (once data is available at ESA's Scientific Hub). The API enables the calculation of spatial indices the ‘‘on the fly’’, but also the ability to download data for further analysis and processing.

The information platform that will be developed will be based on an open / modular architecture with the aim of future scaling and expansion. It will utilize open source software and technologies in order to reduce costs (development / operation / maintenance). This will utilize software such as the PostgreSQL database with the PostGIS extension for spatial data management and the Geoserver spatial data server which implements OGC standards (such as WMS, WFS, WCS, CSW, WPS) which are the basis for implementing modern spatial analysis applications. In addition, other free programming and application development libraries will be used, such as the python programming language, the javascript web application libraries Cesium (3D maps), openlayers (2D maps), GDAL (conversion of spatial grid data) and others. For mobile applications, technologies will be used that enable the development of applications for multiple operating system platforms (Android, iOS) such as AngularJS, Apache Cordova and Ionic.

The basic functionality of the proposed application will be the following:

- The user (farmer or agronomist) will use the application from his computer as well as his mobile phone or tablet where he will easily enter the fields of interest.
- The application will run the irrigation and forecasting models of the green worm that will be developed in local scale, then it will process the data received from the sensors and the electronic capture traps, as well as the latest satellite data.
- The application will then refer to a decision support system installed on Farmacon servers, which will retrieve the necessary information, compose the appropriate advices and send them to the application. Finally, the advices will be presented to the user.

The next figure presents the flow chart of the project, as well as all the subsystems that compose the final product

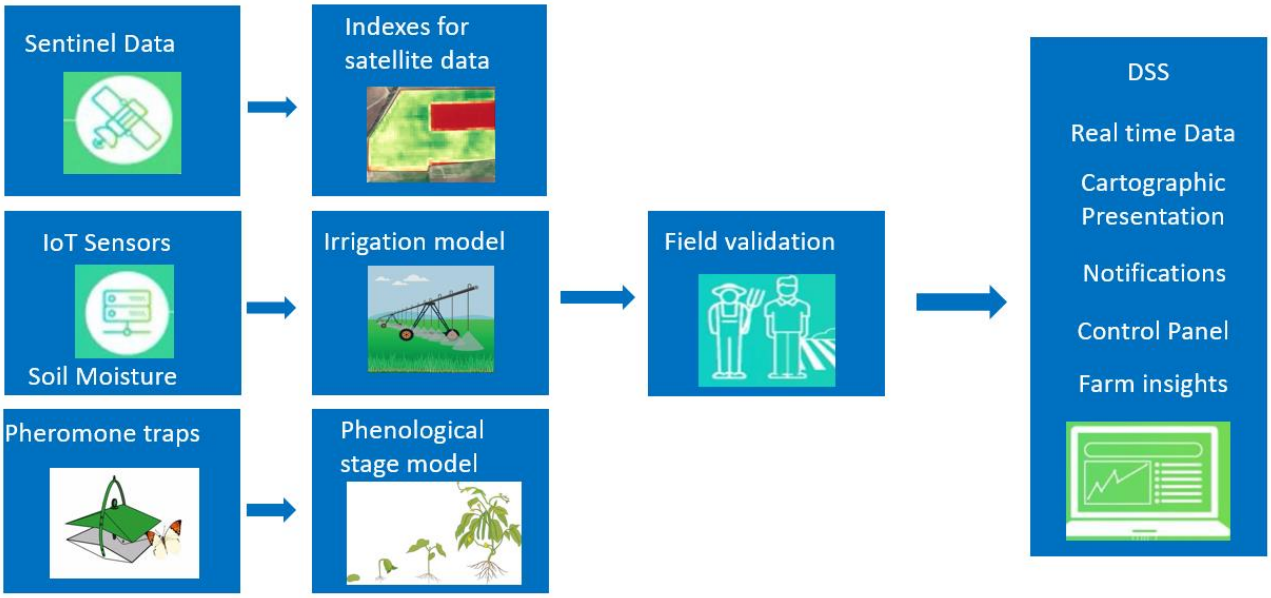

Figure 1. Flow chart of the project.

3 Results

The implementation of the DSS will optimize the use of the irrigation water, reducing it to the necessary amount. Moreover, it will alert the farmer for irrigation, improving time management. In addition, spray application will be reduced. All the above will lead to the reduction of cost and minimizing working hours. The quality and the yield of cotton crops will increase using sustainable ways. This project as well as the innovative products that will be created will give the opportunity for the first time in Greece, for the creation and operation of a support system for the cotton production. It will cover the two major issues concerning the cotton cultivation, irrigation and treatment of the green worm. It is expected that the tool will significantly contribute to cost reduction, product improvement and sustainability of cultivation areas. The system can be extended in the future to other areas, while it will be able to find application outside Greece.

Funding

Co-financed by the European Regional Development Fund of the European Union and Greek national funds through the Operational Program Competitiveness, Entrepreneurship and Innovation, under the call RESEARCH – CREATE - INNOVATE (project code:T2EDK-00746, MIS:5055967).

References

Aubert, B.A., Schroeder, A., Grimaudo, J., 2012. IT as enabler of sustainable farming: An empirical analysis of farmers' adoption decision of precision agriculture technology. Decis. Support Syst. 54, 510–520. https://doi.org/10.1016/j.dss.2012.07.002

Costopoulou, C., Ntaliani, M., Karetsos, S., 2016. Studying Mobile Apps for Agriculture.

Eichler Inwood, S.E., Dale, V.H., 2019. State of apps targeting management for sustainability of agricultural landscapes. A review. Agron. Sustain. Dev. 39, 8. https://doi.org/10.1007/s13593-018-0549-8

Garnett, T., Appleby, M.C., Balmford, A., Bateman, I.J., Benton, T.G., Bloomer, P., Burlingame, B., Dawkins, M., Dolan, L., Fraser, D., Herrero, M., Hoffmann, I., Smith, P., Thornton, P.K., Toulmin, C., Vermeulen, S.J., Godfray, H.C.J., 2013. Sustainable Intensification in Agriculture: Premises and Policies. Science 341, 33–34. https://doi.org/10.1126/science.1234485

Karetsos, S., Costopoulou, C., Sideridis, A., 2014. Developing a smartphone app for m-government in agriculture. J. Agric. Inform. 5. https://doi.org/10.17700/jai.2014.5.1.129

Kasimatis, C.-N., Psomakelis, E., Katsenios, N., Katsenios, G., Papatheodorou, M., Vlachakis, D., Apostolou, D., Efthimiadou, A., 2022. Implementation of a decision support system for prediction of the total soluble solids of industrial tomato using machine learning models. Comput. Electron. Agric. 193, 106688. https://doi.org/10.1016/j.compag.2022.106688

Navarro-Hellín, H., Martínez-del-Rincon, J., Domingo-Miguel, R., Soto-Valles, F., Torres-Sánchez, R., 2016. A decision support system for managing irrigation in agriculture. Comput. Electron. Agric. 124, 121–131. https://doi.org/10.1016/j.compag.2016.04.003

Patel, H., Patel, D., 2016. Survey of Android Apps for Agriculture Sector. Int. J. Inf. Sci. Tech. 6, 61–67. https://doi.org/10.5121/ijist.2016.6207

Rose, D.C., Sutherland, W.J., Parker, C., Lobley, M., Winter, M., Morris, C., Twining, S., Ffoulkes, C., Amano, T., Dicks, L.V., 2016. Decision support tools for agriculture: Towards effective design and delivery. Agric. Syst. 149, 165–174. https://doi.org/10.1016/j.agsy.2016.09.009

Schröer-Merker1, E., Bowie, N., Hammond, H., Schröer-Merker1, E., Bowie, N., Hammond, H., 2016. STATUS AND FUTURE PERSPECTIVES OF SMART TOOLS AND APPS IN NEW ZEALAND AGRICULTURE. https://doi.org/10.22004/AG.ECON.260806

Sundmaeker, H., Verdouw, C.N., Wolfert, S., Freire, L.P., 2016. 4 Internet of Food and Farm 2020.

Scenario-Wise Comparison of Water Balance and Seawater Intrusion in the Coastal Agricultural Watershed of Almyros Basin in Greece

Lyra A.[1*], A. Loukas[2], N. Mylopoulos[1], G. Tziatzios[1], P. Sidiropoulos[1,2], A. Alamanos[1], L. Vasileiades[1]
[1]Laboratory of Hydrology and Aquatic Systems Analysis, Department of Civil Engineering, School of Engineering, University of Thessaly, Volos, Greece
[2] Laboratory of Hydraulic Works and Environmental Management, Department of Agronomy and Surveying Engineering, Aristotle University of Thessaloniki, Thessaloniki, Greece

Abstract. Seawater intrusion is a significant concern for coastal aquifer systems throughout Europe, particularly along the Mediterranean coast, making water resources management complicated. This study presents a scenario-wise comparison of the water balance, seawater intrusion, the indices of Crop Water Productivity (CWP), and Economic Water Productivity (EWP), for irrigation and water storage scenarios for the coastal agricultural Almyros Basin and its aquifer, in Thessaly, Greece. The analysis is based on the simulation results for the Almyros water system from 1991 to 2018, with the use of an Integrated Modeling System (IMS) for agricultural coastal watersheds, which consists of coupled simulation models of surface water hydrology (UTHBAL), reservoir operation (UTHRL), and groundwater models for the simulation of groundwater flow (MODFLOW), and chlorides (SEAWAT). The Multi-Criteria Decision Analysis methods (MCDA), TOPSIS and PROMETHEE I and II, have been applied to evaluate the beneficial ranking of water resources management plans for the Almyros Basin. The results indicate that the most beneficial policy for the quantity and quality of water resources and local agriculture for the TOPSIS method, is the Deficit irrigation combined with Rain-fed cultivation and reservoir operation, whereas, for PROMETHEE I and II methods, the best scenario is the Deficit irrigation with reservoir operation.

1 Introduction

Seawater intrusion is a major hazard for coastal aquifer systems across Europe, especially along the Mediterranean coast, making water resources management complicated (Lyra et al., 2021a; Lyra et al., 2022). The decreasing of water availability and the deterioration of groundwater quality undermines the viability of agricultural production in coastal areas. The chloride water quality regulation for drinking water is 250 mg/L, while chloride concentrations in coastal aquifers range among 25 mg/L to about 12,000 mg/L relying on aquifer attributes, according to European studies (Lyra et al., 2021b). Use of water for irrigation from salinized coastal aquifers may cause adverse problems in irrigated agriculture, and for that special consideration and management should be applied to minimize seawater intrusion. Even though chloride is identified as a nutrient in vegetation at about 100 mg kg^{-1} in soil, higher concentrations are harmful to plants and inhibit nitrogen absorption. Chlorides replace nitrates in agricultural nutrient absorption mechanisms, limiting crop production by inducing crop nitrogen deficit and/or salt buildup in the leaf area and limiting leaf size (based on the crop's resilience to salinity). Alfalfa, maize, olives, trees, vegetables, and vineyards have a maximum permitted soil salinity of 1-2 EC (dS/m), while grains, cotton, and wheat have a maximum allowable soil salinity of 6-8 EC (dS/m). Regarding chlorides, cereals, wheat, and cotton are moderately tolerant to tolerant crops, alfalfa is moderately sensitive to sensitive, most vegetables are fairly sensitive to sensitive, and maize, vineyards, and trees are the most sensitive crops (Lyra et al., 2022). An integrated strategy to agricultural production sustainability, groundwater abstraction, and saltwater intrusion is required to ensure natural resource viability. The comprehension and evaluation of water balance dynamics, as well as improved water quality availability for irrigation and public water use, are crucial features of such a plan (Loukas, 2010). However, the transition of water resources' status to accommodate water requirements in the most sustainable and fruitful mode is a complicated decision-making operation (Alamanos et al., 2018), since the targets to be satisfied cannot all be maximized, and compromise (consensus) instead of an excellent solution is considered as the acceptable solution. A variety of water resources management strategies (decisions, policies, or actions) can be used to tackle complex management challenges, each with its own number of traits and repercussions. Therefore, alternative plans could lack typical comparability metrics, making it difficult to determine which management plan is the most beneficial (Alamanos et al., 2018). Decisions are the product of a well-organized and sophisticated process that prioritizes and selects the best option based on data and criteria (Andreoli and Tellarini, 2000) taking into account the expectations of stakeholders. The difficulty in making decisions lies in the complexity of criteria set to evaluate alternatives (Peniwati, 2007).

The main objective of the present study is to evaluate water resources management plans coupled with the development and reservoir operation, for the improvement of the quantity and quality of the coastal agricultural

Almyros basin in Thessaly, Greece, and determine which plan is the most beneficial to local agriculture and water resources using the TOPSIS and the PROMETHEE family Multi-Criteria Decision Analysis (MCDA) methods. The analysis is based on the results and resources' efficiencies obtained from the calibrated, validated, and high efficiency Integrated Modeling System (IMS) for agricultural coastal watersheds, developed in earlier studies by Lyra et al. (2021;2022), which consists of coupled and interlinked models of surface water hydrology, an agronomic/crop growth model, and groundwater models for the simulation of groundwater flow and seawater intrusion.

2 Materials and Methods

2.1 Study area

The Almyros Basin's primary land use is agricultural, with a mere portion of the basin allocated for urban, sub-urban, and non-cultivated lands. The basin's hydrography is defined by ephemeral torrential streams and the lack of substantial surface water storages. The Almyros aquifer is mostly covered by irrigated farmland. Natural vegetation covers areas at higher altitudes (e.g. forests and bushland). Cereals, olive groves, vineyards, and wheat varieties have been the main crops grown in the study area from 1991 to 2018 (Lyra et al., 2021a). The average annual agricultural water supply amount is about 30 hm^3, whereas the average annual urban water delivery amount is about 2 hm^3. All water needs are satisfied by groundwater abstractions. The past and ongoing unsustainable groundwater withdrawals for agriculture, the lack of surface water reservoirs, the vicinity to the coastline, and the underlying hydrogeological setting and characteristics have led to a significant watershed freshwater imbalance and seawater intrusion along the shores of the Almyros Basin (Lyra et al., 2021b). The last decade three (3) reservoirs have been proposed and designed to increase the use of surface water and decrease the use of groundwater. The Xirias reservoir, with a storage capacity of about 4 hm^3 was designed to address the agricultural water needs of 7 km^2 of farmland and the Mavromati reservoir, situated in the southern highlands, is designed to provide water to cover the urban water demands of nine settlements, and has a water usuable storage capacity of about 1.2 hm^3 (Fig.1). Finally, the Klinovos reservoir was planned to meet the irrigation water demands of the southern area of the basin and to allow the recovery of Almyros aquifer (Fig 1). The designed reservoir will have an operational storage capacity close to 14 hm^3 and the ability to irrigate 10.2 km^2 of arable land, as is presented in an earlier paper (Lyra et al., 2022). The components of the hydrologic and water cycle are illustrated in Figure 1a.

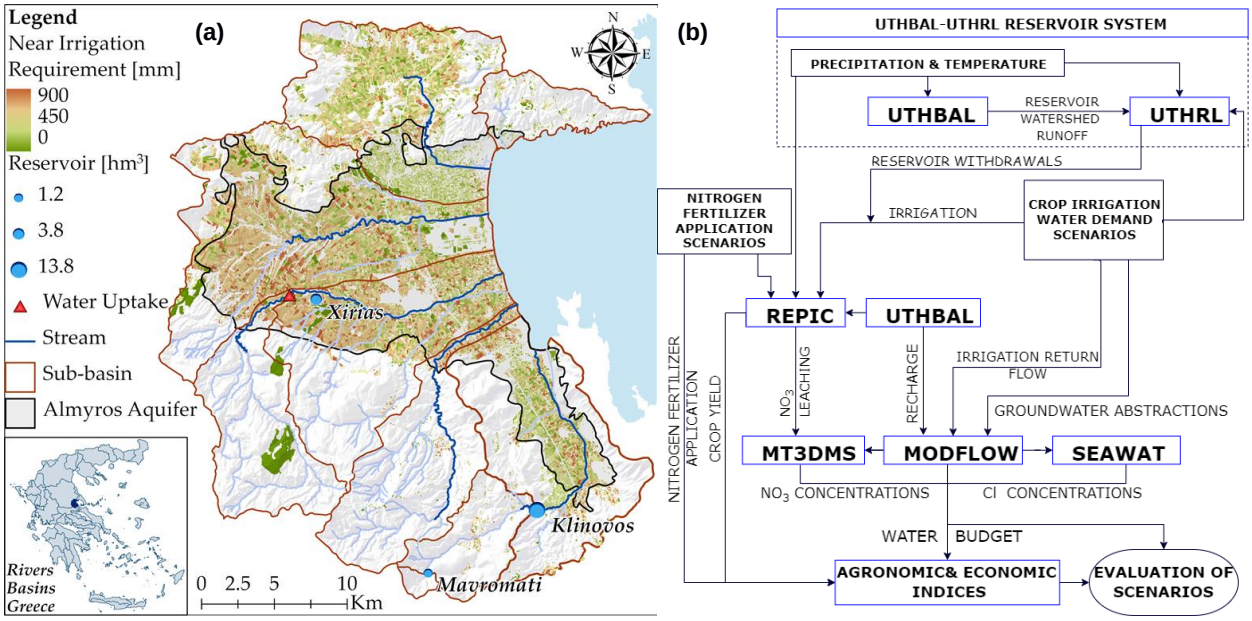

Figure 1. a) Map of Almyros basin, aquifer, sub-watersheds, irrigated agricultural areas, and location of the Xirias reservoir (under construction), the Klinovos reservoir (planned), and the Mavromati reservoir (constructed but not operate) (by Lyra et al., 2022) b) Flowchart of the Integrated Modeling System (IMS) (by Lyra er al 2021, April).

2.2 Integrated Water Resources Modeling System (IMS)

An Integrated Water Resources Modelling System (Fig. 1b) simulated the water resources in the Almyros Basin for the different management plans in previous study by (Lyra et al., 2022). Surface hydrology (UTHBAL) and reservoir operation (UTHRL) models (Loukas et al., 2007), groundwater hydrology (MODFLOW) (Harbaugh et al., 2000), crop growth (REPIC) (Lyra et al., 2021b), and seawater intrusion (SEAWAT) (Guo and Langevin, 2002) models are all coupled and interconnected for a holistic approach of the simulation of the hydrologic and water cycle. The modeling system has been successfully calibrated and verified in the Almyros Basin, simulating groundwater flow, seawater intrusion, and agricultural yields with increased accuracy in an earlier study (Lyra et al., 2021b).

2.3 Crop and Economic Water Productivity

The irrigation water amounts and the crop yields for the Almyros' arable land facilitate the calculation of the Crop Water Productivity (CWP), while the public data of gross market prices of crop types, retrieved by the Hellenic Statistical Authority, when divided by the irrigation water applied produce the efficiency scores of Economic Water Productivity (EWP) of the arable land of the study area as follows (Fernández et al, 2020;Lyra et al.2021a;2021c;2022):

$$CWP = \frac{Crop\ Yield\ kg\ ha^{-1}}{Irrigation\ Water\ m^3 ha^{-1}} \qquad EWP = \frac{Profit\ €\ ha^{-1}}{Irrigation\ Water\ m^3 ha^{-1}}$$

2.4 Multi-Criteria Decision Analysis

Seawater intrusion will likely impede the prosperity of agriculture since it is a chronic phenomenon, and the accumulation of salts in soil from irrigation water will reduce crop yields (Lyra et al.2022). Seawater intrusion depends on the Almyros aquifer's water balance, and crop yield depends on water quantity and quality, while the marketable potential of crops' yield defines the economic development of the study area. However, it is not easy to determine how the parameters of the water and socio-economic cycle should be prioritized and managed under seawater intrusion phenomena in the Almyros aquifer. Thus, Multi-Criteria Decision Analysis (San Cristóbal,2012) is used to assess the trade-offs of the developed water resources management plans (Lyra et al.2022). Considering the European Commission's guidelines for Best Management Practices in Agriculture, the (CWP) and (EWP) indices estimate the efficiency of the resources' use. The relevant criteria in this research are the water balance, the chlorides' concentrations, the (CWP) and (EWP) indices, being considered equally important (Lyra et al.2022), for the application of the TOPSIS and PROMETHEE methods.

2.4.1 TOPSIS

TOPSIS (Technique for Order Preference by Similarity to Ideal Solution) method developed by Hwang and Yoon (1981) as an alternative method to Electre, distinguishes the alternative plans in *ideal* and *non-ideal*. The ideal solution is formed as a composition of the best performance values of any alternative for every criteria, and the non-ideal solution is a composition of the worst performance values. The selected alternative is the closest to the ideal solution. The basic principle is that the selected alternative should have the shortest Euclidean distance/deviation from the ideal solution and the greater distance/deviation from the non-ideal solution. The method assumes that each trait has a monotonically positive or negative course and the order of preference of the alternatives is rendered through the comparison of their euclidean distances from the ideal solution. The TOPSIS method consists of the following steps (San Cristóbal,2012):

1. Normalization of Decision Matrix. A decision table with the values of m alternatives and n criteria is formulated. Then the normalized value/variable (R_{ij}) is calculated based on the values x_{ij} of each criteria j for each alternative i as follows:
$$R_{ij} = \frac{x_{ij}}{\sqrt{\sum_{j=1}^{m} x_{ij}^2}}$$
2. Weighting of the Normalized Decision Matrix. Weights, (w_j), the sum of which equals to 1, are multiplied to the values (R_{ij}) of the Normalized Decision Matrix.
3. Determination of positive and negative ideal alternatives ($R_{ij}^{ideal/non\text{-}ideal}$). For beneficial criteria, the maximum values between alternatives are chosen, while for non-beneficial criteria the minimum values are required.
4. Calculation of deviations (D+ and D-). Using the n-dimensional Euclidean distance, the deviation of each alternative solution from the ideal is given by the relationship:
$$D_j^+ = \sqrt{\sum_{i=1}^{n} \left(w_i \cdot R_{ij} - w_i \cdot R_i^{ideal}\right)^2}$$

Similarly, the deviation from non -ideal solutions is given by the relationship:

$$D_j^- = \sqrt{\sum_{i=1}^{n} \left(w_i \cdot R_{ij} - w_i \cdot R_i^{non-ideal}\right)^2}$$

5. Relative approach of the ideal solution, Performance score (P), and Classification of the order of preference (Rank). The performance of each alternative solution/plan is estimated as:

$$P_i = \frac{D_j^-}{D_j^+ + D_j^-}$$

and the alternatives are ranked on the basis of P_i values in descending order. The proposed solution is the maximum value in the ranking order.

2.4.2 PROMETHEE I & II

PROMETHEE (Preference Ranking Organization Method for Enrichment Evaluation) method is a Multi-Criteria Analysis method (MCDA) developed by Brans et al. (1986). PROMETHEE I performs partial ranking, while PROMETHEE II complete ranking. PROMETHEE uses superiority relations to classify alternative options, based on a pre-determined set of criteria. The method is applied in six steps. In the first step the Decision Matrix is constructed. In the second step, a preference/superiority function that indicates the preference of an alternative A over an alternative B is set separately. The third step concerns the pair-comparison of alternatives using the preference function. As a fourth step, the results of the comparisons are presented in a value table as the estimated/calculated values of each criterion for each alternative. The ranking is realized in the last two steps: The fifth step includes PROMETHEE I, and the sixth step is PROMETHEE II. The method follows (San Cristóbal,2012):

1. Normalization of Decision Matrix. A decision table of m alternatives and n criteria is formulated. Then the normalized value/variable (R_{ij}) is calculated based on the values x_{ij} of each criteria j for each alternative i as follows:

   $R_{ij} = \frac{x_{ij} - min(x_{ij})}{max(x_{ij}) - min(x_{ij})}$ Beneficial criteria $R_{ij} = \frac{max(x_{ij}) - x_{ij}}{max(x_{ij}) - min(x_{ij})}$ Non-beneficial criteria

2. Difference of the normalized i^{th} alternative from the other normalized options.
3. Value estimation of the preference function P_j (α, β) for each difference:

$$P_j(\alpha, \beta) = 0, \quad if \ (R_{\alpha j} - R_{\beta j}) \leq 0$$

$$P_j(\alpha, \beta) = (R_{\alpha j} - R_{\beta j}), \quad if \ (R_{\alpha j} - R_{\beta j}) > 0$$

4. Value estimation of the aggregated preference function index π (α, β) for all criteria, by multiplying the weights of criteria, (w_j), the sum of which equals to 1, with the values of the preference function. The closer to 1 the bigger the preference.

$$\pi(\alpha, \beta) = \frac{\sum_{j=1}^{n} w_j P_j(\alpha, \beta)}{\sum_{j=1}^{n} w_j}$$

5. Outranking flows for each alternative option $\varphi^{+/-}(\alpha)$:

$\varphi^+(\alpha) = \sum_{\beta=1}^{m} \pi(\alpha, \beta)$ (Outflow PROMETHEE I) $\varphi^+(\alpha) = \sum_{\beta=1}^{m} \pi(\alpha, \beta)/m$ (Outflow PROMETHEE II)

$\varphi^-(\alpha) = \sum_{\beta=1}^{m} \pi(\beta, \alpha)$ (Inflow PROMETHEE I) $\varphi^-(\alpha) = \sum_{\beta=1}^{m} \pi(\beta, \alpha)/m$ (Inflow PROMETHEE II)

6. Net outranking flow for each alternative option, φ(α):

$$\varphi(\alpha) = \varphi^+(\alpha) - \varphi^-(\alpha)$$

3 Results

3.1 Integrated Water Resources Modelling System (IMS), CWP and EWP

The simulation of water resources with the Integrated Modeling System (IMS) resulted in the determination of the water balance, the estimation of crop yields and of chlorides concentrations in the Almyros study area and aquifer. Crop Water Productivity and Economic Water Productivity have been estimated based on the applied irrigation schemes and crop market prices as described in the companion paper by Lyra et al (2021a). The averaged annual water deficit/surplus, the average monthly maximum chlorides concentration that indicates seawater, the Crop Water Productivity (CWP), and Economic Water Productivity (EWP) indices are displayed in Table 1. More specifically, the chlorides concentrations and the variation between the water resources management plans and the historical simulated values are displayed in Figure 2.

Table 1. Average Annual Results of the Integrated Modeling System (IMS), Crop Water Productivity and Economic Water Productivity for the simulation period of 1991-2018.

Criterion/Scenario	Water Balance (hm^3)	CL (mg/L)	CWP (tn/m^3)	EWP (€/m^3)
S0 (Baseline scenario)	-12	11289	9.8	1.08
S1 (Deficit Irrigation)	-7.9	6953	11.8	1.29
S2 (Deficit Irrigation & Rain)	-0.3	3520	6.4	0.82
SR1 (Deficit Irrigation from aquifer & reservoirs)	-7	6977	12.9	1.36
SR2 (Deficit Irrigation & Rain - aquifer & reservoirs)	0.7	3520	6.8	0.9

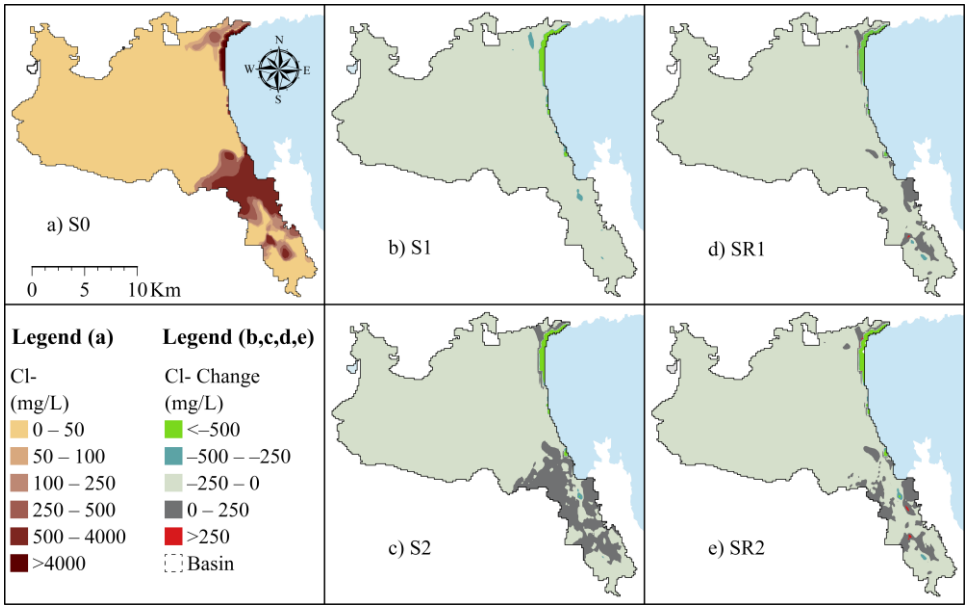

Figure 2. Chlorides Concentrations (a) and Chlorides Concentrations Variation (b,c,d,e) in (mg/L) of Almyros aquifer at the end of the simulation period (September 2018) between the baseline scenario (S0) and the water resources scenarios (a) S0 (b) S0-S1, (c) S0-S2, (d) S0-SR1 (e) S0-SR2.

3.2 TOPSIS

The application of the TOPSIS method indicated as the best water resources management plan the Deficit irrigation combined with Rain cultivation and reservoir operation for irrigation. The Euclidean distances from the ideal and non-ideal solution for equally important criteria are displayed in Table 2.

Table 2 Performance of water resources management plans using the TOPSIS method.

Criteria	Di+	Di-	Pi	Rank
S0	0.238	0.047	0.16	5
S1	0.146	0.122	0.45	4
S2	0.093	0.220	0.70	2
SR1	0.132	0.138	0.51	3
SR2	0.083	0.234	0.74	1

3.3 PROMETHEE I & II

The application of the PROMETHEE method indicated as the best water resources management plan the Deficit irrigation combined with the reservoir operation for irrigation. The outflows and inflows of the superiority relations among the alternatives for equally important criteria are displayed in Table 3 for PROMETHEE I and Table 4 for PROMETHEE II.

Table 3 Performance of water resources management plans using the PROMETHEE I method.

Criteria	φ+, Outflow	φ-, Inflow	φ(a)	Rank
S0	0.215	0.300	-0.085	4
S1	0.320	0.114	0.206	2

S2	0.118	0.493	-0.375	5
SR1	0.385	0.109	0.276	1
SR2	0.233	0.255	-0.021	3

Table 4 Performance of water resources management plans using the PROMETHEE II method.

Criteria	φ+, Outflow	φ-, Inflow	φ(a)	Rank
S0	0.859	1.201	-0.342	4
S1	1.280	0.457	0.823	2
S2	0.472	1.971	-1.499	5
SR1	1.542	0.438	1.104	1
SR2	0.934	1.019	-0.086	3

4 Conclusion

The Multi-Criteria Decision Analysis (MCDA) methods, TOPSIS and PROMETHEE I and II, indicate that the acceptable solution to minimize the water deficit and seawater intrusion and to maximize the Crop and Economic Water Productivity in irrigated agriculture of the Almyros study area could be either the application of deficit irrigation with rain cultivation utilizing the operation of reservoirs, or the application of deficit irrigation also utilizing the operation of reservoirs. In TOPSIS method it was concluded the ideal water management plan is SR2 and in descending order S2, SR1, S1, S0, while in PROMETHEE methods both for partial and complete ranking it was concluded that the most superior management plan among all others is SR1, and then in descending order S1, SR2, S2,S0. The results of this study agree with the results of previous research (Lyra et al,2021a;2022) where it was also concluded that for water resources the best management plan is deficit irrigation with rain cultivation and operation of reservoirs, but for the integration of the sustainability of local agriculture the deficit irrigation with the operation of reservoirs is the most beneficial scenario. Hence, the TOPSIS method requires additional configuration of the criteria weights for the study area to provide an acceptable sustainable solution, whereas the PROMETHEE I and II methods reach out to the most beneficial water resources management plan for the phenomenon of seawater intrusion, by performing a holistic evaluation of the agricultural, environmental, water and socio-economic factors included in water resources management planning in the study area.

Acknowledgements

"This research is co-financed by Greece and the European Union (European Social Fund-ESF) through the Operational Programme «Human Resources Development, Education and Lifelong Learning» in the context of the project "Strengthening Human Resources Research Potential via Doctorate Research" (MIS-5000432), implemented by the State Scholarships Foundation (IKY)".

References

Alamanos A, Mylopoulos N, Loukas A, Gaitanaros D (2018) An Integrated Multicriteria Analysis Tool for Evaluating Water Resource Management Strategies. 10 (12):1795

Andreoli M, Tellarini V (2000) Farm sustainability evaluation: methodology and practice. Agriculture, Ecosystems & Environment 77 (1):43-52.

Brans JP, Vincke P and Mareschal B (1986) How to select and how to rank projects: The Promethee method. European Journal of Operational Research 24(2):228-238

Fernández JE, Alcon F, Diaz-Espejo A, Hernandez-Santana V and Cuevas MV (2020) Water use indicators and economic analysis for on-farm irrigation decision: A case study of a super high density olive tree orchard. Agricultural Water Management 237, 106074

Guo W, Langevin CD (2002) User's guide to SEAWAT; a computer program for simulation of three-dimensional variable-density ground-water flow. Techniques of Water-Resources Investigations, Supersedes OFR 01-434 edn.

Harbaugh AW, Banta ER, Hill MC, McDonald MG (2000) MODFLOW-2000, The U.S. Geological Survey modular ground-water model: User guide to modularization concepts and the ground-water flow process. Open-File Report.

Hwang, CL and Yoon, K (1981) Multiple Attribute Decision Making: Methods and Applications. Springer-Verlag, New York.

Loukas A (2010) Surface water quantity and quality assessment in Pinios River, Thessaly, Greece. Desalination 250 (1):266-273.

Loukas A, Mylopoulos N, Vasiliades L (2007) A Modeling System for the Evaluation of Water Resources Management Strategies in Thessaly, Greece. Water Resources Management 21 (10):1673-1702.

Lyra A, Loukas A, Sidiropoulos P (2021a) Impacts of irrigation and nitrate fertilization scenarios on groundwater resources quantity and quality of the Almyros Basin, Greece. Water Supply 21 (6):2748-2759.
Lyra A, Loukas A, Sidiropoulos P, Tziatzios G, Mylopoulos N (2021b) An Integrated Modeling System for the Evaluation of Water Resources in Coastal Agricultural Watersheds: Application in Almyros Basin, Thessaly, Greece. 13 (3):268
Lyra, A, Loukas, A, Voudouris, K., Mylopoulos, N (2021c) Evaluation of water resources management and agronomic scenarios using an integrated modelling system for coastal agricultural watersheds: The case of Almyros Basin, Thessaly, Greece. In EGU General Assembly Conference Abstracts (pp. EGU21-13137).
Lyra A, Loukas A, Sidiropoulos P, Voudouris K, Mylopoulos N (2022) Integrated Modeling of Agronomic and Water Resources Management Scenarios in a Degraded Coastal Watershed (Almyros Basin, Magnesia, Greece). 14 (7)
Peniwati K (2007) Criteria for evaluating group decision-making methods. Mathematical and Computer Modelling 46 (7):935-947.
San Cristóbal JR (2012) Multi criteria analysis in the renewable energy industry. Springer Science & Business Media.

Collective pressure irrigation networks: Monitoring and Analysis for Management improvement.

N. Dercas[1] and A. Stefopoulou[1]

[1] Laboratory of Agricultural Hydraulics, Department of Natural Resources Management and Agricultural Engineering, Agricultural University of Athens, 75 Iera Odos str., 11855, Athens, Greece.

Abstract. Greek collective irrigation networks under pressure have been built systematically since the 70's. These networks have not been properly maintained, and this resulted to bad conditions of infrastructure and reduced capacities to serve the users (pressure regulators and flow reducers were removed, hydrometers were broken etc). It is necessary to rehabilitate and modernize the networks. In this respect, systematic monitoring and identification of problems are necessary in order to make targeted interventions. The aim of this study is precisely to present such a pilot monitoring and analysis of a collective pressurized irrigation network.The network that was monitored for three years is the network of Kandia (Eastern Peloponnese: 37.524375˚N 22.958088˚E), which irrigates 273ha of citrus, olive trees and vegetables. The network is supplied by a 700m^3 reservoir, which is watered by a pumping station located near the city of Nafplio (Aria area) and a ~25Km long pipeline. The network has 91 hydrants that irrigate respective irrigation units.Pressure traducers with data loggers were installed in three hydrants of the network as well as a water level recorder system in the reservoir. In all the data loggers, measurements were taken every 4 minutes, and the average value was stored on an hourly basis. An ultrasonic flowmeter was also installed at the head of the network, which, despite repeated efforts, could not function reliably because the inner lining of the steel conduit created conditions of instability in the flow. This article presents results from the monitoring and the hydraulic analysis of the network and its potential capabilities to serve the users. This study demonstrates that the behaviour of a pressurized collective irrigation network can be analysed even based on restricted data; such analysis allows us to draw important conclusions for the improvement of projects management.

1 Introduction

Collective irrigation networks under pressure were initially built on a pilot basis in Greece in the 1960s (3-4 networks) in order to be evaluated under Greek conditions. Since 1970, most collective irrigation projects have been under pressure networks. So today we have reached ~ 400.000ha of collective networks under pressure, which usually operate on demand, and ~ 200.000ha old networks with gravity which operate by rotation (with irrigation scheduling). The design of collective irrigation networks on demand is based on the model of Clément (Clément, 1966; Clément and Galand, 1979) and on the discontinuous method of Labye (Labye, 1966) for the discharge evaluation and the diameters optimization, respectively. In these networks the irrigation methods used are mainly sprinkler and to a lesser extent drip irrigation.

Given that the farms in Greece are small (~ 5ha in average) and fragmented (in average 7 plots per farm) usually every hydrant is not used by a sole farmer, but it is shared by more people who own fields nearby. This leads to the need to charge the water according to the irrigated area and not the volume consumed. This method of charging is inappropriate as it leads to significant overconsumption (Karantounias and Dercas, 1999). Of course, in some networks water is charged on the basis of the volume consumed; this is case of the modern network of TOEB Hera-Kourtaki in Peloponnese, and also some networks in Crete where each hydrant is divided into more hydrants with volumetric meters (Photo 1)). In the case of Crete this is possible because the predominant method is drip irrigation, and the flow rates are small. In the case of sprinkler irrigation, a hydrant cannot support the simultaneous operation of many irrigation systems.

Photo 1. A water uptake serving 9 hydrants in Crete (by A. Stefopoulou)

Many collective pressurized irrigation networks are already obsolete and their actual development deviates from the predictions made in the original study (crops and / or irrigation growth rates differed from those initially predicted.) (Karantounias and Dercas, 1999). Maintenance is not appropriate and many control and regulation systems (pressure regulators, flow reducers, flow meters) must be checked and often reinstalled (Karantounias and Dercas, 1999; Kanakis et al. 2014).

This work analyzes the hydraulic behavior of the irrigation network under pressure in Kantia in the Peloponnese, with the view to suggest to project managers and to competent administrative authorities at central and regional level how to monitor a network in order to detect failures and timely face them. The aim of the effort was to achieve these goals with the minimum means and data and this methodology of monitoring and analysis become a common practice in the country.

2 Methods and Materials

For the analysis of on-demand collective pressure irrigation networks several models have been developed. At network level, the analysis is implemented with the indexed characteristic curves (Labye et al. 1975; Bethery et al., 1981; Bethery 1990; CEMAGREF, 1983; Lamaddalena and Sagardoy, 2000; Stefopoulou, 2013, Stefopoulou and Dercas, 2017). At hydrant level several also models have been proposed (CEMAGREF, 1983; Lamaddalena and Sagardoy, 2000; Khadra and Lamaddalena, 2010, Stefopoulou, 2013, Stefopoulou and Dercas, 2017). Models that implement performance analysis at hydrant level may assume a steady-flow state (CEMAGREF, 1983; Lamaddalena and Sagardoy, 2000; Stefopoulou, 2013, Stefopoulou and Dercas, 2017) or a non-steady flow state (Lamaddalena and Pereira, 2007; Estrada et al., 2009; Rossman,2000).

The case study network

The network of Kantia (Eastern Peloponnese: 37.524375˚N 22.958088˚E), irrigates 273ha of citrus, olive trees and vegetables. (Figure 1). The network is supplied by a 700m^3 reservoir, which is watered by a pumping station located near the city of Nafplio (Aria area) and a ~25Km long pipeline. The network has 91 hydrants (6L/s) that irrigate respective irrigation units (size 3ha each). The specific continuous discharge is 0.44L/s/ha. The Clément discharge at the head of the network is 222L/s and the cumulative flow rate at the head of the network is 546L/s.

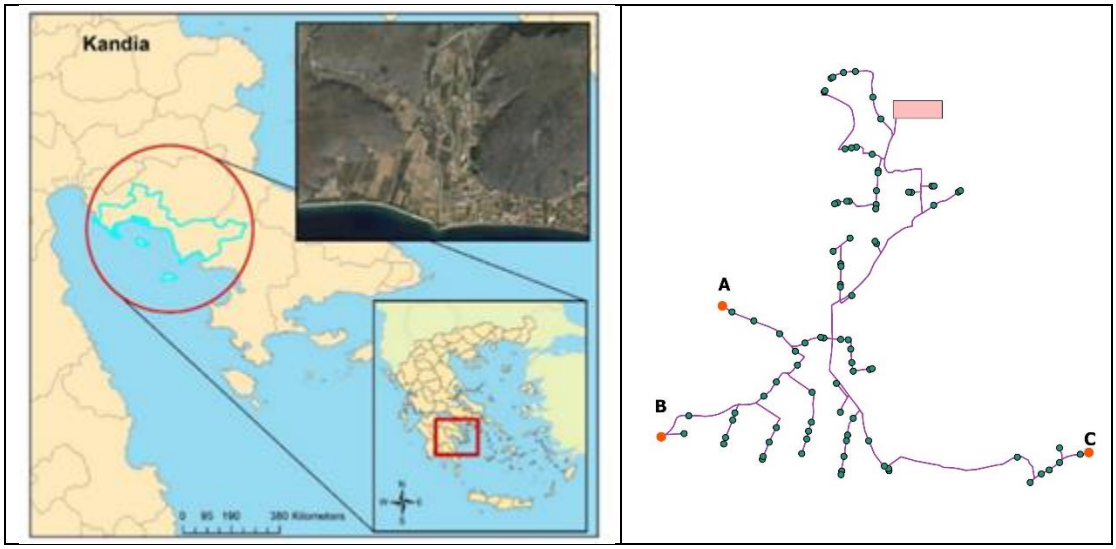

Figure 1. The on-demand pressure irrigation network in Kantia (Stefopoulou and Dercas,2017)

Three pressure transducers with corresponding data loggers were installed in the network at three extreme hydrants in order to monitor the pressure (Figure 1). These data indicate how often pressure drops occur, but at the same time they will allow us to calibrate the hydraulic analysis model.

An ultrasonic flowmeter was installed at the head in order to obtain a continuous recording of the flow rate. This action was not successful because, while the outer liner of the steel pipeline was carefully removed for the placement of the sensors, the inner liner of the pipeline was blocking the signal. Another ultrasonic flowmeter was then used, and the sensor was placed inside the pipeline after perforation. In this case also, the system could not give reliable measurements because the inner lining has detached in many parts of the pipeline and its movement caused instability in the flow.

A pressure level sensor with datalogger was installed in the reservoir that supply water to the network in order to monitor the piezometric elevation.

Eventually the entire hydraulic analysis is based on the data we have on the water head in the supply reservoir and the pressures we collected on the three water hydrants of the network.

For the analysis the COPAM program of FAO is used (Lamaddalena and Sagardoy, 2000), as well as the program NIREUS which has been developed in the Agricultural Hydraulics Laboratory of AUA (Stefopoulou, 2013). A comparative evaluation of the two programs showed that they give similar results (Stefopoulou, 2013, Stefopoulou and Dercas, 2017); however, the

second has more possibilities (more types of load losses, improved reliability index of the hydrants) and is more user friendly in terms of network numbering.

3 Results

3.1 Water level recording in the head reservoir

Figures 2 to 4 show recordings of the water level in the head reservoir (the level ranges from +50m to +54m). The level gauge is installed at +51m. Frequent water supply shortages were observed, which lead to the emptying of the reservoir. The impact of this fact is more important than the interruption of irrigation: the emptying of the network and its refilling lead to hydraulic hammer events that strains the piping system.

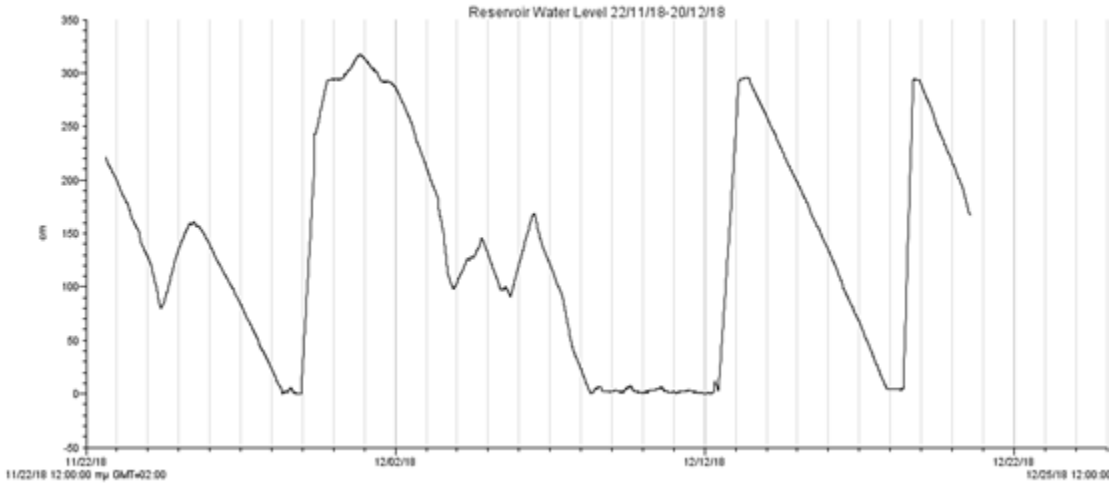

Figure 2. Water level variation in the Head Reservoir (22/11/18-20/12/18)

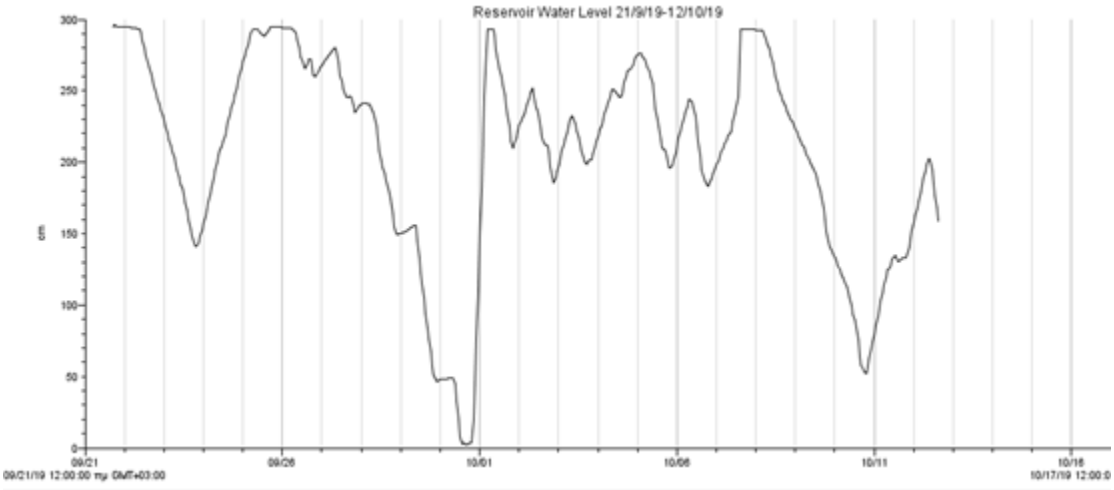

Figure 3. Water level variation in the Head Reservoir (21/09/19-12/10/19)

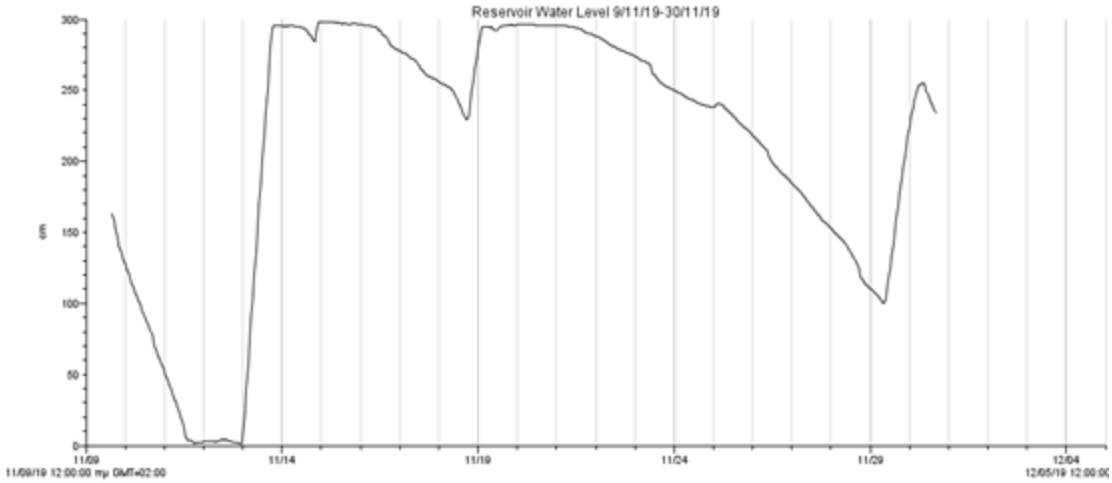

Figure 4. Water level variation in the Head Reservoir (9/11/19-30/11/19)

3.2 Pressure head recording in the hydrants

Figures 5,6,7 show pressure recordings at the three hydrants A, B and C (figure 1). It is apparent that the pressure is usually above 30m, which allows producers to use micro-irrigation systems (micro-sprinklers and drippers) as well as medium pressure irrigation. According to the water level recordings (figures 3,4), it becomes obvious that the pressure drops are due to the lack of water in the suppling reservoir.

Frequent hydraulic hammer events caused by refills of the network led to damage in the three pressure traducers: all three began to systematically show + 10m-+15m more pressure than the actual one (as evidenced by hand pressure gauge measurement).

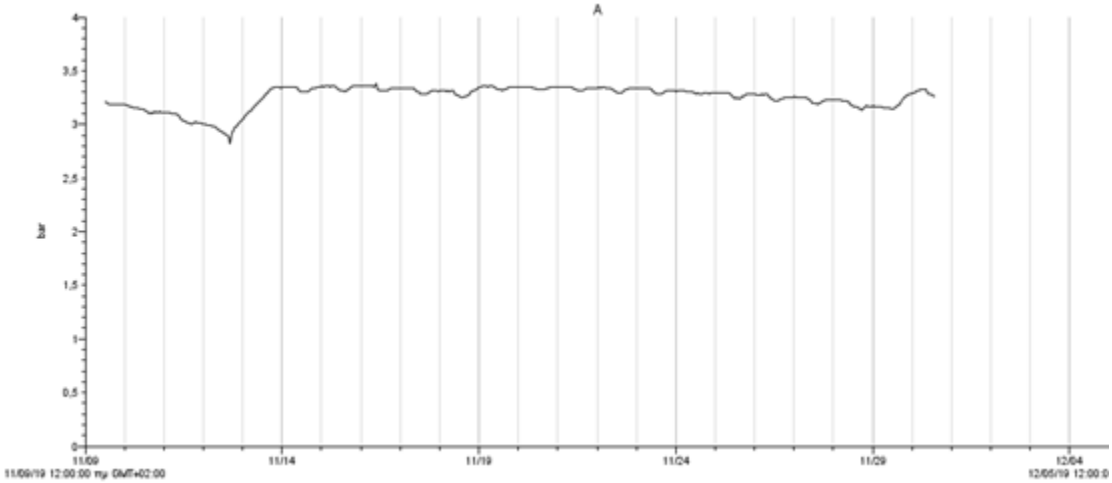

Figure 5. Pressure variation in Hydrant A (9/11/19-30/11/19)

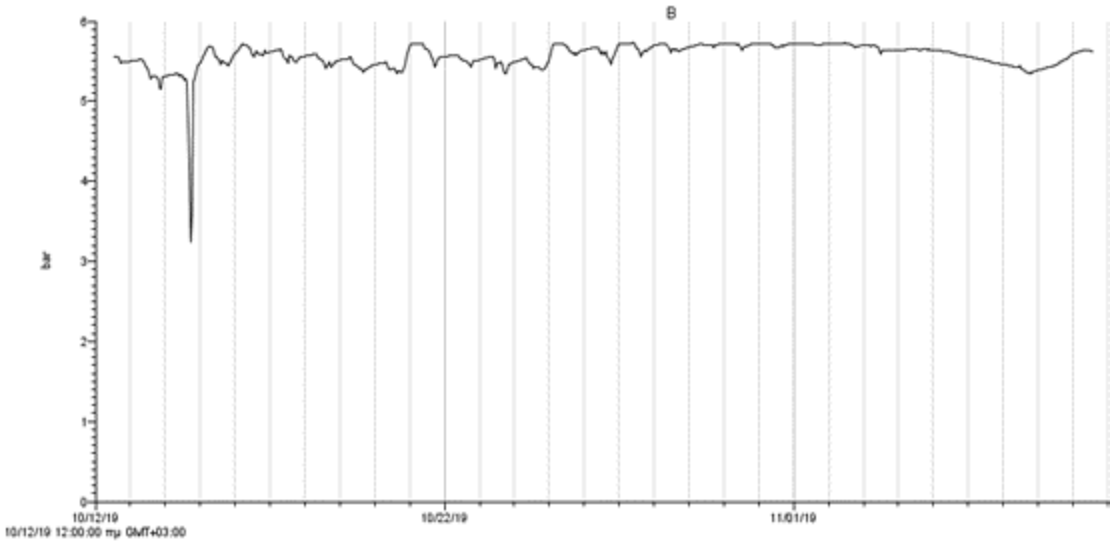

Figure 6. Pressure variation in Hydrant B (9/11/19-30/11/19)

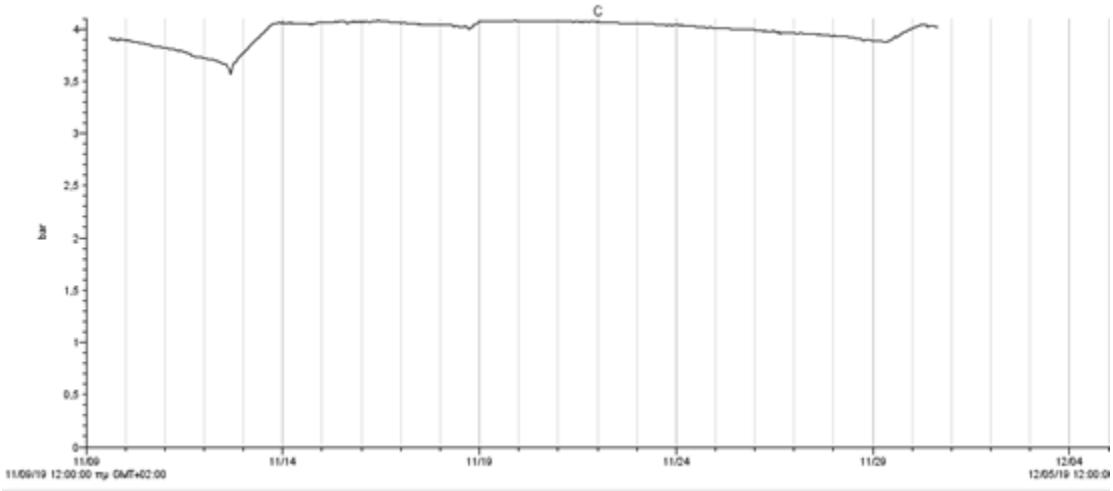

Figure 7. Pressure variation in Hydrant C (9/11/19-30/11/19)

3.3 Hydraulic analysis

The pressure values of the three pressure recordings at the three selected hydrants were used to estimate the average monthly pressure of each hydrant for July 2018 and July 2019. NIREUS program (Stefopoulou and Dercas, 2017) was then used to simulate the hydraulic performance of the network at hydrant level.

Afterwards, the simulated pressures were compared with the actual recording and the comparisons are presented in the following table.

Table 1. The recorded and simulated pressures for each hydrant, for July 2018 and July 2019

		Recorded pressure (m)	Simulated pressure (m)
Hydrant A	July 2018	31.25	21.62
	July 2019	30.76	
Hydrant B	July 2018	57.51	42.14
	July 2019	56.39	
Hydrant C	July 2018	33.96	25.71
	July 2019	36.90	

The results present a difference of 11 m on average, which could be mainly attributed to the frequent hydraulic hammer events occurring in the piping system.

Initially, the characteristic curves with indices (10%, 50% and 90%) were drawn in order to evaluate the overall behavior of the network. For this analysis the specifications of the study were not considered since in the network there are zones with different pressures (0-0.5, 0.5-1.0, 1.0-1.5, 1.5-2.0, 2.0-2.5,> 2.5bars). The reason for this variation is the low head that does not allow the entire network to have a pressure of at least 2.5-3.0 bars that would allow sprinkler operation and low / medium pressure irrigation. For this analysis a uniform minimum pressure head at the hydrants was adopted (20.00 m). We consider that this is the minimum in order to use micro-irrigation system in the field.

Figure 9 shows the network indexed characteristic curves (CC_i) calculated with the COPAM software.

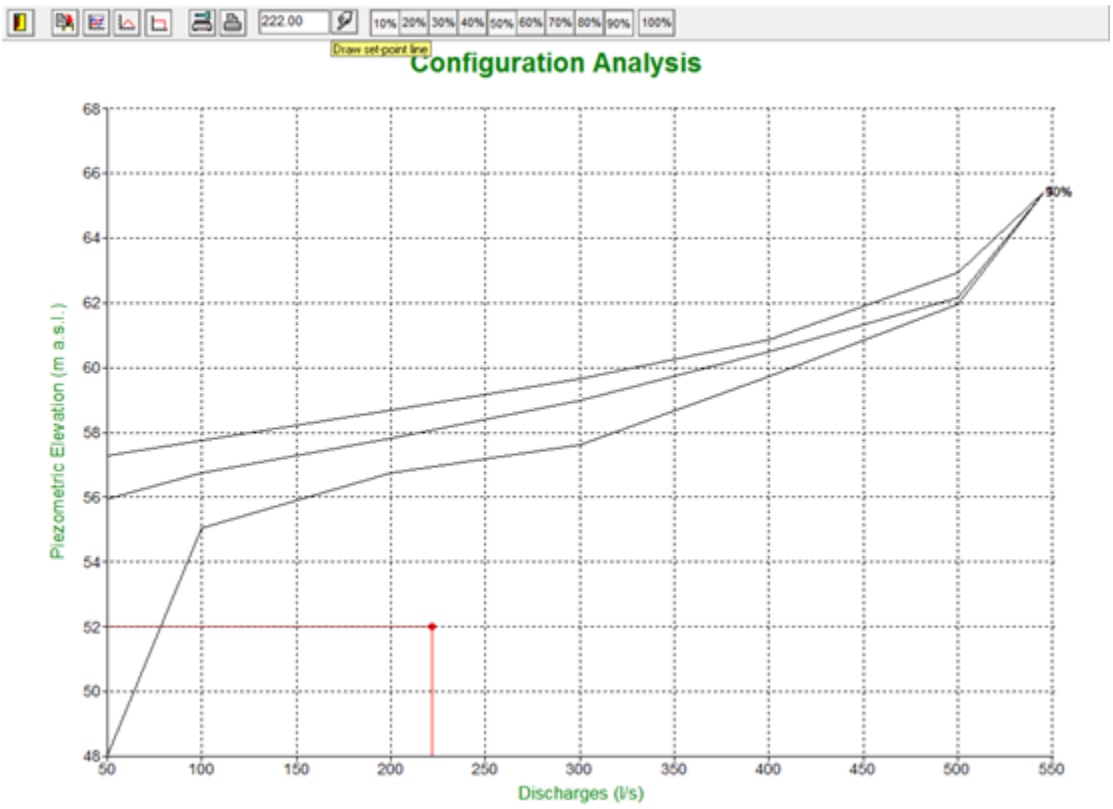

Figure 9. The indexed Characteristic curves (CCi) of the Kantia network (10%, 50%, 90%)

It is well known, from international literature (CEMAGREF, 1983), that a network operating close to the characteristic curve 50% does not suffer from serious failures. This is due to the fact in order to draw the characteristic curves with indices, a very strict criterion was used regarding the operation of the hydrants. From Figure 9 it is obvious that the general behavior of the network is low. This is due to several hydrants that do not have the necessary piezometric head in order to operate with the minimum +20.00 adopted in the analysis.

Analysis was performed, again with COPAM software, at the hydrants level. Figure 10 shows the relative pressure deficit/excess in each hydrant with a piezometric elevation at the suppling reservoir + 52m and a discharge of 222L/s (Clément discharge). A number of 150 simulations were performed. It is noted that the relative pressure deficit/excess is also calculated at the junctions even though they do not have hydrants. There, a pressure head of 0.00m was adopted.

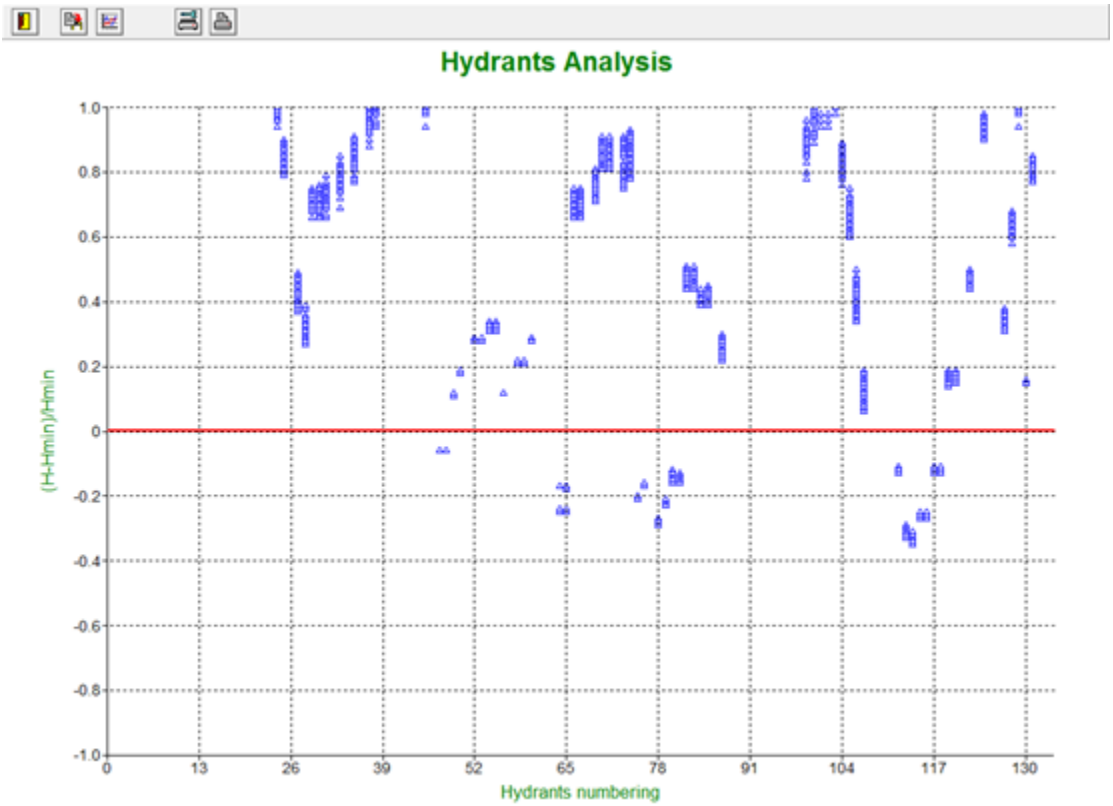

Figure 10 Relative pressure deficit/excess in the hydrants (for $Q_{Clém}$=222L/s, H_{head} = + 52m).

The majority of hydrants have an excess relative pressure which may reach + 100% of 20.00m. But there are several hydrants (~17) that are permanently unable to operate with 20.00m.

In Figure 11 the Hashimoto index (Hashimoto, 1980) for each hydrant is presented. It is obvious that the majority of hydrants are 100% reliable (except 17 hydrants that failure permanently, Hashimoto index equal to 0.0).

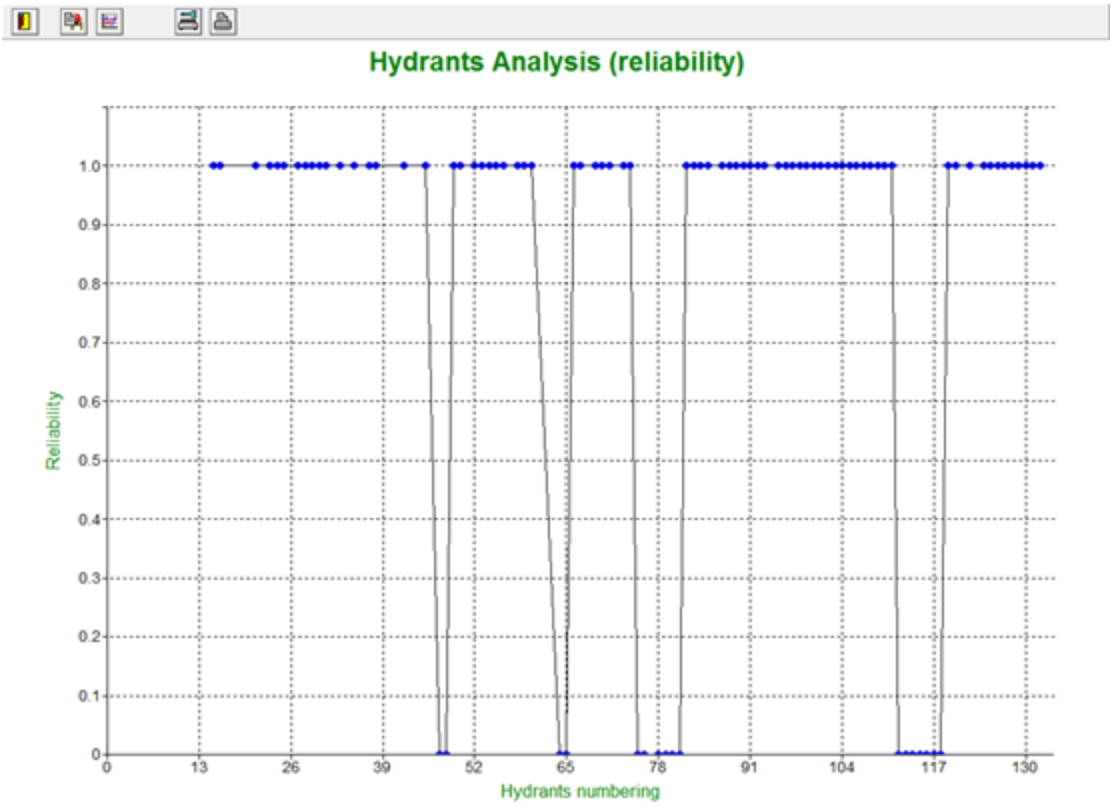

Figure 11 Hydrants' reliability index (for $Q_{Clém}$=222L/s, H_{head} = + 52m)

4 Discussion

As mentioned above, the network design accepts zones with particularly low pressure (0-0.50, and 0.50-1.00bars) which create operating problems even in drip irrigation systems. The simulation was carried out without the assumptions of the study, but with a minimum pressure in the hydrants of 2.00bars in order to allow the operation of micro-irrigation systems (micro-sprinklers and drippers). With this simulation a limited number of hydrants (17) were identified that cannot meet these conditions due to lack of necessary piezometric head).

A producer of the area that irrigates near the hydrant C (point of pressure measurement), expressed his dissatisfaction for lack of pressure while we recorded pressures close to 4bars. In such cases, where there may be others within the network, the design of the individual network within the field should be checked (it may be designed for operation with a flow rate greater than 6L/s which is the nominal operation of the hydrants).

Another important problem is the management of the water supply. The reservoir of Kantia is often without water, this leads to emptying of the network and frequent refills resulting in the occurrence of many hydraulic hammers events to the piping system.

Also, the difficulty and finally the inability to measure the flow rates should concern us regarding the characteristics of the selected pipelines.

5 Conclusion

In the on-demand irrigation network of Kantia due to the low piezometric elevation in the supply reservoir there are hydrants whose pressure is insufficient even for drip irrigation. Using the indexed characteristic curves (CCi) and the piezometric elevation at the head of the network we were able to estimate the general level of user satisfaction. An important issue that affects the operation status of the network is the supply of the head reservoir from the pumping station of Aria close to Nafplio. This issue must be addressed by the management organization (TOEB Iria) together with GOEB of Argonafplia (manager of the pumping station in Aria) in order to avoid frequent emptying and refilling of the network. Finally, the primary goal of the monitoring and analysis of this collective irrigation network is to serve as a pilot application that management organizations should follow in order to know the operating status and to be able to identify the points of failure in time. The analysis also revealed the need to use pipes with characteristics that facilitate the flow rate monitoring. It will be useful for the consolidation of the methodology to be repeated in other networks of the country and to become a systematic way of monitoring on-demand collective irrigation networks.

Acknowledgement: We thank the Land Reclamation Agency of Iria (TOEB of Iria) for their collaboration in the framework of this project.

References

Bethery, J., Meunier, M., Puech, C., 1981. Analyse des défaillances et étude du renforcement des réseaux d'irrigation par aspersion. Proc. XIe Cong CIID 36, 297-324.

Bethery, J., 1990. Réseaux collectifs Ramifiés Sous Pression, Calcul et Fonctionnement, Études hydrauliques agricoles, no 6. Antony, France.

CEMAGREF, 1983. Calcul des réseaux ramifiés sous pression. No 506. Antony, France

Clément R., 1966. Calcul des débits dans les réseaux d'irrigation fonctionnant à la demande. Houille Blanche, No 5, 553-575.

Clément, R., Galand, A., 1979. Irrigation par aspersion et réseaux collectives de distribution sous pression. Editions Eyrolles, p. 182.

Estrada, C., Gonzalez, C., Aliod, R., Pano, J., 2009. Improved pressurized pipe network hydraulic solver for applications in irrigation systems. J.Irrig. Eng. 135(4), 421-430.

Hashimoto, T., 1980. Robustness, Reliability, Resiliency and Vulnerability Criteria for Planning Water Resources System, Ph.D. Dissertation. Cornell University.

Kanakis, P.C., Papamichail, D.M., Georgiou, P.E., 2014. Performance analysis of on-demand pressurized irrigation network designed with linear and fuzzy linear programming. Irrig. Drain. 63 (4), 451-462.

Karantounias, G., et Dercas, N., 1999, “Problèmes de fonctionnement et de gestion des réseaux d’irrigation en Grèce - Étude de deux cas typiques”, *ICID Journal*, vol. 48, No 2, pp. 11-32.

Khadra, R., Lamaddalena, N., 2010. Development of a decision support system for irrigation analysis. Water Resour. Manage. 24, 3279-3297.

Labye, Y., 1966, Etude des procédés de calcul ayant pour but de rendre minimal le coût d’un réseau de distribution d’eau sous pression. La Houille Blanche, No 5/1966.

Labye, Y., Lahaye, J.P., Meunier, M., 1975. Utilisation des caractéristiques indicées. In Proc. Congrès de la ICID, p. 30.

Lamaddalena, N., Sagardoy, J.A., 2000. Performance analysis of on-demand pressurized irrigation systems, Irrigation and drainage paper No 59. FAO, Rome.

Lamadallena, N., Pereira, L.S., 2007. Pressure-driven modelling for the performance analysis of irrigation systems operating on demand. Agric. Water Manag. 90, 36-44.

Rossman, L.A., 2000. EPANET User Manual US Environmental Protection Agency, Drinking Water Research Division Risk Reduction Engineering Laboratory, Cincinnati.

Stefopoulou, A., 2013. Development of a simulation model for the performance analysis of pressurized irrigation networks operating on-demand. PhD Thesis. Agricultural University of Athens.

Stefopoulou, A., Dercas, N., 2017, NIREUS: A new software for the analysis of on-demand pressurized collective irrigation networks, Computer and Electronics in Agriculture 140 (2017) 58-69.

Water Resources Management Scenarios in a Mediterranean Xirias Watershed

M. Kollaiti[1*], A. Lyra[1], G. Tziatzios[1], P. Sidiropoulos[1,2], N. Mylopoulos[1], A. Loukas[2], L. Vasiliades[1]

[1]Laboratory of Hydrology and Aquatic Systems Analysis, Department of Civil Engineering, School of Engineering, University of Thessaly, Volos, Greece
[2] Laboratory of Hydraulic Works and Environmental Management, Department of Agronomy and Surveying Engineering, Aristotle University of Thessaloniki, Thessaloniki, Greece.
* e-mail: mariakollaiti@gmail.com

Abstract. The scope of this study is the management of water resources of the Xirias watershed, in Almyros, Greece. Xirias watershed is an agricultural region with Mediterranean climate, that is irrigated by groundwater abstractions from the Almyros aquifer system. The Almyros aquifer system has undergone degradation of its quantity and quality status, and, in order to alleviate the deficit water balance of the region and increase the sustainability of agriculture, the Xirias irrigation reservoir is intended to be completed in the central area of the watershed, in the near future. The stored water volume of the reservoir will irrigate a proportion of the arable land. The crops cultivated in the area are alfalfa, cereals, cotton, maize, olive groves, orchards, vegetables, vineyards, and wheat. The water resources budget of Xirias watershed have been simulated using the WEAP model (Water Evaluation and Planning Systems) under two different scenarios of water irrigation supply, with i) irrigation water from the Almyros aquifer and ii) irrigation water from the Almyros aquifer and the operation of Xirias reservoir, under two land use scenarios, for the historical period of 1992 to 2018. The results indicate that the reservoir is capable of fully covering the crop water demands of the Xirias watershed. The construction and operation of the Xirias irrigation reservoir will have a significant positive impact on the sustainability of the agriculture and the water balance of the region.

1 Introduction

The term "Water Resources Management" refers to all methods and activities required for the rational utilization of water potential, in order to meet the water needs as fully as possible (Mylopoulos, 2006). It uses all the administrative measures and scientific methods to restore water systems for their total exploitation based on the criteria and the reasons they have been determined (Serageldin, 2009). In the modern era the intensification of economic activities and agriculture has caused significant qualitative and quantitative degradation in aquatic life resources (Georgiadou, 2015). The concern is mainly caused by the declining trend observed in the basements water reserves as their renewal and resurrection are particularly time consuming. In many cases, it is the only source of water either due to lack of surface water or misuse of surface runoff. Thus, it is considered important to examine and deal with this phenomenon and to maintain the quality and quantity of exploited water resources (Georgiadou, 2015). In a similar situation is the underground aquifer of hydrology of the Almyros basin and in particular the Xirias Almyros watershed (Kollaiti, 2021).

The paper analyzes several scenarios that reflect the existing and expected water resources management of the area (for 27 years) as well as new proposals - sustainable solutions based on the investigation of sustainable management policies suitable for the Xirias watershed. Water resources scenarios are presented for the first time focusing on the Xirias watershed, and they are a consequence of the diploma thesis of Kollaiti (2021) regarding the sustainable management of water resources of the Xirias watershed and the Xirias reservoir.

2 Materials and Methods

2.1 Study area

Xirias watershed is an agricultural region which is irrigated by the Almyros aquifer system (Lyra et al., 2021b). The region has a semi-arid Mediterranean climate with hot summers and cold winters (Lyra et al., 2016). The average maximum temperature (1992-2018) is 592 mm, and the average temperature is 14.8 ° C. The mean annual runoff is 120 mm, the mean potential evapotranspiration is 22 mm, and the mean groundwater recharge is 58 mm (Lyra et al, 2021b). The main land use in the Xirias watershed is agriculture and, to a lesser extent, urban, interurban, and uncultivated land. The crops of the area are alfalfa, cereals, cotton, maize, olive groves, vineyards, vegetables as well as other types of trees and cereals for the period 1992-2018 (Lyra et al, 2021a). The cultivated areas are irrigated by deep groundwater abstractions. The irrigation methods used in the watershed are sprinkler and drip irrigation (Georgiadi, 2015). Due to the extensive agricultural activity, the use

of pesticides and fertilizers and the groundwater abstractions, the aquifer underlying the watershed has a continuous quantitative and quality degradation. Water supply to urban settlements is also provided by groundwater abstractions. There is a high risk of water resources problems and unsustainable agriculture, due to the continuous water deficit and the ongoing groundwater quality deterioration. For this reason, a water intake dam in the stream of Xirias and a reservoir of 3,840,000 m^3 is being constructed to irrigate a specific area of crops of 6.4 km^2 and alleviate the negative water balance of the Almyros aquifer system (MEEC, 2017). The reservoir of Xirias will collect and store the partial streamflow of Xirias stream and use the stored volume of water for the irrigation of the cultivated crops of the specified irrigation area (YPETHE, 2022). Groundwater pumping for irrigation will be ceased in the reservoir irrigated area. The construction of the Xirias reservoir may alleviate the groundwater resources problems and help the restoration of the aquifer (MINAGRIC, 2015).

2.2 Simulation of Water Resources Management Scenarios

The WEAP (Water Evaluation and Planning) software (Sieber, 2006; 2015), which is considered suitable for water balance simulations and water resources management, was used to create the model and the management scenarios. WEAP software simulates the water mass balance and requires the estimated agricultural and urban water needs, the mean monthly surface rainfall, temperature, potential evaporation, surface runoff, environmental/ecological streamflow, maximum reservoir capacity, groundwater recharge and other parameters, as input data (Alamanos et al., 2018). The monthly irrigation needs of the crops were calculated using the Near Irrigation Requirement (NIR) method based on the crops of the previous years from 1992 to 2018. The mean monthly surface rainfall, temperature, potential evaporation, surface runoff, and groundwater recharge have been determined in a recent study by Lyra et al. (2021b) using the UTHBAL surface hydrology model (Loukas et al., 2007), which has been successfully implemented in other areas of Thessaly (Sidiropoulos et al. 2016). The environmental/ecological streamflow is the minimum flow requirement for the Xirias stream before the water is taken up from its watercourse and routed to the Xirias reservoir. The environmental flow of the Xirias stream was set equal to the 10% of the surface runoff of the upstream watershed of the dam, according to the reservoir's Environmental Impact Study (MINAGRIC, 2015). The maximum stored usable water volume of the Xirias reservoir, is equal to the capacity of the reservoir, while the operation stored usable water reservoir volume will be defined between the minimum and maximum operating levels. The reservoir's total storage will be 3,824 hm^3 and the Maximum Water Level will be at the altitude of +177 m leaving 1,00 m of margin from the crest level (+178 m). The overflow of the reservoir takes place at an altitude of +177.25 m, 0.75 m lower than the elevation of the crest, given that the Maximum Water Level is 1,00 m (MINAGRIC, 2015; 2018). The sluice gate, which determines the minimum level, will occur at the lowest point of the reservoir. The evacuation will take place from the same pipeline. Thus, the inactive volume of the reservoir, in which the debris materials are deposited, is zero (Kollaiti, 2022).

2.2.1 Land Use

The Xirias reservoir is intended to irrigate approximately 6.4 km^2 with a total annual water requirement of 3×10^6 m^3. The crops that are intended to be cultivated after the construction, and for the operation of the Xirias reservoir are vegetables (34%), pear trees (13%), peach and almond trees (48%), and apple trees (5%) to ensure that the annual water supplied for irrigation won't exceed the volume capacity of the reservoir (MINAGRIC, 2015). Currently and historically, the crops cultivated in the area are distributed on average in alfalfa (12%), cereals (29%), cotton (8%), maize (3%), olive trees (9%), vineyards (2%), vegetables (5%) and wheat (34%) (Lyra et al., 2022). The total area occupied by each one of the nine (9) crop types changes annually from 1992 to 2018 (Kollaiti, 2021).

2.2.2 Water Resources Management Scenarios

Two cases of scenarios were created, depending on the operation or not of the reservoir, for the evaluation and proposal of the most efficient one. Case A refers to the existing and historical condition without the operation of the reservoir (Scenario 1) and Case B refers to the situation with the operation of the Xirias reservoir (Kollaiti, 2021). Case B was distinguished in two scenarios in order to assess if the runoff of the Xirias stream will provide adequate water to Xirias reservoir to cover the monthly irrigation needs on a monthly time-step, taking into account the environmental flow requirement/constraint of the downstream watershed. Scenario 2 evaluates the capacity of the water system to cover the irrigation demands of the current crop types cultivated in the region historically, and Scenario 3 evaluates the capacity of the water system to cover the irrigation demands of the crop types intended to be cultivated after the construction of the reservoir. If the stored water volume in Xirias reservoir can satisfy the irrigation needs of Scenario 2, it will be beneficial for the successful water resources management in Xirias watershed and Almyros aquifer and no further restructuring

of cultivated crops will be required for the successful operation of the reservoir and the undisturbed environmental status of the downstream area. Table 1 describes the water resources management scenarios.

Table 1. Analysis of scenarios examined in depth of 27 years (1992-2018) on monthly time-step.

Scenario	Sc.1-2	Sc.3
Case A: Irrigation from groundwater abstractions	Current situation: This scenario refers to the case of the current situation in which the reservoir has not been constructed and the existing crops are irrigated by groundwater.	---
Case B: Irrigation from groundwater abstractions and Xirias reservoir	This scenario is like the corresponding 1st of the case A. The main difference is the operation of the reservoir for irrigation purposes. A percentage of the crop area is irrigated by the reservoir and the rest by groundwater	It is assumed that the cultivated crops are these which were intended to be irrigated from the reservoir, according to the Environmental Impact Study (2015).

The data for the study area were processed and entered on a monthly time-step for the period 1992-2018. The conceptual model of the Xirias watershed and reservoir with the components of the water balance were created for each scenario in the WEAP software (Sieber, 2006; 2015), as shown in Figure 1.

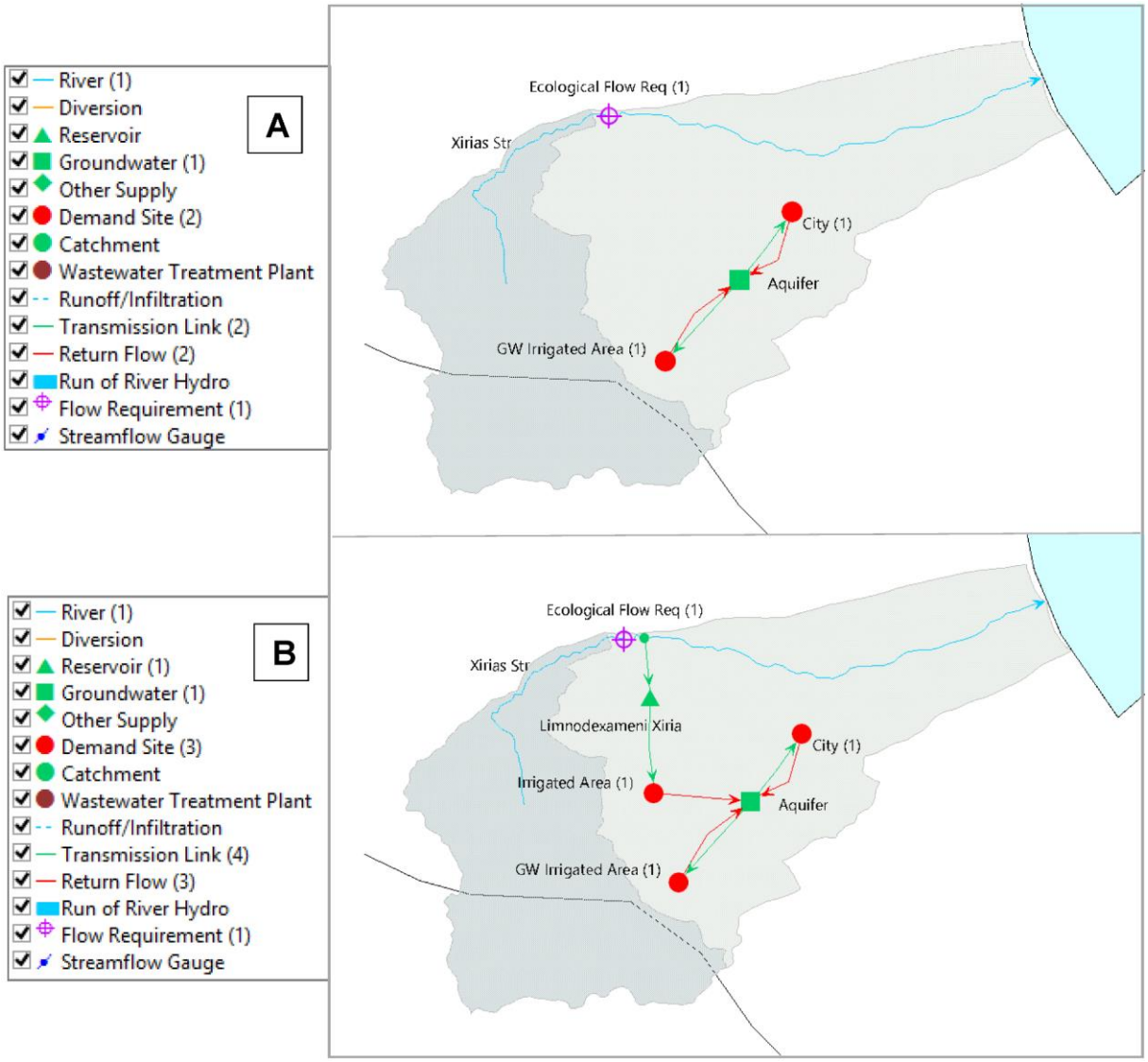

Figure 1. WEAP schematic view of Xirias watershed, Xirias stream, irrigated areas, and water systems. A) schematic view of Scenario 1 and B) schematic view of Scenarios 2 and 3.

3 Results and Discussion

The simulation of the water resources management scenarios in the Xirias watershed was performed using the WEAP model. The scenarios' results are presented and discussed in the next sections.

3.1 Water Evaluation and Planning of Scenario 1 (Historical-Reference Scenario)

For the Scenario 1, the input data for the WEAP model included the study period (1992-2018), the Xirias stream's surface runoff on a monthly time-step (estimated with the UTHBAL model), the areal precipitation and temperature, as well as and other climate data and parameters for the study area. The analysis is based on evaluation of the variation of the groundwater storage deficit. In WEAP software the groundwater storage has a double meaning. Initially, at the beginning of the simulation, in the first time step, the storage volume is defined as the stored volume of water, which cannot be less than the total water inflows (infiltration, irrigation returns, losses of water/irrigation systems) and outflows (agricultural water crop requirements, urban water requirements, surface runoff, etc.). But then, the storage is defined as the change in the theoretically maximum accessible capacity of water of the aquifer system and this definition is equivalent to the concept of lack of storage capacity of the aquifer. At the end of each month, the fluctuation of the storage or the storage deficit is the sum of the storage deficit at the beginning of the month and the inputs and outputs of the current month of the simulation. Storage deficit values cannot be negative, so they indicate a surplus of the storage (Sieber, 2006; 2015). The simulation results for Scenario 1 are shown in Figure 2 and indicate that the aquifer reserves more water for the scenario of crops that are irrigated (current situation).

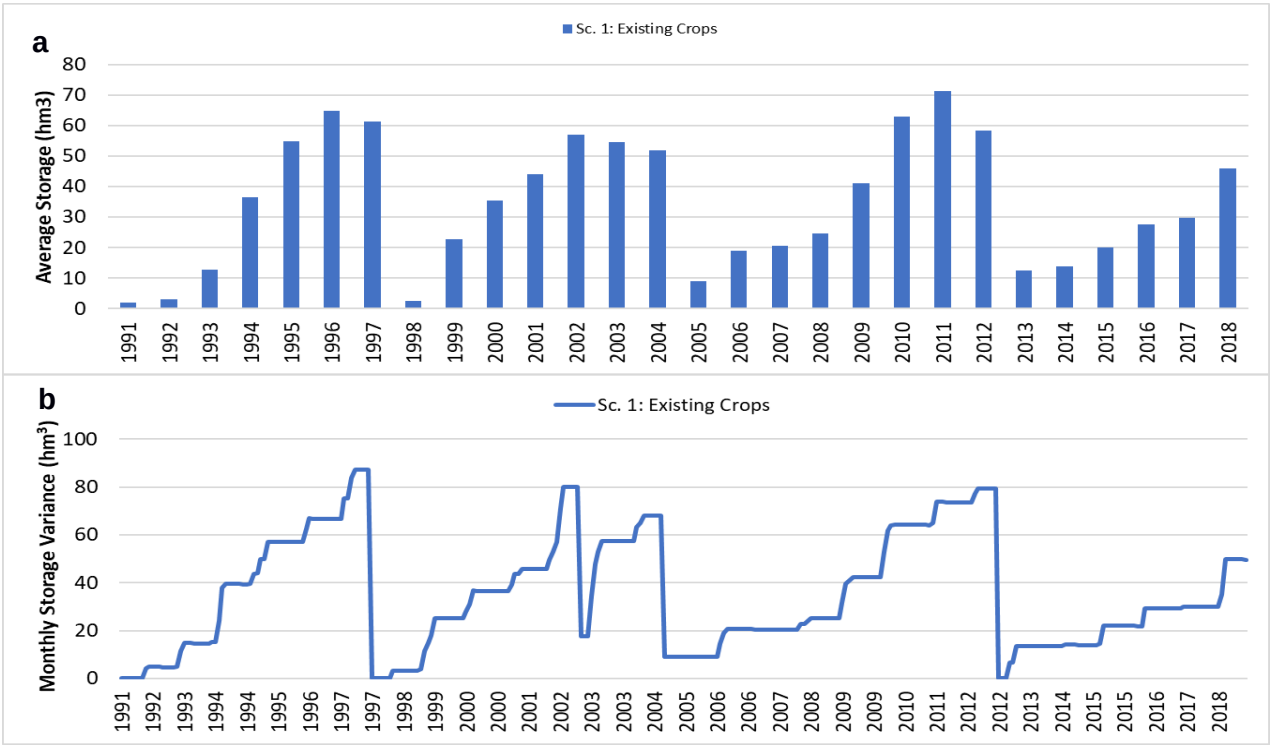

Figure 2. Groundwater storage deficit for all the scenarios of the case A in a) average annual variation and b) monthly variation

3.2 Water Evaluation and Planning of Scenarios 2 and 3

Based on the WEAP model created for Scenario 1 the volume capacity of the reservoir, the environmental flow requirement, the irrigated crop types by Xirias reservoir were entered in the model, and additional relevant changes were made for the simulation of the Scenarios 2 and 3.

The aquifer's storage deficit, and the changes of the reservoir's volume are shown in Figure 3 and 4, respectively. In the Scenario 2 the crops that are irrigated lead to larger groundwater reserves from 1997 and onwards as shown in Figure 3. The aquifer has lower storage when Scenario 3 the crops that were intended to be irrigated, is applied.

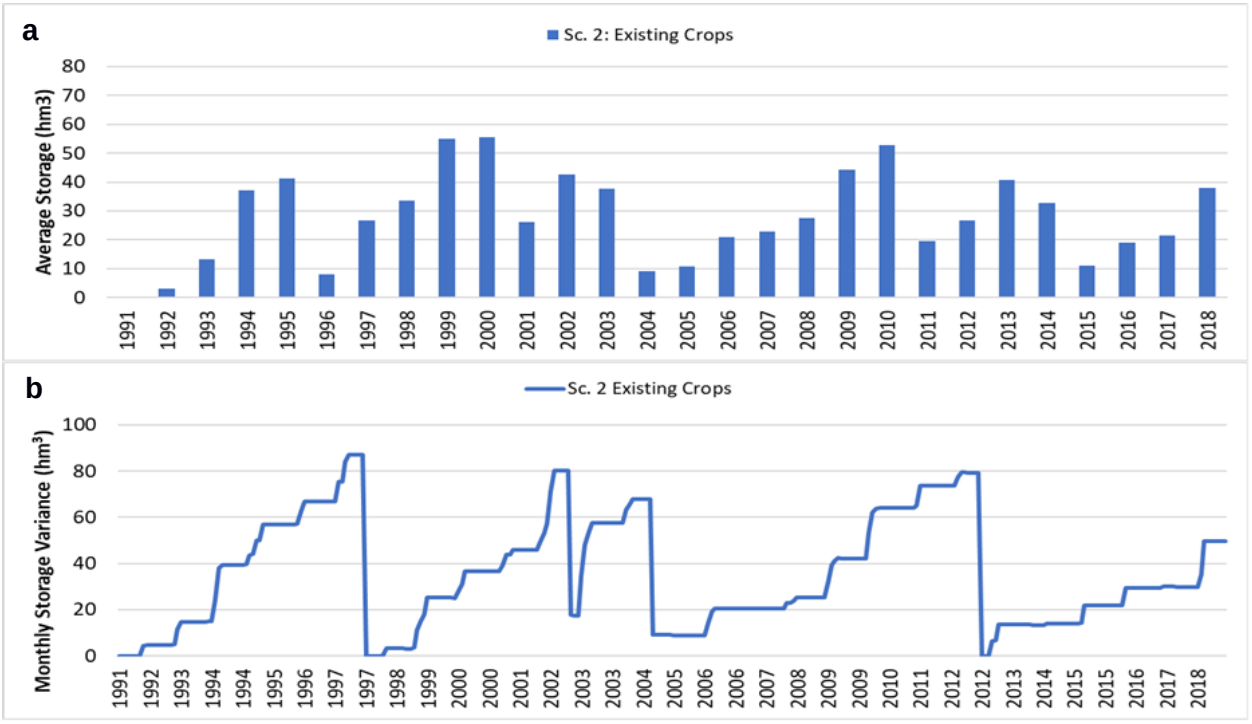

Figure 3. Groundwater aquifer storage deficit for Case B a) average annual variation and b) monthly variation

According to Figure 4, the scenario 3 with the crops that were intended to be irrigated resets and draws to zero the stored water volume of the reservoir several times in October. On the other hand, in the Scenario 2 the Xirias reservoir operates successfully and satisfies the irrigation crop water demands of the irrigated are.

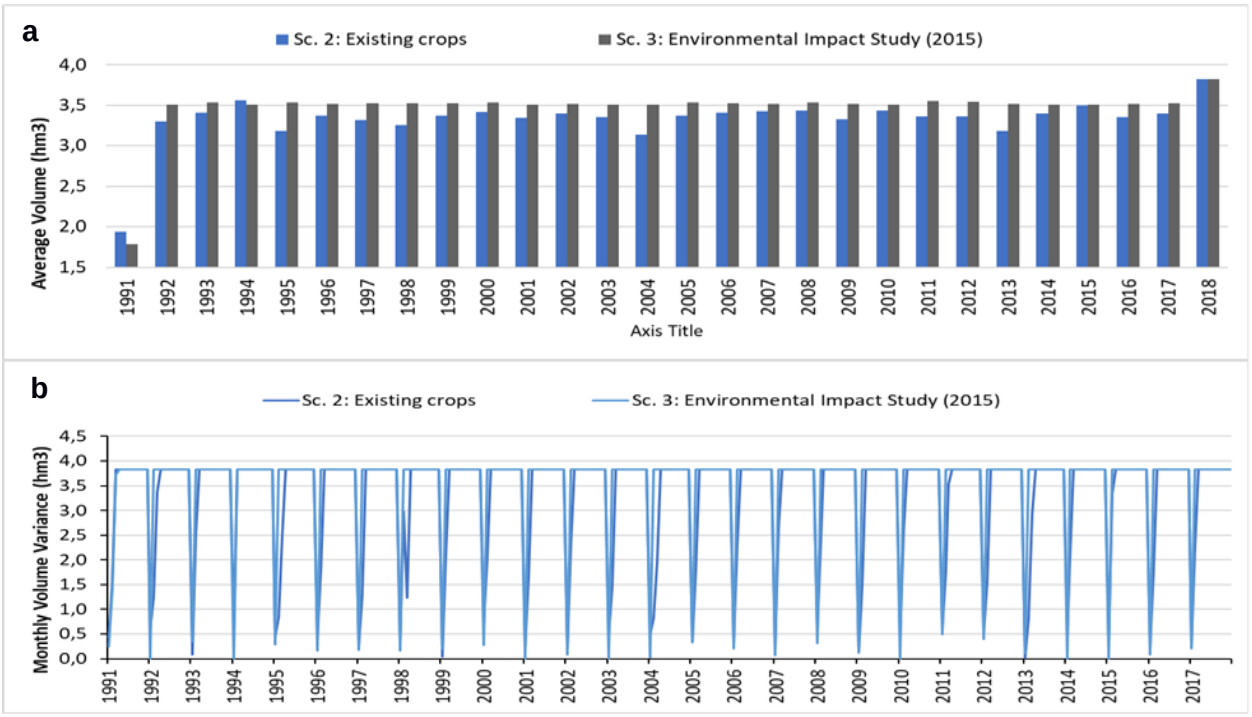

Figure 4. Comparative reservoir water volume diagram for each scenario for a) average monthly annual volume and b) monthly variation

3 Conclusions

The results of the simulation of water resources management scenarios in the Mediterranean Xirias Watershed with the WEAP software indicate that the operation of the reservoir (Case B) is a more efficient policy than the current situation (Case A). The most appropriate water resources Scenario was selected based on the comparison and analysis of the simulation results. The best is Scenario has the least negative impact on the aquifer of the watershed, and satisfies the irrigation needs of the crops to the greatest extent. According to Figure 2 and 3 the reduction of the deficit water balance of the aquifer is achieved with the operation of the Xirias reservoir. According to Figure 4, it is observed that the Scenario 2 of the irrigation of existing crops is the most ideal since the average monthly stored volume of water in the reservoir is within the capacity and at lower levels than the Scenario 3. The operation of Xirias reservoir is capable of irrigating the current cultivated crops and facilitate the irrigation of a wider area than it was initially designed to irrigate. In conclusion, Scenario 2, the operation of the reservoir to irrigate the current crop types cultivated is the best proposal for the efficient management of the water resources of Xirias watershed.

References

Alamanos, A, Mylopoulos, N, Loukas, A, Gaitanaros, D (2018) An Integrated Multicriteria Analysis Tool for Evaluating Water Resource Management Strategies. Water 10(12), 1795. https://doi.org/10.3390/w10121795

Georgiadou, I (2015) Simulation and Management of the Groundwater Aquifer in the Almyros Basin. Master Thesis, Department of Civil Engineering, School of Engineering, University of Thessaly, Volos. (In Greek) https://opac.seab.gr/record=b1208811~S11*gre

Kollaiti, M (2021) Sustainable Water Resources Management in Areas with Water Scarcity Phenomena: The case of Xirias basin, in Almyros. Diploma Thesis, Department of Civil Engineering, School of Engineering, University of Thessaly, Volos. (In Greek) http://hdl.handle.net/11615/57625

Loukas A, Mylopoulos N, Vasiliades, L (2007) A Modeling System for the Evaluation of Water Resources Management Strategies in Thessaly, Greece. Water Resources Management 21(10), 1673-702. https://doi.org/10.1007/s11269-006-9120-5

Lyra A, Loukas, A, Sidiropoulos, P (2021a) Impacts of irrigation and nitrate fertilization scenarios on groundwater resources quantity and quality of the Almyros Basin, Greece. Water Supply 21(6), 2748-59. https://doi.org/10.2166/ws.2021.097

Lyra, A, Loukas, A, Sidiropoulos, P, Tziatzios, G, Mylopoulos, N (2021b) An Integrated Modeling System for the Evaluation of Water Resources in Coastal Agricultural Watersheds: Application in Almyros Basin, Thessaly, Greece. Water 13(3), 268. https://doi.org/10.3390/w13030268

Lyra, A, Loukas, A, Sidiropoulos, P, Voudouris, K, Mylopoulos, N. (2022) Integrated Modeling of Agronomic and Water Resources Management Scenarios in a Degraded Coastal Watershed (Almyros Basin, Magnesia, Greece). Water. 14(7):1086. https://doi.org/10.3390/w14071086

Lyra, A, Pliakas, F, Skias, S, Gkiougkis, I (2016) Implementation of DPSIR framework in the management of the Almyros basin, Magnesia Prefecture. Bulletin of the Geological Society of Greece, Proceedings of the 14th International Congress L(2), 825-34. https://doi.org/10.12681/bgsg.11789

MINAGRIC (2015) Environmental Impact Study for the Modification of the Decision on the Approval of the Environmental Conditions. Xirias Reservoir in Almyros, Magnesia Prefecture. Directorate of Technical Works and Rural Infrastructure, Hellenic Ministry of Rural Development and Food.

MINAGRIC (2018). Amending Project for the Construction of Xirias Reservoir in Almyros, Magnesia Prefecture.

MEEC (2017) 1st Revision of the River Basin Management Plan of the River Basin District of Thessaly (GR08). Ministry of Environment, Energy and Climate Change (Special Secretariat for Water). http://wfdver.ypeka.gr/el/consultation-gr/1revision-consultation-gr/

Mylopoulos, N (2006) Water Resources Management. Teaching Notes, University of Thessaly, Department of Civil Engineering, School of Engineering, University of Thessaly, Volos.

Serageldin, I (2009) Water: conflicts set to arise within as well as between states. Nature 459, 163https://doi.org/10.1038/459163b

Sidiropoulos, P, Loukas, A, Georgiadou, I (2016) Response of a degraded coastal aquifer to water resources management. European Water 55, 67-77. https://www.ewra.net/ew/pdf/EW_2016_55_06.pdf

Sieber J (2006) WEAP Water Evaluation and Planning System. International Congress on Environmental Modelling and Software, 397. https://scholarsarchive.byu.edu/iemssconference/2006/all/397

Sieber J (2015) Water Evaluation and Planning System (WEAP) USER GUIDE. Stockholm Environment Institute (SEI). www.weap21.org

YPETHE (2022) Xeria Almyros Reservoir, Magnesia. Thessaly Water Utilization Projects [Smaller Regional Projects] https://www.ypethe.gr/archive/limnodexameni-xeria-almyroy-magnisias

Earth observation techniques for the assessment of water surfaces quality. A review of current methodologies

Samarinas N.[1,4], M. Spiliotopoulos[2], D. Malamataris[2], N. Tziolas[3,4], G. Zalidis[3,4] and A. Loukas[1]

[1] Department of Rural and Surveying Engineering, Aristotle University of Thessaloniki, Thessaloniki, Greece
[2] Department of Civil Engineering, University of Thessaly, Volos, Greece
[3] Forestry and Natural Environment, Aristotle University of Thessaloniki, Thessaloniki, Greece
[4] Interbalkan Environment Center, Lagadas, Greece

Abstract. At this work, an initial literature review has been carried out, relating remote sensing with the condition of aquatic environment and how satellite data is expected to dominant at the near future. The growing demand for continuous information and data on water quality is impossible to achieve using only traditional in-situ techniques, as they present a number of limitations in their implementation thus creating a rather costly and time-consuming water monitoring process. This is largely an obstacle to achieve the objectives of European directives such the Water Framework Directive (WFD), bringing the EU Member States to the brink of collapse with several difficulties in complying with its requirements. On the other hand, Earth Observation (EO) has an immense potential as an enabling tool for the effective implementation of EU directives and national priorities. Undoubtably, the synergy between remote sensing and in-situ techniques can provide a strong monitoring system and near real time information of various water quality indicators, mainly due to their geospatial stability and repeatability. In this regard, at the current review, a thorough analysis of innovative EO and remote sensing technologies based on the results of research and scientific analysis is presented. Subsequently, it is attempted to determine an appropriate way of contributing modern surveillance techniques for surface water in the design and decision-making related to WFD by the competent bodies. The main objective of this effort is to investigate the appropriate ways and methods for disseminating data for the information produced to reach and exploit the actual actors involved.

1 Introduction

Access to clean, safe drinking water is a key determinant of quality of life, as it is directly linked to human health. Surface-inland water are the main source of drinking water and other several uses such as irrigation, industry, energy etc., depends on the availability and quality of the water (Cravalho *et. al* 2013). The Water Framework Directive (WFD) (European Commission, 2000) recognized that quality information about the environmental state of surface and ground waters is essential for water management and for improving the environmental quality of Europe's waters. Nowadays, there is a growing realization among the policymakers, as highlighted by Blueprint to safeguard Europe's Water Resources, that a systemic approach is key to resolving challenges in water domain.

The limitations that traditional-conventional monitoring approaches present could be an obstacle for EU Member states to achieve the WFD objectives bringing them to the brink of collapse with several difficulties in complying with its requirements. On the other hand, Earth Observation (EO) provides unique capabilities for addressing the enormous challenges inherent to the water quality/quantity status (i.e., regular monitoring of large areas, global reach). As an example, EO can be used to estimate key parameters that are related to water status in aquatic systems, like algae presence and bloom to informed decision making. Research studies showed that satellites and especially Copernicus program can improve global inland water mapping and they can offer a useful information for several water quality parameters (Drush *et al.* 2013, Du *et al.* 2016) in combination with computer science techniques (Peterson *et al.* 2018, Saberioon *et al* 2020).

This work provides a high-level overview of different innovative tools and techniques, based on a recent literature review, for monitoring, that can be used to generate useful quality data and information for catchment management and reduce both the cost and the monitoring frequency. The primary goal is the future application of the new EO technologies, by the competent bodies, in order to improve the current monitoring methods and to provide the transfer of know-how for the smooth integration of the developing European countries into the general European community and their future compliance with European directives such as the WFD.

2 Limitations of conventional techniques for water quality assessment

To highlight the vital importance of the synergy between conventional and remote sensing techniques, first we must clarify the limitations and the existing gaps that arise. In the absence of technological development and for many years, traditional water quality monitoring techniques have generously offered their services. However, most of the surface large water bodies remain unsampled, due to their large number and cost of

field visits, equipment, and maintenance (Ritchie *et al* 2003). In addition, field sampling has in recent decades focused on water bodies that are affected by eutrophication, which has left large gaps in the data availability from other sites. Therefore, until today the surface quality monitoring especially for large water bodies could not be considered as reliable and it is under dispute. Briefly in the following figure (Figure 1) are the most important limitations and gaps associated with conventional techniques that lead to using new tools based on airborne and spaceborne methods.

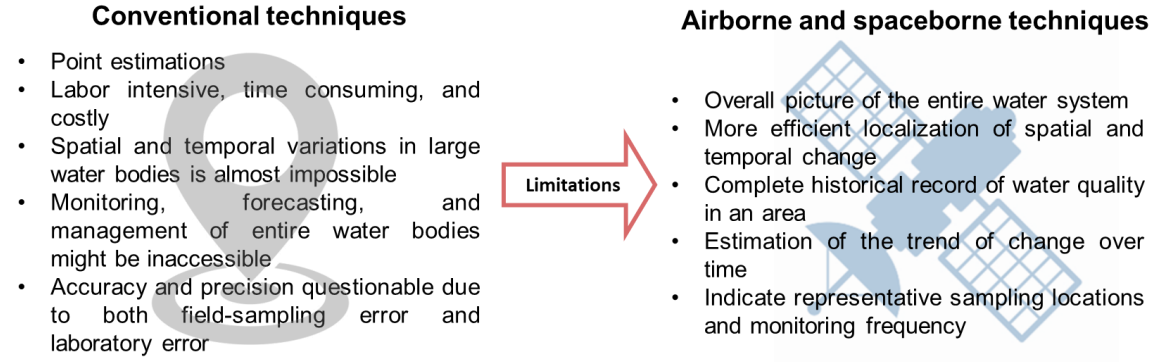

Figure 1. Fill the limitations of the conventional techniques with airborne and spaceborne techniques

3 Existing Earth Observation landscape and methodologies

In the present work a comprehensive literature review from 2015 to 2021 using the Scopus database and Google's scientific search engine took place to get a reliable picture of the current surface water monitoring process, under the WFD umbrella, using innovative monitoring technologies. The selection period is considered representative as the first goal of the WFD was to achieve good status by 2015. Most of the work related to the improvement of the monitoring under the WFD came after the problems and failures to achieve the goals by completing the 1st Review of River Basin Management Plans (RBMPs). Additionally, however, a thorough literature review not directly related to WFD was conducted by Gholizadeh et al. (2016) and therefore the time chosen is a continuation of it. Also, a thorough analysis of the protection of European waters as well as the adoption of new technologies and methodologies for dealing with the crisis that the European waters are facing, has been carried out by Carvalho *et al.* (2019). Their analysis took place through an online conference (eConference), questionnaires and experts on the implementation of WFD with the aim of providing practical ideas and solutions to improve the existing way of water monitoring and the future development of sustainable management.
The review was conducted using keywords and emphasis was placed on the scientific work that covered the following request:

["Earth observation" or "Remote Sensing"]
and
["Water Framework Directive" or "Water quality monitoring"]

The keyword “water quality monitoring” refers to the potential monitored water properties based on the WFD requirements for information on the quality status of water systems. In this context, 28 scientific papers in English were founded and separated accordingly and a detailed description is provided in the Appendix (Table 1) at the end of this paper. An in-depth analysis of the works on the current status was then conducted with the following questions highlited:

1. What are the main EO data sources, sensors and types that have been used?
2. What are the observed and predicted water quality indicators?

The review was carried out with emphasis on the new EO technologies such as spaceborne systems, autonomous floating and aerial systems as well as static-in situ sensors. Their applications in most of the examined works (> 50%) had as main purpose to provide knowledge about their use for a rational water management as well as to promote these technologies and to be a basis for future research and utilization under the WFD. Examining the above technologies in the context of the work, satellite systems undoubtedly offer greater spatial coverage with large time series, present non-destructive sampling methods and are also more cost-effective.

As a search was carried out from 2015 onwards, some of the above technologies were not identified in the context of scientific literature work but are presented in the review of related research projects. It is also fully

understood that in the graphs presented below (see section 3.1 and 3.2) the total number of sensors presented exceeds the total number of examined works, as the authors in many cases used for example more than one sensor and examined more than one indicator.

3.1 Earth Observation systems in use

The arrival of Sentinel's from the European Space Agency under the auspices of the Copernicus program has been and continues to be the most ambitious EO technology with global coverage, with more than 300.000 registered users who are likely to increase in the future with the upcoming Sentinel satellites (Sentinel 5P, 6) (European Commission, 2019).

Considering the collected literature, regarding the satellite systems, the three most widespread satellites for the determination of surface water quality indicators were identified: Sentinel 2 (> 30%), Sentinel 3 (12%) and Landsat 8 (>8%) of the US National Aeronautics and Space Administration (NASA). The satellites have multispectral sensors with medium spatial resolution (10-60m). Furthermore, and to highlight the size of the contribution of satellite systems to water monitoring, the Sentinel-2 satellite gives estimates of chlorophyll-*α* every 5 days with a spatial resolution of 10-60m while Sentinel-3 gives daily estimates with a spatial resolution of 300m.

In addition, to satellite systems, a significant number of works used new technologies (> 28%) based either on point measurements or using aerial systems such as unmanned aerial vehicles (UAVs) and airborne flights with spectral and hyperspectral sensors.

The following graph (Figure 2) shows the sensors used in the examined papers and their occurrence number in the total work. With the term other are meant, new technologies based either on point measurements or using aerial systems and airborne flights.

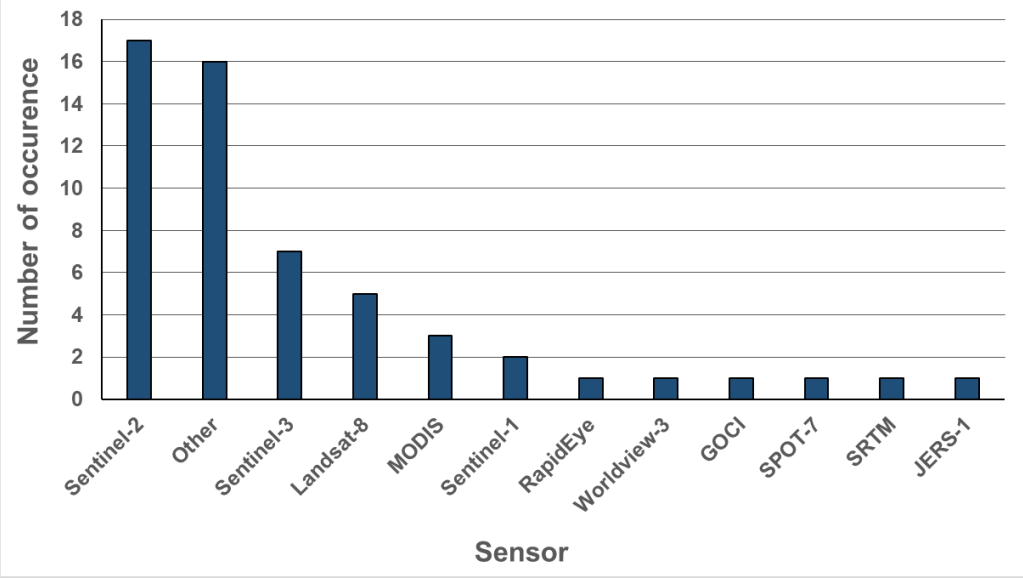

Figure 2. The total number of sensors appeared in the 28 examined research papers

3.2 Observed water quality status indicators

As mentioned above a thorough review of the literature on the use of satellite systems for the determination of water quality parameters was done by Gholizadeh et al. (2016) recognizing a total of 11 quality parameters. In addition, Shang et al. (2018) present an existing status of the remote sensing technologies and the sensors used to monitor water quality indicators in relation to the nutrient cycle. In most of the 28 examined works, emphasis was placed on the determination of the chlorophyll-*α* index (> 45%), a fact that is expected and completely acceptable as it is perhaps the most important or one of the most important water quality indicators and an indicator largely recognizable in the context of WFD. The following are the indices of turbidity (> 19%) and total suspended solids (> 7%). It should also be noted that in the current work included as indicator also the land use changes, as land use change in a River Basin could lead to potentially large-scale pressures on water bodies. Figure 3 presents the most important water quality indicators based on the 28 examined papers.

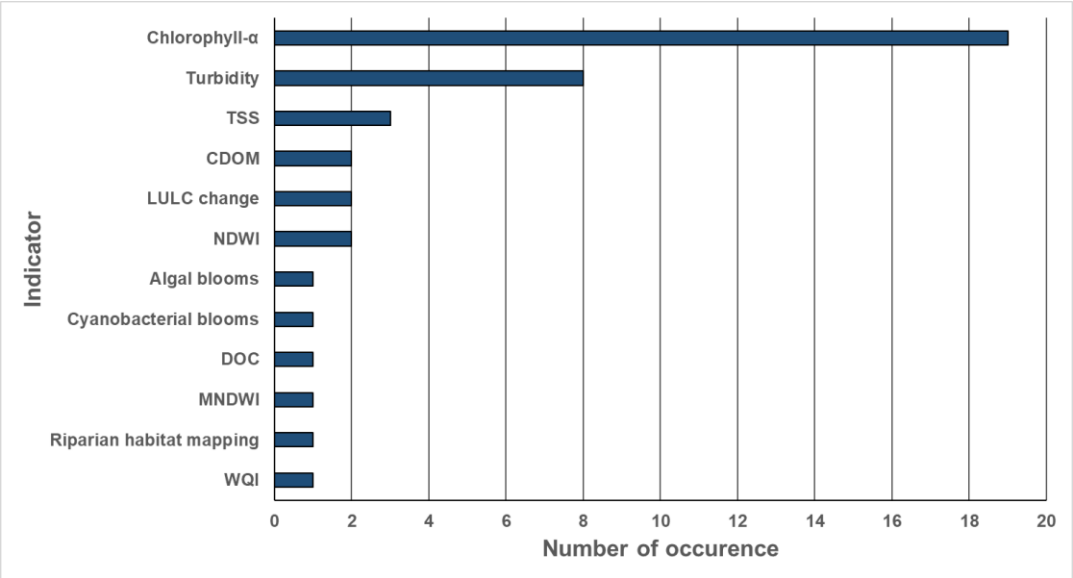

Figure 3. Most important water quality indicators based on the 28 examined scientific papers

4 The proposed and ambitious future with innovative EO services in the forefront for WFD implementation

4.1 The importance to adopt the new EO technologies under the EU countries cooperation

Burning issues such as climate change, population growth and the impact on food security, over-exploitation of natural resources, migration, social stability and economic prosperity require cooperation between countries. The success of such efforts is undoubtedly based on the development of a long-term and structured dialogue between EU countries and the transformation of this dialogue into substantive action. This has been pursued for many years through the definition of common strategies and the implementation of relevant policies at national, regional or international level. The latter takes place through the mobilization of many specific actions (eg ENI, IPA), development programs and partnership programs (PRIMA, Africa-EU partnership, etc.).

To achieve the above, innovative technological tools should be fully utilized. In this context, is where the new EO techniques could offer a range of near-real-time services to provide reliable information and data to end users such as decision and policy makers, researchers, advisors, public sector etc., enabling them to take effective action to address different environmental challenges and also to ensure urban security.

4.2 An ambitious proposed synergistic framework in support of the WFD

Since the launch of Group on Earth Observations (GEO) and European Copernicus Program (Copernicus Land Monitoring Service and Copernicus Marine Environment Monitoring Service), a wide range of activities promoting EO as a key enabler for accurate and timely provision of information for enhanced management of the environment have been carried out. These range from EU projects (e.g., EO-MORES, Rheticus) to ESA-funded projects (Coastal Thematic Exploitation Platform) and large-scale demonstrators under the different GEO Initiatives (e.g. GEOGLOWS). Whilst these activities have made great strides towards developing technological solutions, the use of coordinated EO and its in situ part (e.g., unmanned vehicles, drones, handheld sensors) as a key tool in the service of water bodies monitoring, is still not adequately taken up.
Figure 4 presents 4 different pillars where their synergistic use can offer innovative and integrated solutions in surface water monitoring. In essence, gives the immediately available services and solutions that have been developed but have not yet been sufficiently utilized for the near-real time and reliable monitoring of water resources.
Based on the work done by GEO and taking advantage of subsequent opportunities (e.g. EUROGEO thematic networks), the effort to involve the regional management bodies in specific initiatives should be a key guideline. In the same context, the NEREUS network (Network of European regions using space technologies) can be used as a bridge between the private sector and regional decision-making bodies and management to promote mature solutions from Central European regions.

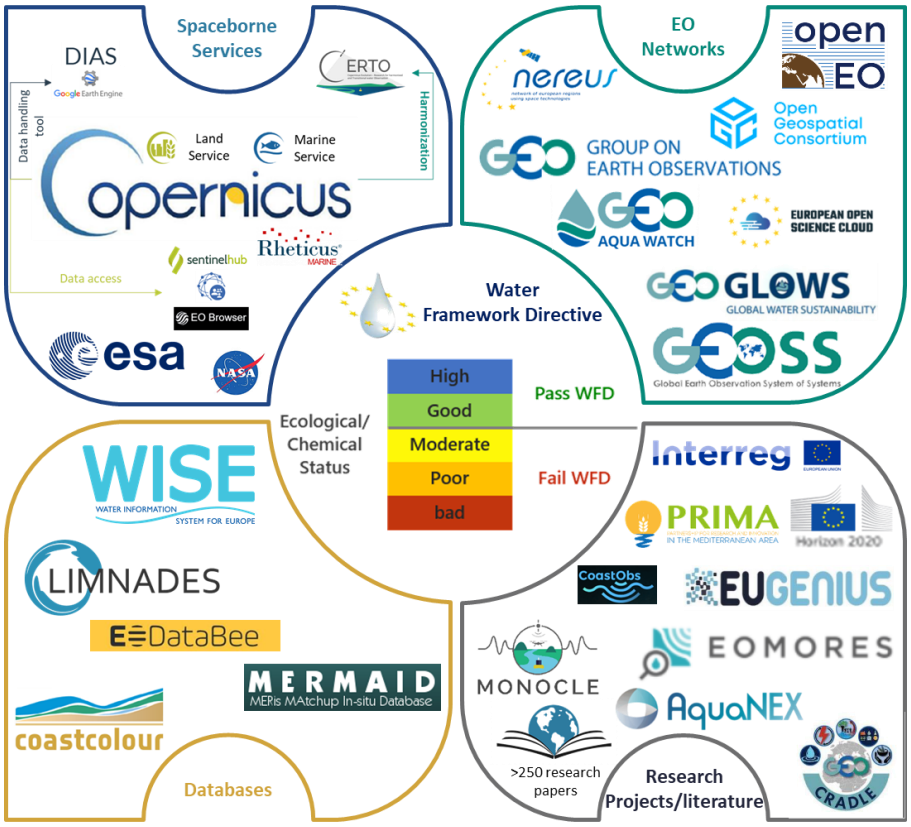

Figure 4. An overall framework which can provide near-real time and reliable monitoring system for supporting the WFD objectives

Business agreements, as well as networking actions, should also be try to structure the supply-demand interaction in selected sectors at regional and international level. In addition, we must highlight the need for existence of data that have been collected with specific protocols and their systematic reuse.
The specific data as well as products developed through research projects such as MONOCLE, AquaNEX, GEO-CRADLE etc., should be promoted and presented at a higher level in order to ensure the direct information of the stakeholders about the current status of each water system of the country, through thematic maps and further promote the research process through the development of innovative services by other groups utilizing existing information. To achieve this, it is necessary to harmonize existing platforms and data nodes by promoting the use of common standards and protocols taking into account international standards such as the Open Geospatial Consortium (OGC). The ultimate goal for the platforms and data nodes is to be supported and promote fundamental efforts such GEO and Copernicus DIAS.
Promoting a culture of data sharing is an essential component of promoting EO data with the aim of developing services for the benefit of different users. In this context, the GEO through the Global Earth Observation System of Systems (GEOSS) node provides a unique solution to the value of geospatial nodes and their role not only as a data entry gateway but also as a support mechanism for their open use. It is therefore strongly recommended that such efforts be scaled up and reproduced, considering regional solutions such as the GEO-CRADLE and NEXTGEOSS project data repositories as well as open databases such as LIMNADES and WISE (Water Information System for Europe). The previous are examples that facilitate access to useful data sets and portals from open data sites, and many of them refer to water body monitoring. In the light of the above, open data repositories play an important role in promoting the idea of data sharing, the further development of innovative services, as well as in the direction of the implementation of EU policies for the protection of natural resources by exploiting these media.

4 Summary

Without a doubt, designing a sustainable water quality monitoring program remains a challenge due to the complexity of the problem. In addition, the water management authorities should be in line with the latest technological developments and trends. Certainly, to support the WFD and achieve the target for 2027, the infrastructure and monitoring methods should be able to cover in real time the monitoring of at least those water bodies that are not in good ecological status or are borrowing their overall status from neighboring water

bodies due to lack of monitoring. According to the results of the literature review that took place in the present work and the proposal for synergy between existing satellite services, networks, databases and proper utilization of research projects results, such goals could now be achieved due to technological progress in water monitoring through innovative EO tools and remote sensing methods. The direct benefits are focused on dramatically reducing the overall operating and maintenance costs, thus enabling the establishment of permanent and reliable water monitoring methods as well as enhancing the often-weak existing national monitoring networks. Also, new methods of dissemination, management, and final utilization of data, further enhance the ability of competent authorities to take timely protection measures and proper management decisions for the water bodies, fully supporting the compliance of European countries with the growing demands of WFD requirements.

Acknowledgements

This research was partly funded by the "AquaNEX" project, funded by the Interreg IPA Cross-border Cooperation Programme "Greece-Albania 2014–2020".

References

Ansper A. & Alikas K., 2019. Retrieval of chlorophyll-a from Sentinel-2 MSI data for the European Union water framework directive reporting purposes. *Remote Sensing*. 11, Issue 11 January 2019 Article number 64.

Beck, R., Zhan, S., Liu, H., Tong, S., Yang, B., Xu, M., Ye, Z., Huang, Y., Shu, S., Wu, Q., Wang, S., Berling, K., Murray, A., Emery, E., Reif, M., Harwood, J., Young, J., Nietch, C., Macke, D., Su, H.,2016. Comparison of satellite reflectance algorithms for estimating chlorophyll-a in a temperate reservoir using coincident hyperspectral aircraft imagery and dense coincident surface observations. *Remote Sensing of Environment*. Vol. 178, pp. 15–30. https://doi.org/10.1016/j.rse.2016.03.002.

Bresciani, M., Cazzaniga, I., Austoni, M., Sforzi, T., Buzzi, F., Morabito, G., & Giardino, C., 2018. Mapping phytoplankton blooms in deep subalpine lakes from Sentinel-2A and Landsat-8. *Hydrobiologia*. Vol. 824(1), pp. 197–214. https://doi.org/10.1007/s10750-017-3462-2.

Carvalho, L., Poikane, S., Solheim, L.A., Phillips, G., Borics, G., Catalan, J., Hoyos, D.C., Drakare, S., Dudley, B., Jrvinen, M., Laplace-Treyture, C., Maileht, K., McDonald, C., Mischke, U., Moe, J., Morabito, G., Nges, P., Nges, T., Ott, I., Pasztaleniec, A., Skjelbred, B., Thackeray, S., 2013. Strength and uncertainty of phytoplankton metrics for assessing eutrophication impacts in lakes. Hydrobiologia 704, 127–140. https://doi.org/10.1007/s10750-012-1344-1.

Chatziantoniou, A., Petropoulos, G.P., and Psomiadis, E., 2017. Co-Orbital Sentinel 1 and 2 for LULC Mapping with Emphasis on Wetlands in a Mediterranean Setting Based on Machine Learning. *Remote Sensing*. Vol. 9(12), p.1259.

Coelho, C., Heim, B., Foerster, S., Brosinsky, A., and de Araújo, J., 2017. In-situ and Satellite Observation of CDOM and Chlorophyll-a Dynamics in Small Water Surface Reservoirs in the Brazilian Semiarid Region. *Water*. Vol. 9(12), p. 913. https://doi.org/10.3390/w9120913

Delegido, J., Urrego, P., Vicente, E., Sòria-Perpinyà, X., Soria, J. M., Pereira-Sandoval, M., Ruiz-Verdú, A., Peña, R., & Moreno, J., 2019. Turbidez y profundidad de disco de Secchi con Sentinel-2 en embalses con diferente estado trófico en la Comunidad Valenciana. *Revista de Teledetección*, Vol. 54, p.15. https://doi.org/10.4995/raet.2019.12603.

Drusch, M., Bello, D.U., Carlier, S., Colin, O., Fernandez, V., Gascon, F., Hoersch, B., Isola, C., Laberinti, P., Martimort, P., Meygret, A., Spoto, F., Sy, O., Marchese, F., Bargellini, P., 2012. Sentinel-2: ESA's optical high-resolution mission for GMES operational services. Remote Sens. Environ. 120, 25–36. https://doi.org/10.1016/j.rse.2011.11. 026.

Du, Y., Zhang, Y., Ling, F., Wang, Q., Li, W., & Li, X., 2016. Water Bodies' Mapping from Sentinel-2 Imagery with Modified Normalized Difference Water Index at 10-m Spatial Resolution Produced by Sharpening the SWIR Band. *Remote Sensing*. Vol.8(4), p. 354. https://doi.org/10.3390/rs8040354.

Elhag, M., Gitas, I., Othman, A., Bahrawi, J., & Gikas, P., 2019. Assessment of Water Quality Parameters Using Temporal Remote Sensing Spectral Reflectance in Arid Environments, Saudi Arabia. *Water*. Vol. 11(3), p. 556. https://doi.org/10.3390/w11030556.

Erena, M., Domínguez, J.A., Aguado-Gimenez, F., Soria, J., and García-Galiano, S., 2019. Monitoring Coastal Lagoon Water Quality Through Remote Sensing: The Mar Menor as a Case Study. *Water*. Vol. 11(7), p. 1468. https://doi.org/10.3390/w11071468.

European Commission, 2000. Directive 2000/60/EC of the European Parliment and of the Council of 23 October 2000 establishing a framework for community action in the field of water policy. Official Journal of the European Communities.

European Commission, 2019. Copernicus Market report. Prepared by PwC. 164. https://www.copernicus.eu/sites/default/files/2021-03/Copernicus_Market_Report_2019.pdf

Gholizadeh, M., Melesse, A., Reddi, L.,2016. A Comprehensive Review on Water Quality Parameters Estimation Using Remote Sensing Techniques. *Sensors*, Vol.16, p. 1298.

Gómez, D., Salvador, P., Sanz, J., Casanova, J.L., 2021. A new approach to monitor water quality in the Menor sea (Spain) using satellite data and machine learning methods. *Environmental Pollution*. 286, 10.1016/j.envpol.2021.117489.

Hess, L. L., Melack, J. M., Affonso, A. G., Barbosa, C., Gastil-Buhl, M., and Novo, E. M. L. M., 2015. Wetlands of the Lowland Amazon Basin: Extent, Vegetative Cover, and Dual-season Inundated Area as Mapped with JERS-1 Synthetic Aperture Radar. *Wetlands*. Vol. 35(4), pp. 745–756. https://doi.org/10.1007/s13157-015-0666-y

Jeong, S. G., Mo, Y., Kim, H. G., Park, C. H., and Lee, D. K., 2016. Mapping riparian habitat using a combination of remote-sensing techniques. *International Journal of Remote Sensing*. Vol. 37(5), pp. 1069–1088. https://doi.org/10.1080/01431161.2016.1142685.

Kislik, C., Dronova, I.,and Kelly, M., 2018. UAVs in Support of Algal Bloom Research: A Review of Current Applications and Future Opportunities. *Drones*. Vol. 2(4), p. 35. https://doi.org/10.3390/drones2040035.

Kudela, R. M., Palacios, S. L., Austerberry, D. C., Accorsi, E. K., Guild, L. S., and Torres-Perez, J., 2015. Application of hyperspectral remote sensing to cyanobacterial blooms in inland waters. *Remote Sensing of Environment*, Vol. 167, pp. 196–205. https://doi.org/10.1016/j.rse.2015.01.025.

Li, X., Ding, J., and Ilyas, N., 2021. Machine learning method for quick identification of water quality index (WQI) based on Sentinel-2 MSI data: Ebinur Lake case study. *Water Supply*. Vol. 21(3), pp. 1291–1312. https://doi.org/10.2166/ws.2020.381

Lyu, H., Zhang, J., Zha, G., Wang, Q., & Li, Y., 2015. Developing a two-step retrieval method for estimating total suspended solid concentration in Chinese turbid inland lakes using Geostationary Ocean Color Imager (GOCI) imagery. *International Journal of Remote Sensing*. Vol. 36(5), pp. 1385–1405. https://doi.org/10.1080/01431161.2015.1009654.

Matthews, M. W., 2017. Bio-optical Modeling of Phytoplankton Chlorophyll- a. In *Bio-optical Modeling and Remote Sensing of Inland Waters*, Elsevier. pp. 157–188. https://doi.org/10.1016/B978-0-12-804644-9.00006-9.

Pahlevan, N., Smith, B., Schalles, J., Oppelt, N., Stumpf, R., 2020. Seamless retrievals of chlorophyll-a from Sentinel-2 (MSI) and Sentinel-3 (OLCI) in inland and coastal waters: A machine-learning approach. *Remote Sensing of Environment*. Vol. 240, 111604.

Palmer, S. C. J., Hunter, P. D., Lankester, T., Hubbard, S., Spyrakos, E., N. Tyler, A., Présing, M., Horváth, H., Lamb, A., Balzter, H., and Tóth, V. R., 2015. Validation of Envisat MERIS algorithms for chlorophyll retrieval in a large, turbid and optically-complex shallow lake. *Remote Sensing of Environment*. Vol. 157, pp.158–169. https://doi.org/10.1016/j.rse.2014.07.024

Pizani, F. M. C., Maillard, P., Ferreira, A. F. F., and de Amorim, C. C., 2020. Estimation of Water Quality in a reservoir from Sentinel-2 MSI and Landsat-8 Oli Sensors. *ISPRS Annals of the Photogrammetry, Remote Sensing and Spatial Information Sciences*. Vol 3. pp.401–408. https://doi.org/10.5194/isprs-annals-V-3-2020-pp. 401-2020.

Peterson, K.T., Sagan, V., Sidike, P., Cox, A.L., Martinez, M., 2018. Suspended sediment concentration estimation from landsat imagery along the Lower Missouri and Middle Mississippi rivers using an extreme learning machine. Remote Sensing 10, 1503. https://doi.org/10.3390/rs10101503

Pyo, J., Duan, H., Baek, S., Kim, M. S., Jeon, T., Kwon, Y. S., Lee, H., and Cho, K. H., 2019. A convolutional neural network regression for quantifying cyanobacteria using hyperspectral imagery. *Remote Sensing of Environment*. Vol. 233, 111350. https://doi.org/10.1016/j.rse.2019.111350.

Ritchie, J.C.; Cooper, C.M.; Schiebe, F.R., 1990. The relationship of MSS and TM digital data with suspended sediments, chlorophyll, and temperature in Moon Lake, Mississippi. Remote Sens. Environ., 33, 137–148.

Saberioon, M., Brom, J., Nedbal, V., Souček, P., and Císař, P., 2020. Chlorophyll-a and total suspended solids retrieval and mapping using Sentinel-2A and machine learning for inland waters. *Ecological Indicators*. Vol. 113, 106236. https://doi.org/10.1016/j.ecolind.2020.106236.

Song, W., J. Dolan, D. Cline, G. Xiong, 2015. Learning-based algal bloom event recognition for oceanographic decision support system using remote sensing data. *Remote Sensing*. Vol. 7 (10), pp. 13564-13585.

Stumpf, R.P., Davis, T.W., Wynne, T.T., Graham, J.L., Loftin, K.A., Johengen, T.H., Burtner, A., 2016. Challenges for mapping cyanotoxin patterns from remote sensing of cyanobacteria. *Harmful Algae*. Vol.54, pp. 160-173.

Toming, K., Kutser, Laas, T. A., Sepp, Paavel, M. B., Nõges, T., 2016. First experiences in mapping lake water quality parameters with Sentinel-2 MSI imagery. *Remote Sensing.* Vol.8 (8), p. 640.

Wang, M., Yao, Y., Gao., H., Li, J., Zhang, F., Wu, Q., 2021. Time-Series Analysis of Surface-Water Quality in Xiong'an New Area, 2016–2019. *Journal of the Indian Society of Remote Sensing. V*ol. 49, pp. 857–872.

Wang, L., M. Xu, Y. Liu, H. Liu, R. Beck, M. Reif, Q. Wu, 2020. Mapping freshwater chlorophyll-*α* concentrations at a regional scale integrating multi-sensor satellite observations with google earth engine. *Remote Sensing*. Vol. 12 (20), p. 3278.

Zheng, G., DiGiacomo, P.M., 2017. Remote sensing of chlorophyll-a in coastal waters based on the light absorption coefficient of phytoplankton. *Remote Sensing of Environment*. Vol. 201 (2017), pp. 331-341.

Appendix

The table below presents the 28 examined research papers with specific details.

Table 1. The 28 examined scientific papers

	Reference	Sensor	Indicator	Goal
1	Ansper and Alikas 2019	Sentinel-2	Chlorophyll-*α* TSS Secchi depth	Estimate the ecological status of water in Estonian lakes
2	Beck *et al*. 2016	Airborne hyperspectral imagery Landsat-8 Sentinel-2 Sentinel-3 MODIS Worldview-3	Chlorophyll-*α*	Develop simple proxies for algal blooms in water bodies sensitive to algal blooms (especially toxic or harmful algal blooms (HABs)) and to facilitate portability between multispectral satellite imagers for regional algal bloom monitoring
3	Bresciani *et al*. 2018	Sentinel-2 Landsat-8 in-situ measur.	Chlorophyll-*α*	Mapping phytoplankton blooms in 2016 in the five largest Italian subalpine lakes
4	Chatziantoniou *et al*. 2017	Sentinel-1 Sentinel-2 SRTM	NDWI LULC change	Mapping land use and land cover in the National Park of Koronia and Volvi Lakes
5	Coelho *et al*. 2017	Landsat-8 RapidEye in-situ measur.	Chlorophyll-*α* CDOM	Retrieving water-quality parameters in three small surface reservoirs
6	Delegido *et al*. 2019	Sentinel-2	Secchi depth Turbidity	Turbidity and Secchi disc depth with Sentinel-2 in different trophic status reservoirs at the Comunidad Valenciana
7	Du *et al*. 2016	Sentinel-2	NDWI MNDWI	A novel 10-m spatial resolution MNDWI is produced from Sentinel-2 images by downscaling the 20-m resolution SWIR band to 10 m based on pan-sharpening
8	Elhag *et al*. 2019	in-situ measur. Sentinel-2	Chlorophyll-*α* Turbidity	The research findings support the use of remote sensing data of Sentinel-2 to estimate water quality parameters in arid environments
9	Erena *et al*. 2019	in-situ measur. Sentinel-2 Landsat-8 Sentinel-1 Sentinel-3 SPOT-7	Chlorophyll-*α* Turbidity	A methodology and monitoring system were generated to track the water quality in the Mar Menor in real-time and space
10	Gomez *et al*. 2021	in-situ measur. Sentinel-2	Chlorophyll-*α*	Derive chlorophyll-a (chl-a) concentrations in the Menor sea lagoon (Spain) using a machine learning approach with S2 data
11	Hess *et al*. 2015	JERS-1	LULC change	Wetland extent, vegetation cover, and inundation state were mapped for the first time at 100 m resolution for the entire lowland Amazon basin, using mosaics of Japanese Earth Resources Satellite (JERS-1) imagery acquired during low- and high-water seasons in 1995–1996
12	Jeong *et al*. 2016	in-situ measur. UAV	ripanian habitat mapping	Investigate methods to classify multispectral data and lidar for riparian habitat mapping, and to identify major habitat components for two target species
13	Kislik *et al*. 2018	in-situ measur UAV	Algal blooms	Reviews current literature focusing on UAVs and algal blooms, and assesses the current state of research, primary barriers to conducting these studies, and what the future holds for this research
14	Kudela *et al*. 2015	MODIS	Cyanobacterial blooms	Spectral-shape algorithms requiring minimal atmospheric correction can be used across a range of legacy sensors to detect cyanobacterial blooms and that, with the availability of high spectral resolution data and appropriate atmospheric correction, it is possible to separate the cyanobacterial genera Aphanizomenon and Microcystis
15	Li *et al*. 2021	in-situ measur. Sentinel-2	WQI	Analysis of the contribution rate of different water quality parameters in water by Z-score and PCA. Comparison of classical water quality index, correlation between spectral modeling and water quality parameters. Modeling and

				predicting Water Quality Index (WQI) using machine learning and linear correlation methods
16	Lyu *et al*. 2015	GOCI	Total Supsended Solids	Develop a two-step retrieval method for estimating TSS concentration in Chinese turbid inland lakes with high retrieval accuracy, particularly for the GOCI imagery
17	Matthews 2017	Sentinel-3	Chlorophyll-*α*	Investigate bio-optical modeling of chl-a, the primary indicator of phytoplankton production, and its estimation using various techniques of detection through different “optical pathways”
18	Pahlevan *et al*. 2020	in-situ measur. Sentinel-2 Sentinel-3	Chlorophyll-*α*	Machine-learning algorithm with potential utility in seamless construction of Chl-a data records in inland and coastal waters, i.e., harmonized, comparable products via a single algorithm for MSI and OLCI data processing
19	Palmer *et al*. 2015	Sentinel-3	Chlorophyll-*α*	Presents the first extensive validation of algorithms for chlorophyll-a (chl-a) retrieval by MERIS in the highly turbid and productive waters of Lake Balaton, Hungary
20	Pizani *et al*. 2020	Landsat-8 in-situ measur. Sentinel-2	Chlorophyll-*α* Secchi depth Turbidity	Compare the performance of Sentinel-2 MSI and Landsat-8 OLI sensors to produce multiple regression models of water quality parameters in a hydroelectric reservoir in Brazil
21	Pyo *et al*. 2019	Airborne hyperspectral imagery	Chlorophyll-*α*	The study demonstrates that Convolutional Neural Network (CNN) regression has the potential to detect and quantify cyanobacteria with high accuracy and can be an alternative to bio-optical algorithms
22	Saberioon *et al*. 2020	Sentinel-2	Chlorophyll-*α* TSS	Develop a semiempirical model for predicting water quality parameters by combining Sentinel-2A data and machine learning methods using samples collected from several water reservoirs within the southern part of the Czech Republic
23	Song *et al*. 2015	in-situ measur. MODIS Sentinel-3	Chlorophyll-*α*	The paper describes the use of machine learning methods to build a decision support system for predicting the distribution of coastal ocean algal blooms based on remote sensing data in Monterey Bay
24	Stumpf *et al*. 2016	Sentinel-3	Chlorophyll-*α*	The paper attempts to estimate microcystins (MCs) from satellite data by examining: (1) the issues involved with choosing surrogate pigment, (2) the characteristics of the MC surrogate relationship, (3) the strengths and limitations of the classes of remote sensing models used for cyanobacterial blooms, and (4) the strategies and considerations for determining whether, and how, to implement the dual models in cyanotoxin mapping
25	Toming *et al*. 2016	Sentinel-2	Chrolophyll-*α* CDOM DOC	Test suitability of Sentinel-2 MSI data for mapping different lake water quality parameters (Chl-a, water color, CDOM and DOC) by means of band ratio type algorithms, which have demonstrated good performance in previous lake remote sensing studies using other multispectral sensors
26	Wang *et al*. 2020	Sentinel-2	Chlyrophyll-*α*	Presents a methodological framework for automatically pairing surface reflectance values from multi-sensor satellite observations with ground water quality samples in time and space to form match-up points, using the Google Earth Engine cloud computing platform
27	Wang *et al*. 2021	Sentinel-2	Chlorophyll-*α*	The chlorophyll-a concentration and turbidity data of the surface waterbodies of the Xiong’an New Area from 2016 to 2019 were retrieved from higher-resolution Sentinel-2 data, and the time-series changes in water quality were statistically analysed
28	Zheng and DiGiacomo 2017	in-situ measur. Sentinel-2	Chlorophyll-*α*	Revsit the semi-analytical pathway of deriving [Chl-a] based on the light absorption coefficient of phytoplankton by introducing the generalized stacked-constraints model (GSCM) to partition satellite-derived total light absorption coefficient of water (with pure water contribution subtracted), anw(λ), into phytoplankton, aph(λ), and non-phytoplankton components, where anw(λ) is derived from satellite remote-sensing reflectance, Rrs(λ), using the Quasi-Analytical Algorithm

Water-saving irrigation practices for maize and cotton crops using the FAO Aquacrop model

Pantelis Sidiropoulos[1], Georgios Tziatzios[1], Marios Spiliotopoulos[1], Ioannis N. Faraslis[3], Nicholas Dercas[2], Nicolas R. Dalezios[1]

[1]Laboratory of Hydrology and Aquatic Systems Analysis, Department of Civil Engineering, School of Engineering, University of Thessaly, 38334 Volos, Greece.
[2]Laboratory of Agricultural Hydraulics, Department of Natural Resources Management & Agricultural Engineering, Agricultural University of Athens, 75 Iera Odos, 11855 Athens, Greece.
[3]Department of Environmental Sciences, School of Technology, University of Thessaly, 41110 Larisa, Greece.
* e-mail: psidirop@civ.uth.gr

Abstract. The scope of this study is the determination of water-saving irrigation practices for maize and cotton crops in Thessaly, Greece with the use of FAO Aquacrop model and it is a contribution to the "HUBIS" research project. A comparison is made between two irrigation practices for the two crops: 1) the first is the common irrigation practice that the farmer applies based on his experience and 2) the second is a water-saving irrigation practice based on the use of precision agriculture tools. These tools are the application of the FAO Aquacrop model for the simulation of the yield response of crops to water, the installation of low-cost soil water sensors and hydrometers for irrigation scheduling, the use of the Weather Research and Forecasting (WRF) atmospheric model to produce high-resolution weather forecasts and the use of Earth Observation Data for the computation of energy balance and acquisition of evapotranspiration values. In order for this comparison to be achieved, two crop fields have been selected as experimental fields for the two crops: 1) the "Farmer" field for the application of the common irrigation practice and 2) the "Hubis" field for the application of the water-saving irrigation practice. The study was carried out throughout the life of the two annual plants in 2021, i.e. from the sowing until harvest. The results indicate that for the cotton the water-saving percentage is 24.45% and for the maize, the percentage reaches the 50.4%.

1 Introduction

The cultivation period of maize and cotton, in Greece, starts in the spring and lasts till the first two months of the fall (Georgopoulou et al., 2017). This means that most days of these two annual crops' life occur in Mediterranean summer, which is characterized by high values of temperature, evapotranspiration, and lack of precipitation. Farmers must apply supplementary irrigation, based on their experience. Due to this fact, in most cases, the irrigation is not proper regarding both the programming and the water volume applied. Specifically, the farmers apply greater volumes of water than the crop needs in their attempt to achieve crop-yield maximization. But this leads to waste of water while water resources in the Mediterranean are limited (Allam et al., 2020). To save water, precision agriculture tools ought to be applied combined with a variety of field data such as climatic, soil, and crop ones. The core of this save water process is the application of a crop simulation model which can use a water-driven strategy. For this reason, Aquacrop (Steduto et al., 2009) is selected as it links crop yield and crop water use under different management and biophysical conditions (Raes et al., 2009). Specifically, it assumes a linear relationship between biomass production and crop transpiration (Steduto et al., 2007) for predicting water requirement, crop productivity, and water use efficiency under water stress and unstressed conditions. In comparison to other crop models, Aquacrop requires a very small number of explicit and mainly straightforward parameters to be established, and it has been tested and applied effectively for numerous crop types in a variety of environmental and agronomic circumstances (Vanuytrecht et a., 2014). The calibration of Aquacrop against observed field data is crucial for successful prediction and sustainable management. To achieve this, the appropriate equipment ought to be established on the farm, as well as a weather forecast tool should be applied (Lalić et al., 2018).
This paper presents the methodological approach of water-saving irrigation practices for maize and cotton crops in Thessaly, Greece, based on the use of precision agriculture tools. These tools are the application of the FAO Aquacrop model for the simulation of the yield response of crops to water, the installation of low-cost soil water sensors and hydrometers for irrigation scheduling, the use of the Weather Research and Forecasting (WRF) atmospheric model to produce high-resolution weather forecasts and the use of Earth Observation Data for the computation of energy balance and acquisition of evapotranspiration values. A comparison is made between two irrigation practices for the two crops: 1) the first is the common irrigation practice that the farmer applies based on his experience and 2) the second is a water-saving irrigation practice based on the use of precision agriculture tools. The study was carried out throughout the life of the two annual plants in 2021, i.e. from the sowing until harvest.

2 Materials and Methods

2.1 Field Experiments and Data

The field experiments took place on farms of cotton and maize near the village of Falani (Larisa, central Greece) at the altitude of 60 m. For the comparison purposes of the two irrigation practices, two crop fields have been selected as experimental fields for each crop: 1) the "Farmer" field for the application of the common irrigation practice and 2) the "Hubis" field for the application of the water-saving irrigation practice. The area of the experimental fields for cotton is 2.5 hectares each, while for maize 2 hectares each. The climate is the temperate Mediterranean characterized by cold humid winters and hot and arid summers (Bsk—Csa according to Köppen's climatic classification) (Köppen, 1936). Based on historical data, the average precipitation is about 560 mm/year, the mean annual temperature is around 14 °C, the mean annual potential evapotranspiration is about 775 mm/year, and the average relative humidity of 67%. During the March to October growing season of 2021, the total rainfall was 307.4 mm (Figure 1b) and the temperature varied from -0.3 °C (min of March) to 44.9 °C (max of August) (Figure 1a).

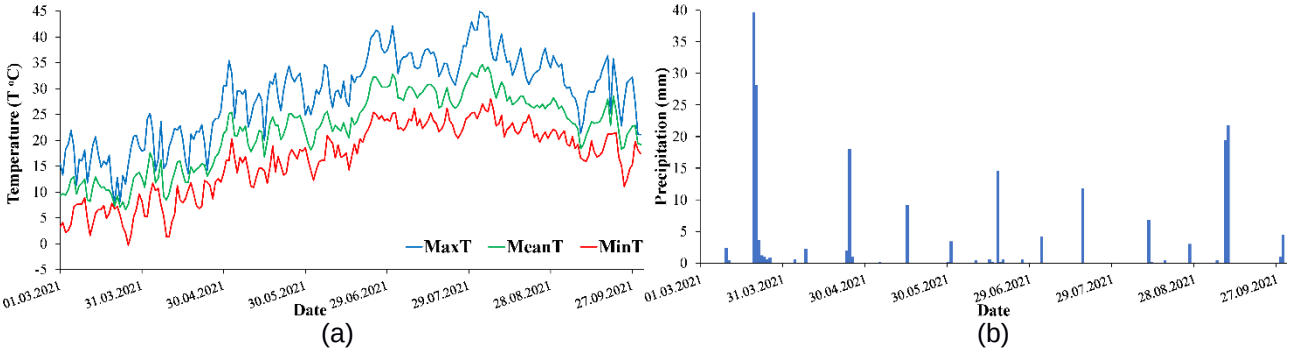

(a) (b)

Figure 1. Daily values of (a) maximum, mean, and minimum temperature and (b) precipitation for the growing season of 2021 (1-3-2021 to 31-10-2021).

One soil sampling was performed for each experimental field located at the center of it. A composite soil sample (0–20 cm, 20–30 cm, 30-60 cm, and 60-90 cm depth, n = 4) was collected from 1 m^2 sub-plot for cotton. A composite soil sample (0–30 cm, 30-60 cm, and 60-90 cm depth, n = 3) was collected from 1 m^2 sub-plot for maize. Soil samples were analyzed in the laboratory for soil texture as determined by physical fractionation (Bouyoukos, 1951), and for soil organic matter as determined by the Walkley–Black method of wet oxidation (Nelson and Sommers, 1982). For cotton, the Hubis field is characterized as clay to clay loam and the Farmer one as clay loam. For maize, the Hubis field is characterized as loam to sandy clay loam and the Farmer one as clay loam (Table 1).

Table 1. Soil properties

Crop Type	**Cotton**								**Maize**					
Field Type	**Hubis**				**Farmer**				**Hubis**			**Farmer**		
Depth (cm)	0-20	20-30	30-60	60-90	0-20	20-30	30-60	60-90	0-30	30-60	60-90	0-30	30-60	60-90
Sand (%)	29	32	26	34	30	24	28	36	43.4	46.7	54.4	31.7	31.2	41
Clay (%)	39	35	53	41	33	37	33	31	27.9	25.3	26.4	32.7	36.2	29.3
Loam (%)	32	33	31	25	37	39	39	33	28.7	28	19.2	35.6	32.6	29.7
Soil Type	CL	CL	C	C	CL	CL	CL	CL	CL	L	SCL	CL	CL	CL
pH	8	8.1	8.2	8.6	8.1	8	8.5	8.6	8	8.2	8.3	8.2	8.3	8.3
El. Conductivity (μS/cm)	396	377	498	487	423	417	340	347	512	380	432	395	437	432
$CaCo_3$ (%)	2.5	3	3.5	4.1	3.5	5.5	4.4	3.8	4	19	15.4	12.9	15.4	14
Organic matter (%)	-	-	-	-	-	-	-	-	0.9	0.7	0.8	0.6	0.3	0.3

Soil samples are also taken for the trenches for texture, gravimetric soil moisture, and bulk density allowing for the estimation of initial conditions. Multi-sensor systems were installed (TEROS 10) in the center of each field and at 15, 30, 60, and 90 depths to monitor the soil moisture. A data logger is installed next to the sensors recording the soil moisture on an hourly basis.

The grown cotton cultivar was ST318 of Pioneer, a Greek early variety. It was selected as it has new genetic material, excellent quality, fiber performance (>38%), and high production. The plant density was 20-22 plants per meter. The seeds of cotton were sawn at 3 cm depth on 19 April 2021. Table 2 presents the supplementary irrigation. The cotton was harvested on 29 September 2021, while the yield was 4,500 kg/ha. The grown maize cultivar was DKC 6897 of Dekalb, a French variety of FAO 700 class that is popular among Greek farmers. It was selected as it combines a new genetic material, excellent germination, excellent agronomic characteristics, and adaptation to high sowing density in good and fertile fields leading steadily to increased yields. The seed density was high and equal to 9,500 plants per hectare. The seeds of maize were sawn at 3.5 cm depth on 19 March 2021. Table 2 presents the supplementary irrigation. The maize was harvested on 24 September 2021, while the yield was 16,120 kg/ha.

Table 2. Irrigations events

Irr. Event	Cotton		Maize	
	Date	Net Application (mm)	Date	Net Application (mm)
1	18.06.2021	50	25.05.2021	60
2	28.06.2021	50	31.05.2021	60
3	04.07.2021	75	12.06.2021	60
4	12.07.2021	75	19.06.2021	60
5	16.07.2021	50	27.06.2021	60
6	23.07.2021	75	03.07.2021	90
7	30.07.2021	75	11.07.2021	90
8	05.08.2021	50	17.07.2021	90
9	14.08.2021	50	24.07.2021	90
10	19.08.2021	50	30.07.2021	60
11	25.08.2021	25	05.08.2021	60
12			12.08.2021	60

2.2 Weather Research and Forecasting Model

For weather forecasting, the Weather Research and Forecasting Model (WRF) was used. It is a state-of-the-art next-generation mesoscale Numerical Weather Prediction system designed to serve both operational forecasting and atmospheric research needs. It features multiple dynamical cores, a 3-dimensional variational (3DVAR) data assimilation system, and a software architecture allowing for computational parallelism and system extensibility. WRF is suitable for a broad spectrum of applications across scales ranging from meters to thousands of kilometers. WRF produces a principal 5-day weather forecast for the study area. To ensure reliability and maintain a standard of more than 97% accuracy automated mechanisms are developed that monitor and review the quality of the forecast daily.

2.3 Aquacrop development and calibration

For the cultivation period, the reference evapotranspiration was calculated by the model using as input the minimum, mean, and maximum daily temperature according to FAO 56 protocol (Allen et al., 1998). The cotton was simulated with the use of Default Cotton, GDD (Cordoba, 15Apr86) crop file, and the maize was simulated with the use of Default Maize, GDD (Davis, 1Jun96) crop file. For both crops, adjustments were made to days of phenological stages, plant density according to field measurements, and Reference Harvest Index (HI_o) according to crop yields. Specifically, for cotton, the duration of the initial stage, canopy development, mid-season stage, and the late-season stage were 45, 35, 56, and 48 respectively, while for the maize the days were 46, 36, 62, and 18 respectively. The plant density was presented in the previous chapter. The HI for cotton was 35% and for maize 55%. The irrigation method for all the fields was drip irrigation with a 40% percentage of soil surface wetted by irrigation. There was not any specific field management and not any shallow groundwater table was observed. The physical soil characteristics of all the plots were processed with Soil Water Hydraulic Properties Calculator (USDA, 2007) to calculate the hydraulic parameters required by AquaCrop. These included volumetric soil water content at field capacity (FC), permanent wilting point (PWP), saturation (SAT), and saturated hydraulic conductivity (K_{sat}). The final values of the parameters were determined by the calibration procedure of Aquacrop through the trial-and-error method till the simulated soil moisture values match the observed ones. Table 3 presents the hydraulic

parameters values and the calibration statistics of the “Hubis” fields for the two crops. Figure 2 presents the observed (black line) and simulated (blue area) soil water content of the 1 m profile. The initial soil water profile was determined by the soil samples’ laboratory analyses. For cotton the soil water content (vol %) was 45 % for the 1 m profile, while for maize 20.87% for 0-35 cm, 21.66 for 35-47 cm, and 17.68% for 47-100 cm depth. Soil salinity was equal to 0.45 dS/m for both crops’ fields.

Table 3. Hydraulic parameters values and calibration statistics of the “Hubis” fields for the two crops

	Hydraulic parameters				Calibration Statistics				
	Sat (mm)	**FC (mm)**	**WP (mm)**	**K_{sat} (mm/d)**	**Pearson Correlation Coefficient (r)**	**Root Mean Square Error - RMSE (mm)**	**Normalized Root Mean Square Error - CV(RMSE) (%)**	**Nash-Sutcliffe Model Efficiency Coefficient (EF)**	**Willmott's Index of Agreement (d)**
Cotton	470	330	250	200	0.86	14.8	4.3	0.63	0.91
Maize	293	210	140	45	0.76	7.4	3.8	0.51	0.87

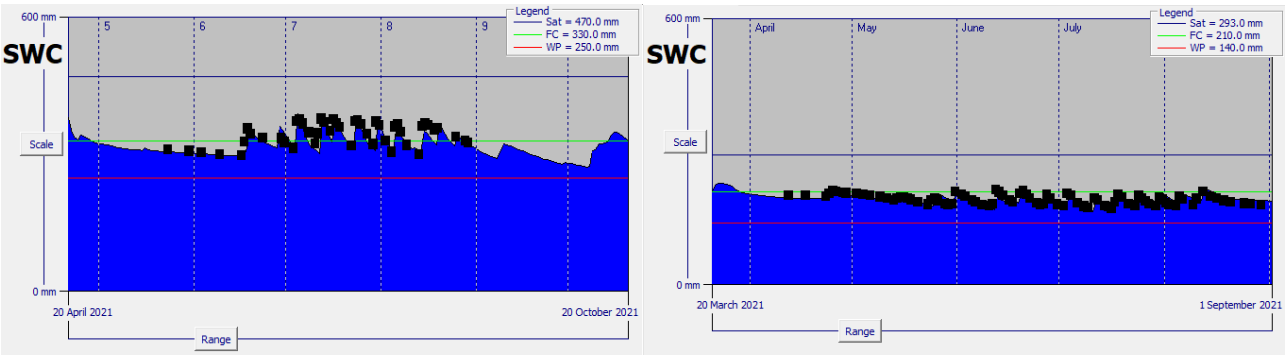

Figure 2. Observed (black line) and simulated (blue area) soil water content of the 1 m profile.

2.4 Calculation of actual evapotranspiration

The actual evapotranspiration (ET_a) was calculated for each plot using MSI Sentinel-2 radiometric data and Sentinel-3 SLSTR thermal data. MSI Sentinel-2 optical data were used to characterize the biophysical condition of the soil surface at a resolution of 20 m. This resolution was chosen because it corresponds to the native resolution of the MSI infrared red and shortwave bands. Sentinel-3 SLSTR thermal data are used to determine the lower limit state of the earth's energy model. The ET_a calculation procedure is based on the relevant methodology of the European Space Agency (ESA), but with significant improvement as meteorological data are derived from the Research and Weather Forecast (WRF) model instead of ERA5 data from the European Center for Medium Weather Forecast (ECMWF). The results produced by the WRF model are real-time data (e.g. air temperature, wind speed, etc.) at any time step requested. The final product of the UTH methodology is ET_a in mm / day with a spatial resolution of 20 m x 20 m. The proposed methodology consists of 17 sub-steps, which are: 1) Downloading of Sentinel images; 2) Pre-processing Sentinel 2 data by downscaling. Resampling of: i) Sentinel 2 image at 20 m, ii) the required channels of the image subsets and storing them as separate products for the evaluation of the biophysical parameters (FAPAR, LAI, F-cover) of the reflection channels; 3) Creation of a Digital Terrain Model of the study area in high resolution; 4) Creation of a land use map of the study area in high resolution from the land use database of the ESA CCI of 2015; 5) Leaf reflection and transmission assessment based on the chlorophyll and water content of the plants; 6) Estimation of green vegetation. The procedure calculates the fraction of vegetation that is green based on the Leaf Area Index (LAI), the fraction of absorbed photosynthetic active radiation (FAPAR), and the channels according to the angle of inclination with the zenith of the sun; 7) Production of maps with its structural parameters (e.g. vegetation height and coverage, forest cover height etc.); 8) Aerodynamic roughness assessment: The procedure calculates the length of the aerodynamic roughness for instantaneous transfer in (m) and the displacement height of the zero level (m) based on the leaf area index (LAI) and the maps created with the structural parameters of the vegetation; 9) Pre-processing Sentinel -3 data by downscaling. The L2A image of Sentinel 3 is retrieved in the required channels of the received AOIm subsets and stored as separate products; 10) Correction of distortion in the prototype: The subset of a source image is viewed and re-sampled into a prototype image using GDAL Warp; 11) Creation of a clearer picture of surface ground temperature. The Python application "Data Mining

Sharpener" is used to improve SLSTR ground temperature in Sentinel-2 spatial analysis; 12) Download WRF meteorological data from 3D S.A; 13) Preparation of WRF meteorological data based on the High-Resolution Digital Soil Model of the study area; 14) Long-wave radiation estimation based on WRF meteorological data; 15) Estimation of net shortwave radiation based on WRF meteorological data and biophysical parameters; 16) Estimation of energy flows of the earth's surface: The process estimates soil surface energy flows (latent and perceptible heat, ground heat and net radiation) using the single-source energy balance model for bare soil pixels and the two-source energy balance model for vegetated pixels; 17) Estimation of actual daily evapotranspiration: The process calculates the actual daily evaporation by extending/extruding the instantaneous latent heat flow using daily solar radiation.

3 Results

Aquacrop estimates the yield of cotton equal to 4.605 tn/ha and for maize 16.205 tn/ha for the “Farmer” fields. These simulated values are very close to the real ones, and this good agreement validates the model’s reliability. For the “Hubis” field the Determination of Net Irrigation water requirement procedure was applied to calculate the exact date on which the field must be irrigated, as well as the exact amount of water to be applied. The user must choose the intervals between each irrigation application, which in the case of corn and cotton is estimated from 7 to 10 days. For cotton, the sum of the irrigation to be applied is 472.2 mm for the whole life of the plant. Since the area of the field is 2.5 ha, i.e. 25,000 m^2, the total volume of water amounts to 11,805 m^3. In other words, a reduction of water volume by 24.45% is achieved in relation to the one applied by the farmer in the field in 2021 (15,625 m^3). However, the impressive result of this comparison scenario is not this, but the yield of the crop, which amounts to 5.459 tn/ha, 18.54% higher than the yield achieved by the application of irrigation from the farmer (4.605 tn/ha). For maize, the sum of the irrigation to be applied is 416.7 mm for the whole life period of the plant. Since the area of the field is 2 ha, i.e. 20,000 m^2, the total volume of water amounts to 8,334 m^3. In other words, a reduction of water volume by 50.4% is achieved in relation to the one applied by the farmer in the field in 2021 (16,800 m^3). However, the impressive result of this comparison scenario is not only this but also the yield of the crop, which amounts to 18.101 tn/ha (Figure 13), 11.70% higher than the yield achieved by irrigation application by the farmer (16.205 tn/ha).

Although these encouraging results are based on a proposed methodological approach, which was not applied in the “Hubis” fields in 2021, its application has already started on the farms this year (2022). The percentages of water reduction in 2021 have already guided us to know the irrigation that ought to be applied in the “Hubis” fields for 2022. From the operational application of the proposed methodology in maize for the first three irrigations, the “Hubis” field is irrigated with almost half the water of the “Farmer” one, which is exactly the proposed percentage for 2021. But improvement is needed for the estimation of actual evapotranspiration since there is not a good agreement between the values calculated by Aquacrop and Sentinel (Figure 3).

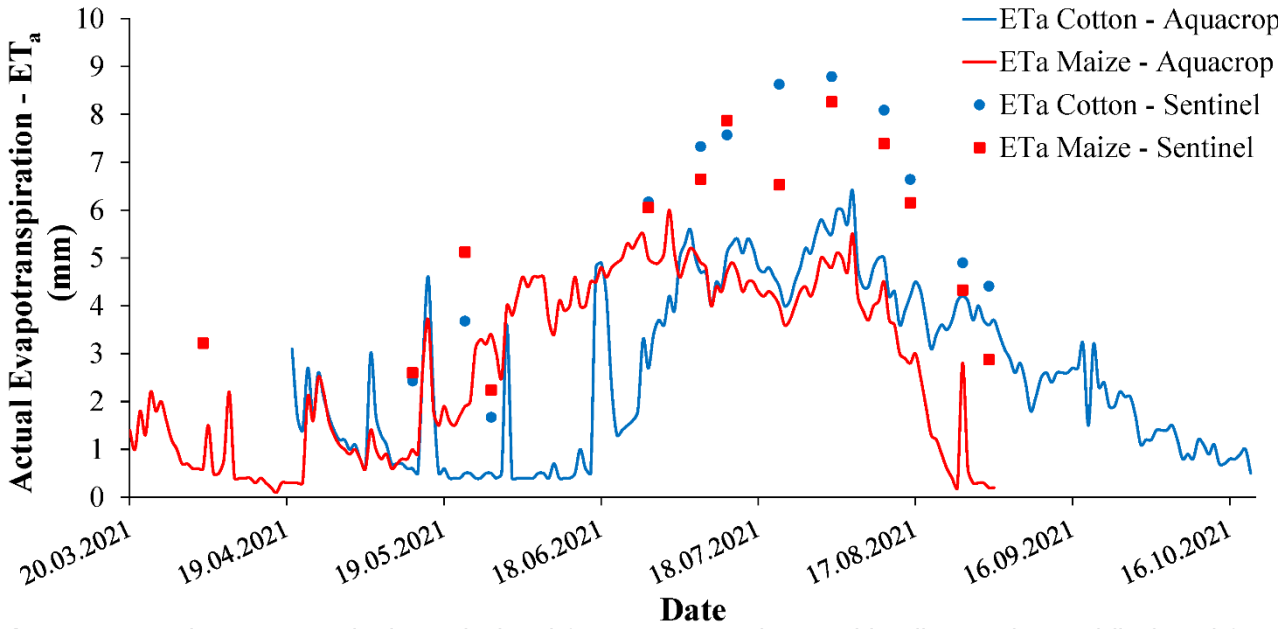

Figure 3. Actual evapotranspiration calculated from Aquacrop (cotton: blue line, maize: red line) and from Sentinel (cotton: blue circle, maize: red square).

4 Summary

In this study, a methodology is proposed for the application of water-saving irrigation practices for maize and cotton crops using precision agriculture tools. These tools are the application of the FAO Aquacrop model for the simulation of the yield response of crops to water, the installation of low-cost soil water sensors and hydrometers for irrigation scheduling, the use of the Weather Research and Forecasting (WRF) atmospheric model to produce high-resolution weather forecasts and the use of Earth Observation Data for the computation of energy balance and acquisition of evapotranspiration values. The results are quite impressive since the water-saving reaches almost 50% of the amounts applied and simultaneously crop yield increase is achieved. This methodology has already been applied in the field in 2022 and new results are expected.

Acknowledgements

The research was funded by «Open innovation Hub for Irrigation Systems in Mediterranean agriculture» with the acronym «Hubis» of PRIMA (Partnership for Research and Innovation in the Mediterranean Area) programme (Section 2 Call 2019 – multi-topic) supported under Horizon 2020.

References

Georgopoulou, E., Mirasgedis, S., Sarafidis, Y., Vitaliotou, M., Lalas, D.P., Theloudis, I., Giannoulaki, K.D., Dimopoulos, D., and Zavras, V., 2017. Climate change impacts and adaptation options for the Greek agriculture in 2021–2050: A monetary assessment. Clim. Risk Manag., 16, 164-182. https://doi.org/10.1016/j.crm.2017.02.002

Allam, A., Moussa, R., Najem, W., and Bocquillon, C., 2020. Hydrological cycle, Mediterranean basins hydrology. Book chapter 1, in: Water Resources in the Mediterranean Region. Editor(s): Mehrez Zribi, Luca Brocca, Yves Tramblay, François Molle, Publisher: Elsevier, Amsterdam, 1-21. https://doi.org/10.1016/B978-0-12-818086-0.00001-7

Steduto, P., Hsiao, T.C., Raes, D., and Fereres, E., 2019. AquaCrop—the FAO crop model to simulate yield response to water: I. Concepts and underlying principles. Agron. J.,101, 426–437. https://doi.org/10.2134/agronj2008.0139s

Steduto, P., Hsiao, T., and Fereres, E., 2007. On the conservative behavior of biomass water productivity. Irrig. Sci., 25, 189–207. https://doi.org/10.1007/s00271-007-0064-1

Raes, D., Steduto, P., Hsiao, T.C., and Fereres, E., 2009. AquaCrop–The FAO crop model to simulate yield response to water: II. Main algorithms and software description. Agron. J., 101, 438–447. https://doi.org/10.2134/agronj2008.0140s

Vanuytrecht, E., Raes, D., Steduto, P., Hsiao, T.C., Fereres, E., Heng, L.K., Garcia-Vila, M., and Moreno, P.M., 2014. AquaCrop: FAO's crop water productivity and yield response model. Environ. Model. Softw., 62, 351–360. https://doi.org/10.1016/j.envsoft.2014.08.005

Lalić, B., Firanj Sremac, A., Eitzinger, J., Stričević, R., Thaler, S., Maksimović, I., Daničić, M., Perišić, D., and Dekić, L., 2018. Seasonal forecasting of green water components and crop yield of summer crops in Serbia and Austria. J. Agric. Sci., 156(5), 658–672. https://doi.org/10.1017/S0021859618000047

Köppen, W., 1936. Das geographische System der Klimate [The geographic system of climates]. In Handbuch der Klimatologie; Verlag von Gebrüder Borntraeger: Berlin, Germany, 1936.

Bouyoukos, G.H., 1951. A recalibration of the hydrometer method for making mechanical analysis of soils. Agron. J., 43, 434–438. https://doi.org/10.2134/agronj1951.00021962004300090005x

Nelson, D.W., Sommers, L.E., 1982. Total carbon, organic carbon, and organic matter. In Methods of Soil Analysis, Part 2, 2nd ed. Editor(s): Page, A.L., Miller, R.H., Keeney, D.R. Publisher: Cambridge, MA, USA, pp. 539–579.

Allen, R.G., Pereira, L.S., Raes, D., and Smith, M., 1998. Crop Evapotranspiration. Guidelines for Computing Crop Water Requirements, FAO Irrigation and Drainage Paper No. 56, FAO, Italy, 333p.

United States Department of Agriculture—USDA, 2007. Soil, Plant, Atmosphere, Water, Field & Pond Hydrology Model; USDA Agricultural Research Service, Beltsville, MD, USA.

Climate change and water resources management impacts on a water-stressed agricultural watershed.

Tzabiras J.[1], A. Loukas[2]

[1] Department of Civil Engineering, University of Thessaly, Volos, Greece
[2] Department of Rural and Surveying Engineering, Aristotle University of Thessaloniki, Thessaloniki, Greece

Abstract. Uncertainty analysis investigates the uncertainty of variables used in decision-making problems in which observations and models represent the knowledge base. This paper is dealing with the bias correction of five coupled (GCM+RCM) ensemble climatic models of quantile mapping. The corrected hydro-meteorological variables were incorporated to an integrated water resources management system applied in the Lake Karla watershed. Previous application of the system where various water management strategies were investigated under climate change conditions by use of CGCM3 output, revealed that the use of rational water management techniques are far more significant in terms of water balance than the climatic projections. In this case where the uncertainty was assessed, two main water management strategies were combined with the climatic projections of five coupled models and the calculations referred to the long-term period 2080-2100. The results showed that future estimates of hydro-meteorological variables (rainfall and temperature) significantly affect and introduce uncertainties in surface hydrological processes, irrigation water demand and the overall water balance of the catchment area. However, the effect of the estimates and uncertainties of the climate models is reduced in the simulation of the underground aquifer. Furthermore, for the degraded aquifer in the study basin, water resources management measures have a more significant effect than the impact of climate change and the uncertainty of future climate assessments.

1 Introduction

Climate change means the change in the global climate and in particular the changes in weather conditions extending to large time scale. Climate change is specifically defined as change in climate that is directly or indirectly caused by human activities, distinguishing the term from climate variability which has natural causes. Due to climate change the sea level is rising, the glaciers are melting and the typology of atmospheric precipitation changes. Extreme weather phenomena - more intense and more intensively-, reduction of atmospheric ozone, changes in the ecosystem due to the loss of biodiversity, changes in hydrological systems and fresh drinking water supplies, soil degradation and urbanization are some of the effects.

Climate models are currently the most useful tools for monitoring global climate, the investigation of past times and future estimates of climatic living conditions on our planet in the next hundreds of years. A climate model uses numerical methods to simulate the interactions between atmosphere and the oceans, the earth's surface, and the polar regions. They are used for a variety of purposes, starting with the study of dynamic climate phenomena mechanisms and ending at future climate assessments. The most common use of climate models in recent years is the assessment of the course of the global average temperature due to the greenhouse effect (climate change).

According to the IPCC definition, General Circulation Models (GCMs) are numerical models that represent the physical processes that take place in atmosphere, oceans, cryosphere and land surface and are the most sophisticated tools, so far, as it relates to global climate simulation at the level of dynamical, chemical and biological processes and their interaction, in combination with the increasing concentration of greenhouse gases. On the other hand, Regional Climate Models (RCMs) are widely used for climate simulation of the earth at a higher spatial resolution, compared to GCMs, and with respect to a specific and spatially limited area. The main role that these models possess is the addition of detail to topography and natural parameters, at the specific scale for which they were originally developed.

Both global (GCMs) and regional (RCMs) climate models have systematic errors (biases) in their results. Errors in climate models can be caused by a number of factors. Errors or biases are due to limited spatial resolution (large grid sizes), simplified thermodynamic processes, and physical or incomplete understanding of the global climate system. To overcome large biases in climate models, a number of bias correction methods have been developed.

In this work, the uncertainty of a statistical downscaling procedure that is incorporated in a water management system is found mainly in two fields. The first has to do with the proposed statistical downscaling methodology and the investigation of the results of the system based on the output of a different downscaling method. On the other hand, the second uncertainty field of the system is introduced by the uncertainty of the

global climate model (GCM) and the requirement to investigate the results using outputs of different global climate models is evident.

2 Study area and data base

2.1 Study area

The hydrological basin of Karla is defined in the most south-eastern part of the water division of Thessaly, between the cities of Volos and Larissa (Figure 1). it is essentially the southeastern end of the Larissa plain and is the deepest part. It is a closed basin because it is surrounded by mountains, with the lowest altitude point (+44 m) being between Stefanovikio and Kanalia. The total area reaches 1660 Km^2, which is located at 39^{o}20'56'' S to 39^{o}45'15'' N and 22^{o}26'10'' E to 23^{o}0'27'' W. As mentioned, it is a closed type basin given that it does not communicate hydraulically with the sea and is surrounded by mountains. The underground aquifer is the main supplier of water needs, it occupies approximately 500 km^2 and is located in the lowland part of the basin, while the remaining water requirements are covered by surface irrigation networks.

The area is characterized by a Mediterranean type microclimate, with a continental character, where the summer is dry and hot while the winter period is cold and wet. Historical data from rain gauges describe higher rainfall during the period of Lake Karlas' existence. The value of the mean annual rainfall in the basin is 560 mm. The mean annual temperature is positive, but the minimum observed temperature during the winter period is -21.6 ^{o}C while the maximum observed during the summer period is 45.2 ^{o}C. Frosts are still very common, especially in the December-March period. The average relative humidity in the Lake Karla watershed is 66%.

Figure 1. Lake Karla watershed (Tzabiras et al, 2016).

2.2 Existing water resources management infrastructure

In Lake Karla watershed there are hydro-technical storage structures and the accompanying storage projects of small reservoirs and ponds. There are two irrigation networks operating in the area and responsible for their operation are the Local Authorities of Land and Reclamation of Pinios and Karla (LALR Pinios and LALR Karla).

The irrigation network of the LALR Pinios serves areas of 15400 hectares, using reservoirs. The reservoirs are fed mainly from Pinios River but also from a limited number of pumping wells. The network works with open earthen channels which are unmaintained and full of dense vegetation with the result that water losses

are very large. The network operates with the help of three pumping stations A', E' and B' located near the river. A more recent one (D') has been built in Gyrtoni, but it is not working. Pumping station A is located near the Omorfohori junction, while E is located near A.

LALR Karla initially served a smaller area of 1000 hectares, which is located between the settlements of Stefanovikeio and Rizomylos and in ditches 3T and 2T. LALR Karla operates various pumping wells that supply the surrounding areas. The newly constructed pressurized irrigation network is designed to serve 8440 hectares around the reservoir area but although it is in operation it is unknown whether the entire area is covered or not.

2.3 Meteorological data base

Monthly precipitation of 12 rain gauges and temperature data of 26 meteorological stations uniform distributed rain gauges across the watershed were available for 20 hydrological years from October 1980 to September 2000. Monthly areal precipitation and temperature of the basin were estimated by the Thiessen polygon method modified by the monthly gradients using the stations, which are within or in the vicinity of the watershed.

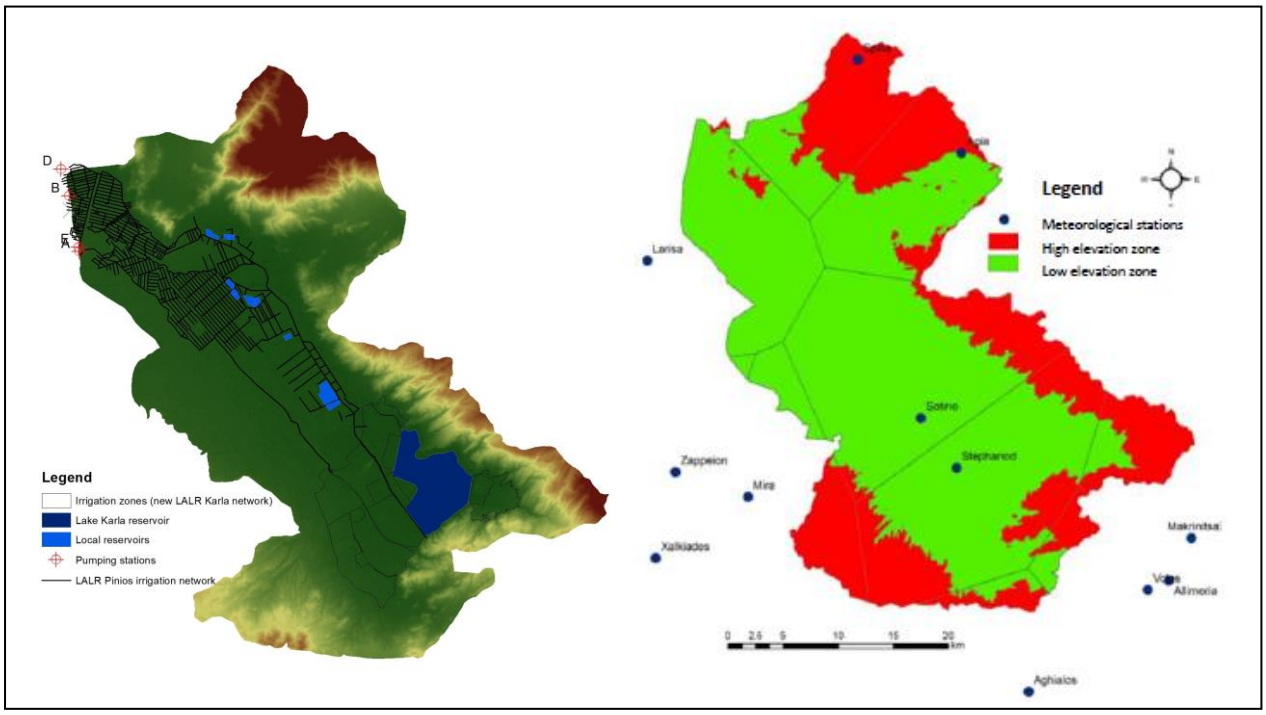

Figure 2. Hydro-technical projects and meteorological database (Tzabiras et.al, 2015)

3 Application of the integrated water resources management system

3.1 General structure

The integrated water management system consists of two sub-systems: a) The District Information System (DIS) (Tzabiras et. al., 2014) and b) The Watershed Information System (WIS) (Tzabiras et.al 2015, 2016). Both sub-systems are interacting and provide critical information for the water management strategies in Lake Karla watershed (Figure 3). Although the system was calibrated and evaluated in Lake Karla basin there is the capability of application in a random catchment.

As for DIS the basic stages of the process are presented below:

- Development of a geographic information system, which includes maps of the Army Geographical Service (Army Geographical Service), orthophoto maps of the Minister of Agriculture, satellite images of Hellenic cadastre, an operational map of LALR Pinios, maps of the study of the restoration of Lake Karla, the Digital Elevation model (DEM), and digitized irrigation networks.
- Development of the remote sensing database which includes high resolution satellite images of LANDSAT TM

- Extraction of real evapotranspiration values using the SEBAL algorithm (Surface Energy Balance Algorithm for Land)
- Estimation of water needs and irrigation requirements in historical conditions with the CROPWAT model
- Simulation of the operation of the surface network of LALR Pinios with the Technologismiki model
- Simulation of the operation of the LALR Karla new network with the WaterCad model.
- Coupling of hydrological models with the WEAP management model

On the other hand, WIS includes a) the water balance model of the University of Thessaly UTHBAL (University of THEssaly water BALance model) for the calculation of the water balance and the (infiltration) loading of the aquifer b) the University of Thessaly Reservoir/Lake model UTHRL (University of Thessaly Reservoir/Lake model) for the modeling of the reservoir c) the lake/aquifer simulation model LAK3 (Lake/Aquifer simulation model) and d) the underground water resources model MODFLOW for the simulation of the aquifer.

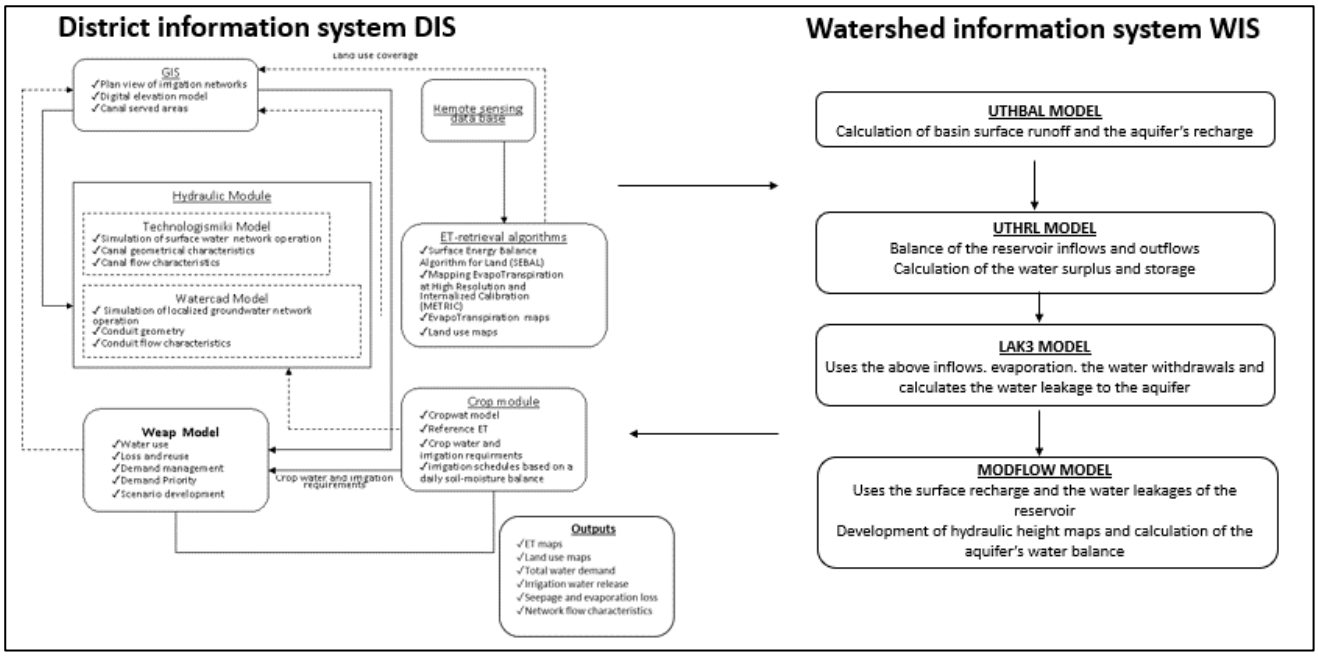

Figure 2. General structure of the integrated water resources management system (Tzabiras et.al, 2015)

3.2 Statistical downscaling

In a previous study, the third generation GCM (CGCM3.1) of the Canadian center for climate monitoring and analysis was used for the choice of predictor variables in downscaling procedure, a spectral model with resolution 3.75º latitude and 3.75º longitude (Flato and Boer 2001). Details of the statistical downscaling procedure and the stochastically generated residuals could be found in the Tzabiras et al. (2015, 2016). Application of the statistical downscaling method for two future periods (2030-2050 and 2080-2100) and three climatic scenarios (SRES) and estimation of future precipitation and temperature timeseries showed small changes relative to the historical period. The stochastically generated timeseries of areal precipitation and temperature, as well as potential evapotranspiration which was calculated from the temperature timeseries were used for running Lake Karla watershed modelling system.

3.3 Water resources management strategies

Two operational strategies of hydrotechnical project development (present situation without operation of the reservoir and future situation with the operation of the reservoir) were coupled with three water demand strategies. In total, eight (8) water management strategies were evaluated and compared. The results showed that, under the existing operational water resources management strategies, the water deficits are quite large and they are largely satisfied by unsustainable groundwater pumping. Overall, water resources management strategies are more important than the climate change impact scenarios because climate change effects on the water balance using the Hydromentor modelling system showed negligible to mild changes. However, the

operation of the proposed hydro-technical projects (reservoir operation and the new irrigation network) in Lake Karla watershed coupled with water demand management measures, like improvement of existing water distribution systems, change of irrigation methods, and changes of crop cultivation could alleviate the problem and lead to sustainable and ecological use of water resources in the study area.

4 Uncertainty analysis

4.1 Climatic Models

In this stage five different global circulation models were used to investigate the uncertainty. The use of multiple simulations is clearly a more analytical method given that a single simulation usually presents many and different fields of uncertainty, especially at a spatial level (Pavlidis, 2015). The multiple simulations analyze the variations of factors that may show uncertainty, and in this way the confidence limits are captured in which the simulation models of future conditions should work (Kerr, 2013).

Typical programs that contain ensembles of simulations from different models are ENSEMBLE and now the successor program CORDEX from the World Research Climate Program (WRCP), the International Council for Science (ICSU), the World Meteorological Organization (WMO), and the Intergovernmental Oceanographic Commission (IOC of UNESCO). In particular, CORDEX (Coordinated Regional climate Downscaling Experiment) aims to develop, coordinate and systematize research and conduct regional climate simulation (Pavlidis, 2015; Hourdin et al., 2016).

The output of the five General Circulation Models from 10 simulations with RCMs, (dynamic downscaling) in which the historical reference period was the 30-year 1960-1990 while the models were applied for the period 2006-2100. The temperature and precipitation output data used in this study come from the Data Extraction Application for Regional Climate program developed at the Aristotle University of Thessaloniki (DearClima, 2018) based on Representative Concentration Pathways (RCPs) Emission Scenarios (Moss et al., 2010), for dynamical downscaling with spatial climate models (RCMs) and bias correction of General Circulation Models (GCMs). Table 1 lists the simulations with RCMs corresponding to each GCM.

Table 1. Climatic models (RCM + GCM) used in this study

GCM	RCM	Body
CNRM-CM5.1	CLMcom-CCLM4-8-17	CLM Community (CLMCOM)
	CNRM-ALADIN53	Centre National de Recherches Météorologiques (CNRM)
	SMHI-RCA4	Swedish Meteorological and Hydrological Institute (SMHI)
EC-EARTH.2	KNMI-RACMO22E	Royal Netherlands Meteorological Institute (KNMI)
IPSL-CM5	IPSL-INERIS-WRF331F	Institut Pierre Simon Laplace/Institut National de l'Environnement Industriel et des Risques (IPSL- INERIS)
	SMHI-RCA4	Swedish Meteorological and Hydrological Institute (SMHI)
HadGEM2-ES	CLMcom-CCLM4-8-17	CLM Community (CLMCOM)
	SMHI-RCA4	Swedish Meteorological and Hydrological Institute (SMHI)
MPI-ESM	CLMcom-CCLM4-8-17	CLM Community (CLMCOM)
	MPI-CSC-REMO2009	Helmholtz-Zentrum Geesthacht, Climate Service Center, Max Planck Institute for Meteorology

4.2 Quantile mapping

The precipitation and temperature output data of the above simulations through the DearClima program refer to the results of the RCP2.6, RCP4.5 and RCP8.5 scenarios. The integrated system was applied for previous generation climate change scenarios (SRES emission scenarios), but given that the RCPs were developed, it was considered appropriate to investigate the field of uncertainty according to the projections of these scenarios. In addition, during the implementation of the system for the SRES emission scenarios the analysis was made for three SRES scenarios B1, A1B and A2 (two extreme and one moderate in terms of climate change signal). On the other hand, the available data from the DearClima program existed for the RCP2.6, RCP4.5 and RCP8.5 scenarios. Hence, the mild scenario was chosen in both sets of scenarios and the comparison of global climate models is carried out for SRES B1 and RCP4.5. Also given that the short-term climate change period (2030-2050) for which the system was applied is a period in which the climate change signal is moderate, the long-term climate period (2080-2100) was chosen to apply the results of the five Global Climate Models (GCMs).

The impact of climate change on water resources is usually assessed at a local scale. However, Regional Climate Models (RCMs) are known to exhibit systematic biases. Hence, RCM simulations must be post-processed to produce reliable estimates of regional scale climate. In this study the parametric transformation of equation 4.1 was used for the quantile mapping of precipitation and temperature derived from GCMs. The calibration of the method was based on the results of global climate models for the period Oct. 1980-Sep. 2000.

$$\widehat{P_0} = bP_m^c \tag{4.1}$$

Figure 3a shows the results of the procedure for the rainfall in the two altitudinal zones of the Lake Karla watershed and it is easy to conclude that the method works well given that all models satisfactorily simulate the observed rainfall. However, a closer look reveals that the method performs better in the high elevation zone as in this zone from the third quartile (75%) and after in the Box-Whisker diagram all GCMs overestimate the precipitation and the only exception maybe the IPSL model. On the other hand, the application of the method for the long-term period 2080-2100 shows quite useful conclusions. Figure 3b presents the multiple Box-Whisker plots for the precipitation of the two altitudinal zones of the catchment during the period 2080-2100.

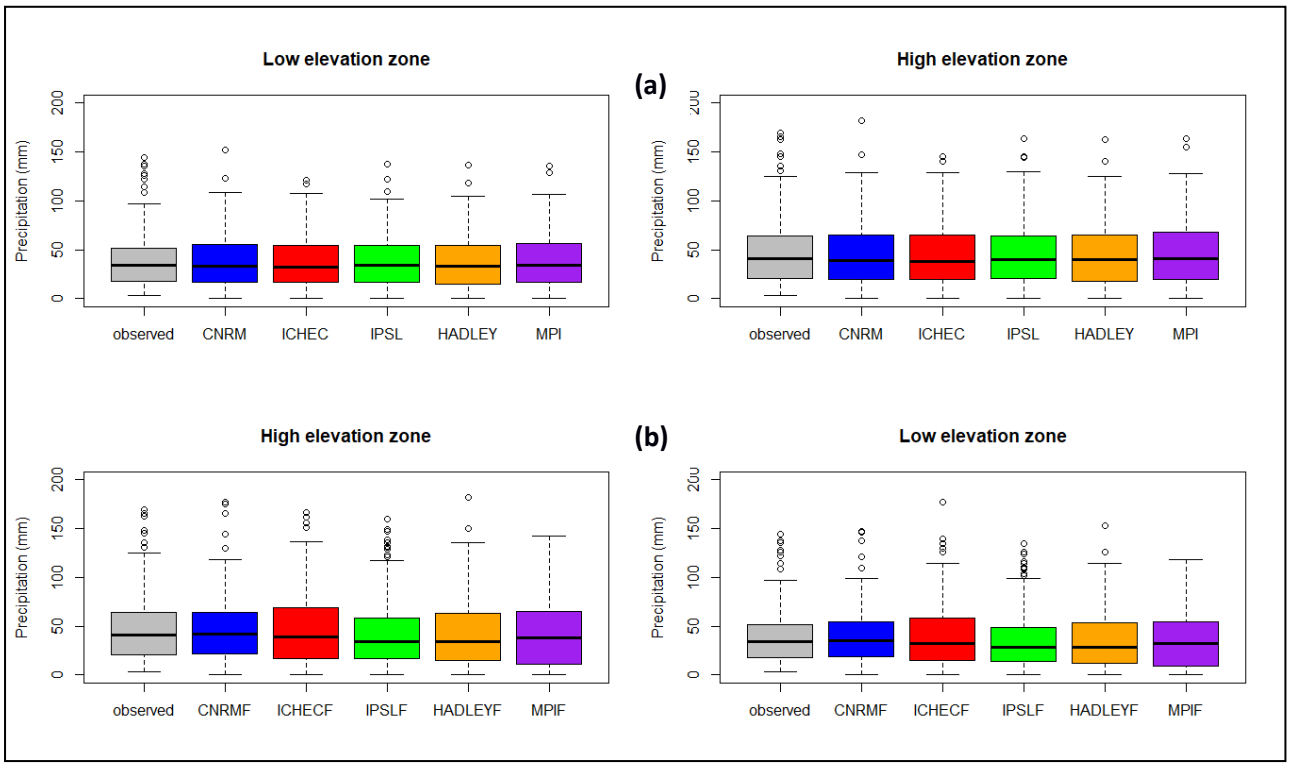

Figure 3. Quantile mapping results (Precipitation) for a) historical period b) long-term period 2080-2100

It is clear that the ICHEC, HADLEY and MPI model project a small increase in precipitation while the CNRM and IPSL model project a decrease for the long-term future period and the RCP4.5 climate scenario which can be seen from the first (25%) and third (75 %) quartile where it appears that the range between the two has

been increased in the case of the ICHEC, HADLEY and MPI model while it has been decreased for the CNRM and IPSL model. The IPSL model projects the greatest decrease in precipitation, something that can be seen from the minimum and maximum value, the median which is smaller, but also in the interquantile range which decreases (1st and 3rd quartile range).
Regarding the temperature, the results during the calibration of the method are presented in figure 4a. It is evident that the CNRM, HADLEY and MPI models overestimate the observed temperature of the period 1980-2000. On the other hand, the ICHEC and IPSL models seem to simulate the observed temperature quite satisfactorily.

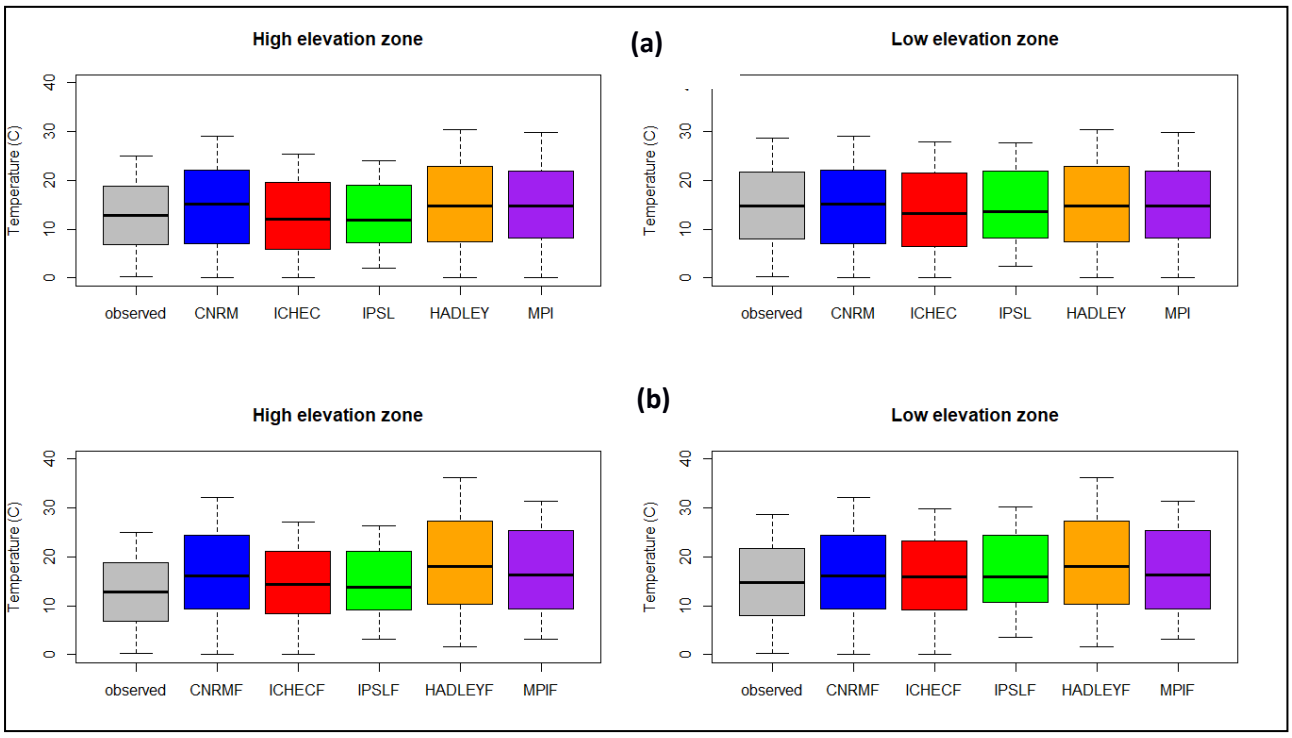

Figure 4. Quantile mapping results (Temperature) for a) historical period b) long-term period 2080-2100

The method was applied for the long-term climate change period 2080-2100 and the results for the two elevation zones of the study area are presented in figure 4b. It is clear that all five global climate models project a significant increase in temperature with the HADLEY model projecting the largest and the ICHEC model the smaller for both altitude zones.

5 Results

5.1 Irrigation requirements

The procedure followed to estimate the water requirements based on the projections of the five global climate models has been extensively described in a previous paper (Tzabiras et al., 2016). Table 2 presents the comparative results between the quantile mapping method for the five global climate models and the basic statistical downscaling methodology that the system was applied. The water requirements for the historical period 1980-2000 and the basic management strategy 2 were 322.5 hm^3 while for the scenario 2a 244.2 hm^3. Regarding to the projection of the CGCM3 model and the SRES A1B climate scenario, the water requirements for the period 2080-2100 are 335.1 hm^3 and 253.6 hm^3 respectively. During the process of uncertainty analysis, the GCM that shows the lowest water requirements is ICHEC with 340.88 hm^3 and 253.34 hm^3 respectively, while the one with the highest water requirements is HADLEY with 440.97 hm^3 and 330.28 hm^3 respectively.

Table 2. Irrigation requirements of Lake Karla watershed and the corresponding climatic models and reference periods

Climatic Model & Reference period	Strategy 2: Future situation (reservoir operation)	Scenario 2a: Future situation Reservoir operation & reduction of canal losses)
Base period 1980-2000	322.5	244.2
CGCM3 SRES 2080-2100	335.1	253.6
CNRM-CM5.1 RCP 4.5 2080-2100	360.84	272.07
EC-EARTH.2 RCP 4.5 2080-2100	340.88	253.34
IPSL-CMS RCP 4.5 2080-2100	378.22	284.92
HadGEM2-ES RCP 4.5 2080-2100	440.97	330.28
MPI-ESM RCP 4.5 2080-2100	381.93	287.64

5.2 Results of the hydraulic module

After the calculation of the irrigation requirements for the five GCMs, the models of the hydraulic module of the system were applied for the basic management strategy 2 (operation of the Karla reservoir) and the scenario 2a (reduction of channel losses) with reference to the long-term period and the climate scenario RCP4.5. The results of the individual models of the system and the individual water balances are presented below.

5.3.1 Hydrological balance

The irrigation requirements were used to calculate the hydrological balance of the Lake Karla watershed. Table 3 presents the annual hydrological balance for the five GCMs (period 2080-2100 and climate scenario RCP4.5) and compares it with the historical period 1980-2000 and the global climate model CGCM3 (SRES B1 2080-2100). The average annual temperature of Lake Karla basin during the historical period 1980-2000 was 14.24 ^{o}C while the CGCM3 model projects an increase to 14.70 ^{o}C. Conversely, the largest increase is projected by the HADLEY model at 17.94 ^{o}C, while the ICHEC (EC-EARTH) model gives the smallest increase at 14.95 ^{o}C.

Table 3. Annual hydrological balance of Lake Karla watershed

UTHBAL RESULTS	T(^{o}C)	P(mm)	PET(mm)	AET(mm)	Runoff (mm)	Recharge (mm)
Base period 1980-2000	14.24	552.77	806.41	407.42	59.78	81.35
CGCM3 SRES 2080-2100	14.70	530.95	805.21	397.62	53.79	75.81
CNRM-CM5.1 RCP 4.5 2080-2100	15.83	493.08	867.06	369.25	49.95	70.41
IPSL-CMS RCP 4.5 2080-2100	16.59	470.42	908.82	352.29	47.65	67.17
EC-EARTH.2 RCP 4.5 2080-2100	14.95	521.95	819.10	390.87	52.87	74.53
HadGEM2-ES RCP 4.5 2080-2100	17.94	403.48	1059.60	302.16	40.87	57.61
MPI-ESM RCP 4.5 2080-2100	16.75	465.85	917.73	348.86	47.19	66.52

5.3.2 Reservoir water balance

The calculation of the water balance of the reservoir was based on the UTHRL reservoir model and the results are presented in Table 4. As already mentioned, the reservoir is planned to be fed with 80 hm^3 from the Pinios river. The analysis of the table below shows that during the historical period 1980-2000, inflows to the reservoir were 156.21 hm^3, while the CGCM3 model projects for the long-term period 2080-2100 and the SRES A1B climate scenario a reduction to 149.04 hm^3. With reference to the other five global climate models, the reservoir inflows are projected at 144.12 hm^3 for CNRM, at 147.87 hm^3 for ICHEC, at 141.17 hm^3 for IPSL, at 132.47 hm^3 for HADLEY and at 140.58 hm^3 for MPI. On the other hand, the outflows from the reservoir for the historical period were calculated at 154.60 hm^3, while the CGCM3 model projects a reduction to 147.44 hm^3 for the long-term period 2080-2100 and the SRES B1 climate scenario. Average annual discharges from the reservoir for

the RCP4.5 scenario are projected to decrease to 142.98 hm^3 for the CNRM model, 146.34 hm^3 for ICHEC, 140.50 hm^3 for IPSL, 134.28 hm^3 for HADLEY and at 140.02 hm^3 for MPI.

Table 4. Lake Karla reservoir water balance

Base period 1980-2000		Future period 2080-2100					
		CGCM3	CNRM-CM5.1	EEC-EARTH	IPSL-CM5	HadGEM-ES	MPI-ESM
Mean annual surface runoff	61.13	54.65	50.75	53.73	48.42	41.53	47.95
Annual Pinios River inflow	80.00	80.00	80.00	80.00	80.00	80.00	80.00
Direct annual precipitation on the reservoir	15.09	14.39	13.36	14.15	12.75	10.94	12.63
Mean annual inflows into the reservoir	156.21	149.04	144.12	147.87	141.17	132.47	140.58
Mean annual evaporation	34.62	27.39	25.44	26.93	24.27	20.81	24.03
Deep percolation losses to groundwater	18.00	18.00	18.00	18.00	18.00	18.00	18.00
Mean annual overflow of the reservoir	70.70	69.82	64.84	68.63	61.86	53.06	61.26
Withdrawals for the irrigation needs	31.27	32.23	34.70	32.78	36.37	42.41	36.73
Mean annual outflows of the reservoir	154.60	147.44	142.98	146.34	140.50	134.28	140.02
(hm^3)							

5.3.3 Groundwater balance

The groundwater model was applied to the five GCMs for the long-term period 2080-2100 and the RCP4.5 climate scenario. Table 5 presents the results of the quantile mapping methodology for the five global climate models. It is obvious that for the case of water management strategy 2 the strongest result is provided by the HADLEY model with a deficit of -258.86 hm^3, followed by MPI with 222.73 hm^3, then IPSL with -220.45 hm^3, followed by CNRM which shows a deficit of -209.76 hm^3 and lastly ICHEC with -197.45 hm^3. On the other hand, the results are similar for scenario 2a (reduction of channel losses in combination with operation of the reservoir). In this scenario again, the HADLEY model is the most intense with a deficit of -229.53 hm^3, then MPI with -197.33 hm^3, followed by IPSL with -195.30 hm3 and milder results show the CNRM with - 185.76 hm^3 and ICHEC with -174.78 hm^3.

Figure 5 graphically represents the comparison for a random cross section BB' of the underground aquifer of Lake Karla. The results follow the intensity of the five GCMs with the HADLEY model projecting the smallest rise in groundwater levels and the ICHEC the largest.

Similar are the results about the spatial distribution of the hydraulic heads of the underground aquifer and are presented in figure 6 On the other hand, table 16.5 presents the results of the water balance for the entire watershed of Lake Karla, both for management strategy 2 and for scenario 2a. In the first case, the water balance of the basin is in deficit during the historical period by 74.60 hm^3, while the CGCM3 model projects the smallest deficit by 84.2 hm^3 and the HADLEY model the largest by 122.51 hm^3.

Table 5. Lake Karla aquifer water balance

	Future period 2080-2100

	CGCM3 SRES B1	CNRM-CM5.1 RCP 4.5	EC-EARTH.2 RCP 4.5	IPSL-CM5 RCP 4.5	HadGEM2-ES RCP 4.5	MPI-ESM RCP 4.5
Scenario 2						
Deep percolation	6.71	6.23	6.60	5.95	5.10	5.89
Return from irrigation	18.24	19.64	18.55	20.58	24.00	20.78
Total	24.95	25.87	25.15	26.53	29.10	26.67
Pumping	218.82	235.63	222.60	246.98	287.96	249.40
Water balance	-193,88	-209.76	-197.45	-220.45	-258.86	-222.73
Scenario 2a						
Deep percolation	6.71	6.23	6.60	5.95	5.20	5.89
Return from irrigation	16.21	17.45	16.49	18.29	21.33	18.47
Total	22.92	23.69	23.09	24.24	26.43	24.36
Pumping	194.51	209.45	197.86	219.54	255.96	221.69
Water balance	-171.59	-185.76	-174.78	-195.30	-229.53	-197.33
(hm3)						

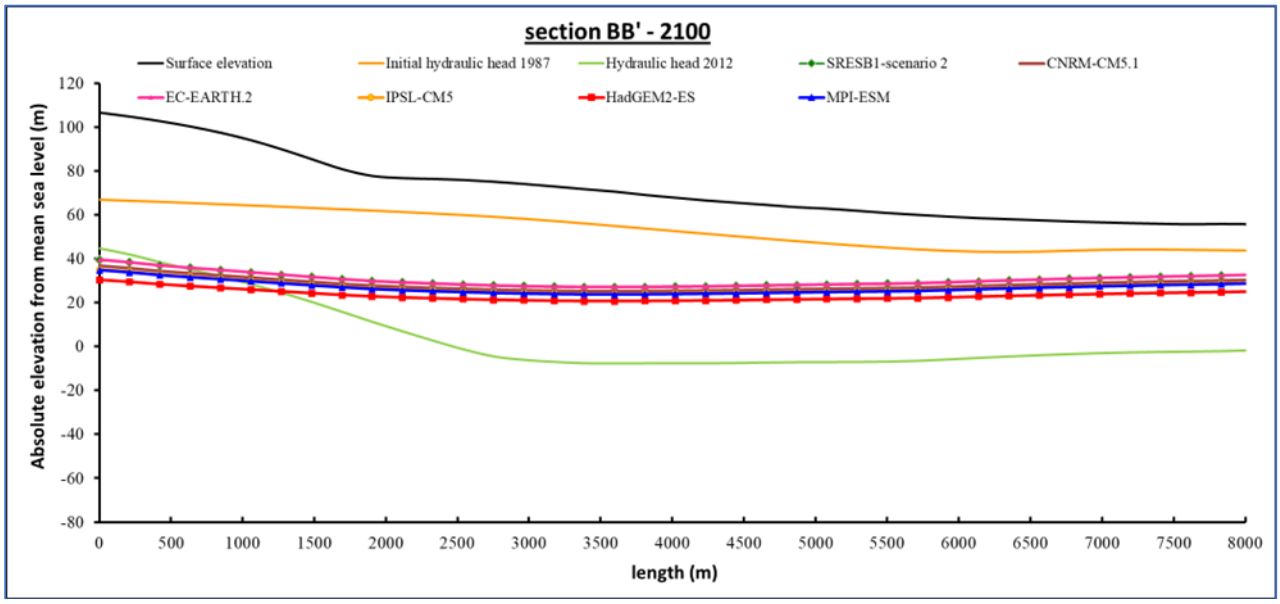

Figure 5. Random cross section of Lake's Karla aquifer

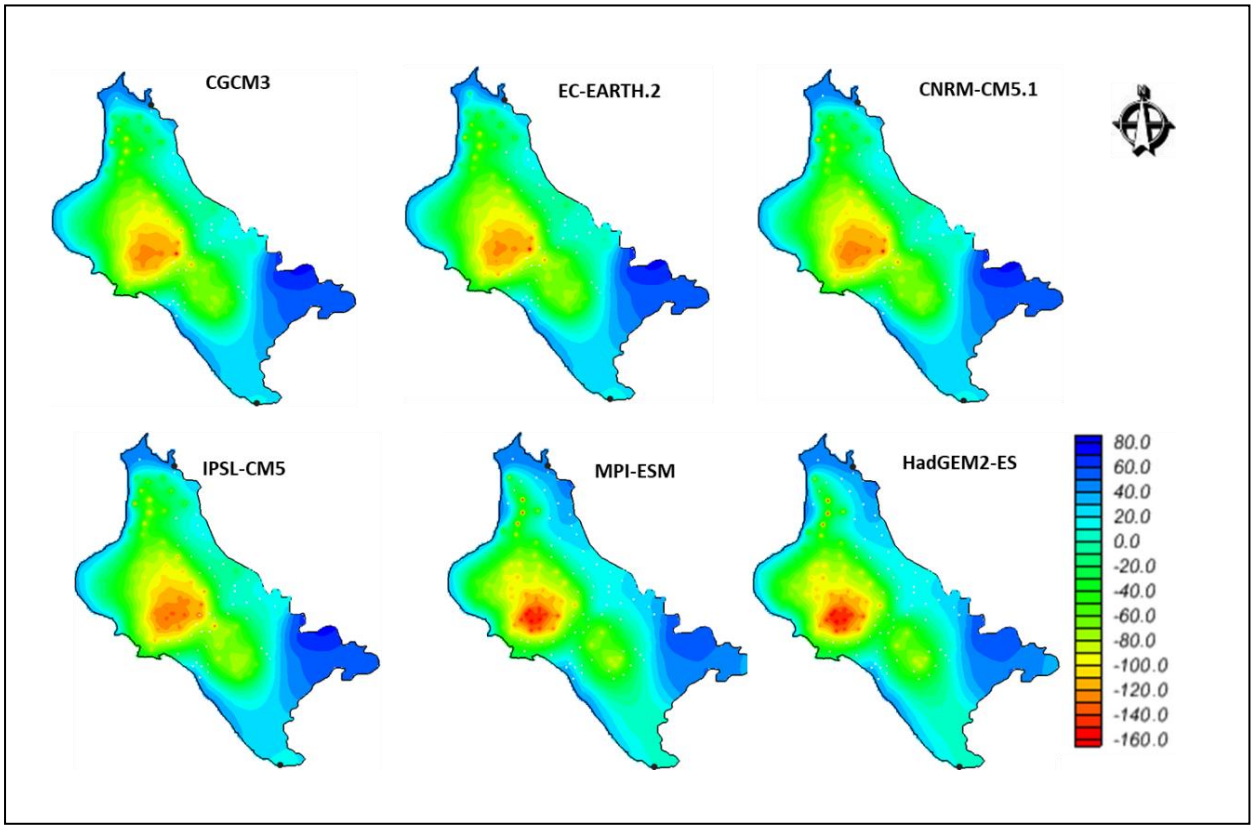

Figure 6. Maps of hydraulic heads for water management strategy 2 for: a)SRES B1 b) EC-EARTH.2 c) CNRM-CM5.1 d) IPSL-CM5 e) MPI-ESM f) Had.GEM2-ES

6 Summary

In this work, the uncertainty of the climate models was assessed using five (5) different climate models (GCMs+RCMs) and the results were compared with the initial simulation based on the CGCM3 climate model. The results showed that future estimates of hydro-meteorological variables (precipitation and temperature) significantly affect and introduce uncertainties in surface hydrological processes, water demand for irrigation and the overall water balance of the watershed. However, the impact of climate model estimates and uncertainty is reduced in the groundwater aquifer simulation (Fig. 5,6). The results show that for the degraded aquifer of the study basin, water resource management measures have a more significant effect than the effect of climate change and the uncertainty of future climate estimates. Specifically, the water balance of the catchment basin is in deficit during the historical period by 74.60 hm^3, while the simulations with the CGCM3 model project an increased future water deficit, which is the smallest and equal to 82.40 hm^3 compared to the simulations with the other climate models. The HADLEY model projects the largest future water deficit by 122.51 hm^3.

Table 6. Lake's Karla watershed water balance

Base period 1980-2000	Future period 2080-2100						
		CGCM3	CNRM-CM5.1	EEC-EARTH	IPSL-CM5	HadGEM-ES	MPI-ESM
Strategy 2: Future situation (Reservoir operation)	-74.60	-93.10	-100.25	-94.71	-105.08	-122.51	-106.11
Scenario 2a: Future situation (Reservoir operation & eaduction of canal losses)	-0.20	-16.50	17.77	-16.78	-18.62	-21.71	-18.81

On the other hand, the application of the management scenario 2a significantly improves the situation since for the historical period 1980-2000 the water deficit of the catchment basin is minimized (-0.2 hm^3) and the

simulations with global climate models show clearly reduced future water values deficit from -16.5 hm^3 for CGCM3 to -21.71 hm^3 for HADLEY. It is clear that during the simulations it is the implementation of the management scenarios that significantly improves the water balance of the Lake Karla watershed.

Thus, with the application of the optimal combination of water management strategies (scenario 2a, operation of the reservoir & reduction of channel losses) which during the historical period provided conditions for minimizing the water deficit of the watershed, an equally remarkable improvement of the water balance is achieved in all used climate models. This fact is confirmed by the significant reduction in the irrigation requirements of the watershed (Table 2) in each applied climate model but also from the results of the underground aquifer where its characteristic cross-section (Figure 5) shows that the hydraulic heights are improved by the application of rational management practices while the effect of the uncertainty of the climate models is significantly less influential.

References

Flato G. and Boer G., 2001. Warming Asymmetry in Climate Change Simulations. Geophysical Research Letters, 28, 195-198. doi:10.1029/2000GL012121

Hourdin, F. et al. (2016). The art and science of climate model tuning. Bulletin of the American Meteorological Society, (98), pp. 589-602. doi:10.1175/BAMS-D-15-00135.1.

Kerr, R.A. 2013. Forecasting regional climate change flunks its first test. Science, 2013 (6120), pp. 339-638. doi: 10.1126/science.339.6120.638.

Moss, R. H., Edmonds, J. A., Hibbard, K. A., Manning, M. R., Rose, S. K., Vuuren, D. P., . . . Wilbanks, T. J., 2010. The next generation of scenarios for climate change research and assessment. Nature, 463(7282), 747-756. doi:10.1038/nature08823.

Pavlidis, B., 2015. Evaluation of climatic model simulations over Europe for the period 1990-2008. Master Thesis. Aristotle University of Thessaloniki, School of sciences, Department of Geology, Sector of Meteorology and Climatology, Program of Post-graduate studies ""Meteorology, Climatology and Atmospheric Environment", Thessaloniki, 2015.

Tzabiras J., Spiliotopoulos M., Kokkinos K., Fafoutis C., Sidiropoulos P., Vasiliades L., Loukas A., Mylopoulos N., 2014. A GIS based district information system for water resources management and planning. EGU General Assembly 2014, 27 April - 2 May 2014, Vienna, Austria. Geophysical Research Abstracts, Vol. 16, 2014.

Tzabiras, J., Vasiliades L., Loukas A. and Mylopoulos N., 2015. Climate Change Impacts on Hydrometeorological Variables using a Bias Correction Method: The Lake Karla Watershed Case, Greece. Mathematics in Engineering, Science and Aerospace Vol. 6, No. 4, pp. 683-700, 2015

Tzabiras, J., Vasiliades L., Sidiropoulos P., Loukas A. and Mylopoulos N., 2015. Investigation of water resources management practices and climate change effects. Case study: Lake Karla watershed. Water resources management 30:5819–5844, 2016.

SESSION 5:

DIGITAL AGRICULTURE-GEOINFORMATICS

The Environmental Justice Atlas: a GIS tool for Monitoring Global Environmental Justice Challenges

Nektaria E. Adaktylou[1], Rick E. Landenberger [1][2],

[1] West Virginia University, Department of Geology & Geography, P.O. Box 6300, Morgantown, WV 26505-6300.
[2] West Virginia Land Trust, P.O. Box 304, Morgantown, WV 26507.

Abstract
This paper describes the fairly recent concept of environmental justice. It provides some context regarding the definition of environmental justice, its origins and the existing legal framework in the United States. The Environment Justice Atlas, a GIS tool that has been developed in order to document and communicate environmental conflicts all over the world is presented. The cases of conflict that have been documented in Greece are highlighted.

Origins of environmental justice
Environmental justice did not enter the public eye as a term, until the early 1980's. In 1982 a landfill designed to accept PCBs (Polychlorinated biphenyls, a highly toxic product of the chemical industry) was proposed to be placed in Warren County North Carolina (Figure 1a &1b), a predominately low income African American community. This plan initiated a massive protest to stop the project. Inspire of the reactions, the dumping did not stop. However this was a defining moment in the environmental movement, and is recognized to be the birth of environmental justice.

(a)

Figure 1 (a).North Carolina. (b). Warren County in North Carolina.

This was not the first related incident. In the early 1960's Cesar Chavez organized Latino farmworkers in California, to improve working conditions and fought against the use of toxic insecticides. In 1968 black residents of Harlem in NY campaigned -unsuccessfully- against a sewage plant in their community (North River). Love Canal in New York (Figure 2) is another well known history. It began when Hooker Chemical Co. used the abandoned canal for eleven years (1942 to 1953) to dump 21,800 tons of industrial hazardous waste.
The Warren County incident was the one that led to foundational studies, designed to explore and uncover the accuracy of the claims made by communities that felt they were targeted by polluting industries. Communities that were primarily found in America's Black Belt (Alabama, Florida, Georgia, Kentucky, Mississippi, North and South Carolina and Tennessee) (Figure 3). Two studies that were conducted in 1986

tried to determine to what extent minority and low income populations were disproportionally exposed to uncontrolled toxic waste and hazardous industrial waste facilities in their communities.

These reports were the first national studies of this kind, and were used to develop another study, issued in 1987: 'Toxic Wastes and Race in the United States: a National report on the racial and socioeconomic characteristics of communities with Hazardous Waste Sites'.

Figure 1. Love Canal. Source: US Environmental Protection Agency

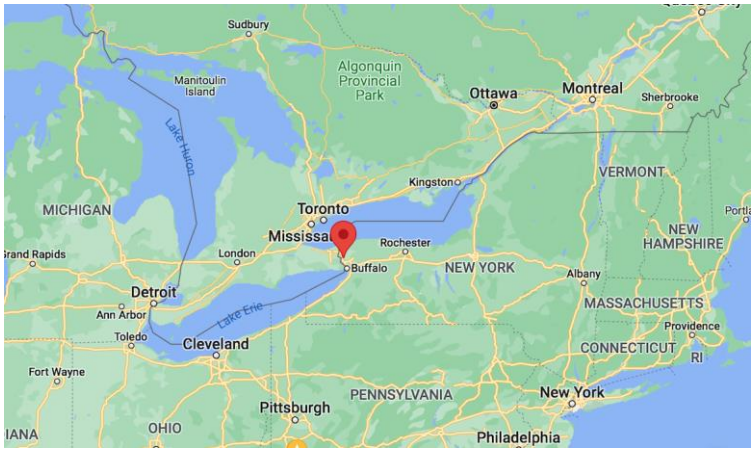

Figure 2 a&b. Love Canal is a (a) km² landfill that became the site of an neighborhood in Niagara Falls, New York. It was the location of a 0.28 enormous environmental disaster in the 1970s.

(b)

This report originated from the United Church of Christ Commission for Racial Justice. According to this report socioeconomic factors did determine the choices about hazardous waste facilities, but race was the most significant variable. According to the report's findings three out of five black and Hispanic Americans

and approximately half of all Asians, Pacific Islanders and American Indians lived in communities where uncontrolled toxic waste was present.

Southern counties with at least 30% African-American population in 2000.

Figure 3. Though strictly the name of a physical region, the term Black Belt has been borrowed by social scientists to denote those areas of the South where the plantation system, with its large number of black slaves, predominated before the Civil War (Britannica).

This report and the leadership of the African American communities in the civil right movement laid a foundation for other marginalized groups and communities to build upon and made the the environmental justice focus progressively broader.

Definition, dimensions, and legal framework of environmental justice

The EPA defines Environmental Justice αs: ´the fair treatment and meaningful involvement of all people regardless of race, color, national origin, or income, with respect to the development, implementation, and enforcement of environmental laws, regulations and policies.'(Gilio_Whitaker, 2019). The definition of environmental justice in the US has come with the re-definition of the 'environment'. The dominant wilderness, greening and natural resource focus now includes urban disinvestment, racism, homes, jobs, neighborhoods and communities. The 'environment' became discursively different; it became 'where we live, where we work and where we play' (Alston, 1991).

Scholars and activists consider environmental justice as an analytical approach to thinking about contested environmental problems. A simple analytical framework based on three dimensions (distribution, procedure and recognition) is the one more broadly used and is presented below in Figure 4.

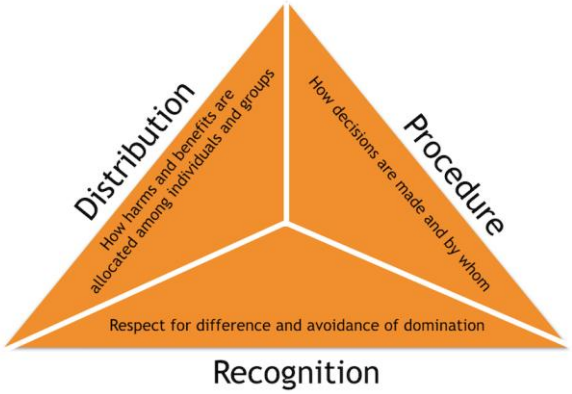

Figure 4. The dimensions of environmental justice.

The concept of environmental justice began to find its way in the US Federal Regulatory terrain with the work and support of the Congressional Black Caucus, that was formed as a group n 1971. In 1990 the Environmental Protection Agency (EPA) established the 'Environmental Equity Work Group' in response to the existing findings that: 'racial minority and low-income populations bear higher environmental risk burden than the general population' and that the EPA's inspections have failed to adequately protect low-income communities of color.' (Ewall, 2013). In 1992 the EPA formed the 'Office for Environmental Equity' and in 1993 the 'National Environmental Justice Advisory Council' was created. Public criticism -in activist, academic and legal circles- led to the use of the word 'justice' instead of that of 'equity' and the 'Office of Environmental Equity' became the 'Office of Environmental Justice' in 1994. That same year, the then President Bill Clinton, issued federal Actions to address the issues of environmental justice for minority and low-income populations, with the Executive order 12898. This executive order remains the cornerstone of environmental justice regulation in the US, with the EPA as a main player/arbiter. Rachtschaffen et al.(2009) state that overall, 'integrating environmental justice into environmental regulations in a meaningful way, has proven to be extremely complex'. The environmental justice movement has been very effective at addressing the challenges of vulnerable communities who are heavily affected by environmental 'bads', such as toxic facilities, or increased air pollution and who have restricted access to environmental 'goods' such as quality green and open play spaces. (Agyeman, 2007).

The Environmental Justice Atlas

In recent decades environmental justice movements and local communities affected by environmental injustices have become increasingly interconnected. Communities are now participating in data gathering of the impacts -social and environmental- of projects. This is what is referred to as 'citizen science'. These networks are progressively engaging with wider political, geographical, and historical contexts.
In 2012 Leah Temper and Joan Martinez-Alier from the Institute of Science, Technology and the Environment (ICTA) of the Autonomous University of Barcelona (UAB) in Spain developed the Environmental Justice Atlas (EJ Atlas) as part of the EJOLT project to document global environmental

conflicts. (add the EJ notes).The EJ Atlas is an GIS tool, with data collections related to a variety of environmental issues (Figure 5).

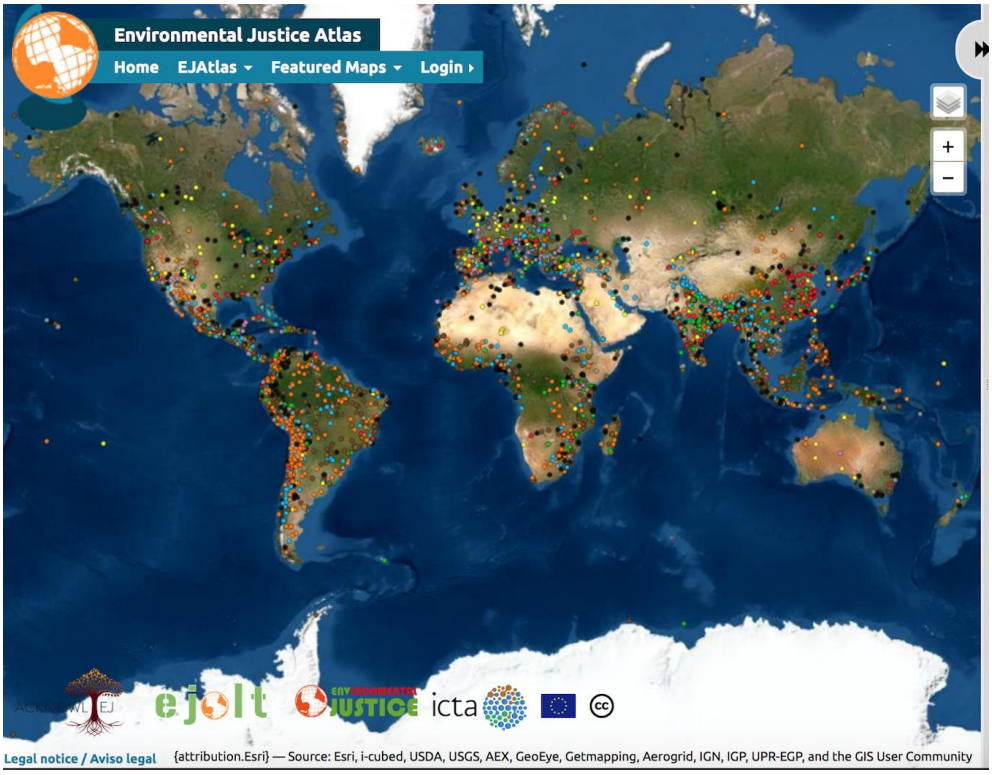

Figure 5. The EJ Atlas

Professor Martinez-Alier and her group received an Advanced Grant from the European Research Council to continue the project for the period 2016-2021. This has allowed to expand the previous FP7 project EJOLT (Environmental Justice Organizations, Liabilities and Trade), creating the current one, named EnvJustice, A Global Movement for Environmental Justice: The EJAtlas.It is important to mention that the atlas is also supported by the Acknowl-EJ (Academic-Activist Co-Produced Knowledge for Environmental Justice) project, directed by Dr. Leah Temper at the ICTA-UAB (SOMM Excellence Alliance).

Atlas Methodology

The Atlas is organized in ten main categories based on the types of conflicts:

- Industrial and Utilities Conflicts
- Waste Management
- Water Management
- Tourism Recreation
- Mineral Ores and Building Extractions
- Biomass and Land Conflicts
- Fossil Fuels and Climate Justice
- Infrastructure and Built Environment
- Biodiversity Conservation Conflicts
- Nuclear

Each conflict is documented by researchers and activists from around the world. One can find detailed information including photos, technical details, stakeholders and population affected, the forms of mobilization strategies being adopted, and the social and environmental impacts
There is a section on the current status of the conflict, where this information is available. Only 17% of the cases reported in the Atlas have been reported as 'solved', which says a lot about the challenges in the effort to achieve environmental justice worldwide. It also important to add that at least 260 cases in which environmental activists have been killed have been identified in the Atlas; the majority of them being in Latin America and Southern and South East Asia.

Environmental Atlas conflicts documented in Greece

The environmental conflicts that have been documents in the EJ Atlas can be seen in Figure 6 and are the following, starting from the south and moving towards the north part of the country:

Figure 6. The Environmental Atlas, here focusing on the area of Greece.

1. Industrial Renewable energy resources on Chios, Greece
2. Landfill construction in Keratea, Athens
3. Development of the former airport of Hellinikon and he coastal front of Agios Kosmas, Attica
4. Coastal fishermen against government policies of trawl fishing, Attica
5. Elefsina Bay Industrial activities
6. Roma living next to a landfill under constant threat of eviction in Aspropyrgos
7. Acheloos river diversion (Western Greece)
8. Aoos river diversion and hydroelectric projects (Northwestern Greece)
9. Waste transfer station in Efkarpia (suburb of Thessaloniki)
10. Water and sewage anti-privatization movement in Thessaloniki
11. Gold mining in Chalkidiki

Discussion

One can argue that there are both intrinsic and instrumental reasons why environmental justice is so important. The intrinsic reason is basically that justice is inherently a good thing. But going beyond this, it important to consider that the improvement of environmental justice will actually make it more likely tor stakeholders to effectively tackle environmental problems, such as biodiversity loss or water insecurity.
Decisions at the level of environmental governance usually create winners and losers and these decisions can therefore be perceived as just by some stakeholders and unjust by others. Where such justices and

injustices are not understood and are left unaddressed, there can be negative impacts on sustainability, including lack of cooperation amongst stakeholders.
In summary, injustice can be both a cause of environmental problems but also a constraint to resolving problems. In this sense promoting environmental justice can be a an important way to break out of unsustainable and uncooperative practices and to find mutually beneficial ways forward. This is why environmental justice is considered to be of instrumental importance for sustainability (Adrian Martin, 2019). The most recent report from the Intergovernmental Panel on Climate Change (IPCC, 2022), is the most comprehensive study available of how communities, countries and companies are exposed to climate change-related physical risks, and how they must adapt to lessen the damage. According to the report, leaving equity and justice out of climate transitions could lead to 'maladaptation, aggravated poverty and reinforce existing inequalities and entrenched gender bias. This could slow, rather than accelerate, the pace of a sustainable transition.'
One way to facilitate this equitable transition is to involve Indigenous and marginalized communities in adaptation planning decisions and in implementation processes. The Environmental Justice Atlas is a GIS tool that has proven to be effective as a communication, engagement and networking, as well as an advocacy resource for pressing environmental conflicts in the entire globe. It currently serves as a virtual space for those working on EJ issues to get information, find other groups working on related issues, and increase the visibility of environmental cases of concern.

References

Agyeman, J., 2007 in: Environmental justice and sustainability, editors: Giles Atkinson, Simon Dietz, Eric Neumayer (2007).

Alston, J., M. Marra, P. Pardey and P. Wyatt (2000), 'Research return redux: a meta-analysis and the returns of R&D', *Australian Journal of Agricultural Economics*, **44**: 1364–85.

EJAtlas - Global Atlas of Environmental Justice at: https://ejatlas.org

Ewall, M. (2013). Legal tools for environmental equity vs. environmental justice. Sustainable development law and policy 13, noI(2012-13).

Gilio_Whitaker, D.2019. As long as grass grows, The indigenous fight for environmental justice, from colonization to Standing Rock.

IPCC, 2022: Climate Change 2022: Mitigation of Climate Change. Contribution of Working Group III to the Sixth Assessment Report of the Intergovernmental Panel on Climate Change [P.R. Shukla, J. Skea, R. Slade, A. Al Khourdajie, R. van Diemen, D. McCollum, M. Pathak, S. Some, P. Vyas, R. Fradera, M. Belkacemi, A. Hasija, G. Lisboa, S. Luz, J. Malley, (eds.)]. Cambridge University Press, Cambridge, UK and New York, NY, USA. doi: 10.1017/9781009157926

Martin, A., 2019. Environmental Justice, Global Environmental Justice Group, University of East Anglia.

Rachtschaffen, C., Gauna, E., O'Neil, C. (2009). 'Introduction: History of the movement'. Environmental Justice: Law, policy and regulation (Durham, NC: Carolina Academic Press, 2009).

Evaluation of applying foliar fertilizers using an Unmanned Aerial Spraying Systems (UASS, drones) in a high density olive grove based on aerial photos and NDVI mapping

Athanasios Gertsis[1], Stavroula Tsimpliaraki[1], Ifigeneia Logotheti[1], Konstantinos Tsarsitalidis[1,] Antonios Panagopoulos[1]and Panagiotis Tziachris[2]

[1]Perrotis College/American Farm School, MSc dept. Sustainable Agriculture & Management, Thessaloniki, Greece
[2] ELGO-Demetra, Soil and Water Resources Institute, Thessaloniki, Greece

Abstract. The production efficiency of any agricultural crop system depends largely on the accurate management practices applied during the entire biological plant cycle. Olive production systems comprise the largest area and income for the Greek agricultural economy. New high density olive production systems offer new potential for increasing productivity and reducing costs. New technologies offer very potential tools to enhance the increase of efficient management. One technology receiving high attention is spraying drones, with different tank capacities (currently at 10, 16, 20 or 30 liters). However, there is no adequate research on the efficiency and efficacy of spraying. This study was undertaken to evaluate the possibility of using Unmanned Aerial Spraying systems UASSs (*aka* Drones) for spraying a high density olive system at Perrotis College and determine the cost and benefits by reducing spraying volumes and active ingredients. The study includes spraying with UASS based on aerial photos obtained with a drone equipped with two georeferenced cameras (RGB and NIR) and processed with a GIS to create maps of Normalized Difference Vegetation Index (NDVI) and adjusting the spray volumes to evaluate droplet distribution with appropriate softwareInitial data indicated that the drones provide a significant cost reduction, compared with ground systems and also mapping of the olive canopy can be used as a good practice to differentiate spraying volumes. Also, there was an increase on leaf nutrient concentration even from the 1st spraying, indicating that an improvement was achieved by the foliar application even at early stages. This study is an ongoing and long term effort to evaluate other aspects of aerial spraying with drones in a holistic approach. The main goal is to facilitate management and increase inputs use efficiency for a sustainable production system.

1 Introduction

The use of drones for spraying started for environmental reasons, and to limit human exposure to agrochemicals, while at the same time having more precise spraying (Khan et al. 2021). Also, spraying can now be done without stamping the vegetation, or affecting the crop in any way other than with the spraying substance. With drones for spraying operations, labor worker's cost can be decreased, and time can be saved for the farmer (Rahman et al. 2021). Drones have the ability to communicate with other drones, or sensors through Internet of Things (IoT) to apply in the most efficient manner pesticides, insecticides, fertilizers or biostimulants. Drones are a good choice for isolated locations, and difficult to approach fields, like in hillsides etc (Zhang et al. 2022). Spraying drones can be used for pesticide/insecticide applications, for fertilizing, or to boost the production. In this paper, we will focus on biostimulant application on olive trees, in a super high density grove.
In order to study the effect of the sprayed substance to the crop, another, smaller drone was used, which had installed two georeferenced cameras, one for the visible light spectrum (RGB), and one capturing at Near Infrared (NIR)

2 Spaying, remote sensing drones and biostimulants for crop production

Biostimulants on olive trees

Biostimulants are natural substances resulting from fine pulverization of inorganic minerasl, alage extarcts, microorgansms hydrolysed, fermented or extracted, (i.e. proteins, amino acids, nitrogen containing compounds etc) from animal and plant tissues, that promote plant growth, and strengthen plants, protecting them from infections (Drobek et al. 2019). The new EU legislation to become affective form 2022,(https://eur-lex.europa.eu/legal-content/EN/TXT/?qid=1583934899523&uri=CELEX:32019R1009) outlines all these products and they are compatible with organic agriculture applications. Almadi et al. (2020) experimented on young olive trees, achieving greater growth rates both in potted, and field plants, by using biostimulant solution of animal origin, containing amino acids. In adult olive trees, melatonin has been found to decrease the negative effects of water stress (Gholami et al. 2022), opening the possibility to use melatonin as a biostimulant. Although biostimulant is a generic term that can include even fertilizers, their effectiveness can be confirmed through research (Zouari et al. 2020), even if it's a time consuming procedure.

Unmanned Aerial Spraying systems UASSs (aka Drones)

Drifting is a parameter not to be neglected, because the finer droplets and the height from which the spraying occurs, facilitate the distribution to other locations than on the crop that is originally sprayed (Wang et al. 2021). Verma et al. (2022) estimated that 2 m above canopy is a good height to spray, to minimize drift, and have uniform distribution of droplets. Also, the airflow generated by the motors of the drones is surely affecting the droplet distribution inside the canopy, although studying it through computational fluid dynamics is lacking (Zhang et al. 2022). Chojnacki and Pachuta (2021) found that there was no statistically significant difference between the distributions of sprayed material in cherry trees spaced at 0.5m and 1m, whereas the rotational speed of the drone and nozzle type altered the spraying distribution. The nozzle plays an important role in the effectiveness of the aerial treatment, for example the diameter of the nozzle (Ru et al. 2020), or its type, for example conventional and centrifugal jet nozzles, that are used in this study. An extensive study was conducted at Perrotis College in a high density olive grove with evaluation of spraying characteristics of ground and aerial systems (Gertsis and Karampekos, 2021) indicating some more advantages of drones in terms of time and amount od application volume.

Monitoring and remote sensing drones and mapping

Monitoring through UAVs has become a trend in modern agriculture, allowing farmers and advisors to create models that will help understand what the crop needs, for example 3D model reconstruction, to study plant parameters on a plant basis (Boursianis et al. 2022). Other UAV applications include sensing of canopy discoloration to detect pests or diseases, mapping, and synergy of UAVs with static sensors like e-traps for insects (Psirofonia et al. 2017). Probability mapping can offer insights to infection risks in any crop, and is a very useful tool to prevent pest and disease infestation, which is valuable both for the economics of the farmer, and the environment, since prevention leads to less pesticide use (Castrignanò et al. 2021). Many authors suggest the use of multiple drones (swarms), for more accurate results despite the technological issues that arise (Ribeiro et al. (2015), Boursianis et al. (2022)). For this study, we used cameras on a small drone, to take pictures in NIR and RGB spectra, in order to later on construct NDVI and other index maps.

3 Materials and Methods

Final results from the entire study are expected at the end of the harvesting period (late December to early January). Therefore, only partial data will be presented in this paper, due to the deadline for submission. Data will be collected from the entire Soil Plant Atmosphere continuum (SPAC). Included are: weather and soil moisture data for a telemetric Weather Station, agronomic data (critical growth stages using the BBCH system for olives), spraying coverage and droplet distribution and characteristics (using Water Sensitive papers-WSP) and final yield weight and infestation levels. Granular ground fertilization was the same for all Treatments in earlier stages with a complete fertilizer (20-10-10)..

The olive grove consists of 3 Planting densities, SHD, HD and MD corresponding to Super High Density, High Density and Medium Density at 1670, 100 and 500 trees/ha))

The foliar treatments were performed with the Topxgun 16 liters drone (Figure 1, www.topxgun.gr) equipped with the centrifugal nozzles, while the WSP test comparison was done using a 16 L Joyance 606 model (Figure 2, www.joyance.tech).

Figure 1. The Topxgun 16 liters drone used for spraying, with centrifugal nozzles.

Figure 2. The Joynace 16 liter drone used with dual conventional nozzles

The experimental olive grove of high density used in this study, is located at Perrotis College, Greece, was divided to four sections, each having its own treatment:

- **Section A** –**Z20** (a finely pulverized mineral water soluble with a macro+micro elements) 30 g +30 ml **Amino acid**+3 ml **Fluisan** (algae extract)
- **Section B** - **Trainer** [Organic N 5%, Organic C=19%, Plant peptides 31%] 30 ml + **MyR Micro** [Organic N 1%, B 0.6%, Fe 2.4 %, Mn 3.2%, Organic C 11,3%) 30 ml of each
- **Section C**: **Auxym** [plant peptides, vitamins, enzymes, auxins and trace elements] 10 ml + **MyR Ca** [organic N 3%, CaO 5%, organic C 16,5%] 30 ml+ **MyR K** [K2) 12%] 30 ml
- **Section D=** Control (not sprayed)

The area of each section was 13 m X 60 m= 780 m^2 and the total area was 4 X 780 =3120 m^2

Spraying Drone settings: 5 m height from the ground- 3 m/s speed – 60 liters/ha spray (5 liter/0.078 ha)

Leaf samples were collected from all 4 treatments on ca. 10-15 days for major and micro elements tissue analyses.

Hypothesis:

- Ho= The applied products have no significant effects of productivity, level of infestation (insects or diseases) and olive oil quality.
- Ha= There are significant effects on all traits measured caused by the applied products.

Statistical analyses will be performed with JMP v 16 software (www.jmp.com), at the end of the harvesting period (late December to early January), when all data required will be collected.

The last procedure followed was the mapping of the four sections, to create NDVI maps. The GEP 4/2 drone (Fig 3) was used, provided by Gep Drones (www.gepdrones.com), which is equipped with two cameras, one in NIR and the other in RGB spectra.

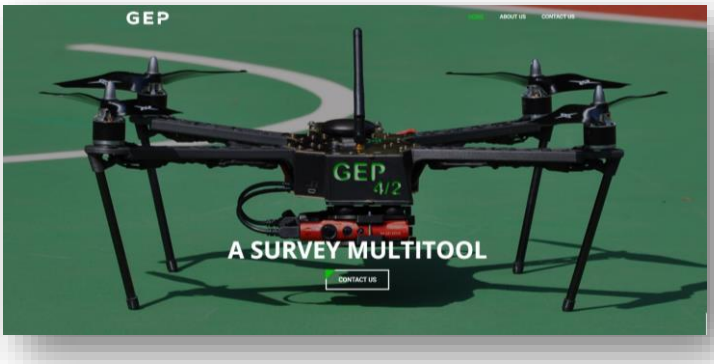

Figure 3. The surveillance drone used to establish NDVI maps

4 Results and Discussion

The results from the initial and 10 days after the 1st aerial spraying are shown in Table 1.

Table 1. The leaf analysis from samples of each section, 10 days after the foliar application by drones and before the application *H=High, A=Adequate, PA= Partially Adequate, IN= INADEQUATE*

Section	N	P	K	Ca	Mg	B	Mn	Zn	Fe	Cu
A	1,786	0,15	0,9	1,93	0,2	20,03	31,54	29,44	66,35	11
B	1,91	0,13	0,81	1,31	0,14	22,02	29,84	28,99	62,8	11,9
C	2,106	0,17	0,82	1,16	0,13	20,31	25,51	36,38	51,92	12,7
D =CONTROL Before 1st application	1,982	0,14	0,84	1,4	0,13	8,89	27,89	31,95	72,02	11,4
	1,287	0,12	1,08	1,23	0,10	7,96	25,34	28,32	55,67	

From Table 1 we cannot conclude any major difference in leaf nutrients, assuming that more conclusive results will be shown after the 2nd and 3rd sprayings and leaf analyses towards the later growth stages, with the olive fruits well established. However, an initial increase of some elements in Sections A, B and C as compared with the Control, is visible, mainly in B, an essential element for olive production. However, there was a difference shown as compared to the leaf analysis before the spraying, indicating that the 1st application has increased the nutrient levels in levels.

From the NDVI map resulting after the 1st spraying (Fig.4) it was not quite visible any major effect of the treatments on leaf canopy (further analysis will be conducted when all 3 spraying terminate). A 3D pictutre of the olive grove (Fig. 5)

5 Summary

The study includes spraying with UASS based on aerial photos obtained with a drone equipped with two georeferenced cameras (RGB and NIR) and processed with a GIS to create maps of Normalized Difference Vegetation Index (NDVI) and adjusting the spray volumes to evaluate droplet distribution with appropriate software. The results presented are yet preliminary, since the biological cycle of olive production will be terminated at the harvesting period, expected in December 2022. The available data supported the hypothesis that

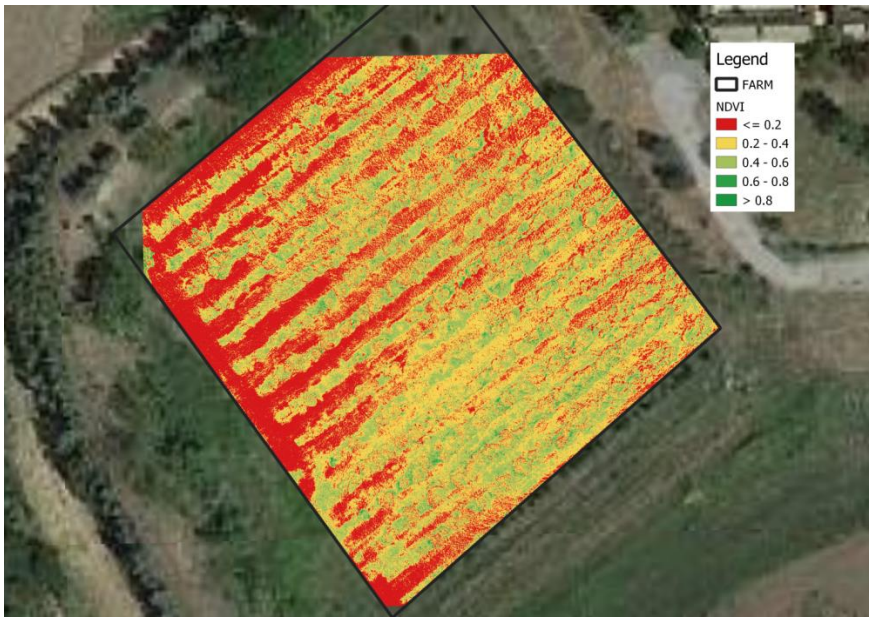

Figure 4. NDVI map fo the olive grove

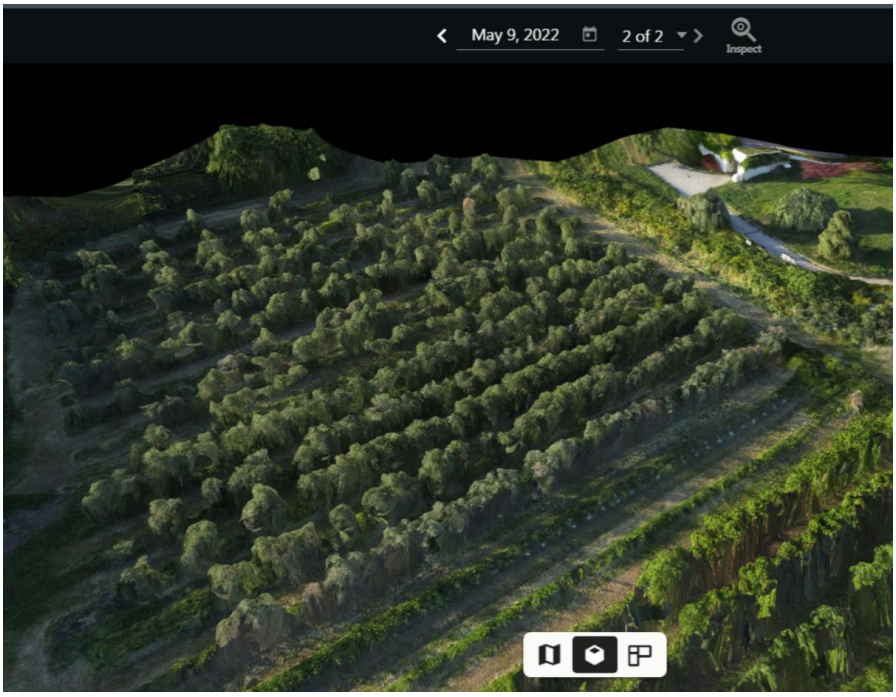

Figure 5. A 3D image of the olive grove

Acknowledgements

The authors express their gratitude to Spyridonakis S.A.(www.topxgun.gr) for supplying the spraying drone with centrifugal nozzles and for his technical support. Also to 3D S.A.. (www.3dsa.gr) for supplying their drone with conventional nozzles for the study. And finally, to BIOSOLIDS S.A. (www.biosoldis.gr) and STEFES (https://www.stefes.eu/) for supplying the biostimulant products used

References

Almadi, L., Paoletti, A., Cinosi, N., Daher, E., Rosati, A., Di Vaio, C. and Famiani, F. 2020. A Biostimulant Based on Protein Hydrolysates Promotes the Growth of Young Olive Trees. *Agriculture* 10(12), p. 618. doi: 10.3390/agriculture10120618.

Boursianis, A.D. et al. 2022. Internet of Things (IoT) and Agricultural Unmanned Aerial Vehicles (UAVs) in smart farming: A comprehensive review. *Internet of Things* 18, p. 100187. doi: 10.1016/j.iot.2020.100187.

Castrignanò, A. et al. 2021. A geostatistical fusion approach using UAV data for probabilistic estimation of Xylella fastidiosa subsp. pauca infection in olive trees. *Science of The Total Environment* 752, p. 141814. doi: 10.1016/j.scitotenv.2020.141814.

Chojnacki, J. and Pachuta, A. 2021. Impact of the Parameters of Spraying with a Small Unmanned Aerial Vehicle on the Distribution of Liquid on Young Cherry Trees. *Agriculture* 11(11), p. 1094. doi: 10.3390/agriculture11111094.

Drobek, M., Frąc, M. and Cybulska, J. 2019. Plant Biostimulants: Importance of the Quality and Yield of Horticultural Crops and the Improvement of Plant Tolerance to Abiotic Stress—A Review. *Agronomy* 9(6), p. 335. doi: 10.3390/agronomy9060335.

Gertsis, A. and L. Karampekos. 2021. Evaluation of Spray Coverage and Other Spraying Characteristics from Ground and Aerial Sprayers (Drones: UAVs) Used in a High-Density Planting Olive Grove in Greece https: Information and Communication Technologies for Agriculture—Theme IV: Actions, Pages255-268. Publisher Springer, Cham//link.springer.com/chapter/10.1007/978-3-030-84156-0_13

Gholami, R., Fahadi Hoveizeh, N., Zahedi, S.M., Gholami, H. and Carillo, P. 2022. Melatonin alleviates the adverse effects of water stress in adult olive cultivars (Olea europea cv. Sevillana & Roughani) in field condition. *Agricultural Water Management* 269, p. 107681. doi: 10.1016/j.agwat.2022.107681.

Khan, S., Tufail, M., Khan, M.T., Khan, Z.A., Iqbal, J. and Wasim, A. 2021. Real-time recognition of spraying area for UAV sprayers using a deep learning approach. *PLOS ONE* 16(4), p. e0249436. doi: 10.1371/journal.pone.0249436.

Psirofonia, P., Samaritakis, V., Eliopoulos, P. and Potamitis, I. 2017. Use of Unmanned Aerial Vehicles for Agricultural Applications with Emphasis on Crop Protection: Three Novel Case - studies. *International Journal of Agricultural Science and Technology* 5(1), pp. 30–39. doi: 10.12783/ijast.2017.0501.03.

Rahman, M.F.F., Fan, S., Zhang, Y. and Chen, L. 2021. A Comparative Study on Application of Unmanned Aerial Vehicle Systems in Agriculture. *Agriculture* 11(1), p. 22. doi: 10.3390/agriculture11010022.

Ribeiro, A. et al. 2015. A fleet of aerial and ground robots: a scalable approach for autonomous site-specific herbicide application. In: *Precision agriculture '15*. The Netherlands: Wageningen Academic Publishers, pp. 167–173. Available at: http://dx.doi.org/10.3920/978-90-8686-814-8_20 [Accessed: 29 May 2022].

Ru, Y., Liu, Y., Qu, R. and Kumar Patel, M. 2020. Experimental study on spraying performance of biological pesticides in aerial rotary cage nozzle. *International Journal of Agricultural and Biological Engineering* 13(6), pp. 1–6. doi: 10.25165/j.ijabe.20201306.5511.

Verma, A., Singh, M., Parmar, R.P. and Bhullar, K.S. 2022. Feasibility study on hexacopter UAV based sprayer for application of environment-friendly biopesticide in guava orchard. *Journal of Environmental Biology* 43(1), pp. 97–104. doi: 10.22438/jeb/43/1/mrn-1912.

Wang, C. et al. 2021. Assessment of spray deposition, drift and mass balance from unmanned aerial vehicle sprayer using an artificial vineyard. *Science of The Total Environment* 777, p. 146181. doi: 10.1016/j.scitotenv.2021.146181.

Zhang, H., Qi, L., Wan, J., Musiu, E.M., Zhou, J., Lu, Z. and Wang, P. 2022. Numerical simulation of downwash airflow distribution inside tree canopies of an apple orchard from a multirotor unmanned aerial vehicle (UAV) sprayer. *Computers and Electronics in Agriculture* 195, p. 106817. doi: 10.1016/j.compag.2022.106817.

Zouari, I. et al. 2020. Mineral and carbohydrates changes in leaves and roots of olive trees receiving biostimulants and foliar fertilizers. *South African Journal of Botany* 135, pp. 18–28. doi: 10.1016/j.sajb.2020.07.032.

Monitoring of broccoli crop before and after biofortification: Toward revealing potential transient stressful periods during development

Dimitris Bouranis[1,2], Evangelos N. Karousis[1], Georgios Stylianidis[1], Andriani Tzanaki[1,3], Despina Dimitriadi[3], Vassilis Siyiannis[4], Styliani Chorianopoulou[1,2]

[1] Plant Physiology and Morphology Laboratory, Crop Science Department, Agricultural University of Athens, Iera Odos 75, 11855 Athens, Greece
[2] PlanTerra Institute for Plant Nutrition and Soil Quality, Agricultural University of Athens, Iera Odos 75, 11855 Athens, Greece
[3] Karvelas AVEE, Ypato, Viotia, Greece
[4] Geoponiki SA, Koropi, Attiki, Greece

Abstract. Broccoli plants present an interesting effect during growth and development: the lower (older) leaves enter senescence mode to support the current developing leaves during vegetative phase, and both young leaves and flower heads during the reproductive phase. To identify potential transient periods where crop might face stress, we monitored the optical properties profiles of both the current 2nd leaf from bottom-up and the 6th one from top-down at the time of measuring. NDVI, PRI, SPAD, and chlorophyll fluorescence (Fv/F0) were used as indices, along with photosynthetic rate, at the measuring time.
One hundred and fifty plants were transplanted in pots containing vermiculite, perlite, and sand in a ratio of 1:1:1, at 2021/10/25 (d0) in a greenhouse. Heads appeared at day 60 post transplantation and were harvested at d107. During growth period, the outside temperature was recorded. Data were collected at days 54, 60, 76, 82, 89, 96, and 103. Once a week, plants were receiving full nutrient solution. In each measuring day, measuring was starting 09:00 and ending 14:00. Photon flux density was recorded along with leaf temperature. During cultivation period, the outside temperature presented fluctuations, and dynamics of the aforementioned parameters are discussed in each type of studied leaves, senescing vs fully developed ones. Toward revealing potential transient stressful periods during development, a potential stress factor index is proposed.

1 Introduction

Senescence is the process of aging in plants. Aging in plants can be either stress-induced or developmental, i.e., age-related one. During leaf senescence, chlorophyll degradation reveals the carotenoids, i.e., carotenes and xanthophylls. Leaf senescence has the important function of recycling nutrients, to growing and storage organs of the plant. Plants continually form new organs and older organs undergo a highly regulated senescence program to maximize nutrient export (Guo et al., 2021). In broccoli plants the lower (older) leaves enter senescence mode to support the current developing leaves during the vegetative phase, and both young leaves and flower heads during the reproductive phase. Therefore, we can roughly distinguish three developmental types of leaves, the old leaves that possess the lower 25% of the shoot, the fully mature leaves in the middle, not yet old, that occupy the 60% of the shoot, and the developing, young ones that occupy the upper 15% of the shoot. The transition state from mature to senescing leaf can be reflected by the changes in its optical properties. Apart from development, stress can also be the cause for such transition.
Live green plants absorb solar radiation in the photosynthetically active radiation (PAR) spectral region, which they use as a source of energy in the process of photosynthesis. Leaf cells have been evolved to re-emit solar radiation in the near-infrared spectral region (which carries approximately half of the total incoming solar energy). A strong absorption at these wavelengths would result in overheating the plant and possibly damaging the tissues. Hence, live green plants appear relatively dark in the PAR and relatively bright in the near infrared. Chlorophyll strongly absorbs visible light (from 400 to 700 nm) for use in photosynthesis. The cell structure of the leaves, on the other hand, strongly reflects near-infrared light (from 700 to 1100 nm). The more leaves a plant has, the more these wavelengths of light are affected (Sellers, 1985; Lichtenhaller and Rinderie, 1988; Gamon et al., 1997; Baker and Rosenqvist, 2004; Kuckenberg et al., 2009).
To identify potential transient periods where broccoli might face stress, in this work we monitored the profiles of the optical properties of both the current 2nd leaf from bottom-up and the 6th one for top-down at the time of measuring (Fig.1). NDVI, PRI, SPAD, and Fv/Fo, were used as indices, along with photosynthetic rate, photosynthetically active radiation, and leaf temperature at the measuring time. Because light and temperature influence the values of these indices within the day, it is important to know the behavior of the control plant to evaluate the behavior of the same plant that received a treatment, applied foliarly of through the soil. Therefore,

in this work we present the kinetics of the optical properties of the aforementioned broccoli leaves without treatment.

2 Experimental

2.1 Plant material

One hundred and fifty plants were transplanted in pots containing vermiculite, perlite, and sand in a ratio of 1:1:1, at 2021/10/25 (d0) in a greenhouse. Once a week, plants were receiving full nutrient solution. During growth period, the outside temperature was recorded. Data were collected at days 54, 60, 76, 82, 89, 96, and 103. Heads appeared at day 60 post transplantation and were harvested at d107. In each measuring day, measuring was starting 09:00 and ending 14:00. Photon flux density was recorded along with leaf temperature. During cultivation period, the outside temperature presented remarkable fluctuations. Dynamics of the studied parameters is presented in each type of studied leaves, senescing vs young fully developed ones.

Fig.1 (Left) Picture of broccoli plant at day 54 post transplantation. A lower leave is at senescence mode. (Right) Both leaves have been marked for measuring; red marker: leaf 6 from top-down, black marker: leaf 2 (the 2nd green one) from bottom-up . Below it, the oldest, now dead, leaf.

2.2 Prevailing environmental conditions

The data of the atmospheric temperature were collected from the database of Hellenic National Meteorological Service (Fig.2, left). Data of leaf temperature (Fig.2, right), and Photosynthetically Active Radiation (PAR; Fig.3, right) were measured using LCproT (ADC BioScientifc Ltd.).

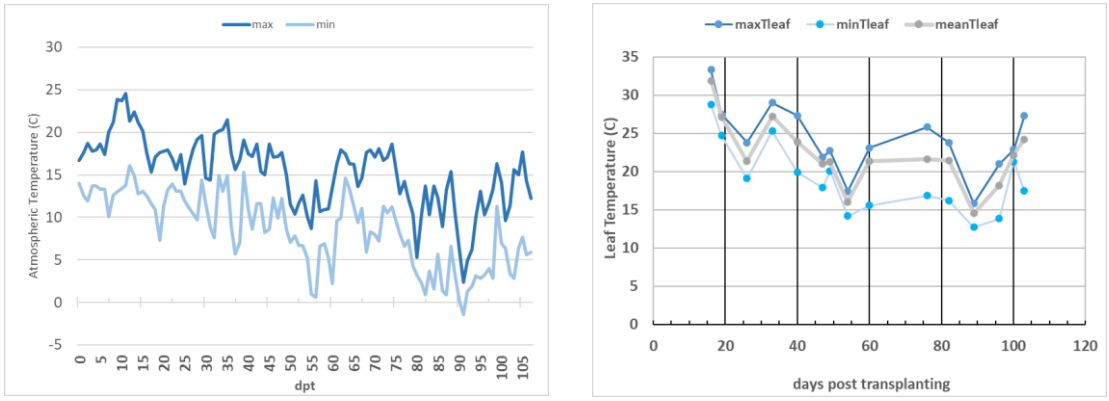

Figure 2. (Left) The kinetics of atmospheric temperature in Koropi, Attiki, during the experiment. (Right) The kinetics of leaf temperature range of control plants in each measuring day. The selected leaves did not differ in temperature.

2.3 Measurements and data collection

The PlantPen model PRI 210 and NDVI 310 were used to measure PRI and NDVI values, respectively. The SPAD values were measured by the Chlorophyll Meter SPAD-502+. Fv/F0 was measured by OS30p+, OptiSciences chlorophyll fluorometer**.** Measurements were taken in the upper one third of each leaf, one measurement per leaf x 3 plants per treatment (leaf 6 or 2). Prior to measuring Fv/F0, the measuring site of the leaf was kept in dark for 30 min. PAR and photosynthetic rate were measured by means of LCproT (ADC BioScientific Ltd.)

3. Results and Discussion

Control plants were measured at 09:00, 10:30, 12:00, and 13:30, in each measuring day, and the kinetics of each parameter is as follows:

3.1 Leaf temperature and PAR

Within the measuring day, leaf temperature was increasing with time, and the fluctuations (Fig.3) were the same in both measuring leaves. D89 and d54 presented the same level, which is in accordance with the external temperature fluctuations.
Photosynthetically active radiation presented a distribution profile (Fig.3), with the peak depending on the presence of clouds and the corresponding decrease of the external photon flux.

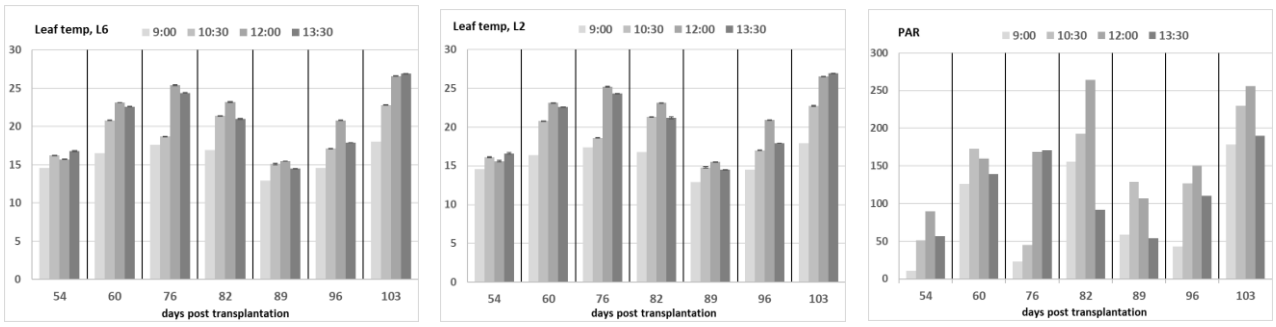

Figure 3. Leaf temperature kinetics of control plants within and between the measuring days, at leaf 6 from top-down (left) vs leaf 2 from bottom-up (middle). Error bars represent standard error. Kinetics of Photosynthetically Active Radiation of control plants in each measuring day (right).

3.2 Photosynthetic rate

The photosynthetic rate presented a significant increase within the measuring time (Fig.4), and in most cases the measurement at 09.00 was significantly lower compared with the others. Lower leaf presented lower photosynthetic rate, with the same distribution pattern with the measuring time.

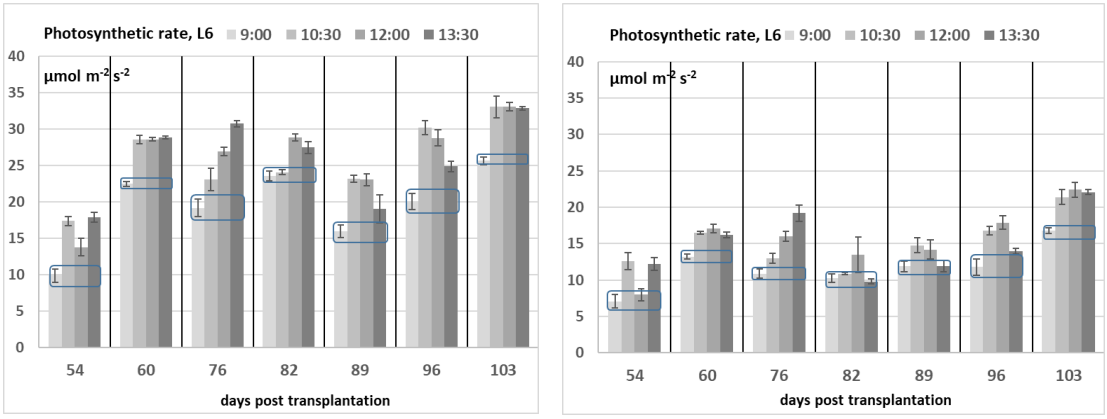

Figure 4. Photosynthetic rate kinetics of control plants in each measuring day, at leaf 6 from top-down (left) vs leaf 2 from bottom-up (right). Error bars represent standard error.

3.3 SPAD index

Leaf 6 presented SPAD values between 60 and 80 with most probable 70, and between measuring days results were comparable (Fig.5). In contract, leaf 2 presented a decreasing pattern with time. D82 and d103 presented extended range of value (30-65) with a mean value of 50.

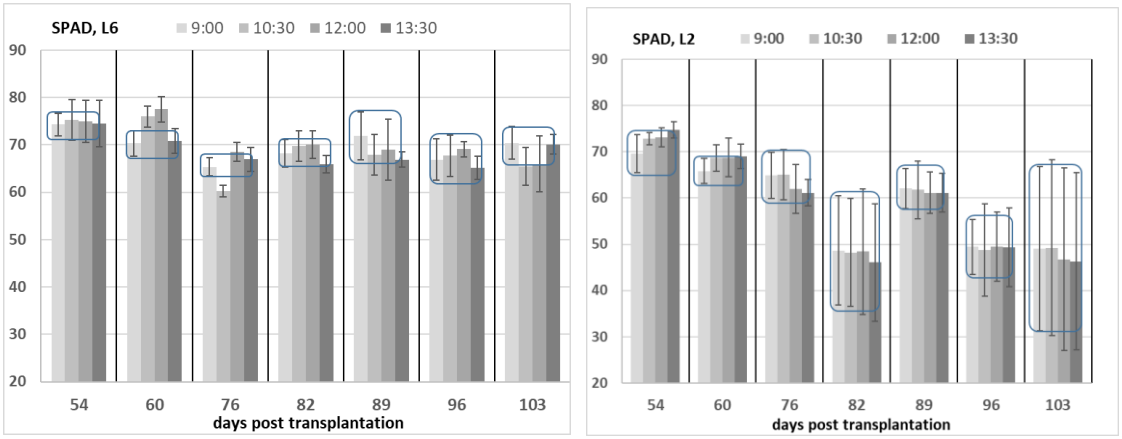

Figure 5. SPAD kinetics of control plants within and between the measuring days, at leaf 6 from top-down (left) vs leaf 2 from bottom-up (right). Error bars represent standard error.

3.4 NDVI

NDVI values ranged between 0.78 and 0.82 in leaf 6, whilst values of leaf 2 were between 0.75 and 0.80 (Fig.6). Again, d82 and d103 presented an exception with values at 0.70 and 0.65 respectively.

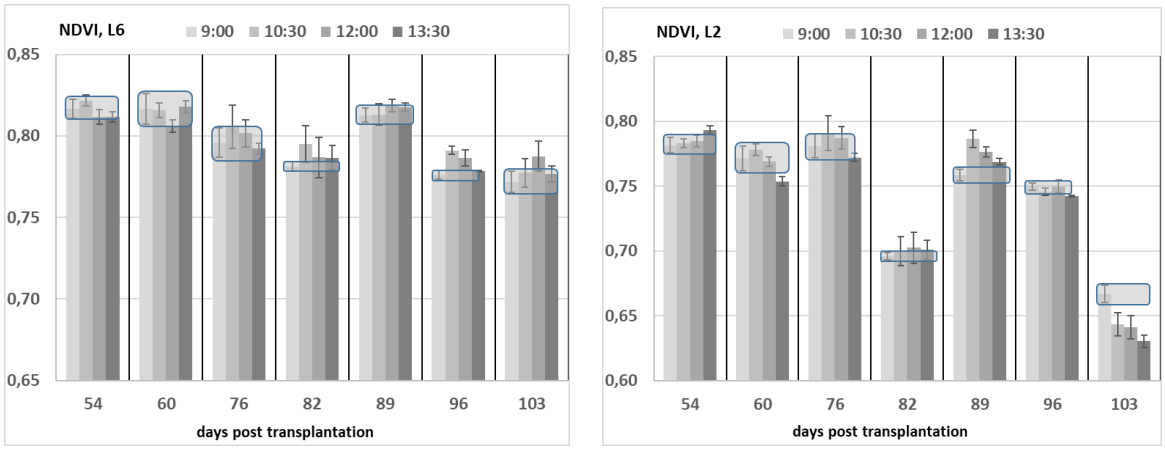

Figure 6. NDVI kinetics of control plants within and between the measuring days, at leaf 6 from top-down (left) vs leaf 2 from bottom-up (right). Error bars represent standard error.

3.5 PRI

PRI values were all positive in leaf 6, ranging from 0.025 to 0.045 (Fig.7). In contrast, leaf 2 presented negative values, in days 82, 96, and 103. Moreover, the variation was very extensive within these days, with negative values as low as -0.22.

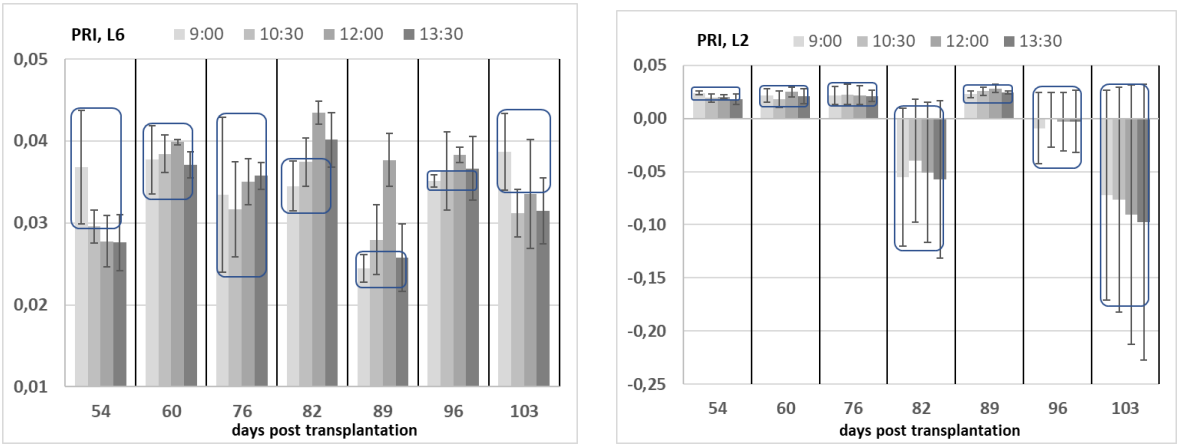

Figure 7. PRI kinetics of control plants within and between the measuring days, at leaf 6 from top-down (left) vs leaf 2 from bottom-up (right). Error bars represent standard error.

3.6 Fv/F0

The ratio of Fv/F0 values of leaf 6 ranged between 3.8 and 5.2 (Fig.8), whilst values below 3.5 were found in leaf 2 at d82, 96, and 103. In both leaves within day, there were cases of differentiation with time, significantly lower compared with that of 09:00.

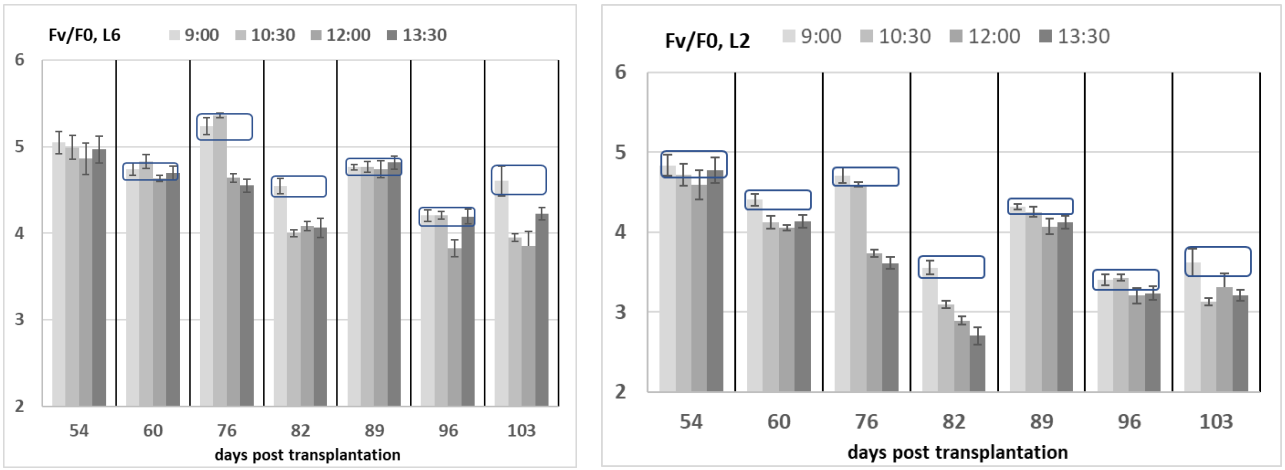

Figure 8. Fv/F0 kinetics of control plants within and between the measuring days, at leaf 6 from top-down (left) vs leaf 2 from bottom-up (right). Error bars represent standard error.

3.7 Development of a potential stress factor index

Utilizing the mean values of PRI for L6 from top-down and L2 from bottom-up, as well as the Fv/F0 corresponding values, we developed a new index, as potential "stress factor" index (Sf), towards depicting the plant's broader situation.

(Eq.1) **Sf = Fv/F0 × [PRI (Leaf 6) +PRI (Leaf 2)]**

Combination 1: PRI (L6) ↑ + PRI (L2) ↓: Biofortification of the upper plant part by the senescing leaf.
Combination 2: PRI (L6) ↑ + PRI (L2) ↑: Both leaves are not under stress, based on PRI values.
Combination 3: PRI (L6) ↓+ PRI (L2) ↓: Both leaves are under stress, based on PRI values.

In Fig.9 we see the results. At days 82 and 103, Sf of control plants presented negative values, whilst at d96 a lower, however positive value is shown. Values between 0.2 and 0.3 seem to be the normal situation.

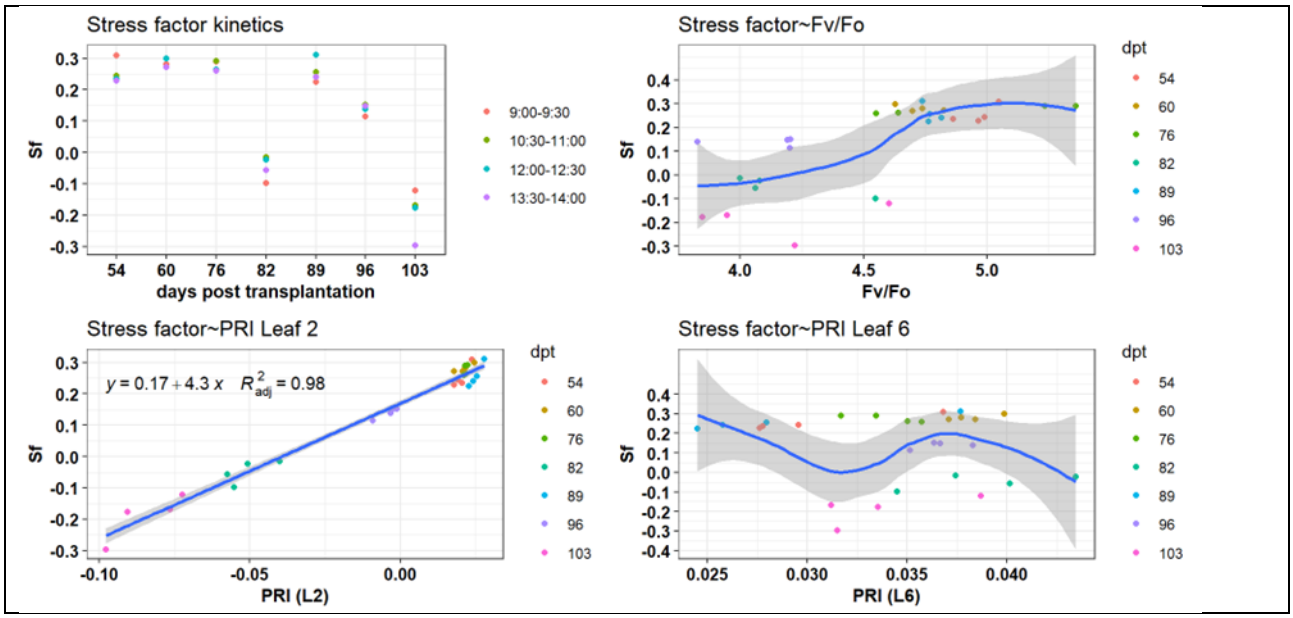

Fig.9 The potential stress factor was calculated according to Eq.1, and its kinetics is depicted (upper, left), along with the correlations between Sf and Fv/F0 (upper, right); PRI (L2) (lower, left), and PRI (L1) (lower, right). Treadlines have been produced according to Local Polynomial Regression Fitting method, and the area in grey represents the confidence interval.

4 Summary

Putting these findings together we conclude that leaf 2 presents systematically lower values. It seems that the following turn points can be used as potential "stress indicators": SPAD < 50, NDVI < 0.70, PRI < 0, Fv/F0 < 3.5. A potential stress factor index was developed, and its range seems to provide a tool towards distinguishing between the measuring days and evaluating the environment inside the greenhouse and its impact on control plants.

References

Baker, N. R., & Rosenqvist, E. (2004). Applications of chlorophyll fluorescence can improve production strategies: An examination of future possibilities. Journal of Experimental Botany, 55, 1607–1621. doi: 10.1093/jxb/erh196.

Gamon J.A., L. Serrano, J.S. Surfus (1997) The photochemical reflectance index: an optical indicator of photosynthetic radiation use efficiency across species, functional types, and nutrient levels. Oecologia 112, 492−501.

Kuckenberg J., I. Tartachnyk, G. Noga (2009) Temporal and spatial changes of chlorophyll fluorescence as a basis for early and precise detection of leaf rust and powdery mildew infections in wheat leaves. Precision Agric 10, 34-44.

Lichtenthaler, H. K., & Rinderle, U. (1988). The role of chlorophyll-fluorescence in the detection of stress conditions in plants. CRC Critical Reviews in Analytical Chemistry, 19, 29–85.

Sellers P. J. (1985) Canopy reflectance, photosynthesis, and transpiration. International Journal of Remote Sensing, 6, 1335-1372.

Guo Y., G. Ren, K. Zhang, Z. Li, Y. Miao, H. Guo (2021) Leaf senescence: progression, regulation, and application. Guo et al. Molecular Horticulture 1, 5. https://doi.org/10.1186/s43897-021-00006-9.

Monitoring of broccoli crop before and after biofortification: The use of photochemical reflection index

Evangelos N. Karousis[1], Georgios Stylianidis[1], Andriani Tzanaki[1,3], Despina Dimitriadi[3], Styliani Chorianopoulou[1,2], Dimitris Bouranis1[,2]

[1] Plant Physiology and Morphology Laboratory, Crop Science Department, Agricultural University of Athens, Iera Odos 75, 11855 Athens, Greece
[2] PlanTerra Institute for Plant Nutrition and Soil Science, Agricultural University of Athens, Greece
[3] Karvelas AVEE, Ypato, Viotia, Greece

Abstract. The photochemical reflectance index (PRI) was originally defined as an index of the xanthophyll cycle activity on a diurnal time scale. Xanthophyll cycle pigments adjust the energy distribution at the photosynthetic reaction center; hence they provide a measure of photosynthetic light-use efficiency and an indicator of stress.
Towards potential biofortification of broccoli heads, several trials were studied by applying sodium selenate in various concentrations (3, 1.5, and 0.2 mM Se), alone or in combination with selected amino acids. One hundred and fifty plants were transplanted in pots containing vermiculite, perlite, and sand in a ratio of 1:1:1, at 2021/10/25 (d0) in a greenhouse. Heads appeared at day 60 post transplantation and were harvested at d107. During growth period, the outside temperature was recorded. Data were collected at days 54, 60, 76, 82, 89, 96, and 103. Once a week, plants were receiving full nutrient solution. In each measuring day, measuring was starting 09:00 and ending 14:00. Foliar applications took place on d73, i.e., at the beginning of head development, when the exponential growth started. Dynamics of PRI is discussed.

1 Introduction

The Photochemical Reflectance Index (PRI) is an index based on leaf reflectance at 531 nm. This index has been found useful for tracking variations in photosynthetic activity of a leaf (Filella et al., 2009). PRI has been correlated with xanthophyll interconversion and photosynthetic radiation-use efficiency, as it is strongly correlated with the de-epoxidation state of xanthophylls, as an expression of the relative concentration of the three xanthophyll cycle pigments. PRI is also correlated with carotenoids/chlorophyll ratio. However, following momentary decreases in light due to clouds, PRI changes following the changes of the de-epoxidation state of xanthophylls, while the carotenoids/chlorophyll ratio remains constant. Filella et al. (2009) showed that PRI was able to reveal short-term changes in de-epoxidation state, i.e., the signal of xanthophyll interconversion, but it also tracked long-term changes in carotenoids/chlorophyll. Carotenoids other than xanthophylls, e.g., b-carotene, are also related to photoprotective processes, thus also making PRI effective as a measure of changes in photosynthetic light-use efficiency in response to stress on a long-term level.
Senescence is the process of aging in plants. Aging in plants can be either stress-induced or developmental, i.e., age-related one. During leaf senescence, chlorophyll degradation reveals the carotenoids, i.e., carotenes and xanthophylls. Leaf senescence has the important function of recycling nutrients to growing and storage organs of the plant. Plants continually form new organs and older organs undergo a highly regulated senescence program to maximize nutrient export (Guo et al., 2021). In broccoli plants the lower (older) leaves enter senescence mode to support the current developing leaves during vegetative phase, and both young leaves and flower heads during the reproductive phase. Therefore, we can roughly distinguish three developmental types of leaves, the old leaves that possess the lower 25% of the shoot, the fully mature leaves in the middle, not yet old, that occupy the 60% of the shoot, and the developing, young ones that occupy the upper 15% of the shoot. The transition state from mature to senescing leaf can be reflected by the changes in its optical properties. Apart from development, stress can also be the cause for such transition.
To identify potential transient periods where broccoli might face stress, we monitored the profiles of the optical properties of both the current 2nd leaf from bottom-up and the 6th one for top-down at the time of measuring (Bouranis et al. 2022). PRI, and Fv/F0, were used as indices (Sellers, 1985; Lichtenhaller and Rinderie, 1988; Gamon et al., 1997; Baker and Rosenqvist, 2004; Kuckenberg et al., 2009). In this work we present the kinetics of PRI of the two selected broccoli leaves of plants that have received a number of treatments towards biofortification of broccoli heads. Several trials were studied by applying sodium selenate in various concentrations (3.0, 1.5, and 0.2 mM Se), alone or in combination with selected amino acids. How did the selected leaves respond to treatments? PRI provided the following answers.

2 Experimental

2.1 Plant material

One hundred and fifty plants were transplanted in pots containing vermiculite, perlite, and sand in a ratio of 1:1:1, at 2021/10/25 (d0) in a greenhouse. Once a week, plants were receiving full nutrient solution. Data were collected at days 54, 60, 76, 82, 89, 96, and 103. Heads appeared at day 60 post transplantation and were harvested at d107. In each measuring day, measuring was starting 09:00 and ending 14:00.

2.2 Treatments

Treatments included application of selenium as sodium selenate in concentrations 3.0 mM, 1.5 mM, and 0.2 mM. The lower concentration applied either at the beginning of the exponential part of the sigmoid curve of head growth (d73) or at the end of it (d92), Moreover, the concentration of Se 0.2 mM was combined with cysteine (0.05 mM), or/and methionine (0.10 mM), or tryptophane (0.05 mM) / methionine (0.10 mM) / phenylalanine (0.25 mM) mix. This mix was applied also without selenium. The amino acids of the mix are precursors of glucosinolates, active compounds of broccoli heads, hence their selection.

The order of monitoring was as follows: between 09:30 and 11:00 the leaves that received the foliar treatments with SW7 as wetter, between 11:00 and 12:30 the leaves that received the corresponding treatments with Saldo as wetter, followed by the corresponding treatments applied by fertigation between 12:30 and 14:00.

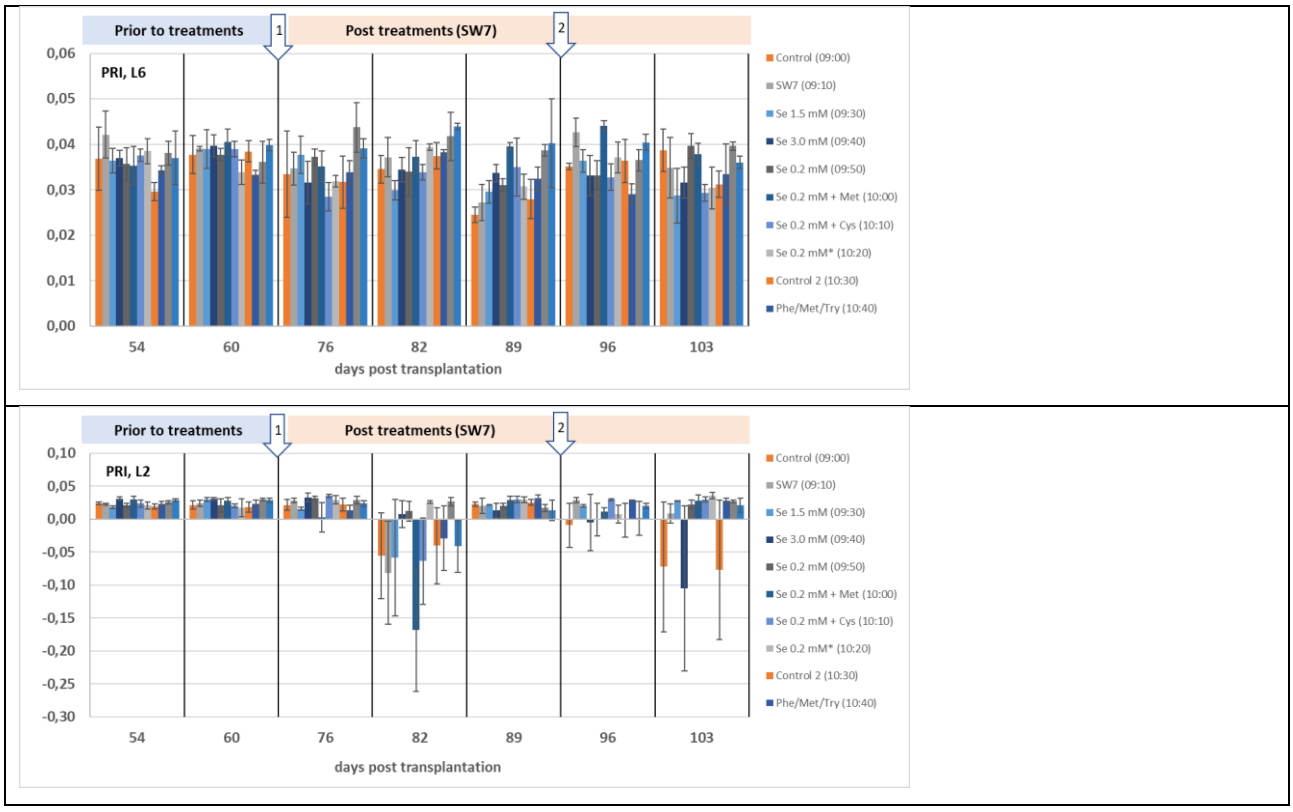

Figure 1. Treatments with foliar application and SW7 as wetter. Error bars represent standard error. SW7 as treatment denotes foliar application of SW7 alone as control.

2.2 Measurements

The PlantPen model PRI 210 was used to measure PRI. The Photochemical Reflectance Index is calculated by the equation: PRI = (R531 – R570) / (R531 + R570).

3 Results and Discussion

Leaf senescence, the last stage of leaf development, is a type of postmitotic senescence and is characterized by the functional transition from nutrient assimilation to nutrient remobilization which is essential for plants' fitness. The initiation and progression of leaf senescence are regulated by a variety of internal and external factors such as age, phytohormones, and environmental stresses (Guo et al., 2021).

3.1 Treatments via foliar application and SW7 as wetter

Leaf 6 presented PRI values above 0.02 (Fig.1, L6) with a mean value of 0.035. Leaf 2 presented negative values at d82, d96, and d103 (Fig.1, L2), especially the control. Heads appeared at d60 and ceased enlarging by d96. Therefore, it seems that aging caused the appearance of negative values, due to alterations in the measuring wavelengths. Measurements of this Group of treatments were taken between 09:30 and11:00.

3.2 Treatments with foliar application and Saldo as wetter

The same pattern held true in plants that received foliar application with different wetter (Fig.3). Leaf 6 presented positive values, above 0.02 (Fig.3, L6). Senescing leaves presented negative values from d86 onwards. Measurements of this Group were taken between 11:00 and12:30.

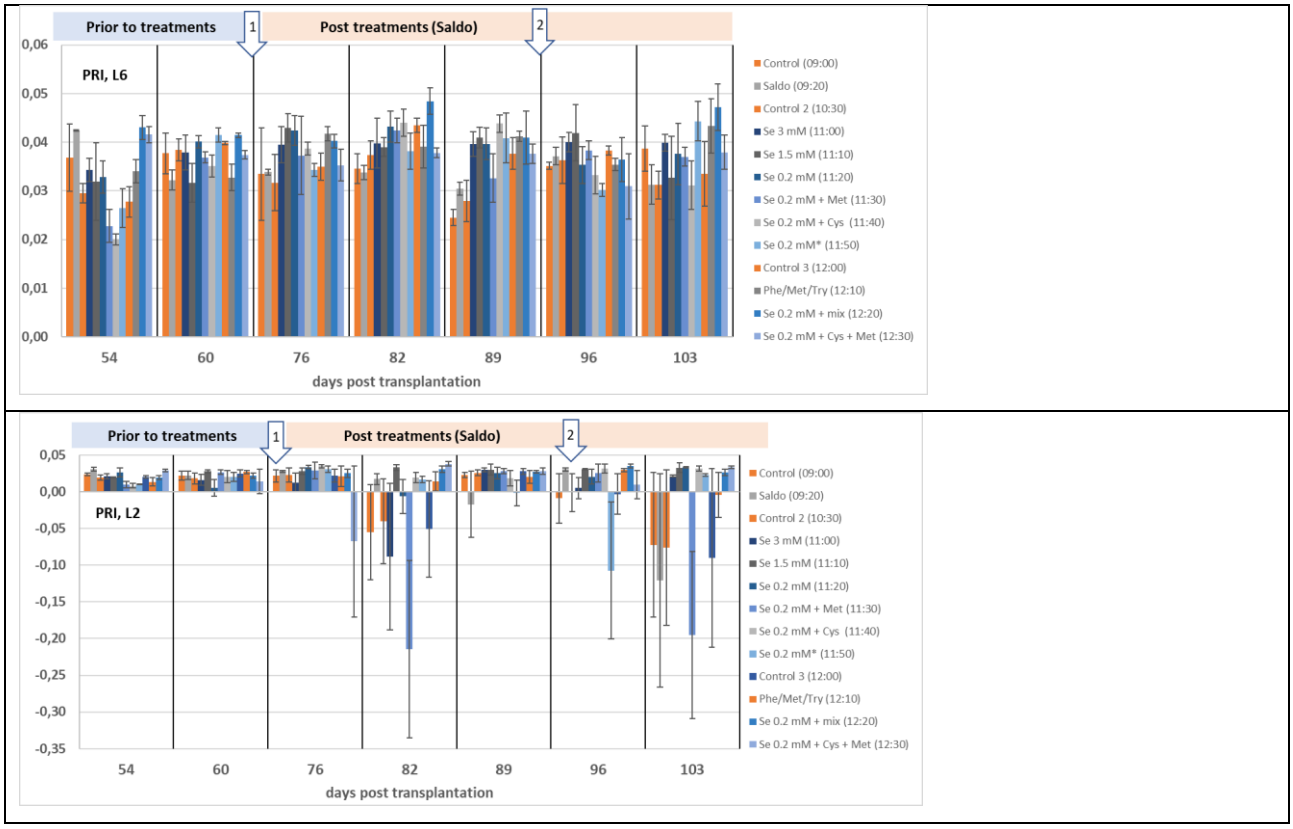

Figure 2. Treatments with foliar application and Saldo as wetter. Error bars represent standard error. Saldo as treatment denotes foliar application of Saldo alone as control.

3.3 Treatments via fertigation

Leaf 6 presented PRI values above 0.02 (Fig.4, L6) with a mean value of 0.035. Leaf 2 presented negative values at d82, d89, d96, and d103 (Fig.4, L2). Measurements of this Group were taken between 12:30 and14:00.

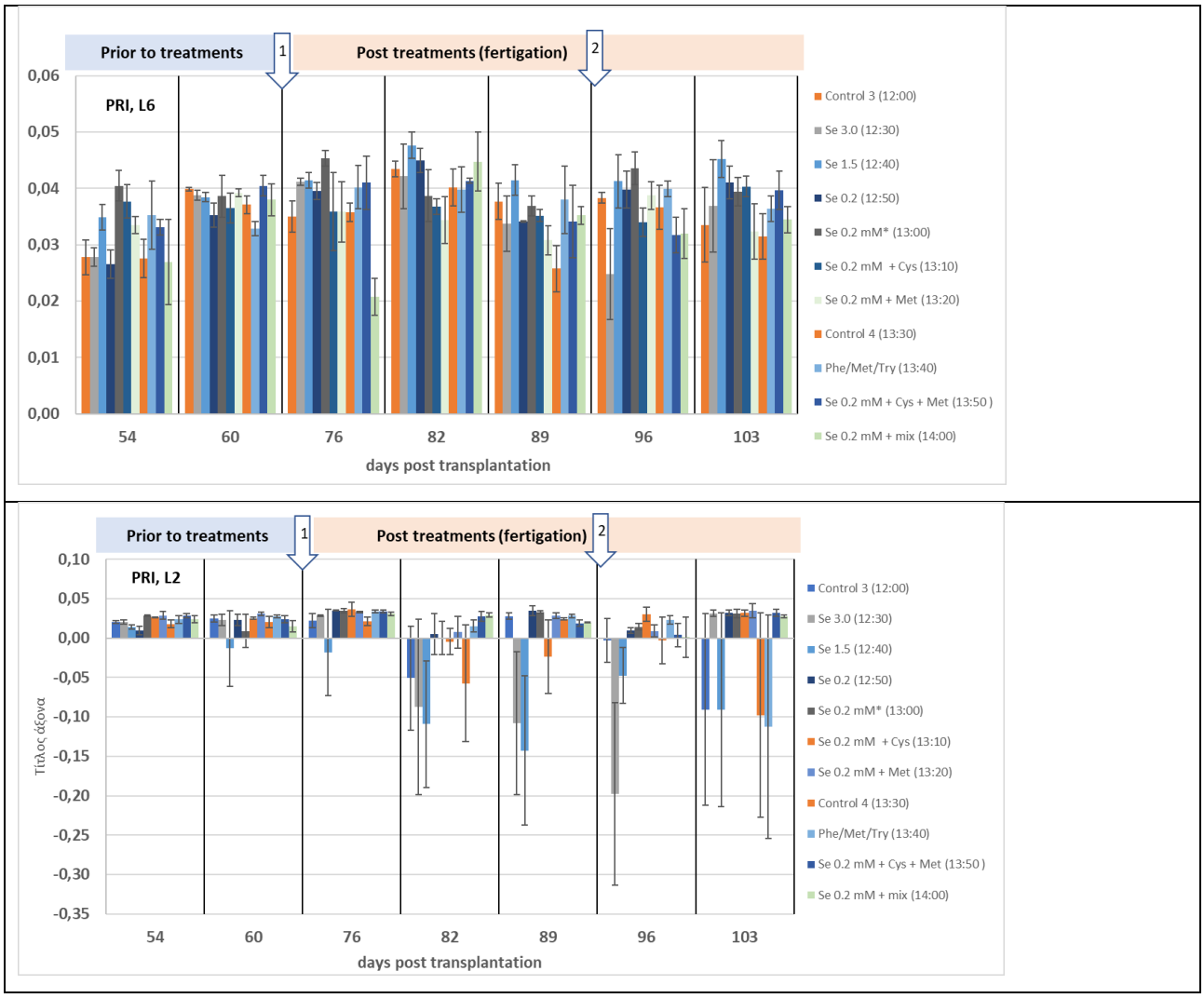

Figure 3. Treatments applied by fertigation. Error bars represent standard error.

3.4 Application of the potential stress factor index

Utilizing the mean values of PRI for L6 from top-down and L2 from bottom-up, as well as the Fv/F0 corresponding values (data not shown), we developed a new index, as potential “stress factor” index (Sf), towards depicting the plant’s broader situation (Bouranis et al., 2022).

(Eq.1) $\mathbf{Sf = Fv/F0 \times [PRI\ (Leaf\ 6) + PRI\ (Leaf\ 2)]}$

The results are presented in Fig.4. At days 82 and 103, Sf presented an extensive range of values including negative one, whilst at d96 a lower, however positive value is shown. Values between 0.2 and 0.3 seem to be the normal situation.

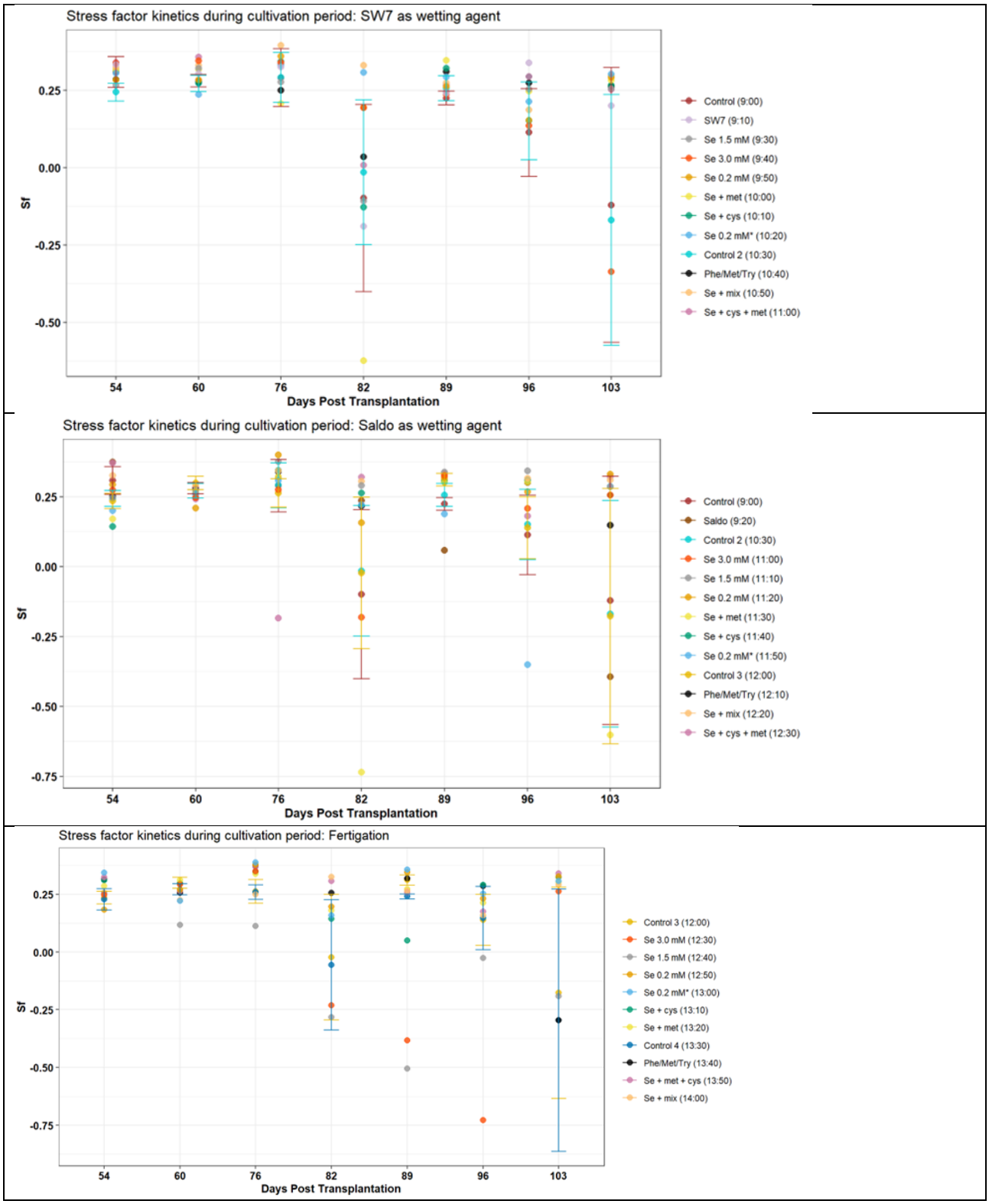

Fig.4 The potential stress factor index was calculated according to Eq.1, and its kinetics is depicted. Upper diagram: foliar application, wetter: SW7; middle diagram: foliar application, wetter: Saldo; lower diagram:

fertigation. The error bars represent the control range. Cycles above or below this range show positive or negative response of plants respectively to corresponding treatment.

4 Summary

The general picture highlights the following: In d54 and d60 plants received no treatments. Therefore, the figures show the kinetics of PRI as control plants within 1.5 hour for each group. Values were positive in both leaves 2 and 6. After d60 two events affected the situation. First, there were growing heads. Second, we applied selenium, alone or in combination with amino acids (d73). At d76, we still received positive values. Then L2 started to differentiate. At d82 we received negative values in several cases, and with large variation between repetitions: hence the wide standard error bars. L6 continued to provide positive values. This experiment shows that the senescing leaves can be distinguished from the mature ones. Moreover, growing heads seem to press for support. To elaborate on the effect of each treatment within the application method and measuring day, as well as for each treatment between measuring days, we need to develop a normalization approach. The proposed potential stress factor index that combines the PRI with the corresponding Fv/F0 index could be useful towards understanding plant behavior post treatment.

References

Baker, N. R., & Rosenqvist, E. (2004) Applications of chlorophyll fluorescence can improve production strategies: An examination of future possibilities. Journal of Experimental Botany, 55, 1607–1621. doi: 10.1093/jxb/erh196.

Bouranis D., A. Tzanaki, G. Stylianidis, E. Karousis, D. Dimitriadi, V. Siyiannis, S. Chorianopoulou (2022) Monitoring of broccoli crop before and after biofortification: Toward revealing potential transient stressful periods during development. 2nd AGROECOINFO, 30/6/2022-2/7/2022, Volos, Greece.

Filella I., A. Porcar-Castel, S. Munne-Bosch, J. Back, M.F. Garbulsky, J. Penuelas (2009) PRI assessment of long-term changes in carotenoids/chlorophyll ratio and short-term changes in de-epoxidation state of the xanthophyll cycle. International Journal of Remote Sensing 30 (17), 10 September 2009, 4443–4455

Gamon J.A., L. Serrano, J.S. Surfus (1997) The photochemical reflectance index: an optical indicator of photosynthetic radiation use efficiency across species, functional types, and nutrient levels. Oecologia 112, 492−501.

Guo Y., G. Ren, K. Zhang, Z. Li, Y. Miao, H. Guo (2021) Leaf senescence: progression, regulation, and application. Guo et al. Molecular Horticulture 1, 5. https://doi.org/10.1186/s43897-021-00006-9.

Kuckenberg J., I. Tartachnyk, G. Noga (2009) Temporal and spatial changes of chlorophyll fluorescence as a basis for early and precise detection of leaf rust and powdery mildew infections in wheat leaves. Precision Agric 10, 34-44.

Lichtenthaler, H. K., & Rinderle, U. (1988). The role of chlorophyll-fluorescence in the detection of stress conditions in plants. CRC Critical Reviews in Analytical Chemistry, 19, 29–85.

Sellers P. J. (1985) Canopy reflectance, photosynthesis, and transpiration. International Journal of Remote Sensing, 6, 1335-1372.

A Wireless IoT System for Precision Agriculture in Greece

Spachos P.[1]

[1]Department of Computer Science and Biomedical Informatics, University of Thessaly, Lamia, Greece

Abstract. Wireless Internet of Things systems is a promising solution for smart farming and precision agriculture. In this work, we present some preliminary results of a wireless IoT system that is deployed in a testbed in Greece. The system has nine solar powered wireless nodes, and each node has two sensors. Three different wireless technologies are examined in terms of energy performance.

1 Introduction

Precision Agriculture (PA) is an ever-expanding field that takes advantage of several new technologies and applies them to farming practices in order to increase the output while reducing the waste. Wireless technologies are an important component of PA, since they are used to transfer time sensitive information from the monitoring field to the control room for further processing and storage (Ahmed 2018). At the same time, the is a plethora of cost efficient and small-scale Internet of Things (IoT) devices with several sensors and at least one communication unit, they can be used to collect data and forward them to the control room (Elijah 2018). In this study, we extend our work (Sadowski 2020, Sadowski 2018, Spachos 2020) and examine the performance of a solar powered wireless IoT system, for agricultural monitoring in Greece. Specifically, each node of the system has two sensors to monitor the temperature and the humidity, a micro controller for basic data processing and a wireless unit for further transmission of the data. Each node is powered through a solar panel that can provide sufficient energy for the nodes to operate unattended. An initial experiment in our testbed in Lamia is conducted to examine the energy requirements of the system when different wireless technologies are used.

2 Real time monitoring System

The proposed IoT system monitors two important parameters from an agricultural field in Lamia, Greece. The data are transmitted in real time while some of the data are stored in a control room at our department, which is located nearly 7 km away from the monitoring field. In the following subsections, we will describe the components of the system, as well as the wireless technologies that are used and the data management processes, we follow in collecting the data.

2.1 Components

Our system has in total 9 wireless sensor nodes that are deployed in the monitoring area. Each of the nodes has the following components.

2.1.1 Sensors. Sensors play an important role in the overall design of the proposed system. We selected sensors based on their accuracy as well as their cost, since a cost efficient IoT system is preferred. Each of the nodes has the following two sensors.

Soil Moisture sensor. The first sensor we selected is the Sparkfun soil moisture sensor, shown in Figure 1. The sensor was selected because it is sufficient to characterize the soil, it has low energy requirements and it has a low-cost. Other soil moisture sensors that have better accuracy exist in the market, however, that would significantly increase the cost per monitoring node. The sensor needed some initial calibration; however, the accuracy of the sensor is sufficient for the proposed application.

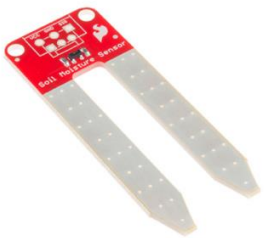

Figure 1. *Soil moisture sensor.*

Soil temperature sensor. The second sensor we selected was the DS18B20 temperature sensor, which is a waterproof temperature sensor, shown in Figure 2. Similar to the soil moisture sensor selection, this sensor was preferred over other temperature sensors due to its low-cost and low energy requirements.

Figure 2. *Soil temperature sensor.*

2.1.2 Central Processing Unit (CPU). As a processing unit, a microcontroller was used. The microcontroller collects the sensor data, processes them and forwards them to the control room. To keep a low energy consumption, a low power microcontroller is required. There are several low-cost microcontrollers in the market. Due to its low power consumption, low-cost and ease of integration with other devices, an Arduino from MKR family was selected, shown in Figure 3. It has available pins to connect up to 8 sensors, for instance 4 for soil moisture, and 4 for soil temperature, it is small and has low power requirements, while it can provide different wireless connectivity. The processing unit forwards the data to the communication unit. The proposed prototype has three different communication units that are described in a following section.

Figure 3. *Arduino MKR.*

2.1.3 Solar Panel. For external harvesting, we use the Star Solar D165X165 monocrystalline solar panel, shown in Figure 4. The panel is small enough for the proposed system and can provide sufficient energy for each node to operate. A power converter was also used in order to connect the solar panel with the main CPU. The converter provides power not only to the CPU but also to a rechargeable Lithium Polymer battery, that is also attached to each node.

Figure 4. *Solar panel.*

2.2 Wireless technologies

There is a plethora of wireless technologies that can be used, from traditional WiFi at 2.4GHz and Zigbee to LoRa and 5G. These technologies can be prioritized based on their cost, availability, and overall performance for the proposed system. Energy consumption is a major concern for the proposed agricultural nodes; hence, we did some initial testing with the three technologies that are currently available in Lamia, Greece, and they have low energy requirements. We used traditional WiFi, Zigbee and LoRa. All three technologies are available to deliver the data from the monitoring area to the control room, within the available time frame. All the technologies can work with the proposed prototype, hence, in the initial testing we mainly focus on the expected lifetime of each of the nodes.

3 Data collection and Results

We deployed the 9 nodes in the field and run experiments for one month. There are three nodes that are equipped with WiFi units, three with Zigbee and finally 3 with LoRa units. The results of the energy consumption are shown in the Figures bellow:

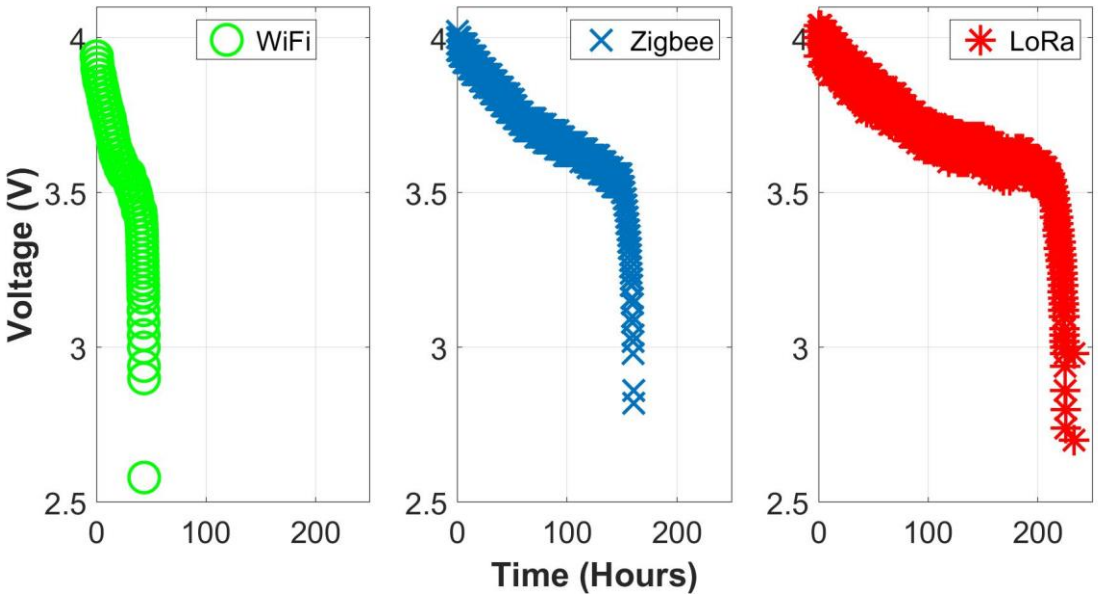

Figure 5. *Residual energy in the nodes*

It is clear that LoRa has a promising performance for the proposed system. It can keep the nodes up and running for very long time, especially with the low duty cycle that the nodes currently have. If the duty cycle is increased, it is expected that there will be challenges, especially in the proper routing between the data from different nodes. However, for the current testbed, with only 9 nodes and a low duty cycle of monitoring for each of the nodes, the performance when the LoRa unit is used is promising.

4 Summary

In this work, we briefly introduce an IoT system for precision agriculture in a testbed in the area of Lamia, Greece. We present some preliminary results on the energy consumption of the nodes when different wireless technologies are used. According to the experimental results, LoRa is a promising approach for the proposed data set. However, if the number of the sensors changes, and the duty cycle is increased, further experimentation is necessary to properly calibrate the proposed system.

References

Ahmed N., De D., Hussain I., 2018, Internet of Things (IoT) for Smart Precision Agriculture and Farming in Rural Areas, *IEEE Internet of Things Journal*, vol. 5, no. 6, pp. 4890-4899.

Elijah O., Rahman T., Orikumhi I., Leow C., Hindia M., 2018, An Overview of Internet of Things (IoT) and Data Analytics in Agriculture: Benefits and Challenges, *IEEE Internet of Things Journal*, vol. 5, no. 5, pp. 3758-3773.

Sadowski S., Spachos P., 2020, Wireless technologies for smart agricultural monitoring using internet of things devices with energy harvesting capabilities, Computers and Electronics in Agriculture, Volume 172, 2020, 105338, ISSN 0168-1699.

Sadowski S., Spachos P., 2018, Solar-Powered Smart Agricultural Monitoring System Using Internet of Things Devices, *2018 IEEE 9th Annual Information Technology, Electronics and Mobile Communication Conference (IEMCON)*, 2018, pp. 18-23.

Spachos, P. Towards a Low-Cost Precision Viticulture System Using Internet of Things Devices. *IoT* **2020**, *1*, 5-20.

Modeling and Estimation of Actual Evapotranspiration in 3 Mediterranean agricultural areas in France, Greece, and Portugal by merging Sentinel-2 and Sentinel-3 data.

Alpanakis N.[1], G. Tziatzios[1], I. Faraslis[2], M. Spiliotopoulos [1], P. Sidiropoulos[1], S. Sakellariou[3] A. Blanta [1], V. Brisimis [1], Karoutsos G.[5], N.R. Dalezios[1], N. Dercas [4]

[1] Laboratory of Hydrology and Aquatic Systems Analysis, Department of Civil Engineering, University of Thessaly, Volos, Greece
[2] Department of Environmental Sciences, University of Thessaly, Larisa, Greece
[3] Department of Spatial Planning and Regional Development, University of Thessaly Volos, Greece
[4] Laboratory of Agricultural Hydraulics, Department of Natural Resources Development and Agricultural Engineering, Agricultural University of Athens, 11855 Athens, Greece
[5] General Aviation Applications "3D" S.A., 2 Skiathou str, 54646, Thessaloniki, Greece

Abstract

Evapotranspiration (ET) is a critical parameter for the hydrological cycle as it determines the water availability and the water management through irrigation. In this paper, a new and innovative methodology is described which is developed for the estimation of the actual daily evapotranspiration (ETa). This is a contribution to the European-funded research project "HubIS". The proposed methodology combines simulation programs and remote sensing. The proposed methodology is applied in three Mediterranean agricultural areas in France (Crau Plain), Greece (Thessaly plain), and Portugal (Lucefecit irrigation area). The simulation program used is the Sen-ET SNAP software. In this paper, the Sen - ET SNAP graphical user interface uses satellite images from Sentinel 2 and Sentinel 3 and meteorological data from the Weather Research and Forecast (WRF) model. The proposed methodology framework consists of 17 individual stages having as the outcome the actual daily evapotranspiration flows estimation. The proposed methodology is applied to several crops, such as maize, cotton, vineyards, olives, hay. The results indicate the suitability of the Sen-ET SNAP software that can be applied for effective irrigation management in data-scarce rural regions.

1 Introduction

Plant water uptake is directly related to transpiration with both mechanisms contributing significantly to the transfer of water to the system: soil-plant-atmosphere, especially in rural basins. In irrigated agricultural fields, water availability improves plant water absorption mechanisms (Uniyal and Dietrich, 2019).

ET explains the exchange of water and energy between soil, land surface and atmosphere but it is very difficult to estimate it due to the high heterogeneity of soils and the characteristics of vegetation found and the wide variety of crops, which are cultivated in agricultural ecosystems (Castelli et al., 2018, Dimitriadou and Nikolakopoulos, 2021, Ochoa-Sánchez et al., 2019). ET valuation methods fall into two main categories: direct and indirect. The direct ones include the vertical deviation systems, the lysimeters (weighing or non-weighing), the sheet temperature measuring systems, as well as the systems that measure the gas exchanges. These are the main direct methods of estimating the ET, giving accuracy to the estimates but are characterized by the high cost (Ghiat et al., 2021, Vishwakarma et al ,2022). In addition, there are indirect methods, which are further distinguished into temperature methods, such as the Thornthwaite method, mass transfer methods, such as the Penman method, water balance methods, irradiation methods such as the Turc method, and finally combined methods. Penman – Monteith (Celestin et al., 2020; Vishwakarma et al., 2022). According to Valipour et al. (2015), radiation methods are the most widely used methods of estimating potential evapotranspiration.

The fundamental difference between actual evapotranspiration (ETa) and ET is that ETa determines the actual amount of plant-water consumption throughout its life, from its phenological stages to its aging. ETa is determined by climatic conditions, crop characteristics and water availability as it is affected by climate / seasonal change, land use and land cover, as well as changes that can be made to these parameters over time. Therefore, the assessment of ETa is particularly important for the management and utilization of water resources management both in the current conditions and for dealing with future adverse conditions in water

systems, such as emerging climate variability / change (Dimitriadou and Nikolakopoulos, 2021, Ochoa-Sánchez et al., 2019).

In recent decades various methods and algorithms have been developed for estimating actual ETa via satellite. Most of them are based on the method of calculating the surface energy balance. Some of these methods used in remote sensing to calculate ETa are the Penman – Monteith method, the Priestley-Taylor method, combinatorial methods, which use the earth's surface temperature in combination with vegetation indices (Karimi and Bastiaanssen, 2015, Zhang et al., 2016). Various approaches have been developed for ETa modeling, which can be classified into predictive and diagnostic models. Predictive models are based on the water balance and require spatially distributed rainfall as input data. In contrast, diagnostic models link ET to ground surface temperature (LST) derived from thermal infrared (TIR) remote sensing. The main advantage of the latter approach is that it does not require spatially distributed measurements of rainfall and soil hydraulic properties. This is a huge benefit in areas characterized by a lack of observed data and strong heterogeneity (Castelli et al., 2018).

This paper presents a new and innovative methodology developed and applied for estimating daily actual evapotranspiration (ETa) through modeling based on Sen - ET SNAP software developed by DHI in collaboration with IRTA (Research and Technology Food and Agriculture) and Sandholt on behalf of the European Space Agency (ESA). The proposed methodology uses the SNAP software to estimate daily Eta, which includes satellite imagery from Sentinel 2 and Sentinel 3, as well as meteorological data from the Weather Research and Forecast (WRF) model.

2 Methodology

The proposed methodology calculates the actual daily ET for each plot using MSI Sentinel-2 radiometric data and Sentinel-3 SLSTR thermal data. The methodology is based on the relevant methodology of the European Space Agency (ESA). Specifically, the initial (by ESA) Sen-ET (Sentinels for evapotranspiration) plugin in SNAP uses the two-source energy balance (TSEB) model with Sentinel-2, Sentinel-3 and meteorological data from ECMWF (ESA, 2020). In this study, the adopted methodology also follows seventeen steps and is based on the TSEB model. However, there is a modification of the initial Sen-ET SNAP by ESA, and the proposed methodology uses meteorological data from the WRF model, instead of ECMWF. Specifically, the required meteorological data used from the plug-in are retrieved from WRF model, and this stands as a modification and improvement from the original designed plug-in. The results produced by the WRF model are real-time data (e.g., air temperature, wind speed and similar parameters) at any time step requested. The final product of the new proposed methodology is ETa in mm / day with a spatial resolution of 20m x 20m. The seventeen steps of the new proposed and adopted methodology are summarized in Table 1.

Table 1. The 17 steps of the new proposed and adopted methodology

Steps	Process
1°	Download Sentinel images
2°	Pre - processing Sentinel 2 data by downscaling. Planning / sampling again: • the Sentinel 2 image at 20 m • the required channels of the image subsets and stores them as separate products and evaluates the biophysical parameters (FAPAR, LAI, F-cover) of the reflection channels.
3°	Creation of a Digital Elevation Model (DEM) of the study area in high resolution
4°	Creation of a land use map of the study area in high resolution from the land use database of the ESA CCI of 2015
5°	Leaf reflection and transmission assessment based on the chlorophyll and water content of the plants
6°	**Estimation of fraction of green vegetation** The procedure calculates the vegetation fraction that is green based on the Leaf Area Index (LAI), the fraction of absorbed photosynthetic active radiation (FAPAR) and the channels according to the angle of inclination with the zenith of the sun
7°	**Production of maps with the structural parameters of vegetation such as**: • Creation of vegetation height maps • Creation of vegetation coverage maps in fractions • Creation of forest cover height and width maps • Create sheet width maps • Create leaf gradient distribution maps • Creating land use maps with classes
8°	**Aerodynamic roughness assessment**

	The procedure calculates the length of the aerodynamic roughness for instantaneous transfer in (m) and the displacement height of the zero level (m) based on the leaf area index (LAI) and the maps created with the structural parameters of the vegetation
9°	Pre-processing Sentinel -3 data by downscaling, The L2A image of Sentinel 3 is retrieved in the required channels of the received AOIm subsets and stores them as separate products.
10°	**Warp to Template** The subset of a source image is viewed and re-sampled into a standard image using GDAL Warp
11°	**Sharpen Land Surface Temperature** Creating a clearer picture of land surface temperature**.** The Data Mining Sharpener Python application is called that can be used to improve SLSTR land surface temperature in Sentinel-2 spatial analysis.
12°	Download WRF meteorological data by 3D S.A partner
13°	Preparation of WRF meteorological data based on the High-Resolution Digital Elevation Model (DEM) of the study area
14°	**Long-wave irradiance** estimation based on WRF meteorological data
15°	**Estimation of net shortwave radiation** based on WRF meteorological data and biophysical parameters
16°	**Estimation of energy fluxes of the land surface** The process estimates soil surface energy flows (latent and perceptible heat, ground heat and net radiation) using the single-source energy balance model for bare soil pixels and the two-source energy balance model for vegetated pixels.
17°	**Estimation of daily evapotranspiration** The process calculates the actual daily evaporation by extending / extruding the instantaneous latent heat flow using daily solar radiation.

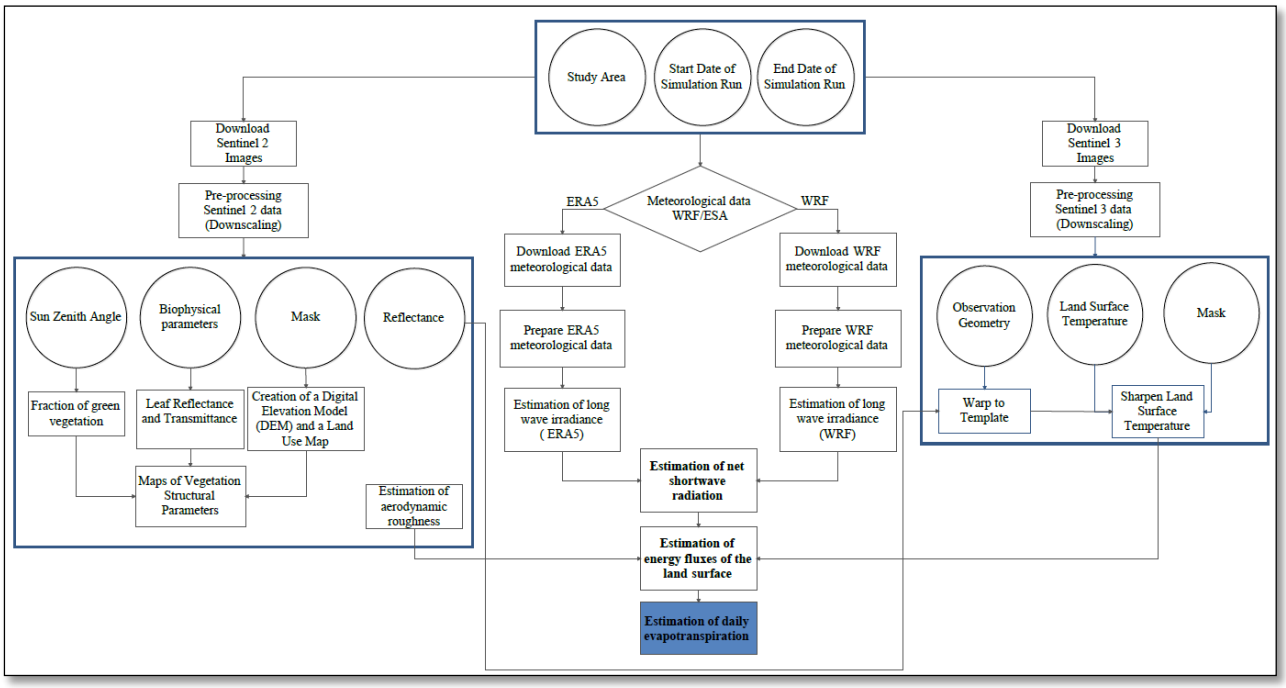

Figure 1. Flow chart of the new proposed methodology.

2 Study areas

The HubIS research project is a European project involving various Mediterranean countries with common problems and issues related to different irrigation systems and water resources management. Therefore, pilot fields were used in all participating countries. The Thessaly plain is the study area in Greece, the Crau plain is the study area in France, and the irrigated area by the Lucefecit reservoir is the study area in Portugal. In all three study areas, the climate is characterized as Mediterranean type with mild rainy winters and hot and dry summers, and intense irrigation activity met.

2.1 France (Crau Plain)

The Crau Plain covers 520 Km^2 and about 60000 ha and is illustrated in Figure 2a (Buisson and Dutoit 2006, Beltrando, 2015). In the Crau Plain, there are no natural surface water systems, but groundwater systems are abundant as they are mainly enriched by irrigation for coverage of agricultural needs applied in parts of the Crau plain.

2.2 Greece (Thessaly)

Thessaly is the second largest plain in Greece presented in Figure 2b but is the most dynamic plain as it is cultivated more intensively than all the other plains. In the Thessalian plain, the annual water consumption amounts to 1.422 hm3, with 92%, i.e., approximately 1305.5 hm3, being used to meet the irrigation needs. Specifically, in Thessaly, about 500000 ha are cultivated, of which about 250000 are irrigated. 76% of irrigation water comes from groundwater systems through legal or illegal drilling, while only 24% comes from surface water systems. The condition of the groundwater systems of Thessaly is not very good both in quantitative terms as it presents a deficit water balance, but also in quality (SDYTH, 2017). The study area is the Thessalian plain and specifically seven (7) experimental plots, which participate in the research program "HubIS".

2.3 Portugal (Lucefecit Irrigation Area)

The Lucefecit irrigation area is in the south of Portugal shown in Figure 2c. It is in the basin area of the Guadiana River and covers an area of approximately 1.179 ha. In this area no abstraction is recorded from groundwater systems as the required quantities of irrigation needs are fully covered by the Lucefecit reservoir, which is essentially a mainstream of the Guadiana River. The main crops are winter wheat, maize, olive, vegetable gardens and vineyards. As observed from the 5 main crops, 4 belong to the irrigated ones.

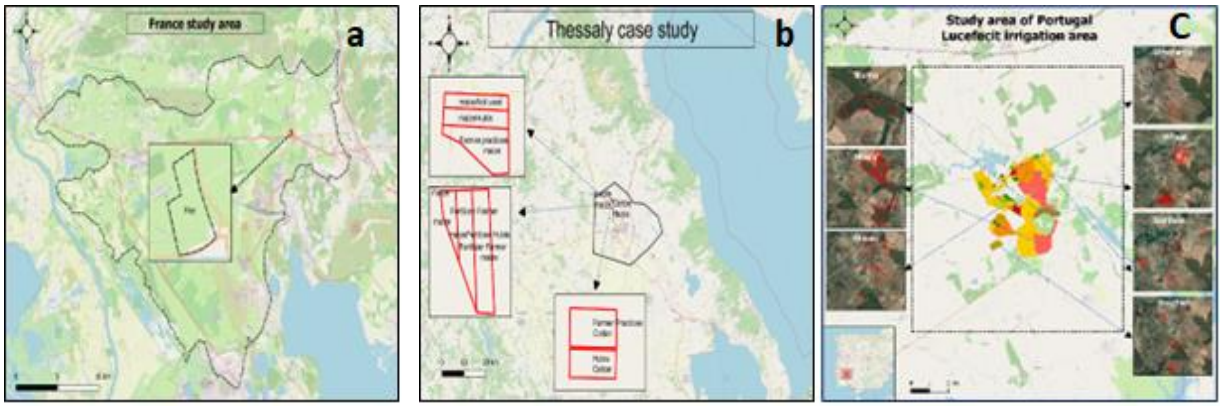

Figure 2. The three study areas and the experimental fields. Figure 2a is the France plain, 2b is the Thessaly plain, and Figure 2c is the Lucefecit plain.

3 Results

The results from the three Mediterranean countries participating in the HubIS program are presented in the following figures. Figure 3 shows the variations of actual daily Eta for the hay crop (France) during the irrigation period when appropriate images from Sentinel 2 and Sentinel 3 were available, as well as the area covered by the hay crop.

3.1 France

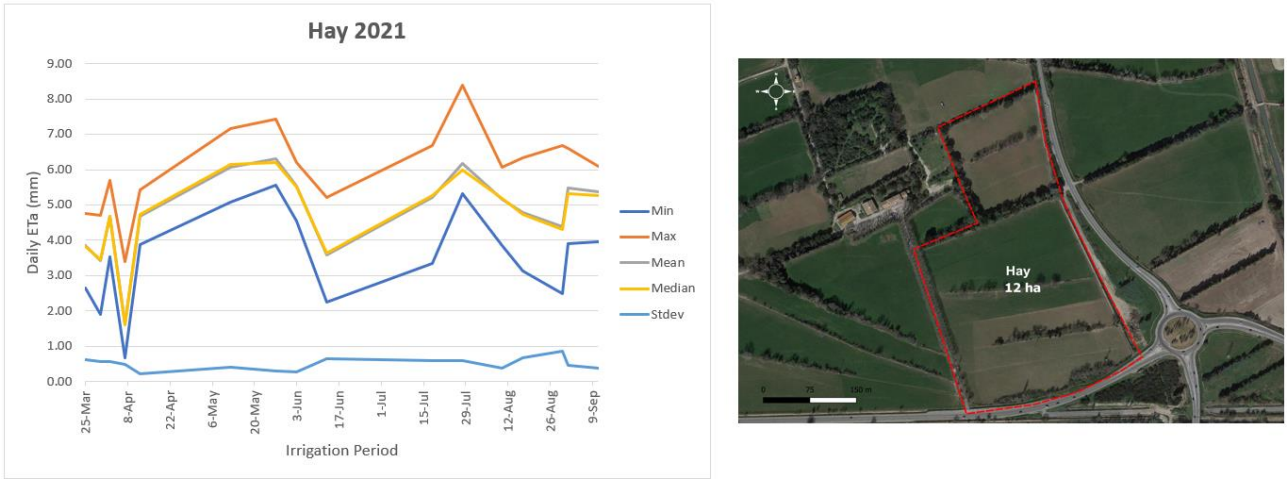

Figure 3. Actual Daily ETa Results in France (Crau Plain)

Figure 4 shows the spatial distribution of the actual daily ETa for the cultivation of hay, for the whole period when Sentinel 2 and Sentinel 3 images were available. The actual daily ETa ranges from the minimum value of 0 mm recorded in January 2021 to maximum reaching 8.5 mm at the end of July 2021.

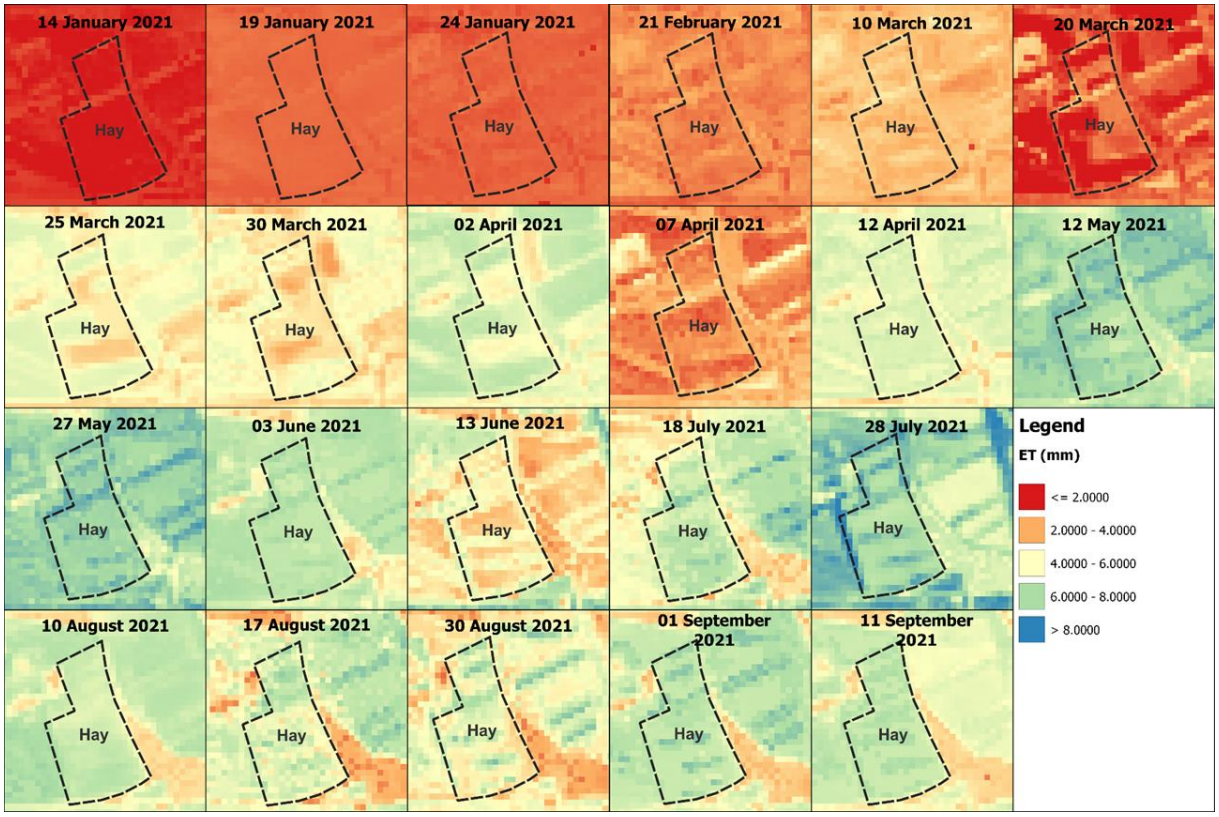

Figure 4. Spatial distribution of the daily ETa for Hay.

3.2 Greece (Thessaly plain)

Before starting the analysis of the results, it is necessary to note that the experimental plots were separated / classified based on the agricultural practices followed and applied in relation to irrigation. Two categories of plots were created, the plots where maize and cotton are grown, where the agricultural / irrigation practices are followed and applied, which are determined by the farmer practices, and the maize and cotton plots where the agricultural / irrigation practices are defined according to the «HubIS» methodology, respectively. Figure 5 shows the variations of actual daily Eta for cotton during the irrigation period when images from Sentinel 2 and Sentinel 3 were available.

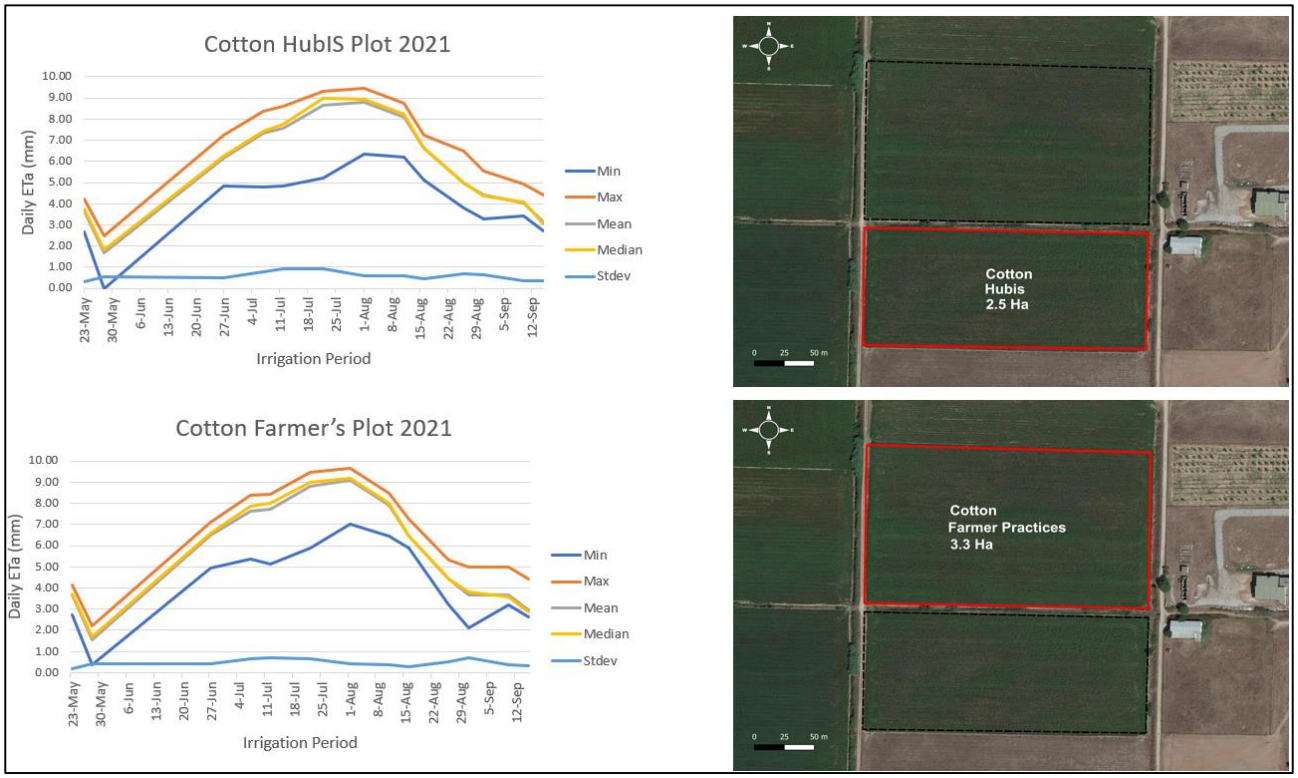

Figure 5. The variation of the actual daily ETa for Cotton plot and a comparison between the Hubis method and the farmer practices.

Figures 6 and 7 show the spatial distribution of the actual daily ETa for the cultivation of Cotton (Farmer practices), for the whole growing season when images from Sentinel 2 and Sentinel 3 were available. The daily ETa ranges from the minimum value of 0 mm which recorded in February to a maximum of 10 mm in early August. In addition, Figure 7 presents the spatial discretization of the daily ETa for the cultivation of Cotton (Hubis), for the whole period that satellite images were available. The daily ETa ranges from a minimum of 0 mm recorded in February 2021 to a maximum of 9.5 mm at the beginning of August 2021.

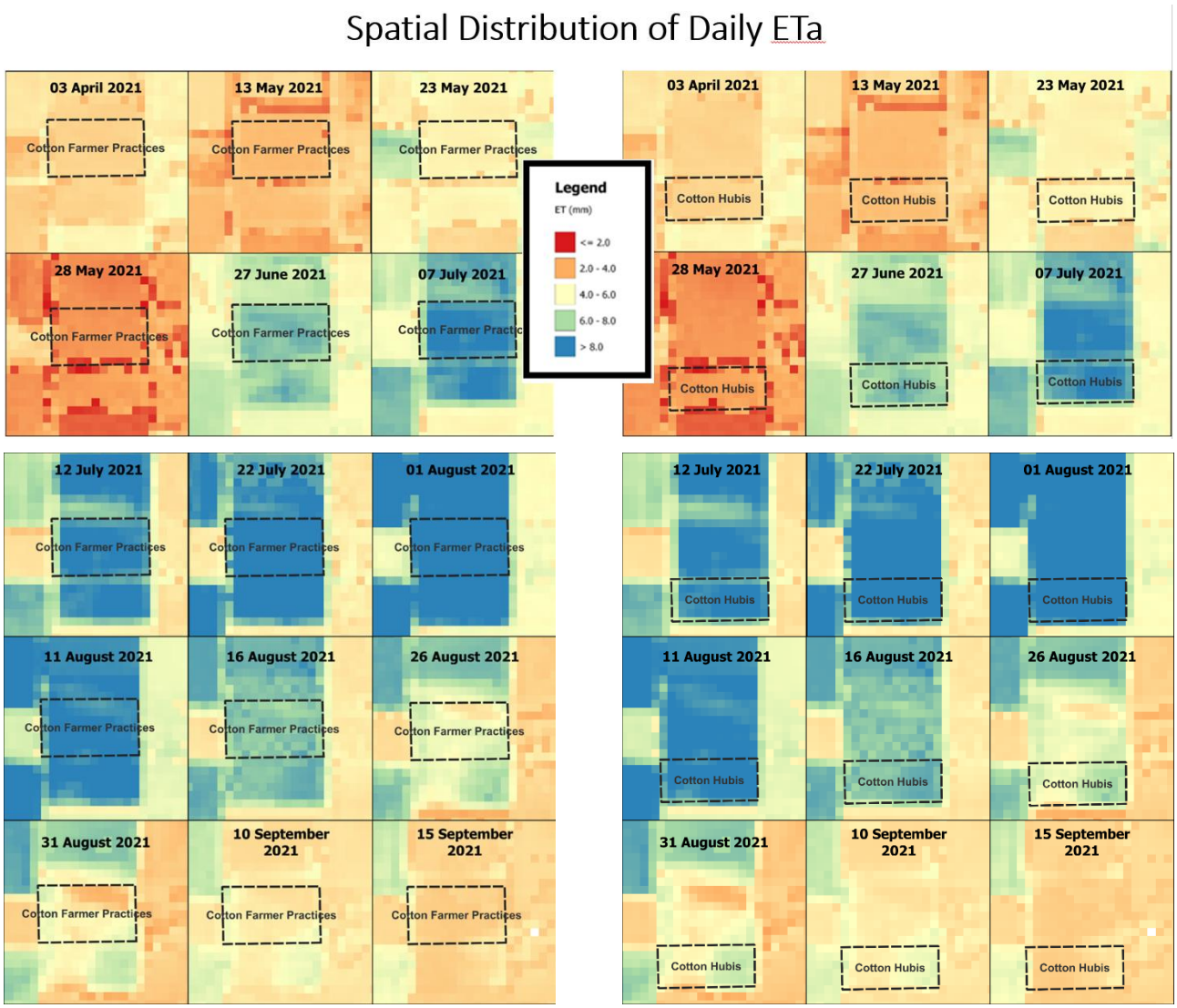

Figures 6(left) and 7(right) show the spatial distribution of the actual daily ETa for the cultivation of Cotton (Farmer practices) and Cotton (Hubis).

3.3 Portugal (Lucefecit Irrigation Area)

Figure 8 shows the variations of actual daily ETa for maize plots during the period when proper images from Sentinel 2 and Sentinel 3 were available. The daily ETa ranges from a minimum of 0 mm in August and a maximum of 9 mm and recorded on 10 June 2021.

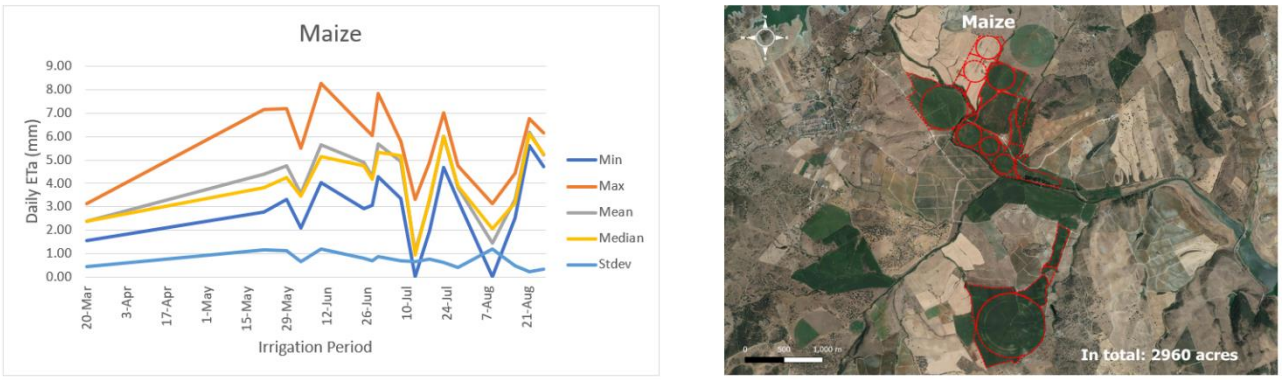

Figure 8. Values of the daily ETA for maize plots.

Figure 9 shows the spatial distribution of the daily ETa for maize plots during the period when suitable images from Sentinel 2 and Sentinel 3 were available. The daily ETA ranges from a minimum of 0 mm in August 2021 and a maximum of 10 mm and recorded on 10 June 2021.

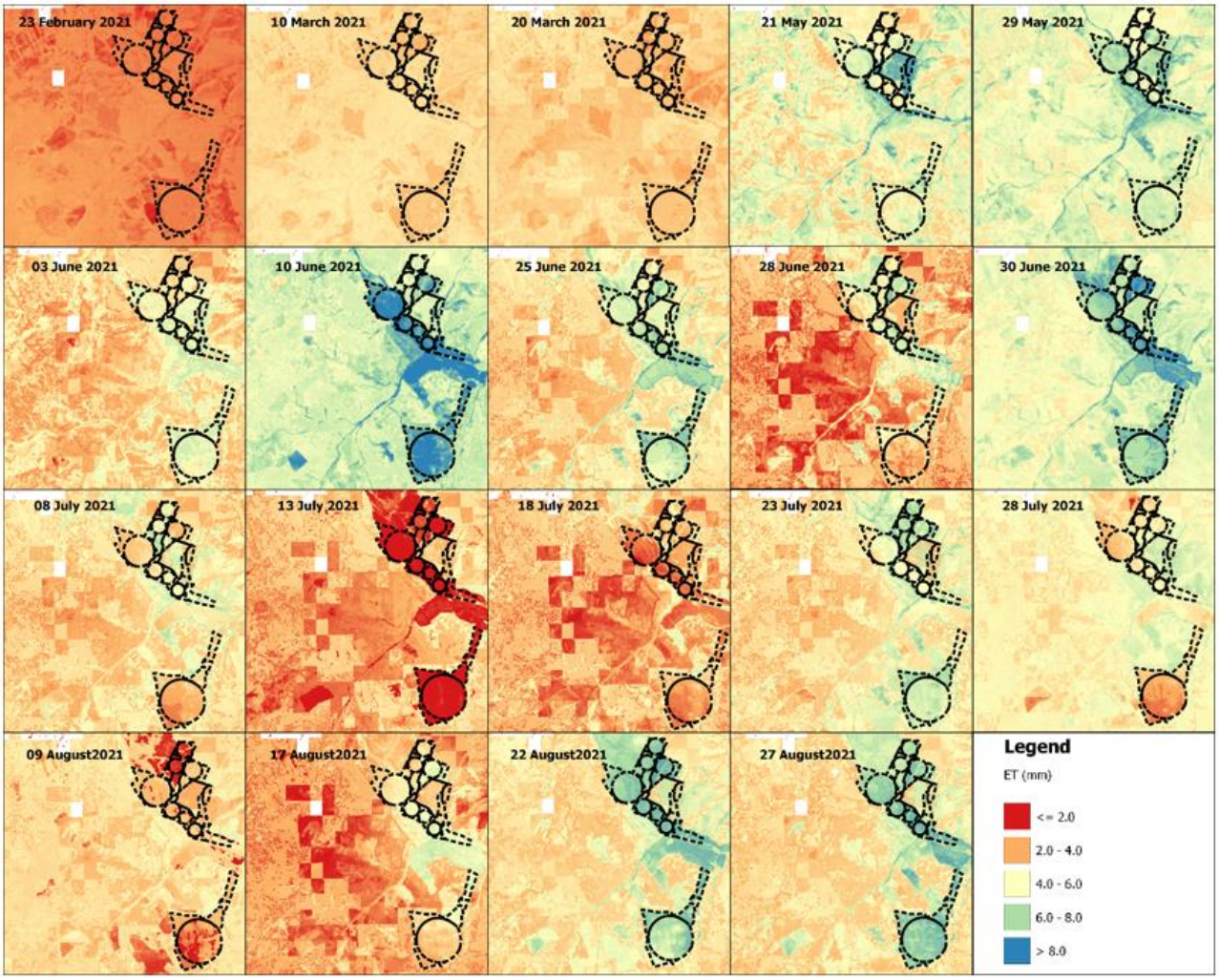

Figure 9. The spatial distribution of the daily ETa for maize plots in Portugal.

4 Summary

In this study, a methodology is presented for the calculation of the actual evapotranspiration, which is developed by the University of Thessaly. This methodology constiutes a modification and improvement of the initial ESA's methodology. The aim is to determine the true daily evapotranspiration (ETa) through modeling using Sen - ET SNAP software developed by DHI in collaboration with IRTA (Research and Technology Food and Agriculture) and Sandholt on behalf of the European Space Agency. SNAP software uses Sentinel 2 and Sentinel 3 satellite imagery to estimate daily ETa, as well as meteorological data from the Weather Forecast and Research (WRF) model. The results of the three areas showed real evapotranspiration values that are very close to the irrigation needs of each crop.

Acknowledgements

The research was funded by «Open innovation Hub for Irrigation Systems in Mediterranean agriculture» with the acronym «HubIs» of PRIMA 2019 (Partnership for Research and Innovation in the Mediterranean Area) programme (Section 2 Call 2019 – multi-topic) supported under Horizon 2020.

References

Uniyal, B., Dietrich, J., Vu, N. Q., Jha, M. K., & Arumí, J. L. (2019). Simulation of regional irrigation requirement with SWAT in different agro-climatic zones driven by observed climate and two reanalysis datasets. Science of the total environment, 649, 846-865.

Beltrando, G, (2015), Groundwater in the Plain of the Crau (South-East of France): between Historical Abundance and Modern Vulnerability, 2nd International Conference - Water resources and wetlands, 11-13 September 2014 Tulcea (Romania); Editors: Petre Gâştescu; Włodzimierz Marszelewski ; Petre Bretcan; ISSN: 2285-7923; Pages: 245-249; Available online at http://www,limnology,ro/water2014/proceedings,html

Buisson, E,, & Dutoit, T, (2006), Creation of the natural reserve of La Crau: implications for the creation and management of protected areas, Journal of Environmental Management, 80(4), 318-326, https://doi,org/10,1016/j,jenvman,2005,09,013

Castelli, M,, Anderson, M, C,, Yang, Y,, Wohlfahrt, G,, Bertoldi, G,, Niedrist, G,, ,,, & Notarnicola, C, (2018), Two-source energy balance modeling of evapotranspiration in Alpine grasslands, Remote Sensing of Environment, 209, 327-342, https://doi,org/10,1016/j,rse,2018,02,062

Celestin, S,, Qi, F,, Li, R,, Yu, T,, & Cheng, W, (2020), Evaluation of 32 simple equations against the Penman–Monteith method to estimate the reference evapotranspiration in the Hexi Corridor, Northwest China, Water, 12(10), 2772, https://doi,org/10,3390/w12102772

Dimitriadou, S,, & Nikolakopoulos, K, G, (2021), Annual Actual Evapotranspiration Estimation via GIS Models of Three Empirical Methods Employing Remotely Sensed Data for the Peloponnese, Greece, and Comparison with Annual MODIS ET and Pan Evaporation Measurements, ISPRS International Journal of Geo-Information, 10(8), 522, https://doi,org/10,3390/ijgi10080522

ESA, 2020, User Manual for SEN-ET SNAP Plugin, V1,1,0 March 19, 2020, 37 pages,

HubIS 2021, Open Innovation Hub for Irrigation Systems in Mediterranean Agriculture, Scientific Programme 2021-2024

Ghiat, I,, Mackey, H, R,, & Al-Ansari, T, (2021), A Review of Evapotranspiration Measurement Models, Techniques and Methods for Open and Closed Agricultural Field Applications, Water, 13(18), 2523, https://doi,org/10,3390/w13182523

Karimi, P,, & Bastiaanssen, W, G, (2015), Spatial evapotranspiration, rainfall and land use data in water accounting–Part 1: Review of the accuracy of the remote sensing data, Hydrology and Earth System Sciences, 19(1), 507-532 https://doi,org/10,5194/hess-19-507-2015

Ochoa-Sánchez, A,, Crespo, P,, Carrillo-Rojas, G,, Sucozhañay, A,, & Célleri, R, (2019), Actual evapotranspiration in the high Andean grasslands: A comparison of measurement and estimation methods, Frontiers in Earth Science, 7, 55, https://doi,org/10,3389/feart,2019,00055

Valipour, M, (2015), Evaluation of radiation methods to study potential evapotranspiration of 31 provinces, Meteorology and Atmospheric Physics, 127(3), 289-303, http://dx,doi,org/10,1007%2Fs00703-014-0351-3

Vishwakarma, Dinesh Kumar, Kusum Pandey, Arshdeep Kaur, N, L, Kushwaha, Rohitashw Kumar, Rawshan Ali, Ahmed Elbeltagi, and Alban Kuriqi, "Methods to estimate evapotranspiration in humid and subtropical climate conditions," Agricultural Water Management 261 (2022): 107378, https://doi,org/10,1016/j,agwat,2021,107378

Zhang, K,, Kimball, J, S,, & Running, S, W, (2016), A review of remote sensing based actual evapotranspiration estimation, Wiley Interdisciplinary Reviews: Water, 3(6), 834-853, https://doi,org/10,1002/wat2,1168

Government Gazette 29/12/2017 "1st Revision of River Basin Management Plan - Thessalia River Basin District

Government Gazette 1132 / B / 19/06/2008. The Thessalian Field, Kopaidiko Field, Argolic Field and the Basin of Pinios in Ilia are defined as vulnerable zones to nitrate pollution of agricultural activity.

Development of two regional-level yield estimation systems for apple orchards and tomato fields in Azerbaijan using Sentinel-2 imagery

S. Fountas[1], V. Psiroukis[1], P. Trojacek [2], I. Bakhish [3] and A. Yashar[4]

[1] Laboratory of Agricultural Engineering, Department of Natural Resources Management & Agricultural Engineering, School of Environment and Agricultural Engineering, Agricultural University of Athens, 11855, Athens, Greece.
[2] International Development Ireland, The Courtyard Building, Carmanhall Road, Sandyford D18 HP90, Dublin 18, Ireland.
[3] Azercosmos, Uzeyir Hajibeyli Street 72, AZ1000, Baku, Azerbaijan.
[4] Ministry of Agriculture of the Republic of Azerbaijan, U. Hajibayli Street 80, AZ1000, Government House, Baku, Azerbaijan.

Abstract. The aim of this paper is to present the development and update process of a large-scale crop production predictive system for apple orchards and tomato fields, and report the performance of the updated crop-specific yield estimation models and their respective projections at both regional and national levels across Azerbaijan and its Economic Areas (Economic Districts). The models used Sentinel-2 satellite imagery-derived cumulative vegetation index (Normalized Difference Vegetation Index, NDVI) values from five (5) selected dates for apples in Guba region and three (3) for tomato fields in Khachmaz region as inputs, with a temporal interval that ranged from 10 to 12 days during the summer of 2021. Following the first data acquisition procedures, a targeted field sampling campaign was performed across the pilot fields of Khachmaz region, to assess the potential of the satellite data to identify productivity variability throughout the season. Moreover, frequent visits on numerous fields in Khachmaz and Guba regions were performed throughout their cultivation seasons, to validate the accuracy of the satellite data through in-situ observations regarding the classified productivity zones of each parcel, for both crops. Finally, the true recorded yield was collected from all pilot fields in order to update the models, fit the yield prediction equations and evaluate their performance in multiple levels (starting from field-level and expanding all the way to National level predictions) and data availability capacities (NDVI cumulative capacity). The models achieved accuracies of 77% and 86% for tomatoes and apples respectively on their respective regional level, while the errors of the National level predictions were 10% for tomatoes and 17% for apples. Finally, the in-situ samples demonstrated a correlation of 0.86 with the recorded yield measurements and 0.92 with their respective productivity zone delineation for tomatoes, indicating that such monitoring and predictive methodologies based on Sentinel-2 imagery can assist multiple producers across large region in making timely, data-driven decisions for their crop management and harvest planning.

1 Introduction

Agriculture has always played an important role in the history of Azerbaijan. Climatic and topographical conditions favour the cultivation of a variety of crops, with half of the country being classified as mountainous and 18% of the land being below sea level. Currently, agriculture generates approximately 6% of Azerbaijan's GDP (Kerimov, 2021). A key element of Azerbaijan's agricultural sector is that it is highly fragmented and includes a large number of smallholder farmers (Valiyev et al., 2022). The number of agricultural producers in 2015 was 1.2 million, with all of them cultivating less than 2.2 million hectares of land in total. In addition, there are over 1,200 state and cooperative farms nationwide. Most of Azerbaijan's cultivated land (over 1 million hectares) is irrigated. After an oil price crisis in 2016 and the downward trend of the country's fossil oil and natural gas prices ever since (Kerimov, 2021), the government has recently adopted a series of strategies to strengthen the agricultural sector. The government's goal is to improve the business climate for the development of a competitive Azerbaijani agrifood sector, to ensure the country's food security and to economically empower the rural population.

The large spatial coverage and high temporal repetition frequency of satellite imagery make it particularly useful for obtaining near real-time information at the regional level. As it is a cost-effective technology, users can minimise field observations and a large number of users can share the same data (Jensen et al., 2000). By using seasonal time series of satellite imagery, various phenological indicators, such as the beginning, peak and end of a crop cycle, can be modelled by specific vegetation indices (VIs). The latter are commonly used for crop phenotyping to assess the physiological state of plants under abiotic stress in different crops (Gianquinto et al., 2011). Among VIs, the Normalised Difference Vegetation Index (NDVI) is probably the most widely used for estimating biomass production, plant vigour, stress level, yield and even as a proxy for

photosynthesis (Fortes et al., 2015). In recent years, several approaches to the quantitative estimation of plant productivity parameters have been elaborated, including methods ranging from simple regression equations (Anastasiou et al., 2018) to the use of more complex plant growth models (Yang et al., 2004). Tucker et al. (1980) were among the first researchers to establish a relationship between NDVI and crop yield using experimental fields and ground-based spectral radiometer measurements. Thereafter, numerous studies have reported the good correlation between vegetation indices provided by RS and crop yield and biomass (Toscano et al., 2019; Fieuzal et al.,2020; Darra et al., 2021).

Early estimates of crop yields enable farmers to optimise their farm planning, field management and product marketing decisions. Data-driven decisions allow for more informed decisions on optimising inputs (e.g. fertilisers, pesticides and water), determining the optimal harvesting method and timing, and most importantly, planning logistics related to product storage, transport and marketing. In the agriculture of the digital age, data is the most valuable currency and the question of "how early" it becomes accessible is the decisive production factor.

In this study the capacity of Sentinel-2 imagery to assess canopy growth, yield and field cultivation of tomato crops and apple trees was evaluated. We used a remote sensing-based vegetation index to extend the approach for early crop yield prediction and to investigate the predictive power of the developed models. A stepwise linear regression method was implemented to select the linear models based on the statistical evaluation of their fit for the entire data set, creating simple equations with easily interpretable coefficients that can forecast crop yield. The inclusion of remote sensing data is carried out to evaluate whether NDVI variables can successfully and accurately quantify yield performance of processing tomatoes at both regional and National levels. Therefore, the objective of this study was to 1) assess the capacity of a cumulative NDVI-based model to accurately predict tomato and apple yields, 2) evaluate NDVI data from the Sentinel-2 satellite platform as a seasonal, near real-time monitoring tool for crop vigour and underlying variability through in situ observations and targeted ground truth sampling campaigns. The results can be used to support policy and regulatory decisions, while the method presented can be transferred to other countries and crops / cultivation systems, contributing to a better understanding of remote sensing data on estimating crop production.

2 Materials and Methods

2.1 Experimental Layout

The trial took place in Khachmaz region, Azerbaijan, where 34 processing tomato fields with a total area of 128 ha (extent of 41°21'40.2"N 48°41'51.8"E : 41°36'07.8"N 48°47'24.8"E), and in Guba region, Azerbaijan, where 91 apple fields with a total area of 225 ha (extend of 41°18'27.2"N 48°30'38.2"E : 41°25'47.0"N 48°47'18.9"E) were selected as pilot fields for this study. The planting date of the tomato fields ranged between the end of May and the beginning of June 2021, while harvesting was completed at the beginning of September. For apple orchards, harvesting was completed by the start of October. All experimental tomato fields were irrigated and planted in rows with average row spacing of about 0.6-0.8 m for tomatoes, which corresponds to the extensive cropping system commonly used in the region. Apple orchards, on the other hand, were further classified into two different categories based on their cultivation system and planting density, into traditional and extensive orchards. The area of the trial regions is shown in Figure 1.

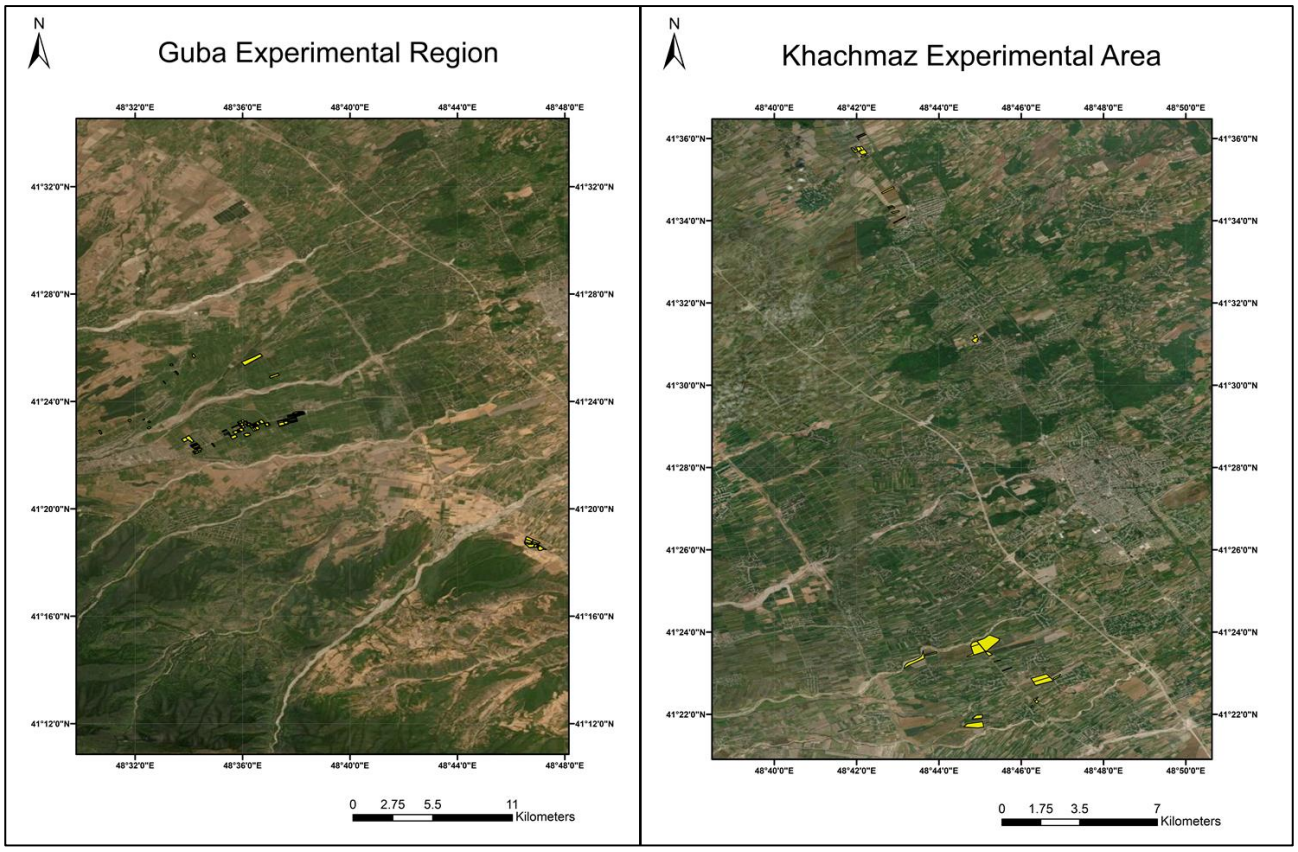

Figure 1. The experimental areas with the trial field boundaries of the apple orchards in Guba region (left) and tomato fields in Khachmaz region (right).

2.2 Data Collection & Preprocessing

The first step of this study was to collect the boundary coordinates for the fields of interest that were to participate in the experiment. For this purpose, topographic field data were collected by agronomists of the Ministry of Agriculture (MOA) of the Republic of Azerbaijan in their respective regions using portable positioning systems in May 2021. These field measurements and the polygon boundary files generated were then checked and possibly fine-tuned using RGB components created from Azersky satellite imagery (SPOT -7) from the same period. An example of the vector layers of field boundaries acquired during these field measurements is presented in Figure 2.

Figure 2. Example of the field boundaries' layer, generated from topographical surveys prior to the start of the cultivation season.

The remote sensing data used in this study are 10x10 m^2 resolution multispectral images obtained from the Multi-Spectral Imager (MSI) sensor of ESA's Sentinel-2 satellite platforms. The atmospherically corrected images (Level-2A, providing Bottom of Atmosphere reflectance values) from the Sentinel-2A satellite in cartographic geometry (UTM/WGS84 projection) were downloaded from the official Copernicus Open Access Hub (scihub.copernicus.eu). A key component of the developed system is the generation of crop growth

status maps for the experimental fields, throughout the cultivation season. After the field boundaries of interest were identified, the next step involved the collection of Sentinel-2 multispectral imagery dataset analysis of Guba-Khachmaz region. More specifically, the steps followed to produce the results of each pilot round (selected date) are described below:

1. Collection of the total number of Sentinel-2 images that covered the entirety of the experimental area.
2. Filtering of all images based on cloud coverage, to ensure that each set of images consisted of high quality, cloud-free data. In the case that high cloud coverage was encountered, and the experimental fields of interest were not fully visible, the next available set of images was used instead.
3. Perform orthomosaicing to “stich” all individual monochromatic Sentinel-2 images from a common date to generate compact orthomaps of the entire experimental area (Figure 2a and 2b).
4. Iteration of the vegetation index (NDVI) formula across all satellite image pixels, creating the NDVI orthomap of the entire area (Figure 2c).
5. Assign a productivity value on each pixel based on the NDVI values. The classification used was a simple 3-class Quantile classification, in order to capture the overall image of the region's crops performance between them.

These maps not only are required for the following steps of the methodology, as yield predictions are essentially generated based on the cumulative values of each field throughout the season, but they can also act as a valuable field management tool for the farmers and agronomists. These maps and the generated time series, or simply the total of generated maps during the cultivation season, can provide information on which field segments need more attention and help easily and timely detect defective areas.

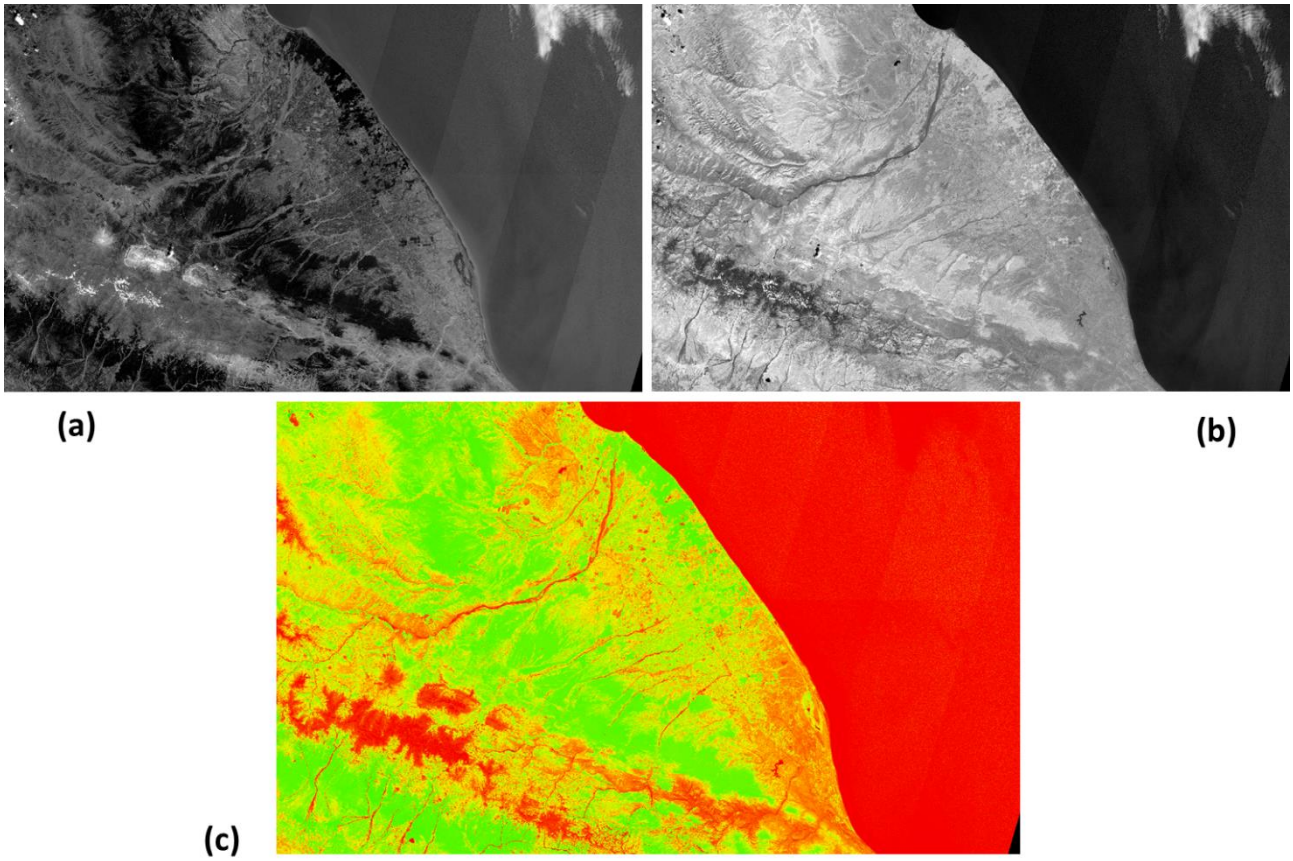

Figure 3. Example of Sentinel-2 Orthomosaics for the Guba-Khachmaz region, on the Red (a) and Near-Infrared (b) spectra, along with the generated NDVI mosaic (c).

2.3 Validation of the accuracy of crop growth status maps

In order to validate the accuracy of the generated crop growth maps, field visits were performed on selected dates (23-26 of August 2021) in the Khachmaz district, in order to collect ground truth samples from targeted tomato crop productivity zones. The sampling spots were selected based on the most recent crop growth

maps generated from satellite imagery, and the overall aim of this activity was to validate the accuracy of the satellite crop growth status maps using data from the actual pilot fields, as it was the first time implemented in this region and for these crops. The ground sampling performed in the selected tomato fields, resulting in a total of 12 samples, consisted on the field-measured production in $1m^2$ cells, accompanied by the respective productivity class of this cell in the most recent crop growth status map. The process of the tomato sampling in a high productivity zone in Qarajik village and a medium one in Sabiroba village are presented below (Figure 6). The final selective sampling maps with the respective productivity class of each sampling target cell are also presented in Figure 7. The methodology and followed steps for the field sampling process are summarised below:

1. Generate the initial 3-class productivity field maps for the selected fields (Low, Medium or High).
2. Identify the most “pure” cells, meaning the areas that are within the center of selected zones characterized entirely by a single class.
3. Select potential alternatives locations for sampling, in case the initial sampling spots are not easily accessible.
4. Integrate a supportive 10x10 m^2 grid to the maps, to assist in locating the selected $1m^2$ sampling areas.

Moreover, aside from the targeted sampling operations in Khachmaz, field visits to evaluate the zone classification and overall accuracy of the crop growth status maps were performed in multiple days, across the cultivation season of both crops, and for both regions (Guba and Khachmaz). These visits provided an additional validity control tool, were performed with the presence of the farmers who cultivate the fields or the responsible agronomists, and the main observations for each field visit and the evaluation of their respective crop growth zones were documented.

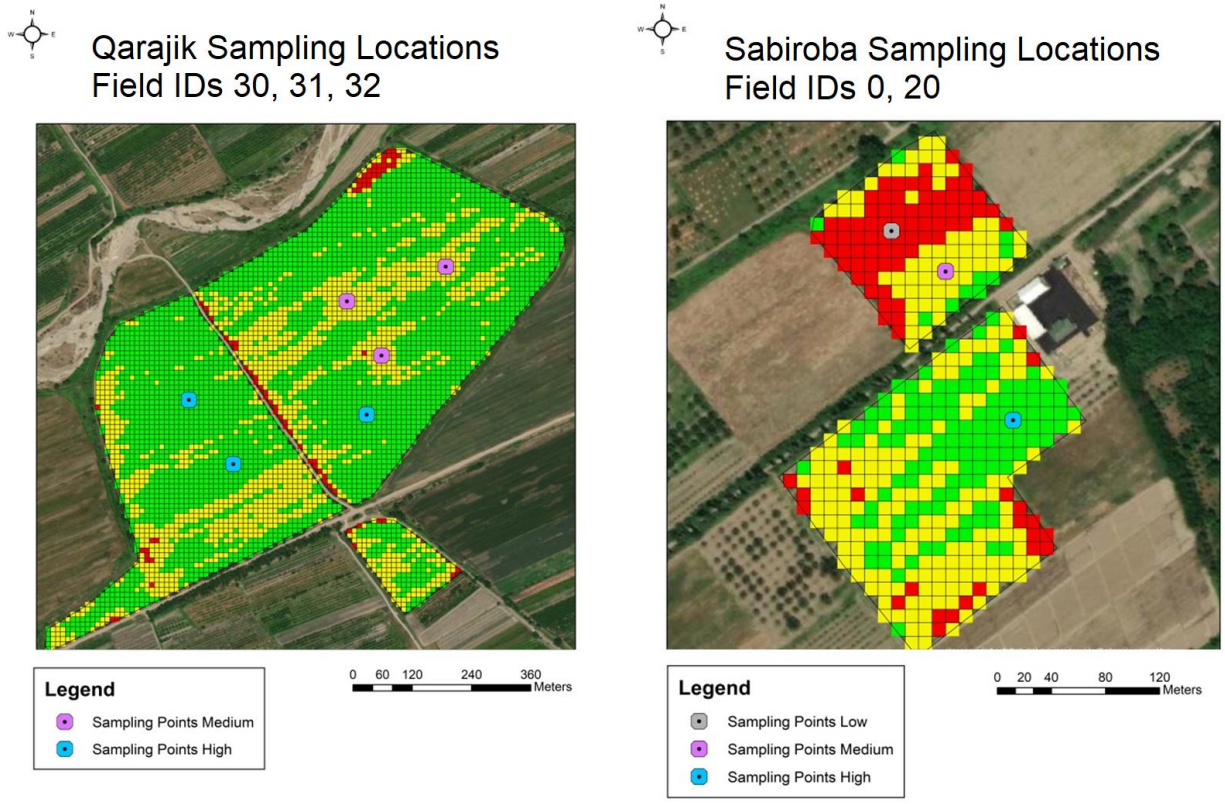

Figure 4. The selective sampling maps with the supporting 10x10m grid and the accompanying productivity class of each target 'pure' cell.

2.4 Collection of actual yields from the farmers

After the end of the cultivation season, once harvesting is completed, the actual produced yields on a field level are collected, expressed in t/ha. This data is necessary to both evaluate and calibrate the model's crop specific equation, since the model is expected to have the smallest error possible to these yield values. Essentially, the model is adapted to how each crop “performed” based on its growth status throughout the season. This process can be repeated for even more years, with the model becoming more robust each year. The actual yield (t/ha) that each pilot field produced was collected directly from the farmers that

cultivated the fields, and the respective ground-truth recorded yield values were assigned to the pilot field vector layer. This way, at the end of the season, each field entry had all cumulative NDVI values and the recorded yield assigned to it. After collection, the yield for tomato fields were categorised normally for all fields, while apple yield, due to significant variations in productivity, were split into two different categories, one for traditional orchards which produced lower yields, and one for intensive cultivation orchards, which demonstrated significantly higher productivity. The initial step of the predictions is to use an adjusted equation, following the approach of Kross et al. (2015), using a biomass conversion function and a harvest index (HI). This linear approach is simple to be implemented, and can be easily calibrated once ground truth yield data become available to increase the models accuracy. Therefore, the initial model was run and conducted with the equation:

$$Predicted\ yield\ (t/ha) = Cumulative\ NDVI * Biomass\ Factor * Harvest\ Index$$

The predictions naturally inherit the linearity of the NDVI and crop growth, and are also classified in 3-class quantiles to identify which fields are expected to perform better than others across the pilot region. For the initial run of the system, a biomass transfer factor of 1.5, and a HI of 0.9 was selected for tomatoes, while for apples, where a lower percentage of biomass in the fields is harvested, the selected values were 0.5 and 0.7 respectively. These predictions however are not calibrated yet. Recorded yield data is necessary for this, since the model is expected to have the smallest error possible to these yield values. Once the actual produced data is collected, the values of the Biomass function and Harvest Index that best describe the yield are identified. These results in the new updated crop specific yield estimation model, which is much more accurate and can even further increase its accuracy with more similar iterations.

3 Results

3.1 Model development

The model was developed using the satellite imagery derived cumulative NDVI values from selected dates, based on the duration of the cultivation season of each crop, with an interval ranging from 15 to 20 days. This resulted in a total of five (5) Sentinel-2 multispectral regional mosaics, with three (3) of them covering the entire Guba and Khachmaz district, while the last two (2) only focused on Guba region, as tomato fields in Khachmaz were already harvested. Each mosaic was “cropped” using the pilot field boundaries as a “mask”, and then for each of the measurement dates, a mean NDVI value was extracted from each field. This results in each tomato field having a total of three (3) NDVI values (one from each measurement / image acquisition) and each apple orchard having five (5), distributed across the growing season. These values were finally integrated with their time interval, to generate the Cumulative NDVI for each field this season, or simply the area below the NDVI curve of each field.

3.2 Accuracy of the growth samples

During the latest stages of the tomato season, before the harvesting, the data of the ground sampling expeditions were analysed. As demonstrated by the results of the analysis, the correlation between the quantile classification and the recorded sample yield was very high, with the Sentinel-2 satellite imagery demonstrating very high capacity in assessing the productivity of the fields in almost real-time. Their correlation with the collected yield, as well as red-only tomatoes harvested, is presented in Table 1.

Table 1. The correlation between sampling data and NDVI values

Correlation	Total Yield	Red tomatoes
Cumulative	**0.858630744**	**0.922595394**
3rd Measurement (06.08.2021)	0.796899808	0.762671216
2nd Measurement (17.07.21)	0.747057138	0.758190575
1st Measurement (04.07.2021)	0.15527121	0.448264217

3.3 Yield estimation models calibration

On the next phase, the equations initially used to generate the first yield predictions were fitted to the ground-truth recorded yield produced from each field. The equations naturally followed the same harvest index approach, using two indices (one for biomass transfer and one for harvest), to convert the cumulative NDVI values to predicted yield in t/ha. The indices that fitted best to the ground truth data was 2 for biomass transfer and 0.9 for HI respectively for tomato. For apples, the model had to be further divided, based on the cultivation system, as variation in productivity and therefore final yield were too high for a single equation to

describe them accurately. To this end, two biomass transfer values of 0.2 and 1.1 and two HIs of 0.5 and 0.55 were used. The results of the calibrated predictions and their respective errors for the pilot fields, after undergoing a simple outlier filtering, are demonstrated below (Tables 2, 3 and 4). These models were developed by using the full number of predefined satellite imagery measurements, meaning that the data from all three (3) dates were used for the model update of the tomatoes, and all five (5) for the apples.

Table 2. The equation and performance of the updated tomato model developed in Khachmaz.

Fitted Equation for Khachmaz tomatoes:	(Cumulative NDVI * 0.9) * 2
% Error	23%
Accuracy	77%

Table 3. The equation and performance of the updated traditional apple orchard model developed in Guba.

Fitted Equation for Guba Apples, Traditional:	(Cumulative NDVI * 0.5) * 0.2
% Error	14%
Accuracy	86%

Table 4. The equation and performance of the updated intensive apple orchard model developed in Guba.

Fitted Equation for Guba Apples, Intensive:	(Cumulative NDVI * 0.55) * 1.1
% Error	18%
Accuracy	82%

3.4 Regional – National upscale

The final step of the methodology is to upscale the predictions of the pilot fields to larger administrative units, such as the entire region, or even across the entire country. The system generates yield predictions for each field, in t/ha, and therefore, by knowing the total number of hectares of our crop of interest cultivated in a certain region, we can use the system's average prediction values, to get yield predictions for this entire area. This projection approach starts from the known fields, uses their predictions and expands to Regional and National level predictions. This method is common for such projections, and is followed by many national organisations and public bodies. FAO, for example, often collects and uses 10-15% of the total cultivated land per crop for each region, to calculate production and yield metrics for larger units. In this applications the Guba and Khachmaz apple and tomato predictions respectively were upscaled, and compared with the most recent recorded statistical values to assess their accuracy. The results of the predictions on a Regional and National level for each crop are presented in Table 5. The system's upscale projections performed very well, with an upscale accuracy of 91% for tomatoes across the Khachmaz district and 81% for apples across the Guba district this year. Moreover, in larger projections, such as predictions on a National level, the models maintain a high accuracy, achieving 83% for apples and 90% for tomatoes using data from 2020 (as 2021 data were not yet available by the time this report was submitted).

Table 5. The equation and performance of the updated traditional apple orchard model developed in Guba.

Tomatoes	Total Ha Cultivated	Tons Produced	Prediction (36.14 t/ha)	Error
Khachmaz (November 2021)	2,015	65,531	72,811	9%
Azerbaijan Republic (2020)	19,371	774,877	700,068	10%

4 Summary

The first run of the models was completed successfully, demonstrating very promising results and great performance. The system can have many uses, not limited to only the intended yield prediction applications but can also act as a valuable field-monitoring tool for farmers. The predictive capacity of the models is very

high, and the applications can also be scaled up in multiple ways, by either expanding the method so that the system includes more crops, or by fine-tune projections for larger regions or at national level through spatial projections, using a total of 10% cultivated land per region next season. One of the most challenging aspects of the method was the collection of field samples and the acquisition of ground truth yield data. These steps were critical for the methodology, and utmost attention should be given so that they are executed in an accurate and efficient manner. Finally, a surprisingly pleasant observation was that most of the future end users we contacted seemed to realise instantly the benefits of the developing system. Regardless of future approaches for the system's expansion, more farmers should be engaged, as they can act as both future users, but also data providers that can help with the systems update each year. To achieve this, an organised and well-thought information campaign is needed, which can potentially include workshops, promotional material and information on the RBIS portal, as well as communication and dissemination of successful cases in order to promote the system and its benefits to future users.

Acknowledgements

The Sentinel-2 data was provided by ESA's Copernicus Open Access Hub. The research was funded by the European "Support to Development of a Rural Business Information System (RBIS)", Contract No: ENI/2019/412-386 program of Azerbaijan.

References

Anastasiou, E.; Balafoutis, A.; Darra, N.; Psiroukis, V.; Biniari, A.; Xanthopoulos, G.; Fountas, S. Satellite and Proximal Sensing to Estimate the Yield and Quality of Table Grapes. Agriculture 2018, 8, 94, doi:10.3390/agriculture8070094.

Darra, N.; Psomiadis, E.; Kasimati, A.; Anastasiou, A.; Anastasiou, E.; Fountas, S. Remote and Proximal Sensing-Derived Spectral Indices and Biophysical Variables for Spatial Variation Determination in Vineyards. Agronomy 2021, 11, 741, doi:10.3390/agronomy11040741.

Fortes Gallego, R.; Prieto Losada, M. del H.; García Martín, A.; Córdoba Pérez, A.; Martínez, L.; Campillo Torres, C. Using NDVI and Guided Sampling to Develop Yield Prediction Maps of Processing Tomato Crop. 2015.

Gianquinto, G.; Orsini, F.; Fecondini, M.; Mezzetti, M.; Sambo, P.; Bona, S. A Methodological Approach for Defining Spectral Indices for Assessing Tomato Nitrogen Status and Yield. European Journal of Agronomy 2011, 35, 135–143.

Jensen, J.R. Remote Sensing of the Environment an Earth Resource Perspective Prentice Hall. Upper Saddle River (NJ), USA 2000.

Kerimov, N. Business Outlook in Azerbaijan 2021.

Kross, A.; McNairn, H.; Lapen, D.; Sunohara, M.; Champagne, C. Assessment of RapidEye Vegetation Indices for Estimation of Leaf Area Index and Biomass in Corn and Soybean Crops. International Journal of Applied Earth Observation and Geoinformation 2015, 34, 235–248.

Toscano, P.; Castrignanò, A.; Di Gennaro, S.F.; Vonella, A.V.; Ventrella, D.; Matese, A. A Precision Agriculture Approach for Durum Wheat Yield Assessment Using Remote Sensing Data and Yield Mapping. Agronomy 2019, 9, 437, doi:10.3390/agronomy9080437.

Tucker, C.; Bn, H.; Jh, E.; Je, M. Relationship Of Spectral Data To Grain Yield Variation: Remote Sensing Of Winter Wheat Field. 1980.

Valiyev, A.; Rustamov, F.V. oglu; Huseynova, R.A.; Orujova, M.S.; Musayeva, S.N. The Digitalization Effectiveness as an Innovative Factor Development of the Agriculture in Azerbaijan. JEECAR 2022, 9, 194–205, doi:10.15549/jeecar.v9i2.902

Yang, P.; Tan, G.X.; Zha, Y.; Shibasaki, R. Integrating Remotely Sensed Data with an Ecosystem Model to Estimate Crop Yield in North China. In Proceedings of the Proceedings of XXth ISPRS Congress Proceedings Commission VII, WG VII/2, Istanbul, Turkey; Citeseer, 2004; pp. 150–156.

Fieuzal, R.; Bustillo, V.; Collado, D.; Dedieu, G. Combined Use of Multi-Temporal Landsat-8 and Sentinel-2 Images for Wheat Yield Estimates at the Intra-Plot Spatial Scale. Agronomy 2020, 10, 327.

Impact of defoliation during the grain filling period on the yield of durum wheat in central Greece

D. Leonidakis[1], D. Bartzialis, K. Giannoulis, I. Gintsioudis, E. Skoufogianni and N.G. Danalatos

[1]University of Thessaly, Department of Agriculture, Crop Production and Rural Environment, Laboratory of Agronomy and Applied Crop Physiology. E-mail: leonidakis.dimitris@gmail.com

Abstract. Seeking the possibility of developing new methods and practices for optimizing crop water use in line with the environmentally friendly sustainable agriculture, an effort was made to examine the impact of defoliation of durum wheat plants on final yield production as a key tool for minimizing the negative effect of transpiration deficit during the grain filling period of the crop in a semi-arid area such as Larissa plain, Central Greece.A durum wheat field experiment was conducted from November 2018 to June 2019 in the Larissa (Giannouli) area, Thessaly plain, Greece. The Zadoks scale was used to estimate the phenological stages at which defoliation took place. Defoliation was performed on 2/4, 8/4, 15/4 and 23/4/2019, when the wheat crop was at stages 65, 70, 71 and 75, respectively. Experimental design was randomized factorial in three blocks. The factors were: a) defoliation dates, and b) defoliation at two levels, e.g. completely defoliated plants and plants in which the flag leaf was maintained. It was found that total defoliation did not significantly affect the yield of durum wheat in any of the defoliation dates and treatments. This finding might suggest that defoliation be a useful practice in maintaining appreciable yield levels of wheat grown in Mediterranean areas characterized by low water availability by reducing the negative effects of transpiration deficit during the grain-filling period. The final yield levels attained by the defoliated plants may be attributed to a no modest assimilation rate of the green plant parts (e.g. stems, flag leaves) or/and a certain assimilates allocation from the reserve pools (stems and roots) to the growing grain, but the subject deserves further research. The work is being continued.

Keywords**:** *wheat, defoliation, yield, Thessaly plain, semi-arid areas*.

1. Introduction

New methods and practices for the optimization of water use efficiency of rainfed crops have been studied in the last decades all over the world. Partial or full defoliation of such crops, e.g. wheat, barley, oats, etc., might be helpful in semi-arid areas in the Mediterranean region and elsewhere, characterized by an accumulated water shortage during grain filling period occurring in May to mid-June, due to increased evapotranspiration deficit. Classical example comprise the low yields of rainfed wheat yields attainable in Central Greek lowlands (2.5-4.5 t/ha). The defoliation method has been referred in various field- and pot experiments as a cultivation technique helping to decrease transpiration and maintain the humidity of the soil. However, the benefit from the reduced consumption of water does not always compensate for the decrease in production (Shao *et al*., 2010). The defoliation during 3 different growth stages of wheat (heading, florescence, 20 days after fluorescence) did not affect the production or the protein content (Ahmadi and Joudi, 2007). Breeders could use the results of this research to create varieties with smaller leaf areas, which can give higher efficiency even if the availability of water in the soil is limited. The effect of the reduced leaf surface on the efficiency and protein content in wheat was analyzed under conditions of full irrigation and water stress. The defoliation took place during the heading or the fluorescence stage. At the 1000 seed weight and protein content measurements, there were no statistically significant differences compared to the control (Ahmadi *et al*., 2009). The present study aims at evaluating the method of defoliation as a potential innovative cultivation technique that could reduce water use in wheat cultivations without negatively affecting the yield.

2. Materials and methods

A durum wheat experiment was conducted from November 2018 to June 2019. The experimental field was established in the rural area of Giannouli (Larissa). The soil is a deep, fertile clay loam formed on carkcareous alluvium of the Peneios River. The sowing was conducted on November 30th, 2018, using the variety Meridiano (Alfa Seeds SA, Greece), with a sowing density of 200 kg/ha. A completely randomized design was used with experimental plots sized 2 m x 2 m and three replications. Defoliation was conducted at four different phenological stages including whole plants and whole plants apart from the flag leaf. Non-defoliated plants

were serving as control.The Zadoks scale was used to estimate the phenological stages at which defoliation was planned. The first defoliation was performed on April 2nd when the cultivation was at stage 65, the second was on April 8th at stage 70, the third on April 15th at stage 71, and the last on April 23rd at stage 75. The harvest of the experimental field took place on June 15th.
Shoot and cob fresh and dry weights (kg/ha) and harvest index were measured in each experimental plot in samples taken in strips of 0.5 m on the rows in the center of each plot to avoid the border effect. The harvest index was calculated by dividing the seed weight over the total dry weight of each sample.

3. Results and Discussion

The results showed no statistically significant differences among the different treatments. In particular, for shoot dry weight, storage organs dry weight, total dry matter weight, crop growth rate, relative growth rate, and harvest index, no significant differences were found.-The total dry matter of wheat production varied between 4,800 and 6,600 kg/ha (Figure 1). The treatments of the whole plant defoliation and the whole plant defoliation except the flag leaf also did not show significant differences compared to the control in all the different phenological stages performed.

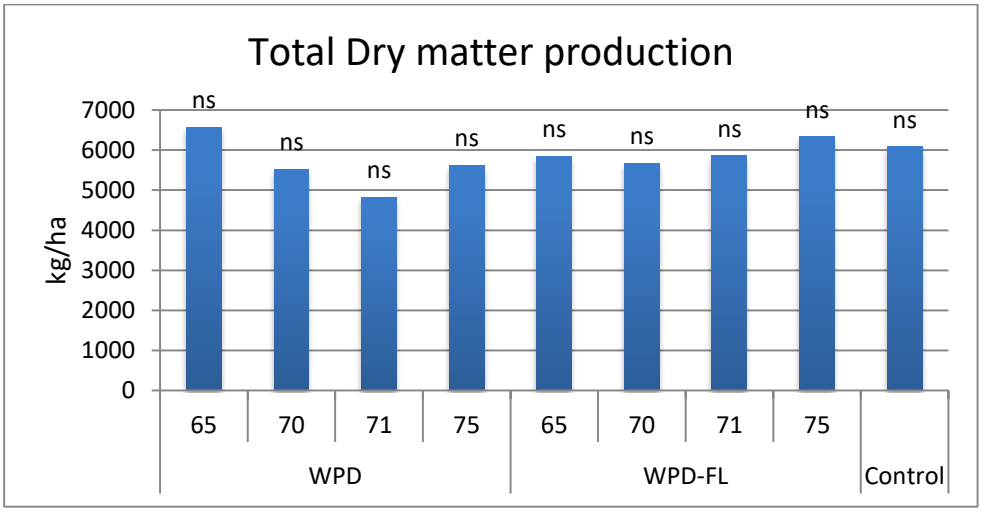

Figure 1. Total dry matter production of durum wheat in the nine different treatments {whole plant defoliation WPD (Zadoks scale stages 65, 70, 71 and 75), whole plant defoliation except flag leaf WPD-FL (Zadoks scale stages 65, 70, 71 and 75) and control}. No significant differences were observed among the treatments.

The harvest index varied from 0.61 to 0.67, with the untreated plants presenting the lowest value (0.61) compared to the other treatments, while the defoliation of the whole plant in Zadoks stage 75 and the defoliation of the whole plant except the flag leaf in stage 71 presented the higher values (0.67) (Figure 2). However, no statistically significant differences were observed according to Analysis of Variance.

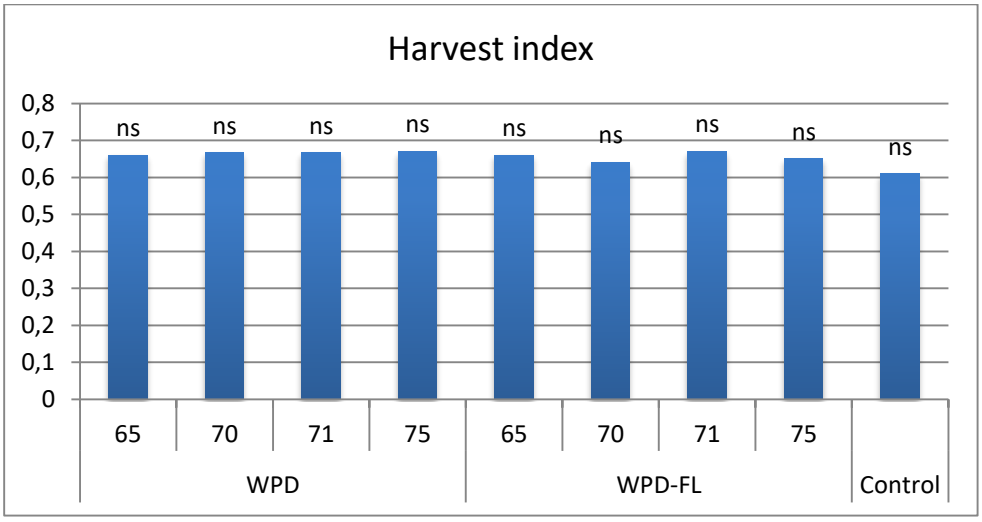

Figure 2. Harvest index of durum wheat in the different treatments {whole plant defoliation WPD (Zadoks scale stages 65, 70, 71 and 75), whole plant defoliation except flag leaf WPD-FL (Zadoks scale stages 65, 70, 71 and 75) and control}. No significant differences were observed among the treatments.

In the durum wheat experiment, whole plant defoliation and whole plant defoliation except flag leaf, conducted at four different phenological stages, did not negatively affect total dry matter production and harvest index with statistically significant differences. Transpiration of the defoliated plants is minimal resulting to a moister soil and a better water use efficiency during the –by all means reduced- process of assimilation by the green plant parts and the flag leaves. Ahmadi and Joudi (2007) evaluated the defoliation intensity and timing in a similar study. They found that the defoliation did not affect the grain yield even after removing the leaves at the anthesis stage. Following up on this research, Ahmadi *et al*. (2009) evaluated the defoliation at the heading and the florescence stage, where no significant statistical differences were observed compared to the untreated plants at the measurements of the 1000 seed weight as well as on the protein content. In another research, post-anthesis defoliation in wheat cultivation reduced dry weight; however, the number of grains was not significantly reduced except for the 100% defoliation of the plants (Aggarwal *et al*. 1990). Aggarwal *et al*. (1990) also found that when the flag leaf was removed, the grain yield was slightly reduced.
Our results indicated no significant differences in the measured traits in both defoliated plants and defoliated plants with the flag leaf remaining on the stand. Relative results are reported by Bijanzadeh and Enam (2010) working with pot experiments. They found that the defoliation treatments did not have a significant result on the number of grains per spike on well-watered cultivars; however, it might be helpful also in regions with low water availability since defoliation did not decrease the number of grains per spike in some cultivars growing under water stress.

4. Conclusion and future prospects

Total defoliation did not affect the yield characteristics of durum wheat, including or not the removal of the flag leaf. These findings justify previous studies showing that defoliation did not affect measurements like total dry matter production, seed yield and harvest index, etc. Further research has to be conducted to monitor the effect of defoliation on earlier stages during the milk and grain filling period of various cultivars of wheat and other winter cereals to investigate the possibility of using this innovative technique of defoliation in agricultural practice in line to the low input sustainable agriculture.

References

Aggarwal, P. K., Fischer, R. A., & Liboon, S. P. (1990). Source–sink relations and effects of post-anthesis canopy defoliation in wheat at low latitudes. The Journal of Agricultural Science, 114(01): 93.

Ahmadi A., Joudi M. (2007). Effects of timing and defoliation intensity on growth, yield and gas exchange rate of wheat grown under well watered and drought conditions. Pakistan Journal of Biological Sciences 10 (21): 3794-3800.

Ahmadi A., Joudi M., Janmohammadi M. (2009). Late defoliation and wheat yield: Little evidence of post-anthesis source limitation. Field Crops Research 113: 90-93.

Bell, L.W., Kirkegaard, J.A., Tian, L., Morris, S., Lawrence, J. (2020). Interactions of Spring Cereal Genotypic Attributes and Recovery of Grain Yield After Defoliation. Frontiers in Plant Science 11:607

Bijanzadeh, E. and Emam, Y. (2010). Effect of defoliation and drought stress on yield components and chlorophyll content of wheat. Pakistan Journal of Biological Sciences 13 (14): 699-705

Collantes H.G., Gianoli E., Niemeyer H.M. (1997). Effect of defoliation on the patterns of allocation of a hydroxamic acid in rye (Secale cereale). Environmental and Experimental Botany 38: 231-235.

Shao L., Zhang X., Hideki A., Tsuji W., Chen S. (2010). Effects of defoliation on grain yield and water use of winter wheat. Journal of Agricultural Science 148: 191-204.

Improvement of Key Performance Indicators in vine crop using a regulated deficit irrigation scheduling tool in a water-scarce Mediterranean agroecosystem

J.A. Martínez-López [1], H. Martínez-López [1], R. López-Urrea [2], A. Martinez-Romero [1], J.J. Pardo [1], C. Casas – Selva [1], J. Montero[1], J.M. Tarjuelo[1] y A. Domínguez [1*]

[1] Centro Regional de Estudios del Agua, Universidad de Castilla – La Mancha, Ctra. De las Peñas Km 3.2, Albacete, España (alfonso.dominguez@uclm.es)
[2] Instituto Técnico Agronómico Provincial de Albacete (ITAP), Parque empresarial Campollano, 2º Avenida, 61, Albacete, España (rlu.itap@dipualba.es)

Abstract Water scarcity is one of the main handicaps for Spanish agriculture and in other areas under semi-arid conditions around the world. This situation, exacerbated by global warming, can have negative effects on crop profitability. Vineyards occupy large areas of the Mediterranean basin, especially in the Castilla-La Mancha region (C-LM), which has the world's largest surface area devoted to grapevines (437,275 ha), of which 236,532 ha are irrigated, mainly using drip irrigation systems. Grapevine irrigation is challenging due to the water/yield/quality relationship. In C-LM, where annual precipitation is lower than 400 mm year^{-1}, vine irrigation is limited by the available water supply. The standard allocation is well below the maximum needs, not exceeding 1500–2000 m^3 ha^{-1} year^{-1}. Under these circumstances, decision support systems to guide farmers in irrigation scheduling would be highly useful, especially those based on Regulated Deficit Irrigation (RDI) techniques. To address these challenges, the SUPROMED project (Sustainable production in water-limited environments of Mediterranean agro-ecosystems) combines, in an online platform (https://dss.supromed.eu/portal/), a series of models and tools for efficient use of water, energy and fertilizer. IS-MOPECO (Irrigation Scheduling module of the Model for Economic Optimization of irrigation water) is one of such models. It generates irrigation schedules according to the amount of available irrigation water, using a simplified water balance in the soil, in accordance with the FAO56 methodology, considering the different sensitivity to water stress at each vineyard crop growth stage. A two-year trial (2020-2021) was carried out to compare traditional management with that proposed by SUPROMED using the IS-MOPECO tool. A set of Key Performance Indicators were analyzed for this purpose. The management proposed by SUPROMED improved yield by 13% and gross margin by 20%. It can be concluded that SUPROMED successfully distributed the available water supply, enhancing the gross agronomic and economic productivity of irrigation water by 2% and 6%, respectively.

1. Introduction

Economically and socially, grapes are one of the most important crops in Spain, especially in the Castilla – La Mancha (CLM) region, which has the world's largest surface area devoted to grapevines (437,275 ha), of which 236,532 ha are irrigated (MAPA 2020), mainly using drip irrigation systems. Irrigation scheduling in vineyards is challenging due to the water/yield/quality relationship (Williams and Mathews, 1990).

In areas with water shortages, where the standard allocation is well below the maximum needs, not exceeding 1500 – 2500 m^{3}ha^{-1} year^{-1}, decision support systems to guide farmers in RDI scheduling would be highly useful. The SUPROMED (Sustainable production in water – limited environments of Mediterranean agro-ecosystems) project is thus intended to enhance the economic and environmental sustainability of Mediterranean farming systems through a more efficient management of land (good agricultural practices), fertilizers (soil analysis and nutrient balance), and water (evaluation of the irrigation systems and a proper irrigation scheduling, taking into account weather forecast and soil moisture). The use of RDI techniques for proper irrigation scheduling is a sensible option for vineyards. In this sense, an RDI scheduling tool has been developed for several tree crops. The irrigation scheduling tool generates schedules according to the amount of available irrigation water, using a simplified water balance in the soil, in accordance with the FAO56 methodology (Allen et al., 1998; Pereira et al., 2020), considering the different sensitivity to water stress at each vine crop growth stage (Intrigliolo and Castel, 2010). The main aim of this work was to demonstrate the impact of applying the SUPROMED models and methodologies on the profitability of a vine crop in comparison with the traditional management of this crop in CLM. Our secondary objectives were as follows: 1) To determine a set of productive, economic, and environmental Key Performance Indicators (KPI); 2) to monitor, using the SUPROMED methodologies, several farms dedicated to the cultivation of vines and manage a subplot within one of the monitored farms; 4) To compare the monitoring results using the KPIs.

2. Material and methods

2.1. Site description

The study was carried out during the 2020 and 2021 growing seasons, in a Monastrell (Vitis vinifera L.) vineyard plot at a spacing of 3 by 1.5 m (2222 vines /ha). The vineyard is located near Ontur (38º35´N;1º29´W; 632 msnm), Albacete, Spain. The available allocation of water in the area is 1200 m^3 ha^{-1}. The vines are trained to a vertical trellis on a bilateral cordon system oriented north-south. Canopy-management practices, all manually

performed, included shoot-thinning and shoot-tip cutting. The study area is characterized by a typical Mediterranean climate (Papadakis, 1966). Bud break for Monastrell in the region usually occurs at the beginning of April, with harvest during September. The crop cycle ends with the leaf fall at the end of October, following the BBCH scale (Meier, 2001).

2.2. Description of monitored vineyard plots

The vineyard plot was divided in two subplots. Consequently, in order to compare traditional management and that proposed by SUPROMED (SUP), one subplot was managed applying the SUPROMED (SUP) techniques and the other was managed by the farmer. In each monitored plot, the group of plants representing the average conditions of the sector was selected to monitor the experiment. Before bud break, the soil profile of each subplot was sampled to determine the effective soil depth, and physical (texture) and chemical (nutrient content) properties. The soil has a depth of 0.5 m, with a sandy loam texture, highly calcareous, and of medium-low fertility (1.15% organic matter). SUP soil analyses were used to determine the irrigation scheduling and fertilization by SUP management and to simulate the farmer's irrigation scheduling

2.3. Irrigation system

The plot is equipped with a drip irrigation system with 5 l h^{-1} pressure compensating emitters spaced at 1 m and located in the plant lines. During the first irrigation event, an evaluation of the irrigation system was carried out to determine the spatial distribution of the water applied by the irrigation system and to determine the actual amount of water applied at each irrigation event at working pressure. All this information (Table 1) was used by SUP to calculate the proper irrigation scheduling and to improve the uniformity of the SUP plot, if necessary.

To compute the soil balance using the RDI scheduling tool, a general irrigation application efficiency of 90% was assumed. This value was based on values for Emission Uniformity (EU) obtained in the evaluation of the irrigation system (between 88% for farmer and 93% for SUP, Table 2), and the low evaporation losses considered for a drip irrigation system.

Table 1: Evaluation of the drip irrigation system

Date	Management	Irrigation frame (m x m)	EU (%)	$Q_{avg}e$ (l h^{-1})	Q_{avg} (q_a) (l h^{-1})	P_{avg} (m)	$P_{min.}$ (m)
23/05/2020	SUPROMED	3 x 1	93	5.00	7.50	17	15
23/05/2020	Farmer	3 x 1	88	5.14	7.70	5	3

EU: Emission Uniformity; $Q_{avg}e$: average emitter flow; Q_{avg}: average flow received by plant; P_{avg}: Average pressure of the subplot; P_{min}: minimum pressure of the subplot.

2.4. Irrigation scheduling

The MOPECO irrigation scheduling tool (https://crea.uclm.es/siar/siarpr/) is a simplification for farmers of the MOPECO model for researchers (Ortega et al., 2004), which determines the irrigation scheduling of a crop using the simplified daily soil water balance proposed by FAO56 (Allen et al.,1998; Pereira et al., 2020). The irrigation scheduling module requires the following information: soil data (texture, depth, stone content); climatic data (temperature, ETo and rainfall); crop parameters (crop coefficient (Kc); duration of crop growth stages in cumulative growing degree days (GDD), previously calibrated according to SIAR (Irrigation advisory service in CLM) crop monitoring in the period 2004 – 2011 and calculated following Sevacherian et al. (1977); lower and upper developmental threshold temperatures; and irrigation system data (Table 2). Additionally, to generate RDI irrigation schedules MOPECO considers the different sensitivity to water stress at each crop growth stage; in the case of vines, the values are based on the studies by Intrilgliolo and Castel (2010).

To generate irrigation schedules, MOPECO updates the daily water balance considering the actual amount of water received by the crop (irrigation or rainfall) and the actual weather data. In addition, to calculate the irrigation water requirements of the crop for the next week, MOPECO uses the seven-day forecast climatic data provided by the Spanish National Institute of Meteorology and the actual phenological stage of the crop. The meteorological variables used for the proper determination of the irrigation requirements of the crop were measured by the SIAR meteorological station located in Ontur. Rainfall was measured using a rain gauge located in the plot.

2.5. Plot monitoring and harvest

Over the two experimental seasons, crop phenology was monitored weekly, following the BBCH scale (Meier, 2001) to fit the irrigation scheduling and supply fertilizers at a proper time.

In each monitored plot, we installed a pressure transducer (Pessl Instruments Pipe Pressure, Weis, Austria), previously calibrated over a range of 0 – 10 bar, and a soil moisture probe with 6 sensors at 10 cm spacing (Drill&Drop, Senteck, Australia), both connected to a data logger (ECO D3, Pessl Instruments, Weiz,Austria). The pressure transducer was installed in the drip emitter line to monitor the duration and the water applied in each irrigation event. The soil moisture probe was placed in the row line between two vine trunks and ≈ 33 cm from a dripper, to monitor the evolution of the volumetric soil water content.

Once the crop reached maturity, eight groups of three vines from each subplot were sampled to obtain the total yield of each crop management type. Quality parameters (Soluble solids, potassium, rot, acidity and pH) were determined in a winery in Ontur.

2.6. Key Performance Indicators

To compare SUP and traditional management, various Key Performance Indicators (KPIs) were calculated (Fernández et al., 2019).

Table 2: Key Performance Indicators

Indicator	Units	Definition and details
$GM = Ya\ PV - Cv - Ig\ \mathrm{Cw} + \mathbf{Subs}$	€ ha $^{-1}$	**Gross Margin**; where Ya (Yield); Yield (kg ha^{-1}); Pv: Sale price (€ kg $^{-1}$) ; Cv: Variable costs (€ ha^{-1}) (all these cost data were provided by the farmers); I_g: Gross Irrigation Water applied (m^3 ha^{-1}); Cw: Water cost (€ m^{-3}); Sub: Subsidies (€ ha^{-1}) (150 € ha^{-1}) (provided by the farmers)
$WP_I = \frac{Y_a}{I_g}$	kg m^{-3}	**WP_I: Irrigation Water Productivity**: ratio between Y_a: grain yield (12% moisture) (kg ha^{-1}) and I_g: gross irrigation (m^3 ha^{-1}).
$NEWP_I = \frac{GM}{(I_N + Re)}$	€ m^{-3}	**Net Economic Irrigation Water Productivity**: Ratio between GM: Gross Margin (€ ha^{-1}) and I_N: Net Irrigation (m^3 ha^{-1}) plus Re: Effective Rainfall (m^3 ha^{-1})
$GEWP_I = \frac{GM}{I_g}$	€ m^{-3}	**Gross Economic Irrigation Water Productivity**: Ratio between GM: Gross Margin (€ ha^{-1}) and I_g; gross irrigation (m^3 ha^{-1}).

3. Results and discussion

3.1. Evaluation of the irrigation system

The evaluation of the irrigation system (Table 1) showed that the SUP subplot achieved better results (93% of UE) than the farmer subplot (88%). Despite both management schedules having the same correctly maintained irrigation system (i.e., there were no water leaks, obstructions, etc.), the farmer subplot showed poorer results because it worked with a very low pressure (0.5 bar) due to its irrigating a larger surface area (1 ha) than the SUP (1.6 bar irrigating 0.5 ha).

3.2. Soil analysis and fertilization requirements

During both campaigns, the amount of fertilizer applied by SUP was based on the soil analysis carried out before sowing and the vineyard requirements. SUP calculated the nutrient balance using the methodology proposed by Dominguez Vivancos, 1989. Before bud break, SUP satisfied the P_2O_5 requirements of the crop, using phosphoric acid (to clean the irrigation system) and an organic fertilizer that also covered part of the N and K_2O requirements. For N, SUP applied the rest of N requirements before veraison, with the aim of halting vegetative growth, avoiding shoot growth potentially competing for the carbohydrates available for fruit ripening and impairing fruit light exposure (Smart, et al; 1985). The rest of potassium requirements were applied between fruit set and veraison, when potassium migrates from leaves to fruits, ensuring a proper ripening.

The farmer applied the same amount of P_2O_5 as SUP, but slightly less N and K_2O.

Table 3: Fertilization of vineyard crop during 2020 and 2021

Year		N/P_2O_5/K_2O (kg ha^{-1})	Cost (€ ha^{-1})
2020	**SUP**	41/41/73	172
	Farmer	32/41/53	145
2021	**SUP**	43/70/104	267
	Farmer	39/70/85	241

SUP: SUPROMED management

3.3. Irrigation scheduling and analysis of KPIs

In 2021, SUP applied RDC irrigation scheduling according to MOPECO, applying all the available irrigation water (around 120 mm) (Table 4). Meanwhile, the farmer underestimated the RDI scheduling by 30% compared to SUP (Fig. 1a.). This effect was simulated by the irrigation scheduling tool (Fig. 1a. and 1c.), finding it occurred when the available water (AW line) reached values below the deficit line, which represents the limit of the RDI irrigation scheduling.

In 2021, the effective rainfall was 6% higher than in 2020, mostly concentrated during spring and the final stage of maturity, and, consequently, SUP applied 70% of the available water allocation. Despite applying 16% more irrigation water, the farmer showed lower AW and volumetric soil water content than SUP (Fig. 1c. and 1d.), as a result of applying a greater amount of irrigation water at the beginning of the crop cycle, when crop requirements were lower (Fig.1c).

Table 4: Total water received by the crop according to management type

Year		Ig (mm)	In (mm)	Re (mm)	In + Re (mm)
2020	SUP	123	107	134	241
	Farmer	87	76	134	210
2021	SUP	84	73	142	215
	Farmer	97	84	142	226

Ig: Gross Irrigation; In: Net Irrigation; Re: Effective rainfall. SUP: SUPROMED management; Farmer: Farmer management.

In 2020, the SUP management type achieved a higher yield than the farmer type (Table 5) and also improved Gross Margin (GM). This was due to SUP applying more water (Table 4), thus keeping soil moisture content higher than the farmer (Fig. 1a. and 1b.), according to the RDI irrigation scheduling. Additionally, the lower amount of K_2O applied by the farmer, which reduced node fruitfulness (g fruit/node) (Cawthon et al.; 1982), was a determining factor. Furthermore, in 2020, SUP achieved better quality parameters, thus obtaining a higher sale price. Meanwhile, the farmer obtained better irrigation water productivity (WP_I) and Gross Economic Water Productivity of Irrigation water ($GEWP_I$).

In 2021, yields were lower than 2020 due to rainfall during the last stage of ripening, which caused hail damage and decreased yield and sale price, affecting quality parameters (causing rot and a lower amount of soluble solids). Nonetheless, SUP achieved a 17% higher yield than farmer, the possible causes of which were the higher amount of water and fertilizers applied the previous year (Tables 3 and 4) and the higher soil moisture content of SUP from fruit set to harvest (Fig 1c. and 1d.). SUP achieved these results with 13% less water, improving WP_I, GM, $GEWP_I$ and Net Economic Water Productivity (NEWP) with respect to the farmer.

Table 5: KPIs of SUP and farmer management types during 2020 and 2021 vineyard crop cycle

Year		Yield (kg ha^{-1})	WP_I (%)	GM (€ ha^{-1})	$GEWP_I$ (€m^{-3})	NEWP (€ m^{-3})
2020	SUP	14094	11.43	2093	1.7	0.86
	Farmer	12881	14.54	1886	2.2	0.89
2021	SUP	12118	14.42	1573	1.9	0.73
	Farmer	10345	13.43	1163	1.2	0.51
Average	SUP	13106	12.9	1833	1.8	0.80
	Farmer	11613	12.6	1524	1.7	0.68

WP_I: Water productivity of Irrigation water; APN: Agronomic Productivity of Nitrogen; GM: Gross margin; $GEWP_I$: Gross Economic Productivity of Irrigation water; NEWP: Net Economic Water productivity.

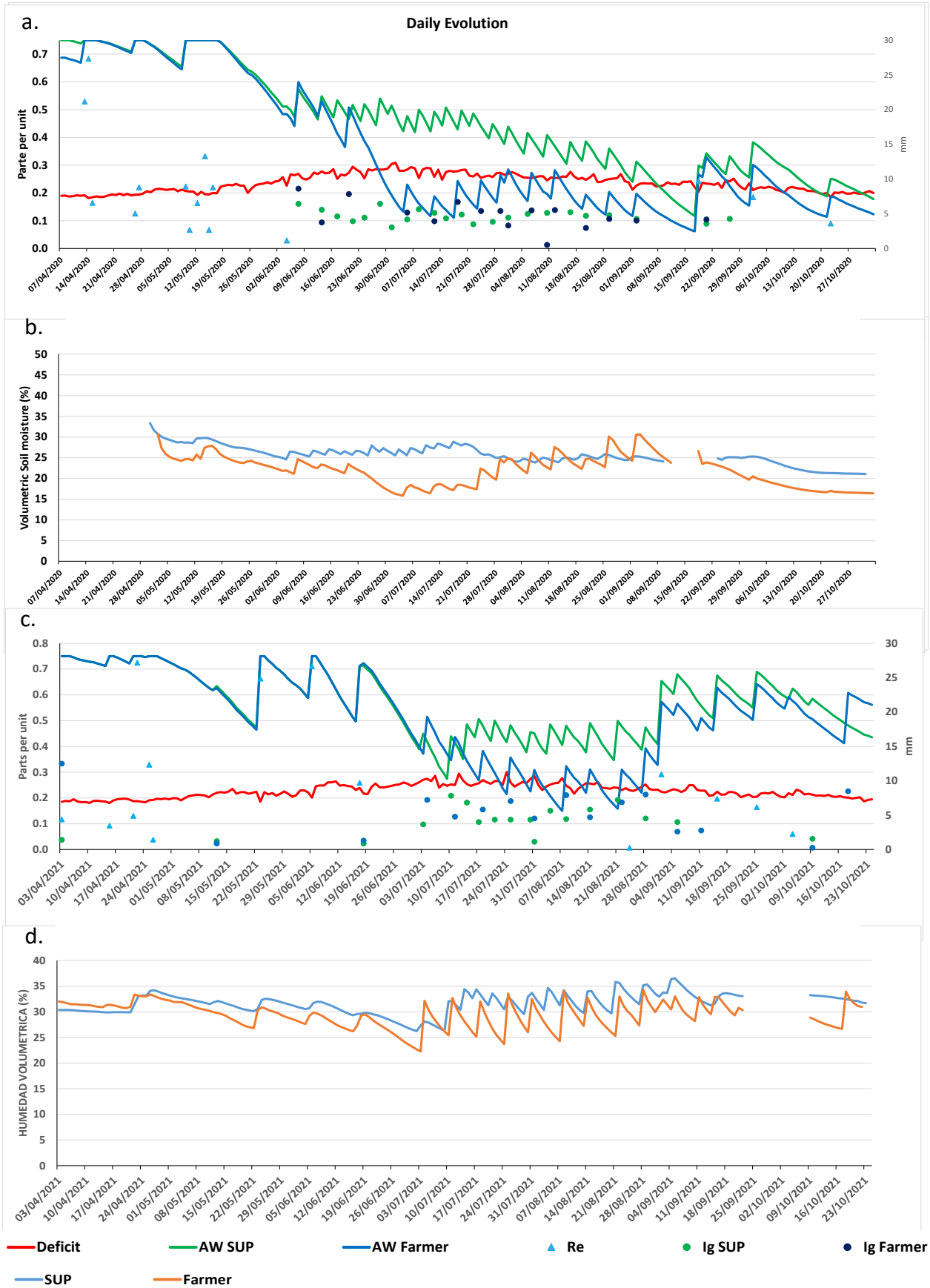

Figure 1: Fig. a. and c.: Evolution of AW (Available soil water) simulated by the MOPECO model for SUP and farmer management types in 2020 and 2021. Fig. b. and d.: Measured (Dill & Drop Senteck) available soil moisture progression for SUP and farmer management types in 2020 and 2021. Re: Effective Rainfall, Ig: Gross irrigation

4. Conclusions

The management of a vineyard crop based on the tools and methodologies included in the SUPROMED platform improved most of the KPIs calculated during the first year of the study. This result was corroborated during the second year, adapting the irrigation scheduling to distribute the available irrigation water allocation despite the variable climatic conditions.

The use of the MOPECO RDI irrigation scheduling tool, in combination with simple methodologies, such as the use of pressure transducers, pluviometers installed on the farm and evaluation of the irrigation system, allows farmers to distribute a limited amount of irrigation water, improving the yield and economic productivity of irrigation water. To determine irrigation scheduling, the MOPECO RDI tool requires calibration for the crops in the area and access to the data registered by a local agrometeorological weather station.

The use of soil analysis to calculate the nutrient balance of the crop may increase yield and reduce the use of fertilizer in some cases.

The widespread use of such tools and methodologies proposed by SUPROMED would help to improve the economic sustainability of Mediterranean-farms, especially those that suffer water scarcity.

Acknowledgements

This research was carried out under the framework of European project SUPROMED “GA-1813” funded by PRIMA, and the Regional project PRODAGUA “Ref SBPLY/19/180501/000144”, funded by FEDER and the Regional Government of Castilla-La Mancha. The authors thank the farmers participating in this research for their support in implementing the tasks and actions carried out over the two monitoring years.

References

Allen et al., 1998; Allen, R.G., Pereira, L.S., Raes, D., Smith, M., 1998. Crop evapotranspiration: guidelines for computing crop water requirements. In: Irrigation and Drainage Paper No. 56. FAO, Italy.

Cawthon et al. 1982. Effect of irrigation, fruit load, and potassium fertilization on yield, quality, and petiole analysis of COncor (Vitis lambrusca L.) grapes. American Journal of Enology and Viticulture 33, 145-148.

Domínguez Vivancos, A., 1989. Tratado de fertilizacion . Mundi-Prensa, Madrid.

Fernández et al. 2020 Fernández J.E.; Alcón. F.; Díaz-Espejo A.; Hernández Santana V.; Cuevas M.V. (2020). Water use indicators and economic analysis for on-farm irrigation decision: A case of study of a super high density olive tree orchard. Agricultural Water Management 237, 106074.

Intrigliolo, D.S. and Castel, J.R. 2010. Response of grapevine cv. ‘Tempranillo’ to timing and amount of irrigation: water relations, vine growth, yield and berry and wine composition. Irrig. Sci 28:113–125.DOI 10.1007/s00271-009-0164-1

MAPA, 2020 https://www.mapa.gob.es/es/default.aspx

Meier, 2001 Meier, 2001. Growth stages of mono- and dicotyledonous plants. BBCH Monograph.Federal Biolo. Res. Centre.Agric. Forestry 158 pp.

Ortega Álvarez, J.F., de Juan Valero, J.A., Tarjuelo Martín-Benito, J.M., López Mata, E., 2004. MOPECO: An economic optimization model for irrigation water management. Irrigation Science 23, 61–75. https://doi.org/10.1007/s00271-004-0094-x

Papadakis, J. 1966. Climates of the World and their Agricultural Potentialities. Hemisferio Sur. Buenos Aires, Argentina.

Pereira et al., 2020 Pereira L.S., Paredes P, Jovanovic N. 2020. Soil water balance models for determining crop water and irrigation requirements and irrigation scheduling focusing on the FAO56 method and the dual Kc approach. Agricultural Water Management 241 (4): 106357.

Sevacherian, V., Stern, V.M., Mueller, A.J., 1977. Heat accumulation for timing Lygus control pressures in a safflower-cotton complex. Joumal of Economic Entomology 70, 399-402.

SIAR – CLM. http://crea.uclm.es/siar/SIAR. https://eportal.mapa.gob.es//websiar/Inicio.aspx

Smart R.E., Robinson I.C., DueG.R., Brien C.J. 1985. Canopy microclimate modification for the cultivar Shiraz. II. Effects on must and wine composition. Vitis 24, 119-128.

Williams and Matthews, 1990 Williams, L.E., Matthews, M.A. (1990) Grapevines. In: Stewart BA, Nielsen DR (eds) Agronomy monograph #30 irrigation of agricultural crops. ASA-CSSA-SSSA Publishers, Madison, pp 1019–1055 .

Smartphone and sensor-based system for Forest Management tasks

Maras J. George[1], Andreopoulou S. Zacharoula[2]

[1]Laboratory of Forestry Informatics, Forestry and Natural Environment School of Forestry, Aristotle University of Thessaloniki, Thessaloniki, Greece
[2] Laboratory of Forestry Informatics, Forestry and Natural Environment School of Forestry, Aristotle University of Thessaloniki, Thessaloniki, Greece

Abstract. This paper presents a smart application for the needs of Forest Service personnel based on smartphone technology that engages inbuilt sensors. It also uses sophisticated artificial intelligence algorithms, as most cell phones or tablets are equipped with, today. It is a smartphone app that radically changes daily important management tasks in the forest by improving and speeding up the process of tasks. Collecting data from test plots, marking trees for logging, registering engineered wood and firewood, processed wood, etc. for forest management can now be done quickly and easily. The specific goals are:
- To be a multitool for forestry personnel that can be used effectively in site, - To collect and manage data in the Forest easily thanks to the new smartphone abilities, - To increase the reliability and validity of the data collected or recorded by forestry personnel during these operations, - To allow forestry personnel to view the data collected by the sensors on their device in a simple and understandable way, either directly on the device or by transferring or sending files from the device itself to a web app to any web browser.

1 Introduction

The adoption of sensor technologies and the advanced software developed for smartphones, contribute to the continuous improvements and expansions of their models. At the same time, their interactions with consumers are becoming increasingly intuitive, in real time, attractive, lovely, and valuable to them (Ajaegbu et al., 2019). This has radically changed the way they are used and now the basic function of the mobile phone, i.e., making calls has been significantly sidelined at the expense of other possibilities provided by advanced mobile devices (Giachetti & Marchi 2010, Gowthami & VenkataKrishnaKumar 2016). These capabilities today cover a huge range of activities and tasks in every area of our lives.
Especially for forests, trees and forest ecosystems, dozens of applications have been developed which focus mainly on the provision of general information and they are targeted to the public (Maras & Andreopoulou, 2019). For the needs of the forest service, a significant number of highly specialized applications have been developed at the same time, which in some cases tend to replace particularly expensive measuring or estimation instruments, such as the clinometer, hypsometer, relascope, GPS, etc.
This paper presents the results of part of the SmartForestry Tools project which is a doctoral thesis research. Some of the initial stages of the research had been presented at the 19th Hellenic Forestry Conference. Here part of our research is presented as well as the first two practical solutions that have already been developed and tested before they become available for wider use in each forest service.

1.1 Study of the forest service

The study of the diverse activities of the forest services and the use of information technology within them was one of the most important parts of the project. Consideration was given to the actions, needs and difficulties of an annual turnover of these services as well as their claims from the collection and registering in an annual database of forests, both for immediate use and for long-term preparation of management studies or even forest policy planning. At this stage, the introduction of informatics in the field of effective connection of the individual units of the Forest Service with each other and with the central administration was explored (Andreopoulou 2009b, Andreopoulou 2011c), in the support of decision-making (Athanasiadis & Andreopoulou, 2011a, Tasoulas & Andreopoulou, 2012, Tzoulis & Andreopoulou, 2013) and the dissemination and exploitation of recent innovations in Information and Communication Technologies (ICT) in forest practice.

1.2 Study of sensors and new intelligence mobile technologies

An important stage before the design and development of the first pilot application was the bibliographic research and then study of the existing applications already developed and used in forest practice, as well as the evaluation, analysis and investigation of the means and methods of their development. Through this stage, the value of the advanced software of smartphones was highlighted in combination with the new generation sensors with which they are now equipped and have radically changed the way they are used not only in

everyday life but even in forest work. The need for a separate sensors study and the new technologies developed in smartphones as well as the components that can be connected to them was considered a milestone in the further continuation of our research, as sensors were the common point in almost all the applications studied. From the initial stages of the sensors study, the possibilities of highlighting new solutions and new practices were revealed through their utilization in our work. Already several researchers have studied the advantages of smartphones that have various sensors and developed smartphone applications mainly for monitoring forest resources (Han & Wang 2011, Hemery 2012, Bijak and Sarzyński. 2015, Wu et al 2019). However, it was found that, in many cases, smartphone sensors, such as gyroscopes and position sensors, because they were designed mainly to meet the needs of the public in entertainment or games, show insufficient measurement accuracy in the professional monitoring of forest data (Molinier et. al 2016). So special category mobile phones were studied, such as some which have an RGB-D camera (Fan et.al., 2018), the use of artificial intelligence to estimate parameters (Kärhä et al. 2019) as well as combinations of smartphones and external devices with more accurate sensors (Lee et. al 2020). The tendency of the latest mobile phone models to be equipped with more than one camera and the ability to extract depth information, augmented reality and specialized artificial intelligence applications in forest data capture was a special stage of our research.

1.3 Purpose - Expected difficulties

The primary objective of the SmartForestry Tools project is to create new tools that will radically change important forest tasks by improving them not only in terms of ease, of application, and speed of execution, but mainly in terms of their standardization, reliability, and validity.

A prerequisite for the achievement of our goal is, beyond the study of the structure and work of the forest services, the recording and processing of data of frequency, gravity, degree of difficulty and achieved accuracy in the various stages of forest tasks execution, mainly on an annual basis. The data was processed using excel spreadsheets.

The difficulties we are expected to face are the in-depth analysis, understanding and learning of new technologies both at hardware level and in the way they are applied using specialized software, libraries, and an appropriate software development environment.

2 Materials and Methods

After the initial bibliographic search, investigation of the current situation in forest services and research of the processes and means of development of applications for mobile devices, the simulation and design of pilot applications began to start the first measurements and tests in practice. The data recordings and field tests of the improved version were carried out in the co-owned Poros Forest and another public forest with name Pyrgos[1]-Olympus. Both forests are in responsibility of the Pieria Forest Service. Initially the application was tested in May 2021 in the Forest Section (F.S.) with number 22, of the Poros Forest and then in the F.S.12 and 13, and in cluster 16b of the Pyrgos-Olympus Forest (Figure 1), during the period June 2021 to November 2021. The first tests were done via a personal mobile. In cluster 16b we had used Forest Service tablet. During the tree selection - marking the forester used the mobile phone or tablet while the ranger next to him, recorded the same data on paper in the traditional way. All tasks' times were recorded and identified advantages, plus any difficulties in the field from the use of the portable device. In cluster 16b, an external hand-held GPS, available to the service, was also used, recording the additional parameters that affect the GPS signal (such as canopy, average trees height, inclination, etc.) to compare it with the GPS of the mobile and to assess its accuracy in relation to purely professional tools.
The application of registers was tested in the above sections and in cluster 16b of the forest Pyrgos – Olympus after the logging. At the same time, we used and the classic way to receiving comparisons and drawing conclusions.
For each firewood stack registering, we took photos via mobile that had multiple cameras and we used a fixed length unit of measurement on the frontage of the stack. Also, we recorded the shooting distance of each photo. This data was then processed to continue the research to automatically estimate stack volume from stereoscopic photographs and artificial neural networks. This specific stage of our research is still in progress.

[1] Pyrgos means Tower

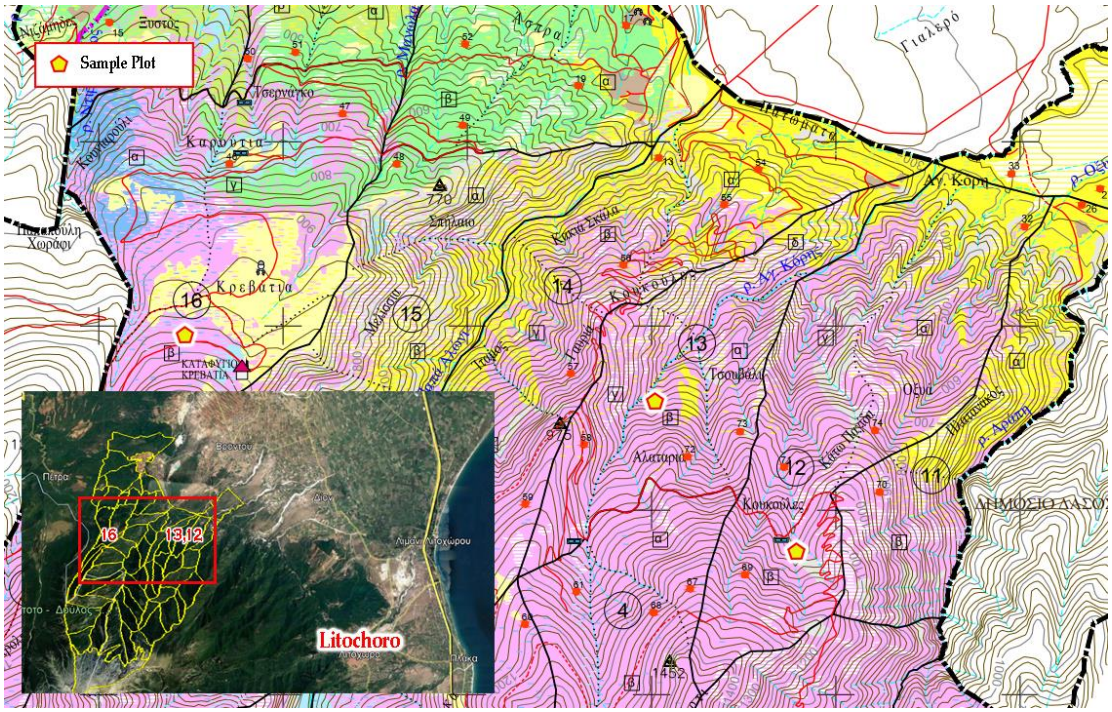

Figure 1. Location of the study area and sample plots. Background map: a) Forest management map & b) Google Earth, 2021.

The first versions of the application had been developed with Angular 2 and the use of the Ionic Framework (Maras & Andreopoulou, 2019) but the research continued, and Flutter came up as the most ideal solution. Flutter is an open-source User Interface (UI) toolkit that allows from one codebase, the creation of applications for different platforms of both Android, iOS, web, and desktop devices such as Windows, macOS and Linux (Katz et. Al, 2021). For the development of the code was used instead of Android Studio, which was the original development environment of Flutter, visual studio code, which is a code development environment that supports many UI such as Flutter, (Website: code.visualstudio.com, 2021). Of course, Android Studio also had to be installed to access the Android SDK and Android emulators. Our code is all in Dart language.

3 Results

The latest version of application has been installed and tested on mobile phones and tablets of the Pieria Forest Service. The two fully functional tools of this version can be used, one in the work of tree marking and the other in the timber and stack registering. The superiority with the use of the application was obvious from the first day. Detailed results will be published at doctoral thesis. As for the most important features of the application, these are:

1. Almost all measurements and data in the application are stored in an external SQLite database which facilitates, in addition to their storage, the execution of complex queries and faster extraction of results. The database was deemed necessary for the information to be continuously stored in it. Suggested to prefer mobile devices with external memory (SD) to protect data in case of accidental fall or destruction of the rest device.
2. Applying relationships between database tables for greater efficiency, control, error reduction, and data integrity.
3. The user can customize too many functions, even the theme (appearance) of the application from the main options menu.
4. Screens (Figure 2) with characteristic themes depending on the tools or forest species selected by the user.
5. In every data recording or registering of any measurement, automatically stored additional sensors information (GPS, compass, 3D accelerometer, etc.). In this way it is possible to display them on a map or specialized diagrams, to search for data based on time or geographical coordinates, but also to ensure the uniqueness and validity of these data.
6. There is a map display for the presentation of registration data in which, in the form of characteristic icons, the data are displayed on a satellite background.

7. It is currently permissible to insert and view on a map of GeoJSON files with the ability to select and display specific characteristics of the geometric objects in this file. For example, the appearance of cluster numbers, forest names, etc.
8. The outgoing file with all registered data, GPS measurements and observations/comments is binary, encoded and almost impossible to hacked by any ordinary user.

Figure 2. SmartForest Tools, version 2.0.0, application architecture diagram

4. Discussion - Conclusions

The development of all code relies on libraries and tools licensed to distribute open source, to avoid technical commitments from third parties (Majchrzak et.al. 2017) Choosing Flutter as the main interface ultimately seems to be perhaps the best choice as Flutter besides exhibits continuous and upward preference and popularity (Website: insights.stackoverflow, 2022), (see Figure 3).

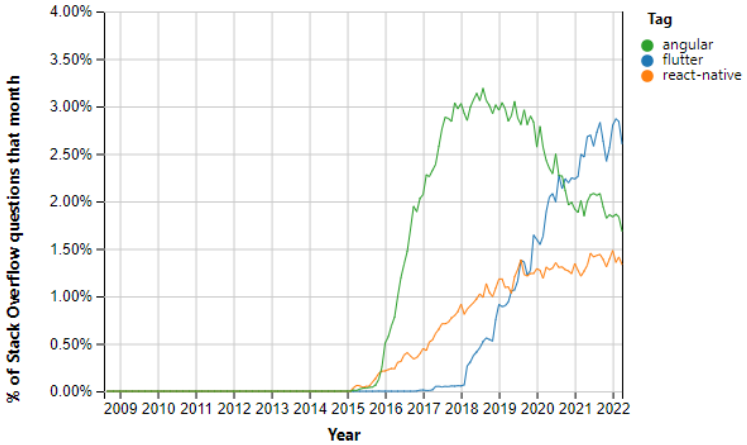

Figure 3. Trends diagram of flutter. Source (Website: insights.stackoverflow, 2022).

The project is aimed at two groups of potential users. Forest personnel of the countryside by radically changing important management tasks within the forest, mainly during data collection, and forest employees - designers in offices, who for the first time they can receive rural data and measurements certified for their validity and enriched with additional information that provides them with new possibilities in their scientific work.
Through research in the context of the implementation of the SmartForestry Tools project, new tools are being developed. Two of them already offer substantial assistance, speed and reliability and will be widely used by forest service personnel. Many are still in the experimental stage, such as those that operate on neural networks. They are currently being tested on simulators. An important part of the research was the standardization and correlation of data and finally the creation of a proper database, capable of immediate future use even in GIS extensions. The research so far to extract the volume of firewood piles from mobile device photos, using convolutional neural networks and image segmentation, will require the greatest effort. Probably a combination of additional parameters and techniques (in a row continuous photos or videos with a few measurements) because as shown in the image 1 below, in Greek forests, the concentration of firewood is usually done in piles, several meters long on either side of the forest roads or in successive parallel stacks with a short distance between them.

Image 1. Two ordinary cases of firewood concentration in Greek forests

To sum up, the main advantages of using the first two tools, that are expected to be used soon in every Greek Forest Service, are:

1. Standardization and ensuring the proper storing of registering or tree-marking data by each employee.
2. Faster measurement recording times with simultaneous recording of information of various sensors. This achieves the projection on a map or table of the positions or values of each measurement and the possibility of additional processing and extra information extraction.
3. Display observations and results straight away in the forest allowing the forest personnel to make appropriate decisions about dependent management tasks.
4. Importing task or information data into database tables with a preview of them at any time and possibility to modify, to addition or deletion them.
5. Validating every registering data to prevent accidental errors when enter them.
6. Certificating and validating of the actual collection data in the field, thanks to the additional unique information's that stored in each recording and the method of creating a coded file which is difficult to hacked.
7. Accessing maps with wealth of important management information, directly in the field
8. Zero use of paper throughout the period of wood registering or tree marking operations in the forest.

Based on the results of this study, the first steps of our work were mapped out and further development was determined. Outcomes was also basis for defining architecture for individual pilot cases. The pilot solution chosen for the implementation of the first applications can be completed within the duration of the thesis and is expected to be a precursor for future upgrading and expansion of these results. This study is also the basis for the preparation of a broader plan for the technical implementation and development of similar projects in Forest Services.
Based on the above and the results of the tests to date, the new tools using smart phones are expected to completely replace years of practice and become the next generation tools in forest practice.

References

Ajaegbu, O.O., Ajaegbu, C., & Sodeinde, O.A. (2019). Smartphone technological advancement trends: A scheme for knowledge acquisition towards societal development. Information Technology Journal, 18, 1-7

Andreopoulou, Z. S. (2007a). E-organization of forest records in Greece. Journal of Environmental Protection and Ecology, 2(8), 455-466.

Andreopoulou, Z. S. (2009b). Adoption of information and communication technologies (ICTs) in public forest service in Greece. Journal of Environmental protection and Ecology, 10(4), 1194-1204.

Andreopoulou, Z. S. (2011c). Introducing computer and network services and tools in forest service and the HR factor. Journal of environmental protection and ecology, 12(2), 761-768.

Athanasiadis, A., & Andreopoulou, Z. S. (2011a). DSS Applications in Forest Policy and Management: Analysis of Current Trends. In HAICTA (pp. 549-557).

Bijak S., Sarzyński.J., (2015). Accuracy of smartphone applications in the field measurements of tree height. Folia ForestaliaPolonica, series A, 2015, Vol. 57 (4), 240–244

Fan, Y., Feng, Z.,Mannan, A., Khan, T.U.,Shen, C., Saeed, S. (2018) Estimating tree position, diameter at breast height, and tree height in real-time using a mobile phone with RGB-D SLAM. Remote Sens. 2018, 10, 1845

Giachetti, C., Marchi, G., (2010) Evolution of firms' product strategy over the life cycle of technology-based industries: a case study of the global mobile phone industry, 1980–2009, Bus. Hist., 52 (2010), pp. 1523-1550

Gowthami, S., & VenkataKrishnaKumar, S. (2016). Impact of smartphone: A pilot study on positive and negative effects. International Journal of Scientific Engineering and Applied Science (IJSEAS), 2(3), 473–478

Han, D., & Wang, C. (2011) "Tree height measurement based on image processing embedded in smart mobile phone," in Proceedings of the in 2011 International Conference on Mul- timedia Technology, pp. 3293–3296, Hangzhou, China, July 2011.

Hemery G. (2012) mensuration on a smartphone. Forest Available on page https://gabrielhemery. com/forest-mensuration-on-a-smartphone/. Visit 15 May 2019

Kärhä K, Nurmela S, Karvonen H, Kivinen V-P, Melkas T, Nieminen M (2019) Estimating the accuracy and time consumption of a mobile machine vision application in measuring timber stacks. Comput Electron Agric 158: 167–182

Katz M, Moore K D and Ngo V (2021) Flutter Apprentice (First Edition): Learn to Build CrossPlatform Apps (McGaheysville: Razeware LLC) 615

Lee, S., Fan, G., Dong, Y., Chen, D., Chen, F., (2020), New Method for Forest Resource Data Collection Based on Smartphone Fusion with Multiple Sensors, Mobile Information Systems, Hindawi, Mai 2020

Maras, G, & Andreopoulou, Z. S. (2019). Application of mobile telephony technologies in forestry, pre-labelling using smart devices, 19th Hellenic Forestry Conference, Litochoro, 29 Sep - 02 Oct 2019, pp. 232-239 Sep 2019

Molinier, M., Lopez-Sanchez, C., Toivanen T., et al., (2016) "Relasphone-mobile and participative in situ forest biomass measurements supporting satellite image mapping," Remote Sensing, vol. 8, no. 10, p. 869.

Tasoulas, E. A., &Andreopoulou, Z. S. (2012). Integrated administration ICT system in forest environments supporting proper management. Journal of Environmental Protection and Ecology, 13(1), 338-344.

Tzoulis, I., &Andreopoulou, Z. (2013). Emerging traceability technologies as a tool for quality wood trade. Procedia Technology, 8, 606-611.

Website: code.visualstudio.com [online]. [Access Date: 10 Mar 2021]. Dikt. Place: <https://code.visualstudio.com/docs>

Website: insights.stackoverflow [online]. [Access Date: 7 Mai 2022]. Dikt. Place: <https://insights.stackoverflow.com/trends?tags=flutter%2Creact-native%2Cangular>

Wu, X., Zhou, S., Xu, A., and Chen, B. "Passive measurement method of tree diameter at breast height using a smartphone," Computers and Electronics in Agriculture, vol. 163, Article ID 104875, 2019.

Combining the use of Sentinel-2 radiance and Sentinel-3 thermal bands to retrieve actual evapotranspiration values: Application in central Spain.

Spiliotopoulos, M.[1], I. Faraslis[2], N. Alpanakis[1], G. Tziatzios[1], S. Sakellariou[1], P. Sidiropoulos[1], V. Brisimis[1], A. Blanta[1], G. Karoutsos[3], N. Dercas[4], N.R. Dalezios[1]

[1] Department of Civil Engineering, University of Thessaly, Volos, Greece
[2] Department of Environmental Sciences, University of Thessaly, Larisa, Greece
[3]General Aviation Applications "3D" S.A., 2 Skiathou str, 54646, Thessaloniki, Greece
[4] Department of Natural Resources and Agricultural Engineering, Agricultural University of Athens, Greece

Abstract. Obtaining useful spatial information and describing difficult physical processes is important for developing better agricultural practices. In this study a combination of Sentinel-2 and Sentinel-3 images for daily crop evapotranspiration estimation is presented and applied to the region of "La Mancha Oriental", Spain. The applied approach has been first operated by ESA, using the Sen-ET plugin. In this study, the purpose of the Sen-ET SNAP plugin is to enable estimation of daily actual evapotranspiration (and other land-surface energy fluxes) at field scale using Sentinel-2 (S2) and Sentinel-3 (S3) satellite observations, as well as meteorological data outputs available from WRF Model. The applied methodology follows seventeen separate steps and is well described and applied at the study area. The results seem very satisfactory and in accordance with new economic optimization model for irrigation water management – MOPECO tested and used at the study area.

1 Introduction

The role of effective irrigation management for optimal food production is well recognized in literature (Tilman et al., 2002). This problem can be possibly solved through the improvement of water use efficiency (WUE) for irrigation to achieve sustainable intensification of irrigated agriculture. At the farm level, to control the adequacy of the water applied to actual crop requirements, net irrigation water requirements (NIWR) are needed. Indeed, NIWR is the water that must be supplied by irrigation to satisfy evapotranspiration, leaching and additional water supply, which is not provided by water stored in the soil, as well as precipitation entering the soil (Jensen et al., 1990). Specifically, computation of NIWR is based on the estimation of crop water requirements (CWR) and soil water balance, where crop evapotranspiration (ET_c) is the main component. There is a continuous research effort to estimate ET_c, CWR and NIWR (Mateos *et al*., 2013; Calera *et al*., 2017; Campos et al., 2017). Irrigation water management generally requires continuous monitoring and reliable information at specific spatial and temporal scales about the soil and plant conditions across farms (Pinter *et al*., 2003).

Earth observation (EO) using Remote sensing (RS) has already become an important tool for the quantification and the detection of the spatial and temporal distribution and variability of several environmental variables at different scales. Remotely sensed models are currently considered suitable for crop water use estimation at field, as well as regional scales (Bastiaanssen, 2000; Calera et al., 2017). Having the knowledge of crop water requirements, irrigation can be supplied either to satisfy full requirements, or to manage a deficit-controlled irrigation. The most prevailing group of Earth Observation methodologies for the estimation of ET_c today is the Energy Balance (EB) algorithms and more specifically the residual methods (Romaguera et al., 2014). Remote sensing-based EB algorithms convert satellite sensed radiances into land surface characteristics, such as albedo, leaf area index, vegetation indices, surface roughness, surface emissivity and surface temperature to estimate ET as a "residual" of the land surface energy balance equation.

Most recent EB models differ mainly in how Sensible Heat H is estimated (Gowda et al., 2007). These models include the Two Source Model (TSM) (Kustas and Norman 1996), where the energy balance of soil and vegetation are modeled separately and then combined to estimate total LE. Such models are the Surface Energy Balance Algorithm for Land (SEBAL) (Bastiaanssen et al., 1998a and 1998b), the Mapping Evapotranspiration with Internalized Calibration (METRIC) (Allen et al., 2007) that uses hot and cold pixels within the satellite images to develop an empirical temperature difference equation and the Surface Energy Balance Index (SEBI) (Roerink et al.,2000; Menenti and Choudhury, 1993) based on the contrast between wet and dry areas. Other variations of SEBI include the Simplified Surface Energy Balance Index (S-SEBI) (Roerink et al., 2000), and the Surface Energy Balance System (SEBS) (Su, 2002). All the above are the prevailing EB methodologies until now (Jaber et al., 2016; Jaafar and Ahmad, 2019).

2 Methodology

2.1 Merging Sentinel-2 and Sentinel-3 for daily actual evapotranspiration estimation

The use of Sentinel-2 and Sentinel-3 satellite data to estimate daily actual evapotranspiration has been first initiated by ESA, called Sen-ET (ESA, 2020). The initial (by ESA) Sen-ET (Sentinels for evapotranspiration) plugin in SNAP uses the two-source energy balance (TSEB) model with Sentinel-2, Sentinel-3 and meteorological data from ECMWF. The Sentinel-2 MSI sensor provides optical reflectance data, while the Sentinel-3 SLSTR TIR sensor is used to obtain land surface temperature (LST). It was developed as part of the Sen-ET project (http://esa-sen4et.org/) and consists of open-source Python libraries and thin wrapper enabling execution from within SNAP graphical user interface (GUI). The Sen-ET SNAP plugin is designed to process a whole Sentinel-2 scene and a corresponding subset of a Sentinel-3 LST product sharpened to Sentinel-2 resolution, while TSEB model requires many inputs and internal parameters. TSEB methodology uses a system of temperature gradient-resistance equations that are solved by an iterative secant procedure developed by Norman et al. (1995) in which an initial estimate of canopy latent heat flux (i.e., plant transpiration) under non-water-stressed conditions is related to the other energy components, as described below. The TSEB model was first proposed in Norman et al. (1995), with important adjustments described in Kustas and Norman (1999). Its main inputs are LST, derived from thermal infrared (TIR) radiation, vegetation structural properties (e.g LAI, canopy height) and meteorological forcing. In this study, the adopted methodology follows seventeen steps and is based on the TSEB model. There is a modification of the initial Sen-ET SNAP by ESA, and the proposed methodology uses meteorological data from WRF model, instead of ECMWF.

Previously, methodologies like METRIC model are based on satellite images and meteorological data using the SEB methodology (Allen *et al*., 2007). The methodology considers that evaporation consumes energy. Since satellite images provide information only for the overpass time, METRIC computes an instantaneous ET flux for the image time. The related ET values can be extrapolated then using a ratio of ET to reference crop ET to obtain daily or seasonal levels of ET. ET flux is calculated for each pixel of the image as a “residual” of the surface energy budget equation, where soil heat flux (G) and sensible heat flux (H) are subtracted from the net radiation flux at the surface (R_n) to compute the “residual” energy available for evapotranspiration (λET) (eq.1).

$$LE = \lambda ET = R_n - H - G \quad (1)$$

where LE is the latent heat flux (W/m^2), λ is the latent heat of vaporization, R_n is net radiation (W/m^2), G is soil heat flux (W/m^2) and H is sensible heat flux (W/m^2).

Net radiation flux at the surface (R_n) represents the actual radiant energy available at the surface, considering losses and gain as follow:

$$R_n = R_{S\downarrow} - \alpha R_{S\downarrow} + R_{L\downarrow} - R_{L\uparrow} - (1-\varepsilon_o)R_{L\downarrow} \quad (2)$$

where:

$R_{S\downarrow}$ is the incoming shortwave radiation (W/m^2), α is the surface albedo (dimensionless), $R_{L\downarrow}$ is the incoming longwave radiation (W/m^2), $R_{L\uparrow}$ is the outgoing longwave radiation (W/m^2), and ε_o is the surface thermal emissivity (dimensionless). Further details about METRIC methodology can be found on literature (Monin and Obukhov, 1954; Bastiaanssen et al., 1998a;1998b, Allen et al., 2007).

The principal source of uncertainty within TSEB lies in the estimation of the sensible heat flux (H), which is calculated through the heat transport equation (eq. 3).

$$H = \frac{rC_p(T_0 - T_A)}{R_H} \quad (3)$$

where H is sensible heat flux (W m^{-2}); is the volumetric heat capacity of air (J m^{-3} K $^{-1}$); is the aerodynamic temperature of the surface (K); is the air temperature at a reference/measurement height (K); and is the aerodynamic resistance to heat transport (s m^{-1}).

LST obtained from TIR remote sensing can differ up to several degrees compared to the aerodynamic surface temperature (Norman et al., 1995; Burchard-Levine *et al*., 2019), and their relationship is not well established (i.e. Colaizzi *et al*., 2004). TSEB, thus, tackles this by assuming that the total blackbody thermal radiance that is emitted by the bulk surface is weighted by the fraction of vegetation observed by the sensor and the emission of both soil and vegetation surfaces, as expressed in eq. 4 taken from Norman *et al*. (1995):

$$LST(\theta) = [f(\theta)T_c^4 + (1 - f(\theta)T_s^4)]^{1/4} \quad (4)$$

where f(θ) is the fraction of vegetation observed by the TIR sensor at an angle θ and is mainly a function of LAI; T_c is the vegetation canopy temperature (K); and T_s is the soil surface temperature (K). Using this scheme, TSEB avoids the use of an empirical method to link radiometric and aerodynamic surface temperature, such as the use of excess resistance in SEBS (Su, 2002) or the use of hot and cold end member pixels in METRIC (Allen et al., 2007) and SEBAL (Bastiaanssen *et al*., 1998;). Further information about TSEB methodology can be found in the literature (Norman et al., 1995; Colaizzi *et al*., 2004; Burchard-Levine *et al*., 2019).

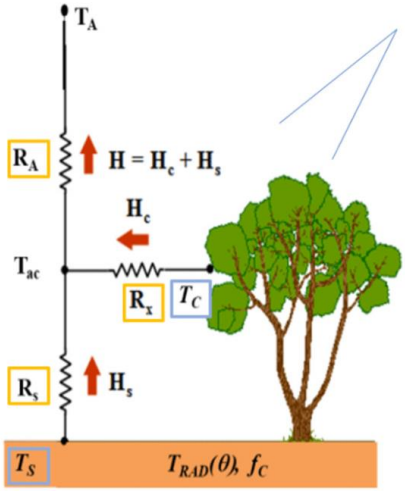

Figure 1.TSEB Sensible Heat model scheme (adapted from Kustas and Anderson, 2009)

2.2 MOPECO model

MOPECO (Economic optimization Model for Irrigation Water Management) developed by University of Castilla-La-Mancha in Spain (Domínguez et al., 2012), is a simulation model helping with the decision-making process for the management of the agricultural systems at farm level, taking into account both human and livestock feeding. The model uses different growth stages of the crop, and optimizes production, taking into account the effect on the quality of the crops. The model's outputs are mainly water irrigation management strategies, among others (Alvarez et al., 2004). It uses the concept where when ET values are larger than the available irrigation or/and precipitation water, then the plant may suffer from stress having serious impacts to the final crop yield (Domínguez et al., 2012). MOPECO has user-friendly graphics and has been used worldwide to support the availability of water, as well as crops' behavior under different climatic scenarios (López-Urrea et al., 2009).

The objectives of the present study were to compute Sen-ET SNAP outputs for the study region and to validate the results through MOPECO outputs for selected agricultural crops.

3 Data Base and Study Area

3.1 Data Base

Thirteen (13) Sentinel-2 scenes for the study area during the year 2020 were selected and downloaded. Finally, five out of thirteen Sentinel-2 images passed the quality control for the present study (Table 1).

Table 1. Selected Sentinel-2 scenes for central Spain

A/A	Sentinel -2	Acquisition Date	Max Cloud Cover %	Quality control	Comments
1	2 Scenes Level2	03 March 2020	99	Failed	Clouds over the area
2	2 Scenes Level2	09 March 2020	86.5	Failed	Clouds over the area
3	2 Scenes Level2	14 March 2020	11.3	Failed	Clouds over the area
4	**2 Scenes Level2**	**29 March 2020**	**3**	**Passed**	**Good**
5	2 Scenes Level2	03 April 2020	17	Failed	Clouds over the area
6	**2 Scenes Level2**	**08 April 2020**	**12.3**	**Passed**	**Good**
7	2 Scenes Level2	18 April 2020	83.4	Failed	Clouds over the area
8	2 Scenes Level2	28 April 2020	77	Failed	Clouds over the area
9	**1 Scene Level2 & 1 Scene level1**	**03 May 2020**	**6.8**	**Passed**	**Level 2, has corrupted bands. Level 1, Atmospheric correction was performed**
10	2 Scenes Level2	08 May 2020	14.2	Failed	Clouds over the area
11	2 Scenes Level2	13 May 2020	98.2	Failed	Clouds over the area
12	**1 Scene Level2 & 1 Scene level1**	**18 May 2020**	**0.9**	**Passed**	**Almost good**
13	**2 Scenes Level2**	**23 May 2020**	**26**	**Passed**	**Good**

3.2 Spanish Case study area.

The study area is the Spanish region “La Mancha Oriental”, which occupies about 7,150 km^2. The region is located at the South-east of the Iberian Peninsula. It is characterized by relatively flat surface averaging 500 to 600 meters in altitude (**Σφάλμα! Το αρχείο προέλευσης της αναφοράς δεν βρέθηκε.**).

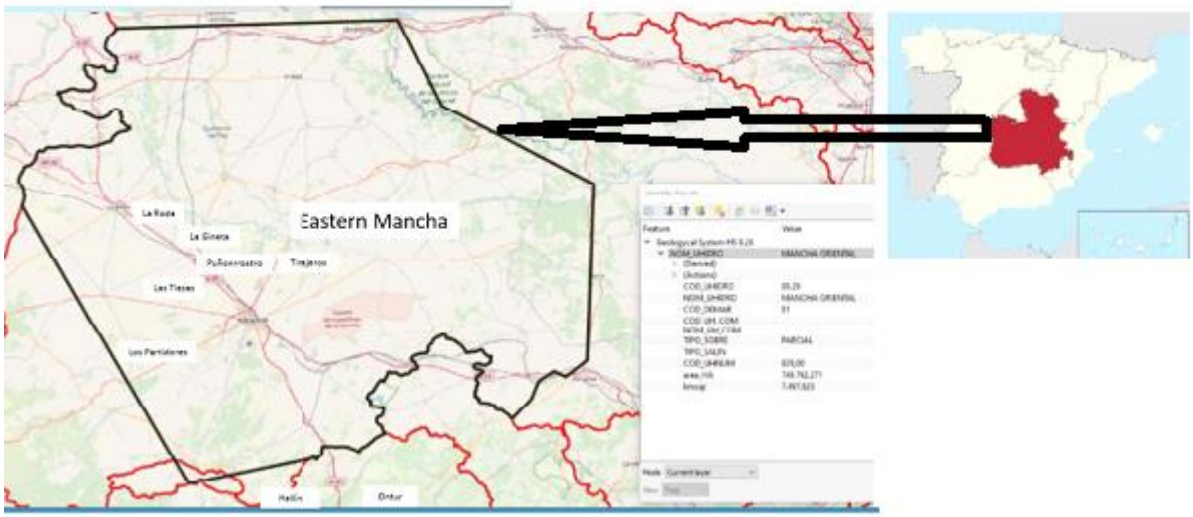

Figure 2. Map of the study area: “La Mancha Oriental”, Albacete, Spain.

Twenty five (25) plots in total located within the study area are selected and processed. Details about the plots and crop types are depicted in Table .

Table 2. Location and type of plots in study area

Crop	Region	Number of fields
Barley	Los Partidores, La Chericoca	5
Garlic	Aguas Nuevas, Los Partidores,	3
Forage Oat	Los Partidores	3
Alfalfa	Tinajeros, Punon Rostro	3
Almond	Las Tiesas, Hellin, La Roda Photovoltaic energy	4
Pistachio	Las Tiesas, La Gineta	2
Vineyard	Ontur	4
Olive	Ontur	1

4 Results and discussion

ET values taken as output of Sen-ET plugin are derived for the study area. The values are mapped as an image and are assigned to the specific fields under consideration. This task has undertaken for all the crop fields of the study. Figure 3 illustrates an example of ET_a values for a Pistachio field with a spatial resolution of 20x20m for 29/03/2020, 08/04/2020, 03/05/2020, 18/05/2020, and 23/05/2020.

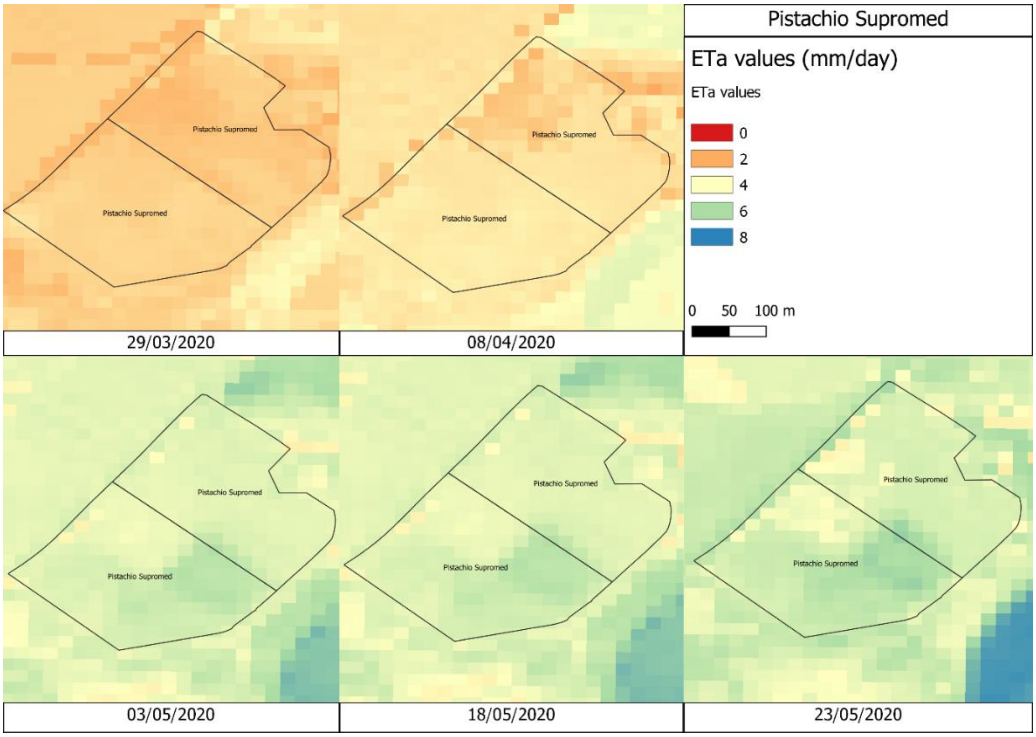

Figure 1. ETa values for Pistachio: Sentinel-2 & Sentinel-3 satellite images (per pixel: 20x20m) for the following dates: 29/03/2020, 08/04/2020, 03/05/2020, 18/05/2020, 23/05/2020 for Albacete,Spain

Tabulated values from MOPECO are also derived and tested against the satellite-based values. Separate correlation procedures for all crops under consideration were undertaken and the related statistics have been computed. Figure 4 illustrates an example for Barley and Oat mean values

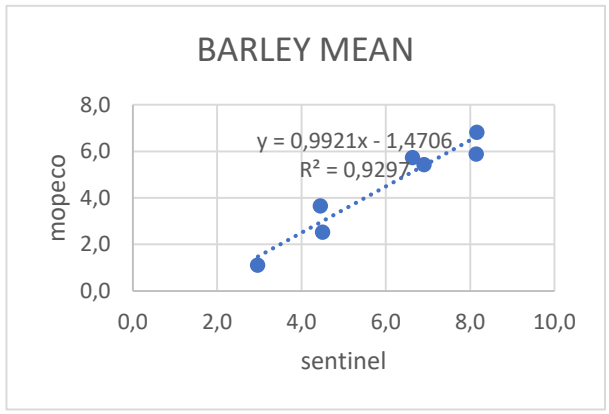

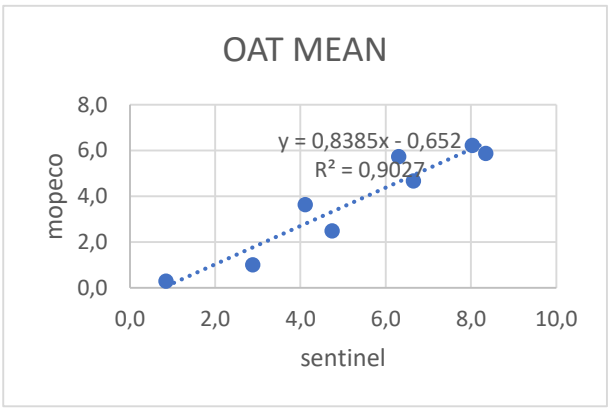

Eff	RMSE	BIAS	CORREL	R^2
0,30	2,45	-1,5	0,96	0,93
1	0	0,0	1	1

Eff	RMSE	BIAS	CORREL	R^2
0,38	2,61	-1,5	0,95	0,90
1	0	0,0	1	1

Figure 4. ETa values for Pistachio Supromed: Sentinel-2 & Sentinel-3 satellite images (per pixel: 20x20m) for the following dates: 29/03/2020, 08/04/2020, 03/05/2020, 18/05/2020, 23/05/2020 for Spain

A significant variation between the crops was found. For example, for barley fields Eff index is 0,5964 and RMSE is 0.47 while R^2 is 0.8287. For garlic Eff index is 0.56, RMSE is 0.61 and R^2 is 0.8648. For oat fields, Eff index is 0.43, RMSE is 0.57and R^2 is 0.76. For alfalfa, Eff index is 0.16, RMSE is 0.35 and R^2 is 0.21. The reason for the different response of alfalfa might be assigned to the different agricultural practices among the farmers (Spiliotopoulos *et al*., 2015). For that reason, all the values for all crops are combined in one graph, and it seems that the total procedure has an improved R^2 (0.59). The total graph is depicted in Figure 5. A simple linear relationship between Sentinel and MOPECO derived values seems to be very encouraging

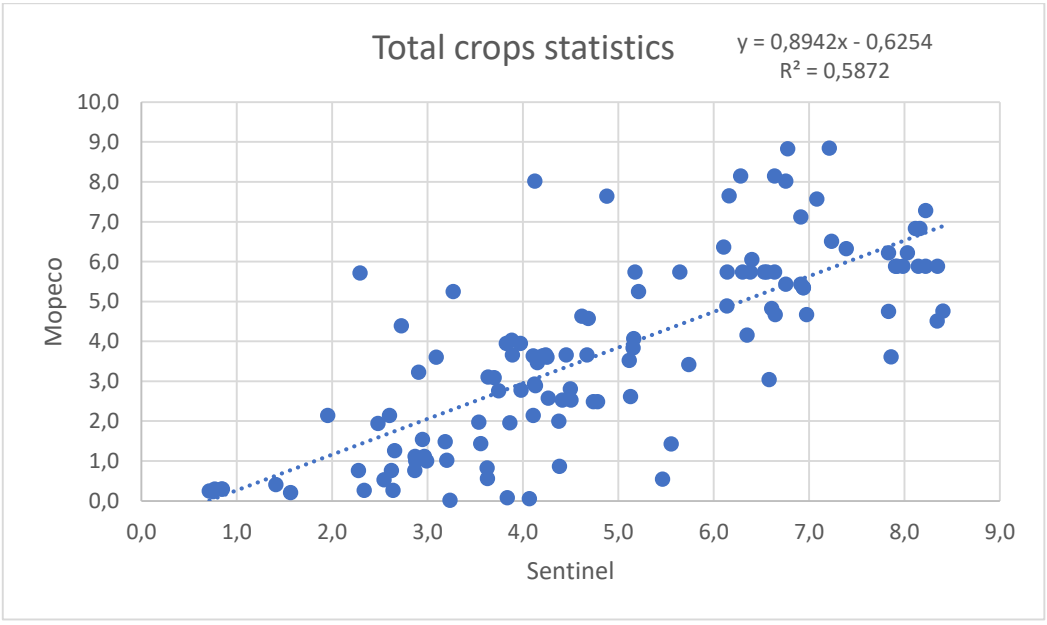

Figure 5. ETa values derived from Sentinel-2 & Sentinel-3 satellite images (per pixel: 20x20m) versus MOPECO outputs for Albacete Spain

5 Summary and conclusions

At this study, a new Sentinel-2/Sentinel-3 satellite-based approach has been utilized in Albacete, central Spain, considered meteorological data from WRF model. Comparisons between satellite and in-situ based ET values through MOPECO model were undertaken for all the crops in the study area. Significant differences between different crop fields were tested and examined, but the total appearance of the procedure seems to be very satisfactory as it seems from the total statistics. With the advancement of technology, new Sentinel sensors will improve the existing accuracy and the errors are expected to minimize.

Acknowledgements

This work has been funded by SUPROMED "Sustainable Production in water limited environments of Mediterranean agroecosystem". R&I project funded under the PRIMA 2018 program section I.

References

Allen, R., Tasumi, M. and Trezza, R., 2007. Satellite-Based Energy Balance for Mapping Evapotranspiration with Internalized Calibration (METRIC)-Model. Journal of Irrigation and Drainage Engineering 133, 380-394, doi:10.1061/(asce)0733-9437(2007)133:4(380) (2007).

Alvarez, J. F. O., de Juan Valero, J. A., Martin-Benito, J. M. T. and E. L. Mata. 2004. MOPECO: an economic optimization model for irrigation water management. Irrigation Science, 23(2), 61-75.

Bastiaanssen, G.M.W.,2000. 'SEBAL-based sensible and latent heat fluxes in the irrigated GedizBasin, Turkey', Journal of Hydrology, Vol. 229, Nos. 1–2, pp.87–100.

Bastiaanssen, W. G. M., Menenti, M., Feddes, R. A. and Holtslag, A. A. M., 1998. A remote sensing surface energy balance algorithm for land (SEBAL) 1. Formulation. Journal of Hydrology 212, 198-212, doi:http://dx.doi.org/10.1016/S0022-1694(98)00253-4 (1998). (a)

Bastiaanssen, WGM, Pelgrum, H, Wang, J, Ma, Y, Moreno J, Roerink, GJ, van der Wal T, 1998b. The Surface Energy Balance Algorithm for Land (SEBAL): Part 2 validation, J. Hydrology, 212-213: 213-229.

Burchard-Levine, V., Héctor Nieto, H., Riaño,D., 3, Migliavacca, M., El-Madany, T.S., Perez-Priego, O., Carrara, A., and Martín, P.M., 2019. Adapting the thermal-based two-source energy balance model to estimate energy fluxes in a complex tree-grass ecosystem.Hydrology and Earth System Sciences Discussions, https://doi.org/10.5194/hess-2019-354 Preprint.

Calera, A., Campos, I., Osann, A., D'Urso, G., Menenti, M., 2017. Remote Sensing for Crop Water Management: From ET Modelling to Services for the End Users. Sensors 17(5), pp.1104.

Campos, I., Neale, C.M.U., Suyker, A.E., Arkebauer, T.J. and Gonçalves, I.Z. (2017) 'Reflectance-based crop coefficients REDUX: for operational evapotranspiration estimates in the age of high producing hybrid varieties', Agricultural Water Management, Vol. 187, pp.140–153.

Colaizzi, P.D., Evett, S.R., Howell, T.A., and Tolk, J.A.: Comparison of aerodynamic and radiometric surface temperature using precision weighing lysimeters, Remote sensing and modeling of ecosystems for sustainability, 5544, 215-230, 700 International Society for Optics and Photonics. https://doi.org/10.1117/12.559503, 2004.

Domínguez, A., R.S. Martínez, J.A. de Juan, A. Martínez Romero and J.M. Tarjuelo. 2012. Simulation of maize crop behavior under deficit irrigation using MOPECO model in a semi-arid environment. Agricultural Water Management, 107:42–53. DOI: 10.1016/j.agwat.2012.01.006

ESA, 2020. USER MANUAL FOR SEN-ET SNAP PLUGIN. V1.1.0 March 19, 2020, 37 pages.

Gowda PH, Chávez JL, Howell TA, Marek TH, New LL. (2008). Surface Energy Balance Based Evapotranspiration Mapping in the Texas High Plains. Sensors. 8(8):5186-5201.

Jaafar, H.H., Ahmad, F.A., 2020. Time series trends of Landsat-based ET using automated calibration in METRIC and SEBAL: The Bekaa Valley, Lebanon. Remote Sensing of Environment Volume 238, 1 March, 111034, https://doi.org/10.1016/j.rse.2018.12.033.

Jaber, H.S., Mansor, S., Pradhan, B., Ahmad, N., 2016. Evaluation of SEBAL model for Evapotranspiration mapping in Iraq using remote sensing and GIS. International Journal of Applied Engineering Research, 11 (6), pp. 3950-3955.

Jensen, E.M., Burman, D.R. and Allen, G.R., 1990. 'Evapotranspiration and irrigation water requirements', in ASCE Manuals and Reports on Engineering Practices, American Society of Civil Engineers, New York, NY, No. 70, p.360.

Kustas, W. P. and Norman, J. M.,1996. Use of remote sensing for evapotranspiration monitoring over land surfaces. Hydrological Sciences Journal 41, 495-516, doi:10.1080/02626669609491522 (1996).

Kustas, W.P., and Anderson, M.C.: Advances in thermal infrared remote sensing for land surface modeling, Agricultural and Forest Meteorology, 149, 2071–2081, 2009.

Lopez-Urrea, R., Olalla, F.M.D., Montoro, A., and P. Lopez-Fuster. 2009. Single and dual crop coefficients and water requirements for onion (Allium cepa L.) under semiarid conditions. Agricultural Water Management, 96, pp.1031–1036.

Mateos, L., González-Dugo, M.P., Testi, L. and Villalobos, F.J., 2013. 'Monitoring evapotranspiration of irrigated crops using crop coefficients derived from time series of satellite images, I: method validation', Agricultural Water Management, Vol. 125, pp.81–91.

Menenti, M. and Choudhury, B.,1993. Parameterization of land surface evavotranspiration using a location dependent potential evapotranspiration and surface temperature range. IAHS Publ 212, 561-568 (1993).

Monin, A.S., Obukhov, A.M., "Basic laws of turbulent mixing in the surface layer of the atmosphere". Tr. Akad. Nauk SSSR Geofiz. Inst 24: 163–187 (1954).

Norman JM, Kustas WP, Humes KS (1995) Source approach for estimating soil and vegetation energy fluxes in observations of directional radiometric surface temperature. Agric For Meteorol 77(3–4):263–293. 10.1016/0168-1923(95)02265-Y.

Pinter, P., Ritchie, J., Hatfield, J. and Hart, G.,2003. 'The agricultural research service's remote sensing program: an example of interagency collaboration', Photogrammetric Engineering & Remote Sensing, Vol. 69, No. 6, pp.615–618.

Roerink, G. J., Su, Z. and Menenti, M., 2000. S-SEBI: A simple remote sensing algorithm to estimate the surface energy balance. Physics and Chemistry of the Earth, Part B: Hydrology, Oceans and Atmosphere 25, 147-157, doi:http://dx.doi.org/10.1016/ S1464-1909 (99)00128-8 (2000).

Romaguera, M., Toulios, L., Stancalie, G., Nertan A., Spiliotopoulos, M., Struzik, P., Calleja, E., Papadavid, G.,, 2014. Identification of the key variables that can be estimated using Remote Sensing data and needed for Water Footprint (WF) assessment. Presented, during the Second International Conference on Remote Sensing and Geoinformation of Environment, RSCy 2014, Paphos, Cyprus 7-10 April 2014.

Spiliotopoulos, M., Loukas, A., Mylopoulos, N., 2015. A new remote sensing procedure for the estimation of crop water requirements. Third International Conference on Remote Sensing and Geoinformation of the Environment 2015, 16-19 March 2015, Cyprus (doi:10.1117/12.2192688)Su, Z., 2002. The surface energy balance system (SEBS) for estimation of turbulent heat fluxes," Hydrology and Earth System Sciences 6, 85-99.

Tilman, D., Cassman, G.K., Matson, A.P., Naylor, R. and Polasky, S.,2002. 'Agricultural sustainability and intensive production practices', in Nature, Vol. 418, pp.671–677. Townshend, R.G.J. and Justice, O.C. (2002) 'Towards operational monitoring of terrestrial systems by moderate-resolution remote sensing', Remote Sensing of Environment, Vol. 83, Nos. 1–2, pp.351–359.

Compliance of EU Water Framework Directive by using Sentinel-2 data.

O. R. Belfiore.[1], C. Gandolfi[2], C. De Michele[3], G. D'Urso[1]

[1] Department of Agricultural Sciences, University of Naples Federico II, Portici, ITALY
[2] Department of Agricultural and Environmental Sciences, Università degli Studi di Milano, Milan, ITALY
[3] Ariespace s.r.l. Spin-off company of University of Naples Federico II, Naples, ITALY

Abstract. The implementation of the EU Water Framework Directive (WFD) is hampered by the lack of suitable data on the actual extension of irrigated areas and the corresponding abstracted volumes. National statistical data often are unable to provide correct data at regional and local scales. To this end, Sentinel-2 (S2) satellites are representing a very valuable source of information to fill the gap between national and local scales for the assessment of water uses in agriculture. The present research is carried out within the INCIPIT project (funded by Italian Min. Univ. and Research) covering different hydrologic and meteorological conditions in six Italian regions (Apulia, Campania, Emilia Romagna, Lombardia, Sardinia, and Sicily). The proposed procedures exploit the full spectral range of S2 data, from visible to shortwave infrared, and the temporal domain. In the first instance, machine learning algorithms have been applied for mapping irrigated and non-irrigated areas from dense temporal series of vegetation indexes, and surface water status derived on SWIR bands with the OPTRAM model. The assessment of the irrigation volumes has been carried out by using the IRRISAT© methodology, based on the Penman-Monteith equation, properly adapted with canopy parameters namely crop height, Leaf Area Index and surface albedo also derived from Sentinel-2 data. The results have been compared for the irrigation seasons 2019 and 2020 in two Irrigation and Land Reclamation Consortium located in the Campania and Sardinia regions, where the accuracy assessment of the proposed procedures has performed with field data related to effective irrigated areas and measured irrigation volumes at district scales.

1 Introduction

The Water Framework Directive (WFD, 2000/60/EC) defines the main objectives in relation to the use of water, in order to guarantee a sustainable and integrated approach to the management of water resources in Europe (Wriedt et al., 2009). As agriculture is still the main source of pressure on water resources (European Environment Agency, EEA), accurate estimates of irrigation demands play a key role in sustainable water management. In Italy, the declaration about the measurements and estimates of water uses in agriculture is regulated by the Decree of the Ministry of Agricultural, Food and Forestry Policies (Mipaaf) of 31 July 2015. Since the Italian irrigation systems are very heterogeneous, for the purposes of the most effective application of the decree, there is a need to develop and validate methodologies for the evaluation of the temporal evolution of the irrigated areas and the irrigation water abstraction in compliance with the WFD. In this context, the **INCIPIT** (**IN**tegrated **C**omputer modeling and monitoring for **I**rrigation **P**lanning in Italy) project (funded by Italian Min. Univ. and Research) is focused on the definition of a methodological framework to support the control and planning of irrigation water uses at different spatial scales and in different conditions of availability of hydrometric and meteorological data in six Italian regions (Apulia, Campania, Emilia Romagna, Lombardia, Sardinia, and Sicily). The present research is carried out for the irrigation seasons 2019 and 2020 in two Irrigation and Land Reclamation Consortium located in the Campania and Sardinia regions, exploiting the full spectral range of ESA Sentinel-2 (S2) data, from visible to shortwave infrared for mapping irrigated areas and estimating spatially-distributed irrigation water requirements. The detection of the actual irrigated areas has been performed by and supervised classification applied to dense temporal series of vegetation indices (Falanga et al., 2020), while the quantification of the irrigation water abstraction has been performed by means of the IRRISAT methodology, the first satellite-based irrigation advisory service developed in Italy and operating in the Campania region (D'Urso et al, 2009).

2 Materials and methods

2.1 Pilot areas

The study areas are related to two Irrigation and Land reclamation consortium: The ConsBIV (Consorzio Generale di Bonifica del Bacino Inferiore del Volturno) and the CBSC (Consorzio di Bonifica della Sardegna Centrale) respectively located in Campania and Sardinia regions for a total cover area of 25,159 hectares. The ConsBiv pilot area is divided into three irrigation districts for a total of 13,289 hectares: Parete, Mazzafarro, and Santa Maria la Fossa (**Figure 1a**). The area of Parete has an extension of 7,937 hectares for three sub-districts called "A" (high), "M" (medium), and "B" (low). The Mazzafarro (MAZ) district covers an area of 2,805

hectares, while that of Santa Maria la Fossa (SMF) covers an area of 2,547 hectares. The main crops are maize, tomato, alfalfa, tobacco, fruit trees, and greenhouse crops such as vegetables and strawberries. The most common irrigation method for herbaceous crops is sprinkling, while localized irrigation prevails for trees. The irrigation season extends from April to October. The CBSC pilot area, based in Nuoro - Sardinia, is divided into three irrigation districts with a total extension of 19,273 hectares: Cedrino, Posada, and Media Valle del Tirso. For the INCIPIT project have been selected the Cedrino (4,711 ha) and Posada (7,126 ha) for a total extension of 11,837 hectares (**Figure 1b**). The main crops are meadows, pastures, alfalfa, maize, sorghum, vegetables, and tree crops such as vineyards, olives, and, citrus. As for the ConsBIV, the most common irrigation method is sprinkling for herbaceous crops and localized for tree crops. Irrigation is guaranteed for twelve months per year, with an intensification of the water demand during the spring-summer irrigation season (from April to September).

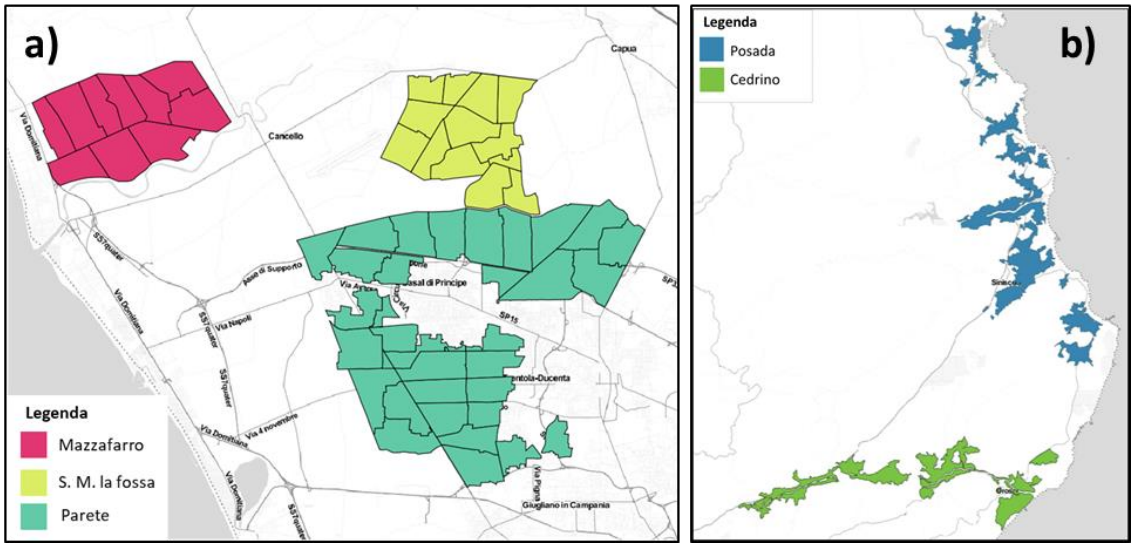

Figure 1. a) ConsBIV and b) CBSC irrigation districts selected in the INCIPIT project.

2.2 Maps of Irrigated areas

For accurate quantification of the irrigation water volumes at the district scale, the identification of the actual irrigated areas is required. Often this information is not available to water managers, who have also to deal with unauthorized water withdrawals for irrigation. For this purpose, for both pilot areas, the detection of the actual irrigated areas is performed by using a time-series of NDVI (Normalized Difference Vegetation Index) maps and rainfall data as input data in a supervised classification process (Falanga et al., 2020). In detail, the basic assumption is that, in conditions of hydrological deficit, typical of the summer period in arid and semi-arid environments (like the Mediterranean basin), the crop growth is compatible only with irrigation. In other terms, high trends of vegetation stand for irrigated crops when the rainfall or the rise of the water table is not sufficient to provide the water supplies necessary for their growth, in reverse for the rainfed crops (**Figure 2**) (Ozdogan et al., 2010).

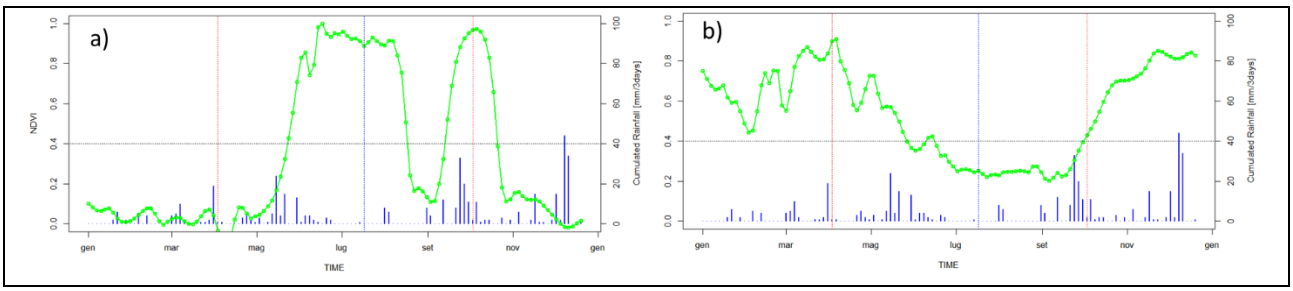

Figure 2. Examples of the NDVI temporal pattern labelled as irrigated crop (a) and rainfed crop (b).

The pre-processing is related to the atmospheric correction of S2 data, performed by using the MAJA (MACCS ATCOR Joint Algorithm) processor, and the cloud masking and gap-filling process carried out by means of the Whittaker smoother (WS), proposed by Eilers (2003) and implemented in the MODIS package into the R environment (Mattiuzzi et al., 2012). In particular, the time series filtering has been performed on the NDVI

maps replacing clouds and shadows, previously detected by means of the binarization of each cloud mask derived with the Multi-Temporal Cloud Detection method (MTCD) implemented in the MAJA processor (Hagolle et al., 2010) (**Figure 3**).

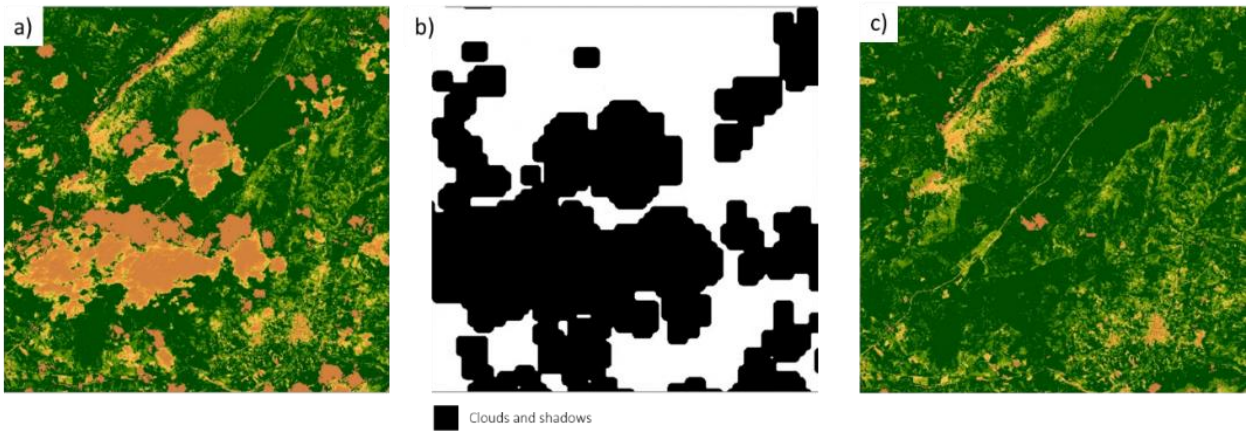

Figure 3. Example of a) raw NDVI map, b) Cloud and shadow mask, and c) gap-filled NDVI data.

Subsequently, the smoothed and gap-filled NVDI maps and three-day cumulated rainfall data derived from Persiann dataset (Nguyen et al., 2019) are considered as input data for supervised classification. In detail, six Machine Learning Algorithms (MLA) as Random Forest (RF), Support Vector Machine (SVM), Boosted Decision Tree (BDT), Single Decision Tree (SDT), Artificial Neural Network (ANN), k-Neigherst Neighbour (k-NN) are tested by using the R studio CARET package (Kuhn et al., 2016), in order to detect the following thematic classes: bare soil, rainfed crops and herbaceous irrigated crops. The map of irrigated areas for the ConsBIV is shown in (**Figure 34*)***, with the irrigated tree crops and the greenhouse classes detected by using pre-existing maps and photointerpretation analysis.

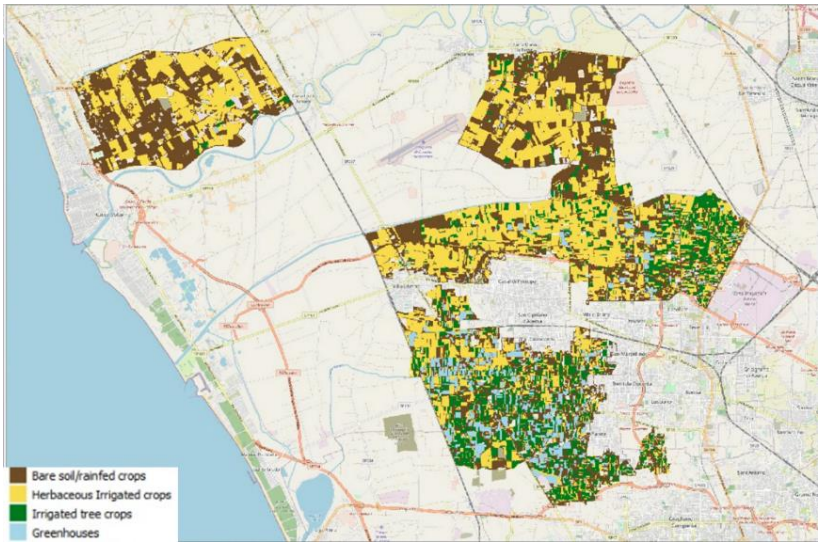

Figure 4. Map of irrigated areas for ConsBIV pilot areas for the irrigation season 2020 derived with the SVM algorithm (Overall Accuracy OA = 95.13%, Kappa statistics (K) = 0.893).

In the CBSC pilot area, the VIS-NIR-Rainfall paradigm is not sufficient, given that many pastures and tree crops such as olives and vineyards are irrigated occasionally during the dry periods in winter-spring and autumn for the pastures, and in the summer for the tree crops. For this reason, from the “rainfed” and “tree crops” classes it was necessary to derive further classes such as irrigated winter-spring and autumn crops and distinguish irrigated and not-irrigated tree crops, exploiting the full spectral range of Sentinel-2 S2 data. For this purpose, the VIS-NIR-SWIR-Rainfall domain are tested by using the OPtical TRApezoid Model (OPTRAM) (Sadeghi et al. 2017), properly adapted by Belfiore et al (2020). The OPTRAM model is based on the pixel distribution within the Shortwave Infrared Transformed Reflectance (STR)-NDVI space, where the STR index (Sadeghi et al. 2015), computed with the S2 SWIR band (Band 12- 2190 nm), is linearly related to the water

content of the soil-canopy ensemble. As shown in **Figure 5a** in the STR-NDVI space, the upper limit represents the position of pixels corresponding to wet conditions in the soil-plant ensemble ("wet edge"), the lower the drier ("dry edge"). Dividing the region between the two extreme edges in four sub-sections, and selecting S2 images acquired in dry periods without significant rainfall, those pixels previously detected as rainfed and tree crops located in the upper wet regions of the scatterplot are considered as irrigated, while those pixels within the dry part of the scatterplot are considered as not irrigated. The map of irrigated areas for the CBSC is shown in (**Figure 5b*)***.

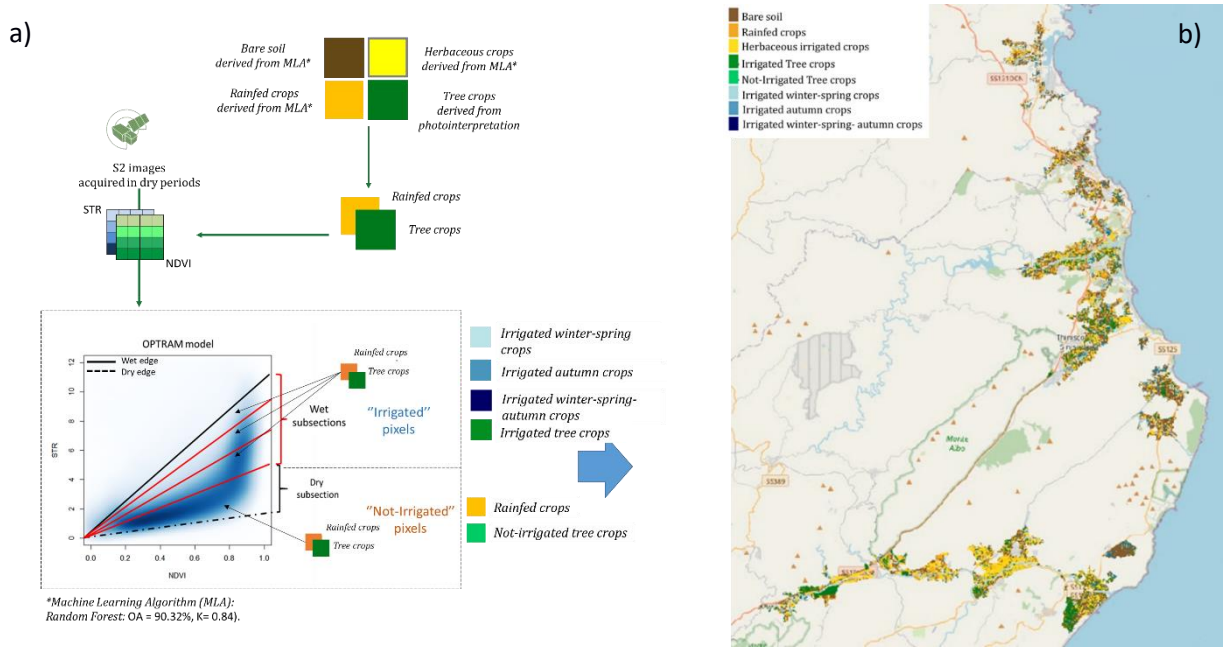

Figure 5. a) OPTRAM model adaptation for the detection of irrigated areas. b) Map of irrigated areas for CBSC pilot area for the irrigation season 2020

2.3 Crop evapotranspiration and crop irrigation water requirements

The crop evapotranspiration (ET) is computed by using the Penman-Monteith (PM) equation based on the "one-step approach" implemented in the IRRISAT© methodology (Vuolo et al., 2015). The ET modeling is carried out deriving canopy parameters, hemispherical albedo (α) (D'Urso & Calera Belmonte, 2006), and Leaf Area Index (LAI) (Weiss & Baret 2016) by using S2 data, while the crop height (hc) is fixed at 0.4 m for the herbaceous crops and 1.2 m for tree crops, assuming that the influence of hc on the estimation of ET is negligible as reported in Vuolo et al. (2015). The agro-meteorological input data (solar radiation, wind speed, air temperature, dew point temperature, atmospheric pressure and precipitation) have been derived from the reanalysis dataset provided by the Copernicus ERA5 single level (https://cds.climate.copernicus.eu/cdsapp#!/dataset/reanalysis-era5-single-levels). The crop irrigation water requirements (IWR) (Eq. 1) have been at monthly scale (mm/month) by subtracting from the ET the effective precipitation (Pe), derived from the total precipitation (P) according to the method proposed by Allen et al. (1998). In conclusion, the gross irrigation water requirements (GIWR) have been derived, only for the irrigated crops classes, by dividing the IWR by irrigation efficiency, which was supposed to be 75 % for the CBSC and 85% for the ConsBIV districts **(Figure 6).**

$$IWR = ET - Pe \text{ (mm/month)} \quad (1)$$

with,

$Pe = 0.8\ P - 25$, if $P > 75$ (mm/month)

$Pe = 0.6\ P - 10$, if $P < 75$ (mm/month)

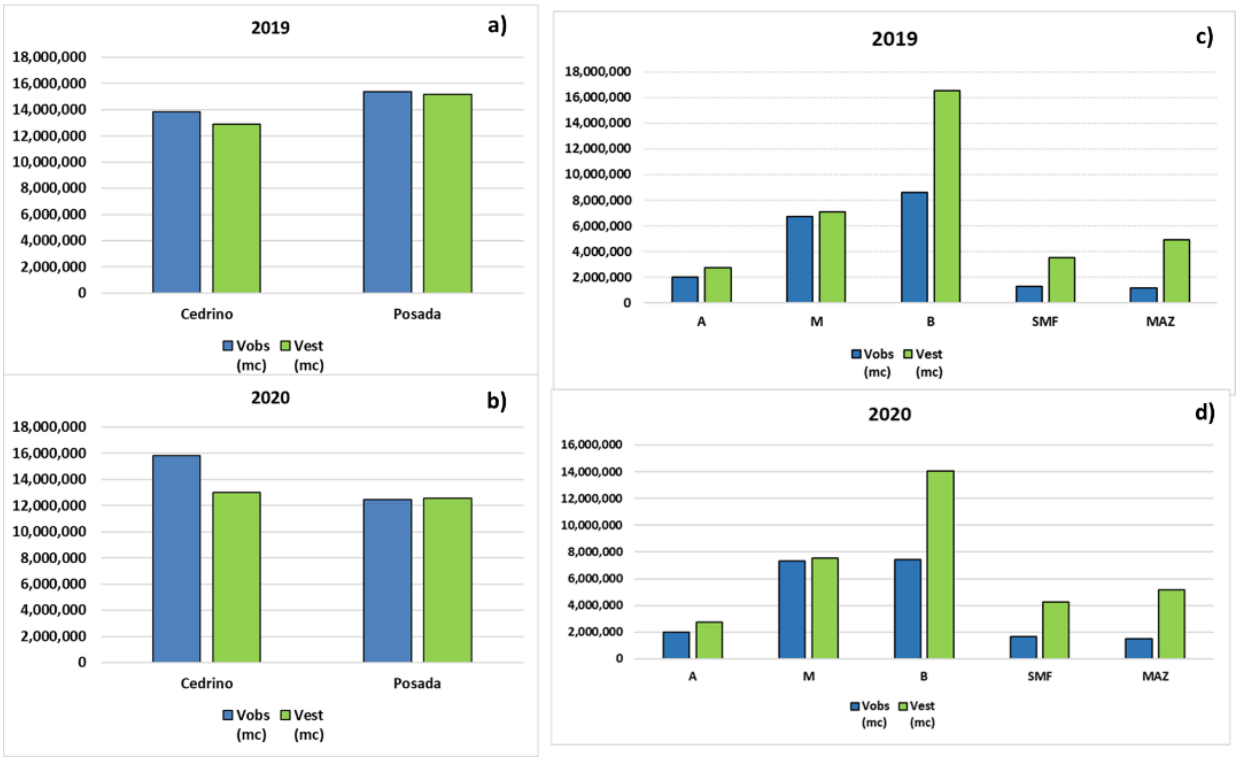

Figure 6. Comparison between measured (V_{obs}) and irrigation seasonal volumes estimated from EO data (V_{est} = GIWR) in 2019-2020 for the CBSC (a, b) and ConsBIV districts (c, d).

3. Discussion and conclusions

The preliminary results of the INCIPIT project confirm the reliability of the Earth Observation data in the mapping of irrigated areas and in the estimation of irrigation water abstraction.
The high revisiting time of the two ESA Sentinel-2A and Sentinel-2B sensors and the high geometric resolution allow constant monitoring of the development of irrigated crops, despite the typical agricultural land fragmentation of the Mediterranean basin.
For the estimation of the irrigation water volumes, the IRRISAT methodology provides reliable estimates with good agreements, as can be seen in particular for the CBSC (Figure 6a-b). For the ConsBIV pilot area, there is a good agreement for sub-districts A and M, while for sub-districts B, and the districts SMF and MAZ there is an overestimation (Figure 6c-d), due to the widespread practice of withdrawing water from irrigation wells (often unauthorized).
In conclusion, the results obtained demonstrate the effectiveness of the proposed methodology as a valid tool for water managers in an operative context, providing valuable information in compliance with the requirements of the WFD.

Acknowledgements

This paper brings together the results of studies performed within the project PRIN 2017 **INCIPIT** (**IN**tegrated **C**omputer modeling and monitoring for **I**rrigation **P**lanning in Italy) with the support of the M.I.U.R (Italian Ministry of University and Research).

References

Allen R.G., Pereira L.S., Raes D., Smith M. 1998. Crop evapotranspiration - guide- lines for computing crop water requirements. FAO irrigation and drainage paper, 56: FAO, Rome, Italy.

Belfiore O. R., Falanga Bolognesi F., D'Urso G., De Michele C. 2020. D2.4 Data products validation report. Zenodo. https://doi.org/10.5281/zenodo.3600256

D'Urso G., Calera Belmonte A. 2006. Operative approaches to determine crop water requirements from Earth Observation data: methodologies and applications. AIP Conf. Proc. 852:14-25.

D'Urso, G., D'Antonio, A., Vuolo, F., & De Michele, C. The irrigation advisory plan of Campania Region: from research to operational support for the water.

Eilers, P.H.C. A perfect smoother. Anal. Chem. 2003, 75, 3631–3636.

European Environment Agency – Water use and environmental pressure. https://www.eea.europa.eu/themes/water/european-waters/water-use-and-environmental-pressures (accessed on 26 May 2022).

Falanga Bolognesi S., Pasolli E., Belfiore O. R., De Michele C., D'Urso G. 2020. Harmonized Landsat 8 and Sentinel-2 Time Series Data to Detect Irrigated Areas: An Application in Southern Italy" Remote Sensing, MDPI, vol.12, no. 8: 1275; doi.org/10.3390/rs12081275, 2020.

Hagolle, O., Huc, M., Pascual, D. V., & Dedieu, G. (2010). A multi-temporal method for cloud detection, applied to FORMOSAT-2, VENμS, LANDSAT and SENTINEL-2 images. Remote Sensing of Environment, 114(8), 1747-1755.

Kuhn, M.;Wing, J.;Weston, S.;Williams, A.; Keefer, C.; Engelhardt, A.; Cooper, T.; Mayer, Z.; Kenkel, B.; R Core Team; et al. Caret: Classification and Regression Training. R Package Version 6.0-86. 2016.

Mattiuzzi, M., Verbesselt, J., Hengl, T., Klisch, A., Evans, B., Lobo, A. 2012: MODIS: MODIS download and processing package. In Processing Functionalities for (Multi-Temporal) MODIS Grid Data. First International Workshop on "Temporal Analysis of Satellite Images", Mykonos Island, Greece, pp. 23-25. (2012).

Nguyen, P., E.J. Shearer, H. Tran, M. Ombadi, N. Hayatbini, T. Palacios, P. Huynh, G. Updegraff, K. Hsu, B. Kuligowski, W.S. Logan, and S. Sorooshian, The CHRS Data Portal, an easily accessible public repository for PERSIANN global satellite precipitation data, Nature Scientific Data, Vol. 6, Article 180296, 2019. doi: https://doi.org/10.1038/sdata.2018.296

Ozdogan M., Yang Y., Allez G., Cervantes C. 2010. Remote sensing of irrigated agriculture: opportunities and challenges". Remote Sensing, MDPI, vol.2:2274-304; doi.org/10.3390/rs2092274, 2010

Sadeghi, M., Babaeian, E., Tuller, M., & Jones, S. B. (2017). The optical trapezoid model: A novel approach to remote sensing of soil moisture applied to Sentinel-2 and Landsat-8 observations. Remote sensing of environment, 198, 52-68.

Sadeghi, Morteza, Scott B. Jones, and William D. Philpot. "A linear physically-based model for remote sensing of soil moisture using short wave infrared bands." Remote Sensing of Environment 164 (2015): 66-76.

Vuolo F., D'Urso G., De Michele C., Bianchi B., Cutting M. 2015. Satellite-based irrigation advisory services: a common tool for different experiences from Europe to Australia". Agricultural Water Management, Elsevier, vol. 147: 82-95; dx.doi.org/10.1016/j.agwat.2014.08.004, 2015.

Weiss, M.; Baret, F. Sentinel-2 ToolBox Level 2 Products: LAI, FAPAR, FCOVER, Version 1.1; European Space Agency: Noordwijk, The Netherlands, 2016. Available online: https://step.esa.int/docs/extra/ATBD_S2ToolBox_L2B_V1.1.pdf (accessed on 26 May 2022).

Wriedt, G., Van der Velde, M., Aloe, A., & Bouraoui, F. 2009. Estimating irrigation water requirements in Europe. Journal of Hydrology, 373(3-4), 527-544.

Assessment of digital promotion of alternative tourism: case study of the Greek island Evia

Andreopoulou Z.[1], Kamila M.[2]

[1] Professor in School of Agriculture, Forestry & Natural Environment Aristotle University of Thessaloniki, Thessaloniki Greece
[2] MSc Aristotle University of Thessaloniki, Thessaloniki Greece

Abstract. The Internet is considered to be the most important and effective mean of communication and information. In regard to the tourism industry, the use of available online tools, contributes significantly to the digital entrepreneurship and the promotion of tourist destinations. At the same time, the internet leads to the emergence of a new consumer-tourist type who organizes their travel experience online and seeks alternative forms of tourism. In the context of this new digital reality, websites provide easy access to a plethora of information, direct communication, interaction, and personalization.

The purpose of this paper is to discover and evaluate websites that promote alternative tourism services on the Greek island of Evia. The websites are being evaluated based on their qualitative and quantitative characteristics and then classified into categories. Ultimately, the paper provides a few suggestions concerning the improvement of these sites. Thus, the promotion of the island will be more efficient and its recognizability will be amplified.

Key words: E-commerce, website assessment, web design principles, alternative tourism

1 Introduction

As early as the 1990s, it became apparent that the Internet would be a powerful force which would transform the whole world. IT experts, politicians, people in the business world foreshadowed the transformation of society and economy through the use of the internet (Curran, Fenton & Freedman, 2012). Three decades later, researchers and scientists create a more realistic picture in order to present the impact of the internet (Morozov, 2011; Foster & McChesney, 2011), and highlight the internet as one of the most important means of communication and information. Businesses, policies, legislation, and citizens need to adapt to a new digital reality.

In the business world, this high intensity digitization redefines entrepreneurship and competition (Nambisan, 2016, 1047; Reuschke & Mason, 2020). Businesses and companies are able to gain more opportunities for the promotion of their products and / or services (Sussan & Acs, 2017), expand their customer base at reduced costs, create new business models, communicate with their customers and collect information (Tsekouropoulos, Tzimitra- Kalogianni & Manos, 2005; Canavari et.al., 2010; Canavari et al., 2011). It is therefore clear that the design and development of an appropriate strategy for the integration of new technologies is a prerequisite for survival, but also a competitive advantage in the digital age (Coskun-Setirek & Tanrikulu, 2021; Andreopoulou, Koutroumanidis & Manos, 2011).

In the tourism sector, the impact of Information and Communication Technologies, and in particular the internet, is significant. Tourism is a global industry with a global and local economic impact (McGrath & More, 2005). It is a hybrid entity that combines the catalytic role of information with services mainly in the physical world (Tanti & Buhalis, 2017). Tourism, as an integral part of the global economy, is being influenced by the internet revolution. The latter redefines the sectors of production, marketing, distribution, and operation of tourism enterprises (Buhalis, 1998). The Internet is now emerging as a primary source of information on tourism products (Andreopoulou, Leandros, Quaranta & Salvia, 2016) and as a tool of digital entrepreneurship, which enhances communication, collaboration, commerce, creating new opportunities and challenges (Buhalis, 2015).

In a parallel manner, these new technologies and the Internet have contributed to the emergence of a consumer-tourist with renewed features. Her/ his consumer behavior is more dynamic, to the point that it qualitatively shapes the tourist product. She/ He uses the internet as a tool in order to discover and access reliable and accurate information, and seeks experiences enhanced through the use of new technologies (Neuhofer, Buhalis & Ladkin, 2015), "smart" destinations, quality connectivity and alternative forms of tourism (Tanti & Buhalis, 2017). In other words, she/ he is a new, more sophisticated, and experienced consumer (Buhalis, Leung & Law, 2011).

Tourism companies respond to the rapid digitization of the tourism industry and the individual needs of consumers by integrating new technologies in their marketing and communication strategy, while digitizing parts of their business (Buhalis, Leung & Law, 2011). They want to create a strong and qualitative presence on the internet, which is a dynamic environment (Tsekouropoulos et al. 2012; Koliouska & Andreopoulou, 2013) that allows access to a large amount of information, transactions with speed and ease, direct communication with consumers and other businesses, interaction, and personalization (Buhalis, 2015; Buhalis,

Leung & Law, 2011). In this process, e-tourism is the key. It is a holistic and integrated system of equipment and software (Buhalis, Leung & Law, 2011), which rapidly changes the traditional processes of promotion, production, and promotion of tourism products.

In order to effectively promote tourism products, businesses need to strengthen their internet marketing policies and put the consumer at the center of the chosen strategy (Tsekouropoulos et al. 2012; Sharma & Sheth, 2004). It is therefore important for each enterprise to take care of its online presence. A website of good quality is a useful tool which provides accurate information to consumers, helps increase customers and facilitates international activity with low investment costs (Tsekouropoulos et al. 2012). The website is a multifaceted construction, whose quality is examined based on various factors: design, security, content quality, transformation speed, interactivity, ease of use and the ability to gather data in order to provide a personalized product (Koliouska & Andreopoulou, 2013; Buhalis, Leung & Law, 2011).

It is obvious that a new, technologically enhanced reality is being formed and tourism is gradually adapting to it. At the same time, the conceptual framework of tourism development is being renewed and new forms of tourism are emerging, such as ecotourism, green and alternative tourism (Theng, Qiong & Tatar, 2015) which offer specialized tourism products and are connected to the concept of sustainability. This term signifies that these types of tourism take into account the current and future economic, social and environmental impact of tourism, but also the needs of tourists, enterprises, ecosystems and local communities (Butler, 2018; Apostolopoulos & Sdrali, 2009 Dodds 2007).

The geomorphological position, the natural and cultural wealth of Greece prove that the mediterranean country is suitable for the development of alternative forms of tourism (Agaliotou, 2015). The internet is the key to effectively promote tourist destinations that offer alternative tourism opportunities.

This paper aims to assess the digital promotion of alternative tourism on the Greek island of Evia. The different characteristics and ICT tools, used to promote different types of alternative tourism, were analyzed.

2 Materials and methods

The methodology used for assessing digital promotion is described in Andreopoulou et. al, 2017.

2.1 Case study: Evia

Evia is the second largest island in Greece and is a part of Central Greece. The prevailing climate is temperate, and there is a high level of biodiversity. The areas with the greatest interest on the island are Eretria, Agia Anna, Edipsos, Chalkida, Steni Dirfis, Karystos. Evia is characterized by rich vegetation and cultural heritage. Sandy beaches, pine forests, mountain paths, archeological and ecclesiastical monuments, festivals, hot springs, and local gastronomy create a beautiful and complex amalgam. It is evident that Evia, as a tourist destination, provides a variety of options for tourists and is suitable for many types of alternative tourism (Chantziantoniou & Dionysopoulou, 2017; Didaskalou, Nastos & Matzarakis, 2004).

2.2 Materials and methods

At first, websites that promote different types of alternative tourism on the Greek island of Evia were retrieved from the Internet using various keywords and combinations such as "Evia alternative tourism", "Evia agritourism accommodation", "Evia winery", "Evia diving", "Evia mountaineering", "Evia paths", "Evia festival", museums, archeological sites ". The websites were retrieved using the large-scale hypertextual search engine “Google” which is very effective (Langville & Meyer, 2006).

Then a two-dimensional table with six columns was created. The first column contained the URLs of all the websites which were retrieved, and the next five columns were used to categorize the websites based on the name of the company / institution, the area of activity, the public / private character of the page, the type of alternative tourism promoted and the use or not of Facebook.

Then, a qualitative analysis was performed in order to identify the features that the websites use to promote the various types of alternative tourism in Evia. Indeed, 6 key features were identified: navigation, design, interactivity, accessibility, usefulness of information, and e-services. Each website was evaluated based on these features. More specifically, the characteristics were used to describe variables x_1, x_2, x_3, x_4, x_5, x_6. These characteristics are presented in Table 1.

Variable x1 refers to the ability of active navigation (use of keywords, sitemap, browsing) and fast response, the existence of a friendly and easy-to-use URL and an independent location (Andreopoulou, 2010; Giannopoulos & Mavragani, 2011). Variable x2 is associated with the appearance of the logo and the brand on the website, the use of a variety of colors (more than four) and music, the offer of information in the form of videos and the existence of multiple pages to highlight each product. Variable x3 refers to the ability of the website to allow the activation of location maps, data sharing, digital downloading of files like tourist guides and brochures, problem-solving communication, consumer feedback, providing useful information (weather,

itineraries) and links (websites of local interest). It also refers to the existence of a social media account which promotes the enterprise (Giannopoulos & Mavragani, 2011).

Variable x4 corresponds to accessibility, and in particular characteristics such as the ability to choose a different language, connection via social media, the ability to support various browser platforms, the existence of a mobile form for the website. Variable x5 refers to the existence of detailed information about the production process, the products, the price list. Finally, variable x6 describes the criterion "electronic services (E-services)", which means that "navigation is inextricably linked to the experience of an electronic market" (Andreopoulou, 2010). More specifically, the website has an online store with a shopping cart, allows the choice of payment and shipping methods and is pays attention to the security of electronic transactions.

VARIABLES	CHARACTERISTICS	VARIABLES	CHARACTERISTICS
X1	Navigation	X4	Accessibility
X2	Design	X5	Usefulness of information
X3	Interactivity	X6	E - Services

Table 1: Variables

Next a quantitative analysis was performed in order to examine the existence or absence of these 6 features. A two-dimensional table was created and then the value 0 and the value 1 were attributed to the variables x1, x2, x3, x4, x5, x6 for the non-existence and the existence of each characteristic respectively.

Furthermore, these 74 websites were classified in four categories, each one representing a stage of adoption of ICT tools. Many researchers present and use a model which describes four stages of ICT tools adoption (Koliouska & Andreopoulou, 2013; Gossain & Kenworthy, 2000; Rao et al, 2003). These stages are the following (Koliouska & Andreopoulou, 2013; Andreopoulou, 2010): 1. presence, 2. interaction, 3. transaction and 4. transformation. The classification depends on the characteristics achieved by each website.

In the first stage, all users who wish to visit the website have access to it and can obtain information. Therefore, the website ensures the presence of the enterprise on the internet and the provision of contact information. In the second stage, the website allows interactive actions of the user, active navigation and includes information about the tourist product and the points of interest that are found in the area, while enabling the social networking of the users. In the third stage, the website environment is configured as an online marketplace with digital applications which facilitates the transaction during payment. In the fourth stage, the website, as a "complete information system", enables the completion of the transaction. The user has a password and is informed about offers based on her/ his search history. At this stage, the quality of communication and the security of electronic transactions are greatly emphasized.

Each of these stages was coded as a number (Table 2), and then all the websites which promote various types of alternative tourism on Evia were categorized based on the stage of ICT adoption that describes them the best. The results were recorded in a separate column of the two-dimensional table.

NUMBER	STAGE	NUMBER	STAGE
1	Presence	3	Transaction
2	Interaction	4	Transformation

Table 2: ICT adoption stage

3 Results

The research through the search engines on the Greek Internet resulted in the retrieval of 74 websites that promote different types of alternative tourism in Evia. First, the majority of websites are private (65 websites). In addition, the leading form of alternative tourism is adventure tourism with 14 websites (Graph 1). Other popular types of alternative tourism are wine tourism, cultural and archaeological tourism (9 websites each). In third place is conference tourism with 7 websites. Geotourism and maritime tourism were placed at the bottom of the ranking because they appear on 1 web page.

Most of the tourism enterprises that offer alternative tourism services on the island of Evia are located in the municipality of Chalkida. In second place are the municipalities of Istiaia-Edipsos and Mantoudi-Limni-Agia Anna. Finally, 10 websites promote more than one area of Evia.

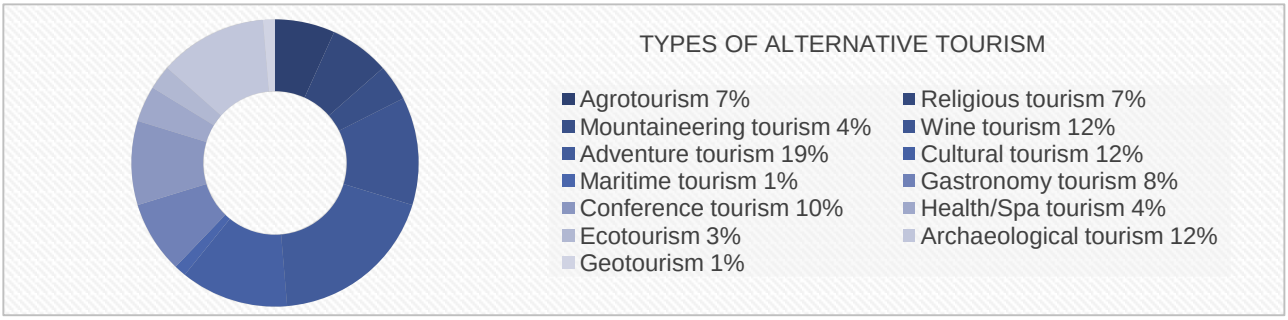

Graph 1: Types of alternative tourism

Regarding the evaluation of websites based on 6 criteria, the results are presented in the graph below. The vast majority of websites (91%), meet the criterion of interactivity (Graph 2). Navigation and design criteria have also high fulfillment rates (88% and 84% respectively). Also, about half of the websites meet the criteria of accessibility and usefulness, while only 19 meet the criterion of e-services. It is important to underline that the criterion of interactivity includes the utilization of social media. Of the 74 websites, 62 have a corresponding Facebook page (Graph 4).

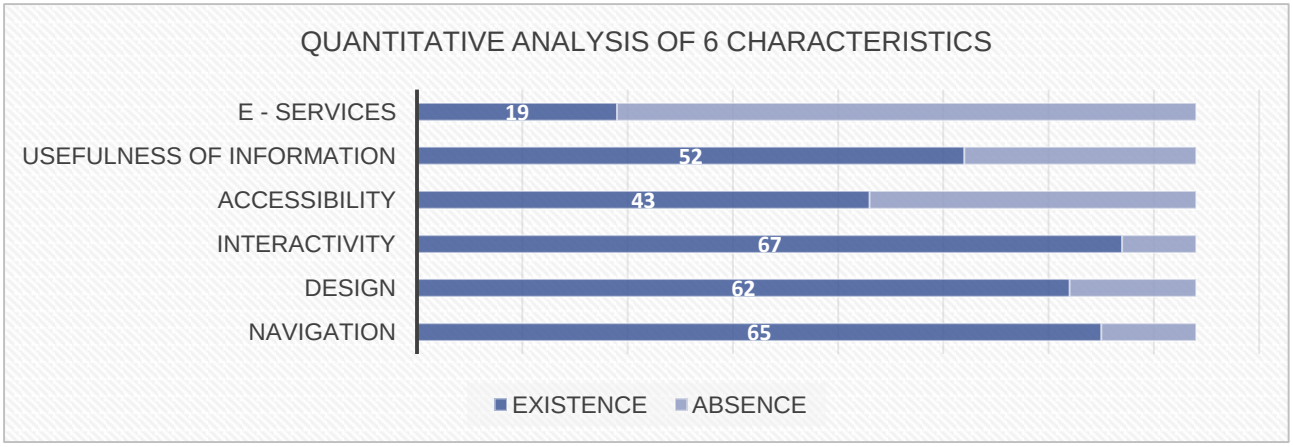

Graph 2: Quantitative analysis of 6 characteristics

Finally, regarding the level of ICT adoption, most companies/ organizations active in the field of alternative tourism, fulfill the characteristics of the second stage (38 companies/ organizations) (Graph 3), while just a small percentage fulfil the characteristics of the fourth stage (only two). About 19% of enterprises belong to the first stage.

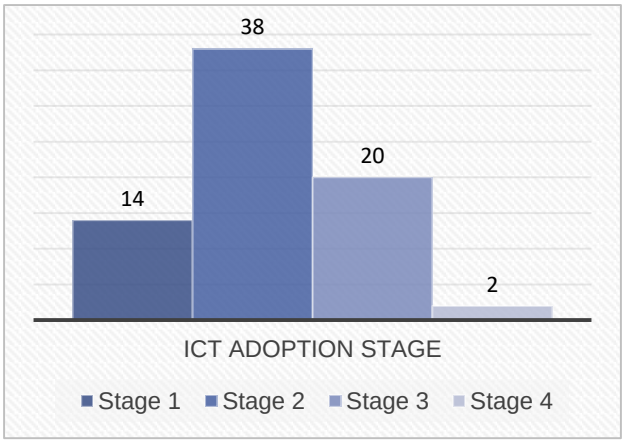

Graph 3: ICT adoption stage

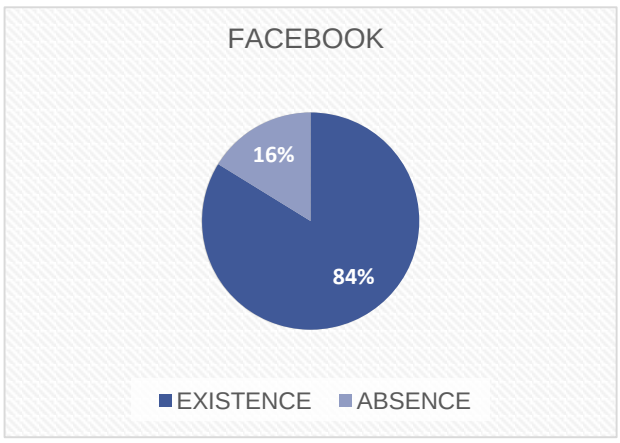

Graph 4: Existence or absence of a Facebook page

4 Summary

In this study, the internet promotion of Evia as an alternative tourism destination is studied. The leading form of alternative tourism is adventure tourism. The rich vegetation and the variety of ecosystems on the island, create a suitable environment for such activities. Other popular types of alternative tourism are wine tourism, cultural and archaeological tourism which are inextricably linked to the rich cultural heritage of Evia. It is important to point out that the majority of the websites have a private character and promote alternative tourism services in the Municipality of Chalkida. The evaluation of the websites in terms of their features showed high fulfillment rates concerning the criteria of interactivity, navigation, and design, while most organizations/ companies have a corresponding Facebook page. It is very positive that most websites (51%) fulfill the characteristics of the second stage of ICT adoption, interactivity. This means that they provide useful material, contact information, interactive maps, photographic material, etc. In this way, the attractiveness of the area is enhanced, and the tourist flow is increasing.

References

Agaliotou C. (2015). Reutilization of industrial buildings and sites in Greece can act as a lever for the development of special interest/alternative tourism. Vol. 175, pp. 291-298. doi: https://doi.org/10.1016/j.sbspro.2015.01.1203.

Andreopoulou, Z., S. (2010). Utilization of the internet for the promotion of eco-agrotourism units in Greece: In the context of the new regional development strategy with a time horizon in 2020. Proceedings of the 16th scientific conference of the association of Greek regionalists. The regional dimension of the new strategy in Europe.

Andreopoulou, Z., Koliouska, C. & Zopounidis, C. (2017). Multicriteria and clustering: Classification techniques in agrifood and environment. Springer. DOI: https://doi.org/10.1007/978-3-319-55565-2

Andreopoulou Z., Koutroumanidis T. and Manos B. (2011) Optimizing Collaborative Ecommerce Websites for Rural Production Using Multicriteria Analysis. *Business Organizations and Collaborative Web – Practices, Strategies and Patterns.* Dr. Kamna Malik and Praveen Choudhary, IGI Global, PA, USA, pp. 102-119

Andreopoulou, Z., Leandros, N., Quaranta, G. & Salvia, R. (2016). Tourism and new media. FrancoAngeli

Apostolopoulos, K. & Sdrali, D. (2009) Alternative and mild tourism: Theoretical approaches and applications in practice. Athens: Ellinoekdotiki SA

Buhalis, D. (1998). Strategic Use of Information Technologies in the Tourism Industry Tourism Management, vol. 19, Issue 5, pp. 409-421. doi: https://doi.org/10.1016/S0261-5177(98)00038-7

Buhalis D. (2015). eEnabled internet distribution for small and medium sized hotels: The case of Athens. Tourism Recreation Research. 33. 10.1080/02508281.2008.11081291.

Buhalis, D., Leung, D. & Law, R. (2011). ETourism: Critical information and communication technologies for tourism destinations. Destination Marketing and Management: Theories and Applications. pp. 205-224. 10.1079/9781845937621.0205.

Butler R. W. (2018). Sustainable tourism in sensitive environments: A wolf in sheep's Clothing? Sustainability 2018, 10(6), 1789. doi: https://doi.org/10.3390/su10061789

Canavari, M., Fritz, M. & Schiefer, G. (Eds.) (2011) Food Supply Networks: Trust and EBusiness, Cab Intl., Oxford.

Canavari, M., Fritz, M., Hofstede, G.J., Matopoulos, A. & Vlachopoulou, M. (2010) The role of trust in the

transition from traditional to electronic B2B relationships in agri-food chains. *Computers and Electronics in Agriculture*, Vol. 70, No. 2, pp.321–327.

Chantziantoniou, A. & Dionysopoulou, P. (2017). The religious tourism in Greece: Case study of Saint John Russian in N. Evia. Journal of Tourism, Heritage & Services Marketing, 3 (2017) 2, p. 15-24. doi: https://doi.org/10.5281/zenodo.1160590

Coskun-Setirek, A. & Tanrikulu, Z. (2021). Digital innovations-driven business model regeneration: A process model. Technology in Society, Vol. 64, February 2021. doi: https://doi.org/10.1016/j.techsoc.2020.101461

Didaskalou, E., Nastos, P.T. & Matzarakis, A. (2004). The development prospects of Greek health tourism and the role of the bioclimate regime of Greece. Advances in Tourism Climatology pp 149-167. Freiburg: Druckerei der Albert-Ludwigs-Universität Freiburg

Dodds, R. (2007). Sustainable tourism and policy implementation: Lessons from the case of Calvi, Spain'. Current Issues in Tourism 10(4): 296-322. doi: 10.2167/cit278.0

Foster, J. & McChesney, R. (2011). The internet's unholy marriage to capitalism, monthly review (March). Online. Available HTTP: < https://monthlyreview.org/2011/03/01/the-internets-unholy-marriage-to-capitalism/> (accessed December 2020)

Giannopoulos, A. & Mavragani, E., P. (2011). Traveling through the web: A first step toward a comparative analysis of European national tourism websites. Journal of Hospitality Marketing & Management. 20:7, pp. 718-739, DOI: 10.1080/19368623.2011.577706

Gossain, S. & Kenworthy, R. (2000). Winning the third wave of E-business-Beyond net markets. NerveWave

Koliouska, C. & Andreopoulou Z. (2013). Assessment of ICT adoption stage for promoting the Greek national parks. Procedia Technology, vol. 8, pp 97-103. doi: https://doi.org/10.1016/j.protcy.2013.11.014

Langville, A.N. & Meyer, C.D. (2006). Google's Pagerank and Beyond: The Science of Search Engine Rankings. Princeton University Press.

McGrath G.M., More E. (2005) An extended tourism information architecture: capturing and modelling change. In: Frew A.J. (eds) Information and Communication Technologies in Tourism 2005. Springer, Vienna. doi: https://doi.org/10.1007/3-211-27283-6_1

Morozov, E. (2011). The Net Delusion, London: Allen Lane.

Nambisan, S. (2016). Digital entrepreneurship: Toward a digital technology perspective of entrepreneurship. Entrepreneurship Theory and Practice, Vol. 41 issue 6, pp. 1029 - 1055. doi: https://doi.org/10.1111/etap.12254

Neuhofer, B., Buhalis, D. & Ladkin, A. (2015). Technology as a catalyst of change: Enablers and barriers of the tourist experience and their consequences. Conference: ENTER2015

Rao, S., Metts, G. & Mora Monge, C. (2013). Electronic commerce development in small and medium sized enterprises: A stage model and its implications. Business Process Management Journal. Vol. 9, No. 1, pp. 11-32. DOI: 10.1108/14637150310461378

Reuschke, D. & Mason, C. (2020). The engagement of home-based businesses in the digital economy. Futures, Available online 5 March 2020. doi: https://doi.org/10.1016/j.futures.2020.102542

Sharma, A. & Sheth, J. N. (2004). Web-based marketing: The coming revolution in marketing thought and strategy. Journal of Business Research. 696-702. 10.1016/S0148-2963(02)00350-8.

Tanti, A. & Buhalis, D. (2017). The influences and consequences of being digitally connected and/or

disconnected to travelers. Inf Technol Tourism 17, 121–141 (2017). doi: https://doi.org/10.1007/s40558-017-0081-8

Theng, S., Qiong,X. & Tatar, K. (2015). Mass tourism vs alternative tourism? Challenges and New Positionings. Etudes Caribéennes 31–32

Tsekouropoulos, G., Andreopoulou, Z., Koliouska, C., Koutroumanidis, T., Batzios, C. & Lefakis, P. (2012). Marketing policies through the internet: The case of skiing centers in Greece. Scientific Bulletin – Economic Sciences. 11. 66.

Tsekouropoulos, G., Tzimitra-Kalogianni, I. and Manos, B. (2005) Logistics in Greek Agricultural Enterprises-Problems-Prospects. Proceedings of ITAFE-International Conference on Information Technology in Agriculture, Food and Environment, Cukurova University, Adana, Turkey. Vol. 2, No. 12-14, pp. 606-613.

Impact of defoliation during the grain filling period on the yield of irrigated maize in central Greece

D. Leonidakis[1], D. Bartzialis, K. Giannoulis, I. Gintsioudis, E. Skoufogianni and N.G. Danalatos

[1]University of Thessaly, Department of Agriculture, Crop Production and Rural Environment, Laboratory of Agronomy and Applied Crop Physiology. E-mail: leonidakis.dimitris@gmail.com

Absrtact. In order to develop alternative practices for increasing water use especially for summer crops grown in semi-arid areas under irrigation in line with the environmentally friendly sustainable agriculture, a field experiment was carried out to examine the impact of defoliation of maize on final yield production as a key tool for minimizing the negative effect of transpiration deficit and for low-input sustainable maize irrigation in semi-arid areas such as the Thessaly plain, Central Greece. A maize experiment was conducted in the Larissa (Giannouli) area, Thessaly plain, central Greece from March to September 2019. Two irrigation treatments were involved, i.e. for matching 100% and 50% of the potential evapotranspiration. The crop was completely defoliated on 12/7, 19/7, 27/7 and 4/8/2019, when the crop was at stages 73, 75, 77 and 83 of the Zadoks scale, respectively. Experimental design was split plot in three blocks, with main plots comprising the irrigation treatments and the subplots comprising the defoliation dates. Soil moisture content was monitored, whereas weather data were collected from an automatic meteorological station installed in the vicinity of the experimental field. It was found that total defoliation reduced cob and total dry matter weight significantly, but only for the earlier defoliation dates. In the late defoliation date, the negative effect of yield reduction was substantially lower. Thus, defoliation at such late stages of the grain filling period may result in an appreciable yield of maize saving in parallel a certain amount of precious irrigation water (last 1-2 applications). This might be of importance in Mediterranean semi-arid areas characterized by low water availability by reducing the negative effects of transpiration deficit during the grain-filling period. The final yield levels attained by the defoliated plants may be attributed to a no modest assimilation rate of the green plant parts (e.g. stems and ear leaves) and a certain assimilates allocation from the reserve pools (stems and roots) to the growing grain, but the subject deserves further research. The work is being continued.

Keywords: *maize, defoliation, yield, irrigation, Thessaly plain, semi-arid areas*.

1. Introduction

Within the frame of the development of worldwide sustainable agriculture especially concerned with the shortage of water in semi-arid areas, much research has been focused on developing new methods and practices for optimization the water consumption by a great variety of crops. Research has shown that maize (*Zea mays*) plants react to defoliation using their resources for their growth and defense (Collantes *et al*., 1998). In field experiments conducted in Nebraska (Piper and Weiss, 1993), maize plants undergone 50% or 100% defoliation at the stage of 7th and 12th visible leaf restored the ratio of aerial versus below ground biomass at the same levels as the control, one week after defoliation. For this balance to be reached, less than 7 days were necessary, whereas the obtained yields were not statistically different than the control yields. Concerning the absorption of nutrients, research showed that in the case of total defoliation, not only the concentration of K was not increased in the husk leaf compared to the control, but also a decrease in the concentration of N, P, and Mg was observed (Fujita *et al*., 1994). In another experiment that was held in Canada, 50% and 100% of leaf blades were removed upon silking, and the results showed that the decrease of the leaves area, which constitutes the plant's energy source at the stage of grain filling advanced maturation. In fact, the defoliation that took place in 50% of the leafage, 6 weeks after the stage of silk creation, reduced only 7% of the 1000 seed weight compared to the control (Tollenaar and Daynard, 1978).
In another research, the effect of defoliation in plants of rye (*Secale cereale*) at the concentration of hydroxamic acids (DIBOA) was studied, which are secondary metabolites in grain and play a significant role in the defense of plants against herbivore insects such as aphids, grasshoppers, etc. It was found that the concentration of the DIBOA was higher than the one in plants of the control in which defoliation did not take place (Collantes *et al*., 1997). In a research that lasted eleven years, the effects of defoliation on the maize at the stage of five leaves were evaluated. The goal of the study was to receive the same results over the years in order to reach reliable conclusions from the correlation between premature defoliation with high yields and the usage of soil

water. The results of the last eight years showed that the defoliation decreased the yields of the first three years and had an insignificant effect during the rest five years. In fact, a shortage of available soil water was observed in these five years. The reduction of leaves' area during the initial stages might help maize plants to undergo fewer adverse effects under the stress of the shortage of water in the following growing stages (Crookston and Hicks, 1988). The defoliation method has been used frequently in order to create a new cultivation technique that will help in maintaining the humidity of the soil. The results of various field and pot experiments with grain crops have shown that the defoliation during the fluorescence reduced the consumption of water (transpiration). However, according to Shao *et al*. (2010), the benefit from the reduced consumption of water does not compensate for the decrease in production. Furthermore, the method of defoliation has been used in maize crops studies where the productive direction of the cultivation is for silage. The results showed that the defoliation in stage R1 had no effect on the content of starch (Roth and Lauer, 2008).The aim of this study was to evaluate the method of defoliation as a potential innovative cultivation technique that could reduce water use in irrigated maize cultivations without a major negative effect in final yield in a semi-arid environment such as the Thessaly plain in Central Greece, comprising the largest lowland formation and agricultural production center of the country.

2. Materials and methods

The maize field experiment was conducted from March to September 2019 in the rural area of Giannouli (Larissa). The soil is a deep, fertile, clay loam formed on calcareous alluvium of the Peneios River. The field received basic fertilization with 700 kg/ha with mixed fertilizer 21-8-14. The sowing was conducted on April 1st 2019 in rows 75 cm apart with a plant population of 80,000 plants/ha. The maize hybrid DKC6728 was used. Sowing depth was 3.5 cm. A completely randomized split plot design was used with plots 5 m x 3 m consisting of 4 rows of plants. The Zadoks scale was used to estimate the phenological stages at which defoliation was programmed. A meteorological station and soil moisture sensors from Pessl were used to assess soil moisture and determine irrigation. Defoliation applications were made on whole plants on four different dates and two soil moisture levels (irrigated plants for matching 100% and 50% of the potential evapotranspiration). The first defoliation took place on the 12th of July (stage 73), the second on the 19th of July (stage 75), the third on the 27th of July (stage 77), and the last on the 4th of August (stage 83). The measurements in each experimental plot were made in a length of 1 m in the two middle rows to avoid the border effect. The samples were separated into stem and cob (and leaves of the control) and dried at 65^{o}C until equal weights. Finally, the dry matter of the stems and seed, were weighted separately as well as the dry weight of the green leaves of the control plots (without defoliation).

3. Results and Discussion

The dry weight of maize cob varied from 6,660 to 16,560 kg/ha (Figure 1). Among the defoliation treatments that were tested, the combination of the defoliation with 100% irrigation on Zadoks stage 83 gave the highest values (13,911 kg/ha), followed by the defoliation with 50% irrigation in the same stage. The lowest cob dry weight (6,660 kg/ha) was measured in the combination of defoliation with 100% irrigation on stage 73 which was the earliest date of defoliation. What is easily noticeable in Figure 1 is that the later the defoliation was performed, the higher the values were observed in the case of dry cob weight. It seems very important that, despite the statistically lower yields, the latest defoliation (ZC83) resulted in a rather acceptable yield of 13.9 t/ha under full irrigation and of 12.5 t/ha with saving 50% of irrigation water. Apparently, a substantial assimilates redistribution from the stems (and roots) to the growing seed was taken place after each defoliation (e.g. about 2-2.5 t/ha; Fig. 1), which at the latest defoliation leaded to obtaining an acceptable final seed yield.

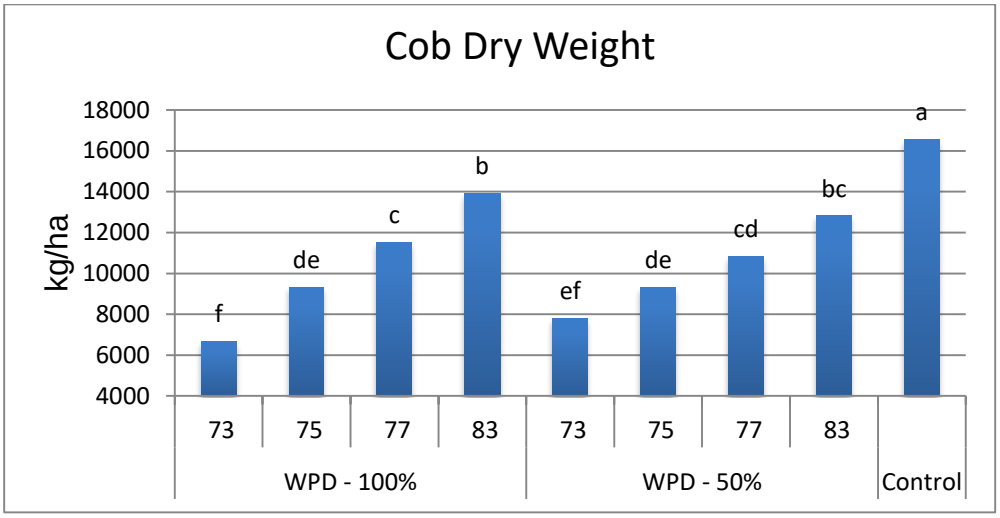

Figure 1. Cob dry weight of maize in the nine different treatments for fully (100%) and partially (50%) irrigated plants (Zadoks scale development stages 73, 75, 77 and 83) versus the control (no defoliation).

Total dry matter also presented statistically significant differences among the treatments, and its value varied from 12,394 to 26,171 kg/ha (Figure 2). The untreated plants presented the highest value of total dry matter (26,171 kg/ha). Among the tested treatments, the defoliation with 100% irrigation on 83 was the best with 13,911 kg/ha, along with the defoliation with 50% irrigation on the same Zadoks stage. The lowest total dry matter (12,394 kg/ha) was observed in the combination of defoliation with 100% irrigation on stage 73 which was the earliest date that the defoliation was performed. In general, the defoliation treatments with any combination of irrigation water decreased the total dry matter production of the maize plants, but the later it is performed, the less significant the decrease.

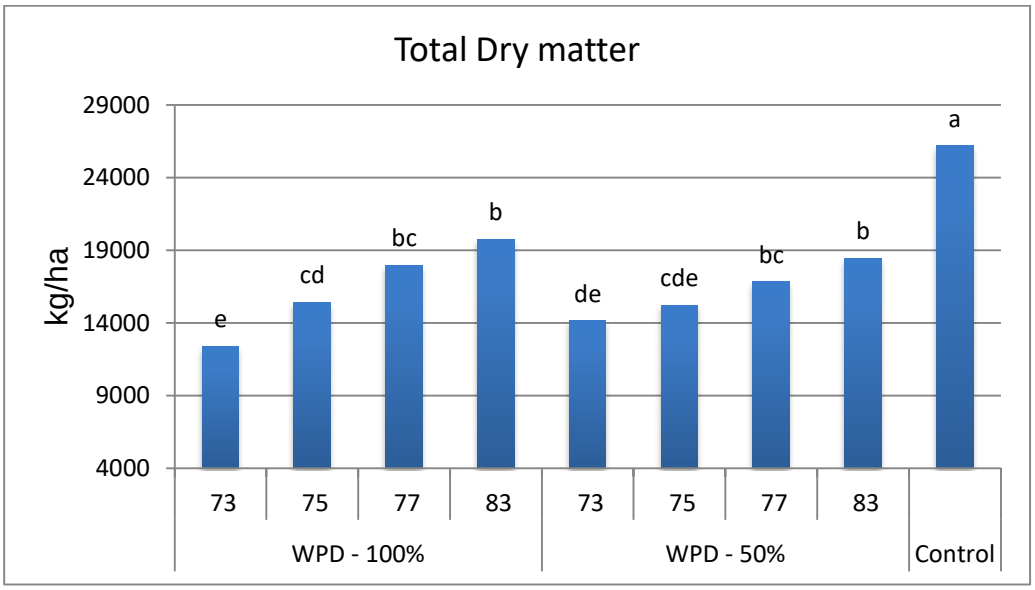

Figure 2. Total dry weight of maize in the nine different treatments for fully (100%) and partially (50%) irrigated plants (Zadoks scale development stages 73, 75, 77 and 83) versus the control (no defoliation).

Since maize is an irrigated cultivation in many countries, including Greece, reduced irrigation (50%) coupled with defoliation at advanced stage during the grain filling period may save considerable amount of irrigation water without greatly harming the final yield. In particular, the later defoliation is performed, the less significant is the reduction of the dry matter yield. As mentioned earlier, after each defoliation, an “assimilate gift” of about

2-2.5 t/ha seems to be is invested to the growing seed apparently from the pools of stem (and root) and this holds also for the partially irrigated crop.

4. Conclusion and future prospects

Total defoliation of maize significantly reduces dry cob weight and total dry matter especially if defoliation takes place long before maturation. However, an increase in dry maize seed of about 2-2.5 t/ha after each defoliation practice results in attaining a considerable yield level at late defoliation dates even under reduced irrigation. This finding might prove that the practice of defoliation can be helpful in areas with low availability of water to maintain an acceptable yield production level with no significant losses due to water stress. Further research has to be conducted to monitor the effect of defoliation on different crop species to investigate the possibility of this innovative technique being used in agricultural practice. The subject deserves further research.

References

Collantes H.G., Gianoli E., Niemeyer H.M. (1997). Effect of defoliation on the patterns of allocation of a hydroxamic acid in rye (Secale cereale). Environmental and Experimental Botany 38: 231-235.

Collantes H.G., Gianoli E. and Niemeyer H.M. (1998). Changes in growth and chemical defences upon defoliation in maize. Phytochemistry Vol. 49, No. 7, pp. 1921-1923.

Crookston R.K. and Hicks D.R. (1988). Effect of Early Defoliation on Maize Growth and Yield: an Eleven-year Perspective. Crop Science 28(2): 371-373.

Fujita K., Furuse F., Sawada O., Bandara D. (1994) Effect of defoliation and ear removal on dry matter production and inorganic element absorption in sweet corn, Soil Science and Plant Nutrition, 40:4, 581-591.

Piper E.L. and Weiss A. (1993). Defoliation during vegetative growth of corn: the shoot-root ratio and yield implications. Field Crops Research, 31, 145-153.

Roth G.W. and Lauer J.G. (2008). Impact of Defoliation on Corn Forage Quality. Agronomy Journal 100 (3): 651-657.

Shao L., Zhang X., Hideki A., Tsuji W., Chen S. (2010). Effects of defoliation on grain yield and water use of winter wheat. Journal of Agricultural Science 148: 191-204.

Tollenaar, M. Daynard, T. B. (1978). Effect of defoliation on kernel development in maize. Can. J. Plant Sci. 58: 207-212.

Evaluation of three gridded data sets in reproducing wheat development and yield with Ceres-Wheat model over the Mediterranean region

Liakopoulou K.S.[1], Mavrommatis T.[1]

[1]Department of Meteorology and Climatology, School of Geology, Aristotle University of Thessaloniki, Greece

Abstract. The availability of ground-based observations continues to be a serious constraint. Although gridded data sets constitute an alternative source, investigators should consider their strengths and weaknesses before its application in climate and weather research. Daily maximum and minimum temperature, precipitation, and solar radiation data from three gridded datasets (E-OBS in 2 spatial resolutions (10km and 25km) and Agri4cast (25km)) and 9 Mediterranean stations (selected for their proximity to wheat crops), during 1980-2019, were compared for its abilities in reproducing wheat development and yield with the crop simulation model CERES-Wheat for the reference period and climate change scenarios. The interactive atlas of IPCC was used for obtaining climate change information. Eobs-0.1 emerged as the best gridded product for anthesis, maturity and harvesting, presenting the lower discrepancies. The RMSE values estimated to 10 days on average for developmental stages both without and with CS, and for yield up to 13% and 9.5% for the reference period and CS, respectively. The correlation was also high to very high.

1 Introduction

In the Mediterranean basin, durum wheat (Triticum turgidum L. subs. Durum [Desf.]) is the most common crop. According to European Commission statistics, Spain, Italy, and France together it is estimated they represent 80% of total durum wheat production in Europe (Rossini et al., 2018). As IPCC (2021) reported, within the next 20 years, global warming is expected to reach or even exceed 1.5°C. Specifically, in the Mediterranean region, temperature is anticipated to rise and precipitation to decrease (EEA 2019). This fact will have an impact on agriculture, and therefore on wheat, as earlier cultivation and reduction of production is expected (Dettori et al., 2017). It is necessary to assess the impact of climate change on wheat production. This can be achieved using crop simulation models, which constitute the main tools for simulating crop growth and harvested yield (Donatelli et al., 2002).
Meteorological data sources can be classified into two main categories 1) observational data and 2) gridded data. The former includes in situ, visual and remote observations (Atlas, 1997) and the later reanalysis and reprocessed data (Ceglar et al., 2017). In climate studies, it is important have accurate and long-term data sets. Such data must have a homogeneous spatial analysis in the area of interest, a long period of time and no gaps. Although many countries around the world have an adequate network of observation stations, in many cases their datasets do not meet the above criteria. Thus, in order to cover this weakness, gridded data of high spatial and temporal resolution have been developed (Tarek et al., 2020).
On this context, the aim of this study is the comparison of three gridded data sets (E-OBS in 2 spatial resolutions and Agri4cast) in reproducing wheat development and yield with the Ceres-Wheat model over the Mediterranean region under a reference period and future climate change scenarios.

2 Data

Daily maximum and minimum temperature, precipitation, and solar radiation (from now on Tmax (C˚), Tmin (C˚), Prec (mm) and QQ (MJ/m^2/day), respectively) data from three gridded datasets (E-OBS in 2 spatial resolutions (10km (Eobs-0.1)) and 25km (Eobs-0.25) and Agri4cast (25km)) and 9 Mediterranean meteorological stations (Obs) (based on their proximity to wheat crops), were selected (Fig. 1). The altitude differences between the gridded data and observed, as well as the reference period for each station are shown in Table 1. Although the differences in longitude and latitude (as shown by the spatial distribution of crosses symbols in Fig.1) between the centres of the grid cells and the stations appear small, the differences in altitude are substantial on some occasions (Malaga, Granada, Melilla and Thessaloniki). The data for Spain, France and Italy stations were assembled from the CDO (Climate Data Online) database of NCEI/NOAA (National Centres for Environmental Information, National

Oceanic and Atmospheric Administration) (https://www.ncdc.noaa.gov/cdo-web/), while for the station in Greece from the meteorological station in Aristotle University of Thessaloniki in Greece. To account for the differences in altitude between the station and the grid centres, the gridded temperature time series was adjusted by 0.65 C˚ for each 100m discrepancy.

The Agri4Cast reanalysis data (http://agri4cast.jrc.ec.europa.eu) covers the EU member states since 1975 and consists of daily a) weather data derived from at least 4.200 synoptic weather stations with an irregular distribution and density; and b) weather from six ECMWF forecast products which have a different number of forecast days (forecast depth) and a varying number of possible realizations called “members”. The two data sources are then interpolated to the centres of a fixed grid of 25 × 25 km (Micale and Genovese, 2004; Baruth et al., 2007).

E-OBS (v23.1e) is a daily gridded reprocessed observational dataset derived from ECA&D (European Climate Assessment and Dataset, http://www.ecad.eu) daily observations. E-OBS includes data for precipitation, temperature and sea level pressure in Europe since 1950 (Haylock et al., 2008; Klok and Tank Klein, 2009; Cornes et al., 2018). The data were interpolated using a three-step methodology (Haylock et al., 2008). The exact number of stations varies over time and is larger for precipitation than temperature, while it decreases from north to south and from west to east (Cornes et al., 2018).

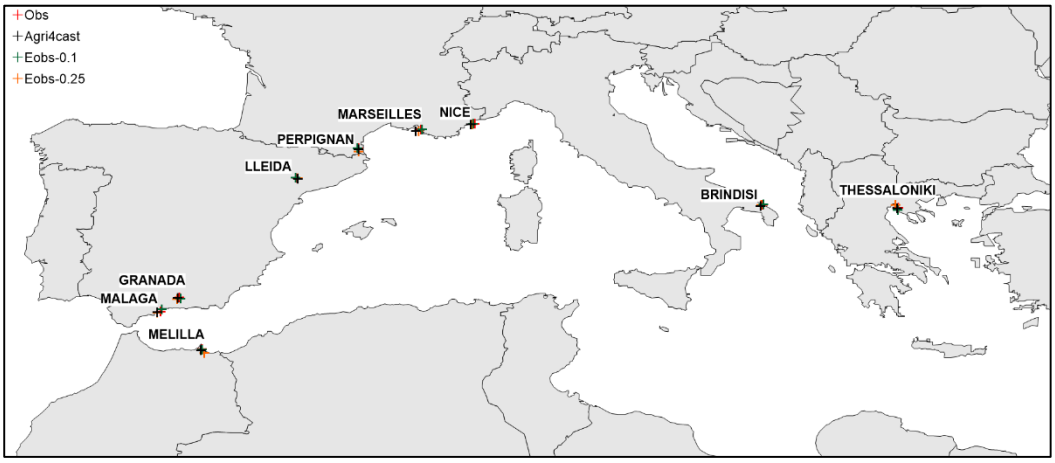

Figure 1. Spatial distribution of Mediterranean meteorological stations and gridded cells’ centres.

Table 1. Altitude differences (m) between the gridded (Eobs-0.1, Eobs-0.25 and Agri4cast) data with the observed (Obs) for each station. The reference period is also shown.

	ALTITUDE DIFFERENCES			REFERENCE
STATION	AGRI4CAST-OBS	EOBS0.1-OBS	EOBS0.25-OBS	PERIOD
MALAGA,SP	62	185	252	1980-2019
GRANADA,SP	198	112	222	1980-2019
MELILLA,SP	203	176	140	1980-2019
LLEIDA,SP	1	31	12	1980-2019
PERPIGNAN,FR	31	3	56	1980-2019
MARSEILLES,FR	5	88	47	1980-2019
NICE,FR	67	55	211	1980-2017
BRINDISI,IT	15	6	31	1980-2017
THESSALONIKI,GR	103	90	82	1980-2009

3 Materials and methodology

3.1 DSSAT (CERES-Wheat crop model)

The decision support system for agrotechnology transfer (DSSAT) was originally developed by an international network of scientists, cooperating in the International Benchmark Sites Network for Agrotechnology Transfer

project (Jones et al. 2003), to simulate the growth and yield of a cultivation system based on the interaction of weather, soil and crop management. In this paper, the DSSAT v4.7.5 version was used, which includes crop models for more than 42 species and improved tools that facilitate the use of crop models. Required input include weather (daily Tmax, Tmin, Prec and QQ) and soil conditions, crop management and plant characteristics (Hunt et al., 2001).
The CERES-Wheat crop model, which simulates wheat crop growth, development and yield considering the effects of weather, genetics, soil (water, carbon and nitrogen), planting, irrigation and nitrogen fertilizer management (Soltani et al. 2004), was selected in this work. The model is designed to have applicability in diverse environments and to utilize a minimum data set of field and weather data as inputs (Jones et al. 2003). It is a widely used model for estimating wheat production (Zhang et al., 2019) and has presented reliable results in Mediterranean conditions (Simeonidis, 2011; Mereu et al., 2019).

3.2 Methodology

Firstly, the time series of weather data were checked for completeness and erroneous values with the use of WeatherMan, a software package, included in DSSAT's tools, designed to assist in preparing daily weather data for use with crop simulation models (Pickering et al., 1994). Then the three gridded data sets (Eobs-0.1, Eobs-0.25 and Agri4cast) were evaluated for their abilities in reproducing wheat development (anthesis and maturity) and harvested yield with the Ceres-Wheat model over the Mediterranean region for the reference period and consequently under climate change conditions. The crop model was run in potential mode (with inactive the subroutines of soil moisture and fertilization simulation). On this mode, yield depends only on temperature, solar radiation, and the variety's genetic characteristics. Iride, the durum wheat variety, which was chosen for this study, is a relatively new variety (released in 1996) of high productivity and adaptability to different environments (Mereu et al. 2019). The genetic coefficients of Iride are presented in Table 2. The same crop management and sowing day (1st November) were chosen for all stations. Incremental climate projections were developed using consistent positive and synchronous adjustments (from 0ºC to +1.6ºC in steps of 0.1 ºC, 289 (17x17) scenarios in total) in historical Tmax and Tmin during the year following the scheme illustrated in Figure 2. The selection of climate scenarios (CS) was guided by the interactive IPCC (https://interactive-atlas.ipcc.ch/) maps for the near future (2021-2040) period over the Mediterranean Region.

Table 2. Genetic coefficients for Iride variety.

Coefficient	Value
P1D (Photoperiod response (% reduction in rate/10 h drop in pp))	62
P1V (Days,optimum vernalizing temperature,required for vernalization)	25
P5 (Grain filling (excluding lag) phase duration (oC.d))	777
G1 (Kernel number per unit canopy weight at anthesis (#/g))	29
G2 (Standard kernel size under optimum conditions (mg))	41
G3 (Standard,non-stressed mature tiller wt (incl grain) (g dwt))	2
PHINT (Interval between successive leaf tip appearances (oC.d))	97

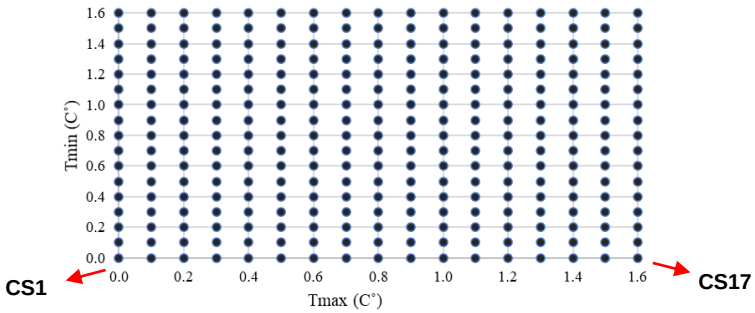

Figure 2. The incremental (from 0ºC to +1.6ºC, in steps of 0.1ºC, 289 (17x17) scenarios in total) and synchronous adjustments for Tmax and Tmin scenarios used in this study.

The comparison between gridded data and Obs was made using boxplots and computing the RMSE and the correlation coefficient (r). RMSE is generally sensitive to extreme values, especially when the sample is not large (Fox, 1981). The correlation coefficient indicates the magnitude of the relation between two variables (Taylor, 1990) and can be either positive or negative, from -1 to 1.

4 Results

The discrepancies of estimated with Ceres-Wheat anthesis, maturity and harvested yield between the gridded products and observed time series for the reference and CS, for each station, are illustrated in Figure 3. Eobs-0.1, followed by Eobs-0.25, presented the lower discrepancies for the reference period, for both developmental stages (anthesis and maturity) and yield production. After the application of climate scenarios, Eobs-0.1 emerged again as the best product, while Eobs-0.25 and Agri4cast followed in small distance. Granada and Thessaloniki tended to present the largest differences, while the stations of France the smallest. For both periods, greater discrepancies were computed for yield than for anthesis and maturity. In addition, the variability (standard deviation) and the range of discrepancies decreased after the climate adjustments.

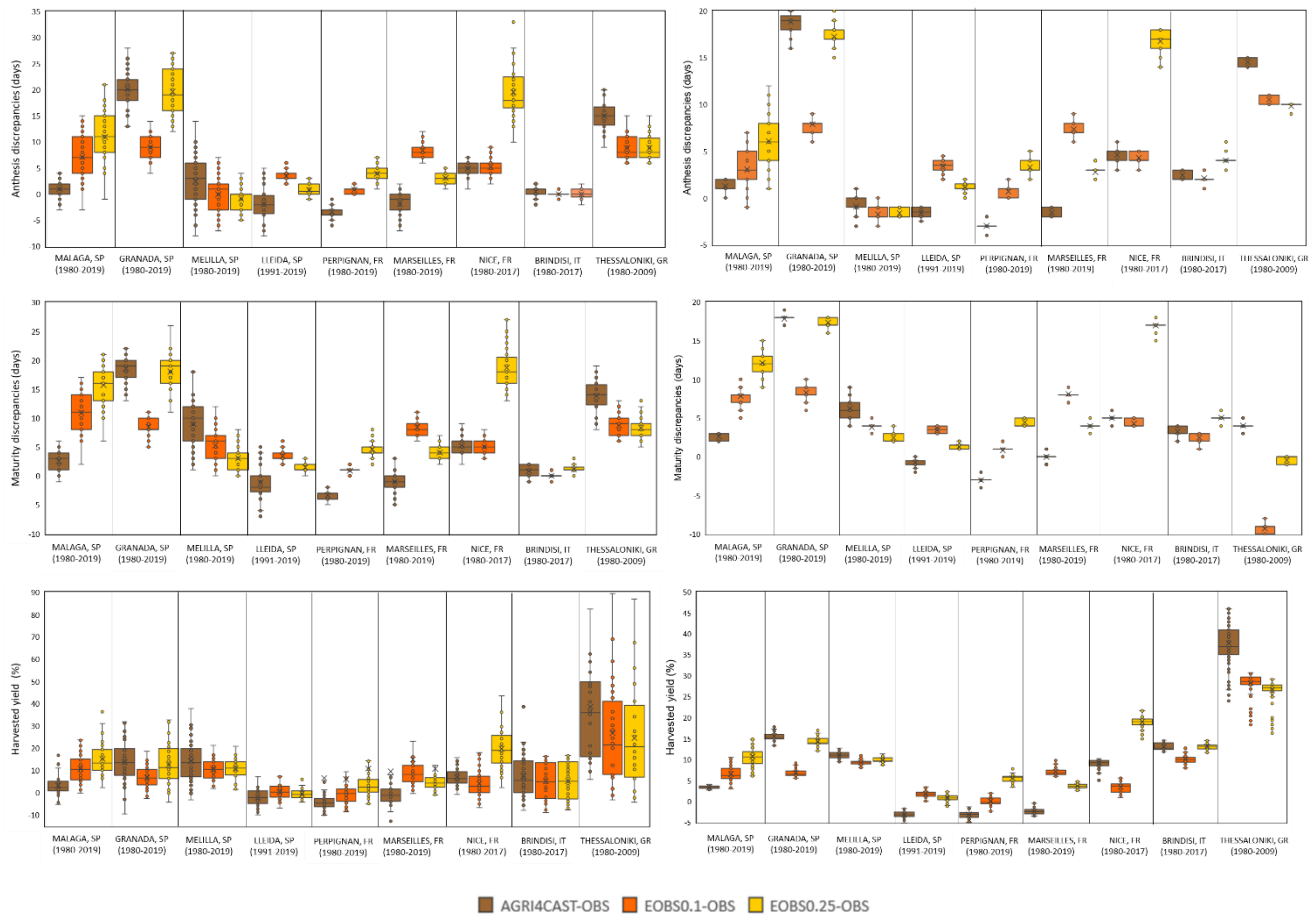

Figure 3. Discrepancies for anthesis and maturity (top and middle figures, respectively) (Re-Obs) and harvested yield (((Re-Obs)/Obs)*100) (bottom figures), estimated with CERES-Wheat between observed and gridded (Eobs-0.1, Eobs-0.25 and Agri4cast) datasets for each station for the reference (left panel) and future projections (right panel) periods.

Table 3 shows the RMSE and r statistics of estimated with Ceres-Wheat anthesis, maturity and yield between the gridded products and observed time series for the reference and near future periods. Eobs-0.1 was again the best product for both periods. RMSE of anthesis, maturity and yield production, ranged for the reference period from 0.3-9 days, 0.2-11 days and 3-13%, while using CS from 1-10.5 days, 1-9 days and 1-9.5%, respectively. Thessaloniki for the reference period and Nice with CS, showed extreme RMSE (27.6 and 21.4%, respectively) compared to the other stations. In addition, high and very high correlation values (greater than 0.9) were found. Note that the correlation was higher with CS than for the reference period.

Table 3. RMSE and r statistics of estimated with Ceres-Wheat anthesis, maturity and yield between the gridded products (Eobs-0.1, Eobs-0.25 and Agri4cast) and observed time series for the reference and future projections.

WITHOUT CLIMATE SCENARIO							WITH CLIMATE SCENARIO					
ADAT							ADAT					
	RMSE			r			RMSE			r		
STATION	Agri4Cast	EOBS-0.1	EOBS-0.25	Agri4Cast	EOBS-0.1	EOBS-0.25	Agri4Cast	EOBS-0.1	EOBS-0.25	Agri4Cast	EOBS-0.1	EOBS-0.25
MALAGA,SP	2.0	8.3	12.0	0.893	0.468	0.343	1.4	3.7	6.6	0.266	-0.851	-0.852
GRANADA,SP	20.4	9.2	20.2	0.899	0.961	0.827	18.9	7.9	17.3	0.982	0.983	0.991
MELILLA,SP	5.4	3.3	2.4	0.317	0.632	0.827	1.3	1.9	1.7	-0.452	0.052	0.414
LLEIDA,SP	3.9	3.6	1.4	0.821	0.977	0.979	1.6	3.5	1.3	0.991	0.985	0.987
PERPIGNAN, FR	3.5	1.0	4.2	0.986	0.996	0.974	3.0	0.9	3.3	0.983	0.969	0.952
MARSEILLES, FR	2.6	8.5	3.3	0.966	0.981	0.990	1.6	7.4	2.8	0.984	0.986	0.988
NICE, FR	5.0	5.5	20.2	0.975	0.961	0.831	4.7	4.3	16.8	0.983	0.982	0.984
BRINDISI, IT	1.1	0.3	0.8	0.984	0.998	0.991	2.5	2.2	4.1	0.960	0.944	0.963
THESSALONIKI, GR	15.2	9.1	9.2	0.898	0.933	0.922	14.6	10.5	9.8	0.980	0.981	0.989
MDAT							MDAT					
	RMSE			r			RMSE			r		
STATION	Agri4Cast	EOBS-0.1	EOBS-0.25	Agri4Cast	EOBS-0.1	EOBS-0.25	Agri4Cast	EOBS-0.1	EOBS-0.25	Agri4Cast	EOBS-0.1	EOBS-0.25
MALAGA, SP	3.0	11.4	16.1	0.941	0.785	0.742	2.7	7.9	12.2	0.857	0.913	0.919
GRANADA, SP	18.7	8.6	18.3	0.947	0.968	0.904	17.9	8.3	17.4	0.988	0.988	0.977
MELILLA,SP	9.8	6.0	3.7	0.499	0.746	0.862	6.4	3.9	2.5	0.919	0.869	0.846
LLEIDA, SP	3.3	3.5	1.6	0.821	0.982	0.988	0.8	3.5	1.3	0.992	0.989	0.993
PERPIGNAN, FR	3.4	1.0	4.8	0.993	0.997	0.978	3.1	1.0	4.5	0.982	0.985	0.983
MARSEILLES, FR	2.1	8.5	4.2	0.968	0.986	0.989	0.3	8.1	4.0	0.992	0.986	0.991
NICE, FR	5.4	5.2	19.1	0.969	0.982	0.921	5.0	4.3	17.0	0.982	0.990	0.988
BRINDISI, IT	1.2	0.2	1.3	0.979	0.999	0.991	3.3	2.6	5.1	0.970	0.955	0.971
THESSALONIKI, GR	14.1	8.9	8.5	0.844	0.925	0.921	4.1	9.3	0.7	0.994	0.981	0.980
HWAM							HWAM					
	(RMSE/mean*100)(%)			r			(RMSE/mean*100) (%)			r		
STATION	Agri4Cast	EOBS-0.1	EOBS-0.25	Agri4Cast	EOBS-0.1	EOBS-0.25	Agri4Cast	EOBS-0.1	EOBS-0.25	Agri4Cast	EOBS-0.1	EOBS-0.25
MALAGA, SP	5.0	12.1	16.4	0.846	0.734	0.655	11.0	8.5	11.1	0.884	0.916	0.911
GRANADA, SP	15.9	8.0	14.7	0.292	0.791	0.397	7.4	3.0	15.4	0.960	0.900	0.944
MELILLA,SP	16.3	11.2	11.5	0.557	0.833	0.857	11.1	9.3	9.9	0.707	0.900	0.843
LLEIDA, SP	4.4	3.2	2.3	0.831	0.885	0.942	3.1	6.2	9.8	0.910	0.927	0.931
PERPIGNAN, FR	14.4	9.7	11.0	0.299	0.786	0.761	3.3	1.0	5.7	0.956	0.970	0.959
MARSEILLES, FR	15.6	12.8	10.1	0.168	0.833	0.857	28.5	21.4	20.0	0.969	0.955	0.978
NICE, FR	7.7	6.6	20.8	0.919	0.787	0.576	19.0	8.4	17.6	0.971	0.964	0.982
BRINDISI, IT	11.0	9.0	9.0	0.774	0.834	0.838	4.4	2.6	1.4	0.971	0.954	0.974
THESSALONIKI, GR	37.7	27.6	25.7	0.423	0.563	0.589	3.3	9.5	4.9	-0.073	0.769	0.773

5 Conclusions

This study compared three gridded data sets (E-OBS in 2 spatial resolutions (10km and 25km) and Agri4cast (25km)) for their abilities in reproducing wheat development and yield with the Ceres-Wheat model over 9 meteorological stations selected for their proximity to wheat crops in the Mediterranean region under the reference and future climate change scenarios. The Iride variety was selected and the crop model was run in potential mode. Overall, Eobs-0.1 was the best gridded product for anthesis, maturity and harvesting presenting the lower discrepancies. The RMSE values estimated to 10 days on average for developmental stages both without and with CS, and for yield up to 13% and 9.5% for the reference period and CS, respectively. The correlation was high to very high.

References

Atlas, R., 1997: Atmospheric Observations and Experiments to Assess Their Usefulness in Data Assimilation, Journal of the Meteorological Society of Japan, 75, No. 1B, 111-130, https://doi.org/10.2151/jmsj1965.75.1B_111.

Baruth, B., Genovese, G. and Leo, O., 2007: CGMS Version 9.2. User Manual and Technical Documentation. JRC Scientific and Technical Reports. EUR 22936 EN, Luxembourg: Office for Official. Publications of the EU, 116.

Ceglar, A, Toreti, A, Balsamo, G., Kobayashi, S., 2017: Precipitation over Monsoon Asia: A Comparison of Reanalyses and Observations, J. Climate, 30, 465–476, https://doi.org/10.1175/JCLI-D-16-0227.1.

Cornes, R. C., van der Schrier, G., van den Besselaar, E. J. M., & Jones, P. D., 2018: An ensemble version of the E-OBS temperature and precipitation data sets, Journal of Geophysical Research: Atmospheres, 123, 9391–9409, https://doi.org/10.1029/2017JD028200.

Dettori, M., Cesaraccio, C., Duce, P., 2017: Simulation of climate change impacts on production and phenology of durum wheat in Mediterranean environments using CERES-Wheat model, Field Crops Research, 206, 43–53, https://doi.org/10.1016/j.fcr.2017.02.013.

Donatelli, M., van Ittersum, M.K., Bindi, M., Porter, R.J., 2002: Modelling cropping systems – highlights of the symposium and preface to the special issues, Eur. J. Agron., 18, 1–11, https://doi.org/10.1016/S1161-0301(02)00104-1.

EEA, 2019: Climate change adaptation in the agriculture sector in Europe. European Environment Agency (EEA), doi:10.2800/537176

Fox, D.G., 1981: Judging air quality model performance: A summary of the AMS workshop on dispersion models performance, Bull. Am. Meteorol. Soc., 62, 599-609, https://doi.org/10.1175/1520-0477(1981)062<0599:JAQMP>2.0.CO;2.

Haylock, M.R., Hofstra, N., Klein Tank, A.M.G., Klok, E.J., Jones, P.D. and New, M., 2008: A European daily highresolution gridded data set of surface temperature and precipitation for 1950-2006, Journal of Geophysical Research, 113, D20119, https:// doi.org/10.1029/2008JD010201.

Hunt, L.A., White, J.W., Hoogenboom, G., 2001: Agronomic data: advances in documentation and protocols for exchange and use, Agricultural Systems, 70, 477-492, https://doi.org/10.1016/S0308-521X(01)00056-7.

IPCC, 2021: Climate Change 2021: The Physical Science Basis. Contribution of Working Group I to the Sixth Assessment Report of the Intergovernmental Panel on Climate Change [Masson-Delmotte, V., P. Zhai, A. Pirani, S.L. Connors, C. Péan, S. Berger, N. Caud, Y. Chen, L. Goldfarb, M.I. Gomis, M. Huang, K. Leitzell, E. Lonnoy, J.B.R. Matthews, T.K. Maycock, T. Waterfield, O. Yelekçi, R. Yu, and B. Zhou (eds.)]. Cambridge University Press, Cambridge, United Kingdom and New York, NY, USA, In press, doi:10.1017/9781009157896. 302.

Jones, J.W., Hoogenboom, G., Porter, C.H., Boote, K.J., Batchelor, W.D., Hunt, L.A., Wilkens, P.W., Singh, U., Gijsman, A.J., Ritchie, J.T., 2003: The DSSAT cropping system model, Europ. J. Agronomy, 18, 235-265, https://doi.org/10.1016/S1161-0301(02)00107-7

Klok, E.J. and Tank Klein, A.M.G., 2009: Updated and extended European dataset of daily climate observations, International Journal of Climatology, 29, 1182–1191, https://doi.org/10.1002/joc.1779.

Mereu, V., Gallo, A., and Spano, S., 2019: Optimizing Genetic Parameters of CSM-CERES Wheat and CSM-CERES Maize for Durum Wheat, Common Wheat, and Maize in Italy, Agronomy, 9, 665, doi:10.3390/agronomy9100665.

Micale, F., and Genovese, G., 2004: Methodology of the MARS crop yield forecasting system, In: Meteorological Data, Collection, Processing and Analysis 1, Luxemburg: Publication EUR 21291 EN of Office for official publication of the EU.

Pickering, N. B., Hansen, J. W., Jones, J.W., Wells, C. M., Chan, V. K., and Godwin, D. C., 1994: WeatherMan: A Utility for Managing and Generating Daily Weather Data, Agron. J., 86, 332-337, https://doi.org/10.2134/agronj1994.00021962008600020023x.

Rossini, R., Provenzano, M.E., Sestili, F., and Ruggeri, R., 2018: Synergistic Effect of Sulfur and Nitrogen in the Organic and Mineral Fertilization of Durum Wheat: Grain Yield and Quality Traits in the Mediterranean Environment, Agronomy, 8, 189; doi:10.3390/agronomy8090189.

Soltani, A., Meinke, H. and deVoil, P., 2004: Assessing linear interpolation to generate daily radiation and temperature data for use in crop simulations, Eur J Agron 21:133-148, doi:10.1016/S1161-0301(03)00044-3.

Symeonidis K., 2011: Contribution to the study of growth and harvest of grains in Greece with agrometeorological models, (Master thesis), doi: 10.26262/heal.auth.ir.129044.

Tarek, M., Brissette, F.P., Arsenault, R., 2020: Evaluation of the ERA5 reanalysis as a potential reference dataset for hydrological modelling over North America, Hydrol. Earth Syst. Sci., 24, 2527–2544, doi: 10.5194/hess-24-2527-2020.

Taylor, R., 1990: Interpretation of the Correlation Coefficient: A Basic Review, Journal of Diagnostic Medical Sonography, 6, 35-39, https://doi.org/10.1177/875647939000600106.

Zhang, D., Wang, H., Li, D., Li, H., Ju, H., Li, R., Batchelor, W., Li, Y., 2019: DSSAT-CERES-Wheat model to optimize plant density and nitrogen best management practices, Nutr. Cycl. Agroecosyst., 114, 19–32, https://doi.org/10.1007/s10705-019-09984-1.

Agroclimatic classification towards sustainable agriculture based on geoinformatics: the case of Sidi Bouzid region in Tunisia

Faraslis[1], I., N. Alpanakis[2], G. Tziatzios[2], M. Spiliotopoulos[2], S. Sakellariou[2], P. Sidiropoulos[2], V. Brisimis[2], A. Blanta[2], N. Dercas[3], N.R. Dalezios[2]

[1] Department of Environmental Sciences, University of Thessaly, Larisa, Greece
[2] Department of Civil Engineering, University of Thessaly, Volos, Greece
[3] Department of Natural Resources and Agricultural Engineering, Agricultural University of Athens, Greece

Abstract

Agriculture is highly dependent on environmental conditions, thus, a quantitative understanding of the climate of an area is essential for sustainable production. The agroclimatic classification has been adopted for identifying sustainable agriculture zones within a climatic region. The objective of this study is to identify sustainable agricultural production zones in Sidi Bouzid region, in Tunisia. To achieve this, Google Earth Engine (GEE) cloud computing platform, and advanced remote sensing and GIS techniques are applied. The agroclimatic zoning methodology is implemented in three steps: firstly, water availability is considered, where hydroclimatic zones are developed leading to water limited growth environment (WLGE) zoning based on drought indices. Secondly, soil and land-use features are considered, which further develop the non-crop specific agroclimatic zoning. Thirdly, crop features and characteristics are considered, leading to crop-specific agroclimatic (CSA) zoning. The final map classifies the study area in seven agricultural suitability zones. The study demonstrates the lack of adequate areas with enough rainfed irrigation. This leads to the necessity of optimal use of underground water supplies. Moreover, the use of continuous high-resolution spatial and temporal remotely sensed data with GEE platform could provide new capabilities in updated agroclimatic zoning with minimizing the in-situ data.

1. Introduction

The population pressure and the high conflicts from different types of land users have made necessary an effective land-use planning. Especially, for food production the sustainable land use is an issue of great concern to governments. The agroclimatic analysis has as objective the assessment of inherent capabilities of land to support specific crops for long periods without degradation. The agroclimatic zones identify areas of sustainable crop production, considering environmental limitations and the sustainable use of natural resources. Many research studies varying in complexity try to identify agroclimatic zones (Araya et al, 2010; Adnan et al., 2017; Falasca et al., 2014). Most of them apply precipitation and evapotranspiration as the most important factors playing a vital role in agrometeorology, hydrology, applied climatology and water resources management. These variables in combination with soil type and landforms could determine high productivity areas avoiding the threat of depletion of natural resources.

Over the last few decades, the methodology of agroclimatic analysis has been developed, based on remote sensing data and methods, and applied in semi-arid regions (Tsiros et al. 2009). Remote sensing techniques and Earth Observation (EO) data have been proposed in many research studies to monitor drought conditions. Specifically, aridity index (AI) and the vegetation health index (VHI) are widely used in detecting subtle changes in vegetation stress (Kogan, 2002; Masitoh and Rusydi, 2019). Moreover, the unique benefits of new satellite EO data include its better spatial and spectral resolution providing improved reliability and accuracy in remote sensing methods with regards to climatic zones (Dalezios et al., 2018). With the advances in information and communication technologies new computer-based web platforms have been developed offering additional computational capabilities, such as the Google Earth Engine (GEE). The GEE is used for cloud-based processing of remote sensing data. It provides a great variety of constantly updated datasets, such as satellite data (Landsat, Sentinels, MODIS, etc), climate data (precipitation, temperature), elevation data, etc (Gorelik et al., 2017).

The aim of this study is twofold: first, to create rapidly, relatively high resolution, agroclimatic zones in arid environments in the Mediterranean basin. Previous agroclimatic zoning studies were more general and less detailed. The second objective is based on the investigation of new remote sensing datasets and the

methodological approaches provided by GEE platform. The study area, where sustainable production zones are created, is in Sidi Bouzid region, in Tunisia.

2. Methodology

The proposed methodology is based on remote sensing and GIS approaches for considering climate, weather, and landform restrictions and then to create sustainable crop production zones. This methodology is divided in three basic stages. (Dalezios et al., 2018): (a) Hydroclimatic zoning, (b) Non crop specific Agroclimatic zoning and (c) Crop specific Agroclimatic zoning. In the following flow-chart the three basic stages, for creating sustainable agricultural zones are illustrated (fig.1). The GEE web platform is the main tool with which scientific analysis of EO data is applied. Moreover, in this platform downscaling Machine Learning techniques are applied, to achieve higher resolution agroclimatic zones (200x200 m pixel size).

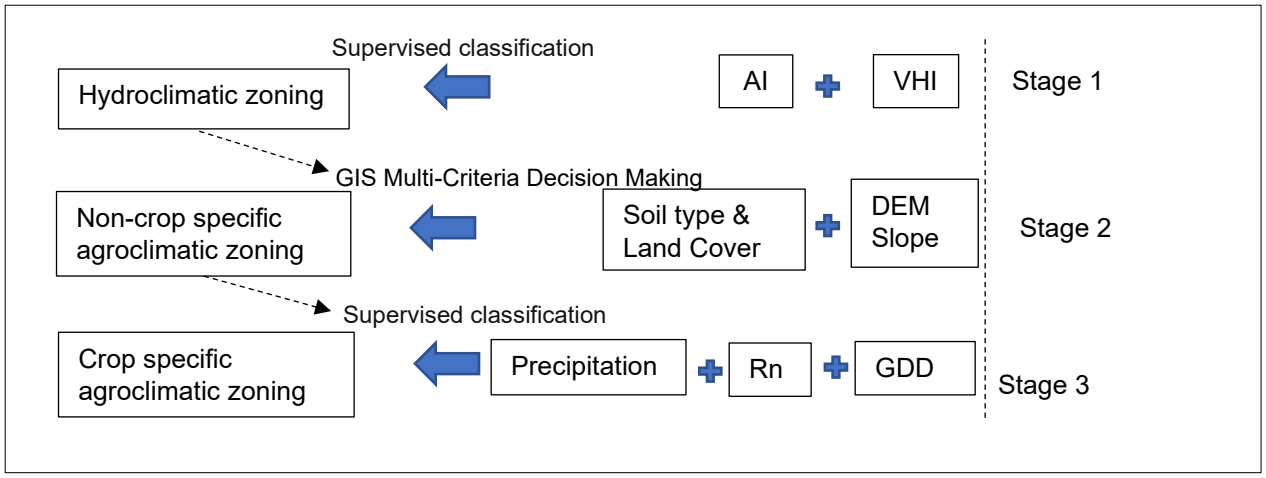

Figure 1The methodological steps of agroclimatic zoning leading to sustainable agricultural zones

The first stage of the methodology is to define suitable zones for agriculture considering the water constraints. In this step, remote sensing techniques are applied creating a map, namely Water Limited Growth Environment (WLGE) zones. These zones describe the hydroclimatic conditions of the study area. To determine the WLGE zones two satellite derived indices are combined, namely Vegetation Health Index (VHI) and Aridity Index (AI) (Wu et al, 2020). The VHI has been used to monitor the areas affected by drought. This index is used to assess vegetation stress, based on climate conditions. It considers the fluctuations of vegetation by defining the minimum and maximum NDVI (Normalized Vegetation Index) and the LST (Land surface Temperature) over a long period of time. The VHI is estimated by the combination of the two indices, the Vegetation Condition Index (VCI) and the Thermal Condition Index (TCI) (Zuhro et al., 2020). The AI, as a climatic index, is calculated by processing meteorological data over a long period of time (e.g., 20-30 years). It is calculated as the ratio between cumulative average monthly precipitation and cumulative average monthly potential evapotranspiration (PET) over a long period of time. The combination of VHI and AI products leads to the definition of three WLGE zones: No limitations, partially limited environment and Limited environment.

The second stage is to define the non-crop specific agroclimatic zoning (or general agroclimatic zoning). That is, sustainable agricultural production zones are classified in terms of water efficiency, soil fertility, and altitude-slope restrictions. These zones are derived by a combination of components, such as WLGE zones, Digital Elevation Model (DEM), slope, soil, and land-use/land cover implementing spatial multi-criteria decision making (MCDM) method (Tsiros et al., 2009). The analytical hierarchy process (AHP) is applied as the most widely accepted MCDM method in agriculture (Kihoro et al, 2013). This method helps to measure the weight of criteria with respect to each other by determining the weight of importance of each criterion. Finally, the derived non-crop specific agroclimatic zoning is classified in five suitable clusters: Good, Fair, Moderate, Poor and Not Suitable.

The third stage is to define crop-specific agroclimatic zoning map, namely sustainable zones according to the special characteristics of the crops, e.g., winter-summer crops. Three components are used, namely the growing

degree-days (GDD), the net radiation (Rn) and the amount of spring precipitation, to identify crop specific agricultural zones. These parameters are estimated over a long period of time (e.g., 20-30 years). The two indices, GDD, which represents the heat demand for crop growth and development and the Rn as the total available energy to influence the climate, could be restricted components at specific type of crops, namely winter or summer annual cultivations. The combination of them leads to high, medium, and low productivity zones. The amount of precipitation in spring is vital for annual crops. Specifically, the amount of precipitation during the last ten days in April and first 10 days in May (20 days in total) are estimated and classified in two clusters, sufficient – insufficient rain for annual crops. Next, a supervised classification of the three components is applied creating three productivity classes: high, medium, and low. Thereafter, Non-crop specific agroclimatic zoning combined with them creates the thematic map of sustainable crop production. The final crop-specific agroclimatic zoning contains seven thematic classes ranging from “Excellent” areas, as the most suitable zones for crop production with sufficient amount of rainfed irrigation, to “Not suitable” areas as inappropriate zones. Particularly, the zones are classified as (a) “Excellent”, “Very Good”, “Good”, which are generally suitable for annual crops, (b) “Fair”, “Moderate”, “Poor” are generally suitable for trees crops, vineyards, or annual crops under restrictions and (c) “Not Suitable”, are unsuitable areas for agricultural use.

3. Study Area and Database

3.1. Study Area

The pilot area in Tunisia is the province “Sidi Bouzid”, which occupies about 7,490 km^2. The region is in the central-western part of Tunisia, in the semiarid land (fig.2). It is characterized by relatively flat surface averaging 300 meters in altitude. The cultivated area is 412 000 hectares based on annual crops like durum wheat, fodder Oat, maize, vegetables, and trees, such as olives and pistachios.

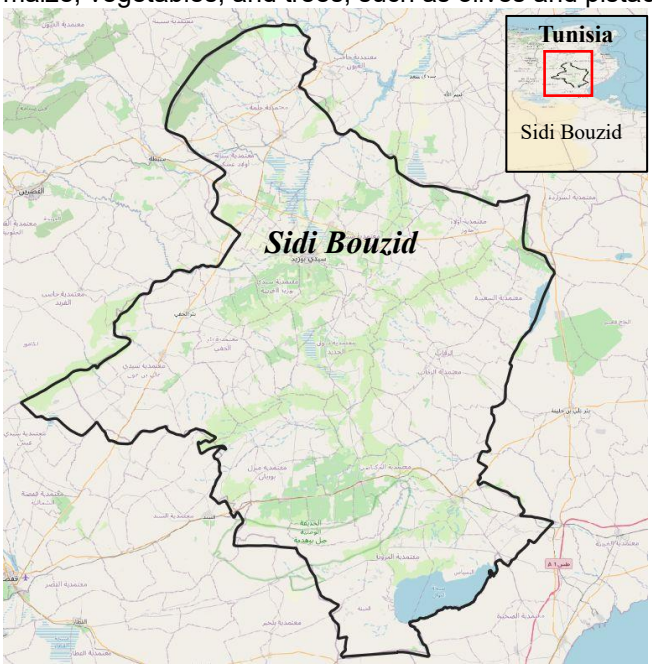

Figure 2 Study area “Sidi Bouzid” in Tunisia

3.2. Database and preprocessing

In this study, earth observation dataset from Google Earth Engine (GEE) and other web-based geoportals are derived. From GEE, the spatial resolution has been used. The available derived Landsat data is for the period of 2013 to 2020. For the Tunisian study area, 820 images are processed.

- Two MODIS products. 8-day Potential Evapotranspiration (MOD16A2) and Land Surface temperature with 500 meters and 1 Km spatial resolution, respectively. The time span for the data availability is 2001 to 2020. For the study area, 1248 8-day images in total are processed.
- Climate Hazards Group InfraRed Precipitation with Station data (CHIRPS) pentad rainfall data with 5 km spatial resolution. For the study area, 1440 pentad data, over the period of 2001 to 2020, are processed.

All the above-mentioned data is elaborated monthly extracting the median values over the last twenty years. Moreover, to achieve better resolution in MODIS and CHIRPS products (200X200 m pixel size) sophisticated techniques, such as machine learning algorithm, (Classification and Regression Trees-CART) is implemented.
From other web portals the following datasets are extracted:

- Digital Elevation Model (DEM). The Shuttle Radar Topography Mission (SRTM) digital elevation data, provided by NASA (National Aeronautics and Space Administration), is derived. The DEM has spatial resolution of about 30 meters.
- Soil Maps. The Soil dataset of the study areas is derived by the International Soil Reference and Information Centre (ISRIC- www.isric.org). The ISRIC soil data hub contains the type of soils at 250 meters resolution.
- Land use/Land Cover (LU/LC). For the Tunisian study area, a land cover thematic map (raster format) is provided by local research institute. This has been followed by the digitizing process to covert it in vector format with the appropriate coding.

4. Results and Discussion

Firstly, the WLGE zoning thematic map is created (fig.3). For the study area, four hydroclimatic classes exist: No Limitations, Partially Limited/No Limitations, Partially Limited and Limited/Partially Limited. As illustrated in figure 3, the two categories Limited/Partially Limited and Partially Limited zones dominate in the study area. In contrast, a small area in the southern part of the study area indicates good climatic conditions (Partial Limited/No Limited zones).

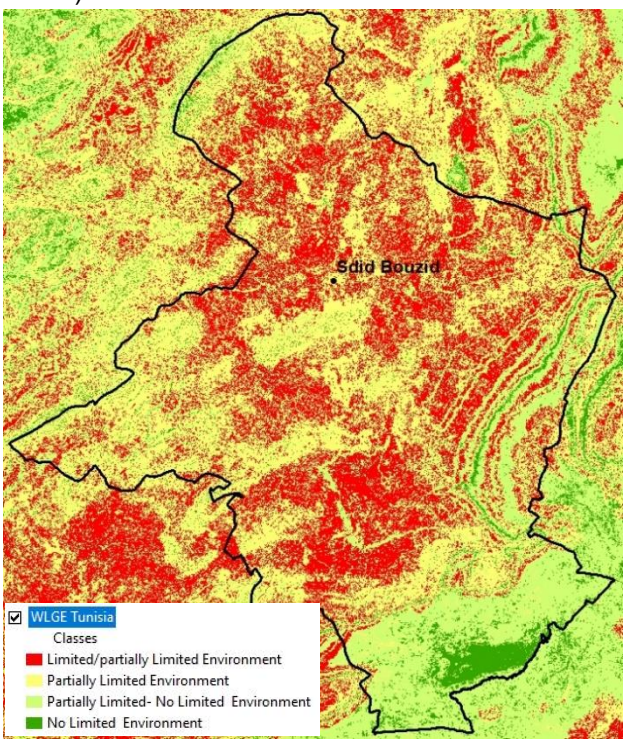

Figure 3 Four WLGE zones for Sidi-Bouzid

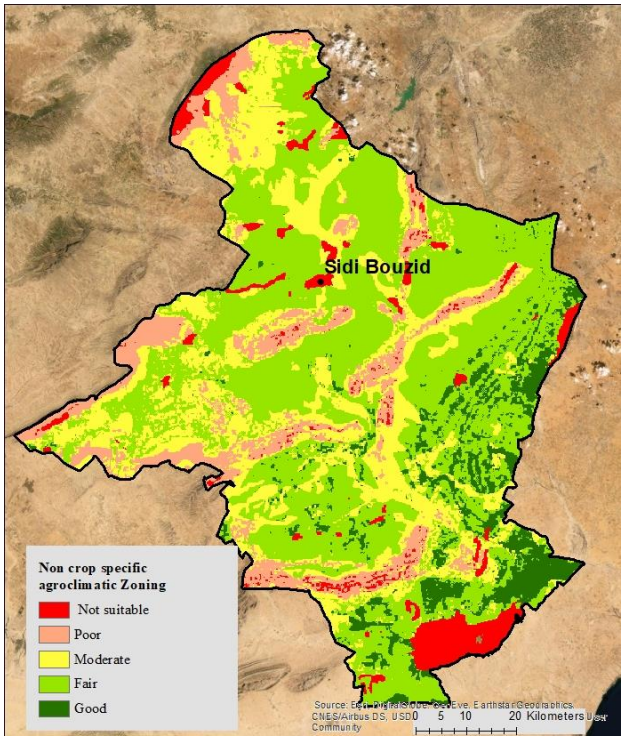

Figure 4 Non-crop specific agroclimatic zoning for Sidi-Bouzid

Secondly, the non-crop specific agroclimatic zoning thematic map is created. There are five classes of land suitability for agricultural purposes: Good, Fair, Moderate, Poor and Not Suitable (fig.4). From the statistical analysis, the first three non-crop specific agroclimatic classes cover 610,000 hectares of the total study area. Thus, 81% of the region can be used for sustainable agricultural production, but under certain conditions. In contrast, only 58,400 ha belong to the first class, which is suitable for agricultural use without restrictions.
From the analysis of the two indices, GDD and Rn, it is found that they aren't limited factor for annual winter crops, such as Oat and wheat. In contrast, the 20 days' spring cumulative precipitation, at the last 10 days of April and the first 10 days of May, is a crucial factor for the above-mentioned crops. To diversify the areas with sufficient amounts of rainfed irrigation a threshold of 10 mm of precipitation in the first two best suitable classes of Non-Specific Agroclimatic zoning, is applied. Finally, the crop-specific agroclimatic zoning thematic map is created (fig.5). In figure 5 the crop-specific agroclimatic zoning map is illustrated with 7 classes in terms of sustainable crop production. "Excellent" areas (dark green color) are identified as the most suitable zones for crop production with sufficient amount for rainfed irrigation and "Not suitable" areas (red color) are identified as inappropriate zones.

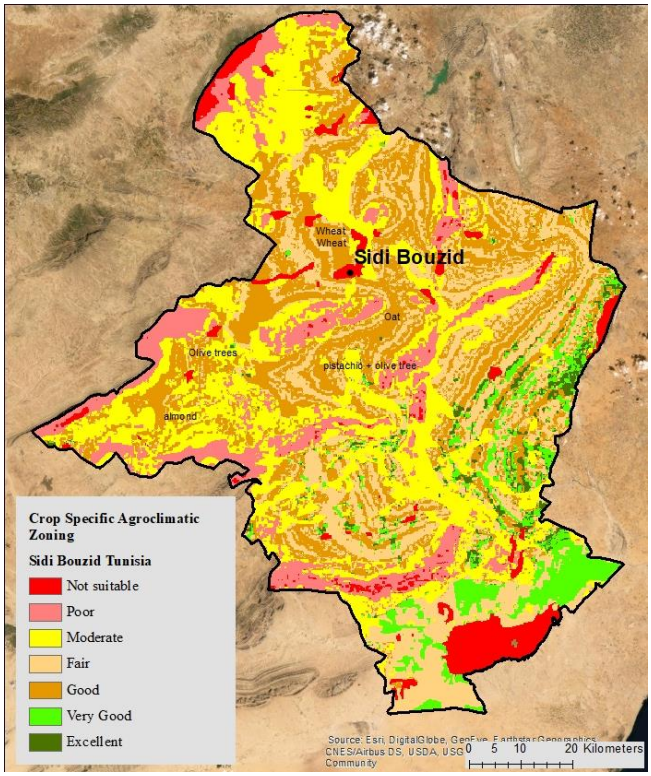

Figure 5 Crop specific agroclimatic zoning in Sidi-Bouzid Tunisia

More specifically, each category could support specific crops in the framework agricultural production as follows:

- Excellent zones: high yield areas for annual crops and arboriculture (vegetables, cereals, almond, pistachio, etc), with enough rainfed irrigation.
- Very Good zones: high yield areas for annual crops and arboriculture (vegetables, cereals, almond, pistachio, etc), with average amount of rainfed irrigation.
- Good zones: good yield areas for annual crops and arboriculture (cereals, oat, almond, pistachio, olive trees, etc), with enough rainfed irrigation.
- Fair zones: medium yield areas for annual crops and arboriculture (cereals, oat, almond, pistachio, olive trees, etc), with average amount of rainfed irrigation.
- Moderate zones: suitable for arboriculture and livestock farming products, etc.
- Poor zones: suitable for agricultural use under conditions (grazing land).

- Not Suitable zones: unsuitable areas for agricultural use, such as settlements, water bodies, etc.

5. Summary and conclusions

The creation of crop specific agroclimatic zones in Sidi Bouzid region in Tunisia, by conducting contemporary agroclimatic classification is applied. This is based on monitoring the impact on weather conditions on vegetation with local soil fertility, altitude and climatic constrains (GDD, Rn, precipitation). The results are encouraging. The first discussions with the local experts from the study area prove the validation of the sustainable production zones. The proposed methodology has three main advantages. Firstly, the identification of suitable agricultural zones is based on continuous spatial and temporal Earth Observation satellite data. This provides more reliable and accurate results compared to conventional data. Secondly, high resolution (200 meters spatial resolution) non-crop specific and crop specific agroclimatic zones, applying Machine Learning interpolation methods, have been achieved. Lastly, the proposed methodology is transferable and relatively easy to process, almost everywhere in the world, via Google Earth Engine platform.
In summary, the described methodology presents new optimal solutions to the main international issues in the field of water – energy – food. The agroclimatic zoning in relation with social, cultural, and economic conditions could provide optimal solutions to farmers reducing crop yield failure and increase their viability.

Acknowledgements

This research was funded by SUPROMED project under the PRIMA 2018 program of the European Commission.

References

Adnan, S., Ullah, K., Gao, S., Khosa, A.H. and Wang, Z., (2017). Shifting of agro-climatic zones, their drought vulnerability, and precipitation and temperature trends in Pakistan. Int. J. Climatol, 37: 529-543. https://doi.org/10.1002/joc.5019

Araya A., Keesstra S.D., Stroosnijder L., (2010). A new agro-climatic classification for crop suitability zoning in northern semi-arid Ethiopia. Agricultural and Forest Meteorology, Vol. 150, Issues 7–8, pp.1057-1064, ISSN 0168-1923, https://doi.org/10.1016/j.agrformet.2010.04.003

Dalezios Nicolas & Mitrakopoulos Kostas & Manos Basil, (2018). Multi-scaling Agroclimatic Classification for Decision Support Towards Sustainable Production. 10.1007/978-3-319-76929-5_1.

Falasca S. L., Fresno M.D. and Waldman C., (2014). Developing an agro-climatic zoning model to determine potential growing areas for Camelina sativa in Argentina. QScience Connect, Vol.2014, Issue 1, Mar 2014, doi: https://doi.org/10.5339/connect.2014.4.

Gorelick, N., Hancher, M., Dixon, M., Ilyushchenko, S., Thau, D., & Moore, R. (2017). Google Earth Engine: Planetary-scale geospatial analysis for everyone. Remote Sensing of Environment.

Kogan, F.N., (2002). World droughts in the new millennium from AVHRR-based vegetation health indices. Eos Trans.Am. Geophys. Union, 83, 557, 562–563.

Kihoro, J.; Bosco, N.J.; Murage, H., (2013). Suitability analysis for rice growing sites using a multicriteria evaluation and GIS approach in great Mwea region, Kenya. SpringerPlus, 2, 265.

Masitoh F. and Rusydi N. A., (2019). Vegetation Health Index (VHI) analysis during drought season in Brantas Watershed. IOP Conference Series: Earth and Environmental Science, Vol. 389, Geomatics International Conference 2019, 21–22 August 2019, Surabaya, Indonesia.

Tsiros E., C. Domenikiotis, N.R. Dalezios, (2009). Sustainable production zoning for agroclimatic classification using GIS and remote sensing. IDŐJÁRÁS, 113, No1–2, 55–68.

Wu Bingfang, Ma Zonghan, Yan Nana, (2020). Agricultural drought mitigating indices derived from the changes in drought characteristics. Remote Sensing of Environment, Vol.244, 111813, ISSN 0034-4257, https://doi.org/10.1016/j.rse.2020.111813

Zuhro Asma, Tambunan Mangapul & Marko Kuswantoro. (2020). Application of vegetation health index (VHI) to identify distribution of agricultural drought in Indramayu Regency, West Java Province. IOP Conference Series: Earth and Environmental Science. 500, 012047. 10.1088/1755-1315/500/1/012047.

Monitoring crop phenology applying biophysical parameters from Sentinel-2 data: The case of Albacete region in Spain

Faraslis[1], I., N. Alpanakis[2], G. Tziatzios[2], M. Spiliotopoulos[2], S. Sakellariou[2], P. Sidiropoulos[2], V. Brisimis[2], A. Blanta[2], N. Dercas[3], N.R. Dalezios[2]

[1] Department of Environmental Sciences, University of Thessaly, Larisa, Greece
[2] Department of Civil Engineering, University of Thessaly, Volos, Greece
[3] Department of Natural Resources and Agricultural Engineering, Agricultural University of Athens, Greece

Abstract.
The newest Earth Observation optical sensors, such as Sentinel-2, provide global biophysical products and vegetation indices at high spatial (decametric or densiometric resolution) and temporal resolution (about 5 days retrieval). These biophysical parameters are essential for constant crop status monitoring at local scale. Optimizing the water use for irrigation, the weed mapping, quantifying above ground biomass and crop yield production, are some of the benefits of biophysical parameters in agriculture. This research investigates the crop status during the 2021's growing season in Albacete agricultural area in Spain. Thus, the winter Barley, biophysical variables, and vegetation indices, that is, Leaf Area Index (LAI), fraction of absorbed photosynthetically active Radiation (FAPAR), Fraction of Vegetation Cover (FVC), Leaf Chlorophyll content (Cab), Canopy Water Content (CWC), Normalized Difference Vegetation Index (NDVI) and Normalized Difference Red Edge Index (NDRedEdge) are retrieved. The PROSAIL radiative transfer model by artificial neural network approach is employed (available of the free SNAP® software) to retrieve the biophysical parameters from Sentinel-2 multispectral imagery. The monitoring of the above-mentioned biophysical variables during the growth period of Barley crop shows a uniform behavior. Finally, high consistency among vegetation parameters confirms the usefulness of Sentinel-2 products in agriculture.

1. Introduction

Remote sensing satellites are a unique data source for continuous monitoring crop status at low cost. Especially, the newest Earth Observation optical sensors, such as Sentinel-2, offer biophysical products and vegetation indices at high spatial and temporal resolution (about 5 days retrieval). The Sentinel-2 mission incorporates three red-edge bands with centered wavelength 705, 740 and 784, respectively. Several studies have shown that these red edge spectral bands provide the ability to detect subtle stress in crops before is detectable by the naked eye or by traditional vegetation indices (Campbell and Wynne 2007; Odindi et al. 2016; Ramoelo and Cho 2018). These red edge bands can provide excellent biophysical variables of vegetative health detecting changes in chlorophyll and nitrogen content in the crops. The variables that characterize the inherent characteristics of vegetation are: (a) Leaf area index LAI (m^2/m^2), is defined as one half green leaf area per unit ground surface area. It is a key variable for evapotranspiration and biomass production estimation (Dorigo et al., 2007), (b) Fraction of Absorbed Photosynthetically active radiation (FAPAR), estimates the canopy photosynthetic capacity of vegetation by measuring the proportion of incoming photosynthetically active radiation between 400–700 nm wavelength range (Hu, et al. 2020). FAPAR is applied in agrometeorological models for estimating net primary production, (c) Fraction of vegetation cover (FVC), indicates the fraction of surface covered by vegetation in vertical projection. This parameter is used for monitoring the early stages of plant growth (Ilina and Petar, 2021), (d) Canopy chlorophyll content (Cab) refers to chlorophyll pigments a and b, which are responsible for photosynthetic activity in leaf, thus, is strongly related to nitrogen content on it. Cab is an indicator of vegetation stress, such as nitrogen shortage, plant diseases, and similar aspects (Bester et al., 2020), (e) Canopy water content (CWC) is defined as the mass of water per unit ground area. As the water vegetation ranges from 60% to 80%, the CWC variable can play a vital role in monitoring the health status of plants (Weiss et al, 2020).
Concerning the retrieval of biophysical parameters from remote sensing data, two main categories exist: (a) the empirical methods that establish a statistical model between remote sensing data and ground truth data, and (b) Physical modelling methods using radiative transfer models (Qiaoyun et al., 2019). Regardless of the extensive use of empirical methods, they are time consuming and require a lot of resources especially for mapping over large areas. In contrast, physical modelling approaches are very promising for biophysical parameters estimation, such as look-up tables and neural networks.

Moreover, vegetation indices, such as NDVI (Normalized Difference Vegetation Index) and Red Edge NDVI are widely used for vegetation monitoring. NDVI is a well-known and widely used index of vegetation health. It measures the chlorophyl density in the leaf and is a reliable indicator of dry plant matter (biomass) in plant species, even though it saturates at higher chlorophyll level (Xue & Su, 2017). Unlike NDVI, Normalized Difference RedEdge (NDRE) index is characterized by higher sensitivity and provides better results about the captured chlorophyll content in the middle and late season crops (Jorge et al., 2019).
This research aims to evaluate the above-mentioned biophysical variables over the winter annual crop of Barley in the region of "La Mancha Oriental", in Spain. That is, seasonal Sentinel-2 LAI, FAPAR, FVC, Cab, CWC, NDVI, NDRE vegetation parameters and indices have been generated for monitoring the vegetation status of Barley. Moreover, product intercomparison between Sentinel-2 vegetation variables, such as LAI and NDVI, has been performed providing information on the performance of the products for the region of "La Mancha Oriental".

2. Materials and Methods

2.1. Description of Study area

The pilot area in Spain is the region "La Mancha Oriental", which occupies about 7,150 Km^2. The region is in the South-east of the Iberian Peninsula. It is characterized by relatively flat surface averaging 500 to 600 meters in altitude. The climate is characterized as semi-arid with annual precipitation below 350 mm. The study area consists of annual crops, such as Barley, Garlic, and Maize and trees, such as Almond, Olive, Pistachio and Vineyard. Regarding this research, the growth of the winter Barley crop has been investigated by Sentinel-2 biophysical parameters retrieval.

Figure 1 The crop pilot-sites in the region of "La Mancha Oriental" in Spain

2.2. Dataset

To cover the growing season for the winter Barley crop, 38 Sentinel-2 images were downloaded from the period of 1st November 2020 to the end of June 2021. Specifically, the satellite data was derived from Copernicus Open Access Hub, which provides free and open access to Sentinel-1, Sentinel-2 and Sentinel-3 products. Level-2A Sentinel-2 products were downloaded over the period concerned. Level-2 products are orthorectified, bottom of atmosphere (BOA) reflectance images. Furthermore, a quality assessment of each Sentinel-2 scene was performed concerning the integrity of the data and the cloud cover. Finally, out of thirty-eight, twelve dates (12 images) were suitable for further analysis. Next, the appropriate processes were performed to mask-out the water bodies and clouds. Other preprocessing approaches were the sub-setting and the resampling by converting the multi-size product at 20 meters spatial resolution.

2.3. Biophysical parameters and vegetation Indices retrieval methodology

Regarding the creation of biophysical indices from Sentinel-2 data the open-source software, namely Sentinel for Application Platform (SNAP), from which the Level-2B biophysical processor has been applied. The Level-

2B processor uses neural networks for the estimation of Sentinel-2 biophysical variables. This algorithm is a physically based radiative transfer model based on three sub-models: (a) the leaf optical properties that are considered by the PROSPECT model, such as leaf chlorophyll content, water content, dry matter content, etc., (b) the canopy structure, described by SAIL radiative transfer model as a homogeneous medium, where leaves are randomly distributed, and (c) the background reflectance that corresponds to non- green material, such as soil, water and snow. Especially, the neural network algorithm operates in three stages: (a) generating the training data base by selecting a representative set of tops of canopy reflectance, (b) calibrating the network and (c) estimate the biophysical variables from the neural network, namely LAI, FAPAR, FVC, Cab, CWC. The benefit from this algorithm is twofold. Firstly, no inputs of land cover type are required and secondly all the biophysical variables can be easily retrieved globally through the processor integrated in the SNAP software. Next, the NDVI and the NDRE have been estimated by the SNAP toolbox. For the NDVI, the bands B4 (red) and B8 (NIR), whereas for the NDRE the bands B8 (NIR) and B5 have been applied, respectively, in each one of the 26 Sentinel-2 images. The vegetation biophysical variables and indicators' characteristics are presented in the following Table (Table 1).

Table 1 Characteristics of Biophysical variables and indices estimated from Sentinel-2 images

Parameter	Unit		Minimum	Maximum
LAI: Leaf Area Index	dimensionless		0	8.0
FAPAR: fraction of absorbed photosynthetically active Radiation	dimensionless		0	1.0
FVC: Fraction of Vegetation Cover	dimensionless		0	1.0
Lai_Cab: Leaf Chlorophyll content	g/cm^2		0	600
Lai_cw: Canopy Water Content	g/m^2		0	0.55
NDVI: Normalized Difference Vegetation Index: (842nm-665nm)/(842nm+665nm)	dimensionless		-1	1
NDRedEdge: Normalized difference Red Edge Index: (783nm-705nm)/ (783nm+705nm)	dimensionless		-1	1

SNAP software advance techniques are used to automate the estimation processes. Especially, the graph builder tool was used to execute the raster data operators in batch-mode creating the final products of the 12 images (fig.2).

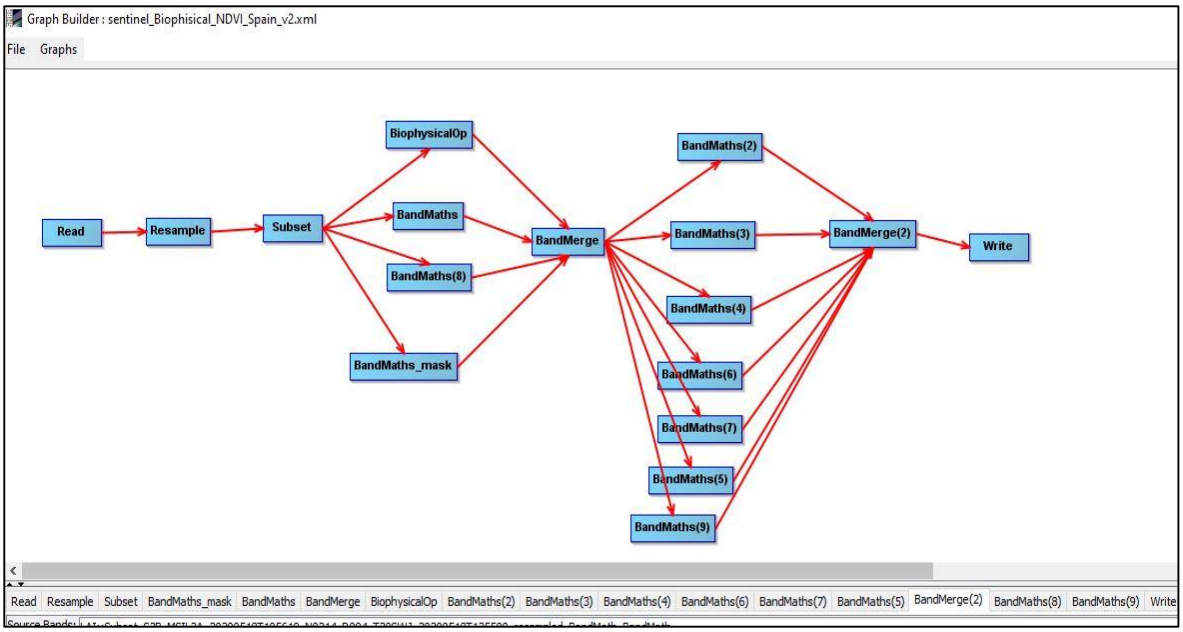

Figure 2 Workflow of the SNAP graph builder tool for producing the biophysical variables and indices of the 26 dates

3. Results and Discussion

Based on the Barley crop calendar, the sowing period begins in December and the harvest starts about the mid of June (Table 2). The growth of the winter Barley crop in the pilot site was monitored through the seven biophysical indices and parameters, showing high consistency during the growing season.

Table 2 Crop calendar for Barley growing season 2020-2021

Date	Stage
4 December, 2020	Sowing
1 January to 10 June, 2021	Mid-Season
10-20 June, 2021	Harvest

The following image represents the evolution of Leaf Area Index (LAI) biophysical parameter for the period from February to June 2021 (fig.3). The shades of green color show the different phenological stages for Barley, i.e., in February the plant is in early stage, on May 13, 2021 (LAI about 6) the crop is on “grain filling” (dark green color) and on June 7, 2021, the crop is on “maturity stage” and the harvest period has already begun (brown-green color).

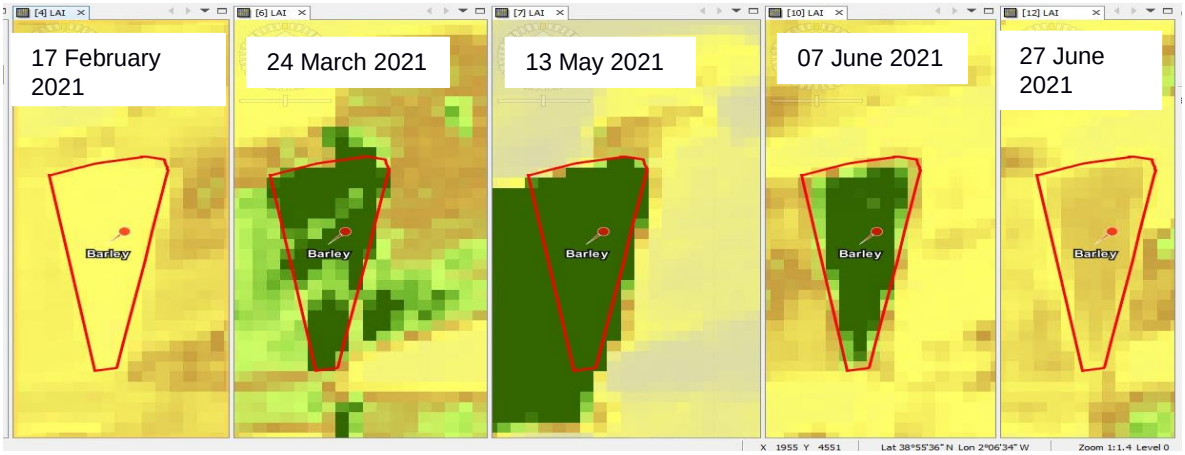

Figure 3 The evolution of Barley crop from January 2021 to June 2021 based on LAI

The following figure 4 portrays the growth pattern for the Barley from seven biophysical/vegetation indices. All the indices indicate almost the same pattern. There are rising values of the indices with the peak occurring at the end of March until the mid of May, followed by a sharp fall until the begin of June (end of season).

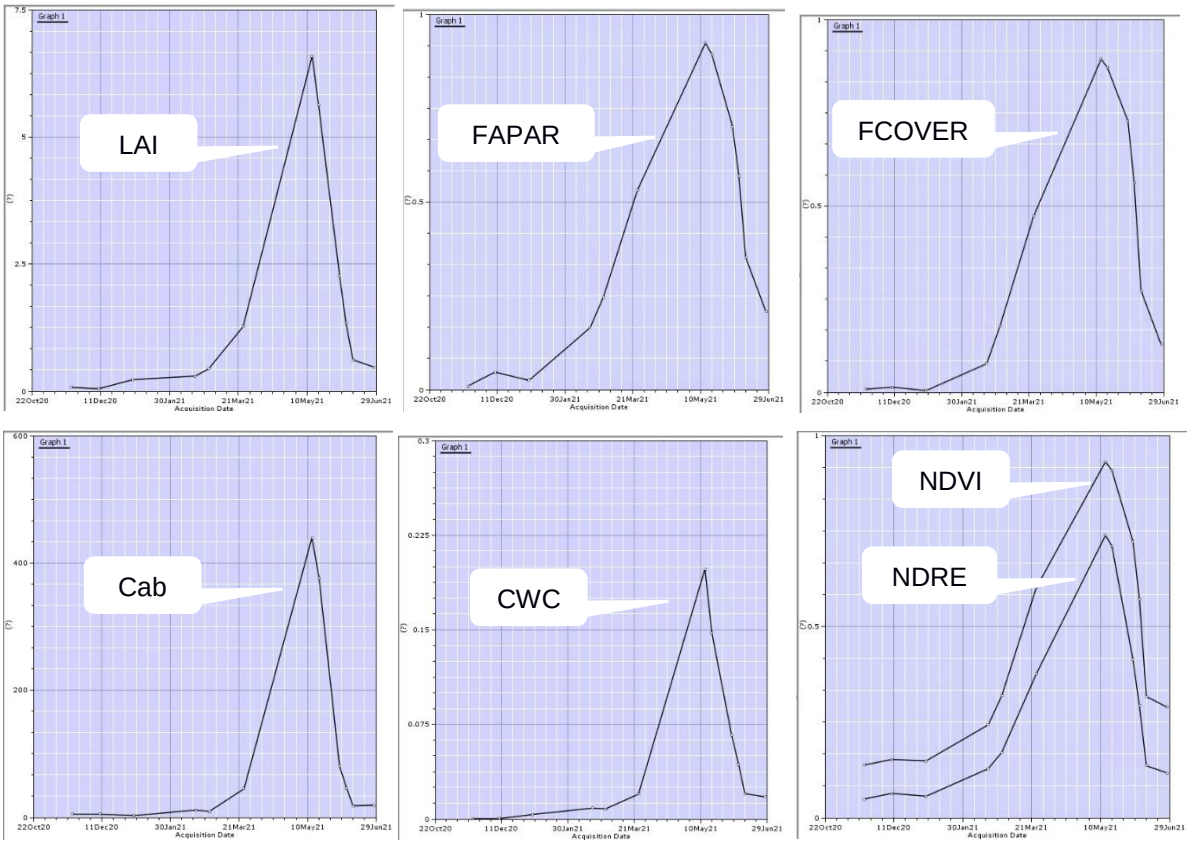

Figure 4 Barley's growth cycle monitored by seven biophysical parameters from November 2020 to end of June 2021

To perform the evaluation of the biophysical parameters, statistical analysis was conducted, in a random set of 100 points, in the region of "La Mancha Oriental" (fig.5). Firstly, the NDVI validates the LAI results, indicating a good agreement (R^2=0.9). Secondly, the validation of LAI, with FCOVER, Cab, CWC, respectively, was performed. The results show a good agreement with coefficient of determination (R^2), above 0.94. Finally, the performance of the FAPAR and FCOVER vegetation variables was evaluated. As presented in figure 5, there is a linear relationship between these parameters with high consistency (R^2 ~ 0.99).

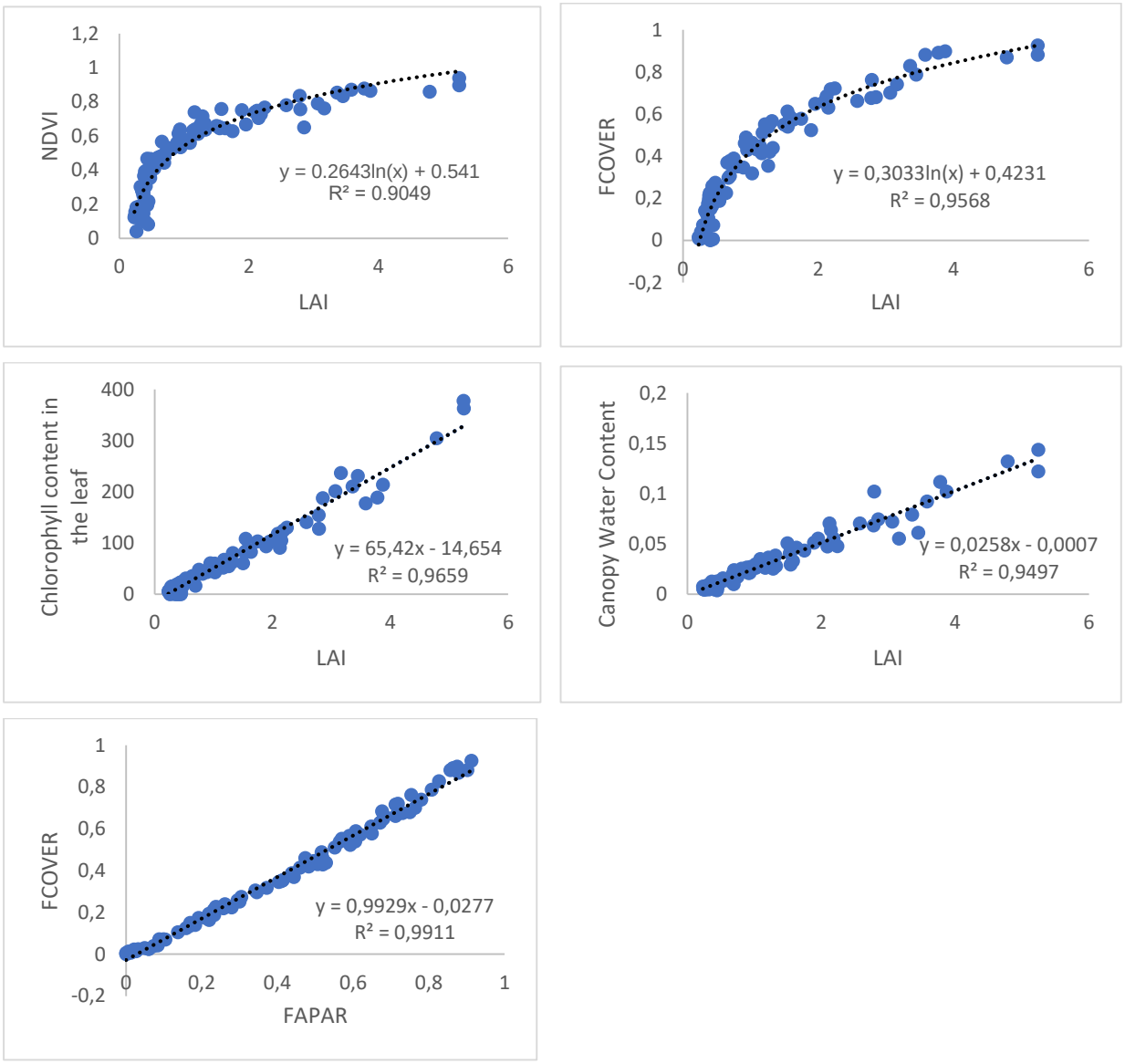

Figure 5 Comparison of biophysical parameters-indices in the region of "La Mancha Oriental", in Spain

It is worth mentioning that the inter-comparison of the biophysical parameters was conducted not only to crop areas but also in natural vegetation. This good synergy of vegetation variables makes them a useful tool for monitoring not only the evolution of crops but also seasonal cycle of natural vegetation.

4. Summary and conclusions

Summarizing, the study estimates seven biophysical parameters and indices for monitoring the winter Barley crop for the period 2020-2021. For this purpose, the Sentinel-2 biophysical products generated by biophysical processor were integrated through SNAP free software. This processor applies neural networks to Sentinel-2 images to create five biophysical variables, namely, LAI, FAPAR, FCOVER, Cad, CWC. Moreover, NDVI and NDRE were estimated. The investigation of Barley's crop calendar shows good agreement and consistency with the biophysical products. Starting from sowing period (December), there is a continuous growth

(germination, seedling establishment and leaf production, stem elongation) with the maximum value being detected in mid-May, following by the maturity stage at the end of June. Moreover, the inter-comparison of biophysical parameters was conducted in the study area of “La Mancha Oriental”. and shows a good correlation between the vegetation parameters.
In conclusion, Sentinel-2 data provide great capabilities to monitor crops. Particularly, the red-edge bands have a great potential in precision agriculture applications. The SNAP free software with the biophysical processor is an exceptionally valuable tool for rapidly retrieving the biophysical parameters from Sentinel-2 (and Landsat 8) multispectral imagery. This tool could furnish useful products and assist farmers and agricultural agencies.

Acknowledgements

This research was funded by SUPROMED project under the PRIMA 2018 program of the European Commission.

References

Bester Tawona Mudereri, Tavengwa Chitata, Concilia Mukanga, Elvis Tawanda Mupfiga, Calisto Gwatirisa & Timothy Dube (2021). Can biophysical parameters derived from Sentinel-2 space-borne sensor improve land cover characterisation in semi-arid regions? Geocarto International, 36:19, 2204-2223, DOI: 10.1080/10106049.2019.1695956.

Campbell J, Wynne R. 2007. Introduction to remote sensing. 5th ed. New York (NY): Guiford Press.

Dorigo, W.A., Jurita-Milla, R., de Wit, A.J.W., Brazile, J., Singh, R., Schaepman, M.E., 2007. A review on reflective remote sensing and data assimilation techniques for enhanced agroecosystem modeling. International journal of applied earth observation and geoinformation, 9(2), 165–193.

Hu, Qiong, Jingya Yang, Baodong Xu, Jianxi Huang, Muhammad S. Memon, Gaofei Yin, Yelu Zeng, Jing Zhao, and Ke Liu. (2020). "Evaluation of Global Decametric-Resolution LAI, FAPAR and FVC Estimates Derived from Sentinel-2 Imagery" Remote Sensing 12, no. 6: 912. https://doi.org/10.3390/rs12060912.

Jorge, J., Vallbé, M., & Soler, J. A. (2019). Detection of irrigation inhomogeneities in an olive grove using the NDRE vegetation index obtained from UAV images. European Journal of Remote Sensing, 52(1), 169-177.

Ilina Kamenova & Petar Dimitrov (2021) Evaluation of Sentinel-2 vegetation indices for prediction of LAI, fAPAR and fCover of winter wheat in Bulgaria, European Journal of Remote Sensing, 54:sup1, 89-108, DOI: 10.1080/22797254.2020.1839359.

Odindi J, Mutanga O, Rouget M, Hlanguza N. 2016. Mapping alien and indigenous vegetaton in the KwaZulu-Natal Sandstone Sourveld using remotely sensed data. Bothalia. 46(2):1–9.

Qiaoyun Xie, Jadu Dash, Alfredo Huete, Aihui Jiang, Gaofei Yin, Yanling Ding, Dailiang Peng, Christopher C. Hall, Luke Brown, Yue Shi, Huichun Ye, Yingying Dong, Wenjiang Huang, (2019). Retrieval of crop biophysical parameters from Sentinel-2 remote sensing imagery, International Journal of Applied Earth Observation and Geoinformation, Volume 80, pp187-195, ISSN 1569-8432, https://doi.org/10.1016/j.jag.2019.04.019.

Ramoelo A, Cho MA. 2018. Explaining leaf nitrogen distribution in a semi-arid environment predicted on Sentinel-2 imagery using a field spectroscopy derived model. Remote Sens. 10(2):269.

Weiss M., Baret F., Jay S., (2020). S2ToolBox level 2 products: LAI, FAPAR, FCOVER. Version 2. European Space Agency. Paris.

Xue, J., & Su, B. (2017). Significant remote sensing vegetation indices: A review of developments and applications. Journal of Sensors, 2017, 1–17. Hindaw Limited. https://doi.org/10.1155/2017/135369.

Identifying agroclimatic zoning for sustainable agriculture, using remote sensing and GIS approach: the case of Beqaa governorate in Lebanon

Faraslis[1], I., N. Alpanakis[2], G. Tziatzios[2], M. Spiliotopoulos[2], S. Sakellariou[2], P. Sidiropoulos[2], V. Brisimis[2], A. Blanta[2], N. Dercas[3], N.R. Dalezios[2]

[1] Department of Environmental Sciences, University of Thessaly, Larisa, Greece
[2] Department of Civil Engineering, University of Thessaly, Volos, Greece
[3] Department of Natural Resources and Agricultural Engineering, Agricultural University of Athens, Greece

Abstract

Agriculture is affected by climate and environmental conditions. The agroclimatic classification zones are defined as areas with similar combinations of climate and soil characteristics and similar physical potentials achieving efficient use of natural resources leading to optimal production. The aim of this study is the identification of agricultural sustainable zones, in Beqaa governorate, Lebanon, by conducting agroclimatic classification based on Google Earth Engine (GEE) platform and advanced remote sensing and GIS techniques. The agroclimatic zoning methodology is a three-stage procedure: firstly, the water limited growth environment (WLGE) zones are created based on water availability; secondly, soil and topographic features are integrated to WLGE zones for developing non-crop specific agroclimatic zoning; thirdly, specific crop features, such as Growing Degree Days and Net Radiation are considered for defining the sustainable production zones, namely, crop specific agroclimatic (CSA) zones. The CSA zones map qualitatively divides the study area in seven productivity zones. The study demonstrates the excess of areas with sufficient amounts of rainfed irrigation. Additionally, it highlights that Bekaa valley is of great importance as high productivity land. Finally, this methodology reveals that GEE could be a valuable tool for creating detailed and up to date agroclimatic zones in a relatively short time.

1. Introduction

Increases in population pressure cause increases in growing demand for food. Agriculture is highly depended on climate conditions causing stress in plants, which affect yield. Therefore, an effective land-use planning is necessary for the sustainable land use in crop production. The agroclimatic analysis has as objective to maximize the production from the available resources and the prevailing climatic conditions in order to support specific crops for long periods without adversely affecting the environment (de Olanda Souza et al, 2022).

Various research studies have developed specific methodological procedures trying to create agroclimatic zones (Adnan et al., 2017; Falasca et al., 2014). Most of them are based on land evaluation using multiple parameters. Temperature and rainfall are two of the most important of them playing an essential role in climatology, hydrology and water resources management in general. These variables, in conjunction with soil type and soil forms, determine the variety of crops that are suitable for high yields cultivation while protecting natural resources.

With the advances in satellite technology new Earth Observation (EO) products and methodological approaches have been developed to creat agroclimatic zones. This modern tools, namely remote sensing and GIS have been well conceived that could play an essential role for sustainable development zoning due to multi-stage character and comprehensive approach (Tsiros et al. 2009). Based on this, different research studies have been conducted to monitor drought conditions. Specifically, drought indices, such as aridity index (AI) and the vegetation health index (VHI), are widely used elaborating EO data over a long period of time, for assessing vegetation stress (Kogan, 2002; Masitoh and Rusydi, 2019). This new EO data provides better spectral and spatial resolution. Moreover, techniques, such as machine learning approaches, could provide more accurate and reliable agroclimatic zones (Dalezios et al., 2018). Previous agroclimatic zoning studies were fuzzier and less comprehensive. Over the last decades, the rapid advances in information technologies, telecommunication networks offer new capabilities in data processing. Specifically, new cloud computing platforms, such as Google Earth Engine (GEE), provide additional capabilities in big data analysis. The GEE can be utilized as geospatial

processing service by processing data over large areas and monitoring them for long periods of time. This cloud platform supplies a great variety of, always up-to-date, satellite data (Landsat, Sentinels, MODIS, etc), climate data (precipitation, temperature), elevation data, etc (Gorelik et al., 2017).
The objective of the paper is to create rapidly high resolution agroclimatic zones in elevated areas in the Mediterranean basin. The approach in this paper is based on the investigation of new remote sensing methodological techniques and high spatial and temporal resolution data, provided by GEE platform. The study area, where sustainable production zones are designed, is located in Beqaa governorate in Lebanon.

2. Methodology

The data processing and modelling, applying remote sensing and GIS techniques, consists of three steps (Dalezios et al., 2018): (a) Hydroclimatic zones, (b) Non crop specific Agroclimatic Zoning, and (c) Crop specific agroclimatic Zoning. In the following flow-diagram, the proposed methodology is illustrated (fig.1). Weather, climate, topography and soil type restrictions, for creating agroclimatic zones, are considered. Scientific research in earth observation dataset is applied, using Google Earth Engine (GEE) through cloud computing technology. Furthermore, Machine Learning algorithms are applied on geospatial data in GEE for downscaling, in order to achieve higher resolution agroclimatic zones (200x200 m pixel size).

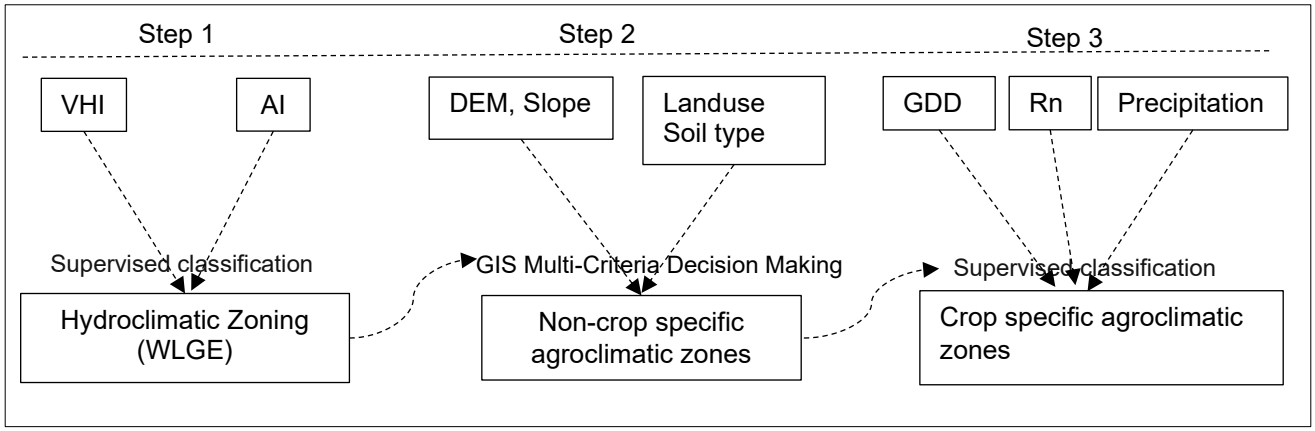

Figure 1The methodological steps of agroclimatic zoning

Identifying zones for sustainable farming according to water limitations is the first step of the proposed methodology. GIS and Remote Sensing tools, are applied for classifying the study area in zones according to hydroclimatic conditions. The product is a thematic map containing Water Limited Growth Environment (WLGE) zones. Two satellite-derived drought indices are combined, the so-called Vegetation Health Index (VHI) and Aridity Index (AI) in order to designate the WLGE zones (Dalezios et al., 2018; Wu et al, 2020). The VHI as an index of agricultural drought has revealed a greater capability in detecting the distribution pattern of drought in the agricultural land. It analyzes the vegetation status, based on the lack of water supply. The variability of vegetation is based on calculating the minimum and maximum Normalized Vegetation Index (NDVI) and the Land surface Temperature (LST) assigned values, on a pixel basis, over a long period of time. The VHI is calculated by combining two indices: (a) The Vegetation Condition Index (VCI), which represents the moisture/vegetation condition, and (b) The Thermal Condition Index (TCI), which represents the temperature condition (Zuhro et al., 2020). The AI is a useful indicator of dryness or wetness in a region. The entire area of drought regions is determined from meteorological data over a long period of time (e.g. 20-30 years). The AI is described as the ratio of cumulative average monthly precipitation to cumulative average monthly potential evapotranspiration (PET) and is a climatic index based on water balance. The WLGE zones are created by a linear combination of the VHI and AI products. Three classes of WLGE zones are defined: No limitations, Partially limited environment and Limited environment.
The creation of non-crop specific agroclimatic zones (or General Agroclimatic Zoning), is described as the second step. Land use suitability analysis classifies areas to be used for agricultural purposes considering land-cover, soil type, altitude, slope and water constrains. A Multi-Criteria Decision Making (MCDM) model is applied taking into

account the following data: WLGE zones, Digital Elevation Model (DEM), slope, soil, and land-use/land cover (Tsiros et al., 2009). The MCDM analysis is a GIS-based approach evaluating various production parameters and weighted them according to their importance on the favorable growth conditions. The Analytic Hierarchy Process (AHP) is implemented as the most reliable MCDM method for agricultural applications (Kihoro et al, 2013). It can help to minimize the subjectivity of the weights of each individual parameter using experts' point of view. This method generates the weight of each criterion in accordance with the pairwise comparison of the decision maker's (Muginyo et al., 2021). Finally, the non-crop specific agroclimatic zones map allocates the area in five suitable agricultural classes, namely Good, Fair, Moderate, Poor and Not Suitable.

Crop-specific agroclimatic zoning map is derived in the third step. Thus, the identification of suitable crops according to their special characteristics (e.g., winter-summer crops) is considered. Three are the most important parameters for the identification of crop suitability classes: the growing degree-days (GDD), the net radiation (Rn) and the amount of spring precipitation. The GDD index is a measure of heat demand of growth and development of plants. The Rn, is a climate-based index which measures the quantity of radiant energy available at a crop. These two parameters are estimated over a period of time (e.g. 20-30 years). Moreover, they may be restricted components at specific type of crops, namely winter, spring or summer annual cultivations. The GDD and Rn indices are combined providing three suitability classes for specific crops, namely high, medium and low productivity zones. Generally, the amount of spring rainfall, is a key component for annual crops. Especially, the last 10 days in April and first 10 days in May (20 days in total) are considered, creating two classes, sufficient and insufficient rain for annual crops. Next, the three above-mentioned parameters with the Non-crop specific agroclimatic zoning are combined, thought the supervised classification procedure, leading to seven crop specific productivity zones. These zones range from "Excellent" areas, as the most suitable zones for crop production with sufficient amount for rainfed irrigation, to "Not suitable" areas as prohibited areas in agriculture. Notably, the zones are classified as (a) "Excellent", "Very Good", "Good" which are generally suitable for annual crops, (b) "Fair", "Moderate", "Poor" are generally suitable for trees crops, vineyards or annual crops under restrictions, and (c) "Not Suitable", which are inappropriate for agricultural use.

3. Study Area and Database

3.1. Study Area

The pilot area in Lebanon is the governorate of Beqaa, which occupies about 1,430 km^2 (fig.2). The altitude in this area fluctuates between 800 m and 1000 m above sea level. It has Mediterranean climate of wet often snow winters and dry, warm summers. The agricultural land is located in the Beqaa Valley cultivated by wheat, barley, potato, winter legumes and summer vegetables, fruit trees, olive and vineyards.

Figure 2 Study area Governorate of Bekaa in Lebanon

3.2. Database and preprocessing

The remote sensing observations mainly are obtained from the Google Earth Engine (GEE) platform for the research study. Especially, from GEE have been used:

- Landsat-8 multispectral satellite data, with 30 meters spatial resolution. The available derived Landsat data is for the period of 2013 to 2020. For Lebanon, study area, 823 images are processed.
- MODIS two products. (a) The MOD16A2 product provides information about 8-day Potential Evapotranspiration at 1 Km pixel resolution. In total 919 images are processed for the period 2001-2020, (b) The MOD11A2 product provides the average land surface temperature at 1 Km spatial resolution. In total 420 images, for the winter and spring seasons and the span between 2001 to 2020, are processed.
- CHIRPS (Climate Hazards Group InfraRed Precipitation with Station) data. This product represents aggregated five days' rainfall with 5 km spatial resolution. For the Beqaa region, 1440 pentad data, over the period of 2001 to 2020, are processed.

The remotely sensed data is elaborated monthly extracting the median values over the last twenty years. Moreover, to achieve better resolutions in MODIS and CHIRPS products (downscaling at 200X200 m pixel size) sophisticated techniques, as machine learning algorithm, (Classification and Regression Trees-CART) is implemented.
Additionally, data from other web portals are extracted:

- Digital Elevation Model (DEM). Thirty meters spatial resolution DEM product from NASA (National Aeronautics and Space Administration) Shuttle Radar Topography Mission (SRTM), is used.
- Soil Map. The International Soil Reference and Information Centre (ISRIC) provides soil maps almost globally (www.isric.org). The soil classification map, at 250 meters spatial resolution, is derived from ISRIC web-portal. Different soil types are ranking according to their suitability for agricultural use.
- Landuse/LandCover (LU/LC). For the Beqaa region, a land cover thematic map (raster format) is provided by local research institute. Next, the digitalization process is applied by converting the map into vector format with the appropriate coding.

4. Results and Discussion

The WLGE zones are created in the first stage (fig.3). In the Beqaa region the two hydroclimatic classes, namely No Limitations, Partial Limited/No Limitations, dominate. Especially, for the Beqaa valley the category Partial Limited/No Limitations prevails, representing the adequate water reserves.

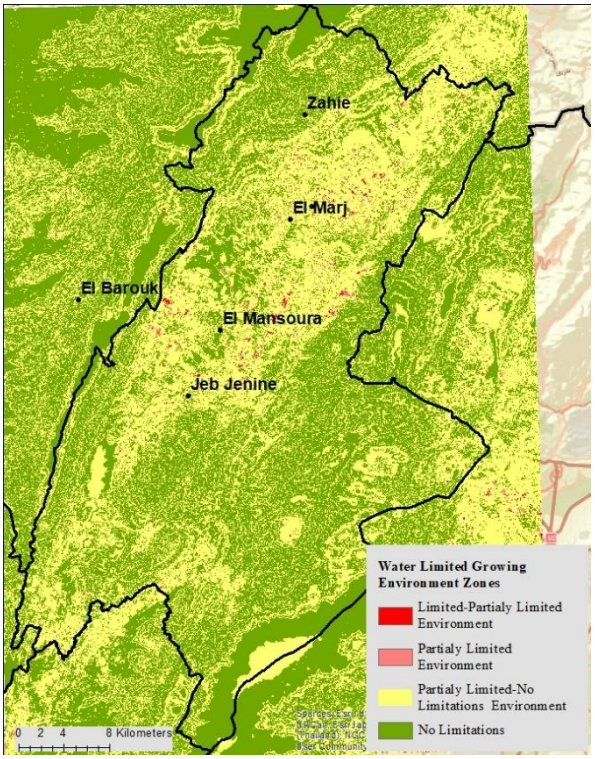

Figure 3 Four WLGE zones for Beqaa

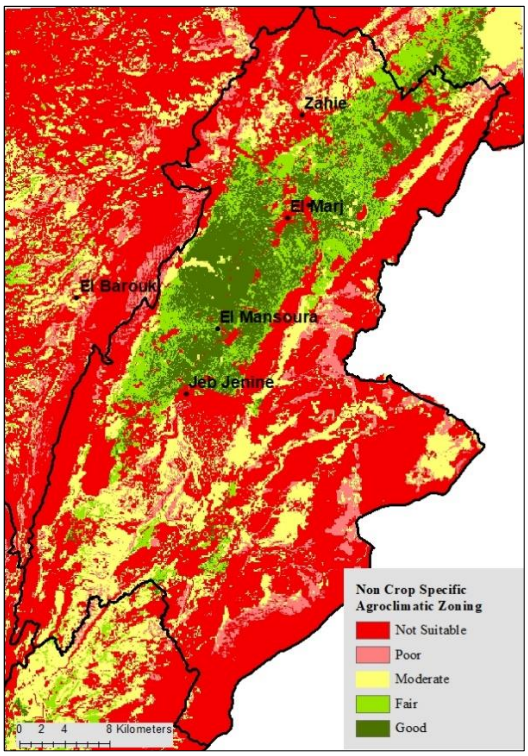

Figure 4 Non-crop specific agroclimatic zoning for Bekaa

The non-crop specific agroclimatic zones, are created in the second stage (fig.4). The study area is classified in five agricultural suitability classes: Good, Fair, Moderate, Poor and Not Suitable. The statistical analysis shows that the first three classes (Good, Fair, Moderate) cover 58,423 hectares of the total study area. Thus, t40.8% of the region can be used for sustainable agricultural production under certain conditions. Moreover, 17,935 ha belong to the first class (Good), which is suitable for agricultural use without restrictions.

The adequacy of Rn and GDD for the annual crops of wheat and potato, are considered in stage 3. The analysis of these two factors shows that they aren't limited factor for the annual crops. On the other hand, the 20 days' spring cumulative precipitation, at the last 10 days of April and the first 10 days of May, is a crucial factor for the wheat as winter crop and potato as spring crop. Two classes of precipitation, below and above the 10 mm, in the first two best of the non-crop specific agroclimatic zoning, is implemented, in order to diversify the areas with sufficient amounts of rainfed irrigation. Lastly, the crop-specific agroclimatic zoning thematic map is created (fig.5). In figure 5 the crop-specific agroclimatic zoning map is classified in 7 clusters in terms of sustainable winter/spring crop production. "Excellent" areas (dark green color) represent the most suitable zones for crop production with sufficient amount for rainfed irrigation and "Not suitable" areas (red color) represent unsuitable zones for crop production.

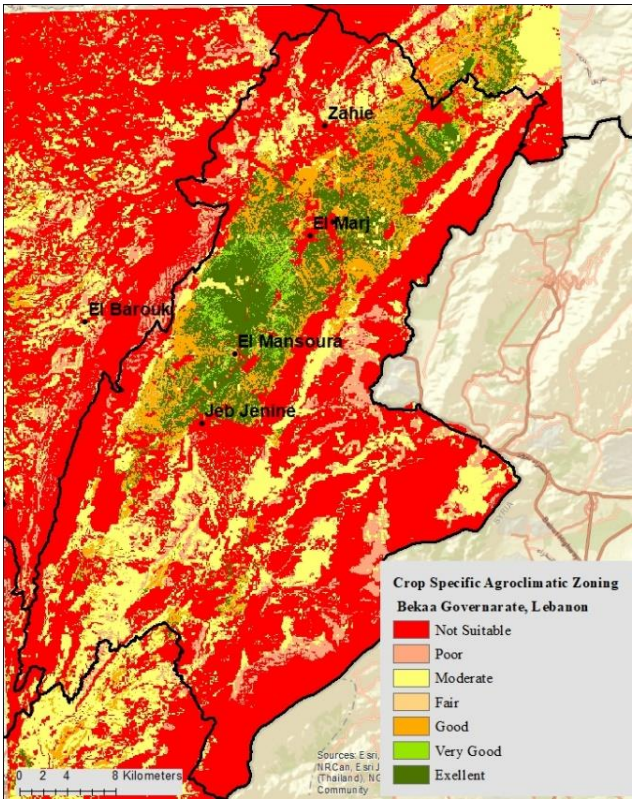

Figure 5 Crop specific agroclimatic zoning in Beqaa governorate, Lebanon

Particularly, for each zone, the following crops are suitable in the framework of sustainable agricultural production:

- Excellent zones: high yield areas for annual crops (wheat, potato, maize), especially for spring crops, with sufficient amounts for rainfed irrigation.
- Very Good zones: high yield areas for annual crops (wheat, potato, maize), especially for spring crops, with average amounts for rainfed irrigation.
- Good zones: good yield areas for annual crops (wheat, potato, maize), especially spring crops, and arboriculture (peach etc), with sufficient amount for rainfed irrigation.
- Fair zones: medium yield areas for annual crops (wheat, potato, maize), especially spring crops, and arboriculture (peach etc), with average amount for rainfed irrigation.
- Moderate zones: suitable for arboriculture and livestock farming products, etc.
- Poor zones: suitable for agricultural use under conditions (grazing land).
- Not Suitable zones: unsuitable areas for agricultural use, such as settlements, water bodies, forests, etc.

5. Summary and conclusions

A three-stage procedure is implemented for defining sustainable agricultural zones in Bekaa governorate in Lebanon. The contemporary methodology is based on the one hand, for monitoring of weather conditions in vegetation through drought indices, such as VHI and AI, and on the other hand to local restriction, such as soil type, altitude, and climatic limitations (GDD, Rn, precipitation). The results highlight the Bekaa valley as high productivity zone and of great importance for food security at state level. The benefits of the proposed methodology are summarized as follows. Firstly, it produces more reliable and accurate results as compared to conventional data, because of the use of continuous spatial and temporal Earth Observation satellite data. Secondly, higher resolution sustainable agroclimatic zones have been attained by implementing contemporary Machine Learning interpolation methods. Thirdly, the implementation of Google Earth Engine platform, provides the proposed methodology applicable almost globally. In summary, the three-stage methodology furnishes a new tool for rapidly monitoring changes in agriculture zones. It can be stated that updated sustainable agroclimatic zoning in

association with economic and social conditions could help farmers to adapt their production systems by increasing their viability.

Acknowledgements

This research was funded by SUPROMED project under the PRIMA 2018 program of the European Commission.

References

de Olanda Souza, G.H., Aparecido, L.E.d.O., de Lima, R.F., Torsoni, G.B., Chiquitto, A.G. and de Moraes, J.R.C. (2022), Agroclimatic Zoning for Bananas Under Climate Change in Brazil. J Sci Food Agric. Accepted Author Manuscript. https://doi.org/10.1002/jsfa.12018.

Adnan, S., Ullah, K., Gao, S., Khosa, A.H. and Wang, Z., (2017). Shifting of agro-climatic zones, their drought vulnerability, and precipitation and temperature trends in Pakistan. Int. J. Climatol, 37: 529-543. https://doi.org/10.1002/joc.5019

Dalezios Nicolas & Mitrakopoulos Kostas & Manos Basil, (2018). Multi-scaling Agroclimatic Classification for Decision Support Towards Sustainable Production. 10.1007/978-3-319-76929-5_1.

Falasca S. L., Fresno M.D. and Waldman C., (2014). Developing an agro-climatic zoning model to determine potential growing areas for Camelina sativa in Argentina. QScience Connect, Vol.2014, Issue 1, Mar 2014, doi: https://doi.org/10.5339/connect.2014.4.

Gorelick, N., Hancher, M., Dixon, M., Ilyushchenko, S., Thau, D., & Moore, R. (2017). Google Earth Engine: Planetary-scale geospatial analysis for everyone. Remote Sensing of Environment.

Kogan, F.N., (2002). World droughts in the new millennium from AVHRR-based vegetation health indices. Eos Trans.Am. Geophys. Union, 83, 557, 562–563.

Kihoro, J.; Bosco, N.J.; Murage, H., (2013). Suitability analysis for rice growing sites using a multicriteria evaluation and GIS approach in great Mwea region, Kenya. SpringerPlus, 2, 265.

Masitoh F. and Rusydi N. A., (2019). Vegetation Health Index (VHI) analysis during drought season in Brantas Watershed. IOP Conference Series: Earth and Environmental Science, Vol. 389, Geomatics International Conference 2019, 21–22 August 2019, Surabaya, Indonesia.

Mugiyo, H.; Chimonyo, V.G.P.; Sibanda, M.; Kunz, R.; Masemola, C.R.; Modi, A.T.; Mabhaudhi, T., (2021). Evaluation of Land Suitability Methods with Reference to Neglected and Underutilised Crop Species: A Scoping Review. Land, 10, 125. https://doi.org/ 10.3390/land10020125.

Tsiros E., C. Domenikiotis, N.R. Dalezios, (2009). Sustainable production zoning for agroclimatic classification using GIS and remote sensing. IDŐJÁRÁS, 113, No1–2, 55–68.

Wu Bingfang, Ma Zonghan, Yan Nana, (2020). Agricultural drought mitigating indices derived from the changes in drought characteristics. Remote Sensing of Environment, Vol.244, 111813, ISSN 0034-4257, https://doi.org/10.1016/j.rse.2020.111813

Zuhro Asma, Tambunan Mangapul & Marko Kuswantoro. (2020). Application of vegetation health index (VHI) to identify distribution of agricultural drought in Indramayu Regency, West Java Province. IOP Conference Series: Earth and Environmental Science. 500, 012047. 10.1088/1755-1315/500/1/012047.

Monitoring crop phenology by applying biophysical parameters from Sentinel-2 data: The case of "Beqaa Valley" in Lebanon

Faraslis[1], I., N. Alpanakis[2], G. Tziatzios[2], M. Spiliotopoulos[2], S. Sakellariou[2], P. Sidiropoulos[2], V. Brisimis[2], A. Blanta[2], N. Dercas[3], N.R. Dalezios[2]

[1] Department of Environmental Sciences, University of Thessaly, Larisa, Greece
[2] Department of Civil Engineering, University of Thessaly, Volos, Greece
[3] Department of Natural Resources and Agricultural Engineering, Agricultural University of Athens, Greece

Abstract.
With the launch of Sentinel-2 mission, multispectral data can provide biophysical products with relatively high spatial and temporal resolution, which are the key requirements for applications in the agricultural sector. The biophysical parameters are vital for monitoring crop status, such as biomass production, sustainable use of irrigation water, disease prevention, and similar aspects. This research investigates the status of the two peach tree plots, via the biophysical indices, during the 2021's growing season in "Beqaa Valley", in Lebanon. Specifically, the Leaf Area Index (LAI), the Fraction of Vegetation Cover (FVC), the Fraction of Absorbed Photosynthetically Active Radiation (FAPAR), the Leaf Chlorophyll Content (Cab), the Canopy Water Content (CWC), the Normalized Difference Vegetation Index (NDVI), and the Normalized Difference Red Edge Index (NDRE) were calculated for the two peach plots by applying the radiative transfer model, namely the PROSAIL model. Sentinel-2 multispectral imagery has been elaborated with open-source SNAP® software for retrieving the biophysical parameters. The results reveal a correlation between the vegetation variables and the crop peach calendar. Finally, the relationship of the two peach tree plots, which follow different cultivation practices, exhibits distinguishing growing pattern. The first plot, in which the farmer followed sustainable agricultural practices, presents better yield characteristics than the other, in which traditional practices were followed.

1. Introduction

Sentinel-2 multispectral imagery offers new products for near-real-time agricultural monitoring. The red-edge spectral bands provide new opportunities in detecting crop stress in early stages (Campbell and Wynne 2007; Odindi et al. 2016; Ramoelo and Cho 2018). These red-edge bands can be used for biophysical parameters retrieval, which are essential for detecting nitrogen and water concentration in crops. In this study, five biophysical variables were explored: (a) Leaf area index (LAI) (m^2/m^2), is the ratio of the amount of leaf area in a canopy per ground area. It is a critical component to evaluate biomass production and evapotranspiration (Dorigo et al., 2007), (b) Fraction of Absorbed Photosynthetically active radiation (FAPAR) estimates the canopy photosynthetic capacity of vegetation in the visible portion of electromagnetic spectrum (400–700 nm) (Hu, et al. 2020). FAPAR is important indicator for monitoring the productivity of vegetation and the impacts of agricultural drought (Rahman et al., 2014), (c) Fraction of vegetation cover (FVC) attributes the portion the surface covered by plant canopy in vertical projection. It is applied in early periods of plants growth for monitoring the transpiration and vigour (Ilina and Petar, 2021), (d) Canopy chlorophyll content (Cab) measures the nitrogen uptake in crops through the chlorophyll pigments, a, and b. Cab is related to nitrogen shortages (Bester et al., 2020), (e) Canopy water content (CWC) describes the mass of water per unit ground area. It is essential variable for monitoring crop water deficiencies (Weiss & al, 2020). The methodology for extracting biophysical parameters from satellite images is based on two broad categories: (a) statistical methods establishing the relationship between ground-truth data and multispectral images (Qiaoyun et al., 2019). Although they are used in many studies, they are time consuming and are not reliable over large areas, and (b) physical models, like artificial neural networks. In contrast to statistical methods, those models indicate good results concerning the measurements of biophysical parameters across different sites and crops.
Apart from biophysical parameters, two very common vegetation indices were retrieved, namely the NDVI (Normalized Difference Vegetation Index) and the NDRE (Normalized Difference Red Edge). The NDVI is the most widely used index for crop assessment by remote sensing data. It addresses crop issues, such as nutritional stress, parasitic attacks, hail damage, etc. On the contrary, several studies show NDVI limitations especially at very low and very high amount of vegetation (saturation effects). (Xue & Su, 2017). The NDRE index is used for measuring the concentration of chlorophyll in plants. It is characterized by high sensitivity, providing better results, as compared to NDVI (Jorge et al., 2019).

The first objective of this study is to evaluate the above-mentioned biophysical variables during the growing period of peach trees in the province of Beqaa Valley, in Lebanon. Thus, the vegetation parameters, namely LAI, FAPAR, FVC, Cab, CWC, NDVI, NDRE, have been calculated using Sentinel-2 imagery for monitoring the vegetation status of peach tree plots. Finally, the relationship between the two peach tree plots, concerning their vegetation characteristics, via the Sentinel-2 biophysical variables have been considered.

2. Materials and Methods

2.1. Description of Study area

The pilot area in Lebanon is the Beqaa Valley, which occupies 371,9 km^2. It is located between the two mountain chains of Lebanon, namely Mount-Lebanon and Anti-Lebanon, with the altitude fluctuating between 800-1000 meters above the sea level. It is of great importance agricultural area for Lebanon (occupies more than 42% of the national agricultural land). The agricultural land consists of annual crops, like wheat, barley, potato, winter legumes, summer vegetables, fruit trees, olives, and vineyards. Concerning this study, two peach tree pilots have been investigated using Sentinel-2 biophysical parameters retrieval. The “supromed plot” (0.88 Ha) implies sustainable cultivation practices, while the “leader plot” (1.55 Ha) implies traditional agricultural practices by the famers (fig.1).

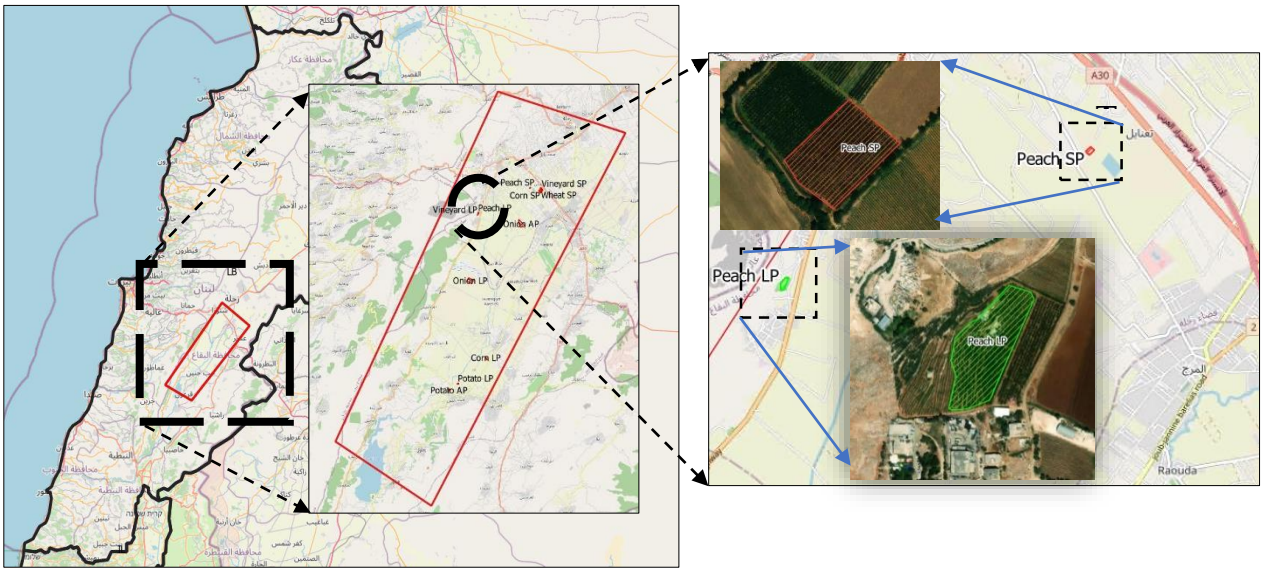

Figure 1 The two-peach pilot-sites in the region of “Beqaa Valley”, in Lebanon

2.2. Dataset

Thirty-five Sentinel-2 images cover the peach growing period from April to September 2021. The satellite data was retrieved from ESA’s (European Space Agency) Copernicus Open Access Hub service. The Copernicus service provides Sentinel products (Sentinel-1, Sentinel-2 and Sentinel-3) free of charge. Level-2A, atmospherically (bottom of atmosphere reflectance images) and geometrically corrected (UTM/WGS84 projection) images were downloaded. Next, a quality assessment was conducted for each Sentinel-2 image for ensuring high standard products. Eventually, twenty-eight images (28) fulfilled the quality criteria. Then, preprocessing procedures were applied to mask-out cloud effects and water bodies. Re-sampling and sub-setting techniques were also implemented creating 20-meter spatial resolution multispectral images in the Beqaa Valley.

2.3. Biophysical parameters and vegetation Indices retrieval methodology

The biophysical parameters and the vegetation indices are created by SNAP (Sentinel for Application Platform) software. It is ESA’s open-source toolbox, integrating many functionalities dedicated to Sentinel-2 imagery, such as Level-2B biophysical processor. The broadly applied PROSAIL model and neural networks are used from biophysical processor to derive Level-2B products: LAI, FAPAR, FCOVER, Cab and CWC. This algorithm belongs to the physical modeling approach using canopy radiative model for the estimation of biophysical parameters. Particularly, this technique is composed of three sub-models: (a) The PROSPECT model, describing the leaf attributes, namely water and chlorophyl concentration, leaf dry matter content, etc, (b) The SAIL (Scattering by Arbitrary Inclined Leaves) is a canopy reflectance model simulating the bidirectional

reflectance factor of turbid medium plant canopies, and (c) the reflectance of non-vegetation areas, that is, water surface, bare soil, and snow. Specifically, the estimation of biophysical parameters is based on the artificial neural network (ANN) algorithm following two steps: (a) a training dataset and the calibration of the network is performed by the canopy reflectance spectral bands, and (b) a backpropagation learning rule was applied to reduce the error between the output biophysical parameters and the input training values. This generic ANN algorithm comes up with two main advantages. Firstly, no field work is required and secondly, the biophysical parameters can be measured almost worldwide depending on Sentinel-2 imagery availability. Subsequently, the NDVI and NDRE were retrieved by SNAP toolbox. The spectral bands B4 (red) and B8 (NIR) were employed for NDVI retrieval, whereas NDRE product was calculated by the bands B8 (NIR) and B5 (red edge). For each of 28 Sentinel-2 images, the five biophysical variables and the two vegetation indices were calculated for the growing period of peach trees. The characteristics of the measured biophysical parameters and indices are described in the following Table (Table 1).

Table 1 Characteristics of biophysical variables and indices estimating from Sentinel-2 images

Parameter	Unit	Minimum	Maximum
LAI: Leaf Area Index	dimensionless	0	8.0
FAPAR: fraction of absorbed photosynthetically active Radiation	dimensionless	0	1.0
FVC: Fraction of Vegetation Cover	dimensionless	0	1.0
Lai_Cab: Leaf Chlorophyll content	g/cm^2	0	600
Lai_cw: Canopy Water Content	g/m^2	0	0.55
NDVI: Normalized Difference Vegetation Index: (842nm-665nm)/(842nm+665nm)	dimensionless	-1	1
NDRedEdge: Normalized difference Red Edge Index: (783nm-705nm)/ (783nm+705nm)	dimensionless	-1	1

To automate the calculation process batch processing methods were applied in SNAP toolbox. Thus, a graph builder tool was created using as input all the 28 images and as output the seven vegetation parameters (fig.2).

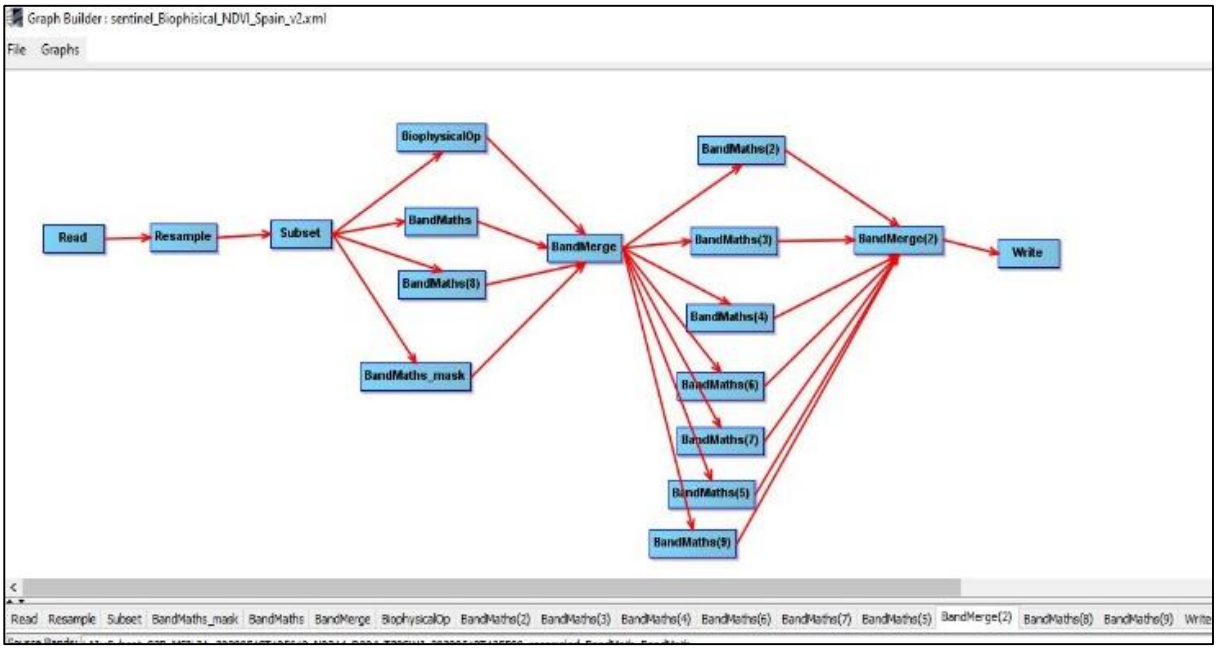

Figure 2 Workflow of the SNAP graph builder tool for producing the biophysical variables and indices of the 28 images

3. Results and Discussion

In agreement with the peach crop calendar, in April occurs leaves emerging, followed by the flowering period in May. Next, the fruit development stage lasts until the mid-August and finally the harvest period stars at the second half of August until September (Table 2). According to the crop calendar, the time series analysis of the biophysical indices was conducted based on the period from April to September 2021. The seven biophysical indices and parameters were calculated for monitoring the growth of the two peach plots (supromed and leader).

Table 2 Crop calendar for Peach growing season in 2021

Date	Stage
April 2021	1st leaf budding
May 2021	Blooming
June-July – August 2021	Fruit Bulking
August 15 - September 2021	Harvest

The following Figure 3 exhibits the evolution of Leaf Area Index (LAI) biophysical parameter for the period from April to September 2021 for the supromed peach plot (fig.3). The shades of yellow-green color indicate the different phenological stages for peach, namely at the end of April the plant is in early stage, in July to mid-August the crop is on “fruit Bulking” stage (shades of green color) and at the end of September the crop is on “maturity stage” (brown color).

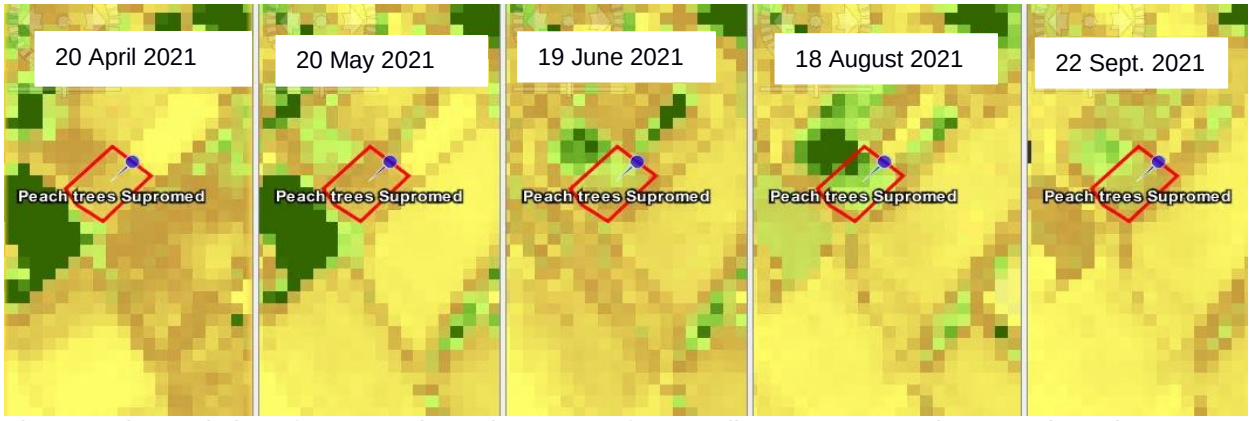

Figure 3 The evolution of supromed peach tree crop from April 2021 to September 2021 based on LAI

Furthermore, the leader and Supromed peach tree plots indicate the same growth pattern concerning the seven biophysical/vegetation indices. The following Figure 4 illustrate the growth pattern for the supromed peach tree plot (fig.4).

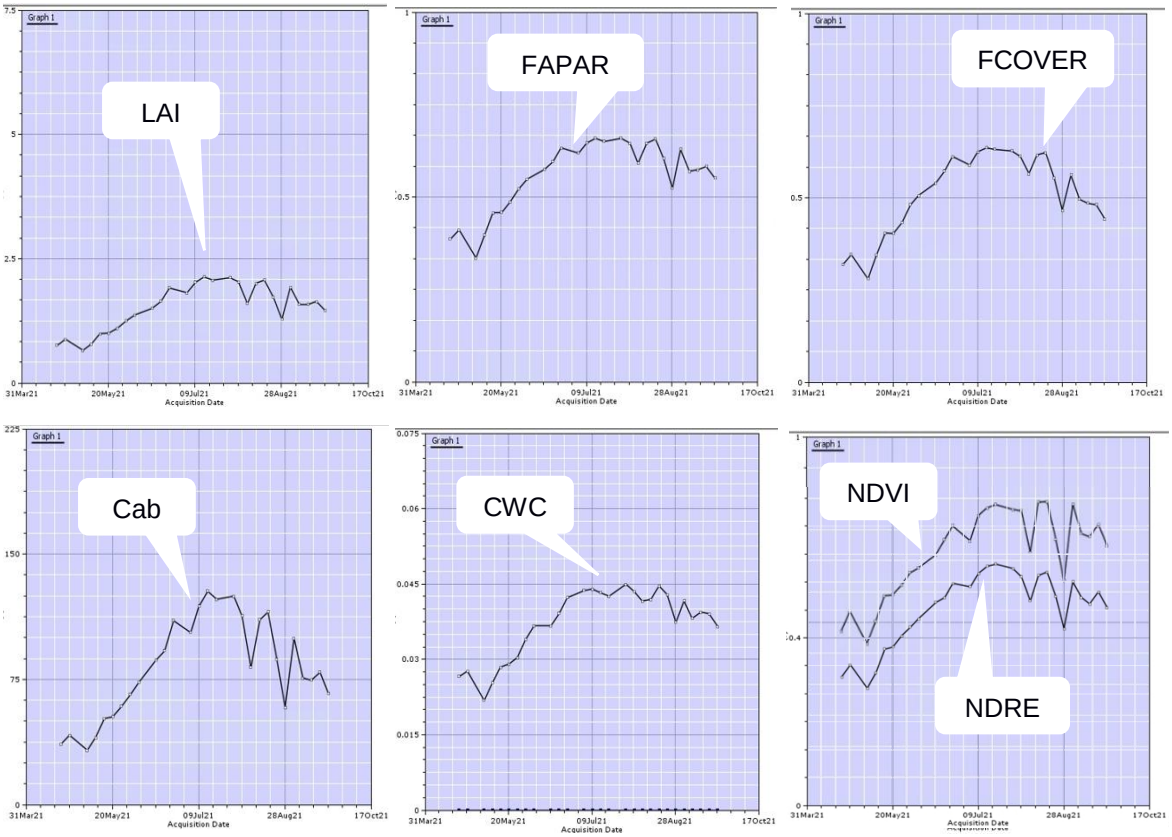

Figure 4 Supromed peach plot growth cycle monitored by seven biophysical parameters from May to September 2021

All the vegetation parameters illustrate almost the same pattern, which is in coherence with the crop calendar for the period of May to September 2021. From the beginning of May there is an increase of values with the maximum occurring about the end of July 2021, which is followed by a sharp fall until the end of September 2021(harvest period). On 3 and 23 of August 2021, a sharp decrease is observed in all vegetation indices. This may indicate temporary stress events on trees canopy (water or nitrogen deficiencies).
Next, the relationship between the two peach tree plots was investigated through the vegetation parameters during the growth period (fig.5). In general, at the first three months of the growing period (from April to 20th of June 2021), the leader peach plot indicates better vegetation characteristics (orange line) than the Supromed one. Next, and for all the bulking period until the end of September (harvest), the Supromed peach plot indicates better characteristics (blue line), than the leader one.

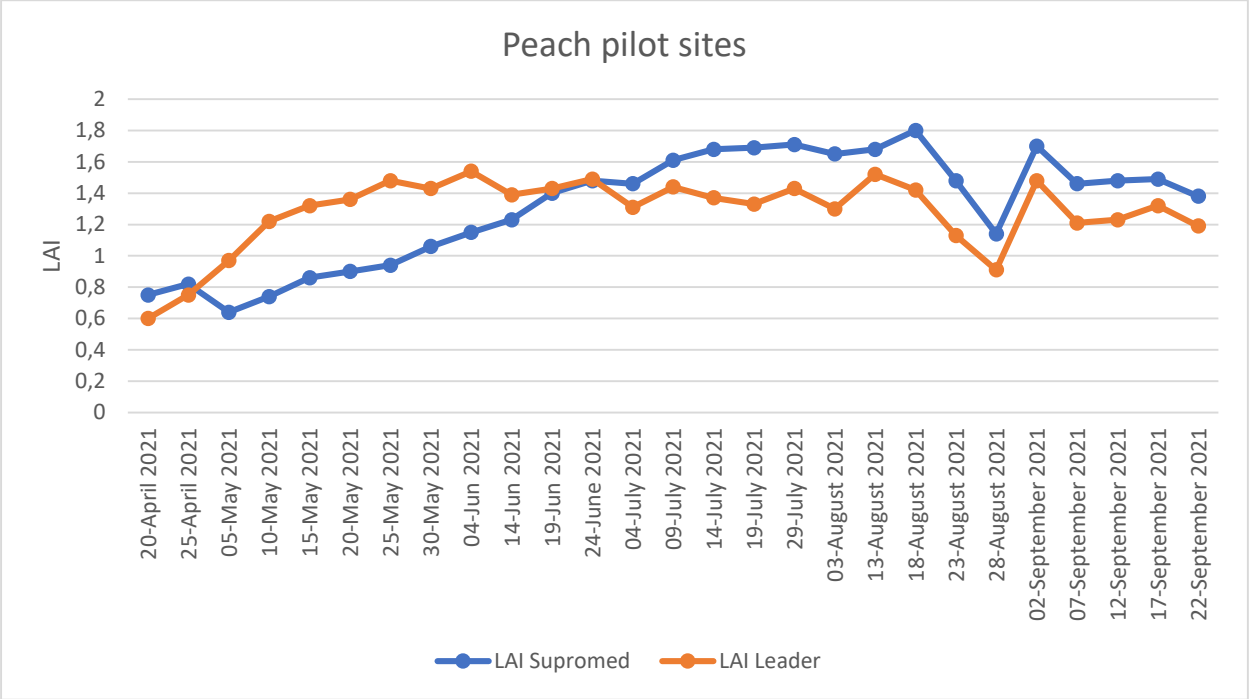

Figure 5 Assessing the two peach tree plots through LAI parameter

This analysis of biophysical parameters shows that the supromed peach plot (with sustainable agricultural practices), has great potential to provide better yield than the leader one.

4. Summary and conclusions

This study investigates the relationship between the seven biophysical parameters and indices for monitoring the two peach tree plots for the period April-September 2021. Twenty-eight Sentinel-2 multispectral images were processed by ESA's SNAP toolbox. The five biophysical variables, namely LAI, FAPAR, FCOVER, Cad, CWC, were calculated by the Level-2B biophysical processor integrated in SNAP. Moreover, the commonly used vegetation indices NDVI and NDRE were computed. The appraisal of the growing patterns of the two peach tree plots, through the biophysical indicators, reveals good correlation according to the crop calendar. From May 2021 and onwards there is a continuous growth (Blooming, Fruit Bulking) with the maximum productivity being detected in mid-August 2021, followed by the harvest period in September 2021. In addition, the comparison between the leader and Supromed peach tree plots was investigated in the study area of "Beqaa Valley" in Lebanon. The assessment of vegetation parameters reveals better performance for the Supromed peach tree plot.
In conclusion, Sentinel-2 missions offer new potential for appraisal crop status. Specifically, the red-edge bands in Sentinel-2 imagery could provide useful products in precision agriculture applications. The SNAP software with the biophysical processor is an exceptionally valuable tool for retrieving almost globally biophysical parameters (Sentinel-2 and Landsat 8). At farm level, these vegetation indicators could be a valuable tool for sustainable use of natural resources, such as irrigation water, or fertilizers.

Acknowledgements

This research was funded by SUPROMED project under the PRIMA 2018 program of the European Commission.

References

Bester Tawona Mudereri, Tavengwa Chitata, Concilia Mukanga, Elvis Tawanda Mupfiga, Calisto Gwatirisa & Timothy Dube (2021). Can biophysical parameters derived from Sentinel-2 space-borne sensor improve land cover characterisation in semi-arid regions? Geocarto International, 36:19, 2204-2223, DOI: 10.1080/10106049.2019.1695956.

Campbell J, Wynne R. (2007). Introduction to remote sensing. 5th ed. New York (NY): Guiford Press.

Dorigo, W.A.,, Jurita-Milla, R., de Wit, A.J.W., Brazile, J., Singh, R., Schaepman, M.E., (2007). A review on reflective remote sensing and data assimilation techniques for enhanced agroecosystem modeling. International journal of applied earth observation and geoinformation, 9(2), 165–193.

Hu, Qiong, Jingya Yang, Baodong Xu, Jianxi Huang, Muhammad S. Memon, Gaofei Yin, Yelu Zeng, Jing Zhao, and Ke Liu. (2020). "Evaluation of Global Decametric-Resolution LAI, FAPAR and FVC Estimates Derived from Sentinel-2 Imagery" Remote Sensing 12, no. 6: 912. https://doi.org/10.3390/rs12060912.

Jorge, J., Vallbé, M., & Soler, J. A. (2019). Detection of irrigation inhomogeneities in an olive grove using the NDRE vegetation index obtained from UAV images. European Journal of Remote Sensing, 52(1), 169-177.

Ilina Kamenova & Petar Dimitrov (2021). Evaluation of Sentinel-2 vegetation indices for prediction of LAI, fAPAR and fCover of winter wheat in Bulgaria, European Journal of Remote Sensing, 54:sup1, 89-108, DOI: 10.1080/22797254.2020.1839359.

Odindi J, Mutanga O, Rouget M, Hlanguza N. (2016). Mapping alien and indigenous vegetaton in the KwaZulu-Natal Sandstone Sourveld using remotely sensed data. Bothalia. 46(2):1–9.

Qiaoyun Xie, Jadu Dash, Alfredo Huete, Aihui Jiang, Gaofei Yin, Yanling Ding, Dailiang Peng, Christopher C. Hall, Luke Brown, Yue Shi, Huichun Ye, Yingying Dong, Wenjiang Huang, (2019). Retrieval of crop biophysical parameters from Sentinel-2 remote sensing imagery, International Journal of Applied Earth Observation and Geoinformation, Volume 80, pp187-195, ISSN 1569-8432, https://doi.org/10.1016/j.jag.2019.04.019.

Rahman Muhammad, Stanley John, Lamb David, Trotter Mark, (2014). Methodology for measuring fAPAR in crops using a combination of active optical and linear irradiance sensors: a case study in Triticale (X Triticosecale Wittmack). In Precision Agriculture. doi -10.1007/s11119-014-9349-6.

Ramoelo A, Cho MA. (2018). Explaining leaf nitrogen distribution in a semi-arid environment predicted on Sentinel-2 imagery using a field spectroscopy derived model. Remote Sens. 10(2):269.

Weiss M., Baret F., Jay S., (2020). S2ToolBox level 2 products: LAI, FAPAR, FCOVER. Version 2. European Space Agency. Paris.

Xue, J., & Su, B. (2017). Significant remote sensing vegetation indices: A review of developments and applications. Journal of Sensors, 2017, 1–17. Hindaw Limited. https://doi.org/10.1155/2017/135369.

Modeling actual evapotranspiration in vulnerable Mediterranean agriculture using satellite-based Sentinel 2 and 3 data: The case of Beqaa Valley in Lebanon

Spiliotopoulos M.[1], G. Tziatzios[1], Faraslis[2], I., N. Alpanakis[1], S. Sakellariou[1], P. Sidiropoulos[1], V. Brisimis[1], A. Blanta[1], G. Karoutsos[3], N. Dercas[4], N.R. Dalezios[1]

[1] Department of Civil Engineering, University of Thessaly, Volos, Greece
[2] Department of Environmental Sciences, University of Thessaly, Larisa, Greece
[3]General Aviation Applications "3D" S.A., 2 Skiathou str, 54646, Thessaloniki, Greece
[4] Department of Natural Resources and Agricultural Engineering, Agricultural University of Athens, Greece

Abstract. Actual evapotranspiration is estimated by many different methods, such as the placement of instruments in the fields such as lysimeters, the use of simulation programs, the use of remote sensing, or/and a combination of the latter two methods. This work utilizes the joining of simulation programs and remote sensing in the Beqaa Valley. Beqaa Valley is the most important rural area in Lebanon, with maize, wheat, onions, and potatoes crops predominating. The simulation program used is the Sen-ET SNAP software. Sen - ET SNAP graphical user interface was developed by the European Space Agency using satellite images from Sentinel 2 and Sentinel 3 and meteorological data from the Weather Research and Forecast (WRF) model to estimate actual daily evapotranspiration. The proposed methodology framework consists of 17 individual stages having the outcome of estimating actual daily evapotranspiration flows. The results indicate the suitability of Sen-ET SNAP software that can be used for effective irrigation management in data scarce rural regions.

1 Introduction

Globally, there is a non-stop research effort to estimate ET_c, as well as crop water requirements (Calera *et al*., 2017; Campos et al., 2017). Remote sensing (RS) has already become an important tool for the quantification and the detection of the spatial and temporal distribution and variability of several environmental variables at different scales. Nowadays, the most prevailing group of Earth Observation methodologies for the estimation of ET_c is the Energy Balance (EB) algorithms and more specifically the residual methods (Salgado and Mateos, 2021). Remote sensing-based EB algorithms estimate ET as a "residual" of the land surface energy balance equation. The computation of sensible Heat H is the parameter, which makes the difference in all the prevailing EB approaches like Two Source Model (TSM) (Kustas and Norman 1996), Surface Energy Balance Algorithm for Land (SEBAL) (Bastiaanssen et al., 1998a and 1998b), Mapping Evapotranspiration with Internalized Calibration (METRIC) (Allen et al., 2007), Surface Energy Balance System (SEBS) (Su, 2002) etc. (Gowda et al., 2007).

2 Methodology

The estimation daily actual evapotranspiration with the use of Sentinel-2 and Sentinel-3 first initiated by ESA, introducing Sen-ET (ESA, 2020). In this study, the adopted methodology follows seventeen steps and is based on the two-source energy balance TSEB model. There is a modification of the initial Sen-ET SNAP by ESA, and the proposed methodology uses meteorological data from WRF model, instead of ECMWF, which stands as a modification and improvement from the original designed plug-in. Sen-ET is designed to process Sentinel-2 radiance scenes and Sentinel-3 LST products sharpened to Sentinel-2 resolution. TSEB methodology requires a system of temperature gradient-resistance equations through an iterative procedure developed by Norman et al. (1995) considering canopy latent heat flux (i.e., plant transpiration) under non-water-stressed conditions and other energy components, as described below. The TSEB model initially proposed in Norman et al. (1995), and then analyzed by Kustas and Norman (1999). utilizes LST derived from thermal infrared (TIR) radiation, vegetation structural properties (e.g LAI, canopy height) and meteorological parameters. Energy balance assumes that evaporation consumes energy, and instantaneous ET flux for the image time is calculated for each pixel of the image as a "residual" of the surface energy budget equation, where soil heat flux (G) and sensible heat flux (H) are subtracted from the net radiation flux at the surface (R_n) to compute the "residual" energy available for evapotranspiration (λET) (eq.1).

$$LE = \lambda ET = R_n - H - G \quad (1)$$

where LE is the latent heat flux (W/m^2), λ is the latent heat of vaporization, R_n is net radiation (W/m^2), G is soil heat flux (W/m^2) and H is sensible heat flux (W/m^2).

The principal source of uncertainty within TSEB lies in the estimation of the sensible heat flux (H) as described above, which is calculated through the heat transport equation (eq. 2).

$$H = \frac{rC_p(T_0 - T_A)}{R_H} \quad (2)$$

where H is sensible heat flux (W m^{-2}); is the volumetric heat capacity of air (J m^{-3} K $^{-1}$); is the aerodynamic temperature of the surface (K); is the air temperature at a reference/measurement height (K); and is the aerodynamic resistance to heat transport (s m^{-1}).

LST obtained from TIR remote sensing generally differs significantly from aerodynamic surface temperature (Norman et al., 1995; Colaizzi *et al*., 2004; Burchard-Levine *et al*., 2019). TSEB methodology assumes that the total blackbody thermal radiance that is emitted by the surface is weighted by the fraction of vegetation observed by the sensor and the emission of soil and vegetation surfaces, as expressed in eq. 3 taken from Norman *et al*. (1995):

$$LST(\theta) = [f(\theta)T_c^4 + (1 - f(\theta)T_s^4)]^{1/4} \quad (3)$$

where θ is the angle of the TIR sensor, f(θ) is the fraction of vegetation observed at this angle, T_c is the vegetation canopy temperature (K), and T_s is the soil surface temperature (K). Further information about TSEB methodology can be found in the original papers or later in the literature (Norman et al., 1995; Colaizzi *et al*., 2004; Burchard-Levine *et al*., 2019).

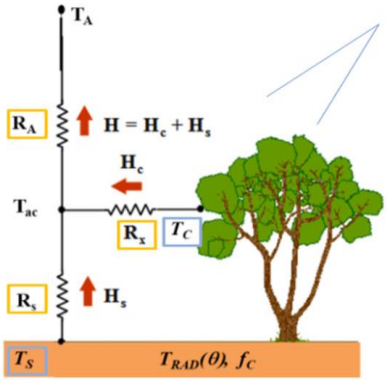

Figure 1.TSEB Sensible Heat model scheme (adapted from Kustas and Anderson, 2009)

3 Data Base and Study Area

3.1 Data Base.

Forty-two (42) Sentinel-2 scenes for the study area during the year 2020 were selected and downloaded. Finally, 29 out of 42 Sentinel-2 images passed the quality control for the present study (Table 1).

Table 1. Selected Sentinel-2 scenes for Beqaa Valley

A/A	Sentinel -2	Acquisition Date	Max Cloud Cover %	Quality control	Comments	A/A	Sentinel - 2	Acquisition Date	Max Cloud Cover %	Quality control	Comments
1	**1 Scene Level2**	**05 February**	**7.8**	**passed**	**Good**	**22**	**1 Scene Level2**	**09 June 2020**	**0.3**	**passed**	**Good**
2	1 Scene Level2	10 February	85.3	failed	Clouds over the area	**23**	**1 Scene Level2**	**14 June 2020**	**3.1**	**passed**	**Good**
3	1 Scene Level2	15 February	76.7	failed	Clouds over the area	**24**	**1 Scene Level2**	**24 June 2020**	**14.7**	**passed**	**Good**

4	1 Scene Level2	20 February	40.3	failed	Clouds over the area	**25**	**1 Scene Level2**	**04 July 2020**	**4.7**	**passed**	**Good**
5	1 Scene Level2	25 February	32.1	failed	Clouds over the area	**26**	**1 Scene Level2**	**09 July 2020**	**20.7**	**passed**	**Good**
6	1 Scene Level2	01 March 2020	60.6	failed	Clouds over the area	**27**	**1 Scene Level2**	**14 July 2020**	**6.4**	**passed**	**Good**
7	1 Scene Level2	06 March 2020	86.2	failed	Clouds over the area	28	1 Scene Level2	19 July 2020	0.1	failed	Data corrupted: bands5,6,7
8	**1 Scene Level2**	**11 March 2020**	**0.8**	**passed**	**partial snow near the area**	**29**	**1 Scene Level2**	**24 July 2020**	**0.4**	**passed**	**Good**
9	1 Scene Level2	05 April 2020	54	failed	Clouds over the area	**30**	**1 Scene Level2**	**29 July 2020**	**4.3**	**passed**	**Good**
10	1 Scene Level2	10 April 2020	77	failed	Clouds over the area	**31**	**1 Scene Level2**	**3 August 2020**	**8.5**	**passed**	**Good**
11	**1 Scene Level2 & 1 Scene level1**	**15 April 2020**	**39.9**	**passed**	**Level-2,corrupted bands.**	**32**	**1 Scene Level2**	**8 August 2020**	**3.9**	**passed**	**Good**
12	1 Scene Level2	20 April 2020	26.9	failed	Clouds over the area	**33**	**1 Scene Level2**	**13 August 2020**	**8.5**	**passed**	**Good**
13	1 Scene Level2	25 April 2020	56.4	failed	Clouds over the area	**34**	**1 Scene Level2**	**18 August 2020**	**0.1**	**passed**	**Good**
14	**1 Scene Level2**	**30 April 2020**	**27.4**	**passed**	**Good**	**35**	**1 Scene Level2**	**23 August 2020**	**0.1**	**passed**	**Good**
15	1 Scene Level2	05 May 2020	80.3	failed	Clouds over the area	**36**	**1 Scene Level2**	**28 August 2020**	**2.7**	**passed**	**Good**
16	**1 Scene Level2**	**10 May 2020**	**5.1**	**passed**	**Good**	**37**	**1 Scene Level2**	**02 September 2020**	**4.43**	**passed**	**Good**
17	**1 Scene Level2**	**15 May 2020**	**10.8**	**passed**	**Good**	**38**	**1 Scene Level2**	**07 September 2020**	**0.33**	**passed**	**Good**
18	**1 Scene Level2**	**20 May 2020**	**0.55**	**passed**	**Good**	**39**	**1 Scene Level2**	**12 September 2020**	**0.08**	**passed**	**Good**
19	1 Scene Level2	25 May 2020	9.6	failed	Clouds over the area	**40**	**1 Scene Level2**	**17 September 2020**	**0.04**	**passed**	**Good**
20	**1 Scene Level2**	**30 May 2020**	**6.4**	**passed**	**Good**	**41**	**1 Scene Level2**	**22 September 2020**	**0.23**	**passed**	**Good**
21	**1 Scene Level2**	**04 June 2020**	**4.5**	**passed**	**Good**	**42**	**1 Scene Level2**	**27 September 2020**	**0.04**	**passed**	**Good**

3.2 Study area.

The pilot area dealing with this study is Beqaa Valley, Lebanon, which occupies 371,9 km^2. The valley is located between the two mountain chains of Lebanon, Mount-Lebanon and Anti-Lebanon, central area of the agriculture production with more than 42% of the Lebanese agricultural lands, where 69% of these lands are irrigated. The altitudes in this area fluctuate between 800m and 1000m above sea level. The population of the area is about 65000 inhabitants (Figure 2).

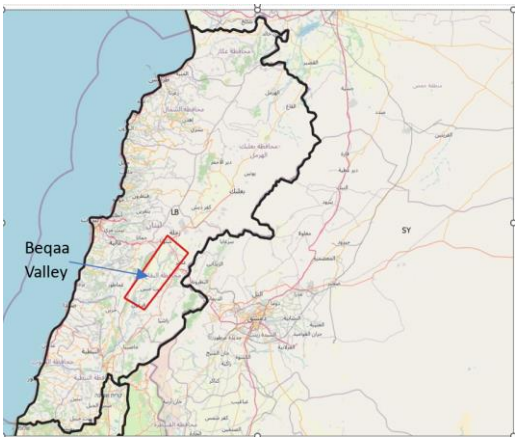

Figure 2. Map of the study area: Bekaa Valley, Lebanon.

The pilot area in Lebanon is depicted in Figure 3.

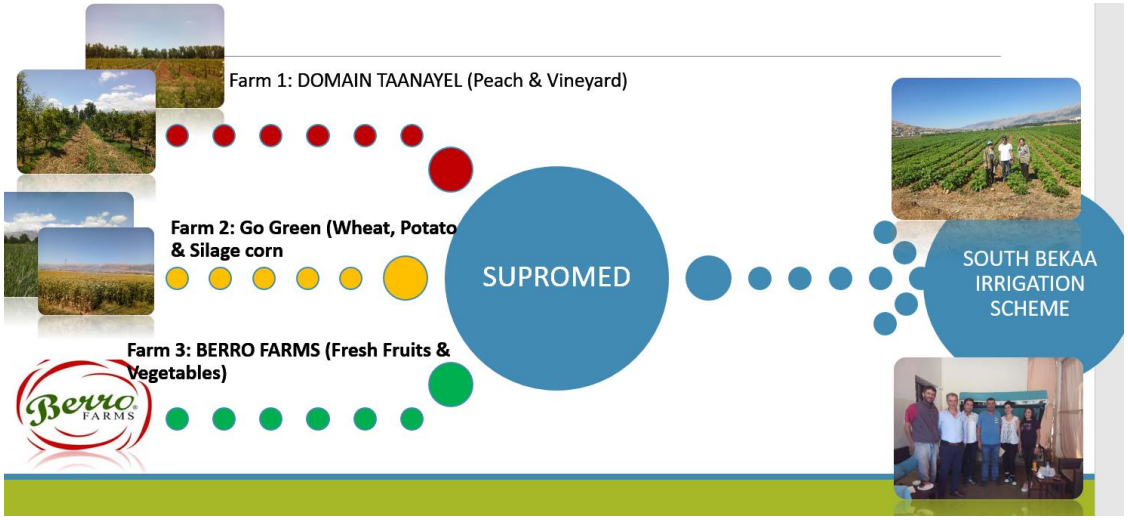

Figure 3. Demo sites in study area *(ULFA, 2020)*

4 Results and discussion

ET values for every image taken as output of Sen-ET plugin are derived for the study area. The values are mapped and assigned to the specific fields under consideration. This task has undertaken for all the crop fields of the study. Tables 2, 3, 4 and 5 illustrate an example of tabulated ET_a statistics for corn, potato, wheat, and peach fields, respectively.

Table 2.Corn ET_a values (Leader plot)

Date	MEAN	MEDIAN	STDEV	MIN	MAX	Date	MEAN	MEDIAN	STDEV	MIN	MAX
5/2/2020	1,5	1,5	0,1	1,1	1,9	24/7/2020	5,7	5,7	0,4	5,1	6,8
11/3/2020	4,6	4,7	0,2	3,2	4,9	29/7/2020	5,5	5,4	0,3	5,3	6,8
15/4/2020	4,4	4,4	0,1	4,0	4,6	3/8/2020	1,8	1,8	0,9	0,0	6,2
30/4/2020	5,1	5,0	0,3	4,4	6,2	8/8/2020	4,3	4,0	0,8	2,6	5,9
10/5/2020	6,9	6,6	2,1	0,7	12,5	13/8/2020	0,3	0,0	0,8	0,0	5,5
15/5/2020	8,3	8,4	0,5	6,8	8,9	18/8/2020	0,4	0,4	0,4	0,0	2,2
20/5/2020	7,0	6,8	0,5	6,2	7,6	23/8/2020	0,6	0,5	0,9	0,0	5,1
30/5/2020	2,4	2,1	0,8	1,8	6,4	28/8/2020	0,6	0,5	0,8	0,0	4,8

4/6/2020	3,5	3,5	0,5	2,1	5,9	2/9/2020	2,7	2,6	0,3	2,5	4,1
9/6/2020	3,9	4,0	0,5	2,8	6,1	7/9/2020	6,3	6,3	0,3	4,6	6,9
14/6/2020	3,2	3,2	0,4	1,9	4,9	12/9/2020	5,0	4,9	0,3	4,4	5,9
24/6/2020	3,4	3,3	0,7	1,8	6,1	17/9/2020	5,9	6,0	0,3	5,0	6,2
4/7/2020	3,1	2,9	0,7	2,5	6,5	22/9/2020	1,1	0,6	1,2	0,1	3,9
9/7/2020	3,2	3,0	0,6	2,4	5,8	27/9/2020	3,9	3,8	0,4	3,2	5,5
14/7/2020	0,7	0,5	1,0	0,0	4,8						

Table 3.Potato ET_a values (Leader plot)

Date	MEAN	MEDIAN	STDEV	MIN	MAX	Date	MEAN	MEDIAN	STDEV	MIN	MAX
5/2/2020	1,4	1,5	0,5	0,2	2,0	24/7/2020	4,1	3,9	0,8	2,4	6,1
11/3/2020	4,2	4,4	0,7	2,9	5,2	29/7/2020	3,6	3,4	0,7	2,1	5,5
15/4/2020	3,9	4,2	0,5	1,2	4,5	3/8/2020	3,1	3,0	0,6	1,7	5,5
30/4/2020	4,0	4,2	0,8	2,7	5,7	8/8/2020	2,8	3,0	0,8	0,3	5,4
10/5/2020	5,8	6,3	0,9	4,1	7,4	13/8/2020	2,6	2,9	0,8	0,4	4,3
15/5/2020	6,6	7,5	1,5	3,8	8,3	18/8/2020	2,3	2,4	0,6	1,1	4,6
20/5/2020	6,6	6,9	1,3	4,3	8,7	23/8/2020	2,8	2,8	0,4	1,5	4,9
30/5/2020	5,2	5,1	0,7	2,9	7,7	28/8/2020	2,7	2,7	0,4	1,4	4,7
4/6/2020	4,3	4,0	0,9	2,1	6,0	2/9/2020	3,4	3,3	0,3	2,7	5,1
9/6/2020	4,9	4,8	0,8	2,4	6,8	7/9/2020	3,3	3,2	0,5	2,3	4,8
14/6/2020	3,4	3,5	1,1	1,6	6,1	12/9/2020	3,1	2,9	0,6	2,1	5,2
24/6/2020	3,6	3,6	0,7	1,7	5,9	17/9/2020	3,2	3,1	0,5	2,4	5,3
4/7/2020	4,1	3,7	1,5	1,8	7,3	22/9/2020	3,2	3,1	0,4	2,3	4,4
9/7/2020	4,2	4,0	0,8	2,4	6,7	27/9/2020	3,9	4,0	0,7	2,2	5,2
14/7/2020	2,2	2,9	1,6	0,0	6,7						

Table 4.Wheat ET_a values (Leader plot)

Date	MEAN	MEDIAN	STDEV	MIN	MAX	Date	MEAN	MEDIAN	STDEV	MIN	MAX
5/2/2020	1,5	1,5	0,1	1,1	1,8	24/7/2020	3,6	3,6	0,3	2,4	4,3
11/3/2020	4,6	4,7	0,3	3,1	5,0	29/7/2020	3,4	3,4	0,4	2,0	4,6
15/4/2020	4,2	4,2	0,2	3,4	4,3	3/8/2020	2,7	2,7	0,3	1,5	3,5
30/4/2020	4,7	4,7	0,4	3,8	5,9	8/8/2020	2,7	2,7	0,3	1,4	4,1
10/5/2020	5,5	5,7	1,2	0,0	7,6	13/8/2020	2,8	2,9	0,3	1,5	3,4
15/5/2020	7,7	7,6	0,4	6,2	8,4	18/8/2020	2,8	2,8	0,4	1,3	3,8
20/5/2020	8,4	8,5	0,8	5,1	10,7	23/8/2020	3,0	3,0	0,3	2,3	3,9
30/5/2020	6,4	6,4	0,4	5,2	7,1	28/8/2020	2,9	2,8	0,3	2,1	3,7
4/6/2020	5,9	5,8	0,5	4,7	6,9	2/9/2020	3,3	3,3	0,1	2,5	3,6
9/6/2020	5,3	5,3	0,7	4,0	6,9	7/9/2020	2,9	2,9	0,1	2,4	3,3
14/6/2020	4,1	4,1	0,4	3,4	6,0	12/9/2020	2,6	2,7	0,3	1,8	3,0
24/6/2020	3,6	3,5	0,8	2,5	6,7	17/9/2020	2,4	2,3	0,3	1,9	3,1
4/7/2020	3,7	3,7	0,5	2,5	5,7	22/9/2020	2,1	2,1	0,2	1,9	2,7
9/7/2020	3,8	3,8	0,4	2,7	5,5	27/9/2020	2,8	2,8	0,4	1,9	4,3
14/7/2020	4,3	4,3	0,7	2,1	7,5						

Table 5.Peach1 ET_a values (Leader plot)

Date	MEAN	MEDIAN	STDEV	MIN	MAX	Date	MEAN	MEDIAN	STDEV	MIN	MAX
5/2/2020	1,6	1,6	0,2	1,1	1,8	24/7/2020	7,3	7,4	0,3	6,7	7,6

11/3/2020	4,6	4,7	0,2	4,4	4,8	29/7/2020	6,1	6,1	0,2	5,9	6,3
15/4/2020	4,4	4,3	0,1	4,2	4,5	3/8/2020	5,6	5,6	0,4	4,9	6,2
30/4/2020	6,0	6,0	0,1	5,8	6,3	8/8/2020	6,7	6,8	0,6	5,8	7,4
10/5/2020	6,2	6,2	0,1	6,1	6,3	13/8/2020	5,0	5,0	0,1	4,9	5,2
15/5/2020	6,9	6,9	0,2	6,4	7,2	18/8/2020	5,4	5,4	0,2	5,1	5,8
20/5/2020	7,5	7,4	0,2	7,2	7,9	23/8/2020	6,1	6,0	0,2	5,9	6,4
30/5/2020	5,8	5,8	0,3	5,4	6,2	28/8/2020	5,8	5,7	0,2	5,6	6,1
4/6/2020	5,2	5,1	0,3	4,9	5,7	2/9/2020	5,0	5,1	0,2	4,8	5,2
9/6/2020	5,7	5,6	0,2	5,4	5,9	7/9/2020	6,2	6,2	0,1	6,0	6,4
14/6/2020	4,7	4,7	0,2	4,6	5,0	12/9/2020	5,4	5,4	0,1	5,2	5,7
24/6/2020	4,7	4,7	0,1	4,6	4,9	17/9/2020	6,4	6,4	0,1	6,3	6,5
4/7/2020	5,3	5,4	0,2	5,0	5,5	22/9/2020	4,5	4,4	0,1	4,3	4,6
9/7/2020	5,6	5,6	0,3	5,1	6,1	27/9/2020	5,5	5,5	0,1	5,4	5,6
14/7/2020	2,6	2,7	0,6	1,7	3,3						

Separate graphs derived from the above Tables are illustrated in Figure 4, where the horizontal axis represents time, and the vertical axis represents daily evapotranspiration values (mm).

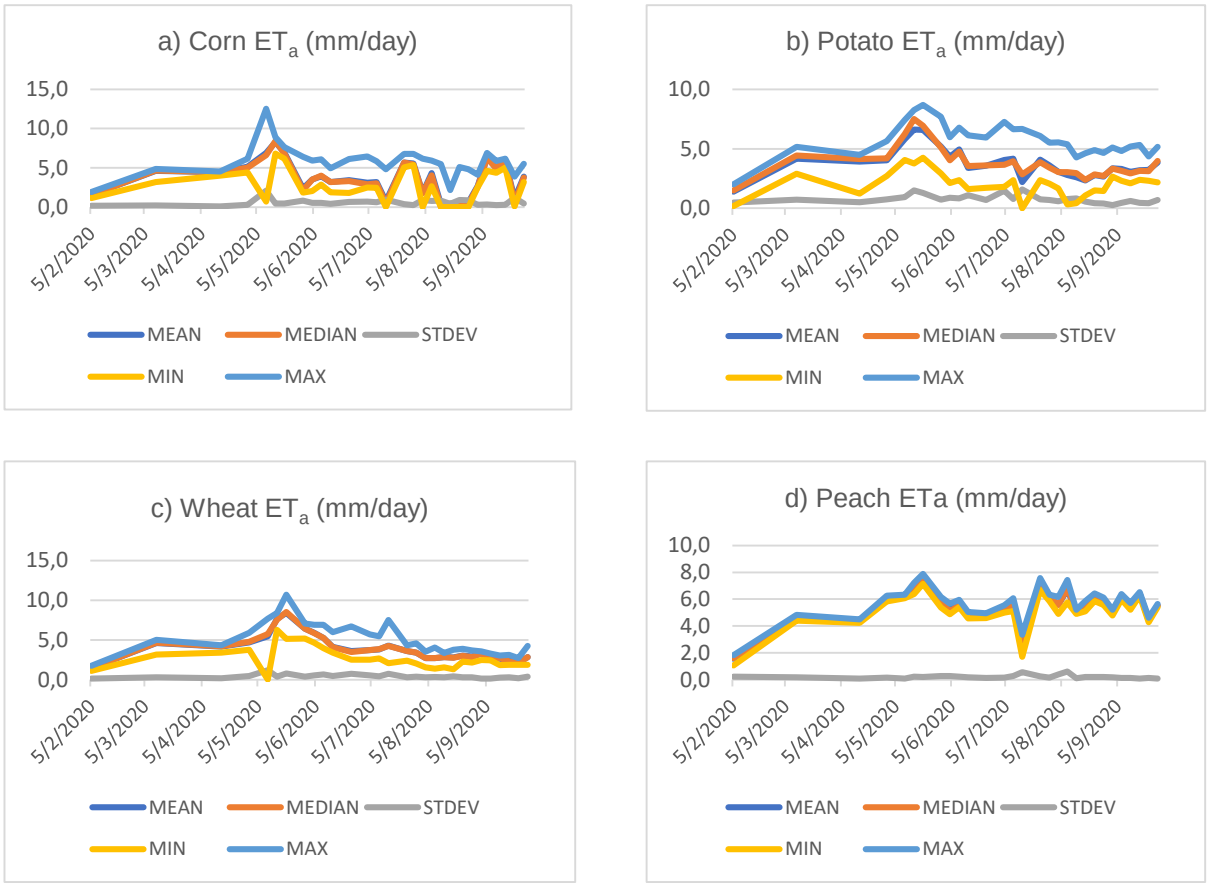

Figure 4. ET_a values for (a) corn, (b) potato, (c) wheat and (D) peach fields - Beqaa Valley

The ET_a time series depicted in the above Figure 4 seem reasonable. The same procedure was repeated for all the available fields for the study area but are not included in this paper due to size restrictions.

5 Summary and conclusions

At this study, a new approach has been utilized in Beqaa Valley, Lebanon, considering WRF modified Sentinel-2 and Sentinel-3 ET_a values taken from Sen-ET plugin. This procedure needs further analysis and additionally a validation procedure using in-situ experiments rationalizing irrigation water requirements. This first approach shows that the use of remote sensing can play a significant role in daily operational agricultural practices, due to continuous technological and scientific advances, as well as the improvement of the related sensors on-board.

Acknowledgements

This work has been funded by SUPROMED “Sustainable Production in water limited environments of Mediterranean agro-ecosystem”. R&I project funded under the PRIMA 2018 program, section I. The authors gratefully acknowledge DIFAF and Lebanese University Faculty of Agriculture & Veterinary (ULFA) groups for providing the field experiments’ data.

References

Allen, R., Tasumi, M. and Trezza, R., 2007. Satellite-Based Energy Balance for Mapping Evapotranspiration with Internalized Calibration (METRIC)-Model. Journal of Irrigation and Drainage Engineering 133, 380-394, doi:10.1061/(asce)0733-9437(2007)133:4(380) (2007).

Bastiaanssen, W. G. M., Menenti, M., Feddes, R. A. and Holtslag, A. A. M., 1998. A remote sensing surface energy balance algorithm for land (SEBAL) 1. Formulation. Journal of Hydrology 212, 198-212, doi:http://dx.doi.org/10.1016/S0022-1694(98)00253-4 (1998). (a)

Bastiaanssen, WGM, Pelgrum, H, Wang, J, Ma, Y, Moreno J, Roerink, GJ, van der Wal T, 1998b. The Surface Energy Balance Algorithm for Land (SEBAL): Part 2 validation, J. Hydrology, 212-213: 213-229.

Burchard-Levine, V., Héctor Nieto, H., Riaño,D., 3, Migliavacca, M., El-Madany, T.S., Perez-Priego, O., Carrara, A., and Martín, P.M., 2019. Adapting the thermal-based two-source energy balance model to estimate energy fluxes in a complex tree-grass ecosystem.Hydrology and Earth System Sciences Discussions, https://doi.org/10.5194/hess-2019-354 Preprint.

Calera, A., Campos, I., Osann, A., D’Urso, G., Menenti, M., 2017. Remote Sensing for Crop Water Management: From ET Modelling to Services for the End Users. Sensors 17(5), pp.1104.

Campos, I., Neale, C.M.U., Suyker, A.E., Arkebauer, T.J. and Gonçalves, I.Z. (2017) ‘Reflectance-based crop coefficients REDUX: for operational evapotranspiration estimates in the age of high producing hybrid varieties’, Agricultural Water Management, Vol. 187, pp.140–153.

Colaizzi, P.D., Evett, S.R., Howell, T.A., and Tolk, J.A.: Comparison of aerodynamic and radiometric surface temperature using precision weighing lysimeters, Remote sensing and modeling of ecosystems for sustainability, 5544, 215-230, 700 International Society for Optics and Photonics. https://doi.org/10.1117/12.559503, 2004.

ESA, 2020. USER MANUAL FOR SEN-ET SNAP PLUGIN. V1.1.0 March 19, 2020, 37 pages.

Gowda PH, Chávez JL, Howell TA, Marek TH, New LL. (2008). Surface Energy Balance Based Evapotranspiration Mapping in the Texas High Plains. Sensors. 8(8):5186-5201.

Kustas, W. P. and Norman, J. M.,1996. Use of remote sensing for evapotranspiration monitoring over land surfaces. Hydrological Sciences Journal 41, 495-516, doi:10.1080/02626669609491522 (1996).

Kustas, W.P., and Anderson, M.C., 2009: Advances in thermal infrared remote sensing for land surface modeling, Agricultural and Forest Meteorology, 149, 2071–2081.

Norman JM, Kustas WP, Humes KS (1995) Source approach for estimating soil and vegetation energy fluxes in observations of directional radiometric surface temperature. Agric For Meteorol 77(3–4):263–293. 10.1016/0168-1923(95)02265-Y.

Salgado, R., and Mateos, L., 2021. Evaluation of different methods of estimating ET for the performance assessment of irrigation schemes. Agricultural Water Management, Volume 243, 1 January 2021, 106450.

Actual evapotranspiration estimation in semi-arid areas using a combination of Sentinel-2 and Sentinel-3 data: The case of Sidi Bouzid, Tunisia

Spiliotopoulos M.[1], I. Faraslis[2], N. Alpanakis[1], G. Tziatzios[1], P. Sidiropoulos[1], S. Sakellariou[1], A. Blanta[1], V. Brisimis[1], G. Karoutsos[3], N.R. Dalezios[1], N. Dercas[4].

[1] Department of Civil Engineering, University of Thessaly, Volos, Greece
[2] Department of Environmental Sciences, University of Thessaly, Larisa, Greece
[3]General Aviation Applications "3D" S.A., 2 Skiathou str, 54646, Thessaloniki, Greece
[4] Department of Natural Resources and Agricultural Engineering, Agricultural University of Athens, Greece

Abstract. The estimation of actual evapotranspiration (ET_a) in semi-arid regions plays a significant role for water resources management and it is very important for peoples' life. This work is dealing with ETa estimation above important crops of the economy of Tunisia like oat, onion, almond and olive trees, among others. Sen - ET SNAP graphical user interface developed by the European Space Agency was used for the estimation of actual daily evapotranspiration. The results indicate the applicability of Sen-ET SNAP software for effective estimation of water needs and irrigation management in sensitive Mediterranean agricultural regions.

1 Introduction

The estimation of ET_c for the computation of crop water requirements in semi-arid regions is very crucial (Calera *et al*., 2017; Campos *et al*., 2017). Remote sensing (RS) has already become an important tool for the quantification and the detection of the spatial and temporal distribution and variability of several environmental variables at different scales. The residual methodologies as a category of Energy Balance (EB) algorithms are the prevailing group of satellite data methodologies for the estimation of ET_c nowadays (Salgado and Mateos, 2021). Remote sensing-based EB algorithms estimate ET as a "residual" of the land surface energy balance equation. The computation of sensible Heat H is the parameter, which makes the difference in all the prevailing EB approaches like Two Source Model (TSM) (Kustas and Norman 1996), Surface Energy Balance Algorithm for Land (SEBAL) (Bastiaanssen *et al*., 1998a and 1998b), Mapping Evapotranspiration with Internalized Calibration (METRIC) (Allen et al., 2007), Surface Energy Balance System (SEBS) (Su, 2002) etc. (Gowda *et al*., 2007).

2 Methodology

The initial Sen-ET (Sentinels for evapotranspiration) plugin in SNAP uses the two-source energy balance (TSEB) model with Sentinel-2, Sentinel-3, and meteorological data from ECMWF (ESA, 2020). In this study, the adopted methodology follows seventeen steps and is based on the TSEB model. There is a modification of the initial Sen-ET SNAP by ESA, and the proposed methodology uses meteorological data from WRF model, instead of ECMWF. Specifically, the required meteorological data used from the plug-in are retrieved from WRF model, and this stands as a modification and improvement from the original designed plug-in. TSEB methodology developed by Norman *et al*. (1995) is an energy balance model dedicated to ET computation. The model utilizes LST derived from thermal infrared (TIR) radiation, vegetation structural properties (e.g., LAI, canopy height) and various meteorological parameters (Kustas *et al*., 1999). Eq.1 gives the concept of the energy balance, while Figure 1 gives the concept of the total methodology

$$LE = \lambda ET = R_n - H - G \quad (1)$$

where LE is the latent heat flux (W/m^2), λ is the latent heat of vaporization, R_n is net radiation (W/m^2), G is soil heat flux (W/m^2) and H is sensible heat flux (W/m^2). Further information about TSEB methodology can be found in the literature (Norman et al., 1995; Kustas et al., 2018; Burchard-Levine *et al*., 2019).

The Weather Research and Forecasting (WRF) Model is a mesoscale numerical weather prediction system designed for both atmospheric research and operational forecasting applications (Powers et al., 2017). The model presents a wide range of meteorological applications to a spatial resolution of tens of meters to thousands of kilometers (Jimenez and Dudhia,2013) Giannaros *et al*., 2017; El-Samra *et al*., 2018). The effort to develop WRF began in the latter 1990's and was a collaborative partnership of the National Center for Atmospheric Research (NCAR), the National Oceanic and Atmospheric Administration (represented by the

National Centers for Environmental Prediction (NCEP) and the Earth System Research Laboratory), the U.S. Air Force, the Naval Research Laboratory, the University of Oklahoma, and the Federal Aviation Administration (FAA) (Giannaros *et al*., 2017; El-Samra *et al*., 2018; Skamrock *et al*.,2019). In this study, meteorological data taken as WRF output are used as an input to the Sen-ET plug-in.

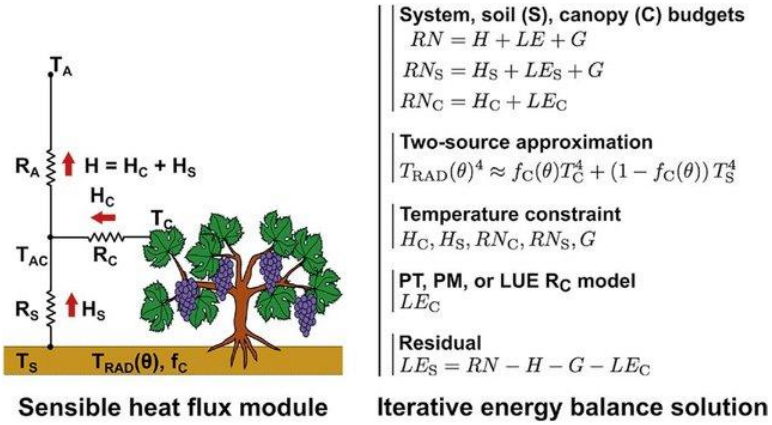

Figure 1. TSEB Sensible Heat model scheme (adapted from Kustas *et al*., 2018)

3 Data Base and Study Area

3.1 Data Base.

Forty-five (45) Sentinel-2 scenes for the study area during the years 2019-2020 were selected and downloaded. Finally, 23 out of 45 Sentinel-2 images passed the quality control for the present study (Table 1).

Table 1. Selected Sentinel-2 scenes for Sidi Bouzid, Tunisia

A/A	Sentinel -2	Acquisition Date	Max Cloud Cover %	Quality control	Comments	A/A	Sentinel - 2	Acquisition Date	Max Cloud Cover %	Quality control	Comments
1	**1 Scene Level2**	**05 December 2019**	**18.8**	**passed**	**Good**	24	1 Scene Level2	08 April 2020	16	failed	Clouds over the area
2	1 Scene Level2	10 December 2019	70.9	failed	Clouds over the area	25	1 Scene Level2	13 April 2020	57.6	failed	Clouds over the area
3	1 Scene Level2	15 December 2019		failed	Clouds over the area	26	1 Scene Level2	18 April 2020	76.2	failed	Clouds over the area
4	1 Scene Level2	20 December 2019	54.8	failed	Clouds over the area	27	1 Scene Level2	23 April 2020	15.3	failed	Clouds over the area
5	**1 Scene Level2**	**25 December 2019**	**0.03**	**passed**	**Good**	**28**	**1 Scene Level2**	**28 April 2020**	**1.4**	**passed**	**Good**
6	1 Scene Level2	30 December 2019	41.8	failed	Clouds over the area	29	1 Scene Level2	03 May 2020	4.8	failed	Bad quality
7	**1 Scene Level2**	**04 January 2020**	**1.9**	**passed**	**Good**	30	1 Scene Level2	08 May 2020	20.2	failed	Clouds over the area
8	1 Scene Level2	09 January 2020	79	failed	Clouds over the area	**31**	**1 Scene Level2**	**18 May 2020**	**2.3**	**passed**	**Good**
9	**1 Scene Level2**	**14 January 2020**	**0.9**	**passed**	**Good**	**32**	**1 Scene Level2**	**23May 2020**	**1.3**	**passed**	**Good**
10	**1 Scene Level2**	**19 January 2020**	**3.3**	**passed**	**Good**	33	1 Scene Level2	28May 2020	17.8	failed	Clouds over the area
11	1 Scene Level2	24 January 2020	34.5	failed	Clouds over the area	**34**	**1 Scene Level2**	**02 June 2020**	**0.6**	**passed**	**Good**
12	**1 Scene Level2**	**29 January 2020**	**5.3**	**passed**	**Good**	35	1 Scene Level2	07 June 2020	23.4	failed	Clouds over the area
13	1 Scene Level2	8 February 2020	45.7	failed	Clouds over the area	**36**	**1 Scene Level2**	**12 June 2020**	**16.4**	**passed**	**Good**

14	1 Scene Level2	13 February 2020	99.5	failed	Clouds over the area	37	1 Scene Level2	17 June 2020	59.7	failed	Clouds over the area
15	**1 Scene Level2**	**18 February 2020**	**1.6**	**passed**	**Good**	**38**	**1 Scene Level2**	**22 June 2020**	**0.2**	**passed**	**Good**
16	**1 Scene Level2**	**23 February 2020**	**0.5**	**passed**	**Good**	39	1 Scene Level2	27 June 2020	58.4	failed	Clouds over the area
17	**1 Scene Level2**	**28 February 2020**	**0.06**	**passed**	**Good**	**40**	**1 Scene Level2**	**02 July 2020**	**0.2**	**passed**	**Good**
18	**1 Scene Level2**	**04 March 2020**	**5.4**	**passed**	**Good**	**41**	**1 Scene Level2**	**07 July 2020**	**1.9**	**passed**	**Good**
19	1 Scene Level2	09 March 2020	25.9	failed	Clouds over the area	**42**	**1 Scene Level2**	**12 July 2020**	**0.7**	**passed**	**Good**
20	**1 Scene Level2 & 1 Scene level1**	**14 March 2020**	**1.5**	**passed**	**Level 2, has corrupted bands.**	**43**	**1 Scene Level2**	**17 July 2020**	**0.7**	**passed**	**Good**
21	1 Scene Level2	19 March 2020	86.2	failed	Clouds over the area	**44**	**1 Scene Level2**	**22 July 2020**	**0**	**Passed**	**Good**
22	1 Scene Level2	24 March 2020	63.7	failed	Clouds over the area	**45**	**1 Scene Level2**	**27 July 2020**	**0**	**passed**	**Good**
23	1 Scene Level2	29 March 2020	83.1	failed	Clouds over the area						

3.2 Study area.

The study area is in the province “Sidi Bouzid”, in central-western Tunisia. The region occupies an area of about 7,490 km^2, located in the central-western part of Tunisia, (Fig.2), and it is characterized by a relatively flat surface with an average altitude of 300 meters above the sea level. The cultivated area is 412000 hectares based on annual crops, like durum wheat, fodder oat, maize, vegetables, and trees, such as olives and pistachios.

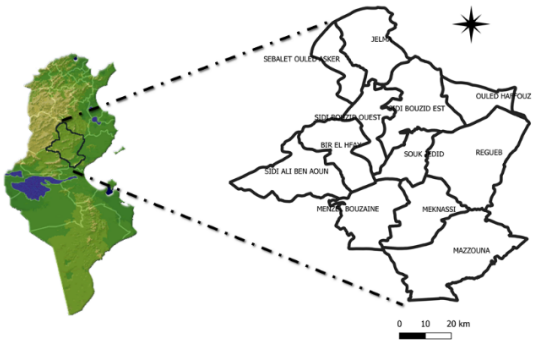

Figure 2. Map of the study area: Sidi Bouzid, Tunisia.

4 Results and discussion

ET values for every image taken as output of Sen-ET plugin are derived for the study area. The values are mapped and assigned to the specific fields under consideration. This task has undertaken for all the crop fields of the study. Tables 2, 3, 4 and 5 illustrate an example of tabulated ET_a statistics for oat, onion, olive trees and almond fields, respectively.

Table 2.Oat ET_a values

Date	MEAN	MEDIAN	STDEV	MIN	MAX	Date	MEAN	MEDIAN	STDEV	MIN	MAX
5/12/2019	1,62	1,61	0,12	1,28	1,93	**2/6/2020**	4,76	4,78	0,22	4,10	5,12
25/12/2019	0,91	0,90	0,10	0,67	1,32	**12/6/2020**	3,61	3,44	0,62	2,72	5,78
4/1/2020	1,06	1,06	0,07	0,80	1,18	**22/6/2020**	2,56	2,56	0,21	2,11	3,25
14/1/2020	1,31	1,31	0,08	1,10	1,51	**2/7/2020**	4,17	4,22	0,30	3,20	4,72
19/1/2020	1,57	1,59	0,12	1,28	1,93	**7/7/2020**	2,15	2,47	1,08	0,00	3,73
29/1/2020	1,60	1,64	0,19	1,13	1,96	**12/7/2020**					

18/2/2020	2,62	2,54	0,39	1,40	3,22	**17/7/2020**	4,00	4,01	0,37	2,54	4,50
23/2/2020	0,91	0,82	0,68	0,00	1,99	**27/7/2020**	2,62	2,61	0,93	0,32	4,28
28/2/2020	0,29	0,00	0,38	0,00	1,4	**1/8/2020**					
4/3/2020	2,66	2,67	1,29	0,00	4,44	**11/8/2020**	3,03	3,10	0,85	1,26	4,99
14/3/2020	2,52	2,48	0,89	0,84	4,91	**16/8/2020**					
28/4/2020	6,01	5,96	0,66	4,09	6,70	**21/8/2020**	3,41	3,52	0,48	1,88	4,04
18/5/2020	0,43	0,00	0,82	0,00	2,90	**26/8/2020**					
23/5/2020	2,23	2,24	0,77	0,68	3,71	**7/9/2020**	4,23	4,25	0,42	3,32	5,04

Table 3.Onion ET_a values

Date	**MEAN**	**MEDIAN**	**STDEV**	**MIN**	**MAX**	**Date**	**MEAN**	**MEDIAN**	**STDEV**	**MIN**	**MAX**
5/12/2019	1,79	1,75	0,08	1,70	1,92	**2/6/2020**	4,76	4,79	0,33	4,15	5,14
25/12/2019	1,29	1,31	0,17	0,98	1,51	**12/6/2020**	4,48	3,89	0,98	3,68	5,91
4/1/2020	1,23	1,27	0,13	0,95	1,36	**22/6/2020**	2,73	2,70	0,27	2,32	3,07
14/1/2020	1,55	1,54	0,21	1,19	1,90	**2/7/2020**	3,86	4,04	0,41	2,95	4,12
19/1/2020	2,09	2,13	0,31	1,53	2,49	**7/7/2020**	2,90	2,98	0,48	1,95	3,54
29/1/2020	2,02	2,15	0,34	1,29	2,32	**12/7/2020**					
18/2/2020	2,57	2,59	0,56	1,53	3,25	**17/7/2020**	3,29	3,60	0,51	2,29	3,64
23/2/2020	1,28	1,65	0,74	0,23	1,96	**27/7/2020**	2,91	2,85	0,29	2,57	3,32
28/2/2020	1,513	1,831	0,734	0,000	2,085	**1/8/2020**					
4/3/2020	2,89	2,74	0,66	2,25	4,21	**11/8/2020**	2,93	3,04	0,33	2,50	3,27
14/3/2020	3,38	3,20	0,54	2,62	4,28	**16/8/2020**					
28/4/2020	4,15	4,18	0,17	3,88	4,36	**21/8/2020**	3,12	3,23	0,25	2,63	3,37
18/5/2020	2,77	3,04	0,68	1,27	3,20	**26/8/2020**					
23/5/2020	2,82	2,77	0,61	1,73	3,69	**7/9/2020**	4,09	4,21	0,32	3,46	4,37

Table 4.Olive Trees ET_a values

Date	**MEAN**	**MEDIAN**	**STDEV**	**MIN**	**MAX**	**Date**	**MEAN**	**MEDIAN**	**STDEV**	**MIN**	**MAX**
5/12/2019	2,05	2,07	0,10	1,63	2,25	**2/6/2020**	4,49	4,55	0,43	3,28	5,38
25/12/2019	1,06	1,10	0,17	0,44	1,38	**12/6/2020**	4,92	5,10	0,66	3,20	6,05
4/1/2020	1,13	1,15	0,11	0,78	1,34	**22/6/2020**	2,34	2,61	0,79	0,55	3,83
14/1/2020	1,36	1,39	0,10	1,04	1,51	**2/7/2020**	4,05	4,15	0,66	2,68	5,51
19/1/2020	1,74	1,79	0,17	1,30	2,01	**7/7/2020**	3,21	3,30	0,93	0,93	5,12
29/1/2020	1,41	1,45	0,20	0,96	1,72	**12/7/2020**	3,91	4,06	0,59	2,76	4,96
18/2/2020	1,87	1,93	0,32	1,02	2,37	**17/7/2020**	3,70	3,89	0,62	2,57	4,81
23/2/2020	1,48	1,61	0,30	0,55	1,87	**27/7/2020**	3,02	3,32	0,58	1,90	3,83
28/2/2020	1,094	1,159	0,417	0,000	1,747	**1/8/2020**					
4/3/2020	2,12	2,23	0,42	0,85	2,85	**11/8/2020**	2,93	3,20	0,59	1,73	3,81
14/3/2020	2,84	2,95	0,35	1,68	3,31	**16/8/2020**					
28/4/2020	5,70	5,79	0,48	3,99	6,50	**21/8/2020**	3,41	3,52	0,48	1,88	4,04
18/5/2020	2,22	2,52	0,68	0,61	3,13	**26/8/2020**					
23/5/2020	3,22	3,31	0,36	1,96	3,75	**7/9/2020**	4,23	4,25	0,42	3,32	5,04

Table 5.Almond ET_a values

Date	**MEAN**	**MEDIAN**	**STDEV**	**MIN**	**MAX**	**Date**	**MEAN**	**MEDIAN**	**STDEV**	**MIN**	**MAX**
5/12/2019	1,61	1,64	0,14	1,17	2,01	**2/6/2020**	2,59	2,73	0,74	0,00	4,09

25/12/2019	1,11	1,06	0,24	0,63	1,73	**12/6/2020**	3,96	4,15	0,79	1,41	6,03
4/1/2020	1,10	1,23	0,25	0,71	1,42	**22/6/2020**	2,59	2,80	0,69	1,19	4,15
14/1/2020	1,29	1,15	0,28	0,84	1,76	**2/7/2020**	3,93	4,01	0,39	2,44	4,78
19/1/2020	1,79	1,81	0,31	1,13	2,53	**7/7/2020**	3,31	3,60	0,83	0,33	5,18
29/1/2020	1,45	1,50	0,19	0,82	1,73	**12/7/2020**	3,73	4,11	0,68	2,51	4,73
18/2/2020	2,02	2,00	0,20	1,16	2,31	**17/7/2020**	3,78	3,97	0,51	2,45	4,58
23/2/2020	1,37	1,42	0,26	0,27	1,73	**27/7/2020**	2,31	2,00	0,81	1,20	3,77
28/2/2020	0,548	0,624	0,308	0,000	1,064	**1/8/2020**					
4/3/2020	2,62	2,64	0,26	1,47	3,00	**11/8/2020**	2,57	2,26	0,69	1,80	3,91
14/3/2020	1,96	1,77	0,46	1,56	3,13	**16/8/2020**					
28/4/2020	6,08	6,24	0,42	4,19	6,48	**21/8/2020**	3,42	3,54	0,40	1,98	4,02
18/5/2020	0,97	0,90	0,45	0,00	2,93	**26/8/2020**					
23/5/2020	1,70	1,46	0,59	1,11	3,97	**7/9/2020**	3,56	3,41	0,31	2,92	4,32

Separate graphs derived from the above Tables are illustrated in Figure 4, where the horizontal axis represents time, and the vertical axis represents daily evapotranspiration values (mm).

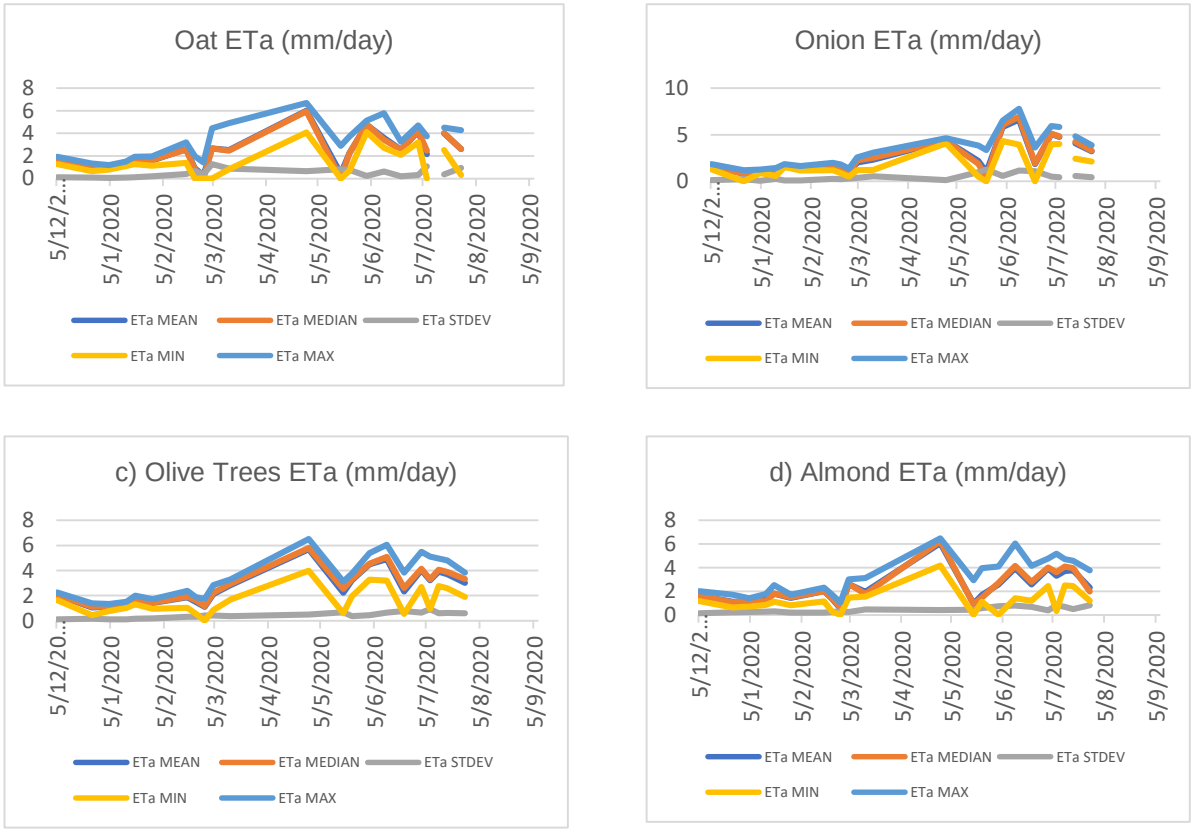

Figure 4. ET_a values for (a) oat, (b) onion, (c) olive trees and (d) almond fields – Sidi Bouzid

The ET_a time series values depicted in the above Figure 4 seem to be reasonable. The same procedure was repeated for all the available fields for the study area but are not included in this paper due to size restrictions.

5 Summary and conclusions

In this study, a new satellite-based approach for the estimation of actual evapotranspiration has been utilized in Sidi Bouzid region, Tunisia. WRF based meteorological data are used instead of initially proposed ERA-5 and are combined with Sentinel-2 and Sentinel-3 ETa earth observation data using the Sen-ET plugin. This

procedure needs further analysis and a validation procedure using in-situ experiments. This first approach shows that the synergy of WRF and remote sensing can play a significant role in daily operational agricultural practices, in environmentally sensitive areas like Tunisia.

Acknowledgements

This work has been funded by SUPROMED "Sustainable Production in water limited environments of Mediterranean agro-ecosystem". R&I project funded under the PRIMA 2018 program section I. The authors gratefully acknowledge INRGREF and NGC groups of Tunisia for providing the field experiments' data.

References

Allen, R., Tasumi, M. and Trezza, R., 2007. Satellite-Based Energy Balance for Mapping Evapotranspiration with Internalized Calibration (METRIC)-Model. Journal of Irrigation and Drainage Engineering 133, 380-394, doi:10.1061/(asce)0733-9437(2007)133:4(380).

Bastiaanssen, W. G. M., Menenti, M., Feddes, R. A. and Holtslag, A. A. M., 1998. A remote sensing surface energy balance algorithm for land (SEBAL) 1. Formulation. Journal of Hydrology 212, 198-212, doi:http://dx.doi.org/10.1016/S0022-1694(98)00253-4.

Bastiaanssen, WGM, Pelgrum, H, Wang, J, Ma, Y, Moreno J, Roerink, GJ, van der Wal T, 1998b. The Surface Energy Balance Algorithm for Land (SEBAL): Part 2 validation, J. Hydrology, 212-213: 213-229.

Burchard-Levine, V., Héctor Nieto, H., Riaño,D., 3, Migliavacca, M., El-Madany, T.S., Perez-Priego, O., Carrara, A., and Martín, P.M., 2019. Adapting the thermal-based two-source energy balance model to estimate energy fluxes in a complex tree-grass ecosystem. Hydrology and Earth System Sciences Discussions, https://doi.org/10.5194/hess-2019-354 Preprint.

Calera, A., Campos, I., Osann, A., D'Urso, G., Menenti, M., 2017. Remote Sensing for Crop Water Management: From ET Modelling to Services for the End Users. Sensors 17(5), pp.1104.

Campos, I., Neale, C.M.U., Suyker, A.E., Arkebauer, T.J. and Gonçalves, I.Z. (2017) 'Reflectance-based crop coefficients REDUX: for operational evapotranspiration estimates in the age of high producing hybrid varieties', Agricultural Water Management, Vol. 187, pp.140–153.

El-Samra, R., Bou-Zeid, E., and El-Fadel, M., 2018. What model resolution is required in climatological downscaling over complex terrain? Atmospheric Research 203 68 – 82 ISSN 0169-8095 URL http://www.sciencedirect.com/science/article/pii/S0169809516305798

ESA, 2020. USER MANUAL FOR SEN-ET SNAP PLUGIN. V1.1.0 March 19, 2020, 37 pages.

Giannaros, T.M., Melas, D., and Ziomas, I., 2017. Performance evaluation of the Weather Research and Forecasting (WRF) model for assessing wind resource in Greece.Renewable Energy 102 190–198 URL http://dx.doi.org/10.1016/j.renene.2016.10.033

Gowda PH, Chávez JL, Howell TA, Marek TH, New LL. (2008). Surface Energy Balance Based Evapotranspiration Mapping in the Texas High Plains. Sensors. 8(8):5186-5201.

Jimenez, P.A. and Dudhia, J., 2013. On the Ability of the WRF Model to Reproduce the Surface Wind Direction over Complex Terrain. Journal of Applied Meteorology and Climatology 52 1610 URL https://journals.ametsoc.org/doi/10.1175/JAMC-D-12-0266.1

Kustas, W. P. and Norman, J. M.,1996. Use of remote sensing for evapotranspiration monitoring over land surfaces. Hydrological Sciences Journal 41, 495-516, doi:10.1080/02626669609491522 (1996).

Kustas WP, Anderson MC, Alfieri JG et al. 2018. The grape remote sensing atmospheric profile and evapotranspiration experiment. Bull Am Meteor Soc 99:1791–1812. https://doi.org/10.1175/BAMS-D-16-0244.1

Norman JM, Kustas WP, Humes KS (1995) Source approach for estimating soil and vegetation energy fluxes in observations of directional radiometric surface temperature. Agric For Meteorol 77(3–4):263–293. 10.1016/0168-1923(95)02265-Y.

Powers, J.G.; Klemp, J.B.; Skamarock, W.C.; Davis, C.A.; Dudhia, J.; Gill, D.O.; Coen, J.L.; Gochis, D.J.; Ahmadov, R.; Peckham, S.E.; et al. The Weather Research and Forecasting Model: Overview, System Efforts, and Future Directions. Bull. Am. Meteorol. Soc. 2017, 98, 1717–1737.

Salgado, R., and Mateos, L., 2021. Evaluation of different methods of estimating ET for the performance assessment of irrigation schemes. Agricultural Water Management, Volume 243, 1 January 2021, 106450.

Skamarock, W. C., J. B. Klemp, J. Dudhia, D. O. Gill, Z. Liu, J. Berner, W. Wang, J. G. Powers, M. G. Duda, D. M. Barker, and X.-Y. Huang, 2019. A Description of the Advanced Research WRF Version 4. NCAR Tech. Note NCAR/TN-556+STR, 145 pp. doi:10.5065/1dfh-6p97

Derivation of the Z-R Relationship for an X-Band Weather Radar System, in the Region of Athens, Greece

A. Bournas[1*], K. Lagouvardos[2], E. Baltas[1]

[1] Department of Water Resources and Environmental Engineering, School of Civil Engineering, National Technical University of Athens, Athens, Greece.

[2] National Observatory of Athens, Institute for Environmental Research and Sustainable Development, Penteli, Athens, Greece.

Abstract.

In this research work, an analysis is conducted in order to derive the Z-R relationship for a newly installed X-Band weather radar, referred to as rainscanner, located within the premises of the National Technical University of Athens campus in the Zographou district and it features a 50km scanning range and a 100m x 100m and two-minute spatial and temporal resolutions. In order to produce Quantitative Precipitation Estimates (QPE), the Z-R relationship must be first derived, which is a power-law equation that relates weather radar reflectivity measurements (Z) with rainfall intensities (R). To derive this relationship, a weather radar – rain gauge correlation analysis is performed, where the Z-R parameters are obtained through an optimization procedure, where a series of rainscanner – rain gauge data pairs that feature a good correlation, are selected in a calibration validation – calibration scheme. The Z-R relationship derived shows good agreement in both calibration and validation and leads to better results than applying well-known Z-R relationships instead.

1 Introduction

The use of weather radars for hydrological and forecasting applications has been gaining increased attention. Floods and flash floods have been observed more frequently, a fact that has been linked with climate change (Alfieri et al. 2012; Caloiero et al. 2017). Under climate change, rainfall events are more likely to reduce in numbers but increase in intensity. This has the impact of producing extreme flooding, where areas that once did not flood, now are prone to flooding (Bournas and Baltas 2021a). In hydrological applications, the most critical parameter is the rainfall input. Traditional rain gauge station networks, being point measurements lack the necessary spatial resolution for producing high-quality rainfall fields required by forecasting models, especially in low accessibility locations which can have high importance regarding rainfall input, such as high elevation areas. Moreover, these networks in order to provide real-time measurements, require a power supply and telemetry systems, i.e. cellar networks, to transmit the datasets in distanced server, which can be unreliable in extreme storm conditions. Therefore, telemetric rainfall measurements such as weather and satellite radar systems, are preferred in such applications. Radar technology as a means for measuring precipitation has been used for over 50 years. The disadvantage of weather radars lies in the fact that they do measure rainfall intensity, R [mm/h], directly but rather indirectly through the measurement of the rain droplets' reflectivity, Z [mm6/m3]. An exponential relationship is then used to transform reflectivity into rain intensity, the Z-R relationship, which has the following form:

$$Z = aR^{\mathrm{b}}, \tag{1}$$

The equation is a product of the work of Marshal n Palmer, which studied the size distribution of rainfall droplets during various rainfall events. They found that parameters a and b range from 1 to 2000 for parameter a and 1 to 3 for parameter b, and they came up with the relationship with parameters a and b having the values of 200 and 1.6 respectively. However, since the relationship is affected by the raindrop's distribution, it is apparent that it depends on the rainfall characteristic, and therefore it varies from event to event. This is well documented through the various research regarding the calibration of weather radar systems and the use of Z-R relationships based on the classification of the storm.

There are two main methodologies in order to estimate the values of the Z-R relationship parameters. The first one is by making use of distrometer measurements, an instrument that measures the raindrop diameter distribution (Joss and Waldvogel 1970; Baltas and Mimikou 2002; Baltas et al. 2015; Feloni et al. 2017), while the second one is through the correlation between radar and rain gauge measurements, assuming that the rain gauges measurements are the actual precipitation (Colli et al. 2013). In the latter case, various approaches can be used such as whether the performing linear or non-linear optimization or adding more parameters to the equation such as the rain gauge-radar distance (Anagnostou and Krajewski 1999; Legates 2000). Overall, this approach is favorable due to the usually high number of rain gauges available, against the low number of distrometers, over a region which makes the calibration better suited to the entire rainfall field.

In Greece, although weather radars have been used for decades, namely C-Band radars, there is limited knowledge regarding the variability of the Z-R relationship. In Athens, after the analysis of distrometers

measurements on convective-based events (Baltas and Mimikou 2002), Baltas and Mimikou derived a convective type Z-R relationship $Z=431R^{1.25}$, while with the study of more datasets including stratiform and convective events, they derived the relationship $Z=261R^{1.53}$ (Baltas et al. 2015). This study focuses on the rain-gauge weather radar correlation and the direct Z-R parameters optimization. The weather radar used is an X-Band weather radar, herein referred to as rainscanner, located in the facilities of the National Technical University of Athens (NTUA) near the center of Athens, Greece (Bournas and Baltas 2020). Previous research has shed a light on the spatial variability of the Z-R (Pappa et al. 2021) and the impact on hydrological applications (Bournas and Baltas 2021b), but currently, we incorporate multiple events and an optimization procedure to extract one Z-R relationship, applicable in Athens.

2 Methods and data used

The study area is defined by the area coverage of the rainscanner system. The rainscanner is located within the facilities of the National University of Athens complex, in the Zografou municipality, near the Hymettus Mountain. The rainscanner oversees a circular area o a total radius of 50km, as seen in Figure 1. Within the scanning range lies the majority of the Attica region, i.e. the entire Athens area and up to Patera's mountain on the west, the mountains of Penteli, Parnitha on the North, and the Saronic Gulf in the Southeast. Concerning the eastward areas, due to orography, mainly due to mount Hymettus, the line of sight is obstructed therefore no reliable datasets can be obtained. These areas are marked in Figure 1 as the groundclutter area, where ground clutter is the signal noise that is generated by stationary objects such as orography, high-height structures, or even stationary signal generation objects such as radio antennas, etc. These areas are flagged within the rainscanner software by the user and are excluded from further processing. Nevertheless, since the majority of storm clouds in Athens have west to east direction, the sight's location is favorable for observing and producing nowcasts over the city of Athens. The rainscanner technical characteristics are showcased in Table 1. The main advantages of the system are its high spatial-temporal resolutions, at 100m x 100m and 2-minute frequency datasets, respectively.

The rain gauge stations used in the study are part of the National Observatory of Athens Automatic Network (NOAAN), providing rainfall datasets with 10-minute precipitation datasets (Lagouvardos et al. 2017), 2017). The datasets are quality controlled in two steps, first, by flagging questionably quality data, e.g. null values of wind for many hours, performed twice per day, and secondly by performing a post-processing reexamination before they are incorporated into the database, of all flagged datasets for spatial and temporal inconsistencies between neighboring stations (Lagouvardos et al. 2017).

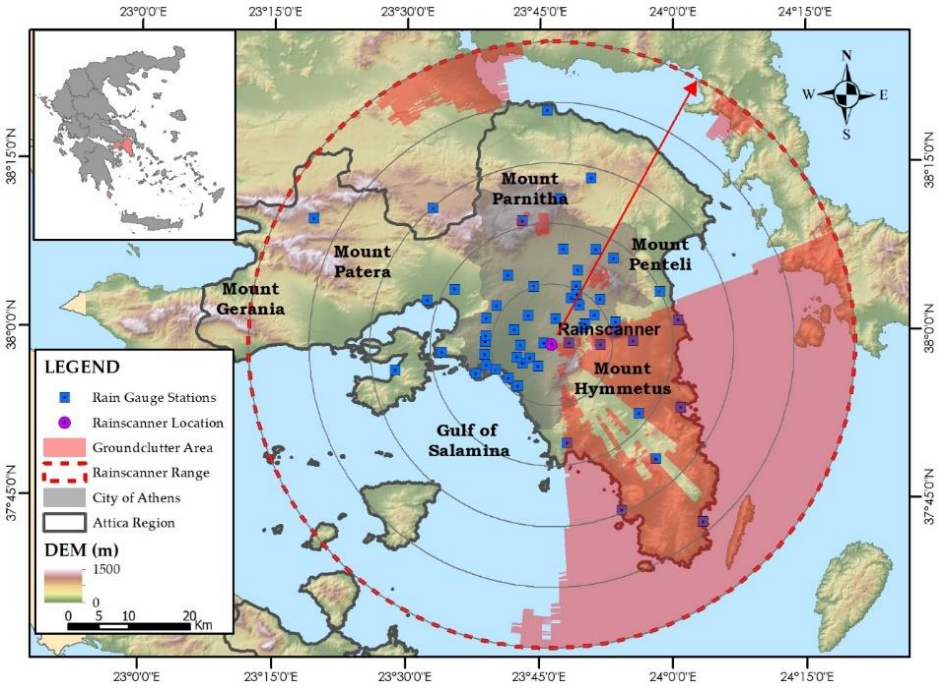

Figure 1. The Study area; the rainscanner area coverage along with the rain gauge stations location

The methodology applied consists of three steps. First, the identification of each station location on the rainscanner grid is made. This is performed by locating the pixel within the rainscanner grid, which center is

closest to the actual rain gauge location (Pappa et al. 2021). The second step is the correlation analysis of the datasets between the rain gauge and the rainscanner. This is achieved by utilizing a default Z-R equation and correlating each dataset since the Z-R relationship does not alter the correlation significantly. This analysis is essential since it highlights bad correlated data pairs, such as zero rain precipitation to high reflectivity, which can be attributed to systematic errors by the rainscanner or errors on the rain gauge station itself. Moreover, this analysis reports whether temporal inconsistencies exist between the two datasets which may disrupt the calibration process. Through this analysis, only the good correlated event datasets per station are utilized for the calibration process, which is the third step. The calibration is performed on the Z-R parameters, a and b, by minimizing the root mean square error (RMSE) first on station level, i.e. each station individually, and secondly by incorporating the entire datasets. The results are then compared, as well as, with Z-R relationships derived for Athens through the use of distrometers. The criteria upon which the comparison is being made are the RMSE, the Normalized Mean Bias (NMB), the Normalized Mean Absolute Error (NMAE), between the rainscanner estimate (R_i) and the rain gauge G_i rainfall height, which are defined as follows:

$$NMB = \frac{\sum_{i=1}^{n}(R_i - G_i)}{\sum_{i=1}^{n} G_i} \quad (2)$$

$$NMAE = \frac{\sum_{i=1}^{n}|R_i - G_i|}{\sum_{i=1}^{n} G_i} \quad (3)$$

$$RMSE = \sqrt{\frac{1}{\mathrm{n}}\sum_{i=1}^{n}(R_i - G_i)^2} \quad (4)$$

3 Results

In Figure 2 the correlation coefficient of each station is shown. Specifically, in Figure 1b, the correlation coefficient including all data pairs for each station is shown, while in Figure 2b, the correlation efficiency is shown, after removing bad correlated events for each station. In the second figure, the datasets are quality controlled, by removing for each station the events where the correlation between the rainscanner and the rain gauge, for the particular station, was below the 0.6 threshold. The comparison of Figures 2a and 2b, leads to the fact that incorporating multiple events, it is important to exclude badly correlated datasets since they may disrupt the calibration and lead to bad results. For instance, station 47, Chaidari, showcases a bad correlation overall, below 0.5, but when some events are removed the correlation rises to over 0.8, which is more than acceptable. This change is attributed to bad events in the specific location, either due to systematic errors or near-zero values that are badly correlated due to the rain gauge measurement resolution. Instead of removing the entire station datasets, in this way, we can incorporate the well-correlated datasets and thus maximize the number of data pairs to be used in the calibration process. Moreover, we do not disrupt the temporal consistency of the datasets, since we do not exclude data pairs within a single event, except from zero values, but rather the entire event.

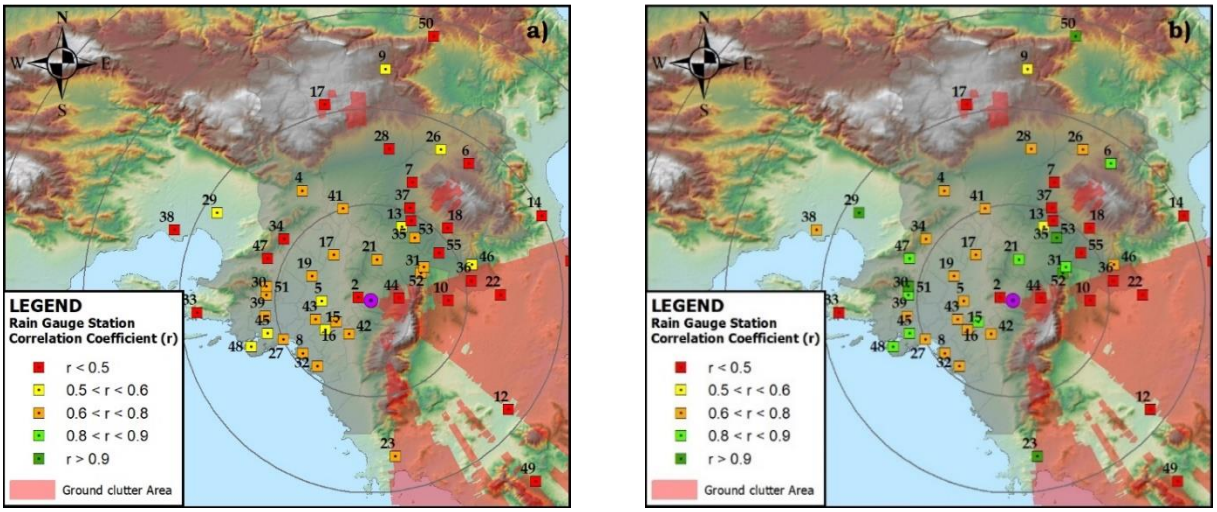

Figure 2. Correlation Coefficient, between rain gauge and rainscanner datasets a) using all available events, b) excluding events with a correlation coefficient less than 0.6 for each station

From Figure 2b, it is evident that the best correlation stations are located in the southwest area of Athens, in the area near the coast, while the worst correlated stations are located in the higher elevation stations. This bad correlation is also due to the proximity of these stations to the ground clutter region, and thus the quality of the rainscanner measurements is hampered. Overall, multiple stations featured a correlation above 0.8 which is more than enough to provide datasets with a good Z-R calibration process.
We continue with the calibration process. We perform the optimization by incorporating all well-correlated datasets in a calibration/validation scheme. Half of the available stations are used in calibration, while the other half is for validation. The selection process was performed based a) on the correlation coefficient of the stations, i.e. the best-correlated stations were chosen for calibration, and b) on the spatial distribution of the stations, i.e. the selection was made so that the calibration and validation groups would have a good distribution over the entire Athens area. In Table 1, the calibration and validation stations are shown, along with the results of each station optimization and the respected RMSE. The values for each station calibration vary from 168 to 490 for parameter a and between 1.05 and 2.42 for parameter b, with average values are 312 and 1.62 respectively.

Table 1: Individual optimization Z-R parameter results, and the RMSE, r for the derived $Z=321R^{1.53}$ relationship

Calibration Stations						Validation Stations					
index	Station	a	b	RMSE	r	index	Station	a	b	RMSE	r
4	Ano Liosia	168	1.79	0.58	0.79	6	Dionysos	183	1.86	0.36	0.90
5	Athens	316	1.68	0.33	0.78	8	Faliro	433	2.26	0.30	0.75
17	Patissia	423	2.15	0.23	0.76	15	Neasmyrni	239	2.18	0.67	0.75
27	Athens-Marina	430	1.78	0.42	0.65	16	Neos Kosmos	402	1.83	0.39	0.84
28	Tatoi	209	1.52	1.67	0.79	19	Peristeri	261	1.31	0.21	0.73
30	Korydalos	304	1.57	0.27	0.85	21	Phychiko	271	1.42	0.45	0.81
32	Alimos	317	1.14	0.38	0.72	29	Aspropirgos	310	1.42	0.43	0.92
42	Imittos-Dafni	292	1.05	0.58	0.79	34	Petroupoli	272	1.81	1.12	0.78
43	Harokopio-Athens	297	1.98	0.35	0.77	35	Vrilissia	371	1.23	0.27	0.92
45	Pireas-Pedagogiki	192	1.87	0.32	0.81	38	Elefsina	275	1.05	0.25	0.77
47	Chaidari	257	1.87	0.80	0.87	39	Nikaia	419	2.42	0.44	0.69
48	Pireas	261	1.34	0.34	0.83	40	Salamina	490	1.08	0.00	0.83
52	Delacroix-Attiki	448	1.05	0.36	0.87	41	Ska	298	1.63	0.32	0.75
						45	Pireas-Pedagogiki	192	1.87	0.32	0.81
						51	Ano Korydallos	315	1.84	0.43	0.91

From the calibration stations the following Z-R is then derived:

$$Z = 321R^{1.53} \quad (5)$$

The values of the parameters are close the average values calculated by the individual optimization. The high a parameter is an indication that the datasets are closer to the convective types since the larger values of parameter “a” are related to a higher number of high diameters raindrop sizes which are found in convective types of events. This is also related to the fact that in Athens, due to its geographical location, rainfall events are not often and therefore the majority of the rainfall events are usually of convective type, where large amounts of rainfall are discharged in little time.
In order to validate the Z-R relationship, the boxplots for the RMSE the NME, and NMB are drawn in comparison with datasets as formed from the optimum values of each station, shown in Table 1. Moreover, the boxplots of similar Z-R relationships, applicable in the Athens area, which were derived from distrometers measurements are also displayed for comparison. As seen in all boxplots, the optimum Z-R, i.e. the entire dataset consisting of the application of station-based Z-R relationships, as shown in Table 1, displays the best results, showcased by the small RMSE value, and the near to zero NMB and NMAE. The proposed Z-R relationship, $Z=321R^{1.53}$ then shows the second-best application among the others, with small RMSE and lower NMB and NMAE values, which also show small variability. Compared with the other Z-R relationships, the Marshal n Palmer $Z=200R^{1.6}$ shows the worst results, while the convective type $Z=431R^{1.25}$ shows good results, although based on the NMB value it seems that an underestimation is being made against the rain gauge

measurements based on the negative mean value. Overall, the proposed Z-R seems to feature better results and thus is an improvement against the use of the previous Z-R relationships.

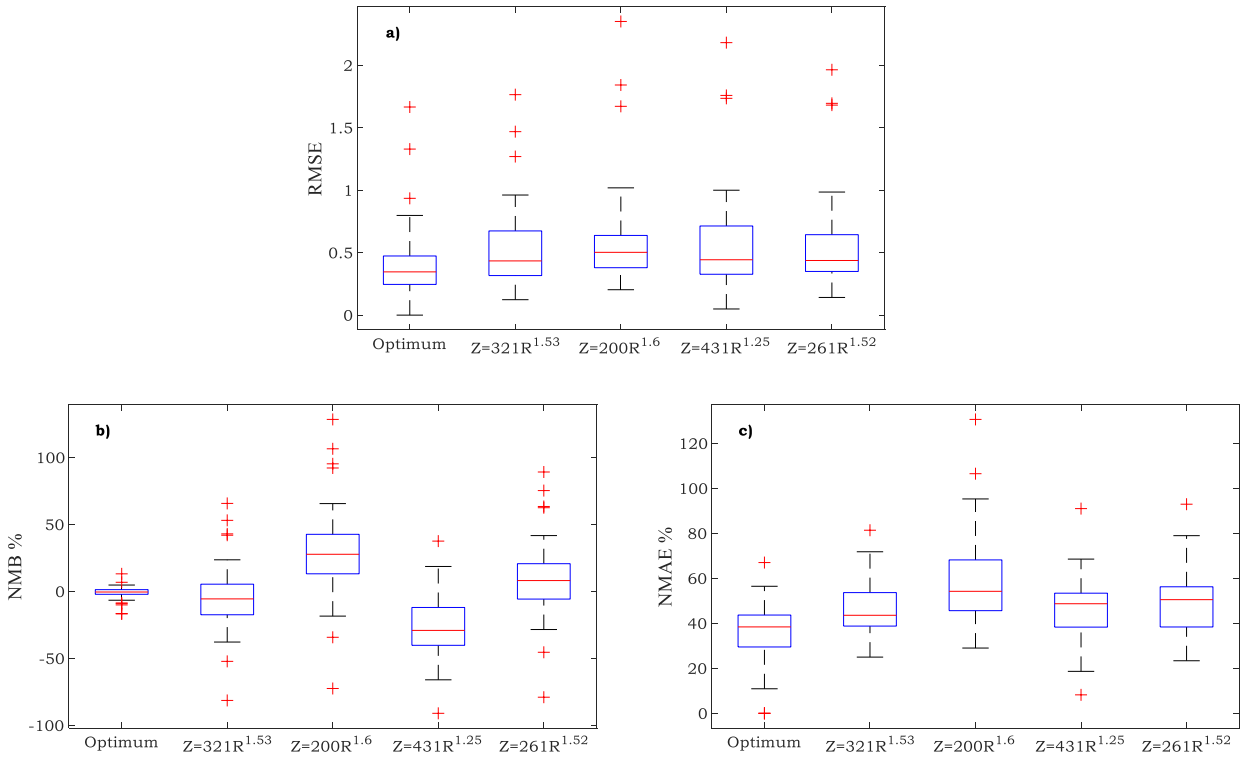

Figure 3. Boxplots of the a) RMSE, b) NMB and c) NMAE values for each Z-R relationship used.

4 Summary

In this study, a framework is applied to determine a Z-R relationship to be used for a newly installed X-Band weather radar system, the rainscanner, in Athens, Greece. The methodology applied consisted of the optimization of the Z-R relationship based on the radar and rain gauge pairs. A correlation analysis is first performed and station-based individual Z-R relationships are derived to extract whether the available datasets are well correlated and whether a Z-R relationship can be established without systematic errors. A correlation threshold is then set to extract only good correlated datasets to improve the quality of the optimization, and a calibration and validation scheme was formed. The derived Z-R relationship, $Z=321R^{1.54}$ is then validated and compared with the optimized results, as well as, with the results for other Z-R relationships derived for the same study area. The results show that the derived Z-R relationship shows good agreement with the used datasets in both calibration and validation while showing an improvement against the previous derived Z-R relationships, and therefore it can be suggested for use to improve quantitative precipitation estimates for hydrological applications. Moreover, it is also evident that the calibration of a Z-R relationship is crucial, since incorporating default relationships, such as the Marshal n Palmer, may lead to large deviations. Finally, the Z-R parameter values from the individual optimization, as well as the derived relationship, highlight the fact that in Athens, convective type events are more frequent than stratiform-based events, based on the high parameter a value. Future research should focus on deriving a more complex Z-R relationship that could incorporate other parameters, e.g., station distance from the rainscanner or bias-driven parameters, as well as deploying a framework for the temporal evolution of the parameter's relationship, based on the rainstorm trajectory.

Acknowledgments

This research is co-financed by Greece and the European Union (European Social Fund-ESF) through the Operational Programme «Human Resources Development, Education and Lifelong Learning» in the context

of the project “Strengthening Human Resources Research Potential via Doctorate Research” (MIS-5000432), implemented by the State Scholarships Foundation (IKY)

References

Alfieri L, Salamon P, Pappenberger F, Wetterhall F, Thielen J (2012) Operational early warning systems for water-related hazards in Europe. Environmental Science & Policy 21:35–49. https://doi.org/10.1016/j.envsci.2012.01.008

Anagnostou EN, Krajewski WF (1999) Real-Time Radar Rainfall Estimation. Part I: Algorithm Formulation. Journal of Atmospheric and Oceanic Technology 16:189–197. https://doi.org/10.1175/1520-0426(1999)016<0189:RTRREP>2.0.CO;2

Baltas EA, Mimikou MA (2002) The use of the Joss-type disdrometer for the derivation of ZR relationships. In: 2nd European Conference on Radar in Meteorology and Hydrology (ERAD). Delft, Netherlands

Baltas EA, Panagos DS, Mimikou MA (2015) An Approach for the Estimation of Hydrometeorological Variables Towards the Determination of Z-R Coefficients. Environ Process 2:751–759. https://doi.org/10.1007/s40710-015-0119-x

Bournas A, Baltas E (2020) Application of a rainscanner system for quantitative precipitation estimates in the region of Attica. In: Sixth International Symposium on Green Chemistry, Sustainable Development and Circular Economy Conference on Environmental Science and Technology, Thessaloniki, Greece. p 8

Bournas A, Baltas E (2021a) Increasing the efficiency of the Sacramento model on event basis in a mountainous basin

Bournas A, Baltas E (2021b) Comparative Analysis of Rain Gauge and Radar Precipitation Estimates towards Rainfall-Runoff Modelling in a Peri-Urban Basin in Attica, Greece. Hydrology 8:29. https://doi.org/10.3390/hydrology8010029

Caloiero T, Coscarelli R, Ferrari E, Sirangelo B (2017) Temporal Analysis of Rainfall Categories in Southern Italy (Calabria Region). Environ Process 4:113–124. https://doi.org/10.1007/s40710-017-0215-1

Colli M, Lanza LG, La Barbera P (2013) Performance of a weighing rain gauge under laboratory simulated time-varying reference rainfall rates. Atmospheric research 131:3–12

Feloni E, Kotsifakis K, Dervos N, Giavis G, Baltas E (2017) Analysis of Joss-Waldvogel disdrometer measurements in rainfall events. In: Papadavid G, Hadjimitsis DG, Michaelides S, Ambrosia V, Themistocleous K, Schreier G (eds) Fifth International Conference on Remote Sensing and Geoinformation of the Environment (RSCy2017). SPIE, Paphos, Cyprus, p 60

Joss J, Waldvogel A (1970) A Method to Improve the Accuracy of Radar Measured Amounts of Precipitation. In: 14th Radar Meteorology Conf. Amer. Meteor. Soc, Tucson, p 776

Lagouvardos K, Kotroni V, Bezes A, Koletsis I, Kopania T, Lykoudis S, Mazarakis N, Papagiannaki K, Vougioukas S (2017) The automatic weather stations NOANN network of the National Observatory of Athens: operation and database. Geoscience Data Journal 4:4–16

Legates DR (2000) Real-Time Calibration of Radar Precipitation Estimates. The Professional Geographer 52:235–246. https://doi.org/10.1111/0033-0124.00221

Pappa A, Bournas A, Lagouvardos K, Baltas E (2021) Analysis of the Z-R relationship using X-Band weather radar measurements in the area of Athens. Acta Geophys. https://doi.org/10.1007/s11600-021-00622-5

SESSION 6:
ECOSYSTEM SUSTAINABILITY

The Role of US Private Land in Ecosystem Sustainability: A case study of the West Virginia Land Trust.

R.E. Landenberger[1, 2], and N.E. Adaktilou[1]. [1] West Virginia University, Department of Geology & Geography, P.O. Box 6300, Morgantown, WV 26505-6300. [2] West Virginia Land Trust, P.O. Box 304, Morgantown, WV 26507.

Abstract

Ecosystem sustainability is a complicated concept that assumes a detailed understanding of the biophysical properties and processes that characterize ecosystems at multiple spatial and temporal scales. In a world that is changing rapidly due to anthropogenic climate change and land use-land cover change, protecting a significant fraction of land from degradation is necessary if earth's ecosystems are to be sustained indefinably. Historically, US public land has been protected and sustained by several large federal land managing agencies, yet large areas of public land do not exist in many places, including in much of the highly developed eastern half of the country, including in West Virginia. Private land protection via conservation easements and conservation land purchases provide flexible, timely, and cost-effective solutions to the otherwise rapid loss of biodiversity and degradation of agricultural land. In West Virginia, a state that lies within the biologically rich, diverse and productive Appalachian Mountains of eastern North America, the West Virginia Land Trust fills an important land protection gap. While only 27 years old, the amount of land that the organization has protected recently adds significant acreage to West Virginia's protected area system and is an example of effective land conservation. Finally, opportunities for ecological restoration of forestland and streams are gaining importance and are taking a larger fraction of the organization's efforts. This very difficult work aims to recover land from an impacted state to a sustainable and ecologically healthy state, adding to the social and ecological services that the state has to offer in the 21st Century.

Introduction – What is 'sustainability'?

Sustainability is the new global paradigm in land protection and management[1], (Shellnhuber et al. 2012; UN 2015) although the basic concept of sustainability has a very long history (Leopold 1933; Muhn 1992). Yet despite its history and contemporary significance, the meaning of sustainability varies depending on context (sensu Foster 2002; van der Schyff 2010). Here we use it to mean that a given terrestrial ecosystem, be it a 'natural' system or an agricultural system, does not decline in ecological diversity or agricultural productivity due to anthropogenic influences[2]. Ecosystem sustainability and ecological sustainability are synonymous as used herein and apply to *natural land cover* characterized primarily by indigenous species and communities, and to *agricultural land cover* (Radwan et al. 2021) characterized by much simpler systems. Although natural and agricultural systems are very different in terms of their ecological structure and function, both can be sustained indefinitely as long as their biophysical properties and processes are protected in such a way as to ensure future use options[3]. Used in this way, ecological sustainability is the opposite of 'ecological degradation', the reduction of biodiversity in natural areas or declining productivity in agricultural systems, over time.

Protected land[4] equates with ecological sustainability, in theory

Undeniably, the concept of sustainability has inherent flaws. Although most reasonable people would agree that it is critically important to protect and sustain some fraction of earth's natural and agricultural land for present and future generations, sustainability of protected land is not guaranteed. Sustainability assumes that ecologists,

[1] Specifically, Goal 15 - Protect, restore and promote sustainable use of terrestrial ecosystems, sustainably manage forests, combat desertification, and halt and reverse land degradation and halt biodiversity loss.
[2] This definition does not require any reference to human use and "development", as does the often-cited 1987 Brudtland Report's definition of sustainable development. But both definitions focus on how present land use-land cover affects the future land use-land cover options. In that respect, they are similar.
[3] Maintaining what economists call 'future option value' is a central underlying assumption of sustainability. The idea is that the land is managed in such a way as to allow all future land use possibilities.
[4] A useful way to think about 'protected land' is to ask "Protected from what, and for whom?" Answers to these two questions define protection in each specific context.

agronomists, and policy makers understand the ecological and social challenges associated with rapidly changing land use patterns (Winkler et al. 2021), growing population, climate change, and other existential threats. Sustainability also assumes that understanding complex ecological and social factors will then transform into actions that maintain ecological diversity and prevent degraded agricultural productivity; understanding how systems operate is simply not enough. In this context, ecological sustainability is an aspirational goal, not an assured outcome because future conditions are largely unknowable (Taleb 2010), let along controllable. Protecting natural and agricultural systems from development is simply the best way to hedge one's bets. Here we address the most common ways of protecting and sustaining private land in the US, using the West Virginia Land Trust as an example. Before we do that, some context is necessary.

Protected public land

In the United States (US), the idea of protecting and sustaining land dates back more than one hundred years to the establishment of the federal 'public domain' (Leshy 2021). The establishment of the US National Forests and Grasslands (USFS), National Parks (NPS), National Wildlife Refuge System (USFWS), and Bureau of Land Management (BLM) lands are generally seen as groundbreaking, even revolutionary, from an ecological sustainability and 'protected area' perspective[5]. As unethical as the creation of the US federal domain was in both historic (Blackhawk 2006; Hämäläinen 2022) and contemporary cultural terms (Echo-Hawk 2013), it resulted in very large, ecologically intact areas of protected public lands that sustain ecological diversity[6]. Today, approximately one-third of the total land area, or 9.24 million km^2, is managed as federal land (Figure 1) under policies that explicitly identify ecological sustainability as a primary goal. State and local governments administer another 0.81 million km^2 (8% of the US), land that is managed either sustainably or not, according to state and local government policy. Thus, somewhere between 35 and 40% of US public land, an area of approximately 340,000 sq. kilometers, is managed sustainably.

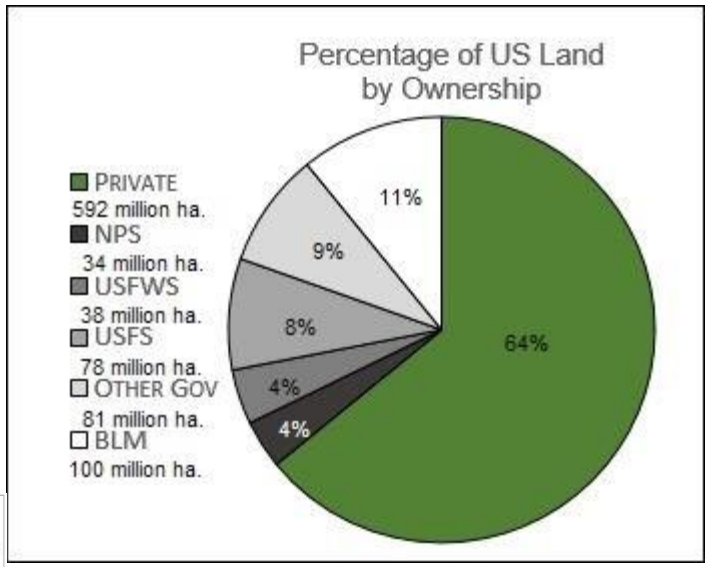

Figure 1. US land ownership by category, in both hectares and percent of total land area. Private land comprises roughly 2/3 of the US. 'NPS' is National Park Service, 'USFWS' is US Fish and Wildlife Service, 'USFS' is US Forest Service, and 'BLM' is Bureau of Land Management. 'Other Gov' includes Department of Defense land, and state and local government land.

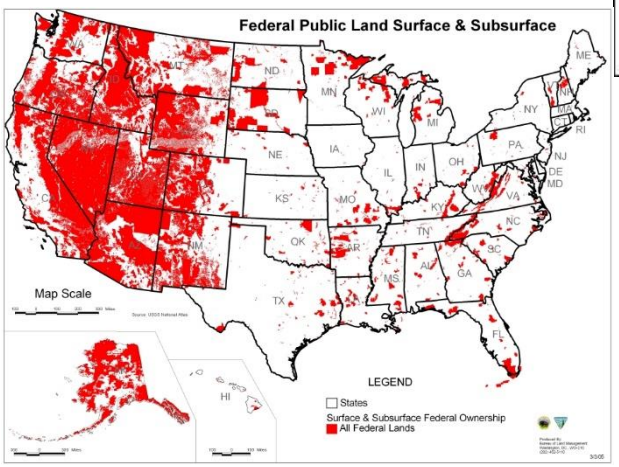

Figure 2. The continental US, with Alaska and Hawaii shown in the lower left. The red areas are federal public lands administered by the federal agencies listed in Figure 1. Note that the vast majority of land is in the western US and Alaska. Alaska and Hawaii are not shown to scale. From https://commons.wikimedia.org/wiki/File:Map_of_all_U.S._Federal_Land.jpg

[5] Protected areas provide the best habitat and offer the highest probability for species and ecosystem viability, particularly in light of the rapidly changing climate..

[6] Also note that significant ecological changes are occurring on federal land, due to fire suppression, non-native species, silviculture and roadbuilding, climate change, fragmentation, and other impacts that operate at multiple scales..

Private land protection

In contrast to the protected public domain shown in red in Figure 2, US private property comprises the vast majority of land in the eastern half of the US. This includes land owned by for-profit businesses such as timber, mining, and agribusiness corporations, land owned by individuals, and land owned by non-profit organizations, often called non-government organizations or 'NGOs'. Taken together, US private land is managed for a wide range of goods and services, and only approximately 3% is protected or managed sustainably; generally, native forest and agricultural lands are declining while urban, residential, and commercially developed lands are increasing (USDA 2017). If the country's ecological diversity is to be sustained, then more private land needs to be protected, particularly in the eastern US where public lands are scarce.

Herein lies one of the biggest challenges to ecological sustainability in the US, because the ability to use private land without restriction is a cherished 'right' claimed by some to be enshrined in the US Constitution[7]. However, the truth about land use rights is somewhat different. Without exception, some combination of federal and state laws, county regulations, and local codes and ordinances partially limit how land use rights are exercised; no area of undeveloped private property can be used in any way that the owner chooses. Conceptually, land use regulations in the US are not very different from land use regulation in European countries or in other 'developed' countries where land conversion from natural areas to developed land use may occur with certain limitations. Yet despite restrictions and limitations, US private land is often subject to ecological degradation. Stated differently, US laws such as the National Environmental Policy Act, the Clean Air and Clean Water Acts, and the Endangered Species Act are not effective vis-à-vis the sustainability of private land.

Fortunately, private land can be protected, sustained, and conserved in a variety of ways and for various durations, ranging from years, to decades, to forever, or 'in perpetuity'. 'Conservation Land Trusts' (hereafter simply called 'land trusts') are non-profit organizations that protect and sustain natural and agricultural land at several geographic scales[8], ranging from the local municipality to the international scale. At the local and state scales, land trusts can maintain a specific focus, protecting areas for family-owned hill-farms and forests for open space, scenery, outdoor recreation, wildlife habitat, and for watershed protection. The emphasis on local cultural and ecological conditions is an advantage given that detailed knowledge of the environment is often a limiting factor when land protection issues are involved. People understand their local area and often have insight that combines an understanding of history with an area's ecological condition. In addition, local decision-making is often seen as more appropriate and more closely aligned with local needs and desires.

[7] See Cato Institute: https://www.cato.org/cato-handbook-policymakers/cato-handbook-policy-makers-8th-edition-2017/property-rights-constitution (accessed November 29, 2022).
[8] Land trusts that focus exclusively on agricultural land are often referred to as 'agrarian land trusts'.

Currently, there are 1,700 land trusts in the US, and together they protect over 25 million ha. The principal land protection tools are 'conservation easements', and 'land acquisitions'. Conservation easements are essentially legal contracts tied to a property's deed that transfers a set of specific land use rights from the landowner, the grantor or 'giver' of the rights, to the land trust, the grantee or receiver of the rights, in perpetuity[9]. Transferred rights typically but not exclusively include the right to subdivide the property into more than one parcel, the right to convert the property from one land use to a more developed land use, the right to construct infrastructure such as buildings and often roads, and the right to alter the topography or extract minerals and other non-renewable resources.

Figure 3.

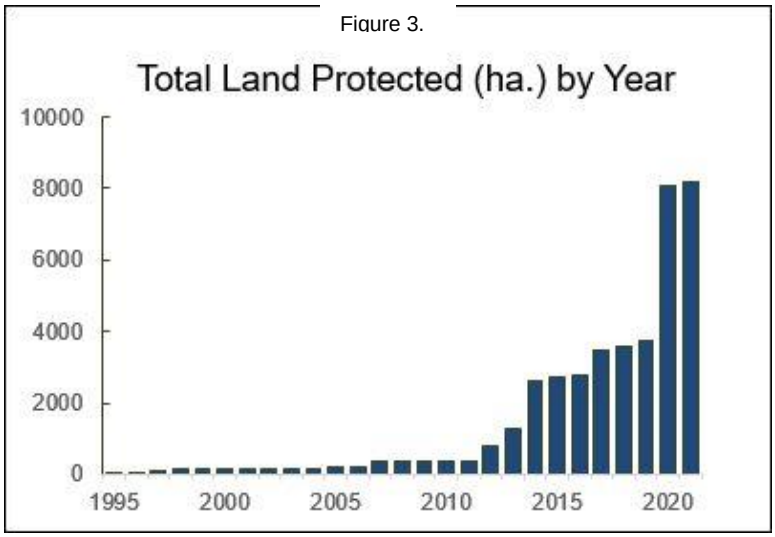

The West Virginia Land Trust -

The West Virginia Land Trust (WVLT) is generally smaller than other state-level land trusts in terms of staffing and budget, because the state is rural and has a low population. Started in 1995 with a single parcel of 35 ha. and no paid staff[10], our protected acreage has grown exponentially in the past three years to 8,100 ha. in 2022 (Figure 3). With a current staff of ten, the organization protects land through conservation easements, acquisitions[11], and through 'partnership projects' whereby we cooperate with another conservation organization to protect an area. Both conservation easements and conservation land by purchases are permanent protections, in perpetuity. Legally, these protections cannot be reversed, only strengthened.

Figure 4. An example of the biologically diverse mixed-mesophytic forest in West Virginia protected by the West Virginia Land Trust. The soils, climate, and wide variety of plans and animals combine to create a very rich group of ecological communities.

Approximately half of the 8,100 ha. total is forestland (Figure 4), and half is in one type of agricultural use or another. Grazing, for example, is a common use because the climate and soils lend themselves to highly productive grassland. Furthermore, approximately half is protected by easement, and half is owned in title by the organization and managed by our staff as public nature preserves. We are currently in the process of opening several forested nature preserves using funds that we raise from state, federal, and foundation grants, but also including a robust internal fundraising program focusing on donations from individuals, families, and local businesses. Clearly, there is an increasingly awareness of the value of nature preserves and other protected land in their communities, for recreation

[9] To 'transfer means to forfeit, to give up. The term can be misleading in that it suggests that the land trust that then 'owns' the rights can exercise them. But it cannot. The rights are more accurately described as being extinguished, ended forever.
[10] In the US, volunteers often manage small land trusts.
[11] Purchases or donations of land or such that the organization owns title.

and scenery, and people are progressively contributing to the organization in various ways including cash donations, donations of equipment, and through volunteer efforts. For example, in the past several years volunteers and staff have built approximately ten kilometers of non-motorized trails, and are developing a volunteer forest restoration program developed around the removal of invasive species, stabilization of stream banks for sediment reduction, and planting of native trees and shrubs for wildlife habitat and other ecosystem services. K-12 schools, an academy for young adults that have entered the judicial system, and West Virginia University all contribute significant time and effort to these projects, totaling hundreds of hours of work and valued at over ten thousand dollars annually. In addition to the improvements that these volunteers make to our nature preserves, they also gain valuable experience and new understanding of the ecological and social benefits associated with protected areas and ecological sustainability. Nature is a wonderful teacher and the forest is an excellent classroom.

Conclusion – land restoration opportunities and the future

Sustainability is the new paradigm for ecosystem-based land protection and management, even though the concept itself is ancient (Foster 2002; van der Schyff 2010). The recent emphasis on sustaining land is at least partially due to our growing awareness of the rapid and often dramatic anthropogenically-driven changes in the earth system. The WVLT's mission is to "*protect land with significant conservation values through the use of conservation easements and real estate acquisitions, and by working with a statewide network of partners to build a passionate land conservation movement in the state"*. Although 'sustainability' is not in our mission statement, we have made the argument here that land protection equates to ecological sustainability, because conservation easements and conservation land purchases are permanent protections from development; they exist in perpetuity. Adding to this line or reasoning, we are now involved in fresh opportunities involving forest and stream restoration. This is the new challenge, restoring former mined land into forest, something that has not yet been accomplished satisfactorily. This opportunity comes with many challenges, but the climate and geology of West Virginia are the foundation of a highly resilient system. The establishment and survival of native forest on former mine land would contribute significantly to the state's economy and cultural identity, both of which have suffered greatly over the past fifty years.

References

Blackhawk, N. 2006. Violence over the land: Indians and empires in the early American West. Harvard University Press. Cambridge.

Echo-Hawk, W. 2013. In the Light of Justice: The Rise of Human Rights in Native America and the UN Declaration on the Rights of Indigenous Peoples. Fulcrum Publishing, Golden.

Foster, S. 2002. Aristotle and the Environment. *The Journal of Environmental Ethics* 24(4), pp. 409-428.

Hämäläinen, Pekka. 2022. Indigenous Continent: The Epic Contest for North America. Liveright Publishing, New York.

Hartmann, M., Six, J. (2022). Soil structure and microbiome functions in agroecosystems. Nature Reviews Earth & Environment. Online at https://doi.org/10.1038/s43017-022-00366-w (accessed November 25, 2022).

IPCC, 2022: Climate Change 2022: Impacts, Adaptation and Vulnerability. Contribution of Working Group II to the Sixth Assessment Report of the Intergovernmental Panel on Climate Change. H.O. Pörtner, D.C. Roberts, M. Tignor, E.S. Poloczanska, K. Mintenbeck, A. Alegría, M. Craig, S. Langsdorf, S. Löschke, V. Möller, A. Okem, B. Rama (eds.). Cambridge University Press. Cambridge University Press, Cambridge, UK and New York, NY, USA, 3056 pp., doi:10.1017/9781009325844.

Kolbert, E. 2014. The Sixth Extinction: An Unnatural History. Picador-Henry Holt and Company. New York.

Leopold, A. 1933. Game Management. University of Wisconsin Press. Madison.

Leshy, J.D. 2021. Our Common Ground: A History of America's Public Lands. Yale University Press, New Haven.

Muhn, J. 1992. Early Administration of the Forest Reserve Act: Interior Department and General Land Office Policies, 1891-1897. *In* Origins of the National Forests: A Centennial Symposium. Steen, H.K. (ed.). Pages 259-275, Forest History Society. Dunham, NC.

Radwan, T.M., Blackburn, G.A., Whyatt, J.D., and Atkins, P. (2021). Global land cover trajectories and transitions. Scientific Reports 11, 12814. https://doi.org/10.1038/s41598-021-92256-2.

Rowling, Megan. Drive for goal to protect 30% of planet by 2030 grows to 50 nations. Thomson Reuters Foundation (https://news.trust.org/item/20210111140220-1qxoj/). Retrieved 11/02/22.

Shellnhuber, H.J., Molina, M. Stern, N., Huber, V. and Kadner, S. Eds. 2012. Global Sustainability: A Nobel Cause. Cambridge University Press. Cambridge.

Simard, S.W. 2021. Finding the Mother Tree. Penguin Random House. New York.

Taleb, N.N. 2010. The Black Swan: The Impact of the Highly Improbable. Penguin Publishing, London.

United Nations. 2022. Transforming Our World: The 2030 Agenda for Sustainable Development. A/RES/70/1.

USDA. 2017. Major Uses of Land in the United States, 2012. US Department of Agriculture, Economic Research Service Economic Information Bulletin No. (EIB-178) 69 pages.

van der Schyff, D.B. 2010. The Ethical Experience of Nature: Aristotle and the Roots of Ecological Phenomenology. *Phenomenology & Practice* 4(1) (2010), pp. 97-121.

Winkler, K., Fuchs, R., Rounsevell, M., and Herold, M. (2021). Global land use changes are four times greater than previously estimated. Nature Communications 12, 2501. https://doi.org/10.1038/s41467-021-22702-2.

Digital Climate Data Organization in Renewable Energy Policies

I. Varvaris [1], Z. Andreopoulou[2], P. Strantzali[3], and E. Varvari[4]

[1] Department of Forecasting in the Regional Meteorological Center Makedonia/Hellenic National Meteorological Service, Thessaloniki, Greece
[2] Professor in School of Agriculture, Forestry & Natural Environment Aristotle University of Thessaloniki, Thessaloniki Greece
[3] MSc in "Sustainable Management of Forests and Natural Ecosystems: Protection, Production and Exploitation", School of Agriculture, Forestry & Natural Environment Aristotle University of Thessaloniki, Thessaloniki Greece
[4] Student in School of Geology Aristotle University of Thessaloniki Greece

Abstract

The issue is approached by the need to assess and manage climate data and the role they play, as a key parameter of participation in a decision-making system for the development and management of green energy technologies (RES) and their development policies. The role of green energy technologies (RES) in green growth, the forms applied and the dynamics they develop for the future were investigated. The climate system and climate data are developed and analyzed. The components of an information system for managing and making climate data are also presented.

A pilot database containing climatic data stored in spreadsheets organized in tables and diagrams has been developed. It was designed to provide climate information to decision support systems (DSS) to meet and adapt to the needs of rational decision-making regarding the installation of RES and the proper management of their energy systems. It was performed with the Ms-Excel software and includes climate recordings from thirteen (13) Meteorological Stations (MS) of the Hellenic National Meteorological Service (HNMS), which are distributed in the central - northern part of Greece. The climatic data were selected based on the availability of long-term measurements (over 30 consecutive years) to represent a normal climatic period, grouped in the form of spreadsheets, and organized into tables with aggregate data for each station. From the comparison of the representations of the tables, diagrams were created, and results were extracted. The need to support RES with climate information leads us to the creation of climate databases to provide and use climate information in decision support systems, to meet and adapt to the needs of rational decision-making for the installation of RES and proper management of their energy systems.

Keywords: Database, Decision Support Systems, Environmental Policies, Green Energy Technologies, Climate Data Management.

1 Introduction

The climate system (Figure 1) is a complex, interactive system with a wide range of complex interactions and interdependencies that occur over time and consists of the atmosphere, the earth's surface, snow and ice, the oceans, and more. aquatic systems and living organisms. Influenced by solar radiation and the radiation of the Earth's surface, the Earth's climate is determined by the interactions between the components of the climate system. The interaction of the atmosphere with the other components plays a dominant role in shaping the climate. The atmosphere acquires energy directly from the incident sunlight or indirectly through processes concerning the Earth's surface. This energy is continuously redistributed vertically and horizontally through thermodynamic processes or large-scale movements in order (essentially impossible) to achieve a stable and balanced state of the system. Climate change has become an important issue for the human community. Human activities, especially the burning of fossil fuels, have led to changes in the composition of the world's atmosphere. Significant increases in carbon dioxide and methane during the industrial age, along with increased aerosols and particulate emissions, significantly affect the global climate.

Climate change and its potential effects on global energy and food production and water reserves, as well as the effects that have already occurred on humanity, have become key issues for decision-makers in recent years. Numerous international conferences have been held to find ways to reduce human impact on the climate and to design strategies for exploiting the climate for social and economic benefit. RES development policies are linked to the WWF's vision of a mid-century world powered by 100% renewable energy. Achieving this goal prevents catastrophic climate change, helps reduce pollution, increases energy security, and improves the health of people around the world (Singer, S. et al, 2017). The most ambitious scientific test (because of Ecofys research on energy consumption- Figure 2) for a future of renewable and clean energy on a global scale, shows that it is technically possible to achieve energy replacement targets of almost 100% from renewable sources of energy over the next three decades. Meeting the energy needs of present and future generations is one of the most important, difficult, and urgent political tasks for any government. Switching to renewable energy is the only and best option. The way people produce and use energy today is not sustainable.

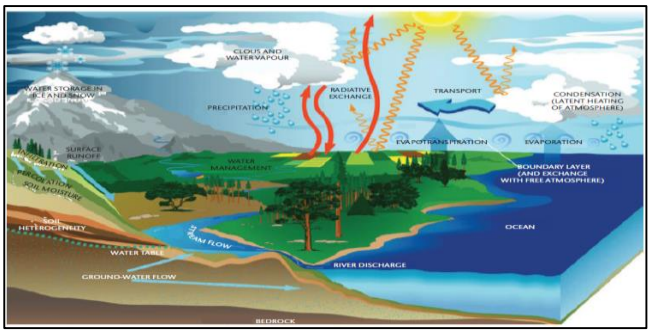

Figure 1. The climate system. Source: (WMO, 2018)

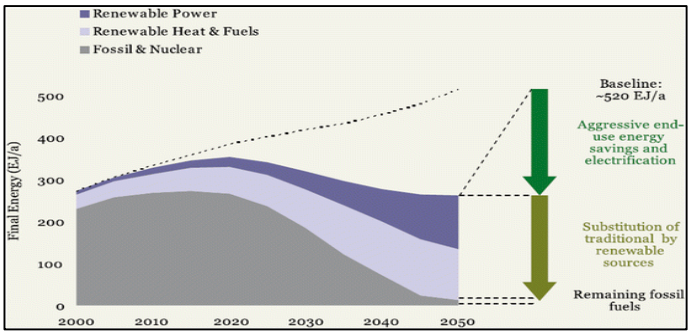

Figure 2. Evolution of energy supply in the energy scenario, presenting the basic developments (Singer, S. et al, 2017).

In the present work, reference is made to wind energy systems, and the case of collection of wind climate data is analyzed. The climatic data were collected from thirteen (13) MS meteorological stations (MS) of the National Meteorological Service (HNMS) that are distributed in the central - northern mainland and island part of Greece. In particular, the three (3) are islanders: Lemnos, Mytilene, and Skyros, the four (4) coastal: Anchialos (Volos), Mikra (Thessaloniki), Alexandroupoli, Chrysoupoli (Kavala), and six (6) mainlands: Larissa, Trikala Kastoria, Drama, Drama (Doxato), Amygdaleonas (Kavala). The availability of long-term measurements was selected as the main criterion, as the recordings are over 30 consecutive years and represent what is known as the normal climatic period (Stathis, D., 2015). A database containing the existing records was then designed and developed on MS.-Excel software. In section 3, the results for the wind case are presented in tables and diagrams and conclusions are drawn for the geographical areas, which are shown to be more suitable for the installation of wind turbines to exploit the wind energy.

2 Climate Data and Decision Support Systems (DSS)

2.1 Climate data recording and monitoring tools

The National Meteorological and Hydrological Services (NMHS) are responsible for recording the climate and creating an "official" climate data repository. Contains meteorological data recorded by observers or instruments according to acceptable observation standards and includes a. Electronic and cartographic records and scanned images, b. Climate observations and metadata, c. Homogenized data, d. Satellite images, e. Radar data. The data included in the recording consist of observation values, over long periods and following routine quality control procedures.

In the climate system, there is a systematic and wide variety of observations of various climate-related phenomena, which are stored, managed, and analyzed using the Climate Data Management System Specifications (CDMS). Examples of media used to make such observations are shown in Figure 3. These observations are systematically analyzed, and a series of generated data is generated (e.g., through climate models). Significant amounts of data generated must be easily and efficiently managed to contribute to improving our understanding of the Earth's climate.

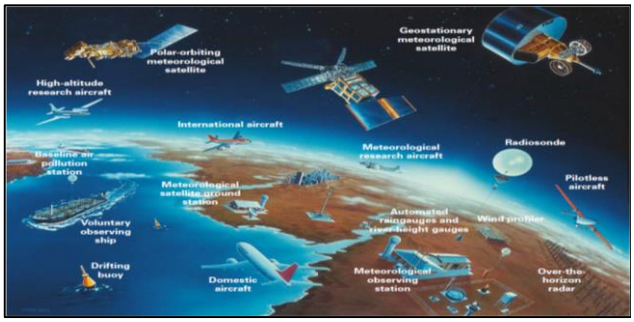

Figure 3. Multiple observation systems. Source: Adapted from a WMO flyer on WMO Integrated Global Observing System (WIGOS) (WMO (2014)

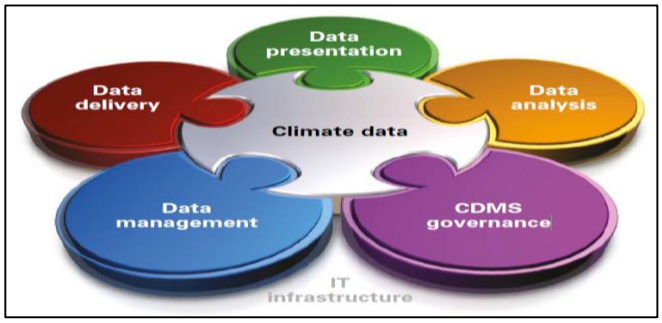

Figure 4. Major components of a climate data management system (WMO (2014)

The components (Figure 4) that make up a Climate Data Management and Decision-Making Information Systems (CDMS) are:/ a. Climate data b. Governance of climate data management information systems c. Data management d. Data provision e. Data analysis f. Data presentation g. IT infrastructure WMO (2014). The "IT infrastructure" component represents the functions required to support a CDMS. The creation of climate databases aims at the availability and provision of climate data. Climate data is used as a parameter by decision support systems (DSS), in the rational decision-making associated with the installation and proper management of RES energy systems.

2.2 Decision Making Support Systems (DMSS)

By Decision Making Support Systems (DMSS) we mean systems that were originally intended to support decision-makers in cases of partially structured problems, but without substituting their judgment capabilities. By design, these systems would be created using computers and had an interactive work environment (Athanasiadis, A., 2018). Decision Support Systems (DSS) evaluate alternative future scenarios for decision making. Decision-Making Support Systems (DMSS) are information systems in which the initial data of some parameters are given as input and produced as outgoing decisions of rational environmental administration and management (Andreopoulou, Z., 2012. Tasoulas, E. A. & Andreopoulou, Z., 2012). The three main parts (figure 5) of an architecture of a D.S.S are:/ the database (or Knowledge Base), the model (e.g., the general decision framework and user criteria), and the user interface. Nowadays, green energy resources can play a very important role in tackling the environmental issues that come with sustainable development. Therefore, developing countries on their way to development can benefit from sustainable and renewable energy sources without disturbing the environment. In recent decades, energy planning methodology has been completely transformed from a single objective simple system to a more complex system, due to the inclusion of multiple benchmarks, interests, and different goals (Mateo, J.R.S.C., 2012).

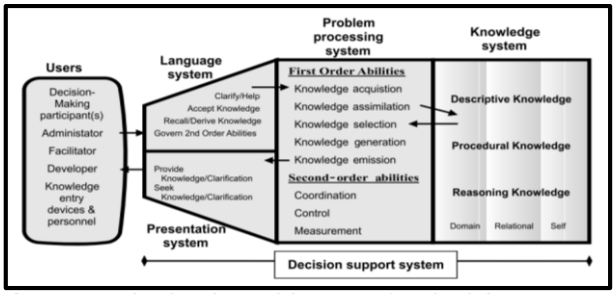

Figure 5. The basic architecture for decision support systems (Holsapple, C. W., 2008).

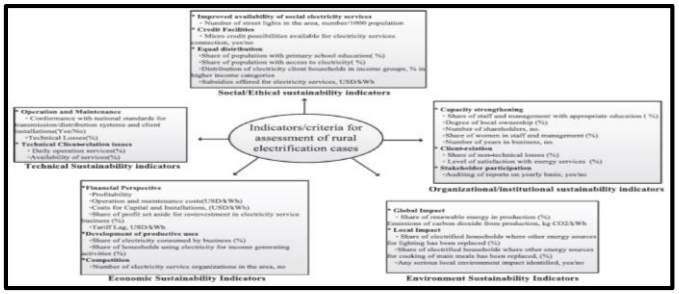

Figure 6. Complex interaction of energy systems (example), (Ilskog, E & B. Kjellström, 2008).

The traditional single decision-making that mainly concerns the maximization or minimization of a specific element remains useful only in a study of the small system. The current energy planning scenario has multiple goals, definitions, and criteria that make it more difficult to achieve a system with a concept of sustainability. Thus, with a vision of sustainable development, a planning system that considers the necessary political, social, economic, and environmental aspects is necessary to overcome the growing energy demand (Figure 6). To solve such complex problems related to energy planning, Multi-Criteria Decision Making (MCDM) has proven to be one of the best tools for energy efficiency planning (Kumar, A. et al., 2017). The MCDM assists the decision-maker in quantifying specific criteria based on their importance, in the presence of other objectives. MCDM techniques are used to find appropriate solutions to the problems of designing an energy system that includes multiple and conflicting goals.

2.3 Wind Energy Systems.

The energy produced by the exploitation of the blowing wind is called wind energy. It is the oldest renewable energy source used to meet human energy needs: sailing ships, windmills, etc. Today it is now widely used for electricity generation. For the utilization of wind energy, today we use wind turbines, which convert the kinetic energy of the wind through the impeller into mechanical energy, which is then converted through the generator into electricity. Wind turbines are used to fully meet or supplement energy needs (Figure 7). The electricity generated by wind turbines is either consumed on-site, injected, and fed into the grid to be consumed elsewhere. Electricity generated by wind turbines, when production is greater than demand, is often stored for later use when demand is greater than production. Storage today is done in two economically viable ways depending on the size of the energy produced. a. In small-scale production units not interconnected to the mains, electric accumulators are used (batteries - which is the most well-known and widespread method of storing electricity). b. When the electricity generated is high, the water storage method is pumped from a fresh or saltwater reservoir using electricity generated by wind turbines. It is then concentrated in artificial lakes constructed at an altitude that can supply a hydroelectric station (hybrid wind - hydroelectric parks) (ypeka.gr, 2019).

Figure 7. Various orientations of horizontal axis wind turbines: (a) Swift type; (b) Eclectic type; (c) Fortis Montana; (d) Scirocco; (e) Tulip; (f-i) Energy ball; (f-ii) Wind wall (Sharikzadeh, M.,2016)

Offshore wind farms have already been set up in northern European countries, such as Denmark and Germany, to minimize the environmental impact of terrestrial wind farms. In Greece, PPC has started in 2008 with the creation of a Hybrid Energy Project in Ikaria (Skodras, 2015). Our country has extremely rich wind potential (the second-best wind potential in Europe), in several areas of Crete, Peloponnese, Evia, and of course the Aegean islands. In these areas, we will find most wind farms, which consist of wind turbine arrays in the optimal layout for the best possible utilization of wind potential. In section 3, the research results are related to the wind potential for the geographical areas of central and northern Greece.

3 Climatic elements of wind in the central, northern mainland, and island parts of Greece

The initial climatic data are checked by homogeneity methods from the climatology department of HNMS and provided in the form of MS.-Excel spreadsheets, organized in rows and columns for each MS (Tables 1, 2). They include monthly wind frequency values and the number of days with Maximum Wind Intensity> = 22 Knots recorded by an anemometer.

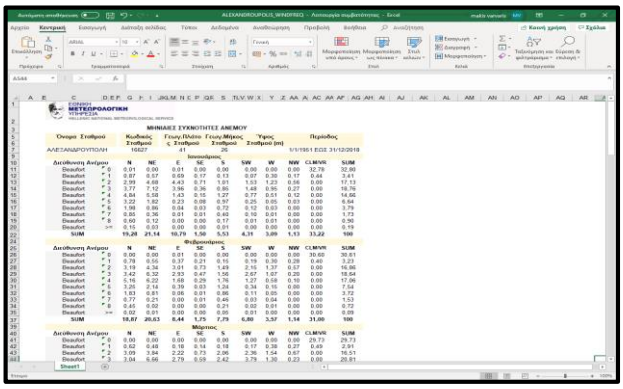

Table 1. Monthly wind frequencies

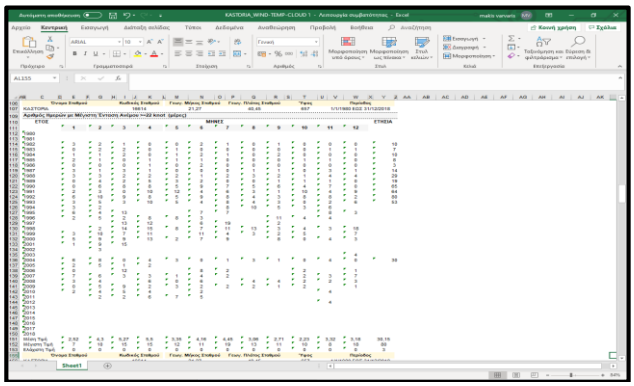

Table 2. Number of Days with Maximum Wind Intensity> = 22 Knots

They were then processed using MS.-Excel software commands and tables with aggregate wind data for thirteen (13) stations were created. The tables are shown in diagrams and conclusions are drawn from their comparison.

3.1 Wind frequency.

Table 3 below calculates the sum of the percentages of annual wind intensity per Beaufort for each station on a scale from 1B to 9B and for the time periods reported in the city column.

Percentage of % of Annual Wind Frequency on Beaufort scale					
City	8->= 9 B	6-7 B	4-5 B	2-3 B	0-1B
Alexandroupoli (1951-2018)	0,34	2,78	20,42	39,25	37,21
Kavala (Chrysoupoli, 1984-2018)	0,02	0,25	7,42	53,93	38,38
Kavala (Amydaleonas, 1956-1984)	0,01	0,24	7,41	31,07	61,27
Lemnos (1973-2018)	0,51	5,59	30,07	38,75	25,07
Mytilini (1955-2018)	0,33	4,86	24,55	46,63	23,63
Skyros (1955-2018)	0,79	7,22	29,66	39,17	23,16
Anchialos (1956-2018)	0,03	0,55	12,00	52,80	34,62
Larissa (1955-2018)	0,02	0,36	6,93	28,62	59,40
Mikra (Thessaloniki) (1959-2018)	0,24	1,90	12,57	47,41	37,88
Trikala Imathia (1980-2010)	0,00	0,08	3,80	50,36	45,76
Kastoria (1980-2018)	0,00	0,08	5,97	37,06	56,88
Drama (1975-2008)	0,00	0,02	0,35	10,34	89,29
Drama (Doxato, 2010-2018)	0,00	0,02	2,83	36,92	60,23

Table 3. Annual wind frequency

In graph 1 that follows the highest frequency percentages, are noted in intensity 0-1b (Apnea or almost apnea) in the stations: Amygdaleonas (Kavala), Larissa, Kastoria, Drama, and Doxato Drama, while in intensity 2-3b (Very sick or patient) at the stations: Alexandroupoli, Chrysoupoli (Kavala), Lemnos, Mytilene, and Skyros, Anchialos and Trikala Imathia. Only Alexandroupoli, Lemnos, Mytilene and Skyros stations show intensity at 4-5b (Almost moderate or moderate) at a rate of over 20%. The analysis of the graph shows that Alexandroupolis, Lemnos, Mytilene, and Skyros, accumulate the highest percentages with an annual wind frequency of 2 to 5B. Therefore, they are indicated as the most suitable geographical areas for the installation of wind turbines, while the type of wind turbines that will be selected for installation, must be suitable for the specific wind intensities.

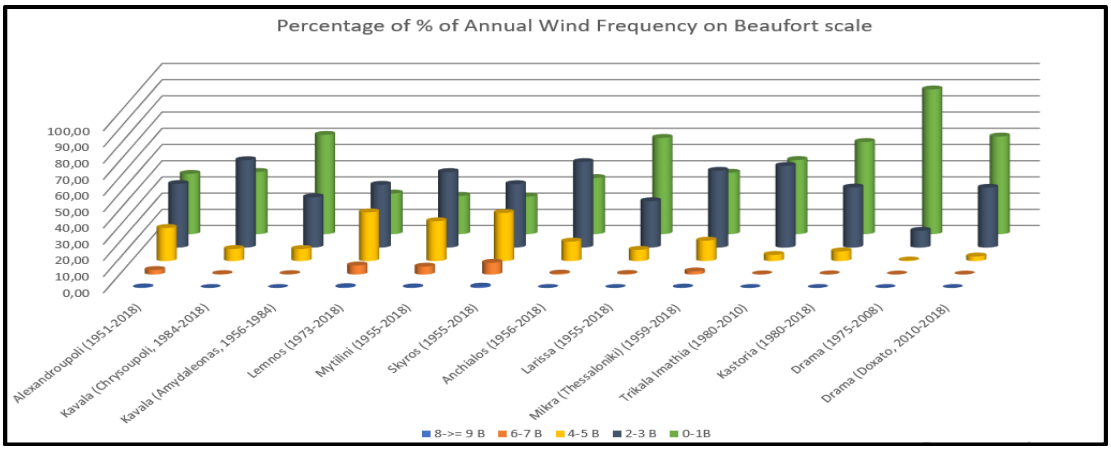

Graph 1. Annual wind frequency

In addition, in coastal areas that show an increased frequency of winds from a specific direction and intensity greater than 4B, ripples are created with a wave height of up to 1.5-2.5m. These areas can be used for the development - installation of offshore power generation systems. With the development of technology, energy production systems are being developed that operate equally efficiently in areas with lower wind intensity and lower wave height (Figures 8,9).

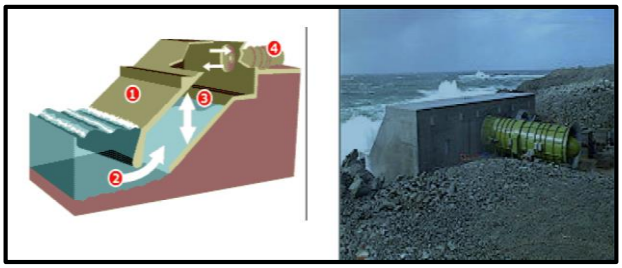

Figure 8. Coastal Limpet Technology systems installation wave energy. (Manalis, SA, 2015).

Figure 9. Wave and ocean energy (Manalis, SA, 2015

3.2 Number of Days with Maximum Wind Intensity> = 22 Knots (Nautical miles per hour).

The following table is a result of the grouping of the initial data and the minimum, average and maximum value of the annual number of days with maximum wind intensity> = 22 Knots (6b – Strong wind) have been calculated.

Annual Number of Days with Maximum Wind Intensity >= 22 Knots			
City	Minimum Number of Days	Average Number of Days	Maximum Number of Days
Alexandroupoli (1951-2018)	39	63,69	97
Kavala (Chrysoupoli, 1984-2018)	28	45,53	65
Kavala (Amydaleonas, 1956-1984)	1	1	1
Lemnos (1973-2018)	162	187,06	218
Mytilini (1955-2018)	96	160,57	193
Skyros (1955-2018)	59	103,12	179
Anchialos (1956-2018)	28	77,3	145
Larissa (1955-2018)	34	57,78	128
Mikra (Thessaloniki) (1959-2018)	50	84,06	129
Trikala Imathia (1980-2010)	5	5	5
Kastoria (1980-2018)	3	30,15	80
Drama (1975-2008)	0	0	0
Drama (Doxato, 2010-2018)	3	3	3

Table 4. Annual Number of Days with Maximum Wind Intensity >= 22 Knots

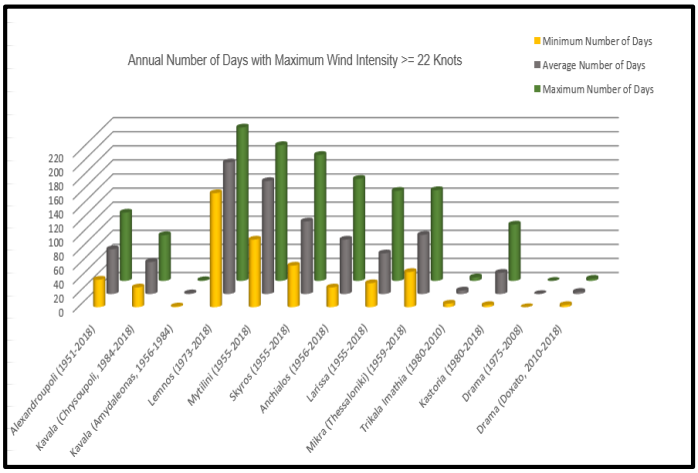

Graph 2. Annual Number of Days with Maximum Wind Intensity >= 22 Knots

Graph 2 shows the highest values of the average annual number of days (with maximum intensity> = 22 Knots) noted at the stations: Lemnos, Mytilene, Skyros, and Mikra (Thessaloniki). The maximum and minimum values of the annual number of days vary.

Therefore, the wind turbine systems that are installed in the areas of Lemnos, Mytilene, Skyros, and Mikra (Thessaloniki), must be suitable, to withstand the frequent prevalence of strong winds. When installing wind turbines in a geographical area, other parameters are taken into account, such as the direction of wind frequency at a higher frequency, the local terrain (e.g. installation in areas with high altitude, while windward areas of mountainous areas, locations with a large slope, areas with favorable conditions for the creation of turbines and gusts of wind, etc.) (Figure 10).

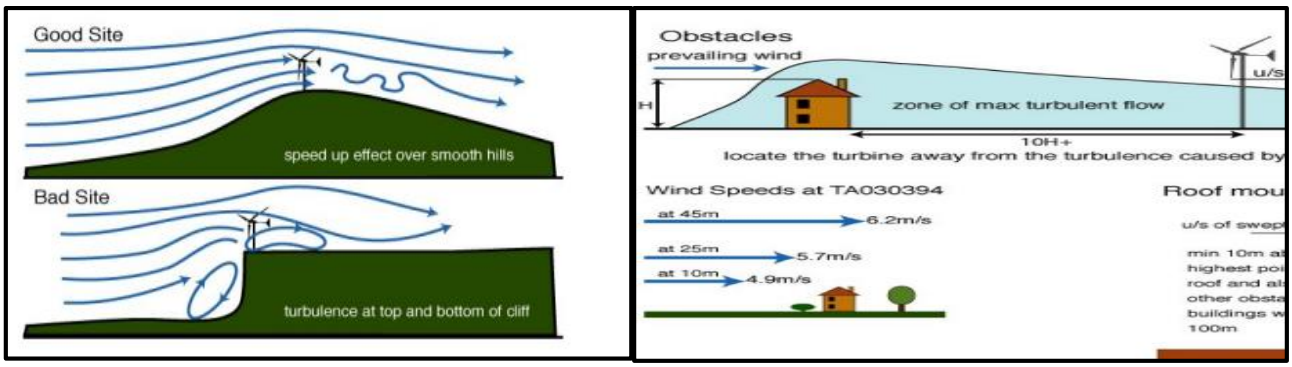

Figure 10. Comparing various site locations for the installation of a wind farm (Green Building, 2020).

4 Summary

In this study, the climatic parameter of the intensity of the winds is examined concerning to their frequency of occurrence and their maximum intensity over 22 knots (5 Beaufort) for the wider region of central and northern Greece. The aim is to use and participate in the research conclusions as individual components of the decision support systems (DSS), to help in the rational decision-making related to the installation and proper management of RES energy systems that exploit the kinetic energy of the wind.

References

Andreopoulou, Z. (2012). Green Informatics: ICT for green and Sustainability. *Agrárinformatika/Journal of Agricultural Informatics*, *3*(2), 1-8.

Athanasiadis, A., Andreopoulou, Z., (2015). A DSS for the identification of forest land types by the Greek Forest Service. *International Journal of Sustainable Agricultural management and Informatics.* Vol. 1, iss.1. pp. 76-88

Holsapple, C. W. (2008). DSS architecture and types. In *Handbook on Decision Support Systems 1* (pp. 163-189). Springer, Berlin, Heidelberg.

Ilskog E, Kjellström B., (2008) And then they lived sustainably ever after? assessment of rural electrification cases by means of indicators. Energy Policy 2008; 36:2674–84, [7//].

Kumar, A., Sah, B., Singh, A. R., Deng, Y., He, X., Kumar, P., & Bansal, R. C. (2017). A review of multi criteria decision making (MCDM) towards sustainable renewable energy development. *Renewable and Sustainable Energy Reviews.* Elsevier Ltd., March 1. https://doi.org/10.1016/j.rser.2016.11.191

Mateo JRSC, (2012). Multi Criteria Analysis in the Renewable Energy Industry. London: *Springer*.

Singer, S., Denruyter, J. P., & Yener, D. (2017). The energy report: 100% renewable energy by 2050. In *Towards 100% renewable energy* (pp. 379-383). Springer, Cham.

Sharikzadeh, M. (2016). Investigate the Performance of a Proposed Micro-Turbine Design in Small Scale Openings in High Rise Buildings.Olabi, A. G., Wilberforce, T., Elsaid, K., Salameh, T., Sayed, E. T., Husain, K. S., & Abdelkareem, M. A. (2021). Selection guidelines for wind energy technologies. *Energies*, *14*(11), 3244.

Skodras, G. (2015). Mild and new forms of energy. Version: 1.0. Kozani 2015. Available from the web address: https: // eclass.uowm.gr/courses/MECH244/ Green Building (2020). Available online: https://www.greenspec.co.uk/building-design/small-wind-turbines/ (accessed on 2 November

Stathis, D. (2015). Courses in forest meteorology and climatology (No. IKEE BOOK-2016-036). Aristotle University of Thessaloniki.

Tasoulas, E. A., Andreopoulou, Z. S., (2012). Integrated Administration ICT System in Forest Environments Supporting Proper Management. *International Journal of Environmental protection and ecology.* Vol. 13, No.1., pp 338-344.

World Meteorological Organization (2014). Climate Data Management System Specifications - No. 1131.

World Meteorological Organization (2017). Guide to the Implementation of Quality Management Systems for National Meteorological and Hydrological Services and Other Relevant Service Providers (WMO-No. 1100). Geneva.

World Meteorological Organization (2018). Guide to Climatological Practices edition.

ypeka.gr (2019). Αιολική ενέργεια. http://www.ypeka.gr/Default.aspx?tabid=287&language=el-gr

DO THE DEMOCRATIC REGIME AND THE MAGNITUDE OF THE INFORMAL ECONOMY DETREMINE HUMAN IMPACTS ON THE ENVIRONMENT- AN EXTREME BOUNDS ANALYSIS

Athanasios Kampas, Michaela Vourvoulia,

[1]Department of Agricultural Economics & Rural Development, Agricultural University of Athens

Abstract

There is a massive literature, which deals with the identification of the major drivers that explain human impacts on the environment. This literature contains two distinct strands, the one labelled as the "environmental Kuznets curve" and the other one as the IPAT, which is the acronym of the basic human ecology equation (Impact equals Population, Affluent and Technology). This paper adopts the stochastic version of the IPAT, known as STIRPAT. In order to address the issue whether the quality of the democratic regime and the size of informal economy determine the human impacts on the environment the paper uses the Extreme Bounds Analysis (EBA) to characterize these drivers as robust or fragile. The is general ambiguity that emerges from the analysis, since the quality of democratic regime and the size of the informal economy can be either robust or fragile variables depending on the how human impacts are defined. The likely policy implications are briefly discussed.

Keywords: Extreme Bounds Analysis, Robust Regression, Varieties of Democracy, Informal Economy, Environmental Performance Index, Ecological Deficit.

INTRODUCTION

There is a bourgeoning literature that examines the drivers behind human impacts on the environment (Chertow, 2000; de Angelis, Di Giacomo, & Vannoni, 2019; Leal & Marques, 2020; Stern, 2004). Against this background, this paper examines two of these controversial drivers, namely the incidence of democracy and the magnitude of informal economy.

Under democratic regimes, people can exercise their right to gather and disseminate environmental information, advocate environmental values and to exercise pressure in favour of environmental friendly projects and policies (Sandler, 1997) In other words, in democracies the possibility of green lobbying is taken for granted (Scruggs, 2003) and very often this is transformed into a relative legislation. Despite the self-evident arguments that a democratic regime is good for the environment (Kashwan, 2017), whole issue is controversial (Iwińska, Kampas, & Longhurst, 2019).

The second issue that this paper wishes to explore is whether the informal sector affects human impacts on the environment. There is no unique definition concerning the concept of informal sector since different theoretical approaches use different vocabulary (see S. Chaudhuri and Mukhopadhyay (2010)) and plethora of phenomena are categorized as such (see Sindzingre (2006)). However, at the simplest level and for all practical reasons we may conceive informal sector as embracing all actors and activities that are not directly regulated by formal institutions. Plausible arguments about the likely positive association between informal sector and environment have been put forward by Briassoulis (1999) and Sarbajit Chaudhuri and Mukhopadhyay (2006), while Biswas, Farzanegan, and Thum (2012) provided empirical evidence that the size of informal sector determines the amount of pollution released by country.

METHODS

This paper adopts a rationale in line with the STIRPAT (the stochastic version of IPAT) (York, Rosa, & Dietz, 2003) which may be expressed :

$$\ln(I) = \alpha + \ln(P) + \ln(A) + \ln(T) + \ln(\mathbf{X}) + \varepsilon \quad (1)$$

where I stands for the human impacts on the environment, α is a constant, P is the population, A refers to affluence, T defines technology, $\mathbf{X}$ is a vector of other variables and ε stands for the error term.

According to Leamer (1985) the Extreme Bounds Analysis (EBA) is an example of global sensitivity analysis that facilitates the proper model selection. The latter requires convincing evidence of inferential sturdiness attached to the variables included in a model. Following (Levine & Renelt, 1992) we express the EBA as a number of equations of the form :

$$\mathbf{Y} = a_I \mathbf{I} + a_M \mathbf{M} + a_Z \mathbf{Z} + \varepsilon \quad (2)$$

Where $\mathbf{Y}$ represents the dependent variables we wish to explain, $\mathbf{I}$ is the set of explanatory variables always included in previous studies, $\mathbf{M}$ includes the variables of we wish to examine whether to include them or not, and $\mathbf{Z}$ is the vector of the variables that have been identified as potentially important by previous studies and ε denotes the error term.

The method works as follows. First, we run the regressions for all the combinations of up to three of the $\mathbf{Z}$ -variables. Then for each variable in question j , one can estimate the extreme bounds. The lower bound is defined as $\min(a_{Mj}) - 2\sigma_{Mj}$, while the upper bound as $\max(a_{Mj}) + 2\sigma_{Mj}$. A variable is said to be robust if it remains significant and of the same sign within the extreme bounds. Otherwise, if a variable in question becomes insignificant or there is a change in its sign, the variable is termed fragile and should not be taken into further consideration in the inference “game”.

Table1 presents the variables used in this study, while Table 2 gives the summary statistics, the normality test and the checks for outliers. Since from Table 2 is evident that we can reject the null hypothesis of normality and the data set contains outliers (Rosner, 1983), the method of OLS is not appropriate (Wilcox, 1996).Hence we opt for Robust regression.

Table 1: Variables' Nomenclature and data Sources

Variable		Name	Abbreviation	Units	Horizon	Source
Dependent		Ecological Deficit	EDEF	10^7 global hectares	1990-2016	Global Footprint Network
		Environmental Performance Index	EPI	free	2002-2012, 2014. 2016	https://sedac.ciesin.columbia.edu/data/collection/epi
Independent	I-set	Affluence	GDP	10^3 US$ per capita in constant 2010 prices	1990-2016	World Bank (indicator code NY.GDP.PCAP.KD)
		Population	POP	10^6 people	1990-2016	World Bank (indicator code SP.POP.TOTL)
		Technology (economic structure)	TECH	Manufacturing, value added (% of GDP)	1990-2016	World Bank (indicator code NV.IND.MANF.ZS)
	M-set	Democracy Index	DEM	Range 0-1	1990-2016	V-Dem Institute, Department of Political Science, University of Gothenburg https://www.v-dem.net/en/
		Index of Shadow Economy	SHAD	Informal economy (% of GDP)	2004-2015	IMF, https://www.elibrary.imf.org/view/journals/001/2018/017/001.2018.issue-017-en.xml.
	Z-set	Global Climate Risk index	CLRI	free	1996-2015	https://germanwatch.org/sites/default/files/Global%20Climate%20Risk%20Index%202021_1.pdf
		Index of Trade Openness	TROP	Trade (% of GDP)	1990-2016	World Bank (indicator code NE.TRD.GNFS.ZS) https://data.worldbank.org/indicator/NE.TRD.GNFS.ZS
		Government effectiveness	GOVE	Range 0-1	1996-2016	World Bank, The Worldwide Governance Indicators https://info.worldbank.org/governance/wgi/
		Globalization Index	GLOB	Range 0-100	1990-2016	KOF Swiss Economic Institute

						https://kof.ethz.ch/en/forecasts-and-indicators/indicators/kof-globalisation-index.html
		Rule of Law	RULW	Range 0-1	1996, 1998, 2000, 2002, 2003-2016	World Bank, The Worldwide Governance Indicators https://info.worldbank.org/governance/wgi/
		International environmental commitments	IEA	free	all	Available at: http://iea.uoregon.edu/ Date accessed: 17 June 2021

Table 2: Summary statistics, Normality test and Outliers checks.

	Dependent Variables		**Independent variables**										
			I-set			**M-set**		**Z-set**					
	EDEF	**EPI**	**GDP**	**POP**	**TECH**	**DEM**	**SHAD**	**CLRI**	**TROP**	**GOVE**	**GLOB**	**RULW**	**IEA**
Sample Size	111	111	111	111	111	111	111	111	111	111	111	111	111
Minimum Value	-2.762	3.095	5.59	-0.919	1.46	-2.723	1.98	2.427	3.121	-1.96	3.277	-3.848	2.079
Maximum Value	5.104	4.46	11.437	7.152	3.662	-0.189	4.172	5.164	5.882	0	4.469	0	5.704
Mean	0.497	3.985	8.725	2.633	2.639	-1.047	3.307	4.332	4.303	-0.698	4.076	-0.979	4.051
Standard deviation	1.124	0.289	1.46	1.508	0.365	0.583	0.508	0.548	0.48	0.435	0.244	0.758	0.698
Coefficient of Variation	2.261	0.072	0.167	0.573	0.138	-0.557	0.154	0.126	0.112	-0.624	0.06	-0.774	0.172
Normality Test													
Shapiro-Wilk	0.963	0.96	0.968	0.987	0.967	0.956	0.956	0.955	0.986	0.971	0.973	0.93	0.981
p-value	0.004	0.002	0.009	0.342	0.008	0.001	0.001	0.001	0.299	0.015	0.021	<0.0001	0.125
Ho Rejected	yes	yes	yes	no	yes	yes	yes	yes	no	yes	yes	yes	no
Outliers Checks													

Extreme Studentized Deviate (ESD)	4.10	3.08	2.15	3.00	3.23	2.87	2.61	3.48	3.29	2.9	3.28	3.79	2.83
ESD critical value (for one outlier : 3.085 for ten outliers 3.158)													
Ho Rejected	yes	no	no	no	yes	no	no	yes	yes	no	yes	yes	no
The MADe method													
Upper limit	2.31	4.62	12.17	5.37	3.23	0.30	4.41	5.57	5.20	0.26	4.57	0.75	5.23
Lower limit	-1.19	3.35	5.20	-0.58	2.15	-2.23	2.48	3.22	3.39	-1.71	3.59	-2.48	2.79
Presence of outliers	10	3	0	6	15	7	5	11	1	3	3	9	4
Ho Rejected	yes	ye	No	yes	yes	yes	yes	yes	yes	yes	yes	yes	yes

RESULTS AND DISCUSSION

A general ambiguity emerges from the results (80 regressions) as it is shown in Tables 4 and 5.

Table 4: Sensitivity analysis for the EDEF

Group M		β	SE	t	R^2	Other Variables	Verdict
SHAD	High:	0,26	0,31	0,45	0,15	CLRI, IEA, RULW	Fragile
	Base:	-0,07	0,29	-0,24	0,09		
	Low:	-0,22	0,33	-0,31	0,09	CLRI, GOVE, GLOB	
DEM	High:	-0,21	0,21	-1,75	0,24	TROP, CLRI, IEA	Robust
	Base:	-0,55	0,18	-3,05	0,17		
	Low:	-0,87	0,2	-3,57	0,2	CLRI, RULW, GLOB	

Πίνακας 5: Sensitivity analysis for the EPI

Group M		β	SE	t	R^2	Other Variables	Verdict
SHAD	High:	0,07	0,04	1,22	0,82	TROP, CLRI, IEA	Fragile
	Base:	-0,01	0,04	-0,39	0,80		
	Low:	-0,04	0,04	-0,31	0,81	TROP, GOVE, RULW	
DEM	High:	0,02	0,03	-0,46	0,81	TROP, CLRI, IEA	Fragile
	Base:	0,01	0,02	0,58	0,80		
	Low:	-0,11	0,03	-2,90	0,85	CLRI, IEA, RULW	

The quality of democratic regime and the size of the informal economy appear to be fragile variables, which means that they cannot explain human impacts on the environment only when the impacts are defined in terms of Environmental Performance Index. On the contrary, if the ecological deficit is used to capture the human impacts, the quality of democratic regime is robust variable, while the shadow economy it is not.

At first glance the results seems to contradict a Parsonian modernization postulate, in the sense that democracy is treated as a crucial determinant (“evolutionary universal”) of society’s change (implicitly through its impact on growth, institutions and organizational capacity) (Marsh, 2014). Arguably, it is the interactions of democracy with other entities, which produces the necessary conditions for an environmental friendly adjustment. Further research is needed to clarify the extentt of the likely interactions.

References

Biswas, A. K., Farzanegan, M. R., & Thum, M. (2012). Pollution, shadow economy and corruption: Theory and evidence. *Ecological Economics, 75*, 114-125. doi:10.1016/j.ecolecon.2012.01.007

Briassoulis, H. (1999). Sustainable development and the informal sector: An uneasy relationship? *Journal of Environment and Development, 8*(3), 213-237. doi:10.1177/107049659900800302

Chaudhuri, S., & Mukhopadhyay, U. (2006). Pollution and Informal Sector: A Theoretical Analysis. *Journal of Economic Integration, 21*(2), 363-378.

Chaudhuri, S., & Mukhopadhyay, U. (2010). *Revisiting the informal sector: A general equilibrium approach*. New York: Springer.

Chertow, M. R. (2000). The IPAT Equation and Its Variants. *Journal of Industrial Ecology, 4*(4), 13-29. doi:10.1162/10881980052541927

de Angelis, E. M., Di Giacomo, M., & Vannoni, D. (2019). Climate Change and Economic Growth: The Role of Environmental Policy Stringency. *Sustainability, 11*(8). doi:10.3390/su11082273

Iwińska, K., Kampas, A., & Longhurst, K. (2019). Interactions between democracy and environmental quality: Toward a more nuanced understanding. *Sustainability (Switzerland), 11*(6). doi:10.3390/su11061728

Kashwan, P. (2017). Inequality, democracy, and the environment: A cross-national analysis. *Ecological Economics, 131*, 139-151.

Leal, P. H., & Marques, A. C. (2020). Rediscovering the EKC hypothesis for the 20 highest CO2 emitters among OECD countries by level of globalization. *International Economics, 164*, 36-47.

Leamer, E. E. (1985). Sensitivity analyses would help. *American Economic Review, 75*(3), 308-313.

Levine, R., & Renelt, D. (1992). A sensitivity analysis of cross-country growth regressions. *American Economic Review, 82*(4), 942-963.

Marsh, R. M. (2014). Modernization theory, then and now. *Comparative Sociology, 13*(3), 261-283. doi:10.1163/15691330-12341311

Rosner, B. (1983). Percentage Points for a Generalized ESD Many-Outlier Procedure. *Technometrics, 25*(2), 165-172. doi:10.1080/00401706.1983.10487848

Sandler, T. (1997). *Global Challenges : An Approach to Environmental, Political, and Economic Problems*. Cambridge: Cambridge University Press.

Scruggs, L. (2003). *Sustaining Abundance: Environmental Performance in Industrial Democracies*. Cambridge: Cambridge University Press.

Sindzingre, A. (2006). The relevance of the concepts of formality and informality: A theoretical appraisal. In B. Guha-Khasnobis, R. Kanbur, & E. Ostrom (Eds.), *Linking the Formal and Informal Economy: Concepts and Policies* (pp. 58-74). Oxford: Oxford University Press.

Stern, D. (2004). The Rise and Fall of the Environmental Kuznets Curve. *World Development, 32*(8), 1419-1439.

Wilcox, R. R. (1996). A review of some recent developments in robust regression. *British Journal of Mathematical and Statistical Psychology, 49*(2), 253-274. doi:10.1111/j.2044-8317.1996.tb01088.x

York, R., Rosa, E. A., & Dietz, T. (2003). STIRPAT, IPAT and ImPACT: analytic tools for unpacking the driving forces of environmental impacts. *Ecological Economics, 46*(3), 351-365.

Spatial crop N management in the Thessaly plain using variable-rate technology

S. Stamatiadis[1], J. S. Schepers[2] and E. Evangelou[3]

[1] Soil Ecology and Biotechnology Lab, Goulandris Natural History Museum, 13 Levidou Street, 14562 Kifissia, Greece
[2] Department of Agronomy and Horticulture, University of Nebraska, 279 Plant Sciences, Lincoln, NE 68583-0915, USA
[3] Institute of Industrial and Forage Crops, Hellenic Agricultural Organization "DEMETER", 1 Theophrastos str. 41335, Larisa Greece

Abstract

Evolution of technologies over the past century have greatly increased the world-wide supply of food, but scrutinization of fertilizer use for environmental reasons has brought about the challenge of dealing with spatial variability. Variable-rate devices for seeds, granules and liquids have been developed, however, the algorithms needed to make rate decision are still an evolving science. This paper reviews the efficiency of the Holland-Schepers algorithm in three major crops of the Thessaly plain when the model was integrated with a sensor-based variable-rate nitrogen (N) application system (VRA) of high spatial resolution. The N response curves indicated that the VRA rate was near the economic optimal N rates. Compared to the farmer uniform practice, VRA reduced total N inputs by 24, 33 and 38% without yield losses in a maize, cotton and wheat field, respectively. These reductions resulted in 27 to 67% increase of agronomic N-use efficiency and 60% decrease of in-season soil nitrate. The increased VRA returns over N cost were also significant in the three crops (€77 to €97/ha) when compared to the conventional practice. Broader scale multi-year trials are needed to verify the comparative yield responses. It is evident, however, that the potential economic incentives for adoption of the real-time integrated VRA system by farmers and policymakers are now stronger than ever. When considering the recent sharp increase of fertilizer prices, the VRA returns over N cost were higher by €154-€196/ha than those of the conventional practice assuming that the value of crop products remains unchanged.

Key words: site-specific management, profitability, environmental benefits, nitrogen, algorithms, N-use efficiency, soil nitrate, cotton, maize, wheat.

1. Introduction

Major innovations and advancements in agriculture that increased food production go back to the early 1900s when Habor and Bosch developed procedures to manufacture anhydrous ammonia. Much of the synthesized nitrogen (N) went into the military activities until after World War II. Availability of N fertilizer for agricultural production in the 1950s complimented the development of the hybrid corn industry. Irrigation contributed significantly to higher corn yields in areas with an abundant supply of ground or surface water. However, furrow and flood irrigation are labor intensive and require a higher level of nutrient management.

Within a decade, the combination of abundant water, high-yielding corn hybrids and inexpensive N fertilizer was resulting in occurrence of unacceptable concentrations of nitrate in groundwater. The obvious solution would have been to scrutinize N and water management practices, but economic incentives enticed a repeating sequence of more water followed by more N fertilizer until human health issues prompted regulations on the amount and timing N fertilizer applications. Public pressure and regulations on fertilizer practices resulted in observations of uneven crop growth and plant color. It soon became obvious that inherent soil fertility was spatially variable in most fields. Satellite and aircraft photos and drone imagery effectively confirmed the extent and severity of spatial variability.

Evolution of technologies over the past century have greatly increased the worldwide supply of food, but presented the current and next generation with challenges that can be transformed into opportunities. Spatial variability is a feature of nature and so a systematic approach will be required to take advantage of what nature has to offer and compensate for any shortcomings to the extent possible. Global positioning systems (GPS) developed are now an integral part of precision agricultural tools.

Various devices have been developed to variably distribute seed, granules and liquids, however, the algorithms needed to make rate decision are still an evolving science.
Many factors influence plant growth and vigor so at one time or another during the growing season they can have a strong influence on crop yields. Crop vigor (plant relative size and color) is a function of preceding growing conditions but can also provide a hint of what might be expected for the remainder of the growing season, especially related to N mineralization. Adequate water will always be a primary consideration. Fortunately, active crop canopy sensors have the ability to quantify the amount of living vegetation (biomass) and greenness (actually reflectance of light used during photosynthesis). Relative differences in these two parameters within a field and over time are the basis for calculating the normalized difference vegetation index (NDVI) that is part of many algorithms used to make variable-rate fertilizer N recommendations.
Variable-rate nutrient algorithms generally fall into two categories. The more intuitive approach relies on the "mass balance" concept that assesses relative plant vigor during the growing season and predicts yields based on canopy sensor values and historical responses to N fertilizer at harvest. The difference in yield times the N concentration in grain is assumed to represent the additional N fertilizer required. The fallacy is that if plants are stressed for nutrients during vegetative growth stages and the deficiency is not corrected, the size of the photosynthetic factory (called plant biomass) will be impaired and the yield potential reduced. Back-calculating fertilizer N requirement from the difference in yield is not adequate because the additional fertilizer must first go toward eliminating the vegetative nutrient deficiency before the grain-fill period begins. In the end, the mass balance approach under-estimates in-season crop N needs. The above type of algorithm was developed by scientists at Oklahoma State University for use with the GreenSeeker sensor (Raun et al., 2005)
The second type of algorithm is based on the observation and fact that biological systems follow a quadratic response to N and other fertilizer additions. This concept implies that fertilizer use efficiency decreases as the application rate increases. The Holland-Schepers algorithm is based on this concept and is universal in that the theory mimics the way plants grow and respond to fertilizer additions (Holland and Schepers, 2010). Calibration is based on producer experiences for the monitored field rather than past data from fields with undocumented cultural practices (Franzen et al., 2016). Both approaches involve the quantitative assessment of relative crop vigor during the vegetative growth period (referred to as Sufficiency Index, SI) (Schepers et al., 1992; Biggs et al., 2002; Varvel et al., 2007). Active crop canopy sensors provide a convenient way to acquire this information because the data generated is not affected by cloud cover, shadows or time of day (Shanahan et al., 2003; 2007).
Both types of algorithms rely heavily on crop color and biomass data. Assumptions are that all other nutrients except N are adequate and soil physical properties are not spatially variable. Herein lies a major consideration because over time erosion has modified the crop's root zone in terms of soil properties, nutrient status and water holding capacity (Bean et al., 2018a; 2018b). For this reason, it is appropriate to somehow integrate these considerations into algorithms. Plants are a good biological indicator of growing conditions before sensing, but at least half of the growing season remains until harvest, so it is appropriate to consider soil chemical and physical properties in the in-season N recommendations when possible. The Holland-Schepers algorithm includes a management zone term that can be activated if the information is available.
This paper reviews the efficiency of the Holland-Schepers algorithm in three major crops of the Thessaly plain when the model was integrated with a sensor-based variable-rate N system (VRA) for granular fertilizer (Opt-N-Air). The VRA system performance was compared to different uniform N treatments in replicated field strips with a randomized complete block design in terms of N inputs, crop yield, N-use efficiency, profitability and residual soil nitrates in the root zone.

2. Materials and Methods

Site description and management practices

Detailed information of the field strip experiments is described by Stamatiadis et al. 2018, 2020 and Evangelou et al. 2020. The field experiments were carried out in three different commercial fields 12 km south (wheat) and 18 km southeast (cotton, maize) of the city of Larissa (central Greece). The soils were classified as Xerochrepts with moderate to low levels of organic matter, variable carbonate content and slightly alkaline pH.
The fields were tilled to a depth of 0.15-0.20 m prior to preplant fertilizer application. The farmer uniformly applied the rates of preplant N shown in Table 1 prior to sowing (15-15-15 in cotton, 25-15-0

in maize, 20-10-10 in wheat). Excluding rainfall, the amounts of applied in-season irrigation water are shown in Table 1. The herbicides and pesticides applied in durum wheat and maize are shown in Table 1. The cotton farmer did not use any chemical methods for pest management, weed control or growth regulation.

Table 1. Crop management practices and N treatment information for each crop trial

	Durum wheat 2016	Cotton 2017	Maize 2017
Crop management practices			
Crop variety	Simeto	Delta Pine	Dekalb DKC6875
Irrigation water, mm	68	158	289
Pesticides	Phosmet, Mancozeb		
Herbicides	Mustang, Senior		Cabatex Extra SC
Strip experimental data			
Strip width and length, m	7, 200	7, 200	7, 190
Blocks	4	4	3
Preplant N, kg N/ha	100	50	80
In-season Nopt, kg N/ha	112	150	190
Total applied N, kg N/ha	212	200	270
Treatment rates (total kg N/ha)	0, 100, 212, 100+VRA	0, 50, 200, 50+VRA	80, 270, 80+VRA

The field experiments and in-season fertilizer application

Part of each field was divided into three or four blocks and treatments were randomly assigned within each block to follow a randomized complete block design. The treatments consisted of a preplant rate without in-season N application, a farmer preplant and in-season application and a preplant plus in-season VRA application. A 0-N control was also included in the wheat and cotton trials (Table 1). Each replicated treatment was a 7-m wide field strip to accommodate the operation of the variable-rate applicator and harvester running a block length of ~200 m. Strip dimensions and treatment rates used in each field trial are shown in Table 1.

In-season granular ammonium nitrate was applied by a VRA prototype consisting of two Crop Circle ACS-430 active crop canopy sensors (Holland Scientific, Lincoln, NE), a GeoScout X data logger (Holland Scientific, Lincoln, NE) that processed the geospatial data under real-time conditions to convey a 1-Hz N rate signal to a hydraulic motor Gandy Orbit Air 66FSC spreader (Gandy, Owatonna, MN) through a Raven SCS 660 controller (Raven Industries, Inc., Sioux Falls, SD). System specifications of the high spatial resolution prototype are described by Stamatiadis et al. (2018). The sensors were mounted in front of the applicator, positioned in a nadir view and centered over individual rows 0.6-m from the crop canopy, and measured three optical channels at 670 nm (red), 730 nm (red edge) and 780 nm (NIR). For fertilizer application on farmer strips, the data logger was set to the uniform mode.

When set in the VRA mode, the prototype first performed an auto-calibration procedure using the "virtual strip approach" as described by Holland and Schepers (2011). Based on this approach, the canopy sensors monitored a portion (one strip) of the existing crop that represented the range in crop vigor within the field. The 95-percentile value was deemed to be non-N limiting and designated as the vegetation index (VI) reference. The software uses data collected during the first 300 s to generate the histogram (300 data points) and calculate the reference value that represents two standard deviation units above the mean. The data logger then switched to application mode by computing N application rate (N_{APP}) based on an algorithm developed by Holland and Schepers (2010):

$$N_{APP} = (N_{opt}) * \sqrt{\frac{(1 - SI)}{\Delta SI}}$$

where Nopt was the maximum in-season N rate prescribed by producers, SI is the sufficiency index (SI=VI sensed/VI reference) (VI is the selected vegetation index) and ΔSI is the sufficiency index difference parameter (set at 0.3 or 1 minus the SI value 0.7 where additional N is assumed to no longer correct a deficiency and attain full yield). Those SI values <0.7 are likely caused by missing plants or those with low vigor caused by unfavorable soil properties. The ΔSI value serves as a threshold in the algorithm. Embedded within Nopt are modifications to the soil N pool from processes that are difficult to quantify like mineralization, immobilization, denitrifcation, and leaching. The vegetation index NDRE was used instead of NDVI because it is more responsive to crop N status under more developed canopies. The Nopt for each crop (Table 1) was set to match the in-season farmer rate.

Soil sampling

Composite soil samples (0–20 and 20–40 cm depth, n = 3) were taken from 1 m2 sub-plots in each field strip and analyzed in the laboratory for soil organic matter as determined by the Walkley–Black method of wet oxidation (Nelson 1982), soil texture as determined by physical fractionation (Bouyoukos 1951) and carbonate content, as an estimate of inorganic C, was determined by using a Bernard calcimeter to measure the released carbon dioxide (CO_2) after addition of dilute hydrochloric acid (HCl) solution (Nelson 1982), pH and EC on a 1:1 soil to water ratio and nitrate-N by a Nitracheck colorimeter (FIAstar 5000 analyzer by Foss, Laurel, Md.) in soil extracts of 2 M KCl (Keeney and Nelson 1982). A harvester was used for measurement of harvested product in the central rows of each treatment strip.

Statistical analysis

A randomized complete block design was used to evaluate the effect of treatments on crop yield and N-use efficiency. Restricted maximum likelihood (REML) for linear mixed models was used for analyses. Treatments were fixed and blocks were random model parameters. For soil data that were taken in sub-plots within treatment strips, a split-plot repeated measures analysis was employed with plot as the repeated measures fixed factor and with block, block-by-treatment interaction and block-by-plot interaction as random effects. The least-significant difference (LSD) was used for mean comparisons of the fixed effects at $P<0.05$. Data analysis was conducted using SAS software, version 9 (SAS Institute, Cary, NC).

3. Results and Discussion

Crop responses to N inputs

The average yield response to N was described by a quadratic function where yield increased linearly with increasing N supply until the asymptote was reached at or around the VRA rate (Fig. 1). This was the rate that in all crop trials produced maximum yield, defined as the economic optimum N rate (EONR). Thereafter, the near plateau portion is where yield became insensitive to increases in N fertilizer additions and represents the excesses in farmer inputs. These excesses ranged between 65 to 81 kg N/ha over the VRA rates.

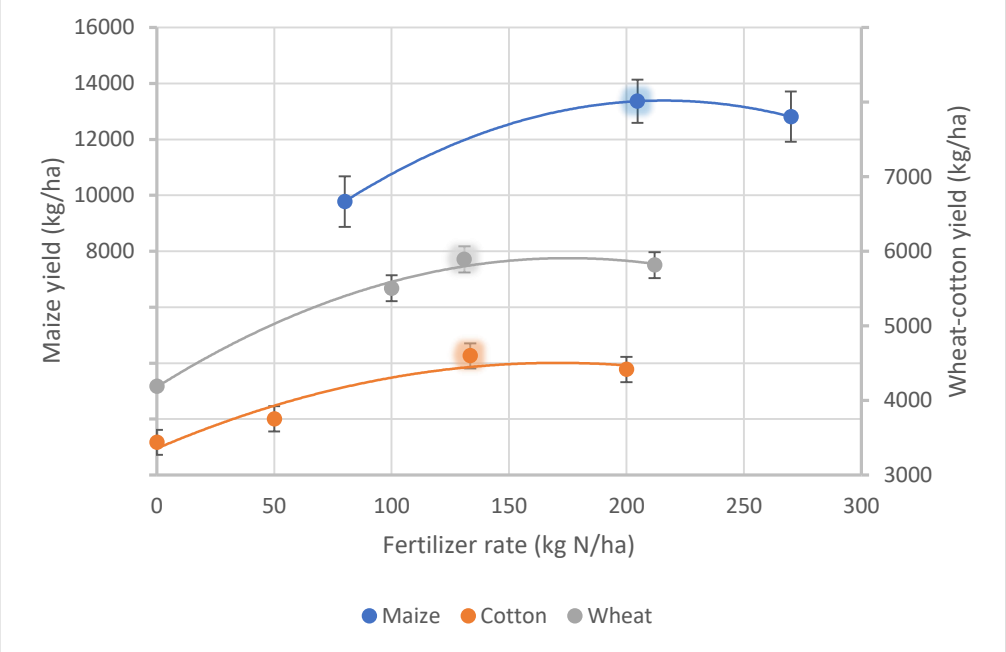

Figure 1. Crop nitrogen response curves (quadratic regressions) of the field strip trials. The mean VRA values are shown with glowing effects. Bars denote standard errors.

Table 2 compares the VRA approach to farmer practice in terms of N-use efficiency parameters. Compared to the conventional rates, the VRA reduced total N inputs by 24, 33 and 38% in the maize, cotton and wheat trials, respectively. Considering that these savings came about without yield losses, the agronomic N-use efficiency and fertilizer N recovery of VRA was greater than that of the farmer practice. The agronomic NUE of 102% in wheat and 118% in cotton indicated that the VRA resulted in N balance or slight depletion of the soil N pool assuming the crop systems were at near steady-state (Meisinger et al. 2008). The VRA also increased NUE in maize (54%), but indicated N losses probably caused by surface runoff as a result of three heavy rainfalls during the summer growing season. The calculation of N recovery further indicated that the VRA resulted in 14 and 20% greater fertilizer N removal in the harvested wheat grain and cotton seed, respectively. This is a large improvement in crop performance considering that only a 1% raise in fertilizer recovery would have a value of at least $235 billion of N fertilizer savings in the global economy (Johnson and Raun 2003). The lack of a 0-N control treatment did not allow estimation of N recovery efficiency in maize.

Table 2. Comparison of N-use efficiency indices between VRA and farmer practice in the three crop fields.

		Wheat 2016		Cotton 2017		Maize 2017	
Parameter	Units	VRA	Farmer	VRA[5]	Farmer	VRA[5]	Farmer
Grain or seed[1] yield[2]	kg/ha	5891	5815	2810	2640	11360	10893
Grain or seed N	%	2.28	2.62	5.63	5.38	0.97	1.05
Grain or seed N	kg N/ha	134	152	158	142	110	114
Total fertilizer N	kg N/ha	131	212	134	200	205	270
Agronomic NUE[3]	%	102	72	118	71	54	42
Fertilizer N recovery[4]	%	58	44	35	15		

1 Assuming 60% of seed cotton is seed (Stamatiadis et al. 2016)

2 Dry yield

3 Agronomic NUE= (grain N/fertilizer N) ×100

4 Fertilizer N recovery= [grain N (treatment—control)/fertilizer N] ×100

5 Average of two VRA treatments (with and without back-off function)

The reduced VRA inputs ultimately resulted in significantly lower levels of soil nitrate when measured after in-season fertilizer application in maize and cotton (Table 3). The high nitrate-N levels of the farmer strips in cotton (45 ppm) were 27 ppm in excess of those of the VRA strips 24 days after N application that corresponded to more than 100 kg N/ha assuming a soil bulk density of 1.3 g/cm^3 for the 0–40 cm depth.

Table 3. Comparison of soil nitrates (ppm at 0-40 cm depth) between VRA and farmer practice in the three crop fields after in-season fertilizer application and at harvest.

		Sampling time	
Crop / year	Treatment	In-season†	Harvest
Wheat 2016	VRA		7.3
	Farmer		8.0
Cotton 2017	VRA	17.9	
	Farmer	44.6	
Maize 2017	VRA	4.2	3.9
	Farmer	10.8	3.3

† 24 days (cotton) and 53 days (maize) after in-season N application

VRA potential for profitability

Based on the unit price of fertilizer N and the unit value of crop product in 2017, the high-resolution VRA provided return over N cost that was €115-219/ha higher than that of the farmer practice (Table 4). The economic benefit of VRA came about because of greater measured yields and less N inputs in comparison to the farmer practice. But the yield difference is probably not real because of lack of statistical significance at the $P<0.05$ level between the two treatments in each crop. Assuming, therefore, that VRA achieves the same yield goals with conventional management, then the economic advantage of VRA as a result of savings in N material cost would be in the range of €77 to €97/ha under 2017 fertilizer prices (Table 4). When considering the recent doubling of fertilizer prices, the VRA returns over N cost are higher by €154-€196/ha than those of the conventional practice assuming that the value of crop products remains unchanged.

Table 4. Comparison of profitability between VRA and farmer uniform application

		Difference (VRA-Farmer)		
Parameter	Units	Wheat	Cotton	Maize
Crop yield[a]	kg/ha	76	283	550
Gross revenue[b]	€/ha	18	142	93
N rate	kg N/ha	-81	-67	-65
N material cost[c]	€/kg N/ha	-97	-77	-78
Return over N cost	€/ha	115	219	171

[a]Maize grain yield adjusted to 15% moisture content
[b]Value of seed cotton was €500/t and value of grain was €240/t and €170/t for wheat and maize, respectively, in 2017.
[c]Cost of N fertilizer was €1.20/kg N in 2017

These comparisons were made with the reasonable assumption that all other production costs are about the same regardless of fertilizer applied or product harvested and excluded the cost of VRA equipment or custom application fees. It is evident, however, that the potential economic and environmental incentives for adoption of the real-time integrated VRA system by farmers and policymakers are now stronger than ever. Broader-scale trials are needed to verify the effectiveness of the Holland-Schepers algorithm as the core of the integrated VRA system in different fields and growing seasons.

4. References

Bean, G.M., N.R. Kitchen, J.J Camberato, R.B. Ferguson, F.G. Fernandez, D.W. Franzen, C.A.M. Laboski, E.D. Nafziger, J.E. Sawyer, P.C. Scharf, J. Schepers, and J.S. Shanahan. 2018a. Active-optical reflectance sensor algorithms evaluated over the United States Midwest Corn Belt. Agron. J. 110:2552-2565. doi.org/10.2134/agronj2018.03.0217

Bean, G.M., N.R. Kitchen, J.J Camberato, R.B. Ferguson, F.G. Fernandez, D.W. Franzen, C.A.M. Laboski, E.D. Nafziger, J.E. Sawyer, P.C. Scharf, J. Schepers, and J.S. Shanahan. 2018b. Improving an active-optical reflectance sensor algorithm using soil and weather information. Agron. J. 110:1-11. doi:10.2134/agronj2017.12.0733

Biggs, G.L., T.M. Blackmer, T.H. Demetriades-Shah, K.H. Holland, J.S. Schepers, and J.H. Wurm. 2002. Method and apparatus for real-time determination and application of nitrogen fertilizer using rapid, non-destructive crop canopy measurements. U.S Patent #6,393,927. May 28, 2002.

Bouyoukos, G. H. (1951). A recalibration of the hydrometer method for making mechanical analysis of soils. Agronomy Journal, 43, 434–438.

Evangelou, E., S. Stamatiadis., J.S. Schepers, A. Glampedakis, M. Glampedakis, N. Dercas, C. Tsadilas, and T. Nikoli. 2020. Evaluation of sensor-based field-scale spatial application of granular N to maize. Precision Agriculture 21:1008-1026 https://doi.org/10.1007/s11119-019-09705-2

Franzen, D. W., N.R. Kitchen, K.H. Holland, J.S. Schepers and W.R. Raun. 2016. Algorithms for in-season nutrient management in cereals. Agronomy Journal, 108(5), 1-7. doi: 10.2134/agronj2016.01.0041

Holland, K.H., and J.S. Schepers. 2010. Derivation of a variable rate nitrogen application model for in-season fertilization of corn. Agronomy J. 102:1415-1424.

Keeney, D. R. and D. W. Nelson. 1982. Nitrogen—Inorganic forms. In A. L. Page, R. H. Miller, D. R. Keeney (Eds.), Methods of soil analysis, Part 2, chemical and microbiological properties. Series Agronomy, No. 9 (pp. 643–698). Madison, WI: ASA and SSSA.

Meisinger, J. J., J. S. Schepers, and W. R. Raun. 2008. Crop nitrogen requirement and fertilization. In Nitrogen in agricultural systems, Agronomy Monograph 49 (pp. 563–612). Madison, WI: ASA.

Nelson, R. E. 1982. Carbonate and gypsum. In A. L. Page (Ed.), Methods of soil analysis, part 2 (2nd ed., pp. 181–197). Madison, WI: ASA and SSSA.

Raun, W.R., J.B. Solie, M.L. Stone, K.L. Martin, K.W. Freeman, R.W. Mullen, H. Zhang J.S. Schepers, and G.V. Johnson. 2005. Optical sensor-based algorithm for crop nitrogen fertilization. Commun. Soil Sci. Plant Anal. 36:2759-2781.

Schepers, J.S., D.D. Francis, M. Vigil and F.E. Below. 1992. Comparison of corn leaf nitrogen and chlorophyll meter readings. Comm. Soil Sci. Plant Anal. Vol. 23, No. 17-20:2173-2187.

Shanahan, J.F., K. Holland, J.S. Schepers, D.D. Francis, M.R. Schlemmer and R. Caldwell. 2003. Use of crop reflectance sensors to assess corn leaf chlorophyll content. p 135-150. In: Digital Imaging and Spectral Techniques: Applications to Precision Agriculture and Crop Physiology. Amer. Soc. Agron. Spec. Publ. 66.

Shanahan, J.F., N.R. Kitchen, W.R. Raun, and J.S. Schepers. 2007. Responsive in-season nitrogen management for cereals. Computer & Electronics in Agric. 61:51-62.

Stamatiadis, S., J.S. Schepers, E. Evangelou, C. Tsadilas, A. Glampedakis, M. Glampedakis, N. Dercas, N. Spyropoulos, N. R. Dalezios and K. Eskridge. 2018. Variable-rate nitrogen fertilization of winter wheat under high spatial resolution. Precision Agriculture 19:570-587. DOI: https://doi.org/10.1007/s11119-017-9540-7

Stamatiadis, S., J.S. Schepers, E. Evangelou, A. Glampedakis, M. Glampedakis, N. Dercas, C. Tsadilas, N. Tserlikakis and E. Tsadila. 2020. Variable-rate application of high spatial

resolution can improve cotton N-use efficiency and profitability. Precision Agriculture 21:695-712 https://doi.org/10.1007/s11119-019-09690-6

Varvel, G.E., W.W. Wilhelm, J.F. Shanahan, and J.S. Schepers. 2007. Nitrogen fertilizer applications for corn based on sufficiency index calculations. Agron. J. 99:701-706.

Weather and satellite sensor data assimilation for monitoring crop performance

Gobin A.[1,2]

[1] Department of Earth and Environmental Sciences, Katholieke Universiteit Leuven, Belgium
[2] Remote Sensing Unit, Flemish Institute for Technological Research, Belgium

Abstract. Agro-ecosystems face the triple challenge of climate resilience, environmental sustainability and high productivity. Advances in satellite sensor technology offer possibilities for monitoring crop performance in relation to yield optimisation while minimising the environmental impact. The contribution of weather data, satellite sensor-derived vegetation indices and soil-water dynamics was analysed in view of estimating agricultural crop yields. Water balance simulations were performed with FAO's Aquacrop model, and yields were subsequently simulated using machine learning methods. Significant differences between low and high crop yields were explained by adverse and extreme weather conditions during the growing season. Time series NDVI and weather explained up to 66% of wheat yield variability at the farm scale in northern Belgium, 74% at the parcel scale in northern France and 83% at the regional scale in Latvia. Weather condition, soil-water depletion and NDVI during the growing season explained 85% of sugar beet and 68% of potato farm yield variability in Belgium. The availability of high resolution satellite sensor and weather data worldwide enabled data assimilation for managing agro-ecosystem performance and agricultural risks.

1 Introduction

Extreme weather events and long-term climate change have marked impacts on crop performance and yield as evidenced by statistical analysis of yield records in relation to extreme or adverse weather events (Kahiluoto et al., 2019; Mäkinen et al., 2018; Moore & Lobell, 2015a; Porter et al., 2014). The 2018 drought in Europe resulted in a 8% decline in cereal harvests compared to the five-year average (European Commission, 2018), and extreme heat waves during several growing seasons have resulted in national cereal production deficits of 9.1% worldwide (Lesk et al., 2016). The occurrence of adverse weather conditions is expected to increase in a warming climate thereby increasing yield variability (Trnka et al., 2016) and yield gaps (Schils et al., 2018). Monitoring crop yield in relation to extreme or adverse weather conditions is therefore necessary to guarantee food security worldwide.

Remote sensing data are available at unprecedented higher spatial, temporal and spectral resolutions from a wide range of platforms. Monitoring crop performance with remote sensing data has shown promising results with certain crops and locations using different vegetation indicators and empirical or process-based modelling methods (Durgun et al., 2020; Schramm et al., 2021; Wright et al., 2020). Some vegetation indicators such as the biophysical parameters Leaf Area Index, fraction of Absorbed Photosynthetically Active Radiation (fAPAR) or fraction of green Vegetation Cover (fCover) are the result of neural network models (Weiss et al., 2020) whereby the uncertainty for a specific location and crop is unknown. Questions arise on the methods used to assimilate remote sensing derived vegetation indices in models and on whether vegetation indices capture soil-water dynamics and extreme weather impacts.

The aim of this paper is to review which weather, soil-water dynamics and Normalised Difference Vegetation Index (NDVI) time series impact arable yields. We tested the methodology for regional scale spring and winter wheat yields in Latvia, farm scale yields of wheat, sugar beet and potato in northern Belgium, and field scale wheat yields in northern France. NDVI series at field level were combined with weather variables, water balance results and crop yield records using a machine learning modelling strategy.

2 Methodology

2.1 Weather characterisation

Meteorological data were retrieved from the national meteorological services for 2014-2015 in France, 1960-2018 in Belgium and 2014-2018 in Latvia. Adverse and extreme weather events were characterised using generalized extreme value analysis based on block maxima (Coles, 2001). Maxima observed at rainfall stations in Belgium by means of max-stable processes using multivariate extreme value theory (Zamani et al., 2015). Spatial extreme modelling through pairwise likelihood inference by a madogram enabled 20-year return levels to be simulated based on geographic coordinates and altitude as covariates (Gobin and Van de Vyver, 2021).

2.2 Weather impacts on arable yield

Yield observations of potato, sugar beet and wheat were analysed in Belgium, Latvia and northern France to characterise their variability. Long-term time series in Belgium allowed to evaluate weather events during the growing season to detrended yields. Yield time series were detrended using linear regression (Gobin, 2010), and the residuals were added to the median 2000-2012 yield (Gobin 2018; Gobin and Van de Vyver, 2021).

2.3 Time series remote sensing indicators in relation to yield

For each parcel where yield was available, NDVI time series were extracted after applying a 10m inward buffer and a threshold of 0.01 km² to ensure that the extracted NDVI profiles for each field were pure. The OpenEO platform (openeo.org; Schramm et al., 2021) was used to extract 5-daily Sentinel-2 NDVI pixels at 10m resolution per field, apply a cloud mask based on the scene classification layer and compute the median NDVI series for each field from the extracted pixels. For all parcels located in Belgium or Latvia, Sentinel-2 NDVI time series were extracted (Vannoppen and Gobin, 2021, 2022), whereas 5-daily 100m and daily 300m resolution Proba-V derived NDVI series were extracted for the central pixel of each parcel in northern France (Durgun et al., 2020).

3 Results and discusion

3.1 Adverse and extreme weather characterisation

Diagnostic plots of time series meteorological variables and indicators such as the number of consecutive dry days (Figure 1) provided information on distributions, return levels and return periods. Agricultural insurances take the 20-year return values to establish pay-out levels (Gobin, 2018). Spatial extreme modelling resulted in ranges (min-max) for the 20-year return period of 29–47 for consecutive dry days across Belgium. The extreme dry year of 2018 showed a clear exceedance of the 20-year return levels in northern Belgium, and predominantly affected summer crops such as potato and maize.

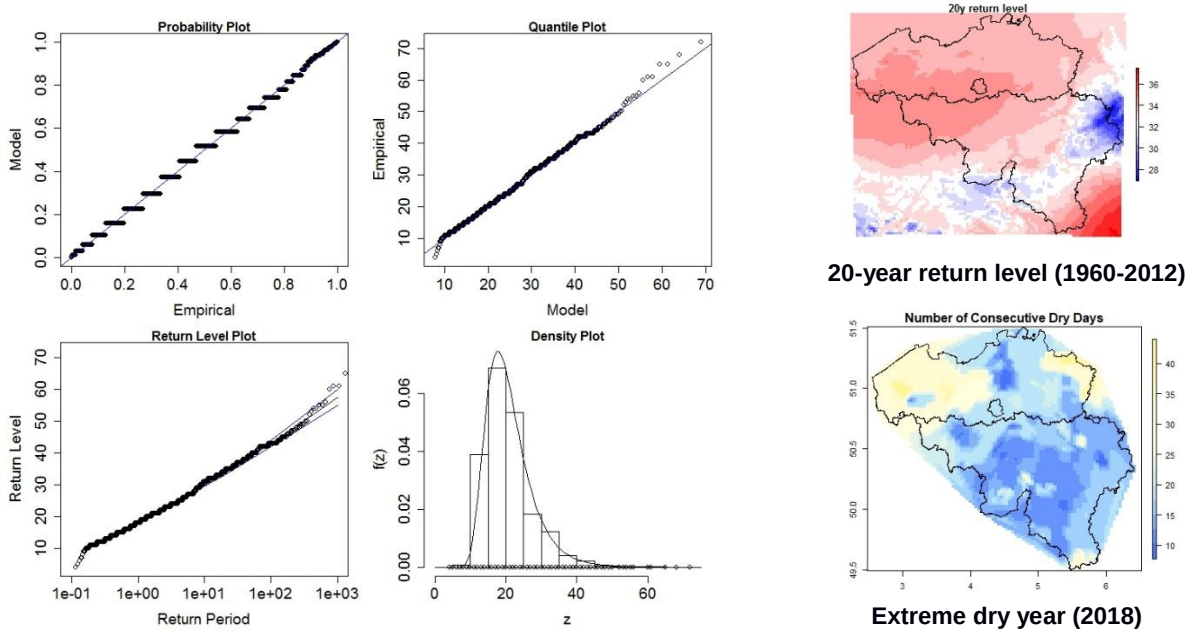

Figure 1. (left) Diagnostic plots showing the goodness-of-fit, probability distribution and return periods of the Number of Consecutive Dry Days (NCDD); (right) spatial 20-year return level of maximum NCDD during 1960-2012 and maximum NCDD extreme dry year during 2018. Adapted from Gobin and Van de Vyver, 2021.

3.2 Weather impacts on arable yields

The 2016 wet season in Belgium resulted in yield reductions in the range 16–39% for winter wheat compared to the median per agricultural region (Figure 2). The negative impact of waterlogging on agricultural productivity has been estimated for observations (Gobin, 2012). Projected yield losses of winter cereals due to excess rainfall were 5 to 12% in a changing climate (Gobin, 2010), which was corroborated by the 2016 observations that showed even higher yield losses.

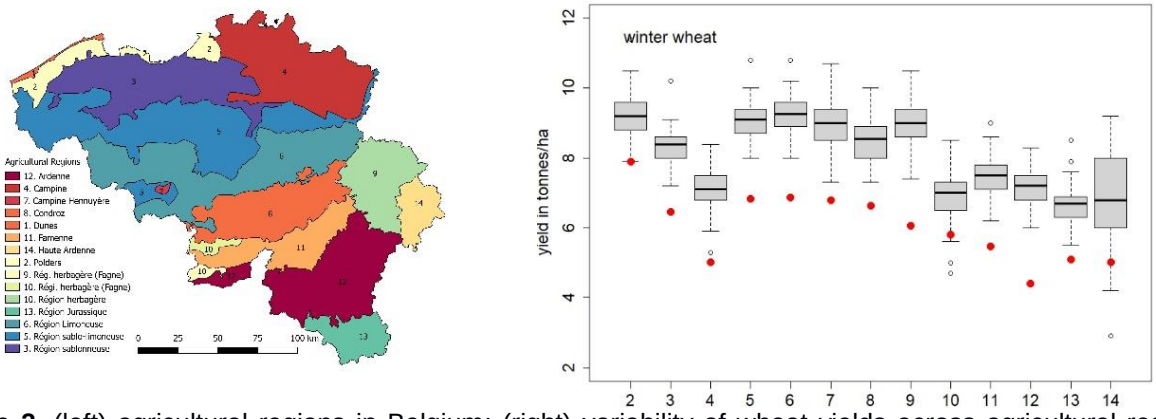

Figure 2. (left) agricultural regions in Belgium; (right) variability of wheat yields across agricultural regions during 1960-2012 (boxplots) and impact of extreme wet weather on yield (red dots). Adapted from Gobin and Van De Vyver (2021).

In Latvia (Figure 3) yields were related to maximum temperatures as interpolated using two different regional climate models. Maximum temperatures during March and June clearly influenced spring wheat yields, whereas January and July maximum temperatures impacted winter wheat yields. The highest spring wheat yields occurred in years with low temperatures in June and high temperatures in March, whereas the highest winter wheat yields coincided with low temperatures in July and high temperatures in January.

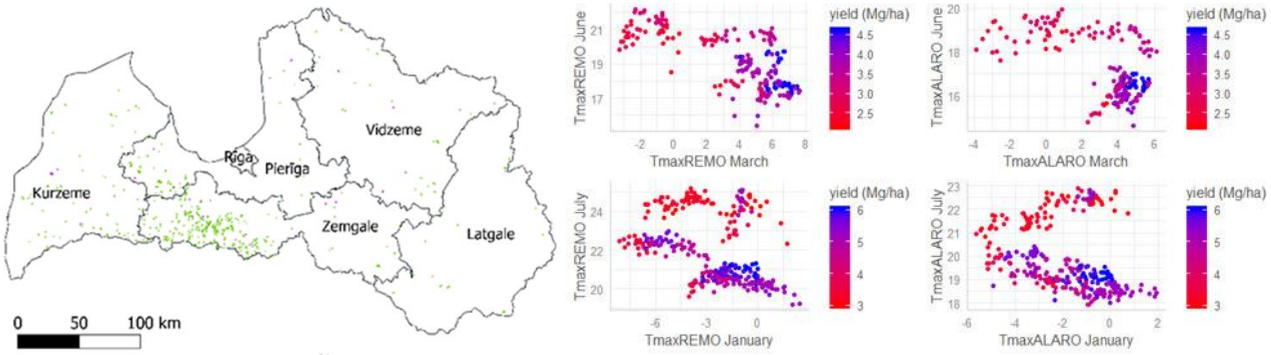

Figure 3. (left) wheat fields in Latvia; (right) 2014-2018 wheat yields in relation to maximum temperatures in January, March and June interpolated with REMO and ALARO climate models. Adapted from Vannoppen et al. (2020).

Single weather variables had a large impact on yields such that the explanatory power of these meteorological variables on yields were interesting to establish. Climate−yield relationships have changed significantly over the past century (1901-2012), and different meteorological predictors have had a greater effect on yields in recent decades 1991 and 2012, as compared to the previous decades (Trnka et al., 2016). The complex weather driven indicators such as the components of a dynamic soil-water balance in relation to crop yield warranted further investigated in conjunction with remote sensing derived vegetation indicators. A remote

sensing derived dry matter productivity (DMP) model was developed to include water stress based on actual evapotranspiration, CO_2 fertilisation, temperature stress and autotrophic respiration. The best relationships between maize and wheat yields and dry matter productivity were obtained by including different combinations of stress factors per region during the phenological stages between the flowering and ripening period (Durgun et al., 2016).

3.3 Time series remote sensing indicators in relation to yield

Remote sensing derived time series vegetation indicators such as the Normalised Difference Vegetation Index (NDVI) integrated over thermal time and calendar time demonstrated the strongest correlation between high spatial resolution thermal time integral and winter wheat yield in northern France (Figure 4). In northern Belgium the relation between the integral of Sentinel-2 derived NDVI and wheat yield was equally strong when integrated over thermal time versus calendar time.

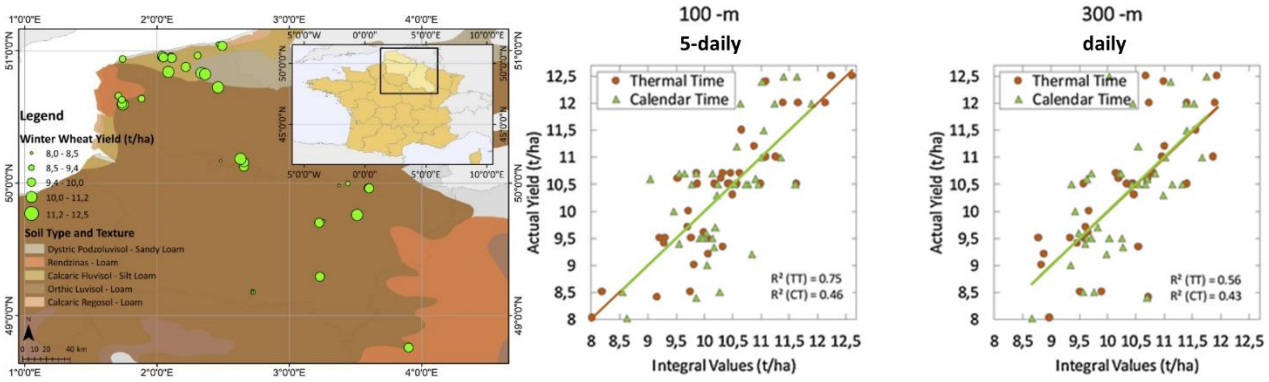

Figure 4. (left) wheat fields and 2015 yields in France; (right) actual wheat yield related to integral values of 100 m 5-daily and 300 m daily NDVI integrated over thermal time (TT) and calendar time (CT). Adapted from Durgun et al. (2020).

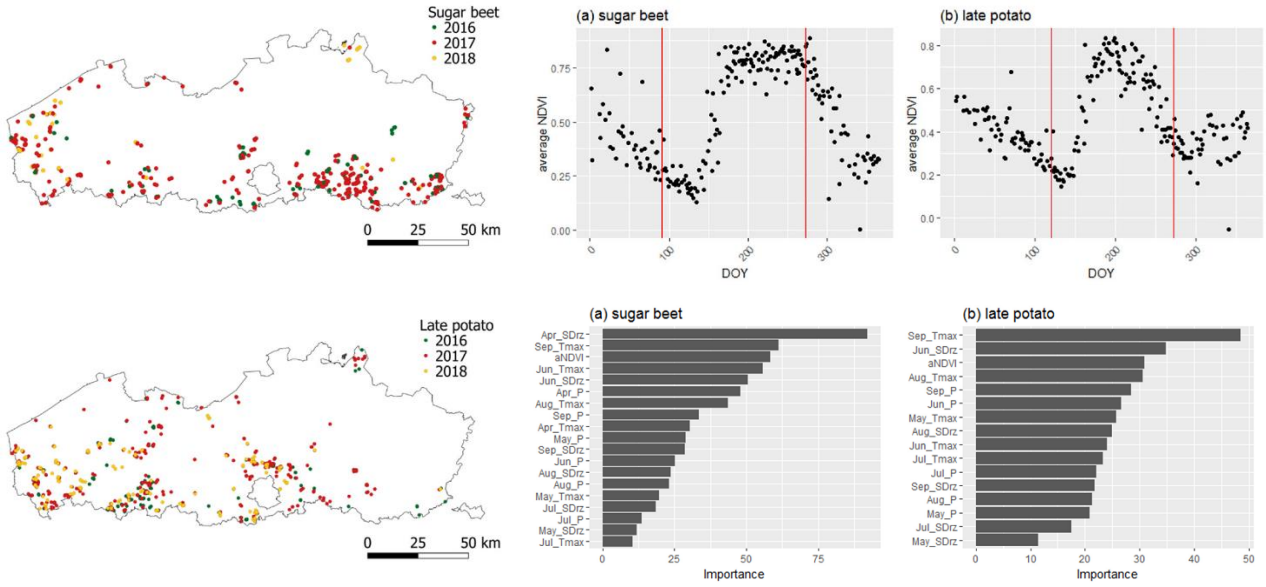

Figure 5. (left) location of sugar beet and late potato fields in northern Belgium; (right top) average NDVI time series of potato and sugar beet fields; (right bottom) monthly variable importance of machine learning models where aNDVI is the integral of NDVI, T is temperature, P is precipitation and SDrz is the rootzone soil-water depletion. Adapted from Vannoppen and Gobin (2022).

The contribution of weather, soil-water dynamics and remote sensing derived vegetation indicators to yield, were investigated with machine learning models to reveal the importance of each of the different contributing factors (Figure 5). The NDVI integral did not explain late potato yield variability and only partly explained sugar-beet yield variability across more than 500 fields during 2016-2018. In combination with rootzone soil-water depletion and maximum temperature during specific months a large part of the yield variability was explained. The method demonstrated that the best models are location and crop specific. The combined modelling methods were commensurate with farm-scale decision making and provided for uniform applications across larger regions.

4 Conclusions

Significant differences between low and high crop yields ($p < 0.05$) were explained by adverse weather conditions during sensitive phenological crop stages (Gobin, 2018), and by extreme dry and wet spells during the cropping season (Gobin and Van de Vyver, 2021). Sentinel-2 derived Normalised Difference Vegetation Index time series did not respond to weather conditions that affected winter wheat yields, but the combination of NDVI, temperature and precipitation explained 66% of the farm wheat yield variability (Vannoppen and Gobin, 2021). Rainfall and temperature during sensitive phenological stages in combination with soil water depletion and NDVI during the growing season explained 85% of sugar beet and 68% of potato farm yield variability (Vannoppen and Gobin, 2022). Machine learning techniques combining weather, soil-water dynamics and remote sensing derived vegetation indicators are promising methods for uncovering the most important variables and for monitoring crop performance at the farm scale across large regions.

Acknowledgements

The research was funded by KU Leuven grant agreement 3E211231 and European Union's Horizon 2020 Research and Innovation Programme, under grant agreements 818346 and 818187.

References

Coles, S., 2001. An Introduction to Statistical Modeling of Extreme Values. Springer Verlag, Berlin.

Durgun, Y.Ö., Gobin, A., Gilliams, S., Duveiller, G., Tychon, B. (2016). Testing the contribution of stress factors to improve wheat and maize yield estimations derived from remotely-sensed dry matter productivity. Remote Sensing, 2016, 8(3), 170. https://doi.org/10.3390/rs8030170

Durgun, Y.Ö., Gobin, A., Duveiller, G., Tychon, B. (2020). A study on trade-offs between spatial resolution and temporal sampling density for wheat yield estimation using both thermal and calendar time. International Journal Of Applied Earth Observation And Geoinformation, 86, Art. No. 101988. https://doi.org/10.1016/j.jag.2019.101988

Gobin, A. (2010). Modelling climate impacts on crop yields in Belgium. CLIMATE RESEARCH, 44 (1), 55-68. https://doi.org/10.3354/cr00925

Gobin, A. (2012). Impact of heat and drought stress on arable crop production in Belgium. NATURAL HAZARDS AND EARTH SYSTEM SCIENCES, 12 (6), 1911-1922. https://doi.org/10.5194/nhess-12-1911-2012

Gobin, A. (2018). Weather related risks in Belgian arable agriculture. Agricultural Systems 159: 225-236. https://doi.org/10.1016/j.agsy.2017.06.009

Gobin, A., Addimando, N., Ramshorn, C., Gutbrod, K. (2021). Climate risk services for cereal farming. Advances in Science and Research, 18, 21-25. https://doi.org/10.5194/asr-18-21-2021

Gobin, A., Van de Vyver, H., 2021. Spatio-temporal variability of dry and wet spells and their influence on crop yields. Agricultural And Forest Meteorology, 308-309, Art. No. 108565. https://doi.org/10.1016/j.agrformet.2021.108565

Kahiluoto, H., Kaseva, J., Balek, J., Olesen, J. E., Ruiz-Ramos, M., Gobin, A., Kersebaum, K. C., Takáč, J., Ruget, F., Ferrise, R., Bezak, P., Capellades, G., Dibari, C., Mäkinen, H., Nendel, C., Ventrella, D., Rodríguez, A., Bindi, M., & Trnka, M. (2019). Decline in climate resilience of European wheat. Proceedings of the National Academy of Sciences of the United States of America, 116(1), 123–128. https://doi.org/10.1073/pnas.1804387115

Lesk, C., Rowhani, P., & Ramankutty, N. (2016). Influence of extreme weather disasters on global crop production. Nature, 529(7584), 84–87. https://doi.org/10.1038/nature16467

Mäkinen, H., Kaseva, J., Trnka, M., Balek, J., Kersebaum, K. C., Nendel, C., Gobin, A., Olesen, J. E., Bindi, M., Ferrise, R., Moriondo, M., Rodríguez, A., Ruiz-Ramos, M., Takáč, J., Bezák, P., Ventrella, D., Ruget,

F., Capellades, G., & Kahiluoto, H. (2018). Sensitivity of European wheat to extreme weather. Field Crops Research, 222, 209–217. https://doi.org/10.1016/j.fcr.2017.11.008

Moore, F. C., & Lobell, D. B. (2015a). The fingerprint of climate trends on European crop yields. Proceedings of the National Academy of Sciences of the United States of America, 112(9), 2670—2675. https://doi.org/10.1073/pnas.1409606112

Porter, J. R., Xie, L., Challinor, A. J., Cochrane, K., Howden, S. W., Iqbal, M. M., Lobell, D. B., & Travasso, M. I. (2014). Food security and food production systems. In Climate Change 2014: Impacts, Adaptation, and Vulnerability. Part A: Global and Sectoral Aspects. Contribution of Working Group II to the Fifth Assessment Report of the Intergovernmental Panel on Climate Change [Field, C.B., V.R. Barros, D.J. Dokken, K.J. Mach, M.D. Mastrandrea, T.E. Bilir, M. Chatterjee, K.L. Ebi, Y.O. Estrada, R.C. Genova, B. Girma, E.S. Kissel, A.N. Levy, S. MacCracken, P.R. Mastrandrea, and L.L. White (eds.)]. (pp. 485–533). Cambridge University Press. https://cgspace.cgiar.org/handle/10568/68162

Schils, R., Olesen, J. E., Kersebaum, K.-C., Rijk, B., Oberforster, M., Kalyada, V., Khitrykau, M., Gobin, A., Kirchev, H., Manolova, V., Manolov, I., Trnka, M., Hlavinka, P., Palosuo, T., Peltonen-Sainio, P., Jauhiainen, L., Lorgeou, J., Marrou, H., Danalatos, N., … van Ittersum, M. K. (2018). Cereal yield gaps across Europe. European Journal of Agronomy, 101, 109–120. https://doi.org/10.1016/j.eja.2018.09.003

Schramm, M., Pebesma, E., Milenković, M., Foresta, L., Dries, J., Jacob, A., Wagner, W., Mohr, M., Neteler, M., Kadunc, M., Miksa, T., Kempeneers, P., Verbesselt, J., Gößwein, B., Navacchi, C., Lippens, S., & Reiche, J. (2021). The openEO API–Harmonising the Use of Earth Observation Cloud Services Using Virtual Data Cube Functionalities. Remote Sensing, 13(6), 1125. https://doi.org/10.3390/rs13061125

Trnka, M., Olesen, J.E., Kersebaum, K.C., Roetter, R.P., Brazdil, R., Eitzinger, J., Jansen, S., Skjelvag, A.O., Peltonen-Sainio, P., Hlavinka, P., Balek, J., Eckersten, H., Gobin, A., Vuceti, V., Dalla Marta, A., Orlandini, S., Alexandrov, V., Semeradova, D., Stepanek, P., Svobodova, E., Rajdl, K. (2016). Changing regional weather-crop yield relationships across Europe between 1901 and 2012. CLIMATE RESEARCH, 70 (2-3), 195-214. https://doi.org/10.3354/cr01426

Vannoppen, A., Gobin, A., Kotova, L., Top, S., De Cruz, L., Vīksna, A., Aniskevich, S., Bobylev, L., Buntemeyer, L., Caluwaerts, S., De Troch, R., Gnatiuk, N., Hamdi, R., Reca Remedio, A., Sakalli, A., Van De Vyver, H., Van Schaeybroeck, B., Termonia, P. (2020). Wheat Yield Estimation from NDVI and Regional Climate Models in Latvia. Remote Sensing, 12 (14), Art.No. 2206. https://doi.org/10.3390/rs12142206

Vannoppen, A., Gobin, A. (2021). Estimating Farm Wheat Yields from NDVI and Meteorological Data. Agronomy-Basel, 11 (5), Art.No. 946. https://doi.org/10.3390/agronomy11050946

Vannoppen, A., Gobin, A. (2022). Estimating Yield from NDVI, Weather Data, and Soil Water Depletion for Sugar Beet and Potato in Northern Belgium. Water, 14(8), Art. No. 1188. https://doi.org/10.3390/w14081188

Weiss, M., Jacob, F., & Duveiller, G. (2020). Remote sensing for agricultural applications: A meta-review. Remote Sensing of Environment, 236, 111402. https://doi.org/10.1016/j.rse.2019.111402

Wright, M. N., Wager, S., & Probst, P. (2020). Package ranger: A fast implementation of random forests [R]. https://www.tandfonline.com/doi/full/10.1080/10618600.2014.983641

Zamani, S., Gobin, A., Van de Vyver, H., Gerlo, J. (2016). Atmospheric drought in Belgium - statistical analysis of precipitation deficit. International Journal of Climatology, 36 (8), 3056-3071. https://doi.org/10.1002/joc.4536

Micrometeorological studies in the Thrace part of Turkey

Levent Şaylan

Istanbul Technical University, Faculty of Aeronautics and Astronautics, Department of Meteorological Engineering, Maslak, Sarıyer, Istanbul, Turkey, e-mail: saylan@itu.edu.tr

Abstract. Specific applied research studies on the exchange of mass and energy between the surface and the atmosphere have been started in Thrace part of Turkey especially since 2009. In this context, our research group aims to understand and increase the basic understanding of atmosphere-biosphere coupling for different surfaces, with practical applications and purposes. In this context, in addition to analysing the effects of climate change on agriculture with models, our research studies have focused on determining the energy and gas fluxes of the surface and their relationships with crop growth indicators such as biomass, leaf area index etc. especially using micrometeorological methods such as Eddy Covariance and Bowen Ratio Energy Balance. In this study, examples will be given from some micrometeorological studies, which we have carried out on different crops (wheat, watermelon etc.) with these micrometeorological methods in Thrace part of Turkey.

1 Introduction

Climate change has occupied an even more important place on the public agenda in recent years. With the effect of the pandemic, the importance of agriculture, and therefore food, has begun to be better understood, especially by those living in cities. The warnings of many national/international institutions and researchers about the possible effects of climate change have become more important today and have contributed to the creation of awareness in the society. Agriculture is one of the most sensitive sectors to climate change and it also affects climate. In this context, many researchers around the world analyse possible impacts of variables such as climate change and/or meteorological, soil, plant, agricultural activities, on yield, water footprint, etc. In addition to this, some of the researchers have focused on the Greenhouse gas exchange over agricultural area. Micrometeorological research on energy and gas transfer has continued to increase with the development of technology, especially after the 1990s. In order to better understand the role of terrestrial ecosystems in the greenhouse gas cycle, micrometeorological methods have been widely used, primarily in developed countries. Today, these methods are used intensively to determine both the emission and sink (storage) amount of greenhouse gases and evapotranspiration (Şaylan et al., 2019).

Greenhouse gas emissions into the atmosphere have been increasing sharply with the industrial revolution. Greenhouse gases are one of the most critical variables on climate researches. For this reason, Greenhouse gas (GHG) exchange between atmosphere and earth surface becomes important with relation to industrial revolution because GHG cause global warming and climate change. In the terrestrial ecosystem, forest and agriculture has one of the key components of global GHG's budget by means of capturing/emission CO_2 from/to the atmosphere.

Terrestrial ecosystems play an important role by sinking of carbon for the national global GHG's budget. CO_2 from the atmosphere is captured by photosynthesis, emitted by respiration and stored by sink (Net ecosystem exchange) within the plant organs. In contrast, there are few studies on this subject for the agricultural crops when compared to the studies on forests. In most of the developing countries the carbon budget of agriculture and forest is calculated according to IPCC values. For his reason, representativeness of the calculated carbon budget should be assessed by comparison with measured data and actual emission and sink coefficients. Energy and gas fluxes over agricultural area are affected by agricultural management like crop rotation, fertilizing, cultivation, irrigation, tillage and meteorological factors. On the other hand, reducing carbon emission from agriculture to atmosphere is an essential subject in global and national greenhouse gas budgets. GHG fluxes from agricultural area are needed to measure in short time interval and continuously and also investigate relationships between meteorological, soil, crop and other variables. In this study, some of the micrometeorological studies are presented which were carried out about the CO_2 and H_2O fluxes over crops in the Thrace part of Turkey. The agricultural production in the Thrace Region in the north-western part of Turkey has been under the effect of various uncontrollable environmental factors, which are mainly meteorological.

The aim of this study is to summarize micrometeorological studies and their results of this subject that have been carried out by us in Thrace part of Turkey so far.

2 Material and Methods

2.1 Study area and measurement systems

Micrometeorological studies are based on an integrated field-and laboratory studies different growing seasons of crops such as winter wheat, watermelon, alfalfa, sunflower crops in the Thrace part of Turkey. In general, the applied micrometeorological studies are carried out at the Atatürk Soil Water and Agricultural Meteorology Research Institute in the Kırklareli city locates at the Thrace part of Turkey.

In these micrometeorological studies, meteorological, soil and plant data were recorded and collected. In this context, agrometeorological and micrometeorological measurement systems were installed in different locations in Thrace, and necessary data for model and CO_2, H_2O fluxes were collected during the development periods. Additionally, agricultural activities were recorded, and the development indicators of crops were measured and observed. The complete agrometeorological measurement system consisted of datalogger, multiplexer (for additional micrometeorological measurements), air temperature/humidity sensors, pyranometer, net radiometer, infrared surface temperature sensor, soil heat flux plates, soil water content sensors, wind speed and direction sensors, rain gauge and soil temperature sensors. Furthermore, the EC system and Bowen Ration Energy Balance systems were installed to measure CO_2 and H_2O fluxes (Figure 1). Phenological stages of crops were observed and recorded during the growing period of crops (Semizoğlu et al., 2011, Şaylan et al., 2012; 2018).

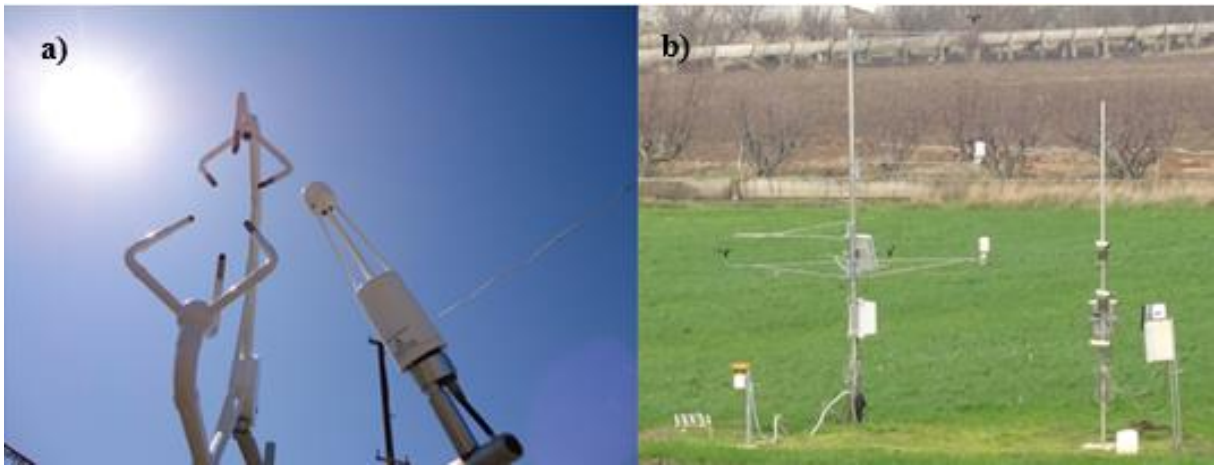

Figure 1: Eddy Covariance system (a); BREB and agricultural meteorological stations (b).

2.2 Eddy Covariance (EC) Method

EC is most widely used method to calculate turbulent fluxes within the atmospheric boundary layer. It bases on the covariance between the concentration of interest and vertical wind speed in eddies (Baldocchi, 2003). Eq. 1 shows the calculation of flux of carbon dioxide (F_{CO2}) according to the EC method (Baldocchi et al., 1998; Foken, 2008):

$$F_c = \rho_a \overline{w' \rho_c'} \quad (1)$$

where; F_c is the CO_2 flux, ρ_a is air density, w' and ρ_c' are the instantaneous deviation from the mean of vertical wind speed and carbon dioxide concentration, respectively (Foken, 2008).

The main output of the EC method is Net Ecosystem Exchange (NEE). Negative values of NEE refers the net carbon accumulation (sink) of the plant. The NEE obtained as a result of the measurements and calculations is fragmented into the Ecosystem Respiration (R_{eco}) values representing the amount of carbon that the plants give to the atmosphere as a result of respiration, and Gross Primary Production (GPP) that shows total carbon production of plants. The relation of these three variable is given in the following Eq. 2:

$$R_{eco} - \mathrm{NEE} = \mathrm{GPP} \quad (2)$$

Detailed information about the EC method can be found in Foken (2008) and Burba (2013).

2.3 Bowen Ratio Energy Balance method

Bowen Ratio Energy Balance (BREB) method based on the following equations:

$$R_n\text{-}G\text{-}LE\text{-}H=0 \quad (3)$$

$$\beta=\gamma(\Delta T/\Delta e)=H/LE \quad (4)$$

$$LE=(R_n\text{-}G)/((1+\beta)) \quad (5)$$

where, β is Bowen ratio, R_n is net radiation (Wm^{-2}); G is soil heat flux (Wm^{-2}); LE is latent heat flux (Wm^{-2}); H is sensible heat flux (Wm^{-2}); γ is psychrometric constant (kPa $^{\circ}C^{-1}$); ΔT is the temperature gradient (^{o}C) and Δe is the vapor pressure gradient (kPa) above canopy surface.

3 CO_2 and energy exchange of crops

In this study, some results of our micrometeorological studies have been presented. First of the EC study has been done on winter wheat in order to estimate CO_2 and energy fluxes between 2009 and 2012 in the Kırklareli city locates at the Thrace part of Turkey. Total NEE, GPP and R_{eco} were estimated as -354.9, 1142.2 and 787.3 gC m^{-2} during the first growing season and -441.3, 1046.8 and 605.5 gC m^{-2} for the second priod of winter wheat, respectively (Fig. 2). GPP/R_{eco}, NEE/GPP and NEE/R_{eco} were calculated as 1.45, 0.31 and 0.45 for the first and 1.73, 0.42 and 0.73 for the second growing periods of winter wheat; respectively. For both growing periods, the relationships between total CO_2 fluxes and biomass of winter wheat were analysed and found a high linear relation between total GPP and biomass (r^2=0.94) for the first growing season. Similarly, high linear relationships between the biomass and total R_{eco} and total NEE were estimated with r^2=0.90 and 0.96, respectively. It showed that total CO_2 fluxes of wheat are strongly related to biomass. That study showed us that the LAI, biomass, NDVI are strongly related to carbon fluxes of winter wheat (Semizoğlu et al., 2011, Şaylan et al., 2012; 2018).

At the same period, we used also BREB method in order to estimate energy fluxes over winter wheat, sunflower and maize crops (Fig. 3) (Şaylan et al., 2012, Başakın et al., 2021). Later EC method was used to measure CO_2/H_2O fluxes over watermelon in 2012 (Fig. 4). The average daily emission value of the watermelon was determined as 6.56 g Cm^{-2} and the sink value was determined as 2.31 g Cm^{-2}. Additionally, the measurements and analyses showed that total gross photosynthesis (GPP) of watermelon was 1160.2 g Cm^{-2} (4246.3 g CO_2m^{-2}), whereas total ecosystem respiration (R_{eco}) was 846.35 g Cm^{-2}. Furthermore, total net ecosystem exchange (NEE) (sink) was determined as -299.03 gCm^{-2} (-1094.45 g $^{-2}$) for watermelon. The daily average GPP, NEE and R_{eco} values were determined as 8.99, -2.31 and 6.56 gCm^{-2} (Aslan, 2014; Şaylan et al., 2019).

Then once again from 2013 to 2014, we have concentrated again on winter wheat CO_2 fluxes by the Eddy Covariance method (Fig. 5). Total NEE, GPP and R_{eco} values between the years 2012-2014 are found as 502.75, 2114.50, 1611.75 gCm^{-2}, respectively. Total NEE, GPP and R_{eco} were -383.94, 1222.17, 838.23 gCm^{-2} for the growing period of winter wheat; -105.14, 671.92, 566.78 gCm^{-2} for the straw and -13.67, 220.41, 206.74 gCm^{-2} for the bare soil, respectively (Yeşilköy et al, 2014; 2017). After that EC research was carried out over sunflower, canola, alfalfa. We are still measuring CO_2/H_2O fluxes over alfalfa during last 3 years by EC method at the same location.

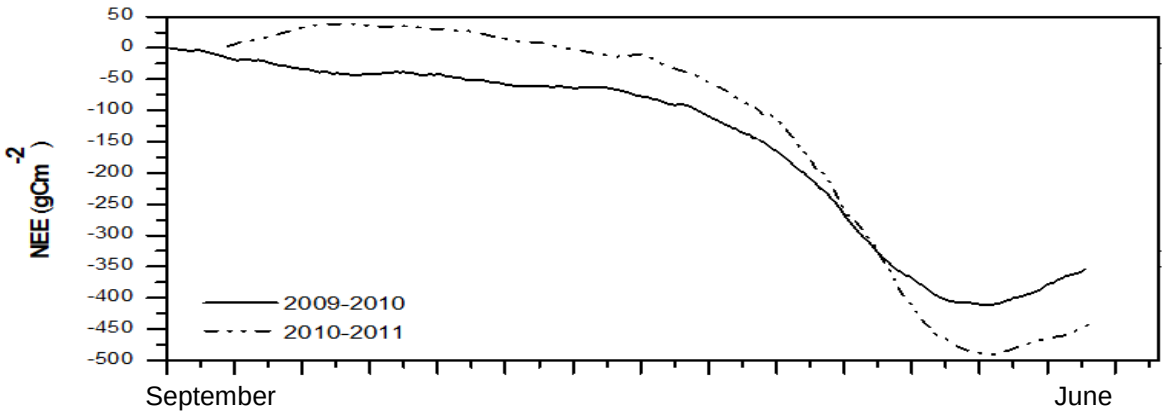

Growing period

Figure 2. Variation of CO_2 fluxes during two growing periods of winter wheat (Şaylan et al., 2012, 2018).

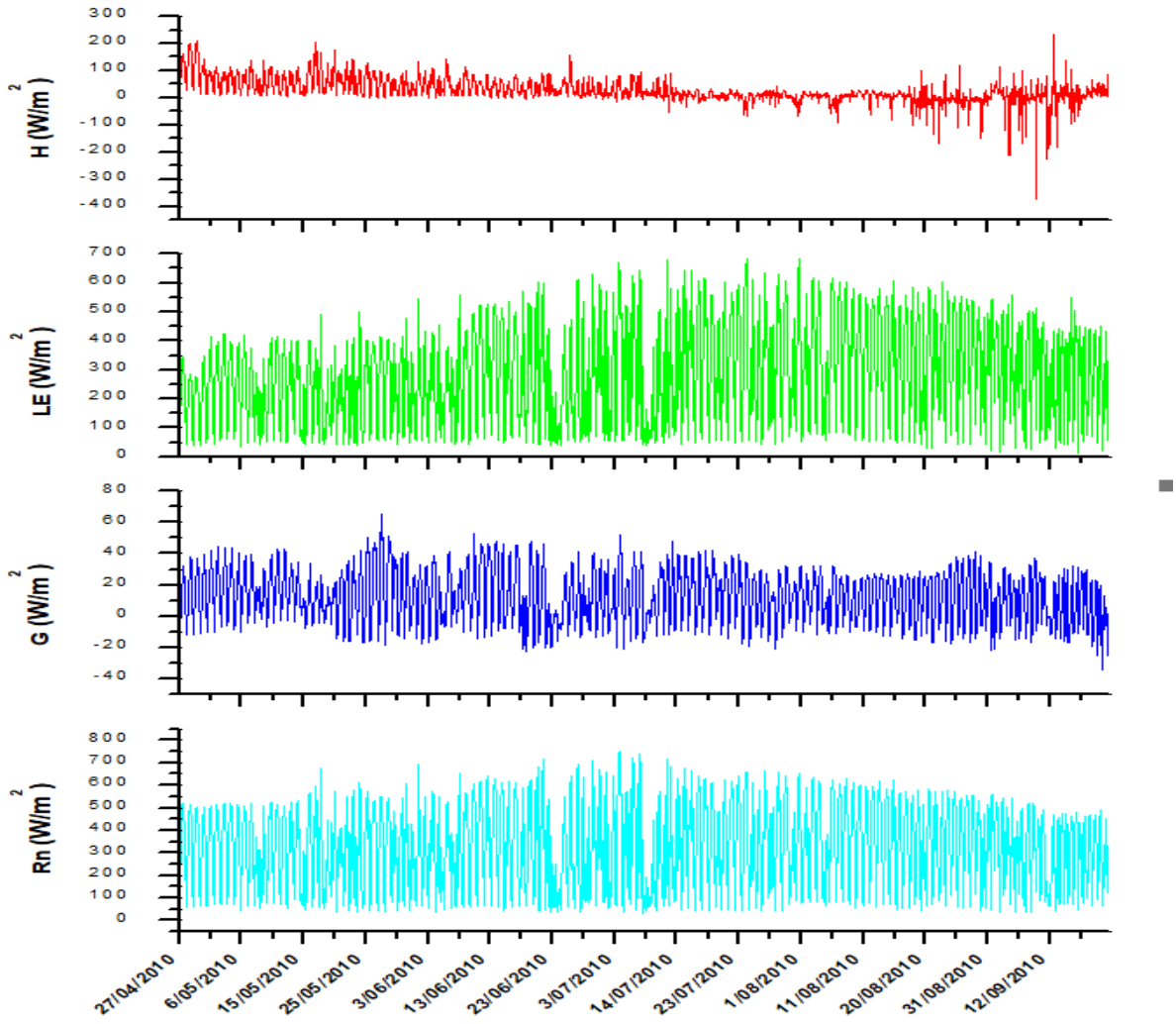

Figure 3. Variation of energy balance components during the growing period of maize (Şaylan et al., 2012).

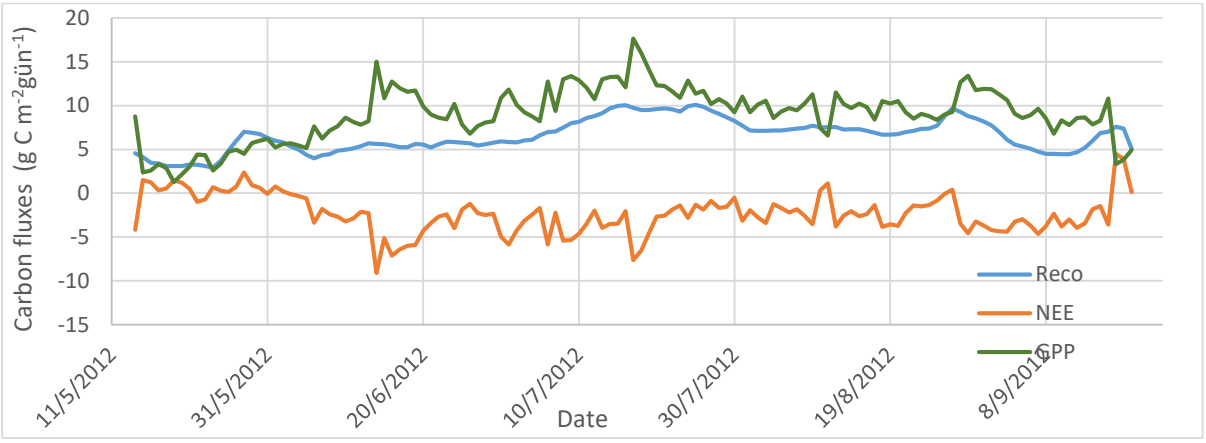

Figure 4. Variations of NEE, GPP and R_{eco} during the growing period of watermelon (Aslan, 2014; Şaylan et al., 2019).

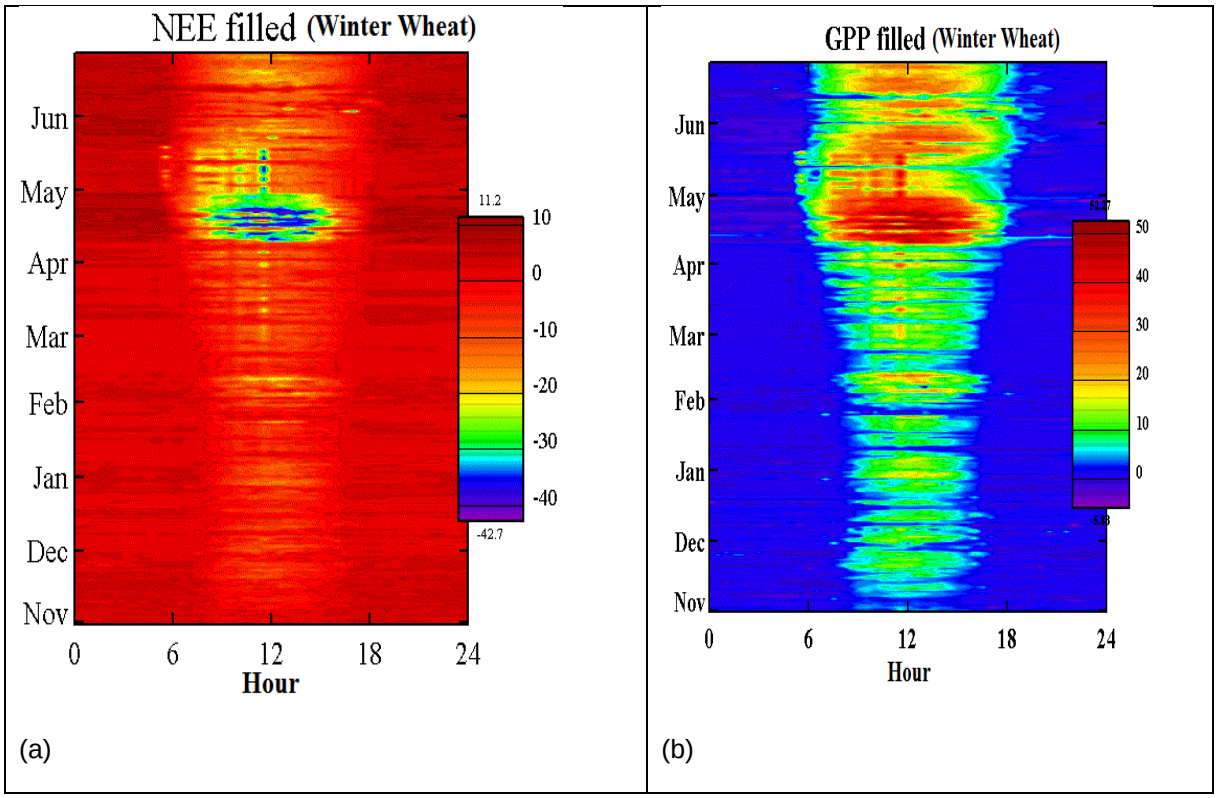

Figure 5. a) NEE b) GPP exchange during the growing period of winter wheat (Yeşilköy et al, 2014; 2017)

4 Conclusion

In this study, some micrometeorological studies on plants and their results, which we started especially in 2009 in the Thrace part of Turkey, are explained. It is possible to carry out these applied studies on other plants in the future. In these studies, only energy and gas flux measurements were made. Also, correlations were found between these fluxes and meteorological factors and plant growth indicators. More data and therefore longer-term studies are needed to find better relationships and develop a model in the future. We also have efforts to expand flux studies to gases other than CO_2 and H_2O, to perennial plants in agricultural areas, and to forests.

Acknowledgements

I would like to thank Istanbul Technical University (BAP), Atatürk Soil Water and Agricultural Meteorology Institute and COST CA20208 for their supports. In addition, I would like to thank Dr. Fatih Bakanoğulları, Assoc. Prof. Barış Çaldağ, Toprak Aslan, Dr. Serhan Yeşilköy, Nilcan Altınbaş, Merve Kızıl Aydın and all the employees who contributed to the project from the Atatürk Soil Water and Agricultural Meteorology Research Institute.

References

Aslan, T., 2014. Determination of CO_2 and H_2O fluxes of vegetation surface by Eddy Covariance Method, Master's Thesis, Istanbul Technical University, Atmospheric Sciences Program (in Turkish).

Baldocchi, D. and Meyers, T., 1998. On using eco-physiological, micrometeorological and biogeochemical theory to evaluate carbon dioxide, water vapor and trace gas fluxes over vegetation: a perspective, Agric. For. Meteorol. 90, 1-25.

Baldocchi, D., 2003. Assessing the eddy covariance technique for evaluating carbon dioxide exchange rates of ecosystems: past, present and future. Global Change Biol. 9, 479-492.

Başakın, E.E., Ekmekcioğlu, Ö., Özger, M., Altınbaş, N. and Şaylan, L., 2021. Estimation of measured evapotranspiration using data-driven methods with limited meteorological variables: Estimation of evapotranspiration, Italian Journal of Agrometeorology.

Burba G., 2013. Eddy Covariance Method for Scientific, Industrial, Agricultural and Regulatory Applications. LI-COR Biosciences.

Foken, T., 2008. Micrometeorology, Springer, Heidelberg, Berlin.

Semizoğlu, E., Şaylan, L., Çaldağ, B. ve Karayusufoğlu, S., 2011. Assessment of Relationship between Winter Wheat Carbon Exchange and Vegetation Dynamics", 10th European Conference on Applications of Meteorology, 12-16 September, Berlin, Germany.

Şaylan, L., B. Çaldağ, F. Bakanoğulları and Kaymaz, Z., 2012. Determination of CO_2 and H_2O and Energy fluxes of wheat crop, TUBITAK Project, Final report (in Turkish).

Şaylan, L., Ceyhan, E. S., Bakanoğulları, F., et al., 2018 Analysis of Seasonal Carbon Dioxide Exchange of Winter Wheat Using Eddy Covariance Method in the Northwest Part of Turkey, Italian Journal of Agrometeorology-Rivista Italiana di Agrometeorologia, 23, 3, 39-52.

Şaylan, L., Aslan, T., Akataş, N., Yeşilköy, S., Çaldağ, B., Bakanoğulları, F., 2019. Assessing greenhouse gas exchange of agrıcultural crops by flux measurements in Thrace part of Turkey. AGROFOR International Journal.

Yeşilköy, S., Akataş, N., Çaldağ, B. and Şaylan, L., 2017. Comparison of modeled and measured CO_2 exchanges over Winter Wheat in the Thrace part of Turkey", FEB – Fresenius Environmental Bulletin, 26 (1), 93-99.

Yeşilköy, S., Şaylan, L., Semizoğlu, E. and Çaldağ, B., 2014. Carbon Capture, Storage and Emission: A Case Study for Winter Wheat in Kırklareli/Turkey, Asia Oceania Geosciences Society, 11th Annual 11. Meeting, 28 July-1 August, Sapporo/Japan, 235 pp.,

"EXPLORING WEAKNESSES AND PROSPECTS FOR THE SUSTAINABLE RURAL DEVELOPMENT THROUGH SMART FARMING TECHNOLOGIES"

Evagelia Koutridi[1*#], Olga Christopoulou[2]

[1]Ph.D Candidate Department of Planning and Regional Development, School of Engineering, University of Thessaly, ekoutridi@uth.gr
[2] Professor Department of Planning and Regional Development, School of Engineering, University of Thessaly, ochris@uth.gr

ABSTRACT
Expanding the agricultural production in an environmentally sustainable way largely depends on the advances of technology and innovation research, while the guidelines provided for the new strategic solutions for agricultural growth, the increase of efficiency and effectiveness of production, will assist the actors/stakeholders in a successful transition towards the digitalization of the sector. The study of the adoption and diffusion of new Smart Farming Technologies (SFTs) in the production of plant and animal products in the previous decades in agricultural economics with emphasis on technological change and innovation, had led to the need to study and understand the role of actors/stakeholders aimed at policy making and marketing practices that would favour the three objectives of sustainable rural development. Therefore an Impact Assessment is in need in order to understand the issues involved in the adoption and diffusion process. In order to predict, analyze and assess the likely impact pathways, an empirical study was conducted among three groups of stakeholders- researchers, politicians and professionals in Greece. Furthermore if the goal is the sustainability (balanced socio-economic and environmental development) the multidisciplinarity of the involved scientists should (a) assist policy decisions as to be of use to the application to rural strategic planning and (b) contribute professionals' in designing, developing and implementing products. With the use of qualitative and quantitative statistical methods, the results not only indicated the challenges rural areas face in relation to the adoption and diffusion of SFT in Greece, such as lack of strategic planning and necessary infrastructures, but also revealed the main drivers for underdevelopment and environmental degradation in those areas which are, of low income and creditability, minor environmental consciousness. Finally the gap between the means (Research and Development) and the goal (sustainable rural development) was affirmed, which probably lays beneath the lack of communication and feedback between the stakeholders. Furthermore this research indicated that rural' area civic involvement in Greece should be studied in order to stimulate rural development perspectives.
Keywords: Sustainable Agriculture, Impact Assessment, Stakeholders, Strategic Rural Planning, Quantitative Analysis, Smart Farming Technologies

1 Introduction

Rural areas are places of great importance for the economy of a country, the well-being of its people; they are carriers of culture and tradition, but of low population density and many other resultant structural and fundamental problems. Sustainable management in Agricultural Systems is crucial for rural development and the research on Smart Farming Technologies (SFTs) seems to be advancing towards that direction. Furthermore, the vulnerability of agricultural systems to weather will increase the frequency of extreme events e.g. droughts, heat and cold waves, associated to climate changes, scarcity of natural resources, soil degradation, environmental pollution, etc. All these raise up the need of the adjustment of the agricultural practice management measures (Stocker et al., 2014). The different actors (stakeholders) who manage the countryside (landowners, farmers, villagers, politicians, etc.), having different beliefs, interests, values and goals regarding landscape conservation, resource management and the goodwill they wish to receive are in constant conflict and its result is reflected in all the elements that make up the countryside (Scherr, et al., 2014). For example, water is the protagonist in many rivalries or synergies of the partners (actors) that concern its disposal, its use or even its pumping (Boelee, 2013).
Expanding the agricultural production in an environmentally sustainable way largely depends both on the advances on technology and innovation research. The guidelines provided for the new strategic solutions for agricultural growth and the increase of efficiency and effectiveness of production will assist the actors/stakeholders in a successful transition towards the digitalization of the sector (Araŭjo, et al, 2021).

The study of the adoption and diffusion of new technologies in the production of plant and animal products in the previous decades in agricultural economics with emphasis on technological change and innovation, had led to the need to study and understand the role of actors / stakeholders) aimed at policy making (Pannell & Claasen, 2020) and marketing practices (Norton & Alwang, 2020) that would favour the three objectives of sustainable rural development of the rural area (Figure 1).

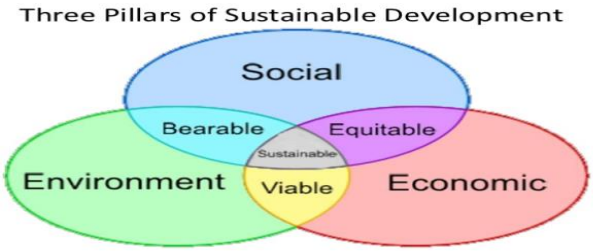

Figure 1. Three objectives of Sustainable Development and their desirable benefits **SOURCE:** VAQAR AHMET SUSTAINABLE DEVELOPMENT POLICY INSTITUTE (SDPI)

Smart Farming or Smart Agriculture is one of the agricultural systems of Sustainable Intensification (SI) (Pretty, et al., 2014). In these agricultural production systems: "crop yields are increased without adverse environmental effects and without cultivating more land" (The Royal Society, 2009). In order to achieve economic, environmental and social results, various partners will have to engage in actions from the level of exploitation (farmers), to the regional level (farmers' associations, investors) to the state level (researchers, companies, public sector). All these partners are therefore also participants in the effort for the Sustainable Rural Development. In a recent (2019) bibliometric study Klerkx, Jukkub & Labarthe on the contribution of sociological studies to the Smart Farming technologies (SFTs) and Agriculture 4.0, identified five thematic clusters of extant social science literature on digitalization in agriculture, one of which concerns the Economics and management of digitalized agricultural production systems and value chains, (Klerkx, et al, 2019).

The technological impetus of Smart Farming Technologies in the agricultural production process, have started as a First Generation Innovation Model, as it has been defined by Rothwell in 1994; a simple linear sequential process that was based on research in new technologies and their development in a productive environment (R&D). However, by the introduction of information and communications technologies systems (ICT systems) and the diffusion of technology, in the frame of sustainability it evolved at Networking- a Fifth Generation Framework of Innovation Modeling, i.e. in a process which emphasizes on knowledge accumulation and external linkages, systems' integration and extensive networking which leads to development efficiency. Feedback and review lead to pervasive innovation. That's why "actors"- those who have the power to implement change (the innovation) and "stakeholders"- those who have direct or indirect interest in the area should be involved in the process of eco-friendly management of Agricultural systems, along with the evolvement and use of SFTs', in order to generate Sustainable Rural Development.

Therefore, an empirical study was conducted among three groups of stakeholders- researchers, politicians and professionals in order to explore the weaknesses and prospects of adopting SFT aiming to sustainable rural development. Rural development requires the insights of several established disciplines or traditional fields of study and needs to be connected to politics in order to achieve successful results, so this approach was implemented. More over if the goal is balanced socio-economic and environmental development- Sustainability- the multidisciplinarity of the involved scientists should assist policy decisions and be of use to the application to Rural Strategic Planning.

So first looking for the dynamics of the relationship in Greece between research, policy and practice in the sector of policy making for sustainable development, then the feedback between actors/stakeholders and network interactions for network transition to a sustainable rural development in the Greek rural area and having as a bibliographic precedent the perceptions of farmers as they have been recorded in the research program SmartAKIS (2019), the empirical study was conducted with the use of a structured questionnaire among three groups of stakeholders: researchers, politicians and professionals.

The presented research was based in a Qualitative Thematic Analysis to explore the profile of Greek rural areas. A Qualitative Content Analysis to investigate the multidisciplinarity in strategic Rural Policy Planning

and stakeholder's participation in Rural Policy Making. That's for a structured questionnaire was addressed to three groups of actors/stakeholders:

- scientists/researchers,
- politicians/policy makers and
- professionals/entrepreneurs

The sample was unstandardized within the groups, insofar as that they were willing to participate and had the experience and the knowledge to answer the questionnaire.

The research took place via google forms between March and August 2021.

All of the twenty researchers that responded are distinguished in their field of expertise- from rural development, environmental science, spatial analysis, economics and sociology, to agriculture, surveying, and computer science. They all are familiar with the topic, even more the majority of them have participated in research projects on SFTs or Precision Agriculture. They are occupied in university research laboratories (mainly), the Greek Agricultural Organization "Demeter" (former National Agricultural Research Foundation) and the Centre of Research and Technology Hellas (CERTH).

The politicians that participated represent (a total of five answers) the four of the six Greek Parliament parties and the Hellenics Republic Ministry of Rural Development & Food, while policy makers category include a respond from the Natural Environment and Climate Change Agency (a Legal Entity of Private Law supervised by the Ministry of Environment and Energy), another respond from the Geotechnical Chamber of Greece and executive's (a total of five answers) from the Specialised Management and Implementation Authority for the Rural Development Programme of Greece and the Payment and Control Agency for Guidance and Community Aid.

Finally five entrepreneurs and professionals at the fields of Smart Agricultural applications, the UAV's industry and the Precision Agriculture appliances replied to the survey conducted.

The participants were asked to describe the profile of Greek rural areas and the weaknesses that led to underdevelopment and environmental degradation. They were called to set their experience to the topic of the existence of multidisciplinarity to Rural Strategic Planning and the necessity of coexistence of the stakeholders' during the process of Rural Making. Finally they were requested to determine the significance on research of SFTs' and relative policies, as a prospect to stimulate rural development perspectives.

A total of thirty-eight responses have been collected in order to explore and understand their perspective, knowledge and thoughts of rural development under the scope of SFTs. Their views and perspectives on Greek rural profile were categorized and then merged into key themes according to similarities, under the Thematic Analysis Method. The generated themes are presented with spider maps. Their insights on the topics of multidisciplinarity and the participation of the stakeholders in Rural Policy making and the interpretations of the groups were analyzed with the Content Analysis Method and there are presented using the concept mapping approach. The maps were created with Lusidchart. The charts with Microsoft excel 360. The notions that were mined were depicted in word clouds with Word Art.

2. Exploring Weaknesses in Geek Rural Areas

2.1 Qualitative Thematic Analysis *Current situation and special conditions formed in Greek rural areas*

The qualitative analysis of the questions regarding the established situation in the Greek rural areas showed 40 repeatable notions as showed in the word cloud bellow (Figure 2) that were categorized into four Themes after the processing.

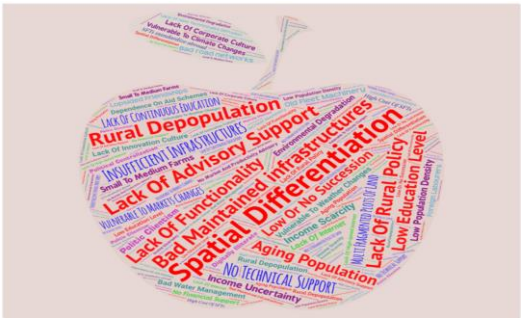

Figure 2: Notions that form the profile of Greek rural areas according to the responders (created in wordart.com)

As of the connotation the themes that were generated reflect the features that could orient science to form policy decisions and initially benefit society (Pannell, et al., 2018). Those themes are:

1st THEME: Environment existing conditions and Spatial connected conditions formed in rural areas

2nd THEME: Infrastructures' issues connected with existing conditions in rural areas

3rd THEME: Policy related issues connected with existing conditions formed in rural areas

4th THEME: Social conditions formed in rural areas (Figure 3).

The 1st THEME that arises is the shaped situation out of the space affected conditions, thus why the first notion that came out of word mining was Spatial Differentiation (Figure 3).

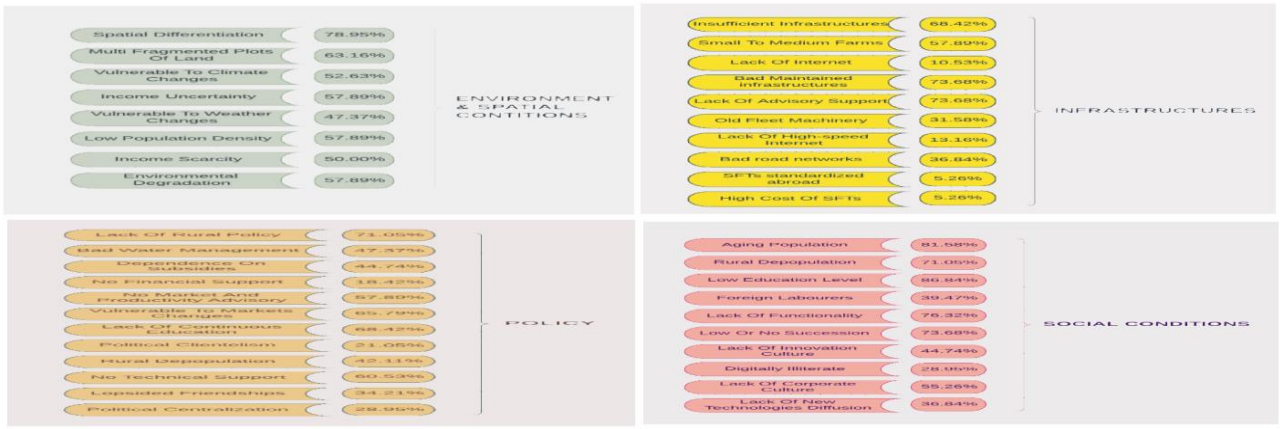

Figure 3: 1st to 4th THEMES generated from the question about the profile of Greek rural areas and special conditions that detain development (created by Lusidchart)

The 2nd Theme was dedicated to infrastructures', thus the backbone of rural economy. Responders noted their absence mainly. They all agree that basic infrastructures' are insufficient or bad maintained and they strongly agree that there is lack of advisory support to people that perform agriculture and animal husbandry.

Policy is crucial regarding development, so there is an all Theme- the 3rd, which deals with policy actions that the responders believe that have a large impact to rural Greek areas, since it's the most popular noted subject. Especially lack of rural policy reaches the top of the theme. Noteworthy in this theme were lack of continuous education of farmers and vulnerability to market changes as well as advisory on productivity and marketing.

Social conditions are omnipresent, constantly encountered and a wide-ranging Theme regarding rural development. The highest score marked in population aging and low education level which leads- according to the majority of the respondents to lack of functionality, lack of innovation and corporate culture. The forth most common answer is connected to aging population, since it is the low rates or complete lack of succession in the farming business. Rural depopulation is present here in this theme, because it's connected to social climbing unlike the 3rd theme that it's connected with rural policies. As expected foreign laboring and lack of technologies' diffusion mark high scores, even if they are low in scale. Overall the social impact in the profile of Greek rural areas is widely discussed.

3. Exploring Prospects in Geek Rural Areas

3.1 Qualitative Content Analysis on multidisciplinnarity in Rural Policy Planning and stakeholder's participation in Rural Policy Making

The participants were asked about the existence of multidisciplinarity in Greek rural policies planning as well as stakeholder's participation in rural policies making and were endorsed to justify their response. The most popular answer within the group A (scientists/researchers) regarding multidisciplinarity is that there is no possibility for that issue because politicians knowingly adopt or adhere to collusive interests of a privileged elite which facilitates the coordination of their political status (Figure 4).

Their opinions shape a political clientelism and centralized state status that works without considering the reconstruction of rural areas or the strategic rural planning and mostly act conjecturally. Group B (politicians and policy makers), divides into three subgroups by their answers. They all agree that multidisciplinarity is a prerequisite. A part of them believes that a NEXUS approach is what is missing, where, another part is talking about a gap in the coexistence of scientists and politicians and that an attempt is made towards it extracted by the EU rural planning program. There is a political party that strongly believes that that is non

compatible with the politics' planning itself. Finally, there is the opinion of another political party, which, out of its political points of view, claims that scientific research is driven from the capital system in order to undermine a holistic scientific approach to the subject (e.g. social needs, environmental protection, etc.). The second most popular view of the subject is coming from the policy makers within the group. They believe that there is a known lack of connectivity between research and development in Greece. It is established through the fact that research's findings' are not connected together and, especially, aren't interconnected with the actual act of farming. They support the idea that there has to be an interaction between policy makers and researchers so that innovation process could be accomplished. From another point of view a lot of them believe that there is no central coordination towards multidisciplinarity or not wish to participate in, due to bad past experiences.

Professionals and entrepreneurs strongly believe (4 out of 5 answers) that there is no multidisciplinary approach to rural policy planning and the one that is differentiated from the others, does that out of the belief that multidisciplinarity is not the dominant and determining factor in the right or wrong choices in Greek state's rural planning.

The concept map (Figure 4 (a)) depicted all the participant groups' insights'. The lines are simple because they have no hesitation about their thoughts; their answers all are firm and strict.

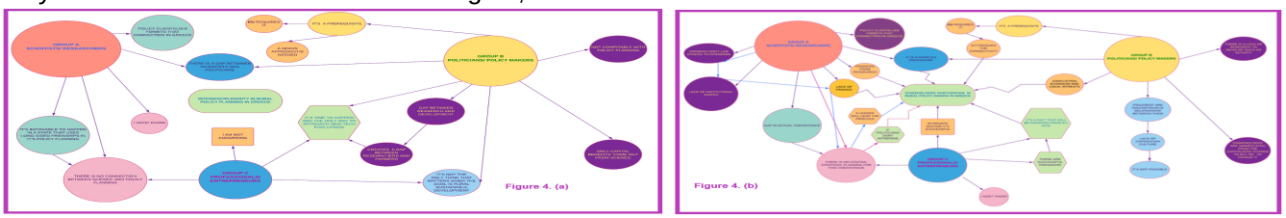

Figure 4: Concept maps generated from the question about the multidisciplinarity (a) in rural policy planning and the possibility of stakeholders' participation in rural policies making (b).

The three groups were asked if there is feasibility for stakeholders' (Producers-Researchers-Local actors-State-Traders-Consumers) to participate in rural policy making in order to be achieved economic, environmental and social results by the use of SFTs. Although the great majority answered positively to stakeholders' participation (Figure 4 (b)), they strongly believe that the whole process will be complicated, because fundamental, financial, and behavioural problems exist. All of them point out the need to that coexistence due to European's Union requisition in order to "Farm to Fork" strategic policy to succeed. There are two political parties that differentiated driven by their political principals. The one believes that there is a lack of systematic research in the field of participatory processes. The other believes that stakeholders' act in favour of the capitalistic system and if they don't, they are doomed to fall apart.

They all have set important issues towards the implementation of stakeholders' participation, mostly driven by the fact that they really want it to happen. A few scientists stated their differentiation since they believe that it's impossible for farmers to be represented in that scheme due to the lack of organized representation and their scepticism towards the state.

3.2 Quantitative Analysis on the research priorities on SFTs and Rural Development

The participants were requested to determine SFTs research priorities with the use of a five point Likert scale and the answers were statistically analyzed using SPSS 26. Descriptive statistics were performed to present sample characteristics and inferential statistics were applied to further reveal significant patterns in the data and test hypotheses. Specifically, Levene's test examined the homogeneity of variances followed by the ANOVA test which detects significant differences in the mean scores regarding the level of agreement between the groups (Figure 5).

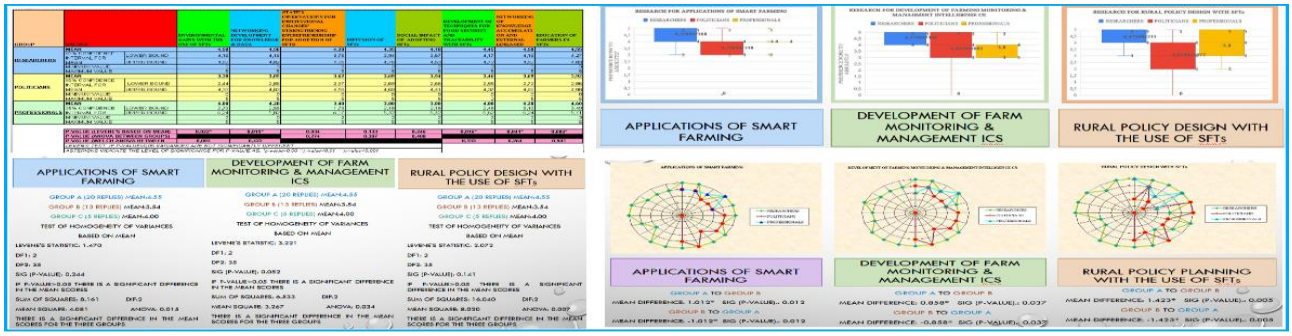

Figure 5: Descriptive statistics, Inferential statistics and Multiple Comparisons about the research priorities on SFTs and Rural Development

The groups' scientists/researchers and politicians/policy makers disagree in the research advance of the two technical subjects posed, vis Smart Farming Applications and Farming Monitoring & Management Intelligence Computer Systems (FIMMCS). Moreover, they strongly disagree that research should focus to engage SFTs in rural policy design. Findings indicated a gap between those groups that should be investigated even more thoroughly. Results suggested that all groups strongly agree that SFTs research should advance towards environmental gains, state's intervention for adaptation, diffusion, farmer's education, food security & traceability and social impact from adopting.

4 Conclusions

The themes and patterns that revealed by the exploratory process of the method followed, affirmed the research questions of the scope and moreover in the process of collecting the data and during the approach of the participants there was a highlight that emerged. The ones that didn't respond into particular questions, systematically preferred not to expose their thoughts out of the belief that, Smart Farming Technologies are not in need of the people of Greek rural areas. They believe that the implementation of the three groups that participated should focus on social and economic revises of the policies applied and to upgrade the existing infrastructures -rather than to embed innovation processes in food production- in order to build resilience to risks and to increase productivity of the sector. Environment's protection was the least discussed topic, since most of them focus in economy and society when they analyze a subject e.g. about rural making involving stakeholders' participation. The Concept mapping method is sufficient enough to create a visual representation of the perspectives and insights from each group. There would be interesting if the social connections between the respondents would be explored, but that wasn't acceptable from the participants. The social network analysis illustrates and quantifies the connections between the responders or the lack thereof. Although the two methods seem to differ, both of them in a similar way underlay data structures thus a network of relationships between data elements, so the rural area and civic involvement should be studied so as if to stimulate Rural Development perspectives.

References

Araŭjo, S. O.; Peres, R. S.; Barata, J.; Lidon, F.; Ramalho J. C.; 2021. Characterising the Agriculture 4.0 Landscape- Emerging Trends, Challenges and Opportunities. *Agronomy*, 11, 667.https://doi.org/10.3390/agronomy11040667

Boelee E.; 2013. *Managing Water and Agroecosystems for Food Security.* Oxford: CAB International.

Klerks L.; Jakkub E.; Labarth P.; 2019. "A review of social science on digital agriculture, smart farming and agriculture 4.0: New contributions and a future research agenda" NJAS - *Wageningen Journal of Life Sciences* 90–91

Norton, G.; & Alwang, J.; 2020. Changes in Agricultural Extension and Implications for Farmer Adoption of New Practices. *Applied Economic Perspectives and Policy*, 1, pp. 8-20.

Pannell, D.; & Claasen, R.; 2020. The Roles of Adoption and Behavior Change in Agricultural Policy. *Applied Economics Perspectives and Policy*, 1, pp. 31-41.

Scherr, S.; Buck, L.; Willemen, L.; & Midle, J. C.; 2014. Ecoagriculture: Integrated Landscape Management for People, Food, and Nature. In: N. V. Alfen, ed. *Encyclopedia of Agriculture and Food Systems, Vol. 3.* San Diego: Elsevier, pp. 1-17.

Smart AKIS Regional Reports Final; 2019. At SmartAkisHub published on line Available at: https://www.smart-akis.com/wp-content/uploads/2018/08/GREECE_RIW_Report.pdf (Accessed 28/08/2021).

Stocker, T.F.; Qin, D.; Plattner, G.K.; Tignor, M.M.; Allen, S.K.; Boschung, J.; Nauels, A.; Xia, Y.; Bex, V.; Midgley, P.M.; Climate Change 2013: The Physical Science Basis, In Working Group I Contribution to the Fifth Asessement Report of the Intergovernmental Panel on Climate Change (IPCC), Cambridge University Press, Cambridge, UK.

The Royal Society.; 2009. *" Reaping the benefits: science and the sustainable intensification of global agriculture",* London: s.n.

BTS signal multi-frequency passive monitoring for rainfall detection

Peter Fabo[1], Pavol Nejedlik[2], Michal Kuba[1]
[1]Alexander Dubcek University of Trencin, Trencin, SK
[2]Earth Science Institute of Slovak Academy of Science, Bratislava, SK

Abstract

Rainfall interfere with electromagnetic signals in the atmosphere. Signal changes can be detected either by detecting the attenuated part of the signal or by a receipt of the different changes in the signal. The first method requires knowledge of the signal parameters and is attached to the wavebands over 10 GHz using usually the microwave links. These demands are fulfilled at meso-meteorological scale at the dimension of a few kilometers usually only in restricted areas. On the other hand, there is a net of base transceiver station (BTS) of mobile network operators which covers in populated areas each square kilometer by respective signal at the waveband of about 1 GHz. Signal attenuation is basically completely lost in the noise at this band.
This paper presents a novel concept of how phase differences between two signals at about 1 GHz arriving at two different antennas can be used to detect precipitation. Based on the utility model of the receiver system measuring parameters of multispectral electromagnetic smog data the time of occurrence and intensity of hydrometeors in the boundary layer were detected and evaluated. Experimental measurements showed the possibility to detect the presence of precipitation in the atmosphere with high spatial resolution in real-time by variations of the signal phase. Phase variations out of the rain periods are much less developed. This gives the opportunity to detect the liquid water in the air and also to monitor the changing rain intensity. Although the results interpret the precipitation occurrence only in a qualitative form so far, they express a certain quantitative view regarding the rain intensity fluctuations. Liquid water in the atmosphere can be detected along the path line of the sight between the signal source and the receiver in a distance of a few kilometers.

Introduction

Hydrometeors occur in the atmosphere both in liquid state or as solid particles and in different forms. There are different methods to detect atmospheric hydrometeors. One of them is based on the changes of the electromagnetic signal penetrating the atmosphere. Use of remote sensing for hydrometeors detection is represented mostly by satellite and radar methods of the detection. Both of them are able to monitor the precipitation on large areas in close to real time but their products suffer with lower level of resolution and further to that earth curvature and ground obstacles make close to ground spaces invisible for radar signal. The development of communication and radar techniques has brought further possibilities to use the signal of different broadcasters for the detection of atmospheric properties, the hydrometeors at first. These methods developed already in the end of the first half of previous century (Atlas and Banks 1951) are based on the signal attenuation and/or reflection. Weather impacts brings some difficulties for the telecommunication services providers which they are trying eliminate. Using the corrections in order to compensate the attenuation of the signal was one of the first methods to detect atmospheric precipitation at about 10 GHz band. Different experiments were done using microwave link networks in the Netherlands and Israel (Leijnse *et al*., 2007; Zinevich *et al*., 2008, Overeem et al. 2011). The results of such measurements were compared to the data measured by rain gauge sets also by other authors (Fencl et al. 2015, Rios Gaona *et al*.2018). Electromagnetic signal of lower frequencies was not used for rain detection so far as it is heavily attenuated and from about 5 GHz it is practically overlapped by noise and any detection of signal attenuation is lost Fig. 1.

Figure 1 Signal attenuation caused by rainfall. Source: Fagiani, A. et al. 2018.

The experiments at the frequencies 10+ GHz showed good results in rainfall detection but a disadvantage of these methods is the lack of the appropriate broadcasters. Further to that the knowledge of the appropriate technical parameters of the signal is necessary for the evaluation of signal attenuation. On the other hand, there is an explosion in the number of broadcasters of mobile service operators in last 20 years basically fully covering densely populated areas by the signal in UHF band. There are activities to use this band for hydrometeors detection (Kuba et al. 2018).

Methods

Mobile service operators usually use the UHF band which covers the frequencies from a hundreds of MHz to a few GHz. This posted a question of using these bands for possible atmospheric property detection. An experiment showed that the mean value of the received signal in these bands includes the noise component which represents interference patterns – reflected and dispersed part of the signal from the surrounding including the atmosphere. The point is to consider if this part of the signal carries an information about the atmospheric properties and possibly to find the way how to use it for a certain interpretation of this properties in sense of atmospheric precipitation. Noise components of an electromagnetic signal coming from one source to two different antennas which are a few wavelength apart one from the other do not correlate. First Fresnel zone is created in the space where signal is propagating. Theoretically, we can assume a correlation of noise components in the part of overlapping Fresnel zones at the output of the antennas due to the inhomogeneity in the respective space of atmosphere. To verify above mentioned theoretical assumptions a signal of BTS station transmitter broadcasting at 935 MHz was used. The experiment happened at a meteorological observatory with 200 m meteorological mast. The transmitter was placed at the mast 30 m above ground and the respective 2 antennas were placed at a roof of an administrative building at a distance of approx. 150 m from the mast. A coherent SDR receiver with two channels brought the signal to a computer for further data processing and evaluation. Data rate from SDR receiver to the computer reaches 400 Mbyte/sec. This produces an enormous amount of data. That is why only one data block of 20 millisecond duration out of each second was processed. In order to compensate the unwanted internal phase shifts caused by the differences in the frequency response of both SDR channels and different lengths of the antenna cables the computer simultaneously handles the measurement configuration by switching the channels by a multiplexer (Fig. 2).

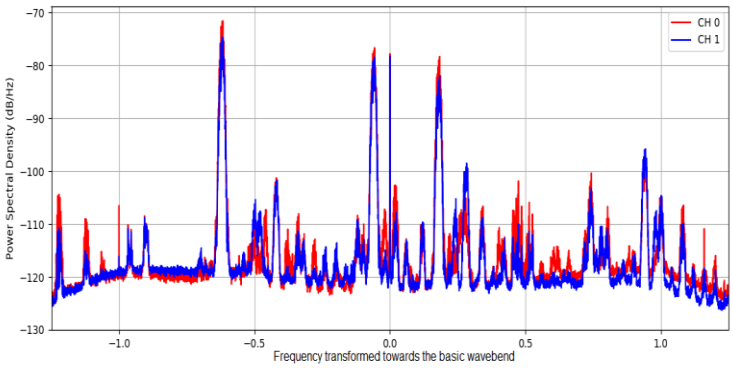

Figure 2 Spectral density distribution of both channels towards the carrier frequency.

Meteorological parameters at the mast in different heights measured each 10 seconds were taken in integrated 10 min. intervals and the precipitation on the ground were recorded continuously by a weighing rain gauge which enabled to express the rain intensity and rain sums in short intervals. The response of the signal to changing atmosphere properties were checked in one day intervals on March 6 and March 22, 2020. Synoptic situation on March 6 was characterized by passing low pressure through over the Central Europe while on March 22 expiring North-East Cyclonic situation occurred being transformed to North-East Anticyclonic situation next day. March 6 was overcast with no direct sunshine duration and with south-east mild wind. An occluded front was passing over the monitored territory early in the morning. Precipitation also started early morning and reached 10.9 mm in total. The course of meteorological parameters and the phase reaction to their changes is on Fig. 3.

The temperature dropped down just after the passing front with further slow steady rise. The daily temperature amplitude reached only 3.5°C. Precipitation is expressed by the vertical glaucous lines at the scale where one vertical line represents 0.1 mm of rain.

Temperature decrease together with the advection of moisty air mass reflected in relative humidity rise and in an impact on phase shift of the signal. Small vibration of the phase before 4 am were caused by mild turbulence and small changes of relative humidity. Phase shift was expressed in much stronger variations during the precipitation period with a certain afterglow with gradual fading of the vibrations. The reaction on the start of the small intensity rain is visible but strong changes in the rain intensity are expressed by strong phase changes of almost 0.5 rad at the level exceeding 2 rad.

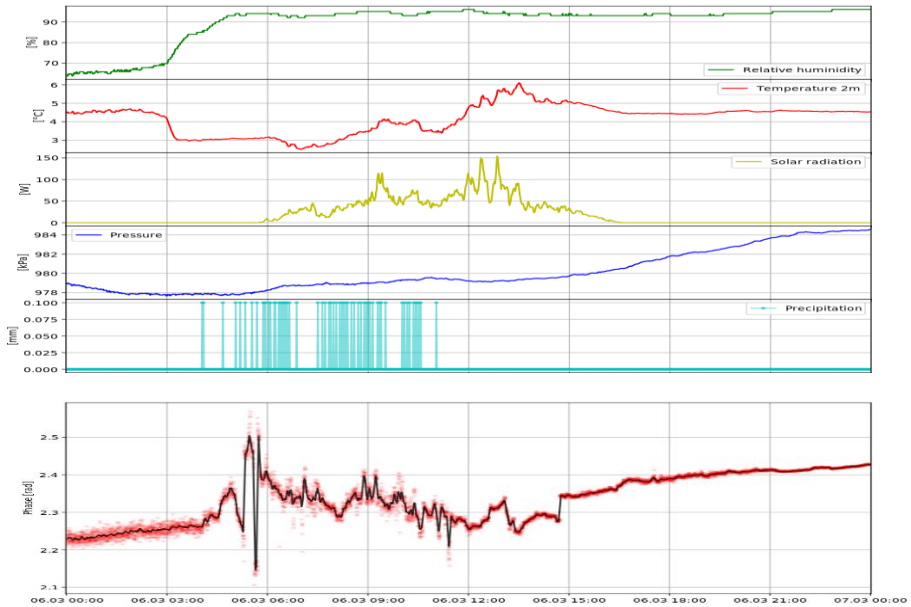

Figure 3 Daily course of meteorological parameters and respective phase shift on March 6, 2020

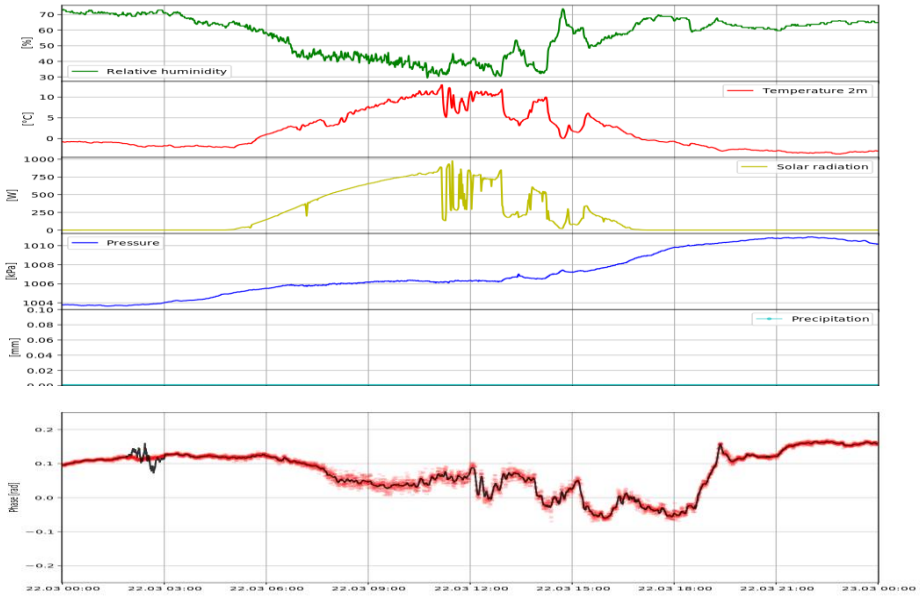

22, 2020

Fig. 4 represents mostly shiny day with higher amplitude of the temperature but with much lower air humidity. The phase response shows much lower vibration of about 0.2 rad at the level close to 0.
Further experiments, when receiving the signal from the sources distant a few kilometers, showed similar reaction of the phase to the rain. Nevertheless, the verification of such results was difficult due to the low knowledge about the rain occurrence and rain intensity in the space between the broadcaster and the receiver.

Concluding results

The experiment showed the impact of the inhomogeneity in the atmosphere on correlational components of the signal noise in the space of overlapping Fresnel zones of the signal coming to 2 different antennas in UHF band at the frequency around 1GHz. Phase difference of the signal coming to 2 antennas distant one from the other a few wavelenghts is related to the frequency of the source of the signal and depends on the properties of the atmosphere. Frequency shifts are in good correlation with the rain occurrence at qualitative level, phase variations out of the rain periods are much less developed, small sudden changes in the air moisture cause only a small vibrations of the phase shift. The method enables to monitor the presence of rain based on the differences in signals propagated along two different trajectories which is expressed as an integral value in the line between the source of the signal and the receiver. Presented method is based on fully passive detection of the BTS signal. Further to the frequency it does not require any knowledge of any technical parameters of the broadcasted signal and does not depend on the strength of the signal once the signal reaches a certain detection level.

Beside above described experiment of receiving signal from one source by two different antennas a method of receiving signal from two different sources by one antenna was tested. The results were similar to one source with 2 antennas composition.

References:

D. Atlas and H. Banks. (1951). The Interpretation of Microwave Reflections from Rainfall, Journal of Meteorology, vol.8, issue.5, pp.271-282, 1951.

Fencl, M., Rieckermann, J., Sýkora, P., Stránský, D. *and* Bareš, V. *(*2015*)* Commercial microwave links instead of rain gauges: fiction or reality? Water Science and Technology, 71, 31–37. https://doi.org/10.2166/wst.2014.466.

Kuba, M., - Fabo, P., Nejedlik, P., - Podhorsky, D. (2018). Possibilities to detect hydrometeors based on the changes of the electromagnetic signal. (In Slovak). In Monitorování přírodních procesů, Lednice 12.-13.9.2018. - Brno : Mendelova univerzita, VÚMOP, v.v.i, [15] p. ISBN 978-80-7509-570-1.

Leijnse, H., Uijlenhoet, R., Stricker, J., N., M. (2007), Rainfall measurement using radio links from cellular communication networks. WATER RESOURCES RESEARCH, VOL. 43, W03201, doi:10.1029/2006WR005631.

Overeem, A., H. Leijnse, and R. Uijlenhoet (2011), Measuring urban rainfall using microwave links from commercial cellular communication networks, Water Resour. Res., 47, W12505, doi:10.1029/2010WR010350.

Rios Gaona, M.F., Overeem, A., Raupach, T.H., Leijnse, H. *and* Uijlenhoet, R. *(*2018*)* Rainfall retrieval with commercial microwave links in São Paulo, Brazil. Atmospheric Measurement Techniques., 11, 4465–4476. https://doi.org/10.5194/amt-11-4465-2018.

Zinevich, A., Alpert, P. *and* Messer, H. *(*2008*)* Estimation of rainfall fields using commercial microwave communication networks of variable density. Advances in Water Resources, 31, 1470–1480. https://doi.org/10.1016/j.advwatres.2008.03.003.

Practices and success factors of business models of Greek agricultural cooperatives

Ioannis Ath. Sfougaris

E-mail: sfouggar@uth.gr

1.I**ntroduction**

Cooperatives around the world contribute to the survival of more than half of the world's population, according to United Nations estimates, and have more than one billion members. They also represent a significant employer, as they provide more than 100 million jobs (Ševarlić and Nikolić, 2013).

The creation of a cooperative company aims to consistently meet the needs of its members, focusing on the benefits of members, but also ensuring a sufficient profit by operating as a company. Cooperatives are companies owned by their members, controlled by them and aimed at their own benefits. They are clearly differentiated in terms of goals from private equity firms (IOF Investor-Owned Firms), which aim to maximize profits (Soboh *et al*., 2011).

Rural Cooperatives produce not only lasting economic results but also social development, inclusion and empowerment. They give farmers a voice in rural policy dialogue and decision-making, and help them exchange ideas across borders (www.ifad.org).

Rural cooperatives enable small-scale producers to expand their range of operations, increase their bargaining power and engage with global market opportunities. Their members utilize natural resources more efficiently and to a greater degree, while also combating the threats of climate change and environmental degradation. Farming families are given access to inputs and services like credit, training, storage facilities and technology, improving the viability of smallholder farming.

With incentives and returns like these, it comes as no surprise that cooperatives are growing internationally. In Brazil, cooperatives were responsible for 37.2 per cent of agricultural gross domestic product and 5.4 per cent of overall GDP in 2009, and earned about US$3.6 billion from exports. In Mauritius, cooperatives account for more than 60 per cent of national food crop production. There are many more examples like these that showcase the effect rural cooperatives can have on sustainability in the future (www.ifad.org).

Agricultural cooperatives have played an important role in market economies and this is evident by their high sales, market share in North America and Western Europe as well as the assets they hold. In the past, the growth capital that fed the aforementioned results came either from debt securities or from domestic revenue. In order to have internal revenue, there had to be flexibility in how members were paid through dividends, redemption of shares and, above all, payments to members for production (Chaddad and Cook, 2004).

The use of purely economic performance indicators in the case of agricultural cooperatives (eg profits, productivity, liquidity, leverage, resource efficiency) does not differentiate them from investment firms (IOFs) and does not take them into account their different goals.

Financial indicators provide information on the financial condition of companies, while non-financial indicators provide an overview of business performance including other factors related to their successful operation (Suklev and Debarliev, 2012).

The Canvas Business Model is a strategic management tool that helps both to create new business models and also to review existing ones. As proposed by Ostewlerder and Pigneur (2010), the canvas renders an organization's business model into nine cohesive building blocks, which can be grouped into four groups: A. Extroversion: 1. Customer segmentation, 2 Value proposition to customers, 3. Channels, 4. Customer relations. B. Introversion: 5. Key activities, 6. Key resources, 7. Key partners. C. Revenue: 8. Revenue flows. D. Expenses: 9. Expenditure structure.

2. **Methodology**

This research aims at investigating both business practices and the application of business models to the operation of six selected agricultural cooperatives in Greece. This research is related to the evaluation of value propositions and business practices from the point of view of agricultural cooperatives and their connection with their successful operation.

The methodology that was followed consists of: 1) Study of the Greek and international literature 2) Collection of data related to the 9 structural features of the canvas business model as well as 3) the collection of financial data and business practices from the websites of cooperatives, as well as balance sheets and their annual reports.

3. **Case Studies**

In this research, six (6) agricultural cooperatives of Greece were analyzed based on the Business Model Canvas: EVOL, THESGALA, TRIKKI, ZAGORIN, Velventos Cooperative "DIMITRA", and PINDOS *. The data of the Ministry of Regional Development show that 734 agricultural cooperatives are registered in the relevant list.

The selection was made among the 24 Agricultural Cooperatives that show a larger turnover.

Evol

The Value Proposition of the cooperative is the production of certified organic milk products combining tradition with the modern rules and procedures that apply in the food industries (HACCP, ISO 22000). More specifically, the products of the cooperative are: goat and cow bottled fresh organic milk, as well as their derivatives - goat yogurt and organic sheep, goat butter organic and goat cheese organic), with attention to careful quality and an aesthetic packaging. As for the Customer Departments, they consist of residents of the mainland and to a small extent from the Aegean, Ionian and Crete islands, while the Key Partners of the cooperative are the farmers who supply the milk and the farmers who supply the feed. The Key Activities for the operation of the cooperative are bottling, cheese-making, yoghurt production, production of plastic bottles and feed production from where the farmers who deliver the milk are supplied with feed for their animals. The above activities require the Key Resources, ie milk, animal feed, bottles and packaging and the brand name. Customer Relationships are created through the sales stores, while the Channels used are the advertising in local newspapers, the distribution of products in well-known supermarket chains, the selected stores in various cities, as well as the website.

Cooperative Costs consist of feed production costs, product transportation costs, refrigerated truck maintenance costs, packaging costs, biological treatment costs, wages and certification costs. Its Revenue comes from the sales of products. (www.evol-easvolou.gr).

Thesgala

The Value Proposition of the cooperative is the provision of high quality milk and dairy products at extremely competitive prices. As for the Customer Departments, they consist of consumers in Athens, Thessaloniki, Larissa. The Key Partners of the cooperative are the partners that arise through the franchising, ELOGAK (Hellenic Milk & Meat Organization), the feed suppliers and the breeders. Finally, crucial partners are other cooperatives such as THESGI (Thessaly farmers' cooperative) for the supply of animal feed. Key Activities for the operation of the cooperative are the daily sampling from all members, with the samples being subjected to a series of laboratory analyzes in the reference laboratories of ELOGAK (Hellenic Milk & Meat Organization). Also, the internal pricing based on 5 quality criteria as described in the contracts with the dairy factories. In the aforementioned activities, the Key Resources are necessary, ie milk and the brand name. Customer Relationships of the cooperative are created through the vending machines and through delivery in Athens and Thessaloniki. The Channels utilized are B2B in dairy industries (Fage, FrieslandCampina, Hellas / Nounou, Delta, EAS Lamia, Trikki and Tositsa foundation), B2B retail in 2 supermarkets, social media and the website (eshop). The Costs of the cooperative consist of salaries, product transportation costs, maintenance costs of refrigerated trucks, operating costs of vending machines and debts to banks. Its Revenue comes from product sales (www.thesgala.gr).

Trikki

The Value Proposition of the cooperative is the processing of exclusively local Greek milk by cooperating producers from livestock units of West Thessaly certified for the use of non-genetically modified feed while maintaining high quality standards at all stages of production: quality certificates: 900 ISO 22000 (HACCP)]. The Customer Departments are made up of consumers from the region. The Key Partners of the cooperative are the stockmen who supply the milk. The Key Activities for the operation of the

cooperative are the receipt of milk and quality control, cheese making, yogurt production, bottling of products, their packaging, monitoring of key parameters and food safety. Key Resources, ie milk, cold storage facilities, and technological equipment are necessary for the above-mentioned activities. Customer Relationships are created through sales stores while the Channels used are some supermarkets in the region, local stores, newspaper advertising as well as the cooperative's website. Product transportation Costs and staff salaries make up the cooperative's costs, while its revenue comes from product sales. (www.trikki.com.gr).

Zagorin

The Value Proposition of the cooperative is the high quality, with a protected designation of origin apples. The cooperative applies the method of "Integrated Production", which is an hybrid state between conventional and organic cultivation. As for the Customer Departments, they consist of consumers in Greece and abroad. Key Partner of the cooperative is the women agritourism cooperative of the market for the production of petimezi from a village of Pelion. The Key Activities for the operation of the cooperative are the harvest, the provision of traceability and plant protection. In the above-mentioned activities, the Key Resources are necessary, ie the fertile and suitable for cultivation soils, the favorable climate, the traceability system, the Smartfresh formulation for the post-harvest protection of the fruits, the privately owned refrigerator-sorting complex, the electronic automatic sorters, the electronic micro-packaging machines in the refrigeration facilities. An important resource is also the brand name of the cooperative which is considered strong. Customer Relationships are created through sales stores as well as through events and competitions organized by the cooperative.

The Channels used are B2B in super market chains, foreign markets (Europe and the Middle East), advertising through sponsorship of TV shows, and through social media, as well as through the cooperative website. The Costs of the cooperative consist of the costs of equipment and depreciation, salaries (permanent and non-permanent employees), plant protection products, the costs of moving and wearing trucks and the cost of advertising. Its Revenue comes from product sales. (https://zagorin.gr/)

Velventos Cooperative (ASEPOP)

The Value Proposition of the cooperative is the production of fruits (peaches, nectarines, apricots, kiwis, cherries, apples) by applying the system of confusion (sexual confusion of insects), which minimizes the use of herbicides and pesticides in the products, making them even safer. The cooperative implements the system of integrated production, is certified according to ISO, HACCP, GLOBALGAP AND EUREPGAP, while since 2002 the integrated management according to AGRO 2.1 is applied 2.2. As for the Customer Departments, they consist of clients in Greece and Russia, Poland, Czech Republic, Hungary, Serbia, Ukraine, Slovakia, Bulgaria, Romania, Cyprus and Egypt. Key Partner of the cooperative is the transport company that undertakes the transport of products, while Key Activities for its operation are the cultivation, harvesting and preservation of fruits and the reach of agreements with the sellers of the products of the cooperative. The above activities require the Key Resources, ie the 11 controlled atmosphere cold rooms, the pesticide warehouse, the storage areas and the sorting rooms. Customer Relationships of the cooperative are created through the stores selling the products. The Channels used are the store in the central market of Athens in Renti and the sale of the products by the cooperative itself in large supermarket chains, but also in various large markets in Greece. The cooperative also carries out large exports to countries such as Russia, Poland, Czech Republic, Hungary, Serbia, Ukraine, Slovakia, Bulgaria, Romania, Cyprus, Egypt. Finally, it utilizes its website as a promotional channel. The Costs of the cooperative consist of the costs of equipment, depreciation cost, salaries (permanent and non-permanent employees), plant protection products, the cost of transporting products and the cost of advertising. Its Revenue comes from product sales. https://asepop.gr

Pindos

The Value Proposition of the cooperative is the fresh chickens that have been raised in a mountainous climate. They develop in modern facilities with strict quality controls and valid certifications. More specifically, per product:

The organic Pindos chicken grows up, in a mountainous environment and at an altitude of over 700m. It feeds only on certified foods, which are produced with organic raw materials (slaughtered after 81

days). In terms of its ready-made baked products, Pindos has employed the most modern methods available and the current technology of poultry farming. The method of packaging in modified atmospheres is followed. The cold cuts are made from selected Pindos chickens and maintain high standards at all stages of the production process. The quality of the products is ensured by the total quality system according to the ISO 22000 standard and the free range chickens have the AGROCERT certification, of OPEGEP. Regarding the Customer Departments, they consist of customers throughout Greece and the foreign countries that the company exports. Key Partners of the cooperative are the subsidiaries of the group. More specifically: Agromark (consulting company, marketing services), Green Pindos (utilization of renewable energy sources for electricity and heat production) and Agrozoi (fully integrated company including slaughterhouse, hatchery and food production unit). Key Partners outside the group are sales representatives, veterinarians and feed suppliers, while Key Activities for the operation of the cooperative are the breeding and slaughter of poultry, their cutting and packaging. Key Resources are needed in the above activities, ie human resources, chicks, and slaughter and cleaning machines.

Customer Relationships are created through advertising, either on television and through sponsorship of shows, or through social media. The Channels used by the cooperative are the 15 branches-distribution centers in Ioannina, Thessaloniki, Veria, Larissa, Trikala, Agrinio, Patras, Corinth, Tripoli, Livadia, Kozani, Athens, Heraklion, Chania and Corfu. It also has exclusive representatives in many more areas of Greece. It also cooperates and supplies supermarket chains, as well as large catering companies. PINDOS products are available in select butchers, restaurants and grills throughout Greece. It also feeds public organizations (hospitals, institutions and meat processing industries. Finally, the cooperative uses its website as a channel to reach customers. The cooperative exports products to selected countries in the Balkans (Bulgaria, Skopje, Albania) as well as to various countries around the world such as Cyprus, Italy, China and Turkey. The Costs of the cooperative consist of the costs of maintenance of equipment, renewal of equipment, costs of transporting products and costs of veterinarians and medicines. Its Revenue comes from product sales. www.pindos-apsi.gr

5. Findings

The factors that emerged from the literature review as important for the successful operation of agricultural cooperatives are the contribution to the rural development of the area in which they operate, the improvement of the economic-social situation of their member farmers, their ability to adapt to change (technological, demand, demographic, etc.) which leads them to extend their viability (multiple life cycles), the active participation of their members (the opposite of opportunistic behavior), the processing which leads to an increase in the added value of the products produced , the use of technology, marketing and standardization, brand development, product differentiation, organizational innovations (eg remodeling into SNG, essentially adapting the organizational characteristics of the Traditional Model to those of private companies), training and education of members and high sales and profits. For the latter, the present research, uses the Net Profit Margin = operating profit / turnover%].

In terms of efficiency indicators, they are presented in Table 1 below.

Table 1: Efficiency Indicators for Agricultural Cooperatives

	2018	**2017**	**2016**	**2015**
EVOL	8%	7%	8%	11%
THESGALA	-7,6%	-2,2%	-6,9%	0,16%
TRIKKI	1,27%	-0,022%	-0,42%	-0,34%
ZAGORIN	0,72%	0,55%	0,06%	0,14%
ASEPOP VELVENTOU	0,39%	0,1%	0,28%	0,07%
PINDOS	3,9%	4,45%	2,34%	3,55%

Sources: www.evol-easvolou.gr,www.thesgala.gr, www.trikki.com.gr, https://zagorin.gr, https://asepop.gr, www.pindos-apsi.gr. Own Processing

In the above table we observe that in THESGALA, there is a continuous decline (-7.6% in 2018 from 1.6% in 2015) due to the reduced response of consumers to the system of milk vending machines, despite the initial enthusiasm. A cornerstone for the restart that the cooperative is called to do, is a new business plan. The total liabilities of the cooperative (to Banks, Greek State, cooperatives, contracted producers, employees, suppliers), amount to 20,840,213.27 euros. The main points of the new business plan of THESGALA are: a) estimate for an annual growth rate of 3% of sales in the existing network, b) gradual reduction of sales of raw milk, which has a low profit margin of 6%, c) cooperation with supermarkets, d) increase sales of ice cream, which have a gross profit margin of 55%, e) scaling down operation with the number of employees reduced in October 2019 to 61, from 164 in June 2017. TRIKKI presents upward trend (1.27% in 2018, -0.34% in 2015), due to a successful market penetration strategy, with the most recent achievement being the consolidation of products in the Athens market. The goals in the near future focus on minimizing costs while maintaining market position. Special importance to direct sales to credible customers will be given, in order to avoid bad debts (Annual Financial Statement for the year 2018). ZAGORIN notes a positive course (0.72% in 2018 from 0.14% in 2015). The increase in 2018 and 2017 is due to the significant increase in production due to the gradual yield of new plantings and due to the reduction of damage due to weather phenomena. ASEPOP Velventou shows an upward trend and according to the president of the Cooperative, in 2018, despite the unfavorable weather conditions (heavy rainfall), and the lower production than other years, the prices were higher, so that the overall result is considered satisfactory. PINDOS from 2015 to 2018, shows a steady increase in turnover and much higher than the other Greek cooperatives examined (2015: 193 million euros, 2016: 209 million euros, 2017: 219 million euros, 2018: 250 million euros). The turn of consumers to chicken in the years of crisis, the recovery of sales in supermarkets, after the transfer of the network of "Marinopoulos" to the "Greek Supermarkets Sklavenitis", but also the strengthening of the products of "Pindos" with new codes, gave boost in sales. The efficiency index fluctuates due to the fluctuation of operating profits. It should be mentioned here that the Bank's bank lending remains high, despite any improvements. Also, the average time of the receivables collection period is significantly high in relation to the average time of the repayment period of the suppliers, a fact that complicates the liquidity of the company. The mismatch of obligations / receivables, as well as the high cost of production of the product due to high prices of suppliers and high non-productive costs, can be considered as reasons for increasing the costs of the Cooperative (Vranias, 2013).

Regarding the processing, as shown in Table 2 below, all the dairy cooperatives (EVOL, THESGALA, TRIKKI) process their products (cheese, yogurt, desserts), while in the same Table is presented the participation status (active or not) of the members in the cooperative, as well as any innovative actions that fall within the scope of its organization and operation.

Table 2: Cooperative performance according to the criteria: processing, standardization, entry into international markets, active participation / engagement incentives and organizational innovations

	Processing	**Standardization**	**Entry into international markets**	**Active participation / Engagement incentives**	**Organizational innovations**
EVOL	Range of dairy products	YES (as they are dairy products)	NO	➢ Active participation because of the benefits that arise ➢ Delivery of 100% of the production according to the articles of association	➢ Dividend payment to members ➢ Corporate Social Responsibility Programs ➢1st Cooperative that buys products from non-members resulting in the increase of quantities and increase of the negotiating role of the cooperative.

THESGALA	Range of dairy products	YES (as they are dairy products)	NO	➢ Defending the interests of member producers [guaranteed price, payment time]	➢ATM and home delivery
TRIKKI	Range of dairy products	YES (as they are dairy products)	NO	➢ Reduced and declining participation (due to poor economic results of the cooperative and disagreements with the management)	➢ Agricultural Corporate Partnership
ZAGORIN	NO	YES	YES (Europe and the Middle East)	➢ Active participation because of the benefits that arise ➢ Delivery of 100% of the production according to the articles of association	
ASEPOP VELVENTOU	NO	YES	YES (Russia, Poland, Czech Republic, Hungary, Serbia, Ukraine, Slovakia, Bulgaria, Romania, Cyprus and Egypt)	➢ the fact that it has certifications, as well as a geotechnical department which all producers consult before applying any crop care practice	ntegrated management system according to AGRO 2.1 2.2.
PINDOS	YES(cold cuts, ready-cooked chicken, sausages)	YES (packaged products)	YES Balkans (Bulgaria, Skopje, Albania) and Cyprus, Italy, China and Turkey.	➢ Active participation due to the continuous supportive presence of the Cooperative to its members (advisory, loan, etc.)	➢ Corporate Social Responsibility Programs ➢ Because there is a significant quality control of the products at all stages (control of diets, chicks from the cooperative and rearing by the poultry farmers), the required additional cost is given in the form of a loan to the poultry farmers. ➢ Establishment of subsidiaries

Sources: www.evol-easvolou.gr,www.thesgala.gr, www.trikki.com.gr, https://zagorin.gr, https://asepop.gr, www.pindos-apsi.gr. Own Processing

From the fruit-producing cooperatives, ZAGORIN and ASEPOP Velventou do not offer any processed product. PINDOS has proceeded with a variety of processed products (indicative: sausage, salami, parizaki).

Entry into international markets is a performance indicator for cooperatives and case studies show that the majority of them (with the exception of EVOL, THESgala and Trikki) are active in markets outside the country where they originated.

5. Conclusions

Overall, evaluating the case studies based on the Business Model Canvas, it was observed that all cooperatives base their revenue streams on product sales and no other model is followed (eg subscription). The differentiation between cooperatives based on performance / success indicators

Most cooperatives make efforts to operate in countries other than their home country of origin and operation. Dairy cooperatives have not been able to penetrate foreign markets, which does not try to do so, recognizing that milk and dairy products are a highly competitive sector and that the task of establishing themselves in foreign markets is a very difficult and precarious process. So they prefer to establish themselves in the local-regional markets and with coordinated steps to gain a large share in the country's markets.

Most cooperatives try to adapt to the changing preferences of consumers, but in terms of differentiation from competitors in similar alliances, this does not seem to exist. THESGALA presented differentiation in the way the consumer can obtain the product. An innovation (at the same time differentiation from the competition) is the fact that THESGALA offers both the sales service (vending machines) and the product of its member producers (fresh milk). This differentiation does not seem to have had a significant effect on its efficiency in the long run.

The agricultural cooperatives that meet most of the performance criteria, as emerged from the literature and mentioned above, show a higher turnover but no higher efficiency index. This could be due to factors such as loan liabilities and higher operating costs (eg payroll, high raw material prices, etc.).

Technology is an important factor for the successful completion of a cooperative's activities and the case studies that have been evaluated show that most of them, as far as they can cover the costs, use the most modern machines and technologies.

In general, from the research carried out, it was found that the commonalities of the Agricultural Cooperatives examined were the brand name, the high quality of products and services ensured by certifications and continuous inspections, the utilization of modern technology and machines, the limited differentiation (except THESGALA, which is in the process of changing channels from B2C to B2B) and the provision of consulting services. Their differences lie in the processing, the adaptability to the changing preferences of the consumers and the new environment (economic, social, etc.), the extent of the advertising (some, mainly the dairy ones, are advertised at local-regional level, preferring to win the local markets for the reasons mentioned) and the range of products produced, including organic (only EVOL produces organic milk, cheese and yogurt).

Finally, it is worth noting that an important indicator of the performance of Cooperatives is the economic and social improvement of the situation of its members. This is proposed to be a subject of future research through questionnaires, which will investigate either the previous and after the entry into the Association economic and social status of its members, or the comparison of the situation between members and non-members.

*
www.ifad.org
www.evol-easvolou.gr
www.thesgala.gr
www.trikki.com.gr
https://zagorin.gr
https://asepop.gr
www.pindos-apsi.gr

References

Chaddad F.R., M.L.Cook, (2004). Understanding New Cooperative Models: An Ownership-Control Rights Typology. Review of agricultural economics 26(3):348-360

Iliopoulos C., R. Värnik, M. Filippi, L. Volli, K. Laaneväli, (2019). Organizational Design Mechanisms Adopted by Estonian Agricultural Cooperatives: A Solution-Focused Approach, Conference Paper [ανακτήθηκε από www.researchgate.net/publication/331742785]

Osterwalder A., Y. Pigneur, (2010). Business Model Generation: a Handbook for Visionaries, Game Changers, and Challengers. John Wiley & Sons.

Ševarlić M.M. and M.M. Nikolić, (2015). Agricultural cooperatives – examples of good practice in the world and Serbia. In: Book of Proceedings The Seminar Agriculture and Rural Development - Challenges of Transition and Integration Processes. Department of Agricultural Economics, Faculty of Agriculture, University of Belgrade.

Soboh, R. A. M. E., Lansink, A. O., and Van Dijk, G. (2011). Distinguishing Dairy Cooperatives From Investor-Owned Firms in Europe Using Financial Indicators. Agribusiness, 27 (1), 34-46.

Suklev, B. & Debarliev, S. (2012). Strategic planning effectiveness comparing analysis of the Macedonian context. Economic and Business Review, 14(1), 63-93.

Vranias N., (2013). The process of preparing a business plan. case study for the poultry cooperative of Ioannina "Pindos". Thesis. School of Management and Economics Department of Finance and Electronics, TEI of Epirus (in Greek).

Large-scale habitat description: utilizing GIS classification tools to describe lesser kestrel foraging habitat in the eastern Thessaly plain.

Christakis C.[1], Sakellariou S.[2], Christopoulou O.[2], Sfougaris A.[1]

[1]Laboratory of Ecosystem and Biodiversity Management, Department of Agriculture, Crop Production and Rural Environment, University of Thessaly
[2]Laboratory of Geographical Research and Environmental Planning, Department of Planning and Regional Development, University of Thessaly

Abstract. The lesser kestrel (*Falco naumanni*) is a small migratory falcon, which usually lives and breeds in colonies and is considered Vulnerable by the Red Book of Endangered Animals of Greece (2009). In Europe, the main breeding ground of the species can be found at the Mediterranean basin, while the main breeding sites of the species in Greece are located in Thessaly plain, which hosts approximately 70% of the total Greek lesser kestrel population. This paper presents a successful implementation of remote sensing and GIS into the creation of the initial database, essential for the implementation of the species conservation plan. The area examined spans about 150km^2 around the villages of Stefanovikio and Rizomilos, an area dominated by arable crops where lesser kestrels forage. Using a Spot satellite image as our initial input data together with ground proofing field observations of land use and cultivation types and utilizing GIS classification tools, we were able to produce a description of the lesser kestrel foraging habitat. The final product of our analysis was a descriptive land use visualization of the species foraging habitat (cultivation types of the area) which provides a concrete base for the implementation of conservation actions.

1 Introduction

The lesser kestrel (*Falco naumanni*) is a small migratory predator that usually lives and reproduces in colonies. In the past, its population in Europe was considered numerous (Bijleveld, 1974, Cramp and Simmons 1980). During recent decades though, the population of the species has been severely reduced (Biber 1990). According to Birdlife International (2012) and Iñigo and Barov (2010), the last decade, the reproductive population in Europe was estimated to be between 25,000 and 42,000 pairs.

The species distribution is South of 55^{o}N in the Palearctic Region (Biber 1994). It reproduces in the areas of the Iberian Peninsula to Mongolia and the Southeast China to North Africa and Levant region (Hollom et al., 1988; Biber, 1994). In Europe, the main breeding grounds of the species are located at the Mediterranean basin, in particular in Spain, which has the largest reproductive population, in Turkey where there is also a significant population, followed by Greece and Italy (Biber, 1994). Furthermore, a small population of the species has been reported to reproduce in North Africa, such as Morocco, Algeria, Tunisia, and occasionally in Egypt (Biber, 1994).

Lesser kestrel nests mainly in wall holes or in holes located under roof tiles (Negro and Hiraldo, 1993). Its preferable foraging habitats are semi-deserts, steppes and cultivated grain areas (Del Hoyo et al., 1994; Biber, 1994, 1996). Its diet consists mainly of large arthropods, such as orthoptera, coleoptera, spiders and some members of the Scolopendridae family (Cramp and Simmons 1980, Negro et al., 1997).

The main breeding sites of the species in Greece are located in Thessaly and at a lesser extend in Southwest Macedonia, but lesser kestrels can also be found in the rest of mainland Greece, where the species appears sporadically (Handrinos and Akriotis, 1997). According to the Red Book of Endangered Animals of Greece (2009), the species is considered Vulnerable. Hallman (1995) and Bousbouras (2006) found that Thessaly maintains the largest part (which accounts for 75%) of the reproductive population in Greece.

The habitats where the species were observed in Thessaly were mainly cereal crops, uncultivated land and pastures. Although a large part of Thessaly is cultivated with cotton, it seems that lesser kestrels do not prefer it (Christakis & Sfougaris, 2021). Its habitat selection depends directly on the availability and abundance of prey (Sfougaris et al, 2004). Cotton crops, due to the increased input of agrochemicals, account for lowest populations of orthoptera and coleoptera, thus it is not favorable by the species (Christakis & Sfougaris, 2021). According to Hallman (1995) the species in Greece uses mostly land dominated by a mosaic of non-intensified

cereals and meadows. However, all arable crops can be selected from lesser kestrels for foraging when vegetation height and plant are favorable for detecting the prey or when agricultural practices in the fields facilitate access to its prey (Rodriguez, et al., 2013).

The purpose of this study was to successfully implement remote sensing and GIS into the creation of the initial database, essential for the implementation of the species conservation plan. The study was conducted within the framework of the LIFE11 NAT/GR/1011 project "Conservation and management of the Lesser Kestrel (*Falco naumanni*) in three Special Protection Areas (SPAs) in Greece", an EU LIFE-NATURE project, aimed to create an effective and sustainable framework for the conservation of Lesser Kestrel in the area. The Lesser Kestrel is one of the designation species for all three SPAs, as it is a threatened avian species using the study area as breeding habitats.

2 Study area

The study area is located within the plain of Thessaly in central Greece. The plain is the most productive in Greece and the second in extent. It supports a population that exceeds 400,000 people, who live in few towns and many smaller villages. This amount of production requires intensive agricultural activity and extensive use of water resources. The largest part of the area is arable land, with cereals, cotton and maize, being the dominant crops cultivated. The remaining part is cultivated by crop rotations with periodic fallows. Crop rotation is done by interchanging the cultivation of cereal and cotton with legumes annually and then by set-aside every three or four years. Grains are usually sown in mid-to-late autumn and harvested from late May to early June. Cotton is sowed in April and is usually harvested in September. Alfalfa, a perennial legume and the most common legume in the region, is mowed all year round. The non-cultivated lands within the area are orchards, olive groves, vineyards or natural vegetation such as maki, phrygana and dry grasslands. Because the plain is put to heavy agricultural use, intensive farming practices are seen as potential sources of pollution, mainly due to the increased use of fertilizers and pesticides (Christakis and Sfougaris, 2021). The climate in this region is Mediterranean continental.

The study area (Figure 1) consists of 150 km^2 area of the Plain of Thessaly and is located around the villages of Stefanovikio (39°27'50.62"N, 22°44'32.02"E) and Rizomilos (39°25'43.11"N, 22°44'47.29"E). The settlements adjacent to and within the study area, namely Rizomilos, Stefanovikio, Armenio, Sotirio and Megalo Monastery, support relatively large Lesser Kestrel colonies.

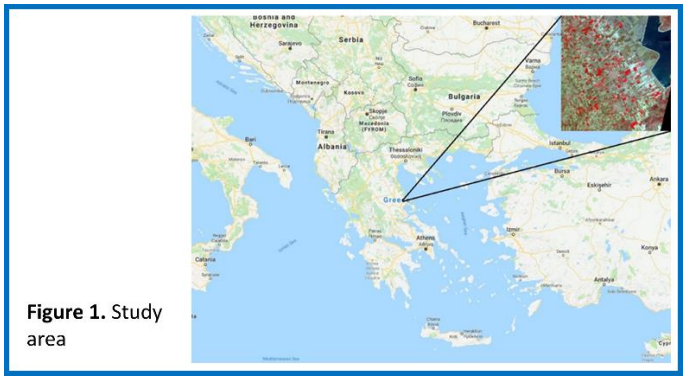

Figure 1. Geographical position of the study area

3 Materials and Methods

One of the critical inputs used in the paper consists of cultivation data that was provided by the local municipality based on farmers' cultivation statements for each year of the study to estimate the surface occupied by the available foraging habitat categories of the study area. The supporting geospatial data used included a SPOT satellite image (10 X 10 m) of June 2014 of the area, as well as ground proofing field observations of land use and cultivation types of the same period. The preprocessing stage of acquired satellite image was conducted using open-source Geographical Information Systems (QGIS 3.0).

Before running the classification process, the selection of the most appropriate classifier (in terms of accuracy) is of utmost importance. Basically, Support Vector Machine (SVM) exploits kernels functions for establishing the decision rules "*to map non-linear decision boundaries in the original data space into linear ones in a high dimensional space*". The effectiveness of SVM is primarily relied on the kernel types and parameters determining the limits of decision rules (Huang et al., 2002). In this study, radial basis function (RBF) kernel used for support vector machine-based classification model, as preferred by Huang et al. (2002). The two most important tuning parameters for SVM model using RBF kernel are cost and sigma. Increasing cost function produces overfitted model and increasing the prediction error; whereas increasing sigma has huge influence on overall classification accuracy which is aftermath of changing the shape of the separating hyperplane (Huang et al., 2002). Hence, we applied supervised classification, using 70% of ground data for classifier training and 30% of the same data for verifying purposes in order to create a land use map appropriate for habitat description. This process would allow us to produce a description of the lesser kestrel foraging habitat. All the geoprocessing procedures took place in a GIS environment.

4 Results

The overall accuracy of the classification amounts to 70% comparing the classified land uses with the ground truth data (Figure 2). We estimated that the percentages of the critical cultivations for the species were divided into the following categories:

The study area was dominated by arable crops, mostly cereals, at 40.5% of the entire study area, followed by irrigated cotton crops (33.8%), other cultivation (11.6%, including irrigated maize and tomato crops, as well as tree plantations and vineyards), as well as a limited area of legumes (8.8%, mainly alfalfa) and non-cultivated land (4.5%). Maize cultivation occupied 5.6% of the study area. Hedgerows and natural vegetation are scarce throughout the study area and therefore were not treated as a separate category.

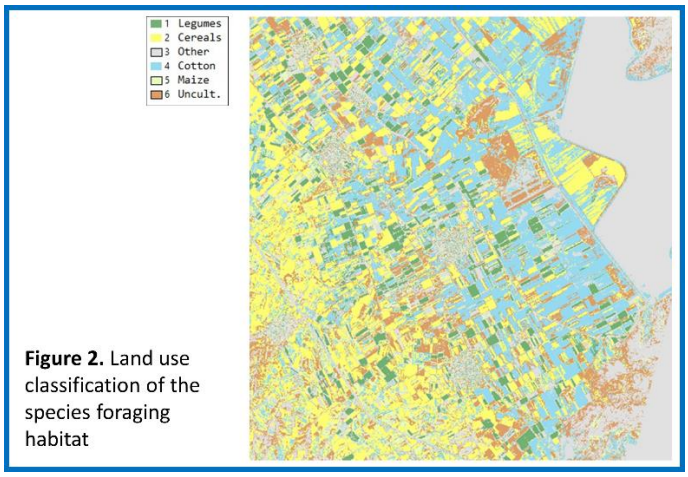

Figure 2. Land use classification for the species foraging habitat

5 Identification and description of foraging habitat

Utilizing the classification of the satellite image and minimum ground-truthing fieldwork, a preliminary description of the foraging habitats of the lesser kestrel was made. The species foraging habitats mainly located in the rural areas around each colony-settlement. These areas are characterized by large areas of crop cultivations, mainly cereals and cotton that dominate the area. There are also crops of legumes, mainly alfalfa, as well as, in lesser extent, uncultivated land or set-aside and maize cultivation. Tree cultivations and fruits as well as vegetables were recorded but are scarce in the study area. The special feature of the rural landscape of the study area is that the average agricultural plot is only 3 acres, including farmers who cultivate larger areas since their cultivating fields are scattered across the area.

During the study period, the area was largely cultivated with cereal and cotton crops (almost 75%of the total cultivation area). Cereals, seems to be one of the important crops for the lesser kestrel in the area (Christakis

& Sfougaris 2021). Sowing takes place from mid-autumn until early December, depending on the weather. Harvesting usually takes place in late May to early June. The cotton is sown at the end of April depending on the weather conditions and the cotton is harvested at the end of September after the species has migrated.

The most input and irrigation demanding crop is cotton cultivation. On the contrary, in this context cereals are a mild form of cultivation. There are generally no tree-lined hedges in the area, yet some individual trees between the boundaries of the fields can be found scarcely. Herbaceous hedges with seasonality are observed. There are trees mainly near livestock facilities as well as in the large drainage canals and parallel to the railway lines. In large crop fields they usually do not exist.

5 Summary

In this paper, we successfully combined remote sensing and GIS for the creation of the initial database which is essential for the implementation of the Lesser Kestrel conservation plan. The study area around the villages of Stefanovikio and Rizomilos is dominated by arable crops where lesser kestrels forage. Using a Spot satellite image as our initial input data together with ground proofing field observations of land use and cultivation types and utilizing GIS classification tools, we were able to produce the description of the lesser kestrel foraging habitat which provides a concrete base for the implementation of conservation actions,

References

Bijeveld, M. (1974) Birds of prey in Europe. London: Macmillan Press Ltd

Cramp, S. and Simmons, K.E.L. (1980) Handbook of the birds in Europe, the Middle East and North Africa: the Birds of the Western Paleartic. Oxford: Oxford University Press.

Christakis C and Sfougaris A (2021) Foraging habitat selection by the Lesser Kestrel *Falco naumanni* during the different phases of breeding and the post breeding period in central Greece Ornithological Science 20 (2) 175-183

Biber J. 1990. Action plan for the conservation of western lesser kestrel *Falco naumanni* populations. ICBP Study Report No. 41. Cambridge (UK): ICBP.

Biber, J.P, (1994) Lesser Kestrel *Falco naumanni* in Tucker, G M and Heath M F (eds) Birds in Europe: Their Conservation status. Birdlife Conservation Series No. 3. Cambridge: Birdlife International, p. 188-189

BirdLife International. 2012. Species factsheet: *Falco naumanni*; [cited 2012 Sep 23] Available from: http://www.birdlife.org

Bousbouras, D. (2009) “Lesser Kestrel (*Falco naumanni*)” in Legakis, A. & Maragkou, P. (eds) The Red data book of Threatened Vertebrates of Greece. Athens: Hellenic Zoological Society.

Bousbouras, D. (2006) “Populations, colonies and foraging sites of lesser kestrels (*Falco naumanni*) in the Thessalian plain: Delineation proposals for Special Protected Areas”. Book of Abstracts of the 10th International Congress on the Zoogeography and Ecology of Greece and Adjacent Regions, p. 18.

Iñigo, A. and Barov, B. (2010) Action plan for the lesser kestrel *Falco naumanni* in the European Union, SEO|BirdLife and BirdLife International for the European Commission, p. 55. Available at: http://ec.europa.eu/environment/nature/ conservation/wildbirds/action_plans/docs/falco_naumanni.pdf

Hollom, P.A.D., Porter, R.F., Christiensen, S. and Willis, I. (1988) Birds of the Middle East and North Africa: a companion guide. London: T. & A.D. Poyser.

Huang, C., Davis, L. S., & Townshend, J. R. G. (2002). An assessment of support vector machines for land cover classification. *International Journal of Remote Sensing*, *23*(4), 725–749. http://doi.org/10.1080/01431160110040323

Negro, J.J., and Hiraldo, F. (1993) “Nestsite selection and breeding success in the Lesser Kestrel *Falco naummani*”. Bird Study. 40(2), p. 115-119

Del Hoyo, J., Elliott, A. and Sargatal, J. (1994) Handbook of the birds of the World. Vol. II: New World Vultures to Guineafowl. Barcelona: Lynx Edicions.

Cramp, S. and Simmons, K.E.L. (1980) Handbook of the birds in Europe, the Middle East and North Africa: the Birds of the Western Paleartic. Oxford: Oxford University Press.

Negro, J.J. (1997) *Falco naumanni* Lesser Kestrel. BWP Update. The Journal of Birds of the Western Palearctic 1. Oxford: Oxford University Press, p. 49–56

Handrinos, G. & Akriotis, T. (1997) The Birds of Greece. London: A & C Black.

Sfougaris, A., Alivizatos, C., Giannakopoulos, A. and Weight, C. (2004) Conservation of a raptor in an intensively cultivated agroecosystem: the case of the Lesser Kestrel (*Falco naumanni*) in Thessaly plain, Central Greece.

Hallmann, B. 1995. Lesser Kestrel survey of Thessaly. Report to HOS, RSPB and BirdLife International.

Rodriguez, C., Tapia, L., Ribeiro, E. & Bustamante, J., 2013. Crop vegetation structure is more important than crop type in determining where Lesser Kestrels forage. Bird Conservation International, pp. 1-15.

Legakis, A.; Maragos, P.; 2009. The Red Book of Endangered Animals of Greece. Athens (Greece): Greek Zoological Society. 528 p.

SESSION 7:

IMPLEMENTATION IN WATER-LIMITED ENVIRONMENTS

Open innovation Hub for Irrigation Systems in Mediterranean agriculture (HubIS): a mid-term perspective on a Research & Development project

G. Belaud[1], L. Mateos[2], S. Bouarfa[1], C. Leauthaud[1], K. Daudin[1], J. Leconte[1], A. Zairi[3], T. Hartani[4], H. Gomez-Mac Pherson[2], A. Hammani[5], M. R. do Cameira[6], N. Dalezios[7], P. Gavilan[8], P. Paredes[6], A. Kettani[5], I. Ferchichi[3], P. Vandôme[1]

[1]UMR G-eau , Institut Agro, INRAE, Cirad, IRD, AgroParisTech, BRGM, Univ. Montpellier, France
[2] CSIC, Instituto de agricultura sostenible, Cordoba, Spain
[3] Institut National de Recherches en Génie Rural, Eaux et Forêts, Univ. Carthage, Ariana, Tunisia
[4] Tipaza University Center, Tipaza, Algeria
[5] Institute for Agronomy and Veterinary Medicine Hassan II, Rabat, Morocco
[6] School of Agriculture - University of Lisbon, Portugal
[7] Faculty of Engineering, Univ. Thessaly, Volos, Greece
[8] IFAPA, Área de Recursos Naturales y Forestales, Cordoba, Spain

Abstract

The modernization of irrigation in Mediterranean countries has boosted irrigated agriculture. Undoubtedly, this transformation has increased performance levels, but new compelling challenges have arisen: (i) in many situations, the irrigation performance gap remains much greater than expected; (ii) irrigation intensification and expansion are at the root of pollution of valuable ecosystems and overdraft of non-renewable water resources; (iii) water savings are not as foreseen due to unexpected rebound effects of irrigation efficiency improvements; (iv) modern energy-eager pressurized systems are costly and environmentally questionable. Furthermore, it is now clear that climate change and its foreseen variability will accentuate the vulnerability of agriculture and ecosystems. The main objective of the innovation hub presented here is to favour the emergence, evaluate and boost innovations aiming at reducing the performance gap and thus improve the sustainability of irrigation systems in the Mediterranean region. These innovations comprise new tools and services for farmers and water users associations, designed to increase water, nutrient and energy use efficiency. Innovation development leading to adoption of new standards will rely on bottom-up processes, understanding of governance settings and implementation of sharing procedures, through innovation hubs developed by the project.

1. Introduction

Significant increases of irrigation performance levels in Mediterranean countries were achieved during the lasts decades' period of modernization, mainly driven by technological developments but also favored through top-down policies and exportation market. Still, some compelling challenges have arisen concerning the gap between actual and attainable performance, the reduction of pollution, the consideration of rebound effects, and the assessment of costs and impacts of transitions towards energy-dependent irrigation. Hence, when designing and promoting innovations, there is a great need to integrate irrigation scales, from farm (with a diversity of farmers) to irrigation schemes (collective management, infrastructure adaptation) towards watershed and territories scales which appear to be more relevant to appreciate environmental impacts. There is also an increasing awareness about the benefit of public participation for natural resources management (Grimble et al. 1999), particularly in the irrigation sector where a lot of efforts have been done to involve farmers in the water governance through water users associations (Roger & Hall 2003). On this basis, a consortium of Mediterranean teams with a strong expertise in irrigation research was constituted with the aim to address most of the above issues through the setup of an "Open innovation Hub for Irrigation Systems in Mediterranean agriculture" (HubIS).

The main objective of HubIS project is to favour the emergence, evaluate and boost innovations aiming at improving the sustainability of irrigation systems in the Mediterranean region. Specific objectives are: (i) strengthen the innovation capacity of the irrigation community; (ii) develop methods and services for precision irrigation and agro-ecosystems conservation; (iii) assess environmental and socio-economic

performances of innovations; (iv) pave the way towards developing a Mediterranean policy framework for sustainable irrigation. The research project started in October 2020 for three years. This mid-term communication presents the set-up of the overall approach and its implementation in each case study.

2. Overall methodology

2.1 Main concepts and methods

HubIS is based on the development, implementation, testing, evaluation and dissemination of new tools and services to farmers and WUA. This constitutes the "**innovation basket**" in which we find cost-efficient technologies such as low-cost sensors, remote-sensing applications, irrigation equipment. These tools and services are thought to be co-designed, or at least integrate local needs and practices from the initiation of the innovation process. Hence, HubIS draws from participatory action research to build a "multi-actor innovation Hub", e.g. an environment for co-working, testing and implementing new practices. The innovation Hub comprises local sites, makerspaces ('**Fab-Labs**' to offer the opportunity for actors to co-design technological innovations), and a web platform making interaction between sites and sharing progress and outcomes of the innovations. While accompaniment of innovation and **participatory processes** are the cornerstone of the project, the scientific challenge consists in the cross-scale assessment of **irrigation performance** through the coupling of advanced methods to integrate farmers with upstream management and downstream effects. The associated research question concerns the role of a collective platform on the emergence and adoption of innovations and its impacts on irrigation water, nutrient, energy use efficiencies. Hence, conceptual and functional modeling of the innovation process will propose to reflect on synergies and trade-off resulting from irrigation development.

2.3 Case studies

A set of eight case studies have been chosen to cover all types of irrigation techniques and agroclimatic zones of the Mediterranean irrigated agriculture except rice addressed specifically in another project. The choice of the case studies was also oriented by the existing relationships with stakeholders. They are listed in Table 1, along with the innovations developed within the project through the set-up of Fablabs. To tackle some of the hottest issues in irrigation management (energy and water conservation, technology adoption, environmental protection, management of collective assets), a range of various challenges is covered by the study sites: irrigation equipment, low-cost sensor and monitoring equipment (improved scheduling), flexibility and energy saving in collective pressurized networks, earth observation tools (precision agriculture), environmental monitoring and collective management.

Table 1: The HubIS cases studies: contexts, issues and innovations tested

Country	Site	Context	Main issue(s)	FabLab	Innovation(s)
Algeria (central)	Ghardaïa region	Sahara region with horticultural crops irrigated by groundwater resources	Low irrigation performance (over-irrigation)	Pivot-lab to support local industry and collective empowerment	Locally adapted low-cost miniature center pivot to enhance irrigation performance and reduce manufacturing and operating costs
France (South-East)	Semi-arid Crau plain	Extensive high-quality hay production irrigated by gravity with inter-basin water transfers	Multi-functionality of the hydraulic network (aquifer recharge, environmental flows, climate change), balance between water application and agricultural labor	SurfIrri-lab to improve water use and accounting at field and scheme scales and increase water application efficiency	Improvement of irrigation practices at field scale (precision, efficiency, labor, adaptation) using low-cost sensors (flowter, arrival detection) paired with a telecom system, automatic connected gates and webservices based on satellite images analysis. Decision support tool at the scheme scale using agrohydraulic modeling to explore scenario of adoption of low-cost technologies

Greece (central)	Thessalic plain	Main agricultural area of the country, various crops (wheat, barley, maize, …), irrigated by groundwater resources	Groundwater levels decline while irrigation water demand increase	Earth Observation lab to prescribe water application and to communicate with farmers	Improvement of irrigation performance at field scale using mapping (water-related indices), spatial modeling (crop evapotranspiration, nitrogen requirement), communication tool (webservice application) and soil sensors and hydrometers (schedule and savings)
Morocco (North)	Gharb scheme	Evolution of cropping systems irrigated with collective channel network and pressurized devices	Low performance of drip irrigation (adaptation of the collective network initially designed for sprinklers)	SmartIrri-lab to optimize water consumption & distribution with wireless monitoring and companion modelling	Equipment and application devices to improve scheduling based on soil moisture sensors, weather forecasts, satellite imagery and crop requirement modeling
Portugal (central)	Lucefecit scheme	Maize, olive orchards, vineyards, pastures and cereals irrigated with collective pipe network (sprinklers and drips)	High production costs due to energy consumption at farm & district levels, recurrent water shortage and heterogeneous efficiencies	Irrigation & Energy monitoring lab to optimize water & energy consumption, develop auditing tool, improve practices and simulate energy-efficient schedules	Improve water and energy efficiencies and increase crop productivity at farm level with soil water sensors & management guidelines (operation, maintenance & evaluation; deficit irrigation). Facilitate monitoring, diagnostic & intervention strategy at district level with measuring devices in distribution pipe (flow, pressure) and spreadsheets for technicians (application for water consumption readings) and managers (water & energy computation tools, optimal energy consumer profile)
Spain	Genil-cabra scheme	Guadalquivir valley with olive trees, citrus, field crops and vegetables irrigated with surface water (drip, sprinkler and furrow)	Low profitability due to energy cost, recurrent water shortage, heterogeneous performances	Catch-lab to develop water accounting at catchment scale based on downstream monitoring.	Reduction in water use and in nutrient disposed at farm and district levels with return flow alarms (flow measuring devices + recording + transmitters)
Spain	Southwestern coast (Huelva)	Greenhouses devoted to intensive production of high value berries, ground and surface water (drip irrigation)	Sandy soils, heterogeneous irrigation performance, environmental impacts	Beirrig-lab to test appropriate equipment design to achieve high irrigation uniformity and efficiency	Increase water energy and nutrient efficiencies using automated drainage lysimeter (measure consumptive water use and diffuse pollution) and smartphone application for irrigation scheduling (update on weather forecasting)
Tunisia (coastal)	Haouaria scheme	Vegetables, field crops and orchards irrigated with groundwater (drip and sprinkler)	Groundwater levels decline with subsequent salinization	CoastAqIS-lab for the conservation of an overexploited coastal aquifer	Rationalize water use by implementing smart measuring devices of water flow and pressure in the water distribution pipe (distribution efficiency), and establishing schedule tools localized irrigation

Table 1 shows that even if each case is grounded in a very specific context, issues are quite similar regarding the need to improve irrigation performance. The cases studies are representative of Mediterranean cropping systems and irrigation management. Each case is generally associated to a given research team (sometimes more), which may have already developed collaborations with local actors (mainly WUA and farmers).

3. Mid-term results

3.1 Implementation of participatory research action

Research action and participation of local stakeholders (SH) are fundamentals in HubIs. They are developed for (1) assessing innovation systems and identifying potential virtuous interventions to match local settings (2) enhance the adoption process by involving a large range of stakeholders. Specific activities were planned to associate the end-users to the project activities and outcomes from the beginning of the project, including the dissemination actions. HubIs highlights the importance of SH at local and regional levels: farmers, WUAs, farmers' associations, extension services, NGOs and local companies providing agricultural inputs or services.

The participation process, designed with experts in participatory approaches (Lisode) is organized as follows:

Step 1. Context analysis: national and site contexts, with baseline/performance analysis

Step 2. Stakeholders' analysis: identifying, characterizing and prioritizing key stakeholders

Step 3. Problems' identification (to detect opportunities)
Step 4. Solutions' identification
Step 5. Determine actions that have the highest potential for sustainable irrigation management, an initial selection of innovations that seem to offer the highest potential for use in practice, so called "plausible promises".
Step 6. Implement actions: Testing and adaption process, with « let-it-go » strategy or joint experimentation strategy

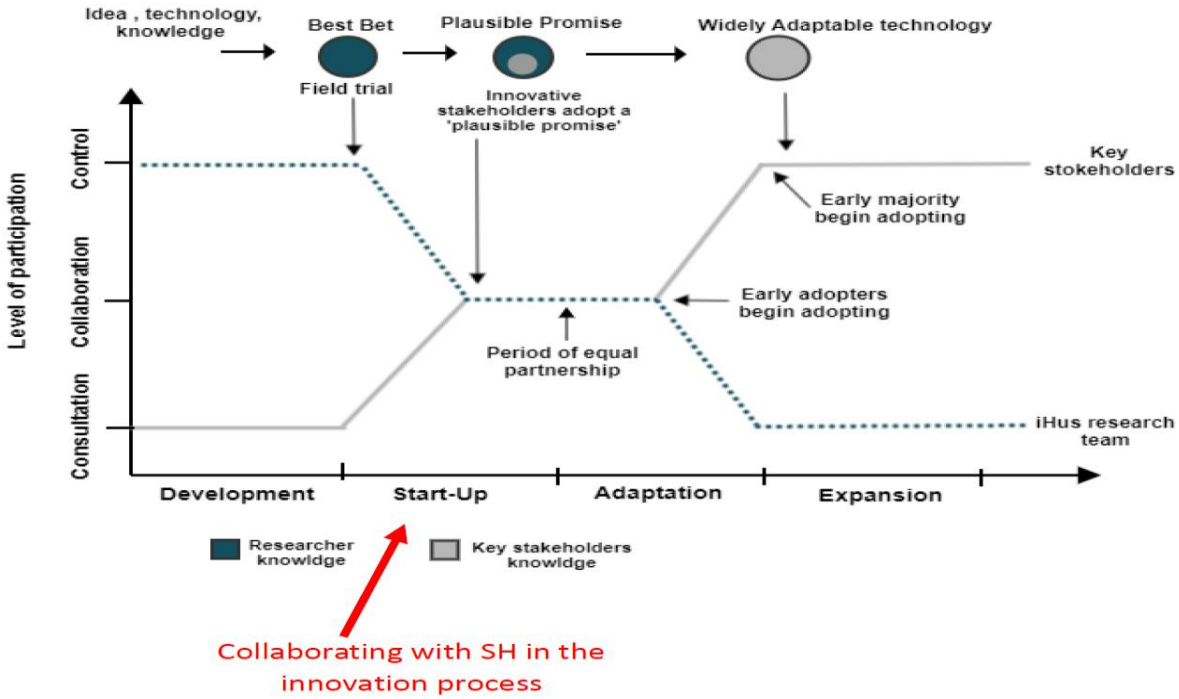

Figure 1: Stakeholders involvement within innovations developed in HubIs Fablabs (adapted from Douthwaite et al.,2001)

The concept of innovation within HubIS was thought to include SH in early stages of innovation processes, in opposition to linear processes where end-users are associated in the late stages of adaptation and expansion. Participation tools for HubIS include problems analysis tools, individual or collective interviews, collective workshops (e.g. **Σφάλμα! Το αρχείο προέλευσης της αναφοράς δεν βρέθηκε.**, Tunisia), role playing games, prioritization tools, participatory mapping, photo safaris, problem or solutions trees, focus groups, priority ranking, participatory modeling… Some HubIS fablabs may be viewed as a novel model of participation in irrigation systems. The whole process is described in Vandôme et al. (2022).

3.2 Irrigation fablabs

The R&D approach lies on the implementation of fab-labs in interaction with the setting of participatory workshops. The Fab-Lab (fabrication laboratory) concept was born at the Massachusetts Institute of Technology for digital fabrication of products generally perceived as limited to mass production. The Fab-Lab movement is closely aligned with the DIY ("Do it yourself" or "bricolage") and the free and open-source movements, and shares philosophy and technology with them. In HubIS we borrowed this concept in most of its dimensions, except that we do not limit it to computer-controlled tools and our Fab-Labs are specialized in specific functions. The irrigation Fab-Labs principle is to share an open innovation environment for small-scale fabrication of technology-enabled products and irrigation practices tailored to local needs. The idea implied small-scale workshops, fabrication of technology enabled products, tailored to local or personal needs. As an illustration, the irrigation fablabs in France

and Tunisia organize participatory workshop to design low-cost sensors (what to measure, how to make it available, where to install the sensors, how to use the information for decision…).

3.3 Evaluation of Irrigation performance

From an irrigation system viewpoint, a multiscale approach is built to propose a set of indicators capable of assessing performance at crossing scales, quantifying the effects of interventions of one scale on higher scales and vis-versa. The set of methods comprises: field experimentation, Rapid Appraisal Process[1](RAP, MASSCOTE 2007), benchmarking, agro-hydrologic modeling, remote sensing, but also participatory workshops, interaction with intermediaries and dissemination tools (from local to regional scales). A reflexive methodology is also implemented to follow-up the innovation adoption process.The main novelty of the indicators is their ability to assess performance at crossing scales, quantifying the effects of interventions at one scale (e.g., field scale), on higher scales (e.g., basin), and vice versa. The results of the RAPs and the computed indicators will be examined, interpreted, and then used as input for benchmarking analyses. Benchmarking techniques will include: (i) Data Envelopment Analysis, (ii) Multi-Regression Models, (iii) Principal Component Analysis, (iv) Cluster Analysis, and (v) other methods.

3.4 Designing and evaluating innovations

From a 'pathway to impact' perspective, the project develops an open basket containing innovations at various Technology Readiness Level (TRL) and intends to complete a set of innovations chains during the project. For example, we will mature a conceptual framework (TRL 2) to characterize basin-scale rebound effects of improved on-farm irrigation efficiency, and we will disseminate existing decision support tools (TRL 7-8) for irrigation scheduling and operation (agrohydrological models, sensors, web-alert systems, index mapping). The variety of TRL will allow an assessment of the innovation process. Since performance gains are expected at farm and district levels, innovations are considered at both levels. They were selected following the site analysis, and completed with those that have emerged from fablabs during the project. They cover the chain of irrigation water use along the water cycle, with different scopes and types of innovations: information at all scales, using low-tech solutions as well as free satellite information (Sentinel 1 and 2) and web-apps, organisation among users, crop planning, irrigation scheduling, effective application… (see Table 1). Therefore, there is a clear focus on practices rather than on application equipment and infrastructures, considering that many large programmes of subsidies for equipment (e.g., for drip irrigation) failed to reach their objectives in term of water saving (see e.g. Kettani et al., *in press*).

3.5 From research to application: upscaling and dissemination

Upscaling at Mediterranean level will be done by extracting generic conclusions from study sites and by evaluating the potential impact of each innovation to increase irrigation performance. This upscaling is relevant thanks to the representativeness, of selected sites, of the various Mediterranean contexts and agroecosystems. It will be achieved using an agroclimatic classification and zoning at the Mediterranean scale (from spatially distributed information), and an evaluation of the potential impact of each innovation type, and conditions of adoption. Dissemination to end-users will be facilitated by the participative approach.

4. Conclusion

The aim of HubIS is to boost and analyse the emergence of, and evaluate, technological innovations that aim at improving the performance and the sustainability of irrigation systems in the Mediterranean

[1] The RAP is a systematic set of procedures for diagnosing the bottlenecks and the performance and service levels within an irrigation system. It also provides key internal and external indicators that can be used as benchmarks in order to compare improvements in performance.

region. These innovations comprise new tools and services for farmers and water users associations, designed to increase water, nutrient and energy use efficiency, such as low-tech sensors, free satellite data, companion modelling of irrigation networks or practices... The gap between actual and attainable performance is tackled from the farm scale, to the irrigation scheme scale, up to the basin level to upscale environmental effects. We expect to demonstrated how the participatory approach setup, declined into stakeholder analysis, identification of potential innovations, fablab design, could boost – or not - the adoption of innovations, compared to top-down public policy approaches.

5. References

Douthwaite, B., Keatinge, J.D.H. and Park, J.R., 2001. Why promising technologies fail: the neglected role of user innovation during adoption. Research policy, 30(5), pp.819-836.

Grimble, R. and Wellard, K., 1997. Stakeholder methodologies in natural resource management: a review of principles, contexts, experiences and opportunities. *Agricultural systems*, *55*(2), pp.173-193.

Kettani, A., Hammani, A., Taky, A., & Kuper, M. (2022). Challenging 'one size fits all': Continued use of sprinkler irrigation in a state-led drip irrigation project in Morocco. *Irrigation and Drainage*. In press

MASSCOTE approach, (2007) Modernizing irrigation management – the MASSCOTE approach Mapping System and Services for Canal Operation Techniques. FAO Irrigation and Drainage Paper.

Rogers, P., & Hall, A. W. (2003). *Effective water governance* (Vol. 7). Stockholm: Global water partnership.

Vandôme P., Belaud G., Leauthaud C., Moinard M., Mekki I., Zairi A., Charron F., Leconte J., Ferchichi I., and Ajmi T., 2022. Exploring ways to improve agricultural water management on two Mediterranean irrigated systems : promises of wireless low-tech sensor networks, IAHS assembly, Montpellier

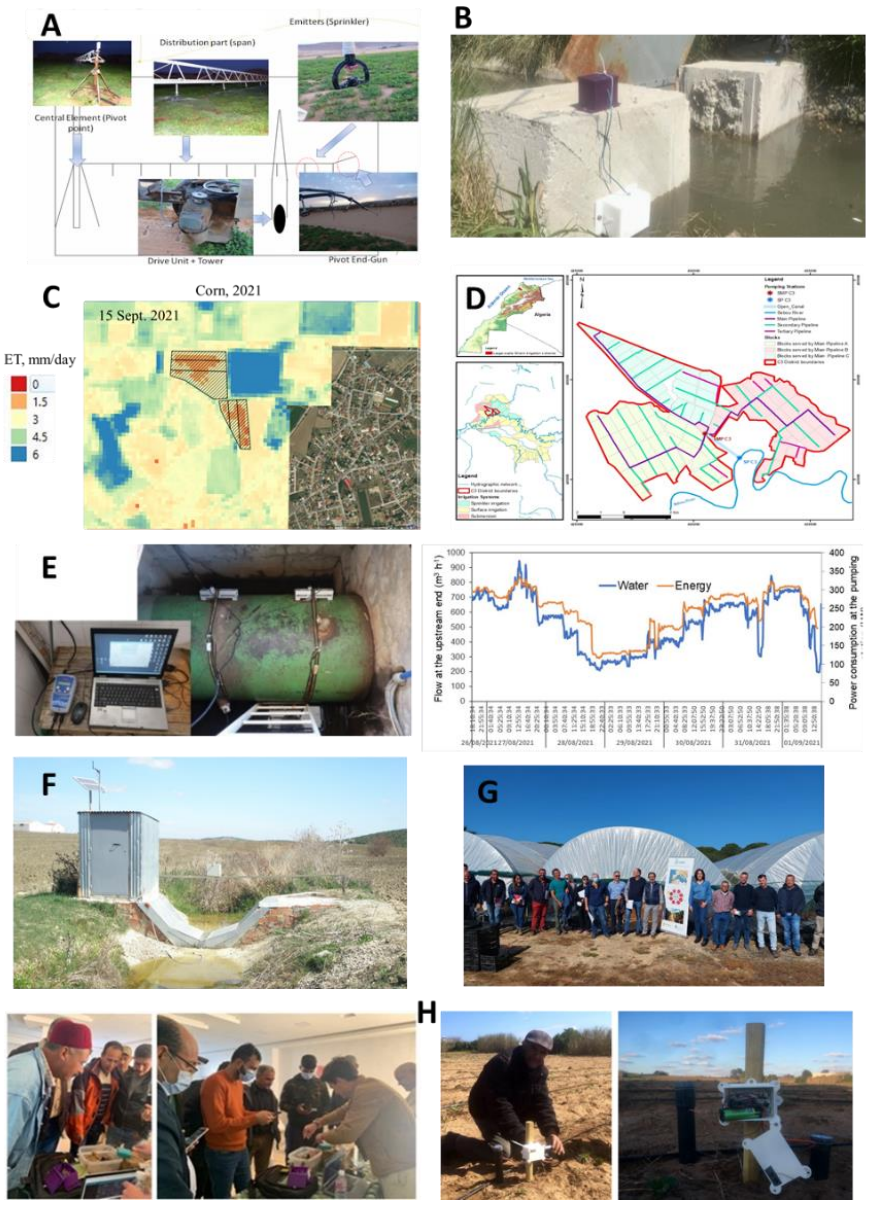

Figure 1: Mosaic of illustration from each case study: A/ Center-pivot innovation from Algeria, B/ SurfIrri-lab flowter sensor, C/ Earth-Observation-lab estimation of daily evapotranspiration (ET) based on Sentinel-2 and Sentinel-3 data, D/ Map of the study site in the Gharb irrigation scheme, E/ Energy monitoring at the pumping station and flows entering the irrigation network in Portugal, F/ Catch-lab gauging station, G/ Beirrig-lab 2022 field day with technicians and farmers and H/ Demonstration of the sensors' prototypes and installation in the irrigated area of Echraf (Tunisia)

From farm to district and basin levels: social technical and environmental efficiency of irrigation systems - The Crau case study

K. Daudin[1], P. Vandôme[1], A. Berkaoui[1], F. Charron[2], G. Belaud[1]

[1] G-EAU, AgroParisTech, Cirad, IRD, INRAE, L'Institut Agro, Univ. Montpellier, Montpellier, France.

[2] G-EAU, AgroParisTech, Cirad, IRD, INRAE, L'Institut Agro, Univ. Montpellier, Salon-de-Provence, France

Abstract

This communication presents the recent advances of the HubIS project on the Crau plain study site. We draw from recent studies in agricultural water management concerning the concept of efficiency to propose a cross-scale assessment framework. The objective is to show the complementarity of a different scale-based analysis, using (a) field measurements of water fluxes, (b) district level evaluation of irrigation performance, (c) documentation of past studies based on groundwater boundaries and (d) basin-scale logics of water transfers. Representative of this nesting issue of "efficiency" assessment, the Crau case study is known for the extensive production of hay thanks to water from outside of hydrological limits (gravity irrigation). In the Crau plain (South East of France), the management of water resources is a multi-stakeholder process in full mutation: naturally dry region, the recharge of the water table is mainly carried out by irrigation water. This recharge plays a role of water tower by allowing other types of uses (drinking water, industries, wetlands). However, the multi-functionality of the hydro-agricultural networks is today under tension, between pressing socio-economic activities (growing demands from farmers and communities), environmental conservation (wetlands: biodiversity, water quality), and potentially reduced water allocation (context of climate change and interaction with upstream territories). By embedding the concept of efficiency into specific spatial and temporal scales, the HubIS project ambitions to compute effective water efficiency and productivity by up-scaling farm efficiency to the irrigation scheme and watershed scales, and to find pathways to improve the overall performance of these farming systems. To do so, there are important challenges to address: evaluate the actual practices, and find affordable ways to improve them. For the Crau plain, we will tackle some promising avenues for research and development: (a,b) recent advances on remote sensing data access and low-cost sensors to improve water accounting and flow management, (c) socio-hydrological observatory to give reflexive insights into knowledge and action interactions, (d) role of hypotheses and uncertainties in a process-based modelling of flow withdrawals.

1. Introduction

Irrigation is the activity of making sufficient soil water available to meet transpiration requirements, dictated by local climate and depending on plant cover and stage of growth. The strategic components of irrigation at the farm level remain unchanged for centuries and related to how much water is delivered and when (e.g. irrigation as the art of delivering the right amount of water at the right time). To evaluate the performance of irrigation, various indices have been defined in the late 1990s (Burt et al., 1997) and a methodology was proposed to systematically and quickly determine key indicators in the aim of facilitating informed decisions (Burt, 2002). The ultimate purpose of performance assessment is to provide relevant feedback to the management at all levels (Bos et al., 2005).

Efficiency in irrigation terminology was introduced more than 100 years ago to provide an indicator of the amount of biomass produced per unit of water used (Hatfield and Dold, 2019). Policies of water savings in agriculture implemented worldwide during the lasts decades mainly relied on the argument of increased efficiency with the modernization of infrastructures and equipment. First, investing in irrigation development (new technology or management measures) to improve efficiency may paradoxically increase water consumption (called rebound effect (Berbel and Mateos, 2014) or

paradox of irrigation efficiency). Second, the investments in management and maintenance were underestimated and the organizational dimension overlooked in collective systems (Bouarfa et al., 2020). Third, physical water accounting must be developed in parallel of water savings policies (Grafton et al., 2018) since for example drip efficiencies are generally only measured in experimental plots (van der Kooij et al., 2013).

The irrigation efficiency classically draws on the ratio between evapotranspiration and water inputs, but many definition haves been proposed over time and applied to a wide range of scales. Since the middle of 2000s, some concerns arose about the use of "efficiency" as an indicator of irrigation performance. The main issues are about:

- spatial bounds: losses at farm scale are generally reused at the watershed scale (Jensen, 2007; Perry et al., 2009; Serra-Wittling et al., 2019);
- temporal scale: time interval is important since both supply and demand constantly evolves (Burt et al., 1997; Pereira et al., 2012);
- rational: engineers focus on design and operation at the farm and district levels while hydrologists on reutilization of return flows as a function of the spatial layout and hydraulic connections (Mateos, 2008);
- perspectives: efficiency has multiple meanings for diverse actors (Lankford et al., 2020), e.g. empirical calculation, management practice, sustainability measure and policy goal, and water used for agricultural production is also a matter of economic and social relevance with political implications.

At the same time, many development opportunities arose in the irrigation sector with Information and Communication Technologies (ICT) that enable accurate monitoring (field measurements with sensors like soil probes and wireless networks, remote-sensing applications) (Nam et al., 2016), automate irrigation (actions through different devices) (Sánchez-Sutil and Cano-Ortega, 2021), and facilitate the continuous exchange of information across the water supply chain (Levidow et al., 2014). Some successful experiments of ICT-based optimization strategy have been achieved, for example Water User Association (WUA) managers that optimize the distribution (Soto-Garcia et al., 2013) or farmers that adjust frequency and quantities (Serra-Wittling et al., 2019). One recognized way forward is thus to continue to develop, implement, test and disseminate tools to support data-oriented irrigation management (Liang et al., 2020). Affordability is clearly a lock for a large adoption of decision support systems and watering methods based on advanced technologies.

In this framework, the HubIS project (2020-2023, Prima funding) intends to produce research-based developments by developing, implementing and evaluating a set of innovations based on local irrigators needs and low-cost technologies. To improve the performance of irrigation systems in the Mediterranean region, the project develops methods, tools and services to improve scale-integration of performance evaluations (technical, socio-economic and environmental assessments). It draws on a set of local experimental sites across the region that merge two concepts: participatory workshops (involving local actors in co-innovation processes) and makerspaces (Fab-Labs to design and maintain technological devices). This communication focuses on the cross-scale evaluation of the efficiency of a specific irrigation system of the French pilot site. The site developments draw on the implementation of innovations to close the performance gap and reduce labor, to establish a performance indicator matrix and to develop a dynamic model of water flows. Since reaching a coherent system definition is not trivial in the irrigation domain (Froebrich et al., 2020) and because we seek to develop an original modeling approach and propose decision support tools in the next steps, a preliminary focus on observations is expected to support the building of the multi-method combination to assess cross-scale efficiency in an adaptive way. We thus propose in this communication a description of the

ongoing research-action process. We draw on the description of the Crau case study to develop a place-based cross-scale multi-dimensional approach and then we present and discuss the results obtained so far. The objective is to trigger the coupling of various observations at different scales (spatial but also administrative with regard to who has responsibilities of water control) and propose a discussion on an exploratory social technical environmental system understanding.

2. Materials & Methods

2.1 The Crau case study

The Crau plain (600 km^2, Fig. 1), located in South Eastern France (Mediterranean climate), is the paleo-delta of the Durance River characterized by stony soils and a unique semi-arid ecosystem receiving annually in average less than 600 mm of precipitations. During the 16th century, the construction of irrigation channels led to the transformation of dry grasslands mainly used for sheep grazing into hay meadows (water transfers in artificial channel network). Irrigation thus introduced a frontier between steppes and irrigated areas, but note that pastoral sheep breeding still uses the two types of grasslands for grazing. Irrigated grasslands produce high quality hay with a controlled designation of origin label.

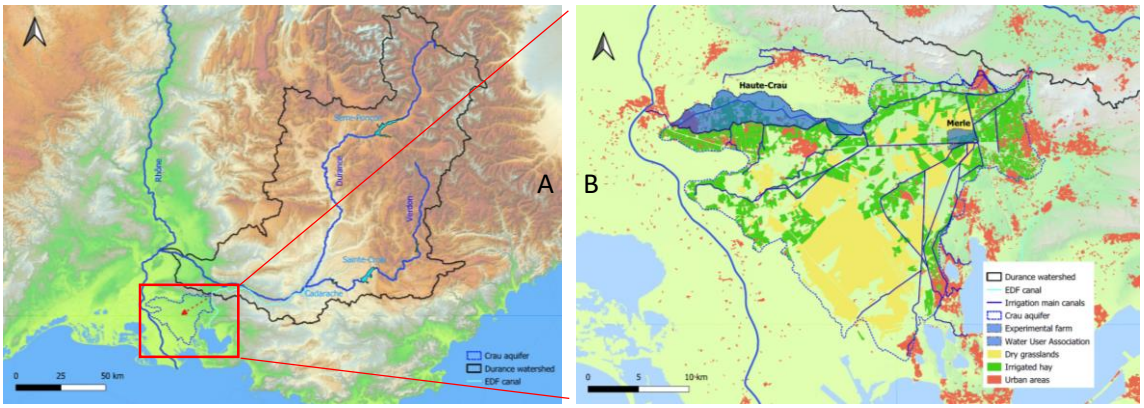

Figure 1: The semi-arid Crau plain: cross-scale analyses of the gravity-irrigation system (A: Durance system with a red arrow to illustrate water transfers; B: Crau system wih an emphasis on the studied sub-systems: Merle farm and Haute-Crau scheme). Source: open-access French databases issued by IGN and Institut Agro Montpellier databases for land cover, irrigation canals and WUA limits.

The Durance water transfer system is unique (water transported by water) and delivers around 0.75 billion m^3/year outside its watershed limits for irrigated agriculture, mainly in the low Durance perimeter that include the Crau plain. Traditional irrigation practices consist in flooding the grassland fields with a high discharge, so that it can reach the downstream end of the plot. The excess is drained through ditches and deep percolation under the plots. Hence, the recharge of the aquifer in the Crau plain depends for around 70% on the irrigation of around 15000 ha of meadow. Still, since 1970s industrial development, other types of agriculture (mainly orchards, 5,000 ha irrigated through drip technics) and urbanization increasingly tap the aquifer, which is currently the main domestic water resource for the 300,000 inhabitants in the area. Moreover, the water channel network participates to the presence of wetlands and supply water to hedgerows (numerous due to strong winds).

Aquifer management thus rely on the sustainability of the hay irrigation system, but many social and technical changes may occur (irrigation practices, replacement of hay production by other crops) and the precipitation regime in the French Alps in the future remains uncertain. Hence, the management of water resources is a multi-stakeholder process in full mutation and the multi-functionality of the hydro-agricultural networks is today under tension, between pressing socio-economic activities (growing demands from farmers and communities), environmental conservation (wetlands:

biodiversity, water quality), and potentially reduced contributions (context of climate change and interaction with upstream territories). In this context, the "inefficiency" of gravity-flow irrigation may be questioned since return flows provide a mix of valuable and interdependent services with regional implications.

2.2 Methods

Based on an experimental farm directly managed by their institution (Merle, Institut Agro Montpellier), scientists in water hydraulics and agriculture management developed knowledge & action researches for more than 20 years. Drawing on previous studies and existing collaborations with key stakeholders engaged in management and governance, the study plans to upscale the farm scale results at the district level while considering allocation mechanisms at the watershed level. The Crau case study appears a good opportunity to implement a network of sensors and improve knowledge on actual practices (farm scale), and also to propose remote-sensing application for scheme operation and maintenance and to put into perspective irrigation losses (district scale). Then we propose a cross-scale multi-dimensional approach based on a place-based perspective of irrigation efficiency.

First, we acknowledge that each irrigation system is embedded into its unique context, and its efficiencies are to be considered highly dynamic in time and space and depending on the set of stakeholders involved in complex socio-technical trajectories (Lankford, 2012). Indeed, integrating stakeholders' perspectives into irrigation efficiency analyses and performances debates is an emerging way to broader irrigation performance analysis (Venot and Kuper, 2019). For example, (Benouniche et al., 2014) propose to analyze performance through the change in farmers' irrigation practices, (Mateos and Araus, 2016) acknowledge that the key to the formulation of the optimization problem relies on the delimitation of the domain of concern which is associated to a community and a decision-maker, and (Lankford et al., 2020) propose a matrix to navigate applications of efficiency employed by different actors at different scales for different purposes (efficiency as a boundary object, a way to think and dialog across scales).

Second, we build on a plurality of methods to investigate the social, technical and environmental dimensions of the multiscale interaction of the Crau irrigation system (Biggs, 2021). We propose to combine quantitative and qualitative approaches to analyze data from various sources: empirical field data, co-produced data through dialogs and sharing among actors, archival information from previous studies, downloaded datasets from public databases. The selection of methods is guided by expertise, research funding (multi-partners project) and relevancy for local developments (insights from the Merle):

- field measurements and monitoring at the plot scale and farm level intend to provide the basis for the evaluation of technical solutions (implementation of innovations like soil sensors and automated gates) with a focus on both water consumption and agricultural labor;
- district level performance evaluation is expected to provide orders of magnitude by the implementation of a systematic set of procedures for diagnosing the bottlenecks and the performance and service levels within an irrigation system (RAP);
- application of tools from participatory action research (collective workshops with stakeholders to illustrate the use of innovation), development of services from remote sensing data in collaboration with farmers and WUA, and implementation of Geographic Information Systems tools and data storage facilities;
- qualitative methods for territorial diagnosis like interviews with farmers and managers (socio-economic study), timelines to represent the evolution of research and development activities, narratives and maps to explore new ways of dissemination.

Third, we develop a dynamic modelling of the agricultural-hydrological irrigation system (with social, technical and environmental dimensions), drawing from the combination of theoretical models and empirically informed models. The modelling objective is to characterize the way in which the system unfolds over time from the interplay of processes, enabling the exploration of outcomes across scales. To investigate the irrigation return flows to the Crau environment (aquifer recharges) we will give a special attention to the consideration of the actors choice (for example to implement an innovation) in the dynamic physical model. Scenarios will be simulated to test several hypotheses, for example on the trade-offs between labor and hydraulic performance and on the influence of water distribution practices on water infiltration through canals. The overall research process would finally provide a useful input for technical reflections while favoring collaborative practices among stakeholders.

3. Results & Discussion

3.1 Field and district performance evaluation

The baseline

The "Merle" center (around 3 Mm^3/year for 150 ha of hay) is both a reference agricultural domain (place of production that need to balance income and expenses) and a place for scientific experimentation. Two modernization steps mark the farm's trajectory over the last 20 years: first the rapid implementation of various technics for gravity-flow irrigation improvement (early 2000s, valves, pipes and liners), second the progressive levelling phase (10-15 ha/year) and suppression of water gates. Since mid-2000s concerns about agricultural labor rose (avoid night watering), but it has been shown that it increases water uses (from 15,000 m^3/ha/year to around 30,000 m^3/ha/year). Today, it is recognized that social and economic dimensions of hay farming systems (work time) are as much important than the capacity to manage water flows, but these two aspects need to be carefully balanced. Moreover, for more than 30 years trials-and-errors on automatic gate systems confront to difficulties in up-scale (from farm to district) due to market opportunities and the need for intermediaries. Hence, the Merle is in a good position 1) to capitalize on past development projects (for example less gates means less maintenance work), 2) to develop situated knowledge through instrumented experiments and 3) to disseminate new knowledge, tools and services to farmers and WUA (important expectations from stakeholders).

In the frame of the HubIS project, field measurements campaigns have been performed in the Merle center for the 2021 irrigation season and is still on going for the 2022 season (Fig. 2A). Two tertiary blocks of the farm have been instrumented with input and output discharges sensors (intake and drainage flow rates). The agronomic monitoring also rely on yield measurements.

The evaluation of irrigation district performance (Fig. 2B) was achieved following the RAP methodology. The main characteristics of the Haute-Crau Water User Association and all relevant information about canal characteristics, boreholes and agricultural productions have been gathered. The irrigated areas covers around 2800 ha and is achieved by gravity for the hay (collective irrigation scheme) and by micro-irrigation for orchards, olive trees and gardening (private tube wells). The 2016 land cover map was used to assess the orders of magnitudes of each crop, and a simplified water balance was computed using local weather station statistics and making hypothesis regarding irrigation practices and crop coefficients.

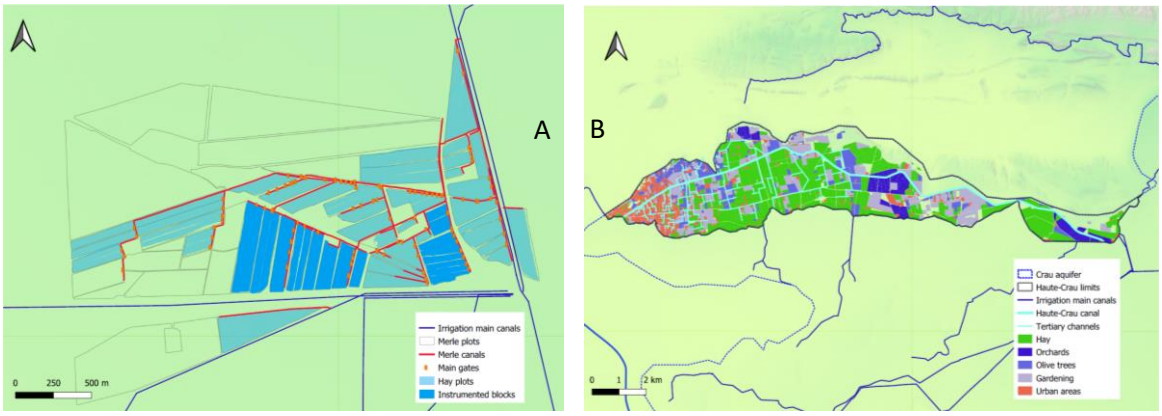

Figure 2: Farm and district performance evaluations (A: Merle farm; B: Haute-Crau district)

The coupling of farm and district evaluation levels will be achieved through a dynamic model to simulate development scenarios of irrigation perimeters at several spatial scales. The objective is to define the performance baseline based on external indicators and compare with the performance that would be achievable supposing that farm-based innovations are widely implemented at the district scale (modeling tool to test various scenario).

Innovations for improved management

Two low-tech low-cost sensors (flowter sensor for frequency and duration of events, and downstream water detection sensor) were specifically developed, based on IoT technologies and connected to a network server (open-source hardware and LoRaWAN communication protocol, alert to the farmer/operator). The objectives are 1) to set the baseline of irrigation performance and check during the second season the influence of sensors implementation, 2) to support irrigation management by avoiding excessive surface drainage (reduce applied volumes) and reduce round trips on the field (less labor and night shifts). The “low-tech” technical solutions implemented in the farm (design, experimentation, evaluation) then feed the simulation of the district behavior in case of large innovation adoption.

At the district scale, the use of low-tech sensors might be a way to know better where and how much water is used. Spatial heterogeneity of water needs and actual withdrawal remains a question. Therefore, opportunities of remote sensing applications based on Sentinel products are explored. While research is mature on the link between satellite information and vegetation indices (e.g. (El Hajj et al., 2016)), going further with possible applications to the detection of irrigation events is still on progress (see e.g. (Bazzi et al., 2022)) as well as the design of tailor-made webservices for WUA.

Together, these studies will provide knowledge on the solutions that may improve the control of irrigation water flows and thus participate to hydro-agricultural development. Note other technical studies are being achieved in parallel, for example concerning the fate of chemical inputs in irrigation canals (used for maintenance) or the deployment of sensors and automated gates in several farms of the Haute-Crau district.

3.2 Water fluxes dynamics in the Crau plain

The sustainability of water transfers may be questioned at the territorial scale (e.g. the Crau aquifer limits). For example, the Durance water resource may come to be reduced by climate change, or the agricultural areas in the Crau plain dedicated to irrigated hay may undergo a transformation towards other crops or urban and leisure land uses. Today, information is thus greatly needed to identify adapted management principles for land and water planning. For example, local authorities wonder if

it is worth continue to invest in boreholes for drinking water, given the state of the hydraulic infrastructures (restoration may be very expensive) and the difficulties to recognize services rendered by irrigation canals (an experimental approach is being implemented to pay farmers for the indirect aquifer recharge). In this context of multi-uses of groundwater resource, it is proposed to describe the water fluxes dynamics in the Crau plain and its evolution through time (e.g. propose a social–historical trajectory of water flows).

Hence, to contextualize water fluxes dynamics in the Crau plain two research activities are being performed in collaboration with stakeholders. First, we trace past research and management studies based on the Crau aquifer spatial limits (systematic indexing) and structure information and data acquired during the last 20 years in the Merle domain. This capitalization study on an experimental sites and its embedding in a broader system will directly benefit from more than 20 years of research and education trainings on water fluxes in agricultural area. The objective is twofold: (i) gather and organize knowledge and datasets to make them visible and reusable (secure information and facilitate sharing), (ii) propose a rapid visualization of previous and on-going projects and give space for a future implementation of a social-hydrological observatory (collaborative mapping, collective learning and adaptive management). Second, water transfers from the Alps to the Crau plain are based on French laws and agreements between hydroelectricity and agriculture stakeholders during the period of major hydraulic developments in the Durance system. These texts specified terms and conditions of water releases of upstream reserve in case of a deficit (resource management during seasonal droughts). The volumes dedicated to agriculture are calculated via a simplified algorithm mainly based on mass balance and measurements of water flows throughout the succession of hydraulic infrastructures. The objective of this critical analysis of inter-basin transfer logics is to propose a didactic explanation on the way the algorithm works (making it understandable by farmers). Specific attention will be given to the definition of terms used, to the translation (from words to calculations) and negotiation processes.

4. Conclusions

The pooling of on-going research activities is expected to produce knowledge on a scale-based adaptive management and to give an illustration on the necessity to have a systemic understanding of irrigation performance. Still one do not forget that the main reasons for farmers to invest in technology remain increased income and convenience, and that high-level performance at the farm-scale need some technicity from irrigators. Hence, farmers need adequate assistance to improve environmental sustainability while maintaining financial and labor objectives (Levidow et al., 2014). Moreover, the data-driven evaluation process supporting effective organization of collaboration and timely provision of monitoring results needs to be complemented by service indicators, first to measure the capability of a collective water system for timely delivery of appropriate volumes (Pereira et al., 2012), second to consider other services than just evapotranspiration in the evaluation of water productivity (Grafton et al., 2018).

5. References

Bazzi, H., Baghdadi, N., Charron, F., Zribi, M., 2022. Comparative Analysis of the Sensitivity of SAR Data in C and L Bands for the Detection of Irrigation Events. Remote Sensing 14, 2312. https://doi.org/10.3390/rs14102312

Benouniche, M., Kuper, M., Hammani, A., Boesveld, H., 2014. Making the user visible: analysing irrigation practices and farmers' logic to explain actual drip irrigation performance. Irrig Sci 32, 405–420. https://doi.org/10.1007/s00271-014-0438-0

Berbel, J., Mateos, L., 2014. Does investment in irrigation technology necessarily generate rebound effects? A simulation analysis based on an agro-economic model. Agricultural Systems 128, 25–34. https://doi.org/10.1016/j.agsy.2014.04.002

Biggs, R. (Ed.), 2021. The Routledge handbook of research methods for social-ecological systems, Routledge international handbooks. Routledge, Taylor & Francis Group, New York.

Bos, M.G., Burton, M.A., Molden, D.J. (Eds.), 2005. Irrigation and drainage performance assessment: practical guidelines. CABI, Wallingford. https://doi.org/10.1079/9780851999678.0000

Bouarfa, S., Brelle, F., Coulon, C., 2020. Quelles agricultures irriguées demain ? répondre aux enjeux de la sécurité alimentaire et du développement durable, Matière à débattre et décider. Éditions Quae, Versailles.

Burt, C.M., 2002. Rapid Appraisal Process (RAP) and Benchmarking Explanation and Tools (No. FAO/Thailand and WB Irrig. Institutions Window).

Burt, C.M., Clemmens, A.J., Strelkoff, T.S., Solomon, K.H., Bliesner, R.D., Hardy, L.A., Howell, T.A., Eisenhauer, D.E., 1997. Irrigation Performance Measures: Efficiency and Uniformity 22.

El Hajj, M., Baghdadi, N., Cheviron, B., Belaud, G., Zribi, M., 2016. Integration of remote sensing derived parameters in crop models: Application to the PILOTE model for hay production. Agricultural Water Management 176, 67–79. https://doi.org/10.1016/j.agwat.2016.05.017

Froebrich, J., Ludi, E., Bouarfa, S., Rollin, D., Jovanovic, N., Roble, M., Ajmi, T., Albasha, R., Bah, S., Bahri, H., Barberá, G., Beek, C., Cheviron, B., Chishala, B., Clercq, W., Coulibaly, Y., Dicko, M., Diawara, B., Dolinska, A., Ducrot, R., Erkossa, T., Famba, S., Fissahaye, D., De Miguel Garcia, A., Habtu, S., Hanafi, S., Harper, J., Heesmans, H., Jamin, J., Klooster, K., Mason, N., Mailhol, J., Marlet, S., Mekki, I., Musvoto, C., Mosello, B., Mweetwa, A., Oates, N., Phiri, E., Pradeleix, L., Querner, E., Rozanov, A., Ker Rault, P., Rougier, J., Shepande, C., Sánchez Reparaz, M., Tangara, B., De Vente, J., Witt, M., Xueliang, C., Zairi, A., 2020. TRANSDISCIPLINARY INNOVATION IN IRRIGATED SMALLHOLDER AGRICULTURE IN AFRICA. Irrig. and Drain. 69, 6–22. https://doi.org/10.1002/ird.2400

Grafton, R.Q., Williams, J., Perry, C.J., Molle, F., Ringler, C., Steduto, P., Udall, B., Wheeler, S.A., Wang, Y., Garrick, D., Allen, R.G., 2018. The paradox of irrigation efficiency. Science 361, 748–750. https://doi.org/10.1126/science.aat9314

Hatfield, J.L., Dold, C., 2019. Water-Use Efficiency: Advances and Challenges in a Changing Climate. Front. Plant Sci. 10, 103. https://doi.org/10.3389/fpls.2019.00103

Jensen, M.E., 2007. Beyond irrigation efficiency. Irrig Sci 25, 233–245. https://doi.org/10.1007/s00271-007-0060-5

Lankford, B., 2012. Fictions, fractions, factorials and fractures; on the framing of irrigation efficiency. Agricultural Water Management 108, 27–38. https://doi.org/10.1016/j.agwat.2011.08.010

Lankford, B., Closas, A., Dalton, J., López Gunn, E., Hess, T., Knox, J.W., van der Kooij, S., Lautze, J., Molden, D., Orr, S., Pittock, J., Richter, B., Riddell, P.J., Scott, C.A., Venot, J., Vos, J., Zwarteveen, M., 2020. A scale-based framework to understand the promises, pitfalls and paradoxes of irrigation efficiency to meet major water challenges. Global Environmental Change 65, 102182. https://doi.org/10.1016/j.gloenvcha.2020.102182

Levidow, L., Zaccaria, D., Maia, R., Vivas, E., Todorovic, M., Scardigno, A., 2014. Improving water-efficient irrigation: Prospects and difficulties of innovative practices. Agricultural Water Management 146, 84–94. https://doi.org/10.1016/j.agwat.2014.07.012

Liang, Z., Liu, X., Xiong, J., Xiao, J., 2020. Water Allocation and Integrative Management of Precision Irrigation: A Systematic Review. Water 12, 3135. https://doi.org/10.3390/w12113135

Mateos, L., 2008. Identifying a new paradigm for assessing irrigation system performance. Irrig Sci 27, 25–34. https://doi.org/10.1007/s00271-008-0118-z

Mateos, L., Araus, J.L., 2016. Hydrological, engineering, agronomical, breeding and physiological pathways for the effective and efficient use of water in agriculture. Agricultural Water Management 164, 190–196. https://doi.org/10.1016/j.agwat.2015.10.017

Nam, W.-H., Hong, E.-M., Choi, J.-Y., 2016. Assessment of water delivery efficiency in irrigation canals using performance indicators. Irrig Sci 34, 129–143. https://doi.org/10.1007/s00271-016-0488-6

Pereira, L.S., Cordery, I., Iacovides, I., 2012. Improved indicators of water use performance and productivity for sustainable water conservation and saving. Agricultural Water Management 108, 39–51. https://doi.org/10.1016/j.agwat.2011.08.022

Perry, C., Steduto, P., Allen, Richard.G., Burt, C.M., 2009. Increasing productivity in irrigated agriculture: Agronomic constraints and hydrological realities. Agricultural Water Management 96, 1517–1524. https://doi.org/10.1016/j.agwat.2009.05.005

Sánchez-Sutil, F., Cano-Ortega, A., 2021. Smart Control and Energy Efficiency in Irrigation Systems Using LoRaWAN. Sensors 21, 7041. https://doi.org/10.3390/s21217041

Serra-Wittling, C., Molle, B., Cheviron, B., 2019. Plot level assessment of irrigation water savings due to the shift from sprinkler to localized irrigation systems or to the use of soil hydric status probes. Application in the French context. Agricultural Water Management 223, 105682. https://doi.org/10.1016/j.agwat.2019.06.017

Soto-Garcia, M., Del-Amor-Saavedra, P., Martin-Gorriz, B., Martínez-Alvarez, V., 2013. The role of information and communication technologies in the modernisation of water user associations' management. Computers and Electronics in Agriculture 98, 121–130. https://doi.org/10.1016/j.compag.2013.08.005

van der Kooij, S., Zwarteveen, M., Boesveld, H., Kuper, M., 2013. The efficiency of drip irrigation unpacked. Agricultural Water Management 123, 103–110. https://doi.org/10.1016/j.agwat.2013.03.014

Venot, J.-P., Kuper, M., Zwarteveen, Margreet Z., 2019. Drip irrigation for agriculture: untold stories of efficiency, innovation and development.

Catchment-scale water accounting and quality monitoring. A Fab Lab for improving irrigation performance

I. Doménech-Carretero, E. Gallego and L. Mateos

Abstract. The Fab-Lab is an irrigated catchment located in the Genil-Cabra Irrigation District (40,000 ha), Córdoba, Spain. The catchment is remotely monitored by irrigation hydrants equipped with water meters, three rain gauges, and a runoff gauging station with an automatic water sample at its outlet. The catchment covers 303 hectares cultivated with olive trees, field crops (cotton, sunflower, wheat), and vegetables (garlic, onion, melon) on 7 small and medium-sized farms. On-field irrigation is with drip and sprinkler systems. The main objective was to improve the conservation of water and soil by supporting the advisory service of the district Water Users Association. Specific objectives were to: 1) explore relationships between water balance components, 2) quantify the runoff through the gauging station, 3) improve irrigation efficiency at the farm and catchment scales based on a detailed analysis of water balance components, and 4) develop irrigation misuse alerts based on runoff monitoring (flow rate and quality). The paper will present water balances of seven hydrological years and discuss measures to improve irrigation performance based on runoff monitoring, distinguishing between the rainy and irrigation seasons (outlining an alert system).

1 Introduction

The watershed scale is the preferred domain for water management and its monitoring under the EU Water Framework Directive. However, the limits of the irrigated areas rarely coincide with the dividing lines of watersheds, so the evaluation of irrigation performance at this scale is not straightforward. Identifying watersheds where return flows can be monitored will help to evaluate water conservation practices and to implement alerts of irrigation water misuse. Criteria and rules for such alerts require previous understanding of the irrigation hydrology and rainfall-runoff relationships in the concerned catchments. The objective of this paper was a preliminary analysis of such relationships and irrigation performance assessment in a Fab-Lab consisting of a monitored irrigated catchment in the Genil-Cabra Irrigation Scheme, Spain.

2 Material and methods

2.1 The study catchment (Catch-Lab)

The study catchment (Fig. 1) is a watershed located in the Genil-Cabra Irrigation Scheme (40,000 ha), in Córdoba, Spain, where the climate is Mediterranean, with hot and dry summer and relatively wet fall and winter. A pressurized pipe network operating on-demand supplies water to the farms. The on-farm irrigation systems are drip/trickle and sprinkler. The main channel of the watershed is 3.6 km long up to the gauging station. The main crops in the catchment are olive, wheat, sunflower and garlic.

Figure 1 Orthophoto of year 2016 showing the catchment boundaries (red), main channel (blue), farms boundaries (green), location of the hydrological station (green circle), hydrants (blue squares) and the rain gauges (black circles) in the Catch-Lab.

2.2 The hydrological station and data collection

The hydrological station consists of a long-throated flume, an ultrasonic water level sensor (Siemens Milltronics, model The Probe; Munich, Germany), an automatic water sampler (Teledyne ISCO, model ISCO 3700C; Lincoln, NE), an automatic tipping bucket rain gauge (Decagon SH2O, model ECRN-100, Pullman, WA), a data logger (Campbell Scientific, model CR1000; Logan, UT), and a GSM communication system (Campbell Scientific, model CS-GSM, Logan, UT). The water level was measured at 2-min intervals.

Two additional automatic tipping bucket rain gauges (like the one installed at the hydrological station) monitor rainfall in the upper and middle watershed (Fig. 1).

Daily applied irrigation was measured with Woltman water meters at the 23 hydrants that supply water to the plots in the watershed (Fig. 1).

Data presented in this paper corresponded to the period 2011-2021. Unfortunately, the gauging station was out of operation during the last two hydrological years.

2.3 Water balance in the study catchment

The watershed water balance components are rainfall (R), irrigation (I), evapotranspiration (ET), surface and subsurface runoff (Q), deep percolation (D) and changes in the water storage in soil (∆S) during the period of study. R, Q, and I were measured. D was considered negligible because of the subsoil in permeability (Fernández et al., 2007). ET was estimated following the dual crop coefficient method proposed by Allen et al. (1998) with the estimation of the basal crop coefficient from a satellite-derived vegetation index (Mateos et al. (2013). Then, a soil root zone water balance was computed to estimate ∆S (as in Duarte and Mateos, 2022). The full water balance was computed for only for year 2016 (Rodríguez-Álvarez et al. (2019).

2.4 Water use indicators

Irrigation performance and catchment water usage were quantified for the irrigation season of the hydrological year 2015-2016 using the indicators Relative water supply (RWS), Relative irrigation supply (SRR), Irrigation efficiency (IE) and Runoff coefficient (ROC) (Molden and Gates, 1990):

$$RWS = \frac{volume\ of\ water\ supplied\ to\ the\ crop}{volume\ of\ crop\ water\ demand} = \frac{R+I}{ET_{crop}} \quad (1)$$

$$SRR = \frac{volume\ of\ irrigation\ water\ applied\ to\ the\ crop}{volume\ of\ crop\ irrigation\ demand} = \frac{I}{I_{required}} \quad (2)$$

$$IE = \frac{I-Q}{I} \quad (3)$$

$$ROC = \frac{Q}{R+I} \quad (4)$$

2.5 Hydrological modelling

The hydrology of the watershed was modelled based on the 100 runoff events identified in the period of analysis. We used general linear models of covariance (ANCOVA) where runoff was the endogenous variable. The three tested models resulted from considering precipitation (X_{t1}) as the only exogenous variable (Model I, Eq. 5), adding soil moisture at the time of the event (here estimated as rainfall during the previous 10-day period, X_{t2}) as the second endogenous variable (Model II, Eq. 6), and adding a third, dummy variable, the four quarters (T_{t3}, T_{t4}, T_{t5}, and T_{t6}, respectively) of the hydrological year (Model III, Eq. 7):

$$Y_t = \beta_1 * X_t + U_t \quad (5)$$

$$Y_t = \beta_1 * X_{t1} + \beta_2 * X_{t2} + U_t \quad (6)$$

$$Y_t = \beta_1 * X_{t1} + \beta_2 * X_{t2} + \beta_3 * T_{t3} + \beta_4 * T_{t4} + \beta_5 * T_{t5} + \beta_6 * T_{t6} + U_t \quad (7)$$

3 Results and discussion

3.1 Watershed hydrology

The period under study was quite variable in terms of rainfall (Fig. 2). The average annual rainfall for the study period was 418 mm. The hydrological year 2012–2013 was considerably wet, while the rest of the years had a rainfall close to (2016–2017, 2017–2018, 2018–2019) or below (2011–2012, 2013–2014, 2014–2015, 2015–2016) the average (Fig. 2).

The runoff coefficient (ROC) was 0.12, a value close to the ones found in Mediterranean environments (Casalí et al, 2008). Irrigation water generated much less runoff than rainfall (Fig. 3) despite contributing slightly more than 33% of the water inflows in the catchment (see runoff from May to September in Fig. 3).

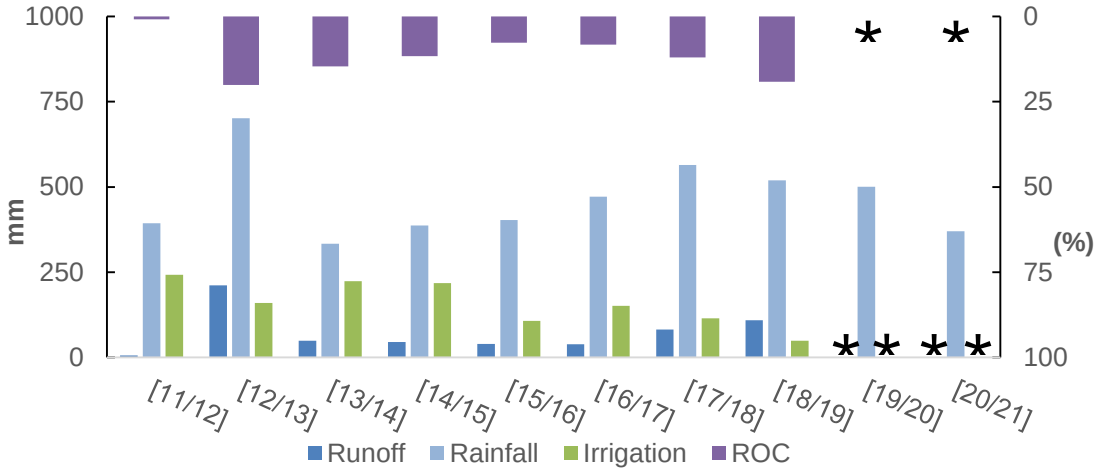

Figure 2. Annual rainfall, irrigation, runoff, and runoff coefficient (ROC) in the study watershed.

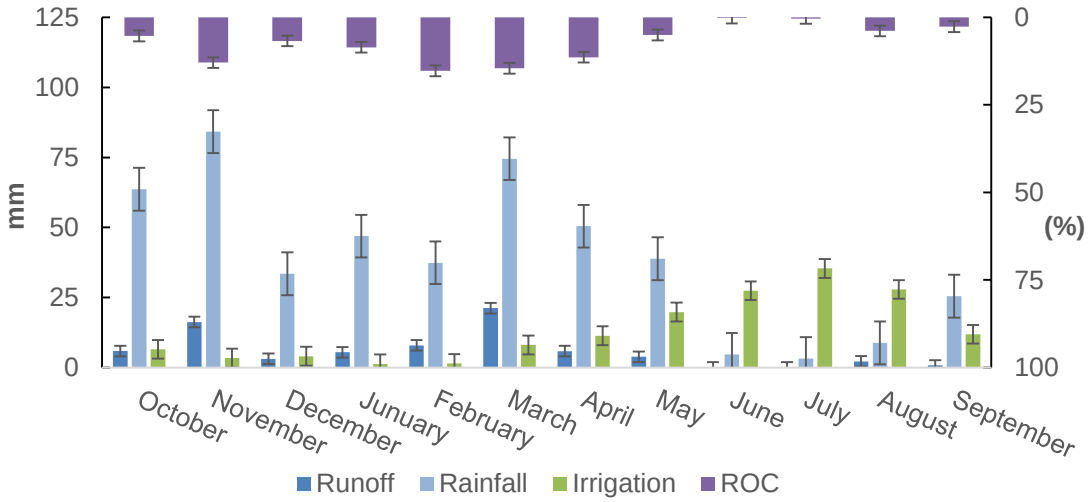

Figure3. Monthly rain, irrigation, runoff, and runoff coefficient (ROC) in the study catchment averaged over the years when these variables were analysed.

The water balance in the irrigation season of 2016 (Table 1) resulted in very low ROC, very high IE, and values of RWS and RIS reflecting deficit irrigation. This good performance prompted to consider sophisticated methods to further close the already narrow performance gap, namely real-time alerts based on runoff monitoring.

Table 1. Indicators of irrigation performance (irrigation season 2016).

Indicator	Value
Relative water supply (RWS)	0.38
Relative irrigation supply (SRR)	0.36
Irrigation efficiency (IE)	0,99
Runoff coefficient (ROC; %)	0.31

The runoff-rainfall relationship was established for the rainy seasons. As expected, runoff increased with rainfall (Fig. 4). However, the slope of the runoff-rainfall relationship increased as the preceding soil moisture increased (Fig. 4). A simple linear regression analysis showed that rainfall explained less than 50% (R^2 = 0.42) of the variance of runoff, while adding the variable 10-day preceding rainfall, through a multiple linear regression it was explained more than 60% of the variance of runoff (R^2 = 0.64). Rainfall intensity surely had an important effect as well (Borga and Morin, 2014); however, the time resolution of our rainfall data did not allow validation of this hypothesis.

The ANCOVA models I, II and II explained over 50%, over 60% and near 75% of the variance of runoff, respectively (statistics in Table 2 and coefficients in Table 4); therefore we chose the last one due to its better fit. The coefficients of the chosen model were statistically significant (Table 3) except for the one for the last four-month period. Therefore, we decided to eliminate this last dummy variable. It should be noted that the model slightly overestimates the lowest runoff values and underestimates the highest values (Fig. 5).

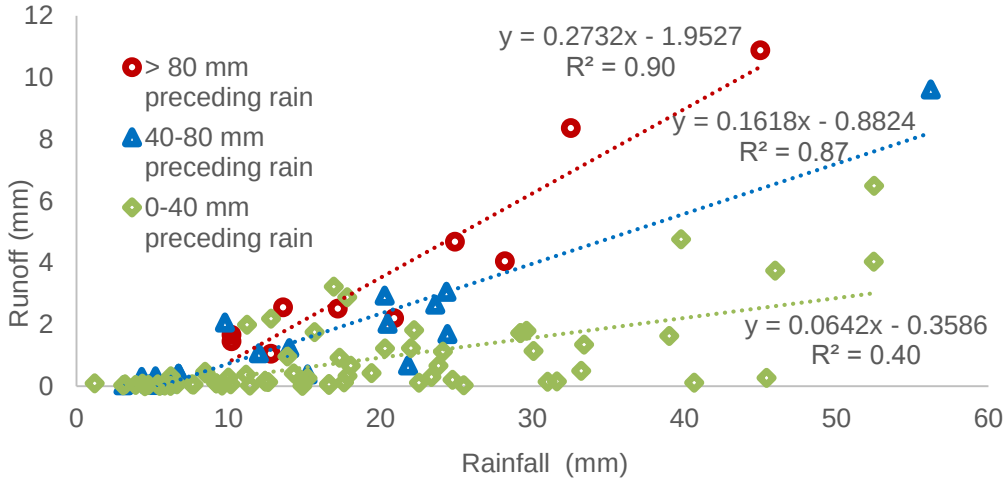

Figure 2. Rainfall-runoff relationships for a set of 100 events along the study period (2011–2021), and classified according to rainfall in the 10 antecedent days (0–40 mm, 40–80 mm and >80 mm).

Table 2. ANCOVA models statistics: Correlation Coefficient (r), R Square (R^2), Adjusted R Square (R_a^2), Standard Error (ST), and the value of the Fisher F statistic and its p-value.

Models	**r**	**R^2**	**R_a^2**	**ST**	**F**	**p-value**
I	0.75	0.57	0.56	1.53	130.2	1.1E-19
II	0.80	0.64	0.62	1.40	86.6	2.6E-08
III	0.86	0.74	0.72	1.22	44.6	1.9E-25

Table 3. Results of the chosen model of Standard Error (ST), and the value of the T-test and its p-value.

	ST	*t stat*	*p-value*
Rainfall in the 10 antecedent days (mm)	0.01	3.85	2.1E-04
Rainfall (mm)	0.02	6.48	4.1E-09
Trimester I	0.45	2.57	1.2E-02
Trimester II	0.46	4.10	8.7E-05
Trimester III	0.47	2.89	4.8E-03

Table 4. Values of the coefficients of the ANCOVA models (Eqs. 5-7).

Model	β_1	β_2	β_3	β_4	β_5
I	0.081	-	-	-	-
II	0.060	0.018	-	-	-
III	0.097	0.025	-1.161	-1.904	-1.361

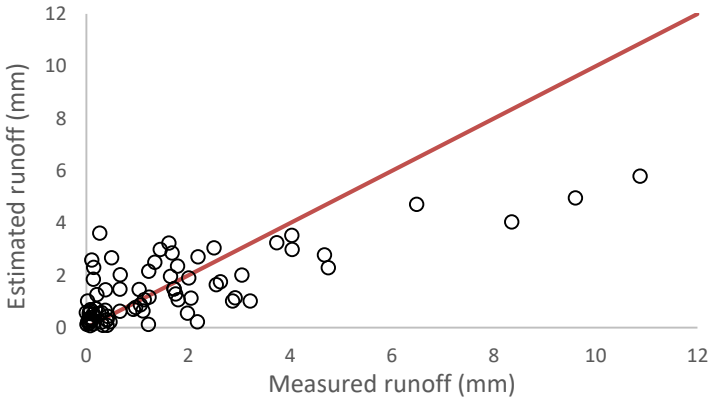

Figure 5. Comparison between the runoff estimated by the model and that measured by the hydrological station, the red diagonal line refers to a fit R2 equal to 1.

3.2 Proposal for irrigation performance alerts

It is proposed to implement irrigation performance alerts in which the intervention threshold will be established based on the quantity and quality of the return flows of the catchment, the second by means of a multiparametric probe and the first will be activated when a runoff rate threshold is exceeded. The threshold illustrated in Figure 5 is one sixth of the irrigation capacity of the hydrants in the catchment. This will be the basis for developing an alarm system that allows better irrigation performance, for which the irrigation runoff events registered during the study period will be analysed.

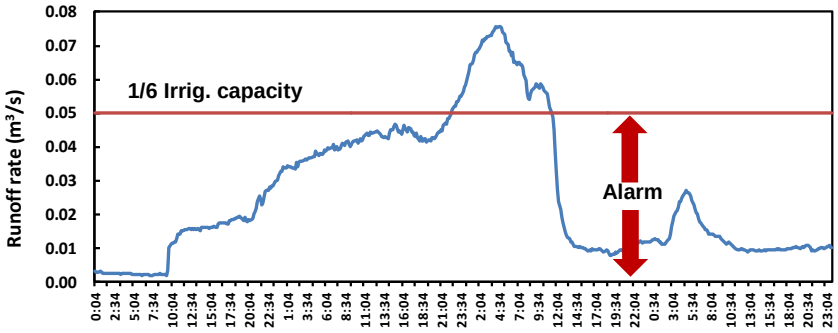

Figure 6. Hydrological event caused by irrigation on July 22, 2014, the red horizontal line delimits the alarm threshold, which is based on the capacity of the hydrants in the watershed.

4 Conclusions

The ANCOVA models allowed reasonable simulation of rainfall runoff when ancillary variables such as preceding rainfall and trimester of the year were included. The year in which irrigation was assessed showed excellent performance. An alert system based on real time runoff monitoring is proposed for further irrigation improvement.

Acknowledgements

This study was part of the Project HubIS of the PRIMA Program (with funds for CSIC from the Agencia Estatal de Investigación. PCI2020-112125). The authors would like to acknowledge support provided by D. Lozano and M. Salmoral for the maintenance of the watershed and also to the staff and farmers of the Genil-Cabra Irrigation District.

References

Allen. R.G., Pereira. L.S., Raes. D., Smith. M., 1998. Crop evapotranspiration. Guidelines for computing crop water requirements. FAO Irrigation and Drainage Paper No. 56. Rome. Italy.

Borga. M., Morín E., 2014. Characteristics of flash flood regimes in the Mediterranean region. In: Diodato. N., Bellochini. G., (Eds.). Storminess and Environmental Change Climate Forcing and Responses in the Mediterranean Region. Springer. Dordrecht. pp. 65-76.

Casalí. J., Gastesi. R., Alvarez-Mozos. J., De Santisteban. L.M., Del Valle de Lersundi. J., Giménez. R., Larrañaga. A., Goñi. M., Aguirre. U., Campo. M.A., López. J.J., & Donézar. M., (2008). Runoff. erosion. and water quality of agricultural watersheds in central Navarre (Spain). Agric. Water Manage.. 95. 1111-1128.

Duarte. A.C., Mateos. L., 2022. How changes in cropping intensity affect water usage in an irrigated Mediterranean catchment. Agric. Water Manag. 260 (2022). Article 107274.

Mateos. L., González-Dugo. M.P., Testi. L., Villalobos. F.J., (2013). Monitoring evapotranspiration of irrigated crops using crop coefficients derived from time series of satellite images. I. Method validation. Agricultural Water Management. 125:81-91.

Molden. D.J., Gates. T.K., 1990. Performance measures for evaluation of irrigation water-delivery systems. J. Irrig. Drain. Eng. 116. 804–823.

Rodríguez Álvarez. F. J., Salgado. R., Lozano. D., García-Vila. M., Soriano. M. A., Mateos. L. (2019). Balance hídrico de una cuenca regable al sur de España utilizando técnicas de teledetección. Actas del XXXVII Congreso Nacional de Riegos. Junio 2019. Don Benito. Badajoz. Spain. DOI 10.17398/AERYD.2019.A12..

Performance assessment of irrigation system undergoing shifting from sprinkler irrigation to drip irrigation

ABLA KETTANI, ABDELILAH TAKY, ALI HAMMANI
Institut Agronomique et Vétérinaire Hassan II, BP6202, 10112, Rabat-Instituts, Rabat, Maroc.

Email: a.kettani@iav.ac.ma.

ABSTRACT

Improving irrigation efficiency and water productivity is a necessary step to mitigate the water scarcity crisis, as well as the problems and pressures on water resources. Hence the importance of assessing the performance of irrigated systems, which supports the planning and implementation of any improvement project. The aim of this research is to understand the irrigation performance gap with the objective of closing it through innovation and improved management. This study was carried out at the C3 irrigation district of the Gharb irrigation scheme. The district of an area of 3,443 ha is undergoing a shifting from sprinkler to drip irrigation consisting on the upgrading of collective pumping station and the irrigation network (works completed in 2014) on one hand, and setting up a drip irrigation system at the farms level (not yet achieved). The performance has been assessed at the farm level. Also a set of performance indicators have been used in the district level based on RAP (rapid appraisal process**),** including system operation indicators, financial indicators, indicators related to agricultural productivity, social, and environmental issues. The results show that the district has many gaps that have to be improved: i) farmers over-irrigate their plots (9.34 Mm^3 of water is delivered annually to farmers' plots while the total net irrigation water requirement (ET – effective rainfall + salt control) is about 5,381 Mm^3; ii) the network distribution efficiency is 69% (The total volume distributed in the network is 13.5 Mm^3/year, while the total volume that reaches the farms is 9.34 Mm^3/year); iii) farmers are facing many problems: 1-The difficulty of managing irrigation. 2- Poor water quality. 3- Poor maintenance of the individual and collective irrigation network. 4- The high price of water and the high costs of inputs, as well as the difficulty of marketing; and iv) The quality of water delivery service to individual property units does not meet project expectations, in fact the actual quality judged by the farmers is lower than that declared by the water irrigation distribution authority (Office), with a ratio (Actual service / declared service) of 0.54…. In general, the indicators are evaluated in detail, which makes it possible to develop a general vision of the various actions that must be taken to improve the overall performance of the services provided by the office. Thus, the increase in yields of agricultural production and the optimal use of water.

Keywords: sprinkler irrigation, drip irrigation, performance assessment, RAP, Gharb.

Introduction

Improving irrigation efficiency and water productivity is a necessary step to solving the water scarcity crisis, as well as the problems and pressures on water resources. Despite the heavy investments undertaken to modernize the collective irrigation systems, the productivity of the resources used remains far from the potential (Kettani et al., 2022) and the sustainability of the irrigated systems is questioned. The performance assessment based on the hydraulic or economic dimension alone do not seem to be the most adopted ones. Moreover, they do not allow for the identification of the actual factors that affect the irrigation systems, nor do they meet the expectations of their users. The understanding of the operation of this system presents an essential first step, followed by the identification of the main constraints perceived by the farmers and the managers lead at the end to the evaluation of the irrigated system. The aim of this research is to understand the irrigation performance gap, using the classical method and by using the RAP (MASSPRESS approach, 2010), with the objective of closing it through innovation and improved management. By answering to the following questions:

- What level of water delivery service does the system currently provide?
- What hardware (infrastructure) and software (operational procedures, institutional setup, etc.) features affect this level of service?
- What are the specific weaknesses in system operation, management, resources, and infrastructure/hardware?

- What simple improvements in various components could make a significant difference in service delivery to users?
- What long-term actions could be taken to improve water delivery service significantly?

Methodology

Our approach comprises two main steps. The first step consists of a diagnostic analysis of the irrigated system (on farm hydraulic performance, …). This step allowed us to assess and identify on farm main constraints. In the second step, we assess the performance at the district level using the RAP.

Rapid performance assessment

The RAP is a tool for identifying the barriers, the performance, and service levels for an irrigation system. It gives a better understanding of where conditions must be amended. It provides internal and external indicators to compare improvements in performance after the implementation of modernisation projects. Its application is based on: i) a combination of field inspections, for evaluating physical system and operations; ii) interviews with the stakeholders and users, for evaluating management aspects; and iii) data analysis, for evaluating a water balance, service indicators and physical characteristics. Thus, it examines (Table 1): a) physical infrastructure; b) water management; and c) project management (MASSPRESS approach, 2010).

Table 1. Summary of the worksheets of a RAP

Sheet	
1	Input – water balance
2	External Indicators (no input required, except for needed "CI" values)
3	Technical indicators/ External Indicators (no input required, except for needed "CI" values)
4	Project Office Questions
5	Project Employees
6	Water User Association (WUA)
7	Main canal
8	Pumping Station
9	Distribution Pipeline
10	Final deliveries Main canal
11	Internal Indicators

Case Study

The study has been carried out in the C3 district of the Gharb large irrigated scheme. It has been equipped with sprinkler irrigation since 1984 and modernised by implementing drip irrigation project (upgrade of collective pumping station completed in 2014) on one hand, and setting up a drip irrigation system at the farms level (not yet achieved). The district has an irrigable area of 3443 ha, supplied by a pumping station (SMPC3) with variable speed drivers. The irrigation is on demand. The irrigation network is organized in 316 collective hydrants, with an average associated area of 12 ha, each collective hydrants feeds individual outlets (1-12). The district is characterized by small-scale agriculture (the average farm size is about 3 ha). The most important crops are sugar crops (sugar beets and sugar cane), wheat, alfalfa and sunflower.

Research approach

Data was gathered using interviews with farmers, field observations and measurements. Multiple interviews were undertaken with ORMVAG staff (engineers, gate keepers, technicians) to fulfil the RAP Sheets (Table 1). Field measurements were carried out on 22 farms (Figure 1). The actual flow was measured to determine the uniformity of distribution.

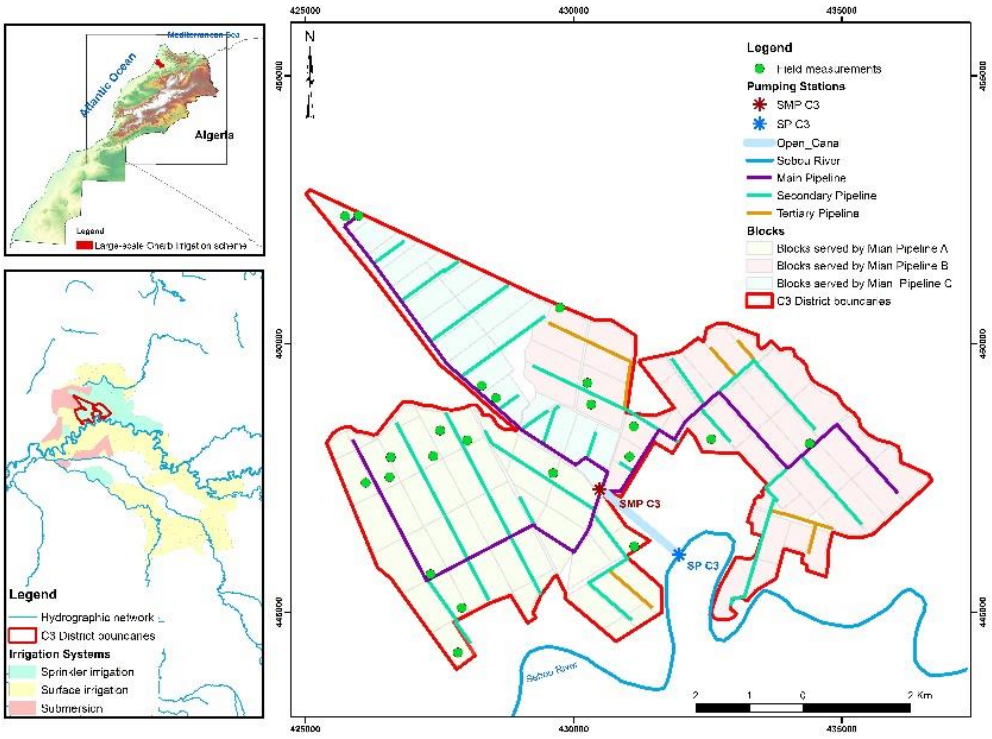

Figure 1. layout of C3 district

Results & Discussion

1. Evaluation of on-farm hydraulic performance

- ***Uniformity of distribution***

The evaluation of the uniformity coefficient gave the following results in the 22 farms studied (Figure 1):

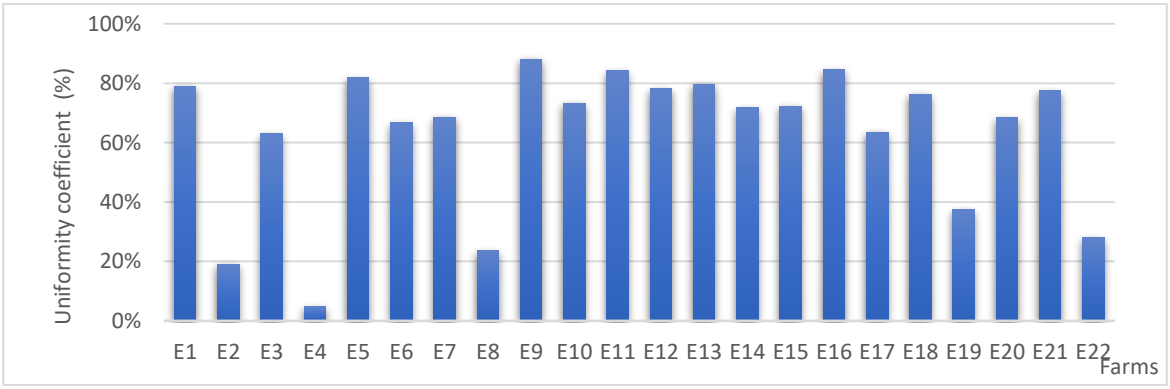

Figure 2. Uniformity coefficient at farm level (22 farms)

According to the results, it can be seen that:

- None of the farms has a uniformity coefficient that exceeds 90;
- 23% of farms have satisfactory uniformity coefficient, which varies between 80 and 90%;
- 32% of farms show uniformity coefficient values between 70 and 80%, i.e. poor uniformity;
- The rest, up to 45 % of the farms, have a poor uniformity of less than 70%.

From what we noticed in the field, the poor uniformity can be explained by:

- The deterioration of the irrigation equipment which has not been renewed since its installation, which justifies the abundance of leaks at the lateral level (Figure 3);

- Clogging of drippers due to irrigation without filtration (farmers remove their filters (Figure 4) because they believe that these filters are causing the pressure drop).

Figure 3. Leaks at the laterals

Figure 4.Irrigation without filter (red)

- ***Rate of satisfaction of crop water needs***

We found that for the same crop, the volume of water provided differs from one farmer to another. This difference is due on the one hand to the variability of farmers' practices in terms of duration and frequency of irrigation applied, and on the other hand to the variation of the flow rate from one farm to another. Which in turn depends even on several factors, in particular, the quality of the installation, the upkeep and maintenance of the network, and the distance from the pumping station.

- The satisfaction rate is about 100% among 31.82% of farmers, thanks to the satisfactory efficiency of application to the plot.
- At farm number “E22” (Figure 2), the satisfaction rate exceeds 100% (142%), this over-irrigation is due to the long duration of irrigation (24 hours per day).
- 31.82% of farms have a satisfaction rate that varies between 71% and 92%, this may be acceptable given that the measurements were carried out during a peak period (July).
- 31.82% of farms have a poor satisfaction rate which varies between 17% and 69%, this is mainly due to the poor uniformity coefficients that have been measured in the plots which reach up to 5%.

2. Performance assessment using the RAP

First, we try to have a clear description and better understanding of the functioning of the system. The main conclusions are as follows:

- Farmers over-irrigate their plots (9.34 Mm^3 of water is delivered annually to farmers' plots while the total net irrigation water requirement (ET – effective rainfall + salt control) is about 5,381 Mm^3.
- The network distribution efficiency is 69% (The total volume distributed in the network is 13.5 Mm^3/year, while the total volume that reaches the farms is 9.34 Mm^3/year).
- There is a difference of 1 Mm^3/year between the volumes consumed by the farmers and the volumes invoiced by the irrigation authority, which is due to estimation instead of reading water meters.

In the second steps we identify the constraints, but focusing on the point of view of the farmers. It is a question of identifying the factors of dysfunction and the determinants of the performance of the irrigated systems through a critical analysis of farmers’ speech. The main constraints are:

- Farmers are facing many problems: 1-The difficulty of managing irrigation. 2- Poor water quality. 3- Poor maintenance of the individual and collective irrigation network. 4- The high price of water and the high costs of inputs, as well as the difficulty of marketing.

- The quality of water delivery service to individual property units does not meet project expectations, in fact the actual quality judged by the farmers is lower than that declared by the water irrigation distribution authority (Office), with a ratio (Actual service / declared service) of 0.54.

Recommendation for closing performance gap

In the light of the results, it is appropriate to recommend the following points:

- Rehabilitation of distribution pipelines to improve transport efficiency (69%);
- Improve the participation of water user associations through: better involvement (since the beginning of the project); Training; awareness; ...
- Reinforce the follow-up of farmers after the installation of the drip equipment, not only in terms of the use of the equipment but by addressing the aspects of the dose and the frequency in order to detach them from the spirit of sprinkler irrigation;
- Initiate a study on the search for the source of frequent clogging of filters for some farmers and improve the quality of the water distributed.
- Study the feasibility of using low-pressure sprinkler irrigation, to face the problem of drippers clogging on the one hand, and to meet the farmers' knowledge on the other hand;
- Use of low cost sensors at farm level to improve the irrigation efficiency.

Conclusion

Irrigation performances in large-scale irrigation schemes depends on how to overcome problems and constraints are which facing development and improvement of the irrigation. The application of performance assessment tools like the RAP are necessary to develop a general vision of the various actions that must be taken to improve the overall performance of the services provided by irrigation authority. Thus, the increase in yields of agricultural production and the optimal use of water.

Acknowledgements

We thank the irrigation authority and the farmers for the fruitful interactions and for sharing information. The research benefited from the reflections in the framework of the HUBIS project, financed by PRIMA Foundation.

REFERENCES

Kettani, A., Hammani, A., Taky, A., & Kuper, M. (2022). Challenging 'one size fits all': Continued use of sprinkler irrigation in a state-led drip irrigation project in Morocco. Irrigation and Drainage. Volume 71, Issue 3 p. 619-634. https://doi.org/10.1002/ird.2675.

MASSCOTE approach, (2007). Modernizing irrigation management – the MASSCOTE approach Mapping System and Services for Canal Operation Techniques. FAO IRRIGATION AND DRAINAGE PAPER.

MASSPRESS approach, (2010). MAPPING SYSTEM AND SERVICES FOR PRESSURIZED IRRIGATION. FAO.

Innovations of "Hubis" Project to be tested at the field/basin and farm level

Sidiropoulos, P.[1], K. Daudin[2], N.R. Dalezios[1], M. do Rosario Cameira[3], P.C.S. Paredes[3] and N. Dercas[4]

[1]Laboratory of Hydrology and Aquatic Systems Analysis, Department of Civil Engineering, School of Engineering, University of Thessaly, 38334 Volos, Greece.
[2] Joint Research Unit Water Management, Actors, Territories (G-EAU), AgroParisTech, Cirad, IRD, INRAE, L'Institut Agro, Univ. Montpellier, Montpellier, France.
[3]Department of Biosystems Engineering, Superior Institute of Agronomy, University of Lisbon, Tapada da Ajuda, 1349-017 Lisbon, Portugal.
[4]Laboratory of Agricultural Hydraulics, Department of Natural Resources Management & Agricultural Engineering, Agricultural University of Athens, 75 Iera Odos, 11855 Athens, Greece.

Abstract. Irrigation performance in the Mediterranean region is below expectations and well below its technological potential. Modernization of irrigation followed a top-down approach not always adapted to the needs and capacities of farmers. The "Open innovation Hub for Irrigation Systems in Mediterranean agriculture" (Hubis) project claims that bridging the actual irrigation performance gap requires inverting the process to a bottom-up interdisciplinary approach, in an open innovation environment making intensive use of emerging technologies. The HubIS consortium integrates 13 partners from 7 countries, including 9 public research institutions and 4 private companies. The partners complement each other in expertise, training and education tasks (from farmer capacity building to postgraduate university programs and supervision), and research vs. extension priorities. The objective of the consortium is to narrow the irrigation performance gap and to improve sustainability of irrigated agriculture in the Mediterranean region, by favoring the emergence and adoption of co-innovations at multiple scales (farm to basin or aquifer scale). The project adopts a participatory action research strategy by implementing a Mediterranean irrigation innovation hub that will link site-specific hubs located in representative irrigated agroecosystems. Each site-hub has a Fab-Lab targeting specific innovations according to the priorities of the corresponding agrosystems. The type of innovations considered in the project range from a novel framework for upscaling irrigation efficiency to advanced open and web-based methods using low-cost spatially distributed information (remote sensing, ground sensors) for site-specific management and automatic operation. Innovations are also expected on application equipment and cropping systems. Environmental conservation is addressed by developing control systems of return flow quality, and optimization of irrigation and crop management. The project's ambitions are to halve the current irrigation performance gap, in terms of both average performance and performance variability, and to reduce water abstraction, agrochemical pollution and C emission below sustainable thresholds.

1 Introduction

The modernization of irrigation in Mediterranean countries has boosted irrigated agriculture. This process has been possible not only through technological developments, but also with top-down public policies (Molle, 2019) and, in some areas where the mild climate allows growing high value crops, the exportation market as main drivers of change. Undoubtedly, this transformation has increased performance levels. However, new compelling challenges have arisen: (i) the irrigation performance gap remains much greater than expected (Benouniche et al., 2014); (ii) irrigation intensification and expansion are at the root of pollution of valuable ecosystems and overdraft of non-renewable water resources; (iii) water savings are not as foreseen due to unexpected rebound effects (Mateos and Araus, 2016; Grafton et al., 2018) of irrigation efficiency improvements; (iv) modern energy-eager pressurized systems are costly and environmentally questionable. Furthermore, it is now clear that climate change and its foreseen variability will accentuate the vulnerability of agriculture and ecosystems, under the combined effect of increased temperature and reduced precipitation in areas already coping with water scarcity. These new challenges require new research paradigms and multiscale approaches:

- The top-down policy that allowed irrigation expansion and modernization must now be transformed into bottom-up actions to close the remaining irrigation performance gap. We advocate that the best strategy to bridge the current performance gap is participatory action research (Chevalier and Buckles, 2013) undertaken in an open innovation environment where technology adoption and co-design can flow fluently between different actors.
- On-farm irrigation performance is conditioned by internal factors, but also by the constraints and the operation of the distribution system when the farm is part of a collective irrigation scheme. In turn, management and performance of both individual and community schemes is conditioned by planning and

management of water resources at a basin scale. Hence, multi-scale approaches are vital to increase irrigation performance.

- Both water accounting and water quality control must become part of standard water management systems at all farms, schemes and basin scales (Bos et. al., 2005). We believe that last generation low-cost sensors, information and communication technology, big data analysis, satellite information at high spatial and temporal resolutions and other emerging technologies provide unforeseen opportunities for this purpose.
- There are vibrant opportunities to reduce external energy consumption and nitrogen leaching in irrigation schemes (Rocamora, 2013).

The aim of this paper is to present the innovations that are tested at the field/basin and farm level, proposed by the "Hubis" project. These innovations comprise new tools and services for farmers and water users' associations (WUA), designed to increase water, nutrient and energy use efficiency. Innovation development leading to adoption of new standards will rely on bottom-up processes, understanding of governance settings and implementation of sharing procedures, through innovation hubs developed by the project.

2 Concept and methodology

2.1 Concept

The hypothesis underpinning the project is that bridging the actual irrigation performance gap requires a substantial paradigm shift, from the top-down approach that has driven irrigation modernization in the last decades to a bottom-up interdisciplinary approach making use of emerging low-cost technologies. Therefore, the project adopts a participatory action research strategy facilitating an open innovation environment where project-promoted site-based irrigation innovation hubs (Site-iHub) face the challenge of bridging the irrigation performance gap. A Site-iHub is an aggregation of different forward-looking communities, entrepreneurs, stakeholders, researchers, public and private organisations that interact and collaborate to surface and take to practice new ideas that solve production, commercial, and organizational challenges within the specific irrigated agroecosystem. The Site-iHubs are interconnected through a common platform, the Mediterranean Irrigation Innovation Hub (Med-iHub). The project has a multiscale approach, from the farm to the basin or aquifer scale, covering management levels that are responsibility of farmers, water users' associations (WUA), and water resources authorities. The Site-iHubs territories are representative irrigated agro-ecosystems in seven Mediterranean countries, reflecting hot issues such as groundwater overexploitation, production of high value crops, high irrigation energy cost, over irrigation, and heterogeneous irrigation performance (Figure 1). The actors include progressive farmers, irrigation advisors, leaders and managers of farmers and water users' organizations, researchers, entrepreneurs, suppliers and installers of irrigation equipment, governmental and non-governmental agencies. Special care is taken to ensure that young professionals and women are properly represented. Project partners play a convener/facilitator role in the Site-iHubs, creating opportunities for interaction and engagement and stimulating serendipitous connections.

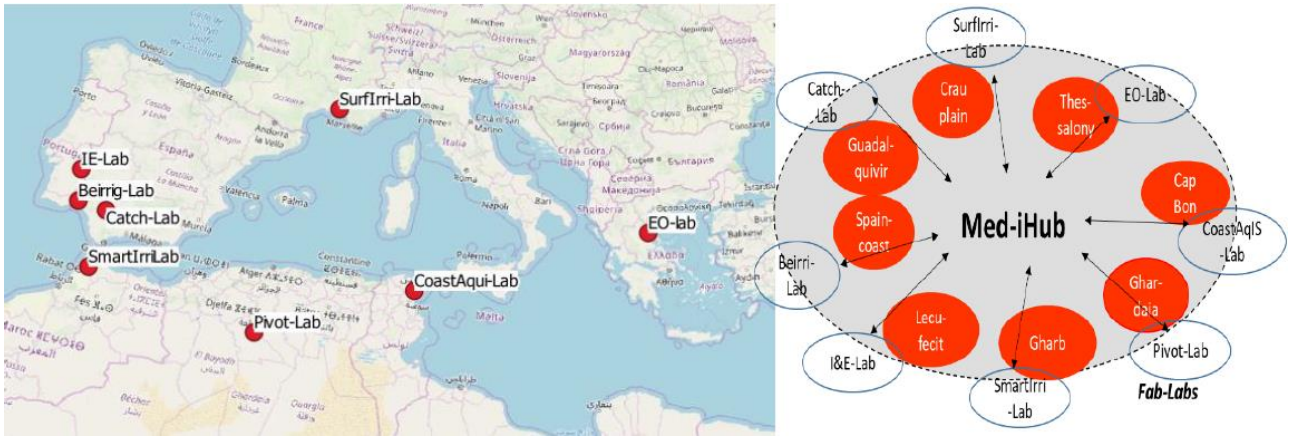

Figure 1. Location map of study sites and attached Fab-Lab (Source: OpenStreetMap). Local Site-iHubs have been assigned names corresponding to local characteristics/challenges. Med-iHub makes connections between all fablabs and site-iHubs.

The Site-iHubs will build upon the Fab-Labs and other local capacities to create an open basket containing innovations at different technology readiness levels (TRL). The aim is to complete multiple innovation chains during the project duration. For instance, the project will offer a conceptual framework to predict basin-scale rebound effects of improved on-farm irrigation efficiency. This may be considered at TRL2 (proof of concept);

however, the proposed framework will mature in the innovation hubs so that it will be transferred as policy recommendation at the end of the project. Other innovation chains will start at TRL 7-8 (prototype demonstration and "flight qualified") so their adoption will take place in an early phase of the project. This is the case of existing decision support tools (i.e., SIC and Optirrig softwares; sensors [MSA]; web alert systems [WRF, 3DSA]; index mapping [Terranis, UTH]) for irrigation scheduling and operation. The Site-iHubs and their innovation baskets will be inter-connected and shared within the Med-iHub, thus the innovations are exchangeable, and the serendipitous environment is widened in space and time, during the project duration and beyond. Med-iHub will be a collaborative platform that will be developed as a web platform within the project to pool all ideas, reflections, methods and tools, innovation process and performance assessment generated by the project. Moreover, the Med-iHub will include a dynamic system to follow up the progress of every innovation chain, monitoring their TRL at each project stage.

2.2 Methodology

HubIS is articulated in 6 Work-Packages (WPs), 8 study sites – the Site-iHubs, and 8 Fab-Labs (Figure 2). The study sites are representative of the main irrigated cropping systems around the Mediterranean basin, of different agroclimatic regions (South-east Europe, Maghreb, Iberian Peninsula, South of France), and of reoccurring tensions over water resources. Irrigation systems in the pilot sites include gravity and pressurized systems, individual and collective systems, thus covering the diversity of situations of Mediterranean irrigated agriculture. The pilot sites in the mid Guadalquivir valley in Spain, the Durance valley in France, North Morocco, Central Portugal (all four using mainly surface water), and the Thessaly plain in Greece (using ground water) are representative of extensive irrigated agriculture and therefore of the largest irrigated areas in the Mediterranean region. The sites in the southwest coastal area of Spain and the coastal area of Tunisia represent intensive agricultural systems producing high value crops in mild climates, using limited ground water resources. The Ghardaia region in Algeria is a paradigmatic example of horticultural production at the expense of non-renewable ground water resources. This careful selection of study sites covers the diversity of Mediterranean situations and therefore will allow exploring all levers needed to increase irrigation performance in the region.

The "basket of innovations" is constituted aiming to improve irrigation performance in the Mediterranean region. This basket includes (though not exclusively) solutions designed within the project and having emerged from the Fab-Labs. The participatory approach is expected to facilitate their adoption and their ability to increase performance. The innovation process is followed-up in order to identify locks and levers, to be considered in the upscaling process and the formulation of recommendations. Each FabLab has prototyped solutions aiming at increasing the performance of irrigation. The actual implementation is expected on the site(s) associated to the FabLab but are expected to be applicable at a larger scale, including the other sites of the project when relevant. Therefore, the associated principles are formalized for each innovation so that they are transferable to other systems. In addition, already existing solutions are included in the innovation basket. The innovation basket covers the whole chain of irrigation water use along the water cycle, with different scopes and types of innovations: information (all scales), organisation among users, crop planning, irrigation scheduling, and effective application. Partners in-charge of each innovation set-up the methodology to be implemented. Since the Fab-Labs create a stimulating innovation environment, these lists are non-exhaustive and subject to evolutions throughout the project. The innovations are tested in two spatial levels: 1) At the district/basin level: They mostly aim at giving relevant information for managers/advisers to have an improved knowledge of actual water status and other indicators, and adjust decisions/recommendations accordingly to shift from supply-based to demand-based delivery, reduce energy consumption, drainage, etc.; 2) At the farm level: They mostly aim at informing farmers on water status at the field and farm levels (uniformity, water status before irrigation, actual water use, energy use, etc.), planning crops and irrigation strategies, applying irrigation efficiently and uniformly.

3 Results

Eleven innovations have been adopted at the district/basin level, and eighteen at the farm level. Table 1 presents the title, site, objective, description, and impacts of the innovations.

Table 1. Innovation basket for the district/basin level and for the farm level.

District/basin level				
Innovation	**Site**	**Objective**	**Description**	**Impacts**
Return flow alarms	Spain Genil-Cabra	Management using downstream observations	Flow measuring devices + continuous recording + transmitters based on a set of consigns	Reduction in water use and in nutrient disposed

Spreadsheet in smartphone application	Portugal Lucefecit	Assist the WUA technician in the recording of hydrant data	Recording of water consumption readings in the hydrants that supply the farms	Facilitate technicians labor and minimize data losses
Flow and pressure continuous observation	Portugal Lucefecit	Monitor flow and pressure in the water distribution pipe	Flow & pressure measuring devices + continuous recording + transmitters	Rapid detection of problems and increase distribution and energy efficiencies
Data computation tool	Portugal Lucefecit	Water and energy balances in pressurized pipe from source to hydrants	Excel spreadsheet to process water and energy databases	Intervention strategy to improve the water and energy use efficiency
Adaptive water consumption based on energy price	Portugal Lucefecit	Determine the optimal energy consumer profile that allows the lowest possible energy cost	Spreadsheet to compare water distribution profiles and consider the energy price curve in water distribution schedules	Significant energy-cost reduction
Irrigation monitoring service	France, Crau	Remote monitoring of irrigation practices	Webservice based on radar and optical satellite images analysis to observe irrigated areas	Adaptation of water supply and improvement of irrigation efficiency
Agro-hydraulic modelling	France, Crau	Decision support tool	Assess the impacts of the adoption of low-cost technologies using a multi-criteria approach (simulation of water use efficiency and crop production)	Improve surface water management by exploring scenario
Flowter wireless sensors	France, Crau	Real time information of water level	Water detection using a magnetic float paired with a LoRaWAN telecom system	Rapid detection of problems (improved maintenance) and increase irrigation efficiency
Farm typologies and trajectories	Tunisia, Haouaria	Decision support tool	Simulation application to predict the evolution of crop types	Assist decision makers and operational management
Smart flow and pressure meters	Tunisia, Haouaria	Monitor flow and pressure in the water distribution pipe	Smart measuring devices of water flow and pressure	Increase water distribution efficiency
Scheduling tool for localized irrigation	Tunisia, Haouaria	Improving water resources management	Establish irrigation schedules in terms of irrigation duration	Reduce water consumption
Farm level				
Innovation	**Site**	**Objective**	**Description**	**Impacts**
Weather forecast data	All	Provide high resolution-accuracy weather monitoring and seasonal climatic forecasting	WRF regional model running (daily and monthly) and presentation of results on a website	Improve irrigation crop schedules, increase irrigation efficiency
Water-related indices mapping	Greece, Thessaly	Produce high-resolution multispectral and advanced thermal imagery	Use of unmanned aerial vehicles and data analytics (correct watering, leaks, and clogs)	Increase irrigation precision
Crop evapotranspiration mapping	Greece, Thessaly	Computation of crop evapotranspiration daily values	Procedure for the synergetic use of Earth Observation data (Sentinel-2 radiometric and Sentinel-3 thermal) in combination with weather forecast	Improve water and crop productivity

Irrigation management service	Greece, Thessaly	Webservice application to notify farmers (irrigation amount and schedule)	Keep farmers informed of possible changes in the weather forecast and support farmers with private pumps	Increase watering efficiency
Soil water sensors and hydrometers	Greece, Thessaly	Assist irrigation scheduling and water pumping	Soil-water sensors at different depth and hydrometers in pipes	Improve irrigation schedule and water savings
Remote estimation of nitrogen requirement	Greece, Thessaly	Optimization of nitrogen inputs	Computation of Nitrogen Nutrition Index through several vegetation indices and local features	Improve nutrient efficiency, reduce environmental impacts
Soil water sensors	Portugal Lucefecit	Assist irrigation scheduling	Installation of sensors at different depth, reading and comparison with thresholds	Water, fertilizers, and energy savings, reduce environmental impacts
Guidelines for irrigation systems operation, maintenance, and evaluation	Portugal Lucefecit	Lay down a set of tasks/practices to be performed before and during the irrigation season	Components evaluation, identification of malfunction and causes, design changes, maintenance requirements	Improve water and energy efficiencies and increase crop productivity
Guidelines for deficit irrigation	Portugal Lucefecit	Implementation of deficit irrigation in olives and vineyards	Impacts on yield quantity and quality of diverse regulated deficit irrigation scheduling	Improved water and crop productivities
Flowter wireless sensor	France, Crau	Real time information of water level	Water detection using a magnetic float paired with a LoRaWAN telecom system	More precision in open channel water management and rapid detection of problems
Water arrival detection sensor	France, Crau	Detect water arrival at the end of the plot and notify the farmer about it	Wireless water sensor paired with a LoRaWAN telecom system	Application efficiency, drainage factor and socio-economic (labour/workload)
Automatic water gates	France, Crau	Water gate automation	Automatic water gates connected to the LoRa network and operated following the water arrival detection	Application efficiency, drainage factor and socio-economic (labour/workload)
Irrigated plot spatial monitoring	France, Crau	Improvement of irrigation practices	Webservices based on satellite images analysis (map of vegetation variability)	Adaptation of water supply and improvement of irrigation efficiency
Automated drainage lysimeter	Spain, Huelva	Measure consumptive water use, irrigation efficiency and diffuse pollution	Automation of ultrasonic flowmeters and drainage lysimeters (IoT devices connected using a LoRaWAN network)	Increased irrigation efficiency, reduction of energy consumption, drainage ratio and diffuse pollution
Smartphone application for irrigation scheduling	Spain, Huelva	Maximum production and not suffer from water stress	Application allows optimizing water consumption and irrigation schedule is daily updated based on weather forecasting	Increased irrigation efficiency, reduction of energy consumption, drainage ratio and diffuse pollution
Return flow alarms	Spain Genil-Cabra	Management using downstream observations	Flow measuring devices + continuous recording + transmitters based on a set of consigns	Reduction in water use and in nutrient disposed
Smart irrigation devices (equipment and application)	Morocco, Gharb	Optimizing irrigation water consumption	Devices to schedule irrigation based on 1) weather, satellite images, crop requirement and 2) soil moisture sensors	Decrease water bills, improve yields, and water productivity, reduce environmental impact of irrigation

Low-cost miniature center pivot	Algeria, Sebseb	Enhance irrigation performance of artisanal pivot	50 m artisanal pivot installed with a single span	Improve irrigation performance

Partners in charge of each innovation are in-charge of its implementation and its monitoring and provide an assessment of the attainable performance gains and the associated conditions. Data supporting the assessment are shared between partners working on each site. As it can be seen from Table 1, each site is the support of one or several innovations that are implemented and monitored. They are operational for one or two years of implementation, considering the necessary involvement of farmers/managers at the district level. The main expected output is the analysis of the adoption process, the constraints, and feedback from farmers/managers that will help to identify the conditions of success and the sustainability of the explored solutions. Adaptations are expected all along with the implementation phase, thanks to this feedback.

4 Summary

In this paper, the innovations that are tested at the field/basin and farm level of eight Mediterranean study sites, proposed by the “Hubis” project, are presented. The concept and the methodology of innovations’ adoption are thoroughly analyzed. A brief description of their objectives, description, and targets is achieved. Although in “Hubis” Full Proposal Template six innovations at the district/basin level and ten innovations at the farm level were proposed, the final innovation basket contains eleven innovations at the district/basin level and eighteen innovations at the farm level. This boost in innovation identification reveals the successful implementation of “Hubis” actions at the study sites.

Acknowledgements

The research was funded by «Open innovation Hub for Irrigation Systems in Mediterranean agriculture» with the acronym «Hubis» of PRIMA (Partnership for Research and Innovation in the Mediterranean Area) programme (Section 2 Call 2019 – multi-topic) supported under Horizon 2020.

References

Benouniche, M., Kuper, M., Hammani, A., and Boesveld, H., 2014. Making the user visible: analysing irrigation practices and farmers’ logic to explain actual drip irrigation performance. Irrig. Sci., 32(6), 405-420. https://doi.org/10.1007/s00271-014-0438-0

Bos, M.G., Burton, M.A., and Molden, D.J., 2005. Irrigation and drainage performance assessment: practical guidelines. CABI Publishing, Wallingford.

Chevalier, J.M., and Buckles, D.J., 2019. Participatory action research: Theory and methods for engaged inquiry. 2nd Edition, Routledge, London. https://doi.org/10.4324/9781351033268

Grafton, R.Q., Williams, J., Perry, C.J., Molle, F., Ringler, C., Steduto, P., Udall, B., Wheeler, S.A., Wang, Y., Garrick, D., and Allen, R.G., 2018. The paradox of irrigation efficiency. Science, 361(6404), 748-750. https://www.science.org/doi/10.1126/science.aat9314

Mateos, L., and Araus, J.L., 2016. Hydrological, engineering, agronomical, breeding and physiological pathways for the effective and efficient use of water in agriculture. Agr. Water Manage., 164(1), 190-196. https://doi.org/10.1016/j.agwat.2015.10.017

Molle, F., Sanchis-Ibor, C., and Avellà-Reus, L., 2019. Irrigation in the Mediterranean: Technologies, Institutions and Policies. Springer, Switzerland. https://doi.org/10.1007/978-3-030-03698-0

Rocamora, C., Vera, J., and Abadía, R., 2013. Strategy for efficient energy management to solve energy problems in modernized irrigation: analysis of the Spanish case. Irrig. Sci., 31, 1139-1158. https://doi.org/10.1007/s00271-012-0394-5

SUPROMED project: improvement of the economic and environmental sustainability of Mediterranean agroecosystems

A. Domínguez [1], R. López-Urrea[2], R.A. Ferrer[3], E. Mino[4], N. Dalezios[5], D. Skepastianos[6], F. Karam[7], H. Hawwa[8], H. Amami[9], R. Nciri[10]

[1] Centro Regional de Estudios del Agua, Universidad de Castilla – La Mancha, Ctra. De las Peñas Km 3.2, Albacete, España (alfonso.dominguez@uclm.es)
[2] Instituto Técnico Agronómico Provincial de Albacete (ITAP), Parque empresarial Campollano, 2º Avenida, 61, Albacete, España (rlu.itap@dipualba.es)
[3] Grupo HISPATEC Informática empresarial S.A., Avenida de la Innovación, 1º Ed. CAJAMAR 4ª Parque Tecnológico PITA, 04131, Almería, Spain (rferrer@hispatec.com)
[4] Euro-Mediterranean Information System on know-how in the Water sector (SEMIDE), BP23, 0690 Sophia antipolis, France (e.mino@semide.org)
[5] University of Thessaly, Argonafton and Filellinon, 38221; Volos, Greece (dalezios.n.r@gmail.com)
[6] General Aviation Applications "3D" S.A., 2 Skiathou str, 54646, Thessaloniki, Greece (dskepastianos@3dsa.gr)
[7] Lebanese University Faculty of Agronomy, Main Road Dekwaneh-Mkales Roundabout, Dekwaneh, Meten, Mount-Lebanon, Lebanon (fadkaram@gmail.com)
[8] Difaf SAL, YASMINA Bldg., 8th Flr., Michael Dabaghi Str., 2036-6403, Ras Beirut, Beirut, Lebanon (hussam.hawwa@gmail.com)
[9] National Institute for Research in Rural Engineering, Water and Forests, Hedi Karray Street, 10th, 2080 Ariana, Tunisia (hacib.amami@gmail.com)
[10] National Institute of Field Crops, Bousalem, 8170, Jendouba, Tunisia (nsiriradouan@yahoo.fr)

Abstract. The activity carried out by the farms located in the Mediterranean basin is conditioned by different climatic, technical, legislative, economic, and environmental restrictions, making irrigation practically essential to generate a sufficient amount of food, achieve adequate profitability and avoid the abandonment of rural areas.
Despite of the technological advances in the irrigation sector, it can be said that this sector has not yet incorporated much of the available technology, or the methodologies developed for improving the management of the farms.
The motives can be of a different nature, highlighting the economic cost of acquiring the corresponding technology; the lack of training of farmers to install and operate the equipment, interpret their data and make the appropriate decisions; or unknowing the impact that certain practices can cause on the profitability and sustainability of their farms.
The SUPROMED project aims to make available to farmers and technicians, through an online platform (www.supromed.eu), a set of models and methodologies that may advise them in making a more efficient use of available resources, thereby improving the profitability of their farms and decreasing the impact on the environment.
These models and methodologies are being validated in 3 demo sites of the Mediterranean basin (Spain, Lebanon and Tunisia). In order to achieve a massive use of them, the tools have been simplified and adapted to the data available to users, to their level of training, and they show the results in an easily interpretable way. In addition, courses and conferences are being organized to disseminate these tools, to demonstrate their impact on farms and to train users in their use.
The results are promising due to all the environmental and economic indicators of those farms where these tools have been applied have improved. For this reason, the interest of users in SUPROMED platform is very high.

1. Introduction

The Mediterranean region presents a strategic location at the crossroads of three continent. It also is one of the most richest regions in ecosystems but it is a high vulnerable zone due to water scarcity caused by the periodical occurrence of drought periods and the irregular distribution of rainfall during the year. Agriculture is the most water demanding sector, with an average demand of 64%. The Mediterranean economy has been growing by relying increasingly in specialized and irrigated agriculture. The agricultural sector generates 6% of Europe Gross Domestic Product and in most countries, agriculture is employing 20-30% population (https://ec.europa.eu/commission/presscorner/detail/en/MEMO_13_631). Nevertheless, the Mediterranean area is greatly conditioned by numerous economic (e.g. harvest price, labor costs, energy price), political (e.g. laws for the protection of the environment), social (e.g. food security and rural abandonment), technical (e.g. machinery and crops) and environmental factors (García – Ruíz et al., 2011; Correia et al., 2009). For these

reasons, irrigation is essential to generate sufficient amount of food, and achieve adequate profitability to ensure the maintenance of rural population. Moreover, the lack of tools or irrigation advisory services for determining the irrigation requirements of crops at farm level, the lack of knowledge about the irrigation system (De Juan et al., 1996; Lopez – Mata et al., 2010) and climatic change that will increase drought periods have all led to an excessive use of resources (water and fertilizers) to compensate for these shortages, decreasing the profitability of Mediterranean farms (Daccache et al. ,2014; Knoxet al., 2012).

Tackling these challenges requires a combination of methodologies and technologies to improve the resilience of agricultural systems. This combination includes enhancing the efficiency of the use of natural resources, improving the design and management of means of production, developing and transferring technology and knowledge to the producers and analyzing scenarios to advise farmers and technicians about the most suitable strategies for dealing with these extreme situations (Tarjuelo et al., 2015).

With this aim, the SUPROMED project (Sustainable production in water-limited environments of Mediterranean agro-ecosystems) is intended to enhance the economic and environmental sustainability of Mediterranean farming systems through a more efficient management of water (evaluation of irrigation scheduling, proper irrigation scheduling taking into account weather forecast and soil moisture), land (good agricultural practices and optimal distribution of crops), energy (audits and solar power) and fertilizers (soil analysis and nutrient balance). For this purpose, SUPROMED combines various models and tools in order to properly manage inputs (mainly water, energy and fertilizers). These tools were simplified and adapted for farmers and technicians and implemented in an end user online platform intended to provide effective advice for more sustainable and profitable crop management. Moreover, the project proposes several complementary methodologies, such as evaluation of the irrigation systems, control of the actual amount of water supplied at each irrigation event, monitoring of the soil moisture content, and fertilization based on a nutrient balance, among others. The tools and methodologies are available on the project webpage (www.supromed.eu).

The main objective of SUPROMED is to provide a holistic crop water management system resilient to climate change. The following secondary objectives have been proposed: 1) Designing an end-user IT (Information technology) platform to advise farmers in the efficient management of Mediterranean cropping systems; 2) integrating a set of models and tools in this platform to increase the production and income of farms, through a reduction and a more efficient use of water and other inputs such as energy and fertilizers; 3) RDI strategies can be very useful to achieve the previous objective, specially in fruit trees and vines, for this reason SUPROMED will consider and promote the use of this strategies; 4) Validation of the end-user IT platform in three different demo-sites located in different countries, to calibrate the different models integrated in the platform, comparing their performance with traditional methods; 5) consolidating them in different farmer´s Training Programs to be performed in the three demo-sites; and 6) the integration of SUPROMED results into water and agricultural policies.

2. Materials and methods

2.1. Duration and budget

SUPROMED is a project funded by PRIMA (Partnership for Research and Innovation in the Mediterranean Area). PRIMA was founded in 2017 and funded by EU Horizon 2020 program and nowadays includes 19 countries of Europe, Asia and Africa, most of them located in the Mediterranean area. PRIMA projects are divided into three themes: water management, agricultural systems and agri-food value chain. SUPROMED belongs to agricultural systems. It started in October of 2019 and has a duration of three years. It has a budget of 2,030,000 €

2.2. Demo-sites

The methodologies and models included in SUPROMED have been tested in three different demo-sites across the Mediterranean area (Spain, Lebanon and Tunisia).

Spanish Demo-site

In Spain the demo-site is located in the hydrogeological Unit “Eastern Mancha” (HUEM), which occupies an area of 8500 km^2 and supplies water to more than 120000 ha of irrigated land. In this area, 95% of irrigation systems are pressurized (mainly sprinkler and surface drip) with an average annual water allocation of 4000 $m3ha^{-1}$. It is a semi-arid area where the average annual precipitation (400 mm) is distributed from September to June. The most common crops in the area are wine grapes, cereals (barley, wheat and maize), garlic, onion. The main problems in this area are the imbalance between water supply and demand because the 90% of the water used in the area is groundwater. Due to the great irrigable land, the HUEM is at risk of overexploitation. Another important problem is the poor animal production and the decrease of agricultural profitability due to the low sale price in combination with the high input costs and the low availability of irrigation water. The main consequence is the young people´s abandonment of rural farms.

Lebanon demo-site

This test site is located in South Bekaa valley of Lebanon and is a part of South Bekaa Irrigation Scheme (SBIS), with an irrigable area about 21500 ha. For economic constrains, only a pilot area of 2000 ha is for the

time equipped with a pressurized irrigation network. It is also a semi-arid climate where the average precipitation (650 mm) is recorded from October to May. The most common crops are wheat and others winter cereals, potato, winter legumes and fruit trees, olive and vineyard. The main problem of this area the lack of knowledge of the farmers to conduct an appropriate irrigation scheduling and also the lack of technical assistance. The poor animal production system is other important problem as occurs in the HUEM.

Tunisian demo-site

In Tunisia, the demo-site is located in Sidi Bouzid area with an irrigated area of 50000 ha, where the 88% belong to farmers and the rest are managed by the government. This region is classified as arid with an average annual precipitation of 190 mm. Annual cultivate crops in the region include vegetables, fodder and cereals. Tree crops include olive, pistachios and almond. All farms are equipped with pressurized irrigation systems using groundwater. Consequently, one the most important problem in this area is the overexploitation of groundwater that causes water shortage an increase pumping cost. Another important problem is the lack of technical assistance and a poor animal production system.

2.3. Partners and tasks

SUPROMED integrates 10 partners of 5 countries located in the Mediterranean area. SUPROMED is coordinated by UCLM (University of Castilla – La Mancha, Spain) which also provided several models integrated in the platform. The rest of models are provided by 3DSA (Greece) UTH (University of Thessaly; Greece), INGC (Institut national des Grandes Cultures, Tunisia). The main responsible partner of each demo - site are ITAP (Instituto Técnico Agronomico Provincial, Spain) which is the responsible of Spanish demo - site, ULFA (University of Lebanon, Faculty of Agronomy) for Lebanon demo - site and INRGREF (Institut National de Reserche en Génie Rural Eaux et Fôrets, Tunisia) for Tunisian demo - site. Three more enterprises are participating in the project for developing the online platform (HISPATEC, Spain), carrying out the socioeconomic analysis about the impact of the project at local, regional and Mediterranean basin levels (DIFAF, Lebanon), and disseminating the results (SEMIDE, France).

2.4. Models integrated in the platform

The overall approach of SUPROMED includes the integration of different models and tools designed by the partners integrated in the project. The models included in the end-users IT platform are:

MOPECO (De Juan et al.,1996) (Model for the ECOnomic Optimization of irrigation water use at farm and plot level) developed by UCLM, MOPECO maximizes the gross margin of farms through a more efficient use of irrigation water. Thus, the model optimizes farms water management and identifies the proper crop rotation in a farm system, optimizing economic and yield water productivity and minimizing environmental impact (Domínguez et al., 2017; Martínez – Romero et al., 2017). The model also offers the possibility to apply ORDI (Optimized Regulated Deficit irrigation) strategies and RDI (Regulated Deficit Irrigation) strategies to fruit trees and vines in combination with TMY (Typical Meteorological Year) in those situations where the amount of water is limited (Domínguez et al., 2012b; Domínguez et al., 2012c; Pardo et al., 2018). MOPECO also generates irrigation scheduling, by using few and simply parameters (climatic, soil, crop and irrigation system data).

IREY (Irrigation Reference to Enhance Yield) developed by INGC is a mobile application for irrigation scheduling,

DOPIR and DOPIR-SOLAR (Carrion et al., 2016; Moreno et al., 2010)**:** both developed by UCLM, with the aim to improve the design of water infrastructures as a whole, based on water and energy savings. DOPIR (Design of Pressurized IRigation**)** optimizes the process of pumping water from an aquifer and its application by pressurized irrigation systems and DOPIR-Solar integrates the hydraulic model managed by DOPIR with a photovoltaic model for power generation.

PRESUD: developed by UCLM. It's a model for optimum designing of irrigation systems at plot level.

WRF (Politri et al., 2018; Skamarock et al., 2008) (Weather Research and Forecasting) provided by 3DSA. WRF is a system that will be used for both high resolution accuracy weather monitoring and climate variability and change, including impacts and adaptations as well as climatic forecasting up to 6 months.

EO-assisted methodology for water and nutrient requirements: provided by UTH: the EO methodology is used for mapping crop water requirements on a pixel-by-pixel basis by using remote sensing (Dalezios et al., 2017; Stamatiadis et al., 2017).

Drought assessment: provided by UTH. It conducts drought analysis in the agroclimatic zones of the selected areas through VHI (Vegetation Health Index), using satellite data to calculate NDVI (Normalized Difference vegetation Index) and temperature.

Fertilizer calculator: developed by UCLM, this tool determines the fertilization requirements of annual crops.

2.5. Main Tasks

The project has a duration of three years, an overview of the methodology and main tasks for each year is described as follows:

Year 1

Two activities ran in parallel 1) End – user platform development (lead by HIPATEC) 2) Preparation of the different tools and models (lead by UCLM), where the deployment of the different in – situ sensors (pressure transducers, soil moisture sensors), in the 3 demo-sites was performed to calibrate models and tools to be used in specific crops and fruit trees. In addition, the management proposed by the models carried out by the research team was compared with the traditional management carried out in each demo-site by the farmers.

Year 2

Once the end-users platform was ready, a second year of validation was carried out, managing and monitoring the same crops and fruit trees, now validating the full potential that end-users platform has. Although in year 2 farmers continued managing their crops, they provided their feedback about the use of the platform. For reaching this aim, farmers were involved in the management of the crops managed by the research team by using the platform. In addition, during year 2, a larger training took place with the aim of involve a large number of farmers.

Year 3

The information collected from the previous years, allow us to improve the end-user's platform and deliver the final version, in addition, different scenarios will be simulated for performing an impact analysis and supply solutions to extreme weather conditions, as well as including the climate change effect. To this aim 1) we will analyze the socio-economic impact of implementing SUPROMED in the demo - site areas, by using the local data generated during the management and monitoring of the demonstration farms for the current situation and for the mid-term including climate change and 2) Extrapolate these results to the Mediterranean basin, promoting policies for facing the problems determined in 1).

3. Results

3.1. Plots monitoring using the models and tool integrated at the end users platform

SUPROMED aims to improve the economic and environmental sustainability of Mediterranean agroecosystems developing an online platform composed of models and methodologies designed for increasing the efficiency in the use of inputs as water, energy, fertilizers and land. For demonstrating the impact of SUPROMED on increasing the profitability of farms and decreasing the impact on the environment, during the two first years, 56 individual farmers were involved in the monitoring of 16 crops in 95 plots (several plot of fruit trees and vineyard were managed using RDI techniques). A set of 16 productive, economic and environmental key performance indicators (KPIs) were calculated for each crop and plot, comparing SUPROMED management with the traditional management of the same crops carried out by farmers. Among them, 13 were selected for testing the models by their own and provide feedback about to improve the tools. Some of them also participated in the workshops for telling their experience to other end users. Despite of the results are very variable depending of the crop SUPROMED, all the indicators have improved (Table 1).

Table 1: Main KPIs improvement analysis

KPI	Average improvement (%)
Yield (kg ha^{-1})	13-40
Agronomic water productivity (kg m^{-3})	22-82
Economic water productivity (€m^{-3})	44-145
Water footprint decrease (m^3 kg^{-1})	12-33
Nitrogen productivity (kg kg^{-1})	29-35
Energy ($kWhm^{-3}$)	15-30
Profitability (€ ha^{-1})	25-88

3.2. Dissemination of end users platform and SUPROMED results

During these 3 years, 30 workshops attended by more than 800 participants have been organized for showing and explaining the KPIs results, promoting the use of the SUPROMED methodologies, and training more than 200 farmers and technicians in the use of the platform (that includes videotutorials and manuals). These data highlight the great interest of the sector for adopting the management solutions proposed.

The web page developed for the project (www.supromed.eu) has received more than 13000 visits, while the number of persons/enterprises registered for the use of "MOPECO irrigation scheduling" model is 171 (the only one that requires registration). This number is exponentially increasing, being 2022 the first-year farmers can use it for determining the irrigation requirements of their crops. It must be highlighted

the most of them are users located in Eastern Mancha demo site. The reason is the higher number of both weather stations (more than 40) connected to the tool (higher advisory area) and crops calibrated. Moreover, in Tunisia farmers have the option of using IREY model (340 users), while in this country and in Lebanon the number of crops and available weather stations is still low.

Moreover, several important farmers associations and enterprises are supporting the project with the objective of promoting the tools among their users and clients: FENACORE (irrigators at national level with more than 700000 people); JCRMO, MO1 and Sidi Bouzid (irrigators at regional level with more than 15000 people); Sistema AZUD and Deda (irrigation equipment enterprises); Zeta GEO Soluciones (consultant); Cooperativas Agroalimentarias de Castilla-La Mancha, Souk Jedid, Majel Bel Abbes and WUA Ouled M'hamed (more than 8000 cooperative members).

Thanks to the success in the implementation of these tools in the demo site areas, several public administrations, including the Spanish Ministry of Agriculture, have contacted SUPROMED members for extending the implementation of these tools at regional and national level.

4. Conclusions

SUPROMED can improve the economic and environmental sustainability of Mediterranean farming systems through a more efficient management of means of production. However, it requires some affordable changes in traditional management, for example having a reliable weather station network, control the irrigation system (with evaluation of the irrigation system, pressure transducers and flowmeters) and soil analysis are key to feed the models included in SUPROMED.

In addition, remote sensing tools can be useful for identifying water or nitrogen deficit at certain parts of the plot due to a poor uniformity distribution of irrigation system (It can be detected carrying out a evaluation of the irrigation system too) or variations in the soil characteristics.

Moreover, the MOPECO crops distribution tool can be complemented with the WRF weather forecast and agroclimatic zone models integrated in the platform, determining the crop distribution that maximizes profitability depending of the drought and water availability for the next moths.

The impact of SUPROMED could be extended to other areas of the world through other research teams that have expressed their interest in the platform. In this sense, MOPECO, that has been validated for many crops, can be easily calibrated for the main crops in each area because it requires a low number of parameters.

Due to the improvements achieved by SUPROMED, relevant regional, national and international institutions are supporting and promoting SUPROMED.

Acknowledgements

This work has been carried out in the frame of the SUPROMED project (ref. grant number 1813) funded by PRIMA and the European Commission. Authors also thank farmers and private and public institutions participating in this research.

5. References

García-Ruiz J M, L.-M.J.I.V.-S.S.M.L.T. and B.S. 2011. Mediterranean Water Resources in a Global Change Scenario.*Earth-Sci. Rev. 105* **2011**, 121–139.

Correia, F.N.; Iwra, M.; Técnico I.S. Water Resources in the Mediterranean Region. *Int. Water Resour. Assoc.* **2009**, *24*, 22–30.

de Juan, J.A.; Tarjuelo, J.M.; Valiente, M.; García, P. Model for Optimal Cropping Patterns within the Farm Based on Crop Water Production Functions and Irrigation Uniformity. I: Development of a Decision Model. *Agricultural Water Management* **1996**, *31*, 115–143, doi:10.1016/0378-3774(95)01219-2.

López-Mata, E.; Tarjuelo, J.M.; de Juan, J.A.; Ballesteros, R.; Domínguez, A. Effect of Irrigation Uniformity on the Profitability of Crops. *Agricultural Water Management* **2010**, *98*, 190–198, doi:10.1016/j.agwat.2010.08.006.

Daccache, A.; Ciurana, J.S.; Rodríguez Díaz, J.A.; Knox, J.W. Water and Energy Footprint of Irrigated agriculture in the Mediterranean Region. *Environmental Research Letters* **2014**, *9*, doi:10.1088/1748-9326/9/12/124014.

Knox, J.; Hess, T.; Daccache, A.; Wheeler, T. Climate Change Impacts on Crop Productivity in Africa and South Asia. *Environmental Research Letters* **2012**, *7*, doi:10.1088/1748-9326/7/3/034032.

Tarjuelo, J.M.; Rodriguez-Diaz, J.A.; Abadía, R.; Camacho, E.; Rocamora, C.; Moreno, M.A. Efficient Water and Energy Use in Irrigation Modernization: Lessons from Spanish Case Studies. *Agricultural Water Management* 2015, *162*, 67–77.

Domínguez, A.; Martínez-Navarro, A.; López-Mata, E.; Tarjuelo, J.M.; Martínez-Romero, A. Real Farm Management Depending on the Available Volume of Irrigation Water (Part I): Financial Analysis. *Agricultural Water Management* **2017**, *192*, 71–84, doi:10.1016/j.agwat.2017.06.022.

Martínez-Romero, A.; Martínez-Navarro, A.; Pardo, J.J.; Montoya, F.; Domínguez, A. Real Farm Management Depending on the Available Volume of Irrigation Water (Part II): Analysis of Crop Parameters and Harvest Quality. *Agricultural Water Management* **2017**, *192*, 58–70, doi:10.1016/j.agwat.2017.06.021.

Domínguez, A.; Martínez, R.S.; de Juan, J.A.; Martínez-Romero, A.; Tarjuelo, J.M. Simulation of Maize Crop Behavior under Deficit Irrigation Using MOPECO Model in a Semi-Arid Environment. *Agricultural Water Management* **2012**, *107*, 42–53, doi:10.1016/j.agwat.2012.01.006.

Domínguez, A.; Jiménez, M.; Tarjuelo, J.M.; de Juan, J.A.; Martínez-Romero, A.; Leite, K.N. Simulation of Onion Crop Behavior under Optimized Regulated Deficit Irrigation Using MOPECO Model in a Semi-Arid Environment. *Agricultural Water Management* **2012**, *113*, 64–75, doi:10.1016/j.agwat.2012.06.019.

Pardo, J.J.; Martínez-Romero, A.; Léllis, B.C.; Tarjuelo, J.M.; Domínguez, A. Effect of the Optimized Regulated Deficit Irrigation Methodology on Water Use in Barley under Semiarid Conditions. *Agricultural Water Management* **2020**, *228*, doi:10.1016/j.agwat.2019.105925.

Carrión F., Sanchez-Vizcaino J., Corcoles J.I., Tarjuelo J.M., Moreno M. A. Optimization of groundwater abstraction system and distribution pipe in pressurized irrigation systems for minimum cost. Irrigation Science. **2016**, 34(2), 145-159.

Moreno, M. A., Ortega J.F., Córcoles, J. I., Martínez A., Tarjuelo, J. M. Energy analysis of irrigation delivery systems: monitoring and evaluation of proposed measures for improving energy efficiency. Irrigation Science. **2010**, Vol 28. 445-460

Politi, N., P.T. Nastos, A. Sfetsos, D. Vlachogiannis and N.R. Dalezios,. Evaluation of the AWR-WRF model configuration at high resolution over Greece. Atmospheric Research **2018**, 208, 229-245 .

Skamarock, W. C., J. B. Klemp, J. Dudhia, D. O. Gill, D. M. Barker, W. Wang, and J. G. Powers,: A Description of the Advanced Research WRF version 3. NCAR. **2008 ,**tech. note TN-475_STR, 113 pp.

Dalezios, N.R., N. Dercas, N.V. Spyropoulos and M. Psomiadis. Water availability and requirement for precision agriculture in vulnerable agroecosystems. European Water **2017**, 59, 387-394.

Stamatiadis S., Schepers J. S., Evangelou L., Tsadilas C., Glampedakis A., Glampedakis M., Dercas N., Holland K. H., Spyropoulos N., Dalezios N. R. and Eskridge K. Variable-rate nitrogen fertilization of winter wheat under high spatial resolution. Precision Agriculture, **2017**, DOI 10.1007/s11119-017-9540-7.

DEVELOPING DECISION SUPPORT TOOLS FOR IRRIGATION SCHEDULING IN TUNISIA

A. Bouselmi[1], R. Nciri[1], R. Kalboussi[1], M. Mark Dougherty[2], T. Jarrahi[1],

[1]National Institute of Field Crops, Tunisia
[2]Auburn University, USA

Abstract. The Smart irrigation app "IREY" was developed to provide real-time irrigation schedules in Tunisia for selected crops (i.e., wheat, barley, sugar beet, oat and corn). Irrigation schedules in the Smartphone app and on the web are based on water balance methodology using weather data from multiple resources. The crop evapotranspiration, ETc, is calculated by multiplying the reference crop evapotranspiration, ETo issued from the WAPOR platform, by a local crop coefficient, Kc are applied based on time after planting, calendar month, or a crop's phenological stage. Soil physical properties are provided from the ISRIC to estimate available water content. App outputs include estimated reference ETc, days between irrigation events, irrigation depth and weather forecast. In addition, the App would require minimum user input and would provide ready-to-use output. A limitation of the App is the spatial variation in rainfall provided from satellites with low resolution. Future efforts will focus on enhancing the rainfall data and integrating AI into the model for more accurate recommendation.

1 Introduction

The North African countries encompass the center of origin, diversity and domestication of wheat and many other globally significant crops. But today, most of these countries face a serious challenge in terms of water resources management and water valuation is becoming an imperative for the decision makers especially in some basins where the water resource is very scarce. Thus, food security is highly dependent on imports. Domestic production and imports account for an equal share of food supplies in these countries, making them the most import-dependent countries in the developing world. Tunisia would experience, according to forecasts, increases in annual and seasonal temperatures as well as decreases in precipitation. The recurrence of dry years, as well as successions of two and three years, would be stronger. Thus, drought would be the highlight of climate projections (MARH and GIZ, 2007). According to FAO the water scarcity has reached a critical point in Tunisia, and severe drought is expected in the future. According to Kurukulasuriya and Rosenthal (2003) The highest concern goes to the agriculture sector as this sector is the main user of the available water. At the moment Tunisia already suffer from severe water shortage, which is defined as less than 500 m3 per inhabitant per year. Despite water scarcity, irrigation in Tunisia continues to represent up to 80% of the total demand in water. Generally, farmers seek to optimize soil-water-plant relationships in order to achieve a maximum yield. They usually try to achieve this desired yield by minimizing inputs and maximizing outputs, so as to optimize profits. Determining crops water requirements ETc will enable to set up a farm model for optimizing water allocation (e.g., Morgan et al., 2006; Zotarelli et al., 2009, 2011; Kiggundu et al., 2012; Dobbs et al., 2014). For this purpose, it is necessary to acquire a modeling tool for farmers and Extension Agents. The growing use of smartphones and availability of remote sensing data have resulted in an ideal situation for designing and implementing smartphone apps for irrigation scheduling. Using this concept, several SmartIrrigation apps and web apps were developed (K. W. Migliaccio, et al., 2016). Thus, this study's objectives were to develop smartphone apps for scheduling irrigation using remote sensing data and meteorological data and provide users with an irrigation schedule for crops based on soil and growth stages and weather conditions.

2 Smart Irrigation App

The Smart irrigation app we named "IREY" it is an abbreviation of "Irrigation Reference to Enhance Yield". We designed this app to provide real-time irrigation schedules in Tunisia for selected crops (i.e., wheat, barley, sugar beet, oat and corn). Irrigation schedules in the Smartphone app and on the web are based on water balance model according to FAO publication N56 "Crop Evapotranspiration - Guidelines for computing crop water requirements "for the calculation of crop water requirements and irrigation requirements based on soil, climate, remote sensing data from the WaPOR platform developed by the food and agriculture organization (FAO) and crop data. Texture, depth and initial soil moisture content (%). These data are required for calculating the soil water balance. The soil texture data comes from the digital soil map in shape file format. It is provided by ISRIC-World Soil Information (https://www.isric.org) to estimate the Available

water content (AWC). However, the IREY application allows the user to modify the type of soil according to the analysis results. In addition, App outputs include estimated reference ET, days between irrigation events, irrigation depth and weather forecast.

3 ET and WEATHER DATA SOURCES

3.1 Use of the FAO WaPOR platform

A large number of empirical or semi-empirical methods have been developed to estimate reference evapotranspiration from different climatic variables. These empirical formulas can be classified into three groups: formulas based on using temperature (Blanney-Criddle, 1951; Hargreaves and Samani, 1985), formulas based on using radiation (Priestly Taylor, 1972; Makkink, 1957), and combined formulas (Penman, 1963; Monteith, 1965). In our case, the evapotranspiration of the IREY app was based on using the WAPOR, FAO's portal for monitoring water productivity through an open access to data derived from remote sensing. It monitors and reports on the water productivity for agriculture in Africa and the Near East and provides access open to the water productivity database and its thousands of layers underlying maps. It allows direct queries of data. Analysis area statistics time series and variable data download associated with water and land productivity assessments. WaPOR data can be downloaded in csv format (values separated by commas) or as a TIFF (Tagged Image File Format) image. To download the csv numerical data, just enter the Latitude and Longitude coordinates of the point desired or the Shape file of the study area. ETo and rainfall data from WaPOR were analyzed to see their accuracy *https://wapor.apps.fao.org/*.

Figure 1. WaPOR data download steps, a) choice of ETo layer, b) choice of location (Lat, Long), c) choice of data series download period, d) display of the result and download.

The objective is to prove that the model generates good estimates of the values studied. To do this, it is necessary to work at least with a data reference of confirmation. This reference is the Local weather station database for the period 2016-2019. Five sites were chosen for this comparison, namely the weather stations of Bizerte,Beja, Jendouba, Kef and Siliana. These areas were chosen to have results comparisons in different bioclimatic stages. These reference data are used to validate the satellite estimation model.

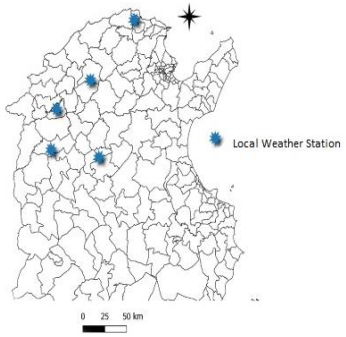

Station	Latitude N	Longitude E
Bizerte	37.25	9.8
Jendouba	36.48	8.8
Kef	36.13	8.73
Béja	36.73	9.23
Siliana	36.07	9.34

Figure 2. (left) weather station location in Tunisia (right) geographical coordinates for each station.

The acquisition of evapotranspiration data was carried out through the WaPOR platform https://wapor.apps.fao.org/home/WAPOR_2/1 with a resolution of 250 for the different study sites. The results in Table 1 of the comparison between ET WaPOR values and ET from local weather stations, showed a good overall correlation with a high R^2 around 0.8 at all study sites during the 2016-2019 period. Low mean absolute deviation around 0.6, confirms the good quality of the prediction obtained with the R^2. Low RMSE values at all the study sites, around 0.8, which means a small amplitude of the deviations. A Bias around 0.2, showing a low average of all deviations, which overestimates the prediction model. The accuracy index $\sigma\varepsilon^2$ has low values, around 0.8, which gives us an idea of the temporal variation of the differences between the values observed and simulated. d Willmott qualitative index, in order of 0.9 which explain good consistency.

Table 1. Statistics comparing ET WaPOR with ET local weather station.

ET					
SITE / INDICE	**Bizerte**	**Beja**	**Jendouba**	**Kef**	**Siliana**
R^2	0.8	0.88	0.84	0.90	0.82
MAE	0.69	0.51	0.68	0.56	0.68
MSE	0.91	0.52	0.94	0.66	1.01
RMSE(mm/d)	0.95	0.71	0.93	0.79	0.99
bias	0.07	-0.27	-0.32	-0.35	-0.22
$\sigma\varepsilon^2$	0.84	0.44	0.80	0.52	0.91
d Willmott	0.94	0.97	0.95	0.96	0.95

The ET-WaPOR generally has good agreement with the ET estimated from in-situ meteorological measurements at the different sites. The correlation at all sites was good to very good (0.8-0.9) and this confirm the results published by the FAO 2020 in the Technical report on the data quality of the WaPOR FAO database version 2 between RET-WPR and RET-EC is high, the agreement between the ETIa-WPR and ETa-EC is also high. This indicates that ET WaPOR is a good input for our IREY model.

3.2 Estimation of Crop ET (ETc)

Crop ET (ETc) is estimated using crop coefficients Kc values based on crop phenology and the reference ET (ETo) (Allen et al. 1998) (eq. 1):

$$ETc = ET0 \times Kc \quad (1)$$

According to Xanthoulis (2010), ETc varies during the development of an annual crop; it gradually increases with the rate of soil cover by the plant to reach ETo and decreases at the end of the vegetative cycle.
We used the Crop coefficients from FAO 56 which are typically vary during the plant's life cycle and validated for use in the Mediterranean basin. Different methods may be used to determine the plant stage and respective Kc value.

Table 2. Crop coefficients from FAO 56

Crop	$Kc_{initial}$	$K_{c\ middle}$	$K_{c\ end}$
Wheat	0.7	1.15	0.25
Barely	0.3	1.15	0.25
Oat	0.3	1.15	0.25
Corn	0.7	1.2	0.35
Sugarbeet	0.35	1.20	0.70

Depending on the information available, two methods was used to assign Kc values in the apps: the growing degree day method (GDD), days after planting method, or calendar-based method. GDDs are calculated using equation 2:

$$GDDs = \frac{Tmax - Tmin}{2} - Tbase \quad (2)$$

Where T_{max}= Daily maximum temperature (°C), T_{min}= Daily minimum temperature (°C) and T_{base}= Base temperature (0°C) below which the process of plant growth does not progress. For DW and Oat, T_{base} is 0.0 °C. Any temperature below T_{base} is set to T_{base} before calculating the average (Matzarakis et *al.,* 2007; Kumar et *al.,* 2020).

3.3 Precipitation

Rainfall is included in the apps using three different sources due to the spatial variability of rainfall and the limited number of weather stations in Tunisia. Measured rainfall points provided by DGRE (General Directorate of Water Resources in Tunisia), and from satellite data we use GPM (Global precipitation measurement NASA) and WaPOR platform. WaPOR do not provide a good accurately predict rainfall compared to DGRE and GPM. Forecast data from weather underground using web service https://www.wunderground.com/ .

4 App Concept and development

4.1 Concept

The concept is based on the water balance model: input: irrigation, rainfall and available water, and output: evapotranspiration and drainage (Allen et al 1998) as showed on Fig 3. In addition, the App allows the development of irrigation schedules for two different managements (deficit irrigation or full irrigation). The web application can also be used to evaluate farmers' irrigation practices.

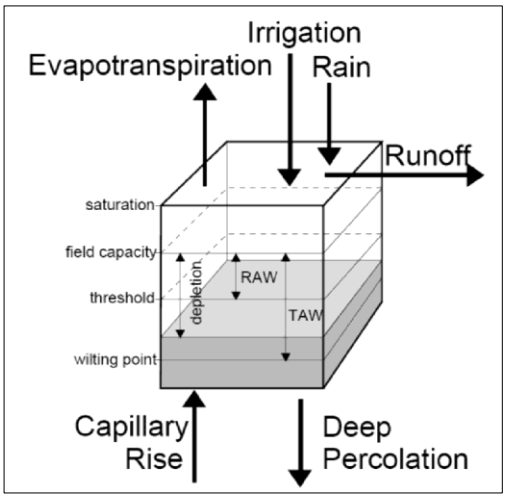

Figure 3. Shematic of the FAO 56 illustrated.

The soil texture data comes from the digital soil map in shape file format. It is provided by ISRIC (International Soil Reference and Information Centre Soil) (https://www.isric.org). However, the IREY application allows the user to modify the type of soil according to the analysis results.

2

Figure 4. SOTER-based soil parameter estimates (SOTWIS) for Tunisia from ISRIC.

4.2 Devlopment

IREY app was developed using Java and Android SDK, with a user friendly design, the web app developed using odoo open source software using Python and JavaScript. The apps communicate with WaPor, DGRE, GPM and weather forecast via specific developed web services and APIs (APIs) to run the models needed for the water balance calculations. A web request to the IREY application extracts the ETo and precipitation values from the matrix according to geographic coordinates (X, Y) entered by the IREY user.

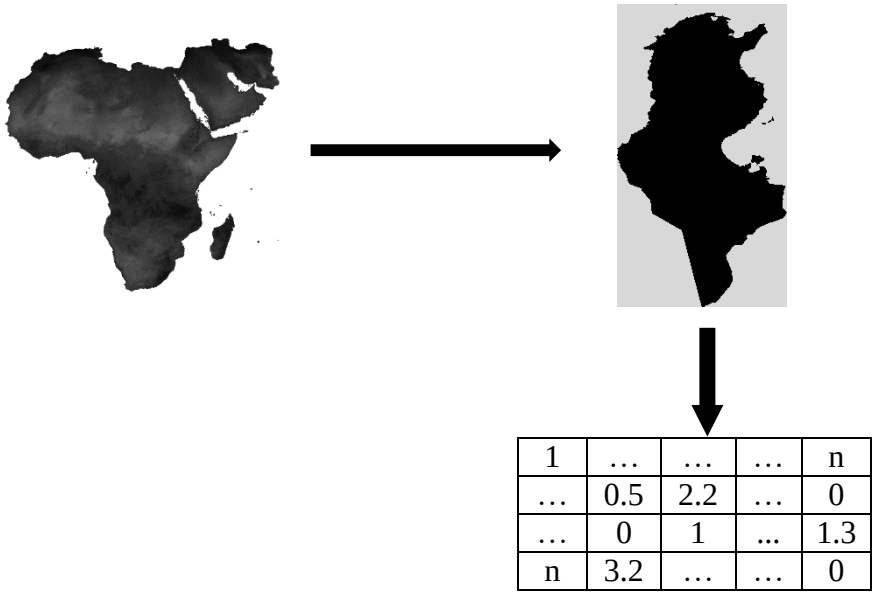

1	…	…	…	n
…	0.5	2.2	…	0
…	0	1	...	1.3
n	3.2	…	…	0

Figure 5. Cutting, downloading TIF raster image and conversion to matrix using python script.

Schedule updates based on observed weather data and the, rain events, and applied irrigation. In addition, soil water balance status will be updated and will indicate with blue and red color if the plant stressed or not.

5 IREY output and functionality

IREY app was released on the google play store in three languages Arabic, English and French with integration of Remote Sensing Data from the WaPOR Platform. This app helps farmers, extension services, researchers and other users to analyses, make decisions and increase the water productivity.
The app, allowing users to easily schedule their irrigation, conserve water with no yield reduction or plant damage. With a user-friendly design, the app allow farmer to schedule their irrigation without any help from extension agent or any technician. With a google account you can sign-in free to the app and on the web too. In few steps farmers could manage their irrigation easily; click 'add a new field'. Name your field. Select the location, crops, irrigation method, precipitation sources and finally the sowing.

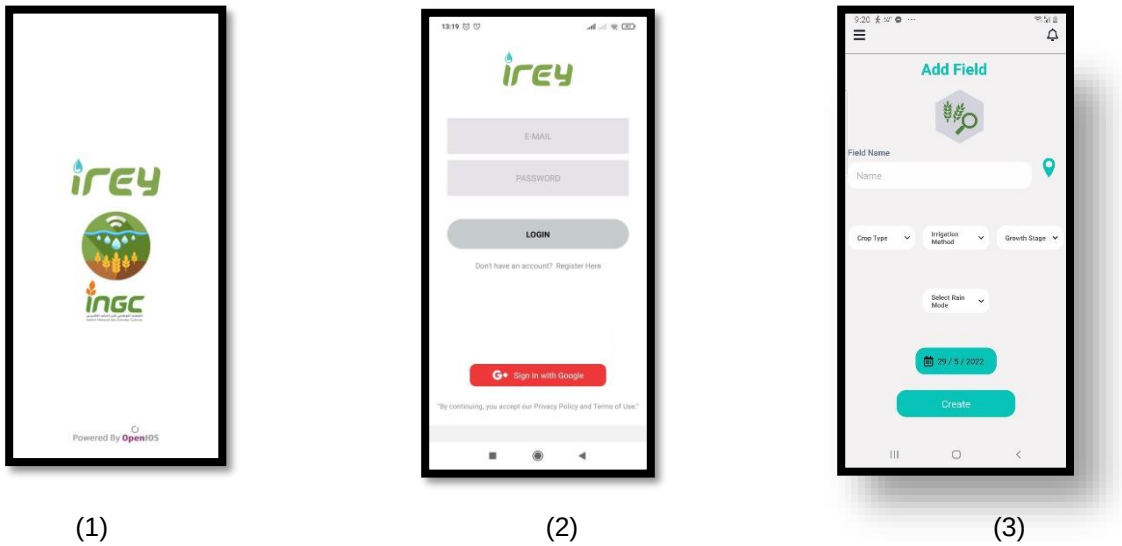

(1) (2) (3)

Figure 6. Screenshot of IREY app (1) IREY Home page (2) Sign-in with google account (3) adding new field.

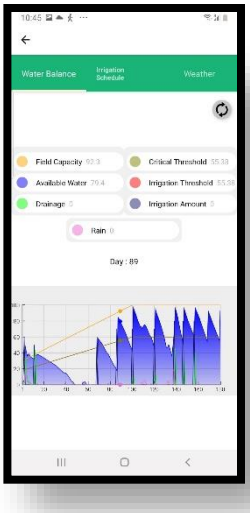

Figure 7. Screenshot of Soil Water Chart.

The App provide a nice graphic 'Soil Water Chart' that shows estimated soil water in your field based on calculated soil water balance model. The red line that indicates where first stress is set at 60% of field capacity as a default. However, the user can adjust this 'management allowable deficit' level in the settings if you prefer a higher or lower threshold to trigger refill of the water profile.

5.1 Evaluation of IREY model output

To Compare IREY model output to observed measurement, an experimentation was conducted in central of Tunisia where two crops were monitored, Durum wheat and Oat during the growing season 2020-2021. Figure 8 and 9 shows the graph of simulated available water AW with IREY model and observed values of AW using Sentek sensors. These values present good results and promising. More experimentation need to be conducted for other crops in different regions to enhance the model output accuracy.

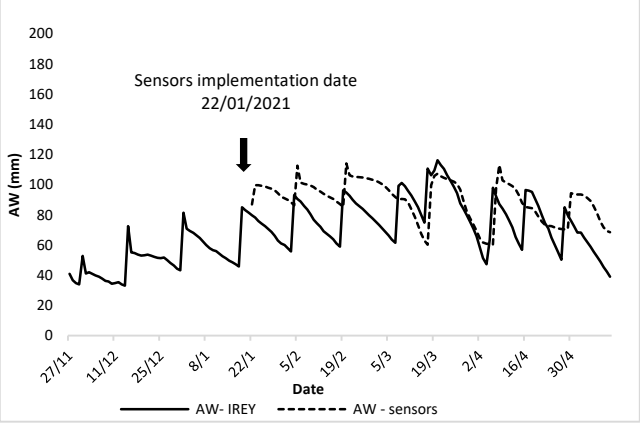

Figure 8. Comparison of simulated available water model with observed measurement for wheat field

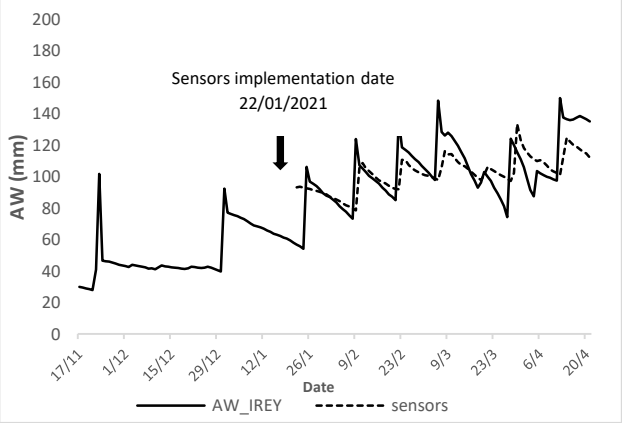

Figure 9. Comparison of simulated available water model with observed measurement for oat field

6 Summary

In order to improve the estimation of the water balance, we integrated the climatic data from WaPOR into the IREY application. This satellite product provides daily updates of climate databases. The integration of WaPOR data has made it possible to increase the meteorological network, covering the entire bioclimatic zone of Tunisia. It also allowed automatic updating avoiding the painful tasks of manual updating. The data was validated by comparing it with the data from the local weather station, and the results were very promising for the reference evapotarnspiration ETo. With these satellite data, IREY estimates crop water needs in real time by recommending the right irrigation application at the right time. A limitation of the App is the spatial variation in rainfall provided from satellites with low resolution. Future efforts will focus on enhancing the rainfall data and integrating AI into the model for more accurate recommendation and to conduct more experimentation for all crops used in IREY App in different regions.

Acknowledgements

This work was made possible by funding from the FAO under FAO-SIDA project "Implementing the 2030 Agenda for water efficiency/productivity and water sustainability in the NENA countries'", Sustainable Production in water limited environments of Mediterranean agro-ecosystem (SUPROMED), financed by PRIMA program Section1 and INGC the National Institute of Field Crops in Tunisia.

References

Allen, R.G., Pereira, L.S., Raes, D., Smith, M., 1998. Crop evapotranspiration: guidelines for computing crop water requirements. In: Proceedings of the Irrigation and Drainage Paper No. 56. Food and Agricultural Organization, United Nations, Rome, Italy.

Blaney, H.F. and Criddle, W.D. 1950. Determining water requirements in irrigated area from climatological irrigation data. Washington, DC: US Department of Agriculture. Soil Conservation Service, Technical Paper No. 96.

Dobbs, N. A., Migliaccio, K. W., Li, Y. C., Dukes, M. D., & Morgan, K. T. (2014). Evaluating irrigation applied and nitrogen leached using different smart irrigation technologies on bahiagrass (Paspalum notatum). Irrig.

FAO. 2020. WaPOR V2 quality assessment – Technical Report on the Data Quality of the WaPOR FAO Database version 2. Rome.

Hargreaves, G.H. and Samani, Z.A. (1985) Reference Crop Evapotranspiration from Temperature. Applied Engineering in Agriculture, 1, 96-99.

ISRIC International Soil Reference and Information Centre Soil ; https://www.isric.org.

Kiggundu, N. Migliaccio, W. Schaffer, B. Yuncong, L. (2012), Water savings, nutrient leaching, and fruit yield in a young avocado orchard as affected by irrigation and nutrient management. Irrigation Science, 30(4), 275- 286.

Kumar et al., 2020). Kumar, P., Herndon, E., and Richter D. (2020): Critical Agents of Change at Earth's Surface.

Kurukulasuriya, P. and Rosenthal, S. (2003) Climate change and agriculture. A review of impacts and adaptations. The World Bank Environment Department.

MARH et GIZ, 2007 : Stratégie nationale d'adaptation de l'agriculture tunisienne et des écosystèmes aux changements climatiques, Cahiers 1à 6.

Makkink GF (1957). Testing the Penman Formula by Means of Lysimeters', J. Instit. Water Engineers 11: 277 288.

Matzarakis, A. Climate, thermal comfort and tourism. Clim. Chang. Tour. Assess. Coping Strateg. 2007, 139–154.

Migliaccio, K.W., Morgan, K.T., Fraisse, C., Vellidis, G., Zotarelli, L., Fraisse, C., Zurweller, B.A., Andreis, J.H., Crane, J.H., Rowland, D., 2016. Performance evaluation of urban turf irrigation smartphone app. Comput. Electron. Agric. 118, 136–142.

Monteith, J.L. 1965. Evaporation and environment. pp. 205-234. In G.E. Fogg (ed.) Symposium of the Society for Experimental Biology, The State and Movement of Water in Living Organisms, Vol. 19, Academic Press, Inc., NY.

Morgan, K.T., Obreza, T.A., Scholberg, J.M.S., Parsons, L.R., Wheaton, T.A., 2006. Citrus water uptake dynamics on a sandy Florida Entisol. Soil Sci. Soc. Am. J. 70, 90–97.

Penman, H.L. 1963. Vegetation and hydrology. Tech. Comm. No. 533. Harpenden, England: Commonwealth Bureau of Soils. 125 pp.

Priestley, C. H. B. and Taylor, R. J.: 1972, 'On the Assessment of Surface Heat Flux and Evaporation Processes in Atmospheric General Circulation Models, Cambridge University Press. Using Large-scale Parameters', Mon. Wea. Rev. 100, 8 1-92.

Xanthoulis (2010), Xanthoulis D., 2010 : Calcul ET0-Penman.pdf. 54 pp

Zotarelli, L.; Scholberg, J. M.; Dukes, M. D.; Muñoz-Carpena, R.; Icerman, J., 2009. Tomato yield, biomass accumulation, root distribution and irrigation water use efficiency on a sandy soil, as affected by nitrogen rate and irrigation scheduling. Agri. Water Management, 96 (1),: 23-34.

Setting out a Decision Support System for farmers in South Bekaa Irrigation Scheme through the involvement of SUPROMED innovative platform

F. Karam[1], V. Kaspard[2], N. Nassif[1], A.H. Mouneimne[1], C. El Hachem[1], S. Samaha[3]

[1]Department of Environmental Engineering, Faculty of Agricultural and Veterinary Sciences, Lebanese University. Main Road to Mkalles Roundabout, Dekwaneh, Meten, Lebanon

[2]Laboratory of Geosciences, Georesources & Environment, Faculty of Sciences, Lebanese University, Hadath Campus

[3]Université Saint Joseph, Faculté des Sciences Humaines, Spécialité Géographie, Environnement et Aménagement du Territoire, Rue de Damas, Beyrouth, Lebanon

Corresponding author: Fadi Karam (fadkaram@gmail.com)

Abstract. Farmers in South Bekaa Valley of Lebanon are facing production challenges due to (i) imbalance between water supply and demand, (ii) lack of technical assistance and (iii) poor animal production systems. SUPROMED (Sustainable Production in Water Limited Environments of Mediterranean Agro-Ecosystem, 2019-2022) aims to establish a Decision Support System (DSS) to help farmers better coping with their agricultural practices under the prevailing climatic conditions. The DSS will integrate models, among which MOPECO (Economic optimization model for irrigation water management) to optimize water productivity (WP) and gross margin (GM) for sustainable agricultural production of both annual crops and fruit trees.

Lebanon's demo site is situated within South Bekaa Irrigation Scheme in the southern plains of the Bekaa Valley, covers an irrigable area about 21,500 ha. For economic constraints, only a pilot area of 2,000 ha is for the time being equipped with a pressurized irrigation network, while the rest of the scheme is still relying on ground wells for irrigation purposes. Agricultural land in test site consists of one-third of wheat and other winter cereals, mainly barley, one-third of potato, winter legumes and summer vegetables and one third of fruit trees, mainly peach and vineyards, and land kept as fallow during the in-between seasons.

SUPROMED integrates a set of models and tools in an online platform to increase the production and income of farms, through more efficient use of water, fertilizers and energy, while decreasing the impact on the environment. SUPROMED also considers *in-situ* data and Earth Observation (EO) imagery, agro-alerts, agro-climatic classification and zoning together with drought forecast tools. The SUPROMED IT Platform has been shown to be easily accessed by farmers, proposing a reserved access area to designated end-users.

1 Introduction

Decision Support Systems (DSSs) are used in agriculture to collect and analyze data from a variety of sources with the ultimate goal of providing end users with insight into their critical decision-making process (FAO, 2004; Zhaoyu et al., 2020). These online systems help farmers to solve complex issues related to crop production. However, these systems are challenging in terms of information overload, system design, and data collection. Therefore, DSS designers are interested in making these systems easily accessible and friendly-use. This study covers current trends and future developments of a decision support system developed by SUPROMED, for which a water management resilient to climate change is proposed. Thus, an end-user IT (Information Technology) platform designed to smartly advise farmers in the efficient water management of Mediterranean crops will be delivered. To this end, SUPROMED will integrate a validated set of models and tools in an online platform to increase the production and income of farms through a reduction and more efficient use of water, and other inputs such as energy and fertilizers, while decreasing the impact on the environment.

This paper aims to align with SUPROMED objectives for the 'Development of an end-user IT platform', as Decision Support System (DSS) and 'Enterprise Resource Planning (ERP) to (i) advise farmers and technicians on the optimal design and management of farming systems infrastructures, (ii) improve their resilience to climate change, by embracing real-time management of water, fertilizers and energy, and (iii) benchmark techniques to optimize the management of production means, mainly with relation to water, energy and fertilization. The

ultimate objective is to propose a quick assessment of the suggested DSS, by means of oriented questionnaire and face-to-face interviews with farmers in the southern plains of the Bekaa Valley of Lebanon.

2 Material and Methods

2.1 Description of the demo site in Lebanon

Lebanon's demo site is located in South Bekaa Valley of Lebanon and is a part of South Bekaa Irrigation Scheme (SBIS), with an irrigated area about 21,500 ha. Many challenges are faced by local farmers in SBIS, mainly, (i) the imbalance between water supply and demand, (ii) weak extension services and (iii) lack of knowledge by farmers on good production practices and handling techniques to improve crop productivity. For all these reasons, SUPROMED proposed to establish an Early Warning System (EWS) to alert farmers on irrigation application timely and properly, and increase the efficiency with which fertilizers are used by crops. To do so, the DSS was designed to include models such MOPECO (Ortega Álvarez et al., 2004), IREY and DOPIR, which are tools to optimize crop production and encourage water savings under the prevailing weather conditions.

Demonstration plots were established within SBIS, covering annual crops (potato, wheat, corn and onion), fruit trees (peach) and vineyard. MOPECO was calibrated and validated using weather, soil and crop data from the 2019-2020 and 2020-2021 growing years. The plots have been selected within a polygon, 100 km^2 in area (20 km long x 5 km wide), covering the whole South Bekaa Irrigation Scheme (SBIS). For each of the selected crops, a leader farmer (LF) and an average farmer (AF) have been identified, either for comparing the results with SUPROMED monitored plots, or for socio-economic purposes. The leader farmer usually has the biggest plot in the demo site, compared to average and associated farmers, while average farmer is more representative of the local farming systems in the demo site. Being advantageous compared to other small or associated farmers, either in term of technology possessed, or knowledge gained, both leader and average farmers are among the potential users of the SUPROMED IT Platform.

2.2 The proposed SUPROMED online DSS

SUPROMED online platform is designed to increase the production and income of farms through a reduction and a more efficient use of water, and other inputs such as energy and fertilizers, while decreasing the impact on the environment (Figure 1). Data are taken from the farm and the weather station, analyzed by the system and generating solutions to the end users. The online system can be considered as a toolbox offering end users the possibility to use different models and information depending on their needs (Figure 2):

- Irrigation scheduling: MOPECO and IREY
- Optimal crops distribution: MOPECO
- Full modelling and optimization of farm management: MOPECO
- Design and optimization of irrigation network: DOPIR (for pressurized irrigation systems), DOPIR-Solar (for solar powered irrigation) and PRESSUD (for sprinkler and drip irrigation systems)
- High resolution weather forecasts: satellite weather and climate forecasts.

These models and tools can be accessed in SUPROMED website through the following link: https://dss.supromed.eu/portal/.

SUPROMED IT Platform has an easiest way to be accessed by logging in into the page and then registration a new personal account to save your own data. SIAR is the Irrigation schedule programmer (Figure 3). The application calculates the water needs of a crop using climatic data and crop data. The results obtained are the consumption of the crop, the precipitation, the consumption forecast for the next 7 days, and a simulation of the crop cycle based on climatic data from a typical year.

The online DSS comprises 4 different steps:

1. Plot location: the user should be familiar with google map to add the location. This step is not very accurate in the DSS, as it is put randomly without the coordinates (x for longitude and y for latitude);
2. Soil data: soil information, such as soil type, depth, soil infiltration rate are needed as input parameters;

3. Crop data: date of sowing, crop growth stages, crop coefficients (K_c) of the selected crops should be known;
4. Irrigation data: including irrigation interval, maximum and minimum irrigation volume, initial soil moisture, depletion level and filling level.

Figure 1. Decision Support System of SUPROMED (*adopted* from SUPROMED, 2021)

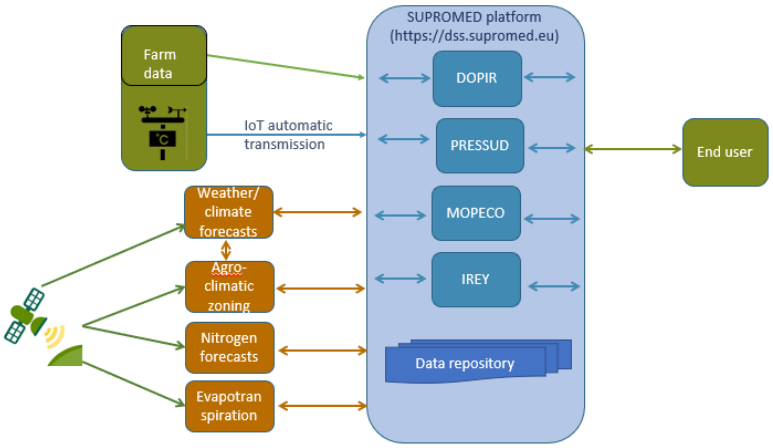

Figure 2. SUPROMED DSS schematic description (*adopted* from SUPROMED, 2021)

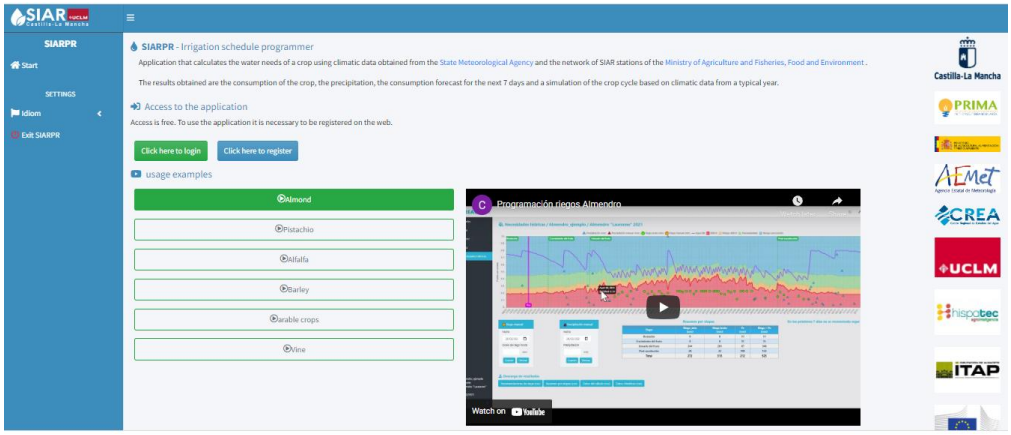

Figure 3. Access to SUPROMED DSS platform https://crea.uclm.es/siar/siarpr (*adopted* from SUPROMED, 2021)

2.3 Description of the questionnaire and end users experience

In order to be able to assess the degree of usage of the proposed SUPROMED online DSS at the farm level, a tailored questionnaire was prepared by ULFA (Lebanese University, Faculty of Agronomy) project team, with the aim to collect information from leader and average farmers, as well as other agricultural engineers and technicians using the DSS. The questionnaire contains two parts; Part (A) on Farmer's Bios information, and Part (B) on Information on farmer's land. In addition, the questionnaire has two Sections; Section I with general questions to farmers and section II with specific questions to farmers on the proposed DSS.

Section I of the Questionnaire includes 5 general questions:

1) What crops do you grow in your farm/field?
2) Do you record/register farm interventions? Yes/No (If yes, specify the interventions you record/register in your farm/field).
3) Do you face real shortages of water during irrigation period? Yes/No (If yes, specify time and duration of last water shortage).
4) Are you willing to apply less water when there are shortages? Yes/No.
5) Do you use any advisory information on time and quantity of irrigation? Yes/No (If yes, specify the name of the provider and the way to access the information (mobile application, computer, etc.…). Are you satisfied with results?

Section II has 6 DSS-oriented questions:

1) Are you willing to use a Decision Support System to help you better coping with agricultural practices in your field/farm? Yes/No
2) Are you willing to use the recommendations proposed by the DSS at a daily basis? Yes/No
3) How did you find SUPROMED DSS? (Easy, Note very easy, Difficult)
4) What did you see as opportunities in the proposed DSS?
5) What did you see as challenges in the proposed DSS?
6) Are you ready to pay the service provided by SUPROMED-DSS?

In summary, the easy-to-use farmer's questionnaire aimed to assess (i) the knowledge of the users regarding the Decision Support System, (ii) accessibility, easiness, and understandability of SUPROMED IT Platform, (iii) level of difficulty, accessibility, satisfaction, readiness to use MOPECO as an irrigation model, and rely on the results generated by the model to apply the right amount of water amounts at the right times, (iv) readiness to pay for the service, and (v) collect suggestions of farmers and end-users to improve the system.

3 Results

With the aim to assess the SUPROMED proposed DSS, as a platform to provide advantages for water, fertilizer and production management, the results of the questionnaire were categorized at two levels of user's type:

i) Farmers: useful experience in general, especially on irrigation scheduling and fertilizers' applications. They are mainly concerned by the way to get the DSS functional. They need assistance for the proper use of the model especially when data are related to the irrigation system and water availability, maximum and minimum dose… They were also inquiring about the use of the MOPECO tool for other crops than the selected one. Finally, regarding the payment, they didn't reject the idea but it needs to be well calculated and the benefits from using the model should be well seen.

ii) Agro-environmental engineers and technicians: this platform provides management consultancy, technical assessments & designs, and equipment procurement to deliver solutions under the different sectors.

To explain the functionality of the online system, a targeted training was conducted in June 2021 to a group of leader farmers, average farmers, and agricultural engineers and technicians, representing different cropping systems within South Bekaa Irrigation Scheme (SBIS). Considering that the proposed online platform depends to a larger extent on the part related to water and irrigation, set of opportunities and challenges were collected from the interviewees *vis-à-vis* the online DSS, which are found in Table 1. Figure 4 contains the results of the oriented questionnaire in terms of responses of the enquired farmers to the set of six DSS-oriented questions.

Table1. Opportunities and Challenges of the SUPROMED-DSS

Opportunities of SUPROMED-DSS as witnessed by the interviewee's farmers and end-users	Challenges of the SUPROMED-DSS as witnessed by the interviewee's farmers and end-users
a. Help in decision-making; b. Allow rapid assessment of agricultural production systems; c. Reduce water loss; d. Improved irrigation efficiency; e. Promote accurate irrigation scheduling; f. Calculate improved ratio of gain/cost; g. Advance introduction of technologies.	a. Identify emerging approaches and future direction of research in the field; b. Change decisions and mind set; c. Change irrigation practices in the field; d. Sophisticated tool for farmers; e. Training and expertise needed; f. Farmers have difficulty to introduce data required, such as crop and irrigation information, needed to calculate the water requirement; g. challenges related to internet connectivity.

Moreover, with the aim to improve the usage of the DSS, a set of suggestions were collected from farmers for further analysis by the research team:

- Developing Short Messaging Service (SMS) technology as a tool to improve farmers' and extensionists timely access to technical knowledge and to increase technology adoption;
- Development of Mobile Application as a decision-making tool for irrigation monitoring;
- Development of Cereal Expert System;
- Development and out-scaling of the appropriate technical and economic packages;
- Organization of training courses for famers and extensionists;
- Assisting in developing enabling policy environment to take stoke of the improved technologies;
- Enhancing capacity of farmers via the organization of field events and Farmer's Schools;
- Development and distribution of technical manuals in local language.

4 Summary

The overall objective of the proposed online SUPROMED DSS is to provide farmers with enough agricultural decision-making suggestions, like farm operation scheduling, irrigation and fertilization programs, detailed operation cost, resources usage, and profitability analysis, alongside specific aspects on the readiness of farmers towards advanced information systems and Internet technologies adopted to the agricultural sector.

Decision Support System for agriculture has become a very attractive topic for both farmers and decision-making. However, exploring the challenges and opportunities of employing DSS in agriculture are among the key factors for successful and sustainable use by farmers. Researchers and engineers may improve the DSS by overcoming the detected challenges and promote opportunities. It is worth noting that lack of tools and/or irrigation advisory services for determining the irrigation requirements of crops at farm level may cause a decrease in both the final yield and the irrigation water productivity. The models suggested by SUPROMED DSS are important tools, as the most relevant issue met by farmers is water, and water scarcity and high water pumping energy costs, which all-in-all have to be addressed in South Bekaa Irrigation Scheme.

Acknowledgements

The authors wish to thank PRIMA (Partnership of Research and Innovation in the Mediterranean Area) and SUPROMED (Sustainable Production in Mediterranean Agricultural Ecosystems) for supporting this research.

References

Zhaoyu, Z, José Fernán Martínez, Victoria Beltran and Néstor Lucas Martínez, 2020. Decision support systems for agriculture 4.0: Survey and challenges. Computers and Electronics in Agriculture, Vol. 170, Issue C, https://doi.org/10.1016/j.compag.2020.105256.

Ortega Álvarez, J. F., de Juan Valero, J. A., Tarjuelo Martín-Benito, J. M. and E. López Mata. 2004. MOPECO: an economic optimization model for irrigation water management. Irrigation Science, 23 92): 61-75. DOI: 10.1007/s00271-004-0094-x

FAO, Land evaluation decision support system (MicroLEIS-DSS) for agricultural soil protection, 2004.

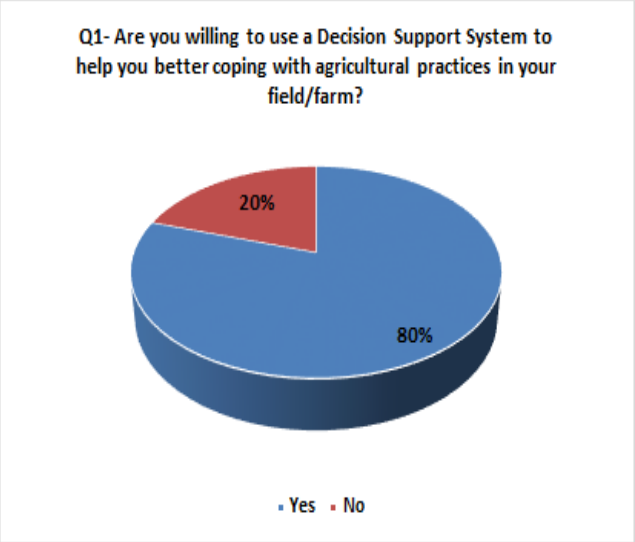

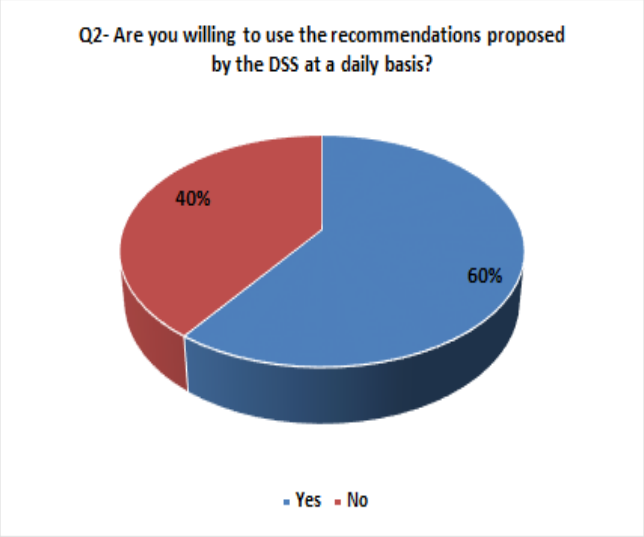

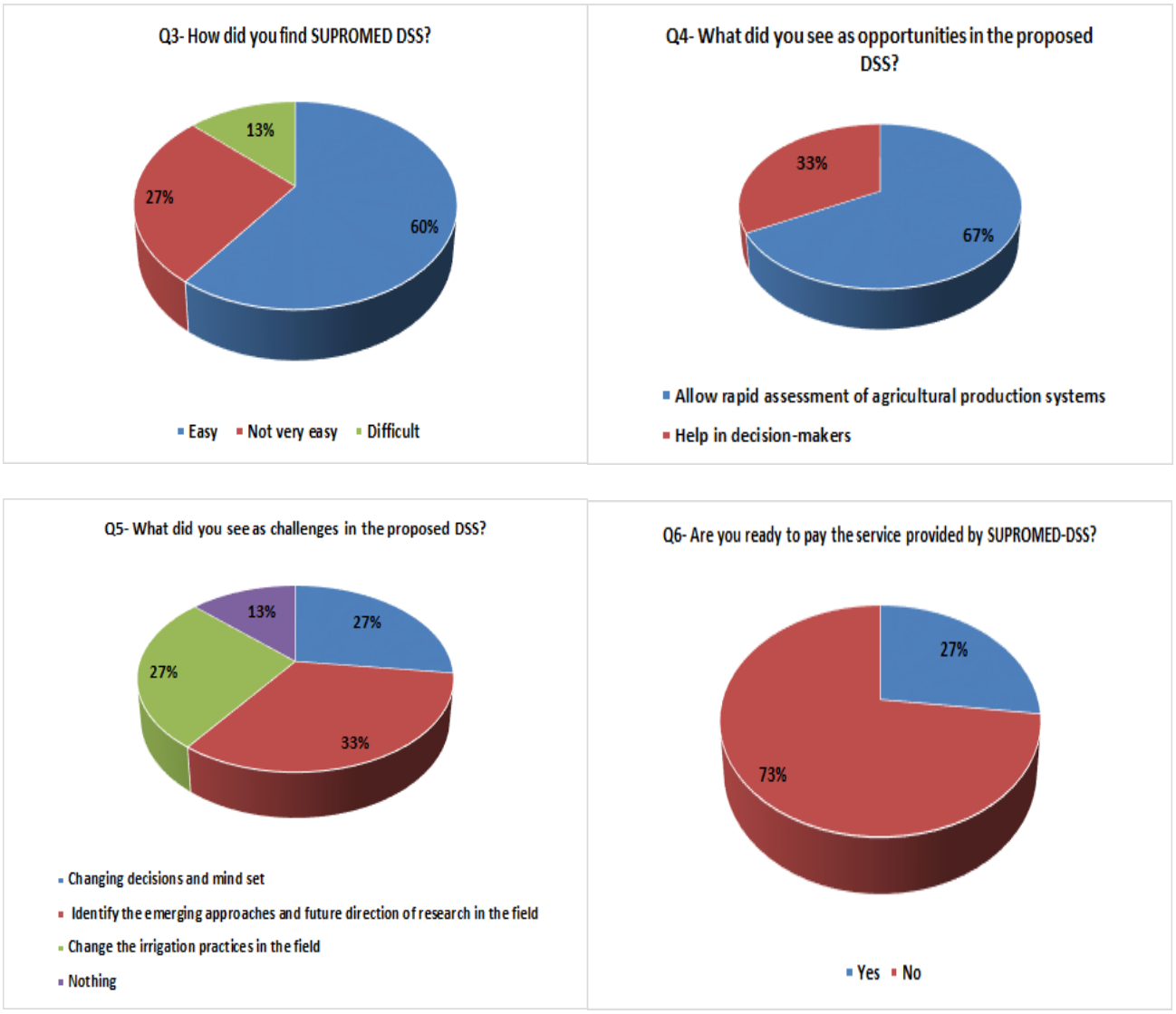

Figure 4. Results of the DSS oriented questionnaire

Remotely sensed Agroclimatic Classification and Zoning towards sustainable agriculture: the case of La Mancha Oriental (Albacete) region in Spain

Faraslis[1], I., N. Alpanakis[2], G. Tziatzios[2], M. Spiliotopoulos[2], S. Sakellariou[2], P. Sidiropoulos[2], V. Brisimis[2], A. Blanta[2], N. Dercas[3], N.R. Dalezios[2]

[1] Department of Environmental Sciences, University of Thessaly, Larisa, Greece
[2] Department of Civil Engineering, University of Thessaly, Volos, Greece
[3] Department of Natural Resources and Agricultural Engineering, Agricultural University of Athens, Greece

Abstract

Temperature and rainfall, in terms of quantity and spatiotemporal variability, are the main variables which determine the type of suitable crops to a given climatic region. The agroclimatic analysis has as objective the assessment of inherent capabilities of land to support specific crops for long periods without degradation. New methodologies based on satellite remote sensing and GIS data and techniques for agroclimatic classification are applied. The purpose of this study is to identify agricultural land for sustainable production in Albacete region in Spain. The current work is based on a three-stage procedure. Firstly, water limited growth environment (WLGE) zones are defined by combining aridity index (AI) and vegetation health index (VHI). Secondly, general, or non-crop specific agroclimatic zones (NCSAZ) are created by associating WLGE zones and landforms. Finally, crop specific attributes (Growing Degree Days, Net Radiation) are combined with NCSAZ forming the crop specific agroclimatic zone for sustainable agriculture production. The results are promising as compared with the current crop production system of the area under investigation. Moreover, new relatively high-resolution satellite data, integrated in sophisticated platforms, like Google Earth Engine, could provide a valuable tool for creating detailed and up to date agroclimatic zones almost worldwide.

1. Introduction

Environmental conditions, such as land availability and water scarcity, highly affect agricultural production. Moreover, the most important factors of the suitability and the yield of a specific crop is specified by local climate and weather conditions (Wall and Smit, 2005; Amber et al., 2021). Agroclimatic zoning (ACZ) permits recognizing agricultural areas with optimal production and efficient use of natural resources. The agroclimatic classification zones are defined as areas with similar combinations of climate and soil characteristics and similar physical potentials for agricultural production (Fischer et al., 2021). There are many agroclimatic classification research studies in the literature trying to identify sustainable production zones within a climatic region (Araya et al, 2010; Adnan et al., 2017; Falasca et al., 2014). Their approaches vary in complexity with most of them based on evapotranspiration and rainfall. The delimitation of areas that crops could or could not be grown, avoiding at the same time the degradation of natural resources, should be a combination of climate regime, such as temperature and rainfall, along with topographic features, soil types and crop parameters. Thus, all aspects of agroclimatic analysis must consider the impact of climate change.

With the entry of 21st century new methodologies based on satellite remote sensing data and GIS techniques for agroclimatic classification are applied (Patel et al., 2000). The lack of long records in many countries, as well as the lack of available data in remote areas is the main driving force behind the increasing use of satellite products (Thenkabail et al., 2004). It is also broadly accepted that remote sensing has become a valuable tool for monitoring the spatial and temporal distribution of climate extreme events, such as droughts, floods, or heat waves. Specifically, remote sensing data and methods have been applied to agroclimatic zones mapping, in semi-arid regions (Tsiros et al. 2009). Furthermore, the new satellite systems offer better spatial and spectral resolution providing increasing reliability and accuracy in Earth Observation (EO) data and remote sensing methods concerning environmental parameters and vegetation (Dalezios et al., 2018; Niemeyer, 2008). Besides, the technological advancements also offer additional computational capabilities. The Google Earth Engine (GEE) is a computer-based platform dedicated to processing a great variety of EO data, over a long period of time. Its database contains a petabyte of satellite imagery (Sentinels, Landsat, Modis, etc) and geospatial of datasets (e.g., climatic and elevation data) (Gorelik et al., 2017).

The objective of this research is to create rapidly relatively high resolution agroclimatic zones for sustainable agricultural production. New remote sensing, datasets and the capability of GEE is considered. The study area, where sustainable production zones are created, is in the region of La Mancha Oriental (Albacete) in Spain.

2. Methodology

In the proposed methodology remote sensing and GIS are used as tools to analyze water, soil, and altitude restrictions in defining appropriate zones for sustainable crop production. Briefly, the methodology for delineating agricultural land suitability assessment is divided in 3 major steps (Dalezios et al., 2018): (a) Hydroclimatic zoning, (b) Non crop specific Agroclimatic Zoning and (c) Crop specific Agroclimatic Zoning. Figure 1 represents the flow chart of the agroclimatic zoning methodological steps. The main processing is conducted in GEE web platform. Moreover, downscaling effective techniques, such as machine learning algorithms, are applied in this platform to achieve relatively high resolution agroclimatic zones (200x200 m pixel size).

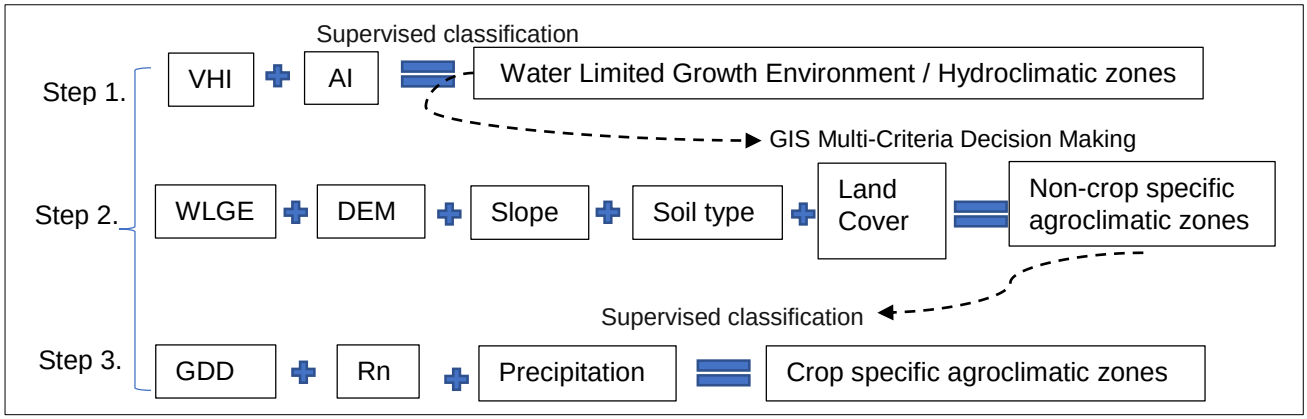

Figure 1The methodological steps of agroclimatic zoning

The first step is to identify zones adequate for sustainable farming according to water limitations using GIS and remote sensing approaches, namely Water Limited Growth Environment (WLGE) zones. The WLGE zones, describing the hydroclimatic component of the agroclimatic zoning, are identified through superposition of the two indices, namely the Vegetation Health Index (VHI) and Aridity Index (AI) (Wu et al, 2020). The VHI monitors the overall vegetation health, according to climate conditions (moisture and thermal conditions) and is used for the identification of vegetative stress and drought affected areas over a period. It is a widely used index of agricultural drought based on remote sensing data. The VHI is a linear combination of two indices, namely the vegetation Condition Index (VCI) and the Thermal Condition Index (TCI) (Zuhro et al., 2020). The AI is a climatic index and is calculated using meteorological data over a period (e.g., 20-30 years). It is a function of the ratio of precipitation to potential evapotranspiration. As soon as both indices (VHI and AI) are computed, the Water Limited Growth Environment Zones (WLGE) are created. The VHI map is combined with the climatic aridity map, by means of supervised classification, leading to the definition of WLGE zones: “No limitations”, “Partially limited-No limited environment”, “Partially Limited environment” and “Limited environment”.

The second step is to identify sustainable production zones to characterize the non-crop specific agroclimatic zones (or General Agroclimatic Zoning) in terms of water efficiency, fertility (appropriate or not for agricultural use), desertification vulnerability and altitude restrictions. Thus, a combination of criteria, such as: WLGE zones, Digital Elevation Model (DEM), slope, soil map and land-use/land cover, are applied (Tsiros et al., 2009). GIS Multi-Criteria Decision Making (MCDM) method is used for the non-crop specific agroclimatic zoning. The MCDM approach evaluates and weights each criterion according to their relative importance on the optimal growth conditions for crops. Besides, the suitable weight of each criterion is calculated by the Analytical Hierarchy Process (AHP). This method is widely accepted and is considered the most reliable MCDM method that helps to measure the weight of criteria with respect to each other. Finally, the non-crop specific agroclimatic zones map is created leading to five suitability classes: Good, Fair, Moderate, Poor and Not Suitable.

In the third step, the crop-specific agroclimatic zoning map is created representing the sustainable zones according to the special characteristics of the crops, e.g., winter-summer crops. Three crop parameters are considered, namely growing degree-days (GDD), net radiation (Rn), and the local climatic conditions focused on the amount of spring precipitation. These parameters are calculated for a period (e.g., 20-30 years). According to the type of crops, such as winter or summer annual cultivations, the two indices, GDD and Rn, are combined to identify where crops are not restricted due to radiation, leading to high, medium, and low productivity zones. Moreover, the 20 days spring precipitation (April – May) is rated in two classes, sufficient – insufficient rain for annual crops. The combination of the above-mentioned indices (GDD, Rn) and spring precipitation classes, applying supervised classification, provides three productivity zones: high, medium, and low. Subsequently, the Non-crop specific agroclimatic zoning is combined with the three classification zones. The result is a 7-class map in terms of sustainable crop production. The classes range from “Excellent” areas, as the most suitable zones for crop production with sufficient amount for rainfed irrigation, to “Not suitable” areas as inappropriate zones. More specifically, the zones classified as (a) “Excellent”, “Very Good”, “Good” are generally suitable for annual crops, (b) “Fair”, “Moderate”, “Poor” are generally suitable for tree crops, vineyards, or annual crops under restrictions and (c) “Not Suitable”, are unsuitable areas for agricultural use.

3. Study Area and Database

3.1. Study Area

The pilot area in Spain is the region “La Mancha Oriental”, which occupies about 7,140 Km^2 (fig.2). It is in the South-east of the Iberian Peninsula and is characterized by relatively flat surface averaging from 500 to 600 meters in altitude. It has semi-arid climate with annual precipitation below 350 mm and evapotranspiration above 1200 mm. In the region there is a strong agriculture sector with annual crops, such as Wheat, Barley, Alfalfa, Onion, Garlic, and Legumes and trees as Almont, Olive, Pistachio and Vineyard.

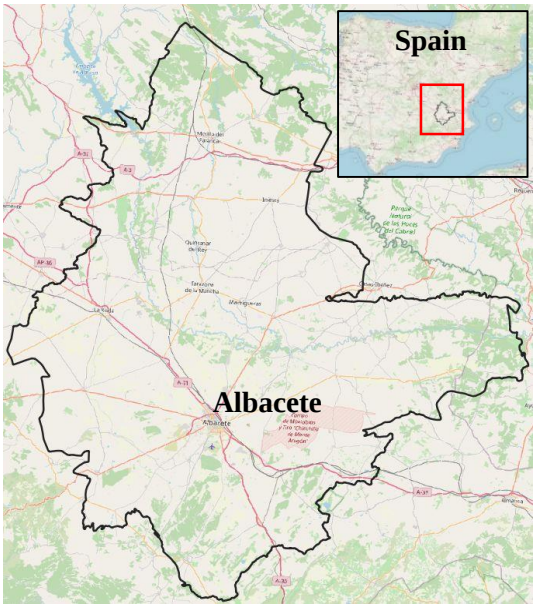

Figure 2 Study area “La Mancha Oriental” in Spain

3.2. Database and preprocessing

The research carried out is based mainly on raster dataset ingested in Earth’s Engine Data Catalog (GEE) and other web-based geospatial resources. Specifically, in the Google Earth Engine:

- Landsat-8 multispectral satellite data, with 30 meters spatial resolution. The available derived Landsat data is for the period of 2013 to 2020. For the Spanish study area, 640 images are processed.

- Two MODIS products are considered: (a) The 8-day Potential Evapotranspiration product (MOD16A2) with 500 meters spatial resolution and (b) Land Surface temperature product with 1 Km spatial resolution. For the study area, 1339 images in total are processed for the period of 20 years (2001-2020)
- Climate Hazards Group InfraRed Precipitation with Station data (CHIRPS). The pentad rainfall data has 5 km spatial resolution. For the study area, 1440 pentad data, over the period of 2001 to 2020, are processed.

The EO data is processed monthly extracting the median values over the last twenty years. Furthermore, advanced techniques, as machine learning algorithms, (Classification and Regression Trees-CART) for improving MODIS and CHIRPS products spatial resolution (200X200 m pixel size) are implemented.

Different sources of datasets are evaluated for the study area. In general, the following datasets are prepared:

- Digital Elevation Model (DEM). Elevation data is derived from the Shuttle Radar Topography Mission (SRTM), provided by NASA (National Aeronautics and Space Administration). The DEM has spatial resolution about 30 meters.
- Soil Map. The World Soil Information (International Soil Reference and Information Centre-ISRIC) is an independent foundation providing soil information globally (www.isric.org). Soil information provisioning is derived from ISRIC soil data hub. The spatial resolution of the soil map is 250 meters.
- Landuse/LandCover (LU/LC). For the Spanish study area, the lu/lc is derived from the Copernicus Land Monitoring Service. Specifically, the Corine Land Cover (CLC) product in 2018 is used. The spatial resolution of the CLC is 100 meters (European Union, 2018).

4. Results and Discussion

The three-stages of the proposed methodology for agroclimatic zoning in the Albacete study area are applied. Firstly, a thematic map, containing the Water limited Growing Environment Zones (WLGEZ) is estimated (fig.3). For the region "La Mancha Oriental" the first three hydroclimatic classes exist in different proportions: “No limitations”, “Partially limited-No limited environment”, “Partially Limited environment”. The Partially Limited zones dominate, unlike to No Limitations zones, which occupy a minimum area. In contrast, the category “Limited environment’ doesn’t exist. This indicates that most of the area has relatively good climatic conditions for the agricultural production, experiencing moderate droughts.

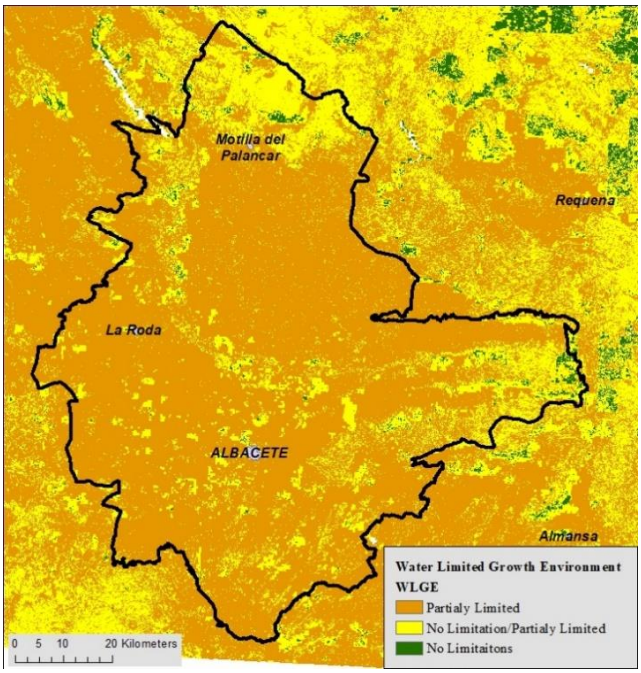

Figure 3 The three WLGE zones for the Spanish study area

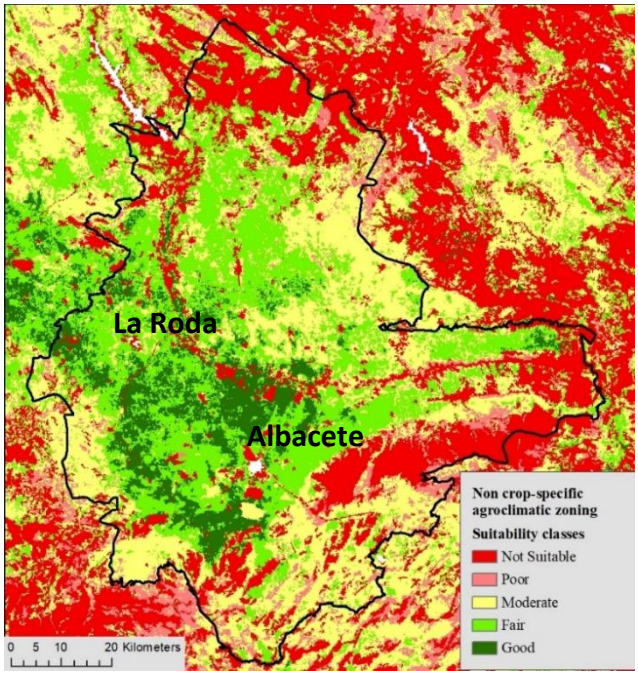

Figure 4 Non-crop specific agroclimatic zoning

Secondly, a thematic map, namely the non-crop specific agroclimatic zones, is produced. The study area is divided in five land suitability classes for agricultural purposes: Good, Fair, Moderate, Poor and Not Suitable (fig.4). The covered surface and the percentage of each zone is calculated. The first three non-crop specific agroclimatic classes represent most of the region “La Mancha Oriental”. Thus, about 74% of the total area can be used for sustainable agricultural production, but under certain conditions.
According to the complementary research from local authorities in the first two classes (good and fair), annual crops, such as Wheat, Barley, Alfalfa, Onion, Garlic, and Legumes, dominate. Moreover, in these classes there are trees, such as olives and pistachios. In the third class (moderate) and especially the northern regions of Albacete are dominated by vineyards.
Lastly, the crop-specific agroclimatic zoning is created (fig.5). The analysis of the GDD and Rn shows that they aren’t a limited factor for the annual crops. In contrast, the 20 days’ spring cumulative precipitation, provided by the last 10 days of April and the first 10 days of May, is a limited factor for annual winter-spring crops. Thus, the crop-specific agroclimatic zoning map for the region of Mancha Oriental in Spain is based on the amount of precipitation in spring. To differentiate the areas with enough rainfed irrigation a threshold of 10 mm of precipitation (for the range of 20 days) in the first two best suitable classes of Non-Specific Agroclimatic zoning, is applied. The result is a 7-classes map in terms of sustainable crop production.

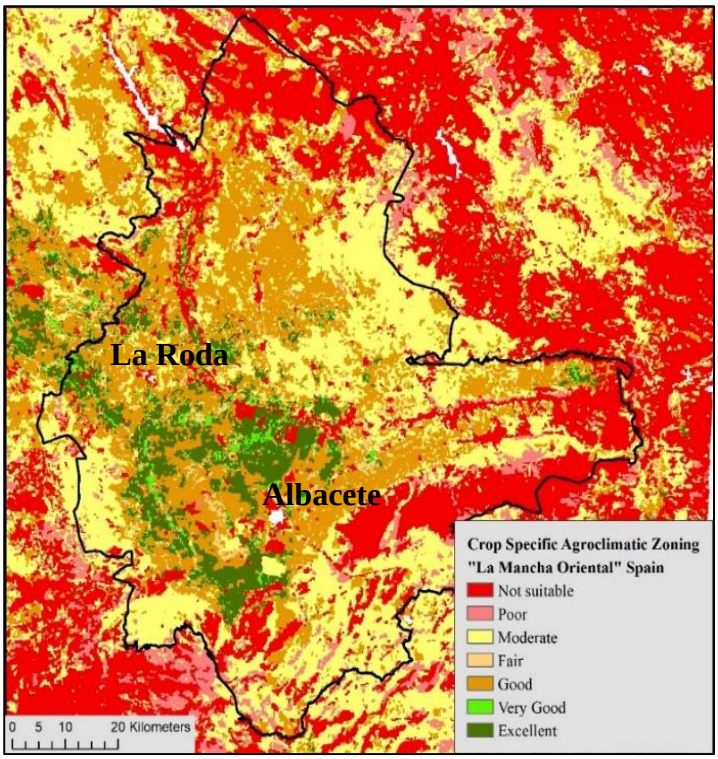

Figure 5 Crop specific agroclimatic zoning in Mancha Oriental in Spain

Specifically, “excellent”, “very good”, “good” and “fair” areas are identified as high yield areas for annual winter crops (Barley, Garlic, Oat and Wheat), with sufficient to average amounts for rainfed irrigation. These four zones cover 45% of the study area. In contrast, the “moderate” zones are suitable for tree crops, such as vineyards.

5. Summary and conclusions

The identification of sustainable production zones through agroclimatic classification in the region of "La Mancha Oriental" in Spain, is based on a three-step procedure. The proposed methodology combines the monitoring of climate conditions on vegetation averaged over a long period of time with local landforms (soil type, altitude) and specific features and characteristics (GDD, Rn, precipitation) of crops. The research results are promising. The first discussions with the local experts from the study area prove the validation of the sustainable production zones.

The advantages of the proposed methodology could be summarizing in three basic domains. Due to continuous spatial and temporal Earth Observation data the results are more precise and reliable in comparison to conventional data. By applying contemporary downscaling methods such as machine learning algorithms better resolution agroclimatic zones have been achieved. Lastly, Google Earth Engine cloud platform could be a great tool for rapidly monitoring changes in agriculture zones almost worldwide

The proposed methodology integrating the latest technological achievements in remote sensing contributes to better management of natural resources optimizing crop yield modeling especially in the Mediterranean basin. Moreover, the resulted fine-resolution sustainable agroclimatic zoning could help farmers within social and economic context to accommodate their production system ensuring their viability.

Acknowledgements

This research was funded by SUPROMED project under the PRIMA 2018 program of the European Commission.

References

Amber J. Fletcher, Margot Hurlbert, Sam Hage & David Sauchyn (2021). Agricultural Producers' Views of Climate Change in the Canadian Prairies: Implications for Adaptation and Environmental Practices, Society & Natural Resources, 34:3, 331-351, DOI: 10.1080/08941920.2020.1823541.

Adnan, S., Ullah, K., Gao, S., Khosa, A.H. and Wang, Z. (2017). Shifting of agro-climatic zones, their drought vulnerability, and precipitation and temperature trends in Pakistan. Int. J. Climatol, 37: 529-543. https://doi.org/10.1002/joc.5019

Araya A., Keesstra S.D., Stroosnijder L., (2010). A new agro-climatic classification for crop suitability zoning in northern semi-arid Ethiopia. Agricultural and Forest Meteorology, Vol. 150, Issues 7–8, pp.1057-1064, ISSN 0168-1923, https://doi.org/10.1016/j.agrformet.2010.04.003.

Dalezios Nicolas, Mitrakopoulos Kostas and Manos Basil, (2018). Multi-scaling Agroclimatic Classification for Decision Support Towards Sustainable Production. by J. Berbel et al., (eds.), Multicriteria Analysis in Agriculture, Multiple Criteria Decision Making, https://doi.org/10.1007/978-3-319-76929-5_1. Springer International Publishing AG, part of Springer Nature 2018,

European Union (2018). Copernicus Land Monitoring Service. European Environment Agency (EEA).

Falasca S. L., Fresno M.D. and Waldman C., (2014). Developing an agro-climatic zoning model to determine potential growing areas for Camelina sativa in Argentina. QScience Connect, Vol.2014, Issue 1, Mar 2014, doi: https://doi.org/10.5339/connect.2014.4.

Fischer G., Nachtergaele F.O., van Velthuizen H.T., Chiozza F., Franceschini G., Henry M., Muchoney D. and Tramberend S. (2021). Global Agro-Ecological Zones v4 – Model documentation. Rome, FAO. https://doi.org/10.4060/cb4744en.

Gorelick, N., Hancher, M., Dixon, M., Ilyushchenko, S., Thau, D., & Moore, R. (2017). Google Earth Engine: Planetary-scale geospatial analysis for everyone. Remote Sensing of Environment.

Niemeyer, S. (2008). New drought indices. Options Méditerranéennes. Série A: Séminaires Méditerranéens, 80: 267–274.

Patel N. R., Umesh K. Mandal, Pande L. M., (2000). Agro-ecological Zoning System - A Remote Sensing and GIS Perspective. Journal of agrometeorology. 2(1), 1-15.

Thenkabail P.S., Gamage M.S.D.N., and Smakhtin V. U., (2004). The Use of Remote Sensing Data for Drought Assessment and Monitoring in Southwest Asia. Research Report, International Water Management Institute, No. 85, 1-25.

Tsiros E., C. Domenikiotis, N.R. Dalezios, (2009). Sustainable production zoning for agroclimatic classification using GIS and remote sensing. IDŐJÁRÁS, 113, No1–2, 55–68.

Wall Ellen & Smit Barry, (2005). Climate Change Adaptation in Light of Sustainable Agriculture. Journal of Sustainable Agriculture, 27:1, 113-123, doi: 10.1300/J064v27n01_07.

Wu Bingfang, Ma Zonghan, Yan Nana, (2020). Agricultural drought mitigating indices derived from the changes in drought characteristics. Remote Sensing of Environment, Vol.244, 111813, ISSN 0034-4257, https://doi.org/10.1016/j.rse.2020.111813.

Zuhro Asma, Tambunan Mangapul & Marko Kuswantoro. (2020). Application of vegetation health index (VHI) to identify distribution of agricultural drought in Indramayu Regency, West Java Province. IOP Conference Series: Earth and Environmental Science. 500, 012047. 10.1088/1755-1315/500/1/012047.

Sustainable production of barley in a water-scarce Mediterranean agroecosystem

J.J. Pardo[1], J.A. Martínez-López[1], R. López-Urrea[2], A. Martínez-Romero[1], J. Montero[1], J.M. Tarjuelo[1] and A. Domíngez[1]

[1] Centro Regional de Estudios del Agua (CREA), University of Castilla – La Mancha, Albacete, Spain
[2] Instituto Técnico Agronómico Provincial de Albacete (ITAP), Albacete, Spain

Abstract. In arid and semi-arid areas, the scarcity of water resources is one of the main constraints on agricultural activity. This situation appears to be worsening due to global warming, which can affect the profitability of crops in Mediterranean agroecosystems (i.e., Castilla -La Mancha, Spain). To tackle these challenges, the SUPROMED project (Sustainable production in water-limited environments of Mediterranean agroecosystems) combines, in an online platform (https://dss.supromed.eu/portal/), a set of models and methodologies for more efficient management of water, energy and fertilizers. A two-year trial (2020-2021) was conducted to demonstrate the effectiveness of SUPROMED as a farm management support tool. The impact of transferring the MOPECO irrigation scheduling model (IS-MOPECO), integrated in the SUPROMED platform, to farmers and technicians, was determined by analyzing a set of productive, economic and environmental key performance indicators (KPIs) for a barley crop. In the first year, the management proposed by SUPROMED technicians achieved the same yield as traditional management with 32% less water, resulting in a 13% and 66% improvement in Gross Margin and Gross Economic Irrigation Water Productivity, respectively. During the second year, the management implemented by the farmer using the SUPROMED platform showed improvements in all KPIs analyzed. The results obtained are promising, indicating that the tools and models proposed in SUPROMED can be easily used by farmers, and can improve the economic and environmental sustainability of Mediterranean agroecosystems. Furthermore, the results have been presented at meetings with farmers and technicians to promote the use of the platform.

1 Introduction

The Mediterranean area is one of the richest regions in ecosystems and one of the most vulnerable zones due to water scarcity caused by frequent drought periods and irregular distribution of rainfall during the year (García-Ruiz, et al., 2011). Thus, the lack of water resources is one of the main handicaps for agriculture in this area (Correia et al., 2009). Moreover, the lack of tools and/or irrigation advisory services for determining the irrigation requirements of crops at farm level, the lack of knowledge of the irrigation system (López-Mata et al., 2010; Nascimento et al., 2019), the low price of harvests in the international market, and climate change have all led to an excessive use of resources, such as groundwater and energy to compensate for these shortages. This, in turn, has decreased the profitability of farms located in Mediterranean areas (Daccache et al., 2014; Knox et al., 2012)

Tackling the challenges of this situation requires a combination of methodologies and technologies that include a more efficient use of natural resources, improving the design and management of the means of production, transferring knowledge to producers, and advising farmers and technicians on the most appropriate strategies to deal with extreme situations (Tarjuelo et al., 2015).

Many crop simulation models and tools (Pereira et al., 2003; Stockle et al., 2003) have been developed in order to act as decision support to be used by managers, but often require a large number of input variables and parameters that are not easily available to end users. In this sense, the SUPROMED project (Sustainable production in water-limited environments of Mediterranean agroecosystems) was designed to support sustainable production of Mediterranean agroecosystems by combining a set of methodologies, tools and models, such as MOPECO (Model for the ECOnomic OPtimization of irrigation water use at farm level, Ortega et al., 2004), in order to properly manage inputs (mainly water, energy and fertilizers). These tools were simplified and adapted for farmers through an online end-user platform that aims to provide effective advice for more sustainable and profitable crop management.

The main objective of this work was to demonstrate the impact of applying the models and methodologies in SUPROMED (https://dss.supromed.eu/portal/) on the sustainability and profitability of a barley crop in comparison with the traditional management of this crop in Castilla-La Mancha (CLM, Spain). The secondary objectives were as follows: 1) To determine a set of productive, economic, and environmental Key Performance Indicators (KPIs); 2) To monitor 4 farms dedicated to the cultivation of barley and manage a subplot within one of the monitored farms using the SUPROMED platform; 3) To train one of the farmers in the use of the methodologies in SUPROMED and monitor, during the second year, their management of the crop; 4) To compare the monitoring results using the KPIs.

2 Materials and Methods

2.1 Site description

The study was carried out during the 2020 and 2021 growing seasons in various barley plots located in the Hydrogeological Unit of Eastern Mancha (HUEM) (CLM, Spain). This agroecological system is characterized by a Mediterranean climate (Papadakis, 1966). Long-term mean annual precipitation in the area is 360 mm (mostly concentrated in the autumn and spring months) and mean cumulative annual reference evapotranspiration (ETo) is around 1300 mm. Soils are defined by a petrocalcic horizon at a depth of 0.5 to 0.7 m, while the first horizons have a clay loam texture with low to medium levels of soil organic matter.

2.2 Barley plots

In 2020, five plots of barley (Hordeum vulgare L., cv. Planet) belonging to four different farmers were monitored. One of the farmers was selected as a "Leader" farmer (LEA), being one of the best-trained and highest-producing farmers in the area. Consequently, in order to compare traditional management and that proposed by SUPROMED (SUP), two plots on his farm, with similar characteristics, were monitored: one managed by LEA and the other by SUP. The other three selected farmers, who we called "Average", were producers with a training level and a way of managing their farms that is representative of the area (AVE 1, AVE 2, AVE 3). In 2021, only one barley plot managed by the Leader farmer using SUPROMED platform (LEA_{SUP}) was monitored to quantify the improvement capacity of individual farmers when using the proposed methodologies. A pressure transducer (Pessl Instruments Pipe Pressure, Weiz, Austria), and a soil moisture probe with 6 sensors at 10 cm spacing (Drill&Drop, Sentek, Australia) were installed in the area, delimited by a set of four sprinklers representing the average conditions of each monitored plot.

2.3 Irrigation scheduling

LEA and AVE farmers performed irrigation scheduling based on their own knowledge, while SUP and LEA_{SUP} used the "MOPECO irrigation scheduling" tool (https://crea.uclm.es/siar/siarpr/). This tool is a simplification for farmers and technicians of the MOPECO model, which determines the irrigation scheduling of a crop by using the simplified daily soil water balance proposed by FAO – 56 (Allen et al., 1998; Pereira et al., 2020). The irrigation scheduling tool requires only a few parameters, such as soil data (texture, depth, stone content), climatic data (daily temperature, ETo, rainfall), crop parameters (crop coefficient (Kc), duration of crop growth stages in cumulative growing degree days (GDD), lower (TL) and upper (TU) developmental threshold temperatures) and irrigation system data (efficiency, precipitation rate).
To generate irrigation schedules, MOPECO updates the daily water balance considering the actual amount of water received by the crop (irrigation or rainfall) and the actual weather data. In addition, MOPECO uses the seven-day forecast climatic data provided by the Spanish National Institute of Meteorology for the area and the actual phenological stage of the crop to calculate the irrigation water requirements for the next week.
The meteorological variables were measured by an automated weather station IMETOS 3.3 (Pessl Instruments, Weiz, Austria), positioned on the LEA farm, at no more than 1 km distance from the rest of monitored plots.

2.4 Key Performance Indicators

To evaluate the differences between traditional and SUPROMED management, various Key Performance Indicators (KPIs) were calculated (Fernández et al., 2020) (Table 1).

Table 1. Key Performance Indicators.

Indicator	Units	Definition and details
$GM = Ya\ PV - Cv - Ig\ \mathrm{Cw} + \mathrm{Subs}$	€ ha $^{-1}$	**GM: Gross Margin**; Ya: Yield (kg ha^{-1}); Pv: Sale price (€ kg $^{-1}$); Cv: Variable costs (€ ha^{-1}) (provided by the farmers); I_g: Gross Irrigation Water applied (m^3 ha^{-1}); Cw: Water cost (€ m^{-3}); Sub: Subsidies (€ ha^{-1}) (150 € ha^{-1}) (provided by the farmers)
$WP_I = \frac{Y_a}{I_g}$	kg m^{-3}	**WP_I: Irrigation Water Productivity**: ratio between Y_a: grain yield (12% moisture) (kg ha^{-1}) and I_g: gross irrigation (m^3 ha^{-1}).
$\mathrm{NEWP} = \frac{GM}{(I_N + Re)}$	€ m^{-3}	**Net Economic Water Productivity**: ratio between GM: Gross Margin (€ ha^{-1}) and I_N: Net Irrigation (m^3 ha^{-1}) plus Re: Effective Rainfall (m^3 ha^{-1})
$GEWP_I = \frac{GM}{I_g}$	€ m^{-3}	**Gross Economic Irrigation Water Productivity**: ratio between GM: Gross Margin (€ ha^{-1}) and I_g; gross irrigation (m^3 ha^{-1}).

3 Results and discussion

A summary of the results of the five monitored barley plots in 2020 (two subplots of the leader farm (LEA and SUP) and the three average farmers (AVE)) and 2021 (leader plot using SUPROMED platform (LEA_{SUP})) is showed in Table 2. It should be noted that these results can only be directly compared in the case of SUP and LEA, as both were obtained in the same farm under similar soil and cropping conditions.

Table 2. Summary of the monitored plots in 2020 and 2021.

Year	2020					2021
Crop management	**SUP**	**LEA**	**AVE 1**	**AVE 2**	**AVE 3**	**LEA_{SUP}**
Sowing date	18/12/19	18/12/19	4/12/19	15/01/20	30/01/20	23/12/20
Harvest date	19/06/20	19/06/20	10/06/20	19/06/20	29/06/20	16/06/21
Re (mm)	234	234	237	231	195	192
I_g (m^3 ha^{-1})	1996	2921	2227	1869	2641	2870
Pr (mm)	90.5	144.6	104.3	96.2	124.6	79.0
PI (mm)	0	19.4	0	0	9.3	19.3
Yield (kg ha^{-1})	9467	9295	8776	9564	7350	9828
GM (€ ha^{-1})	589	523	713	895	291	1424
WP_I (kg m^{-3})	4.74	3.18	3.94	5.12	3.05	3.42
NEWP (€ m^{-3})	0.15	0.11	0.17	0.23	0.08	0.34
$GEWP_I$ (€ m^{-3})	0.30	0.18	0.32	0.48	0.12	0.50

ET_a: Actual crop evapotranspiration; ET_m: Potential crop evapotranspiration; Re: Effective rainfall; Ig: Gross irrigation; Pr: Rain percolation; PI: Percolation due to Irrigation events; GM: Gross Margin; NEWP: Net Economic Water productivity; $GEWP_I$: Gross Economic Irrigation Water Productivity; NEWP: Net Economic Water Productivity.

During 2020, the irrigation water applied varied significantly, depending on who was managing the plot, ranging from 292 mm for LEA to 187 mm for AVE 2. Despite these considerable differences, all the management regimes showed significant percolation during the growing season (Table 2), mainly due to the rainfall events that had occurred by late March (Figure 1). Percolation was higher for LEA because irrigation was managed by the farmer with the aim of maintaining soil moisture close to field capacity, as there are significant restrictions on water availability in some years. This excessive percolation was solved in 2021 when LEA used the "MOPECO irrigation scheduling" tool (LEA_{SUP}) (Figure 2).

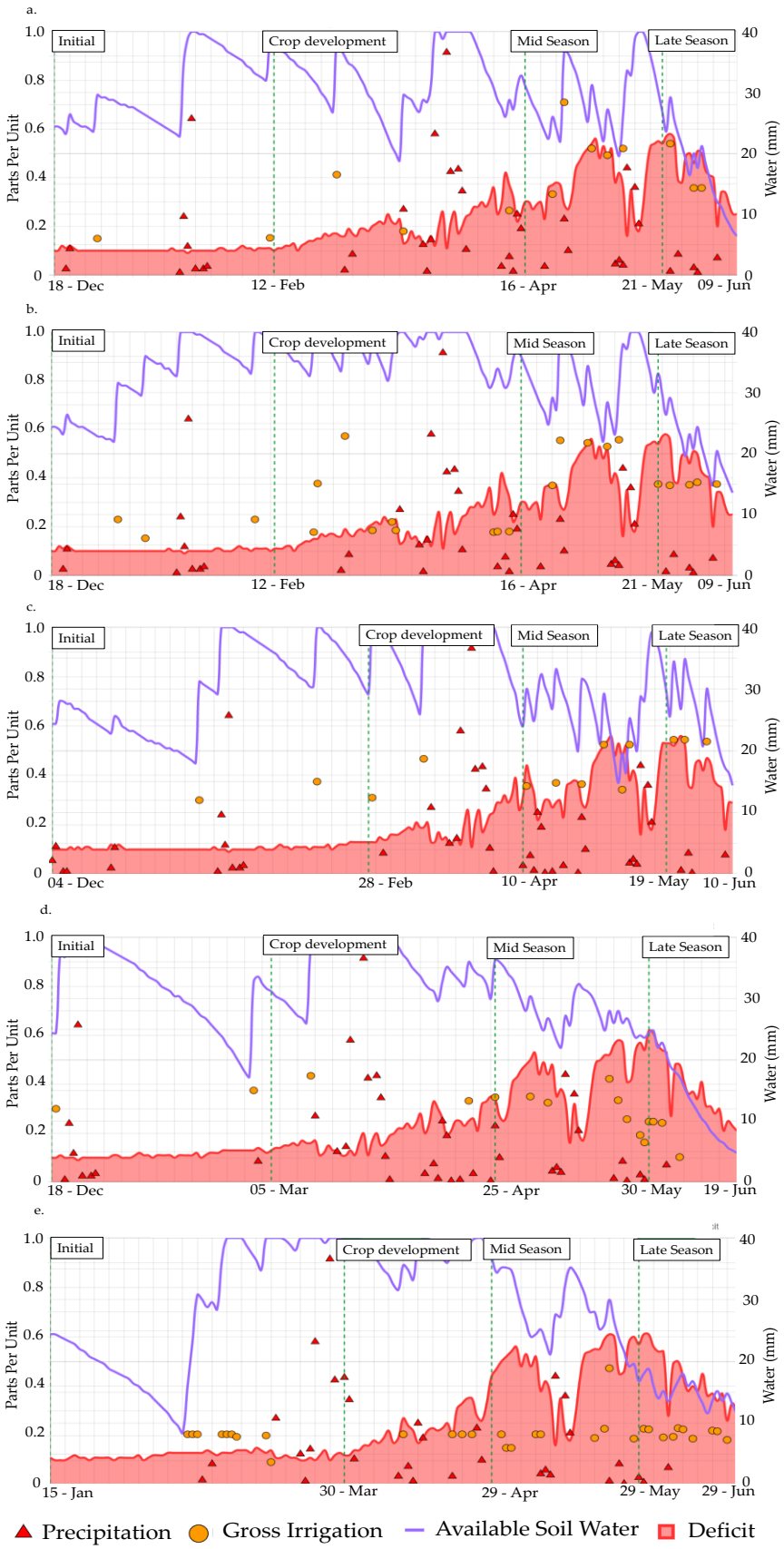

Figure 1. Evolution of available water simulated by the "MOPECO irrigation scheduling" tool in 2020 (a: SUP, SUP: SUPROMED management; b) LEA: LEADER management; c), d) and e): AVE: Average management). Main Y axis: Deficit: 1-p, where p is the fraction of TAW (Total Available Water) that a crop can extract without suffering water stress; Available water. Secondary Y axis: Gross irrigation; Precipitation.

Although, in comparison with LEA, AVE 2 and SUP resulted in water savings in 2020 of 36% and 32%, respectively, there were no significant differences in crop yield between SUP, LEA and AVE 2, resulting in an increase in the WP_I and $GEWP_I$ (Table 2) for SUP and AVE 2 crop management. The possible factors leading AVE 2 to reach a similar crop yield to that of SUP, with 6% less irrigation water applied, include a somewhat deeper soil, the previous crop (maize for AVE 2 and garlic for SUP) and higher nitrogen application. The lowest yield was achieved by AVE 3, although around 32% more irrigation water than SUP was applied. This can be explained by this farm having a very old irrigation system with several breakdowns in the early stages of the crop, waterlogging the plot affecting the final yield (Figure 1e). In addition, the crop in AVE 3 suffered a slight water stress during the grain filling according to the MOPECO estimation, which also affected the final yield. Even though the income reached by AVE 2 was similar to SUP and LEA, AVE 2 had lower total costs due to not having to apply pest and disease treatments (one of the highest production costs), thus achieving better KPIs. Additionally, AVE 1 obtained better GM than SUP and LEA, mainly due to AVE 1 also not applying pest and disease treatments (Table 2).

In 2021, LEA_{SUP}, improved all the indicators compared to LEA. This was due to a 40% increase in the sale price of barley grain, a reduction in the application of pest and disease treatments, better management of the irrigation system and a reduction in the use of fertilizers. Thus, the farmer achieved higher profitability (172%) and a higher yield (6%), applied less irrigation water (2%), and decreased the percolation (45%) (Table 2).

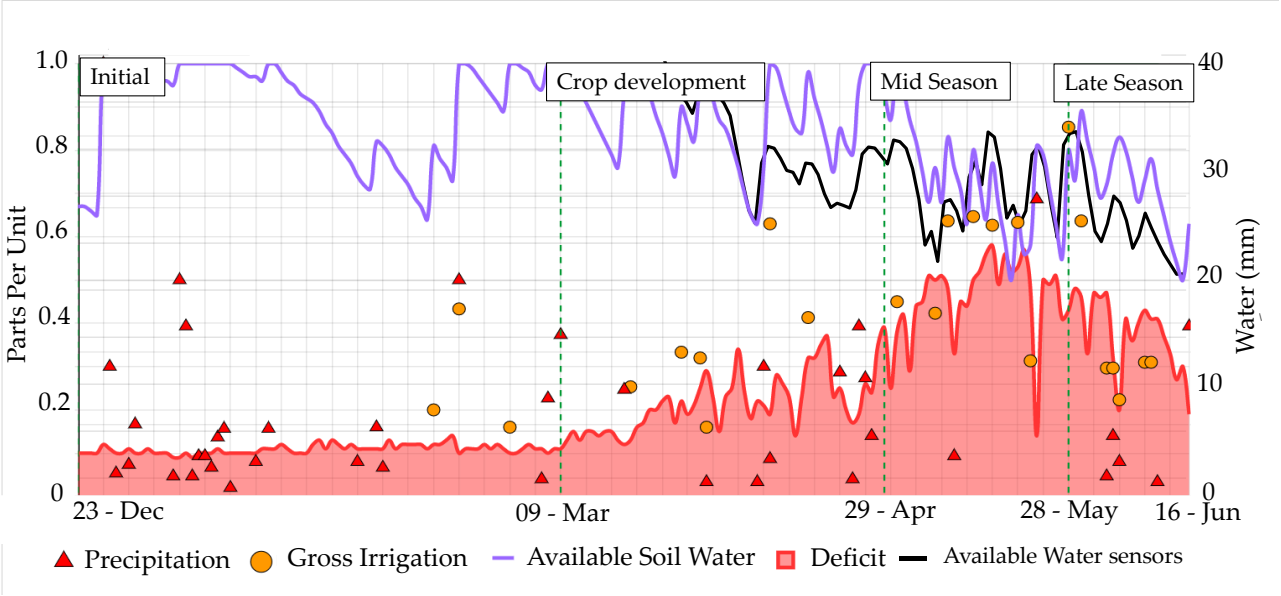

Figure 2. Evolution of AW (Available soil water; main Y axis) simulated by "MOPECO irrigation scheduling" tool for LEA_{SUP} (LEADER using SUPROMED tool) in 2021 and comparison with measured (Drill & Drop, Senteck) available soil moisture progression in LEA_{SUP} (2021) (Available water sensors; Main Y axis). Where Deficit (main Y axis): 1-p, where p is the fraction of TAW (Total Available Water) that a crop can extract without suffering water stress. Secondary Y axis: Gross irrigation; Precipitation.

4 Conclusions

Despite the great professionalism of farmers, the lack of tools and methodologies adapted to their training and necessities negatively affects the profitability and sustainability of farms. Thus, the management of a barley crop based on the tools and methodologies adapted to farmers included in the SUPROMED platform improved most of the productive, economic and environmental indicators calculated during the first-year monitoring of 4 traditional farms. This result was corroborated in the second year of the experiment, when a farmer (LEA_{SUP}) trained in the use of these methodologies improved all the key performance indicators with respect to the values obtained in Year 1 on his farm (LEA).

The results highlight the advantage of using the models and tools included in the SUPROMED platform, helping farmers implement optimized irrigation scheduling to maximize the agronomic (yield) and economic (Gross Economic Irrigation Water Productivity) productivity of rainwater and irrigation, leading to more sustainable and profitable crop management. In this way, SUPROMED contributes to improving the economic and environmental sustainability of Mediterranean agroecosystems through a more efficient management of water, energy and fertilizers.

Moreover, the tool provides farmers with information about excessive or insufficient irrigation doses, which may cause water percolation or stress in the crop due to water deficit. To determine the irrigation scheduling, the “MOPECO irrigation scheduling” tool requires calibration for the crops in the area and access to the data registered by a local agrometeorological weather station.

Acknowledgements

This research was carried out under the framework of European project SUPROMED “GA-1813” funded by PRIMA, and the Regional project PRODAGUA “Ref SBPLY/19/180501/000144”, funded by FEDER and the Regional Government of Castilla-La Mancha. The authors thank the farmers participating in this research for their support in implementing the tasks and actions carried out over the two monitoring years.

References

Allen et al., 1998; Allen, R.G., Pereira, L.S., Raes, D., Smith, M., 1998. Crop evapotranspiration: guidelines for computing crop water requirements. In: Irrigation and Drainage Paper No. 56. FAO, Italy.

Correia, F.N., Iwra, M., Técnico I.S., 2009. Water resources in the Mediterranean region. Int. Water Resour. Assoc. 24, 22–30.

Daccache, A., Ciurana, J.S., Rodríguez Díaz, J.A., Knox, J.W., 2014. Water and energy footprint of irrigated agriculture in the Mediterranean region. Environmental Research Letters 9, 124014.

Fernández J.E., Alcón. F., Díaz-Espejo A., Hernández Santana V., Cuevas M.V., 2020. Water use indicators and economic analysis for on-farm irrigation decision: A case of study of a super high density olive tree orchard. Agricultural Water Management 237, 106074.

García-Ruiz, J.M., López-Moreno, I.I., Vicente-Serrano, S.M., Lasanta-Martínez, T., Beguería, S., 2011. Mediterranean water resources in a global change scenario. Earth-Science Rev. 105, 121–139.

Knox, J., Hess, T., Daccache, A., Wheeler, T., 2012. Climate change impacts on crop productivity in Africa and South Asia. Environmental Research Letters 7, 034032.

López-Mata, E., Tarjuelo, J.M., de Juan, J.A., Ballesteros, R., Domínguez, A., 2010. Effect of irrigation uniformity on the profitability of crops. Agricultural Water Management 98, 190–198.

Nascimento, A.K., Schwartz, R.C., Lima, F.A., López-Mata, E., Domínguez, A., Izquiel, A., Tarjuelo, J.M., Martínez-Romero, A., 2019. Effects of irrigation uniformity on yield response and production economics of maize in a semiarid zone. Agricultural Water Management 211, 178–189.

Ortega Álvarez, J.F., de Juan Valero, J.A., Tarjuelo Martín-Benito, J.M., López Mata, E., 2004. MOPECO: An economic optimization model for irrigation water management. Irrigation Science 23, 61–75.

Papadakis, J. 1966. Climates of the World and their Agricultural Potentialities. Hemisferio Sur. Buenos Aires, Argentina.

Pereira, L.S., Teodoro, P.R., Rodrigues, P.N., Teixeira, J.L., 2003. Irrigation Scheduling Simulation: The Model Isareg. In: Rossi, G., Cancelliere, A., Pereira, L.S., Oweis, T., Shatanawi, M., Zairi, A. (eds) Tools for Drought Mitigation in Mediterranean Regions. Water Science and Technology Library, vol 44. Springer, Dordrecht.

Pereira L.S., Paredes P., Jovanovic N., 2020. Soil water balance models for determining crop water and irrigation requirements and irrigation scheduling focusing on the FAO56 method and the dual Kc approach. Agricultural Water Management 241, 106357.

Sevacherian, V., Stern, V.M., Mueller, A.J., 1977. Heat accumulation for timing Lygus control pressures in a safflower-cotton complex. Joumal of Economic Entomology 70, 399-402.

Stockle, C., Donatelli, M., Nelson, R., 2003. CropSyst, a cropping systems simulation model. European Journal of Agronomy 18, 289–307.

Tarjuelo, J.M., Rodriguez-Diaz, J.A., Abadía, R., Camacho, E., Rocamora, C., Moreno, M.A., 2015. Efficient water and energy use in irrigation modernization: Lessons from Spanish case studies. Agricultural Water Management 162, 67-77.

Calibration and validation of MOPECO as sustainable water management tool within South Bekaa Irrigation Scheme in Lebanon

F. Karam[1], N. Nassif[1], A.H. Mouneimne[1], C. El Hachem[1], L. Moussawi[1]

Department of Environmental Engineering, Faculty of Agricultural and Veterinary Sciences, Lebanese University. Main Road to Mkalles Roundabout, Dekwaneh, Meten, Lebanon

Corresponding author: Fadi Karam (fadkaram@gmail.com)

Abstract. A study was conducted during the 2020-2021 growing years in South Bekaa Irrigation Scheme (SBIS) in Lebanon, on two annual crops (Potato and Onion), using MOPECO (Economic Optimization Model for Irrigation Water Management). The model was calibrated during the 2020 growing year using daily climatic data from Domain Tanayel weather station and soil data from SBIS, and validated during the 2021 growing year in pre-selected plots. A sensitivity test of the model input parameters was conducted using the method of *trial and error*.

Typical Meteorological Year (TMY) was calculated for the study area using daily weather data from 1994 through 2018. Daily weather data included air temperature (T_{max}) and T_{min}), rain and global radiation. Potential evapotranspiration (ET_p) was calculated at daily basis using Hargreaves equation. Moreover, Growing-Degree Day (GDD) was calculated for each crop for the TMY and during the 2020 and 2021 growing years, using real observations on crop phenology. Crop coefficients (K_c) of potatoes were derived from local experiments conducted at Tal Amara Research Station in the Bekaa Valley during 1998-2008, while K_c values of onion were obtained from literature in likely-environmental conditions.

The sensitivity test showed that among all MOPECO inputs parameters, depletion level (*p*), available water (AW), initial soil available water and irrigation interval are the most sensitive. The results of the calibration in 2020 demonstrated that time course evolution of soil water content (SWC) was within the refill (field capacity) and lower (permanent wilting point) limits. Net irrigation requirements were found to be 526 mm for potato and 731 mm for onion. The results of the validation in 2021 showed that the soil water balance approach of MOPECO yielded good results. Gross irrigation requirements during the whole growing season were 540 mm for potato and 728 mm for onion. We concluded that MOPECO is an important tool of water resources management and planning in agriculture, and may save considerable amounts of water that can be used to bring additional land into irrigation.

1 Introduction

The efficient use of water and energy in agriculture is gaining importance due to a general decreasing tendency of water availability for agricultural uses and increasing energy costs. These aspects condition the viability of irrigation activities in many areas of the world (Ortega et al., 2004). Numerous crop simulation models have been developed to improve irrigation management in farms, such as CROPSYST, WOFOST, and APSIM (Ortega et al., 2004; Saseendran et al., 2008; Domínguez et al., 2012) and AquaCrop (Abi Saab, 2014). All these models can simulate the crop yield from a specific irrigation schedule, with varying degrees of precision given the climate conditions. However, they have a certain use limitation due to the high number of soil, crop, and weather parameters.

MOPECO (Economic optimization Model for Irrigation Water Management) is a simulation model that was developed by a group of researchers at the University of Castilla-La-Mancha in Spain, with the aim to offer support in the decision-making process for the management of the agricultural systems at farm level, aiming at both human and livestock feeding (Domínguez et al., 2012). The model uses a typical meteorological year (TMY) as a reference to supply water between at the different growth stages of the crop, and to optimize production, taking into account the effect on the quality of the product obtained. The model is a tool for identifying optimal production plans and water irrigation management strategies (Alvarez et al., 2004). It uses Stewart et al (1997)'s suggested model to estimate crop yields in the various growth phases as a function of the ET_a/ET_m ratio. When $ET_a < ET_m$ that means that the plant suffers from any stress that may cause in yield (actual yield (Y_a) < potential yield (Y_m)).

Being a user-friendly computer model easily accessible by researchers and irrigation managers (López-Mata et al., 2019), MOPECO helps to achieve a sustainable production system at the level of agricultural exploitation, using a risk calculation module associated with a crop plan at the farm level, according to the availability of water and the variability of agricultural products prices and climatic data, therefore it can be adapted to climatic scenarios that involve less water availability, higher energy costs and variability in agricultural prices in a globalized market (López-Urrea et al., 2009). The model has been used worldwide to support the decision on the best-adapted annual crop rotation that maximizes the gross margin of the farm, considering (i) available water, (ii) available surface, (iii) the behavior of crops under different climatic scenarios and (iv) price variability of crops. In Lebanon, the project has been used to simulate deficit irrigation under water stress and salinity conditions (Domínguez et al., 2011).

The objectives of the present study were to (i) provide a water management tool to farmers in face of the water shortage, and (ii) support an end-user IT platform to increase the production and income of farms through an efficient use of water, and other inputs, like energy and fertilizers, while decreasing the impact on the environment.

2 Material and methods

2.1 Plot selection

Plots were selected during the 2020 growing year within South Bekaa Irrigation Scheme (SBIS), the one irrigated area extends over 21,500 ha. For economic constraints, only a pilot area of 2000 ha is for the time being equipped with a pressurized irrigation network, while the rest of the scheme is still relying on ground wells for irrigation purposes. The pilot area is being supplied with water through Canal 900 conveyor. Plots grown with potato and onion have been selected during the 2020 and 2021 growing years within a polygon of 100 km^2 in area (5 km wide x 20 km long), which was identified for the scope of SUPROMED project. South Bekaa has a Mediterranean semi-arid climate, hot and dry from May to September, and cold and wet extending for the remainder of the year.

2.2 Model description

MOPECO (Economic Optimization Model for Irrigation Water Management) comprises three computing modules:

- Module I: Estimation of water requirements

This module is to determine the required number and timing of different irrigations throughout the crop cycle for maximum yield (ET_m). Reference crop evapotranspiration (ET_o) is determined as the average of the Penman-FAO and Penman Monteith methods applied daily (Figure 1).

Module II: Effect of irrigation uniformity on crop yield. Determination of cost and gross margin functions.

MOPECO uses a normal statistical distribution function representing water applied by the irrigation system (Figure 1). This function simulates, for different irrigation application uniformities (known as Christiansen's Uniformity, CU), irrigation quality parameters, which allows to estimate crop yield when integrated in a production function. Tested yields are used to estimate gross revenue, as yield multiplied by unit crop price. A cost function is developed to quantify the global production costs for different crops. The model starts with the production function of Stewart et al. (1977), which estimates the crop yield based on the relation of evapotranspiration (ET_a/ET_m) (Eqn. 1)

$$\frac{Y}{Ym} = \prod_{i=1}^{n} (1 - \mathrm{K}yi \,.\, (1 - \frac{\mathrm{ETa}}{\mathrm{ETm}})i) \qquad (1)$$

Where Y is real harvested yield (kg ha^{-1}); Y_m maximum yield achieved when water availability is not limiting (kg ha^{-1}); K_y proportionality factor (crop sensitivity to water stress); ET_a actual crop evapotranspiration (mm); ET_m crop evapotranspiration for maximum yield (mm) and *i* the crop developmental stages.

The deficit coefficient in the root zone based on the quantity of water in the irrigated field (Cd) (Hart and Reynolds 1965) is integrated by means of its effects on ET_a into the production function as per the following (Ortega, 2004):

$$\frac{Y}{Ym} = \prod_{i=1}^{n} (1 - \mathrm{K}yi\ .\ (\frac{\mathrm{Y}}{\mathrm{Ym}} = \prod_{i=1}^{n} (1 - (Kyi\ .(\mathrm{C}dmi\ .(1-p)i)))) \qquad (2)$$

Where C*dmi* is mean deficit coefficient for each growth and development stage (i), and (1-p)*i* is ET fraction for each of the growth and development stages of a crop whose needs are met through the irrigation water applied.

Module III: Annual crop rotation optimization using genetic algorithms

After establishing for each crop the relationships between gross margin and gross irrigation depth, the objective then is to identify crop planning that optimizes irrigation water use (Ortega, 2004). The optimization criteria are based on two key variables; (i) expected farm profit and (ii) economic risk associated with annual climatic variability.

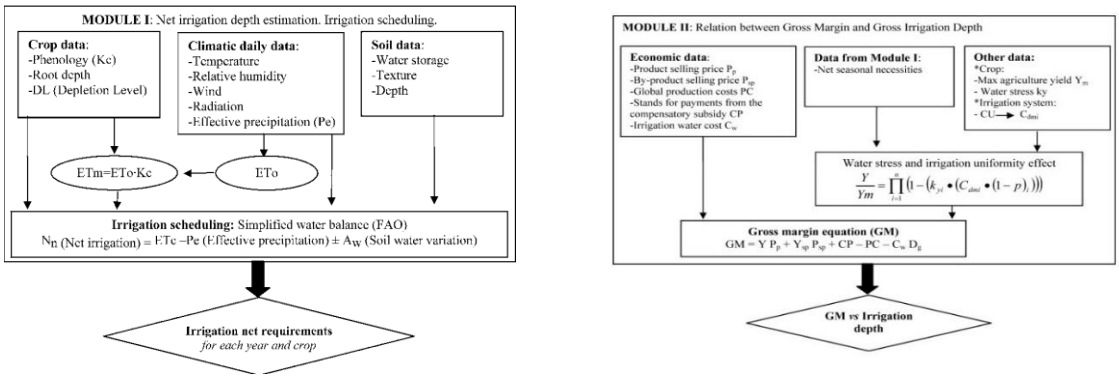

Figure 1. Flowchart of Module I (left) and Module II (right) of MOPECO (Dominiguez et al., 2014)

Glossary: K_c crop coefficient; DL depletion level for the crop at which actual ET_a begins to decline from the potential rate (decimal); P_e effective precipitation (mm), ET_m crop evapotranspiration for maximum yield (mm); ET_o reference evapotranspiration (mm); N_n net irrigation water requirement (mm); A_w variation in soil water storage (mm). Gross margin *versus* gross irrigation depth. Pp selling price of the product (Kg $^{-1}$); Psp selling price of the by-product (Kg $^{-1}$); PC global production costs for actual yield (ha $^{-1}$); CP payments from the compensatory subsidy for some cops (ha $^{-1}$), in Europe by the common agricultural policy (CAP); C_w cost of irrigation water application (m^{-3}); Y_m agronomic maximum yield that can be achieved in a given area when crop development is not limited by water availability or other factors (Kg ha $^{-1}$).

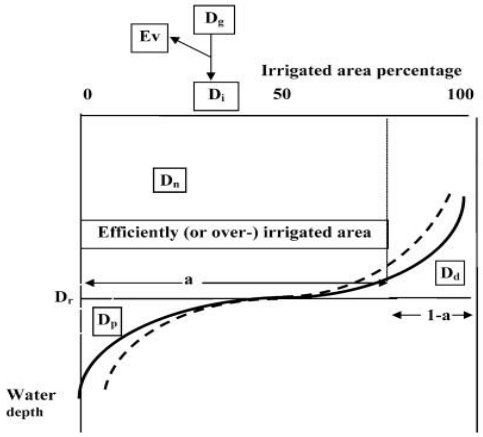

Figure 2. Flowchart of the normal function of irrigation water distribution in MOPECO (Dominiguez et al., 2014)

Glossary: The dashed curve corresponds to CU value lower than the distribution curve (continuous line). D_g gross irrigation depth (mm); E_v losses during the irrigation process (evaporation and drift) (mm); D_i depth applied to the soil and infiltrated (mm); D_n net depth stored in the root zone (mm); D_d deficit depth in the under-irrigated zone (mm); D_p percolated depth in the over-irrigated zone (mm); D_r required depth by the crop (mm); a percentage of adequately or over irrigated area.

2.3 Sensitivity test

A sensitivity test of MOPECO input parameters was conducted using *trial and error* method, to help identifying among all MOPECO inputs parameters, those retained sensitive, *i.e*. their variation induced a variation in the outputs of the model with respect to net irrigation requirements, gross irrigation requirements and soil water content.

2.4 Model calibration

The model was calibrated in 2020 growing year, using daily climatic data from Domain Tanayel weather station, soil data from SBIS, and agronomic information from potato and onion SUPROMED grown-plots. The calibration is used to test if sensitive parameters, *i.e.* available water and soil depletion level, are within the acceptable levels.

Typical Meteorological Year (TMY) was calculated for SBIS using daily weather series from 1994 to 2018, including daily air temperature (T_{max} and T_{min}), rain and global radiation. Potential evapotranspiration (ET_p) was calculated at daily basis using Hargreaves equation (Aguilar and Polo, 2011). Growing-Degree Day (GDD) was calculated for each of crop for the TMY and during the 2020 and 2021 growing years, using real phenological observations. Crop coefficients (K_c) of potatoes were derived from local experiments conducted at Tal Amara Research Station (Karam et al., 2014), while K_c values of onion were obtained from literature in likely-environmental conditions.

3 Results of the model validation

3.1 Results of the sensitivity test

The sensitivity test conducted on MOPECO demonstrates that the model's sensitive parameters are (i) percentage of effective precipitation, (ii) percentage of available water at the beginning of the growing season, (iii) depletion level of water in the soil and (iv) interval of irrigation.

3.2 Results of MOPECO calibration (2020)

For potato, irrigation from mid-season to late tuber ripening stage, includes 22 mm at day of year (d.o.y) 130, 22 mm at d.o.y 136, 25 mm at d.o.y 140, 29 mm at d.o.y 160, 29 mm at d.o.y 163, 29 mm at d.o.y 168 and 29 mm at d.o.y 172 (Figure 3). Crop coefficient (K_c) at mid-development stage reached 1.1, compared to 0.5 early in the season. Net irrigation requirements of the 120-day grown-potatoes from planting to harvest accumulated 526 mm under the pedo-climatic conditions of South Bekaa. For onion, irrigation events from d.o.y 83 to d.o.y 131 were distributed as 20 mm at d.o.y 98, 17 mm at d.o.y 107, 14 mm at d.o.y 114 and 15 mm at d.o.y 122 (Figure 3). During this growth period, K_c increases from 0.4 in the initial stage to 1.1 at mid-season. Seasonal net irrigation requirements of onion were 731 mm for a total growing season of 178 days from sowing to harvest.

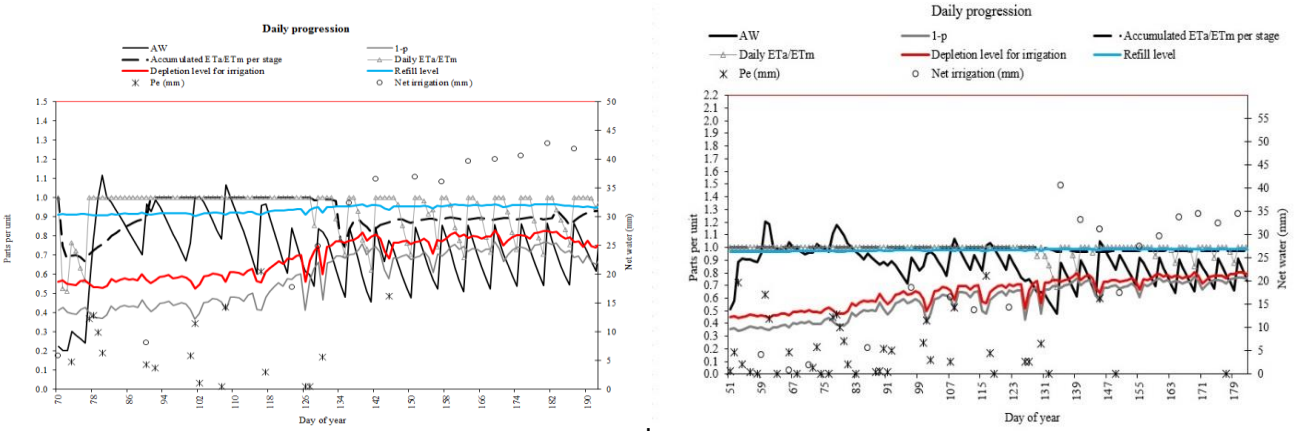

Figure 3. Time course evolution of available water (AW), depletion level (*p*) and simulation of net irrigation as a result of MOPECO calibration on potato (left) and onion (right)

3.3 Results of MOPECO validation (2021)

For potato, an irrigation of 19 mm on d.o.y 76, alongside rainfall events between d.o.y 74 and d.o.y 80, led to an increase in available water about 8 mm above the refill level on d.o.y 82. Slow potato growth was then observed due to percolation, which did not only cause water loss but also stops soil aeration due to water filling the soil pores, thus preventing potato plants from using soil oxygen for their roots growth. After d.o.y 82, soil available water (AW) returns to an optimum level, which is below the refill level and above the depletion level. An irrigation of 9 mm occurred on d.o.y 91, braking the drop in the soil available water, and rising some 2-3 mm above the refill level. Thereafter, AW maintained an optimal level from d.o.y 100 to d.o.y 111, where plants received an irrigation of 16 mm on d.o.y 100. Moreover, an irrigation of 26 mm on d.o.y 112 brakes the drop in AW below the depletion level, which caused a significant decrease in the ET_a/ET_m ratio (Figure 4). From mid-development stage (d.o.y 107) until the end of mid-season (d.o.y 171), daily ET_a/ET_m ratio decreased, decreasing the level of available water in the soil, most probably due an excessive water uptake by tubers. Crop coefficients of irrigated potatoes reached a maximum of 1.1, compared to 0.5 early in the season. At late growth stages, irrigation events were 31 mm at d.o.y 173, 28 mm at d.o.y 177, 28 mm at d.o.y 181, 26 mm at d.o.y 184, 24 mm at d.o.y 189, 29 mm at day 194 and 25 mm at day 199. The results of the model validation in 2021 showed that the gross irrigation requirements during the whole growing season were 540 mm for potato.

For onion, although the soil available water at sowing (20 February 2021) was optimal, it was necessary to provide 23 mm to plants on d.o.y 57, to avoid extra depletion of AW. On the other hand, rain recoded between d.o.y 73 and d.o.y 82 raised water in the soil to a level near the refill level. Moreover, between d.o.y 83 (bulbs development stage) and d.o.y 133 (mid-season), a series of watering events took place (5 mm on d.o.y 85, 13 mm on d.o.y 91, 10 mm on d.o.y 96, 18 mm on d.o.y 99, 15 mm on d.o.y 107, 21 mm on d.o.y 113, 27 mm on d.o.y 122, 22 mm on d.o.y 125 and 22 mm on d.o.y 132, contributing to improved water status in the soil (Figure 4). At d.o.y 133 until the end of mid-season, irrigation increased as water requirements increased (Kc slightly > 1.0), were an irrigation of 32 mm was supplied to plants at d.o.y 139, 33 mm at d.o.y 146, 34 mm at d.o.y 151, 33 mm at d.o.y 156, 33 mm at d.o.y 160, 34 mm at d.o.y 165, 34 mm at d.o.y 171, 35 mm at d.o.y 178 and 35 mm at d.o.y 184. During the period from d.o.y 133 to d.o.y 184, the ET_a/ET_m ratio increased, as shown in Figure 4. The results of the validation in 2021 showed that gross irrigation requirements of onion during the whole growing season from seeds sowing to harvest were 728 mm.

Based on the obtained results, MOPECO should be optimized by taking into account all critical factors affecting the required parameters, especially ET, to calculate crop water requirements and irrigation schedule. For example, crop coefficients (k_c) and yield response to water (k_y) of the simulated crops should be obtained from local experiments, as for potatoes (Karam et al., 2014). A good irrigation scheduling based on MOPECO gives the optimal yield production. Moreover, gained knowledge of the crop different growth stages, in relation to GDDs, contributes to

improving current management practices, taking into account sustainable management practices should be placed at both agricultural and environmental level.

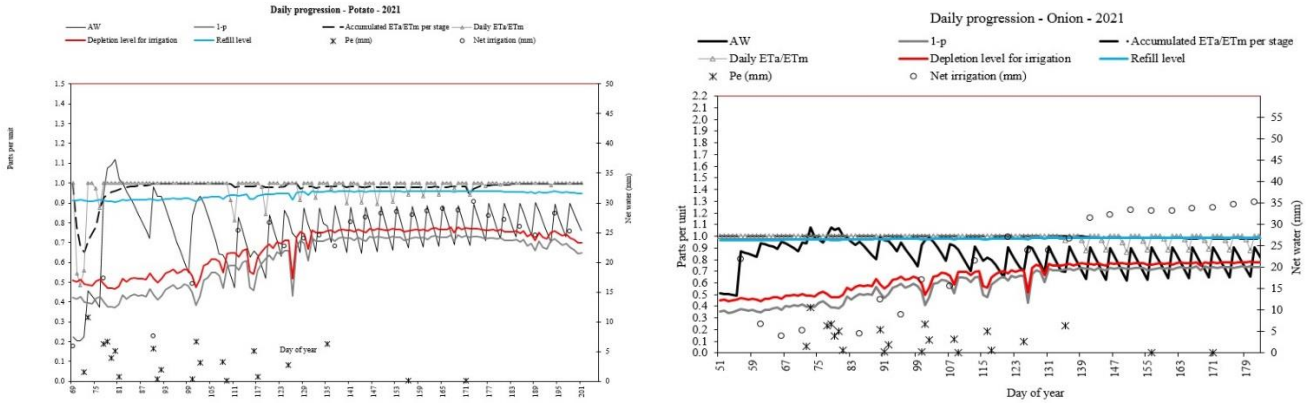

Figure 4. Time course evolution of available water (AW), depletion level (*p*) and simulation of net irrigation as a result of MOPECO validation on potato (left) and onion (right)

4 Summary

The results of the model calibration in 2020 demonstrated that time course evolution of soil water content (SWC) was within the refill (field capacity) and the lower (permanent wilting point) limits. Data showed that soil water content increased after each irrigation supply, thus showing the readiness of plants to extract water in the range of non-deletion. On the other hand, net irrigation requirements of potato and onion were found to be 526 mm and 731 mm, respectively. Moreover, the results of the validation conducted on the same crops in 2021 consolidated the results obtained during the calibration year. Indeed, the simulation of the soil water balance approach by MOPECO yielded sound results concerning time course evolution of the soil water content, which is the key factor of an environmentally-sustained irrigation. In addition, gross irrigation requirement were found to be 540 mm for potato, and 728 mm for onion. A deep knowledge of the irrigation requirements during the growing season help farmers better planning their water resources, given the economic and financial constraints faced by the Lebanese agricultural sector. We concluded that MOPECO can serve an important tool of water resource management and planning in agriculture, and may lead to save considerable amount of water that can be used to bring additional land into irrigation.

Acknowledgements

The authors wish to deeply thank PRIMA (Partnership of Research and Innovation in the Mediterranean Area) and SUPROMED (Sustainable Production in Mediterranean Agricultural Ecosystems, 2019-2022) for supporting the present research.

References

Abi Saab, M.T., Albrizio, R., Nangia, V., Karam, F. and Y. Rouphael. 2014. Developing scenarios to assess sunflower and soybean yield under different sowing dates and water regimes in the Bekaa valley Lebanon: Simulations with Aquacrop. International Journal of Plant Production, (8): 4, 457-482.

Aguilar, c., and M. J. Polo. 2011. Generating reference evapotranspiration surfaces from the Hargreaves equation at watershed scale. Hydrol. Earth Syst. Sci., 15, 2495–2508. doi:10.5194/hess-15-2495-2011

Alvarez, J. F. O., de Juan Valero, J. A., Martin-Benito, J. M. T. and E. L. Mata. 2004. MOPECO: an economic optimization model for irrigation water management. Irrigation Science, 23(2), 61-75.

Dominguez Padilla, A., Tarjuello, J.M., Breidy, J., and F. Karam. 2011. Deficit irrigation under water stress and salinity conditions: The MOPECO-SALT Model. Agricultural Water Management, 98: 1451-1461.

Domínguez, A., R.S. Martínez, J.A. de Juan, A. Martínez Romero and J.M. Tarjuelo. 2012. Simulation of maize crop behavior under deficit irrigation using MOPECO model in a semi-arid environment. Agricultural Water Management, 107:42–53. DOI: 10.1016/j.agwat.2012.01.006

Karam, F. Amacha, N., Fahed, S., EL Asmar, T., and A. Domínguez. 2014. Response of potato to full and deficit irrigation under semiarid climate: Agronomic and economic implications. Agricultural Water Management, 142, 144–151.

López-Mata, E., Tarjuelo, J. M., Orengo-Valverde, J. J., Pardo, J. J., and A. Domínguez. 2019. Irrigation scheduling to maximize crop gross margin under limited water availability. Agricultural Water Management, 223, 105678. https://doi.org/10.1016/j.agwat.2019.06.013.

Lopez-Urrea, R., Olalla, F.M.D., Montoro, A., and P. Lopez-Fuster. 2009. Single and dual crop coefficients and water requirements for onion (Allium cepa L.) under semiarid conditions. Agricultural Water Management, 96, pp.1031–1036.

Ortega Álvarz, J. F., de Juan Valero, J. A., Tarjuelo Martín-Benito, J. M., & López Mata, E. (2004). MOPECO: An economic optimization model for irrigation water management. Irrigation Science, 23(2), 61-75. https://doi.org/10.1007/s00271-004-0094-x.

Saseendran, S.A., L. Ahuja, D.C. Nielsen, Th. J. Trout and L. Ma. 2008. Use of crop simulation models to evaluate limited irrigation management options for corn in a semiarid environment. Water Resources Researches. 44(7). DOI:10.1029/2007WR006181

Stewart, J.I., R.E. Danielson, R.J. Hanks, E.B. Jackson, R.M. Hagan, W.O. Pruitt, W.T. Franklin and J.P. Riley. 1977. Optimizing crop production through control of water and salinity levels in the soil. Utah Water Lab. PRWG 151-1. Logan, Utah. 191 pp.

Tool for irrigation scheduling in herbaceous and woody crops. Supromed project

Martínez-Romero, A.[1], Tarjuelo J.M.[1], López-Urrea R.[2], Martínez-López J.A.[1], Pardo, J.J.[1], Montero, J.[1], Montoya, F.[1] and Domínguez A.[1]

[1] Regional Center of Water Research (CREA), University of Castilla-La Mancha (UCLM), Albacete, Spain. angel.mromero@uclm.es
[2] Provincial Agronomic Technical Institute (ITAP) and FUNDESCAM, Albacete, Spain. rlu.itap@dipualba.es

Abstract. Water scarcity is one of the main handicaps for agriculture in the Mediterranean area and other locations with a semi-arid climate. The PRIMA foundation has funded several European institutions through the SUPROMED project (www.supromed.eu), which aims to improve and safeguard the economic and environmental sustainability of Mediterranean agroecosystems. It provides an online platform with a set of models including the irrigation scheduling module of the Model for Economic Optimization of irrigation water (IS-MOPECO), developed and validated between 2019 and 2021.
The aim of this paper is to present the performance of the IS-MOPECO in herbaceous and tree crops, developed and validated during the SUPROMED project (https://dss.supromed.eu/portal/ and https://crea.uclm.es/siar/siarpr).
Two tools are available, one for irrigation scheduling (IS) in herbaceous crops, and the other for fruit trees and vines. In both, a simplified soil water balance is performed, following the FAO56 methodology. Daily IS is conducted by simulating the evolution of soil water content throughout the crop growth stages, according to the chosen production objective: 1) in herbaceous crops, to supply the crop's water requirements; 2) in tree crops, to supply the crop's water requirements, totally or partially, depending on irrigation water availability, applying Regulated Deficit Irrigation (RDI) techniques.
The information required is:

a) Crop: Crop coefficients adapted to the area (K_c), Crop development threshold temperatures (T_{up}, T_{dow}) and maximum root depth (automatic for the user (AU)). For herbaceous crops, the sowing date (user-input (IU)). For tree crops, the tree spacing and canopy cover, and an RDI strategy selected according to the water available for irrigation (IU).
b) Climate data (AU): Maximum and minimum temperatures, reference evapotranspiration (ET_o) and daily rainfall.
c) Soil data (IU): Texture and maximum depth explorable by roots.

The water balance is updated daily, and the user can adjust the precipitation data, the volume of irrigation applied and the day when the phenological stage of the crop changes.

1 Introduction

The Mediterranean area is one of the world's richest regions in ecosystems. However, it is also one of the most vulnerable zones due to irregular rainfall distribution throughout the year and water scarcity caused by frequent drought periods (García-Ruíz et al., 2011). Thus, the lack of water resources is one of the main handicaps for agriculture in this area (Correia et al., 2009). In addition, the farming sector is greatly conditioned by numerous economic (e.g., harvest price and labor cost), political (e.g., laws for the protection of the environment), social (e.g., food security and maintenance of rural population), technical (e.g., machinery and crops), and environmental (e.g., climate, soil and diseases) factors. Moreover, particular aspects, such as the lack of tools and/or irrigation advisory services for determining the irrigation requirements of crops at farm level, the lack of knowledge about the irrigation system (de Juan et al., 1996; Nascimento et al., 2019), or climate change, have all led to an excessive use of resources, such as groundwater and energy (Knox et al., 2012).
The PRIMA foundation has funded several European institutions through the SUPROMED project (Sustainable production in water-limited environments of Mediterranean agro-ecosystems) (www.supromed.eu), which aims to improve and safeguard the economic and environmental sustainability of Mediterranean farming systems through a more efficient management of water (evaluation of the irrigation systems, proper irrigation scheduling taking into account weather forecast and soil moisture), land (good agricultural practices and optimal distribution of crops), energy (audits and solar power), and fertilizers (soil analysis and nutrients balance). It provides an online platform with a set of models including the irrigation scheduling module of the Model for Economic Optimization of irrigation water (IS-MOPECO), developed and validated between 2019 and 2021.

The aim of this paper is to present the performance of the IS-MOPECO in herbaceous and tree crops, developed and validated during the SUPROMED project (https://dss.supromed.eu/portal/ and https://crea.uclm.es/siar/siarpr).

2 Materials and Methods

2.1 Study area

The irrigation scheduling module of the Model for Economic Optimization of irrigation water (IS-MOPECO), was developed and validated between 2019 and 2021 in the region of Castilla-La Mancha (Spain) (Fig. 1) through the SUPROMED project. In "Eastern Mancha" the average daily maximum temperature occurs in summer (33°C), with great seasonal variability in mean daily temperature (3.8°C in January and 24.4°C in July). Long-term mean annual precipitation is 360 mm (mostly concentrated in the autumn and spring months) and mean cumulative annual reference evapotranspiration (ETo) is around 1300 mm. A petrocalcic horizon is found at a depth of 0.4 to 0.7 m, while the first horizons have a clay loam texture with low to medium levels of soil organic matter. The most common crops in the area are grape ($21 \cdot 10^3$ ha), cereals ($25 \cdot 10^3$ ha), almond ($11 \cdot 10^3$ ha), garlic ($10 \cdot 10^3$ ha), corn ($9 \cdot 10^3$ ha), onion ($5 \cdot 10^3$ ha), and others, such as alfalfa and olive (JCRMO, 2021).

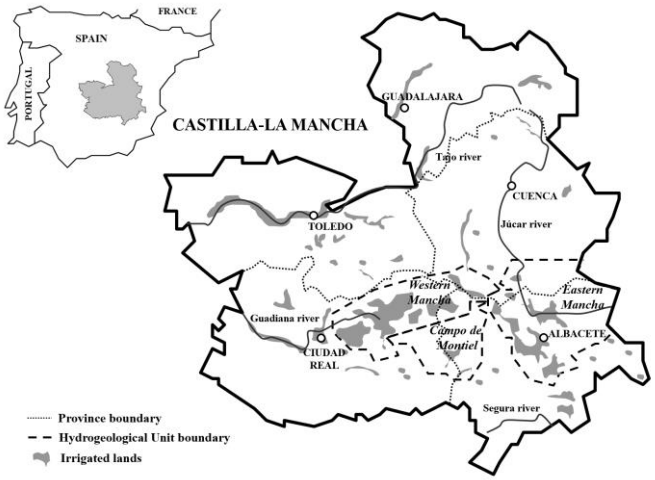

Figure 1. Location of Castilla-La Mancha Region in southeastern Spain. Hydrogeological Unit of "Eastern Mancha".

2.2 Irrigation scheduling

The "MOPECO irrigation scheduling" tool (IS-MOPECO) (https://crea.uclm.es/siar/siarpr/) is a simplification of the MOPECO model for researchers (Ortega et al., 2004), aimed at farmers and technicians. It determines the irrigation scheduling of a crop by using the simplified daily soil water balance proposed by FAO – 56 (Allen et al., 1998) and FAO-66 (Steduto et al., 2012).
Two tools are available, one for irrigation scheduling (IS) in herbaceous crops, and the other for fruit trees and vines. In both, a simplified soil water balance is performed, following the FAO56 methodology. Daily IS is conducted by simulating the evolution of soil water content throughout the crop growth stages, according to the chosen production objective: 1) in herbaceous crops, to supply the crop's water requirements; 2) in tree crops, to supply the crop's water requirements, totally or partially, depending on irrigation water availability, applying Regulated Deficit Irrigation (RDI) techniques. The water balance is updated daily, and the user can adjust the precipitation data, the volume of irrigation applied and the day when the phenological stage of the crop changes.

2.2.1 Irrigation scheduling in herbaceous crops

Logging is required to run the software (https://crea.uclm.es/siar/siarpr). IS-MOPECO module requires certain information, which is provided in several steps (Fig. 2). The information required is:

a) Plots: Plot location **(user-input (IU)**. Climate data (maximum and minimum temperatures, reference evapotranspiration (ET_o) and daily rainfall) are selected by the program from the nearest weather station **(automatic for the user (AU)).**
b) Soil: Texture, maximum depth explorable by roots (soil depth useful) and percentage of stone **(IU).**

c) Crop: Crop and the sowing date **(IU).** Phenological development stages are generated automatically. To obtain the length of the crops growth stages in accumulated growing-degree-days (◦C), MOPECO uses the double triangulation method (Sevacherian et al., 1977). Change of the growth stages can be modified manually by the user. Crop coefficients adapted to the area (K_c), Crop development threshold temperatures (T_{up}, T_{dow}), maximum root depth are **AU**. These must be calibrated for the area by the program managers.

d) Irrigation: data on the irrigation system and its management, such as irrigation depth, intervals between irrigations, efficiency, or rainfall are **UI**.

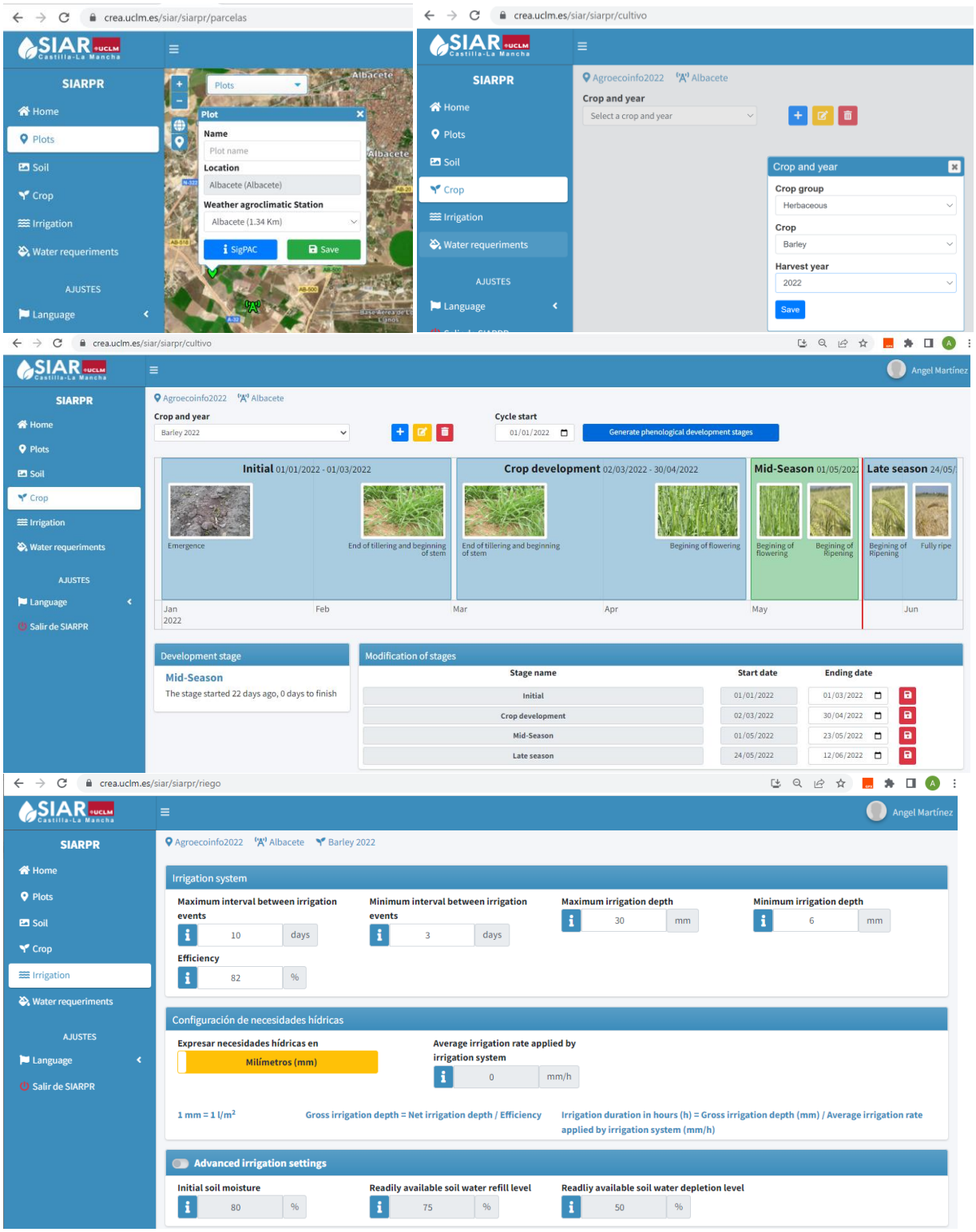

Figure 2. Data required by Irrigation Scheduling software (*https://crea.uclm.es/siar/siarpr*).

2.2.2 Irrigation scheduling in tree crops and vineyards

For tree crops, similar data are required (*2.2.1. irrigation scheduling in herbaceous crops*). With respect to the crop data, the differences are:

- Instead of the sowing date, cycle start date is required **(IU).**
- One option according to irrigation water availability must be selected **(IU)** (Fig. 3)**.** The program will adjust the irrigation water, by applying Regulated Deficit Irrigation (RDI) techniques.
- In addition, the tree spacing and canopy cover must be selected (treetop diameter).

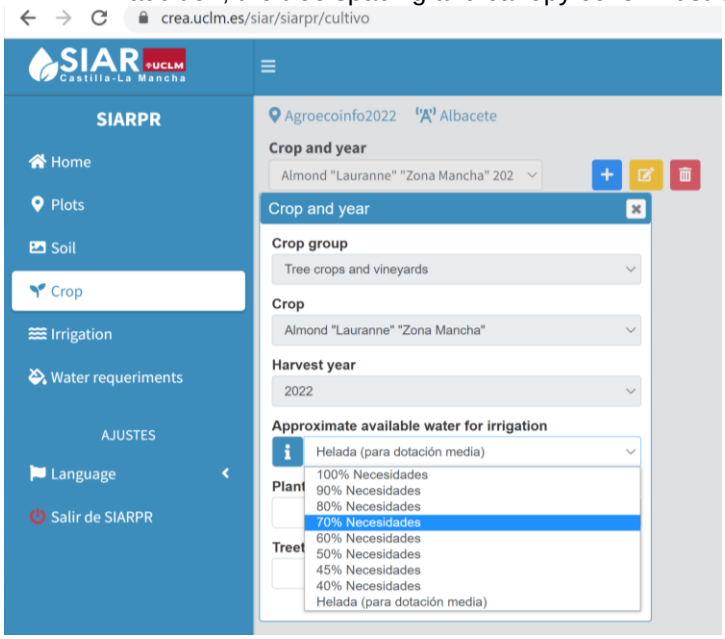

Figure 3. Additional data required in tree crops by Irrigation Scheduling software (*https://crea.uclm.es/siar/siarpr*).

3 Results

3.1. Examples of Irrigation scheduling

Daily IS is performed by IS-MOPECO. Evolution of soil water content is simulated graphically (Fig. 4). Although the water balance is updated daily, these balances are estimated until the end of the cycle, using average climatic data from the corresponding weather station (Fig. 4).

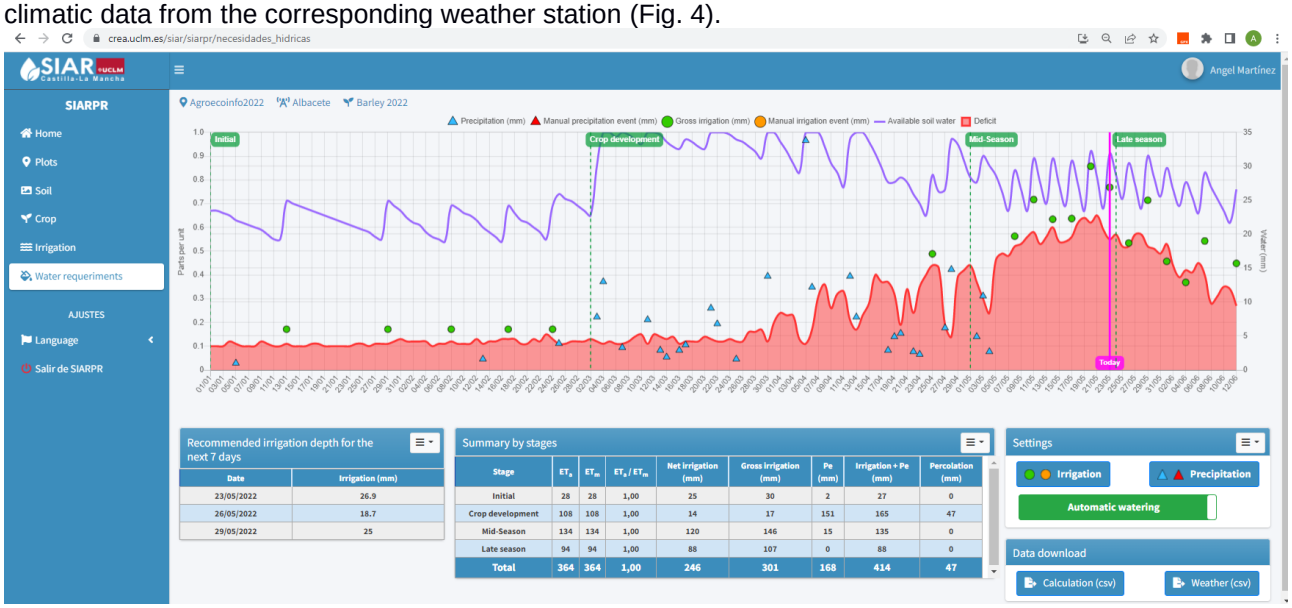

Figure 4*: Evolution of available water simulated by "MOPECO irrigation scheduling" tool in 2022 for barley (Main Y axis: Deficit: 1-p, where p is the fraction of TAW (Total Available Water) that a crop can extract without suffering water stress; Available water. Secondary Y axis: Gross irrigation; Precipitation.*

3.1.1 Examples of Irrigation scheduling in herbaceous crops

The result of the irrigation scheduling for a barley crop in 2022 is shown in Figure 4. The scheduling was performed on May 23, estimating the beginning of the vegetative cycle on January 1, and the end of the cycle on June 12. Therefore, the climatic data are the actual ones up to May 22 and estimated (mean year climatic data) from May 23 to June 12. The pink line named "Today" indicates the current day.
The IS has been performed automatically. Gross Irrigation was 301 mm and the total water 414 mm, where percolation was 47 mm (due to rainfall). ETa/ETm ratio was 1 at all stages. Water use efficiency could be slightly improved if the last two irrigations were manually reduced to decrease the available water in the soil before the end of the cycle.

3.1.2 Examples of Irrigation scheduling in tree crops

The result of the irrigation scheduling for almond crop in the year 2022 is shown in Figures 5 and 6. The scheduling was performed on May 23, estimating the beginning of the annual cycle on February 2, almond harvest on September 12 and leaf fall on November 17. The pink line called "Today" indicates the current day. Note that Figure 5 shows the no deficit irrigation strategy (ND) and Figure 6 shows the strategy with a 20% reduction in maximum water requirements (T80).

Figure 4: Evolution *of available water simulated by "MOPECO irrigation scheduling" tool in 2022 for almond (no deficit) (Main Y axis: Deficit: 1-p, where p is the fraction of TAW (Total Available Water) that a crop can extract without suffering water stress; Available water. Secondary Y axis: Gross irrigation; Precipitation.*

Figure 5: *Evolution of available water* simulated *by "MOPECO irrigation scheduling" tool in 2022 for almond (20% déficit) (Main Y axis: Deficit: 1-p, where p is the fraction of TAW (Total Available Water) that a crop can extract without suffering water stress; Available water. Secondary Y axis: Gross irrigation; Precipitation.*

The IS was performed automatically. Gross Irrigation was 495 mm and 348 mm for ND and T30 respectively (30% reduction in irrigation water). The total water was 801 mm vs 653 mm, accounting for 20% less water.

The difference in percentages between irrigation water and total water is due to the effect of rainfall. Owing to the high rainfall in the area during the first two stages of phenological development, no irrigation was required in either stage. For T30 strategy, the main reduction in water supply was implemented in the period close to harvesting (from 25th August to 12sd September), applying 49 mm and 11 mm of irrigation water for T100 and T80, respectively.

4 Summary

This study describes two tools, one for irrigation scheduling (IS) in herbaceous crops, and the other for fruit trees and vines. The aim for herbaceous crops is to supply the crop's water requirements (maximum yield), and, for tree crops, it is to supply the crop's water requirements, totally or partially, depending on irrigation water availability, applying Regulated Deficit Irrigation techniques.

Acknowledgements

This research was carried out under the framework of European project SUPROMED “GA-1813” funded by PRIMA, and the Regional project PRODAGUA “Ref SBPLY/19/180501/000144”, funded by FEDER and the Regional Government of Castilla-La Mancha.

References

Allen, R.G.; Pereira, L.S.; Raes, D.; Smith, M. 1998. Crop Evapotranspiration-Guidelines for Computing Crop Water Requirements-FAO Irrigation and Drainage Paper 56.

Correia, F.N.; Iwra, M.; Técnico I.S. 2009. Water Resources in the Mediterranean Region. Int. Water Resour. Assoc. 24, 22–30.

de Juan, J.A.; Tarjuelo, J.M.; Valiente, M.; García, P. 1996. Model for Optimal Cropping Patterns within the Farm Based on Crop Water Production Functions and Irrigation Uniformity. I: Development of a Decision Model. Agricultural Water Managemen 31, 115–143, doi:10.1016/0378-3774(95)01219-2.

García-Ruiz J M, L.-M.J.I.V.-S.S.M.L.T. and B.S. 2011. Mediterranean Water Resources in a Global Change Scenario. Earth-Sci. Rev. 105 2011, 121–139.

JCRMO, 2021. Memoria JCRMO 2020-2021. https://www.jcrmo.org/wp-content/uploads/2022/05/memoria-jcrmo-2020-2021.pdf (accessed 20 May 2022).

Knox, J.; Hess, T.; Daccache, A.; Wheeler, T. 2012. Climate Change Impacts on Crop Productivity in Africa and South Asia. Environmental Research Letters, 7, doi:10.1088/1748-9326/7/3/034032.

Nascimento, A.K.; Schwartz, R.C.; Lima, F.A.; López-Mata, E.; Domínguez, A.; Izquiel, A.; Tarjuelo, J.M.; Martínez-Romero, A. 2019. Effects of Irrigation Uniformity on Yield Response and Production Economics of Maize in a Semiarid Zone. Agricultural Water Management 211, 178–189, doi:10.1016/j.agwat.2018.09.051.

Ortega Álvarez, J.F.; de Juan Valero, J.A.; Tarjuelo Martín-Benito, J.M.; López Mata, E. 2004. MOPECO: An Economic Optimization Model for Irrigation Water Management. Irrigation Science, 23, 61–75, doi:10.1007/s00271-004-0094-x.

Sevacherian, V., Stern, V.M., Mueller, A.J., 1977. Heat accumulation for timingLygus control pressures in a safflower–cotton complex. J. Econ. Entomol. 70,399–402.

Steduto, P., Hsiao, T.C. ; Fereres, e., Raes, D. 2012. Crop Yield Response to Water FAO Irrigation and Drainage Paper 66. FAO, Rome, Italy.

Remotely sensed drought assessment in agricultural ecosystems under climate change uncertainty (1982-2020): The case of Albacete region, Spain

Sakellariou S.[1], Alpanakis N. [1], Faraslis I.[2], Spiliotopoulos M. [1], Sidiropoulos P. [1], Tziatzios G.[1], Blanta A. [1], Brisimis V. [1], Dalezios N.[1] & Dercas N. [3]

[1] Department of Civil Engineering, University of Thessaly, 38334, Volos, Greece
[2] Department of Environmental Sciences, University of Thessaly, 41500, Larissa, Greece
[3] Department of Natural Resources Management & Agricultural Engineering, Agricultural University of Athens, 11855, Athens, Greece

Abstract. Drought is considered as a natural hazard recurring at a regional scale throughout history. Drought quantification is usually accomplished through indicators and indices. Primary aim of the paper consists of the remotely sensed drought assessment of an agricultural region under climate change uncertainty in the last 40 years (1982 – 2020). To this end, we used satellite data, as provided by the CHIRPS database (i.e., precipitation data), to estimate the monthly Standardized Precipitation Index (SPI) based on the precipitation evolution for the last 12 months (SPI_{12}). Based on the analysis results, the driest hydrological year was 1994-1995 (SPI = -1.84), whereas the wettest hydrological year was 1989-1990 (SPI = 1.99). The hydrological year with the most normal conditions in terms of drought/wetness was 1991-1992 (SPI = 0.05). Beyond this, the mapping of drought conditions can be a useful tool assessing drought spatial variability and for targeted measures based on drought severity for each pixel. Hence, counterbalancing measures could be taken in the most susceptible regions, especially in the western part of Albacete, whereas the southeastern territory seems to face wetter conditions.

Keywords: Drought; Wetness; Remote Sensing; CHIRPS database; Albacete, Spain

1 Introduction

Drought is considered as a natural hazard recurring at a regional scale throughout history. Essentially, droughts originate from a deficiency or lack of precipitation in a region over an extended period and can be regarded as an extreme climatic event associated with water resources deficit (Dalezios et al., 2017a). Therefore, droughts are also referred to as 'non-events'. Droughts occur in both high and low rainfall areas and virtually all climate regimes. It is recognized that drought is characterized as one of the major natural hazards with significant impact to environment, society, agriculture, and economy, among others (Dalezios et al., 2018a).

Drought quantification is usually accomplished through indicators and indices. There are several commonly used drought indices based on ground (conventional) and/or remotely sensed data (Kanellou et al., 2009a; Kanellou et al., 2009b; Du Pissani et al., 1998; Mishra and Singh, 2010; McVicar and Jupp, 1998; Zargar et al., 2011). Moreover, climate variability and change may affect drought preparedness planning and mitigation measures (IPCC, 2012; Salinger et al., (eds), 2005). Thus, climate change must be considered in all the aspects of drought analysis.

Over the last decades, there is a gradually increasing trend for the use of remote sensing in drought analysis and assessment, and specifically for the detection of several spatial and temporal drought features at different scales (Dalezios et al., 2017b). Moreover, a major consideration for remote sensing use in drought analysis, is the extent to which operational users can rely on a continued supply of data (Thenkabail et al., 2004). Indeed, satellite systems provide temporally and spatially continuous data over the globe and, thus, they are potentially better and relatively inexpensive tools for regional applications, such as drought quantification, monitoring and assessment, than conventional environmental and weather data (Dalezios et al., 2018a). Hence, primary aim of the paper consists of the remotely sensed drought assessment of an agricultural region under climate change uncertainty in the last 40 years (1982 – 2020). To this end, satellite data are used, as provided by the CHIRPS database (i.e., precipitation data), to estimate the monthly Standardized Precipitation Index (SPI) based on the precipitation

evolution for the last 12 months (SPI_{12}), through the transformation of gamma cumulative distribution to standardized normal distribution (Qin et al., 2015).

2 Materials and Methods

2.1 Study area

The study area is Albacete, which is a Spanish province that is in the south-eastern part of the country (Figure 1). The study domain occupies 14,858 km^2. The total population amounts to 387,658 and can be considered sparsely populated with 26 people per km^2. The geographical coordinates are: 38º 50' N, 2º 00' W (Wikipedia, 2022). Albacete mainly constitutes an agricultural region, and the applied methodology has been conducted under the SUPROMED European research project.

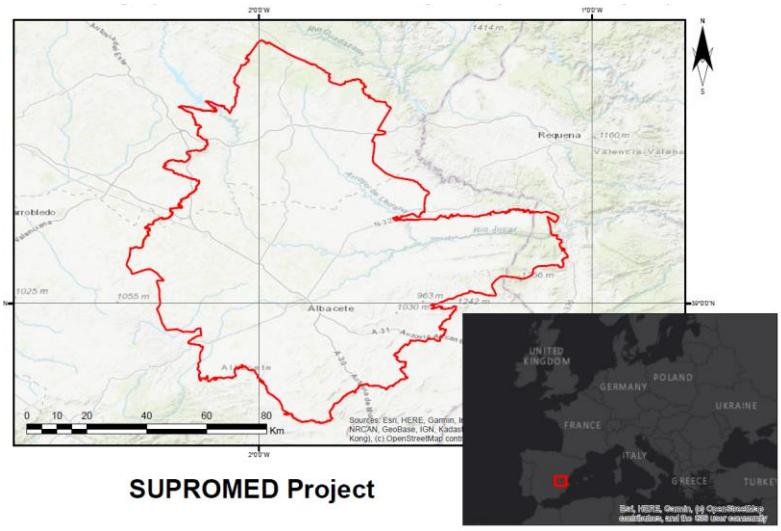

Figure 1. Geographical location of the study area (Albacete, Spain)

2.2 Data

Precipitation in the study area was assessed using the CHIRPS database (Climate Hazards Group InfraRed Precipitation with Station data). The CHIRPS database consists of daily precipitation data at spatial resolution of 0.05 and 0.25º for the quasi-global coverage of 50º N–50º S from 1981 to present (CHG, 2021; Duan et al., 2016). CHIRPS is a fusion of satellite images and data from rain-gauge stations. CHIRPS data perform well at the watershed scale. Monthly CHIRPS products at 0.05º, which corresponds to a spatial resolution of 5 km * 5 km, were used in this study for the period 1982–2020 (Sidiropoulos et al., 2021).

2.3 Methodology

2.3.1 Drought Severity Assessment

Drought severity assessment is conducted with the use of the Standardized Precipitation Index (SPI) (WMO, 2012), which is solely based on precipitation data. The SPI is based on standardized probability to quantify precipitation deficit for multiple time scales, such as for 3-, 6-, 9- and 12-month periods (Qin et al., 2015; Steinemann et al., 2005; Dalezios et al., 2018b; WMO, 2012). Based on historical long-term rainfall data, the maximum likelihood is used to estimate the gamma distribution parameters and fit a gamma distribution. Then, the cumulative probability is used for the inverse normal function, resulting in the SPI (Guttman, 1999). Specifically, the SPI is computed by dividing the difference between the normalized seasonal precipitation and its long-term seasonal mean by the standard deviation. A classification system is used to define SPI drought severities (Table

1). SPI negative values indicate drought and the event ends when the SPI becomes positive. The SPI is flexible and can be calculated for periods from 1 to 72 months, but it is mostly used for periods of 24 months or less. For the current application, a 1-month period is used. Seven classes of SPI are shown in Table 1 (EDO, 2021; Sidiropoulos et al., 2021).

Table 1. SPI classification scheme

SPI values	Class	Probability (%)
> 2	Extremely wet	2.3
1.5 – 1.99	Very wet	4.4
1 – 1.49	Moderately wet	9.2
-0.99 – 0.99	Normal precipitation	68.2
-1 – -1.49	Moderately dry	9.2
-1.5 – -1.99	Very dry	4.4
< -2	Extremely dry	2.3

EDO, 2021 (adjusted)

3 Results and Discussion

This section describes the results of SPI_{12} for a historical period from 1982 to 2020. This type of analysis would allow the identification of the historical driest and wettest conditions occurred in the study area, exploring potential patterns (cycles) in meteorological conditions.

3.1 Historical Drought Severity Assessment in Albacete, Spain

Two types of presentations are considered, namely drought quantification and spatial variability. First, the SPI_{12} values are estimated of the driest and wettest hydrological year, as well as the year with the most normal conditions. Table 2 summarizes the SPI_{12} for each hydrological year. At first glance, it is observed that the driest hydrological year is 1994-1995 (SPI = -1.84), whereas the wettest hydrological year is 1989-1990 (SPI = 1.99). The hydrological year with the most normal conditions in terms of drought/wetness is 1991-1992 (SPI = 0.05).

Table 2. Annual (hydrological year: October to September) SPI_{12} in Albacete, Spain

Hydrological year	SPI_{12}	Hydrological year	SPI_{12}
1982-1983	-0,1385	2001-2002	-0,0601
1983-1984	-1,0007	2002-2003	0,7395
1984-1985	0,1146	2003-2004	0,9772
1985-1986	-0,7433	2004-2005	-0,5931
1986-1987	0,8354	2005-2006	-0,6422
1987-1988	0,4926	2006-2007	0,6641
1988-1989	0,6055	2007-2008	0,7700
1989-1990	1,9915	2008-2009	0,8772
1990-1991	0,2859	2009-2010	0,9549
1991-1992	0,0548	2010-2011	1,0670
1992-1993	-0,3921	2011-2012	-0,3205
1993-1994	-0,9272	2012-2013	0,3040
1994-1995	**-1,8388**	2013-2014	-0,4543

1995-1996	-1,0185	2014-2015	-0,6062
1996-1997	0,5366	2015-2016	-1,1841
1997-1998	0,5727	2016-2017	0,2920
1998-1999	-1,0092	2017-2018	-0,8111
1999-2000	-1,0275	2018-2019	0,3809
2000-2001	-0,1437	2019-2020	0,4068

However, beyond the average values of SPI_{12}, the frequency distribution for the three representative hydrological years is determined, exploring the severity of drought/wetness in the study domain.

Figure 2a presents the histogram of the driest hydrological year (1994-1995) in Albacete for a time frame from 1982 to 2020. It is observed that almost 1,500 pixels of 5 km^2 tend to have values close to -1.5 followed by almost 1,000 pixels, which tend to have values close to -2. The remaining pixels present either extreme conditions (with values < -2) or little slighter drought conditions (with values from -1 to 0). On the other hand, Figure 2b presents the histogram of the wettest hydrological year (1989-1990) in Albacete for the same time frame. In this case it is observed that almost 1,700 pixels of 5 km^2 have SPI_{12} values higher than 2, whereas more than 1,700 receive values lower or equal to 2. Finally, Figure 2c depicts the year with the most normal conditions, where more than 2,000 pixels have values higher or equal to 0.5, whereas the remaining pixels range from 0 to -1.

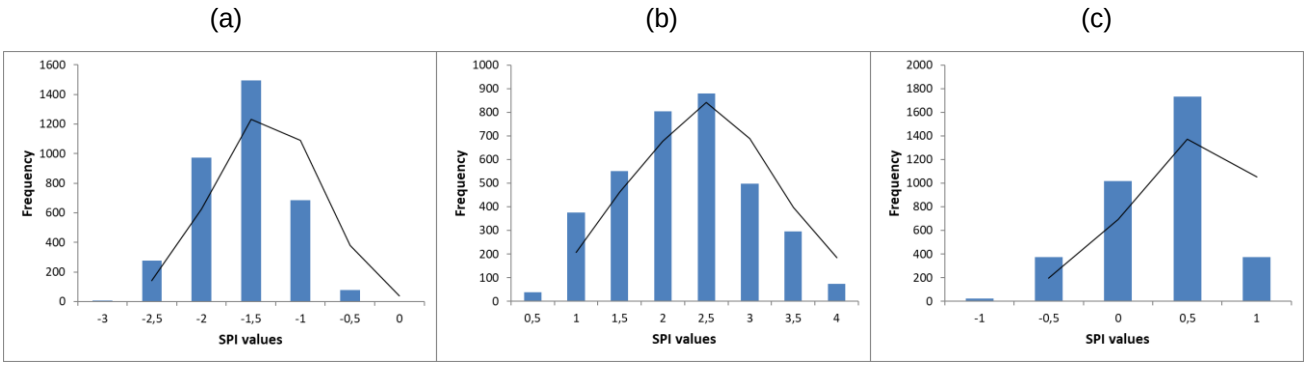

Figure 2. Frequency distribution of SPI_{12} for (a) the driest, (b) the wettest and (c) the hydrological year with the most normal conditions

The second type of presentation refers to drought spatial variability. Beyond the statistical assessment of SPI_{12}, the mapping of extreme conditions for each pixel in the study area can be considered a being of crucial importance. To this end, the average SPI_{12} values are mapped for the driest and wettest year, and one year with quite normal conditions. Consequently, the outputs can be a valuable tool for more spatially targeted measures (where needed) to avoid extreme drought conditions with profound implications on crops viability.

Figure 3a depicts the driest year in Albacete throughout the time reference (1982-2020). The values of SPI range from -2.4 to -1.08. The driest regions are in the central and northern part of Albacete region (-2 < SPI < -2.4), surrounded by a region of milder drought (-1.5 < SPI < -2), whereas there are a few areas in the eastern part of the study domain with the least degree of drought (-1 < SPI < -1.5).

Figure 3b presents the wettest year in Albacete, occurred in the hydrological year of 1989-1990, where the lowest value of SPI_{12} is 1.02 and the highest value is 2.77. From the same figure, it is observed that the study area is divided into three conceivable zones, where the first zone starts from northwest and is characterized by the lowest degree of wetness (1 < SPI < 1.5), followed by a second zone in immediate proximity to the first zone (1.51 < SPI < 2), and a more extensive zone, which is in the southeastern part of Albacete (SPI > 2).

Figure 3c presents the mapping of a quite normal year in terms of drought. Specifically, SPI_{12} ranges from 0.44 – 0.52 throughout the study area without any extremes, either in terms of drought or wetness.

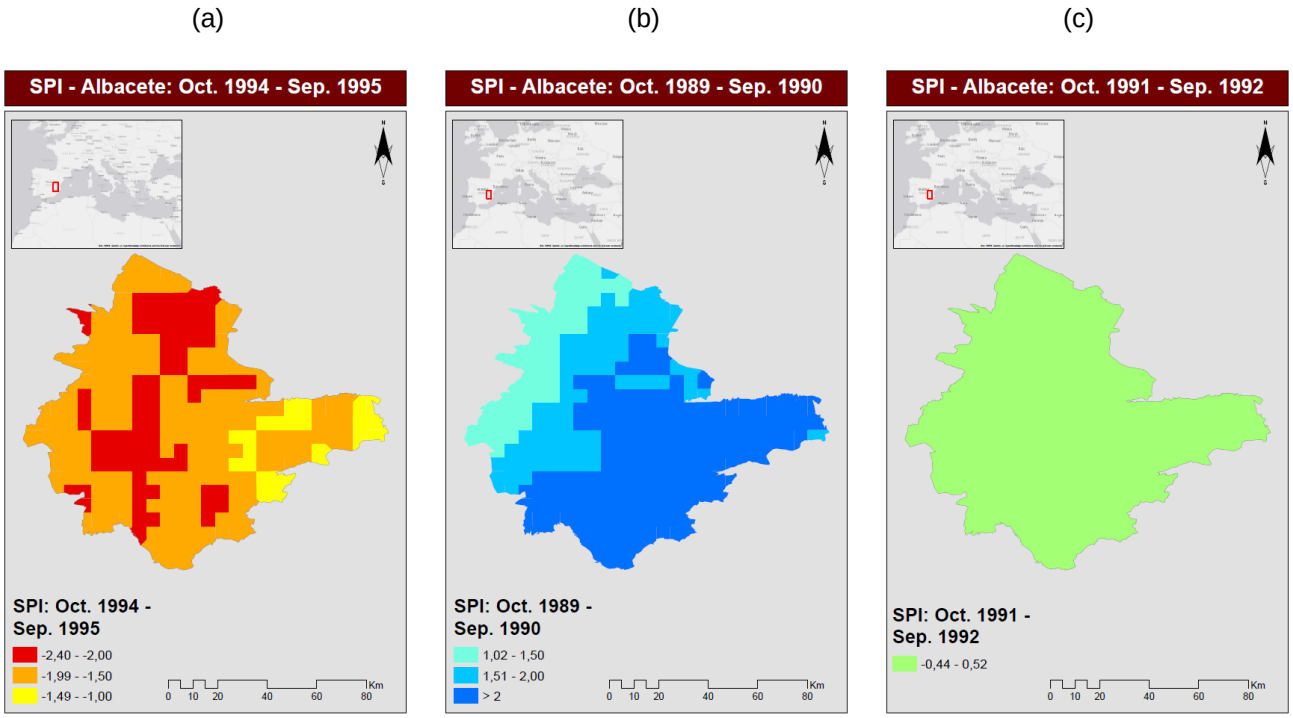

Figure 3. Spatial distribution of SPI_{12} in the (a) driest (b) the wettest and (c) the hydrological year with the most normal conditions

4 Concluding remarks

The quantitative and qualitative drought analysis indicated the hydrological years with the most extreme conditions (extremely dry and extremely wet conditions) in a timeframe of the last 40 years. Beyond this, the mapping of drought conditions can be a useful tool for targeted measures based on drought severity for each pixel. Hence, counterbalancing measures could be taken in the most susceptible regions, especially in the western part of Albacete, whereas the southeastern territory seems to face wetter conditions.

Acknowledgements

The research was funded by the SUPROMED (Sustainable production in water limited environments of Mediterranean agroecosystem) research and innovation (R&I) project funded under the PRIMA 2018 program section I Farming Systems.

References

CHG, 2021. Climate Hazard Group Releases New Version of CHIRPS. Available online: https://geog.ucsb.edu/climate-hazard-groupreleases-new-version-of-chirps/ (accessed on 2 January 2021).

Dalezios, N.R., N. Dercas and S. Eslamian, 2018a. Water Scarcity Management: Part 2: Satellite-based Composite Drought Analysis. I.J.G.E.I., Vol. 17, No 2/3, 267-295.

Dalezios, N. R., Dercas, N., Blanta, A., & Faraslis, I. N. (2018b). Remote sensing in water balance modelling for evapotranspiration at a rural watershed in Central Greece. *International Journal of Sustainable Agricultural Management and Informatics*, *4*(3-4), 306-337.

Dalezios, N.R., Z. Dunkel and S. Eslamian, 2017a: Meteorological Drought Indices: Definitions. Book chapter 3 in Vol. 1 of 3-Volume Handbook of Drought and Water Scarcity (HDWS). Editor: Prof. S. Eslamian. Publisher: Taylor and Francis, 27-44.

Dalezios, N.R., N.V. Spyropoulos and S. Eslamian, 2017b: Remote Sensing in Drought Quantification and Assessment. Book chapter 21 in Vol. 1 of 3-Volume Handbook of Drought and Water Scarcity (HDWS). Editor: Prof. S. Eslamian. Publisher: Taylor and Francis, 377-396.

Du Pissani, C. G., H..J. Fouche and J. C. Venter, (1998): Assessing rangeland drought in South Africa. *Agricultural Systems*: 57: 367-380.

Duan, Z., Liu, J., Tuo, Y., Chiogna, G., & Disse, M. (2016). Evaluation of eight high spatial resolution gridded precipitation products in Adige Basin (Italy) at multiple temporal and spatial scales. *Science of the Total Environment*, *573*, 1536-1553.

EDO, 2021. European Drought Observatory. Available from: https://edo.jrc.ec.europa.eu/documents/factsheets/factsheet_spi.pdf; Accessed on 30/06/2021

Guttman, N. B. (1999). Accepting the standardized precipitation index: a calculation algorithm 1. *JAWRA Journal of the American Water Resources Association*, *35*(2), 311-322.

IPCC, 2012: Managing the Risks of Extreme Events and Disasters to Advance Climate Change Adaptation, Special Report of IPCC, 582p.

Kanellou, E.C., C. Domenikiotis and N.R. Dalezios, 2009a: Description of Conventional and Satellite Drought Indices. pp 23-59. In: G.Tsakiris (ed). PRODIM Final Report, EC, 448p.

Kanellou, E., C. Domenikiotis, E. Tsiros and N.R. Dalezios, 2009b: Satellite-based Drought Estimation in Thessaly. *European Water Association Journal,* 23/24, 111-122.

Mishra, A.K. and V.P. Singh, 2010: A Review of Drought Concepts. J. Hydrology, 39 (1-2), 202-216.

Qin, Y., Yang, D., Lei, H., Xu, K., & Xu, X. (2015). Comparative analysis of drought based on precipitation and soil moisture indices in Haihe basin of North China during the period of 1960–2010. *J. of Hydrology*, *526*, 55-67.

Salinger, J., M.V.K. Sivakumar and R.P. Motha, (Eds), 2005: Increasing Climate Variability and Change: Reducing the Vulnerability of Agriculture and Forestry. Springer, ISBN 1-4020-3354-0,362p.

Sidiropoulos, P., Dalezios, N. R., Loukas, A., Mylopoulos, N., Spiliotopoulos, M., Faraslis, I. N., ... & Sakellariou, S. (2021). Quantitative classification of desertification severity for degraded aquifer based on remotely sensed drought assessment. *Hydrology*, *8*(1), 47.

Steinemann, A. C., Hayes, M. J., & Cavalcanti, L., 2005. Drought indicators and triggers. *Drought and water crises: Science, technology, and management issues*, 71-92.

Thenkabail, P. S., M. S. D. N. Gamage and V. U. Smakhtin, (2004): The use of remote sensing data for drought assessment and monitoring in southwest Asia. *Research Report, International Water Management Institute*, No. 85, 1-25.

Wikipedia, 2022. *Albacete*. Accessible from: https://en.wikipedia.org/wiki/Albacete, on 20/2/2022.

WMO, 2012. World Meteorological Organization: Standardized Precipitation Index. User Guide; WMO: Geneva, Switzerland, 2012.

Zargar, A., R. Sadiq, B. Naser and F.I. Khan, 2011. A review of drought indices. Environ. Rev., 19, 333-349.

Spatiotemporal analysis of drought/wetness extremes in climate change adaptation (1982-2020): The case of Sidi Bouzid Governorate, Tunisia

Sakellariou S.[1], Alpanakis N.[1], Spiliotopoulos M.[1], Faraslis I.[2], Tziatzios G.[1], Sidiropoulos P.[1], Ekklisiarchi P.[4], Tyreli V.[5], Blanta A.[1], Brisimis V.[1], Dalezios N.[1] & Dercas N.[3]

[1] Department of Civil Engineering, University of Thessaly, 38334, Volos, Greece
[2] Department of Environmental Sciences, University of Thessaly, 41500, Larissa, Greece
[3] Department of Natural Resources Management & Agricultural Engineering, Agricultural University of Athens, 11855, Athens, Greece
[4] Pharmacist, Greece
[5] 15th Primary School of Katerini, 60100, Greece

Abstract. Drought is not just a physical phenomenon, because it results from interplay between a natural event and demands placed on water supply by human-use systems. Drought quantification methods rely either on conventional meteorological data or satellite-based data that are consistently available and can be used to detect several drought features and characteristics. Primary aim of the paper consists of the spatiotemporal analysis of drought/wetness extremes in the light of climate change for the last 40 years (1982 – 2020). To this end, the monthly Standardized Precipitation Index (SPI) is calculated based on the precipitation evolution for the last 12 months (SPI_{12}). The results indicated that the driest hydrological year is 2000-2001 (SPI = -1.08), whereas the wettest hydrological year is 1995-1996 (SPI = 1.79). The year with the most normal conditions is 2019-2020 (SPI = 0.03). Concerning the intra-annual analysis of SPI_{12} in the driest hydrological year, there is high degree of fluctuations in drought conditions. The months from February to July and September face extremely drought conditions, where the northern part of the study area being characterized as the driest territory. Beyond this, the mapping of drought conditions through all months in the driest year highlighted that the central and northern part of Sidi Bouzid is characterized by more severe drought conditions as compared to the southern territory. Therefore, a cohesive strategy with specific measures against drought events could be primarily focused on the most susceptible areas, namely the central and the northern regions.

Keywords: Drought intensity; CHIRPS database; SPI12, Sidi Bouzid, Tunisia

1 Introduction

Drought is not just a physical phenomenon, because it results from interplay between a natural event and demands placed on water supply by human-use systems (Heim, 2002). Indeed, there are several regions around the world, which are characterized as vulnerable areas due to the combined effect of temperature increases and reduced precipitation in areas already coping with water scarcity (IPCC, 2012).

Traditional drought quantification methods rely on conventional meteorological data, which are limited in a region, often inaccurate and usually unavailable in near real-time (Thenkabail et al., 2004). On the other hand, satellite-based data are consistently available and can be used to detect several drought features and characteristics. Indeed, the growing number and effectiveness of pertinent Earth Observation (EO) satellite systems present a wide range of new capabilities, which can be used to assess and monitor drought hazard and its effects, such as the activities for droughts of the United Nations International Strategy for Disaster Reduction (UNISDR) (UNIDRS, 2005; UNIDRS, 2015; Dalezios et al., 2018; Dalezios et al., 2017).

Therefore, primary aim of the paper consists of the spatiotemporal analysis of drought/wetness extremes in the light of climate change for the last 40 years (1982 – 2020). To this end, the monthly Standardized Precipitation Index (SPI) is calculated based on the precipitation evolution for the last 12 months (SPI_{12}). The raw precipitation data was retrieved by the CHIRPS database (i.e., Rainfall Estimates from Rain Gauge and Satellite Observations). In addition, the annual and monthly drought conditions are mapped across the study area for the drought extremes.

2 Materials and Methods

2.1 Study area

The study area is *Sidi Bouzid Governorate,* which constitutes one of the 24 governorates (provinces) of Tunisia. It is in the central part of Tunisia. The area of the region amounts to 7,405 km², whereas the population amounts to 429,912 (2014 census). The capital is Sidi Bouzid, which is the most populated part of the region. The geographical coordinates are 35°02′N, 9°30′E. (Wikipedia, 2022). Figure 1 depicts the geographical location of the study area in national (a) and global (b) perspective.

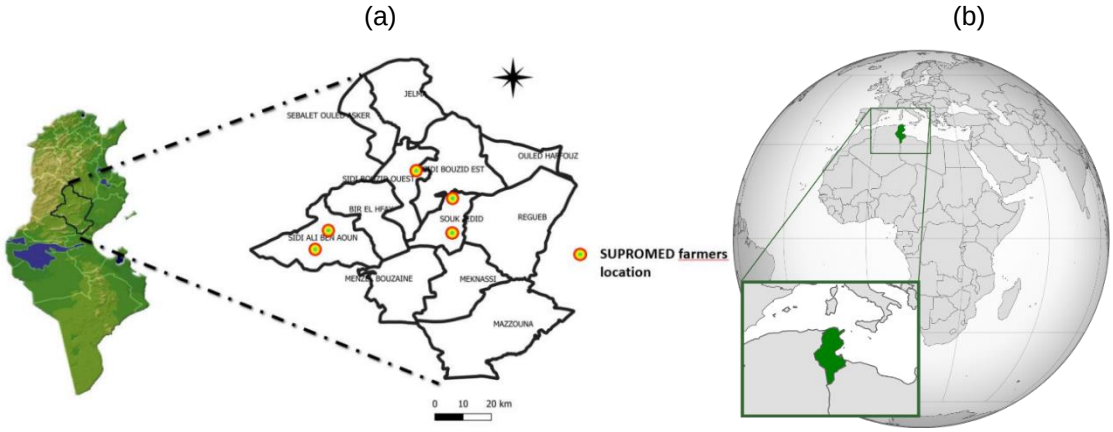

Figure 1. Geographical location of the study area (Sidi Bouzid, Tunisia)

2.2 Data

The precipitation levels in the study domain were estimated through the CHIRPS database (Climate Hazards Group InfraRed Precipitation with Station data). The CHIRPS database incorporates precipitation data on a daily or monthly basis at a spatial resolution of 0.05 and 0.25º, in both cases, for the quasi-global coverage of 50º N–50º S from 1981 up until now (CHG, 2021; Duan et al., 2016). CHIRPS is a fusion of satellite images and data from rain-gauge stations. CHIRPS data perform well at the watershed scale. Monthly CHIRPS products at 0.05º, which corresponds to a spatial resolution of 5 km * 5 km, were used in this study for a timeframe from 1982 to 2020 (Sidiropoulos et al., 2021).

2.3 Methodology

2.3.1 Drought Severity Estimation

Drought severity is conducted exploiting the Standardized Precipitation Index (SPI) (WMO, 2012). This index makes use of precipitation data. The SPI is based on standardized probability to quantify precipitation deficit for multiple time scales, considering the impact of drought for 3-, 6-, 9- and 12-month periods (Qin et al., 2015; Steinemann et al., 2005; Dalezios et al., 2018; WMO, 2012). Based on historical precipitation data, the maximum likelihood is used to estimate the gamma distribution parameters and fit a gamma distribution. Next, the cumulative probability is used for the inverse normal function, resulting in the SPI (Guttman, 1999). In detail, the SPI is computed by dividing the difference between the normalized seasonal precipitation and its long-term seasonal mean by the standard deviation. Certain intervals indicate the degree of drought or wetness across any given area. When SPI value ranges between -0.99 – 0.99, then normal conditions prevail. When SPI value is lower than -1, then differentiated degrees of drought emerge (-1 - -1.49: moderately dry; -1.5 - -1.99: very dry; < -2: extremely dry). On the contrary, when SPI value is higher than 1, then differentiated degrees of wetness emerge (1 - 1.49:

moderately wet; 1.5 - 1.99: very wet; > 2: extremely wet) (EDO, 2021; Sidiropoulos et al., 2021). The monthly SPI_{12} was estimated for this paper.

3 Results and Discussion

This section summarizes the results of SPI_{12} for a historical period from 1982 to 2020. This type of analysis would permit the assessment of the historical driest and wettest conditions occurred in the study area, exploring potential patterns (cycles) in meteorological conditions.

3.1 Spatiotemporal Drought Severity Assessment in Sidi Bouzid (Tunisia) from 1982 to 2020

The results are presented in two ways, namely drought quantification and spatial variability. The first section depicts the estimated values of SPI_{12} for the entire timeframe highlighting the driest and wettest hydrological year as well as the year with the most normal conditions. Table 2 summarizes the SPI_{12} for each hydrological year. At first glance, we observe that the driest hydrological year is 2000-2001 (SPI = -1.08), whereas the wettest hydrological year is 1995-1996 (SPI = 1.79). The year with the most normal conditions is 2019-2020 (SPI = 0.03). Figure 2 depicts the historical evolution of SPI_{12} highlighting the high degree of variability through years.

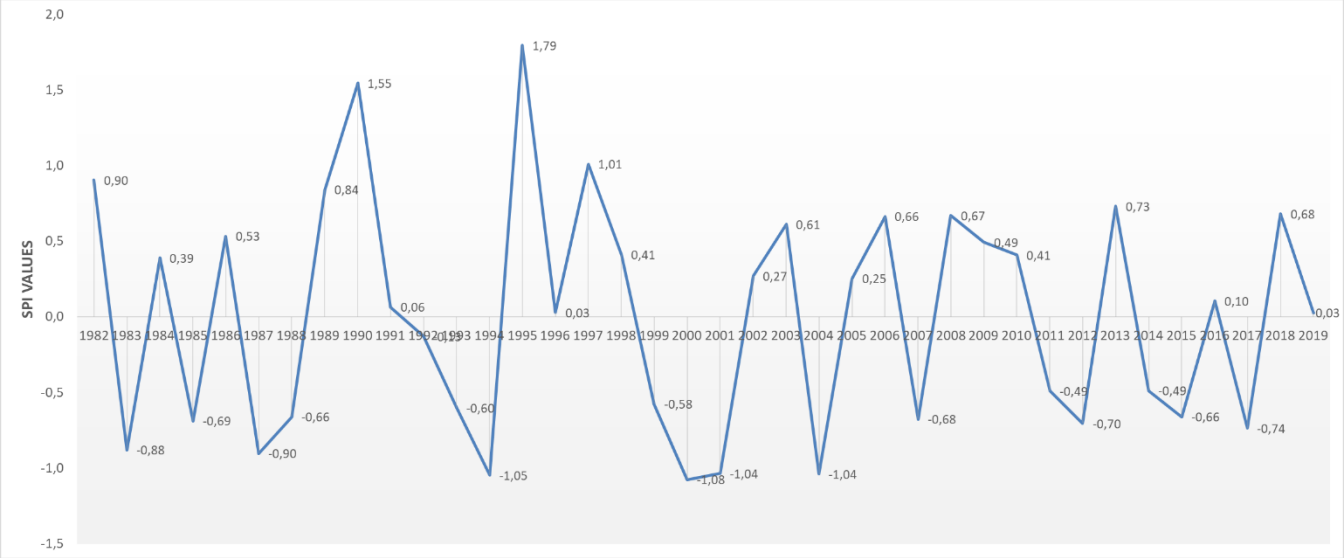

Figure 2. Drought intensity assessment (hydrological years) through SPI_{12} evolution (1982-2020)

The second type of presentation refers to drought spatial variability. Indeed, beyond the average values of SPI_{12}, the frequency distribution for the three representative hydrological years should be determined, exploring the intensity of drought/wetness in the study domain.
Figure 3 presents the number of pixels per drought category in the driest hydrological year (2000-2001). As it is observed, moderately dry conditions prevail in all months, whereas the most severe drought conditions manifest from November to February. Moreover, high number of pixels indicate normal conditions, and a marginal number of pixels show extremely dry conditions.

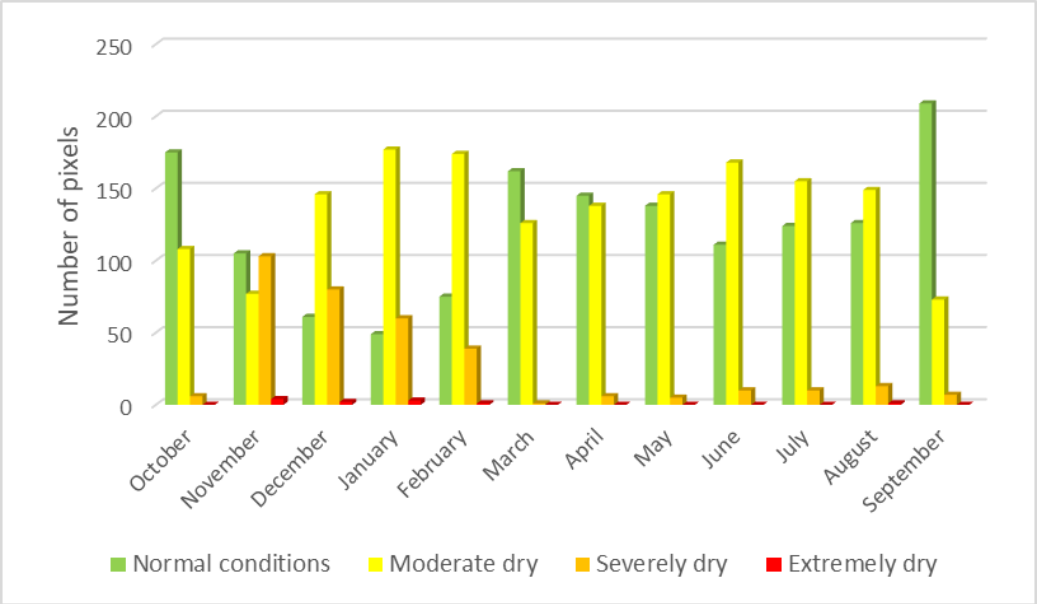

Figure 3. Number of pixels per drought category in the driest hydrological year (2000-2001)

Figure 4 presents the number of pixels per drought category in (a) the wettest and (b) the year with the most normal conditions. As expected, in Figure 4a there is no drought category, however, a few pixels face normal conditions especially from October to December. In Figure 4b, almost all the pixels face normal conditions.

(a) (b)

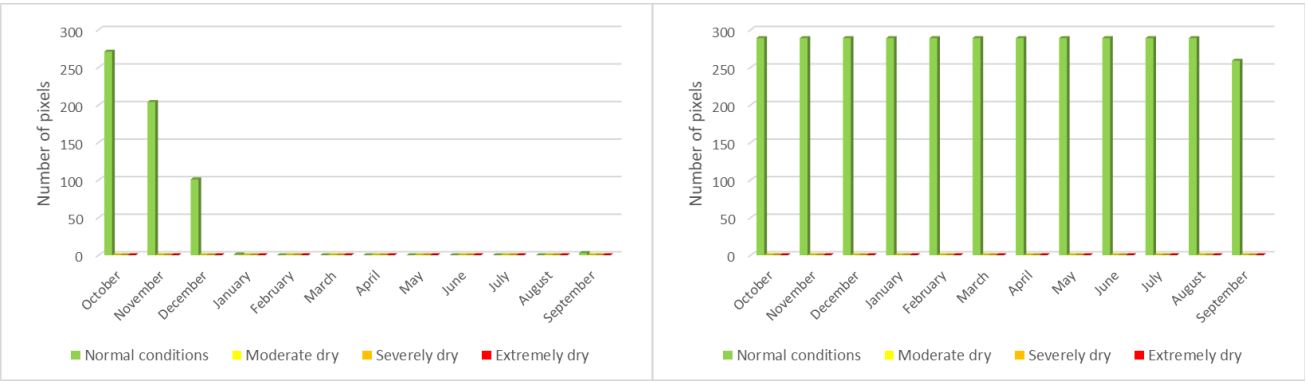

Figure 4. Number of pixels per drought category in (a) the wettest (1995-1996) and (b) the year with the most normal conditions (2019-2020)

In addition to statistical assessment of SPI_{12}, the mapping of extreme conditions can be considered of crucial importance in the study area. Hence, the average SPI_{12} values are mapped for the driest and wettest hydrological years, as well as one year with quite normal conditions. Consequently, the outputs can be a valuable tool for more spatially targeted measures (where needed) to avoid extreme drought conditions with profound implications to crops viability.

Figure 5a shows the second driest hydrological year (1994-1995) in Sidi Bouzid Governorate. The values of SPI range from -1,86 to -1. The driest regions are in the north of the study area (-1.86 < SPI < -1.50), followed by a region in the central part of Sidi Bouzid, which faces moderately drought conditions (-1 < SPI < 1.5), whereas the degree of drought is very close to normal conditions (-1 - 0) in the southern part of the study domain.

Figure 5b depicts the wettest year in Sidi Bouzid occurred in the hydrological year of 1995-1996, where the lowest value of SPI_{12} is 1.18 and the highest value is 2.56. From the same figure, it is observed that the study area is divided by three zones of wetness, where the first one covers almost all the central study area, which is characterized by very wet conditions (1.5 < SPI < 2). A few scattered regions in the north and east part face moderate degree of wetness (1 < SPI < 1.5), whereas the wettest regions of the study area are in the southeastern and northwestern territory (SPI > 2).

Figure 5c presents a quite normal year (2019-2020) in terms of drought. Specifically, SPI_{12} ranges from -0.51 to 0.78 throughout the study area without any extremes, either in terms of drought or wetness.

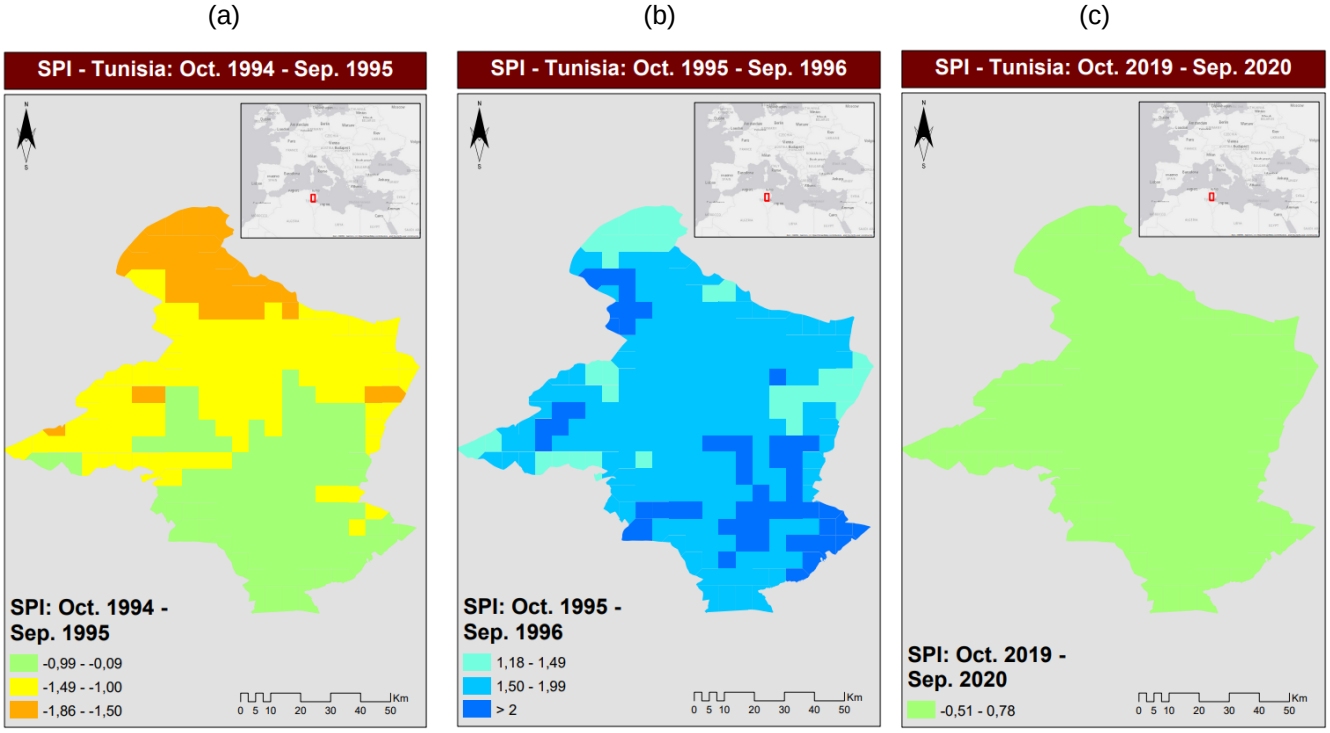

Figure 5. Spatial distribution of SPI_{12} in the (a) driest (b) the wettest and (c) the hydrological year with the most normal conditions

Concerning the intra-annual analysis of SPI_{12} in the second driest hydrological year, there is high degree of fluctuations in drought conditions (Figure 6). Specifically, the months from February to July and September face extremely drought conditions, where the northern part of the study area is characterized as the driest territory (SPI < -2). Moreover, the same months are characterized by moderate and severe drought conditions covering the central part of Sidi Bouzid, where extensive regions are characterized by SPI from -1.5 to -1.99 and from -1 to -1.49. The southern territory of the study area faces normal conditions (-1 < SPI < 1), but it constitutes just a small part of the entire study domain. On the other side, normal conditions prevail from October to December, where extensive regions are characterized by SPI values ranging from -0.99 to 0.99. In addition, a few regions in the north part are characterized by moderate drought conditions (-1.49 < SPI < -1). Almost the entire study domain faces totally normal conditions in September.

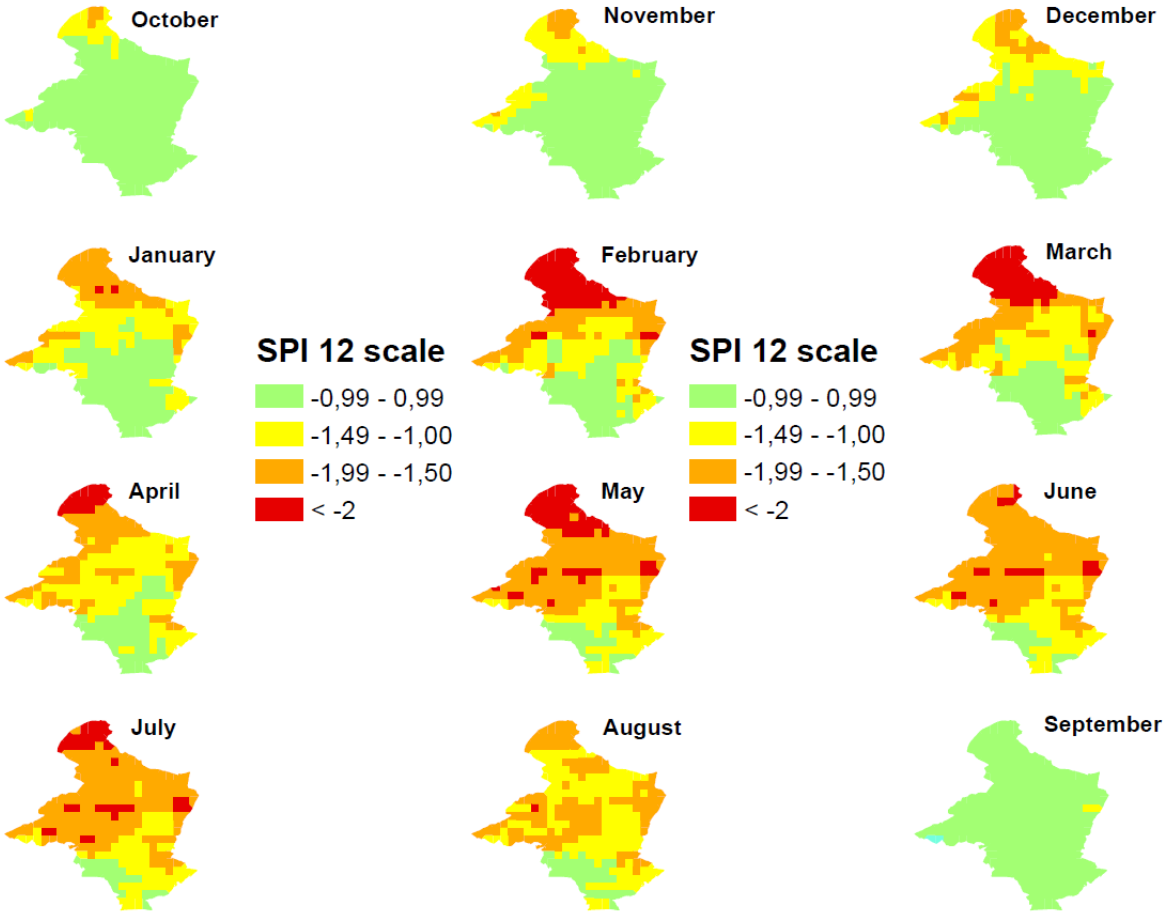

Figure 6. Monthly spatial distribution of SPI_{12} in Sidi Bouzid for the second driest hydrological year (1994-1995)

4 Concluding remarks

The spatiotemporal drought analysis indicated the hydrological years with the most extreme conditions (extremely dry and extremely wet conditions) in a timeframe of the last 40 years. Beyond this, the mapping of drought conditions through all months in the driest year highlighted that the central and northern part of Sidi Bouzid is characterized by more severe dry conditions as compared to the southern territory. Therefore, a cohesive strategy with specific measures against dry events could be primarily focused on the most susceptible areas, namely the central and the northern regions.

Acknowledgements

The research was funded by the SUPROMED (Sustainable production in water limited environments of Mediterranean agro-ecosystem) research and innovation (R&I) project funded under the PRIMA 2018 program section I Farming Systems.

References

Dalezios, N.R., N. Dercas and S. Eslamian, 2018. Water Scarcity Management: Part 2: Satellite-based Composite Drought Analysis. I.J.G.E.I., Vol. 17, No 2/3, 267-295.

Dalezios, N.R., A.M. Tarquis and S. Eslamian, 2017: Drought Assessment and Risk Analysis. Book chapter 18 in Vol. 1 of 3-Volume Handbook of Drought and Water Scarcity (HDWS). Editor: Prof. S. Eslamian. Publisher: Taylor and Francis, 323-343.

EDO, 2021. European Drought Observatory. Available from: https://edo.jrc.ec.europa.eu/documents/factsheets/factsheet_spi.pdf; Accessed on 30/06/2021

Guttman, N. B. (1999). Accepting the standardized precipitation index: a calculation algorithm 1. JAWRA Journal of the American Water Resources Association, 35(2), 311-322.

Heim, R. R. Jr., 2002: A Review of Twentieth-Century Drought Indices Used in the United States. Bulletin of the American Meteorological Society, 83(8), 1149-1165.

IPCC, 2012: Managing the Risks of Extreme Events and Disasters to Advance Climate Change Adaptation, Special Report of IPCC, 582p.

Qin, Y., Yang, D., Lei, H., Xu, K., & Xu, X. (2015). Comparative analysis of drought based on precipitation and soil moisture indices in Haihe basin of North China during the period of 1960–2010. Journal of Hydrology, 526, 55-67.

Sidiropoulos, P., Dalezios, N. R., Loukas, A., Mylopoulos, N., Spiliotopoulos, M., Faraslis, I. N., ... & Sakellariou, S. (2021). Quantitative classification of desertification severity for degraded aquifer based on remotely sensed drought assessment. *Hydrology*, *8*(1), 47.

Steinemann, A. C., Hayes, M. J., & Cavalcanti, L., 2005. Drought indicators and triggers. Drought and water crises: Science, technology, and management issues, 71-92.

Thenkabail, P. S., M. S. D. N. Gamage and V. U. Smakhtin, (2004): The use of remote sensing data for drought assessment and monitoring in southwest Asia. Research Report, International Water Management Institute, No. 85, 1-25.

UNISDR, 2005. Hyogo framework for Action 2005-2015. Building the Resilience of Nations and Communities to Disasters. United Nations, International Strategy for Disaster Reduction, Geneva, Switzerland. http://www.unisdr.org/eng/hfa/hfa.htm.

UNISDR, 2015. Reading the Sendai framework for disaster risk reduction 2015-2030. UNISDR, Geneva, Switzerland, 34p.

Wikipedia, 2022. Sidi Bouzid Governorate. Accessible from: https://en.wikipedia.org/wiki/Sidi_Bouzid_Governorate, on 20/3/2022.

WMO, 2012. World Meteorological Organization: Standardized Precipitation Index. User Guide; WMO: Geneva, Switzerland, 2012.

Long-term assessment of environmental extremes to enhance spatial resilience: The case of drought in Beqaa Valley, Lebanon

Sakellariou S.[1], Alpanakis N. [1], Sidiropoulos P. [1], Tziatzios G.[1], Faraslis I.[2], Spiliotopoulos M. [1], Blanta A. [1], Brisimis V. [1], Dalezios N.[1] & Dercas N. [3]

[1] Department of Civil Engineering, University of Thessaly, 38334, Volos, Greece
[2] Department of Environmental Sciences, University of Thessaly, 41500, Larissa, Greece
[3] Department of Natural Resources Management & Agricultural Engineering, Agricultural University of Athens, 11855, Athens, Greece

Abstract. The impacts of a drought event may be severe and are neither immediate nor easily measured. Drought impacts are very critical and especially costly affecting more people than any other type of natural disaster universally. Consequently, primary aim of the paper is the long-term estimation of environmental extremes (drought and wetness) to enhance spatial resilience. Spatial resilience can be achieved by taking the appropriate counterbalancing measures (spatially determined) against drought. To this end, precipitation data are explored, as provided by the CHIRPS database, to calculate (both statistically and spatially) the monthly Standardized Precipitation Index (SPI) based on the precipitation evolution for the last 12 months (SPI_{12}). Based on the analysis results in the study area of Beqaa Valley, Lebanon, the driest hydrological year was 1989-1990 (SPI = -1.39), whereas the wettest hydrological year occurred in 2018-2019 (SPI = 2.28). The long-term analysis indicated high degree of temporal variability in terms of drought/wetness through years. It is remarkable that in the driest year, the pilot study area was characterized by severe drought, whereas the neighboring regions primarily presented moderate drought or even normal conditions. Such situations should activate specific counterbalancing measures on the ground, so that the spatial resilience of the study area can be enhanced against extreme and damaging conditions as severe drought may heavily affect the agricultural production, as well as the viability of underground resources, which might be crucial for several socioeconomic activities.

Keywords: Drought; SPI; drought / wetness mapping; Beqaa Valley, Lebanon

1 Introduction

The impacts of a drought event may be severe and are neither immediate nor easily measured. It is difficult to determine the effects of drought as it constitutes a complicated phenomenon, evolving gradually in any single region. Drought impacts are very critical and especially costly affecting more people than any other type of natural disaster universally (Keyantash and Dracup, 2002). All the above may accumulate difficulties in drought assessment and response, which may result into slow progress on drought preparedness plans and mitigation actions.

In terms of climate variability, there is medium confidence that since the 1950s some regions of the world have experienced more intense and longer droughts (IPCC, 2012). Land use changes have potential impacts on droughts (Arneth et al., 2014) and anthropogenic forcing has contributed to the global trend towards increased drought in the second half of the 20th century. Extreme climate variables and climate extremes, such as droughts, are projected to experience significant changes over the 21st century, just as they have during the past century, in many areas, including Southern Europe, among others (Nastos et al., (eds.), 2016; Tarquis et al., (eds.), 2013). Remote sensing data and methods can delineate the quantitative spatial and temporal variability of several drought features (Kanellou et al., 2012; Dalezios et al., 2014). Thus, there is a need for proper remotely sensed quantification of drought and drought impacts, so that the spatial drought resilience in any potentially affected region can be enhanced.

Consequently, primary aim of the paper is the long-term estimation of environmental extremes (drought and wetness) to enhance spatial resilience. Spatial drought resilience can be achieved by taking the appropriate

counterbalancing measures (spatially determined) against drought. To this end, precipitation data are used, as provided by the CHIRPS database, to calculate (both statistically and spatially) the monthly Standardized Precipitation Index (SPI) based on the precipitation evolution for the last 12 months (SPI_{12}), through the transformation of gamma cumulative distribution to standardized normal distribution (Qin et al., 2015).

2 Materials and Methods

2.1 Study area

The study area extends into the Beqaa Valley in Lebanon. The valley is situated between Mount Lebanon to the west and the Anti-Lebanon mountains to the east. Beqaa Valley is 120 km long and 16 km wide on average. It has a Mediterranean climate of wet, often snowy winters and dry, warm summers. The geographical coordinates are: 33° 49'N, 36° 0'E. (Wikipedia, 2022). The pilot study area in Lebanon is depicted in Figure 1.

(a) (b)

Figure 1. Geographical location of the study area (Beqaa Valley, Lebanon)

2.2 Data

The precipitation data was retrieved by the CHIRPS database (Climate Hazards Group InfraRed Precipitation with Station data), which is based on satellite and ground data. The CHIRPS database incorporates precipitation data on a daily or monthly basis at a spatial resolution of 0.05 and 0.25º, in both cases, for the quasi-global coverage of 50º N–50º S from 1981 to present (CHG, 2021; Duan et al., 2016). CHIRPS is a fusion of satellite images and data from rain-gauge stations. Monthly CHIRPS products at 0.05º, which corresponds to a spatial resolution of 5 km * 5 km, were used in this study for the period 1981–2020 (Sidiropoulos et al., 2021).

2.3 Methodology

2.3.1 Drought Severity Assessment and mapping

Drought severity assessment is usually estimated using the Standardized Precipitation Index (SPI) (WMO, 2012), which is relied solely on precipitation data. The SPI is based on the standardized probability to quantify precipitation deficit by considering the status of previous months, such as for 3-, 6-, 9- and 12-month periods (Qin et al., 2015;

Steinemann et al., 2005; Dalezios et al., 2018; WMO, 2012). Based on historical long-term rainfall data, the maximum likelihood is used to estimate the gamma distribution parameters and fit a gamma distribution. Then, the cumulative probability is used for the inverse normal function, resulting in the SPI (Guttman, 1999). Specifically, the SPI is computed by dividing the difference between the normalized seasonal precipitation and its long-term seasonal mean by the standard deviation. A classification scheme is used to determine the degree of drought/ wetness conditions (Table 1). When SPI is lower than -1, differentiated degrees of drought occur. Conversely, when SPI is higher than 1, differentiated degrees of wet conditions prevail. The SPI_{12} has been calculated for each month through the entire timeframe (1982-2020). Seven classes of SPI are shown in Table 1 (EDO, 2021; Sidiropoulos et al., 2021). For the spatial distribution of drought/wetness conditions, geostatistical methods are used to accurately depict the variability of SPI and the respective drought / wetness condition per pixel.

Table 1. SPI classification scheme

SPI intervals	Drought / Wetness condition
> 2	Extremely wet
1.5 – 1.99	Very wet
1 – 1.49	Moderately wet
-0.99 – 0.99	Normal precipitation
-1 – -1.49	Moderately dry
-1.5 – -1.99	Very dry
< -2	Extremely dry

EDO, 2021 (adjusted)

3 Results and Discussion

This section describes the results of SPI_{12} for a historical period from 1982 to 2020 for the Bequa Valley region, Lebanon. This type of analysis would allow the exploration of the historical driest and wettest conditions, which occurred in the study area, exploring potential patterns (cycles) in meteorological conditions.

3.1 Drought Severity Estimation and Mapping

Figure 2 presents the estimated values of SPI_{12} for the entire timeframe highlighting the driest and wettest hydrological year in the study area. It is observed that the driest hydrological year is 1989-1990 (SPI = -1.39), whereas the wettest hydrological year is 2018-2019 (SPI = 2.28).

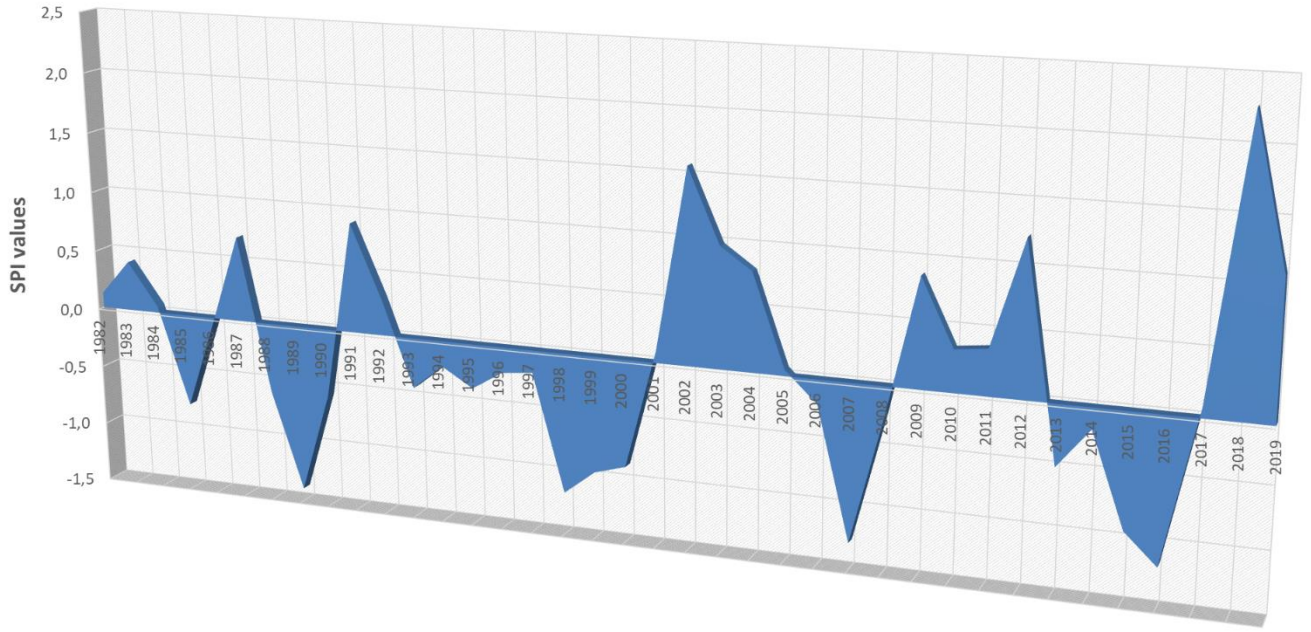

Figure 2. Long-term estimation of dry and wet conditions through SPI_{12} from 1982-2020 in Beqaa Valley, Lebanon.

Next, the extreme conditions are mapped as evolved across the whole territory of the study area. The spatial distribution of environmental extremes is considered of outmost importance since the spatial and territorial resilience against extreme drought may be enhanced. To this end, the average SPI values are mapped for the driest and wettest hydrological year. Consequently, the outputs can be a valuable tool for more spatially targeted measures (where needed) to avoid extreme drought conditions with profound implications to crops viability.

Figure 3a depicts the driest year in Lebanon throughout the time reference (1982-2020). The values of SPI range from -1.92 to -0.67. The driest regions (-1.99 < SPI < -1.5) are in the central part of Lebanon (inside the pilot study area, followed by extensive regions in the east). The southwestern part of Lebanon is characterized by normal conditions, whereas the remaining territory primarily faces moderately drought conditions (-1.49 < SPI < -1). Figure 3b shows the wettest year in the study domain occurred in the hydrological year of 2018-2019, where the lowest value of SPI_{12} is 1.42 and the highest value is 2.9. The greatest part of Lebanon is characterized by extremely wet conditions (SPI > 2), whereas there are some scattered regions with slightly less wetness (1 < SPI < 2). Almost the entire pilot study area faces extremely wet conditions.

(a) (b)

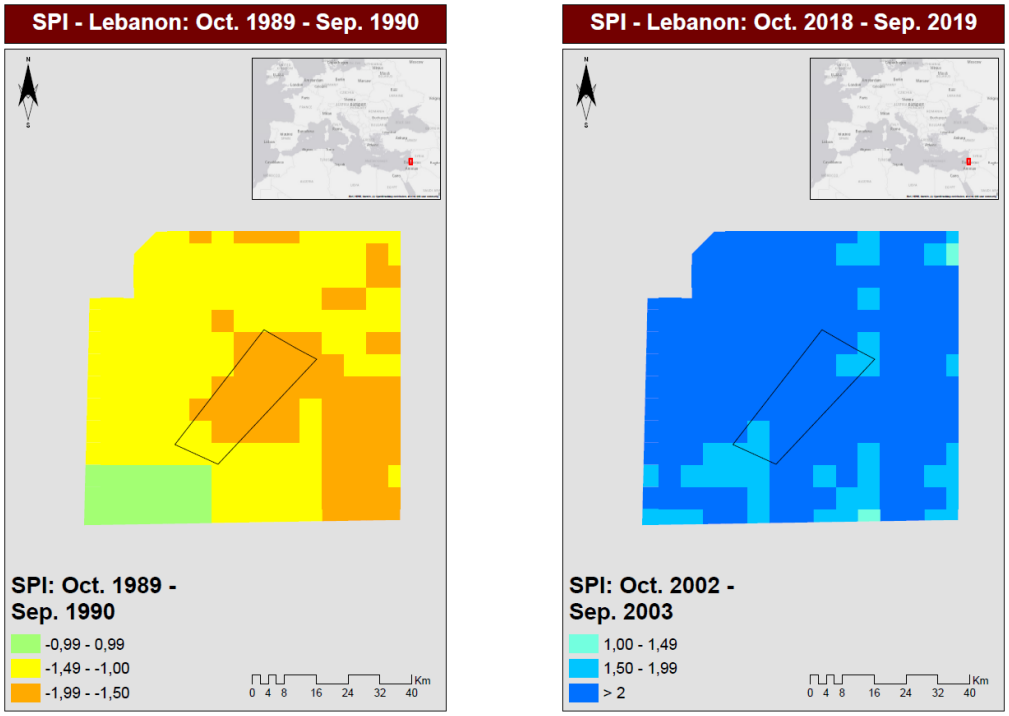

Figure 3. Spatial distribution of SPI12 in Beqaa Valley, Lebanon, in the (a) driest, (b) wettest hydrological year.

From Table 2 and Figure 4 it is observed that there is a mosaic of variable drought conditions. Table 2 presents the percentage contribution of the pixels falling into different levels of drought indicating the dominance of moderately drought conditions from February to September (48-68% of the entire study area); the dominance and strong impact of severely drought conditions from October to January (40-63% of the entire study area); the dominance of extremely drought conditions in December (58% of the entire study area).

Table 2. Percentage contribution of pixels falling into different levels of drought in Lebanon (1989-1990)

Hydrological Year	Month	Normal conditions	Moderate dry	Severely dry	Extremely dry
1989	October	14%	45%	40%	1%
1989	November	8%	39%	44%	9%
1989	December	0%	0%	42%	58%
1990	January	0%	10%	63%	28%
1990	February	38%	54%	8%	0%
1990	March	9%	48%	38%	5%
1990	April	13%	67%	20%	0%

1990	May	14%	67%	19%	0%
1990	June	14%	67%	19%	0%
1990	July	14%	67%	19%	0%
1990	August	14%	67%	19%	0%
1990	September	14%	68%	18%	0%

Most of the regions are primarily characterized by moderate drought conditions (up to 68% of the entire area). Fewer regions face severe drought conditions (up to 68% of the entire area), whereas a few regions face normal conditions and even fewer regions are characterized by extreme drought conditions (especially in December and January).

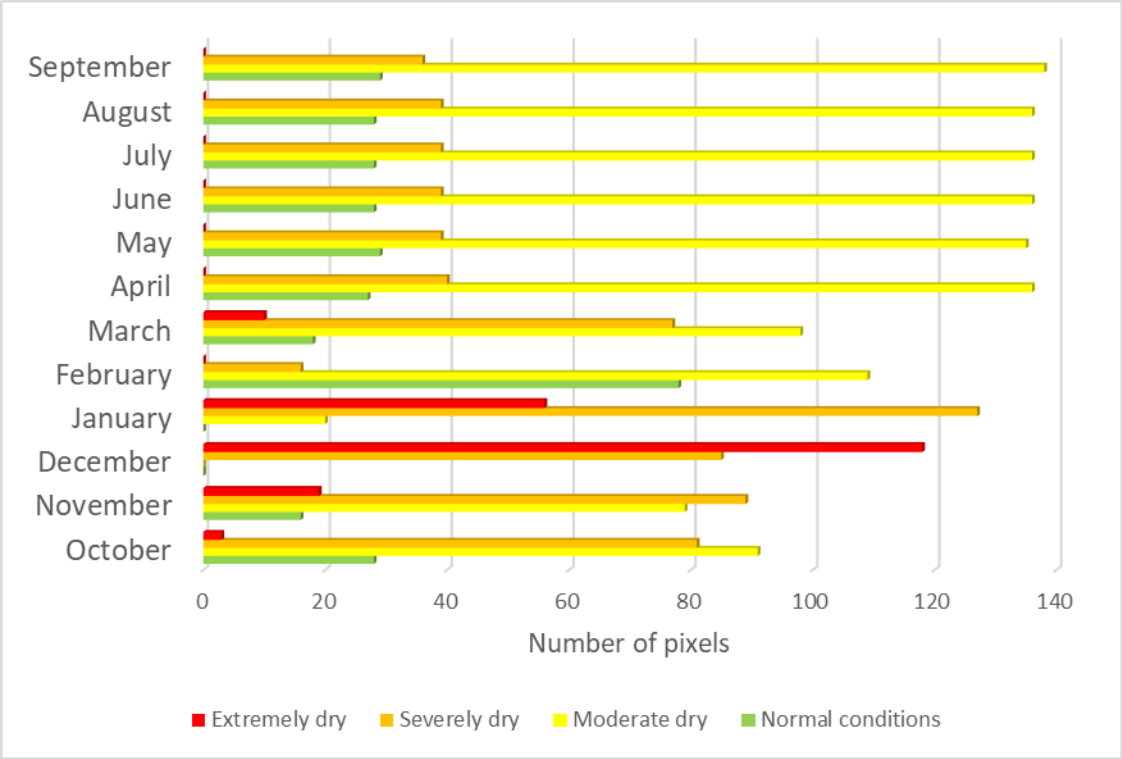

Figure 4. Number of pixels per drought category in the driest hydrological year (1989-1990), in Beqaa Valley

4 Summary and Conclusions

The spatiotemporal analysis of drought evolution highlighted the hydrological years with the most extreme conditions (extremely dry and extremely wet conditions) from 1982 to 2020. The analysis included the statistical and spatial estimation of SPI, a drought index that is widely used for these types of problems. Hence, high degree of drought variability is observed in terms of drought/wetness through time. It is remarkable that in the driest year, the pilot study area was characterized by severe drought, whereas the neighboring regions primarily presented moderate drought or even normal conditions. Such situations should activate specific counterbalancing measures on the ground, so that the spatial drought resilience of the study area can be enhanced against extreme and damaging conditions, as severe drought may heavily affect the agricultural production, as well as the viability of underground resources, which might be crucial for several socioeconomic activities.

Acknowledgements

The research was funded by the SUPROMED (Sustainable production in water limited environments of Mediterranean agro-ecosystem) research and innovation (R&I) project funded under the PRIMA 2018 program section I Farming Systems.

References

Arneth, A., C. Brown, and M. D. A. Rounsevell, (2014). Global models of human decision-making for land-based mitigation and adaptation assessment, Nature Climate Change, 4(7), 550-557.

CHG, 2021. Climate Hazard Group Releases New Version of CHIRPS. Available online: https://geog.ucsb.edu/climate-hazard-groupreleases-new-version-of-chirps/ (accessed on 2 January 2021).

Dalezios, N.R., A. Blanta, N.V. Spyropoulos and A.M. Tarquis, 2014: Risk Identification of Agricultural Drought for Sustainable Agroecosystems. NHESS, 14, 2435-2448.

Dalezios, N. R., Dercas, N., & Eslamian, S., 2018. Water scarcity management: part 2: satellite-based composite drought analysis. International Journal of Global Environmental Issues, Vol.17 (2/3), 267-295.

Duan, Z., Liu, J., Tuo, Y., Chiogna, G., & Disse, M. (2016). Evaluation of eight high spatial resolution gridded precipitation products in Adige Basin (Italy) at multiple temporal and spatial scales. Science of the Total Environment, 573, 1536-1553.

EDO, 2021. European Drought Observatory. Available from: https://edo.jrc.ec.europa.eu/documents/factsheets/factsheet_spi.pdf; Accessed on 30/06/2021

Guttman, N. B. (1999). Accepting the standardized precipitation index: a calculation algorithm 1. JAWRA Journal of the American Water Resources Association, 35(2), 311-322.

IPCC, 2012: Managing the Risks of Extreme Events and Disasters to Advance Climate Change Adaptation, Special Report of IPCC, 582p.

Kanellou, E., N. Spyropoulos, N.R. Dalezios, 2012. Geoinformatic Intelligence Methodologies for Drought Spatiotemporal Variability in Greece. Water Resour. Management, March, Volume 26 (5), 1089-1106.

Keyantash, J., and Dracup, J. A., 2002: The Quantification of Drought: An Evaluation of Drought Indices. Bulletin of American Meteorological Society, 1167-1180.

Nastos. P., Dalezios N.R. and U. Ulbrich (editors), 2016: Advances in Meteorological Hazards and Extreme events. Special Issue of NHESS.

Qin, Y., Yang, D., Lei, H., Xu, K., & Xu, X. (2015). Comparative analysis of drought based on precipitation and soil moisture indices in Haihe basin of North China during the period of 1960–2010. J, of Hydrology, 526, 55-67.

Sidiropoulos, P., Dalezios, N. R., Loukas, A., Mylopoulos, N., Spiliotopoulos, M., Faraslis, I. N., ... & Sakellariou, S. (2021). Quantitative classification of desertification severity for degraded aquifer based on remotely sensed drought assessment. *Hydrology*, *8*(1), 47.

Steinemann, A. C., Hayes, M. J., & Cavalcanti, L., 2005. Drought indicators and triggers. Drought and water crises: Science, technology, and management issues, 71-92.

Tarquis A.M., A. Gobin, U. Ulbrich and N.R.Dalezios (Editors), 2013: "Weather Related Hazards and Risks in Agriculture". Special Issue of NHESS journal.

WMO, 2012. World Meteorological Organization: Standardized Precipitation Index. User Guide; WMO: Geneva, Switzerland, 2012.

Climate change adaptation: water availability in Albacete (Spain) through spatial and temporal drought analysis

Sakellariou S.[1], Alpanakis N. [1], Spiliotopoulos M. [1], Faraslis I.[2], Tziatzios G.[1], Sidiropoulos P. [1], Blanta A. [1], Brisimis V. [1], Dalezios N.[1], Dercas N. [3], Karoutsos G[4]. and Kartsios S.[4]

[1] Department of Civil Engineering, University of Thessaly, 38334, Volos, Greece
[2] Department of Environmental Sciences, University of Thessaly, 41500, Larissa, Greece
[3] Department of Natural Resources Management & Agricultural Engineering, Agricultural University of Athens, 11855, Athens, Greece
[4] General Aviation Applications "3D" S.A., 2 Skiathou Str., 54646 Thessaloniki Greece

Abstract. Any drought event begins with a deficiency of precipitation in a region over a period. The use of remotely sensed drought indices is anticipated to increase significantly in the following years due to the availability of precipitation and temperature satellite-based data platforms at a global scale, besides the increasing technological and computational advances. Primary aim of the paper consists of the water availability estimation in Albacete (Spain) through spatial and temporal drought analysis for the next 30 years (2020 - 2050). To achieve this, monthly precipitation data are simulated and predicted through the Weather and Forecasting Model. Next, the Standardized Precipitation Index (SPI) is estimated based on the precipitation evolution for the last 12 months. The results showed that there is no significant variability, indicating a few years with either moderate dry or wet conditions. The driest hydrological year is projected to be in 2046 – 2047 (SPI = -1.24), whereas the wettest year is projected to be in 2045 – 2046 (SPI = 1.62). However, the intra-annual analysis indicated severe and extreme drought throughout Albacete from April to September. This type of analysis could be a valuable tool for spatially targeted measures based on drought i for each pixel. Thus, counterbalancing measures could be adopted in the most vulnerable regions.

Keywords: Drought; Remote Sensing; Weather Research & Forecasting (WRF); CHIRPS database; Albacete, Spain

1 Introduction

Any drought event begins with a deficiency of precipitation in a region over a period. These early stages of accumulated departure of precipitation from normal or expected are usually considered as meteorological drought (Dalezios et al., 2017). A continuation of these dry conditions over a longer period, sometimes in association with above-normal temperatures, high winds, and low relative humidity, quickly result into impacts in the agricultural and hydrological sectors. Specifically, except for meteorological drought, the other types of droughts, such as agricultural and hydrological, emphasize on the human or social aspects of drought, in terms of the interaction between the natural characteristics of meteorological drought and human activities that depend on precipitation, to provide adequate water supplies to meet societal and environmental demands (Dalezios et al., 2014). For assessing and monitoring droughts, several drought features are usually detected, such as severity, periodicity, duration, onset, end time and areal extent. (Dalezios et al. 2017; Mishra and Singh, 2010).
The use of remotely sensed drought indices is anticipated to increase significantly in the following years due to the availability of precipitation and temperature satellite-based data platforms at a global scale, besides the increasing technological and computational advances (Eslamian & Eslamian, 2017). There are solely precipitation drought indices, such as Effective Drought Index (EDI) (Byun and Wilhite, 1999) and Drought Frequency Index (DFI) (Gonzalez and Valdez, 2006). The Palmer Drought Severity Index (PDSI) is categorized as a "comprehensive" drought index (Niemeyer, 2008) and remains a popular index. Improvements include self-calibration capacity and modifications in the estimation of evapotranspiration by replacing the original Thornthwaite method (Thornthwaite, 1948) with other formulations and/or remotely sensed estimation (Dalezios et al., 2012).

The Standardized Precipitation Index (SPI) is an index that is used for the estimation of meteorological drought for several time scales. The SPI values indicate “the number of standard deviations by which the observed anomaly deviates from the long-term mean”. Its main drawback lies in the fact that it does not account for changes in evapotranspiration (NCAR, 2022a).
The primary aim of the paper consists of the water availability estimation in Albacete (Spain) through spatial and temporal drought analysis for the next 30 years (2020 - 2050). To achieve this, precipitation data are used as provided by the CHIRPS database, so that we can feed the Weather Research and Forecasting (WRF) Model can be fed and predict the monthly precipitation data in the long run. Next, the Standardized Precipitation Index (SPI) is estimated based on the precipitation evolution for the last 12 months (SPI_{12}), through the transformation of gamma cumulative distribution to standardized normal distribution (NCAR, 2022a; Qin et al., 2015).

2 Materials and Methods

2.1 Study area

The proposed methodology has been implemented in Albacete region, which is a Spanish province that is situated in the south-eastern part of Spain (Figure 1). The total area of Albacete is 14,858 km^2. There are 387,658 people that live in the study area, whereas the population density amounts to 26 people per km^2. The geographical coordinates are: 38^o 50’ N, 2^o 00’ W (Wikipedia, 2022). Albacete primarily constitutes an agricultural region, and the applied methodology has been conducted under the SUPROMED European research project.

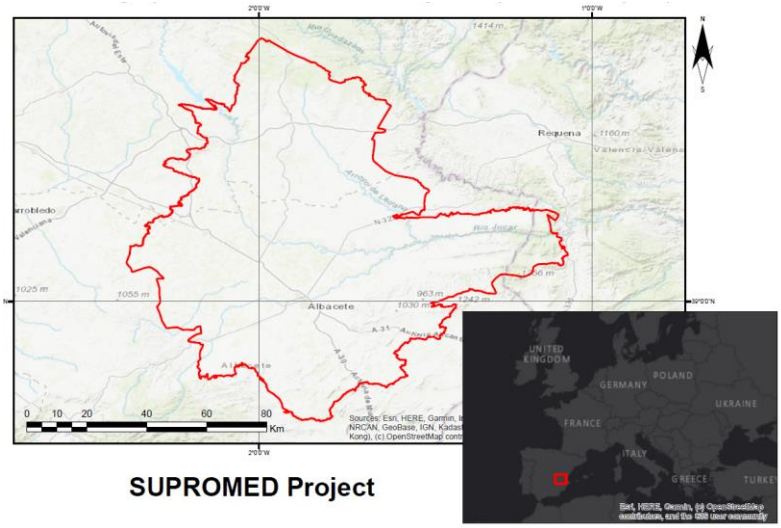

Figure 1. Geographical position of Albacete, Spain

2.2 Data

The primary data used in the current analysis consists of precipitation data that was retrieved by CHIRPS (Climate Hazards Group InfraRed Precipitation with Station data) database. The CHIRPS database consists of daily or monthly precipitation data at spatial resolution of 0.05 and 0.25^o for the quasi-global coverage of 50^o N–50^o S from 1982 to present (CHG, 2021; Duan et al., 2016). CHIRPS is a fusion of satellite images and data from rain-gauge stations. Historical monthly CHIRPS products (1982-2020) with spatial resolution of 5 km * 5 km, were used in this study for the projection of precipitation evolution from 2020 to 2050 (Sidiropoulos et al., 2021).

2.3 Methodology

2.3.1 Projected Drought Severity and Water Availability Estimation (2020 – 2050)

In general, drought severity estimation assessment makes use of the Standardized Precipitation Index (SPI) (WMO, 2012), which is relied on precipitation data. The SPI is based on standardized probability to quantify precipitation deficit for multiple time scales (i.e., from 1 to 36 months) (Qin et al., 2015; Steinemann et al., 2005; Dalezios et al., 2018; WMO, 2012). Based on historical long-term rainfall data, the maximum likelihood is used to estimate the gamma distribution parameters and fit a gamma distribution. Then, the cumulative probability is used for the inverse normal function, resulting in the SPI (Guttman, 1999). In detail, the SPI is computed by dividing the difference between the normalized seasonal precipitation and its long-term seasonal mean by the standard deviation (Sidiropoulos et al., 2021). Hence, to implement the above methodology for the following 30 years, the Weather Research and Forecasting (WRF) Model is used, a model that is employed for the simulation of atmospheric processes based on actual atmospheric conditions (i.e., from observations of historical data retrieved by the CHIRPS database) (NCAR, 2022b). Having estimated the projected precipitation data, the SPI values are calculated for the entire timeframe and mapped the SPI spatial distribution of the study area to determine the differentiated levels of drought/wetness in space. This process would facilitate the targeted measures against severe drought conditions for the regions, which might suffer the most. SPI values among -0.99 to 0.99 indicate normal conditions; SPI values above 1 designate wet condition, whereas SPI values below -1 indicate drought events. The higher the values, the higher the severity of wetness/drought (EDO, 2021).

3 Results and Discussion

This section describes the results of SPI_{12} for the projected period from 2021 to 2050. This type of analysis would allow us to predict the driest and wettest conditions occurred in the study area, providing the necessary information for taking the respective counterbalancing measures against severe drought conditions.

3.1 Projected Drought Intensity and Water Availability Estimation (2020 – 2050)

Figure 2 depicts the predicted SPI evolution based on the projected precipitation data from 2020 to 2049 based on WRF. There is no significant variability since the values range from -1.24 to 1.62 indicating a few years with either moderate dry or wet conditions. As it can be observed, the driest hydrological year is projected to be in 2046 – 2047 (SPI = -1.24), whereas the wettest year is projected to be one year earlier, namely, in 2045 – 2046 (SPI = 1.62). The standard deviation of this time series analysis amounts to 0.79.

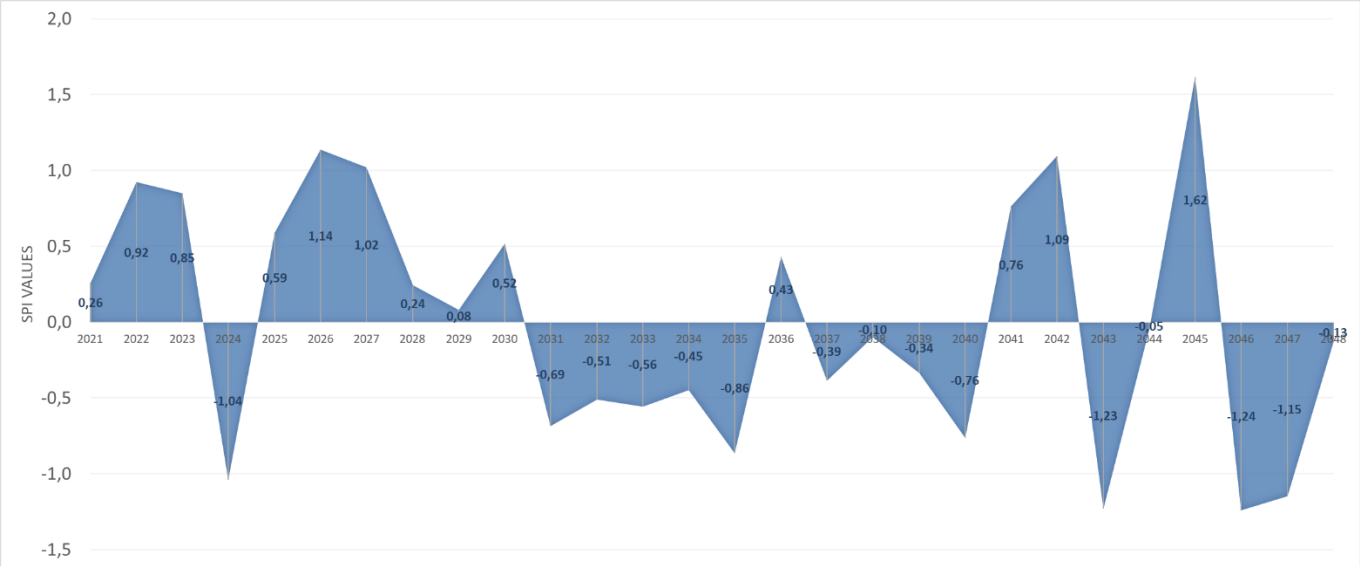

Figure 2. Predicted drought assessment through SPI evolution (2021-2049)

Nevertheless, beyond the average values of SPI_{12}, the severity of drought/wetness is spatially determined in the study domain focusing on the most extreme situations. Beyond the statistical assessment of SPI_{12}, the mapping of extreme conditions for each pixel in the study area can be considered of crucial importance. To this end, the average SPI_{12} values are mapped for the driest and wettest hydrological year. Consequently, the outputs can be a valuable tool for more spatially targeted measures (where needed) to avoid extreme drought conditions with profound implications on crops viability.

The driest hydrological year has been projected to be in 2046-2047. In this hydrological year, the greatest part of the study area is characterized by moderate degree of drought (-1.49 < SPI < -1), whereas a small region in the northeastern part of Albacete tends to face severe drought conditions (-1.99 < SPI < -1.5). Once more, the eastern region is characterized by normal conditions in the driest hydrological year (Figure 3a). On the other side, the previous hydrological year (2045-2046) tends to be the wettest one (Figure 3b). Here, Albacete has been divided into four distinct zones. The northern part, which is characterized by normal conditions; the next adjacent zone which is situated below the previous region and characterized by wetter conditions (1 < SPI < 1.49); the central and southern part of Albacete presents even wetter conditions (1.5 < SPI < 1.99), whereas the wettest region of the study area is located in the eastern Albacete (SPI > 2).

(a) (b)

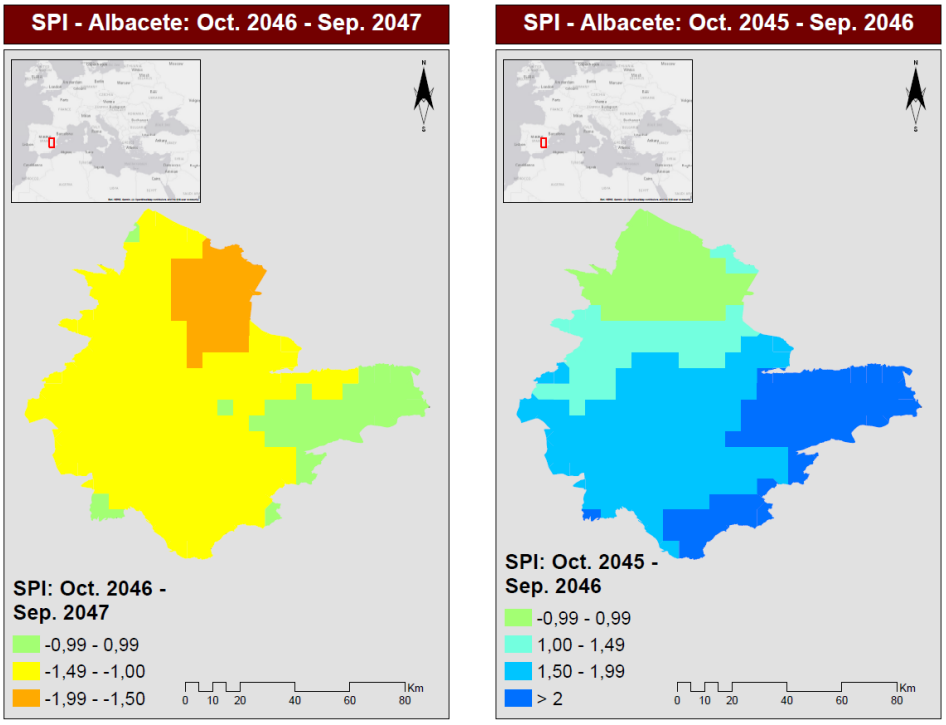

Figure 3. Spatial distribution of predicted SPI_{12} of Albacete, in the (a) driest (b) the wettest hydrological year

Next, an intra-annual analysis is conducted to estimate regions, which suffer the most from severe drought conditions. Figure 4 depicts the predicted monthly SPI_{12} evolution from 2046 to 2047 (dry conditions). At the beginning of this hydrological year (from October to December), normal and wet conditions prevail in almost the entire Albacete. Two diagonally opposite regions emerge from January to March, which face moderate drought conditions. These areas can be in the northeastern and southern part of Albacete. However, almost the entire study area is characterized by extremely drought conditions (SPI < -2), especially from June to September. This phenomenon is less severe in April and May, since ¾ of Albacete faces moderate and severe drought conditions but not extreme.

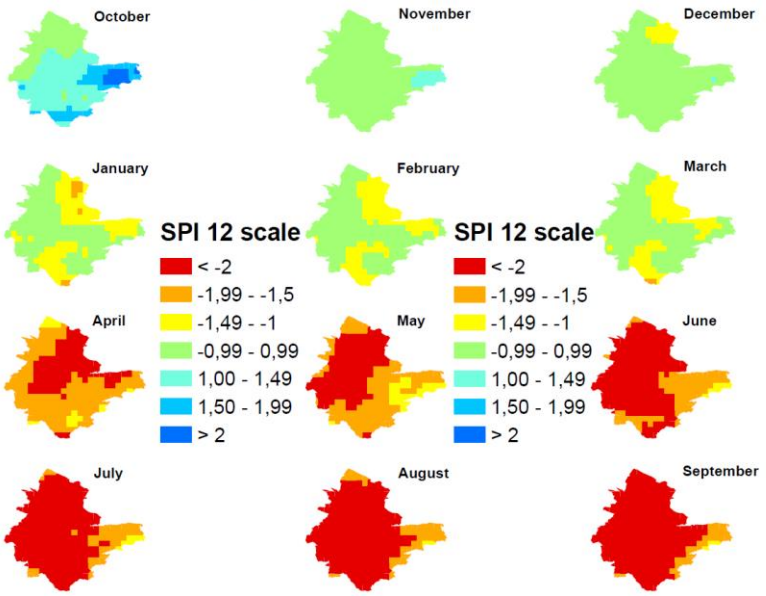

Figure 4. Predicted monthly SPI_{12} in the driest projected hydrological year: 2046 – 2047 in Albacete, Spain

Figure 5 presents the monthly SPI_{12} evolution for 2045-2046 (the wettest hydrological year). The study domain is conceivably divided into four zones. The wettest region tends to be in the eastern and southern part of Albacete (SPI > 2). The central territory is characterized by less wet conditions (1.5 < SPI < 2). Similarly, towards the north, the conditions are getting drier. The intermediate zone is slightly wet (1 < SPI < 1.5), whereas the northern part is characterized by the lowest degree of wetness approaching normal conditions. This pattern is repeating all the months of this year with slight differentiations for each zone.

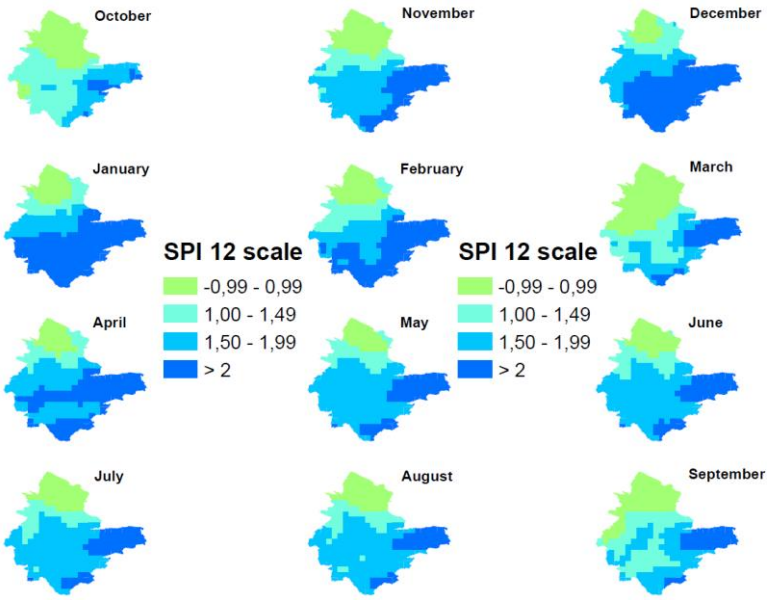

Figure 5. Predicted monthly SPI_{12} in the wettest projected hydrological year: 2046 – 2047 in Albacete, Spain

4 Conclusions

The spatial and temporal drought analysis highlighted the hydrological years with the most extreme conditions (extremely dry and extremely wet conditions) under the prediction of precipitation conditions for the next 30 years (2020 – 2050). Hence, based on the atmospheric simulation for the precipitation variable, it is observed that moderate dry conditions are expected even in the driest hydrological year. However, the intra-annual analysis indicated severe and extreme drought throughout Albacete from April to September. This type of analysis could be a valuable tool for spatially targeted measures based on drought severity for each pixel. Thus, counterbalancing measures could be adopted in the most vulnerable regions. Finally, it is recognized that there is an international research need for drought preparedness plans through the development of Decision Support System (DSS) (Dalezios (ed.), 2017). It is also recognized that the drought policy principle must consider the implementation of preparedness and mitigation measures (Arneth et al., 2014; Wilhite, 2009).

Acknowledgements

The research was funded by the SUPROMED (Sustainable production in water limited environments of Mediterranean agroecosystem) research and innovation (R&I) project funded under the PRIMA 2018 program section I Farming Systems.

References

Arneth, A., C. Brown, and M. D. A. Rounsevell, (2014). Global models of human decision-making for land-based mitigation and adaptation assessment, Nature Climate Change, 4(7), 550-557.

Byun, H.R., and Wilhite, D.A. 1999. Objective quantification of drought severity and duration. J. Clim. 12 (9): 2747–2756.

Dalezios, N.R., (Editor), 2017. Environmental Hazards Methodologies for Risk Assessment and Management. Publisher IWA, London UK, ISBN 9781780407128, 534 pages.

Dalezios, N. R**.,** A. Blanta and N. V. Spyropoulos, 2012: Assessment of remotely sensed drought features in vulnerable agriculture. NHESS, 12, 3139-3150.

Dalezios, N. R., Blanta, A., Spyropoulos, N. V., & Tarquis, A. M. (2014). Risk identification of agricultural drought for sustainable agroecosystems. *Natural Hazards and Earth System Sciences*, *14*(9), 2435-2448.

Dalezios, N.R., Z. Dunkel and S. Eslamian, 2017: Meteorological Drought Indices: Definitions. Book chapter 3 in Vol. 1 of 3-Volume Handbook of Drought and Water Scarcity (HDWS). Editor: Prof. S. Eslamian. Publisher: Taylor and Francis, 27-44.

EDO, 2021. European Drought Observatory. Available from: https://edo.jrc.ec.europa.eu/documents/factsheets/factsheet_spi.pdf; Accessed on 30/06/2021

Eslamian, S., & Eslamian, F. A. (Eds.). (2017). *Handbook of drought and water scarcity: environmental impacts and analysis of drought and water scarcity*. CRC Press.

González, J., & Valdés, J. B. (2006). New drought frequency index: Definition and comparative performance analysis. Water Resources Research, 42(11).

Mishra, A.K. and V.P. Singh, 2010: A Review of Drought Concepts. J. Hydrology, 39 (1-2), 202-216.

NCAR, 2022a. National Centre for Atmospheric Research: *Climate Data: Standardized Precipitation Index (SPI)*. Available from: https://climatedataguide.ucar.edu/climate-data/standardized-precipitation-index-spi; Accessed on 15/11/2021

NCAR, 2022b. National Centre for Atmospheric Research: *Weather and Forecasting Model*. Available from: https://www.mmm.ucar.edu/weather-research-and-forecasting-model; Accessed on 15/11/2021

Niemeyer, S. 2008. New drought indices. Options Méditerranéennes. Série A: Séminaires Méditerranéens, 80: 267–274.

Sidiropoulos, P., Dalezios, N. R., Loukas, A., Mylopoulos, N., Spiliotopoulos, M., Faraslis, I. N., ... & Sakellariou, S. (2021). Quantitative classification of desertification severity for degraded aquifer based on remotely sensed drought assessment. *Hydrology*, *8*(1), 47.

Thornthwaite, C.W. 1948. An approach toward a rational classification of climate. Geog. Rev. 38 (1): 55–94.

Wikipedia, 2022. *Albacete*. Accessible from: https://en.wikipedia.org/wiki/Albacete, on 20/2/2022.

WMO, 2012. World Meteorological Organization: Standardized Precipitation Index. User Guide; WMO: Geneva, Switzerland, 2012.

Wilhite, D.A., 2009: The Role of Monitoring as a Component of Preparedness Planning: Delivery of Information and Decision Support Tools. In: Iglesias, A., A. Cancelliere, F. Cubillo, L. Garrote, and D. Wilhite, eds. Coping with Drought Risk in Agriculture and Water Supply Systems. Springer Publishers, Dordrecht, The Netherlands.

Projecting the environmental extremes (wetness / drought) under climate change uncertainty: A valuable tool for spatial resilience enhancement in Sidi Buzid, Tunisia

Sakellariou S.[1], Alpanakis N. [1], Spiliotopoulos M. [1], Faraslis I.[2], Tziatzios G.[1], Sidiropoulos P. [1], Blanta A. [1], Brisimis V. [1], Dalezios N.[1] & Dercas N. [3], Karoutsos G.[4] and Kartsios S.[4]

[1] Department of Civil Engineering, University of Thessaly, 38334, Volos, Greece
[2] Department of Environmental Sciences, University of Thessaly, 41500, Larissa, Greece
[3] Department of Natural Resources Management & Agricultural Engineering, Agricultural University of Athens, 11855, Athens, Greece
[4] General Aviation Applications "3D" S.A., 2 Skiathou Str., 54646 Thessaloniki Greece

Abstract. Drought constitutes a natural phenomenon, which is directly related with the long-term shortage of precipitation. As a result, agricultural production risks could become an issue in the affected regions as mainly droughts are likely to increase the incidence of crop failure. Remote sensing methodologies and data can be employed in vulnerability and damage assessment, as well as relief, which involves assistance and/or intervention during or after drought. Consequently, main aim of the paper is to explore the environmental extremes (wetness / drought) under the impact of climate change (i.e., from 2020 to 2050) in Sidi Buzid, Tunisia, so the spatial resilience of any given region can be enhanced adopting the most appropriate counterbalancing measures directly on the most vulnerable regions. To this end, the precipitation values are simulated and estimated through the Weather Research and Forecasting (WRF) Model monthly in Sidi Buzid, Tunisia. Following, the Standardized Precipitation Index (SPI) is calculated based on the precipitation evolution for the last 12 months. The results indicated that the driest hydrological year in Sidi Buzid, Tunisia, is projected to be in 2030 – 2031 (SPI = -1.44); the wettest hydrological year is projected to be in 2045 – 2046 (SPI = 2.15); the hydrological year with the most normal conditions is projected to be in 2023 - 2024 (SPI = 0.01). In the intra-annual analysis of the driest year, the most severe drought conditions manifest from February through August. However, it is remarkable that there won't be any year with extremely drought conditions. Hence, the impacts of climate change are expected to be milder in this specific region. However, the mapping of the most vulnerable regions in terms of drought could lead to take the most appropriate (end extensive) measures to tackle the repercussions of this natural phenomenon.

Keywords: Environmental extremes; Climate Change; Weather Research & Forecasting Model; Spatial resilience

1 Introduction

Drought constitutes a natural phenomenon, which is directly related with the long-term shortage of precipitation. As a result, agricultural production risks could become an issue in these regions as mainly droughts are likely to increase the incidence of crop failure. As yield variability increases the food supply is at increasing risk (Sivakumar et al. (eds.), 2005; Dalezios et al., 2017). Moreover, drought monitoring is of critical importance in economically and environmentally sensitive regions and are significant inputs in drought preparedness and mitigation plan.
Traditional methods of drought assessment and monitoring rely on conventional rainfall data, which are usually limited in a region, often inaccurate and, most importantly, difficult to obtain in near-real time (Thenkabail et al., 2004). On the other hand, monitoring the extent of drought is best achieved in areas by using the vegetation coverage. This can be achieved through multispectral visible imagery from polar orbiting satellites for monitoring vegetation conditions and agricultural drought than conventional weather data (Dalezios et al., 2018).
Remote sensing methodologies and data can be employed in vulnerability and damage assessment, as well as relief, which involves assistance and/or intervention during or after drought. The possible contribution of remote sensing could be focused on relief and, possibly, preparedness, although in many cases remote sensing can make a valuable contribution to disaster prevention, where frequency of observation is not a prohibitive limitation (Dalezios et al., 2018). Moreover, remote sensing is a useful tool to analyze the vegetation dynamics on local, regional, or global scales (Keyantash and Dracup, 2002), to assess the vegetative stress and to determine the impact of climate on vegetation. Satellite-derived vegetation indices have been extensively used for identifying periods of vegetative stress in crops, which represents an indication of agricultural drought, or generally vegetation

(Dalezios et al., 2014). Moreover, soil moisture can be directly measured in the microwave region of the electromagnetic spectrum through satellites and interpretation of SAR data may also provide additional information on soil moisture (Dalezios et al., 2018; Petropoulos et al., 2015).
Consequently, main aim of the paper is to explore the environmental extremes (wetness / drought) under the impact of climate change (i.e., from 2020 to 2050), so the spatial resilience of any given region, such as Sidi Buzid under examination, can be enhanced by adopting the most appropriate counterbalancing measures directly on the most vulnerable regions.
To this end, the precipitation values are retrieved by remotely sensed sources, such as the CHIRPS database, so that the rainfall intensity evolution can be predicted through the simulation of this variable using the WRF Model. Next, the Standardized Precipitation Index (SPI) is calculated based on the precipitation evolution for the last 12 months (SPI_{12}) for all the projected time frame (2020 – 2050), through the transformation of gamma cumulative distribution to standardized normal distribution (NCAR, 2022a; Qin et al., 2015).

2 Materials and Methods

2.1 Study area

The proposed methodology has been implemented in *Sidi Bouzid Governorate,* which constitutes one of the 24 governorates (provinces) of Tunisia. The study area lies in the central part of Tunisia. The total area amounts to 7,405 km², whereas the total population amounts to 429,912 (2014 census). The capital (Sidi Bouzid) is characterized by the highest population density. The geographical coordinates are 35°02′N, 9°30′E. (Wikipedia, 2021). The pilot study area in Tunisia is depicted in Figure 1.

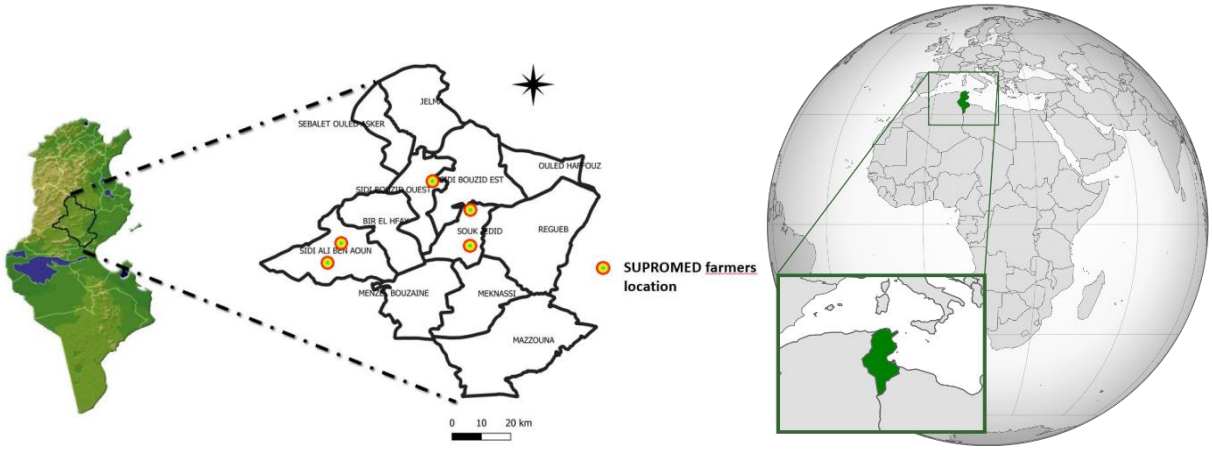

Figure 1. Geographical location of Sidi Buzid, Tunisia

2.2 Data

The main source of geospatial data (i.e., precipitation values) that was used for this analysis consists of the CHIRPS database (Climate Hazards Group InfraRed Precipitation with Station data). The CHIRPS database contains precipitation data on daily or monthly basis at spatial resolution of 0.05 and 0.25º for the quasi-global coverage of 50º N–50º S from 1981 to present (CHG, 2021; Duan et al., 2016). CHIRPS is a fusion of satellite images and data from rain-gauge stations. The projection of monthly precipitation levels in the long run (2020 – 2050) was based on the precipitation history of the previous 40 years (i.e., from 1981 to 2020). The spatial resolution of the data is 5 km (Sidiropoulos et al., 2021).

2.3 Methodology

2.3.1 Projected Drought Severity Estimation (2020 – 2050)

Projected drought severity assessment involves the simulation of atmospheric processes exploiting historical atmospheric measurements (i.e., observations of historical data retrieved by the CHIRPS database) (NCAR, 2022). To this end, the WRF Model is used to estimate the monthly precipitation values from 2020 to 2050. Next, the Standardized Precipitation Index (SPI) (WMO, 2012) is estimated, a drought index which is relied on precipitation data. The SPI is based on standardized probability to quantify precipitation deficit for differentiated time periods, e.g., 1, 3, 6, 9, 12 months and so on (Qin et al., 2015; Steinemann et al., 2005; Dalezios et al., 2018; WMO, 2012). Based on historical long-term rainfall data, the maximum likelihood is used to estimate the gamma distribution parameters and fit a gamma distribution. Then, the cumulative probability is used for the inverse normal function, resulting in the SPI (Guttman, 1999). In detail, the SPI is computed by dividing the difference between the normalized seasonal precipitation and its long-term seasonal mean by the standard deviation (Sidiropoulos et al., 2021). Finally, the annual spatial distribution of SPI is mapped by applying the Delaunay triangulation (Voronoi polygons) for each location. This process may provide the necessary tools to enhance the spatial resilience of any given region. For instance, targeted measures could be applied against severe drought conditions before the drought event breaks out. When SPI values are higher than 1, then, wet conditions are expected (the higher the difference from 1, the higher the wetness). On the contrary, when SPI values are smaller than -1, then, drought conditions are anticipated (the higher the difference from -1, the higher the drought). The middle interval (from -0.99 to 0.99) indicates normal conditions in terms of wetness/drought (EDO, 2021).

3 Results and Discussion

3.1 Projected Drought Severity Estimation (2020 – 2050)

Table 1 presents the monthly evolution of SPI_{12} for the projected time frame (2021 – 2049). As it can be observed, the driest hydrological year is projected to be in 2030 – 2031 (SPI = -1.44); the wettest hydrological year is projected to be in 2045 – 2046 (SPI = 2.15); and the hydrological year with the most normal conditions is projected to be in 2023 - 2024 (SPI = 0.01).

Table 1. Monthly evolution of SPI_{12} for the projected time frame (2021 – 2049) in Sidi Buzid, Tunisia

Hydrological year	SPI_{12}	Hydrological year	SPI_{12}
2021 – 2022	-0.41	2035 – 2036	-0.22
2022 – 2023	0.24	2036 – 2037	-1.07
2023 – 2024	0.01	2037 – 2038	-0.81
2024 – 2025	1.47	2038 – 2039	0.45
2025 – 2026	0.13	2039 – 2040	-0.42
2026 – 2027	-0.10	2040 – 2041	-0.42
2027 – 2028	1.51	2041 – 2042	0.62
2028 – 2029	-0.33	2042 – 2043	0.18
2029 – 2030	-0.04	2043 – 2044	-0.81
2030 – 2031	-1.44	2044 – 2045	0.69
2031 – 2032	-0.29	2045 – 2046	2.15
2032 - 2033	-0.96	2046 – 2047	0.23
2033 – 2034	0.04	2047 – 2048	-0.67
2034 – 2035	-0.13	2048 – 2049	0.28

During the entire projected time frame, the focus is on the driest, wettest, and most normal hydrological years. The hydrological year 2030-2031 tends to be the driest one (Figure 2a). Here, the study domain is conceivably divided in primary two regions with escalating drought conditions. The southeastern part of the study area is characterized by severe drought conditions (-1.99 < SPI < -1.5), whereas the northwestern region faces less severe drought (i.e., moderate drought conditions: -1.49 < SPI < -1). Very few regions (in the north and west) tend to face normal

conditions. On the contrary, the wettest hydrological year has been projected to be in 2045-2046. The largest part of the study area is characterized by extremely wet conditions (SPI > 2), whereas a few regions in the southern, central and eastern part of the study domain are characterized by slightly fewer wet conditions (1.5 > SPI > 1.99) (Figure 2b). Figure 2c presents a quite normal year (in terms of drought) throughout the study area. This year has been projected to be the hydrological year of 2023-2024. It is noticeable that the entire study area is characterized by normal conditions (-0.99 < SPI < 0.99). There is not any indication of drought in any region for this hydrological year.

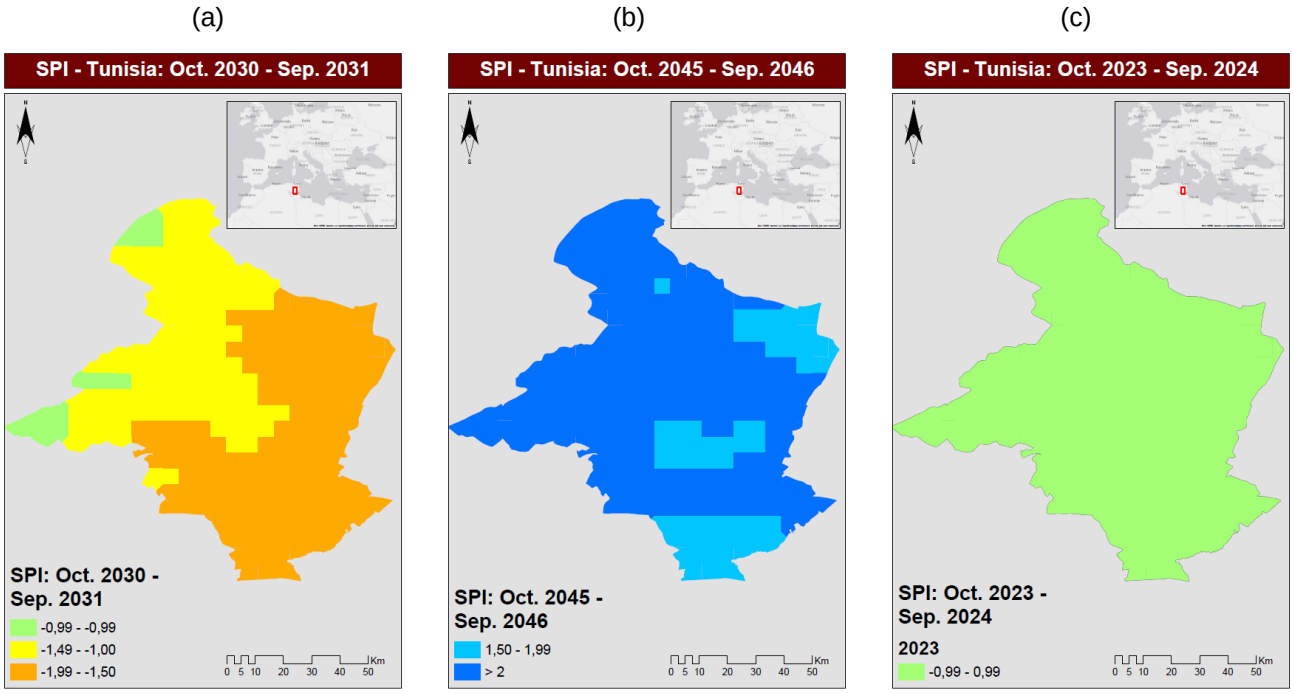

Figure 3. Spatial distribution of predicted SPI_{12} in the (a) driest (b) wettest and (c) the hydrological year with the most normal conditions (SPI ~ 0)

Figure 4 presents the monthly percentage of pixels falling in different drought categories for the projected hydrological year 2030 – 2031. Normal conditions prevail in October and November (from 67-100% of the total area); Moderate drought conditions dominate in December and September (from 58-72% of the total area); Severe drought conditions prevail from January to August (from 40-61% of the total area); Extreme drought conditions heat many regions in April and August (from 41-47% of the total area). Figure 5 shows the same information for the projected hydrological year 2045-2046. The variability is too small, since almost every geographical part of the study area faces quite wet conditions. The relative dry conditions for this hydrological year can be depicted in the summer months, namely from May to September. Even so, these regions are very few (less than 10% of the entire study area). Finally, for the projected hydrological year 2023-2024, it is observed that all the geographical parts of the study area face normal conditions except very few regions, which are characterized by slightly wetter conditions from October to December. There is not any indication of drought conditions this year (Figure 6).

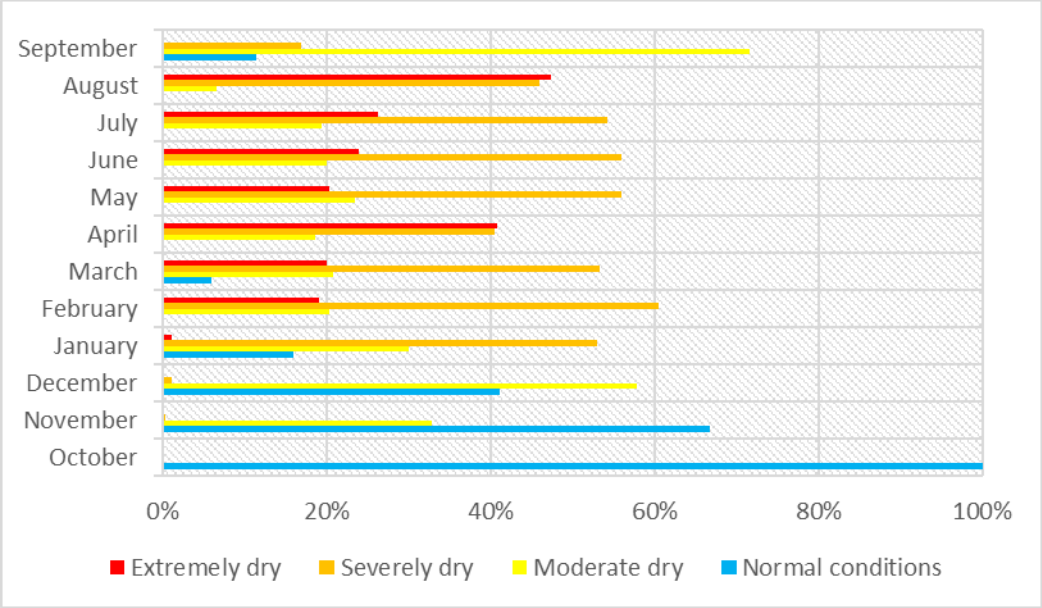

Figure 4. Percentage of pixels falling in different drought categories (2030-2031) in Sidi Buzid

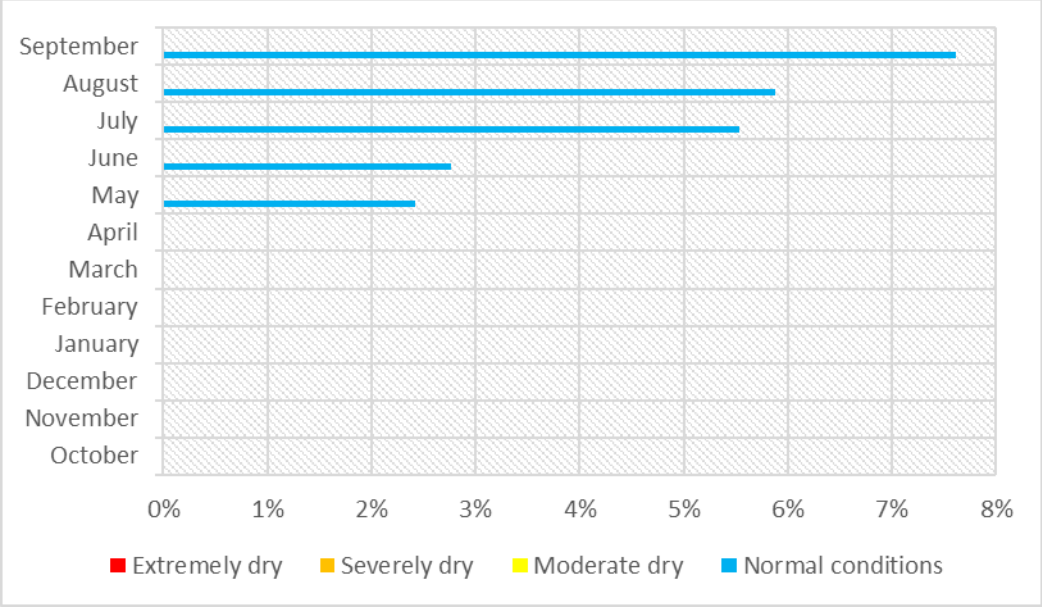

Figure 5. Percentage of pixels falling in different drought categories (2045-2046) in Sidi Buzid

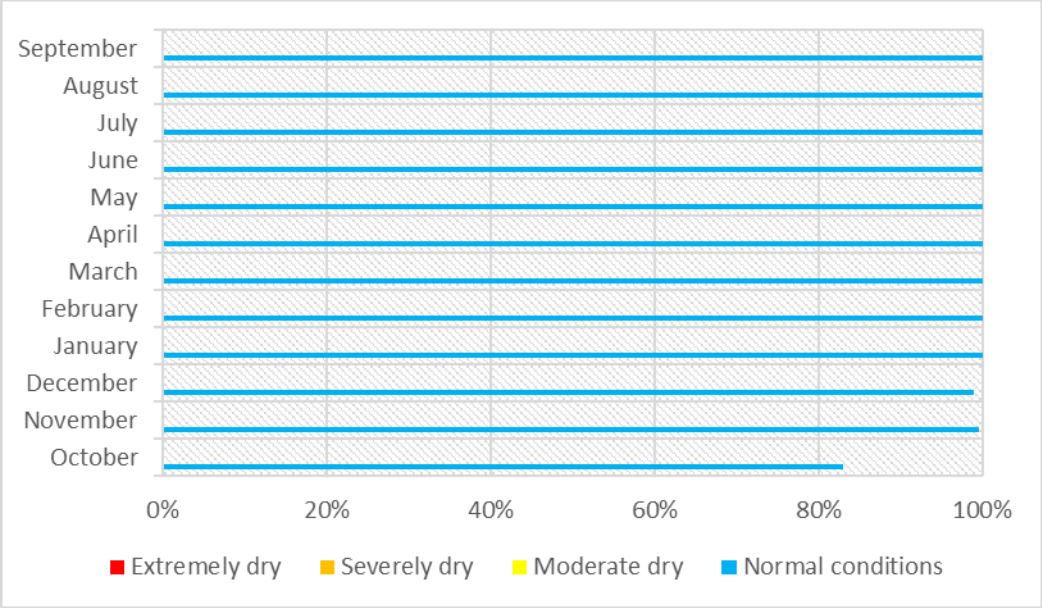

Figure 6. Percentage of pixels falling in different drought categories (2023-2024) in Sidi Buzid

4 Conclusions

The prediction of future rainfall evolution under the impact of climate change constitutes a valuable tool, so that the focus can be on managerial actions to the most susceptible territories in terms of drought severity mitigation. Even though there might be a high variability in SPI (the examined drought index), it is observed that the anticipated conditions indicate normal and wet conditions. There are very few hydrological years with moderate or severely drought conditions, whereas the projected driest year for the entire timeframe indicates severe drought conditions. It is remarkable that there won't be any year with extreme drought conditions. Hence, the impacts of climate change are expected to be milder in this specific region. However, the mapping of the most vulnerable regions in terms of drought could lead to take the most appropriate (end extensive) measures to tackle the repercussions of this natural phenomenon.

Acknowledgements

The research was funded by the SUPROMED (Sustainable production in water limited environments of Mediterranean agroecosystem) research and innovation (R&I) project funded under the PRIMA 2018 program section I Farming Systems.

References

CHG, 2021. Climate Hazard Group Releases New Version of CHIRPS. Available online: https://geog.ucsb.edu/climate-hazard-groupreleases-new-version-of-chirps/ (accessed on 2 January 2021).

Dalezios, N. R., Blanta, A., Spyropoulos, N. V., & Tarquis, A. M. (2014). Risk identification of agricultural drought for sustainable agroecosystems. *Natural Hazards and Earth System Sciences*, *14*(9), 2435-2448.

Dalezios, N. R., Dercas, N., & Eslamian, S., 2018. Water scarcity management: part 2: satellite-based composite drought analysis. International Journal of Global Environmental Issues, 17(2-3), 267-295.

Dalezios, N.R., A. Gobin, A.M. Tarquis and S. Eslamian, 2017: Agricultural Drought Indices: Combining Crop, Climate and Soil Factors. Book chapter 5 in Vol. 1 of 3-Volume Handbook of Drought and Water Scarcity (HDWS). Editor: Prof. S. Eslamian. Publisher: Taylor and Francis Group, 73-89.

Duan, Z., Liu, J., Tuo, Y., Chiogna, G., & Disse, M. (2016). Evaluation of eight high spatial resolution gridded precipitation products in Adige Basin (Italy) at multiple temporal and spatial scales. Science of the Total Environment, 573, 1536-1553.

EDO, 2021. European Drought Observatory. Available from: https://edo.jrc.ec.europa.eu/documents/factsheets/factsheet_spi.pdf; Accessed on 30/06/2021

Guttman, N. B. (1999). Accepting the standardized precipitation index: a calculation algorithm 1. JAWRA Journal of the American Water Resources Association, 35(2), 311-322.

Keyantash, J., and Dracup, J. A., 2002: The Quantification of Drought: An Evaluation of Drought Indices. Bulletin of American Meteorological Society, 1167-1180.

NCAR, 2022a. National Centre for Atmospheric Research: *Climate Data: Standardized Precipitation Index (SPI)*. Available from: https://climatedataguide.ucar.edu/climate-data/standardized-precipitation-index-spi; Accessed on 15/11/2021

Petropoulos, G.P., Ireland, G. & B. Barrett (2015): Surface Soil Moisture Retrievals from Remote Sensing: Current Status, Products & Future Trends. Physics and Chemistry of the Earth. DOI: 10.1016/j.pce.2015.02.009

Qin, Y., Yang, D., Lei, H., Xu, K., & Xu, X. (2015). Comparative analysis of drought based on precipitation and soil moisture indices in Haihe basin of North China during the period of 1960–2010. Journal of Hydrology, 526, 55-67.

Sidiropoulos, P., Dalezios, N. R., Loukas, A., Mylopoulos, N., Spiliotopoulos, M., Faraslis, I. N., ... & Sakellariou, S. (2021). Quantitative classification of desertification severity for degraded aquifer based on remotely sensed drought assessment. *Hydrology*, *8*(1), 47.

Sivakumar, M.V.K., R.P. Motha and H.P. Das, (Eds), 2005: Natural Disaster and Extreme Events in Agriculture. Springer, ISBN-10 3-540-22490-4, 367p.

Steinemann, A. C., Hayes, M. J., & Cavalcanti, L., 2005. Drought indicators and triggers. Drought and water crises: Science, technology, and management issues, 71-92.

Thenkabail, P. S., M. S. D. N. Gamage and V. U. Smakhtin, (2004): The use of remote sensing data for drought assessment and monitoring in southwest Asia. Research Report, International Water Management Institute, No. 85, 1-25.

Wikipedia, 2021. Sidi Bouzid. Available from: https://en.wikipedia.org/wiki/Sidi_Bouzid; Accessed on 15/11/2021

WMO, 2012. World Meteorological Organization: Standardized Precipitation Index. User Guide; WMO: Geneva, Switzerland, 2012.

Assessing future drought hazard under climate change adaptation in Beqaa Valley, Lebanon

Alpanakis N. [1], Sakellariou S.[1], Faraslis I.[2], Spiliotopoulos M. [1], Sidiropoulos P. [1], Tziatzios G.[1], Blanta A. [1], Brisimis V. [1], Dalezios N.[1], Dercas N. [3], Karoutsos G.[4] and Kartsios S.[4]

[1] Department of Civil Engineering, University of Thessaly, 38334, Volos, Greece
[2] Department of Environmental Sciences, University of Thessaly, 41500, Larissa, Greece
[3] Department of Natural Resources Management & Agricultural Engineering, Agricultural University of Athens, 11855, Athens, Greece
[4] General Aviation Applications "3D" S.A., 2 Skiathou Str., 54646 Thessaloniki Greece

Abstract. Drought clearly involves a shortage of water, but realistically can be defined only in terms of a particular need. Primary aim of the paper consists of the assessment of the future drought hazard under a framework of climate change adaptation for the next 30 years (2020 - 2050). Drought severity assessment can be estimated using the Standardized Precipitation Index (SPI), which constitutes a drought index that makes absolute use of precipitation data. Hence, to implement the above methodology, the Weather Research and Forecasting (WRF) Model is used for the simulation of atmospheric processes based on historical measurements. After the estimation of future monthly precipitation values, the SPI is statistically calculated and the spatial allocation of this index is mapped in the study domain, so that the regions with the highest degree of wetness and drought can be specified. The results indicated that the driest hydrological year is projected to be in 2047 – 2048 (SPI = -1.82), whereas the wettest hydrological year is projected to be in 2028 – 2029 (SPI = 1.62). The assessment of future drought hazard in in Beqaa Valley (Lebanon) can help policy and decision makers to take any precautionary measures against severe drought events. Even though the weather simulation indicated that precipitation levels seem to decline leading to drier environment (as represented by the future SPI values), primarily normal conditions are expected in the study area. The pilot study area is characterized by extreme drought in the driest year, whereas the adjacent regions face severe drought. The results call for targeted measures, especially in the pilot study area, to alleviate the extreme drought conditions and support the agricultural ecosystem.

Keywords: Drought hazard; climate change adaptation; Weather Research & Forecasting Model; precipitation; Beqaa Valley, Lebanon

1 Introduction

Drought clearly involves a shortage of water, but realistically can be defined only in terms of a particular need. It is difficult to find a generally accepted definition of drought. Indeed, there is no universally accepted definition of drought, since there is a wide variety of sectors affected by drought, as well as due to its diverse spatial and temporal distribution (Heim, 2002). If drought is considered as a phenomenon, it is certainly an atmospheric phenomenon. Studies in several areas around the world have shown that drought periods are often characterized by a large decrease in the amount of rainfall per rainy day, by an increase in the continentality of clouds and by lack of rain-producing clouds (Dalezios et al., 2018a). In general, droughts have been shown to be associated with persistence of ridges or centers of high-pressure systems at middle-level in the troposphere. Furthermore, the corresponding reduced cloud cover results in positive temperature anomalies in the lower atmosphere, which produces the middle-level pressure anomaly and favors subsidence at high level keeping the atmosphere significantly drier and more stable than normal (Dalezios et al., 2009). Nevertheless, by considering drought as a hazard, there is a tendency to define and classify droughts into different types, however, the relationship between the different types of droughts is complex. In the international literature, three operational definitions are considered, namely meteorological or climatological, agrometeorological, or agricultural and hydrological drought (Wilhite et al., 2000). As a fourth type of drought, the socioeconomic impacts of drought can also be considered.
In drought quantification and assessment, two types of passive remote sensing systems are considered, namely meteorological and environmental or resource satellites. The main differences between the two types of satellites are their spatial and temporal resolutions, which affect their applications and uses. Specifically, meteorological

satellites have a rather coarse spatial resolution, but high temporal re-occurrence, thus, being suitable mainly for operational applications, such as monitoring drought through changes in the index values. On the other hand, environmental satellites have usually fine spatial resolution, but low temporal re-occurrence, being basically used in land-use classification, such as quantitative classification of drought severity (Dalezios et al., 2018b).
The advantage to using remotely sensed data is that they allow for a high-resolution spatial coverage and are updated frequently to allow for near real time analyses, whereas the main drawbacks are the relatively short period of record. Indeed, the number of satellite systems is steadily increasing year by year with a continuous improvement of the spatial resolution. New types of remote sensing systems offer online open information for web platforms and are also utilized for monitoring and detecting drought. Such systems are the European Copernicus system with six Sentinel satellites (2014-2021) to monitor land, ocean, emergency response, atmosphere, security, and climate change (ESA, 2014), or NASA's new online satellites for climate change, Global Precipitation Measurement Core Observatory, Orbiting Carbon Observatory-2, and active-passive Soil Moisture (Dalezios et al., 2018c).
Hence, primary aim of the paper consists of the assessment of the future drought hazard under a framework of climate change adaptation for the next 30 years (2020 - 2050). The precipitation measurements retrieved by the CHIRPS database. This input has been used to feed the WRF Model and predict the precipitation values for each month for the entire time frame (2020-2050). Finally, the Standardized Precipitation Index (SPI) is calculated, which is an index for monitoring the precipitation evolution for 12 consecutive months (SPI_{12}), through the transformation of gamma cumulative distribution to standardized normal distribution (NCAR, 2022; Qin et al., 2015). Complementary objective of this model is the early detection of projected drought conditions, so that the negative effects can be counterbalanced with the corresponding measures to protect the agricultural crops.

2 Materials and Methods

2.1 Study area

The study area extends into the Beqaa Valley in Lebanon (Figure 1). The valley is located between Mount Lebanon to the west and the Anti-Lebanon mountains to the east. The dimensions of Beqaa Valley are 120 km long and 16 km wide. It is characterized by Mediterranean climate indicating wet, occasionally snowy winters and a combination of dry and warm summers. The geographical coordinates are 33° 49'N, 36° 0'E. (Wikipedia, 2021). The pilot study area in Lebanon is delimited by the black rectangle as can be shown in Figure 1.

Figure 1. Geographical location of Beqaa Valley (Lebanon) from national and international perspective

2.2 Data

One the most valuable types of data required for drought assessment constitutes the precipitation levels. The monthly precipitation values were retrieved by CHIRPS database (Climate Hazards Group InfraRed Precipitation with Station data). The CHIRPS database incorporates precipitation data for each calendar day at spatial

resolution of 0.05 and 0.25º for the quasi-global coverage of 50º N–50º S from 1981 up until now (CHG, 2021; Duan et al., 2016). CHIRPS is a fusion of satellite images and data from rain-gauge stations. Historical monthly CHIRPS products (1981-2020) with spatial resolution of 5 km * 5 km, were used in this study for the calculation of future precipitation values from 2020 to 2050 through WRF (Sidiropoulos et al., 2021).

2.3 Methodology

2.3.1 Projected Drought and Wetness Severity (2020 – 2050)

Drought severity assessment can be estimated using the SPI (WMO, 2012), which constitutes a drought index that makes absolute use of precipitation data. The SPI is based on standardized probability to quantify precipitation deficit for multiple time scales (i.e., from 1 to 36 months) (Qin et al., 2015; Steinemann et al., 2005; Dalezios et al., 2018b; WMO, 2012). The historical record has been adjusted to a "gamma" probability distribution, which is then transformed into a normal distribution, such that the mean SPI value for that location and period is zero. Then, the cumulative probability is used for the inverse normal function, resulting in the SPI (Guttman, 1999). Specifically, the SPI is estimated by dividing the difference between the normalized seasonal precipitation and its long-term seasonal mean by the standard deviation (Sidiropoulos et al., 2021). Hence, to implement the above methodology for the next 30 years, the WRF Model capabilities are exploited, a model that is used for the simulation of atmospheric processes based on actual atmospheric conditions (i.e., from observations of historical data retrieved by the CHIRPS database) (NCAR, 2022). After the estimation of future monthly precipitation values, the SPI is calculated statistically and the spatial allocation of this index is mapped in the study domain, so that the regions with the highest degree of wetness and drought can be specified. For any given location, increasingly severe rainfall deficits (i.e., meteorological droughts) are indicated as SPI decreases below –1.0, while increasingly severe excess rainfall are indicated as SPI increases above 1.0 (EDO, 2021).

3 Results and Discussion

3.1 Projected Drought and Wetness Severity (2020 – 2050)

Figure 2 presents monthly evolution of SPI_{12} for the projected time frame (2021 – 2049). As it can be observed, the driest hydrological year is projected to be in 2047 – 2048 (SPI = -1.82), whereas the wettest hydrological year is projected to be in 2028 – 2029 (SPI = 1.62). It is also observed that there will be not any critical dry hydrological year. The potential dry years have values close or lower than -1. On the contrary, two wet years are expected, namely in 2021-2022 and 2022-2023 indicating moderately wet conditions with 1.41 and 1.39 values, respectively. The trend seems to lead to a drier environment, however, inside the normal condition's interval.

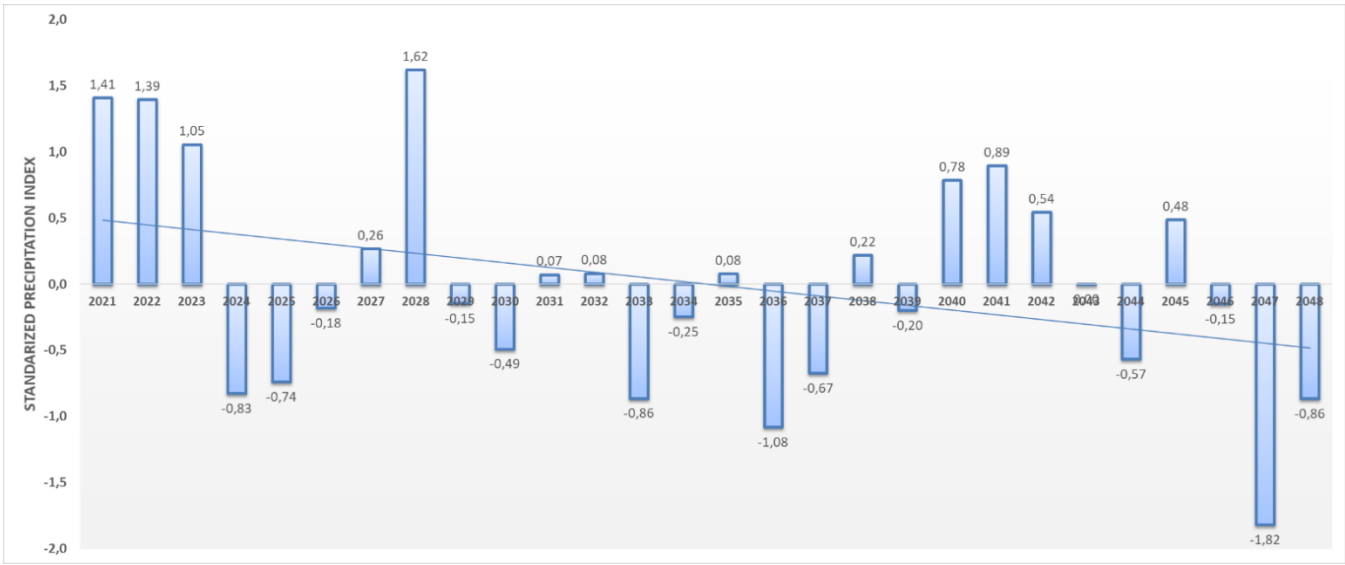

Figure 2. Predicted drought severity assessment based on SPI_{12} evolution (2021-2049) in Beqaa Valley

The hydrological year 2028-2029 tends to be the wettest year (Figure 3a). Based on the projected weather data and the corresponding SPI_{12} values, it is observed that the pilot study area will be characterized by very wet conditions (1.5 < SPI < 1.99). However, there are a few regions in the wider area facing slightly fewer wet conditions (1 < SPI < 1.49).

On the contrary, the driest hydrological year has been projected to be in 2046-2047. The greatest part of the study area is characterized by severe drought conditions (-1.99 < SPI < -1.5), whereas the pilot study area primarily faces extreme drought conditions (SPI < -2) (Figure 3b). This fact will require counterbalancing measures to protect the crops viability for the driest year in the next 30 years.

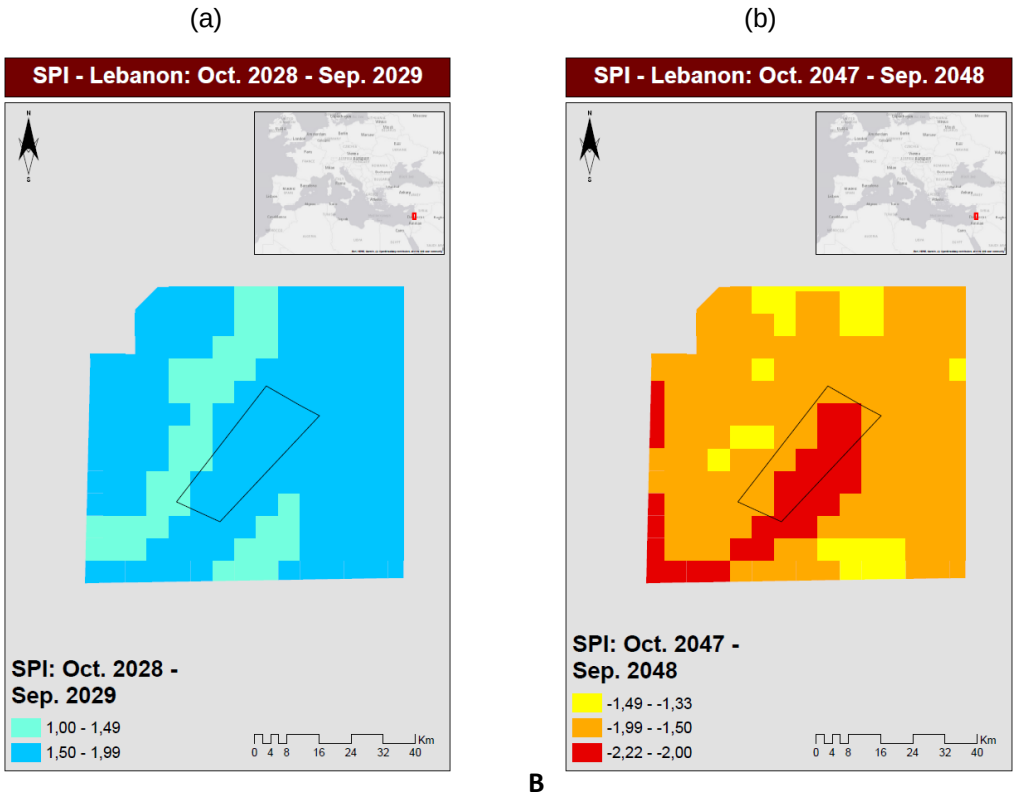

Figure 3. Spatial distribution of predicted SPI_{12} in Beqaa Valley in: (a) wettest (b) the driest hydrological year

Following, an intra-annual analysis is performed to estimate the magnitude of drought / wetness in the driest and wettest hydrological year, respectively. Table 1 summarizes the drought/wetness conditions in Lebanon for the projected hydrological year 2028-2029 in terms of pixels falling into differentiated categories. As it is observed, the entire study area is characterized by quite wet conditions with not any indication of drought. The only exception can be found in the first three months (from October to December) where many regions face normal to wet conditions. Specifically, the entire study domain is characterized by normal conditions in October (99% of the total area) with a descending trend in November and December, where the conditions are wetter and wetter.

Table 1. Frequency of pixels (%) reflecting different levels of drought conditions in the wettest year (2028-2029)

Year	Month	Normal conditions	Moderate dry	Severely dry	Extremely dry
2028	October	99%	0%	0%	0%
2028	November	69%	0%	0%	0%
2028	December	24%	0%	0%	0%
2029	January	0%	0%	0%	0%
2029	February	0%	0%	0%	0%

2029	March	0%	0%	0%	0%
2029	April	0%	0%	0%	0%
2029	May	0%	0%	0%	0%
2029	June	0%	0%	0%	0%
2029	July	0%	0%	0%	0%
2029	August	0%	0%	0%	0%
2029	September	0%	0%	0%	0%

Table 2 summarizes the drought conditions for the projected hydrological year 2047-2048 in terms of pixels falling into differentiated categories. Here, the pattern is variable. There are many regions with normal or moderately drought conditions from October to December, whereas at the remaining parts, an escalating trend is observed by increasing drought conditions from moderate to extreme. Severe and extreme drought conditions prevail from January to September; however, the pilot study area almost exclusively faces extremely dry conditions. The results indicate the dominance of normal conditions in October and November (85% of the entire study area); the dominance of moderate drought conditions in December (40% of the entire study area); the dominance of extreme drought conditions from January to September (45-94% of the entire study area).

Table 2. Frequency of pixels (%) reflecting different levels of drought conditions in the driest year (2047-2048)

Year	Month	Normal conditions	Moderate dry	Severely dry	Extremely dry
2047	October	85%	14%	1%	0%
2047	November	85%	12%	4%	0%
2047	December	16%	40%	33%	11%
2048	January	0%	16%	39%	45%
2048	February	0%	0%	7%	93%
2048	March	0%	0%	6%	94%
2048	April	0%	2%	21%	78%
2048	May	0%	12%	26%	63%
2048	June	0%	11%	26%	63%
2048	July	0%	12%	27%	62%
2048	August	1%	14%	28%	57%
2048	September	2%	14%	28%	57%

4 Summary and Conclusions

The assessment of future drought hazard in the Beqaa Valley (Lebanon) can help policy and decision makers to take any precautionary measures against severe drought events. Even though the weather simulation indicates that precipitation levels seem to decline leading to drier environment (as represented by future SPI values), primarily normal conditions are expected in the study area. Only one hydrological year (2047 – 2048) surpass the normal conditions, indicating extremely dry conditions. The pilot study area seems to be affected the most, since the adjacent regions face severe drought. The results call for targeted measures, especially in the pilot study area, to alleviate the extreme drought conditions and support the agricultural ecosystem.

Acknowledgements

The research was funded by the SUPROMED (Sustainable production in water limited environments of Mediterranean agro-ecosystem) research and innovation (R&I) project funded under the PRIMA 2018 program section I Farming Systems.

References

CHG, 2021. Climate Hazard Group Releases New Version of CHIRPS. Available online: https://geog.ucsb.edu/climate-hazard-groupreleases-new-version-of-chirps/ (accessed on 2 January 2021).

Dalezios, N.R., D. Bampzelis and C. Domenikiotis, 2009: An integrated methodological procedure for alternative drought mitigation in Greece. European Water, 27/28, 53-73.

Dalezios, N. R., Angelakis, A. N., & Eslamian, S. (2018a). Water scarcity management: part 1: methodological framework. *International Journal of Global Environmental Issues*, *17*(1), 1-40.

Dalezios, N. R., Dercas, N., & Eslamian, S. (2018b). Water scarcity management: part 2: satellite-based composite drought analysis. *International Journal of Global Environmental Issues*, *17*(2-3), 267-295.

Dalezios, N.R., K. Mitrakopoulos and B. Manos, 2018. Multi-scaling agroclimatic classification for decision support towards sustainable production. Book chapter in special issue: Multicriteria analysis in agriculture, by Berbel et al., (eds.), Publisher: Springer, DOI: 10.1007/978-3-319-76929-5_1, 1-42.

Duan, Z., Liu, J., Tuo, Y., Chiogna, G., & Disse, M. (2016). Evaluation of eight high spatial resolution gridded precipitation products in Adige Basin (Italy) at multiple temporal and spatial scales. *Science of the Total Environment*, *573*, 1536-1553.

EDO, 2021. European Drought Observatory. Available from: https://edo.jrc.ec.europa.eu/documents/factsheets/factsheet_spi.pdf; Accessed on 30/06/2021

ESA, 2014: "Sentinel, Earth online - ESA", <https://earth.esa.int/web/guest/missions/esa-future-missions/sentinel-1>, 06/04/2014.

Heim, R. R. Jr., 2002: A Review of Twentieth-Century Drought Indices Used in the United States. Bulletin of the American Meteorological Society, 83(8), 1149-1165.

Wilhite, D.A., Hayes, M.J., Kinutson C., and K.H. Smith, 2000: Planning for drought: moving from crisis to risk management. J. Amer. Water Res. Assoc., 36(4), 697-710.

NCAR, 2022. National Centre for Atmospheric Research: *Climate Data: Standardized Precipitation Index (SPI)*. Available from: https://climatedataguide.ucar.edu/climate-data/standardized-precipitation-index-spi; Accessed on 15/11/2021

Qin, Y., Yang, D., Lei, H., Xu, K., & Xu, X. (2015). Comparative analysis of drought based on precipitation and soil moisture indices in Haihe basin of North China during the period of 1960–2010. J. of Hydrology, 526, 55-67.

Sidiropoulos, P., N. R. Dalezios, A. Loukas, N. Mylopoulos, M. Spiliotopoulos, G. N. Faraslis, N. Alpanakis and S. Sakellariou, 2021. Quantitative classification of desertification severity for degraded aquifer based on remotely sensed drought assessment. *Hydrology* **2021**, *8*, 47. https://doi.org/10.3390/hydrology8010047.

Wikipedia, 2021. *Beqaa Valley*. Accessible from: https://en.wikipedia.org/wiki/Beqaa_Valley, on 20/2/2022.

Estimation of Nitrogen requirements through remotely sensing data and methods: The case of Albacete, Spain

Sakellariou S.[1], Alpanakis N. [1], Faraslis I.[2], Spiliotopoulos M. [1], Sidiropoulos P. [1], Tziatzios G.[1], Blanta A. [1], Brisimis V. [1], Karoutsos G.[4], Dalezios N.[1] & Dercas N. [3]

[1] Department of Civil Engineering, University of Thessaly, 38334, Volos, Greece
[2] Department of Environmental Sciences, University of Thessaly, 41500, Larissa, Greece
[3] Department of Natural Resources Management & Agricultural Engineering, Agricultural University of Athens, 11855, Athens, Greece
[4] General Aviation Applications "3D" S.A., 2 Skiathou str, 54646, Thessaloniki, Greece

Abstract. Precision agriculture implies the determination of the fertilizer, the timing, and the doses to be properly distributed in the plot. The paper aims to present the spatialized methods of nitrogen fertilization using satellite remote sensing measurements. The key concept is the determination of Nitrogen Nutrition Index (NNI), which is defined as the ratio between the actual nitrogen content (N) and the canopy optimum N content. Deviations of NNI values from the value around 1 would indicate no proper N management. Time-series analysis of remotely sensed vegetation and nitrogen indices has been conducted, so that a six-day estimation of NNI (temporal frequency of Sentinel-2) can be obtained. Hence, after the computation of several intermediate indices based on the phenological stages of crops (NDVI, RENDVI, Kt, Transpiration etc.) the NNI evolution is monitored from March to May in Albacete. It is observed that the NNI presented a declining trend, which is reasonable, since the fertilization primarily takes place in the initial stages of crop development. However, the fertilization from late of March until beginning of May was considered excessive, whereas the N presence in the following days seems to become optimal. Hence, it is highlighted the fact that a certain number of financial resources could be saved allowing the N presence to be closer to 1, which indicates optimal value. As more concrete time-series data become available, the nitrogen requirement assessment would be more effective in environmental and financial terms.

Keywords: Nitrogen Nutrition Index (NNI); Remote Sensing; Sentinel 2; Albacete, Spain

1 Introduction

Precision agriculture implies the determination of the fertilizer, the timing, and the doses to be properly distributed in the plot. The content of Nitrogen in the canopy (N, grams of N/grams of biomass) is an important diagnostic indicator and its estimation is a key parameter in precision agriculture. Specifically, the Nitrogen Nutrition Index (NNI) is defined as the ratio between the actual nitrogen content (N) and the canopy optimum N content Nup-c, NNI = N/Nup-c. Deviations of NNI values from the value around 1 would indicate no proper N management. Indeed, remote sensing methods can provide the N content in the crop by using different combinations of spectral reflectance bands known as vegetation indices (Gonzalez-Piqueras et al., 2017).

The methodological framework selected is based on the concept of critical N concentration (Colnenne et al. 1998) to obtain the N recommendation via the Nitrogen Nutrition Index (NNI) (Lemaire et al. 2008). This approach was originally based on ground measurements and recently tested and applied with remote sensing data by Houles et al. (2007) and in several other studies (Cilia et al., 2014; Vouillot et al., 1998). The main limitation of the approach is the need for extensive calibration to estimate the two input parameters required for the application of the NNI: the above ground dry mass accumulation (W) and the actual N concentration (%Na) at a specific growing stage. The aim is to apply the NNI approach, using an empirical relationship to derive dry mass accumulation from Leaf Area Index (LAI) and %Na from a spectral chlorophyll index (CI) (Vuolo et al., 2017).

The paper aims to present the spatialized methods of nitrogen fertilization using satellite remote sensing measurements. The Sentinel 2 mission offers a great potential for improvement due to: (1) high temporal repetitiveness, which makes it possible to follow the vegetation during the critical stage revealing the soil / water / nitrogen interactions on the development of the vegetal cover and thus to appreciate the potential of production

and the limiting factors; (2) its high spatial resolution (20m), which is adapted to the spatialized application scale of fertilizers; and (3) an interesting spectral content for the characterization of the nitrogenous state of plants, mainly due to the bands in the red edge spectral domain. As the Sentinel images are freely available and all the processing chains to make spatial registration and atmospheric effect correction are now mature, transfer of the companies able to provide the service to the farmer would be possible at reasonable cost. This manuscript presents the rationale of those methods and the approach applied in SUPROMED Project, including their results, to identify the added value of nitrogen fertilization by remote sensing (Sentinel-2). The goal of the research is to explore the estimated nitrogen as acquired by a series of satellite images throughout the growing season. The NNI will reveal the potential deficit of Nitrogen and the respective requirements to reach optimal supply.

2 Materials and Methods

2.1 Study area

Albacete is a Spanish province, which is in the south-eastern part of the country (Figure 1). The study area occupies 14,858 km^2. The total population amounts to 387,658 and can be considered sparsely populated with 26 people per km^2. The geographical coordinates are: 38^o 50' N, 2^o 00' W (Wikipedia, 2022). Albacete mainly constitutes an agricultural region, and the applied methodology has been conducted under the SUPROMED European research project.

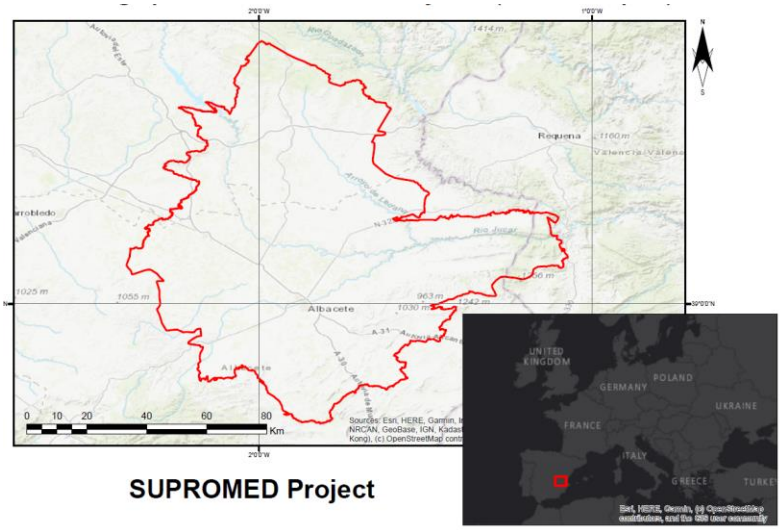

Figure 1. Geographical location of the study area (Albacete, Spain)

2.2 Data

The primary data sources consist of three categories: The Sentinel 2 satellite images (20 X 20 m.), the precipitation data and the crop calendar of the study area. The acquisition of satellite images has been conducted for dates when clear (without cloud interference) images were available. These dates comprise of 29/03/2020; 08/04/2020; 03/05/2020; 18/05/2020 and 23/05/2020. Secondly, the precipitation data (2 X 2 km) has been acquired from the WRF model to calculate the Reference Evapotranspiration. The crop calendar, which describes the quantities of Nitrogen fertilization on selected dates, will be used for the biomass estimation based on its interrelationship with the cumulative evapotranspiration.

2.3 Methodology

2.3.1 Estimation of critical remotely sensed vegetation indices

There are two modules that run simultaneously. The first one is related to the satellite images handling, whereas the second one focuses on purely precipitation data. Specifically, two vital vegetation indices are calculated,

namely the Normalized Difference Vegetation Index (NDVI) and the Red Edge Normalized Difference Vegetation Index (RENDVI). The RENDVI capitalizes on the sensitivity of the vegetation red edge to small changes in canopy foliage content, gap fraction, and is calculated through the following equation:

$$RENDVI= (NIR-RE) / (NIR+RE) \quad (1)$$

where: NIR is the near-infrared band 8 and RE the Red Edge band 6.

The RENDVI has been estimated for all the images, since it constitutes an independent variable for the determination of Nitrogen based on remote sensing measurement. In the same context, the NDVI is calculated for all images through the following equation:

$$NDVI= (NIR-R) / (NIR+R) \quad (2)$$

where: NIR is the near-infrared band 8 and R the Red band 4.

At the same time, the collection of precipitation data allowed the estimation of the Reference Evapotranspiration (Eto). The calculation of this index was conducted through a Weather Research and Forecasting model (WRF). However, the spatial resolution of this type of data was too low (2 km). To deal with this restriction, an Inverse Distance Weighting (IDW) interpolation is applied, so that more reliable measurements of Eto can be obtained for each pixel inside the pilot field. Afterwards, transpiration can be obtained by using an empirical relationship, such as the following regression equation for central Spain (Campos et al., 2018):

$$T = Kt \times Eto \quad (3),$$

$$Kt = 1.64 \times NDVI – 0.14 \quad (4)$$

where: T stands for Transpiration, Kt is the transpiration coefficient, Eto is the Reference Evapotranspiration.

Next, the mean actual transpiration is computed through zonal statistics. This process is critical, so that the biomass can be estimated for the reference days since this type of data does not exist in the crop calendar. Hence, the second-best approach to estimate the biomass is based on the interrelation of cumulative transpiration curve. The only known biomass value is the amount of biomass on the harvesting date according to the crop calendar. This value amounts to 20,133 kg / ha. Relied on this information, the approximate estimation of the biomass values is considered for each reference date, since it has empirically proved that the biomass values coincide with the fitting line of cumulative transpiration curve (Campos et al., 2018).

2.3.2 Estimation of nitrogen indices

Following, the critical Nitrogen (Nc) is estimated, which is the optimal amount of N on the ground (Justes et al., 1994). This index will be compared with actual Nitrogen (Nr) through the Nitrogen Nutrition Index (NNI). To calculate the Nc, the following equation is used (Justes et al., 1994):

$$Nc = 5.35 * Biomass-0.442, \text{ when estimated biomass} > 1 \text{ t. ha-1} \quad (5)$$

On the other hand, once the red-edge vegetation indices are obtained from Sentinel-2, which are a function of N, then they are calibrated/validated with field observations of total nitrogen content N (g/m^2) and x NNI (dimensionless) (Gonzalez-Piqueras et al., 2017). Before estimating the components of NNI, the equation (6) is used, which derived from the linear fit of the red-edge indices applied to the spectral reflectance measurements to broad bands of Sentinel-2 (Vuolo et al., 2017):

$$N = 43 * RENDVI – 5 \quad (6)$$

where N is the Nitrogen captured by satellite images as a function of RENDVI.

After the estimation of N value, the computation of NNI is considered and its structural components, namely the actual N (Nr) and the optimal N (Nc) values (Gonzalez-Piqueras et al., 2017):

$$Nr\ (g/100\ g\ total\ biomass) = [N\ (g/m2) / biomass\ (g/m)] \quad (7)$$

$$NNI\ (dimensionless) = Nr\ (g/100\ g\ total\ biomass) / Nc\ (g/100\ g\ total\ biomass) \quad (8)$$

where Nr is the computed nitrogen N from satellites and Nc is the optimal N (reference). The deviation between actual and optimal N values would provide the framework for optimal amount of fertilization for each plot.

3 Results and Discussion

This section summarizes all the estimated values for barley until the final goal is reached, namely the estimation of NNI, which determines the necessity of intensifying or lessening the fertilization on the pilot crop.

Table 1 depicts all the estimated statistical values of N, as captured by satellite images, as function of RENDVI which is the result of equation (6). In the same context, the results (**Table 2**) are presented of another intermediate but critical index, *Kt* as a function of NDVI, based on equation (4).

Table 1. Statistical values of N for Barley, 2020

Dates	**Plot**	**N as a function of RENDVI**					
Values	**Area**	**Min**	**Max**	**Range**	**Mean**	**Std**	**Sum**
29/3/2020	81,200	9.45	25.19	15.74	19.33	3.00	3,924.43
8/4/2020	81,200	8.68	25.65	16.97	19.96	3.25	4,051.97
3/5/2020	81,200	13.56	26.35	12.78	23.88	2.34	4,847.12
18/5/2020	81,200	6.95	24.24	17.29	20.77	3.07	4,216.71
23/5/2020	81,200	7.62	22.30	14.68	18.02	2.31	3,658.90

Table 2. Statistical values of Kt for Barley, 2020

Dates	**Plot**	**Kt as a function of NDVI**					
Values	**Area**	**Min**	**Max**	**Range**	**Mean**	**Std**	**Sum**
29/3/2020	81,200	0.39	1.28	0.89	1.11	0.15	224.71
8/4/2020	81,200	0.36	1.27	0.91	1.12	0.16	227.45
3/5/2020	81,200	0.52	1.25	0.73	1.18	0.09	238.96
18/5/2020	81,200	0.27	1.31	1.04	1.21	0.18	244.76
23/5/2020	81,200	0.49	1.35	0.86	1.16	0.12	234.56

The pilot field has an area of 8.1 ha. Based on these two tables, it is observed that the average Kt and N indices take the maximum values in May, whereas the harvesting period is completed in June.
The next step constitutes the biomass estimation through the cumulative transpiration curve. This process is based on equation (4), which contains the interaction of Kt and the value of Eto. **Table 3** presents the results of all statistical values for transpiration, as computed inside the pilot field. Once more, the highest values can be found in May, except a sharp decrease on 18/05 which might be due to technical inaccuracies of the satellite image.

Table 3. Statistical values of Transpiration for barley, 2020

Dates	**Transpiration as a function of Kt and Adj Eto**					
Values	**Min**	**Max**	**Range**	**Mean**	**Std**	**Sum**
29/3/2020	0.81	2.73	1.92	2.35	0.32	469.66
8/4/2020	0.90	3.27	2.36	2.86	0.39	572.61

3/5/2020	3.01	7.26	4.25	6.94	0.53	1.387.04
18/5/2020	0.78	3.86	3.08	3.54	0.46	707.10
23/5/2020	3.51	10.01	6.50	8.56	0.82	1,712.42

The only known value for biomass is the value for the harvesting date, which occurred on 19/06/2020. At that date, the measured biomass was 20,133 kg / ha. Hence, a biomass curve is empirically defined in relation to cumulative transpiration (as depicted in the **Figure 3**) to best approach the biomass values required for all the dates. This process constitutes an approximation, which is a limitation of the current project. The enrichment of crop calendar with the exact biomass values would resolve similar issues in the future. **Figure 3** presents the adjustment of biomass to the cumulative transpiration curve for the days when satellite images were available (and operational).

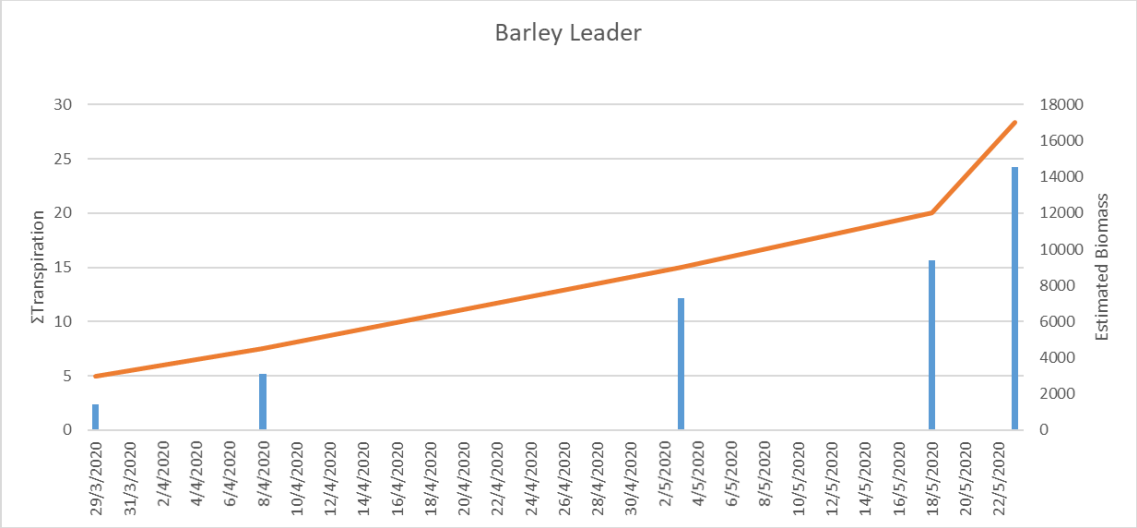

Figure 3. Adjustment of biomass values to cumulative transpiration curve

Table 4 summarizes the average and cumulative transpiration values for each date of reference. The estimated biomass follows the trend of cumulative transpiration.

Table 4. Average / cumulative transpiration and estimated biomass for barley,

Transpiration / Date					
Barley	**29/3/2020**	**8/4/2020**	**3/5/2020**	**18/5/2020**	**23/5/2020**
Mean Transpiration	2.35	2.86	6.94	3.54	8.56
Cumulative Transp.	2.35	5.21	12.15	15.68	24.24
Est. Biomass (kg / ha)	3,000	4,500	9,000	12,000	17,000

The final stage constitutes the calculation of NNI based on equation (8). The N index which is based on satellite measurements seems to increase from late of March till beginning of May following a reverse trend until late of May. **Table 5** summarizes the results for all available dates contrasting the N measured by satellites with the corresponding estimated biomass for each date.

Table 5. Summary of remotely sensed nitrogen and biomass values for barley Leader

Barley	**29/3/2020**	**8/4/2020**	**3/5/2020**	**18/5/2020**	**23/5/2020**
N (Satellite)	19.33	19.96	23.88	20.77	18.02
Est. Biomass (t./ha)	3.0	4.5	9.0	12.0	17.0

Having calculated the intermediate indices, namely the Nr and Nc, the NNI is finally estimated. The results are provided in **Table 6**. It is observed that the NNI is higher than 1 from late of March till beginning of May indicating an excess of Nitrogen presence. Approaching the mid of May (18/05/2020), the index receives the value of 0.97 which indicates optimal Nitrogen presence in environmental and financial perspective. Moving closer to the harvesting day (19/06/2020), the index takes a value of 0.69 highlighting the N deficit for that specific period, however, this is reasonable at this stage.

Table 6. Nitrogen requirements based on NNI (Nitrogen Nutrition Index)

Barley	**29/3/2020**	**8/4/2020**	**3/5/2020**	**18/5/2020**	**23/5/2020**
Nr (Satellite)	6.44	4.44	2.65	1.73	1.06
Nc	3.29	2.75	2.03	1.78	1.53
NNI	**1.96**	**1.61**	**1.31**	**0.97**	**0.69**

4 Concluding remarks

In this paper, the fertilization requirements are computed based on remotely sensed data. A proof-of-concept methodology is developed to examine the comparative advantage of such processes. Most of the data derived from consecutive satellite images of high spatial resolution, which allowed the assessment of Nitrogen presence on the ground. The NNI constitutes a robust index which evaluates the Nitrogen requirements in any agricultural field. Hence, after the computation of several intermediate indices based on the phenological stages of crops (NDVI, RENDVI, Kt, Transpiration etc.) the NNI evolution is monitored from March to May in Albacete. It is concluded that the NNI presented a declining trend which is reasonable, since the fertilization primarily takes place in the initial stages of crop development. However, it is observed that the fertilization from late of March until beginning of May was excessive, whereas the N presence in the following days seems to become optimal. Hence, it is highlighted the fact that a certain number of financial resources could be saved allowing the N presence to be closer to 1 which indicates optimal value. As more concrete time-series data become available, the nitrogen requirement assessment would be more effective in environmental and financial terms.

Acknowledgements

The research was funded by the SUPROMED (Sustainable production in water limited environments of Mediterranean agro-ecosystem) research and innovation (R&I) project funded under the PRIMA 2018 program section I Farming Systems.

References

Campos, I., Gonzalez-Gomez, L., Villodre, J., Gonzalez-Piqueras, J., Suyker, A. E., & Calera, A. (2018). Remote sensing-based crop biomass with water or light-driven crop growth models in wheat commercial fields. *Field Crops Research*, *216*, 175-188.

Cilia, C., Panigada, C., Rossini, M., Meroni, M., Busetto, L., Amaducci, S., ... & Colombo, R. (2014). Nitrogen status assessment for variable rate fertilization in maize through hyperspectral imagery. *Remote Sensing*, *6*(7), 6549-6565.

Colnenne, C., Meynard, J. M., Reau, R., Justes, E., & Merrien, A. (1998). Determination of a critical nitrogen dilution curve for winter oilseed rape. *Annals of botany*, *81*(2), 311-317.

COAH, 2021. Copernicus Open Access Hub. Available from: https://scihub.copernicus.eu/ ; Accessed on 10/03/2020.

González-Piqueras, J., Lopez-Corcoles, H., Sánchez, S., Villodre, J., Bodas, V., Campos, I., ... & Calera, A. (2017). Monitoring crop N status by using red edge-based indices. *Advances in Animal Biosciences*, *8*(2), 338-342.

Houles, V., Guerif, M., & Mary, B. (2007). Elaboration of a nitrogen nutrition indicator for winter wheat based on leaf area index and chlorophyll content for making nitrogen recommendations. *European Journal of Agronomy*, *27*(1), 1-11.

Justes, E., Mary, B., Meynard, J. M., Machet, J. M., & Thelier-Huché, L. (1994). Determination of a critical nitrogen dilution curve for winter wheat crops. *Annals of botany*, *74*(4), 397-407.

Lemaire, G., Jeuffroy, M. H., & Gastal, F. (2008). Diagnosis tool for plant and crop N status in vegetative stage: Theory and practices for crop N management. *European Journal of agronomy*, *28*(4), 614-624.

Vouillot, M. O., Huet, P., & Boissard, P. (1998). Early detection of N deficiency in a wheat crop using physiological and radiometric methods. *Agronomie*, *18*(2), 117-130.

Vuolo, F., Essl, L., Zappa, L., Sandén, T., & Spiegel, H. (2017). Water and nutrient management: The Austria case study of the FATIMA H2020 project. *Advances in Animal Biosciences*, *8*(2), 400-405.

Wikipedia, 2022. Province of Albacete – Wikipedia. Available from: https://en.wikipedia.org/wiki/Province_of_Albacete ; Accessed on 10/01/2022.

Determination of Growth Stage-Specific Crop Coefficients (Kc) of durum wheat and oat in the region of Sidi bouzid –Tunisia

R. Nciri[1], A. Bouselmi[1], T. Jarrahi[1], F. Ghdifi[1]

[1]National Institute of Field Crops

Abstract. This study was conducted in Sidi-Bouzid located in the center of Tunisia. In this region, Irrigated crops present 10 % of the national irrigated area. However, many framers of this region use high amount of water to exceed crop needs, resulting an over exploitation of groundwater (annual depletion of groundwater is more than 0.5 m/year). Irrigation scheduling is required to improve water use efficiency while many methods are available, based on calculating the crop water requirements (ETc = Kc x ETo). This work will focus on improving the calculation of ETc by adjusting the crop coefficient (Kc). Two Kc were adjusted, kc of durum wheat (DW) (*Triticum durgidum* L.) and kc of oat (*Avena sativa* L.) using cumulative growing-degree-days (CGDD) and modeling by multiple regression of local Kc according to the Kc proposed by FAO-56 (FAO Kc). The results shown CGDD for the whole growth cycle is around 2709°C for DW and 2663.86°C for oat. The average error in days for two growing seasons (2019/2020 and 2020/2021) compared with FAO GDD was around -7; 6; 3 and -12 days for DW and 5; 1; -3 and 10 days for oat according to the crop stages (initial, development, mid-season and late-season). The result of Modeling the local Kc gives two relationships for DW and oat (local Local Kc_{DW} =FAO Kc*1,062+GDD*-1,176-0,067 with R^2=0.95 and Local Kc_{Oat} = FAO Kc*0,7788+GDD*5,347+0,131 with R^2=0.88). This results could be useful to adjust irrigation scheduling models i.e. "IREY" and "MOPECO". However, more trials in other region may be necessary for evaluation.

Keywords. Crop coefficient, CGDD, ETc, calibration, Modeling, Irrigation, Durum wheat, Oat, IREY, MOPECO.

1 Introduction

Located in the center-west of Tunisia, the governorate of Sidi Bouzid currently represents one of the main agricultural regions of the country, where irrigation has known a remarkable development for decades. Irrigated areas in the region increased by 60% between 1987 and 2014 (DGAT, 2016). This region is marked by low water resources which are increasingly in demand. (Hamdi et *al.,* 2015). About 80% of these areas are irrigated from surface wells (12334 wells) and by deep drillings (1504 drillings) (DGAT, 2018). The problem of availability of water resources is even more accentuated and influenced by the temporal and spatial variability of precipitation (Ghazavi et *al.*, 2012; Hamdi et *al.,* 2015). In order to ensure optimal use and maximize the water efficiency, it is necessary to use advanced calculation methods based on climate, soil and plant data. The water balance model, which takes into account the inflow and outflow of water into the soil at the root zone, can accurately estimate the exact needs of the crops. (Ávila-Dávila et *al.*, 2021; Soldevilla-Martinez; Allen et *al.,* 1998). There are other methods for estimating crop water requirements based on estimating crop evapotranspiration (ETc), such as the approach proposed by the Food and Agriculture Organization of the United Nations (FAO), using reference evapotranspiration (ETo) and crop coefficient (Kc). This approach has two components: i) climatic component such as relative air humidity, sunlight, solar radiation, wind speed and air temperature, in order to obtain the ETo which refers to a crop reference (the grass) well supplied with water and of uniform height. It is relative to the Penman-Monteith modeling which represents the effect of climate on the water needs of crops (Allen et *al.,* 1998). ii) Kc which represents the effect of crop growth as a function of time as a coefficient. To calculate Kc, FAO proposes a simple approach that integrates ETo and ETc (Kc = ETc/ETo). The Kc is different from a stage of development to another. On the other hand, temperature is an important climatic factor with a significant influence on phenology and crop yield. It is also a better indicator of crop development rate (Kumar et al., 2020). The cumulative growing degree days (CGDD), is an index calculated from temperature data, and allows to estimate the time required for a crop to reach maturity or complete a developmental stage (Paparrizos and Matzarakis, 2017). CGDD is the difference between average air temperature and base temperature (Tb). The CGDD is used to relate the Kc curve of the culture to the phenological development (Kumar et al., 2020). As a result, the management of irrigation requires the combination of several factors and sometimes complex calculations for farmers or policy makers because it must be adjusted to the variability of water requirements depending on the climate, the growth of the crop and technical hazards. This complexity can lead irrigators to apply, as a precaution, more water than the actual needs of the crops. To help farmers make decisions, several simple software and applications have been developed. (Chopart et *al.,* 2008). Two IT irrigation management tools have been tested and calibrated in Sidi

Bouzid region. The first called IREY (Irrigation Reference to enhance Yield) which is a Tunisian model available on Android smartphone and on the web and allows the management of the irrigation of Field crops. The second is a Spanish model, called MOPECO available on the web and ensures the management of the irrigation of a wide range of crops (field crops, vegetables, tree crops, etc.). The main goal of this study is to determine growth stage-specific Kc by comparing and calibrating models and tools used in durum wheat (DW) (*Triticum durgidum* L.) and oat (*Avena sativa* L.) crops with real data obtained from three trials plots installed in Sidi Bouzid region. This data collected by monitoring plots by using traditional methods and by applying "IREY" and "MOPECO" (model for the economic optimization of irrigation water use at farm and plot level) in identic plots.

2. Study Area

The study was conducted in two municipalities in the region of central West of Tunisia (Figure 1). These delegations are Sidi Bouzid-West and Souk Jedid which belong administratively to the Governorate of Sidi Bouzid. The experimental plots were an open fields and implemented in farmers' fields with an average area of 1 ha for DW and 0.4 ha for oat. The area around the plots was dominated by olive trees and vegetables, mainly onion and garlic. The coordinates of the plots and monitored crops are shown in Table 1. The study area is under the influence of an arid climate. The average rainfall is around 250 mm/year. The average monthly temperature is around 19°C. The maximum temperature is recorded in July (33°C). The average evapotranspiration is around 131.5 mm. The average wind speed is 2 m/s with hot Saharan winds in summer and temperate winds in winter (Hamdi et *al.* 2015).

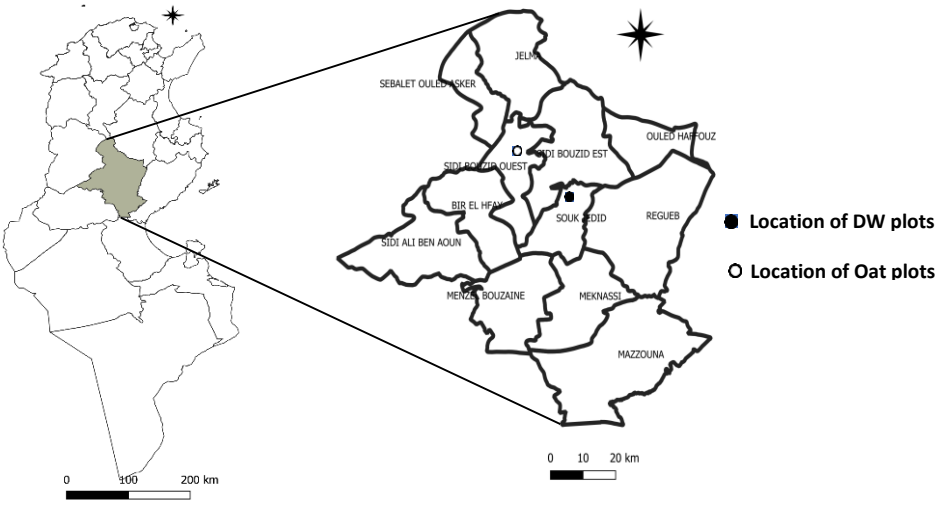

Figure 1. The geographic location of the study area

Table 1. Location of monitored crops

Delegation	Monitored crops	Growing season	Location of plots	
			Latitude	Longitude
Sidi Bouzid-West	Durum wheat	2019-2020	35°05'08.50"N	9°26'42.90"E
		2020-2021	35° 3'27.08"N	9°24'45.02"E
Souk Jedid	Oat	2019-2020	34°57'22.30"N	9°34'16.70"E
		2020-2021	34°57'19.76"N	9°34'15.01"E

3. Crop Management

The experimental plots were monitored during two growing seasons (2019/2020 and 2020/2021). The crops parameters are shown in Table 2.

Table 2. Crop parameters used for determination of crop coefficient and associated seasonal data.

Crop	Variety	growing season	Sowing – Harvest (M/D)	Rainfall (mm)	Irrigation (mm)	ETo (mm)	Temperature[b]		GDD[c] (°C)
							Max (°C)	Min (°C)	
DW[a]	Maali	2019-2020	03/12 – 06/08	127.2	462.6	687.6	25.2	11.5	2793
	Maali	2020-2021	11/27 – 06/14	73.1	412	530	22.8	10.3	2601
Oat	Local	2019-2020	12/23 – 05/12	100.7	320	619.6	23.0	10.3	2790
	Local	2020-2021	11/17 – 05/22	100.7	320	605.8	23.2	12.7	2878

[a] DW : Durum Wheat
[b] the temperatures are averages of maxima and minima calculated from the date of sowing until harvest
[c] GDD, growing degree days, was determined using a base temperature of 0.0 °C for DW and Oat.

The crops were sowed using a precision seed drill at the rate of 450 seeds/m^2 for DW and 400 seeds/m^2 for oats. The distance between the sowing rows is 17 cm. The vegetative cycle until the harvest for DW was 188 days in 2019-2020 and 199 days in 2020-2021. The crop cycle length for oat respectively for the two campaigns was 166 days and 186 days. The fertilization dose was applied according to the recommendations based on soil analysis. The weed and pests were managed according to technical reference of the National Institute of Field Crops of Tunisia (INGC 2017). The irrigation scheduling was performed following the ETc computation with the Drill and Drop capacitance probe with soil moisture precision ±0.03% vol. (METOS SENTEK DRILL & DROP).

4. Determination of field data

The recording ETo and ETc computation are started from crop sowing until harvest. ETo data is provided by METOS weather station by Pessl instruments, which reports data automatically to the www.fildclimate.com webserver (METOS- FieldClimate manual). This device measures temperature, relative humidity, wind speed and global radiation in the field. This data is used to calculate the ETo using the Penman–Monteith equation referred to the FAO Irrigation and drainage paper 56 (METOS- FieldClimate manual; Allen et *al.,* 1998).

The ETc was estimated using capacitance probe based on the creation of electric field between two conductive plates when the voltage is applied (Campora et *al.,* 2020). These sensors have a length of 0.6 m according to the effective root zone depth of monitored crops, and provide measurements every 0.1 m. Several studies have shown a better performance of capacitance probes to estimate ETo in comparison with the FAO model (Hussein Mounzer et *al.,* 2008) and with the Lysimeter method (Zerizghy et *al.,* 2013). The soil moisture depletion for different periods between two successive soil measurements was calculated. In order to determine ETc for all stages of growing cycle between two successive soil moisture measurement dates (Kumar et *al.,* 2020) as shown in figure 2.

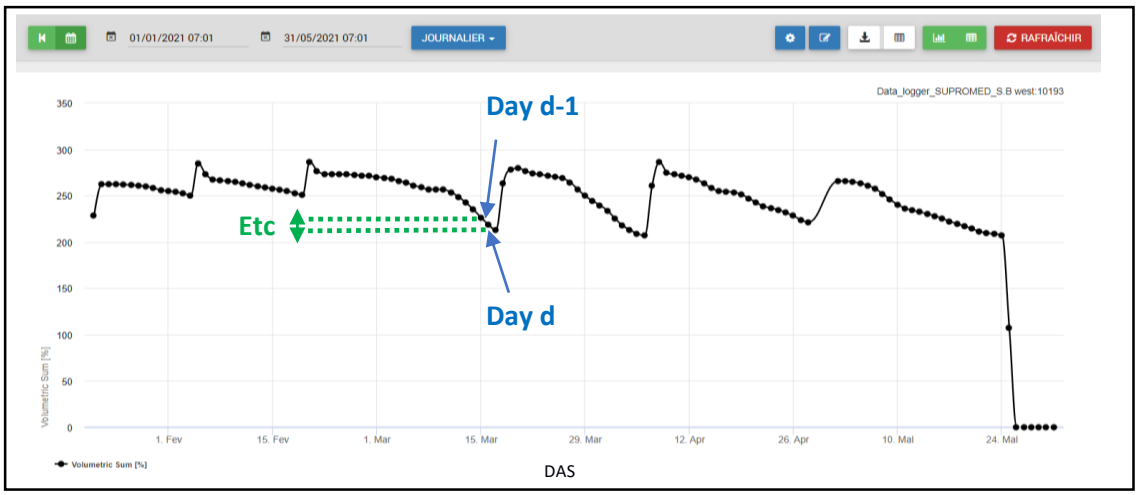

Figure 2. Screenshot from the field climate platform showing the evolution of soil moisture of Durum wheat plot during the growing season 2020-2021. DAS means Day After Sowing. ETc is obtained by the difference in the water storage in the soil in day d-1 and water storage in day d.

The ETo and ETc data were used to calculate Kc values for DW and Oat crops all the time periods using following equation:

$$\mathrm{Kc} = \frac{ETc}{ETo}$$

Where ETc = Crop evapotranspiration (mm) and ETo = Reference evapotranspiration (mm). The local Kc of Sidi Bouzid for DW and oat crops have been determined for a single growing season 2020-2021 due to the delay in acquiring equipment due to covid-19 restrictions.
Growing degree-days (GDD) were calculated during the experiments using daily minimum and maximum temperature data recorded by weather station in the site. The Equation used for calculating GDD was:

$$GDD = \frac{T_{max} + T_{min}}{2} - T_{base}$$

Where T_{max}= Daily maximum temperature (°C), T_{min}= Daily minimum temperature (°C) and T_{base}= Base temperature (°C) below which the process of plant growth does not progress. For DW and Oat, T_{base} is 0.0 °C. Any temperature below T_{base} is set to T_{base} before calculating the average (Matzarakis et *al.,* 2007; Kumar et *al.,* 2020). Growing degree days (GDD) calculated on daily basis were accumulated for the concerned period to know the cumulative growing degree days (CGDD).
We carried out a comparison between the selected parameters from the bibliographical references (Table 3) to adjust irrigation scheduling models "IREY" and "MOPECO".

Table 3. Crop parameters according to bibliographic references

Parameter		**Durum Wheat**		**Oat**	
		values	**References**	**values**	**References**
Kc values	Kc initial	0.7	Allen et al. (1998) (FAO Irrigation & Drainage Paper, 56)	0.30	Allen et al. (1998) (FAO Irrigation & Drainage Paper, 56)
	Kc middle	1.15		1.1	
	Kc end	0.25		0.30	
Length of Kc stages in accumulated GDD (ºC)	Initial	488	Raes et al, 2018 (FAO ANNEX I – AquaCrop paper)	502	SIAR, 2020
	Crop development	1300		837	
	Mid-season	2000		1222	
	Late season	2900		1555	
Threshold temperatures (ºC)	Upper temperature	26.0	Raes et al, 2018 (FAO ANNEX I – AquaCrop paper)	26.0	Raes et al, 2018 (FAO ANNEX I – AquaCrop paper)
	Lower temperature	0.0		0.0	

5. Calibration of growing degree days (GDD)

The climatic data of the first growing season were obtained from weather station of the National Institute of Meteorology (INM – Tunisia), where the geographic coordinates are 35.00 N, 9.48 E. In the second growing season, the climatic data were obtained from METOS weather station where the GPS coordinates 34.955682; 9.570992 GDD were calculated with a 0 °C threshold base temperature (Raes et *al,* 2018). The comparison made between simulated duration of the Kc stages of DW and Oat crops, by using the Growing-degree-days (GDD) and real monitored phenological shown in the Table 4.

Table 4. GDD values of Kc stages for DW and Oat crops

Crop/year		**Accumulated GDD (ºC)**			
		Kc (I)	**Kc (II)**	**Kc (III)**	**Kc (IV)**
Durum wheat	**Reference**	**488**	**1300**	**2000**	**2900**
	1st year	492	1275	2079	2793
	2nd year	317	1143	1786	2601
	Error in days	-7	6	3	-12
Oat	**Refecence**	**502**	**837**	**1222**	**1555**
	1st year	207	901	1703	2374
	2nd year	424	1103	2337	2878
	Error in days	5	1	-3	10

The values provided for the crop GDD in the tables 4, represent estimates values obtained in calibration/validation of IREY and MOPECO models with experimental data. The local GDD values for Sidi Bouzid for DW during the two growing seasons 2019-2020 and 2020-2021 were generally lower than those mentioned by Allen et *al* (1998). In terms of number of days, the highest difference is observed during stage IV, while the lowest difference is observed during stage III. The average error in days are around -7 days, 6 days, 3 days and -12 days respectively for DW Kc stages I, II, II and IV. For oats, the values were generally higher than those mentioned by Siar (2020). The average error in days are around 5 days, 1 day, -3 days and 10 days respectively for oat Kc stages I, II, II and IV.

6. Determination of calculated Kc

Crop coefficient (Kc) values for different periods of growing season of DW and Oat were computed as ratio of crop evapotranspiration (ETc) and reference evapotranspiration (ETo). The ETo was obtained from METOS weather station and the ETc was obtained from sensors. The calculation of ETc is obtained by the difference in the water storage in the soil on day d-1 and water storage in day d. The crop coefficient (Kc) values of wheat and oat were plotted against GDD that have been presented in Figure 3a and 3b respectively. When plotting the crop coefficient values for a particular period, the mid-point of that particular period was taken and the points formed a polynomial function (Figure 3a and 3b). The Kc of wheat (Figure 3a) increased gradually from a low initial value of 0.2 on January 25, 2021 (652 °C) and reaches the maximum value 1.3 on March 10, 2021 (104 days after sowing; 1185 °C) and after that the value started declining to attain a value of 0.18 at the time of harvest (2601 °C). The same trend was obtained by Kumar et *al* (2020) by studying the Kc for wheat and maize. The Kc of oat (Figure 3 b) shows an initial value of 0.23 and the maximum is reaches on April 1, 2021 (1754 °C), and the final value of Kc was 0.25 (2878 °C). Based on these results, the Kc values for DW are 0.44; 1.2 and 0.39 respectively for the different growing stages Initial (Kc I), mid-season (Kc II) and late season (Kc IV). For oat this values are 0.31; 1.23 and 0.32 respectively for Kc I, Kc II, Kc III and Kc IV.

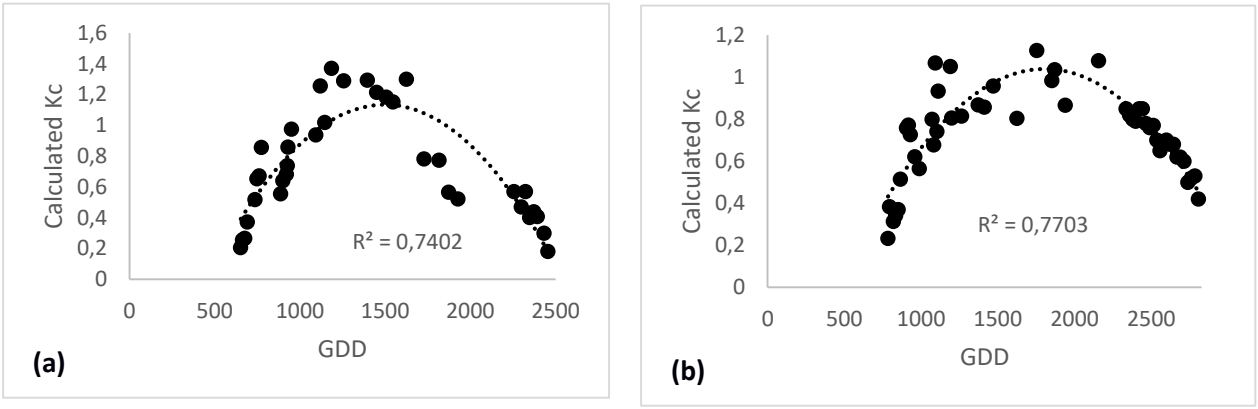

Figure 3. Calculated Kc for Durum wheat (a) and oat (b) during the growing season 2020-2021

7.Calibration of local Kc

The results analysis of local Kc values for DW and oat crop show the same trend with the FAO Kc (Allen et *al.*, 1998). However, the local Kc was lower than the FAO Kc during the initial stage, and then during the mid-season and late season stages the local Kc was higher than FAO Kc. For oat crop, the local Kc is almost similar to the FAO Kc in the initial and late-season stage. However, it was higher during the mid-season stage. The coefficients of determination (R^2) of the local Kc compared to the FAO Kc for wheat and oats respectively were 0.87 and 0.77 (Figure 4).

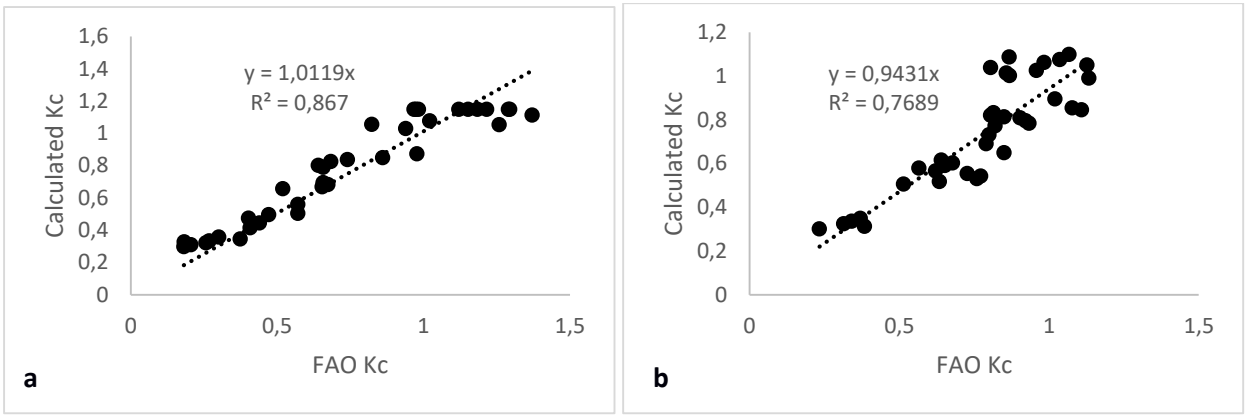

Figure 4. Correlation between calculated Kc during growing season 2020-2021 and the FAO Kc (Allen et *al.,* 1998). a: Durum wheat, b: oat.

8. Modeling of local Kc in Sidi Bouzid

A multiple linear regression was carried out in order to determine the equation of estimation of local Kc in Sidi Bouzid, by using FAO Kc and GDD values. The multiple regression function relating the local Kc values and FAO Kc and cumulative growing degree days (GDD °C) were derived as follows:

$$\textbf{Local } Kc_{DW} \textbf{ = FAO Kc*1,062+GDD*-1,176-0,067}$$
$$\textbf{Local } Kc_{Oat} \textbf{ = FAO Kc*0,7788+GDD*5,347+0,131}$$

The multiple coefficient of determination (R^2) for wheat and oat crops were respectively 0.95 and 0.88. Using the above equations crop coefficient value for any FAO Kc and the corresponding GDD can be estimated. The study will be helpful for deciding the crop water requirement and irrigation scheduling during the growing cycle of these crops (wheat and oat) on the basis of temperature data and FAO Kc. The results will also be used to calibrate the IREY and MOPECO models. The results of regression model of local Kc can therefore, be used for estimation of ETc for these crops to be grown in Sidi Bouzid area, as well as for other areas having similar climatic conditions, where such data either have not been generated experimentally or not available.

In the view of climate change effects and global warming, GDD can be potentially increase in the future and the field crops can achieves growing cycle in shorter period, that will affect distribution of the growing degree days for the crop periods. The model developed in this study will provide valuable information for irrigation management of crops. Therefore, this study can help in better estimation of crops water needs that will promote better irrigation scheduling against the upcoming climate change.

Summary

The center west of Tunisia is an irrigated region par excellence given the scarcity of rainfall and the bad distribution throughout the crop cycle. Tools for measuring soil moisture for irrigation scheduling are less accessible to farmers and are expensive. Therefore, this study was carried out for the calibration of GDD and local Kc in Sidi bouzid and similar regions, and also to develop a powerful model for estimating Kc: multiple R^2 = 0.95 for wheat and 0.88 for oat. the results will be used for the calibration of IREY and MOPECO models which are free, accessible and user friendly.

Acknowledgements

This study was undertaken and supported by the project Sustainable Production in water limited environments of Mediterranean agro-ecosystem (SUPROMED), financed by PRIMA program Section1 and coordinated by University of Castile-La Mancha (Spain).

References

Allen, R.G., Pereira, L.S., Raes, D., Smith, M., 1998. Crop Evapotranspiration-Guidelines for Computing Crop Water Requirements. FAO Irrigation and drainage paper 56. United Nations Food and Agriculture Organization, Rome. 327 p.

Ávila-Dávila, L., Molina-Martínez, J.M., Bautista-Capetillo, C., Soler-Méndez, M., Robles Rovelo, C.O., Júnez-Ferreira, H.E., González-Trinidad, J. 2021. Estimation of the Evapotranspiration and Crop Coefficients of

Bell Pepper Using a Removable Weighing Lysimeter: A Case Study in the Southeast of Spain. Sustainability 2021, 13, 747. https://doi.org/10.3390/su13020747

Ben Nouna B., Zairi A., Ruelle P., Slatni A., Yacoubi S., Ajmi T et Oueslati T (2005) Evaluation de la demande en eau et pilotage de l'irrigation déficitaire des cultures annuelles : Exemple de méthodologie et outils de mesure utilisables. Actes du Séminaire « Modernisation de l'agriculture irriguée dans les pays du Maghreb ». Rabat du 19-23 Avril 2004 pp.

Campora M., Palla A., Gnecco I., Bovolenta R., Passalacqua R. (2020): The laboratory calibration of a soil moisture capacitance probe in sandy soils. Soil & Water Res., 15, pp 75−84

Charef A., Ayed L., Azzouzi R. 2012. "Impact of natural human processes on the hydrochimical evolution of overexploitation coastal groundwater: Case study of the Mornag aquifer refill (South-East Tunis, Tunisia)", Chemie der Erde 72, pp. 61-69.

Chemak F., Issam Nouiri I., Bellali H., Chahed M.K. 2022. Irrigation practices, prevalence of leishmaniasis and sustainable development: Evidence from the Sidi Bouzid region in central Tunisia. Scientific African, Volume 15, Article e01093, pp. 1-9.

Chopart J.L., Mézino M., Le Mezo L.. 2008. Des outils d'aide à la décision pour une irrigation et une gestion de l'eau durables en culture de canne à sucre In : AFCAS. 4ème Rencontre internationale francophone, 11 au 14 mars 2008, Le Gosier, Guadeloupe. Le Gosier : AFCAS, 11 p.. Rencontre internationale francophone de l'AFCAS. 4, 2008-03-11/2008-03-14, Le Gosier (Guadeloupe).

Derwich E., Benaabidate L., Zian A., Sadki O., Belghity D. 2010. "Caractérisation physicchimique des eaux de la nappe alluviale du haut sebou en aval de sa confluence avec oued Fes'', Larhyss Journal 8, pp. 101-112.

DGAT, 2016. schema directeur d'amenagement et de developpement du gouvernorat de sidi bouzid. Report of Directorate General for Regional Planning, Ministry of Equipment, Housing and Territorial Development Tunisia. 204 p.
http://www.mehat.gov.tn/fileadmin/user_upload/Amenagement_Territoire/SDAD/RapportSDADsidiBouzidDec2016fr.pdf

DGAT, 2018, ATLAS DU GOUVERNORAT DE SIDI BOUZID. Report of Directorate General for Regional Planning, Ministry of Equipment, Housing and Territorial Development – Tunisia. 106 p http://www.mehat.gov.tn/fileadmin/user_upload/Amenagement_Territoire/AtlasSidiBouzidFr.pdf

DGRE: Direction Générale des Ressources en Eaux. 2012. Annuaire d'exploitation des nappes phréatiques et profondes, 45p.

Egbuikwem, P.N., Obiechefu, G.C. Evaluation of Evapotranspiration Models for Waterleaf crop using Data from Lysimeter. 2017. In Proceedings of the Spokane, Washington, DC, USA, 16–19 July 2017, American Society of Agricultural and Biological Engineers: St. Joseph Charter Township, MI, USA.

Gammoudi S, Chkir N, Boughattas N.H, Hamdi M, Arraouadi S, Zouari K. 2020. Assessment of urban groundwater vulnerability in arid areas: Case of Sidi Bouzid aquifer (central Tunisia). Journal of African Earth Sciences (IF2.046). doi: https://doi.org/10.1016/j.jafrearsci.2020.103849.

Ghazavi R., Vali A. B., Eslamian S. 2012. "Impact of flood spreading on groundwater level variation and groundwater quality in an arid environment", Water Resources Management 26, pp: 1651-1663.

Grigorieva, E., Matzarakis, A., De Freitas, C. R. Analysis of growing degree-days as a climate impact indicator in a region with extreme annual air temperature amplitude. 2010. Climate Research, , 42(2), pp. 143-154.

Hamdi M., M'Nassri S., Dridi L., Majdoub R., Abida H., 2015. Effet de L'épandage des Eaux de Crues sur les Ressources en Eaux Souterraines dans les Zones Arides: Plaine de Sidi Bouzid (Tunisie Centrale) Euro. J. Sci. Research. ISSN 1450-216X / 1450-202X Vol. 129. pp.33 – 42

Hussein Mounzer O., Hernández R. M., Villena I. A., Muñoz J. V., Ruiz-Sánchez M. C., Vargas L. M. T., Arnaldos V. P., García J. M. A. 2008. Estimating evapotranspiration by capacitance and neutron probes in a drip-irrigated apricot orchard. INCI vol.33 n.8 Caracas ago, pp 586 – 590.

Kumar J., Umesh U. N., and Singh A. K. P. 2020. Derivation of Crop Coefficient Model of Wheat and Maize Using Growing Degree Days to Mitigate Climatic Variability. Int.J.Curr.Microbiol.App.Sci. 9(10): 2915-2924. doi: https://doi.org/10.20546/ijcmas.2020.910.351

Matzarakis, A., Ivanova, D., Balafoutis, C. and Makrogiannis, T. (2007). Climatology of growing degree days in Greece. Clim. Res., 34: pp 233–240.

METOS - SENTEK DRILL & DROP: Probe Manual Version 1.2, For Bluetooth probes, Series II Interface probes, and Series III probes. Copyright © 2001 – 2020 Sentek Pty Ltd All rights reserved. https://www.fondriest.com/pdf/sentek_drill_drop_probe_manual.pdf

METOS - FieldClimate MANUAL & RECENT RELEASES' NOTES. Available online. https://metos.at/fr/fieldclimate-manual/ (accessed on 22 may 2022).

Mileham L., Taylor G. R., Todd M., Tindimugaya C., Thompson J. 2009. “The impact of climate change on groundwater recharge runoff in a humid equatorial catchment: sensitivity of projections to rainfall intensity’’, Hydrological Sciences Journal 54 (4), pp: 727-738.

Paparrizos, S. and Matzarakis, A. 2017. Present and future responses of growing degree days for Crete Island in Greece. Adv. Sci. Res., 14: 1–5.

Raes, D., Steduto, P ., C.HSIAO, T., Fereres, E., Annex I – AquaCrop, Version 6.0 - 6.1, May 2018 Sevacherian, V., Stern, V.M., Mueller, A.J., 1977. Heat accumulation for timing Lygus control pressures in a safflower-cotton complex. J. Econ. Entomol. 70, 399–402.

SIAR, 2020. Irrigation Advisory Service in Castilla-La Mancha. Regional Center of Water Research. http://crea.uclm.es/siar/. Field data from 2001 to 2013.

Soldevilla-Martinez, M., Quemada, M., López-Urrea, R., Muñoz-Carpena, R., Lizaso, J.I. 2019. Soil water balance: Comparing two simulation models of different levels of complexity with lysimeter observations. Agric. Water Manag. 139, pp. 53–63. [CrossRef] 11.

The National Institute of Field Crops of Tunisia. Available online : http://ingc.com.tn/index.php (accessed on 07 april 2022).

Yimam, A.Y., Assefa, T.T., Adane, N.F., Tilahun, S.A., Jha, M.K., Reyes, M.R. 2020. Experimental Evaluation for the Impacts of Conservation Agriculture with Drip Irrigation on Crop Coefficient and Soil Properties in the Sub-Humid Ethiopian Highlands. Water 2020, 12, 947.

Zerizghy, M.G., Van Rensburg, L.D., Anderson, J.J., 2013. Comparison of neutron scattering and DFM capacitance instruments in measuring soil water evaporation. Water SA. 39 (2), pp 183–190.

Analysis of land use in Sidi Bouzid region central Tunisia

Insaf Mekki[1], Rim Zitouna Chebbi[1], Hacib Amami[1], Ameni Touaiti[1], Nesrine Taouajouti[1], Abdelaziz Zairi[1],

[1] INRGREF, University of Carthage, Tunisia.

Correspondence: insaf.mekki.im@gmail.com

Abstract

Semi-arid agricultural zones offer ecosystem services that are driven by land and water resources use. Effective management of these zones requires assessing the land use patterns across several spatial scales. The present study focused on characterizing the main cultivated crop areas in Sidi Bouzid region in central Tunisia. We performed farmers interviews and collected data about farms structures and field spatial distribution. We also observed crop types for these fields in 2021 and 2022. The crops rotation at the plot level and the agriculture practices and irrigation water use are obtained from survey of the farms. The typical crop sowing and harvesting dates for the most important and widespread crops in region are determined. Observations are gathered within a geographical information system (GIS). Producing multi-layer GIS with different georeferenced information such as: soil and crop types, agricultural practices, irrigation system, helped to provide a first indicator of the water irrigation requirement during the cropping season.

Keywords: crop spatial distribution, crop rotation, agricultural practices, irrigated systems.

1. Introduction

Arid and semi-arid agricultural zones offer ecosystem services that are driven by land and water resources use. They depend almost entirely on groundwater resources which are marked by degradation, and an increasing competition between the agricultural, domestic and industrial sectors (Pereira et al., 2009; FAO, 2012). Besides, these agrosystems face climate change pressure that is expected to impact the crop yield and thus affecting the availability of food and interfering in various environmental factors. In the context of global change, the spatiotemporal distribution of crops in the landscape is a major concern to better manage the soil and water resources (Mekki et al., 2018a). For example, the adoption of crops rotation is promoted to increase the agricultural production and the added value per cubic meter of irrigation water used by crops. Contributing, therefore, to increase agricultural production and to preserve soil and water resources. Regarding water management, there is a need to ensure that both the needs for water for rainfed crops and for the storage of water for irrigated agriculture are met. Mekki et al. (2018b) have shown that evapotranspiration is the predominant factor influencing soil moisture dynamics and that evapotranspiration differs significantly depending on the crops, cropping practices, soil properties and climatic conditions. Consequently, they assumed that it is possible to control the amount of downstream water yield by adopting appropriate agricultural practices, including the spatiotemporal distribution of crops. Therefore,

characterizing the drivers of crop allocation to fields is a prerequisite for (1) exploring and simulating spatially explicit plausible land use scenarios, and (2) quantifying the subsequent ecosystem services and disservices (Benoît et al., 2012; Rizzo et al., 2013). Hence, there is a need to explore reasonable choice of cropping system that increases the crop yield, optimize water resources management while ensuring a decent income for farmers. The objective of this study is to characterize the main cropping systems within the Sidi Bouzid plain.

2. Materials and methods

2.1 Study site

The study area was the Sidi Bouzid Governorate in the central-western part of Tunisia (Figure 1). The climate regime is at the boundary between semiarid and arid (Carte Agricole, 2003) with cold and humid winters and hot and dry summers. The mean annual evaporation of about 1,470 mm exceeds considerably the mean annual rainfall that range from 188 mm to 251 mm (Carte agricole, 2003). Soils are deep with an organic matter content ranging from 0.5 to 1.5%, being suited for the majority of the crops. Water supply in Sidi Bouzid plain comes from groundwater reserves held by multi-layer Mio-Plio-Quaternary aquifer systems (Yangui et al., 2010). As described by Yangui et al., (2010), the exploitation of the aquifer is carried out through dug wells for the shallow levels (40-100 m) and by tube-wells with depths ranging from 100 to 400 m (Figure 1).

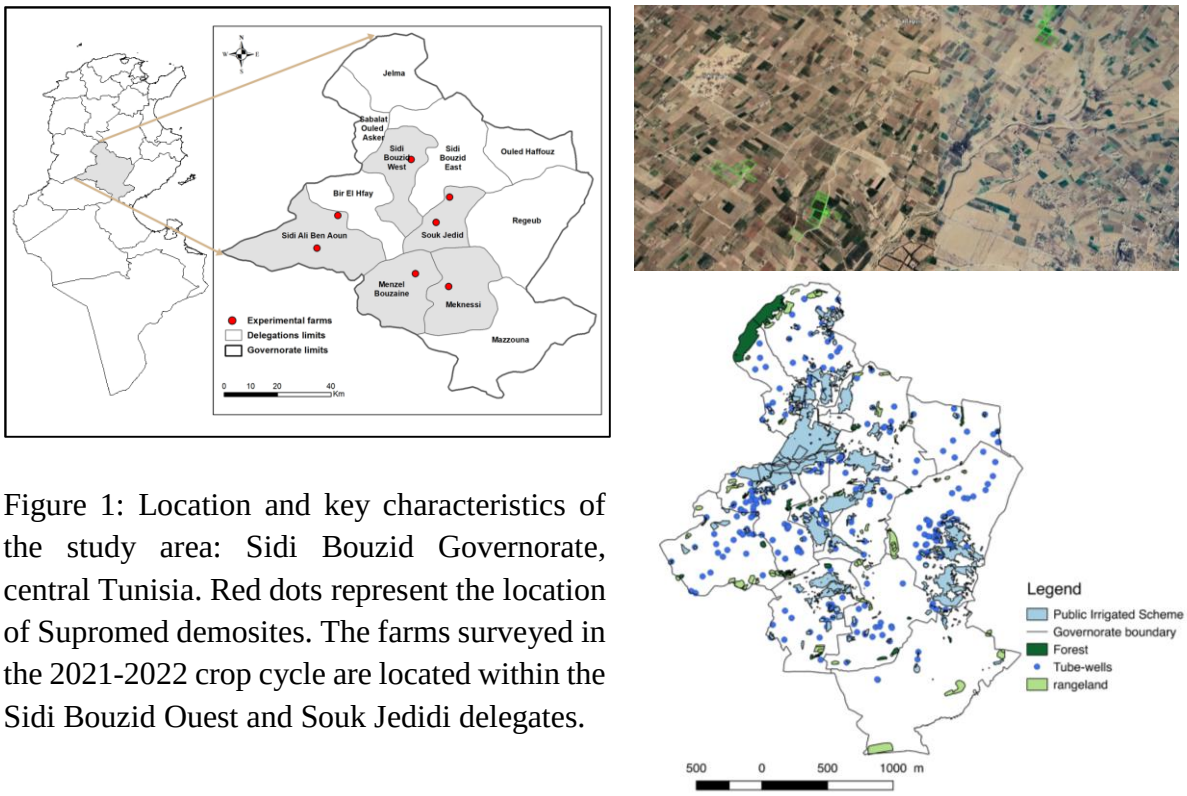

Figure 1: Location and key characteristics of the study area: Sidi Bouzid Governorate, central Tunisia. Red dots represent the location of Supromed demosites. The farms surveyed in the 2021-2022 crop cycle are located within the Sidi Bouzid Ouest and Souk Jedidi delegates.

Agriculture remains one of the main economic activity in Sidi Bouzid governorate, with almost 30% of its population involved in this activity (INS, 2014). The socio-economic development of the Sidi Bouzid governorate relies on groundwater resources and is suffering from depletion

and quality deterioration of the shallow and deep aquifers. The irrigated agricultural practices developed since the 60s thanks to the creation of the public irrigated schemes (Figure 1). The irrigated area covers more than 50,000 ha, where 88% of them are private farms whilst 12% are within the public irrigated schemes. Cropping patterns in Sidi Bouzid plain have long consisted of traditional homogeneous system of pastoral producers based on self-consumption and mixed agro-pastoral system with low inputs of fodder crops for livestock. With the introduction of cash crops and the intensification of phreatic and then deep groundwater pumping in the 1960s and 1980s, farmers gradually shifted towards high value vegetable crops, olive and almond. The governorate has therefore been one of the leaders in onion and almond production in the country along with a considerable production of olives and pistachios.

2.2. Data collection

The present study focused on characterizing the main cultivated crop areas. We performed farmers interviews and collected data about farms structures and field spatial distribution. A survey form was designed to collect data at the scale of the farms. Farmers were interviewed on: the types of grown crops, the type of raised livestock; the agricultural practices in terms of crop rotation, the allocation to the agricultural field and the strategies behind their choice.

We also observed crop types for these fields in 2021-2022 cropping cycle. The crops rotation at the plot level and the agriculture practices and irrigation water use are obtained from survey of the farms. The typical crop sowing and harvesting dates for the most important and widespread crops in region are determined.

In a second step the use of the sentinel images and the observations at different agricultural fields is envisaged to produce land use maps. The required georeferenced data were acquired by using existing data and classifying sentinel images. Data on the crops present in the fields during the growing season were obtained through field observations and a database is built to train the supervised classification of the sentinel images series. The observed fields were distributed among the existing types of crops (wheat, forage crops, vegetables, olive, …).

3. Results

Farming system is based on wheat, fodder, vegetables, olive trees and livestock. The livestock is a main component of the farming system to increase the soil fertility by supplying manure and/or ensuring liquidity throughout the year. Livestock husbandry includes cattle, sheep and goat breeding. Livestock feeding relies on forage production, the grazing of natural vegetation and crop residues, and the use of external feed supplements. Annual cultivated crops in the observed farms include: vegetables (onion, garlic, tomato, pepper), fodder (oat) and cereals (wheat). Tree crops mostly include olive where two interviewed farms practiced the intercropping with fodder crops using sprinkler irrigation systems. According to interviewed farmers, the choice of the cultivated crops is mainly impacted by the access to land, water and energy resources. Farmers consider that the limited financial resources play a decisive role in the choice of crops to be cultivated. Farmers with small landholdings (less than 3 ha) are constrained by the size of the farm; they do not practice crop diversification because they are

constrained by the limited area. The local market and the neighboring practices are also identified as driving factors for cultivated crop choices. The identified drivers should be perceived as constraints to be considered when defining agricultural policies.

The irrigation system depends on the type of cultivated crops: drip irrigation for vegetables and young olive trees, and surface or sprinkler irrigation for cereals, fodder and old olive trees.

The crops rotation at the plot level and the agriculture practices are obtained from survey of the farms. Crop sequences representing possible combinations of the four types of crops (onion, wheat, oat, vegetables) were observed and classified into five types of succession (oat/onion; onion/wheat/oat; onion/wheat/vegetable, wheat/ fallow/oat). The data shows that the onion/wheat/oat type is dominant. Wheat is mainly rotated with vegetables to capture the benefits of fertilization and/or to control pests or weeds. However, forage crops and fallow may sometimes replace vegetable crops in the succession. The reason behind this is the irrigation water scarcity and/or the need to feed the livestock.

4. Conclusion

The preliminary results of this study characterize the main crops and the agricultural practices within the plain of Sidi Bouzid. The results are currently to be validated using high number of field observations and satellite images over several years and dates (three cropping cycles). The observations are gathered within a geographical information system (GIS). Producing multi-layer GIS with different georeferenced information such as: soil and crop types, agricultural practices, irrigation system. The combination with the remote sensing and the crop coefficient data will help providing a first indicator of the total water irrigation requirement during the cropping season with the objective to assess the groundwater uses and to improve the monitoring capabilities.

Acknowledgements
The main financial support for this study was provided by the PRIMA SUPROMED "Sustainable Production in water limited environments of Mediterranean agro-ecosystem" project. The cooperation of the farmers in the Sidi Bouzid Ouest Souk Jedidi delegates regions by providing access to their land was highly appreciated.

References

Benoît, M., Rizzo, D., Marraccini, E., Moonen, A.C., Galli, M., Lardon, S., Rapey, H., Thenail, C., Bonari, E., 2012. Landscape agronomy: a new field for addressing agricultural landscape dynamics. Landsc. Ecol. 27, 1385–1394. https://doi.org/10.1007/s10980-012-9802-8.
FAO, 2012. Coping with Water Scarcity. An Action Framework for Agriculture and Food Security. (Water Reports 38) FAO, Rome.
INS, 2014. (Institut National des Statistiques). Sidi Bouzid à travers le Recensement Général de la Population et de l'Habitat 2014, Tunis.
Mekki, I., Bailly, J.S., Jacob, F., Chebbi, H., Ajmi, T., Blanca, Y., Zairi, A., Biarnes, A., 2018a. Impact of farmland fragmentation on rainfed crop allocation in Mediterranean landscapes: a case study of the Lebna watershed in cap bon. Tunisia. Land Use Policy 75, 772-783. https://doi.org/10.1016/j.landusepol.2018.04.004.

Mekki, I., Zitouna-Chebbi, R., Jacob, F., Ben, Mechlia N., Pr´evot, L., Albergel, J., Voltz, M., 2018b. Impact of land use on soil water content in a hilly rainfed agrosystem: a case study in the cap bon peninsula in Tunisia. AGROFOR Int. J. 3, 64-75. https://doi.org/10.7251/AGRENG1801064M.
Pereira, L.S., Cordery, I., Iacovides, I., 2009. Coping with Water Scarcity-Addressing the Challenges. Springer, Netherlands (ISBN: 978-1-4020-9578-8)(Print) (978-1-4020-9579-5)(Online).
Rizzo, D., Marraccini, E., Lardon, S., Rapey, H., Debolini, M., Benoît, M., Thenail, C., 2013. Farming systems designing landscapes: land management units at the interface between agronomy and geography. Dan. J. Geogr. 113, 71-86. https://doi.org/ 10.1080/00167223.2013.849391.
Yangui, H., Zouari, K., Trabelsi, R., Rozanski, K. 2010. Recharge mode and mineralization of groundwater in a semi-arid region: Sidi Bouzid plain (central Tunisia). Environ. Earth. Sci. DOI 10.1007/s12665-010-0771-4.

A participatory process for exploring sustainable groundwater management options: A case study in Northern Tunisia

Intissar Ferchichi[1], Insaf Mekki[1], Mohamed Elloumi[2], Abdelaziz Zairi[1]

[1]INRGREF, University of Carthage, Tunis, Tunisia
[2]INRAT, University of Carthage, Tunis, Tunisia

Abstract. Environmental sustainability problems are typically complex and multiscale. Solving sustainability problems requires balancing the socio-economic well-being of farmers and the protection of natural environment and water resources. Finding sustainable solutions could be accomplished through a collaborative process that includes the diversity of knowledge and values of all affected stakeholders. In the irrigated area of Echraf, located in the Haouaria Plain, in Northern Tunisia, farmers are currently dependent upon groundwater use for their livelihood and food security. Today, the sustainability of this agrosystem is threatened by the depletion and quality deterioration of groundwater resources. The purpose of this paper is to present results from a participatory process based on a territory game approach to explore the main issues of the study site, the drivers of change and evolution scenarios for the area. Through the territory game method, local stakeholders identified conditions that hinder or facilitate the implementation of scenarios and the pathways of actions. Participants agreed that one of the key problems identified for the groundwater exploitation is the lack of collective action amongst farmers. Farmers invest individually in illegal abstraction given the availability of drilling technology, with limited knowledge or awareness of the collective negative consequences of uncoordinated and unregulated abstraction. Small scale farmers must face emerging constraints such as the increase of production and abstraction costs related to the cost of energy for pumping and the intensive use of inputs. Participants emphasized the need for local initiatives and innovations to strengthen farmers' collective organization and to improve water resources management. Local innovations in the irrigated area of Echraf are being tested within the project PRIMA-HubIs to explore more sustainable managements options of groundwater resources.

1. Introduction

Recent studies highlight the fragility of the Mediterranean basin which is undergoing rapid social and environmental changes with negatives implications towards current and future sustainability. Climate and land cover change are likely to amplify water stress in the Mediterranean region, caused by a combination of decreased water resource availability and increased water use pressure resulting from economic growth and urban expansion (Garcia-Ruiz et al., 2011). Groundwater resources play a vital role, in meeting irrigation water demands, they have been and continue to be the largest buffer in water scarcity situations (Garrido and Iglesias 2006). Given the character of groundwater (a classic 'common-pool resource'), it is inherently vulnerable to the so-called 'tragedy of the commons' in which actual users and potential polluters act solely in their individual short-term interest, rather than considering long-term communal considerations (Ostrom, 1990). Concerns over groundwater depletion and ecosystem degradation have led to the incorporation of the concept of groundwater sustainability as a groundwater policy instrument in several water codes and management directives worldwide. 'Groundwater sustainability' may refer to the development and use of the resource in a manner that can be maintained for an indefinite time without causing unacceptable environmental, economic, or social consequences (Alley et al., 1999). Groundwater sustainability is not only a function of the aquifer performance, but also of the larger participatory and adaptive governance processes. Water security and sustainability should be framed beyond just the focus on the water quality and quantity to better understand possible co-evolving scenarios between water systems, ecosystems, and society (Elshall, 2020). In the context of water scarcity and increasing competition in access to water resources, farmers who had to face water scarcity and uncertainty favored short-term gains by arranging the institutions in a way that suits their particular needs. Thus, it appears that only by strengthening collective action and expanding the role of water users in preserving groundwater resources in cooperation with the state is it likely that efficient and equitable management of water resources will be achieved (Ferchichi et al., 2017).

In this paper, we focused on an example of inadequate groundwater governance arrangements found in the Haouaria plain and particularly in the irrigated area of Echraf. Conflicts have emerged between agricultural and industrial water users over access to groundwater. Declining groundwater levels and

increasing salinity, industrial pollution and contamination is also reported in this region. Existing institutions are currently unable to support sustainable or equitable water management outcomes. A participatory process was implemented to initiate interactions between different stakeholders involved in the management of the irrigated area. Rather than imposing exogenous practices and technologies, the participatory process aims at giving essential support to groundwater resource users to propose solutions based on their context and available options.

2. The case of the irrigated system Echraf in the Haouaria plain, Tunisia

The study focuses on the public irrigated area of Echraf, located in the Haouaria plain, in north-eastern Tunisia (Figure 1). The plain is surrounded by the forest of Dar Chichou and Djebel Haouaria, and the Mediterranean Sea on both sides. The climate is Mediterranean upper sub-humid, with irregular precipitation and wind 300 days per year on average. The annual rainfall is about 568 mm/year (1972-2007) with erratic rains mainly between September and April. Summers are very dry as rain during this season contributes only 2% of the annual total precipitation. Monthly evaporation average is 104 mm, ranging from 176 mm in July to 35 mm in December. Dominant sandy soils and a rather flat topography favor direct rain infiltration, explaining why the hydrographic network is almost nonexistent in the plain of Haouaria (Mekki et al. 2017). Agriculture remains the main economic activity in the Haouaria region, with almost 70% of its population involved in this activity (INS, 2010). The agricultural development relies on groundwater resources which are currently suffering from depletion and quality deterioration of the shallow and deep aquifers. The exploitation increased between 1970 and 2006 fivefold for the shallow aquifer and twofold for the deep aquifer, respectively (CRDA, 2011), has led to the qualitative and quantitative degradation of water resources in the plain. The Public Irrigated Area of Echraf covers around 312 ha. Irrigation water is supplied to farmers through a collective network, alimenting 60 hydrants, and managed by the water users' association, called GDA. Initially, the groundwater was pumped from seven boreholes, managed by the administration (CRDA), with a flow rate capacity at the head system estimated at 180 CMS. The boreholes serve a buffer reservoir whose capacity is around 5000 m^3. The water is then distributed through the pumping station of Echraf, to the collective network. Currently, only three boreholes are functional due to the increasing salinity or the decreasing of the groundwater level. The flow rate capacity at the head system is currently estimated at 70 CMS.

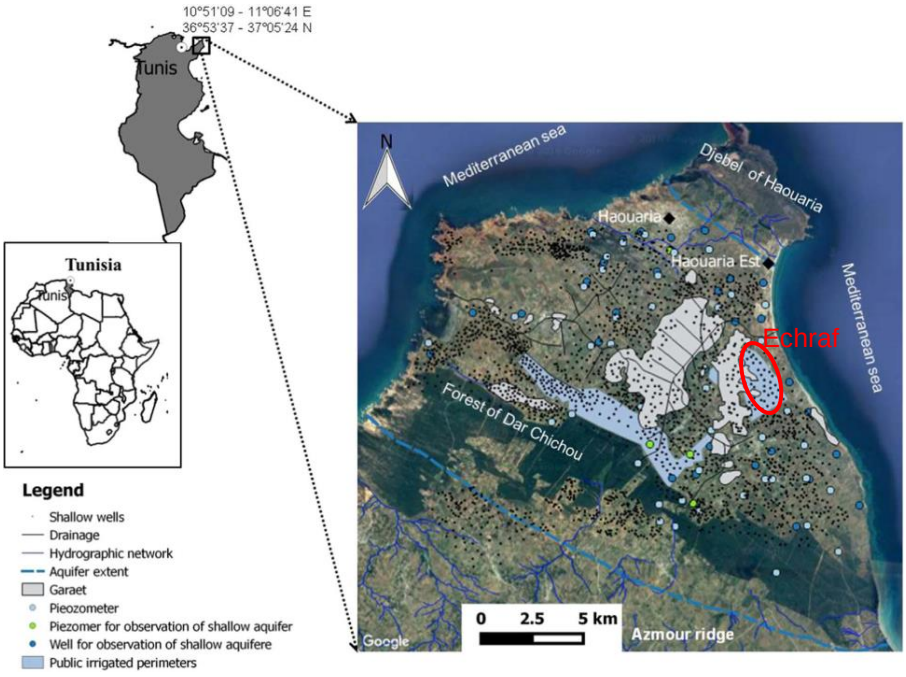

Figure 1. Localization and key characteristics of the study area. Garaet/Garâa is a natural wetland **(Mekki et al., 2017)**

Since 1975, the Ministry of Agriculture in Tunisia is in charge of water management, assisted by two bodies, the National Water Council, and the Commission of the Public Water Domain. Within the Ministry of Agriculture, several technical departments are involved in the management of water resources. The

most important are: (i) In each governorate, the Regional Commission for Agricultural Development (CRDA) is the decentralized body representing the Ministry of Agriculture. It has financial autonomy and is responsible for the implementation of policies from the Ministry in each governorate and (ii) Farmers associations called Development Grouping of Agriculture "GDA" sharing one aquifer are in competition with each other as well as with other types of users. There are no structures that work linking the different GDAs in one aquifer system together, making joint monitoring and rule-making difficult given the absence of coordination (Elloumi, 2016).

3. Implementation of the participatory process

The planification for the participatory process started from 2015 within the framework of previous projects on groundwater governance (Mekki et al., 2017; Closas et al., 2017). Individual and collective interviews were conducted with 30 farmers, 10 government agencies, 7 suppliers and NGO. During this time, discussions covered the institutions, actors, interactions, and outcomes associated with water management. Participatory workshops were also organized with water management actors and the administration. The discussions helped to clarify: (i) whether there really are coordination challenges related to water management, (ii) in which fields institutions fail to address water related social dilemmas, (iii) the historical or current rules and norms farmers refer to. Together, this information helped us to design the territory game conceptual idea. Players (particularly well-informed on the topic) become more engaged. Since 2017, field visits and interviews were conducted to characterize the current spatial agricultural dynamics, linked to the groundwater use, trends and impacts on agricultural practices, species diversity and local food systems. Interviews performed during field investigations concerned these issues: Collection of data from previous projects conducted within the case study: farm systems (characteristics), Main potentialities and threats of the farm systems / drivers of change? What changes in the last 30 years and reasons of change; What was the foreseen future in the next 30 years? Desirable/or not future for the local actors?

Cartographical and statistical material made from old projects and government websites and reports were combined with qualitative data collected from the conducted interviews. This information was used to prepare for a territory game. The territory game is a concertation tool between territory stakeholders, it aims to support territorial development processes (Lardon et al., 2016). This tool is based on an analysis of the main organizers of the space expressed as graphic models that serve as the thread for comparing and integrating the knowledge generated throughout the procedure. A multi-actor workshop was held on 27 mars 2018 in Kelibia city, Cap Bon. Three groups of actors participated in the territory game separately. Four research facilitators were present, including a main facilitator who conducted the workshop, one observer who recorded workshop proceedings, and two co-facilitators who organized game materials, assisted participants, and recorded discussions during the game debriefings. The workshop was attended by 27 participants that were invited formally. Participants represented key stakeholders' groups from the community. 12 participants were from local administrations (CRDA, GDA, municipality…), 5 participants from different associations (farmers' association, rural woman association, …), 1 research engineer, 4 farmers and 1 supplier were also present.

In April 2021, a participatory workshop was organized with 19 local stakeholders: 12 farmers from the irrigated area Echraf, two participants from the CRDA and 5 participants from the GDA. This workshop aimed to discuss collective solutions and potential innovations, based on the results of the multi-actor workshop and the analysis of water consumption of different farmers, collected from the GDA.

4. Stakeholders'' perceptions of key issues and innovations pathways

Among the three focus groups formed during the multi-actor workshop, organized in mars 2018, one group focused on water resource sustainability in the irrigated area of Echraf. The main issues identified with participants were relatives to: (i) the lack of collective action amongst farmers; (ii) the limited knowledge or awareness of the negative consequences of uncoordinated and unregulated abstraction of water, (iii) the environmental impacts of the development of the agro-industry in the area, (iv) production costs especially for small farmers and (v) marketing difficulties (Ferchichi et al., 2020).

During the workshop of April 2021, the distribution of the crops irrigated from the collective network of the GDA during the Fall-Winter 2020 season and then during Spring-Summer 2020 season, and the water consumption of farmers irrigating from the collective network of the GDA, have been illustrated

through graphs (Figure 2). These graphic supports were used to detect levers to improve the competitiveness of farmers through the amelioration of the water productivity at the farm level. Participants identified five key issues relative to the groundwater management in their system: (i) the increasing costs of inputs and pumping, (ii) the deterioration of the quality and quantity of groundwater, (iii) irrigation systems are not adapted to the farm requirement, (iv) the deterioration of the irrigation service provided by the GDA and (v) the lack of maintenance of the collective network.

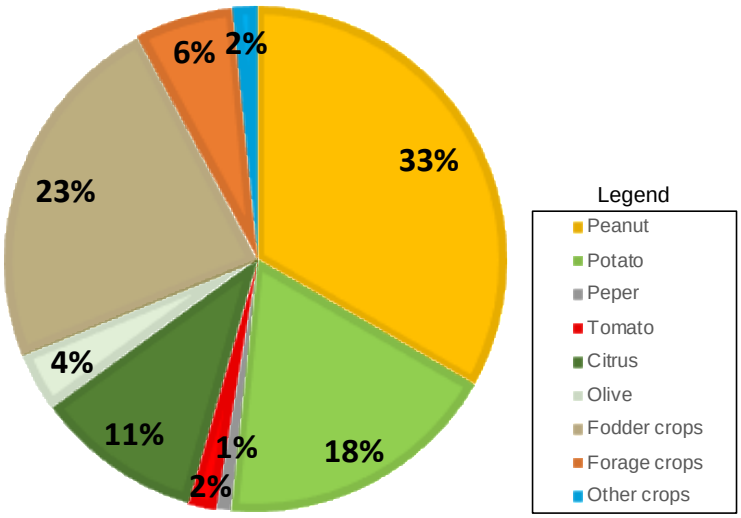

Figure 2. Irrigated crops' distribution in the irrigated area Echraf, during the Spring-Summer-2020 season

Based on Figure 2, the two crops of peanut and potato are taken as an example to discuss the possibility of improving the techno-economic performance of the farm. During the Spring-Summer 2020 season, peanut occupied an area of 33% while potato was grown on 18% of the total area of the farmers operating the collective network of GDA Echraf. The importance of the area of these two crops is explained by their profits that are quite significant despite the high costs of fertilizers, pesticides, and water. Tomato cultivation occupies only 2% of the area, whereas previously this crop was among the main crops grown in the region. The near disappearance of this crop indicates that farmers in the region have not been able to secure a high profit; the competitiveness of this crop has been judged to be low compared to other regions. Regarding the water consumptions for two types of crops (potato and peanuts), the farmers explained the excess of the applied quantity of water by the quality of the soil. The access for many farmers to the groundwater through individual wells can also explain the observed sur-irrigations. The majority of participants indicated that they don't know exactly the water requirements of their farms.

Many farmers explained that they had to deepen their wells because of the decrease of the groundwater level. Managers from the WUA and the administration also explained the impact of the degradation of the quantity and quality of the groundwater on the irrigation service quality. Currently, the allocated water to the irrigated area is pumped through only three collective boreholes. The other four boreholes are no more functional because of the decrease of the water level and the increasing salinity. Between 1996 and 2019, a decrease in piezometric levels of 20 m has been observed for the Haouaria aquifer (Figure 3).

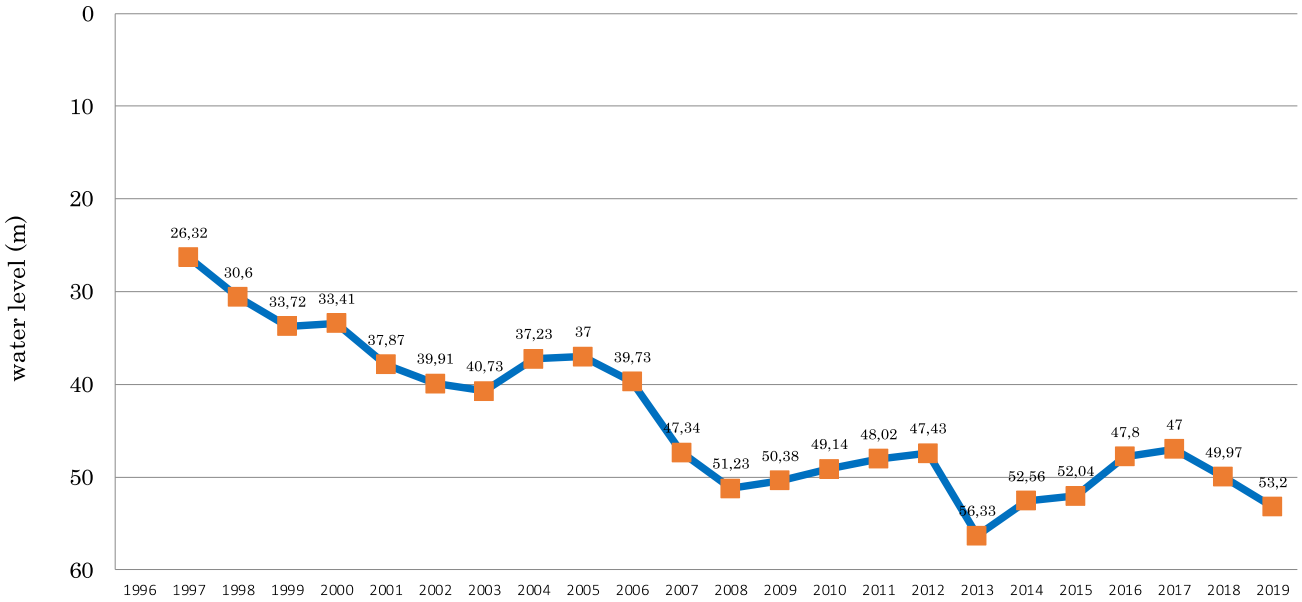

Figure 3. Evolution of the piezometric level of the Haouaria aquifer from 1996 to 2019

Farmers showed their interest in co-developing decision support tools for a better management of the water resources. According to participants, these tools should consider the marginal and vulnerable environment and the limited socio-economic infrastructure in the Echraf irrigated area. Participants approved the necessity to conduct a more in-depth diagnosis of factors explaining the poor performance at the level of the farm and the district.

5. Conclusion

The implemented process aims to develop innovations for sustainable irrigation water management in collaboration with local stakeholders. We believe that through this process of joint innovation, farmers can experiment and adapt new technologies and management practices. The need for farmer participation and innovation is justified by the fact that most water management problems tend to be site specific. This calls for the need to provide farmers with a set of flexible options to fit specific niches depending on perceived constraints rather than wholesome recommendations that promote a single technological and institutional package in all areas.

Acknowledgements

This research was supported by the Arimnet2-funded regional project “DIVERCROP” (land system dynamics in the Mediterranean basin across scales as relevant indicator for species diversity and local food systems) and is currently supported by the HubIs project (Open Innovation Hub for Irrigation Systems in Mediterranean Agriculture). The main objective of HubIS is to favor the emergence, evaluate and boost innovations aiming at reducing the performance gap and thus improve the sustainability of irrigation systems in the Mediterranean region. We gratefully acknowledge all the actors involved in water management in the irrigated area of Echraf (local extension services, farmers, water user associations, etc.) for their kind cooperation and for making data available and accepting to respond to our interviews and to participate in different workshops.

References

Alley, W.M., Reilly,T.E and Franke, O.L., 1999. Sustainability of ground-water resources U.S. Geol. Surv. Circ. 1186, pp 79.

Closas, A.; Molle, F.; Hernández-Mora, N. 2017. Sticks and carrots to manage groundwater over-abstraction in La Mancha, Spain. Agric. Water Manag. 194, 113–124.

CRDA-Nabeul. 2011. Annual Report of 2011 Activities. Technical Report. Regional planning Commission for Agricultural Development: Nabeul, Tunisia. (In French)

Elloumi, M. 2016. La Gouvernance des Eaux Souterraines en Tunisie, Report No. 6; IWMI Project Publication 'Groundwater Governance in the Arab World'; IWMI: Cairo, Egypt.

Elshall, A. S., Arik, A. D., El-Kadi, A. I., Pierce, S., Ye, M., Burnett, K. M., and Chun, G. 2020. Groundwater sustainability: A review of the interactions between science and policy. Environmental Research Letters, 15(9), 093004.

Ferchichi, I., Marlet, S., & Zairi, A. 2017. How Farmers Deal with Water Scarcity in Community-Managed Irrigation SYSTEMS: A Case Study in Northern Tunisia. Irrigation and Drainage, 66(4), 556-566.

Ferchichi, I., Mekki, I., Elloumi, M., Arfa, L., & Lardon, S. 2020. Actors, scales and spaces dynamics linked to groundwater resources use for agriculture production in Haouaria plain, Tunisia. A territory game approach. Land, 9(3), 74.

García-Ruiz, J.M., López-Moreno, J.I., Vicente-Serrano, S.M., Lasanta–Martínez, T. and Beguería, S., 2011. Mediterranean water resources in a global change scenario. Earth-Science Reviews, 105(3-4), pp.121-139.

Garrido, A. and Iglesias, A., 2006, January. Groundwater's role in managing water scarcity in the Mediterranean region. In International Symposium on Groundwater Sustainability, 113-138.

INS.2010. Annuaire des Statistiques 1998–2010; Institut National des Statistiques: Tunis, Tunisia.

Lardon, S.; Marracini, E.; Filippini, R.; Gennai-Schott, S.; Johany, F.; Rizzo, D. Prospective participative pour la zone urbaine de Pise (Italie). 2016. L'eau et l'alimentation comme enjeux de développement territorial. Cah. Geog. Québec, 170, 265–286.

Mekki, I.; Ghazouani, W.; Closas, A.; Molle, F. 2017. Perceptions of groundwater degradation and mitigation responses in the Haouaria region in Tunisia. Groundw. Sustain. Dev. 5, 101–110.

Ostrom, E., 1990. Governing the commons: The evolution of institutions for collective action. Cambridge university press.

A modern approach to irrigation management

Markinos A.[1], Koufopoulou M.[1], Kiourtsis K.[1] and Alexiou E.[1]

[1]Local Organisation of Land Improvement (TOEV) Tavropou Karditsas, Karditsa, Greece

Abstract
Land improvement infrastructure aim to obtain and conserve water to meet the irrigation needs of crops, the rational management of soil and water resources, the quality of irrigation water and the protection of soil. Land improvement infrastructure include works serving irrigation, i.e. pumping stations, canals, pressurised pipeline networks, reservoirs, tanks. In Greece, after 1960, the preparation of the first land improvement programmes began. During the same period, the operation of the Land Improvement Organisations was established. Their establishment arose from the need to manage certain land improvement works as collective irrigation projects, where the operation and maintenance of the projects was not feasible by each user individually. Today, in our country there are more than 450 Local Land Improvement Organisations (TOEV) and General Land Improvement Organisations (GOEV), which are the legally responsible bodies responsible for the management (i.e. administration, operation and maintenance) of land improvement infrastructure in their area of jurisdiction and distribute irrigation water to farmers through irrigation networks, either closed under pressure or open with free flow. TOEV Tavropou Karditsas is a case study where modern practices are applied in both administrative operation and irrigation management, ensuring maximum benefits for its thousands of Members.

Keywords
Irrigation, Water, Management, Land Improvement Organisation

1. Local Organisation of Land Improvement (TOEV) Tavropou Karditsas

TOEV Tavropou Karditsas is a Local Organisation of Land Improvement. It is a self administered Organisation by its own members. Every four years the members, land owners in the area of TOEV, elect a general assembly of 85 members, as well as a seven member administrative board. TOEV is responsible, on behalf of the public sector, acting as a utility Organisation, for the operation and maintenance of the irrigation network of the area (Land Improvement Infrastructure of Tavropos). TOEV Tavropou main scope of work is the administration, operation and maintenance of land improvements, which contribute to the utilisation and development of agriculture through the application of rational irrigation and drainage models in Karditsa Regional District. All TOEV in the country fall under the administration of the Regional Authorities, which in turn fall under the Ministry of Rural Development and Food.

2. Land Improvement Project of Tavropos

The existing Land Improvement Infrastructure of Tavropos is managed by TOEV Tavropou. The construction of the existing Infrastructure originally started at 1963, its gradual operation at 1965 and its construction was completed in 1973. The project's water supply is derived from N. Plastiras Lake through the Hydroelectric Station and the post-regulatory tank of volume 600.000 m^3. Tavropos Infrastructure consists of an extended open gravity irrigation network, with channels, which extend to almost 890 km alongside with the drainage network and the rural road network (Table 1). The irrigation network consists of the central, primary, secondary and tertiary irrigational channels, that distribute the water to the producers. Tavropos network irrigates an area of 12.000 ha, around the city of Karditsa (Fig. 1, 2), within Land Reclamation Fields in 19 Local Communities of Karditsa and Mouzaki Municipalities, concerning 8.000 Members. Figures 3-8 delineate aspects of the existing network.

Table 1. Elements of the existing Land Improvement Infrastructure of Tavropos

Network Category	Length
Open gravity irrigation network	887 km
○ Central	28.460 m
○ Primary	19.900 m
○ Secondary	140.835 m
○ Tertiary	697.675 m
Drainage network	824 km
○ Primary	37.713 m
○ Secondary	175.951 m
○ Tertiary	610.017 m
Rural road network	851 km
○ Primary	38.500 m
○ Secondary	223.929 m
○ Tertiary	588.401 m

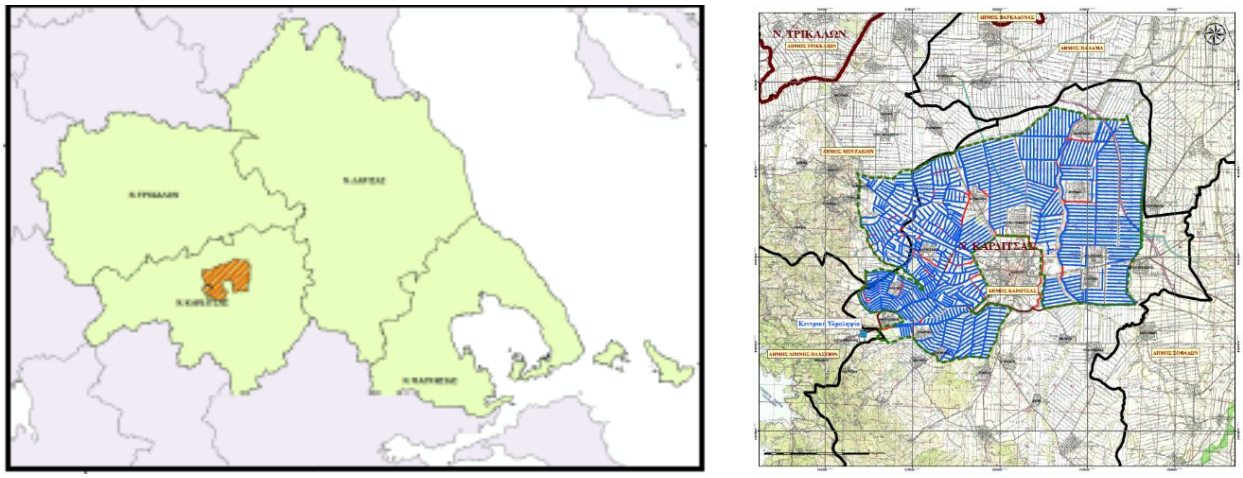

Figures 1-2. Positioning of the existing Land Improvement Infrastructure of Tavropos (left) in the region of Thessaly (right); in the District of Karditsa

Figures 3-8. Aspects of the existing Land Improvement Infrastructure of Tavropos (irrigation network): water tank, central channel, primary, secondary and tertiary channels

3. Actions of TOEV Tavropou Karditsas

TOEV Tavropou Karditsas, starting from the year 2016, managed to decrease expenses, apply KPIs and manage the finances, so it succeeded in only one year to more than double the available funds, and this trend continues up to the present, through strict economic control and rationalization of expenses, without changing the contribution fee of its Members. This achievement gave the opportunity to TOEV Tavropou to invest over 700.000 € in the acquisition of modern operation machinery (Fig. 9), without financing.

More specifically, TOEV acquired two new excavators (purchase cost 176.849 € and 207.576 €, vat included), a new tractor and new hedge and grass cutters (purchase cost 117.412 €, vat included) and a new contemporary grader (purchase cost 197.160 €, vat included) (Fig. 10-13). Today, the new machinery can produce 1 km of cleaning work in the network, instead of 150 meters, in an 8hour shift. This work now costs 200 €, instead of 1.000 € that used to be spent in the past. TOEV also invested in equipment, in order to fight water absorbing vegetation. It is very important to mention that in the past all this vegetation was combated with chemicals, more than 12 tones of glyphosate were applied in the area, with whatever this implies about public health. Resulted the chemical control stopped.

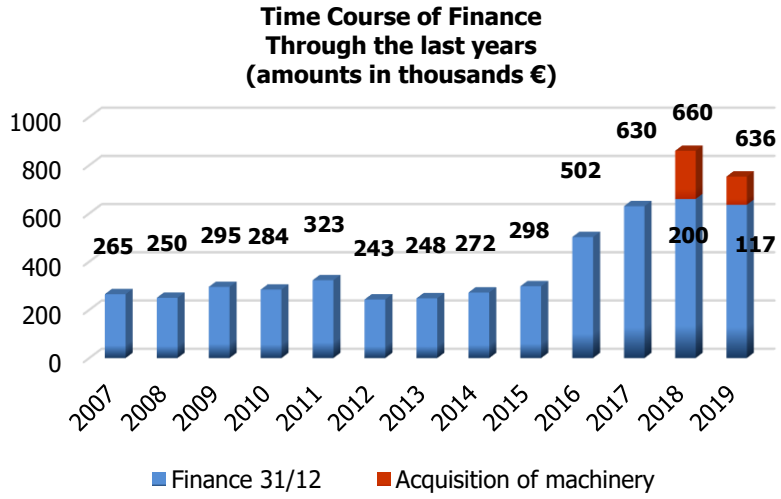

Figure 9. Time course of TOEV Tavropou finance through the last years

Figures 10-13. Acquisition of modern operation machinery

4. Water management in TOEV Tavropou network in the past

Apart from the financial management, the most important thing in TOEV Tavropou Karditsas' operation is irrigation. Water management in the past was practised in a free demand network, with no storage space, with water distribution in an average irrigation cycle of cultivations of 15 days. Irrigation water is distributed through Tavropos network per irrigation sector and water supply is delivered according to the total and not the actual irrigated area of each sector, so as a result, excess water is delivered in specific sectors and lack of water derives in others. Figures 14-16 delineate aspects the irrigation sectors of the existing network.

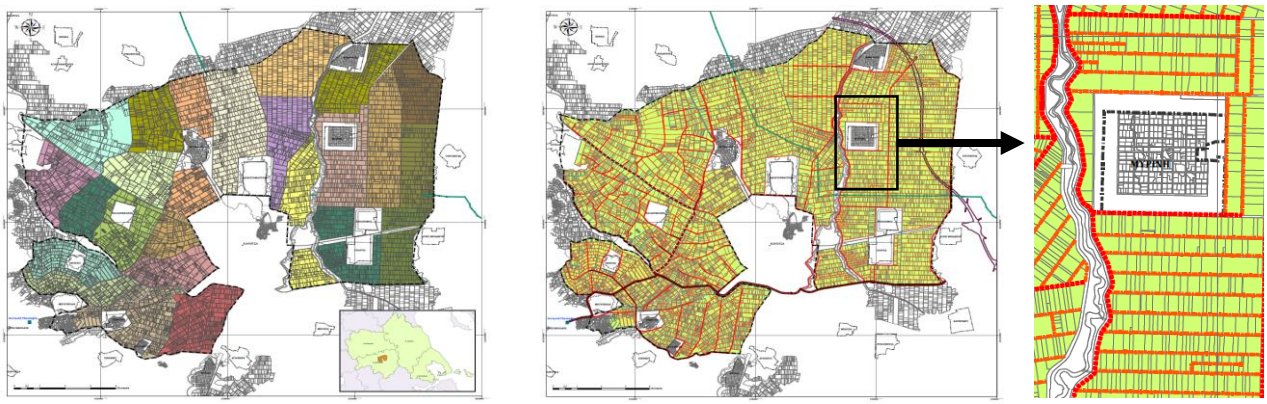

Figures 14-16. (left) Irrigation sectors of Tavropos network; (right) details of an irrigation sector

5. Automated operation of the central post-regulatory tank's gate and hub points of the network

TOEV Tavropou Karditsas' belief is that no one should irrigate without control, so there should be a programmed irrigation. All water inspection agents note the water records, according to the producers' needs and when they are about to irrigate, so all these created a schedule before the beginning of irrigation. Consequently, having all these data, an information system was developed, called "Kalliroi" software, using electric motors, sensors and gate controls, in order to schedule the changing daily supplies depending on demand, to have the right water supply, and some kind of precise irrigation with a small deviation. This application is used by the water inspector agents, embedded in military type mobile phones. They enter real time data, as who irrigates, for how long, as well as the type of cultivation. This way TOEV managed to decrease the amount of water that ends up in the outfalls. Moreover, TOEV practices remote control by means of telemetry and has applied an appropriate hydrometer downstream of the water supply position (Fig. 17-28).

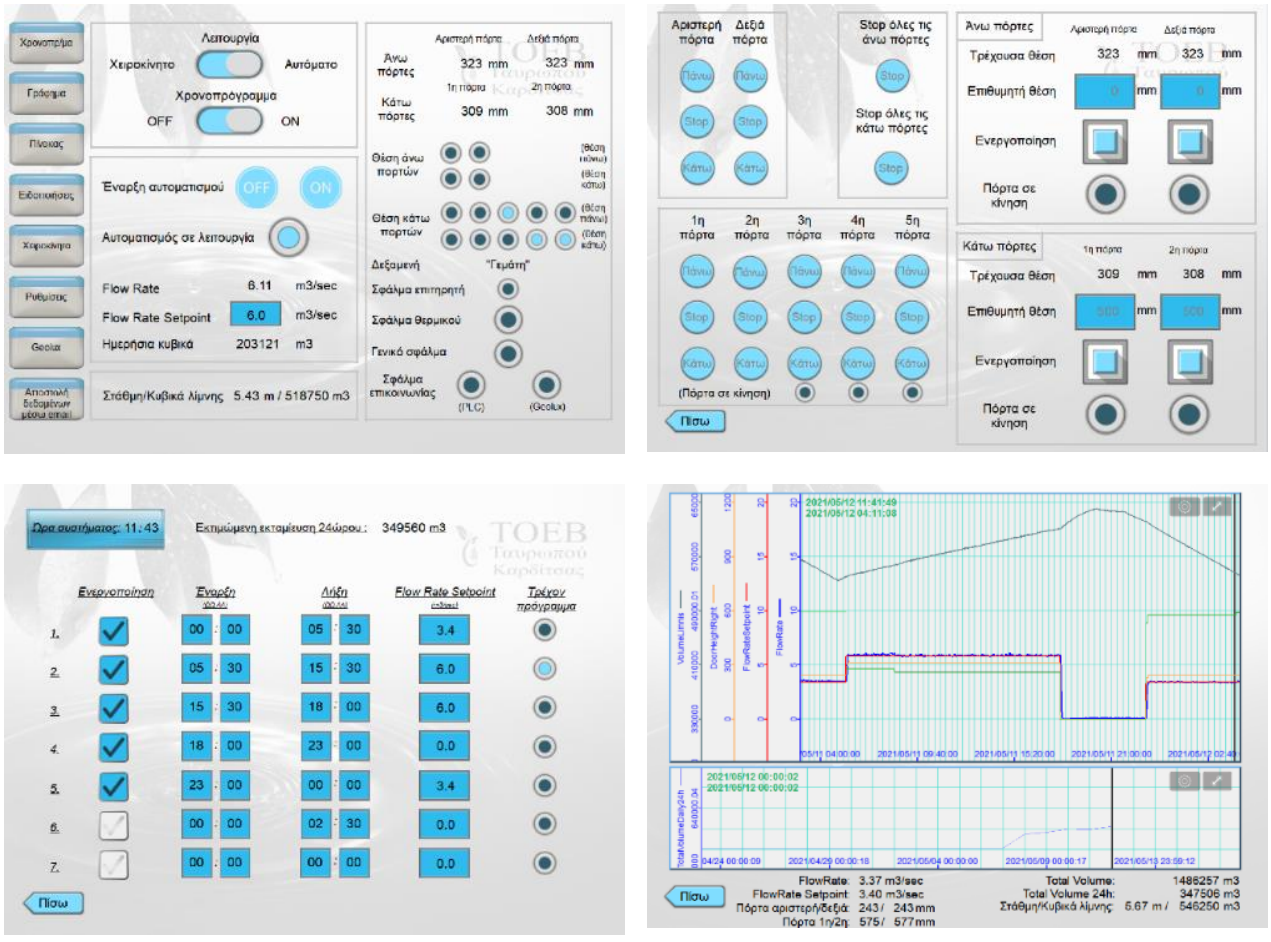

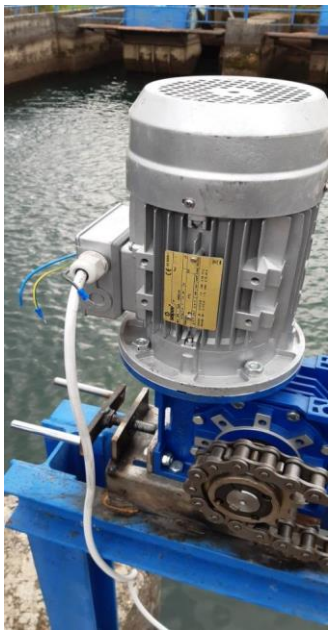

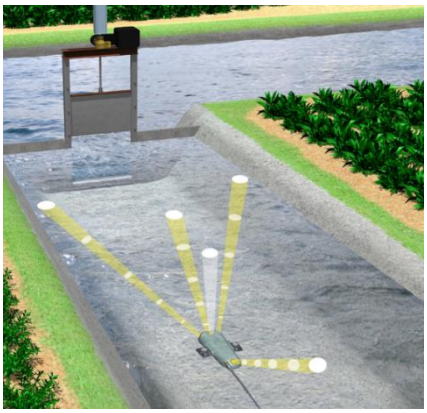

Figures 17-23. Remote control by means of telemetry

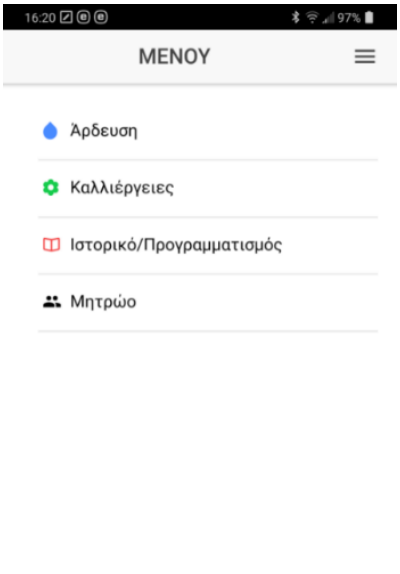

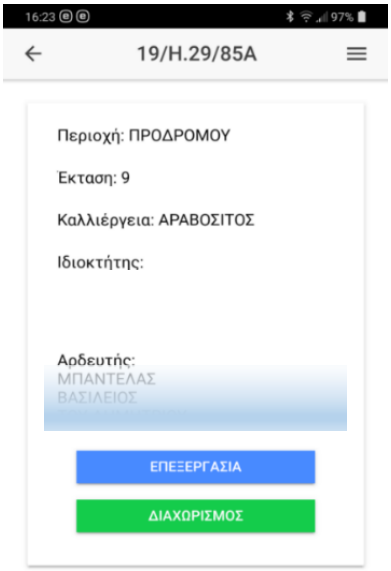

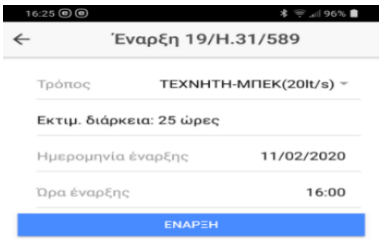

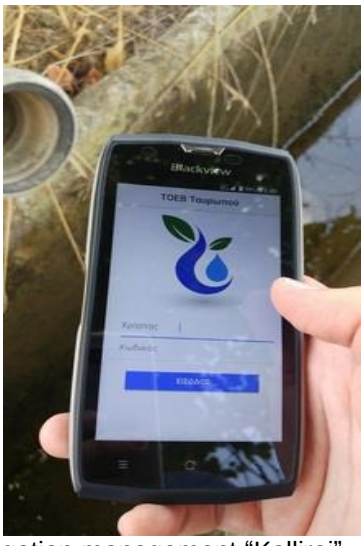

Figures 24-28. Information System of irrigation management “Kalliroi”

Water Management Rationalization Results

Through automated operation TOEV Tavropou Karditsas managed to increase its total irrigated area by 33% (from 6.000 ha to 8.000 ha), to manage water supply based on the actual irrigated area of each sector and reduce the average irrigation cycle of cultivations up to 8 days.

6. Operational problems of the existing irrigation infrastructure of Tavropos

The existing irrigation infrastructure faces operational problems, as it was designed for free demand irrigation and flood method application, which is an old fashioned method that leads to lower crop yields, great loss of water, and a non accepted practice based on Agricultural Best Practices. From the beginning and up to the growth of the plants, in the middle of the cultivating season, the sprinkler method is used.

Despite of the low irrigation fees (40 €/ha) and drainage fees (40 €/ha), the irrigation cost really exceeds 500 €/ha, due to diesel oil use, for the required pumping operation.

More specifically, the existing irrigation network disadvantages are:

- Designed for free demand irrigation and flood method application:
  - *Lower irrigation efficiency (less than 30%)*
  - *Great loss of water*
  - *Soil erosion (reduced fertility, weed growth etc.)*
  - *Burden groundwater pollution caused by nitrates*
  - *Non accepted method nowadays*
- From the beginning and up to the growth of the plants, in the middle of the cultivating season, the sprinkler method is used:
  - *Use of pumping units for the necessary pressure - Exclusive diesel oil use in absence of rural electricity*
  - *Increase of irrigation production cost*
- Despite of the low irrigation fees (40 €/ha) and drainage fees (40 €/ha), the irrigation cost really exceeds 500 €/ha.
- High operational and maintenance costs, due to oldness especially after the Mediterranean cyclone “IANOS”, 18th September 2020.
- Increased water loss due to leaks and vaporization.

7. Modernization of the Irrigation Network - New irrigation project

Since 2017 a closed irrigation network study has been launched with funding of TOEV Tavropou itself and design based on its own needs and modern requirements. A new closed pressurized irrigation network with underground pipelines has been designed, providing the required energy naturally, due to the geomorphology altitude difference of 90 meters from the point of water intake to the hydrant outlets. It is a network that will lead by design in 35% water savings. Figures 29 to 31 delineate the horizontal design of the new project and the results of the simulation of the operation of the new network (available pressure of hydrant outlets).

The benefits of the New irrigation project include:

- A fully closed network of 800 km length, under pressure network
- Direct water saving of 35% by design
- Operational pressure of at least 4 atm in all hydrant outlets without the use of energy
- Favors the use of high efficiency irrigation methods by users (drip)
- Fully automated based on IoT technology for control and operation of hydrant outlets

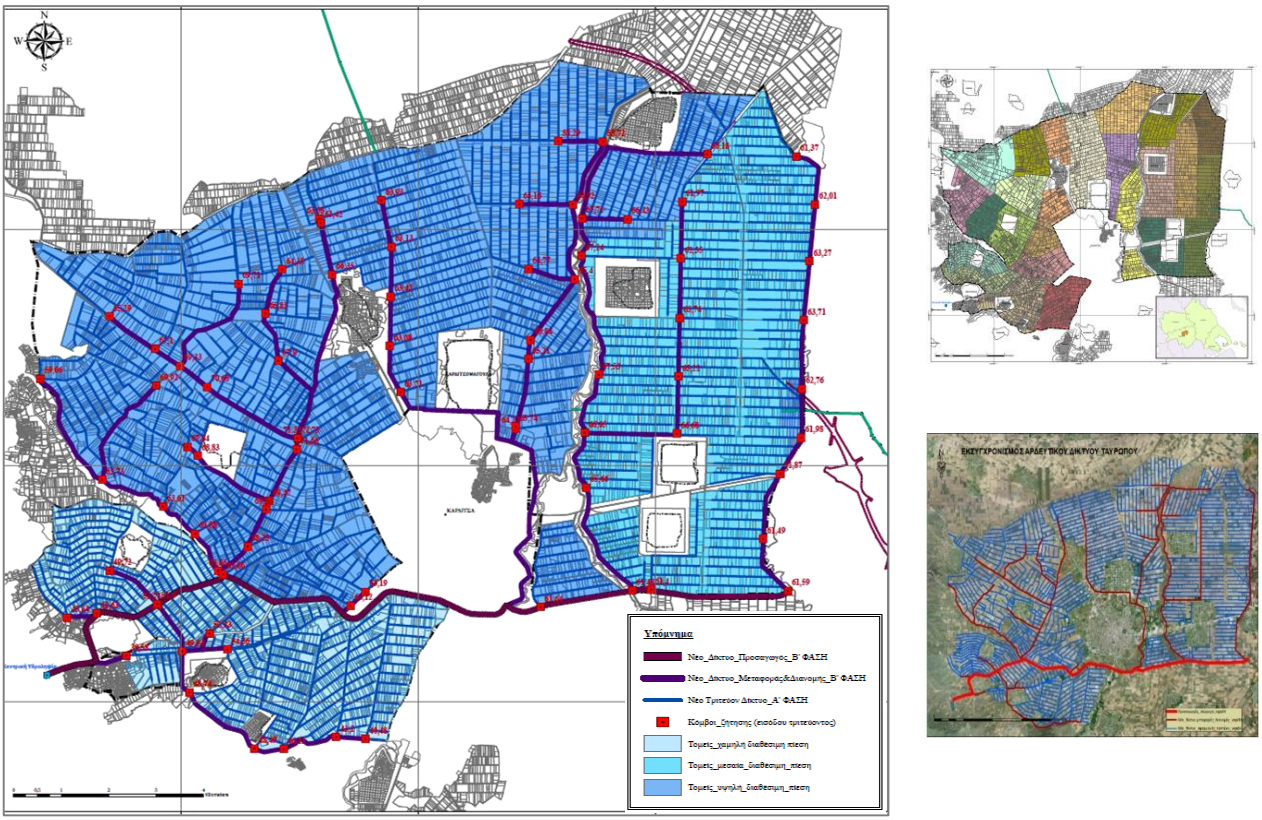

Figures 29-31. Horizontal design of the New Project

Remote control of network devices - hydrant outlets

The hydrant outlets of the new irrigation network will consist of a hydro outlet, an electronic hydrometer, a flow limiter, a closing valve and will operate energy sufficiently. Its control system will operate through Internet of Things (Fig. 32-33). Built-in sensors will be installed in the hydrant outlets (network devices) and acquired data will be delivered through the platform (cloud) to the central control-management system.

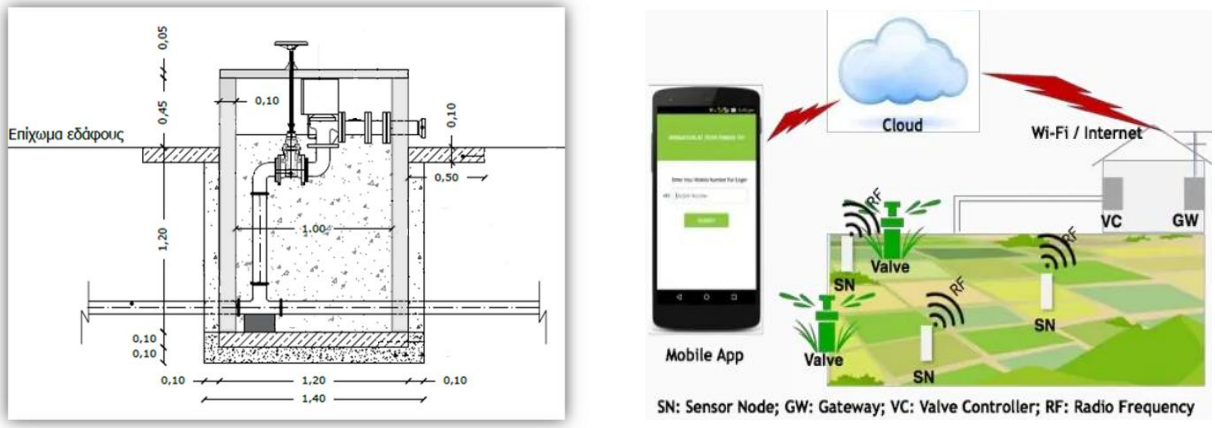

Figures 32-33. Operation of a hydrant outlet (left) through Internet of Things (right / Source: Suthar J.V.; Krishna V.)

8. Integration progress of the TOEV Tavropou New irrigation project

On the 8th of November 2021 there has been an announcement, by the Minister of Rural Development and Food, that the new project was included in the Investment Project in land improvement infrastructure “Υδωρ 2.0” by Public Private Partnerships (PPPs). The project was characterized as a significant pilot one. The European Bank of Reconstruction and Development has undertaken the proceedings in order to promote the project and the tender procedure. On the 9th of June 2022 representatives of EBRD visited the existing site. The implementation of the project plays an important role for the primary sector and for the entire local economy.

References

Clément R (1966) Calcul des debits dans les réseaux d'irrigation fonctionnant à la demande. Huille Blanche, No5, 553-575.

Clément R, Galand A (1979) Irrigation par aspersion et réseaux collectives de distribution sous pression. Editions Eyrolles, pp.182.

Decision of the National Water Committee (2014) Nr 909 Approval of Plan Management of the Rivers Basins of Thessaly water district, Greek Official Gazette, Vol B, 2561/25.09.2014

Decision of the National Water Committee (2017) Nr 897 Approval of the 1st Revision of Plan Management of the Rivers Basins of Thessaly water district and the corresponding Strategic Environmental Impact Assessment, Greek Official Gazette, Vol B, 4682/29.12.2017

Decision of the National Water Committee (2018) Nr 41337/329 Approval of Flood Risk Plan Management of the Rivers Basins of Thessaly water district and the corresponding Strategic Environmental Impact Assessment, Greek Official Gazette, Vol B, 2685/06.07.2018

Dercas N (1989) Contribution au calcul des réseaux sous pression à la demande libre et restreinte. Proposition d'un modèle de simulation Thèse de doctorat, Université des Sciences et Techniques du Languedoc (Université Montpellier II), France, 201pp.

Dercas N (2020) Agricultural Water Management in Greece. In: Negm, A., Romanescu, G., Zelenakova, M. (eds) Water Resources Management in Balkan Countries. Springer Water. Springer, Cham. pp 421-453

Dercas N, Londra P, Karamanos A (2007) Proposals for improved irrigation water management according to WFD 200/60, Proc. of 5th National Congress of Agricultural Engineering, Larissa, Greece, pp 328-336

Hellenic Statistics Service (2011) Agricultural statistics of Greece, Year 2011.

Kanakis PC, Papamichail DM, Georgiou PE (2014) Performance analysis of on-demand pressurized irrigation network designed with linear and fuzzy linear programming. Irrigation and Drainage. 63(4): 451–462

Karamanos A, Aggelides S, Londra P (2004) Irrigation systems performance in Greece. 2nd Workshop on Water Saving in Mediterranean Agriculture. Hammamet, Tunisia.

Karantounias G, Dercas N (1999) Problèmes de fonctionnement et de gestion des réseaux d'irrigation en Grèce - Etude de deux cas typiques, ICID Journal, vol. 48, No 2, pp. 11-32.

Khadra R, Lamaddalena N, Inoubli N (2013) Optimization of on demand pressurized irrigation networks and on-farm constraints. Procedia Environmental Sciences 19: 942 – 954.

Labye Y, Lahaye JP, Meunier M (1975) Utilization des caracteristiques indices. Proc. Congres de la ICID, Moscou, p30

Lamaddalena N, and Pereira L.S (2007) Pressure-driven modelling for the performance analysis of irrigation systems operating on demand. Agric Water Manag 90:36-44

Lamaddalena N, Sagardoy JA (2000) Performance analysis of on-demand pressurized irrigation Systems, Irrigation and Drainage Paper no 59. FAO, Rome

Law 414 (1976) Amending and complementing of the provisions of L.D. 3881/1958 on land reclamation works,as subsequently amended. Vol A, 212/14.08.1976

Law 1739 (1987) Management of water resources and other provisions, Greek Official Gazette, Vol A, 201/20.11.1987

Law 3199 (2003) Water Protection and Management – Harmonization with Directive 2000/60/EC of European Parliament and Council of 23 October 2000, Greek Official Gazette, Vol A, 280/09.12.2003

Law 3852 (2010) New architecture of local government and regional administration – Kallikratis Program, Greek Official Gazette, Vol A 87/07.06.2010

Law 4456 (2017) Complementary measures of application of Regulation EU, Euratom, 1141/2014 on European political parties and foundations measures for the acceleration of Government's work and other provisions, Greek Official Gazette, Vol A 24/01.03.2017

Legislative Decree 1218 (1972) Replacing and repealing certain provisions of L.D. 3881/1958 on land reclamation works, Greek Official Gazette, Vol A, 133/29.07.1972

Legislative Decree 1277 (1972) Amending and complementing L.D. 3881/1958 on land reclamation works, Greek Official Gazette,Vol A, 213/01.12.1972

Legislative Decree 3881 (1958) On land reclamation works, Greek Official Gazette, Vol A, 181/30.10.1958

Mantzou A (2008) Agricultural Policy and Water Resources Management in the Framework of a Sustainable Economic Development, PhD Thesis, National Kapodistrian University of Athens.

Ministry of Agriculture (2000) Water management in the agricultural sector, pp 43.

Presidential Decree 499 (1975) Concerning policy of irrigation water and works governed by LRA, Greek Official Gazette, Vol A, 163/05.08.1975

Presidential Decree 332 (1983) Transfer of competences from the Minister of Agriculture and the Inter-prefecture Services of the Ministry of Agriculture to the Prefects, Greek Official Gazette, Vol A, 119/08.09.1983

Royal Decree 709 (1970) On the definition of the competences remaining upon he Minister of Agriculture and the Inter-Prefectures Authorities of the Ministry of Agriculture, Greek Official Gazette, Vol A, 235/05.11.1970

Stamouli P, Dercas N, Baltas E (2017) Performance analysis of on-demand pressurized irrigation networks – Case study in Greece, Water Utility Journal 16: 39-55.

Stefopoulou A (2013) Development of a simulation model for the performance analysis of pressurized irrigation networks operating on-demand. PhD Thesis. Agricultural University of Athens. Pages. 232 pp.

Stefopoulou A, Dercas N (2012) The effect of head losses evaluation on the analysis of pressurized irrigation networks operating on-demand. Water Utility Journal. 3: 3-18.

Stefopoulou A, Dercas N (2017) NIREUS: A new software for the analysis of on-demand pressurized collective irrigation networks. Computers and Electronics in Agriculture, Volume 140, August 2017, 58-69.

Tsakiris G (1991) Course of Land Reclamations Works, Publ. NTUA, Athens, p 325.

Monitoring crop phenology by applying biophysical parameters from Sentinel-2 data. The case in "Sidi Bouzid" in Tunisia

Faraslis[1], I., N. Alpanakis[2], G. Tziatzios[2], M. Spiliotopoulos[2], S. Sakellariou[2], P. Sidiropoulos[2], V. Brisimis[2], A. Blanta[2], N. Dercas[3], N.R. Dalezios[2]

[1] Department of Environmental Sciences, University of Thessaly, Larisa, Greece
[2] Department of Civil Engineering, University of Thessaly, Volos, Greece
[3] Department of Natural Resources and Agricultural Engineering, Agricultural University of Athens, Greece

Abstract.
Biophysical products, from relatively new Sentinel-2 optical imagery, indicate a promising dataset for crop monitoring. These products can be retrieved globally at relatively high spatial and temporal resolution. The benefits of biophysical parameters in crop monitoring focused on optimizing water irrigation, prevent stress events, weed mapping, calculating crop yield production, etc. This paper considers the summer crop status of maize during the 2021's growing season in "Sidi Bouzid" agricultural area, in Tunisia. The biophysical variables and vegetation indices, that is, Leaf Area Index, Fraction of absorbed photosynthetically active Radiation, Fraction of Vegetation Cover, Leaf Chlorophyll content, Canopy Water Content, Normalized Difference Vegetation Index and Normalized Difference Red Edge Index are retrieved for the two maize plots by applying the PROSAIL radiative transfer model. The free SNAP® toolbox has been implemented for retrieving the biophysical parameters from Sentinel-2 multispectral imagery. The biophysical variables indicate uniform behavior during the growing season. Moreover, the comparison of the two maize plots, which follow different cultivation practices, reveals distinct growing pattern. With the one, this with sustainable agricultural practices, to present better yield characteristics. Finally, the Sentinel-2 biophysical products could provide a valuable tool for crop monitoring at farm scale.

1. Introduction

Earth observation satellites, such as Sentinel-2, allows new opportunities for continuous agricultural monitoring. The Sentinel-2 missions comprise red edge spectra bands that can reveal subtle stress in crops before is detectable by the naked eye (Campbell and Wynne 2007; Odindi et al. 2016; Ramoelo and Cho 2018). Thus, biophysical products and vegetation indices, with high spatial and temporal resolution, can be retrieved from red edge bands. These parameters, which are essential in several applications in precision agriculture, are used for crop yield prediction, nitrogen deficiency and water improper irrigation. In the context of agricultural monitoring five biophysical variables, which identify the inherent characteristics of vegetation, are investigated: (a) Leaf area index LAI (m^2/m^2), is the ratio of green leaf area over the surface area. It's a critical indicator for modelling evapotranspiration and water balance and biomass estimation (Dorigo et al., 2007), (b) Fraction of Absorbed Photosynthetically active radiation (FAPAR), is defined as the amount of proportional incoming photosynthetically active radiation (400–700 nm) absorbed by plants for photosynthesis (Hu, et al. 2020). FAPAR is important parameter in plant growth modeling and biomass production (Rahman et al., 2014). (c) Fraction of vegetation cover (FVC), refers to the fraction of vertical projected area of vegetation observed on the surface. It's important indicator for plant transpiration and especially for monitoring the early stages of plant growth (Ilina and Petar, 2021). (d) Canopy chlorophyll content (Cab) measure for photosynthetic activity in leaf through the chlorophyll pigments a and b. Cab is associated to nitrogen deficiencies, and plant diseases (Bester et al., 2020). (e) Canopy water content (CWC), indicates the amount of water in leaves per unit ground area. It is a key parameter in monitoring crop water shortages (Weiss & al, 2020).
There are two categories for calculating the biophysical parameters from remote sensing data: (a) the statistical methods, applying regression models between remote sensing data and in-situ data and (b) physical modeling employing radiative transfer models (Qiaoyun et al., 2019). The statistical models are broadly used although their major disadvantage is that they need a lot of resources for large areas. Instead, physical modelling, such as artificial neural networks have exhibited good results concerning the measurements of biophysical parameters.
Moreover, the two vegetation indices, the NDVI (Normalized Difference Vegetation Index) and the NDRE (Normalized Difference RedEdge) were employed for crop monitoring. The NDVI, extensively used to agricultural production, such as fertilizer application and irrigation, although it has been reported saturation issues over high biomass conditions (Xue & Su, 2017). The NDRE index is defined by high sensitivity and

provides better results, compared to NDVI, about the chlorophyll concentration in the plants (Jorge et al., 2019).
The objective of this study is to evaluate the above-mentioned biophysical variables over the summer of annual crop maize in the province "Sidi Bouzid", in Tunisia. That is, seasonal Sentinel-2 LAI, FAPAR, FVC, Cab, CWC, NDVI, NDRE vegetation parameters and indices have been estimated for monitoring the vegetation status of Maize plots. Furthermore, relationships between the two maize crops concerning the vegetation characteristics, via the Sentinel-2 biophysical variables, have been considered.

2. Materials and Methods

2.1. Description of Study area

The pilot area in Tunisia is the province "Sidi Bouzid", covering an area of 7,490 km^2. The region is in the central-western part of Tunisia. It is characterized by relatively flat surface averaging 300 meters in altitude and semi-arid climate. The underline alluvial deposits in the study area, led to development of vegetable crops and olive. The agriculture consists of annual crops like durum wheat, fodder oat, maize and trees as olives and pistachios. Regarding this research, the growth of the two maize crops has been investigated by Sentinel-2 biophysical parameters retrieval. The first plot (hereafter "supromed plot") indicates the farmer, who has followed sustainable cultivation practices, whereas the second plot (hereafter "leader plot") is the farmer who has followed the traditional practices (fig.1). The covered area by supromed and leader plots are 0.07 & 0.06 hectares, respectively.

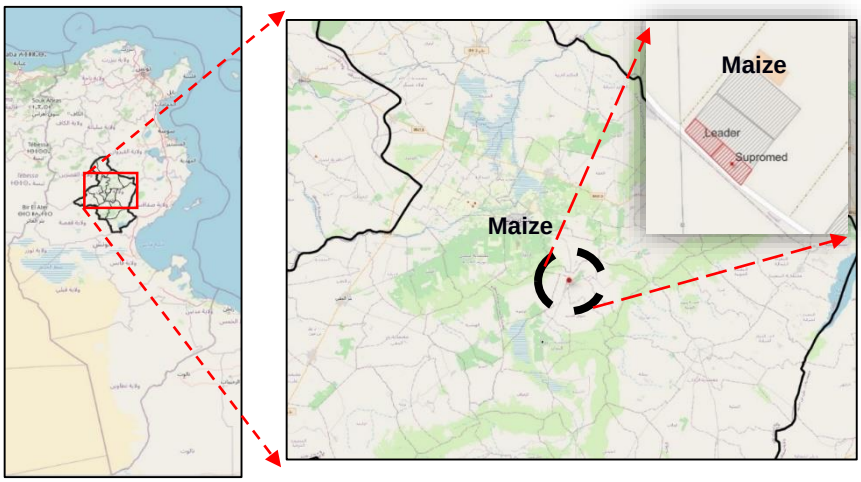

Figure 1 The two maize pilot-sites in the region of "Sidi Bouzid" , in Tunisia

2.2. Dataset

To cover the growing season for maize crop, 24 Sentinel-2 images from the period June 1, 2021, to the end of September 2021 was downloaded. The satellite data was derived from Copernicus Open Access Hub. ESA's (European Space Agency) Copernicus service supplies, free of charge, Sentinel products (-1, Sentinel-2 and Sentinel-3). The multispectral Sentinel-2 images were Level-2A. Thus, they are atmospherically (bottom of atmosphere reflectance images) and geometrically corrected (UTM/WGS84 projection). Moreover, for each Sentinel-2 product a quality assessment was conducted for minimizing cloud effects and other artifacts. At the end, seventeen images (17) fulfilled the quality criteria, which have been used for further study. Following, the appropriate processes were performed to mask-out the water bodies, etc. Resampling and subsetting, preprocessing techniques were implemented, creating 20-meter spatial resolution multispectral images for the area under investigation.

2.3. Biophysical parameters and vegetation Indices retrieval methodology

The ESA's open-source toolbox SNAP (Sentinel for Application Platform) has been applied for estimating the biophysical parameters and the vegetation indices. Especially, the biophysical processor integrated in SNAP derives Level-2B products such as: LAI, FAPAR, FCOVER, Cab and CWC. The Level-2B processor, make use of the common applied PROSAIL model and neural networks, for the biophysical variables' computation. This algorithm belongs to physical modeling approach, which uses radiative transfer model for simulation the canopy characteristics. In details, there are three submodels: (a) The PROSPECT model that defines the leaf characteristics namely, water content, leaf dry matter content, chlorophyll content, etc, (b) The SAIL radiative

transfer model, describing the reflectance of canopy structure as homogeneous medium where leaves are randomly distributed, and (c) the reflectance of non-green material, namely bare soil, water, and snow. To estimate the biophysical parameters this physical model is based on the artificial neural network method following two steps: (a) the canopy reflectance bands were used for the creation of a training dataset and calibrating the network, and (b) a back-propagation learning rule was applied to reduce the error between input training values and predicted outputs biophysical parameters. The Level-2B processor offers two main benefits. Firstly, no in-situ data are required and secondly, based on a pre-trained neural network, the biophysical parameters can be retrieved globally through Sentinel-2 dataset.
Afterwards, the two vegetation indices, NDVI and NDRE were obtained by SNAP software. The NDVI was retrieved by the bands B4 (red) and B8 (NIR), whereas the NDRE by the bands B8 (NIR) and B5 (rededge). Finally, the five biophysical variables and the two vegetation indices were calculated in each one of the 17 Sentinel-2 images for the summer period. The characteristics of the above-mentioned vegetation parameters are illustrated in the following table (table 1).

Table 1 Characteristics of Biophysical variables and indices estimating from sentinel-2 images

Parameter	Unit	Minimum	Maximum
LAI: Leaf Area Index	dimensionless	0	8.0
FAPAR: fraction of absorbed photosynthetically active Radiation	dimensionless	0	1.0
FVC: Fraction of Vegetation Cover	dimensionless	0	1.0
Lai_Cab: Leaf Chlorophyll content	g/cm^2	0	600
Lai_cw: Canopy Water Content	g/m^2	0	0.55
NDVI: Normalized Difference Vegetation Index: (842nm-665nm)/(842nm+665nm)	dimensionless	-1	1
NDRedEdge: Normalized difference Red Edge Index: (783nm-705nm)/ (783nm+705nm)	dimensionless	-1	1

Batch processing techniques were applied for automating the calculation process. The SNAP graph builder tool was implemented, in 17 images, to retrieve the seven vegetation parameters (fig.2).

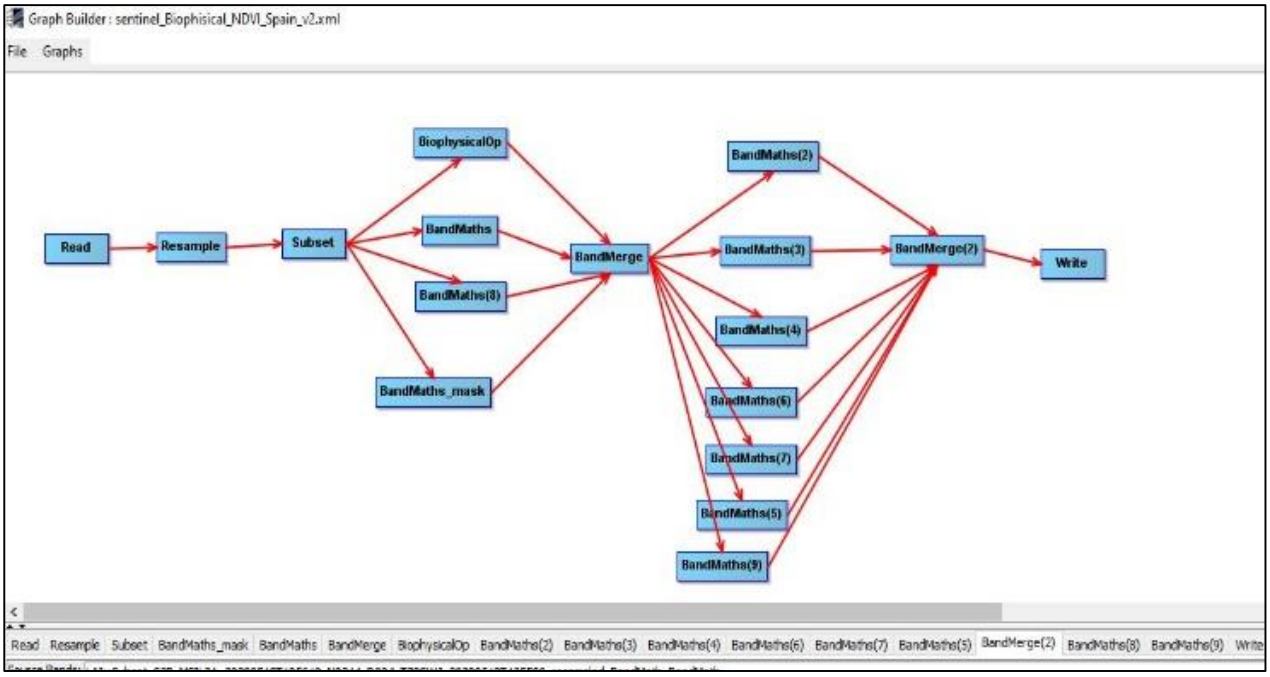

Figure 2 Workflow of the SNAP graph builder tool for producing the biophysical variables and indices of the 17 images

3. Results and Discussion

According to crop calendar, for maize growing season 2021, begins in June (sowing period) and ends at the end of September (end season) (table 2). Thus, the time series analysis of the biophysical indices, was conducted based on the period from 7 June (sowing/germination) until 30 September 2021 (late season/harvest period). The growth of the two maize plots (supromed and leader) was monitored through the seven biophysical indices and parameters.

Table 2 Crop calendar for Maize growing season 2020-2021

Date	Stage
June 4, 2021	Sowing
June 12, 2020	Germination
July 11, 2021	4-5 leaf stage
August 8-14, 2021	Flowering
Aust 30, 2021	Plat with fruit
September 16, 2021	Fruit with seeds

The following image represents the evolution of Leaf Area Index (LAI) biophysical parameter for the period from June to September 2021 for the two maize plots (fig.3). The shades of green color show the different phenological stages for Maize, namely in June the plant is in early stage, in July to mid-August (LAI about 1) the crop is on “flowering” stage, (dark green color) and at the beginning of September the crop is on “maturity stage” (brown-green color).

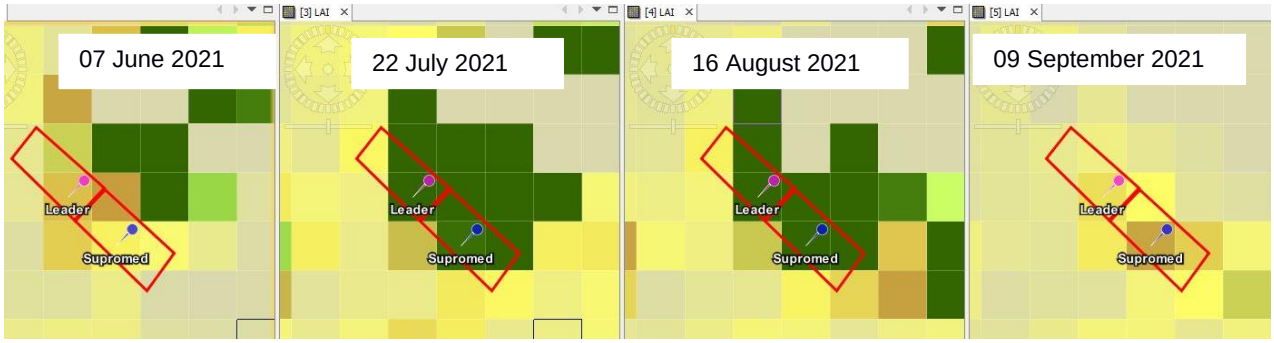

Figure 3 The evolution of Maize crop from June 2021 to September 2021 based on LAI

Moreover, the leader and supromed maize plots indicate the same growth pattern concerning the seven biophysical/vegetation indices. The following images portray the growth pattern for the supromed maize plot (fig.4).

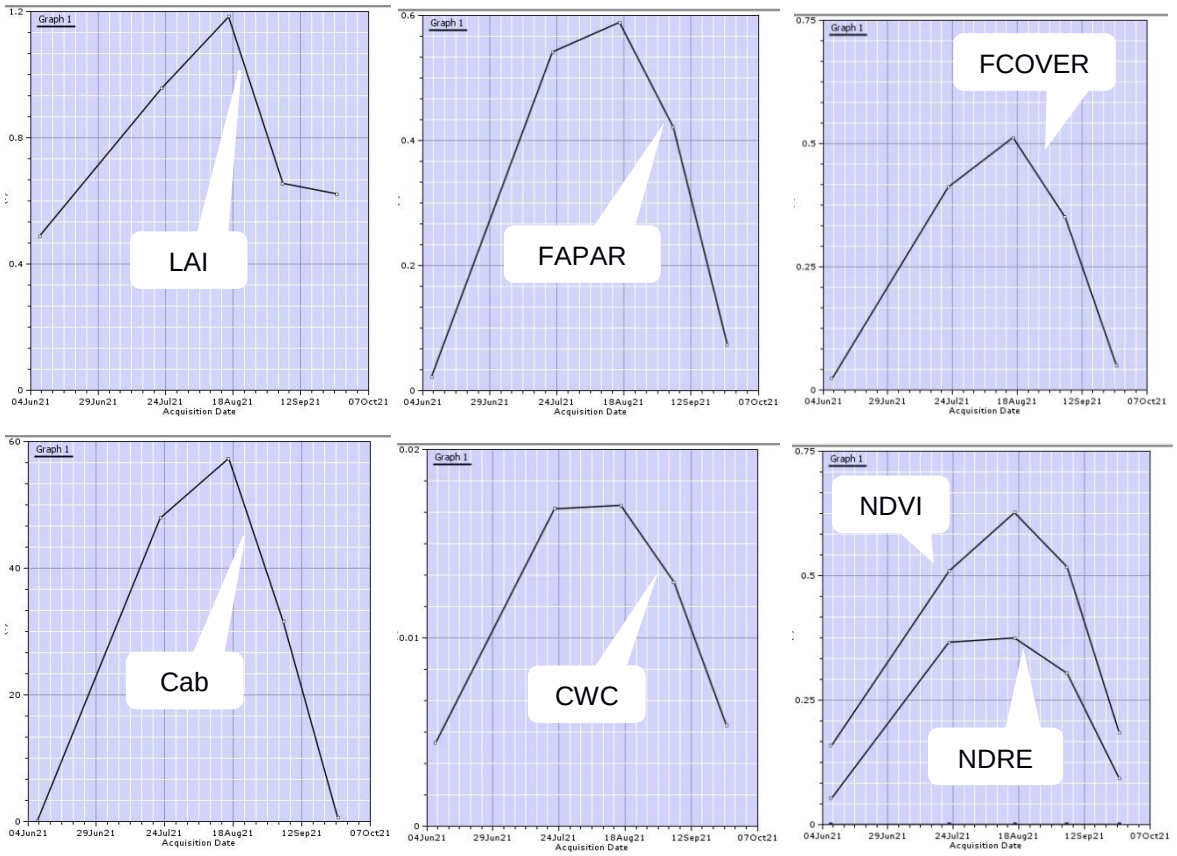

Figure 4 Supromed Maize plot growth cycle monitoring by seven biophysical parameters from June to September 2021

All the vegetation parameters illustrate almost the same pattern, which is in consistency with the crop calendar. From the beginning of June there is an increase of values with the peak occurring by mid-August, followed by a sharp fall until the end of September (end of season).
Next, the relationship of the two plots, via the vegetation parameters, during the growth period, was investigated. Generally, the supromed plot indicates better inhered vegetation characteristics than the leader one. For instance, considering the LAI parameter the supromed maize plot indicates better characteristics (blue line) about the amount of foliage in the plant canopy than the leader one, especially at the growth period i.e., from July to mid-August (fig.5).

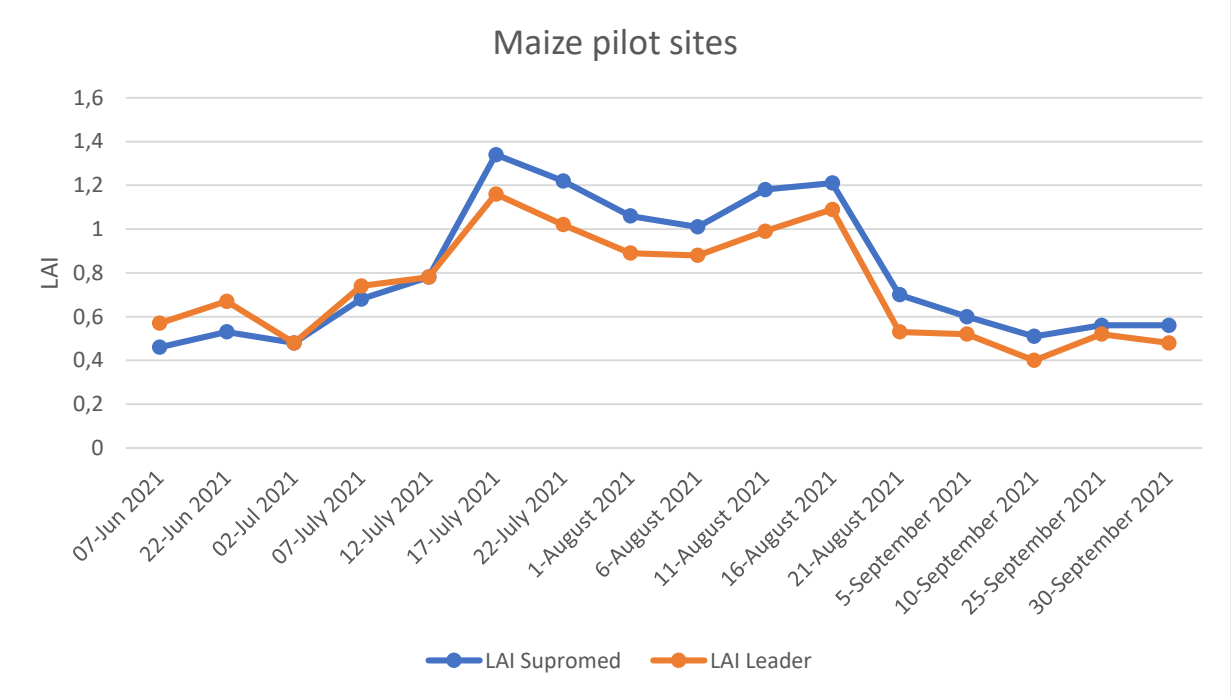

Figure 5 Assessing the two maize plot sites by LAI vegetation parameter

In summary, the correlation of biophysical parameters during the growing period of maize makes them a useful tool for monitoring the crop status.

4. Summary and conclusions

The research calculates the seven biophysical parameters and indices for monitoring two maize plots for the period June-September 2021. 17 Sentinel-2 images were elaborating by open-source software SNAP. The biophysical processor integrated in SNAP have been applied to estimate five biophysical variables, namely, LAI, FAPAR, FCOVER, Cad, CWC. In addition, the vegetation indices NDVI and NDRE were calculated. The investigation of growth maize plots via the biophysical indicators implies a good synergy according to the crop calendar. From June and onwards there is a continuous growth (Germination, 4-5 leaf stage, flowering) with the maximum productivity being detected in mid-August, following by the maturity stage at the end of September. Moreover, the comparison between the leader and supromed maize plots was conducted in the study area of “Sidi Bouzid”. The vegetation parameters reveal better performance for the supromed maize plot. In summary, Sentinel-2 imagery is a great tool to monitor crop status. Notably, in the field of precision agriculture the red-edge bands play a vital role. The open toolbox SNAP with the biophysical processor is an exceptional tool for retrieving almost globally biophysical parameters (Sentinel-2 and Landsat 8). These parameters could help farmers for sustainable use of resources (irrigation water, fertilizers, etc).

Acknowledgements

This research was funded by SUPROMED project under the PRIMA 2018 program of the European Commission.

References

- Bester Tawona Mudereri, Tavengwa Chitata, Concilia Mukanga, Elvis Tawanda Mupfiga, Calisto Gwatirisa & Timothy Dube (2021). Can biophysical parameters derived from Sentinel-2 space-borne sensor improve land cover characterisation in semi-arid regions? Geocarto International, 36:19, 2204-2223, DOI: 10.1080/10106049.2019.1695956.
- Campbell J, Wynne R. 2007. Introduction to remote sensing. 5th ed. New York (NY): Guiford Press.
- Dorigo, W.A.,Jurita-Milla, R., de Wit, A.J.W., Brazile, J., Singh, R., Schaepman, M.E., 2007. A review on reflective remote sensing and data assimilation techniques for enhanced agroecosystem modeling. International journal of applied earth observation and geoinformation, 9(2), 165–193.
- Hu, Qiong, Jingya Yang, Baodong Xu, Jianxi Huang, Muhammad S. Memon, Gaofei Yin, Yelu Zeng, Jing Zhao, and Ke Liu. (2020). "Evaluation of Global Decametric-Resolution LAI, FAPAR and FVC Estimates Derived from Sentinel-2 Imagery" Remote Sensing 12, no. 6: 912. https://doi.org/10.3390/rs12060912.
- Jorge, J., Vallbé, M., & Soler, J. A. (2019). Detection of irrigation inhomogeneities in an olive grove using the NDRE vegetation index obtained from UAV images. European Journal of Remote Sensing, 52(1), 169-177.
- Ilina Kamenova & Petar Dimitrov (2021) Evaluation of Sentinel-2 vegetation indices for prediction of LAI, fAPAR and fCover of winter wheat in Bulgaria, European Journal of Remote Sensing, 54:sup1, 89-108, DOI: 10.1080/22797254.2020.1839359.
- Odindi J, Mutanga O, Rouget M, Hlanguza N. 2016. Mapping alien and indigenous vegetaton in the KwaZulu-Natal Sandstone Sourveld using remotely sensed data. Bothalia. 46(2):1–9.
- Qiaoyun Xie, Jadu Dash, Alfredo Huete, Aihui Jiang, Gaofei Yin, Yanling Ding, Dailiang Peng, Christopher C. Hall, Luke Brown, Yue Shi, Huichun Ye, Yingying Dong, Wenjiang Huang, (2019). Retrieval of crop biophysical parameters from Sentinel-2 remote sensing imagery, International Journal of Applied Earth Observation and Geoinformation, Volume 80, pp187-195, ISSN 1569-8432, https://doi.org/10.1016/j.jag.2019.04.019.
- Rahman Muhammad, Stanley John, Lamb David, Trotter Mark, (2014). Methodology for measuring fAPAR in crops using a combination of active optical and linear irradiance sensors: a case study in Triticale (X Triticosecale Wittmack). In Precision Agriculture. doi -10.1007/s11119-014-9349-6.
- Ramoelo A, Cho MA. 2018. Explaining leaf nitrogen distribution in a semi-arid environment predicted on Sentinel-2 imagery using a field spectroscopy derived model. Remote Sens. 10(2):269.
- Weiss M., Baret F., Jay S., (2020). S2ToolBox level 2 products: LAI, FAPAR, FCOVER. Version 2. European Space Agency. Paris.
- Xue, J., & Su, B. (2017). Significant remote sensing vegetation indices: A review of developments and applications. Journal of Sensors, 2017, 1–17. Hindaw Limited. https://doi.org/10.1155/2017/135369.

INDEX OF AUTHORS